

R-06-10

Preliminary site description

Laxemar subarea – version 1.2

Svensk Kärnbränslehantering AB

April 2006

Svensk Kärnbränslehantering AB

Swedish Nuclear Fuel
and Waste Management Co
Box 5864

SE-102 40 Stockholm Sweden

Tel 08-459 84 00

+46 8 459 84 00

Fax 08-661 57 19

+46 8 661 57 19



ISSN 1402-3091

SKB Rapport R-06-10

Preliminary site description

Laxemar subarea – version 1.2

Svensk Kärnbränslehantering AB

April 2006

Preface

The Swedish Nuclear Fuel and Waste Management Company (SKB) is undertaking site characterisation at two different locations, the Forsmark and Simpevarp areas, with the objective of siting a geological repository for spent nuclear fuel. An integrated component in the characterisation work is the development of a site descriptive model that constitutes a description of the site and its regional setting, covering the current state of the geosphere and the biosphere as well as those ongoing natural processes that affect their long-term evolution.

The Simpevarp candidate area consists of two subareas, named the Laxemar subarea and the Simpevarp subarea, which were prioritised for further investigations. The present report documents the site descriptive modelling activities (version 1.2) for the Laxemar subarea. The overall objectives of the version 1.2 site descriptive modelling are to produce and document an integrated description of the site and its regional environments based on the site-specific data available from the initial site investigations and to give recommendations on continued investigations. The modelling work is based on primary data, i.e. quality-assured, geoscientific and ecological field data available in the SKB databases Sicada and GIS, available November 1, 2004.

The work has been conducted by a project group and associated discipline-specific working groups. The members of the project group represent the disciplines of geology, rock mechanics, thermal properties, hydrogeology, hydrogeochemistry, transport properties and surface ecosystems (including overburden, surface hydrogeochemistry and hydrology). In addition, some group members have specific qualifications of importance in this type of project e.g. expertise in RVS (Rock Visualisation System) modelling, GIS-modelling and in statistical data analysis.

The overall strategy to achieve a site description is to develop discipline-specific models by interpretation and analyses of the primary data. The different discipline-specific models are then integrated into a site description. Methodologies for developing the discipline-specific models are documented in methodology reports or strategy reports. A forum for technical coordination between the sites/projects is active and also sees to that the methodology is applied as intended and developed if necessary. The group consists of specialists in each field as well as the project leaders of both modelling projects.

The following individuals and expert groups contributed to the project and/or to the report:

- Anders Winberg – project leader and editor,
- Henrik Ask – investigation data,
- Carl-Henric Wahlgren, Jan Hermanson, Philip Curtis, Ola Forsberg, Paul La Pointe, Eva-Lena Tullborg, Henrik Drake – geology,
- Eva Hakami, Flavio Lanaro, Anders Fredriksson, Isabelle Olofsson – rock mechanics,
- Jan Sundberg and co-workers – thermal properties,
- Ingvar Rhén, Lee Hartley, Sven Follin and the HydroNet Group – hydrogeology,
- Marcus Laaksoharju and the members of the ChemNet group – hydrogeochemistry,
- James Crawford, Sten Berglund, Johan Byegård, Eva-Lena Tullborg – transport properties,
- Tobias Lindborg and the members of the SurfaceNet group – ecosystems,
- Johan Andersson – confidence assessment,
- Fredrik Hartz and Anders Lindblom – production of maps and figures.

The report has been reviewed by the following members of SKB's international Site Investigation Expert Review Group (Sierg): Per-Eric Ahlström (Chairman); Jordi Bruno (Enviros, Spain); John Hudson (Rock Engineering Consultants, UK); Ivars Neretnieks (Royal Institute of Technology, Sweden); Mike Thorne (Mike Thorne and Associates Ltd, UK); Gunnar Gustafson (Chalmers University). The group provided many valuable comments and suggestions for completion of this work and also for future work, and is not to be held responsible for any remaining shortcomings of the report. Review comments on the report were also provided by Geoffrey Milnes (GEA Consulting).

Summary

A site descriptive model constitutes a description of the site and its regional setting, covering the current state and characteristics of the geosphere and the biosphere, as well as of those ongoing natural processes that affect the latter's long-term evolution. The overall objectives of the site descriptive modelling of the Laxemar subarea, version 1.2, are to produce this integrated description based on site-specific data available from the initial site investigations, as well as to give recommendations on continued investigations. The modelling work is based on quality-assured, geoscientific and ecological field data from the Laxemar and Simpevarp subareas available at the time of data freeze Laxemar 1.2, i.e. November 1, 2004.

The local scale model area (24 km²) for the Laxemar 1.2 modelling encompasses both the Laxemar and the Simpevarp subareas. The local model area is located in the centre of a regional scale model area (273 km²). The focus of the modelling is on the Laxemar subarea.

Important new surface data in terms of a new bedrock map, covering the Laxemar and Simpevarp subareas, have been made available for the Laxemar 1.2 modelling. The new borehole data available are foremost related to the Laxemar subarea where full characterisation data are available from two new deep cored boreholes (KLX03 and KLX04). Furthermore, data collected during the drilling process and a preliminary geological mapping are available from the new deep boreholes KLX05 and KLX06.

Modelling results and main characteristics of the site

The integrated description of the surface system has been further developed. Quantitative modelling of the distribution and stratigraphy of the overburden has been performed that provide support for existing conceptual models. The process-based hydrology model has been enlarged. The ecosystem models (terrestrial, limnic and marine) have been developed for the complete Laxemar subarea and marine sub-basins along the coast from Uthammar to Kråkelund. The finding that major pools of carbon are present in the soils and sediments has been substantiated and provide improved constraints on potential variations of in future states.

The Laxemar subarea is in its entirety located above sea level, and is characterised by a relatively flat topography (c. 0.4% topographical gradient), which largely reflects the surface of the underlying bedrock surface, and is also characterised by a high degree of bedrock exposures (38%). Till is the dominant Quaternary deposit which covers about 45% of the subarea.

The dominant rock domain in the central and northern parts of the Laxemar subarea (RSMA01) is principally made up of Ävrö granite. In the south are found domains dominated by quartz monzodiorite (RSMD01) flanked in the north by an arc-shaped mixed domain with a high frequency of diorite to gabbro (RSMM). The latter two domains are assumed to dip to the north. Embedded in the RSMM domain is found smaller domains RSMBA made up of a mix of Ävrö granite and fine-grained dioritoid. The eastern boundary of the subarea coincides with a domain (RSMP) which is characterised by high frequency of ductile deformation zones. Lithological heterogeneity is introduced in the Laxemar subarea as various forms of subordinate rock types and various types of compositional variations. The ore potential in the area is considered negligible, with a real potential only for quarrying of building- and ornamental stone associated with the Götemar and Uthammar granite intrusions to the north and south of the investigated area, respectively.

A conspicuous characteristic of the gabbroid-dioritoid-syenitoid-granite rocks of the Simpevarp area is their low quartz content. The higher the quartz content the higher the thermal conductivity. The results of the modelling of thermal conductivity show mean values of the thermal conductivity on the 0.8 m scale in the order of 2.7 to 2.9 W/mK and also show a high variability. The bimodal characteristics of the distribution of thermal conductivity, particularly seen in RSMA and RSMBA domains, suggest possible future needs to further divide these domains in quartz-rich and quartz-poor varieties.

In total, 35 deterministic deformation zones of high confidence of existence have been interpreted in the local scale model area, five of which have been added since SDM Simpevarp 1.2. Changes to the model are foremost related to the Laxemar subarea. However, most of the medium confidence zones are still without verification e.g. by drilling. Three main orientations of deformation zones are seen among the principal high confidence zones at Laxemar. A major regional zone with east-west strike and southerly dip to forms the northern boundary of the subarea. Likewise, an east-west local major zone with variable, steep to shallow northerly dip divides the Laxemar subarea. A north-south local major zone bounds the subarea in the west, and a parallel north-south zone, further to the east, further divide the subarea. Additional medium confidence zones of local major character with north-south strike also exist at Laxemar. The third main orientation is associated with ductile north-east deformation zones, forming the eastern bound of the Laxemar subarea, and also coinciding with rock domain RSMP. A single local subhorizontal deformation zone is interpreted, although at great depth in the central parts of the Laxemar subarea (> 770 m). Possible subhorizontal zones of local major character (or smaller) cannot be ruled out at present and will be further investigated.

The fracturing in the rock mass between interpreted deterministic deformation zones, and the variation in local fracture orientations suggests, together with results from the deformation zone model, that the Simpevarp subarea is located within a belt of shear zones. The Laxemar subarea, with significantly different behaviour and lower degree of fracturing, is located outside and west of this belt.

Statistical analyses of fracture orientation are based solely on fracture patterns observed in outcrop, and may not necessarily match conditions found at depth. Fracture size analysis shows that regional fracture sets can be approximated by power-law size models. Fracture intensity is shown to be dependent on subarea, somewhat dependent on the rock domain, and locally dependent on host rock lithology, fracture ages, degree of alteration, and presence of ductile or brittle deformation zones. This is indicated by intensities (P_{32} of all fractures) of the regional sets in the domain RSMA of the Laxemar subarea varying between 1.4 and 1.7 m^{-1} , and the corresponding intensities in the Simpevarp subarea being some 30–100% higher.

The current stress model indicates volumes (domain II) in the local model area where rock stresses are interpreted to be lower than in the surrounding bedrock. The former rock volumes are interpreted to be associated with stress relief induced in wedge-formed rock volumes formed at one location in the Simpevarp subarea, and at one location in northern Laxemar, the latter defined by the two EW-striking zones discussed above. The magnitude of the maximum principal stress (σ_1) at 500 m in the remainder of the rock (domain I), where the most of the potential deposition areas at Laxemar are located, is interpreted to vary between 25 to 42 MPa. Quantification of mechanical properties of the naturally fractured rock mass and rock associated with interpreted deformation zones is supported by new laboratory data on intact rock samples, underpinned by empirical and theoretical relationships.

Analysis of hydraulic test data from one deep borehole drilled in rock made up of rock domains RSMM and RSMD indicates that these domains are less permeable than rock domain RSMA01. It should be pointed out that the low hydraulic conductivity of RSMD (dominated by quartz monzodiorite) at present is only supported by a small number of data above the measurement limit. Analysis of borehole hydraulic test data on a 100 m test scale also suggests the existence of a depth trend in hydraulic conductivity in boreholes, although additional analysis of the significance in the depth trends is warranted. A few major deformation zones have been intercepted by boreholes, and it appears that they, at least in some instances, are significantly more conductive than the rock mass in between these zones. The general flow direction through the modelled area is determined by the overall topographical gradient towards the Baltic sea. The controls of the flow are, apart from the hydraulic gradient, also the geometry and properties of the hydraulic rock domains (rock mass) and the hydraulic conductor domains.

Four groundwater types have been identified in the Simpevarp area, including the Laxemar subarea; the Type A (dilute and mainly Na-HCO₃) is found at shallow depths (< 100 m), Type B (brackish, mainly Na-Ca-Cl) at shallow to intermediate depths (150–300 m), Type C (saline (6,000–20,000 mg/l Cl, 25–30 g/L TDS), mainly Na-Ca-Cl) at intermediate to deep levels (> 300 m). Type D (highly saline, > 20,000 mg/l, max TDS ~ 70 mg/l) is only seen in KLX02 at depths > 1,200 m. The marked differences in the groundwater flow regimes (in terms of depth

penetration of local flow cells) between the Laxemar and Simpevarp subareas are reflected in differences in measured groundwater chemistry. Furthermore, our current understanding is that the hydrochemical stability criteria as set up by SKB are met for all principal components, i.e. Eh, pH, TDS, DOC and Ca+Mg.

An original base case hydraulic DFN model has been slightly modified to better match the measured present hydrogeochemistry. The resulting regional case hydraulic DFN model features a modified depth relationship and an adjusted anisotropy (reduced transmissivity of NE and NNE fracture sets). Transient simulation of present day salinity distribution, on the basis of inferred transient boundary and initial conditions (shore-line displacement due to isostatic land uplift and variable salinity of the water of the Baltic Sea and its predecessors), show results, trends and distributions that are compatible with measured geochemical signatures in selected reference boreholes.

Specific surface area measurements (BET) on intact rock samples indicate that relative sorption strengths (strongest to weakest retention) should approximately follow the order: Fine-grained dioriteoid/Fine grained diorite to gabbro > Ävrö granite > diorite to gabbro > quartz monzodiorite, although the differences between the various rock types are likely to be very small.

From the available data, Ävrö granite appears to have roughly a factor four times higher formation factor (associated with higher retention) than the other rock types, the latter which appear to have formation factors of roughly the same magnitude. Estimates and discussion of the transport resistance (F-factor) are also provided.

Uncertainties and confidence in the site description

Important modelling steps have been taken in the development of model version Laxemar 1.2 and many uncertainties are now quantified or explored as alternative hypotheses/models. The uncertainties of the mechanical properties, rock stresses and thermal properties are quantified. Uncertainties in the occurrence of deformation zones are illustrated by providing an alternative model where low confidence zones are excluded, and are explored further in the hydrogeological flow modelling. The regional flow modelling has also assessed the sensitivity of the results to various assumptions regarding boundary conditions (water table), initial conditions (salt distribution) and material properties of the deformation zones and the rock mass. Uncertainties in the hydrogeochemical description have been explored by employing various modelling approaches to the same data set. Furthermore, the sensitivity of modelled mixing proportions (M3) has been assessed by introducing uncertainty to the definition of end member extreme waters.

The understanding of the Simpevarp area has been largely confirmed and the detailed understanding of the Laxemar subarea has increased since SDM Simpevarp 1.2. In this process no major surprises have been encountered. One element of this finding is a stabilising 3D geological rock domain model. The rock mechanics and thermal descriptions are associated with enhanced confidence given that the analyses and modelling, now based on a larger primary data set, overall confirm the ranges obtained in model version Simpevarp 1.2.

New subsurface data provide limited verification to the deformation zone model. The updated model of deformation zones includes an increased number of high confidence zones in Laxemar subarea, but still many medium confidence zones occur and remain to be substantiated further. There is still much uncertainty associated with the hydraulic conductivity of the rock mass, the representativity of hydraulic test data from individual boreholes for given hydraulic rock domains, the transmissivity of deformation zones, and the variability of transmissivity within individual zones.

Sammanfattning

En platsmodell utgör en beskrivning av en plats och dess regionala omgivning, inkluderande dess nuvarande tillstånd och egenskaper hos geosfär och biosfär, och de pågående naturliga processer som kan förväntas påverka platsens utveckling över längre tid. De huvudsakliga målen med den platsbeskrivande modelleringen för delområde Laxemar, version 1.2, är att producera denna integrerade beskrivning baserad på platsspecifika data som finns tillgängliga från den inledande platsundersökningen, samt att ge rekommendationer för fortsatta undersökningar. Det aktuella modellarbetet är baserat på kvalitetssäkrade geovetenskapliga och ekologiska fältdata från delområdena Laxemar och Simpevarp, tillgängliga vid tidpunkten för datafrysningen den 1 november 2004.

Det lokala modellområdet (24 km²) för Laxemar 1.2 modelleringen innefattar både delområde Laxemar och Simpevarp, Det lokala modellområdet är lokaliserat till centrum av det regionala modellområdet (273 km²). Fokus för den platsbeskrivande modelleringen är på delområde Laxemar.

Viktiga nya ytdata i form av en ny berggrundskarta, täckande delområdena Laxemar och Simpevarp, är tillgängliga för Laxemar 1.2 modelleringen. Ny borrhålsdata kommer främst från två nya djupa kärnborrhål (KLX03 och KLX04). Dessutom finns olika former av data insamlade under borrhning och en preliminär geologisk kartering av de nya djupa kärnborrhålen KLX05 och KLX06.

Modellresultat och viktiga egenskaper hos platsen

Den integrerade beskrivningen av ytsystemen har utvecklats ytterligare. Kvantifierande modellering av fördelning av jordlager och dess stratigrafi har genomförts som ger ytterligare stöd för utvecklade konceptuella modeller. Den processbaserade hydrologiska modellen täcker nu ett större område. Ekosystemmodellerna (terrest, limnisk och marin) har tagits fram för hela delområdet Laxemar och för marina del-bassänger längs kusten mellan Uthammar och Kråkelund. Indikationen att de större ackumulationerna av kol återfinns i jordlager och i sediment har nu belagts och ger därmed ökat stöd för avgränsningar av möjliga variationer i framtida förhållanden.

Delområde Laxemar är i sin helhet lokaliserat ovan havsnivån och karakteriseras av en relativt flack topografi (c. 0,4 % topografisk gradient), som dessutom överlag motsvarar variationen i berggrundens överyta. Delområdet karakteriseras också av en hög andel berg i dagen (38 %). Morän är den huvudsakliga kvartära avlagringen och täcker c. 45 % av delområdet.

Den dominerande bergdomänen i de centrala och norra delarna av delområde Laxemar (RSMA01) består till största delen av Ävrögranit. I söder återfinns en bergdomän som domineras av kvartsmonzodiorit (RSMAD01) som flankeras i norr av en bågformad blanddomän med ett stort inslag av diorit till gabbro (RSMMD). Dessa två bergdomäner antas stupa mot norr. Inneslutna i blanddomänen återfinns mindre domäner RSMB som består av en blandning av Ävrögranit och finkornig dioritoid. Den östra randen av delområdet sammanfaller med en bergdomän (RSMP) som karakteriseras av ett stort inslag av plastiska deformationszoner. Litologisk heterogenitet i Laxemar utgörs av olika typer av underordnade bergarter och olika former av sammansättningsvariationer. Malmpotentialen i området bedöms som försumbar, med en verklig potential endast för brytning av byggnads- och prydnadssten i anslutning till Götemar- och Uthammargraniten, norr respektive söder om delområdet.

En framträdande egenskap hos gabbro-diorit-syenit-granit bergarterna i Simpevarpsområdet är deras låga kvartsinnehåll. En högre kvartshalt medför en ökad termisk ledningsförmåga. Resultatet från modelleringen av termiska egenskaper påvisar medelvärden på den termiska ledningsförmågan mellan 2,7 och 2,9 W/mK (0,8 m skala) och en hög variabilitet. Den bimodala formen på fördelningen av termisk ledningsförmåga som noterats, speciellt i bergdomänen RSMA och RSMB, indikerar ett möjligt behov att ytterligare dela upp dessa domäner i kvartsrika och kvartsfattiga varieteter.

Inom det lokala modellområdet har 35 deterministiska deformationszoner tolkats med hög konfidens kopplad till deras existens. Av dessa har 5 stycken tillkommit sedan modellversion Simpevarp 1.2. Ändringar i modellen har främst genomförts i delområde Laxemar. De flesta zoner av medelhög

konfidensgrad saknar dock fortfarande verifiering, exempelvis genom borrhning. Tre huvudsakliga orienteringar hos tolkade deterministiska deformationszoner kan noteras. En större regional deformationszon med östvästlig strykning och relativt flack stupning mot söder utgör den norra avgränsningen av delområdet. På motsvarande sätt delar en östvästlig zon, med variabel brantstående till flack stupning mot norr, upp delområde Laxemar. En nordsydlig större lokal zon avgränsar delområdet i väster, och en parallell zon öster om denna delar upp delområdet ytterligare. Ytterligare lokala större zoner (medelhög konfidens) med nordsydlig stupning återfinns i Laxemar. Den tredje huvudsakliga riktningen är associerad med nordöstliga plastiska zoner som bildar den östra begränsningen av delområdet. De senare zonerna sammanfaller med bergdomän RSMP. En enskild lokal subhorisontell deformationszon har tolkats i de centrala delarna av delområde Laxemar, om än på stort djup (> 770 m). Förekomst av subhorisontella zoner av lokal karaktär (eller mindre) kan inte uteslutas och är föremål för fortsatt analys.

Sprickigheten mellan tolkade deformationszoner och variationen i lokala sprickriktningar indikerar, sammantaget med resultat från deformationszonsmodellen, att delområde Simpevarp är beläget inom ett bälte med skjuvzoner. Delområde Laxemar, med en distinkt annorlunda och lägre sprickighet, är beläget utanför och väster om detta bälte.

Statistiska analyser av sprickorienteringar baseras endast på sprickmönster observerade på håll, och behöver inte nödvändigtvis återspegla förhållandena på större djup. Analys av sprickstorlek visar att regionala set kan approximeras med en potensmodell för fördelningen av sprickstorlek. Sprickintensitet (frekvens) är beroende på delområde, delvis beroende av bergdomän, och är lokalt beroende på bergart, sprickålder, omvandlingsgrad, och förekomst av plastiska och spröda deformationszoner. Detta påvisas av variationen i intensitet (P32 för alla sprickor) av de regionala sprickseten i bergdomän RSMA i delområde Laxemar som varierar mellan 1,4 och 1,7 m⁻¹, där motsvarande intensiteter i delområde Simpevarp är 30–100 % högre.

Den aktuella spänningsmodellen uppvisar volymer (domän II) i det lokala modellområdet där bergspänningarna tolkas vara lägre än i omkringliggande berg. Dessa volymer tolkas vara associerade med spänningsavlastning i kilformiga bergvolymer som formats dels i delområde Simpevarp och på ett ställe i delområde Laxemar, den senare definierad av de två östvästliga deformationszonerna som diskuteras ovan. Storleken på huvudspänningen (σ_1) på 500 m djup i återstoden av berget (domän I), som utgör merparten av tillgänglig deponeringsvolym i Laxemar, tolkas variera mellan 25 och 42 MPa. Kvantifiering av de mekaniska egenskaperna i den naturligt spruckna bergmassan och i tolkade deformationszoner stöds av nya laboratedata baserat på intakt bergmaterial, understödda av empiriska och teoretiska samband.

Analys av hydrauliska testdata från ett djupt kärnborrhål som penetrerar bergdomänerna RSMM och RSMD tyder på att dessa domäner är mindre vattenförande än bergdomän RSMA01. Det bör också påpekas att den lägre hydrauliska konduktiviteten hos RSMD (dominerad av kvartsmonzodiorit) i dagsläget endast understöds av ett fåtal mätningar över mätgränsen. Analys av hydrauliska testdata från borrhål (100 m testskala) indikerar ett möjligt djupavtagande i hydraulisk konduktivitet. Ytterligare analys för att belägga detta djupavtagande behöver utföras i kommande modelleringsarbete. Ett fåtal större deformationszoner har genomborrats av borrhål, och testdata från dessa påvisar att de åtminstone i vissa fall, är väsentligt mer vattenförande än bergmassan mellan deformationszoner. Den huvudsakliga flödesriktningen genom det modellerade området bestäms av den rådande topografiska gradienten mot Östersjön. De element som, förutom den hydrauliska gradienten, bestämmer flödets storlek och variation är geometri och egenskaper hos de hydrauliska bergdomänerna (bergmassan) och de hydrauliska strukturdomänerna.

Fyra huvudsakliga grundvattentyper har identifierats i Simpevarpsområdet, inkluderande delområde Laxemar; Typ A (utspätt och i huvudsak av Na-HCO₃-karaktär) återfinns på mindre djup (< 100 m), Typ B (bräckt och i huvudsak av Na-Ca-Cl-karaktär) återfinns på ytligt till intermediärt djup (100–300 m), Typ C (salt (6 000–20 000 mg/l Cl, 25–30 g/l TDS, i huvudsak av Na-Ca-Cl-karaktär) på intermediärt till stora djup (> 300 m). Type D (mycket salt (> 20 000 mg/l, max TDS ~ 70 mg/l)), har bara noterats i borrhål KLX02 på djup större än 1 200 m. Markerade skillnader i flödesregimer (beroende på topografistyrd djuppenetration av lokala flödesceller) mellan delområde Laxemar och Simpevarp återspeglas i uppmätta skillnader i grundvattenkemi. Med vår nuvarande förståelse så uppfylls de stabilitetskriterier som ställts upp av SKB för viktiga kemiska komponenter; Eh, pH, TDS, DOC och Ca+Mg.

Den hydrauliska DFN-modellen (basfall) har modifierats en aning för att ge en förbättrad överensstämmelse mellan simulerad och uppmätt hydrogeokemi. Den resulterande hydrauliska DFN-modellen (regionalt fall) kännetecknas av ett modifierat djupavtagande i hydrauliska bergdomäner, liksom ett förändrat anisotropiförhållande (minskad transmissivitet hos sprickset i nordöstlig och nordnordöstlig riktning). Transienta simuleringar av nuvarande fördelning av salinitet, på grundval av valda transienta rand- och initialvillkor (strandlinjeförskjutning på grund av landhöjningen och variabel salthalt i Östersjön och dess föregångare), visar resultat, trender och fördelningar som är överstämmande med mätta geokemiska signaturer i valda referensborrhål.

Bestämda specifika ytor (BET) på intakt bergmaterial indikerar att den relativa sorptionsstyrkan översiktligt och approximativt skulle följa följande ordning: finkornig dioritoid/finkornig dioritgabbro > Ävrögranit > diorit till gabbro > kvartsmonzodiorit, även om skillnaderna mellan enskilda bergarter förmodligen är små.

Baserat på tillgängliga data så verkar Ävrögranit uppvisa en formationsfaktor (kopplad till en högre retention) som är ungefär en faktor fyra högre än för andra bergarter, där de senare uppvisar formationsfaktorer i ungefärligen samma storleksordning. Uppskattningar och diskussion av transportmotstånd (F-faktorn) redovisas också.

Osäkerheter och tilltro till platsbeskrivningen

Viktiga modelleringssteg har tagits i framtagandet av modellversion Laxemar 1.2 och många osäkerheter är nu kvantifierade eller undersökta som alternativa hypoteser eller modeller. Osäkerheter kopplade till mekaniska egenskaper, bergspänningar och termiska egenskaper är kvantifierade. Osäkerheter i deformationszoners existens illustreras med en alternativ modell, där zoner med låg konfidens har tagits bort, som sedan analyseras i den hydrogeologiska modelleringen. Den regionala flödesmodelleringen har också undersökt känsligheten i beräknade resultat kopplade till olika antaganden om randvillkor (grundvattenytans läge), initialvillkor (saltfördelning) och material-egenskaper hos deformationszoner och bergmassa. Osäkerheter i den kemiska beskrivningen har undersökts genom att tillämpa flera modellkoncept på samma datamängder. På motsvarande sätt har känsligheten hos modelleringen av blandningsförhållanden (M3) har testats genom att introducera osäkerhet i definitionerna av typvatten (end members).

Vår förståelse av Simpevarpsområdet som helhet har på det hela bekräftats och vår detaljerade förståelse av delområde Laxemar har ökat sedan modellversion Simpevarp 1.2. I denna process har inga större överraskningar påträffats. Ett element som reflekterar detta konstaterande är en stabilisering av den tredimensionella bergdomänmodellen. De bergmekaniska och termiska beskrivningarna karakteriseras av en ökad konfidens, där analyser och modellering baserade på ett större dataunderlag, överlag bekräftar de parameterintervall som bestämdes för modellversion Simpevarp 1.2

Nya underjordsdata för Laxemar 1.2 ger en begränsad verifikation av den upprättade deformationszonsmodellen som dock uppvisar ett större antal zoner med hög konfidens i delområde Laxemar, men fortfarande är andelen zoner med medelhög konfidens stor, och återstår att belägga. Stora osäkerheter är fortfarande kopplade till den hydrauliska konduktiviteten i bergmassan, representativiteten av hydrotestdata från enskilda borrhål för enskilda hydrauliska bergdomäner, deformationszoners transmissivitet, och dess variabilitet inom enskilda zoner.

Contents

1	Introduction	19
1.1	Background	19
1.2	Objectives and scope	20
1.3	Setting	21
1.4	Methodology and organisation of work	22
1.4.1	Methodology	22
1.4.2	Interfaces between disciplines	24
1.4.3	Organisation of work	24
1.4.4	Changes compared to Simpevarp 1.2 work	25
1.5	This report	26
2	Available data and other prerequisites for the modelling	27
2.1	Overview	27
2.1.1	Investigations and primary data acquired up to data freeze Simpevarp 1.1	27
2.1.2	Investigations and primary data acquired for data freeze Simpevarp 1.2	27
2.1.3	Data freeze Laxemar 1.2 – investigations performed and acquired data	28
2.2	Previous model versions	29
2.2.1	Version 0	29
2.2.2	Models developed as part of Äspö HRL and Ävrö work	30
2.2.3	Laxemar test application	30
2.2.4	Simpevarp 1.1	30
2.2.5	Simpevarp 1.2	31
2.3	Geographical data	32
2.4	Surface investigations	32
2.4.1	Bedrock geology and ground geophysics	32
2.4.2	Overburden	33
2.4.3	Meteorology, hydrology and hydrogeology	34
2.4.4	Surface ecology	35
2.5	Borehole investigations	36
2.5.1	Borehole investigations during and immediately after drilling	37
2.5.2	Borehole investigations after completion of drilling and analysis of drill core and drill cuttings	38
2.6	Other data sources	39
2.7	Databases	40
2.8	Model volumes	59
2.8.1	General	59
2.8.2	Regional model volume	60
2.8.3	Local model volume	61
3	Evolutionary aspects	63
3.1	Crystalline bedrock	63
3.1.1	Introduction	63
3.1.2	Lithological development	64
3.1.3	Structural development	70
3.2	Overburden including Quaternary deposits	77
3.2.1	Quaternary development of Sweden	77
3.2.2	The Pleistocene	78
3.2.3	The latest deglaciation	79
3.2.4	Climate and vegetation after the latest deglaciation	80
3.2.5	Development of the Baltic Sea after the latest deglaciation	81
3.2.6	Quaternary history of the Simpevarp area	81

3.3	Premises for surface and groundwater evolution	84
3.3.1	Development of permafrost and saline water	84
3.3.2	Deglaciation and flushing by meltwater	84
3.4	Development of surface ecosystems	86
3.4.1	Population	86
3.4.2	Farms and land use	86
4	The surface system	89
4.1	State of knowledge at the previous model version	89
4.2	Evaluation of primary data	89
4.2.1	Quaternary deposits and other regoliths	90
4.2.2	Climate, hydrology and hydrogeology	90
4.2.3	Chemistry	91
4.2.4	Biota	91
4.2.5	Humans and land use	92
4.3	Model of Quaternary deposits and other regoliths	92
4.3.1	Background	92
4.3.2	The surface distribution and stratigraphy of Quaternary deposits	93
4.3.3	Soils	95
4.4	Climate, hydrology, hydrogeology and oceanography	97
4.4.1	Conceptual-descriptive and quantitative water flow modelling	97
4.4.2	Some observations from quantitative water flow modelling	99
4.4.3	Coastal oceanography of the Simpevarp area	101
4.5	Chemistry	102
4.5.1	Chemical characteristics of near-surface ecosystems in the Simpevarp area	103
4.6	Biota	105
4.6.1	Terrestrial	105
4.6.2	Limnic	110
4.6.3	Marine	112
4.7	Humans and land use	115
4.8	Development of the ecosystem model	115
4.8.1	Terrestrial ecosystem description	115
4.8.2	Limnic ecosystem description	117
4.8.3	Marine ecosystem description	120
4.9	Evaluation of uncertainties	125
4.9.1	Abiotic descriptions	125
4.9.2	Biotic description	125
5	Bedrock geology	129
5.1	State of knowledge at previous model version	130
5.2	Evaluation of primary data	131
5.2.1	Surface geology	131
5.2.2	Outcrop mapping and complementary analytical studies	132
5.2.3	Rock type distribution on the surface – bedrock map	134
5.2.4	Lineament identification	144
5.2.5	Observation of ductile and brittle structures from the surface	145
5.2.6	Surface geophysics	153
5.2.7	Fracture statistics from borehole data	155
5.2.8	Geologic interpretation of borehole data	158
5.3	Rock domain model	169
5.3.1	Basis for modelling	169
5.3.2	Division into rock domains at the surface and in cored boreholes	170
5.3.3	Construction of the 3D rock domain model	173
5.3.4	The 3D rock domain model	174
5.3.5	Property assignment	174
5.3.6	Evaluation of uncertainties	178
5.4	Deterministic deformation zone modelling	181

5.4.1	Modelling assumptions and input from other disciplines	181
5.4.2	Conceptual model of the kinematic evolution of deformation zones	183
5.4.3	Conceptual deformation zone model with potential alternatives	183
5.4.4	Property assignment to the base case model with specification of selected high confidence zones	189
5.4.5	Evaluation of uncertainties	202
5.5	Statistical model of fractures and deformation zones	204
5.5.1	Modelling assumptions and input from other disciplines	204
5.5.2	Conceptual model with potential alternatives	206
5.5.3	Verification demonstration	210
5.5.4	Discussion and guidelines for usage	212
5.5.5	Summary of parameters of geological DFN models	215
5.5.6	Evaluation of uncertainties	218
6	Rock mechanics model	219
6.1	State of knowledge at previous model version	219
6.2	Evaluation of primary data	219
6.2.1	Laboratory tests of intact core samples	219
6.2.2	Laboratory tests on fracture samples	220
6.2.3	Rock mechanics interpretation of borehole data	222
6.2.4	Other data	223
6.2.5	Stress measurements	224
6.3	Rock mechanics property models	225
6.3.1	Assignment of properties for the intact rock	225
6.3.2	Assignment of properties to single fractures	226
6.3.3	Conceptual models for rock mass characterisation	227
6.3.4	Empirical approach to rock mass mechanics properties	227
6.3.5	Theoretical approach to rock mass mechanics properties	228
6.3.6	Assignment of rock mass mechanics properties in the model volume	230
6.4	State of stress	236
6.4.1	Modelling assumptions and input from other disciplines	236
6.4.2	Conceptual model with potential alternatives	236
6.4.3	Modelling of stress distribution	236
6.4.4	Evaluation of uncertainties in stress model	240
7	Bedrock thermal model	241
7.1	State of knowledge at the previous model version	241
7.2	Evaluation of primary data	241
7.2.1	Thermal conductivity and diffusivity from measurements	241
7.2.2	Thermal conductivity from mineral composition	243
7.2.3	Thermal conductivity from density	245
7.2.4	Statistical rock type models of thermal conductivity	246
7.2.5	Heat capacity	246
7.2.6	Coefficient of thermal expansion	248
7.2.7	In situ temperature	248
7.3	Thermal modelling of lithological domains	249
7.3.1	Modelling assumptions and input from other disciplines	249
7.3.2	Conceptual model of spatial variability	250
7.3.3	Modelling approach for domain properties	250
7.3.4	Domain modelling results	255
7.3.5	Evaluation of domain modelling results	259
7.3.6	Summary of domain properties	261
7.4	Evaluation of uncertainties	261
7.4.1	Thermal conductivity	262
7.4.2	Heat capacity	263
7.4.3	In situ temperature	263
7.4.4	Thermal expansion	264
7.5	Feedback to other disciplines	264

8	Bedrock hydrogeology	265
8.1	State of knowledge at previous model version	265
8.2	Evaluation of primary data	266
8.2.1	Hydraulic evaluation of of single hole tests	266
8.2.2	Hydraulic evaluation of interference tests	277
8.2.3	Joint hydrogeology and geology single hole interpretation	278
8.3	Hydrogeological model – general conditions and concepts	282
8.3.1	Modelling objectives and premises	282
8.3.2	General modelling assumptions and input from other disciplines	284
8.3.3	General modelling strategy	287
8.4	Assignment of hydraulic properties	288
8.4.1	HSD – overburden	289
8.4.2	HCD – deterministic deformation zones	290
8.4.3	HRD – bulk properties based on statistics of the hydraulic tests	296
8.4.4	HRD – hydro DFN model	304
8.4.5	HRD – hydroDFN base case – block modelling	313
8.5	Regional flow modelling	315
8.5.1	Initial and boundary conditions	316
8.5.2	Effects of model size and model resolution	318
8.5.3	Resulting groundwater flow model	320
8.5.4	Present-day flow conditions	326
8.6	Conclusions from the regional flow modelling	329
8.7	Evaluation of uncertainties	330
8.7.1	Overburden – HSD	330
8.7.2	Geometry of deformation zones and rock domains	331
8.7.3	Hydraulic properties of deformation zones and rock domains	332
8.7.4	Boundary conditions and initial conditions	334
8.8	Feedback to other disciplines	334
8.8.1	Important observations related to other disciplines	334
8.8.2	Can new boreholes resolve some of the issues raised?	335
8.8.3	What other data or tests can discriminate between models?	335
9	Bedrock hydrogeochemistry	337
9.1	State of knowledge at the previous model version	337
9.2	Hydrogeochemical modelling	338
9.2.1	Modelling assumptions and input from other disciplines	338
9.2.2	Conceptual model with potential alternatives	339
9.3	Hydrogeochemical data	339
9.3.1	Groundwater chemistry data sampled in boreholes	340
9.3.2	Representativeness of the data	341
9.4	Explorative analysis	343
9.4.1	Examples of evaluation of scatter plots	343
9.4.2	Descriptive observations – main elements	345
9.4.3	Descriptive observations – isotopes	347
9.4.4	Microbes	350
9.4.5	Colloids	351
9.4.6	Gases	352
9.4.7	Pore water composition in the rock matrix	352
9.4.8	Fracture fillings	354
9.4.9	Palaeorecord investigations of fracture filling minerals	355
9.4.10	Origin of brine water	355
9.5	Mass balance, reaction path and mixing calculations	356
9.5.1	Sensitivity and uncertainty analysis of the mixing models	357
9.6	Conclusions used for the site descriptive model	363
9.6.1	Modelling and visualisation of the near surface properties	363
9.6.2	Modelling and visualisation of the groundwater properties	365
9.6.3	Groundwater samples in relation to major deformation zones	374
9.6.4	Resulting conceptual model	375
9.6.5	Revisitation of hydrogeochemical stability criteria	375

9.7	Integration between between hydrogeological and hydrogeochemical models	376
9.7.1	Paleo-hydrogeological calibration of the reference case	377
9.7.2	Present-day flow conditions	383
9.7.3	Conclusions	385
9.8	Evaluation of uncertainties	386
10	Bedrock transport properties	389
10.1	State of knowledge at the previous model version	389
10.2	Modelling methodology and input from other disciplines	390
10.3	Conceptual model with potential alternatives	391
10.3.1	Basic conceptual model	391
10.3.2	Alternative models	393
10.4	Description of input data	393
10.4.1	Data and models from other disciplines	393
10.4.2	Transport data	395
10.5	Evaluation of transport data	396
10.5.1	Methods and parameters	396
10.5.2	Porosity	397
10.5.3	Diffusion	397
10.5.4	Sorption	399
10.5.5	Specific flow-wetted surface	401
10.5.6	Field scale tracer tests	402
10.6	Transport properties of rock domains	404
10.6.1	Methodology	404
10.6.2	Description of rock domains	404
10.7	Transport properties of fractures and deformation zones	406
10.7.1	Methodology	406
10.7.2	Description of fractures	406
10.7.3	Description of deformation zones	409
10.7.4	Application of the retardation model	409
10.7.5	Supporting evidence from process-based modelling	410
10.8	Transport properties of flow paths	410
10.8.1	Generic, first order estimation of the F-factor	410
10.8.2	Estimations of the F-factor using site specific data	412
10.9	Evaluation of uncertainties	414
11	Resulting description of the Laxemar subarea	417
11.1	Surface properties and ecosystems	417
11.1.1	Quaternary deposits and other regoliths	417
11.1.2	Climate, hydrology, hydrogeology and oceanography	417
11.1.3	Chemistry	418
11.1.4	Ecosystem description	419
11.2	Bedrock geological description	421
11.2.1	Rock domain model	421
11.2.2	Deterministic deformation zone model	424
11.2.3	Statistical model of fractures and deformation zones	427
11.3	Rock mechanics description	428
11.3.1	Mechanical properties	428
11.3.2	In situ stress conditions	429
11.4	Bedrock thermal properties	430
11.5	Bedrock hydrogeological description	430
11.5.1	Hydraulic properties	431
11.5.2	Groundwater flow pattern	433
11.6	Bedrock hydrogeochemical description	434
11.6.1	Summary of groundwater types	435
11.6.2	Comparison between modelled and measured geochemistry	437

11.7	Bedrock transport properties	438
11.7.1	Effective diffusivities of major rock types	438
11.7.2	Sorption properties of major rock types	439
11.7.3	Overall retention properties and migration of solutes along potential flow paths	440
12	Overall confidence assessment	441
12.1	How much uncertainty is acceptable?	441
12.1.1	Safety assessment needs	441
12.1.2	Repository engineering needs	442
12.1.3	Assessing the importance of the uncertainties	442
12.2	Are all data considered and understood?	443
12.2.1	Answers to auditing protocol	443
12.2.2	Overall judgement	444
12.3	Uncertainties and potential for alternative interpretations?	444
12.3.1	Auditing protocol	444
12.3.2	Main uncertainties	445
12.3.4	Overall assessment	458
12.4	Consistency between disciplines	459
12.4.1	Important and actually considered interactions	459
12.4.2	Overall assessment	464
12.5	Consistency with understanding of past evolution	464
12.6	Comparison with previous model versions	465
12.6.1	Auditing protocol	465
12.6.2	Assessment	466
13	Conclusions	469
13.1	Major developments since the previous model version	469
13.2	Current understanding of the site	470
13.2.1	General understanding of the Laxemar subarea	470
13.2.2	Uncertainties, alternatives and integration of models	477
13.3	Implications for future modelling	479
13.3.1	Technical aspects and scope of the Laxemar 2.1 modelling	479
13.3.2	Modelling procedures and organisation of work	480
13.4	Implications for the ongoing investigation programme	480
13.4.1	Recommendations provided during the modelling work	481
13.4.2	Recommendations based on uncertainties in the current site descriptive model Laxemar 1.2	481
13.5	General conclusions	485
14	References	487
Appendix 1	Geographical and topographical overview	513
Appendix 2	Nomenclature of rock types (in English and Swedish), including rock codes applied in the site investigation at Oskarshamn	515
Appendix 3	Bedrock map	517
Appendix 4	Composites of geological, hydrogeological and hydrogeochemical borehole logs	519
Appendix 5	Property tables for rock domains	529
Appendix 6	Property tables for deformation zones	565
Appendix 7	Correlation of flow anomalies (PFL-f) with Boremap data from new boreholes analysed for model version Laxemar version 1.2	601
Appendix 8	Concepts for assignment of hydraulic properties to the hydraulic rock domains (HRD)	607
Appendix 9	Overall confidence assessment	613

1 Introduction

1.1 Background

The Swedish Nuclear Fuel and Waste Management Company (SKB) is undertaking site characterisation at two different locations, the Forsmark and Simpevarp areas, with the objective of siting a deep repository for spent nuclear fuel. The characterisation work is divided into an initial site investigation stage and a complete site investigation stage, /SKB 2001a/. The results of the initial investigation stage will be used as a basis for deciding on a subsequent complete site investigation stage. The results of the complete site investigations will form the basis for selection of a repository site and the license application to construct a repository at that site. During the subsequent Construction and Detailed Investigation Phase additional (detailed) investigations will be performed.

An integrated component in the characterisation work is the development of a site descriptive model (SDM) that constitutes the description of the site and its regional setting, covering the current state of the geosphere and the biosphere as well as those ongoing natural processes that affect their long-term evolution. The site description includes two main components:

- a *written synthesis* of information relating to each site summarising the current state of knowledge as well as describing ongoing natural processes which affect its long-term evolution, and
- one or several *site descriptive models*, in which the collected information is interpreted and presented in a form that can be used in numerical models for rock engineering, environmental impact and long-term safety assessments.

Before the start of the initial site investigations in the Simpevarp area (including the Simpevarp and Laxemar subareas), a version 0 of the site descriptive model for the Simpevarp area was developed /SKB 2002b/. This model version served as a point of departure for the development of the subsequent versions of the site description during the initial site investigation phase. Each model version is coupled to a “data freeze” in time that defines the database available at that time for the model version in question. The results of the descriptive modelling also serve to provide feedback to, and set priorities for, the ongoing site characterisation. This interplay between site descriptive modelling, Site Investigation, Repository Engineering (Design), and Environmental Impact Assessment and Safety Assessment is illustrated in Figure 1-1.

There has been a successive development of site descriptive models, from version 0, through version 1.1 for the Simpevarp area and version 1.2 of the Simpevarp subarea to the SDM 1.2 for the Laxemar subarea presented here. The experience from previous site descriptive modelling work on the Simpevarp and Forsmark areas have been utilised in the current preliminary site description for the Laxemar subarea. This report concludes the modelling of the initial site investigation phase at Oskarshamn. With reference to Figure 1-1, this most recent site description (Laxemar version 1.2) is being used by Repository Engineering (Design) to produce the facility description layout D1. Together with the D1 layout, it also forms the basis for a Preliminary Safety Evaluation (PSE) of the Laxemar subarea and a Safety Assessment (SR-Can) based on the repository layout D1 of the Laxemar subarea. Furthermore, the preliminary site description for the Laxemar subarea has also provided input for devising the complete site investigation programme for the Laxemar subarea /SKB 2005c/. Another important recipient of the SDM Laxemar 1.2 is the Environmental Impact Assessment.

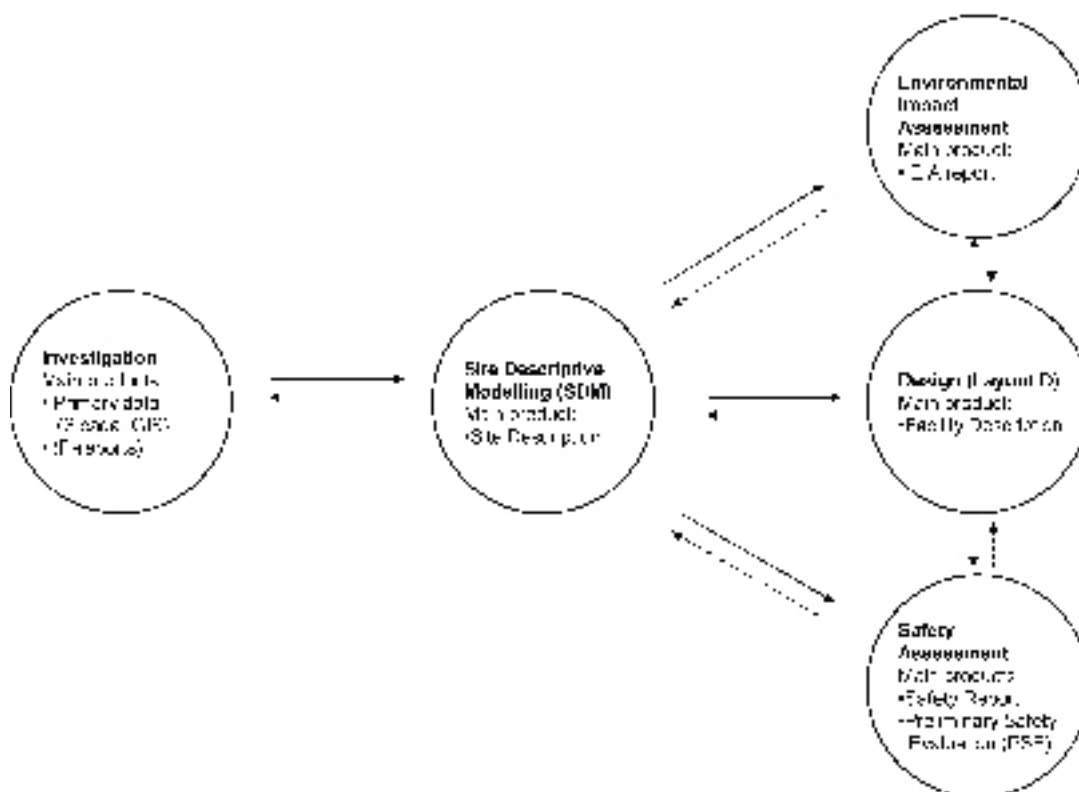


Figure 1-1. Site Descriptive Modelling (SDM) and its main products in a context. Illustrated also is the exchange of information between the main technical activities that provide data to the site modelling, or which makes use of the site modelling and associated description.

1.2 Objectives and scope

The development of the preliminary site description of the Laxemar subarea (version 1.2) was made with the main objective of presenting a site descriptive model on a local and a regional scale, together with a synthesis of the current understanding of the site. This is based on field data collected during the initial site investigations up to the data freeze point (November 1, 2004). An additional outcome is the recommendations given on continued field investigations based on results and experiences gained during the work with the development of the various site descriptive model versions.

The specific objectives of the work were to:

- produce and document an integrated description of the site and its regional environment based on the site-specific data available from the initial site investigations,
 - analyse the primary data available in data package Laxemar 1.2,
 - build a three-dimensional site descriptive model,
 - perform an overall confidence assessment including systematic treatment of uncertainties and evaluation of alternative interpretations,
 - develop, document and evaluate alternative models in a systematic way,
 - perform modelling activities in close interaction with safety analysis and repository engineering,
- perform the safety related geosphere and biosphere analyses as specified as Site Modelling in the planning document for the Preliminary Safety Evaluation (PSE) /SKB 2002a/,
- highlight and, when the available data allow, answer all current site specific geoscientific and ecological key issues for understanding the site,
- give recommendations on continued investigations in the reporting as well as on a continuous basis.

The basis for the preliminary site description (version 1.2) of the Laxemar subarea is quality-assured, geoscientific and ecological field data from the Simpevarp area, including the Laxemar subarea, available in the SKB databases Sicada and GIS at the time of data freeze. All information available up to this date has been used to re-evaluate and extend the pre-existing knowledge embedded in model version 1.2 of the Simpevarp subarea. The latter is made possible by the fact that the two subareas are located close to one another and actually share the same local scale model area, cf. Section 1.3. A detailed description of underlying primary data for the site descriptive model, including geographical information and definition of modelling areas is provided in Chapter 2.

As is to be expected at this stage of the site investigation, and given the delayed start of the site investigations in the Laxemar subarea, there are still substantial uncertainties in the site description, and in many aspects the confidence is low. However, many significant steps have been taken in the descriptive modelling of the Simpevarp and Laxemar subareas as a whole, and it is expected that future exploratory analysis and modelling based on a larger set of primary data will resolve many of the uncertainties in the preliminary site description of this subarea.

1.3 Setting

The Simpevarp area is located in the province of Småland, within the municipality of Oskarshamn, and immediately adjacent to the Oskarshamn nuclear power plant and the Central interim storage facility for spent fuel (Clab), cf. Figure 1-2 and Appendix 1. The Simpevarp area (including the Simpevarp and Laxemar subareas) is located close to the shoreline of the Baltic Sea. The eastern-most part (Simpevarp subarea) includes the Simpevarp peninsula (which hosts the power plants and the Clab facility, cf. Figure 2-1) and the islands Hålö and Ävrö. The island of Äspö, under which the Äspö Hard Rock Laboratory (Äspö HRL) is developed, is located some two kilometres north of the Simpevarp peninsula. The area of the Laxemar subarea covers some 12.5 km² whereas the Simpevarp subarea is approximately 6.6 km².

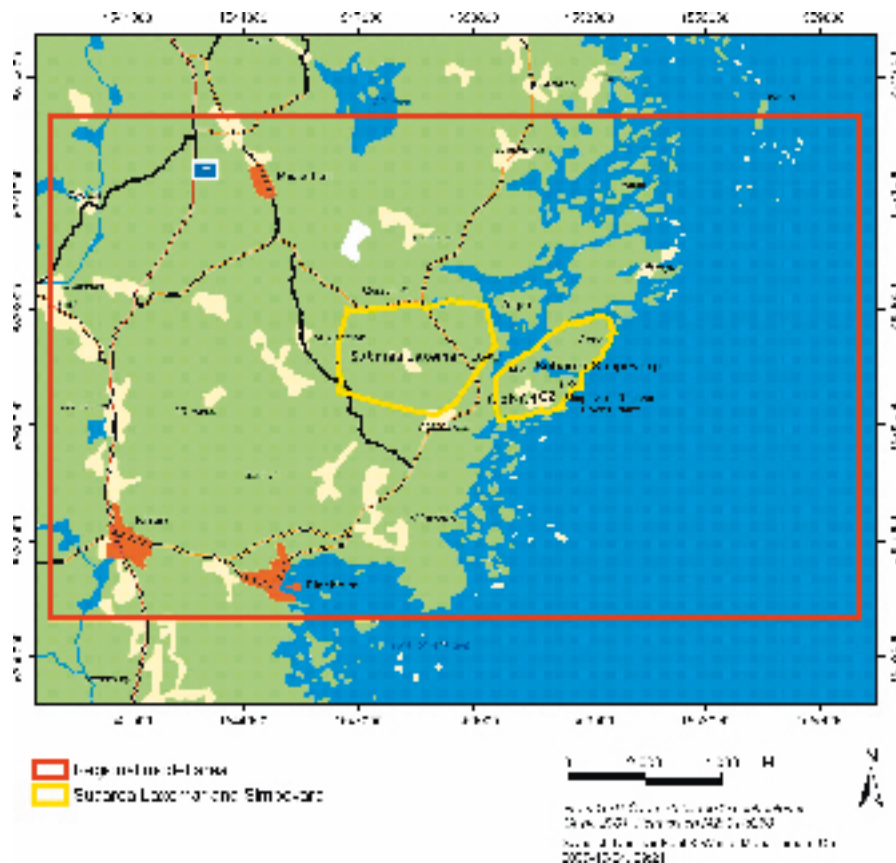


Figure 1-2. Overview of the Simpevarp regional model area and identification of the Simpevarp and Laxemar subareas, cf. Section 2.8.

1.4 Methodology and organisation of work

1.4.1 Methodology

The project is multi-disciplinary in that it covers all potential properties of the site that are of importance for the overall understanding of the site, for the design of the deep repository, for safety assessment and for the environmental impact assessment. The overall strategy to achieve this (illustrated in Figure 1-3) is to develop discipline-specific models by interpretation and analyses of the quality-assured primary data stored in the two SKB databases. The developed discipline models are subject to discipline-wise and cross-discipline quality control, both through the use and application of the models and associated data, but also through audit and seminars involving the working groups, cf. Table 1-1, sometimes also involving appointed SKB internal reviewers (the Sierg group). The different discipline-specific models are then integrated into a unified site description. Old existing data from the construction of the power plants, the Clab facility and the Äspö Hard Rock Laboratory (Äspö HRL) are, to a variable extent, also incorporated in the analysis, as discussed below.

The site descriptive modelling comprises the iterative steps of primary data evaluation, descriptive and quantitative modelling in 3D, and of overall confidence evaluation. A strategy for achieving sufficient integration between disciplines for producing site descriptive models is documented in a separate strategy document on integrated evaluation /Andersson 2003/, but has been developed further during the work with model versions 1.1 for Forsmark and Simpevarp and versions 1.2 for the Simpevarp subarea /SKB 2005a/ and the Forsmark area /SKB 2005b/.

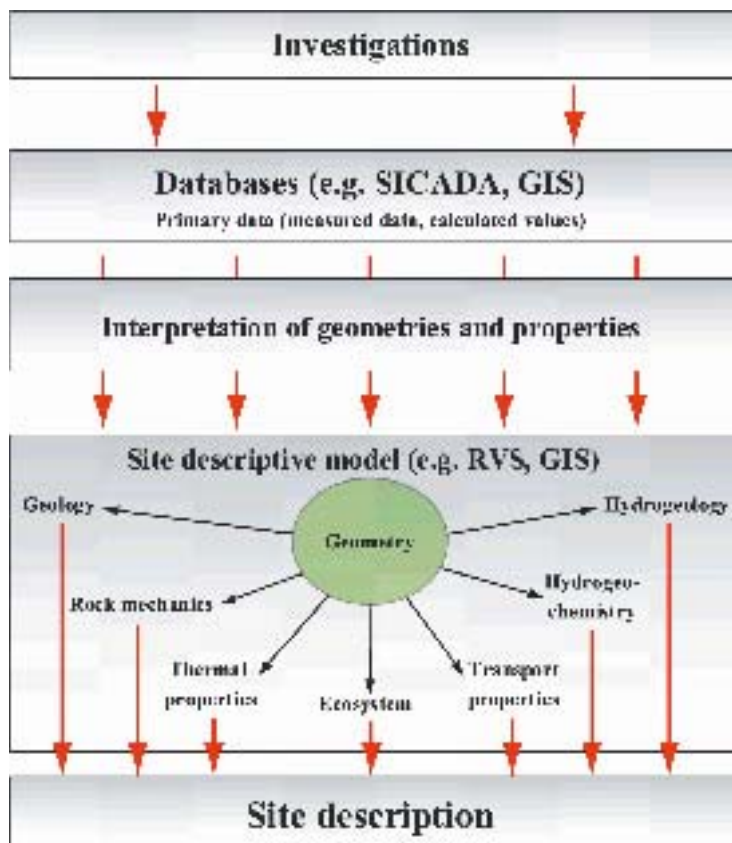


Figure 1-3. From site investigations to site description. Primary data from site investigations are collected in databases. Data are interpreted and presented in a site descriptive model, which consists of a description of the geometry of different units in the model and the corresponding properties of the site /from SKB 2002a/.

Data are first evaluated within each discipline and then the evaluations are cross-checked between the disciplines. Three-dimensional modelling, with the purpose of estimating the distribution of parameter values in space, as well as their uncertainties, follows. The geometrical framework for modelling is taken from the geological model, and is subsequently used by the rock mechanics, thermal and hydrogeological modelling etc. (see Figure 1-4). The three-dimensional description aims to present the parameters with their spatial variability over a relevant and specified scale, with the uncertainty included in this description. If required, different alternative descriptions are provided.

The current methodologies for developing the discipline-specific models are documented in methodology reports or strategy reports. In the present work, the guidelines given in those reports have been followed to the extent possible with the data and information available at the time for data freeze for model version Simpevarp 1.2. How the work was carried out is described further in Chapters 4 through 11. For more detailed information on the methodologies the reader is referred to the methodology reports. These are:

- Geological Site Descriptive Modelling /Munier et al. 2003, Munier 2004/.
- Rock Mechanics Site Descriptive Modelling /Andersson et al. 2002b/.
- Thermal Site Descriptive Modelling /Sundberg 2003a/.
- Hydrogeological Site Descriptive Modelling /Rhén et al. 2003/.
- Hydrogeochemical Site Descriptive Modelling /Smellie et al. 2002/.
- Transport Properties Site Descriptive Modelling /Berglund and Selroos 2003/.
- Ecosystem Descriptive Modelling /Löfgren and Lindborg 2003/.

According to the strategy report for integrated evaluation /Andersson 2003/, the overall confidence evaluation should be based on the results of the individual discipline modelling and involve the different modelling teams. The confidence is assessed by carrying out checks concerning e.g. the status and use of primary data, uncertainties in derived models, and various consistency checks such as between current models and with previous model versions. This strategy has been followed when assessing the overall confidence in model version Laxemar 1.2. The core members of the project and the activity leaders from the Oskarshamn site investigation group together utilised protocols addressing uncertainties and biases in primary data, uncertainty in models and potential for alternative interpretations, consistency at interfaces between disciplines, consistency with understanding of past evolution and consistency with previous model versions. The results are described in Chapter 12.

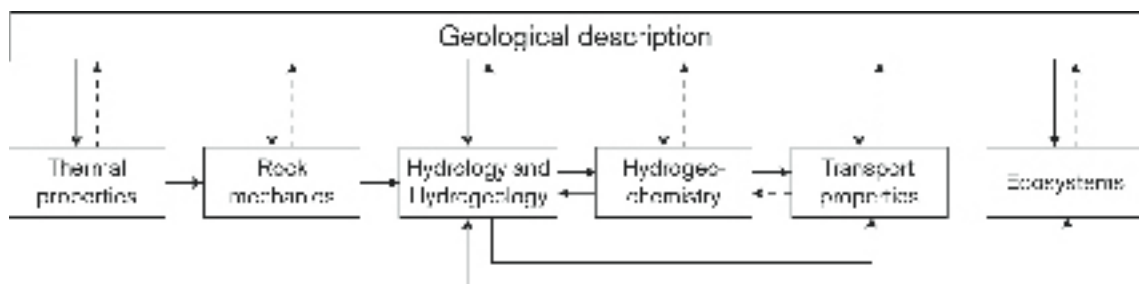


Figure 1-4. Interrelations and feedback loops between the different disciplines in site descriptive modelling where geology provides the geometrical framework /from Andersson 2003/.

1.4.2 Interfaces between disciplines

Central in the modelling work is the geological model which provides the geometrical context in terms of the characteristics, location, geometry and extent of deformation zones¹ and the rock mass units between the zones. Using the geological and geometrical description as a basis, descriptive models for other scientific disciplines (hydrogeology, hydrogeochemistry, rock mechanics, thermal properties and transport properties) are developed. Development of these models has in turn highlighted issues of potential importance for the geological model. Some of these issues have been discussed in conjunction with specific interfaces, e.g. connectivity of deformation zones (Hydrogeology), importance of mineralogy (Thermal model). However, the main feedback to the Geological model is expected during the course of the subsequent site descriptive modelling steps 2.1 and 2.2. The interface between hydrogeology and hydrogeochemistry has been handled e.g. by regional palaeo-hydrogeological simulations of variable-density groundwater flow between 5,000 BC and 2,000 AD. Another example of successful integration of surface data, information and models is the Ecosystems modelling, cf. Chapter 4 and /Lindborg 2006/.

The interface between the surface and bedrock systems was considered in the evaluation of deep and shallow groundwater movement as well as in the groundwater chemistry description. The present relatively detailed conceptualisation of the distribution of Quarternary deposits and their hydraulic properties is implemented in the hydrogeological modelling and also in the evaluation of the impact of groundwater recharge on the present groundwater composition, and of the chemical and biogeochemical reactions that influence the chemistry of recharging waters. A first attempt to model the shallow groundwater system was made as part the SDM Simpevarp 1.2 of the Simpevarp subarea /SKB 2005a/. In the current modelling, this has been expanded to incorporate more run-off areas. In this context, the flow conditions in the bedrock have been adapted from the Simpevarp 1.2 regional hydrogeological model. The link between water flow and chemistry in the shallow system is so far restricted to comparisons between the location and areal distribution of zones of recharge and discharge from the hydrology modelling and the corresponding characteristics evaluated from the chemical composition of water samples.

The handling of interfaces between disciplines is described in more detail in Chapters 4 through 12.

1.4.3 Organisation of work

The work has been conducted by a project group and associated discipline-specific working groups, or persons engaged by members of the project group. The members of the project group represent the disciplines of geology, rock mechanics, thermal properties, hydrogeology, hydrogeochemistry, transport properties and surface ecosystems.

Each discipline representative in the project group was given the responsibility for the assessment and evaluation of primary data and for the modelling work concerning his/her specific discipline. This task was then done either by the representatives themselves, or together with other experts or groups of experts outside the project group. In this context, the discipline-specific groups set up by SKB play an important role. These groups are the same for the Laxemar and Forsmark site-modelling projects and they are essentially run by the person responsible, as appointed by SKB. The purpose of these groups is to carry out site modelling tasks and to provide technical links between the site organisations, the site modelling teams and the principal clients (Repository Engineering, Safety Assessment and Environmental Impact Assessment). The discipline-specific working groups actively involved in the site modelling work are identified in Table 1-1. Supporting reports have been produced for some of the discipline-specific work carried out within the framework of model version Laxemar 1.2. References to these supporting reports are given at the appropriate places in subsequent chapters of this report.

¹ The term deformation zone is used to designate an essentially 2-dimensional structure (sub-planar structure with a small thickness relative to its lateral extent) along which deformation has been concentrated /Munier et al. 2003/. See also Chapter 5 for its use in modelling.

Table 1-1. Discipline-related analysis groups active in the site modelling work and their mandates/objectives.

Dicipline	NET-group	Mandate
Geology	GeoNET	GeoNet promotes synchronisation between the two modelling projects within the framework of the overall methodology. In addition, it constitutes a forum for technical discussions on issues mainly related to structural geology. Furthermore, GeoNet manages feedback from other disciplines by distributing specific tasks to appropriate experts.
Rock mechanics and thermal properties	MekNET	Coordination of modelling tasks for rock mechanics and thermal properties at both sites. Resource for development and maintenance of method descriptions.
Hydrogeology	HydroNET	Execution of the hydrogeological modelling, constitute a forum for all modellers within hydrogeology (needs of Site modelling, Safety Assessment and Repository Engineering), promote technical exchange of experience.
Hydrogeochemistry	ChemNET (formerly denoted HAG)	To model the groundwater data from the sites and assure that the data quality is sufficient. Produce site descriptive hydrogeochemical models. Integrate the description with other disciplines and make recommendations for further site investigations.
Transport properties of the bedrock	RetNET	Execution of the Transport properties modelling, constitute a forum for all transport related modellers within site modelling and safety assessment, and promote technical exchange of experiences.
Surface system	SurfaceNET	To describe and model the surface system by subdiscipline (biotic and abiotic), modelling the properties in a distributed way over space and time (maps and 3D), describe the different ecosystems (conceptually and in a site specific way), describe and model the flow of matter in the landscape, describe and model the flow of matter in the landscape by defining and connecting ecosystems, produce site descriptions to support environmental impact assessment (EIA).

The project group has met at regular intervals to discuss the progress and integration of the work, and specific questions that have emerged during the modelling work. In addition, the project group has had a workshop addressing uncertainties, integration of, and interactions between, disciplines, and overall confidence in the analyses made and models produced. The information exchange between the modelling project and the site investigation team is an important component of the project, which is facilitated by the fact that some of the project members are also engaged as experts in the site investigation team. In addition, the leader of the site investigations at Simpevarp has participated in most of the modelling project meetings.

1.4.4 Changes compared to Simpevarp 1.2 work

There are no major changes in the work modes or reporting strategies of the Laxemar 1.2 work compared with those employed for the preceding Simpevarp 1.2 work. Worth mentioning, however, is the setting up of a separate NET group for the treatment of the transport modelling in the bedrock and surface systems.

The fact that the Simpevarp 1.2 and Laxemar 1.2 models share the same locals scale model volume provides the opportunity for tracking the evolution of the site descriptive models of the two subareas. Compared to the situation at the time of the data freeze for Simpevarp 1.2, there is for Laxemar 1.2 a considerable amount of information from the Laxemar subarea.

1.5 This report

This report presents the preliminary site description for the Laxemar subarea. For reasons explained in Section 2.8, the local model volume also includes the Simpevarp subarea.

This report follows the updated structure for descriptive modelling reports for the initial investigation phase which has already been applied for the SDM Simpevarp 1.2 /SKB 2005a/ and the SDM Forsmark 1.2 /SKB 2005b/.

- Chapter 2 summarises available primary data and provide an overview of their usage.
- Chapter 3 provides an account of the development of the geosphere and the surface systems in an evolutionary perspective.
- Chapters 4 through 10 in sequence provide accounts of the modelling of surface ecology, geology, rock mechanics, thermal properties, hydrogeology, hydrogeochemistry and transport properties, respectively. Each chapter includes the discipline-based accounts of evaluation of the primary data, three-dimensional modelling and discussion of identified uncertainties associated with the developed models.
- Chapter 11 encapsulates the resulting descriptive model of the Simpevarp subarea in a condensed form.
- Chapter 12 discusses overall consistency between the various disciplines and identifies the interactions between disciplines, and finally outlines possible alternative interpretations in the light of observed uncertainties.
- Chapter 13 provides the overall conclusions of the work performed and discusses implications for the continued site investigation work and the future modelling process.

2 Available data and other prerequisites for the modelling

This chapter defines the database used for the Laxemar 1.2 modelling, and other associated premises and prerequisites related to the modelling work. The account given here is provided primarily for future reference and for traceability. Specific data are not provided, nor discussed. Referenced reports in the SKB P-series² of reports display data and also provide references to data in the SKB Sicada and GIS databases. These reports also provide descriptions of the performance of investigations and other relevant matters associated with data acquisition. Discussions on specific data and how they have been used in the modelling process are found Chapters 4 through 10. Chapter 12 discusses what data were available, but not used, and explains why those data were not used.

2.1 Overview

This section primarily presents a summary of the investigations conducted between data freezes for Simpevarp 1.2 and Laxemar 1.2. The majority of those investigations were completed and made available to site modelling during the period April 1 2004 through November 1, 2004. Also, a short retrospective review is provided of the data previously acquired, i.e. data used in model versions Simpevarp 1.1 /SKB 2004a/ and Simpevarp 1.2 /SKB 2005a/.

2.1.1 Investigations and primary data acquired up to data freeze Simpevarp 1.1

Investigations have been in process at the Simpevarp area from about March 2002. The data freeze for the Simpevarp 1.1 model version was set at July 1, 2003.

The *surface investigations* consisted of airborne photography and airborne and surface geophysical investigations, for the most part regional scale in character. The surface investigations in the Simpevarp subarea included lithological mapping of rock surfaces, scan line mapping of structural characteristics and mapping of Quaternary deposits and soils. Furthermore, marine geological investigations, hydrogeochemical characterisation of surface waters and various types of surface ecological inventories and investigations were included.

The *borehole activities* included drilling of two vertical cored c.1,000 m deep boreholes (KSH01A and KSH02), drilling of the 100 m deep complementary cored borehole KSH01B and three percussion-drilled boreholes (HSH01, HSH02 and HSH03) with lengths up to 200 m and reaching depths of 185–200 m. Several methods of borehole investigations after drilling were applied to these boreholes. These were: geological and rock mechanics sampling and testing of drill cores, TV logging of the borehole wall using the Borehole Image Processing System (BIPS), radar logging, conventional geophysical logging, Boremap logging of core-drilled and percussion-drilled boreholes using the core and BIPS in combination, rock stress measurements using the overcoring technique, and different types of hydraulic testing and groundwater sampling.

2.1.2 Investigations and primary data acquired for data freeze Simpevarp 1.2

The data freeze for version Simpevarp 1.2 was set at April 1, 2004. A decision had already been taken to define a local scale model volume for Simpevarp 1.2 that included both the Simpevarp and Laxemar subareas. At the time of the data freeze, the lineament data and interpretation covered the whole regional scale modelling area. However, one important component – the lithological mapping of the Laxemar subarea and selected regional surroundings – was yet to be completed and delivered. In fact, access to the Laxemar subarea was not granted until December 2003. Apart from the above geological components, the database at April 1, 2004 comprised additional elements of surface and borehole investigations.

² The P-series report the results of the ongoing site investigations at Oskarshamn (Simpevarp and Laxemar subareas) and Forsmark. These reports are available on the SKB web page together with reports in the SKB R- and TR-series (www.skb.se).

The *surface investigations* consisted of; detailed mapping of structural characteristics of fractures across four cleared rock surfaces, hydrogeochemical characterisation of surface waters and various types of surface ecological inventories and investigations.

Borehole activities included drilling of two new c. 1,000 m long cored boreholes (KSH03A and KAV04) and the complementary 100 m deep cored borehole KSH03B. To these boreholes should also be added the cored borehole KLX04, drilled in the Laxemar subarea (from which only limited investigation data were available, e.g. stress measurement data. Drilling in the overburden included soil/rock augering of 19 boreholes for total depth of overburden). Four of the latter boreholes were drilled for environmental monitoring in conjunction with drill sites on the Simpevarp peninsula. In addition, manual augering of 17 boreholes and weight soundings at 23 sites were conducted in conjunction with mapping of the overburden.

The same package of borehole logging and characterisation as applied in conjunction with Simpevarp 1.1 was also applied for Simpevarp 1.2. One exception was the undertaking of rock stress measurements using the hydrofracturing technique. Furthermore, complementary data were collected from two existing cored boreholes (KLX01 and KLX02). Investigations in these boreholes included BIPS, Boremap logging, geophysical logging, boremap radar (RAMAC) and Posiva flow logging (PFL), the latter only in KLX01.

It was identified that review of old geological data from the construction of the nuclear power plants and the Clab facility had not been carried out to the extent originally proposed. This is not considered critical for the description of the Laxemar subarea.

2.1.3 Data freeze Laxemar 1.2 – investigations performed and acquired data

The data included in data freeze Laxemar 1.2 and available for the Laxemar 1.2 modelling work are the data used in previous models versions, as described in the preceding sections, and data acquired between data freezes Simpevarp 1.2 and Laxemar 1.2 (i.e. during the period April 1 2004 through November 1, 2004). The investigations associated with data collection during this period comprised the following main items:

- Geoscientific and ecological surface investigations. Note that no additional airborne measurements have been performed for use in Laxemar 1.2.
- Drilling, measurements during drilling, investigations of drill core and drill cuttings and investigations in boreholes after completion of drilling.

The surface investigations comprised:

- Bedrock mapping (lithology, structural characteristics).
- Investigations of Quaternary deposits including indirect assessments of marine and lacustrine sediments in the Baltic and in Lake Frisksjön. The investigations have included stratigraphy, distribution of chemical composition of the overburden, sediment samples and peat land investigations.
- Surface geophysical investigations, including acquisition of new data and updated/extended interpretations of data collected before data freeze Simpevarp 1.2 (primarily reflection seismic data).
- Meteorological and hydrological measurements and monitoring (precipitation, snow depth, ground frost, ice cover, surface water levels, run-off in streams and brooks).
- Hydrogeochemical sampling and analysis of precipitation, surface waters and shallow groundwater.
- Various ecological inventories and investigations.

The drilling activities comprised (see Figure 2-3 for borehole locations).

- Drilling of deep cored boreholes KLX03, KLX04, KLX05 and KLX06.
- Drilling of percussion boreholes HLX13 through HLX29, HSH04 through HSH06 and HAV09–HAV14.
- Drilling of additional boreholes through Quaternary deposits.

Borehole investigations during drilling of all core-drilled and percussion-drilled boreholes were carried out according to standardised programmes presented in Section 2.5. The measurements and activities performed after drilling can be outlined as follows:

- **Geology:** Boremap logging and geological single-hole interpretation of the boreholes drilled after data freeze Simpevarp 1.2. For the core-drilled parts also drill core sampling and analyses of petrographical, geochemical, petrophysical properties and fracture mineralogy. Single-hole interpretations were only available for the cored boreholes KLX03 and KLX04. Only results from drilling and preliminary geological mapping of cored boreholes KLX05 and KLX06 were available and used in the modelling of rock domains, deformation zones and geological SDN model. However, data from these boreholes were used in the fracture mineralogical analysis.
- **Geophysics:** BIPS- and radar logging, conventional geophysical logging and interpretation of geophysical measurements in the boreholes drilled after data freeze Simpevarp 1.2.
- **Rock mechanics:** Sampling and rock mechanics testing of drill core samples from boreholes KLX03 and KLX04.
- **Thermal properties:** Sampling and testing in the laboratory of drill cores from boreholes KLX03 through KLX04.
- **Hydrogeology:** Difference flow logging in cored boreholes KLX03 and KLX04, single-hole injection tests in cored boreholes KLX03 and KLX04, pumping tests and flow logging in the percussion boreholes HAV09–HAV10, HLX13, -14, -18, -20, -22, HLX24–HLX25 and in the percussion-drilled parts of telescopic core-drilled boreholes KLX03 and KLX04. In addition, a series of superficial interference tests have been conducted focused primarily on the connectivity of interpreted deformations zones.
- **Hydrogeochemistry:** hydrogeochemical logging and complete hydrogeochemical characterisation in telescopic core-drilled boreholes KLX03–KLX06, investigations of microbes in flushing water during drilling, sampling and analysis of groundwater from percussion-drilled boreholes, and investigations of fracture minerals sampled from drillcores from boreholes KLX03 and KLX04.
- **Transport properties:** laboratory resistivity measurements on core material from KLX04, in situ resistivity measurements from KLX03 and KLX04, laboratory determined formation factors (through-diffusion) on core material from KLX02, porosity data relating to core samples from KLX02, KLX03, KLX04, and KLX06. Also tracer dilution tests in KLX02, a combined pumping and tracer test between KLX02 and HLX10, and one single-well injection withdrawal (SWIW) test in KSH02.

The performed site investigations and subsequent testing and analyses in the laboratory of samples from the Simpevarp area (including the Laxemar subarea) has resulted in a significant increase in the amount of data compared with that available at the onset of the Simpevarp 1.2 modelling. This said, it should be acknowledged that the new amount of information from deep boreholes is relatively limited in the Laxemar subarea. In the case of surface information, the new bedrock map covering the Laxemar subarea, paired with more surface data including an improved map of Quaternary deposits, has resulted in an overall improved platform for the modelling.

2.2 Previous model versions

2.2.1 Version 0

The version 0 report provided a regional scale site-descriptive model for the geosphere covering the disciplines geology, rock mechanics, hydrogeology and hydrogeochemistry. Within each discipline, identified uncertainties and alternative models were discussed to variable levels of detail, depending on the availability of data. For the surface system, version 0 provided a systematic overview of data availability and data needs for future development of a site-descriptive model for the surface ecosystems (the biosphere). Worth noting is that information from cored boreholes KAV01, KLX01 and KLX02 and percussion boreholes HAV01–HAV08 and HLX01–HLX12 already existed prior to version 0.

An important result of the work with the version 0 model was the data inventory, in which the locations and scope of all potential sources of data were documented, and the evaluation of those data was provided with respect to their usefulness for site descriptive modelling. This inventory contains data that, at that time, were already stored in the SKB databases Sicada and GIS (primarily data from Äspö HRL, see Section 2.2.2, and from the construction of Clab), but also data that had not been evaluated and/or inserted in the databases, but which were, nevertheless, relevant for site descriptive modelling (e.g. old data related to the construction of the power plants).

2.2.2 Models developed as part of Äspö HRL and Ävrö work

Models preceding the version 0 model of the Simpevarp area included models developed on the basis of characterisation data produced for the siting and construction of the Äspö HRL. In this process, descriptive models were developed for the Äspö island and its immediate environs /Rhén et al. 1997c/. As part of the operational phase of the Äspö HRL, descriptive models, including conceptual models of fractures and fracture systems were developed as part of the TRUE Programme /Winberg et al. 2000, Andersson et al. 2002c/, the Fracture Classification and Characterisation Project (FCC) /Mazurek et al. 1997, Bossart et al. 2001/, Äspö Task Force work /Dershowitz et al. 2003/ and the Prototype Repository Project /Rhén and Forsmark 2001/. More recently, an effort has been made within the so-called GEOMOD project to revisit the 1997 site-scale descriptive models of Äspö, also attempting to incorporate the new information from the experimental work undertaken during the operational phase on a larger scale /e.g. Berglund et al. 2003/.

In preparation for the SKB site investigation programme, the Rock Visualization System (RVS) was tested out using information from the island of Ävrö /Markström et al. 2001/. A series of models of deformation zones and lithology was developed, incorporating successively more information starting from using surface information only, adding surface geophysics (reflection seismics), and finally incorporating data from existing core-drilled and percussion-drilled boreholes. Important feedbacks to the modelling process using RVS were also provided.

2.2.3 Laxemar test application

A more full fledged test of the developed methodology for site descriptive modelling was made on the Laxemar area /Andersson et al. 2002b/. The intent was to explore whether the available methodology for site descriptive modelling using surface and borehole data was adequate, and further to identify needs for new developments and improvements. With limitations in scope – thermal properties and transport properties and surface ecology were not included – a descriptive model more or less equivalent to a version 1.2 descriptive model on a local scale was developed. The underlying data consisted of various types of surface data and data from two deep core-drilled boreholes (KLX01 and KLX02). Controls of internal consistency and processing of the primary data for use in 3D modelling were undertaken.

In order to promote cross-discipline interpretation and check for consistency, the evaluation/modelling was performed individually for each discipline followed by cross-checking. Despite its limited scope, the resulting description was viewed as an illustration of the type of product that will emerge at the end of the initial site investigation stage. This indicated that the type of descriptive modelling outlined in the general execution programme was indeed achievable. Hence, the Laxemar test application served as a preliminary and provisional model for the ongoing site-descriptive modelling in the Forsmark and Simpevarp areas.

2.2.4 Simpevarp 1.1

For the Simpevarp version 1.1 modelling, the surface-based data sets were, in a relative sense, extensive compared with data sets from deep boreholes, for which the information largely was limited to information from one new c. 1,000 m deep cored borehole (KSH01A) and two old cored boreholes (KLX01 and KLX02, in the Laxemar subarea).

Compared with version 0 there were considerable additional features in the version Simpevarp 1.1, especially in the geological description and in the description of the near surface. The developed geological models of lithology and deformation zones were based on borehole information and surface data of much higher resolution. The lithology model included four interpreted rock domains and the deformation zone model included 14 zones of interpreted high confidence (of existence). A discrete fracture network (DFN) model was developed, including attempts to assess fracturing imposed by interpreted deformation zones. The rock mechanics material property model was based on information from the Äspö HRL and an empirical mechanical classification of data from KSH01A and data from outcrops. A first model of thermal properties of the rock was developed largely based on data from the Äspö HRL, and projections based on density and mineral content.

The hydrogeological description was based solely on the version 0 regional structural model. Hydrogeological simulations of the groundwater evolution since the last glaciation were compared with the developed hydrogeochemical conceptual model. A first model of the transport properties of the rock was presented, although still rather immature, due to lack of site-specific data in support of the model. There was information regarding the distribution of Quaternary deposits, and some information about the stratigraphy of the overburden.

There was much uncertainty in the version Simpevarp 1.1 site descriptive model. However, the main uncertainties were regarded as being identified.

2.2.5 Simpevarp 1.2

For the Simpevarp 1.2 modelling, the amount of information from deep boreholes was significantly improved compared with Simpevarp 1.1 with data primarily from four approximately 1,000 m deep cored boreholes (KSH01A, KSH02, KSH03A and KAV04). Data from percussion holes were the same as for Simpevarp 1.1, (HSH01, HSH02 and HSH03), with lengths ranging up to 200 m and reaching depths of 185–200 m. The surface information at the time suffered from the fact that there was no bedrock map of the complete local model area.

The SDM Simpevarp 1.2 has developed considerably compared to Simpevarp 1.1 with geological models of rock domains and deformation zones that are based on more borehole information. The geological DFN model was developed and used by other disciplines. The rock stress model was intimately tied to the geometry of deformation zones with lower stresses in the Simpevarp subarea compared with the area west thereof (including the Laxemar subarea) attributed to unloading of a wedge-formed rock volume underneath the Simpevarp peninsula as delineated by the intersecting deformation zones. Quantification of bedrock mechanical properties was based on new laboratory data on intact rock samples, underpinned by empirical and theoretical relationships. The model of the thermal conductivity has developed considerably since Simpevarp 1.1, indicating that the thermal conductivity in the Simpevarp subarea generally is low.

The hydrogeological description was based on the model of deformation zones and hydraulic properties of the rock mass based on a hydraulic DFN model developed on the basis of the geological DFN and hydraulic test data from KSH01A and KSH02. Subsequent modelling identified the Simpevarp subarea as an area of groundwater discharge (upward directed flow) at repository depth. Hydrogeological simulations of the evolution of the salinity distribution from the latest glaciation showed results compatible with measured geochemical signatures. The results further suggest that Littorina water, indicated by the characterisation, may be present near the coast and below the Baltic Sea. The developed retardation model provides a parameterisation for rock domains and their constituents as well as for fractures and deformation zones. The model, is however, mainly based on imports and inferences from Äspö paired with formation factors derived from resistivity logging in KSH01A and KSH02. Surface ecosystem models in terms of pools and fluxes of carbon were developed for the terrestrial (e.g. plants and animals) and limnic (e.g. algae and fish) systems using the Lake Frisksjön drainage area. Furthermore, a first marine ecosystem model was developed for the Basin Borholmsfjärden.

2.3 Geographical data

The Simpevarp area, cf. Figure 1-2, is located close to the shoreline of the Baltic Sea and the investigated area extends out into the sea. The eastern-most land masses in the area include the Simpevarp peninsula, the Ävrö and Hälö islands and associated smaller islets. The western limit is located immediately west of the main highway (Route E22) that runs essentially north-south. The geographical data available for the Simpevarp version 0 site descriptive model are presented in /SKB 2002b, Section 2.1/. This report includes the applicable coordinate system, available maps (general map, topographic map, cadastral index map), digital orthophotography and elevation data.

The applicable coordinate system used for spatial coordinates for the version Laxemar 1.2 modelling are:

- X/Y (N/E): The national 2.5 gon V 0:–15, RT90 system (“RAK”).
- Z (elevation): The national RH 70 levelling system /Wiklund 2002/.

Elevation data covering the land area are available for the whole of Sweden from the GSD-Elevation database. For most parts of the country, including the Laxemar area, a digital elevation model called 4600DEM (sometimes termed DTM-model, Digital Terrain Model), based on the GSD-Elevation database, is available. This elevation model, which is derived from aerial photographs taken at a height of 4,600 m, is produced on a 50×50 m grid. Metria, National Land Survey of Sweden, guarantees that the average error in elevation data is less than ± 2.5 m for each 50×50 m grid cell.

A more detailed digital elevation model of the Laxemar area, called 2300DEM, has also been developed by Metria. This is based on flying at 2,300 m height and uses 10 m grids, i.e. the distances between data points in both X and Y direction is 10 m. The 2300DEM has served as the basis for further elaboration of elevation data in several steps, of which the first was reported in /Brydsten 2004/. The 2300DEM in its primary version has served as the standard elevation database in the site investigations performed between data freezes 0 and 1.2 and further developed versions have been applied for special purposes. The most recent version is described in /Brydsten and Strömngren 2005/ and /Lindborg 2006/.

2.4 Surface investigations

The surface investigations (including marine and lacustrine investigations) performed in the Simpevarp regional model area (and its surroundings) carried out between data freezes Simpevarp 1.2 and Laxemar 1.2 involved the following disciplines:

1. Bedrock geology.
2. Quaternary geology.
3. Geophysics.
4. Meteorology, hydrology and hydrogeology.
5. Hydrogeochemistry (boreholes in overburden and surface waters).
6. Surface ecology.

In the following, the investigations that have provided data for the data freeze Laxemar 1.2 are described in a greater detail according to discipline. Bedrock geology and geophysical information are treated as one group, given their close interrelation.

2.4.1 Bedrock geology and ground geophysics

Bedrock mapping of the Laxemar subarea was completed for the data freeze and has produced a bedrock map of the local model area including the Simpevarp and Laxemar subareas (1:10,000), with associated outcrop databases /Wahlgren et al. 2005a/. With this added information, the bedrock mapping in the Simpevarp area has essentially reached its goals. This does not rule out minor complementary, targeted mapping tasks in the future.

Scan-line mapping in the Laxemar subarea and in the corridor between the Simpevarp and Laxemar subareas.

Bedrock characterisation from pits dug to the rock surface in the southern parts of the Laxemar subarea.

Reflection seismic survey/-s in the Laxemar subarea included collection of about 9.9 km of high resolution seismic data along three separate profiles /Juhlin et al. 2004b/. In addition, reflection seismic data were also acquired on the Ävrö island (Simpevarp subarea) /Juhlin et al. 2004a, Schmelzbach and Juhlin 2004/.

Ground geophysical information included refraction seismic profiling in the Laxemar subarea and off-shore refraction profiling on Ävrö and off the coasts of the Ävrö island and the Simpevarp peninsula. In addition, gravimetrical data were collected along roads in the Laxemar area. Finally, ground geophysical profiles were collected in the Laxemar subarea.

2.4.2 Overburden

Overburden here refers to all surficial deposits irrespective of their origin. Mapping of Quaternary deposits in the Laxemar subarea was completed in early fall 2004. For clarity, the short boreholes used to map the depth and the stratigraphy of the overburden are included in this section. Detailed information about the types of boreholes completed in the overburden and their spatial distribution is provided in /SKB 2006b/.

Surface data

The surface data available for data freeze Laxemar 1.2 comprised, cf. Figure 2-1:

- Field data from mapping of Quaternary deposits in the terrestrial and most of the marine parts of the Simpevarp regional model area.
- Map of soils in the terrestrial parts of the Simpevarp regional model area.

Stratigraphical and overburden depth data

- Results from 47 percussion bore holes and 17 cored bore holes to establish the total depth of Quaternary deposits.
- Results from 327 manually augered boreholes and weight soundings to establish the stratigraphy of the uppermost overburden.
- Stratigraphical data from 38 monitoring wells.
- Stratigraphy and analytical data from characterisation of dug pits to the rock surface in the southern parts of the Laxemar subarea.
- Vertical electrical sounding (VES) at 22 sites to determine the total depth of the overburden.
- Refraction seismic from 31 profiles in the Laxemar and Simpevarp subareas to determine total depth of the overburden.
- Total depth and stratigraphy from 19,237 points in the marine area, gained from seismic and sediment echo sounding.

Analyses

- Analytical data, including grain size, organic carbon, nitrogen, sulphur, soil pH and calcium carbonate.

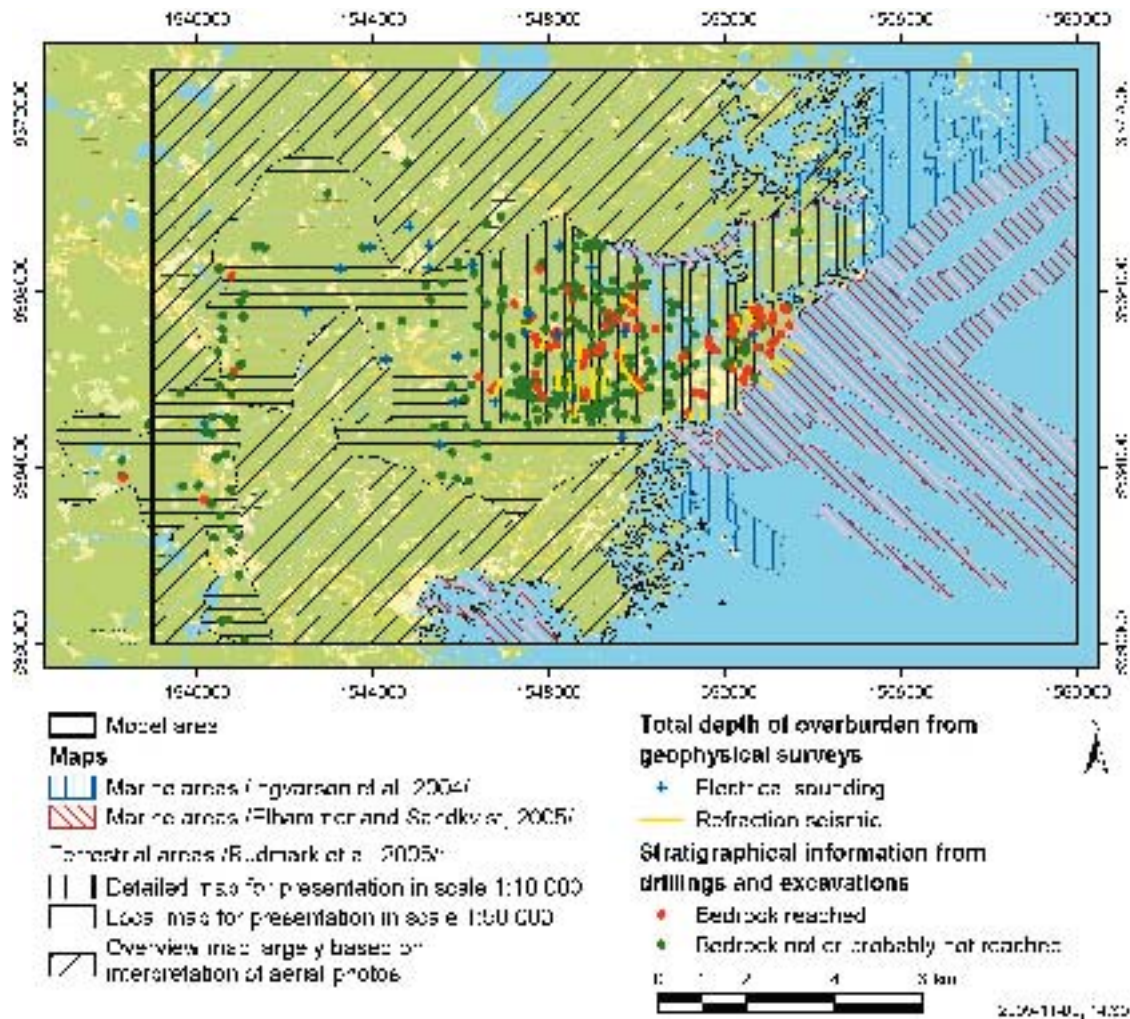


Figure 2-1. Data used for modelling the surface and stratigraphical distribution of Quaternary deposits in the Simpevarp regional model area. In addition, a soil map covering the whole terrestrial part of the regional model area has been produced by /Lundin et al. in press/. Data from the marine areas mapped by /Elhammer and Sandkvist 2005/ include stratigraphy and total depth data of overburden from 19,237 points. The refraction seismic profiles include overburden depth data from 1,087 points.

2.4.3 Meteorology, hydrology and hydrogeology

Between the Simpevarp 1.2 (April 1, 2004) and Laxemar 1.2 (November 1, 2004) data freezes, the meteorological, hydrological and hydrogeological investigations have comprised the following main components, cf. Figure 2-2:

- Additional time series from the meteorological station on Äspö.
- Establishment of a new meteorological station in Plittorp, located in the western part of the Simpevarp area c. 10 km west of the station on Äspö.
- Establishment of new hydrological stations for discharge measurements.
- Measurement of cross sections along the main water courses in selected catchment areas.
- Continued manual discharge measurements in water courses.
- Drilling and additional slug tests of groundwater monitoring wells in Quaternary deposits (QD) in Laxemar.
- Continued manual groundwater level measurements in wells in QD.
- Installation of equipment for automatic measurements of groundwater levels in wells in QD.

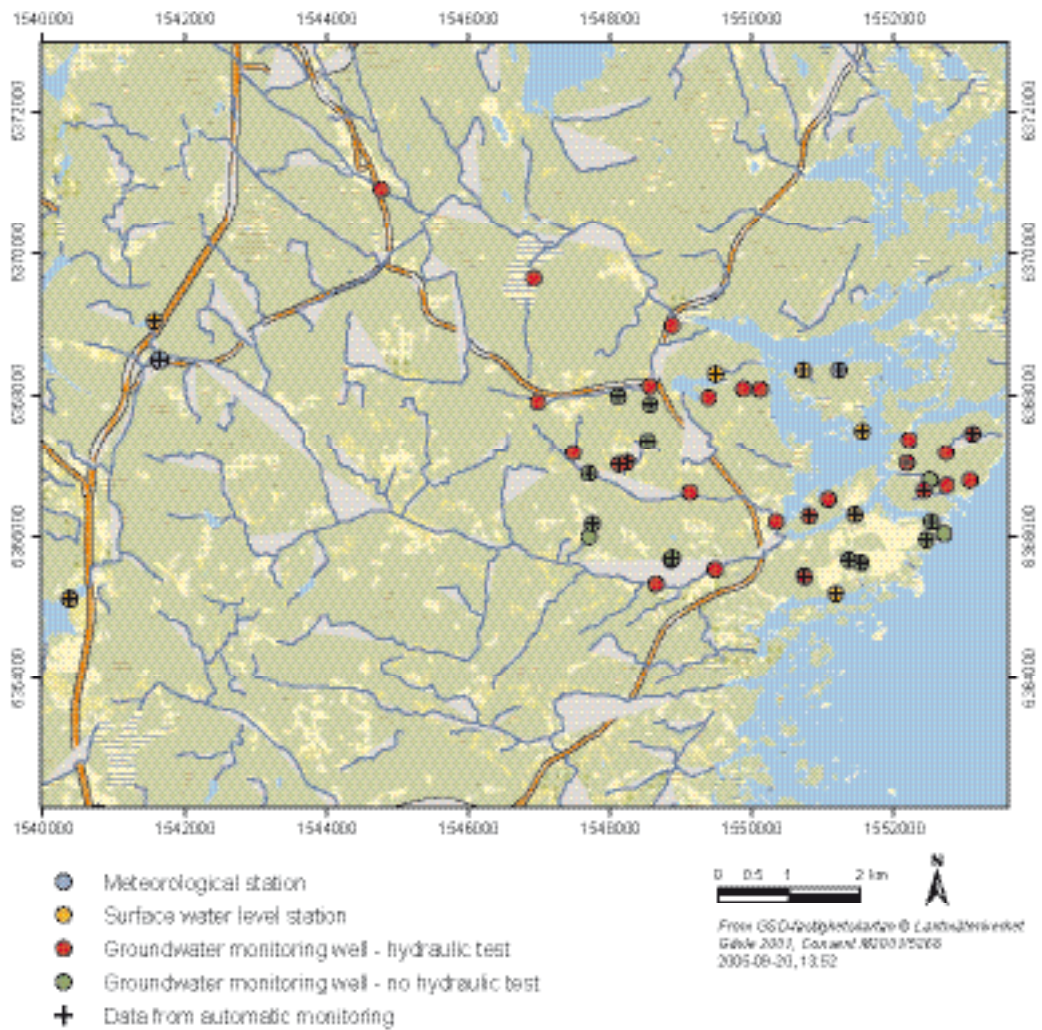


Figure 2-2. Hydrological measurement stations and groundwater monitoring wells providing data used to produce the description of climate, surface hydrology and near-surface hydrogeology. Stations and monitoring wells for which data from automatic monitoring are available in the Laxemar 1.2 database are marked by “+” in the figure. In addition, data from manual groundwater level measurements are available for most monitoring wells.

2.4.4 Surface ecology

The surface investigations made exclusively as part of the surface ecological programme, and producing data for data freeze Laxemar1.2 comprised:

Terrestrial (biotic)

- Bird population survey.
- Mammal population survey.
- Vegetation mapping.

Surface waters (biotic)

- Benthic fauna survey.
- Fish fauna survey.
- Phytoplankton and zooplankton survey.
- Macrophyte survey.

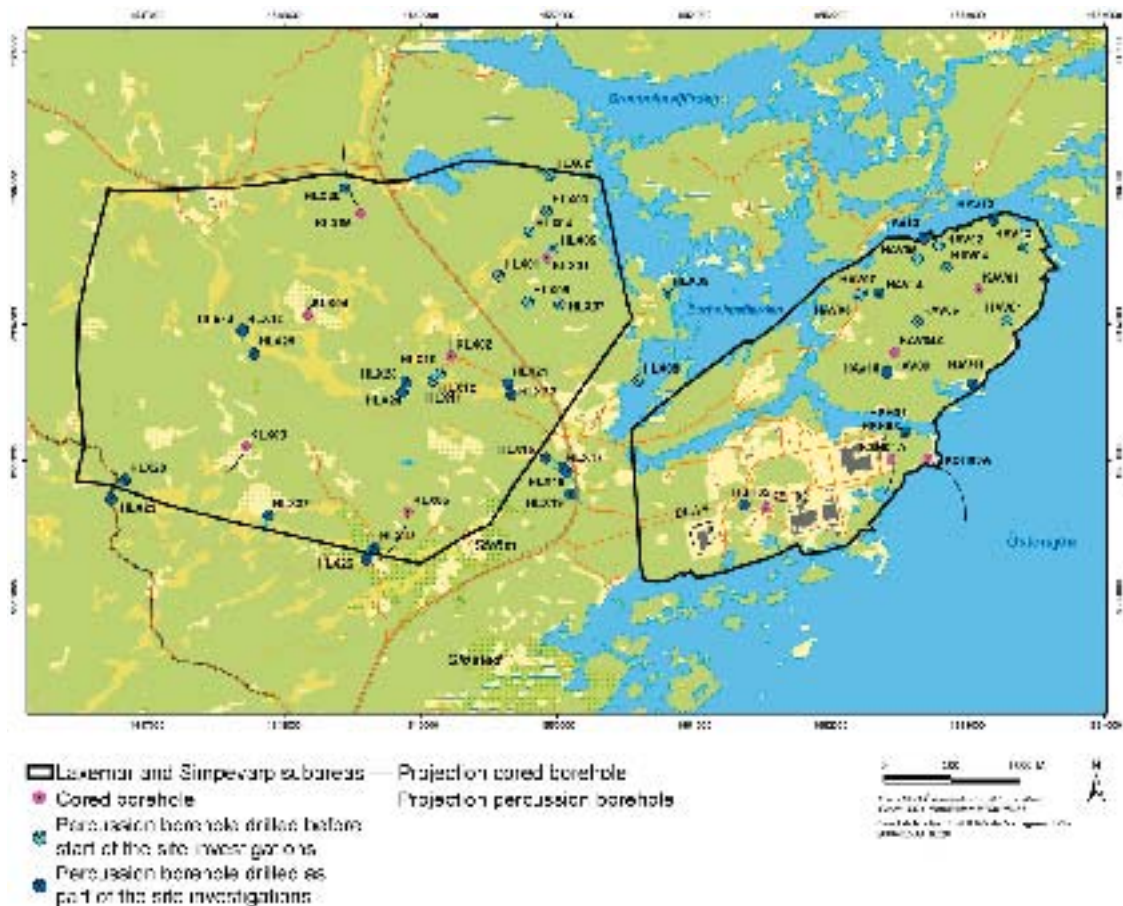


Figure 2-3. Overview map of core-drilled and percussion-drilled boreholes in the Laxemar and Simpevarp subareas.

2.5 Borehole investigations

Primary data from boreholes for data freeze Laxemar 1.2 originate from investigations performed in cored boreholes and percussion-drilled boreholes shown in Figure 2-3. The corresponding boreholes dedicated to mapping the depth and stratigraphy of the overburden are discussed in Section 2.4.2. In the following, only those boreholes that have been added to the databases between data freeze Simpevarp 1.2 and Laxemar 1.2 are discussed. Details on the boreholes included in data freeze Simpevarp 1.2 are discussed in /SKB 2005a/. The investigations performed in boreholes may roughly be divided in two categories:

- 1) Investigations conducted during and immediately following completion of the drilling, and
- 2) Investigations conducted after drilling.

Each of the two borehole categories, cored boreholes and percussion-drilled boreholes in bedrock, was associated with a specific investigation programme during drilling and another programme after drilling. These programmes are presented in Sections 2.5.1 and 2.5.2, followed by comments on any deviations from the standard procedures, if any. New borehole data included in the Laxemar 1.2 modelling include:

- Data from cored boreholes KLX03, KLX04, KLX05 and KLX06, used to a variable extent (as discussed below),
- Data from the percussion-drilled boreholes HAV09–HAV14 and HLX13–HLX29.

2.5.1 Borehole investigations during and immediately after drilling

Core-drilled boreholes

Borehole investigations during and immediately after core drilling normally include the following items (cf. SKB MD 620.004): overview mapping of the drill core, hydraulic tests with a special test tool (the wireline probe), absolute pressure measurements with the wireline probe, water sampling with the wireline probe, measurements of borehole deviation and weighing of drill cuttings. In addition, registration of the following flushing and return water parameters is made: flushing water and return water flow rate, flushing water pressure, content of dissolved oxygen in flushing water and electric conductivity of flushing and returned water from the borehole. Moreover, the flushing and returned water is sampled for determination of the content of tracer dye. Technical drilling parameters, some of which may be useful for geoscientific evaluation, e.g. penetration rate and feed pressure, are also registered. If the core-drilled borehole is selected for rock stress measurements using the overcoring technique, these tests are also carried out during the drilling process.

The core-drilled boreholes produced during the site investigation may be divided into two categories: 1) telescopic boreholes and 2) core-drilled boreholes of traditional type (without telescoped section). Most of the deep boreholes (down to c. 1,000 m) belong to the former category, and this also applies to the new cored boreholes included in data freeze Laxemar 1.2. Telescopic drilling implies that the upper 100 m is percussion-drilled with a large diameter (≥ 200 mm). In the case of friable rock or large inflows this upper 100 m is cased with stainless steel casing, and the annular space between the casing and borehole wall is grouted. A casing is always emplaced 10 m into the rock in order to prevent shallow groundwater from discharging into deeper parts of the bedrock during the continued drilling below 100 m. If casing and grouting is required, the diameter of the upper 100 m has to be increased to c. 250 mm in order to allow a casing with an inner diameter of 200 mm.

The borehole section between approximately 100–1,000 m, i.e. the major part of the telescopic borehole, is core-drilled. Because a telescopic borehole consists of a percussion-drilled as well as a core-drilled section, the investigation programmes for both percussion-drilled and core-drilled boreholes are applied.

The telescopic boreholes are categorised as boreholes of standard type (including boreholes dedicated for rock mechanics (overcoring)) or of chemistry type. During drilling of both these categories of holes, severe requirements are placed on cleaning the down-hole equipment, in order to avoid contamination of the groundwater and borehole walls. However, the cleaning procedures for boreholes of chemistry type also include disinfection of the down-hole equipment, in addition to the degreasing and cleaning used for both categories of telescopic boreholes.

The full data sets from two c. 1,000 m deep telescopic boreholes, KLX03 and KLX04, became available during the period from data freeze Simpevarp 1.2 till data freeze Laxemar 1.2. These are KLX03 and KLX04. In addition, the drilling data and preliminary geological mapping results from boreholes KLX05 and KLX06 were available for the geological modelling at the time of the data freeze.

Comments, telescopic boreholes KLX03, KLX04, KLX05 and KLX06

Overcoring stress measurements were made in two length intervals, 233–245 m and at 374–451 m in borehole KLX04.

No serious deviations from the measurement programme occurred in relation to telescopic boreholes drilled between data freezes Simpevarp 1.2 and Laxemar 1.2.

Percussion-drilled boreholes

Borehole investigations during (and immediately after) percussion drilling in bedrock comprise:

- sampling of soil with a frequency of one sample per metre while drilling through the unconsolidated overburden (if any) and a preliminary on-site examination,
- sampling of drill cuttings from the solid rock with a frequency of one sample per metre and a preliminary on-site examination,

- manual measurement or automatic logging of penetration rate,
- observation of return water colour at every metre or at levels of observed change,
- measurement of return water flow rate at each major flow change observed,
- measurement of the electrical conductivity of the groundwater every third metre: (measured after completion of drilling),
- deviation measurements after completion of drilling.

Comments, percussion-drilled boreholes HAV09–HAV14 and HLX13–HLX29

No deviations from the measurement programme occurred in relation to the percussion-drilled boreholes included between data freezes Simpevarp 1.2 and Laxemar 1.2.

2.5.2 Borehole investigations after completion of drilling and analysis of drill core and drill cuttings

A base programme was carried out after drilling in all core-drilled boreholes and another base programme in percussion-drilled boreholes. Depending on whether the borehole is prioritised for hydrogeochemical measurements or not, the supplementary data acquired after the base programme may differ between boreholes /SKB 2000/. In the case of data freeze Laxemar 1.2 borehole KLX03 was prioritised for hydrogeochemical investigations and rock stress measurements using the overcoring technique were conducted in borehole KLX04.

Cored boreholes – telescopic

Data from the telescopic boreholes KSH01A, KSH02 and KSH03A and KAV04 plus data from complementary investigations in KAV01 and KLX02 were included in data freeze LSimpevarp 1.2. For data freeze Laxemar 1.2, data from telescopic boreholes KLX03, KLX04 and early data (preliminary geological mapping) from the drilling of KLX05 and KLX06 were made available. Similarly, hydrogeochemical data from KLX06 were also analysed.

The upper c. 100 m long borehole section is percussion-drilled in all mentioned telescopic boreholes. Normally, BIPS-logging should be performed in this section (below the upper casing of 10–15 m) after the first drilling step which provides a borehole diameter of 165 mm. Borehole radar, conventional borehole geophysics and HTHB (Swedish acronym for Hydraulic Test Equipment for Percussion-drilled Borehole) tests are a bit difficult to carry out with good results at this borehole diameter. The results in the telescopic parts are often poor due to a large annular space between the logging tool and the borehole wall. Above all, the latter investigations are, like BIPS-logging, difficult to accomplish from a logistics point of view, due to the narrow time window available during the different sequences of percussion drilling. Therefore, it has not been possible to perform some of these methods in all telescopic boreholes.

BIPS-logging and the samples of drill cuttings provide the basis for (a simplified) Boremap logging of the percussion-drilled part. However, BIPS-logging may be difficult to perform from a technical standpoint. This is because the time available is not always long enough to permit drill cuttings to settle, entailing the risk of poor water quality (with respect to light penetration) in the borehole. BIPS-logging was performed in KLX04 (12–97 m) and in KLX06 (11–97 m) but was not reported for KLX03 and KLX06. No simplified Boremap logging was undertaken in any of the telescopic parts.

Borehole geophysics was only performed in the telescopic part of KLX05. No HTHB tests were performed in any of the telescopic parts of the new cored boreholes.

The borehole investigations performed in the *borehole section 100–1,000 m* and reported as part of data freeze Laxemar 1.2 comprise (if not otherwise indicated applicable to KLX03 and KLX04 but not to KLX05 and KLX06):

- BIPS-logging, borehole radar logging, geophysical logging, Boremap-logging using drill core and BIPS images with support from geophysical logging, geological and rock mechanics single-hole interpretation.

- Difference flow measurements (PFL) and single-hole injection tests with the PSS equipment (employing various test section lengths).
- Hydrochemical logging.
- Complete hydrogeochemical characterisation of selected packed-off water-yielding sections in KLX03. Pumpings conducted in KLX04 and KLX06 using the PSS equipment in conjunction with injection tests.
- Microbial investigations in KLX01, KLX02, KAV01, KSH01, KSH02 and KAS02, KAS03, KAS04 and KAS06 at Äspö. Investigations of fracture minerals were available from boreholes KLX03, KLX04, KLX05 and KLX05.
- Sampling of the drill core for geological, rock mechanics, thermal properties, geochemical and transport laboratory analyses (all boreholes, although not all data and reports available from KFM05A): the rock mechanics testing comprised porosity and density determinations, indirect tensile strength tests, uniaxial and triaxial compression tests, normal stress tests and shear tests on joints, tilt tests, and determination of the P-wave velocity transverse to the drill cores.

Percussion-drilled boreholes

The borehole investigations performed in the bedrock parts have involved the following percussion-drilled boreholes; HAV05, HAV07–HAV14 and HLX12–HLX29 were:

- BIPS-logging, borehole radar logging, geophysical logging and simplified Boremap-logging using drill cuttings and BIPS images with additional support from geophysical logs.
- HTHB-logging.

Hydraulic interference tests have been performed between HLX10(p), KLX02 and HLX12 and HLX22(p) and HLX21 in the Laxemar subarea, HSH03 (p) and HSH01, HSH04 (p), HSH01 and HSH06 and various tests targeted on interpreted lineaments on Ävrö involving KAV01, KAV03, KAV04A, KSH03A, HAV02, HAV05, HAV07, HAV08, HAV12, HAV13 and HAV14. The subscript (p) implies pumped borehole.

Single-hole tests (air-lift tests or pumping tests) were performed in percussion boreholes HAV09, HAV10, HLX13, HLX14, HLX18, HLX20, HLX22, HLX24 and HLX25.

2.6 Other data sources

Other relevant data sources for the site modelling in the Simpevarp area are “old” data already stored in relevant official SKB databases.

One obvious extensive source of information is that provided by the characterisation data and associated descriptive models available from the Äspö HRL. The position taken by the site descriptive modelling project is to make use of selective information important for filling voids in the data needs of the modelling process. The ambition is by no means to integrate the vast Äspö HRL database in its entirety. Examples of data of interest from Äspö HRL are various generations of geological data, models of deformation zones and various compilations of hydraulic test results that have been used when developing the geological and hydrogeological site-descriptive models. Likewise, compilations of transport properties relevant to Äspö conditions (and the associated data on geology/mineralogy) have been used in developing the bedrock transport models.

Additional old data include surface and borehole information from investigations performed on the islands of Ävrö and Hålö. Old data are also available from the construction of the three nuclear power reactors on the Simpevarp peninsula (and associated tunnels and storage caverns).

A third source of old data is related to the site characterisation and construction of the central storage facility for spent nuclear fuel (Clab I and Clab II).

References to any old data used as input to the descriptive modelling for model version Laxemar 1.2 are summarised in Section 2.7.

2.7 Databases

This section summarises the data that were available at the time of the data freeze for Laxemar 1.2 and distinguishes data used and data not used in the site descriptive modelling. The basis for the presentation is a series of tables developed for each discipline. In each table, the first two columns set out the data available, columns 3 and 4 identify the data that were used, whereas column 5 identifies data not used, and presents arguments in support of their not being used. It is noted that the use of data from individual boreholes by the various disciplines varied depending on the state of down-hole discipline-wise characterisation in the individual boreholes.

Table 2-1. Available bedrock geological and geophysical data and their handling in Laxemar 1.2.

Available primary data Data specification	Ref.	Usage in Laxemar 1.2 Analysis/Modelling	Cf. Section	Not utilised in Laxemar 1.2 Motivation/Comment
Surface-based data				
Bedrock mapping – outcrop data (rock type, ductile and some brittle structures at 353 observation points in the Simpevarp subarea and 1,169 observation points in the Laxemar subarea).	P-04-102	Rock type, ductile deformation in the bedrock, fracture statistics and identification of possible fracture zones at the surface.	5.2.2	
	P-04-221		5.2.4	
	P-05-180		5.3.3	
			7.3.1	
Bedrock map of the Äspö island	PR-25-88-12	Rock domain modelling.	5.2.2	
Marine geological survey	P-05-35	Identification of lineaments/ deformation zones.	5.2.3	
Scan-line mapping of fractures at 16 outcrops in the Simpevarp subarea and 24 outcrops in the Laxemar subarea	P-04-102 P-04-244	Frequency and orientation of fractures.	5.2.4	
Detailed fracture mapping at four sites in the Simpevarp subarea and 2 sites in the Laxemar subarea	P-04-35 P-04-274	Fracture orientation, tracelength and other geological parameters (mineral infilling, alteration etc).	5.2.4	
Modal analyses and geochemical analyses	P-04-102 P-05-180	Mineralogical and geochemical properties of the bedrock. Assessment of thermal properties.	5.2.1	
			5.2.2	
			11.2	
Petrophysical rock parameters and in situ gamma-ray spectrometric data	P-03-97 P-04-294	Physical properties of the bedrock.	5.2.1	
			5.2.2	
			5.2.4	
			11.2	
Airborne geophysical data (magnetic, EM, VLF and gamma-ray spectrometric data)	P-03-25	Identification of lineaments/ deformation zones and lithological boundaries.	5.2.3	
	P-03-63			
	P-03-100			
Detailed topographic data from airborne photography	P-02-02 P-03-99	Identification of lineaments/ deformation zones.	5.2.3	
High resolution reflection seismics	P-03-71	Identification of inhomogeneities in the bedrock that may correspond to boundaries between different types of bedrock or to deformation zones. Supportive information used from previous models (Laxemar, Ävrö and Äspö 96). Rock domain modelling.	5.2.5	
	P-03-72			
	P-04-52			
	P-04-204			
	P-04-215			
	TR-97-06			
	TR-02-04			
	TR-02-19			
	R-01-06			
	R-01-07			
	Geophysics 64, 662-667 Tectono- physics 355, 201–213			
Surface geophysical data (magnetic, EM, refraction seismic and in situ gamma ray spectrometric data)	P-02-05	Identification of lineaments/ deformation zones.	5.2.5	
	P-03-66		5.2.5	
	P-04-128	Rock domain modelling.		
	P-04-134			
	P-04-201			
	P-04-211			
	PR 25-89-13			
PR 25-89-23				

Available primary data Data specification	Ref.	Usage in Laxemar 1.2 Analysis/Modelling	Cf. Section	Not utilised in Laxemar 1.2 Motivation/Comment
Regional gravity data and gravity data from profile measurements in the Laxemar subarea	P-04-128	Rock domain modelling.	5.3.1 5.3.3	
Interpretation of airborne geophysical and topographical data (linked lineament map)	P-03-100 P-03-99 P-04-49	Deterministic structural model.	5.2.3 5.4.4	
Simpevarp site descriptive model v. 0	R-02-35	Rock domain model and deterministic structural model.	5.3.1 5.4.1 5.5.1	
Simpevarp site descriptive model v. 1.2	R-05-08	Bedrock map, Rock domain model and deterministic structural.	5.2.2 5.3	
Laxemar area – testing the methodology for site descriptive modelling	TR-02-19	Deterministic structural model.	5.4.1	
RVS modelling, Ävrö	R-01-06	Deterministic structural model.	5.4.1	
Äspö HRL, geological model	IPR-03-34	Deterministic structural model.	5.4.1	
Cored borehole data				
Geophysical, radar and BIPS logging, interpretation of geophysical data, Boremap data, single-hole interpretation in KSH01A/B	P-03-15 P-03-16 P-03-73 P-04-01 P-04-28 P-04-32 P-04-218 P-04-250	Fracture statistics (including mineralogical analyses), rock type proportion down to borehole depth 1,000 m in DFN (Discrete Fracture Network), rock domain and deformation zone models.	5.2.6 5.2.7 5.3.2 5.3.5 5.4 5.5	
Geophysical, radar and BIPS logging, interpretation of geophysical data, Boremap data, single-hole interpretation in KSH02	P-03-16 P-03-73 P-03-109 P-03-111 P-04-28 P-04-77 P-04-131 P-04-133 P-04-218	Fracture statistics (including mineralogical analyses), rock type proportion down to borehole depth 1,000 m in DFN (Discrete Fracture Network), rock domain and deformation zone models.	5.2.6 5.2.7 5.3.2 5.3.5 5.4 5.5	
Geophysical, radar and BIPS logging, interpretation of geophysical data, Boremap data, single-hole interpretation in KSH03A/B	P-04-132 P-04-214 P-04-231	Fracture statistics (including mineralogical analyses), single hole interpretation, rock type proportion down to borehole depth 1,000 m in DFN (Discrete Fracture Network), rock domain and deformation zone models.	5.2.6 5.2.7 5.3.2 5.3.5 5.4 5.5	
Geophysical, radar and BIPS logging, interpretation of geophysical data, Boremap data, single-hole interpretation in KAV01	P-03-120 P-04-77 P-04-130 P-04-133 P-04-218	Fracture statistics (including mineralogical analyses), rock type proportion down to borehole depth 1,000 m in DFN (Discrete Fracture Network), rock domain and deformation zone models.	5.2.6 5.2.7 5.3.2 5.3.5 5.4 5.5	
Geophysical, radar and BIPS logging, interpretation of geophysical data, Boremap data, single-hole interpretation in KAV04A/B	P-04-217 P-04-308 P-05-22	Fracture statistics (including mineralogical analyses), single hole interpretation, rock type proportion down to borehole depth 1,000 m in DFN (Discrete Fracture Network), rock domain and deformation zone models.	5.2.6 5.2.7 5.3.2 5.3.5 5.4 5.5	
Petrocore data, geophysical loggings and interpretation of geophysical data for KLX01 Note: Petrocore is a predecessor to the Boremap system.	P-05-34	Single hole interpretation, rock type proportion down to borehole depth 1,000 m, rock domain and deformation zone models.	5.2.6 5.2.7 5.3.2 5.3.5 5.4 5.5	
Geophysical, radar and BIPS logging, interpretation of geophysical data, Boremap data, single-hole interpretation in KLX02	P-03-111 P-03-120 P-04-214 P-04-129 P-04-231	Fracture statistics (including mineralogical analyses), single hole interpretation, rock type proportion down to borehole depth 1,000 m in DFN (Discrete Fracture Network), rock domain and deformation zone models.	5.2.6 5.2.7 5.3.2 5.3.5 5.4 5.5	

Available primary data Data specification	Ref.	Usage in Laxemar 1.2 Analysis/Modelling	Cf. Section	Not utilised in Laxemar 1.2 Motivation/Comment
Geophysical, radar and BIPS logging, Boremap data, single-hole interpretation in KLX03	P-05-24 P-05-34	Fracture statistics (including mineralogical analyses), single hole interpretation, rock type proportion down to borehole depth 1,000 m in DFN (Discrete Fracture Network), rock domain and deformation zone models.	5.2.6 5.2.7 5.3.2 5.3.5 5.4 5.5	
Geophysical, radar and BIPS logging, Boremap data, single-hole interpretation in KLX04	P-05-23 P-05-34	Fracture statistics (including mineralogical analyses), single hole interpretation, rock type proportion down to borehole depth 1,000 m in DFN (Discrete Fracture Network), rock domain and deformation zone models.	5.2.6 5.2.7 5.3.2 5.3.5 5.4 5.5	
Simplified mapping, radar and geophysical logging and interpretation of geophysical data of the cored borehole KLX05	P-05-189	Rock domain and deformation zone models.	5.2.7 5.3.2 5.3.5	
Simplified mapping, radar, geophysical logging and interpretation of geophysical data of the cored borehole KLX06	P-05-44	Rock domain and deformation zone models.	5.2.7 5.3.2 5.3.5	
Geophysical, radar and BIPS logging, interpretation of geophysical data, Boremap and single-hole interpretation in HSH01, HSH02 and HSH03	P-03-15 P-04-02 P-04-28 P-04-32 P-04-218	Rock domain and deformation zone models.	5.2.6 5.2.7 5.3.2 5.3.5 5.4 5.5	
Geophysical, radar and BIPS logging, interpretation of geophysical data, Boremap and single-hole interpretation in HAV09 and HAV10	P-04-214 P-04-231	Rock domain and deformation zone models.	5.2.7	
Geophysical logging, interpretation of geophysical data in HLX13	P-04-217	Rock domain and deformation zone models.	5.2.6 5.2.7 5.3.2 5.3.5 5.4 5.5	
Geophysical, radar and BIPS logging, Boremap and single-hole interpretation in HLX15	P-04-217 P-04-308	Rock domain and deformation zone models.	5.2.6 5.2.7 5.3.2 5.3.5 5.4 5.5	
BIPS, radar, geophysical logging and single-hole interpretation HLX21-28	P-05-34	Rock domain and deformation zone models.	5.2.7 5.4	

Table 2-2. Available rock mechanics data and their handling in Laxemar 1.2.

Available data Data specification	Ref	Usage in Laxemar 1.2 Analysis/Modelling	Cf. Section	Not utilised in Laxemar 1.2 Motivation/Comment
Data from core-drilled boreholes				
Uniaxial compressive strength – Intact rock		Characterisation of the intact rock; Empirical determination of the rock mass mechanical properties by means of RMR and Q; Theoretical determination of the rock mass mechanical properties by means of numerical modelling.	6.2.1 6.3.1	
KSH01A	P-04-207			
KSH02A	P-04-209			
KLX02	P-04-255			
KLX04A	P-04-261			
Triaxial compressive strength – Intact rock		Characterisation of the intact rock; Empirical determination of the rock mass mechanical properties by means of RMR and Q; Theoretical determination of the rock mass mechanical properties by means of numerical modelling.	6.2.1 6.3.1	
KSH01A	P-04-208			
KSH02A	P-04-210			
KLX04A	P-04-262			

Available data Data specification	Ref	Usage in Laxemar 1.2 Analysis/Modelling	Cf. Section	Not utilised in Laxemar 1.2 Motivation/Comment
Indirect tensile strength		Characterisation of the intact rock;	6.2.1	
KSH01A	P-04-62	Theoretical determination of the rock	6.3.1	
KSH02A	P-04-63	mass mechanical properties by means of		
KLX02	P-04-256	numerical modelling.		
KLX04A	P-04-263			
Crack initiation stress	Sicada	Evaluation of the elastic limit of	6.2.1	
KSH01A		deformation.	6.3.1	
KSH02A				
KLX02				
KLX04A				
Direct shear tests on rock fractures		Characterisation of the rock fractures – strength and stiffness; Theoretical	6.2.2 6.3.2	
KSH01A	P-05-06	determination of the rock mass		
KSH02A	P-05-07	mechanical properties by means of		
KAV01	P-05-05	numerical modelling.		
KLX02	P-04-257			
KLX04A	P-04-264			
Tilt tests on fractures		Characterisation of the rock fracture	6.2.2	
KSH01A	P-03-107	properties and of the rock mass by RMR	6.3.2	
KSH02A	P-04-10	and Q.		
KAV01	P-04-42			
KLX02	P-04-44			
KLX04A	P-04-265			
Empirical characterisation		Characterisation of the rock mass (RMR,	6.3.4	
KSH01A and B	In prep.	Q) – rock mass mechanical properties.		
KSH02A	In prep.			
KSH03A and B	In prep.			
KAV01	In prep.			
KAV04	In prep.			
KLX01	In prep.			
KLX02	In prep.			
KLX03	In prep.			
KLX04	In prep.			
P-wave velocity measurements		Stress state determination.	6.2.5	
KSH01A	P-03-106			
KSH02A	P-04-11			
KAV01	P-04-43			
KAV04A	P-04-206			
KLX02A	P-04-45			
KLX03	P-05-03			
KLX04A	P-04-266			
Overcoring data from the site investigation program:		Stress state determination.	6.2.5 6.4	
KSH02A	P-04-23			
KAV04	P-04-84			
KLX04	P-05-69			
Hydraulic fracturing data from the site investigation program:		Stress state determination.	6.2.5 6.4	
KSH01A	P-04-310			
Other borehole and tunnel data				
Older overcoring data from the region:		Stress state determination.	6.2.5 6.4	
KF0093A01	R-02-26			
KA3376B01	IPR-03-16			
KAS05	PR-25-89-17			
KOV01	IPR-02-18			
KK0045G01	IPR-01-67			
KA3579G	IPR-01-67			
Older hydraulic fracturing data from the region:		Stress state determination.	6.2.5 6.4	
KOV01	IPR-02-01			
KA2599G01	IPR-02-02			
KF0093A01	IPR-02-02			
KLX02	PR U-97-27			
KAS02, KAS03	PR-25-89-17			

Table 2-3. Available data on thermal properties and their handling in Laxemar 1.2.

Available data Data specification	Ref		Usage in Laxemar 1.2 Analysis/Modelling	Cf. Section	Not utilised in Laxemar 1.2 Motivation/Comment
Data from core-drilled boreholes					
Temperature logging	Results	Interpret.	Temperature and temperature gradient distribution.	7.4.3	
KLX01	Sicada ID 3012572	P-05-34			
KLX02	P-03-111	P-04-214			
KLX03	P-04-280	P-05-34			
KLX04	P-04-306	P-05-34			
KAV04A	P-04-202	P-04-217			
Density logging	Results	Interpret.	Density distribution to indicate the distribution of thermal properties.	7.2.3 7.2.4	Data from KAV04A not used in the modelling, borehole located outside the model area.
KLX01	Sicada ID 12924140	P-05-34			
KLX02	Sicada ID 12947164	P-04-214			
KLX03	P-04-280	P-05-34			
KLX04	P-04-306	P-05-34			
KAV04A	P-04-202	P-04-217			
Boremap logging	KLX01 –		Dominant and subordinate rock type distribution.	7.2.4 7.3	Data from KAV04A not used in the modelling, borehole located outside the model area.
KLX02	P-04-129, P-04-231				
KLX03	P-04-275				
KLX04	P-04-239				
KAV04A	P-04-195, Sicada				
Laboratory test of thermal properties			Thermal conductivity and specific heat capacity.	7.2.1 7.2.4 7.2.6	
KLX02	P-04-258				
KLX04	P-04-267				
KAV01	P-04-55				
KAV04A	P-04-270				
KSH01A	P-04-53				
KSH02	P-04-54				
KA2599G01	R-02-27, /Sundberg et al. 2005a/ IPR-99-17				
Äspö prototype repository tunnel					
Modal analysis			Estimation of thermal conductivity.	7.2.2 7.2.4	
KLX01	–				
KLX02	P-04-258				
KLX03	–				
KLX04	P-04-267				
KAV01	P-04-55				
KAV04A	P-04-270				
KSH01A	P-04-56				
KSH02	P-04-54				
Laboratory test of thermal expansion			Thermal expansion coefficient.	7.2.7	
KLX02	–				
KLX04	P-04-269				
KAV01	P-04-61				
KAV04A	P-04-272				
KSH01A	P-04-59				
KSH02	P-04-60				
Surface-based data					
Modal analyses			Estimation of thermal conductivity.	7.2.2 7.2.4	
Surface samples	P-04-102, Sicada field note no. 538				

Table 2-4. Available data on hydrogeological properties and their handling in Laxemar 1.2.

Available primary data Data specification	Ref.	Usage in Laxemar 1.2 Analysis/Modelling	Cf. Section	Not utilised in Laxemar 1.2 Motivation/Comment
Geometrical and topographical data				
Digital elevation Model (DEM)	P-04-03 Sicada	Basic input to flow and models.	8.5	
Geological data				
Map and model of Quaternary deposits in the terrestrial part and sea bottom of the Simpevarp regional model area	R-05-54, R-05-61, R-06-11	Description of surface distribution of Quaternary deposits in the Simpevarp regional model area and the hydraulic properties of the deposits.	8.3, 8.4	
Rock types	Sicada	Interpreting borehole data for assignment of hydraulic properties to rock types.	8.4	
Bedrock model, geometry	R-06-69, Chapter 5, SIMONE	Interpreting borehole data for assignment of hydraulic properties to deformation zones and rock domains.	8.4	
Cored borehole data				
Wireline tests, drilling information	TR-94-02, TR-01-11, P-03-113, P-04-151, P-04-233, P-05-25, P-05-111, P-05-167	Borehole data and (prel) transmissivity distribution in large scale.	8.2	
Difference flow logging	IPR-01-06, R-01-52, P-03-70, P-03-110, P-04-213, P-04-216, P-05-67, P-05-68,	Conductive parts of the borehole, Statistics of conductive fractures.	8.2	
Hydraulic injection tests, pumping tests (single hole)	TR-94-02, TR-01-11, P-04-247, P-04-288, P-04-289, P-04-290, P-04-291, P-04-292, P-05-16, P-05-184,	Transmissivity distribution along the borehole in different scales.	8.2	
Percussion hole data				
Drilling, and hydraulic tests	P-03-56, P-03-114, P-04-150, P-04-234, P-04-235, P-04-236, P-04-287, P-05-55, P-05-190,	Hydraulic test data for the bedrock.	8.2	Data in P-04-287 were not possible to include in the analysis as the corresponding data were not available in Sicada at the time of the data freeze for Laxemar 1.2.
Interference tests				
Interference tests using percussion and core holes	P-03-56, P-04-287, P-05-20	Infer connectivity between deformation zones and estimate transmissivity and (if possible) storage coefficient for deformation zones.	8.2	

Available primary data Data specification	Ref.	Usage in Laxemar 1.2 Analysis/Modelling	Cf. Section	Not utilised in Laxemar 1.2 Motivation/Comment
Other borehole, construction, tunnel data and models				
Hydraulic tests in areas Äspö, Ävrö, Håltö, Simpevarp, Mjälén and Laxemar areas	TR-97-03, TR-97-05, TR-97-06, TR-02-19, R-98-55, IPR-01-44, IPR-00-28, IPR-03-13, IPR-01-65, P-05-65, P-05-241, Sicada database	Previous made evaluations compared to new data and for assessment of properties not known or with few data from SI.	8.2, 8.4	Not used in detail.
Other hydraulic data	R-04-09, TR-98-05	Previous made evaluations compared to new data and for assessment of properties not known or with few data from SI.	8.4	

Table 2-5. Available hydrogeochemical data and their handling in Laxemar 1.2. For further details see Appendix 9 in SKB R-06-12.

Available data Data specification	Ref	Usage in Laxemar 1.2 Analysis/Modelling	Cf. Section	Not utilised in F1.2 Motivation/Comment
Surface based data				
Precipitation, running water, soil pipes, Sea water samples	R-06-12 P-04-317 P-04-75 P-04-13	Manual evaluation and mathematical modelling such as PHREEQC, M3 and coupled transport modelling. The results of the modelling is presented in the conceptual model of the site. The use of the data in the specific modelling approaches are described in SKB R-06-12.	9 and 11.6	Non representative samples were not used in the detailed modelling (see motivation in SKB R-06-12).
Cored borehole data				
KSH01, KSH02, KSH03, KAV01, KAV04, KLX01, KLX02, KLX03, KLX04, KLX06	P-04-12 P-05-89 P-05-88 P-05-05 R-06-12 P-05-54 P-04-304 P-04-299 P-03-89 P-04-281 P-04-220 P-04-219 P-04-51 P-04-12 P-03-89 P-03-88 P-03-87			
Percussion hole data	R-06-12 P-03-113 R-04-12			
HSH02/03/04/05 HAV04/05/06/07 HAV09/10/11/12/13/14 HLX01/02/03/04/05/06/07/08/10/ HLX14/18/20/22/24				
Other available data				
Äspö and other Nordic Sites	R-06-12			

Table 2-6. Available bedrock transport data and their handling in Laxemar 1.2.

Available data Data specification	Ref	Usage in Laxemar 1.2 Analysis/Modelling	Cf. Section	Not utilised in Laxemar 1.2 Motivation/Comment
Data from core-drilled boreholes				
Resistivity measurements and determination of formation factors on samples from KLX04 and KSH02	P-05-75	Assignment of porosity and diffusion parameters.	10.5.2 10.5.3	
Formation factor logging in situ by electrical methods in KLX03 and KLX04	P-05-105			
Laboratory data from the site investigation programme for the transport properties of the rock	P-05-106 Sicada			
Tracer dilution and SWIW tests in KSH02 and KLX02	P-05-28	(P-05-106) contains only representative diffusivity measurement at steady state for Ävrö granite in the Laxemar subarea (KLX02). (P-05-28) Field-scale demonstration of tracer transport and retention.	10.5.6	
Combined interference tests and tracer test between KLX02 and HLX10	P-05-20			
Input from other disciplines				
Geological data and description: – lithology and mineralogy of identified rock types (LM)	SDM chapter P-04-221	Identification of site-specific rock types, fractures and fracture zones, as well as properties of site-specific geological materials. Used as a basis for retardation model and descriptive transport model.	10.6 10.7	
– boremap mapping KLX02 KLX03 KLX04	P-04-129 P-05-24 P-05-23			
– fracture mineralogy	P-05-174 P-04-250 P-05-241			
Hydrogeological data and description PFL data from KLX02 PFL data from KLX03 PFL data from KLX04 PFL data from KAV04A and KAV04B PSS data from KLX02 PSS data from KLX04	SDM Chapter 8 R-01-52 IPR-01-06 P-05-67 P-05-68 P-04-216 P-04-288 P-04-292	– Identification of conductive fractures and correlations between fracture types and hydraulic properties. – Assignment of specific flow-wetted surface for modelling of site specific transport resistance (F-factor). – Hydraulic properties used for the estimation of site specific transport resistance (F-factor).	10.5.5 10.7 10.8	
Hydrogeochemical data and description	SDM Chapter 9 Sicada R-06-12	Identification of site-specific water types and water-rock interactions.	10.4 10.5.4	
Other borehole and tunnel data				
Data and models from the TRUE project and Äspö Task Force (Task 6C)	TR-98-18 ICR-01-04 IPR-03-13	Conceptual modelling. Assignment of sorption and diffusion parameters.	10.3.1 10.5.4 10.6 10.7	Some old data not used due to differences in methods and insufficient sample characterisation.

Table 2-7. Available abiotic data from the surface system and their handling in Laxemar 1.2.

Available site data Data specification	Ref.	Usage in Laxemar 1.2 Analysis/Modelling	Cf. Section	Not utilised in Laxemar 1.2 Arguments/Comments
Geometrical and topographical data				
Digital Elevation Model (DEM)	P-04-03 Sicada	Basic input to flow and mass transport models.	4.3, 4.4, 4.6, 4.8	
Geological data				
Map of Quaternary deposits in the terrestrial part of the Simpevarp regional model area	P-04-22 P-05-49	Description of surface distribution of Quaternary deposits in the terrestrial part of the Simpevarp regional model area.	4.3	
Maps of Quaternary deposits covering a large part of the sea bottom in the regional model area	P-04-254 P-05-35	Description of surface distribution of Quaternary deposits at the sea floor.	4.3	
Map of soils in the terrestrial part of the Simpevarp regional model area	P-04-243 GIS database	Distribution of soil types in the Simpevarp regional model area.	4.3	
Stratigraphy and total depth of Quaternary deposits from the sea and lake floors	R-02-47 P-04-254 P-04-273 P-05-35	Description of stratigraphical distribution and total depth of Quaternary deposits at the sea and lake floors.	4.3	
Drilling and sampling of Quaternary deposits	P-03-80 P-04-22 P-04-121 P-04-317 P-05-49	Description of stratigraphical distribution and total depth of overburden in the terrestrial parts of the Simpevarp and Laxemar subareas.	4.3	
Helicopter borne survey data	P-03-100	Description of surface distribution of Quaternary deposits in parts of the Simpevarp regional model area.	4.3	The new map /Rudmark et al. 2005/ gives more accurate information.
Electric soundings	P-03-17	Total depth of Quaternary deposits in the Laxemar and Simpevarp subareas.	4.3	
Refraction seismic	P-04-134 P-04-201 P-04-298	Total depth of Quaternary deposits in the Laxemar and Simpevarp subareas.	4.3	
Analytical data, including grain size, organic carbon, nitrogen, sulphur, soil pH and calcium carbonate.	P-04-243 P-04-273 P-05-49 R-02-47 Sicada	Chemical and physical properties of Quaternary deposits.	4.3	
Meteorological data				
“Regional” meteorological data prior to the site investigations.	TR-02-03 R-99-70	Description of “regional” meteorological conditions.	4.4	
Meteorological data from Äspö (Sep. 2003–Jun. 2005) and Plittorp (Jul. 2004–Jun. 2005).	P-05-227	Comparison with “regional” meteorological data. Input to quantitative water flow modelling (MIKE SHE).	4.4	
Hydrological data				
“Regional” discharge data prior to the site investigations.	TR-02-03 R-99-70	Description of “regional” hydrological conditions (e.g. average regional specific discharge).	4.4	
Investigation of potential locations for hydrological stations.	P-03-04	Size of catchment areas for manual and automatic discharge measurements.	4.4	
Geometric data on catchment areas, lakes and water courses	P-04-242	Delineation and characteristics of catchment areas, lakes, and water courses. Input to quantitative water flow modelling (MIKE SHE-MIKE 11).	4.4	

Available site data Data specification	Ref.	Usage in Laxemar 1.2 Analysis/Modelling	Cf. Section	Not utilised in Laxemar 1.2 Arguments/Comments
Manual discharge measurements in water courses.	P-04-13 P-04-75 P-04-246	Description of spatial and temporal variability of discharge.	4.4	
Surface-water levels in lakes and the sea	P-05-227	Description of spatial and temporal variability of surface-water levels.		
Surveying of water courses in catchment areas 6–9.	P-06-05	Input to quantitative water flow modelling (MIKE 11).		
Characterisation of running waters, including vegetation, substrate and technical encroachments.	P-05-40	Identification of “missing” (parts of) water courses. Interpretation of discrepancies between actual and model-calculated “flooded” areas.		“Missing” water courses and near-surface ditching/drainage operations will be included in future model versions.
Discrepancies between actual water courses and water courses in the SKB GIS database.	P-05-70	Identification of “missing” (parts of) water courses. Interpretation of discrepancies between actual and model-calculated “flooded” areas.		“Missing” water courses and near-surface ditching/drainage operations will be included in future model versions.
Hydrogeological data				
Inventory of private wells	P-03-05	General description of available hydrogeological information.	4.4	
Manually measured groundwater levels in QD.	P-05-205 Sicada	Description of spatial and temporal variability of groundwater levels in QD.	4.4	
Automatically measured groundwater levels in QD.	P-05-205	Description of spatial and temporal variability of groundwater levels in QD.		
Geological data from drilling in QD and installation of groundwater monitoring wells.	P-03-80 P-04-46 P-04-121 P-04-317	Conceptual-descriptive model of HSD geometry.		
Hydraulic conductivity from slug tests in groundwater monitoring wells in QD.	P-04-122 P-04-318	Conceptual-descriptive modelling of hydraulic conductivity in QD.	4.4	
Hydrogeological inventory in the Oskarshamn area.	P-04-277	General description of ditching-, draining- and other water related activities in the Simpevarp area.	4.4	
Oceanographic data				
Regional oceanographic data	TR-02-03 R-99-70	Quantitative modelling.	4.4	
Chemistry data				
Surface water sampling	P-04-13 P-04-75	Characterisation and description of spatial and temporal variability of surface water chemistry.	4.5	
Shallow groundwater	P-03-80 P-04-46 P-04-121 P-04-317	Characterisation of the chemistry in shallow groundwater.	4.5	
Overburden	P-03-80 P-04-46 P-04-121 P-04-243 P-04-273 P-04-317	Characterisation of the chemistry in the regolith.	4.5	

Table 2-8. Available biotic data from the surface system and their handling in Laxemar 1.2.

Available site data Data specification	Ref.	Usage in Laxemar 1.2 Analysis/Modelling	Cf. Section	Not utilised in Laxemar 1.2 Arguments/Comments
Terrestrial biota				
Compilation of existing information 2002	R-02-10	Description.	4.6 4.8	
Bird population survey	P-04-21 P-05-42	Description.	4.6 4.8	
Mammal population survey	P-04-04 R-05-36	Description, modelling.	4.6 4.8	
Amphibians and reptiles	P-04-36, /Andrén 2004/	Description, modelling.	4.6 4.8	
Soil fauna	/Lohm and Persson 1979/	Generic description.	4.6 4.8	
Vegetation inventory	P-04-20	Description.	4.6 4.8	
Vegetation mapping	P-03-83	Description, modelling.	4.6 4.8	
Biomass and Net Primary Productivity (NPP) of the vegetation	NFI	Modelling, tree layer.	4.6 4.8	
Biomass and NPP of the vegetation	P-04-315	Modelling, shrub layer.	4.6 4.8	
Biomass and NPP of the vegetation	P-05-80	Modelling, field layer and ground layer.	4.6 4.8	
Biomass and NPP of the vegetation	/Vogt et al. 1982/	Modelling, fungi.	4.6 4.8	
Biomass of the vegetation	P-04-20, /Berggren et al. 2004/ P-03-90	Modelling, dead organic material.	4.6 4.8	
Data from soil mapping	P-04-243	Description, modelling.	4.6 4.8	
Ecosystem modelling	P-06-x, manuscript	COUP.	4.6 4.8	
Limnic biota				
Limnic producers	P-04-242 P-04-253 P-05-40 P-05-173	Description, modelling.	4.6 4.8	
Habitat borders	P-04-242	Description.	4.6 4.8	
Limnic consumers	P-04-253 P-04-251 P-04-252	Description, modelling.	4.6 4.8	
Marine biota				
Compilation of existing information 2002	R-02-10	Description.	4.6 4.8	
Barythymetical measurements	P-04-254	Description, modelling.	4.6 4.8	
Light penetration depth	P-04-13 and field measure- ments (Sicada)	Description.	4.6 4.8	
Zooplankton, phytoplankton	P-04-253	Description, modelling.	4.6 4.8	
Identification of dominating species	P-03-68	Description.	4.6 4.8	No quantitative data
Macrophyte communities	P-03-69	Description, modelling.	4.6 4.8	

Available site data Data specification	Ref.	Usage in Laxemar 1.2 Analysis/Modelling	Cf. Section	Not utilised in Laxemar 1.2 Arguments/Comments
Soft bottom infauna	P-04-17	Description, modelling.	4.6 4.8	
Hard bottom infauna	(in press)	Description, modelling.	4.6 4.8	
Reed	P-04-316	Description, modelling.	4.6 4.8	
Fish sampling	P-04-19	Description, modelling.	4.6 4.8	Investigation used to sample fish for future chemical analyses
Fish population estimates	In Press	Description, modelling.	4.6 4.8	
Bird population survey	P-04-21	Description.	4.6 4.8	
Humans and land use				
Humans and land use	R-04-11	Description, modelling.	4.7	

Table 2-9. Reports in the SKB P, IPR, ICR, R, and TR-series referenced in Tables 2-1 through 2-8.

P-02-02	Wiklund S. Digitala ortofoton och höjdm modeller. Redovisning av metodik för platsundersökningsområdena Oskarshamn och Forsmark samt förstudieområdet Tierp Norra (in Swedish).
P-03-04	Lärke A, Hillgren R. Rekognoscering av mätplatser för ythydrologiska mätningar i Simpevarpsområdet (in Swedish).
P-03-05	Morosini M, Hultgren H. Inventering av privata brunnar i Simpevarpsområdet, 2001–2002. (in Swedish).
P-03-07	Curtis P, Elfström M, Stanfors R. Oskarshamn site investigation Compilation of structural geological data covering the Simpevarp peninsula, Ävrö and Hälö.
P-03-15	Nilsson P, Gustafsson C. Simpevarp site investigation. Geophysical, radar and BIPS logging in borehole KSH01A, HSH01, HSH02 and HSH03.
P-03-16	Nielsen U T, Ringgaard J. Simpevarp site investigation. Geophysical borehole logging in borehole KSH01A, KSH01B and part of KSH02.
P-03-17	Thunehed H, Pitkänen T. Simpevarp site investigation. Electrical soundings supporting inversion of helicopterborne EM-data. Primary data and interpretation report.
P-03-25	Rønning H J, Kihle O, Mogaard J O, Walker P. Simpevarp site investigation. Helicopter borne geophysics at Simpevarp, Oskarshamn, Sweden.
P-03-31	Green M. Platsundersökning Simpevarp. Fågelundersökningar inom SKB:s platsundersökningar 2002 (in Swedish).
P-03-56	Ludvigson J-E, Levén J, Jönsson S. Oskarshamn site investigation. Hydraulic tests and flow logging in borehole HSH03.
P-03-63	Byström S, Hagthorpe P, Thunehed H. Oskarshamn site investigation. QC-report concerning helicopter borne geophysics at Simpevarp, Oskarshamn, Sweden.
P-03-66	Triumf C-A. Oskarshamn site investigation. Geophysical measurements for the siting of a deep borehole at Ävrö and for investigations west of Clab.
P-03-67	Borgiel M. Makroskopiska organismers förekomst i sedimentprov. En översiktlig artbestämning av makroskopiska organismer (in Swedish).
P-03-68	Tobiasson S. Tolkning av undervattensfilm från Forsmark och Simpevarp (in Swedish).
P-03-69	Fredriksson R, Tobiasson S. Simpevarp site investigation. Inventory of macrophyte communities at Simpevarp nuclear power plant. Area of distribution and biomass determination.
P-03-70	Rouhiainen P, Pöllänen J. Oskarshamn site investigation. Difference flow measurements in borehole KSH01A at Simpevarp.
P-03-71	Vangkilde-Pedersen T. Oskarshamn site investigation. Reflection seismic surveys on Simpevarpshalvön 2003 using the vibroseismic method.
P-03-72	Juhlin C. Oskarshamn site investigation. Evaluation of RAMBØLL reflection seismic surveys on Simpevarpshalvön 2003 using the vibroseismic.
P-03-73	Aaltonen J, Gustafsson C, Nilsson P. Oskarshamn site investigation. RAMAC and BIPS logging and deviation measurements in boreholes KSH01A, KSH01B and the upper part o KSH02.

- P-03-74 **Barton N.** Oskarshamn site investigation. Q-logging of KSH 01A and 01B core.
- P-03-80 **Ask H.** Installation of four monitoring wells, SSM000001, SSM000002, SSM000004 and SSM000005 in the Simpevarp subarea.
- P-03-83 **Boresjö Bronge L, Wester K.** Vegetation mapping with satellite data of the Forsmark, Tierp and Oskarshamn regions.
- P-03-87 **Wacker P.** Oskarshamn site investigation. Hydrochemical logging in KSH01A.
- P-03-88 **Berg C.** Hydrochemical logging in KSH02. Oskarshamn site investigation.
- P-03-90 **Fridriksson Georg, Öhr J.** Assessment of plant biomass of the ground, field and shrub layers of the Forsmark area.
- P-03-93 **Lindqvist L, Thunehed H.** Oskarshamn site investigation. Calculation of Fracture Zone Index (FZI) for KSH01A.
- P-03-97 **Mattsson H, Thunehed H, Triumf, C-A.** Oskarshamn site investigation. Compilation of petrophysical data from rock samples and in situ gamma-ray spectrometry measurements.
- P-03-99 **Triumf, C-A.** Oskarshamn site investigation. Identification of lineaments in the Simpevarp area by the interpretation of topographical data.
- P-03-100 **Triumf C-A, Thunehed H, Kero L, Persson L.** Interpretation of airborne geophysical survey data. Helicopter borne survey data of gamma ray spectrometry, magnetics and EM from 2002 and fixed wing airborne survey data of the VLF-field from 1986. Oskarshamn site investigation.
- P-03-106 **Chryssanthakis P, Tunbridge L.** Borehole: KSH01A. Determination of P-wave velocity, transverse borehole core. Oskarshamn site investigation.
- P-03-107 **Chryssanthakis P.** Borehole: KSH01A. Results of tilt testing. Oskarshamn site investigation.
- P-03-109 **Aaltonen J, Gustafsson C.** RAMAC and BIPS logging in borehole KSH02.
- P-03-110 **Rouhiainen P, Pöllänen J.** Oskarshamn site investigation – Difference flow measurements in borehole KSH02 at Simpevarp.
- P-03-111 **Nielsen T, Ringgaard J, Horn F.** Geophysical borehole logging in boreholes KSH02 and KLX02.
- P-03-113 **Ask H, Morosini M, Samuelsson L-E, Stridsman H, 2003.** Oskarshamn site investigation – Drilling of cored borehole KSH01. SKB P-03-113. Svensk Kärnbränslehantering AB.
- P-03-114 **Ask H, Samuelsson L-E, 2003.** Oskarshamn site investigation – Drilling of three flushing water wells, HSH01, HSH02 and HSH03. SKB P-03-113. Svensk Kärnbränslehantering AB.
- P-03-120 **Aaltonen J, Gustafsson C.** RAMAC logging in boreholes KAV01 and KLX02.
- P-04-01 **Ehrenborg J, Stejskal V, 2004.** Oskarshamn site investigation. Boremap mapping of core drilled boreholes KSH01A and KSH01B.
- P-04-02 **Nordman C, 2004.** Oskarshamn site investigation. Boremap mapping of percussion boreholes HSH01–03.
- P-04-03 **Brydsten L.** A method for construction of digital elevation models for site investigation program at Forsmark and Simpevarp.
- P-04-04 **Cederlund G, Hammarström A, Wallin K.** Surveys of mammal populations in the areas adjacent to Forsmark and Oskarshamn. Results from 2003.
- P-04-10 **Chryssanthakis P.** Oskarshamn Site Investigation – Borehole KSH02, Results of tilt testing,
- P-04-11 **Chryssanthakis P, Tunbridge L.** Borehole: KSH02A Determination of P-wave velocity, transverse borehole core. Oskarshamn site investigation.
- P-04-12 **Wacker P, Berg C, Bergelin A.** Complete hydrochemical characterisation in KSH01A. Results from four investigated sections, 156.5–167.0, 245.0–261.6, 586.0–596.7 and 548.0–565.4 m.
- P-04-13 **Ericsson U. and Engdahl A.** Surface water sampling at Simpevarp 2002–2003. Oskarshamn site investigation.
- P-04-14 **Ericsson U.** Sampling of precipitation at Äspö 2002–2003.
- P-04-17 **Fredriksson, R.** Inventory of the soft-bottom macrozoobenthos community in the area around Simpevarp nuclear power plant. Oskarshamn site investigation.
- P-04-19 **Engdahl A, Ericsson U.** Fish sampling in connection with geophysical measurements at Simpevarp 2003.
- P-04-20 **Andersson J.** Vegetation inventory in part of the municipality of Oskarshamn.
- P-04-21 **Green M, 2004.** Bird surveys in Simpevarp 2003. Oskarshamn site investigation.
- P-04-22 **Rudmark L.** Investigation of Quaternary deposits at Simpevarp peninsula and the islands of Ävrö and Hälö. Oskarshamn site investigation.
- P-04-23 **Sjöberg J.** Overcoring rock stress measurements in borehole KSH02. Oskarshamn Site Investigation.
- P-04-28, **Mattsson H, Thunehed H.** Interpretation of geophysical borehole data from KSH01A, KSH01B, KSH02 (0–100 m), HSH01, HSH02 and HSH03 and compilation of petrophysical data from KSH01A and KSH01B.

- P-04-32 **Mattsson H, Stanfors R, Wahlgren C-H, Stenberg L, Hultgren P.** Geological single-hole interpretation of KSH01A, KSH01B, HSH01, HSH02 and HSH03. Oskarshamn site investigation.
- P-04-35 **Hermanson J, Hansen L, Wikholm M, Cronquist T, Leiner P, Vestgård J, Sandah K-A.** Detailed fracture mapping of four outcrops at the Simpevarp peninsula and Ävrö. Oskarshamn site investigation.
- P-04-36 **Andrén Claes.** Oskarshamn site investigation, Amphibians and reptiles in SKB special area of investigation at Simpevarp.
- P-04-37 **Triumf C-A.** Joint interpretation of lineaments in the eastern part of the site descriptive model area. Oskarshamn site investigation.
- P-04-42 **Chryssanthakis P.** Oskarshamn Site Investigation – Borehole KAV01, Results of tilt testing.
- P-04-43 **Chryssanthakis P, Tunbridge L.** Borehole: KAV01 Determination of P-wave velocity, transverse borehole core. Oskarshamn site investigation.
- P-04-44 **Chryssanthakis P.** Oskarshamn Site Investigation – Borehole KLX02, Results of tilt testing.
- P-04-45 **Chryssanthakis P, Tunbridge L.** Borehole: KLX02 Determination of P-wave velocity, transverse borehole core. Oskarshamn site investigation.
- P-04-46 **Ask H.** Drilling and installation of two monitoring wells, SSM 000006 and SSM 000007 in the Simpevarp subarea.
- P-04-49 **Triumf C-A.** Oskarshamn site investigation. Joint interpretation of lineaments.
- P-04-50 **Nielsen T, Ringgaard J, 2004.** Geophysical borehole logging in borehole KSH03A, KSH03B, HAV09 and HAV10.
- P-04-51 **Berg C.** Hydrochemical logging in KSH03A.
- P-04-53 **Adl-Zarrabi B.** Drill hole KSH01A Thermal properties: heat conductivity and heat capacity determined using the TPS method and mineralogical composition by modal analysis.
- P-04-54 **Adl-Zarrabi B.** Drill hole KSH02 Thermal properties: heat conductivity and heat capacity determined using the TPS method and mineralogical composition by modal analysis, Svensk Kärnbränslehantering AB.
- P-04-55 **Adl-Zarrabi B.** Drill hole KAV01 Thermal properties: heat conductivity and heat capacity determined using the TPS method and mineralogical composition by modal analysis.
- P-04-56 **Savukoski M, Carlsson L.** Drill hole KSH01A. Determining of porosity by water saturation and density by buoyancy technique.
- P-04-59 **Åkesson U.** Drill hole: KSH01A. Extensometer measurement of the coefficient of thermal expansion of rock.
- P-04-60 **Åkesson U.** Drill hole: KSH02. Extensometer measurement of the coefficient of thermal expansion of rock.
- P-04-62. **Jacobsson L.** Oskarshamn Site Investigation – Drill hole KSH01A, Indirect tensile strength tests.
- P-04-63 **Jacobsson L.** Oskarshamn Site Investigation – Drill hole KSH02, Indirect tensile strength tests.
- P-04-75 **Ericsson U, Engdahl A.** Surface water sampling in Oskarshamn – Subreport October 2003 to February 2004.
- P-04-77 **Mattsson H, Thunehed H.** Oskarshamn site investigation. Interpretation of geophysical borehole data and compilation of petrophysical data from KSH02 (80–1,000 m) and KAV01.
- P-04-84 **Sjöberg J.** Overcoring rock stress measurements in borehole KAV04. Oskarshamn Site Investigation.
- P-04-102 **Wahlgren C-H, Ahl M, Sandahl K-A, Berglund J, Petersson J, Ekström M, Persson P-O.** Oskarshamn site investigation. Bedrock mapping 2003 – Simpevarp subarea. Outcrop data, fracture data, modal and geochemical classification of rock types, bedrock map, radiometric dating.
- P-04-110 **Rouhiainen P, Pöllänen J.** Oskarshamn site investigation. Difference flow measurements in borehole KSH02 at Simpevarp.
- P-04-121 **Johansson T, Adestam L.** Drilling and sampling in soil. Installation of groundwater monitoring wells.
- P-04-122 **Johansson T, Adestam L.** Slug tests in groundwater monitoring wells in soil in the Simpevarp area.
- P-04-128 **Triumf C-A.** Gravity measurements in the Laxemar model area with surroundings.
- P-04-129 **Ehrenborg J, Stejskal V.** Oskarshamn site investigation. Boremap mapping of core drilled borehole KLX02.
- P-04-130 **Ehrenborg J, Stejskal V.** Oskarshamn site investigation. Boremap mapping of core drilled borehole KAV01.
- P-04-131 **Ehrenborg J, Stejskal V.** Oskarshamn site investigation. Boremap mapping of core drilled borehole KSH02.
- P-04-132 **Ehrenborg J, Stejskal V.** Oskarshamn site investigation. Boremap mapping of core drilled boreholes KSH03A and KSH03B.
- P-04-133 **Mattsson H, Stanfors R, Wahlgren C-H, Carlsten S, Hultgren P.** Oskarshamn site investigation. Geological single-hole interpretation of KSH02 and KAV01.

- P-04-134 **Lindqvist G.** Refraction seismic measurements in Laxemar. Oskarshamn site investigation.
- P-04-150 **Ask H, Samuelsson L-E.** Drilling of two flushing water wells, HAV09 and HAV10.
- P-04-151 **Ask H, Morosini M, Samuelsson L-E, Stridsman H.** Oskarshamn site investigation – Drilling of cored borehole KSH02.
- P-04-185 **Chryssanthakis P.** Simpevarp Site Investigation – Drill hole: KSH01A, The normal stress and shear tests on joints.
- P-04-195 **Gustafsson J, Gustafsson C.** RAMAC and BIPS logging in boreholes KAV04A, KAV04B, HLX13 and HLX15.
- P-04-201 **Lindqvist G.** Refraction seismic measurements in the water outside Simpevarp and Ävrö and on land on Ävrö. Oskarshamn site investigation.
- P-04-202 **Nielsen U T, Ringgaard J.** Geophysical borehole logging in borehole KAV04A, KAV04B, HLX13 and HLX15.
- P-04-204 **Schmelzbach C, Juhlin C.** 3D processing of reflection seismic data acquired within and near the array close to KAV04A on Ävrö, 2003.
- P-04-206 **Chryssanthakis P, Tunbridge L.** Borehole: KAV04A. Determination of P-wave velocity, transverse borehole core.
- P-04-207 **Jacobsson L.** Oskarshamn Site Investigation – Drill hole KSH01A, Uniaxial compression test of intact rock.
- P-04-208 **Jacobsson L.** Oskarshamn Site Investigation – Drill hole KSH01A, Triaxial compression test of intact rock.
- P-04-209 **Jacobsson L.** Oskarshamn Site Investigation – Drill hole KSH02, Uniaxial compression test of intact rock.
- P-04-210 **Jacobsson L.** Oskarshamn Site Investigation – Drill hole KSH02, Triaxial compression test of intact rock.
- P-04-211 **Thunehed H, Triumf C-A, Pitkänen T.** Geophysical profile measurements over interpreted lineaments in the Laxemar area.
- P-04-212 **Svensson T.** Oskarshamn site investigation, Pumping tests and flow logging in boreholes KSH03 and HSH02.
- P-04-213 **Rouhiainen P, Pöllänen J.** Oskarshamn site investigation – Difference flow measurements in borehole KAV01 at Ävrö.
- P-04-214 **Mattsson H.** Interpretation of geophysical borehole data and compilation of petrophysical data from KSH03A (100–1,000 m), KSH03B, HAV09, HAV10 and KLX02 (200–1,000 m).
- P-04-215 **Juhlin C, Bergman B, Palm H.** Reflection seismic studies performed in the Laxemar area during 2004.
- P-04-216 **Pöllänen J, Sokolnicki M.** Difference flow measurements in borehole KAV04A and KAV04B.
- P-04-217 **Mattsson H.** Interpretation of geophysical borehole data and compilation of petrophysical data from KAV04A (100–1,000 m), KAV04B, HLX13 and HLX15.
- P-04-218 **Carlsten S.** Oskarshamn site investigation. Geological interpretation of borehole radar reflectors in KSH01, HSH01–03, KAV01 and KSH02.
- P-04-219 **Berg C.** Hydrochemical logging in KLX04A.
- P-04-220 **Berg C.** Hydrochemical logging in KAV04A.
- P-04-221 **Nilsson, Katarina P, Bergman T, Eliasson T.** Bedrock mapping 2004 – Laxemar subarea and regional model area. Outcrop data and description of rock types.
- P-04-231 **Hultgren P, Stanfors R, Wahlgren C-H, Carlsten S, Mattsson H.** Geological single-hole interpretation of KSH03A, KSH03B, KLX02, HAV09 and HAV10.
- P-04-232 **Nielsen T, Ringgaard J, Horn F.** Geophysical borehole logging in borehole KAV01.
- P-04-233 **Ask H, Morosini M, Samuelsson L-E, Ekström L, Håkansson N.** Drilling of cored borehole KSH03.
- P-04-234 **Ask H, Samuelsson L-E.** Drilling of two percussion boreholes, HLX13 and HLX14.
- P-04-235 **Ask H, Samuelsson L-E, Zetterlund M.** Percussion drilling of boreholes HLX15, HLX26, HLX27, HLX28, HLX29 and HLX32 for investigation of lineament NW042.
- P-04-236 **Ask H, Samuelsson L-E.** Percussion drilling of borehole HLX20 for investigation of lineament EW002.
- P-04-239 **Gustafsson J, Gustafsson C.** RAMAC and BIPS logging in borehole KLX04.
- P-04-242 **Brunberg A-K, Carlsson T, Brydsten L, Strömgren M.** Identification of catchments, lake-related drainage parameters and lake habitats. Oskarshamn site investigation.
- P-04-243 **Lundin L, Björkvald L, Hansson J, Stendahl J.** Surveillance of soils and site types in the Oskarshamn area.
- P-04-244 **Berglund J.** Scan line fracture mapping. Subarea Laxemar and passage for tunnel.

- P-04-246 **Morosini M, Lindell L.** Compilation of measurements from manually gauged hydrological stations, October 2002–March 2004. Oskarshamn site investigation.
- P-04-247 **Rahm N, Enachescu C.** Hydraulic injection tests in borehole KSH01A, 2003/2004, Simpevarp.
- P-04-250 **Drake H, Tullborg E-L.** Oskarshamn site investigation. Fracture mineralogy and wall rock alteration. Results from drill core KSH01A+B.
- P-04-251 **Engdahl A, Ericsson U.** Sampling of freshwater fish. Description of the fish fauna in four lakes.
- P-04-252 **Ericsson U, Engdahl A.** Benthic macro invertebrates. Results from sampling in the Simpevarp area 2004.
- P-04-253 **Sundberg I, Svensson J-E, Ericsson U, Engdahl A.** Phytoplankton and zooplankton. Results from sampling in the Simpevarp area 2003–2004. Oskarshamn site investigation.
- P-04-254 **Ingvarson N, Palmeby A, Svensson O, Nilsson O, Ekfeldt T.** Oskarshamn site investigation, Marine survey in shallow coastal waters Bathymetric and geophysical investigation 2004.
- P-04-255 **Jacobsson L.** Borehole KLX02. Uniaxial compression test of intact rock.
- P-04-256 **Jacobsson L.** Drill hole KLX02. Indirect tensile strength test.
- P-04-257 **Jacobsson L.** Borehole KLX02 Normal stress and shear tests on joints.
- P-04-258 **Adl-Zarrabi B.** Drill hole KLX02. Thermal properties: heat conductivity and heat capacity determined using the TPS method and mineralogical composition by modal analysis.
- P-04-261 **Jacobsson L.** Borehole KLX04A Uniaxial compression test of intact rock.
- P-04-262 **Jacobsson L.** Borehole KLX04A Triaxial compression test of intact rock.
- P-04-263 **Jacobsson L.** Drill hole KLX04A: Indirect tensile strength test.
- P-04-264 **Jacobsson L.** Borehole KLX04A Normal stress and shear tests on joints.
- P-04-265 **Chryssanthakis P.** Borehole KLX04A Tilt testing.
- P-04-266 **Chryssanthakis P, Tunbridge L.** Borehole KLX04A Determination of P-wave velocity, transverse borehole core.
- P-04-267 **Adl-Zarrabi, B.** Drill hole KLX04A Thermal properties: heat conductivity and heat capacity determined using the TPS method and Mineralogical composition by modal analysis.
- P-04-269 **Åkesson U.** Drill hole KLX04. Extensometer measurement of the coefficient of thermal expansion of rock.
- P-04-270 **Adl-Zarrabi B.** Drill hole KAV04A. Thermal properties; heat conductivity and heat capacity determined using the TPS method and mineralogical composition by modal analysis.
- P-04-273 **Nilsson G.** Investigation of sediments, peat lands and wetlands. Stratigraphical and analytical data.
- P-04-274 **Cronquist T, Forssberg O, Maersk Hansen L, Jonsson A, Koyi S, Leiner P, Sävås J, Vestgård J.** Detailed fracture mapping of two outcrops at Laxemar.
- P-04-277 **Nyborg M, Vestin E, Wilén P.** Oskarshamns site investigation. Hydrogeological inventory in the Oskarshamn area.
- P-04-280 **Nielsen U T, Horn F.** Geophysical borehole logging in borehole KLX03, HLX21, HLX22, HLX23, HLX24 and HLX25.
- P-04-281 **Wacker P, Berg C.** Water sampling in KSH02A. Summary of water sampling analysis in connection with Pipe String System (PSS) and Single Well Injection Withdrawal (SWIW) measurements.
- P-04-287 **Rahm N, Enachescu C.** Hydraulic testing of percussion drilled lineament boreholes on Ävrö and Simpevarp, 2004.
- P-04-288 **Rahm N, Enachescu C.** Hydraulic injection tests in borehole KLX02, 2003, Laxemar.
- P-04-289 **Ludvigson J-E, Levén J, Källgården J.** Oskarshamn site investigation. Single-hole injection tests in KSH02.
- P-04-290 **Rahm N, Enachescu C.** Hydraulic injection tests in borehole KSH03, 2004, Simpevarp.
- P-04-291 **Rahm N, Enachescu C.** Hydraulic injection tests in borehole KAV04A, 2004. Subarea Simpevarp.
- P-04-292 **Rahm N, Enachescu C.** Hydraulic injection tests in borehole KLX04, 2004. Subarea Laxemar.
- P-04-294 **Mattsson H, Thunehed H, Triumf C-A.** Compilation of petrophysical data from rock samples and in situ gamma-ray spectrometry measurements. Stage 2 – 2004 (including 2002).
- P-04-298 **Lindqvist G.** Refraction seismic measurements in Laxemar autumn 2004. Oskarshamn site investigation.
- P-04-299 **Berg C, Wacker P.** Hydrochemical logging in KLX03A.
- P-04-304 **Berg C.** Hydrochemical logging in KAV04A.

- P-04-306 **Nielsen U T, Ringgaard J, Horn F.** Geophysical borehole logging in boreholes KLX04, HLX26, HLX27 and HLX28.
- P-04-308 **Carlsten S, Hultgren P, Mattsson H, Stanfors R, Wahlgren C-H.** Geological single-hole interpretation of KAV04A, KAV04B, KLX01 and HLX15.
- P-04-310 **Kolla om detta är en reell referens!? – Hydraulic fracturing KSH01A, Table 2-3! RC!!!**
- P-04-315 **Alling V, Andersson P, Fridriksson G, Rubio Lind C.** Estimation of biomass and primary production of birch. Birch biotopes in Forsmark and Oskarshamn.
- P-04-316 **Alling V, Andersson P, Fridriksson G, Rubio Lind C.** Biomass production of Common reed (*Phragmites australis*), infauna, epiphytes, sessile epifauna and mobile epifaunal, Common reed biotopes in Oskarshamn's model area.
- P-04-317 **Johansson T, Adestam L.** Drilling and sampling in soil. Installation of groundwater monitoring wells in the Laxemar area.
- P-04-318 **Johansson T, Adestam L.** Slug tests in groundwater monitoring wells in soil in the Laxemar area.
- P-05-03 **Chryssanthakis P, Tunbridge L.** Borehole KLX03A. Determination of P-wave velocity, transverse borehole core.
- P-05-05 **Jacobsson L.** Oskarshamn Site Investigation – Drill hole KAV01, Normal loading and shear tests on joints.
- P-05-06 **Jacobsson L.** Oskarshamn Site Investigation – Drill hole KSH01A, Normal loading and shear tests on joints.
- P-05-07 **Jacobsson L.** Oskarshamn Site Investigation – Drill hole KSH02, Normal loading and shear tests on joints.
- P-05-18 **Gustavsson E, Gunnarsson M.** Oskarshamn site investigation. Laboratory data from the site investigation programme for the transport properties of the rock. Boreholes KSH01A, KSH02 and KLX02.
- P-05-20 **Gustafsson E, Ludvigson J-E.** Combined interference test and tracer test between KLX02 and HLX10.
- P-05-23 **Ehrenborg J, Dahlin P.** Boremap mapping of core drilled borehole KLX04.
- P-05-22 **Ehrenborg J, Stejskal V.** Boremap mapping of core drilled boreholes KAV04A and KAV04B.
- P-05-24 **Ehrenborg J, Dahlin P.** Boremap mapping of core drilled borehole KLX03.
- P-05-25 **Ask H, Morosini M, Samuelsson L-E, Ekström L, Håkansson N.** Drilling of cored borehole KAV04.
- P-05-27 **Löfgren M, Neretnieks I.** Oskarshamn site investigation. Formation factor logging *in situ* and in the laboratory by electrical methods in KSH01A and KSH02. Measurements and evaluation of methodology.
- P-05-28 **Gustafsson E, Nordqvist R.** Groundwater flow measurements and SWIW tests in boreholes KLX02 and KSH02.
- P-05-34 **Mattsson H, Thunehed H, Keisu M.** Interpretation of geophysical borehole measurements and compilation of petrophysical data from KLX01, KLX03, KLX04, HLX21, HLX22, HLX23, HLX24, HLX25, HLX26, HLX27 and HLX28.
- P-05-35 **Elhammer A, Sandkvist Å.** Detailed marine geological survey of the sea bottom outside Simpevarp.
- P-05-40 **Carlsson T, Brunberg A-K, Brydsten L, Strömgren M.** Characterisation of running waters, including vegetation, substrate and technical encroachments.
- P-05-42 **Green M.** Bird monitoring in Simpevarp 2002–2004.
- P-05-44 **Mattsson H.** Interpretation of geophysical borehole measurements from KLX06.
- P-05-49 **Rudmark L, Malmberg-Persson K, Mikko H.** Investigation of Quaternary deposits 2003–2004.
- P-05-54 **Berg C.** Hydrochemical logging in KSH03A. Results from isotope determinations.
- P-05-55 **Ask H, Samuelsson L-E, Zetterlund M.** Percussion drilling of boreholes HLX21, HLX22, HLX23, HLX24, HLX25, HLX30, HLX31 and HLX33 for investigation of lineament EW007.
- P-05-65 **Forsman I, Zetterlund M, Forsmark T, Rhén I.** Correlation of Posiva Flow Log anomalies to core mapped features in KSH01A, KSH02A and KAV01.
- P-05-67 **Rouhiainen P, Pöllänen J, Sokolnicki M.** Difference flow logging of borehole KLX 03. Subarea Laxemar.
- P-05-68 **Rouhiainen P, Sokolnicki M.** Difference flow logging of borehole KLX04.
- P-05-69 **Kolla om detta är en reell referens?! – Overcoring KLX04, Table 2-3! RC!!!**
- P-05-70 **Svensson, J.** Fältundersökning av diskrepanser gällande vattendrag i GIS-modellen. Platsundersökning Oskarshamn.
- P-05-75 **Thunehed H.** Resistivity measurements and determination of formation factors on samples from LX04 and KSH02.

- P-05-80 **Löfgren A.** Estimation of biomass and net primary production in field and ground layer, and biomass in litter layer of different vegetation types in Forsmark and Oskarshamn. Oskarshamn/Forsmark site investigation.
- P-05-88 **Berg C.** Hydrochemical logging in KLX04 Results from isotope determinations (3H, δD and δ18O).
- P-05-89 **Berg C.** Hydrochemical logging in KLX03 Results from isotope determinations (3H, δD and δ18O).
- P-05-105 **Löfgren M, Neretnieks I.** Formation factor logging in situ by electrical methods in KLX03 and KLX04.
- P-05-111 **Ask H, Morosini M, Samuelsson L-E, Ekström L, Håkanson N.** Drilling of cored borehole KLX04.
- P-05-167 **Ask H, Morosini M, Samuelsson L-E, Ekström L, Håkanson N.** Drilling of cored borehole KLX03.
- P-05-173 **Aquilonius K.** Vegetation in lake Frisksjön.
- P-05-174 **Drake H, Tullborg E-L.** Fracture mineralogy and wall rock alteration. Results from drill cores KAS04, KA1755A and KLX02.
- P-05-180 **Wahlgren C-H, Bergman T, Persson Nilsson K, Eliasson T, Ahl M, Ekström M.** Bedrock map of the Laxemar subarea and surroundings. Description of rock types, modal and geochemical analyses, including the cored boreholes KLX03, KSH03 and KAV01.
- P-05-184 **Rahmn N, Enachescu C.** Pumping tests and hydraulic injection tests in borehole KLX06.
- P-05-189 **Mattsson H, Keisu M.** Interpretation of geophysical borehole measurements from KLX05.
- P-05-190 **Ask H, Zetterlund M.** Percussion drilling of boreholes HLX16, HLX17, HLX18 and HLX19.
- P-05-205 **Nyberg G, Wass E, Askling P.** Groundwater monitoring program. Report for December 2002 – October 2004. Oskarshamn site investigation.
- P-05-227 **Lärke A, Hillgren R, Wern L, Jones J, Aquilonius K.** Hydrological and meteorological monitoring at Oskarshamn during 2003–2004. Oskarshamn site investigation.
- P-05-241 **Forsman I, Zetterlund M, Forsmark T, Rhén I.** Correlation of Posiva Flow Log anomalies to core mapped features in KLX02, KLX03, KLX04, KAV04A and KAV04B.
- P-06-05 **Strömgren M.** Surveying of water courses in the Simpevarp area. **(NB Tentative title – Bevaka!)**
- PR-25-89-17 **Bjarnason B, Klasson H, Leijon, B, Strindell L, Öhman T 1989.** Rock stress measurements in boreholes KAS02, KAS03 and KAS05 on Äspö.
- PR-25-89-23 **Rydström H, Gereben L.** Regional geological study – Seismic refraction survey.
- PR U-97-27 **Ljunggren C, H Klasson, 1997.** Drilling KLX02 – Phase 2 Lilla Laxemar Oskarshamn – Deep hydraulic fracturing Rock stress measurements in Borehole KLX02, Laxemar.
- IPR-99-17 **Sundberg J, Gabrielsson A.** Laboratory and field measurements of thermal properties of the rock in the prototype repository at Äspö HRL.
- IPR-00-28 **Andersson P, Ludvigson J-E, Wass E, Holmqvist M.** TRUE Block Scale. Tracer Test Stage. Interference tests, dilution tests and tracer tests, phase A.
- IPR-01-06 **Rouhiainen P.** Difference flow measurements in borehole KLX02 at Laxemar.
- IPR-01-44 **Andersson P, Ludvigsson J-E, Wass E.** TRUE Block Scale project. Preliminary characterisation stage. Combined interference tests and tracer tests. Performance and delivery evaluation.
- IPR-01-65 **Forsmark T, Rhén I.** Summary report of investigations before the operation phase. Prototype Repository (D27).
- IPR-01-67 **Klasson H, Persson M, Ljunggren C.** Overcoring rock stress measurements at the Äspö HRL. Prototype Repository: Borehole KA3579G (Revised data) and K – tunnel: Borehole KK0045G01.
- IPR-02-01 **Rummel F, Klee G, Weber U.** Äspö Hard Rock Laboratory. Rock Stress measurements in Oskarshamn. Hydraulic fracturing and core testing in borehole KOV01.
- IPR-02-02 **Klee G, Rummel F.** Äspö Hard Rock Laboratory. Rock Stress measurements at the Äspö HRL. Hydraulic fracturing in boreholes KA2599G01 and KF0093A01.
- IPR-02-03 **Collin M, Börgesson L.** Äspö Hard Rock Laboratory. Prototype Repository. Instrumentation of buffer and backfill for measuring THM processes.
- IPR-02-18 **Klasson H, Lindblad K, Lindfors U, Andersson S.** Äspö Hard Rock Laboratory. Overcoring rock stress measurements in borehole KOV01, Oskarshamn.
- IPR-03-13 **Dershowitz W, Winberg A, Hermanson J, Byegård J, Tullborg, E-L, Andersson P, Mazurek M.** Äspö Hard Rock Laboratory. Äspö Task Force on modelling of groundwater flow and transport of solutes. Task 6c. A semi-synthetic model of block scale conductive structures at the Äspö HRL.
- ICR-01-04 **Byegård J, Widestrand H, Skälberg M, Tullborg E-L, Siitari-Kauppi M.** First TRUE Stage. Complementary investigations of diffusivity, porosity and sorbtivity of Feature A-site specific geologic material.
- R-97-13 **Carbol P, Engkvist I.** Compilation of radionuclide sorption coefficients for performance assessment.
- R-98-05 **Axelsson C-L, Mærsk Hansen L.** Update of structural models at SFR nuclear waste repository, Forsmark, Sweden.

- R-98-55 **Follin S, Årebäck M, Axelsson C-L, Stigsson M, Jacks G.** Förstudie Oskarshamn. Grundvattnets rörelse, kemi och långsiktiga förändringar (in Swedish).
- R-99-70 **Lindell S, Ambjörn C, Juhlin B, Larsson-McCann S, Lindquist K.** Available climatological and oceanographical data for site investigation program.
- R-01-06 **Markström I, Stanfors R, Juhlin C.** Äspölaboratoriet RVS-modellering, Ävrö Slutrapport (in Swedish).
- R-01-52 **Ludvigson J-E, Hansson K, Rouhiainen P.** Methodology study of Posiva difference flow meter in borehole KLX02 at Laxemar.
- R-02-06 **Boresjö Bronge L, Wester K.** Vegetation mapping with satellite data of the Forsmark and Tierp regions.
- R-02-10 **Berggren J, Kyläkorpi L.** Ekosystemen i Simpevarpsområdet Sammanställning av befintlig information (in Swedish).
- R-02-10 **Berggren J, Kyläkorpi L.** Ekosystemen i Simpevarpsområdet – Sammanställning av befintlig information (In Swedish: Ecosystems in the Simpevarp area – A list of available information).
- R-02-26 **Janson T, Stigsson M.** Test with different stress measurement methods in two orthogonal bore holes in Äspö HRL.
- R-02-27 **Sundberg J.** Determination of thermal properties at Äspö HRL. Comparison and evaluation of methods and methodologies for borehole KA 2599 G01.
- R-02-35 **SKB.** Simpevarp – site descriptive model version O.
- R-02-47 **Risberg J.** Holocene sediment accumulation in the Äspö area. A study of a sediment core.
- R-03-10 **Sundberg J.** Thermal Site Descriptive Model. A strategy for the model development during site investigations. Version 1.0.
- R-04-09 **Smellie J.** Recent geoscientific information relating to deep crustal studies.
- R-04-11 **Miliander S, Punakivi M, Kyläkorpi L, Rydgren B.** Human population and activities at Simpevarp.
- R-04-12 **Kyläkorpi, L** Tillgänglighetskartan (/Map of accessibility).
- R-04-16 **Laaksoharju M, Smellie J, Gimeno M, Auqué L, Gómez J, Tullborg E-L, Gurban I.** Hydrogeochemical evaluation of the Simpevarp area, model version 1.1.
- R-04-74 **SKB, 2004.** Hydrogeochemical evaluation for Simpevarp model version 1.2. Preliminary site description of the Simpevarp area.
- R-05-54 **Nyman H.** Depth and stratigraphy of Quaternary deposits. Preliminary site description Laxemar subarea – version 1.2
- R-05-61 **Werner K, Bosson E.** Description of climate, surface hydrology, and near-surface hydrogeology. Preliminary site description Laxemar subarea – version 1.2.
- R-06-11 **Lindborg T (ed.).** Description of surface systems, Preliminary site description Laxemar subarea – version 1.2.
- R-06-12 **SKB.** Hydrogeochemical evaluation. Preliminary site description, Laxemar subarea – version 1.2.
- TR-94-02 **Wersin P, Spahiu K, Bruno J.** Time evolution of dissolved oxygen and redox conditions in a HLW repository.
- TR-97-03 **Rhén I (ed.), Bäckblom G (ed.), Gustafson G, Stanfors R, Wikberg P.** Äspö HRL – Geoscientific evaluation 1997/2. Results from pre-investigations and detailed site characterization. Summary report.
- TR-97-05 **Rhén I, Gustafson G, Wikberg P.** Äspö HRL – Geoscientific evaluation 1997/4. Results from pre-investigations and detailed site characterization. Comparison of predictions and observations. Hydrogeology, groundwater chemistry and transport of solutes.
- TR-97-06 **Rhén I (ed.), Gustafson G, Stanfors R, Wikberg P.** Äspö HRL – Geoscientific evaluation 1997/5. Models based on site characterization 1986–1995.
- TR-97-20 **Ohlsson Y, Neretnieks I.** Diffusion data in granite. Recommended values.
- TR-98-05 **Juhlin C, Wallroth T, Smellie J, Eliasson T, Ljunggren C, Leijon B, Beswick J.** The Very Deep Hole Concept: Geoscientific appraisal of conditions at great depth.
- TR-98-18 **Byegård J, Johansson H, Skälberg M, Tullborg E-L.** The interaction of sorbing and non-sorbing tracers with different Äspö rock types. Sorption and diffusion experiments in the laboratory scale.
- TR-01-11 **Ekman L.** Project Deep Drilling KLX02-Phase 2. Methods, scope of activities and results. Summary.
- TR-02-03 **Larsson-McCann S, Karlsson A, Nord M, Sjögren J, Johansson L, Ivarsson M, Kindell S.** Meteorological, hydrological and oceanographical information and data for the site investigation program in the community of Oskarshamn.
- TR-02-19 **Andersson J, Berglund J, Follin S, Hakami E, Halvarson J, Hermanson J, Laaksoharju M, Rhén I, Wahlgren C-H.** Testing the methodology for site descriptive modelling. Application for the Laxemar area.
- SKI 98:41 **Xu S, Wörman A.** Statistical patterns of geochemistry in crystalline rock and effect of sorption kinetics on radionuclide migration.

2.8 Model volumes

The site descriptive modelling is performed using two different model volumes (or domains) of different scales, the *regional* and the *local* scale model volumes. Generally, the local model is required to cover the volume within which the repository is expected to be positioned, including accesses and the immediate environs. In addition to the description on the local scale, a description is also devised for a much larger volume, the regional model. The latter model provides boundary conditions and puts the local model in a larger context. It is noted that the defined modelling areas and their vertical extents, which in combination defined three-dimensional modelling domains, are the areas for which a parameterised description in some form is expected. They are by no means to be regarded as strict model volumes for e.g. numerical hydrogeological modelling. In the latter case, other considerations come into play when defining the modelling domain, e.g. topographical considerations (groundwater divides) and/or the positioning of interpreted deformation zones.

This section presents and motivates the models volumes selected for the model version Laxemar 1.2 modelling.

2.8.1 General

By necessity, the site characterisation efforts need to focus on the volumes of primary interest for the repository location. Demands for increased information density are higher in these volumes than outside. The local volume description should be detailed enough for the needs of the repository engineering and safety assessment groups. It is primarily these users of the descriptions who can judge whether the local volume is sufficiently large. However, the site modelling needs to ensure a sufficient understanding of the evolution of the natural system. This means that the size and level of resolution needed, especially in the regional volume, should be dictated by what is required in order to capture the most relevant physical phenomena for describing this evolution.

In selecting the model volumes for version 1.1 models for Simpevarp and Forsmark the following rules of thumb, taken from the SKB strategy document for integrated evaluation /Andersson 2003/ were applied:

- The local site descriptive model should cover an area of about 5–10 km², i.e. large enough to include the potential repository and its immediate surroundings. This also means that the location of this model area needs to be agreed upon by both the Repository design and Site modelling groups.
- The regional descriptive model should be large enough to allow for a sensitivity analysis of boundary conditions and to provide site understanding to the local model.
- If possible, model domains selected in previous versions should be retained. Deviations should be well motivated and their basis fully documented.
- The models should include the main sources of new information (e.g. deep boreholes and areas of extensive surface geophysics).
- The local domain should be large enough to allow meaningful hydrogeological flow simulations within the domain, though information for boundary conditions or an encompassing regional scale hydrogeological model will often need to be taken from the regional domain – or beyond.
- Potentially important features, such as lineaments, rock type boundaries etc., should be considered when selecting the size of the model volumes.

These rules also apply for model versions 1.2. It needs also be understood that the distinct model sizes primarily concern the development of the geological model in the SKB Rock Visualisation System, RVS. The following clarifications are noted:

- Model boundaries for numerical simulations, e.g. in the hydrogeological model, are to be set to suite the purpose of these simulations and do not need to be restricted to the size of the RVS-representation.
- In modelling the hydrogeological and hydrogeochemical evolution, the numerical model assesses the importance of the location of boundaries and the importance of different boundary conditions at these boundaries, see Chapter 8. These studies are in principle not restricted by the size of the regional volume for the RVS representation.

The regional and local model volumes differ with respect to amount of detailed data and degree of determinism, but not with regard to the scale of resolution of the spatial variability. For example, outside the local model volume the geological model only has large deterministic deformation zones, whereas small zones are represented by expanding the DFN-model in this volume, see Chapter 5. This means that in the regional hydrogeological modelling, see Chapter 8, the resolution is the same in the entire model domain, whereas, of course the uncertainty in the domain outside the local volume is indeed much higher than inside that volume.

2.8.2 Regional model volume

Generally, the geographic scope of the regional models depends on the local premises and requirements and is controlled by the basic need to achieve understanding of the conditions and processes that determine the conditions at the site /SKB 2001a/. The regional model volume should encompass a sufficiently large area that the geoscientific conditions that can directly or indirectly influence the local conditions, or help in understanding the geoscientific processes in the repository area, are included. In practical terms, this may entail a surface area of “a few hundred square kilometres.”

Figure 2-4 shows the regional model area selected for Laxemar1.2. It is the same model area used in the version 0 report /SKB 2002b/, the version Simpevarp 1.1 /SKB 2004b/ and version Simpevarp 1.2 /SKB 2005a/. The depth of the model volume is set to 2.2 km (from 100 m above sea level and extending down to 2,100 m below).

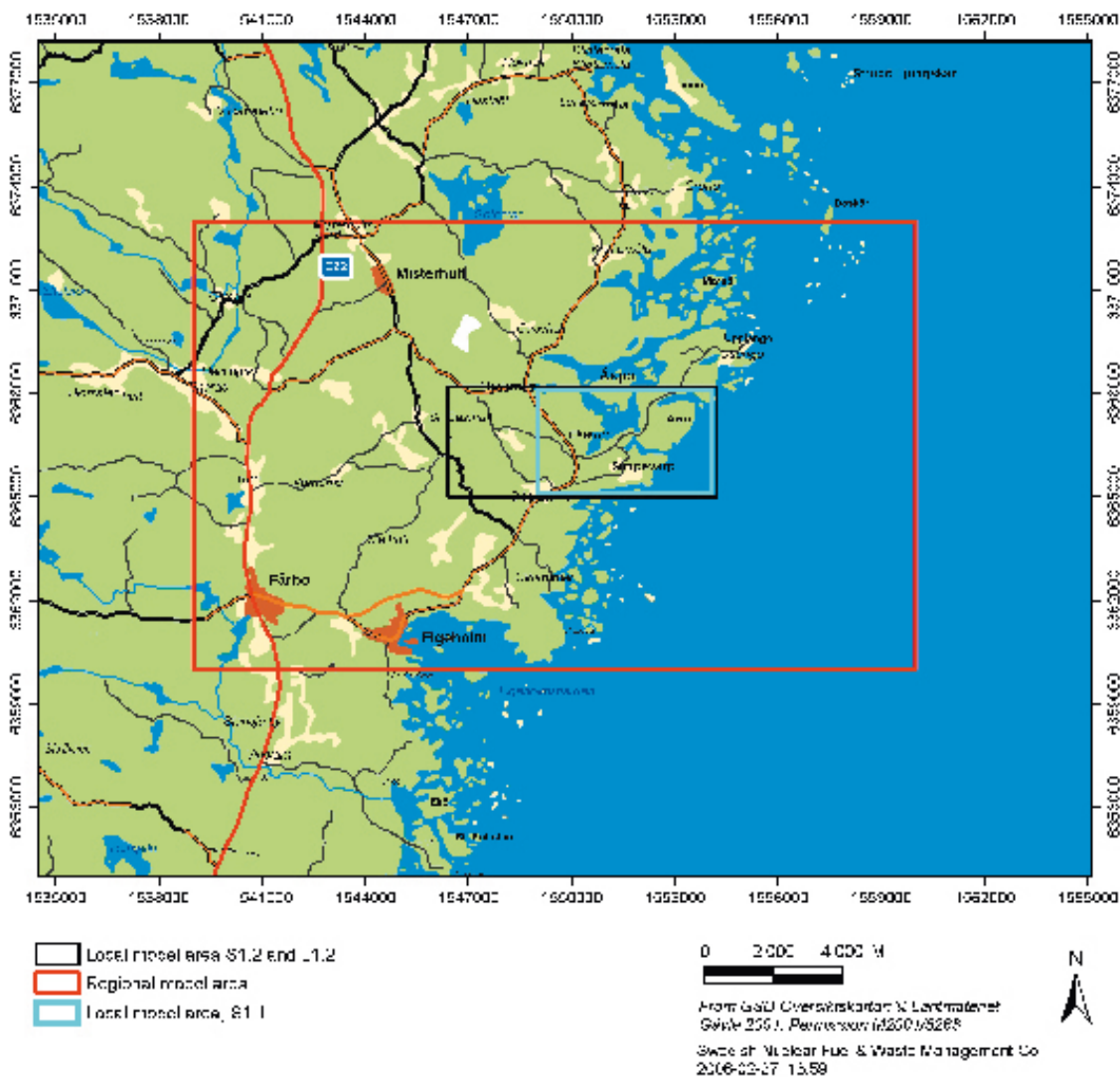


Figure 2-4. Regional and local model areas used for Laxemar 1.2. The areal coverages of the local and regional models are the same as those employed in version Simpevarp 1.2 /SKB 2005a/.

The regional model volume has been selected on the basis of the following considerations and arguments:

- It includes the prioritised area for site investigations in the Simpevarp area /SKB 2001b/ and it is not prohibitively large, with an approximate surface area of $(21 \times 13) 273 \text{ km}^2$.
- It captures the extensive regional deformation zones that strike in northnortheasterly and near east-west directions, and surround the prioritised area for site investigations. Any expansion of the regional model area to the east or west would not provide any significant changes in the regional geological picture.
- It adequately covers the variations in rock type in the candidate area and its immediate surroundings.
- It captures the main features in the region interpreted to be of hydrogeological importance as the east-west boundaries are judged to be sufficiently well separated in space not to influence the groundwater flow in the region. Furthermore, the western boundary lies on the western side of a local topographic divide and the boundary to the east lies in the Kalmar Sund strait (between the mainland and the island of Öland). The area includes potential discharge areas for groundwater resulting from future shoreline displacement. The proper locations of the boundaries in the regional hydrogeological model – as well as the proper boundary conditions are assessed through a series of sensitivity analyses in the hydrogeological modelling for Simpevarp 1.2 /SKB 2005a/.
- A depth of 2.2 km (of which 100 m is above sea level) is considered to provide a reasonable context for the local description. Furthermore, this depth is considered the maximum down to which any meaningful extrapolations of deformation zones can be made.

The coordinates outlining the surface area of the Regional model for Laxemar 1.2, cf. Figure 2-4, are (in metres):

(X, Y): (1539000, 6373000), (1560000, 6373000), (1539000, 6360000), (1560000, 6360000).

Z: +100 m, -2,100 m

2.8.3 Local model volume

The area covered by the repository (at repository depth) should ideally not be more than about 2 km². This should be sufficient for a repository with approximately 6,000 canisters, under the assumption of a 90% utilisation of possible canister positions and centrally located space for the required infrastructure. The surface facility and the access to the deep repository are not included in this area, as their areal needs depend on whether a straight ramp, a spiral ramp or a shaft access will be employed. A geometrically ideal case will not be achieved in reality, since the layout of the deep repository will be adapted to conditions in the bedrock (deformation zones, etc.). The more deposition subareas the deep repository is made up of, and the more irregular these are, the greater the total repository area that will be required, since intervening unutilised “corridors” must also be included in the total “encompassing” area. The local (investigation and) model area should be considerably larger than the repository area, above all because it is not otherwise possible to try out alternative repository layouts and gradually arrive at the optimal placement and adaptation to the rock conditions. The local model volume should therefore encompass a surface area of 5–10 km² /SKB 2001a/.

In the version 0 report /SKB 2002b/, a near circular-shaped “candidate area” with a size of some 50 km² was presented. The ambition of subsequent characterisation and analysis has been to reduce the candidate area to a “prioritised area for site investigation”. In the case of the Simpevarp area, the prioritised area for site investigations is made up of two separate subareas. The first area, where drilling commenced during the summer of 2002, is denoted the “Simpevarp subarea” and is made up of major portions of the Simpevarp peninsula, together with the islands of Ävrö, Hålö and Bockholmen. The second, the “Laxemar subarea” was selected early in 2003 /SKB 2003/ following complementary regional investigations and subsequent evaluation /Wahlgren et al. 2003/, cf. Figure 1-1. The two areas are in essence neighbouring one another. This suggested that including the two “subareas” in one single local model would provide synergy and facilitate co-interpretation of data which will emerge from the two sites over time. Characterisation of the Laxemar subarea commenced with selected surface investigations in late 2003 and drilling in February 2004, in

this context comes second in time to the Simeparp subarea. Also, the area of Hålö/Bockholmen, positioned in between the two subareas, is a candidate area for the surface installations associated with a future deep repository. By including the two subareas in one local model volume, satisfactory coverage is also provided for any type of access tunnel and/or tunnel connection from a shaft access to either of the two.

The coordinates (X,Y) outlining the surface area of the local scale model for Laxemar 1.2, cf. Figure 2-4, are (in metres):

(1546400, 6368200), (1554200, 6368200), (1554200, 6365000), (1546400, 6365000).

Figure 2-4 shows the local model area for the Laxemar 1.2 model version as embedded in the Regional Scale Model. The vertical extent of the local model is set to 1,200 m, 1,100 m below sea level and 100 m above sea level. It is noted that the southern parts of the Äspö island is included in the model, cf. Section 2.3. For comparison, also the local model area employed for Simeparp 1.1 is shown in Figure 2-4.

The local model volume has been selected on the basis of the following considerations:

- It provides a volume that includes the Laxemar subarea and the area for potential surface facilities, access ramps and tunnels connecting from Clab facility or the islands of Hålö and Bockholmen.
- In addition it contains the Simeparp subarea. This allows co-interpretation of data emerging from the two subareas in an efficient and flexible manner.
- By retaining the same local model area as used for model version Simeparp 1.2, a direct comparison between the Laxemar 1.2 and Simeparp 1.2 local models is possible. However, for the continued modelling associated with the complete site investigations (CSI), a reduction (focusing) of the local model will be considered.
- The north boundary is positioned along an interpreted fracture zone (ZSM0002A0, The Mederhult zone) that was interpreted already for v. 0, cf. Table 5-5 and associated Figure 5-53. The south boundary coincides with a topographically/geophysically identified lineament, respectively. The north-south boundaries of the model are not associated with any particular geographical feature.
- A depth of 1,100 m below sea level will permit inclusion of all information from the deep boreholes that will be completed at the site.
- The local scale model area has a surface area of approximately 24 (8×3) km² (see Figure 2-4).

3 Evolutionary aspects

3.1 Crystalline bedrock

3.1.1 Introduction

The following brief outline of the geological evolution in the Oskarshamn region is a slightly modified version of that presented in /Andersson et al. 2002b/. It is mainly based on results published in reports in various SKB series as well as in research papers in scientific journals. The Oskarshamn region is put into a regional geological context, but the description is focussed on the geological evolution of rock types and structural elements that characterize the bedrock in the Oskarshamn municipality and its immediate surroundings.

The geological evolution of cratonic (stabilised) bedrock regions is generally the result of consecutive large-scale processes, e.g. orogenies, which have operated over a considerable period of time. In order to understand the geological development of the bedrock in southeastern Sweden, it is necessary to take into account also post-cratonization (after c. 1,750–1,700 Ma), i.e. large-scale processes more or less remote from the Oskarshamn region that might have had a far-field effect on the already cratonised crust.

The geological development in the Oskarshamn region, including the formation of existing rocks, as well as structural and tectonic overprinting, is complex and spans a period of c. 1,900 Ma. The following text gives a brief summary and for further information of the geological evolution and processes that might have affected the bedrock in the Oskarshamn region and the rest of the southern part of the Fennoscandian Shield, the reader is referred to e.g. /Larson and Tullborg 1993/ and /Milnes et al. 1998/.

As a reference for the following text, the geological time units and nomenclature used are displayed in Figure 3-1.

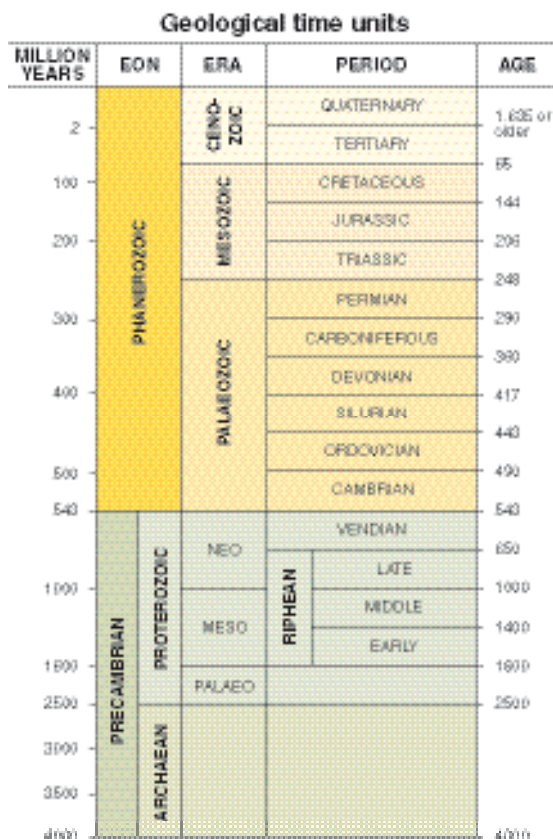


Figure 3-1. Geological time scale. Modified after /Koistinen et al. 2001/.

In order to put the Oskarshamn region in a large-scale geological evolutionary perspective, the successive growth of the Fennoscandian Shield and subsequent formation of Phanerozoic cover sequences from c. 1,910 Ma until the Quaternary period is displayed in Figure 3-2 through Figure 3-6. In each figure, previously formed rocks are marked in grey. The following abbreviations are used:

GP = granite-pegmatite,

GDG = granitoid-dioritoid-gabbroid,

GSDG = granite-syenitoid-dioritoid-gabbroid.

3.1.2 Lithological development

The position of the Oskarshamn region in a regional geological-evolutionary perspective can be seen in Figure 3-2 through Figure 3-7. The oldest rocks in the Oskarshamn region, though subordinate, comprise more or less strongly deformed and metamorphosed supracrustal rocks of predominantly sedimentary but also of volcanic origin. The formation of the metasedimentary rocks is constrained to the time interval c. 1,870–1,860 Ma /Sultan et al. 2004/, and the rocks have their main expression in the Blankaholm-Västervik area, cf. Figure 3-8 /Bergman et al. 1998, 1999, 2000/.

In the area immediately north of Oskarshamn and westwards, metagranitoids belonging to the E-W to WNW-ESE trending so-called Oskarshamn-Jönköping belt /Mansfeld 1996/ constitute an important lithological component. These rocks were formed c. 1,834–1,823 Ma ago /Mansfeld 1996, Åhäll et al. 2002/ and display a varying degree of tectonometamorphic overprinting and in many places they are relatively well-preserved.

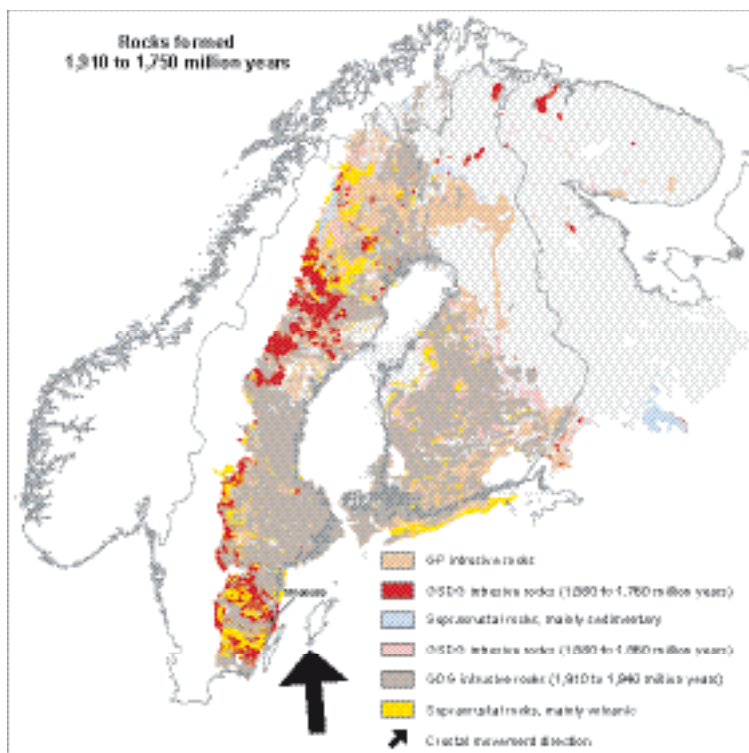


Figure 3-2. Rocks formed in the time interval 1,910–1,750 Ma. The figure is based on the database presented by /Koistinen et al. 2001/.

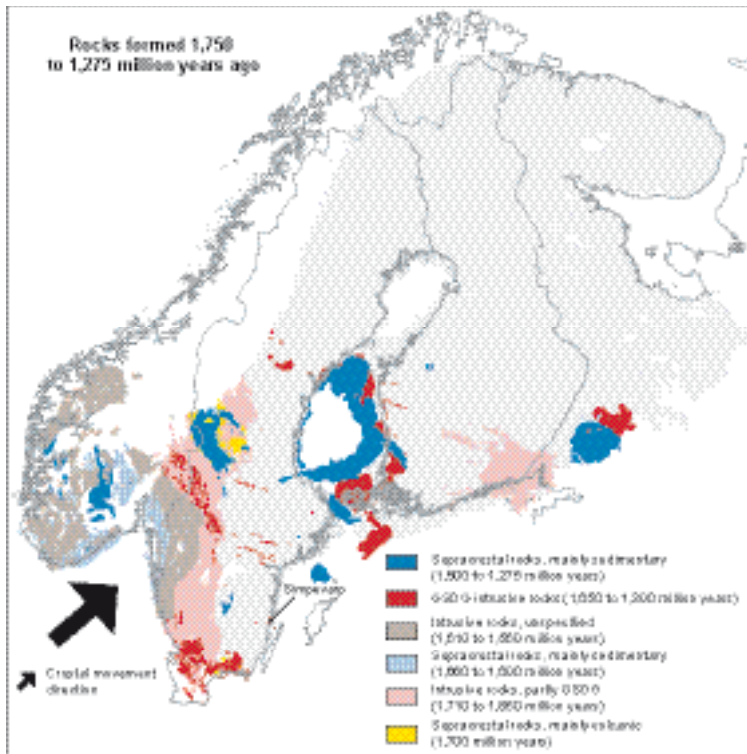


Figure 3-3. Rocks formed in the time interval 1,750–1,275 Ma. The figure is based on the database presented by /Koistinen et al. 2001/.

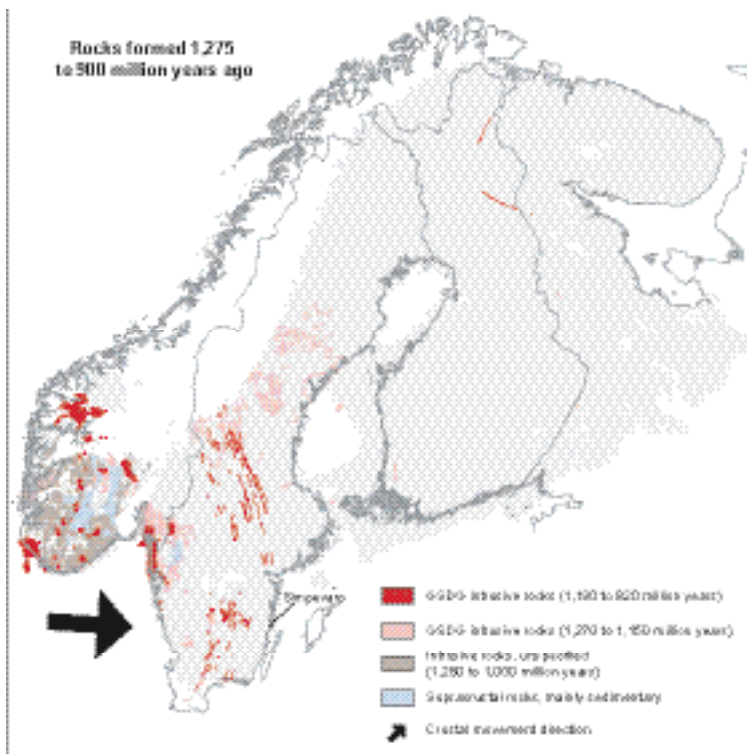


Figure 3-4. Rocks formed in the time interval 1,275–900 Ma. The figure is based on the database presented by /Koistinen et al. 2001/.

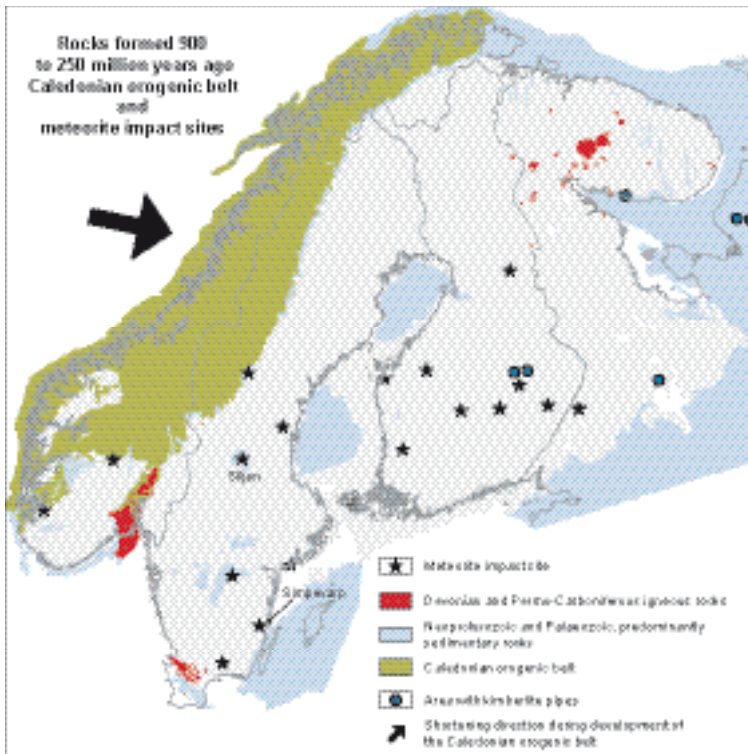


Figure 3-5. Rocks formed in the time interval 900–250 Ma. The figure is based on the database presented by /Koistinen et al. 2001/.



Figure 3-6. Rocks formed in the time interval 250 Ma to the Quaternary period. The figure is based on the database presented by /Koistinen et al. 2001/.

The majority of the rocks at the present day erosional level in southeastern Sweden were formed during a period of intense igneous activity c. 1,810–1,760 Ma ago /e.g. Wikman and Kornfält 1995, Kornfält et al. 1997/, during the waning stages of the Svecokarelian orogeny. The dominant rocks comprise granites, syenitoids, dioritoids and gabbroids, as well as spatially and compositionally related volcanic rocks. The granites and syenitoids, as well as some of the dioritoids are by tradition collectively referred to as Småland “granites”. Both equigranular, unequigranular and porphyritic varieties occur, and the compositional variation is displayed in Figure 3-9. Hence, the Småland “granites” comprise a variety of rock types regarding texture, mineralogical and chemical composition.

This generation of igneous rocks belongs to the so-called Transscandinavian Igneous Belt (TIB), which has a NNW extension from southeastern Sweden through Värmland and Dalarna into Norway, where it finally disappears beneath the Scandinavian Caledonides (Figure 3-7). It is characterised by repeated alkalicalcic-dominant magmatism during the period c. 1,860–1,650 Ma ago. Magma-mingling and -mixing processes, exemplified by the occurrence of enclaves, hybridization and diffuse transitions etc. between different TIB rocks indicate a close time-wise and genetic relationship between the different rock types. At mesoscopic scale, these processes often resulted in a more or less inhomogeneous bedrock regarding texture, mineralogical and chemical composition. However, if larger rock volumes are considered, these may be regarded as being more or less homogeneous, despite some internal variations.

Locally, fine- to medium-grained granite dykes and minor massifs, and also pegmatite occur frequently. Though volumetrically subordinate, these rocks constitute essential lithological inhomogeneities in parts of the bedrock in the Oskarshamn region, e.g. in the Simpevarp area. They are roughly coeval with the TIB host rock /Wikman and Kornfält 1995, Kornfält et al. 1997/, but have been intruded at a late stage in the magmatic evolution. Furthermore, TIB-related mafic and composite intrusions occur locally.

After the formation of the TIB rocks, the next rock-forming period in the Oskarshamn region, including southeastern Sweden, did not take place until c. 1,450 Ma ago. It was characterised by the local emplacement of granitic magmas in a cratonized crust. However, this granitic magmatism was presumably a far-field effect of ongoing orogenic processes elsewhere, in all likelihood farther to the southwest of present Scandinavia. In the Oskarshamn region, the c. 1,450 Ma magmatism is exemplified by the occurrence of the Götemar, Uthammar and Jungfrun granites, cf. Figure 3-8 /Kresten and Chyssler 1976, Åhäll 2001/. Fine- to medium-grained granitic dykes and pegmatites that are related to the c. 1,450 Ma granites occur as well, e.g. in the Götemar granite. However, these dykes are inferred to occur only within the granite and in its immediate surroundings.

The youngest magmatic rocks in the region are scattered dolerite dykes that presumably are related to the regional system of N-S trending, c. 1,000–900 Ma old dolerites that can be followed from Blekinge in the south to Dalarna in the north /Johansson and Johansson 1990, Söderlund et al. 2004/. The dykes are emplaced in and to the east of the frontal part of the Sveconorwegian orogen. Due to the generally high content of magnetite, they usually constitute linear, positive magnetic anomalies, and their occurrence and extension may, thus, be identified on the magnetic anomaly maps. Time-wise they are related to the c. 1,100–900 Ma Sveconorwegian orogeny which is responsible for the more or less strong reworking and present structural geometry in the bedrock of southwestern Sweden.

In late Precambrian and/or early Cambrian time, i.e. c. 600–550 Ma ago, arenitic sediments were deposited on a levelled bedrock surface, the so-called sub-Cambrian peneplain. The sediments were subsequently transformed to sandstones, which constitute the youngest rocks in the region, cf. Figure 3-7 and Figure 3-8. The remainder of these former extensively occurring sedimentary rocks covers the Precambrian crystalline rocks along the coast of the Baltic Sea from the area south of Oskarshamn in the north to northeastern Blekinge in the south. Furthermore, fractures filled with sandstone are documented in the Oskarshamn region in e.g. the Götemar granite, east of the N-S trending fault (cf. Figure 3-8) that transects the granite /Kresten and Chyssler 1976/ and at Enudden, c. 4 km northeast of Simpevarp /Talbot and Ramberg 1990, see also Röshoff and Cosgrove 2002/. During the ongoing site investigation in Oskarshamn, sandstone of presumed Cambrian age has been documented in a cored borehole. The sandstone occurs in a deformation zone and occupies c. 0.1 m of the drill core.

BEDROCK OF SWEDEN

Fossil-bearing bedrock outside the Caledonides

Bancalton, shale and limestone, 645-65 m.y. in age

Caledonides

Rocks 750-430 m.y. in age

- Granite and gabbro
- Bancalton, shale, limestone and volcanic rocks, mainly metamorphosed
- Mica schist, mica gneiss and amphibolite
- Bancalton with dolerite dykes
- Bancalton, fossil-bearing shale and limestone

Rocks older than 1500 m.y.

- Granite, gabbro, volcanic rocks and mica gneiss

Precambrian shield

Rocks 1570-700 m.y. in age

- Granite and pegmatite
- Bancalton, shale and meta-volcanic rocks, partly metamorphosed
- Granite, monzonite, gabbro and dolerite, partly gneissose

Rocks 1650-1600 m.y. in age

- Mica gneiss and amphibolite
- Post-volcanic rocks, gneissose
- Volcanic rocks, partly metamorphosed
- Granite, mainly granitic, granodioritic or tonalitic in composition
- Granite, pegmatite, monzonite, gabbro and dolerite, partly gneissose

Rocks 1680-1650 m.y. in age

- Granite, monzonite, gabbro and dolerite, partly metamorphosed
- Granite, granodiorite, tonalite and gabbro, partly gneissose
- Bancalton and shale, partly gneissose
- Volcanic rocks, metamorphosed

Rocks 1800-1780 m.y. in age

- Meta-volcanic rocks, serpentinite, shale and limestone, metamorphosed

Rocks older than 2000 m.y.

- Granite, granitic, granodioritic or tonalitic in composition, gabbro

Structures

- Impact structure
- Form line of tectonic foliation
- Fault, symbols in downthrown block
- Thrust in the Caledonides, symbols in elevated block
- Thrust or reverse deformation zone in the Precambrian shield, symbols in elevated block
- Deformation zone, symbols in downthrown block
- Deformation zone, arrows indicate horizontal component of movement
- Deformation zone, unspecified

LLDZ Lalleharanna - Linköping Deformation Zone

SFDZ Sveonorwegian Frontal Deformation Zone

PZ Proterogine Zone

SBDZ Småland - Blåhinge Deformation Zone

TIB Transscandinavian Igneous Belt

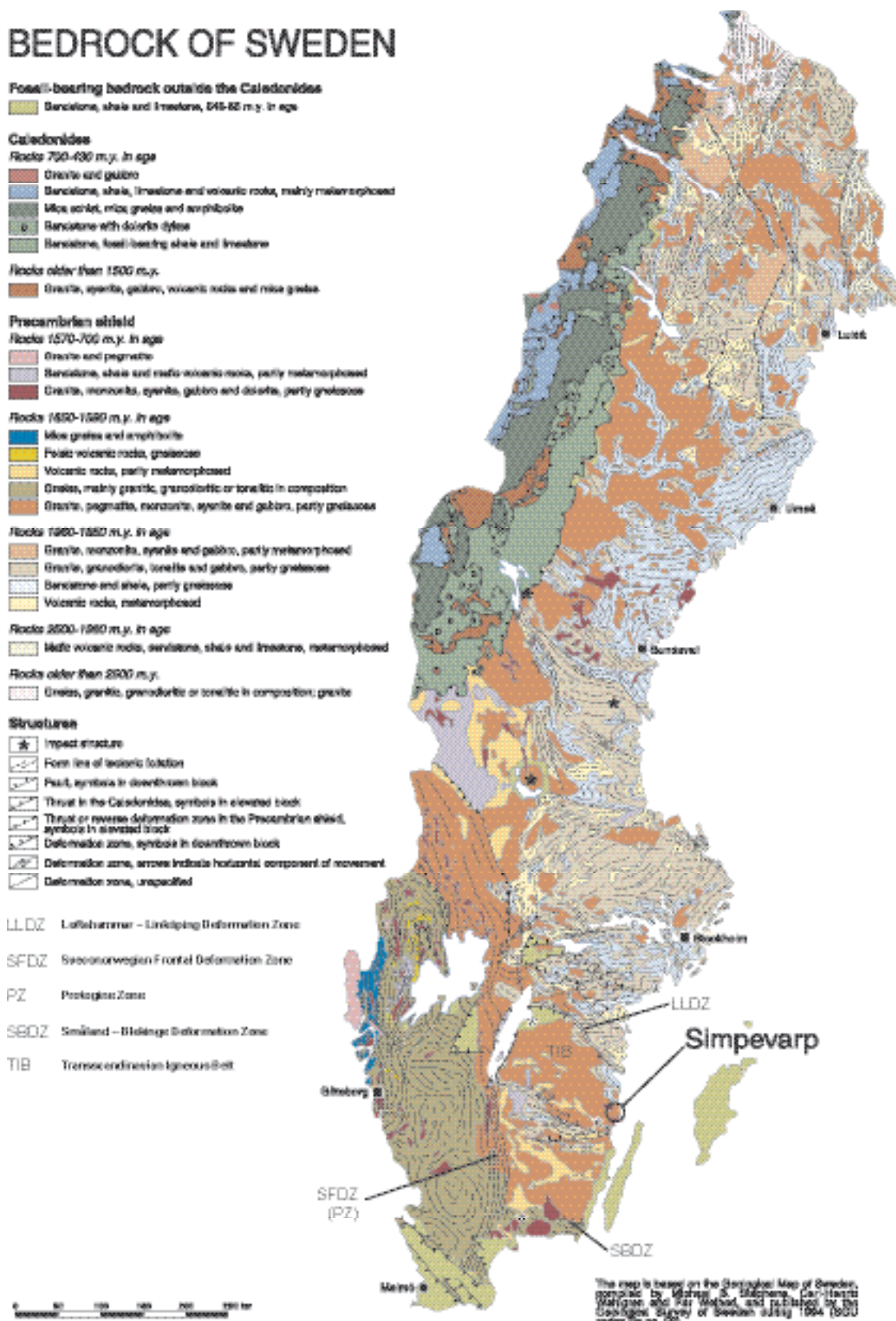


Figure 3-7. Simplified bedrock map of Sweden. The geological province in which the Simpevarp area lies is bounded by major deformation zones along its northern /LLDZ/, southern /SBDZ/ and western /SFDZ/ boundaries. Modified after /Stephens et al. 1994/.

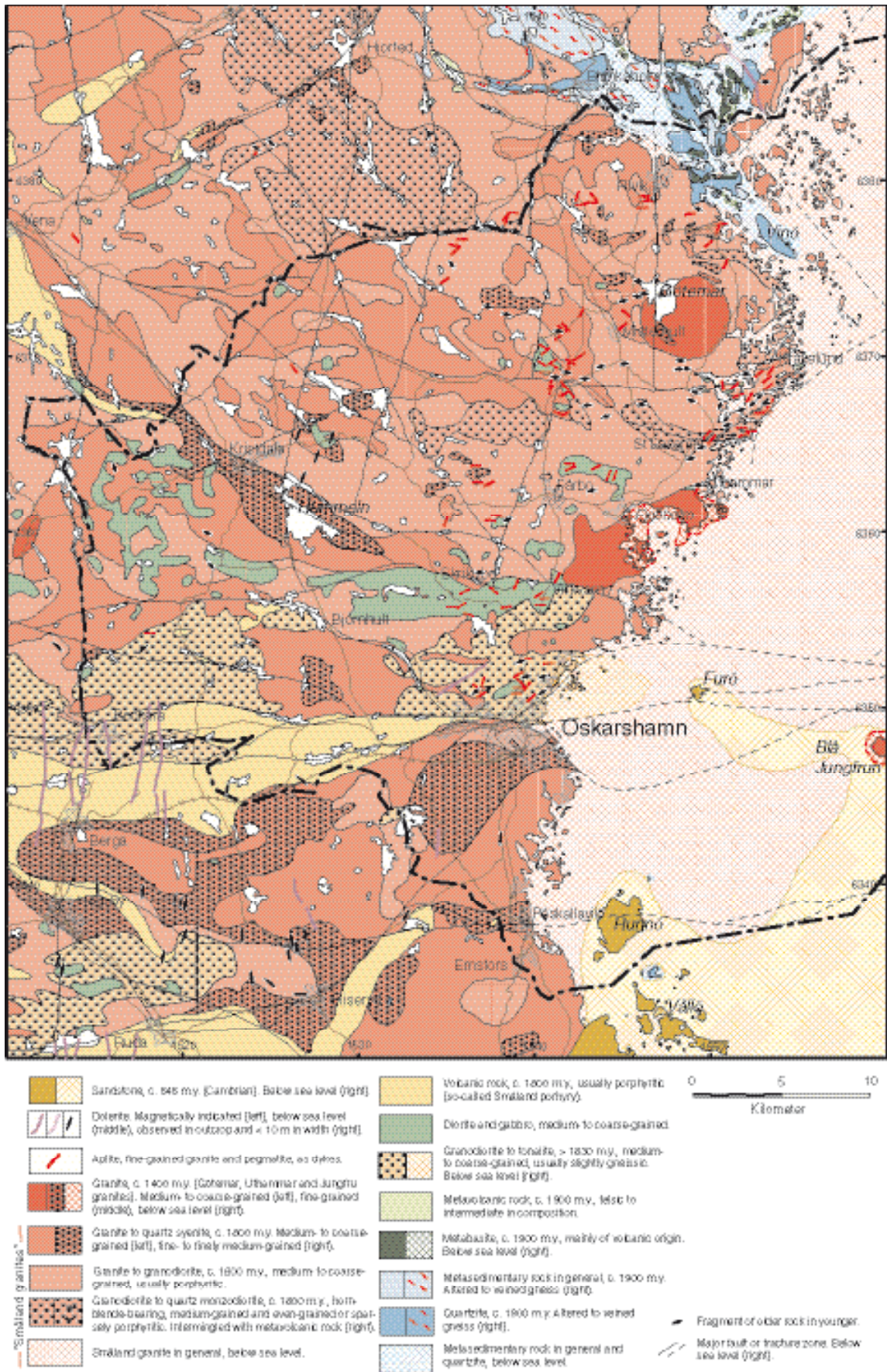


Figure 3-8. Bedrock map of the Oskarshamn municipality and the surrounding area. Slightly modified after /Bergman et al. 1998/.

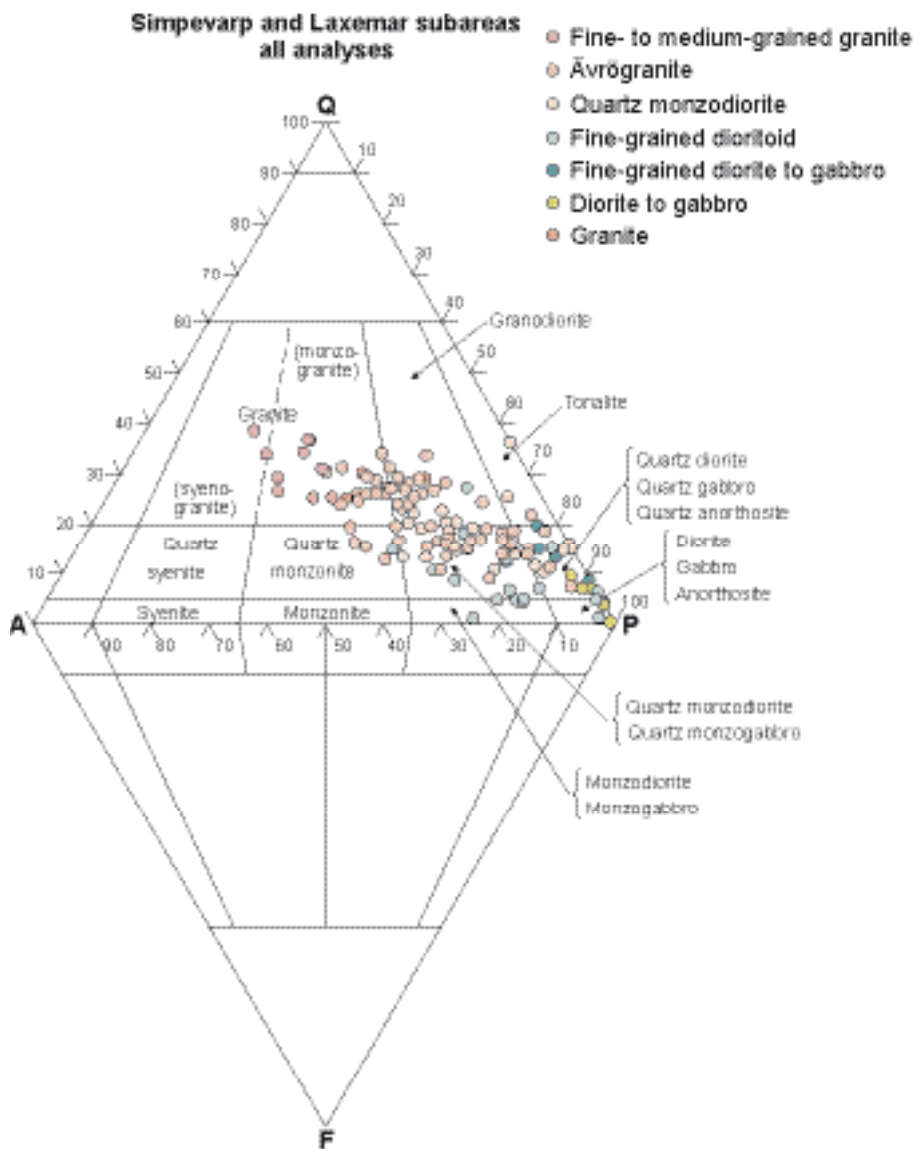


Figure 3-9. QAPF-diagram displaying the compositional variation of magmatic rocks, exemplified with modal analyses of rocks from the Simpevarp and Laxemar subareas.

In general, the sandstone infilling has been intruded by force downward into the basement /Röshoff and Cosgrove 2002/. A close spatial relationship between the sandstone dykes, the sub-Cambrian peneplain and Cambrian cover rocks indicates that the sandstone dykes are Cambrian in age. A characteristic feature is the local occurrence of fluorite (\pm calcite and galena) mineralisations within the pores of the sandstone dykes and along the dyke/country rock interface. The timing of formation of the mineralisations is uncertain, but they post-date the formation of the sandstone dykes. /Alm and Sundblad 2002/ claimed that the mineralisations are post-Cambrian and pre-Silurian in age, whereas /Röshoff and Cosgrove 2002/ suggested that they are pre-Permian in age.

3.1.3 Structural development

Ductile deformation

The bedrock of southeastern Sweden has gone through a long and complex structural development, including both ductile and brittle deformation, since the formation of the oldest c. 1,890–1,850 Ma supracrustal rocks. The oldest deformation, which was developed under medium- to high-grade metamorphic conditions, is of regional, penetrative character, and is recorded in the supracrustal rocks in the Blankaholm-Västervik area. It pre-dates the intrusion of the c. 1,860–1,850 Ma generation of TIB rocks which, however, are deformed themselves. At variance from the more or less

penetrative pre-1,860 Ma deformation in the supracrustal rocks, the deformation that has affected the 1,860–1,850 Ma generation of TIB rocks, as well as the older supracrustal rocks, was heterogeneous in character. It was caused by dextral transpression under medium-grade metamorphic conditions in response to c. N-S to NNW-SSE regional compression (see Figure 3-2), is constrained to the time-interval c. 1,850–1,800 Ma, and is exemplified by the dextral, strike-slip dominated Loftahammar-Linköping deformation zone, cf. Figure 3-7 /Stephens and Wahlgren 1996, Beunk and Page 2001/. However, the folding of the foliation in the pre-1,850 Ma rocks was also supposedly developed in response to the same stress field /Stephens and Wahlgren 1996, Beunk and Page 2001/.

The 1,810–1,760 Ma generation of TIB rocks, that dominates the bedrock in the Oskarshamn region, is post-tectonic in relation to the regional, penetrative deformation related to the peak of the Svecokarelian orogeny. However, these rocks are characterised by a system of ductile deformation zones of the same character as the Loftahammar-Linköping deformation zone, though developed during more low-grade metamorphic conditions, i.e. at shallower levels in the crust than the initial phase of shearing in the Loftahammar-Linköping deformation zone. However, the latter zone displays ductile reactivation during low-grade metamorphic conditions, which presumably is contemporaneous with the shearing in the 1,810–1,760 Ma TIB rocks. In the Oskarshamn region, these low-grade, ductile deformation zones are exemplified by the E-W trending Oskarshamn-Bockara and NE-SW trending Oskarshamn-Fliseryd deformation zones /Bergman et al. 1998/. Presumably, also the NE-SW trending Äspö shear zone /Gustafson et al. 1989, Bergman et al. 2000/, which is characterised by a sinistral strike-slip component, belongs to this system of ductile deformation zones (Figure 3-10).

Independent of the syn-deformational metamorphic grade, the dextral and sinistral strike-slip component in the WNW-ESE to NW-SE and NE-SW trending ductile deformation zones, respectively, indicate that a regional, c. N-S to NNW-SSE compression prevailed during their formation and subsequent ductile reactivation. Consequently, this regional stress field is inferred to have prevailed for a considerable period, at least from the time of the intrusion of the 1,850 Ma TIB generation, or possibly earlier, until c. 1,750 Ma ago. Most of the lithological contacts in the region, and also in the whole of southeastern Sweden, are more or less concordant with the orientation of the ductile deformation zones, which indicates that the emplacement of the TIB magmas was facilitated by ongoing shear zone activity. Together with the subsequent deformation of the TIB rocks, this testifies to the influence of the deformation zones in the present structural and lithological frame-work in the bedrock of southeastern Sweden.



Figure 3-10. Strongly deformed, protomylonitic porphyritic granite in the Äspö shear zone

The structural and metamorphic overprinting in rocks in the Oskarshamn region in relation to their age of formation is summarised in Table 3-1.

Apart from the mylonitic foliation in the ductile deformation zones, the 1,810–1,760 Ma TIB rocks locally display a more or less well-developed foliation /Kornfält and Wikman 1987, Persson Nilsson et al. 2004, Wahlgren et al. 2004, Wahlgren et al. 2005a/, e.g. preferred orientation of feldspar phenocrysts, mafic enclaves, biotite etc. However, it is often difficult to decide whether the foliation is syn-intrusive or caused by a subsequent tectonic overprinting. Independent of origin, field relationships indicate a time wise relationship between foliation development outside the ductile deformation zones and the shear zone activity.

The kinematics in the ductile shear zones is focussed on in an ongoing study in connection with the complete site investigation in Oskarshamn.

Brittle deformation

To unravel the brittle tectonic history in the bedrock in southeastern Sweden during the last c. 1,450 Ma is difficult. It is plausible that tectonic activities that are related to more or less remote large-scale processes, such as e.g. the Gothian, Hallandian, Sveconorwegian and Caledonian orogenies, the opening of the Iapetus Ocean, the Late Palaeozoic Variscan and the Late Mesozoic to Early Cenozoic Alpine orogenies, as well as the opening of the present Atlantic Ocean, have had a far-field effect within the shield area, cf. Table 3-2. In a global tectonic perspective, the Sveconorwegian orogeny, which corresponds to the Grenville orogeny in North-America and elsewhere, ultimately resulted in the assembly of the supercontinent Rodinia c. 900 Ma ago. Likewise the Caledonian orogeny (collision between the Laurentian and Fennoscandian Shields) was the first step in the formation of the supercontinent Pangaea, the latter part of which was finally assembled in connection with the Hercynian-Variscan orogeny in central Europe c. 250 Ma ago.

To what degree these large-scale processes have affected the bedrock in the Oskarshamn region and the rest of southeastern Sweden, and especially which brittle structure, may have been formed or have been reactivated is difficult to decipher. The main reason for this uncertainty is the great lack of time markers for relative dating, except for the sub-Cambrian peneplain and the Cambro-Ordovician cover rocks, and the difficulties in dating brittle structures radiometrically.

Since no ductile deformation has been observed in the c. 1,450 Ma granites /e.g. Talbot and Ramberg 1990, Munier 1995/ or younger rocks, it is evident that only deformations under brittle conditions have affected the bedrock in the Oskarshamn region during at least the last c. 1,450 Ma. However, the transition from ductile to brittle deformation presumably took place during the time interval c.1,750–1,700 Ma, i.e. during uplift and stabilization of the crust after the Svecokarelian orogeny.

During the subsequent geological evolution, faults and older ductile deformation zones have been reactivated repeatedly, due to the increasingly brittle behaviour of the bedrock. Brittle reactivation of ductile deformation zones is a general phenomenon. The Oskarshamn-Bockara, Oskarshamn-Fliseryd and Äspö shear zones display clear evidence of being reactivated in the brittle régime /see also e.g. Munier 1995/. An inversion of the strike-slip component in the Äspö shear zone from sinistral during the older ductile deformation, to dextral during the younger brittle reactivation has been proposed by /Talbot and Munier 1989/ and /Munier 1989/.

Table 3-1. The relation between age of rocks and the structural and metamorphic overprinting.

Age (Ma)	Structural and metamorphic overprinting
540	Brittle deformation. The rocks are well-preserved.
1,100–900	Brittle deformation. The rocks are well-preserved.
1,450	Brittle deformation. The rocks are well-preserved.
1,810–1,760	Spaced ductile shear zones developed under low-grade metamorphic conditions. Although the majority of the rocks are structurally more or less well-preserved, a low- to very low-grade alteration has occurred.
1,834–1,823	Inhomogeneous ductile deformation under low- to medium-grade metamorphic conditions.
1,860–1,850	Inhomogeneous ductile deformation under medium-grade metamorphic conditions.
1,880–1,870	Penetrative, ductile deformation under medium- to high-grade metamorphic conditions.

K-Ar dating of biotites from the “Småland granites” /Åberg 1978/ has yielded ages of c. 1,500–1,400 Ma. According to /Åberg 1978/, the obtained ages are caused by the c. 1,500–1,400 Ma magmatic activity in southern Sweden. However, /Tullborg et al. 1996/ considered the closure of the K-Ar system in this time interval to be the result of an uplift scenario. Independent of the interpretation of the c. 1,500–1,400 Ma K-Ar ages, these ages imply that the present day erosional level of the bedrock in the Oskarshamn region passed through the closure temperature of c. 300°C for the K-Ar isotope system in pre-Sveconorwegian time.

The occurrence of c. 1,000–900 Ma dolerite dykes in southeastern Sweden testifies to a Sveconorwegian tectonic influence, as the intrusion of the parent magmas was tectonically controlled. However, whether individual faults or fracture zones, which were not injected by mafic magma, were formed or reactivated during the Sveconorwegian orogeny, and if so which of them, is uncertain.

On the basis of titanite and zircon fission track studies in the Oskarshamn region, it has been suggested that sediments that were derived from the uplifted Sveconorwegian orogenic belt and deposited in a Sveconorwegian foreland basin reached a thickness of c. 8 km in southeastern Sweden at around 850 Ma /Tullborg et al. 1996, Larson et al. 1999/. Subsequent exhumation of southeastern Sweden and erosion of the sedimentary pile were completed by the establishment of the sub-Cambrian peneplain at the end of the Neoproterozoic. Remnants of this sedimentary pile are found in the Almesåkra Group in the vicinity of Nässjö /Rodhe 1987/. Furthermore, apatite fission track ages in the Oskarshamn region indicate that Upper Silurian to Devonian sediments, which were derived from the uplift of the Caledonian orogenic belt and deposited in a Caledonian foreland basin, covered most of Sweden and reached a thickness exceeding 2.5 km /Tullborg et al. 1995, 1996, Larson et al. 1999/. Exhumation and subsequent erosion during the Early Mesozoic removed the sedimentary cover almost completely /Tullborg et al. 1995, 1996, Larson et al. 1999/. During the Cretaceous, a transgression occurred which resulted in a thin cover of marine sediments. In the Oskarshamn, region the sedimentary cover was not completely removed until the Tertiary /Lidmar-Bergström 1991/.

The above-mentioned repeated large-scale events of subsidence, deposition of sediments, and subsequent exhumation and erosion, reasonably must have been accompanied by tectonic activity, i.e. movements along faults. However, there is no information that helps to decipher which fracture zones (faults) formed or were reactivated during these periods.

A recently performed (U-Th)/He geochronological study on apatites from rocks sampled in the access tunnel to the Äspö Hard Rock Laboratory and the cored boreholes KLX01 and KLX02 in the Laxemar area, yields decreasing ages with increasing depth (c. 270 Ma at the surface and c. 120 Ma at 1,700 m). This indicates that exhumation took place primarily during Late Palaeozoic to Mid Mesozoic and that no, or very little, exhumation has taken place after approximately 100 Ma /Söderlund et al. 2005/. Movement during the exhumation probably reactivated old fault zones, e.g. the Äspö shear zone. An ongoing complementary (U-Th)/He geochronological study will try to estimate offset and movements in some of the faults in the Simpevarp area. Furthermore, a complementary $^{40}\text{Ar}/^{39}\text{Ar}$ study will focus on the older uplift history of the bedrock in the Simpevarp area.

According to /Milnes and Gee 1992/ and /Munier 1995/, the Ordovician cover rocks along the north-western coast of Öland are tectonically undisturbed, except for displacements at the centimetre scale. This suggests that the E-W trending fracture zones/faults in the Oskarshamn-Bockara deformation zone, which can be seen in the magnetic anomaly maps to continue eastwards under Öland, have not affected the Cambro-Ordovician cover sequences on Öland. Thus, this indicates that these brittle deformation zones of regional character were not active in post-Cambrian time, but are related to the Precambrian tectonic evolution. However, post-Cambrian fracture zones/faults do occur in the Oskarshamn region. On the northwestern part of Furö, a small island c. 10 km east of Oskarshamn, cf. Figure 3-8, a brecciated fault contact between a Cambrian sandstone and a red granite is recorded /Bergman et al. 1998/. Furthermore, the observed sandstone in the deformation zone in a cored borehole as mentioned above indicates fault movements in post-Cambrian time. Another indication of post-Cambrian deformation is the occurrence of joints filled with sandstone only east of the N-S trending fault in the western part of the Götemar granite, i.e. the eastern block has been down-faulted in relation to the western block /Kresten and Chyssler 1976, Bergman et al. 1998/.

As mentioned above, the sub-Cambrian peneplain is a potential marker to demonstrate post-Cambrian brittle tectonics. In general, all pronounced depressions and distinct differences of topographic level in the sub-Cambrian peneplain constitute potential fracture zones or faults. /Tirén et al. 1987/ studied the relative movements of regional blocks in southeastern Sweden which were bounded by fracture zones and ranged in size between 25 km² and 100 km². Differential movements were interpreted to have occurred along existing faults both during periods of uplift and subsidence. Furthermore, it was concluded that block faulting occurred at different scales, e.g. minor block faulting occurred inside large fault bounded rock blocks.

A general problem is to decipher the relation between the formation and subsequent reactivation of faults and fracture zones. Especially, the mutual age relationship between fracture zones with different orientation is difficult to determine, mainly due to the complex relationship between age of formation and age of (latest?) reactivation. Another, and perhaps the most important complicating factor is that brittle deformation zones are very poorly exposed, since they mostly constitute topographical depressions filled with glacial cover, rivers, swamps etc.

The brittle deformation history of a region can be regarded as the combined effect of generation of new fractures or faults and reactivation of old fractures or faults. The ratio between generation of new structures and reactivation of older structures is presumed to decrease with time, since the orientation spectrum of pre-existing structures increases with every new event of brittle deformation /Munier 1995/. Relative age determinations of fractures, based on orientation and a succession of mineral filling with decreasing age, have been recorded on Äspö /e.g. Munier 1995/, and it is reasonable to assume that these findings can be extrapolated to the surrounding parts of the Oskarshamn region. The oldest fractures are epidote- and quartz-bearing, and with decreasing age chlorite, zeolite and calcite appear as fracture fillings. Since the mineralogy in individual fractures within fracture zones is essentially similar to that of fractures in the intervening blocks /Munier 1995/, the fracture filling is a tool for relative age determination of movement (reactivation) of the former. Consequently, the calcite-bearing fracture zones/faults represent the youngest reactivation, but its absolute age is uncertain. However, an ongoing study of fracture fillings and hydrothermal alteration shows that different generations of calcite occur, whereas zeolite and calcite represents the youngest fracture filling (see Section 5.2.7). At least one generation of calcite fracture fillings is assumed to be of Palaeozoic age since the calcite overprints fractures filled with sandstone of presumed Cambrian age.

Based on data from Äspö, the orientation of the maximum compressive stress during the formation of the epidote- and quartz-bearing fracture zones was N-S/subhorizontal /Munier 1989/, but had changed orientation to NE-SW when the chlorite-filled fracture zones/faults formed /Talbot and Munier 1989/. The maximum horizontal compression in the region was still NE-SW when the fractures formed which are filled with Cambrian sandstone /Talbot and Munier 1989/. However, this does not necessarily indicate the orientation of the large-scale, regional stress field. The orientation of the maximum horizontal compressive stress during the subsequent tectonic evolution is presumed to have been the same as the present stress regime, i.e. NW-SE in relation to the present geographic coordinate system. Consequently, a roughly NW-SE maximum compressive stress is inferred to have prevailed for a considerable period of time, i.e. possibly for hundreds of million of years.

Attempts have been made to use palaeomagnetic, electron spin resonance (ESR) and isotopic dating (K-Ar, Rb-Sr) techniques on some brittle structures at the Äspö site /Maddock et al. 1993/, in order to constrain the minimum age of the most recent movements. Characterization of the sampled fault gouge material demonstrated that many fracture zones contain sequentially developed fault rocks and verifies that reactivation has occurred.

The ages given by the various dating methods reflect both inherent differences in the techniques and differences in the phase or phenomenon being dated. The interpretation of the ESR dating, which was limited by the resolution of the method, yielded minimum ages of movements in the order of several hundred thousand to one million years. The results of the palaeomagnetic and K-Ar analyses strongly suggest that growth of the fracture infilling minerals took place at least 250 million years ago. The most recent fault movements are interpreted to have preceded this mineral growth. /Maddock et al. 1993/ concluded that any Quaternary and Holocene activity had little effect on the fracture zones.

According to /Mörner 1989/, a great number of supposed post-glacial faults occur on Äspö. However, none of the faults reported showed any positive evidence of movements /SKB 1990/. Some of the reported faults did not display any disturbance of Precambrian markers, others had their bases exposed by excavation and ice plucking could be positively demonstrated. /Talbot and Munier 1989/ discussed post-glacial faults in connection with studied fault scarps, i.e. abrupt steps in the glacially polished bedrock surface on Äspö. According to /Munier 1995/, post-glacial reactivation of individual fractures has most likely occurred, but despite searches no evidence of such features has been found on outcrops.

Ongoing tectonic activity is manifested in seismic events and aseismic slip /Larson and Tullborg 1993/. According to /Slunga et al. 1984/, the so-called Protogine Zone of southern Sweden (cf. Figure 3-7), has been shown to be the border between a more seismic western Sweden and a more aseismic southeastern Sweden. Even though southeastern Sweden is a seismically very quiet area (Figure 3-11), an earthquake of magnitude 3.3 and a focal depth of 5.0 km was recorded c. 100 km south of Gotland in December 2002 /Bödvarsson 2003/. In addition, an earthquake of magnitude 2.0 was recorded c. 21 km northwest of Oskarshamn 28th March, 1996 (Bödvarsson pers. comm.), and in September 1988, an earthquake of magnitude 1.0 and focal depth of c. 16 km was recorded c. 30 km south of Oskarshamn /Slunga and Nordgren 1990/. The orientation of the maximum horizontal principal stress relaxed by this earthquake, as well as other seismic events in Sweden, was c. NW-SE /Slunga et al. 1984, Slunga and Nordgren 1990/. This is in agreement with the results from rock stress measurements at depths of more than 300 m /Stephansson et al. 1987/, and also with the stress field generated by plate movements in the North Atlantic Ocean

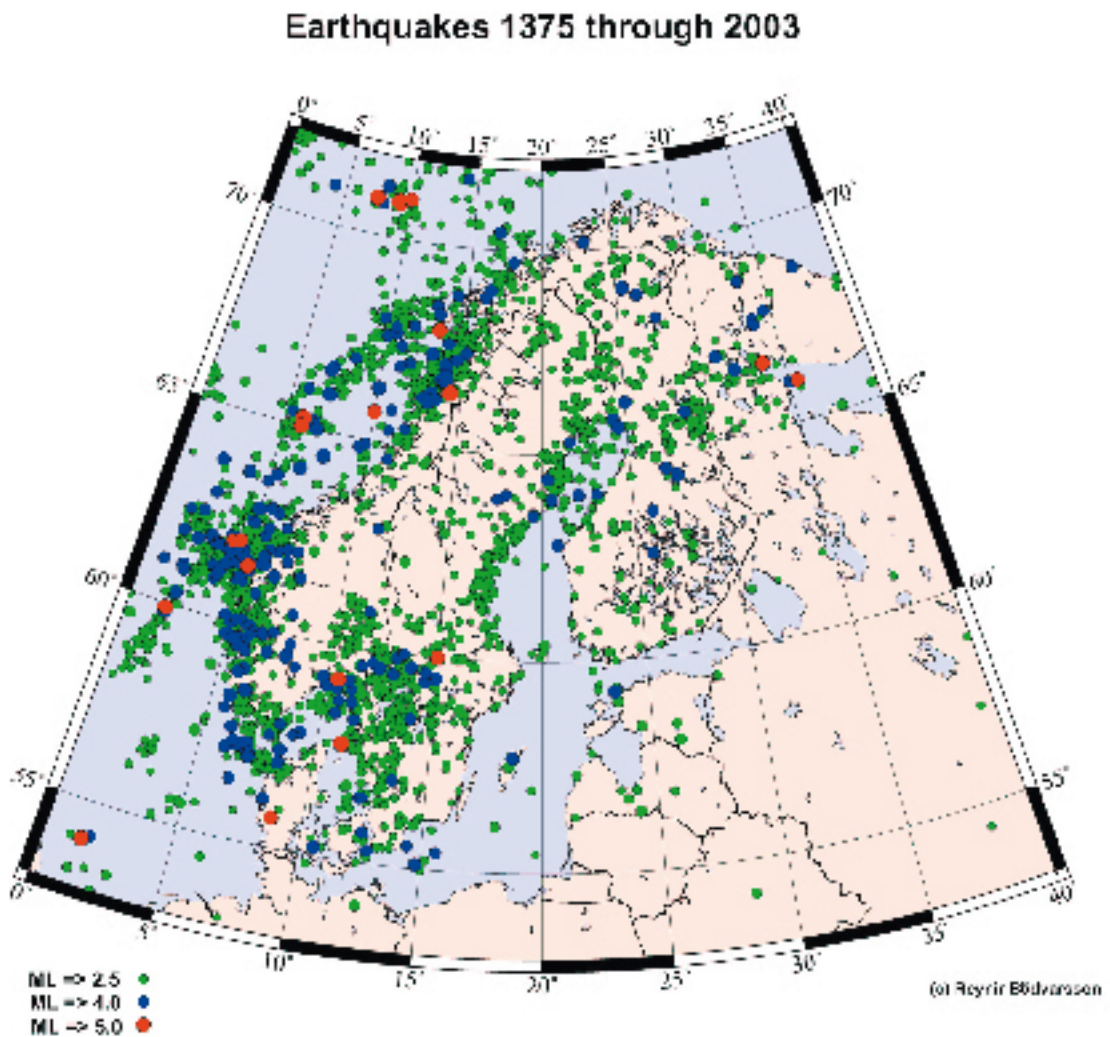


Figure 3-11. Earthquake epicentra in Scandinavia and Finland 1375–2003. Data from the University of Uppsala.

/cf. Slunga 1989, Gregersen et al. 1991, Gregersen 1992/. According to /Slunga and Nordgren 1990/, recent seismic activity in southeastern Sweden is related to plate-tectonic forces and not directly to land upheaval subsequent to and consequent on the last glaciation. /Gregersen et al. 1991/ and /Gregersen 1992/ came to the same conclusion based on focal mechanisms for present-day earthquakes in Fennoscandia. However, /Muir-Wood 1993/ and /Wu et al. 1999/ suggested that post-glacial rebound appears to be the cause of post-glacial seismic activity in Fennoscandia.

The geological evolution in southeastern Sweden, with focus on the Oskarshamn region, is tentatively summarised in Table 3-2.

Table 3-2. Tentative synopsis of the geological evolution in southeastern Sweden with a focus on the Oskarshamn region.

Age (Ma)	Geological event
0.115-0	Glaciation; syn- to post-glacial fault movements?; NW-SE to WNW-ESE maximum horizontal principal stress
95-0	Alpine orogeny (central Europe); Final break-up of the supercontinent Pangaea; opening and spreading of the North Atlantic Ocean; <i>brittle deformation in the cratonic Oskarshamn region as a far-field effect?</i>
> 250	<i>Latest fault movements at Äspö? (K-Ar dating of gouge material)</i>
295-60	Tectonic activity in the Tornquist Zone (Fennoscandian border zone); <i>brittle deformation in the cratonic Oskarshamn region as a far-field effect?</i>
360-295	Hercynian-Variscan orogeny (central Europe). Final assembly of the supercontinent Pangaea; <i>Brittle deformation in the cratonic Oskarshamn region as a far-field effect?</i>
420-220	Subsidence related to the development of a Caledonian foreland basin, sedimentation followed by exhumation and erosion; <i>brittle deformation in the cratonic Oskarshamn region?</i>
510-400	Caledonian orogeny ; closure of the Iapetus Ocean; formation of the Scandinavian Caledonides; WNW-ESE shortening (regional compression?) followed by extensional collapse; <i>brittle deformation in the cratonic Oskarshamn region as a far-field effect of orogenic deformation in western Baltica?</i>
600-550	Peneplanation; Sub-Cambrian peneplain; Marine transgression and extensive sedimentation
700-600	Final break-up of the supercontinent Rodinia and opening of the Iapetus Ocean; <i>far-field effect in the cratonic Oskarshamn region?</i>
900-700	Subsidence related to the development of a Sveconorwegian foreland basin, sedimentation followed by exhumation and erosion; Almesåkra group; Rifting, graben formation, sedimentation in the Vättern area; Visingsö group; <i>brittle deformation in the cratonic Oskarshamn region?</i>
1,100-900	Sveconorwegian orogeny ; formation of the Sveconorwegian Frontal Deformation Zone ("Protogine Zone"); WNW-ESE to E-W regional compression; intrusion of dolerites - E-W extension; Assembly of the supercontinent Rodinia; <i>Brittle deformation in the cratonic Oskarshamn region as a far-field effect of orogenic reworking of the crust in southwestern Sweden?</i>
1,460-1,420	Hallandian orogeny ; <i>Brittle deformation in the cratonic Oskarshamn region as a far-field effect?</i>
1,450	Intrusion of granite (e.g. Götemar and Uthammar granites)
1,610-1,560	Gothian orogeny ; <i>Brittle deformation in the cratonic Oskarshamn region as a far-field effect?</i>
1,750-1,700	Transition from ductile to brittle tectonic régime
1,800-1,750	Formation of transpressive, ductile deformation zones in response to c. N-S to NNW-SSE regional compression under low-grade conditions. Deformation zones with NW-SE to WNW-ESE and NE-SW direction display dextral and sinistral horizontal component, respectively.
1,810-1,760	Intense igneous activity; Intrusion of granite-syenitoid-dioritoid-gabbroid ("Småland granite"), composite dykes; Sedimentation and volcanic activity
1,830-1,810	Regional, inhomogeneous deformation under (low)- to medium-grade conditions
1,830-1,820	Intrusion of granitoids; volcanic activity?
1,850(-1,800)	Formation of transpressive, ductile deformation zones with a dextral horizontal component of movement, in response to c. N-S to NNW-SSE regional compression under medium-grade metamorphic conditions; <i>folding of foliation in pre-1,850 Ma rocks</i>
1,850	Intrusion of granite-syenitoid-dioritoid-gabbroid
1,890-1,850	Volcanic activity and sedimentation; regional deformation under medium- to high-grade conditions
1,960-1,750	Svecokarelian orogeny

3.2 Overburden including Quaternary deposits

The Quaternary record gives information about past processes and climatic variations. The interpretation of this development is of fundamental importance when explaining the distribution of Quaternary deposits. This information can also be used when discussing future scenarios for the Simpevarp area. Most results and interpretations that are discussed in this section are based on investigations that have been carried out outside the Simpevarp model area.

3.2.1 Quaternary development of Sweden

The Quaternary is the present geological period and is characterised by alternating cold glacial and warm interglacial stages. The glacial stages are further subdivided into cold phases, stadials, and relatively warm phases, interstadials. A combination of climatic oscillations of high amplitude, together with the intensity of the colder periods, is characteristic of the Quaternary period. At the Geological Congress in London, 1948 the age of the Tertiary/Quaternary transition, as used here, was determined to be 1.65 million years. More recent research, however, suggests that the Quaternary period started c. 2.4 million years ago /e.g. Šibrava 1992, Shackelton 1997/. The Quaternary period is subdivided into two epochs: the Pleistocene and the Holocene. The latter represents the present interglacial, which began c. 11,500 years ago.

Results from studies of deep-sea sediment cores suggest as many as fifty glacial/interglacial cycles during the Quaternary /Shackelton et al. 1990/. The climate during the past c. 900,000 years has been characterised by 100,000 years long glacial periods interrupted by interglacials lasting for approximately 10,000–15,000 years. The coldest climate, and largest ice sheets, occurred toward the end of each of the glacial periods. Most research indicates that the long-term climate changes (> 10,000 years) are triggered by variations in the earth's orbital parameters. However, there is not universal agreement on this point. The warm interglacials are relatively short compared to the glacial periods. It is therefore likely that the present interglacial Holocene will be followed by a long period of colder climate and Scandinavia will probably be covered by ice once more. However, the anthropogenic burning of fossil fuel is causing increasing atmospheric concentrations of green house gases, mainly CO₂. These gases will probably cause a warmer global climate in the nearest future, the so-called greenhouse effect. Quaternary climatic conditions, with a focus on Sweden, have been reviewed by /e.g. Morén and Pässe 2001/.

The most complete stratigraphies used in Quaternary studies are from the well-dated sediment cores retrieved from the deep sea, which have been used for studies of e.g. oxygen isotopes /e.g. Shackelton et al. 1990/. The marine record has been subdivided into different Marine Isotope Stages (MIS), which are defined based on changes in the global climatic record. Quaternary stratigraphies covering the time before the Last Glacial Maximum (LGM) are sparse in areas that have been repeatedly glaciated, such as Sweden. Furthermore, these stratigraphies are often disturbed by erosion and are difficult to date absolutely. Our knowledge of the pre-LGM Quaternary history of Sweden is, therefore, to a large extent based on indirect evidence from non-glaciated areas.

In most parts of Sweden, the relief of the bedrock is mainly of Pre-Quaternary age and has only been slightly modified by glacial erosion /Lidmar-Bergström et al. 1997/. In Sweden, the average erosion during the Quaternary period has been estimated to represent 12 m of fresh bedrock /Pässe 2004/. In the same report, the average erosion of bedrock during one glacial cycle is estimated to be 1 m. The magnitude of the glacial erosion seems, however, to vary considerably geographically. Pre-Quaternary deep weathered bedrock occurs in areas such as the inland of eastern Småland, southern Östergötland and the inner parts of northernmost Sweden /Lundqvist 1985, Lidmar-Bergström et al. 1997/. The occurrence of saprolites indicates that these areas have only been affected to a small extent by glacial erosion.

In some areas, such as in large parts of inner northern Sweden, deposits from older glaciations have been preserved, which indicates that the subsequent glaciations have had a low erosional capacity /e.g. Hättestrand and Stroeven 2002, Lagerbäck and Robertsson 1988/. However, such deposits occur also in some areas, e.g. Skåne, which have been glaciated during a relatively short period of time.

3.2.2 The Pleistocene

The global oxygen isotope record indicates numerous glaciations during the Quaternary Period. Several of these glaciations have probably affected Sweden. It is, however, at present impossible to state the total number of Quaternary glaciations in Sweden.

In Sweden, the preserved geological information from Pleistocene is, as mentioned above, fragmentary. Pleistocene deposits have mainly been found in areas, which have been subjected to glaciations during a short period of time, e.g. Skåne, or where the glacial erosion has been low due to cold-based ice conditions. It has been suggested that these latter conditions occurred in the inner parts of northern Sweden during the middle and late parts of the latest glaciation, the Weichselian, cf. Figure 3-12. Most Pleistocene deposits have been correlated with the stadials and interstadials that occurred during the latest glaciation. There are, however, a few sites with older Pleistocene deposits. Inorganic deposits such as glacial till have not been dated with absolute methods and such deposits from early stages of the Quaternary Period may therefore exist.

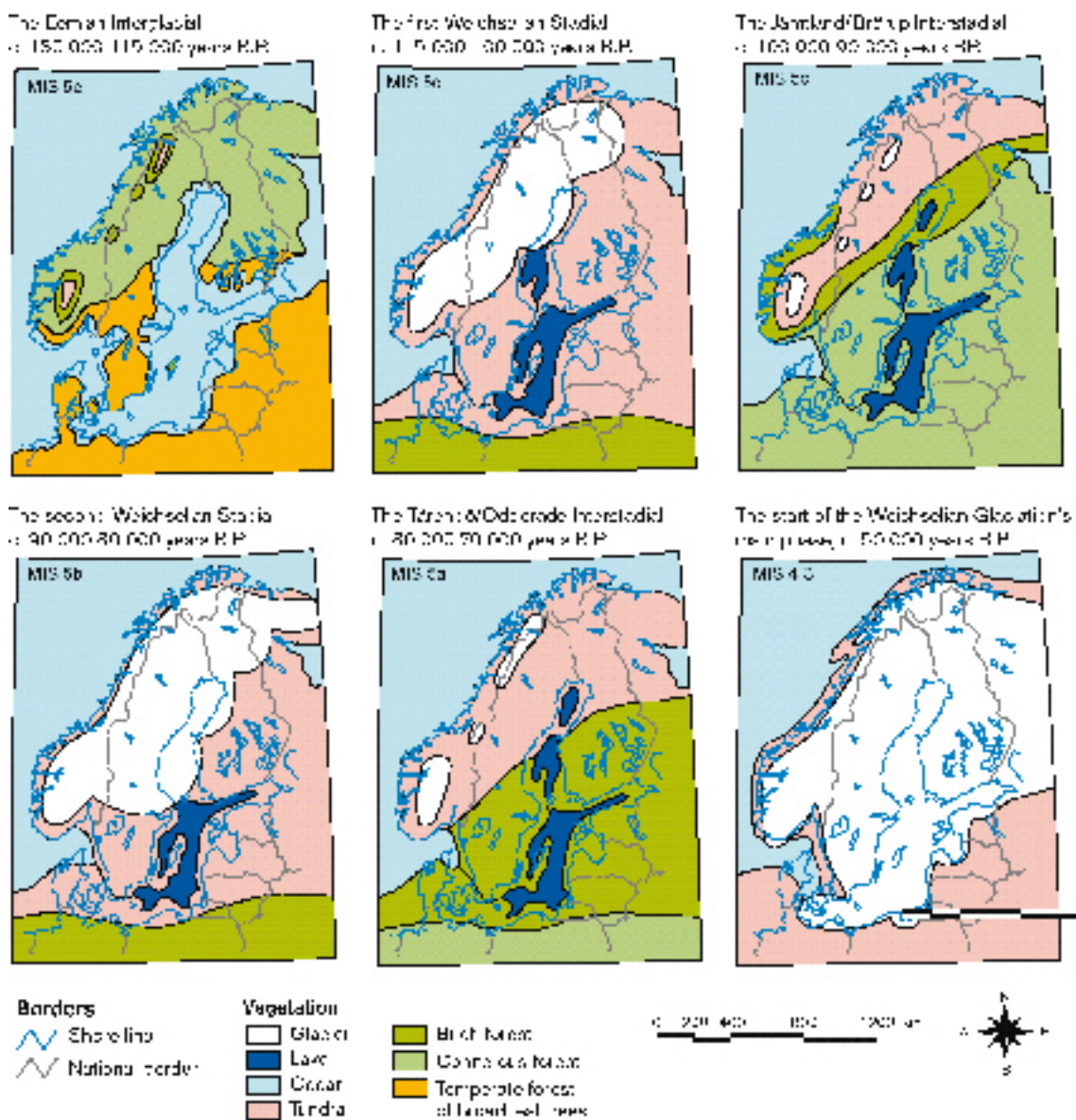


Figure 3-12. The development of vegetation and ice cover in northern Europe during the latest interglacial (Eem) and first half of the last ice age (Weichsel). The different periods have been correlated with the Major Isotope stages (MIS). The maps should be regarded as hypothetical due to the lack of well dated deposits from the different stages /from: Sveriges Nationalatlas, www.sna.se/.

There are traces of three large glaciations, Elster (MIS 8), Saale (MIS 6) and Weichsel (MIS2–5d), that reached as far south as northern Poland and Germany /e.g. Fredén 2002/. Saale had the largest maximum extension of any known Quaternary ice sheet. There were two interglacials, Holstein and Eem, between these three glacials.

The oldest interglacial deposits in Sweden, dated by fossil composition, were probably deposited during the Holstein interglacial (MIS 7, c. 230,000 years ago) /e.g. Ambrosiani 1990/. The till underlying the Holsteinian deposits may have been deposited during Elster and is the oldest known Quaternary deposit in Sweden.

Deposits from the Eemian interglacial (MIS 5e, 130,000–115,000 years ago) are known from several widely spread sites in Sweden /e.g. Robertsson et al. 1997/. The climate was periodically milder than it has been during the present interglacial, Holocene. The sea level was, at least periodically, higher than at present and large parts of the Swedish lowland were probably covered with brackish or marine water.

The latest glacial, the Weichselian started c. 115,000 years ago. It was characterised by colder phases, stadials, interrupted by milder interstadials. Numerous sites with deposits from the early part of Weichsel are known from the inner parts of northern Sweden. The model presented by /e.g. Fredén 2002, Lundqvist 1992/ is often used to illustrate the history of Weichsel (Figure 3-12). Two interstadials took place during the early part of Weichsel, approximately 100,000–90,000 (MIS 5c) and 80,000–70,000 years ago (MIS 5a). Most of Sweden was free of ice during these interstadials, but the climate was considerably colder than today and tundra with shrub vegetation probably characterised northern Sweden.

Southern Sweden was covered with coniferous forests during the first of these interstadials. The second interstadial (correlated with MIS 5a) was colder and the vegetation in southern Sweden was probably characterised by a sparse birch forest. Most researchers agree that the ice did not reach further south than the Mälaren Valley during the Early Weichselian stadials. The ice advanced south and covered southern Sweden first during the Mid Weichselian (c. 70,000 years ago). Most of Sweden was thereafter covered by ice until the deglaciation. Parts of Skåne were, however, free of ice until a few thousand years before the LGM.

The models presented by /Fredén 2002/ and /Lundqvist 1992/ have been debated (Figure 3-12). Most researchers agree that at least two interstadials, with ice-free conditions, did occur during the Weichselian glaciation. However, since the dating of such old deposits is problematic, the timing of these interstadials is uncertain. Investigations from both Finland and Norway suggest that most of the Nordic countries were free of ice during parts of Mid Weichselian (MIS 3–4) /e.g. Olsen et al. 1996, Ukkonen et al. 1999/. That may imply that one of the interstadials attributed to Early Weichselian by /Fredén 2002/ may have occurred during Mid Weichsel. In large parts of Sweden, the total time of ice cover during Weichsel may therefore have been considerably shorter than previously has been suggested by /e.g. Fredén 2002/.

During the last glacial maximum (LGM), c. 20,000 years ago (MIS 2), the continental ice reached its southernmost extent (Figure 3-13). The Weichselian ice sheet reached as far south as the present Berlin, but had a smaller maximal extent than the two preceding glacials (Saale and Elster).

3.2.3 The latest deglaciation

A marked improvement in climate took place about 18,000 years ago, shortly after the LGM and the ice started to withdraw, a process that was completed after some 10,000 years. The timing of the deglaciation of Sweden has been determined with ¹⁴C dates and clayvarve chronology. The deglaciation of eastern Sweden, including the Simpevarp and Forsmark areas, has mainly been studied by using clayvarve chronologies /Kristiansson 1986, Strömberg 1989, Brunnberg 1995, Ringberg et al. 2002/, whereas the timing of the deglaciation in other parts of Sweden has been determined with ¹⁴C dates. These two chronologies have recently been calibrated to calendar years /e.g. Fredén 2002, Lundqvist and Wohlfarth 2001/.

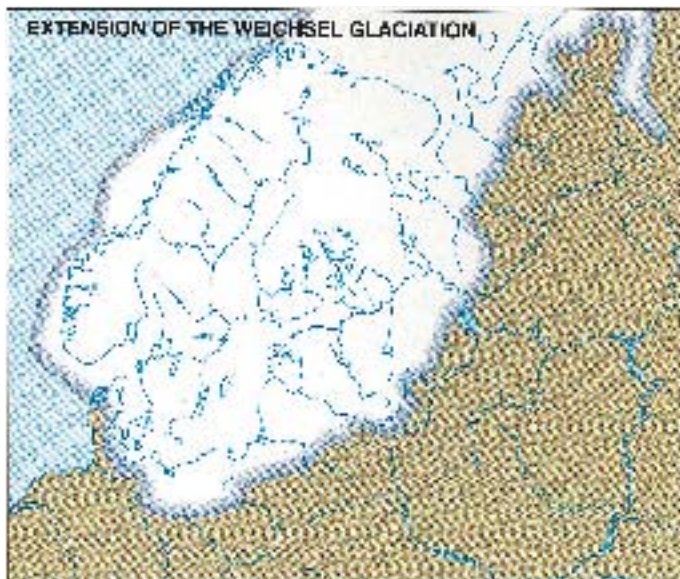


Figure 3-13. The maximum extent of the Weichselian ice sheet during MIS 2 approximately 20,000 years ago /from: Sveriges Nationalatlas, www.sna.se/.

There were several standstills and even readvances of the ice front during the deglaciation of southern Sweden. In western Sweden, zones with end moraines reflect these occasions. The correlations of ice marginal zones across Sweden are, however, problematic. In south-eastern Sweden, few end moraines developed because a lot of stagnant ice remained in front of the retreating ice sheet.

There was a major standstill and in some area readvances of the ice front during a cold period called the Younger Dryas (c. 13,000–11,500 years ago). The ice front then had an east west extension across Västergötland and Östergötland. The end of Younger Dryas marks the onset of the present interglacial, the Holocene. The ice retreated more or less continuously during the early part of the Holocene.

3.2.4 Climate and vegetation after the latest deglaciation

Pollen investigations from southern Sweden have shown that a sparse *Betula* (birch) forest covered the area soon after the deglaciation /e.g. Björck 1999/. There was a decrease in temperature during a cold period called the Younger Dryas (c. 13,000–11,500 years ago) and the deglaciated parts of Sweden were consequently covered by a herb tundra. At the beginning of the Holocene c. 11,500 years ago the temperature increased and southern Sweden was first covered by forests dominated *Betula* and later by forests dominated by *Pinus* (pine) and *Corylus* (hazel). The timing and climatic development of the transition between the Pleistocene and the Holocene has been discussed by /e.g. Björck et al. 1996, Andrén et al. 1999/.

Northern Sweden was deglaciated during the early part of Holocene when the climate was relatively warm. These areas were therefore covered by forest, mainly birch and pine, shortly after deglaciation.

Between 9,000 and 6,000 years ago the summer temperature was approximately 2° warmer than at present and forests with *Tilia* (lime), *Quercus* (oak) and *Ulmus* (elm) covered large parts of southern Sweden. These trees then had a much more northerly distribution than at present. The temperature has subsequently decreased, after this warm period, and the forests became successively more dominated by coniferous trees. During the Holocene, *Picea* (spruce) has spread successively from northernmost Sweden towards the south. This tree has not yet spread to Skåne and the Swedish west coast. The composition of vegetation has changed during the last few thousand years due to human activities, which have decreased the areas covered by forest. The ecological history of Sweden during the last 15,000 years has been reviewed by /e.g. Berglund et al. 1996/.

3.2.5 Development of the Baltic Sea after the latest deglaciation

A major crustal phenomenon that has affected and continues to affect northern Europe, following melting of the latest continental ice, is the interplay between isostatic recovery on the one hand and eustatic sea level variations on the other. During the latest glaciation, the global sea level was in the order of 120 m lower than at present, due to the large amounts of water stored in ice /Fairbanks 1989/.

In northern Sweden, the heavy continental ice load depressed the Earth's crust by as much as 800 m below its present altitude. As soon as the pressure started to decrease, due to thinner ice coverage, the crust started to rise (isostatic land uplift). This uplift started before the final deglaciation and is still an active process in most parts of Sweden. In Sweden, the highest identified level of the Baltic Sea or the West Sea is called the highest shoreline. This shoreline is situated at different altitudes throughout Sweden depending on how much the crust had been depressed. The highest levels, nearly 300 m, are found along the coast of northern Sweden but decrease to levels below 20 m in southern-most Sweden.

The development of the Baltic Sea since the last deglaciation is characterised by changes in salinity, which have been caused by variations in the sea level. This history has therefore been divided in four main stages /Björck 1995, Fredén 2002/, which are summarised in Table 3-3. Freshwater conditions prevailed during most of the deglaciation of Sweden. Weak brackish conditions prevailed 11,300–11,100 years ago during the Yoldia Sea stage /Andrén et al. 2000/. The salinity in the open Baltic proper (south of Åland) varied between 10–15‰ during the brackish phase of the Yoldia Sea /Schoning et al. 2001/. The Baltic was thereafter characterised by freshwater conditions until the onset of the Littorina Sea around 9,500 years ago /Fredén 2002, Berglund et al. 2005/. Salinity was probably low during the first c. 1,000 years of the Littorina Sea stage but started to increase 8,500 years ago. Salinity variations since the onset of the Littorina Sea have been summarised by /Westman et al. 1999/. The most saline period occurred 6,500–5,000 years ago when the surface water salinity in the Baltic proper (south of Åland) was 10–15‰ compared with approximately 7‰ today /Westman et al. 1999/. Variations in salinity during the Littorina Sea stage have mainly been caused by variations of freshwater input and changes of the cross-sectional areas in the Danish Straits /cf. Westman et al. 1999/.

The shoreline displacement in northern Sweden has been mostly regressive due to a large isostatic component. Along the southern part of the Swedish east and west coasts, the isostatic component was less and declined earlier during the Holocene, resulting in a complex shoreline displacement with alternating transgressive and regressive phases. The shoreline displacement in Sweden has been summarised by e.g. /Påsse 2001/.

Table 3-3. The four main stages of the Baltic Sea. The Littorina Sea here includes the entire period from the first influences of brackish water 9,500 years ago to the present Baltic Sea.

Baltic stage	Calendar year BP	Salinity
Littorina Sea <i>sensu lato</i>	9,500–present	Brackish
Ancylus Lake	10,800–9,500	Lacustrine
Yoldia Sea	11,500–10,800	Lacustrine/Brackish /Lacustrine
Baltic Ice Lake	15,000–11,550	Glacio-lacustrine

3.2.6 Quaternary history of the Simpevarp area

No studies dealing with Quaternary history have been carried out within the regional model area and our understanding of that history is therefore dependent on information from other areas.

All known overburden in the Simpevarp regional model area has been deposited during or after the Weichselian glaciation. Older glacial till and fluvial sediment of unknown age were, however, found during the SGUs mapping of Quaternary deposits in Västervik, c. 40 km north of Simpevarp /Svantesson 1999/. It can therefore not be excluded that Quaternary deposits, older than the last glaciation, exist also in the Simpevarp area. Furthermore several sites with saprolites of Pre-Quaternary

age are known in the inland of Småland, the closest c. 50 km west of the Simpevarp regional model area /Lidmar-Bergström et al. 1997/. These deposits indicate that the intensity of glacial erosion has been low in the areas west of Simpevarp. The occurrence of such “old” saprolite deposits in the regional model area can therefore not be excluded.

The marine isotope record suggests numerous glaciations during the Quaternary Period. The number of glaciations covering the Simpevarp area is, however, unknown. End moraines from three glaciations are known from northern Poland and Germany. It can therefore be concluded that the Simpevarp area has been glaciated at least three times, but probably more, during the Quaternary Period.

The Baltic Sea level was higher than at present during the Eemian interglacial and it is therefore likely that the local model areas were covered with brackish water during the main part of that interglacial.

The area was probably free of ice during the early Weichselian stadials and interstadials (Figure 3-13). It has been assumed that tundra conditions prevailed during the stadials /Fredén 2002/. The vegetation during the first Weichselian interstadial was probably dominated by coniferous forest, whereas the second interstadial was colder, with the forest sparse and dominated by *Betula* (Birch). The ice advanced south and covered the Simpevarp area first during Mid Weichselian (c. 70,000 years ago). The exact timing of the Mid Weichselian glaciation is, however, unknown and there are indications of ice free condition in large parts of Fennoscandia during parts of Mid Weichsel /Ukkonen et al. 1999/. The total time of ice coverage in the Simpevarp area may therefore have been considerably shorter than in the model presented by /Fredén 2002/.

According to glaciological models, the maximum thickness of the ice cover in the Oskarshamn region was more than 1.5 km at 18,000 years BP /Näslund et al. 2003/. Glacial striae on bedrock outcrops indicate a youngest ice movement from N30°W-N45°W and N40°W-N60°W in the Västervik and Oskarshamn areas, respectively /Svantesson 1999, Rudmark 2000/. Also, in the Simpevarp region, glacial striae as well as the orientation of eskers indicate a main ice movement direction from NW–NNW. Subordinate older striae indicate more westerly and northerly directions. In the Oskarshamn area, striae formed from north-east have been observed on the islands outside the present coast /cf. Rudmark 2000/, which indicates a period with an ice moving from the Baltic depression.

According to the calibrated clay-varve chronology, the Oskarshamn area was deglaciated almost 14,000 years ago /Lundqvist and Wohlfarth 2001/, during the Bölling chronozone. The ice front had a north-east south-west direction during the deglaciation, which is perpendicular to the latest ice movement (see above). Results from studies of clayvarves, along the coast of Småland, indicate that the ice margin retreated more or less continuously with a velocity of c. 125–300 m/year /Kristiansson 1986/. There are, however, indications of an ice marginal oscillation in the Vimmerby area /Agrell et al. 1976/ 40 km north-west of the regional model area. This oscillation has resulted in a series of ice marginal deposits which can be followed to Vetlanda c. 50 km south-west of Vimmerby /Lindén 1984/. This presumed oscillation may have taken place during or after the Older Dryas chronozone (c. 14,000 years ago).

The highest shoreline in the Oskarshamn region is c. 100 m above sea level /Agrell 1976/, and, thus the whole Simpevarp regional model area is situated below the highest shoreline. In the Simpevarp region, shoreline regression has prevailed and the rate of land uplift during the last 100 years has been c. 1 mm/year /Ekman 1996/.

The late Weichselian and early Holocene shoreline displacement in the Oskarshamn region has been studied with stratigraphical methods by /Svensson 1989/. According to that investigation, and several other publications /e.g. Björck 1995/, the shoreline dropped instantaneously c. 25 m due to drainage of the Baltic Ice Lake 11,500 years ago. This drainage was followed by the Yoldia Sea stage, which was dominated by freshwater conditions, but was influenced by brackish water for about 100–150 years. The onset of the following Ancylus Lake stage was characterised by a transgression of c 11 m. There are no studies from the Oskarshamn area dealing with the shoreline displacement during the Littorina Sea stage.

Salinity variations in the open Baltic proper, offshore from Oskarshamn, since the onset of the Littorina Sea is shown in /Westman et al. 1999/. However, since the Simpevarp area has been situated close to the coast during most of the Littorina stage it can be assumed that salinity has been generally lower than what is shown in /Westman et al. 1999/. Results from a study c. 100 km north of Simpevarp /Robertsson 1997/ suggest a regressive shore displacement during Littorina time. However, more detailed stratigraphical studies of sediments from areas north (Södermanland) and south (Blekinge) of the Simpevarp area has shown that three respectively six transgressions occurred during that period /Risberg et al. 1991, Berglund 1971/. It is therefore likely that several transgressions have occurred in the model area during Littorina time.

The estimated shore line displacement since the last deglaciation has been reviewed and modified more recently by /Påsse 2001, Påsse 1997/ (Figure 3-14). Påsse's curve is similar to the curve presented by /Svensson 1989/. Påsse suggests, however, that the reason for the fast shoreline displacement during the end of the Baltic Ice Lake was caused a fast isostatic component and not due to a sudden drainage as has been suggested earlier /e.g. Svensson 1989, Björck 1995/.

Pollen stratigraphical investigations from Blekinge show the succession of terrestrial plants in south-eastern Sweden from the latest deglaciation to the present /Berglund 1966/. The Simpevarp area was probably deglaciated before or during the relatively cold Older Dryas chronozone /cf. Lundqvist and Wohlfarth 2001/, which was characterised by a tundra vegetation dominated by herbs and bushes and a low coverage of trees. During the following Alleröd chronozone a sparse *Pinus* and *Betula* forest dominated the vegetation.

The following cold Younger Dryas chronozone was characterised by tundra vegetation reflected by a high proportion of *Artemisia* pollen. At the beginning of the Holocene c. 11,500 years ago the temperature increased and south eastern Sweden was first covered by forests dominated *Betula* and later by forests dominated by *Pinus* (pine) and *Corylus* (hazel). 9,000–6,000 years ago a forests by *Tilia* (lime), *Quercus* (oak) and *Ulmus* (elm) covered southeastern Sweden. *Picea* (spruce) reached the Simpevarp area only c. 2,000 years ago.

A pollen investigation, covering the last c. 1,500 years, have been carried out on sediments from two lakes situated 20 and 25 km west of Fårbo /Aronsson and Persson, unpublished data/. The results show an increase of *Juniperus* (Juniper) and *Cerealea* (e.g. wheat and barley) c. 1,200 years ago, which indicates that areas used as arable land and for pasture increased during that time.

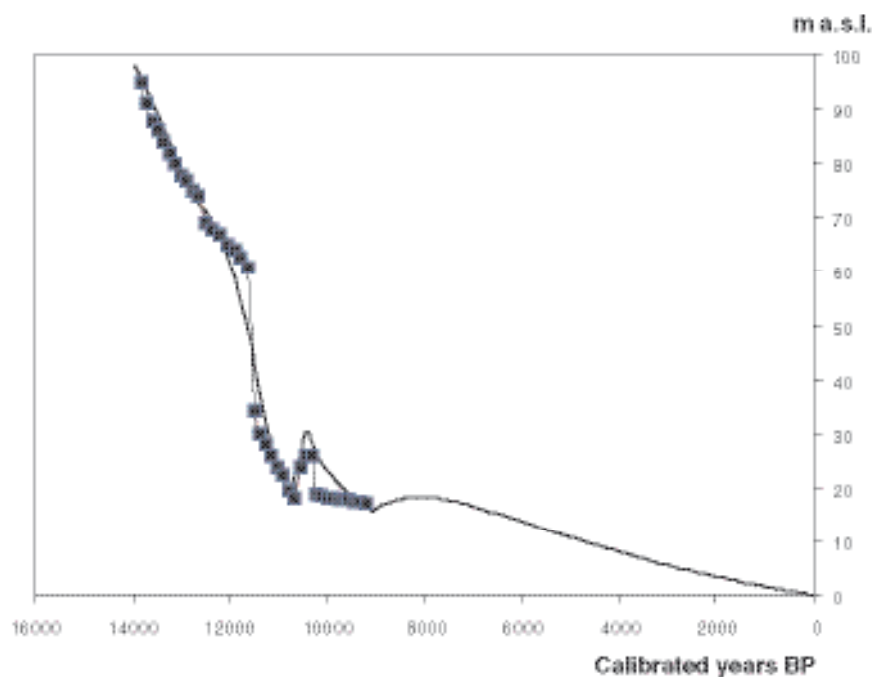


Figure 3-14. The shore line displacement in the Oskarshamn area after the latest deglaciation. The blue symbols show a curve established by /Svensson 1989/ based on a study of lake sediments in the region. The curve without symbols has been calculated by the use of a mathematical model /Påsse 2001/.

3.3 Premises for surface and groundwater evolution

The first step in the groundwater evaluation is to construct a conceptual postglacial scenario model for the site (Figure 3-15) based largely on known palaeohydrogeological events from Quaternary geological investigations. This model can be helpful when evaluating data since it provides constraints on the possible groundwater types that may occur. Interpretation of the glacial/postglacial events that might have affected the Simpevarp area is based on information from various sources including /Fredén 2002, Pässe 2001, Westman et al. 1999/ and /SKB 2002b/. This recent literature provides background information which is combined with more than 10 years of studies of groundwater chemical and isotopic information from sites in Sweden and Finland in combination with various hydrogeological modelling studies of the postglacial hydrogeological events /Laaksoharju and Wallin 1997, Luukkonen 2001, Pitkänen et al. 1998, Svensson 1996/. The model is therefore based on Quaternary geological studies, fracture mineralogical investigations and groundwater observations. These facts have been used to describe possible palaeo events that may have affected the groundwater composition in the bedrock.

3.3.1 Development of permafrost and saline water

When the continental ice sheet was formed at about 100,000 BP permafrost formation ahead of the advancing ice sheet probably extended to depths of several hundred metres. According to /Bein and Arad 1992/ the formation of permafrost in a brackish lake or sea environment (e.g. similar to the Baltic Sea) produced a layer of highly concentrated salinity below the advancing freezing front. Since this saline water would be of high density, it would subsequently sink to lower depths and potentially penetrate into the bedrock where it would eventually mix with formational groundwaters of similar density. Where the bedrock was not covered by brackish lake or sea water, similar freeze-out processes would occur on a smaller scale within the hydraulically active fractures and fracture zones, again resulting in formation of a high-density saline component which would gradually sink and eventually mix with existing saline groundwaters. Whether the volume of high salinity water produced from brackish waters by this freeze-out process would be adequate to produce such widespread effects is presently under debate.

With continued evolution and movement of the ice sheet, areas previously subjected to permafrost would eventually become covered by ice accompanied by a rise in temperature and slow decay of the underlying permafrost layer. Hydrogeochemically, this decay may have resulted in distinctive signatures being imparted to the groundwater and fracture minerals.

3.3.2 Deglaciation and flushing by meltwater

During subsequent melting and retreat of the ice sheet the following sequence of events is thought to have influenced the Simpevarp area (Figure 3-15).

During the recession and melting of the continental ice sheet, glacial meltwater was hydraulically injected into the bedrock (> 14,000 BP) at considerable pressure close to the ice margin. The exact penetration depth is still unknown, but depths exceeding several hundred metres are possible according to hydrodynamic modelling /e.g. Svensson 1996/. Some of the permafrost decay groundwater signatures may have been disturbed or destroyed during this stage.

Different non-saline and brackish lake/sea stages then transgressed the Simpevarp area during the period c. 14,000–4,000 BP. Of these, two periods with brackish water can be recognised; Yoldia Sea (11,500 to 10,800 BP) and Littorina Sea starting at 9,500 BP and continuing to the present. The Yoldia period has probably resulted in only minor contributions to the subsurface groundwater, since the water was very dilute to brackish because of the large volumes of glacial meltwater it contained. Furthermore, this period lasted only for 700 years. The Littorina Sea period in contrast had a maximum salinity of about twice that of the present Baltic Sea and this maximum prevailed at least from 6,500 to 5,000 BP; during the last 2,000 years the salinity has remained almost equal to the present Baltic Sea values /Westman et al. 1999 and references therein/. Because of increased density, the Littorina Sea water was able to penetrate the bedrock resulting in a density turnover which affected the groundwater in the more conductive parts of the bedrock. The density of the intruding seawater in relation to the density of the groundwater determined the final penetration depth. As the Littorina Sea stage exhibited the most saline groundwater, it is assumed to have had the deepest penetration depth, eventually mixing with the glacial/brine groundwater mixtures already present in the bedrock.

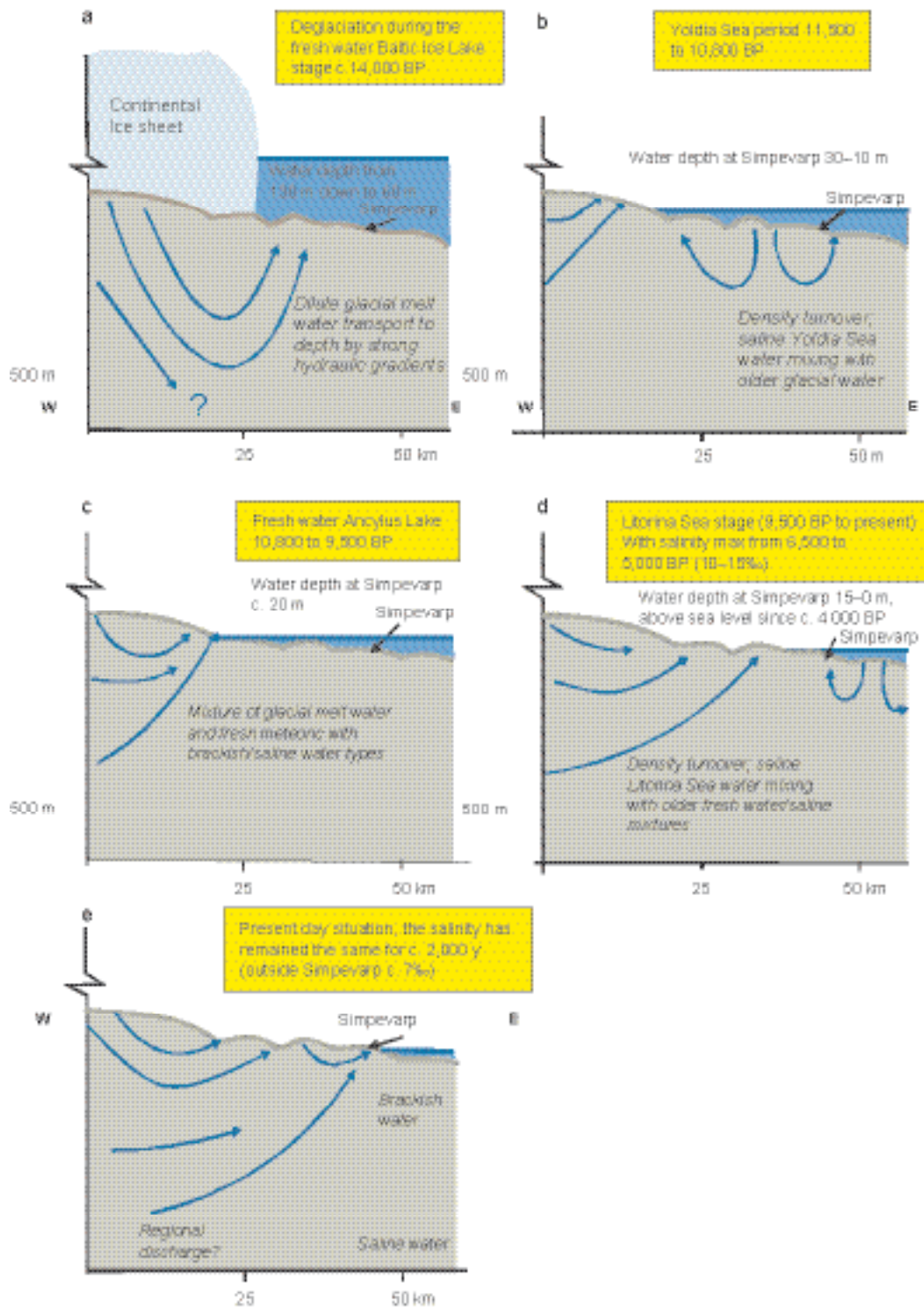


Figure 3-15. Conceptual postglacial scenario model for the Simpevarp area. The figures show possible flow lines, density driven turnover events and non-saline, brackish and saline water interfaces. Possible relation to different known postglacial stages such as land uplift which may have affected the hydrochemical evolution of the site is shown: a) deglaciation of the continental ice, b) Yoldia Sea stage, c) Ancylus Lake stage, d) Littorina Sea stage, and e) present day Baltic Sea stage. From this conceptual model it is expected that glacial melt water and deep and marine water of various salinities have affected the present groundwater. Based on the shoreline displacement curve compiled by /Påsse 2001/ and information from /Fredén 2002; Westman et al. 1999/ and /SKB 2002b/.

When the Simpevarp region was subsequently raised above sea level 5,000 to 4,000 years ago, fresh meteoric recharge water formed a lens on top of the saline water because of its low density. However, local hydraulic gradients resulting from higher topography to the west of the Simpevarp area may have flushed out varying amounts of these older waters, at least to depths of 100–150 m, with the freshwater lens mostly occupying these depths today, depending on local hydraulic conditions.

Many of the natural events described above may in the future be repeated several times during the lifespan of a repository (thousands to hundreds of thousands of years). As a result of these events, brine, glacial, marine and meteoric waters are expected to be mixed in a complex manner at various levels in the bedrock, depending on the hydraulic character of the fracture zones and groundwater density variations. For the modelling exercise which is based on the conceptual model of the site, groundwater end members reflecting, for example, Glacial melt water and Littorina Sea water composition, were added to the data set /cf. Appendix 4 in SKB 2006a/.

The uncertainty of the updated conceptual model increases with time into the past. The largest uncertainties are therefore associated with the stage showing the flushing of glacial melt water. The driving mechanism behind the flow lines in Figure 3-15 is the shore level displacement due to the land uplift.

3.4 Development of surface ecosystems

In this section, some illustrative results from the region are presented. For further details see /Jansson et al. 2004/ or /Lindborg 2006/.

Data sources used include historical maps, cadastral material, interviews and field work. The investigated areas in the Simpevarp area consist of parishes. This is due to the fact that most of the sources for historical periods are organised in parishes. It is also a level that enables us to study local human activities, e.g. follow the use of forests in the context of a village.

3.4.1 Population

In the year 1571, the estimated population in the three investigated parishes in this part of the province of Småland was c. 1,266 persons. The population growth was quite moderate in the parishes of Misterhult, Döderhult and Kristdala until the middle of the 18th century. However, after c. 1,800, there was rapid population growth, especially in Döderhult. Kristdala and Misterhult showed a quite similar population trend, although Misterhult's population size generally was larger. Döderhult followed the same trend as Kristdala and Misterhult, until c. 1865, when a very high rate of population growth began in Döderhult and lasted until c. 1900. This peak might be explained by the fact that the town of Oskarshamn was established in 1856. During the early 20th century there was a negative population trend in the three investigated parishes. After 1960, the trend has turned into a population growth in Döderhult, and the same thing happened in Misterhult after 1980. In 1990, the population size was calculated to 10,640 persons in Misterhult, Döderhult and Kristdala, taken together.

3.4.2 Farms and land use

The number of farms has changed over the years in this part of the province of Småland. In Döderhult, nearly 50% of the settlement units were wholly or partially deserted in 1631 according to the cadastral book of the same year. In Kristdala, the deserted farms reached c. 17% and in Misterhult c. 22% of the farmsteads were deserted at this time. A possible explanation for this can perhaps be found in the expensive Swedish wars that had a great impact on the population.

In the municipality of Oskarshamn, the changes in the landscape were dramatic between 1940 and 1980. About 74 km² of arable land were abandoned over that interval. According to calculations, only 3.8 new km² were ploughed in 1980. Of the original 114 km² of arable land in 1940, only 41 km² remained in 1980. If we study the changes spatially, we can detect that some areas were more affected than others. A lot of the smaller fields have been completely abandoned.

During the 18th and 19th century, the arable land and meadows increased. This was particularly true of the number of meadows. Drained wetlands in the woods were now used as meadows. At the same time, the old meadows, near the settlements, were transformed into arable land. The increase of the population and the increase of the number of farms during the period may partly explain this. Another explanation may be that fishery and incomes from the sea decreased in relation to other incomes and agriculture increased as the source for incomes at the same time.

In the mid-18th century enclosure (*Sw: laga skifte*) took place in Ekerum and Lilla Laxemar. At that time, the number of farms in the area had increased and the arable land area had increased even more. A consequence of the enclosure in Ekerum and Lilla Laxemar was that some farms were forced to move from the former toft of the villages. Another direct consequence of enclosure was the establishment of the boundaries of the properties. From that time, all the farms in the area were single farms, managing their lands on their own.

4 The surface system

This chapter constitutes a description of the work performed within the site modelling for Laxemar 1.2 concerning the surface system, i.e. meteorology, overburden characterisation, hydrology, hydrochemistry, oceanography, biota and development of ecosystem models. A comprehensive description of the surface system is reported in /Lindborg 2006/ and the underlying modelling and description strategy is given in /Löfgren and Lindborg 2003/.

The surface system starts where the deep bedrock ends, except where the bedrock reaches the surface and thereby becomes a part of the surface system as outcrops, and extends to the atmosphere which affects the site, e.g. through the climate. This means that a number of different disciplines are represented in addressing discipline specific patterns and processes at various spatial and temporal scales. Each discipline-specific description (e.g. hydrology) is developed independently, but they are then integrated to provide a deeper understanding of environmental patterns and processes at the site.

At the end of this chapter, three descriptive ecosystem models are presented, describing terrestrial, limnic and marine environments. The overall aim of the ecosystem modelling is to describe the carbon cycle for the different environments. A deep understanding of the carbon cycle will be one important tool to estimate and predict flows and accumulations of matter at a landscape scale (regional or sub regional) in the subsequent safety assessment. The carbon cycle is described in two steps; 1) a conceptual model is presented for the three environments, 2) site specific quantitative data are used to create carbon budgets for the terrestrial part of several discharge areas and a lake within the Laxemar subarea and several marine basins adjacent to the Simpevarp area. These descriptive ecosystem models use data from a number of disciplines e.g. overburden characterisation (Quaternary deposits), hydrology, biota etc. that are presented in the preceding sections within the surface ecosystem description.

The overall aim of the modelling is to produce a detailed description of the present conditions in the Simpevarp area, with focus on the Laxemar subarea. However, it is also of value to know the history of the studied site, not only to understand the present patterns, to provide a basis for predictions of future conditions.

4.1 State of knowledge at the previous model version

In the Simpevarp 1.2 site-descriptive model, the modelling of the abiotic components of the surface system was included in the discipline-specific geological, hydrogeological and hydrogeo-chemical modelling. The site data available for the descriptions of the abiotic components were quite limited for the Laxemar subarea. The geology of the Quaternary deposits was described based on the detailed map of the Quaternary deposits within the Simpevarp subarea, and available data from soil drillings within the Simpevarp subarea. The Simpevarp 1.2 description of the biotic components of the surface system included a vegetation map over the regional model area, results of biomass and production calculations for different vegetation types, some data on aquatic producers, and a description, to large extent based on generic data, of terrestrial and aquatic consumers. In addition, an assessment of the available information on humans and land use was provided.

4.2 Evaluation of primary data

A complete list of abiotic and biotic data from the surface system available for use in Laxemar 1.2 is provided in Tables 2-7 and 2-8.

4.2.1 Quaternary deposits and other regoliths

The overburden model is based on results from field mapping in larger parts of the Simpevarp regional scale model area (Table 2-7). Drillings and geophysical investigations have gained information that has been used to construct a model demonstrating the stratigraphical and total depth distribution of Quaternary deposits in the Simpevarp regional model area /Nyman 2005/. The uppermost part of the overburden, the soil, has been carefully described at 20 selected sites distributed over the regional model area. The reader is referred to /Lindborg in press/ for details of the data used in the description of the overburden in the Simpevarp regional model area. The terrain relief was modelled by interpolation of elevation data creating a DEM (digital elevation model) /Brydsten 2004/.

4.2.2 Climate, hydrology and hydrogeology

This section gives a brief overview of the site investigation data used in the Laxemar 1.2 modelling of the meteorological, hydrological and hydrogeological characteristics of the area. For a detailed presentation and evaluation, the reader is referred to /Werner et al. 2005/. It should be noted that the Laxemar 1.2 data freeze has not been applied strictly as a last date for input to the present work. In particular, the time series for presentation of meteorological parameters have been extended to June 2005. The motivation is that these types of data are crucial for the development of the conceptual-descriptive and quantitative water flow models of the site; since the available site-specific time series are very short, the basis for the modelling is considerably improved when a few additional months of measurements are utilised.

In the Laxemar 1.2 dataset, local meteorological data are available from two meteorological stations, one on the island of Äspö (September 2003–June 2005), and another in Plittorp (July 2004–June 2005), located c. 10 km west of the Äspö station. Furthermore, snow depth, soil freezing and ice cover are measured in the Laxemar subarea and in three sea bays. The data evaluation indicates that the annual precipitation in the Simpevarp area is c. 100 mm higher than that at the SMHI station at Ölands norra udde, which previously was selected as a “reference” meteorological station for the Simpevarp area /Larsson-McCann et al. 2002/.

New hydrological data in the Laxemar 1.2 dataset include cross-sectional data (bottom levels and widths) from field surveys of the main watercourses in catchment areas 6 (Mederhultsån), 7 (Kåreviksån), and 9 (Ekerumsån) /Strömgren 2005/. Furthermore, data are available from continued manual discharge measurements in some of the watercourses. There are also data on automatically measured water levels in some of the lakes (Lake Jämsen, Lake Plittorpsgöl, and Lake Frisksjön, see Appendix 1) and in the sea. However, there are as yet no data on automatically measured water levels or calculated discharges in watercourses. The surface-water levels in the lakes demonstrate a clear co-variation. Even though the amplitude is small, the data clearly show a typical seasonal variation of the discharge.

The bottom stratigraphy of wetlands, peat areas and lakes in the Simpevarp area has been investigated /Nilsson 2004/. These types of areas are not included in the “regular” mapping of Quaternary deposits (QD).

In addition to the Simpevarp 1.2 dataset, data from slug tests in 12 new groundwater monitoring wells (all located in the Laxemar subarea) are included in the Laxemar 1.2 data freeze /Johansson and Adestam 2004cd/. Data from grain-size analyses (particle-size distribution curves, PSD) of soil samples are also available and have been used in order to obtain supplementary hydraulic conductivity data on the QD, using the Hazen and the Gustafson evaluation methods /Werner et al. 2005/. The slug tests and the Hazen method provide approximately similar mean/median values for the hydraulic conductivity of the till, whereas the Gustafson method gives somewhat lower K-values, see /Werner et al. 2005/ for details on the evaluation of hydraulic conductivity data.

Up to December 2004, 42 groundwater monitoring wells in QD have been installed in the Simpevarp and Laxemar subareas. Automatic and/or manual groundwater level measurements have been performed in 37 of them. Except for three wells, the available time series are relatively short. More detailed analyses would require groundwater level data, and associated meteorological and hydrological data, for a period of at least one (hydrological) year.

4.2.3 Chemistry

The description of chemical properties of surface ecosystems in the Simpevarp area is based on data from surface waters (sampling sites in streams, lakes and the sea), shallow groundwater (soil tubes and private wells), and regolith (samples from till, soil and sediment). Moreover, there are also some data available on the concentration of different elements in precipitation, and of the elemental content in roots of amphibious plants. A detailed compilation and statistical evaluation of the primary data on chemical characteristics in surface ecosystems in the Simpevarp area is given in /Tröjbom and Söderbäck 2006/, and the reader is also referred to /Lindborg 2006/ for an account of the data used in the description.

4.2.4 Biota

A complete list of abiotic and biotic data from the surface system available for use in Laxemar 1.2 is found in Tables 2-7 and 2-8.

Terrestrial

Producers

The descriptive model contains a large number of components that describe biomass, NPP (Net Primary Production) and turnover of plant tissues. For information about the site specificity of the data, where it is published and some information about the methods used to estimate/calculate results, see /Lindborg 2006/. The sources from where the data have been obtained are shown in Table 2-8.

Consumers

Site-specific data and generic data obtained from different reports are listed in Table 2-8. A new mammal report /Truvé and Cederlund 2005/, with calculations of species consumption, production, respiration and egestion (fecal material) based on site-specific density data, has been published since Simpevarp 1.2.

Limnic

The Simpevarp regional model area contains relatively few lakes. Six lakes, situated partly or entirely within the regional model area, have been investigated for habitat characterisation during the site investigations. For some of the lakes there are also other biotic data collected, e.g. relating to plankton, macrophytes, fish, and invertebrates. This chapter gives an account based on data from four lakes; Lake Jämsen, Lake Frisksjön, Lake Söråmagasinet and Lake Plittorpsgöl (see Appendix 1).

Macrophyte biomass was investigated along 7 transects in Lake Frisksjön in August 2004 /Aquiloni 2005/. Along these transects, frames with 0.5 m or 0.25 m sides were placed once in each 0.5 m depth interval, until the water depth and light penetration limited plants from growing. The water depth was established for each frame. All plant individuals within the frames were identified and counted. Samples from each identified plant species were dried and weighed. The total dry weight of macrophyte biomass in each square was calculated from the number of individuals for each plant species and the dry weight/plant species. The calculations were often based on only one weighted sample of each plant species, and the result must therefore be considered as rough estimates of the total plant weight in each square.

Data have also been collected in streams, where a characterisation of the watercourses concerning has been performed. A number of *stream parameters* were measured while walking along the streams, each of them estimated for every 10-m length section /Carlsson et al. 2005/. Notes were taken regarding morphometry, water velocity, shading, bottom substrate, vegetation and human constructions, such as pipes, bridges and filled channels. For each investigated section, vegetation abundance was noted according to five abundance classes, also up to five dominating plant species were recorded. Moreover, invertebrate data have been collected in two of the streams.

Marine

Producers

Data from six site-specific studies were used for the description of primary producers (Table 2-8).

The major source for this description of the benthic marine environment is the vegetation map presented in /Fredriksson and Tobiasson 2003/. It is based on three different data sets; a general survey of over 1,000 localities with recordings of dominant macrophytes and degree of cover, 20 diving transects with quantitative sampling and 40 video recordings and finally bathymetrical data from Swedish nautical charts. The map was drawn by hand and the accuracy is dependant on the density of observations – generally higher in the inner bays and coastal areas and lower in the offshore area. The site observations and diving transects present the data in terms of degree of cover, i.e. the percentage of the sea bottom that is covered by macrophytes. The biomass in the basins is calculated by using the average degree of cover of the vegetation type and a biomass linearly related to percentage cover. The quantitative sample size for each vegetation type ranged between two and twelve. Data is presented per vegetation type in dry weight per square metre and degree of cover. As a complementary measure, biomass has been recalculated into gC using species specific conversion factors presented in /Kautsky 1995/. In addition, data on reed (*Phragmites australis*) was presented in a separate report /Alling et al. 2004/. Data on measured chlorophyll and irradiance /Ericsson and Engdahl 2004/ were used to calculate phytoplankton biomass and production. Data on phytoplankton presented by /Sundberg et al. 2004/ were used as temporal averages from three sampling occasions (December 2003, April and June 2004) at four localities. Data were presented per taxon (or species) and in dry weight per litre. The sampling sites were the same as those used for water chemistry samples taken during the year 2002.

Consumers

Data from five site-specific studies were used for the description of the consumers (Table 2-8).

There are three main sources of biomass data used in the descriptions: (i) the vegetation mapping study by /Fredriksson and Tobiasson 2003/ where epifauna associated with the vegetation were sampled, and (ii) a study of the soft bottom fauna /Fredriksson 2004/ and (iii) a study of the hard bottom fauna /Fredriksson 2005/. The quantitative data presented in these reports, i.e. biomass per unit biomass of vegetation (g dry weight per 100 g dry weight) and biomass per unit area (g dry weight per m²), respectively, were used to calculate the total biomass per functional group and basin. The species were grouped into functional groups according to the classification given in /Kautsky 1995/.

4.2.5 Humans and land use

In order to arrive at an overall assessment of the human population and human activities in the model area, a wide range of different human-related statistics were acquired from Statistics Sweden. These statistics include data and times series on demography, labour, health situation, land use, agriculture etc. Beside this, some additional information was searched for and acquired from other sources, such as the National Board of Fisheries, the Swedish Association for Hunting and Wildlife Management, the County Administrative Board. A detailed presentation of the data and results is given in /Miliander et al. 2004/.

4.3 Model of Quaternary deposits and other regoliths

4.3.1 Background

This section describes the surface characteristics and stratigraphical distribution of the overburden in the Simpevarp regional model area. The overburden includes all unconsolidated deposits covering the bedrock and is sometimes, for convenience, referred to as QD (Quaternary deposits) in the following text. The upper part of the overburden is affected by local climate, hydrology, vegetation etc. and is referred to as the soil.

The overburden models are used as input for modelling hydrological, chemical and biological processes taking place in the uppermost part of the geosphere. In the current description, the overburden description is used for modelling the near surface hydrology (Section 4.4). The near surface hydrology model uses both the surface and depth distribution data on the overburden. The total depth and (simplified) stratigraphical distribution of the overburden has been summarised in a model, which is used in for this purpose. The distribution of overburden in the discharge areas is of special interest, since groundwater from the more deep-seated bedrock may reach the surface through the overburden in these areas. Several of the site investigations have and will continue to be focused on the distribution of overburden in wetlands and areas covered by water. Results from soil and peat investigations have been used for constructing a carbon budget for the Laxemar subarea (Section 4.8). In forthcoming analyses the transport of elements (e.g. radionuclides) in the overburden will be modelled. The distribution of QD can be used for discussing potential future land use of the area. The studies of QD also improve the knowledge of the Late-glacial and Holocene development in the area.

4.3.2 The surface distribution and stratigraphy of Quaternary deposits

The Simpevarp regional model area, in its present state, is a relatively flat area with a coastline well exposed to the Baltic Sea. All known QD in the area were formed during or after the latest glaciation, the Weichselian. The oldest deposits are of glacial origin and have been deposited either directly by the ice or by water from the melting ice. The whole model area is located below the highest coastline and fine-grained water laid glacial and post-glacial sediments have consequently been deposited in sheltered positions. Isostatic land uplift (still an active process (1 mm/year)) and coastal processes are continuously changing the properties and distribution of the overburden. Exposed areas have been, and at some sites still are, subjected to wave washing, which has caused erosion and redeposition of some of the overburden. Sand and gravel is currently being transported at the bottom of the most exposed parts of the sea. A layer of sand and gravel therefore often covers the valleys on the sea bottom. Accumulation of clay is an ongoing process in the present narrow bays along the coast.

The properties of the soils are of crucial importance for the composition and richness of the vegetation. Different types of soils are characterised by horizons with specific chemical and physical properties. It often takes many thousands of years for soil horizons to develop. In Sweden, the soils have been formed during the period following the latest deglaciation, which is a relatively short period of time for soil formation. At the lowest altitudes in the Simpevarp area the time available for soil forming processes is even shorter, since these areas quite recently have emerged from the sea (Figure 3-3).

The bedrock surface is often rough in the regional model area indicating a low degree of glacial erosion. The absence of overburden predating the last glacial cycle indicates, however, that the most recent ice sheets have eroded older loose deposits. Glacial striae on outcrop surfaces indicate a dominant latest ice movement from the north-west. There are, however, striae indicating older ice-movements from the north-east, i.e. from the Baltic Sea basin /Rudmark et al. 2005/ (see also Chapter 3).

The surface distribution of QD (Figure 4-1) in the terrestrial part of the model area was mapped by /Rudmark et al. 2005/ whereas the distribution of QD in the marine areas were mapped by /Elhammer and Sandkvist 2005/ and /Ingvarson et al. 2004/. Both in the marine and terrestrial parts of the investigated area, the highest altitude zones comprise almost entirely exposed bedrock (Figure 4-1). There are probably several reasons for the relatively low coverage of QD. One reason may be that a relatively small amount of glacial till was deposited in the area during the latest ice age. Another reason is the fact that large parts of the investigated area are exposed towards the open Baltic Sea. That has caused, and is still causing, erosion and redeposition of overburden by waves and streams.

Glacial till is the oldest known component of the overburden and was deposited directly by the Quaternary glaciers. Till is the dominant QD and covers approximately half of the marine and terrestrial areas mapped by /Ingvarson et al. 2005, Rudmark et al. 2005/, respectively. The marine geological map by /Elhammer and Sandkvist 2005/ indicates that only a small fraction of the seafloor is covered by till (Table 4-1). It is, however, likely that the till areas were underestimated in that investigation, as further discussed in /Lindborg 2006/. Most of the till has a sandy matrix,

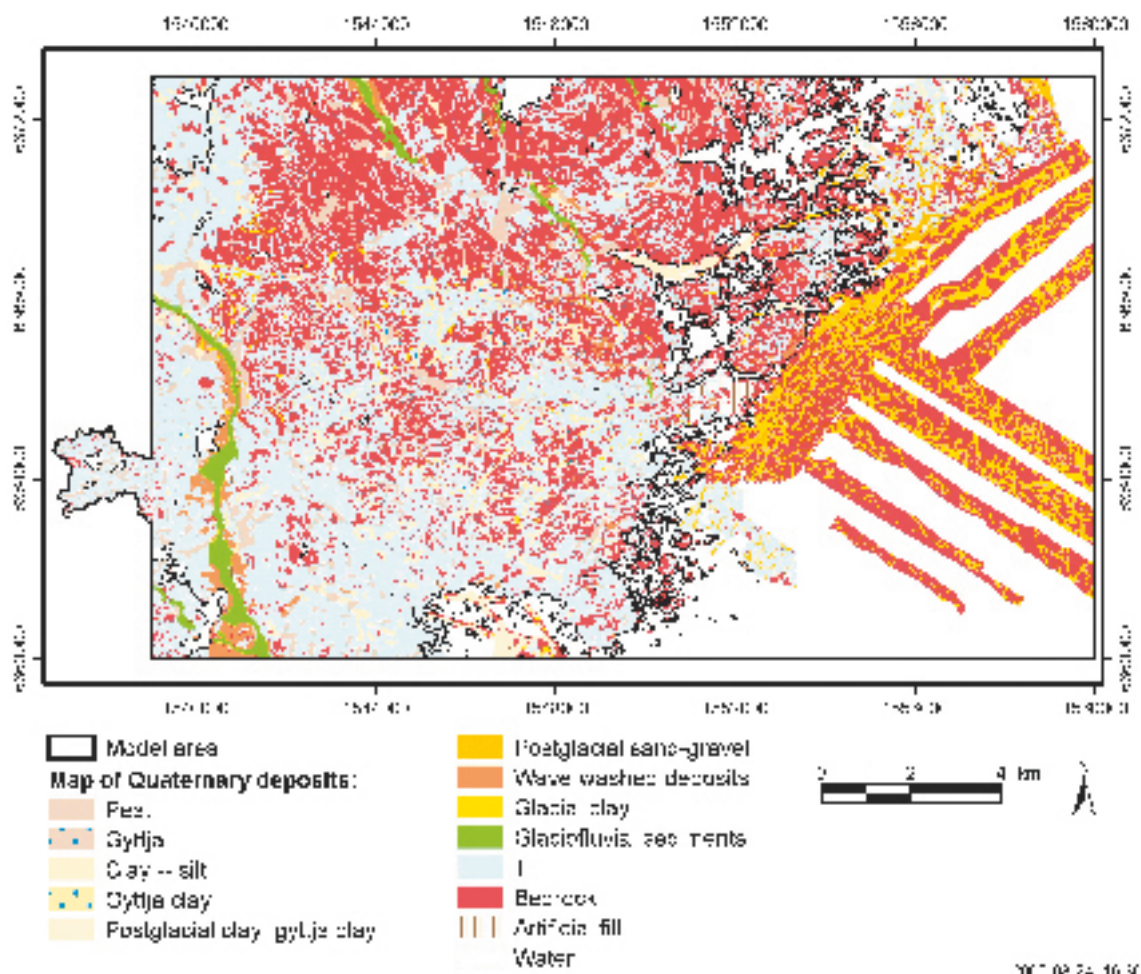


Figure 4-1. The distribution of Quaternary deposits in the Simpevarp regional model area.

but gravelly till does also occur /Rudmark et al. 2005/. The characteristics of the till indicate short distance of transportation and the mineral composition of the till should therefore reflect that of the local bedrock. The morphology of the till in the subarea normally reflects that of the bedrock surface. There is, however, a more coherent till coverage in the central part of the Laxemar subarea and the south-western part of the regional model area, where small hills of till occurs. At all investigated sites, the till rests directly on the bedrock surface /Johansson and Adestam 2004a, Rudmark et al. 2005/. It has been estimated that the till has an average thickness of 3.6 m in the clay covered valleys, whereas the average thickness is 2 m in terrestrial non-clay areas /cf. Nyman 2005/.

Table 4-1. The proportional distribution of Quaternary deposits in the Simpevarp regional model area.

Quaternary deposit	Terrestrial areas (%) /Rudmark et al. 2005/	Marine areas (%) /Elhammer and Sandkvist 2005/	Marine areas (%) /Ingvarson et al. 2004/
Peat	7.6	0	0
Gyltja clay	3.3 (all clay and silt)	4.2	11.6
Glacial clay and silt		38.4	0
Glaciofluvial deposits	1.4	0	0
Post-glacial sand and gravel	1.3	1.5	21.8
Till	51.7	1.1	49.3
Precambrian bedrock	34.6	54.8	17.3
Artificial fill	0.13	0	0

During the latest deglaciation, glaciofluvial material was deposited in tunnels created beneath the ice by melt water running from the north. The occurrences of subglacially formed eskers indicate bottom-melting conditions during the deglaciation. There are three relatively small and one large (Tunaåsen) glaciofluvial eskers in the regional model area. One of these small eskers reaches the northern part of the Laxemar subarea. These deposits may have hydrological importance and will be a focus for studies during the forthcoming site investigations.

The distribution of fine-grained water laid QD is mainly an effect of the local bedrock morphology. These sediments are mostly restricted to the long and narrow valleys which are characteristic for the investigated area. The oldest fine-grained deposits, glacial clays, were deposited during the latest deglaciation when the water was relatively deep. As the water depth decreased, streams and waves started to erode the uppermost clay, and then deposited a layer of sand/gravel on top of the clay. The lowest areas became sheltered bays as the water depth decreased and post-glacial clays containing organic material (clay gyttja) started to deposit. The processes of erosion and deposition are still active at the sea floor and along the present coast. The floors of many of the valleys, in the terrestrial areas, are former or present wetlands where layers of peat have formed. The areas of wetlands have, however, decreased significantly due to ditching. There remain, however, a number of small, not raised, bogs, which occur in depressions in the areas dominated by exposed bedrock. The bog peat is often underlain by fen peat.

Information about the depth and stratigraphy of overburden has been gained from drillings and geophysical investigations. A general stratigraphy for the area is presented in Table 4-2. The results from all these investigations were used to construct a model, with the GeoEditor graphical tool /DHI Water&Environment 2001/, which shows the distribution of overburden depths for the whole regional model area /Figure 2 from Nyman 2005/. The clay/peat-covered valleys and the glaciofluvial Tunaåsen esker are clearly visible as zones with thick overburden (Figure 4-2). Further drillings, excavations and geophysical investigations will give more information regarding the thickness and stratigraphy of the overburden, which will be used to update the model.

4.3.3 Soils

Soils are formed as a result of the interaction of the overburden, climate, hydrology and biota. In the investigated area, soil forming processes started as the land was lifted above sea level. The lowermost investigated localities are situated more than one meter above the present sea level and have consequently been exposed to soil forming processes for at least one thousand years.

Soils from ten different land types have been classified /Lundin et al. 2004/. These land types were defined based on vegetation, land use, and wetness. The distribution of different soil classes is presented in a map /Lundin et al. in press/, which is based on data from the field classifications and geographical information, such as maps of Quaternary deposits and vegetation types (Figure 4-3).

Table 4-2. The stratigraphical distribution of Quaternary deposits in the Simpevarp regional model area.

Quaternary deposit	Relative age
Bog peat	Youngest
Fen peat	↑
Gyttja clay/clay gyttja	
Sand/gravel	↑
Glacial clay	
Till	↑
Bedrock	Oldest

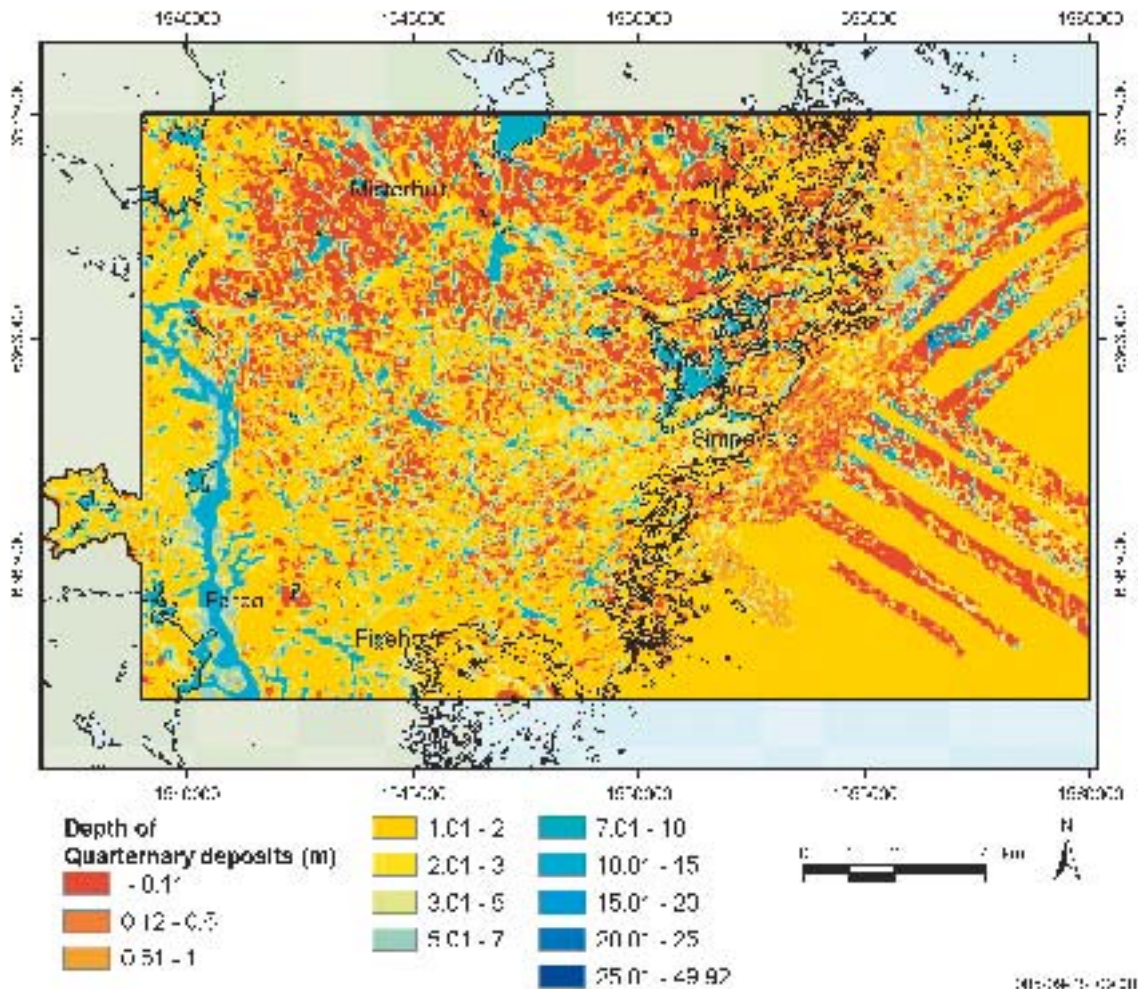


Figure 4-2. The distribution of total depth of overburden in the Simpevarp regional model area. The map was constructed after calculations with Geoeditor /Nyman 2005/. The marine part of the regional model area partly lacks field information. In these areas, the average depth of QD in the marine areas mapped by the SGU was used.

The most common soil types in the Simpevarp area are:

- Leptosol* – areas with a thin layer of overburden overlying the bedrock.
- Podzol* – a soil type with low pH, which has a subsurface, often rust coloured, spodic horizon.
- Gleysol* – a soil type that has periodically reducing conditions due to water saturation.
- Regosol* – characterised by incomplete development of soil horizons.
- Umbrisol* – a soil type, which often develop on arable land, with an upper horizon rich in organic material.
- Histosol* – formed from materials with a high content of organic matter (often peat).

Podzol and regosol dominate areas where the underlying deposit is till or glaciofluvial material. The areas with leptosol occur mostly where there are bedrock exposures. It must be pointed out that some of the areas classified as podzol/regosol (Figure 4-3) are areas, which according to the QD maps consists of exposed bedrock or thin soil covers (Figure 4-1). Umbrisol and gleysol dominate the fine-grained water laid sediments, which are used as arable land or meadows. Histosol is the most common soil type in the wetlands.

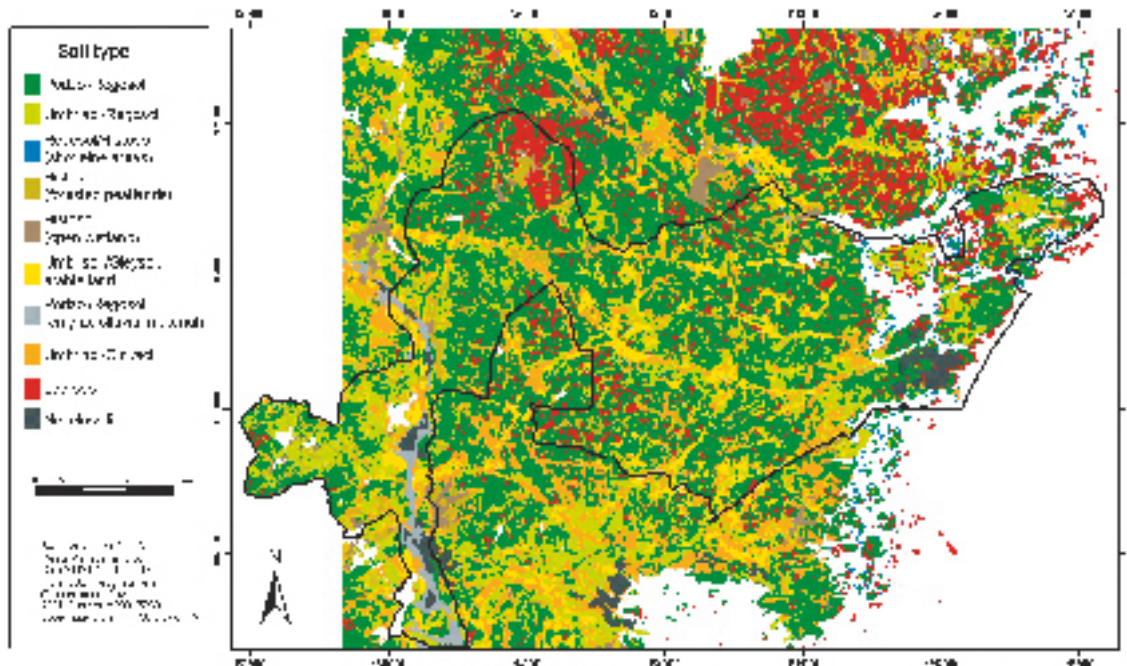


Figure 4-3. The distribution of soils in the Simpevarp regional model area. The map is based on field studies and interpretations of other geographical information such as maps of QD and vegetation. Since the most detailed mapping of QD took place in the Laxemar subarea the soil map is most reliable in that area.

4.4 Climate, hydrology, hydrogeology and oceanography

4.4.1 Conceptual-descriptive and quantitative water flow modelling

The conceptual-descriptive and quantitative modelling of the meteorological, surface hydrological and near-surface hydrogeological conditions in the Simpevarp area is presented in /Werner et al. 2005/. The conceptual-descriptive model is based on three types of “elements”: type areas, flow domains, and interfaces between flow domains. The identified type areas are (1) *high altitude areas* (dominated by exposed or very shallow bedrock), (2) *valleys* (with thicker QD, and postglacial sediments at the surface), (3) *glaciofluvial deposits* (of which the Tuna esker in the western part of the regional model area is the largest), and (4) *hummocky moraine areas* (primarily existing in the south-western part of the regional model area and in the central part of the Laxemar subarea).

The identified flow domains are Hydraulic Soil Domains (HSD), lakes, watercourses, and wetlands. A geometrical model of the HSD has been developed /Nyman 2005/. In this model, the HSD are divided into three QD layers, denoted Z1–Z3. The model also includes three additional QD layers, referred to as M1–M3. The latter layers represent peat (M1), glaciofluvial deposits (M2) and artificial fill (M3; not strictly QD). The QD types assigned to the layers in the conceptual-descriptive model are based on the geometrical model of the HSD and the detailed QD map /Rudmark 2004, Rudmark et al. 2005/. The description of the QD types is expected to be further developed in future model versions when more site investigation data are available. The assigned hydraulic properties of QD types in the Laxemar 1.2 model version are shown in Table 4-3. Note that the hydraulic properties of “near-surface bedrock” shown in the table apply to the upper few metres of the bedrock. For larger depths into the bedrock, the modelling results and the associated data used in the flow modelling described below are taken from the Simpevarp 1.2 model of the hydraulic properties of the bedrock /SKB 2005a/, as presented by the DarcyTools modelling team.

Table 4-3. Assignment of hydraulic properties to Quaternary deposits (QD) /Werner et al. 2005/.

QD no	QD	Horizontal hydraulic conductivity, K_H ($m \times s^{-1}$)	K_H/K_V	Specific yield, S_Y (-)	Storage coefficient, S_S (m^{-1})
1	Gyttja (only present below open water)	$1^1 \times 10^{-8}$	1	$1^0.03$	$1^6 \times 10^{-3}$
2	Gyttja clay, clay gyttja	$2^1 \times 10^{-7}$	1	$1^0.03$	$1^6 \times 10^{-3}$
3	Clay (postglacial/glacial), silt				
	Z1 (on land)	$4.5.6^1 \times 10^{-6}$	1	$3^0.03$	$4^6 \times 10^{-3}$
	Z2 (not in Z3)	$4.5.6^1 \times 10^{-8}$			
4	Till, artificial fill, unclassified				
	Z1	$7^4 \times 10^{-5}$	1	$8^0.15$	$4^1 \times 10^{-3}$
	Z2–Z3	$7^4 \times 10^{-5}$		$8^0.05$	
5	Fluvial outwash, gravel	$5.15^1 \times 10^{-2}$	1	$3^0.25$	$9^0.025$
6	Fluvial outwash, sand	$5^1 \times 10^{-3}$	1	$3^0.25$	$9^0.025$
7	Flood sediments, clay-gravel	$10^1 \times 10^{-6}$	1	$1^0.03$	$1^6 \times 10^{-3}$
8	Peat	11.5×10^{-6}	1	$11^0.24$	$11^5 \times 10^{-2}$
9	Bedrock (near-surface)	12.05×10^{-7}	1	$12^0.005$	$12.1.5 \times 10^{-6}$
10	Glaciofluvial deposits (coarse sand, gravel) ²	13.1×10^{-4}	1	$14^0.25$	$9^0.025$

¹ Assumed equal to the corresponding parameter for clay.

² Assigned 10 times the K_H -value for clay.

³ Generic data from the literature /Domenico and Schwartz 1998/.

⁴ Generic data from Blomquist-Lilja, 1999 (unpublished SKB report).

⁵ Generic data from the literature /Knutsson and Morfeldt 1993/.

⁶ K_H for near-surface clay assigned 100 times K_H for deeper clay.

⁷ Site-specific data from slug tests /Johansson and Adestam 2004bd/ and particle-size distribution curves.

⁸ Based on the conceptual-descriptive model of till in the Forsmark 1.2 model /Johansson et al. 2005/.

⁹ Assigned 1/10 of S_Y .

¹⁰ Assumed to be 100 times the K_H -value for clay and 10^{-4} times the K_H -value for gravel.

¹¹ Generic data from the literature /Kellner 2003/.

¹² K_H and S_Y are the same as for the uppermost part of the bedrock in the DarcyTools data set (Simpevarp 1.2 model version), S_S is calculated based on an empirical relation between S_S and K_H in bedrock /Rhén et al. 1997c/.

¹³ Assigned 1/10 of the K_H -value for gravel.

¹⁴ Assumed to be equal to sand and gravel.

¹⁵ A K_H -value of $1 \times 10^{-2} m \times s^{-1}$ is reasonable for gravel, but the value was decreased to $1 \times 10^{-3} m \times s^{-1}$ in the MIKE SHE-MIKE 11 quantitative water flow modelling due to numerical instability.

Three interfaces between flow domains are used in the modelling; (1) “near-surface” bedrock and “deep” bedrock (this interface is placed at 150 m below sea level), (2) QD and bedrock, and (3) groundwater and surface water; the QD at the bottom of lakes are assumed to consist of low-permeable layers of gyttja and clay, whereas QD below peat areas (wetlands) and QD at the bottom of the sea are assumed to consist of gyttja (peat areas) and clay (the sea), respectively.

The interpretation of the surface and near-surface flow system can be summarised as follows:

- The Simpevarp area has a relatively small-scale topographical undulation and shallow QD. This implies that there are a large number of relatively small catchments with mostly small watercourses. A crude long-term regional-scale water balance, applying the general water balance equation $P = E + R + \Delta S$ has previously been presented for the Simpevarp area, based on selected “representative” data on precipitation P and runoff R (specific discharge) /Larsson-McCann et al. 2002/. Considering a time period of one year, it was assumed that the storage change $\Delta S = 0$. The average (corrected) precipitation in the Simpevarp area (P) is c. 600–700 $mm \times y^{-1}$, and the average specific discharge (R) is estimated to be in the interval 150–180 $mm \times y^{-1}$ /Larsson-McCann et al. 2002/. Hence, the evapotranspiration (E) was estimated to be in the interval 550 (700 minus 150) to 420 (600 minus 180) $mm \times y^{-1}$. The Laxemar 1.2 modelling shows that there are large variations of the specific discharge between years (and, of course, also during years) due to variations in the meteorological conditions. There is also a spatial variability in the specific discharge, e.g. between different catchment areas, in the Simpevarp area. This variability is likely due to differences in, for example, the fractions of exposed bedrock and open water, and the land use (vegetation).

- There is a large degree of surface runoff taking place in the exposed/shallow bedrock areas, from which water is diverted into the valleys, and further into watercourses, lakes and wetlands. Hence, the near-surface groundwater flow mainly takes place in the valleys. The discharge in the watercourses is highly transient, and most watercourses have a low discharge or are dry during large parts of the year. There are relatively short periods with large discharges, associated with heavy precipitation events and/or snowmelt.
- Even though there is yet no field evidence that precipitation and snowmelt are the only sources of groundwater recharge, the Laxemar 1.2 modelling (which includes Lake Frisksjön) indicates that the lakes do not contribute to groundwater recharge during dry periods, when groundwater levels are low. As the groundwater table generally is located close to the ground surface, evapotranspiration-precipitation cycles are assumed to have a strong effect on the groundwater level in the QD.
- Each catchment area can be divided into recharge areas and discharge areas. In general, recharge takes place in areas of relatively higher altitudes and discharge in lower-lying areas. However, the transient nature of the system implies that the recharge and discharge areas most likely vary during the year.
- Investigations of the QD stratigraphy below some lakes, wetlands, and peat areas indicate that the QD in such areas typically consist of low-permeable layers, limiting the contact between groundwater and surface water. Discharge from the bedrock into the QD probably mostly takes place in the topographically defined major discharge areas.

Some of the above concepts are illustrated in Figure 4-4.

4.4.2 Some observations from quantitative water flow modelling

The Laxemar 1.2 quantitative water flow modelling included detailed process modelling of catchment areas 6–9 (see Figure 4-12) including near-coastal parts of land, i.e. areas with direct runoff to the sea and extending some distance into the Baltic Sea. The flow modelling was performed using the MIKE SHE-MIKE 11 software packages /DHI Software 2004/, and by means of large-scale GIS-based hydrological modelling applying the PCRaster-POLFLOW modelling approach /Jarsjö et al. 2005/.

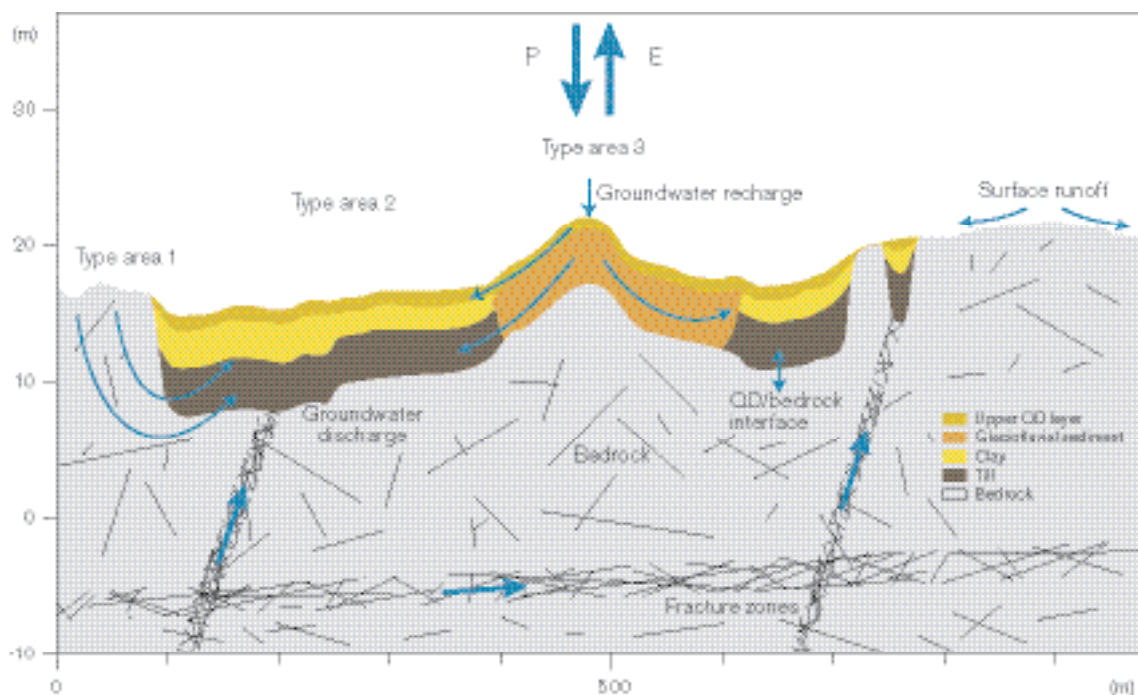


Figure 4-4. Schematic cross section, illustrating the descriptive model of the surface-hydrological and near-surface hydrogeological conditions in a hypothetical valley in the regional model area /Nyman 2005/. The figure also indicates type areas 1–3 and the QD/bedrock interface.

The quantitative water flow modelling serves two main purposes:

- To produce output data necessary for other models and applications (e.g. modelling of groundwater in the bedrock, ecosystems modelling, Environmental Impact Assessment). To achieve this purpose, the MIKE SHE-MIKE 11 modelling includes the definition and simulation of an “initial base case” and an “updated base case”, where the latter is identified by simulation of a series of “sensitivity cases” (see below). All these simulations use local meteorological data, measured at the Äspö meteorological station during the year 2004.
- To investigate the sensitivity of the modelling results to various input parameters. In the MIKE SHE-MIKE 11 modelling, a series of “sensitivity cases” was defined and simulated, in order to investigate the sensitivity of the model output to the hydraulic properties of the QD, and the vegetation-related parameters leaf area index (*LAI*) and crop coefficient (*K_c*). The sensitivity analysis and the resulting updated base case were used to evaluate the conceptual-descriptive model, in order to further develop the overall understanding of the hydrological, meteorological and hydrogeological conditions in the Simpevarp area, and to provide a basis for future model versions.

The main observations from the quantitative water flow modelling can be summarised as follows:

Water balance and specific discharge: Figure 4-5 illustrates the model-calculated water balance ($\text{mm} \times \text{year}^{-1}$) for the updated base case, and the exchanges of water between different compartments of the model. In the updated base case in the present Laxemar 1.2 modelling, the average specific discharge is 189 mm (c. $6 \text{ l} \times \text{s}^{-1} \times \text{km}^{-2}$), calculated as the accumulated discharge (sum of overland and groundwater flow into the watercourses and the sea), divided by the land area within the model area (hence including near-coastal land areas, with direct runoff to the sea). The modelling shows that there are some differences in annual average specific discharge between the modelled catchment areas, and also that the vegetation-related parameters leaf area index (*LAI*) and crop coefficient (*K_c*) have rather large influence on the modelled water balance.

The calculated specific discharge is slightly higher than the “regional” long-term average value of $150\text{--}180 \text{ mm} \times \text{year}^{-1}$ /Larsson-McCann et al. 2002/, and the results obtained in the previous Simpevarp 1.2 modelling and in the PCRaster-POLFLOW modelling /Jarsjö et al. 2005/. It should

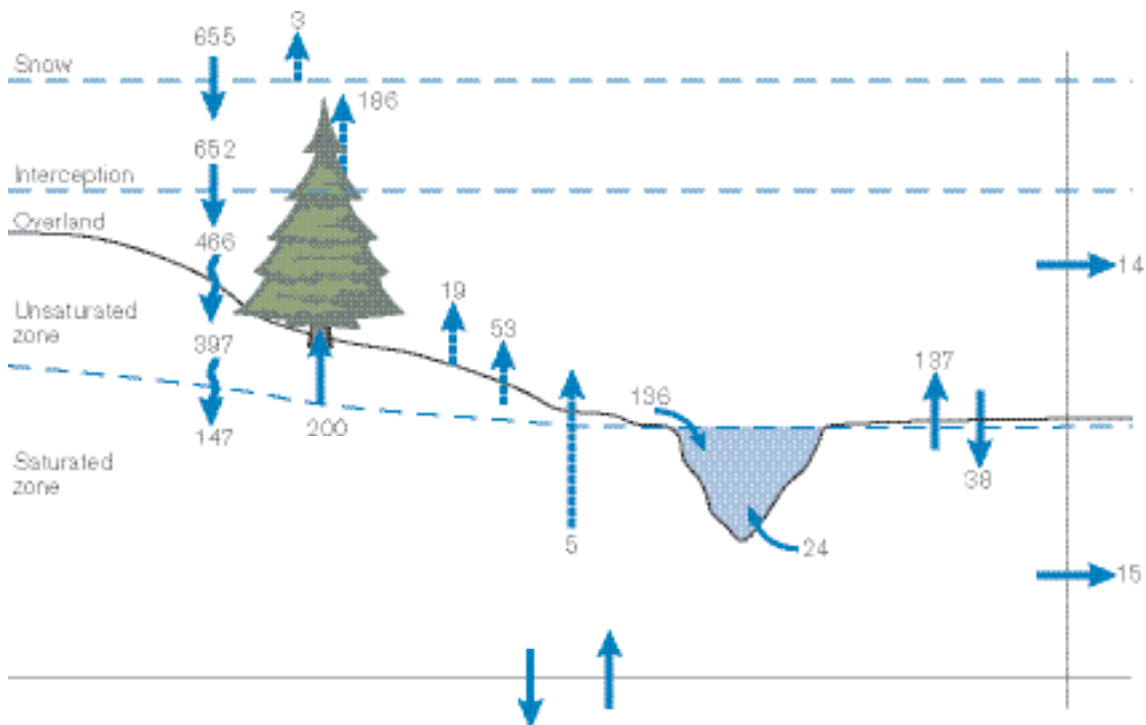


Figure 4-5. Illustration of the water balance for the model area ($\text{mm} \times \text{year}^{-1}$) for the updated base case. Note that the water balance is calculated for all land-based parts of the model area.

be noted that in the previous Simpevarp 1.2 simulations, the regional long-term average annual precipitation measured at the Ölands norra udde station was used, which is on the order of 100 mm smaller than the annual precipitation used in the Laxemar 1.2 base case simulations (Äspö meteorological data from 2004).

Groundwater levels: For the updated base case, the model-calculated average groundwater level in QD is shallow, which is in agreement with site investigation data. The deeper groundwater levels are mainly found in higher-altitude areas, associated with groundwater recharge. There are also areas where the simulated groundwater pressure head is above the ground surface. Hence, these are groundwater discharge areas, including e.g. Lake Frisksjön and areas in the vicinity of the main watercourses. However, there are not actual lakes, wetlands and/or watercourses in all areas where there is surface water in the model. In most cases, this is due to the fact that these areas have been drained (by open ditches or subsurface pipes), which is a general characteristic of the Simpevarp area /Nyborg et al. 2004/. Ditches, drainages, and “missing” watercourses that have been characterised /Carlsson et al. 2005, Svensson 2005/ but not included in the Laxemar 1.2 model version will be considered in future model versions.

The modelling results show that the annual amplitude of the groundwater level is smaller in discharge areas than in recharge areas. The groundwater levels demonstrate an expected seasonal variability, with decreasing levels during the late spring, summer, and early autumn, and increasing levels during late autumn. The sensitivity cases show that the effect of the hydraulic conductivity on the groundwater level (and the associated temporal fluctuations) is rather small.

Surface water levels and discharge: In accordance with site investigation data, the modelling results show large temporal variability of the discharge in the watercourses during the year.

Groundwater recharge and discharge areas: As hypothesised in the conceptual-descriptive modelling, the (long-term average) discharge areas are found in the vicinity of the main watercourses, in and around Lake Frisksjön, and also along the coastline towards the Baltic Sea. The modelling results also show that the distribution of recharge and discharge to some extent varies with time, due to (seasonally) variable meteorological conditions; there are somewhat larger discharge areas during a dry period compared with a wet period.

4.4.3 Coastal oceanography of the Simpevarp area

For aquatic ecosystems the rate of water exchange is a basic parameter for determining the material turnover. The overall objective of the oceanographic model is to quantify the water turnover of the coastal area outside Simpevarp regional model area in such terms that projection into the distant future is made possible.

To obtain a quantitative estimate of the water turnover, the concept of Average Age (AvA-) time defined by /Bolin and Rodhe 1973/ is consistently used. This well-defined concept was independently adapted to water circulation models by introducing its volume-specific counterpart /England 1995, Engqvist 1996/. AvA-time denotes the length of time a particular water parcel (or parts thereof) of specified exogenous water on the average spends within a defined connected body of water see e.g. /Engqvist 1999/. The AvA concept gives a comprehensible measure of the bulk water exchange. However, the water turnover between sub-basins (SBs) in the marine ecosystem model (see Section 4.8) is used in the form of corresponding volume fluxes.

The coastal area has been partitioned into a number of non-overlapping SBs based on consideration of present underwater structures, e.g. sills and ridges (see Figure 4-14), that potentially in the future with the current land rise will progressively accentuate the confinement of the water movements. The bathymetry is based on the DEM /Brydsten and Strömngren 2005/. For some shallow areas, complementary data have been obtained by manual sounding. One of the areas is considerably greater than all the others combined, and represents the open coastal area that is regarded as an intermediate stage for the eventual water exchange to the Baltic; this is referred to as the inshore water coastal zone (IWCZ).

The response of the basins to the exchanged water adds to the influence of the local forcing, of which wind normally is the major cause, of vertical mixing /Stigebrandt 1985/. Basins that receive freshwater discharge also display a notable estuarine circulation mode. Even with an established estuarine circulation flow regime, the varying density stratification in the offshore waters is often the dominant cause of ventilation of coastal basins /Stigebrandt 1990, Engqvist and Omstedt 1992/.

The Baltic model (AS3D) employed in this study /Andrejev and Sokolov 1989, 1990/ has been developed for the main purpose of providing insight into the circulation of the central Baltic. The complete set of equations of the AS3D-model, including boundary formulation and numerical scheme is given in /Andrejev and Sokolov 1997/. This model together with its nested fine-resolution variants of local coastal sections are under continued development and is presently being used in several ongoing Baltic oceanographic studies /Engqvist and Andrejev 2003, Andrejev et al. 2004ab/. The water exchange of semi-enclosed landlocked waters is different from that of the open offshore waters because the confinement to channels means a reduced degree of freedom of current directions. The water exchange of landlocked basins has therefore been quantified in a specific way employing a hydraulically coupled 1-D discrete basin (DB) model that resolves each SB in the vertical, see /Engqvist 1996, 1997, Engqvist and Andrejev 2003/.

Computational results of AvA time for the SBs are presented in Table 4-4.

Table 4-4. Collective basin AvA-time (days) estimates for 13 sub-basins (SB). The major inshore water coastal zone (IWCZ) is regarded as exogeneous water. DB = discrete basin model, 3D = three-dimensional model.

	Minimum (days)	Mean-S.D. (days)	Mean (days)	Mean + S.D. (days)	Maximum (days)	Model type	Remark
SB1	9.7	26.2	38.1	49.9	68.4	DB	
SB2	33.5	48.2	60.3	72.5	78.8	DB	Split SB
SB3	2.8	6.5	12.8	19.1	38.9	DB	Split SB
SB6	0.2	0.3	1.4	2.5	4.4	DB	
SB9	0.6	1.3	3.2	5.0	11.9	DB	
SB10	22.3	41.4	52.3	63.3	71.0	DB	
SB11	1.2	3.3	5.4	7.5	11.1	DB	
SB12	0.7	2.6	4.7	6.7	10.7	DB	Split SB
SB13	0.4	0.6	1.8	3.1	5.0	DB	
SB14	0.2	0.3	1.5	2.7	4.8	DB	
SB15	0.09	0.38	0.58	0.79	1.00	3D	
SB17	0.03	0.07	0.09	0.11	0.13	3D	
SB18	0.02	0.08	0.13	0.17	0.22	3D	
IWCZ	0.36	0.85	1.29	1.74	2.16	3D	Individual AvA-time – all adjacent SBs are considered as exogenous water.
IWCZ	0.04	1.05	1.85	2.66	3.78	3D	Collective AvA-time – all SBs are included in IWCZ.

4.5 Chemistry

Data on surface water chemistry have been collected biweekly to monthly from October 2002, and the sampling programme includes 18 streams, 4 lakes and 5 sea sampling sites. The number of sampling sites has been reduced since the start of the programme, but for all sites there is a time series of at least one year. Analysed parameters include, for most samples, major cations and anions, nutrients, organic compounds and oxygen. Water temperature, pH, conductivity, salinity and turbidity were determined in the field. Moreover, trace elements were analysed at one sampling occasion, whereas stable and radiogenic isotopes were analysed at 1–4 sampling occasions per year. Data on the water chemistry of precipitation have been collected regularly from one sampling location.

Shallow groundwater has been sampled from 30 soil tubes (shallow boreholes). Each soil tube has been sampled at 1–3 sampling occasions. The number of analysed parameters varies greatly, from only pH and electrical conductivity in some cases, to a complete chemical characterisation, including also stable and radiogenic isotopes. In addition, groundwater has been sampled from 47 private wells during the period 1989–2005. The location of the wells are illustrated in /Morosini and Hultgren 2003/.

The chemical analyses of Quaternary deposits performed hitherto mainly include total contents of organic carbon, calcium carbonate (CaCO_3), nitrogen and sulphur. In total, 27 till samples have been analysed for CaCO_3 . The contents of carbon, nitrogen, hydrogen and sulphur have been analysed in samples of sediments from peatlands (7 samples), and in marine and lacustrine sediments from bays and lakes (20 samples). The contents of carbon and nitrogen have been analysed in different soil horizons from ten typical site types in the Simpevarp area. For a more detailed description of the samples collected from surface waters, groundwater and overburden, and of the parameters analysed, see /Tröjbom and Söderbäck 2006/ and /Lindborg 2006/.

4.5.1 Chemical characteristics of near-surface ecosystems in the Simpevarp area

Surface water

The freshwater systems in the Simpevarp area can generally be classified as mesotrophic, brown-water types. Most freshwaters are markedly coloured due to a high content of humic substances, indicating very high levels of dissolved organic carbon. Both streams and lakes are also relatively rich in nitrogen and phosphorus. These high levels of dissolved organic carbon and nutrients imply poor light penetration conditions in the lakes, and periodically also high levels of chlorophyll in the surface water and low oxygen concentrations in the bottom water of the lakes.

Most freshwater sampling sites show almost neutral or ‘moderately acid’ pH values and an alkalinity corresponding to ‘good buffering capacity’ according to the Swedish Environmental Quality Criteria /Naturvårdsverket 2000/. However, there are a few stream sampling sites which show ‘very acid’ pH values and ‘no or negligible’ buffering capacity, indicating the presence of acidified surface waters in the Simpevarp area. A substantial proportion of the Simpevarp area is covered by a very thin layer of Quaternary deposits or is characterised by outcrop bedrock, thereby giving the necessary prerequisites for acidification in the small watercourses which drain the catchments dominated by these thin soils.

Both the electrical conductivity and the content of dissolved ions are slightly higher than in most lakes and watercourses in Sweden. The concentrations of major ions, e.g. calcium, sodium and chloride, seem to increase downstream in the watercourses, and the highest levels are observed at sampling sites near the outlets in the Baltic. There is also a tendency for an increasing concentration gradient from north-west to south-east, coinciding with increasing depth of the Quaternary deposits.

The five sea sampling sites can be divided into two different types. The first type represents the open sea and outer archipelago and consists of three sites; Kråkelund, Ekö and Fågelöfjärden. These sites are situated quite close to the open sea and show similar electrical conductivity and similar concentrations of most analysed parameters. The other type of site is situated in relatively confined bays close to the mainland and consists of two sites; Basin Borholmsfjärden and Basin Granholmsfjärden. These sites show lower concentrations of ions than the open sea sites, whereas the concentrations of organic compounds and nutrients, especially the nitrogen fractions, are considerably higher. For a comprehensive compilation of selected chemical parameters at stream, lake and sea sites in the Simpevarp regional model area, the reader is referred to /Lindborg 2006/.

Many parameters show temporal variations related to run-off or primary production. In the lakes, nutrients and carbon, especially the particulate species, show typical seasonal variations connected to the primary production during the warm season. The relatively closed coastal basins Granholmsfjärden and Borholmsfjärden show large variations of most parameters due to varying mixing proportions between sea water and fresh water runoff from the streams. This dilution-derived variation is, in most cases, dominant relative to other sources of variation in these closed basins.

The 'open sea' coastal sites show only minor variations compared with the lakes and brackish basins. There are slow changes in the contents of the major dissolved ions, coupled to the large scale variations of salinity in the Baltic, as well as seasonal variations of e.g. calcium and silicon, coupled to primary production. In streams, the concentrations of most elements show more or less strong variation, both due to dilution effects caused by variations in the run-off, and seasonal variations coupled to the mobility of e.g. carbon species and primary production. During winter when the water in the superficial soil layers is frozen, the contents of carbon and carbon related elements are usually low in the stream water. The seasonal variations of dissolved ions are less accentuated and probably principally controlled by variations in water flow.

Shallow groundwater

The chemical composition of shallow groundwater is an integrated result of both present and past processes. Shallow groundwater in the Simpevarp area is characterised by neutral or slightly acid pH values, an alkalinity ranging from high to very low, and a normal or slightly elevated content of major constituents in a national context. The groundwater in the area is influenced by marine relics, resulting in elevated content of e.g. chloride and sulphate in both shallow groundwater and fresh surface waters. When the Simpevarp area is compared to normal conditions in Sweden, several parameters show large deviations. Iron and manganese show markedly elevated concentrations (about an order of magnitude), and also fluoride, iodide, strontium, and some trace elements, show higher concentrations in the area compared to Swedish reference data from shallow groundwater and surface waters. For a more detailed discussion of the results, see /Tröjbom and Söderbäck 2006/ and /Lindborg 2006/.

Overburden

Till

When data on the chemical composition of till from the Simpevarp area are compared with regional and national data, only minor differences are revealed, indicating that the till in the Simpevarp area is relatively normal in a Swedish context. However, all till samples from the Simpevarp area show very low contents of calcium carbonate in a national context.

Sediment

The content of calcium carbonate in the sediments is usually negligible. One gyttja sample from Långenmossen (PSM006564) contains, however, 12% calcium carbonate at a depth of 220–227 cm, which probably is of biogenic origin. There is a large spread in the content of carbon, nitrogen, hydrogen and sulphur, depending on both sampling location and depth in the sediment profile. For many of the sampling sites, the content of carbon, nitrogen, sulphur and hydrogen decreases with depth. The carbon content ranges from 0–60%, nitrogen from 0–2%, sulphur from 0–4% and hydrogen from 0–6%.

Soil

The chemical composition of top soil samples from the Simpevarp area is in general close to the Swedish average values, indicating rather normal pH values and normal contents of carbon and nitrogen.

Element content in amphibious plants

Many metals, e.g. iron, cobalt, chromium, copper and especially molybdenum, occur in elevated levels in amphibious plants in the Simpevarp area when compared to regional and national conditions. Lead occurs at normal levels, whereas manganese occurs at lower levels when data from the Simpevarp area are compared with the available reference data.

4.6 Biota

4.6.1 Terrestrial

Producers

The vegetation is very much influenced by the bedrock, Quaternary deposits and human land management. The bedrock mainly consists of granites. The Quaternary deposits are mainly wave washed till, whereas silt and clay have been deposited in the valleys. This is manifested in the vegetation where pine forests dominate on till and all the arable land and pastures (abandoned arable land) are found in the valleys. The dominant wetland type is the poor mire (low in nutrients) that is accumulating peat /Rühling 1997, SNV 1984/. Human management has been restricted to agricultural activities in the valleys, while forestry has been the dominating activity elsewhere. The spatial distribution of different vegetation types is presented in the vegetation map stages. A more detailed description of the different vegetation types is found in /Lindborg 2006/.

Species composition and red listed species

The flora in this region has been investigated within the project “The flora of Oskarshamn” /Rühling 1997/ which is a description of the distribution of vascular plants that is found within the municipality of Oskarshamn. The flora has also been investigated by SLU (Swedish University of Agricultural Sciences) within the “National survey of forest soil and vegetation” that has included 38 sampling localities in the area. Their results include abundance data for 230 species of vascular plants, lichens and mosses. Moreover, an additional 24 sampling localities were selected by SKB within the area using the same methodology for taxa as the “National survey of forest soil and vegetation” /Andersson 2004/. All information concerning red listed plants from the site has been obtained from the Swedish Species Information Centre (*Sw: Artdatabanken*). Further information concerning the actual species is presented in /Berggren and Kyläkorpi 2002/.

Protected areas

A number of sensitive areas of conservation interest are located within the Simpevarp area. Some of these areas have extensive protection whereas others lack protection so far. The sensitive areas are extensively listed in /Kyläkorpi 2005/. There are today three areas that are legally protected as nature reserves. These are Stenhagen, Tallungen and Misterhults archipelago (more information about the nature reserves and other protected areas can be found in /Lindborg 2006/).

Woodland Key Habitats

Forest key habitats are areas where red listed animals and plants exist or could be expected to exist /Nitare and Norén 1992/. A nationwide survey of these habitats has been conducted in Sweden, administrated by the Swedish Board of Forestry /SBF 1999/. As a complement to this survey, SKB initiated a more detailed survey at the site where 46 habitats were identified with the total area of 61 ha /Sturesson 2003/. The dominating key habitat type, both in number of objects and total area, at the site is old semi-natural grasslands or meadows with old pruned (*Sw: hamlade*) deciduous trees in close proximity to old settlements. Generally, the woodland key habitats are dominated by deciduous trees. These habitats are often a relict of an older and more open landscape created by intensive management.

Descriptive biomass and NPP models

Photosynthesis provides the carbon and the energy that are essential for many important processes in ecosystems. Photosynthesis directly supports plant growth and produces organic matter that is consumed by animals and soil microbes. The photosynthesis at an ecosystem level is termed gross primary production (GPP). Approximately half of the GPP is respired by plants to provide the energy that supports the growth and maintenance of biomass /Chapin et al. 2002/. The net carbon gain is termed net primary production (NPP) and is the difference between GPP and plant respiration. However, GPP can not be measured directly and total respiration is difficult to measure, especially in multi-species forests /Gower et al. 1999/.

The different components, constituting the NPP for a certain ecosystem may be measured separately /Clark et al. 2001/ (Figure 4-6). NPP is here the sum of all materials that have been produced and are retained by live plants at the end of the interval and the amount of organic matter that was both produced and lost by the plants during the same interval /Clark et al. 2001/.

The vegetation constitutes the major part of living biomass and comprises the main primary producers in terrestrial ecosystems. The biomass and necromass will therefore be an important measure of how much carbon may be accumulated in a specific ecosystem. Similarly, the net primary production (NPP) will provide the basis for an estimate of how much carbon (and other elements) is incorporated in living tissue. Thus, combining net primary production and decomposition rates will give a rough estimate of the carbon turnover in the ecosystem. The primary producers covering the terrestrial landscape are described by their biomass, NPP and turnover, in order to inform the conceptual ecosystem model with data (see Section 4.8). This section describes the components, the data, the resolution of the data and the methodology that is used to build the quantitative descriptive models of biomass and NPP that are further treated in Section 4.8.

The total plant biomass in an area consists of a number of different components that all have to be measured or estimated, cf. Figure 4-6 and Figure 4-7.

Quantitative descriptive models

In order to describe the ecosystem, a number of simplifications have to be made in regard of the descriptive units. These simplifications are based on their ecosystem function, e.g. the different organisms in the ecosystem are lumped together into functional groups based on structural properties, e.g. the field layer includes all herbs, grasses and ferns. Below the methodology and procedure applied in the modelling are described in brief. The results and a more detailed methodology description are given in /Lindborg 2006/. The quantitative figures are used in the corresponding terrestrial ecosystem model, as described in Section 4.8.

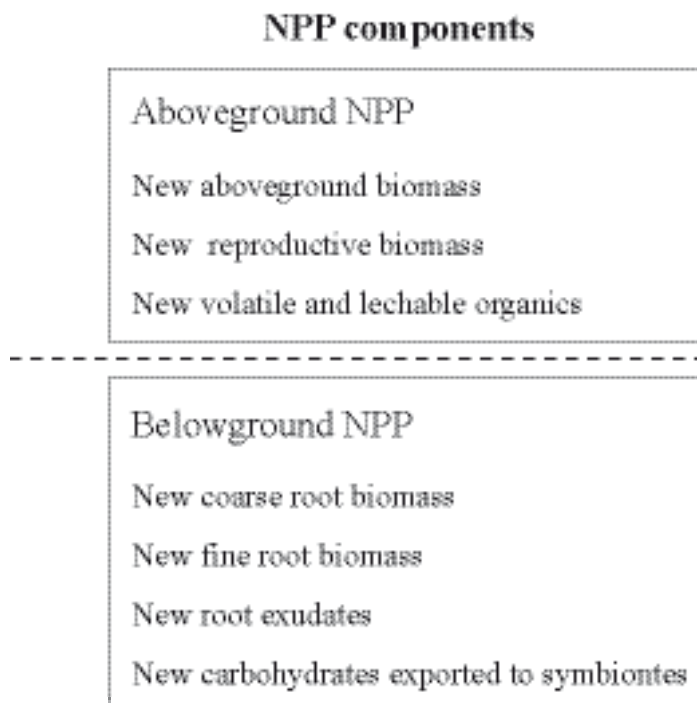


Figure 4-6. The changes in biomass components that together constitutes the NPP during a specific time interval /after Clark et al. 2001/.

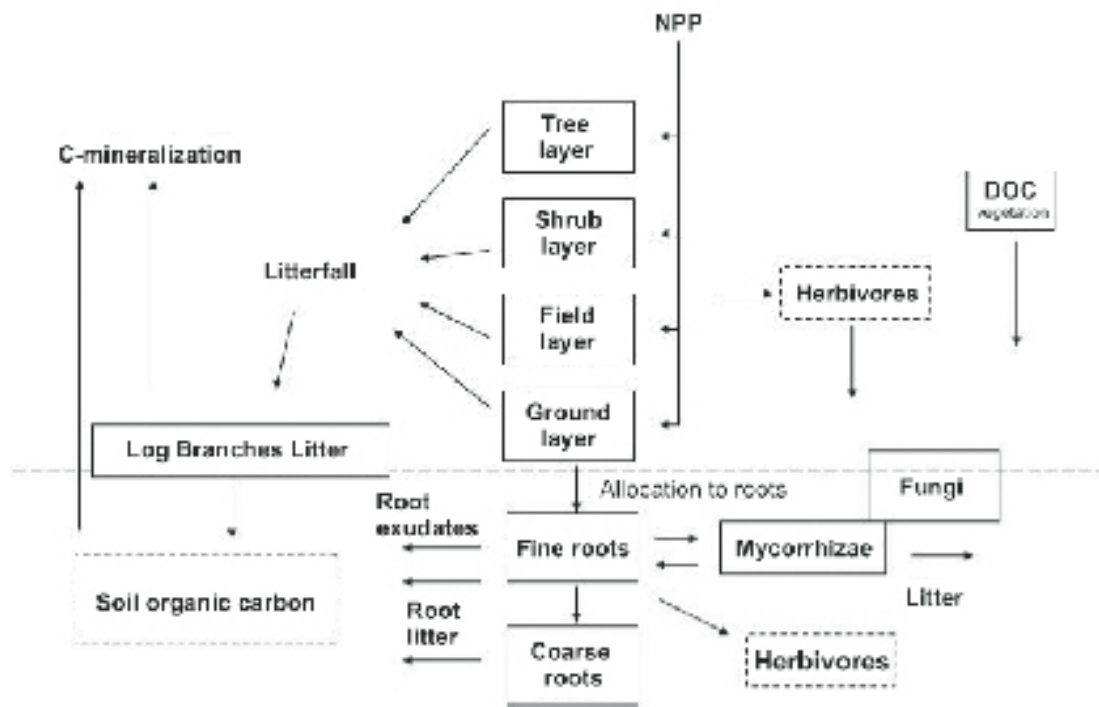


Figure 4-7. An illustration of the different pools and fluxes of matter in a terrestrial ecosystem with the focus on the producers. Pools with a broken line are treated elsewhere.

Tree layer

Biomass and NPP for four fractions of the tree layer have been calculated (woody parts (above ground), green parts, coarse roots and fine roots). Furthermore, the annual amount of litterfall and other falling components have been calculated for four forest classes. The forest classes used to describe the tree layer (young-, dry- and old- coniferous forest and deciduous forest) and the GIS sources from which the information has been obtained to construct the classes are described in /Lindborg 2006/, as well as the methodology and the data used in the calculations.

Shrub layer

Biomass and NPP of the shrub layer have been calculated. Field inventories /Andersson 2004/ indicated that the shrub layer most often is insignificant when a tree layer is present in the area. A habitat that had a very significant shrub layer was clear cuts of varying age where *Betula pendula* (silver birch) is very dominant. *Salix sp.* (Willow sp.) can be abundant on mires and was identified by /Boresjö Bronge and Wester 2003/ in their shrub layer. Therefore, the focus is on *Betula* (Birch) and *Salix* (Willow) in the shrub layer. However, due to lack of biomass and NPP data for *Salix sp.* the values for Birch are used throughout. The classes used to describe the shrub layer and the GIS sources from where the information was obtained to construct the classes is described in /Lindborg 2006/ jointly with the methodology and the data used in the calculations.

Dead wood

The biomass of dead wood has been calculated according to the description in /Lindborg 2006/, and is presented in $\text{gC}\times\text{m}^{-2}$ for different vegetation types.

Field and ground layer

Biomass and NPP of the field and ground layer have been calculated. The classes used to describe field and ground layer and the GIS sources from where the information is obtained to construct the classes is described in /Lindborg 2006/ as well as the methodology and the data used in the calculations. The results, assigning biomass and NPP values in $\text{gC}\times\text{m}^{-2}$ and $\text{gC}\times\text{m}^{-2}\times\text{y}^{-1}$ for the different field and ground layer classes are presented in /Lindborg 2006/.

Fungi/mycorrhizae

Biomass and NPP for fungi in the forest habitats (young-, dry- and old- coniferous forest and deciduous forest) have been calculated according to the approach described in /Lindborg 2006/.

Consumers

Mammals

The most common larger mammal species in the Simpevarp area is roe deer (5 deer \times km⁻²) /Truvé and Cederlund 2005/. Moose is also fairly common (0.7 moose \times km⁻²), but unevenly distributed, which is normal for this part of Sweden due to variations in hunting pressure, snow depth and distribution of food. European and mountain hare are fairly low in abundance, compared to other regions (see Table 4-6). A more detailed description of the mammals is found /Lindborg 2006/.

No observations of Badger, Beaver, Fallow deer, Lynx, Otter or Wolf were made during the investigations in 2003.

Birds

In total, 126 species were found in the regional model area in 2003 (112 in 2002), and 28 of these are red listed as endangered bird species in Sweden /Green 2004/. Both the number of species and individuals/territories were similar (or even higher) in 2004 compared to earlier years. The most common species on land in 2004 were Chaffinch and Willow Warbler /Green 2005/. A major part of the nesting species was small birds, associated with the open or semi-open landscape. A coarse density estimate of birds in the area has been given by (Green 2005 pers.comm.). The terrestrial bird fauna make up 98% of the total bird fauna. In the Simpevarp regional model area this means a density of 637 pairs or 1,274 individuals \times km⁻².

Cattle

A significant part of the terrestrial biomass of consumers in the Simpevarp area is domestic animals. There were 4.3 cows and calves per km² in the Simpevarp area /Miliander et al. 2004/, which can be compared with the densities given in Table 4-6.

Table 4-6. Estimated abundances of mammal species in 2003/2004 in the Simpevarp regional model area /Truvé and Cederlund 2005/.

Species	Animals per km²
European hare (field)	3.51
Mountain hare (forest)	0.52
Fox	Observed
Marten	0.13
Mink	Observed
Moose	0.68
Red deer	0.03
Roe deer	4.9
Small mammals field (mice and voles)	1,060
Small mammals forest (mice and voles)	1,160
Small mammals water areas (water vole)	570
Small mammals (common shrew)	850
Wild boar	0.15

Amphibians and reptiles

Site-specific data concerning the species that are likely to occur in the Simpevarp area have been obtained through field studies by /Andrén 2004a/. There are no site-specific density data for amphibians and reptiles. Generic data concerning these species have been obtained from /Andrén 2004b/. These data are compiled in /Lindborg 2006/.

Soil fauna

Three examples of soil fauna densities and biomass figures have been obtained from Tryggve Persson, professor in Soil biology at SLU. The three examples come from a pine moor in Gästrikland, a deciduous forest in Uppland (Andersby-Ångsbacka in Dannemora) and a grassland in Uppland /Lohm and Persson 1979/. The densities and biomass for the different soil species are given in /Lindborg 2006/.

Quantitative model

A biomass and production model, with carbon flows for the terrestrial consumers in the subareas within Simpevarp area, has been produced. The calculations are based on the site-specific density data for mammals and birds and generic data for amphibians and reptiles. As there are no site-specific data concerning the agriculture in these subareas, theoretical values have been used for the cattle biomass and production, as well as the crop production. These values are based on the grazing and arable areas in each subarea. These data are compiled in /Lindborg 2006/.

The applied methodology with carbon pools and flows are presented in /Lindborg 2006/. An illustration of the carbon budget is given in Figure 4-8. The model for the terrestrial consumers is used in the terrestrial ecosystem model, described in Section 4.8.

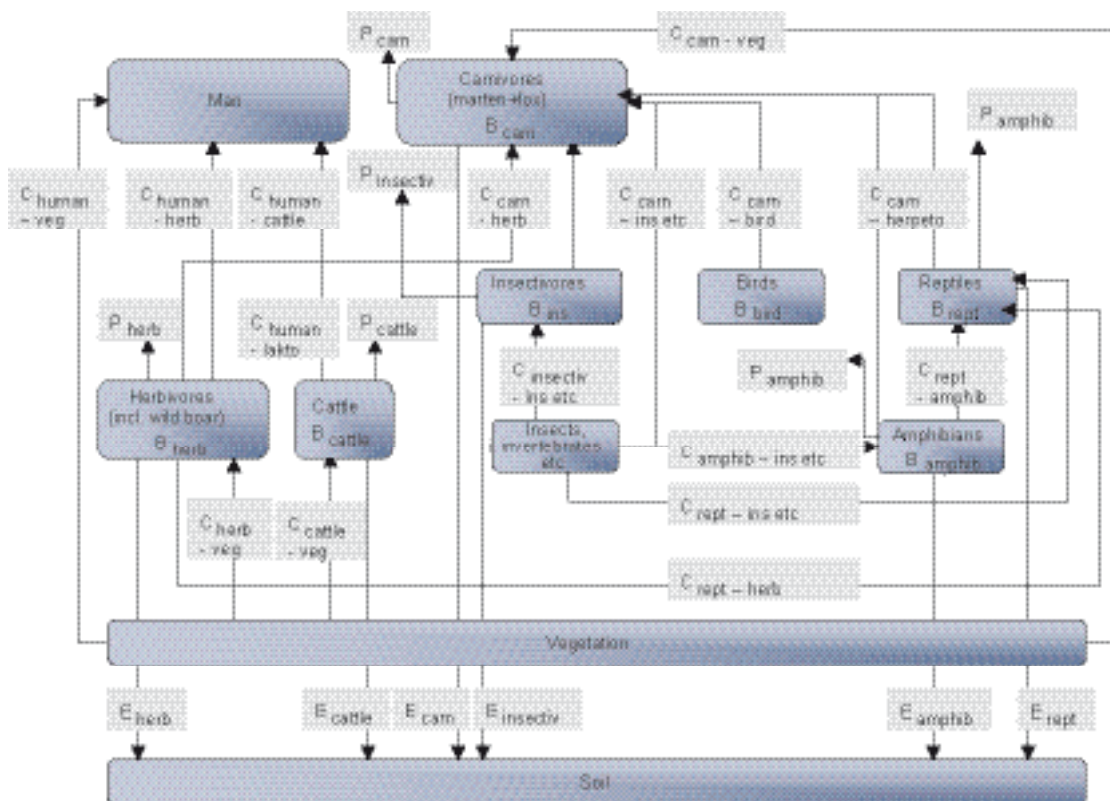


Figure 4-8. An illustration over the pools and flows of carbon in a terrestrial ecosystem, with focus on the consumers. B = Biomass, P = Production, C = Consumption and E = Egestion (mass of faeces).

4.6.2 Limnic

Limnic producers

Methodology

The *lake characterisation* includes, besides the identification of watersheds, a recording of lake morphometric parameters using a Differential Geographical Position System and an echo-sounder equipment /Brunberg et al. 2004/. From these data, bathymetric maps, and depth grids were constructed for each lake. Using the same equipment, the distribution of different lake habitats was determined in the field.

Phytoplankton was sampled at 12 occasions during the period July 2003–June 2004 /Sundberg et al. 2004/. Three of the samples were analysed (July and December 2003, April 2004). Phytoplankton samples were taken with a so-called “Ramberg-rör” (a 2 m tube sampler with a diameter of 3.5 cm). Five sub-samples were taken within a radius of 50 m. Species composition and biomass of phytoplankton were determined using an inverted phase-contrast microscope.

Description/models

The lakes in the Simpevarp area have been divided into five different habitat types; the Littoral types I, II and III, Pelagial and Profundal /Brunberg et al. 2004/.

Littoral type I: The littoral habitat with emergent and floating-leaved vegetation. This habitat is developed in wind-sheltered, shallow areas where the substrate is soft and allows emergent and floating-leaved vegetation to colonise.

Littoral type II: The littoral habitat with hard substrate. This habitat develops in wind-exposed areas of larger lakes, but also in smaller lakes, where the lake morphometry includes rocky shores. The photosynthesising organisms colonising these areas include species that are able to attach to the hard substrate, e.g. periphytic algae.

Littoral type III: The littoral habitat with submerged vegetation. This habitat is found in deeper areas of the lakes, where light enough to sustain photosynthetic primary production penetrates down to the sediment.

The profundal habitat: This habitat develops in the sediments of lakes where light penetration is less than that required to sustain a permanent vegetation of primary producers. Non-photosynthesising organisms dominate this habitat. The profundal organisms are dependent on carbon supplies imported from other habitats of the lake, or from allochthonous sources.

The pelagic habitat: This habitat includes the open lake water, where a pelagic food-web based on planktonic organisms is developed. Depending on the availability of light, these plankton are dominated by either photosynthetic production (i.e. by autotrophic phytoplankton) or, if the water is strongly coloured or turbid, by heterotrophic carbon processing (e.g. by heterotrophic or mixotrophic bacterioplankton and phytoplankton). The pelagic habitat covers the same area as the sum of areas corresponding to littoral type II, littoral type III and profundal habitats within a lake.

Lakes

The relative distribution of different habitats in four of the lakes are presented in Table 4-7. All five major habitats are present in Lake Frisksjön (Figure 4-9). Despite the relative shallowness of this lake (maximum depth 2.8 m), the brown colour of the water prevents light from penetrating some parts. Thus, the profundal habitat covers a substantial part of the bottom area (41%). The dominant littoral habitat is of type III.

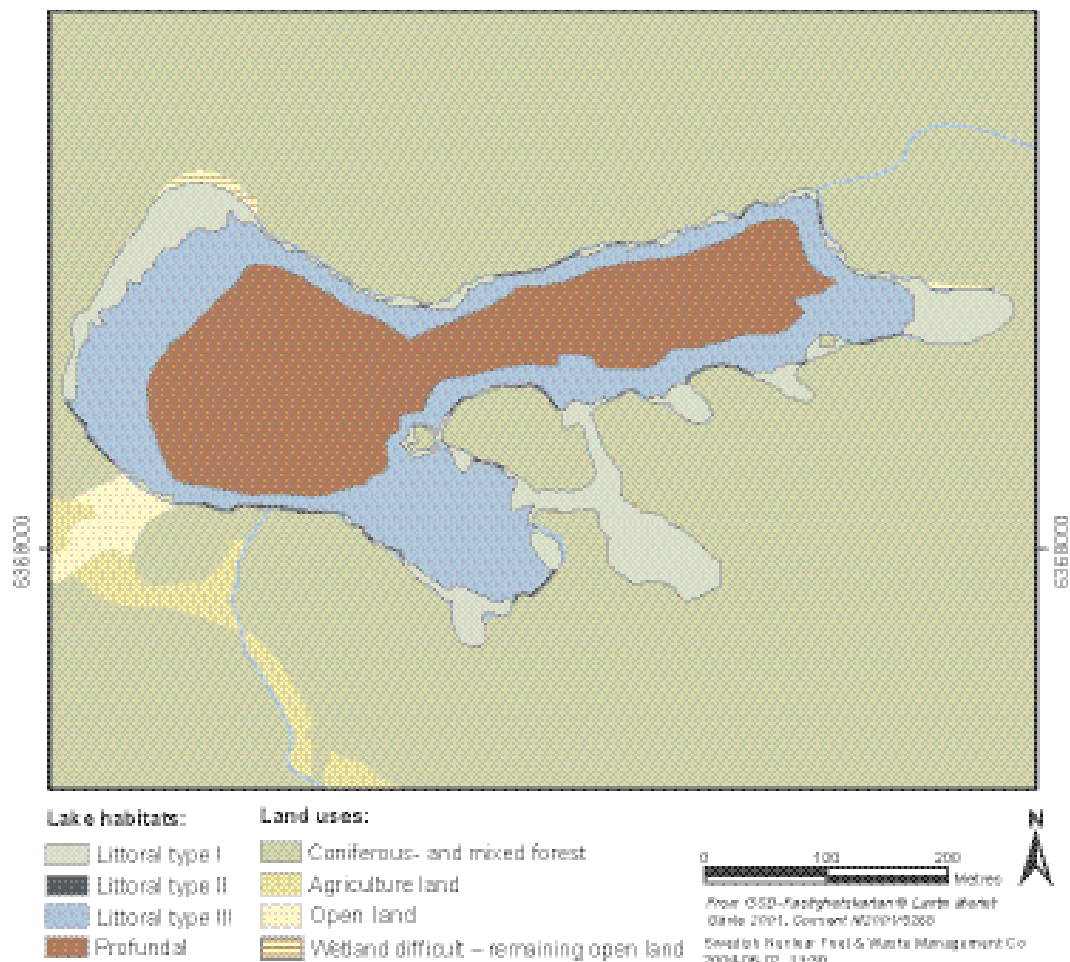


Figure 4-9. Distribution of major habitats in Lake Frisksjön /Brunberg et al. 2004/.

Table 4-7. Distribution of major habitats in four lakes /Brunberg et al. 2004/.

Habitats	Area (%)			
	Lake Frisksjön	Lake Plittorpögöl	Lake Jämsen	Lake Söråmagasinet
Littoral type I	18	20	21	20
Littoral type II	< 2	< 1	< 1	< 1
Littoral type III	38	13	5	40
Pelagial	82	80	79	80
Profundal	41	67	75	38

Macrophyte biomass was studied in Lake Frisksjön in August 2004, when the vegetation had reached its maximum biomass for the season. The calculations were often based on only one weight of each plant species and are therefore to be considered as rough estimates. In Littoral III, no vegetation was found. Littoral II hosted low vegetation biomass, whereas the biomass was higher in Littoral I (see Table 4-8). This indicates that the bottom area with light conditions below the compensation level, i.e. where it is too dark to enable primary production, is larger than the area classified as Profundal in /Brunberg et al. 2004/. In the ecosystem model for Lake Frisksjön presented below, the area of Littoral III has therefore been included in the Profundal.

Table 4-8. Vegetation biomass in Lake Frisksjön (data from /Aquilonius 2005/).

Habitat	Biomass (g DW m ⁻²)
Littoral I	13.2
Littoral II	2.1
Littoral III	0

Detailed information on the composition and biomass of phytoplankton in Lake Frisksjön is to be found in /Lindborg 2006/.

Running waters

In the River Mederhultsån (catchment Simpevarp 6, cf. Figure 4-12) the vegetation cover was often 50% or more, the exception was in the downstream sections close to the outlet to the sea, where the growth was sparse or lacking. The often dominant species in upstream sections was *Lemna minor*, which was found in substantial amounts. Further downstream, commonly dominating species were *Alisma plantago-aquatica*, *Juncus effusus*, and *Sparganium sp.* In the most upstream part of the River Kåreviksån (catchment Simpevarp 7, cf. Figure 4-12) where water was present, there were a few sections with dense growth of vegetation. Downstream of Lake Frisksjön, where the channel was densely shaded, the vegetation was characterised by isolated plants, and in many of the sections vegetation was lacking. Species that often dominated in this part of the stream were *Alisma plantago-aquatica*, but there were also sections with substantial amounts of *Lemna minor*. In the River Ekerumsån (catchment Simpevarp 9, cf. Figure 4-12) there was a substantial and intense growth of vegetation in most parts. Among the dominating species were *Alisma plantago-aquatica* and *Juncus effusus*. In the River Laxemarsån (catchment Simpevarp 10, cf. Figure 4-12), the vegetation abundance fluctuated from “Lacking” to “Intense growth”, however, “Lacking” was the most common abundance class. Species that frequently dominated the investigated sections were *Alisma plantago-aquatica* and *Nymphaeaceae*. *Phragmites australis* was commonly found in the most downstream part.

Limnic consumers

Detailed information on the composition and biomass of zooplankton, benthic fauna and fish in Lake Frisksjön are found in /Lindborg 2006/. The fish community can be regarded as typical for small brownwater lakes in the Simpevarp area. It contains six species (with Swedish translation in italics); perch (*abborre*), bream (*braxen*), ruffe (*gärs*), roach (*mört*) and pike (*gädda*), of which perch is dominating both in number and in biomass.

4.6.3 Marine

The marine system in the Simpevarp area encompasses three major habitats; semi-enclosed bays to a varying degree affected by the fresh water effluence, coastal archipelago with sheltered areas and a Baltic Sea coastal habitat exposed to sea currents and wave action. The bays have a variable geometry, large shallow areas (less than 1 m) are found as well as depths down to 18 m. The bay areas have an average surface water salinity of 3.5–4.5‰, whereas the bottom water (18 m) has a salinity close to the surrounding coastal area of 6‰. The bay areas are characterised by humic, low transparency conditions, averaging a light penetration of 2–3 m in enclosed bays, 4–7 m in the archipelago and 12 m in the open sea.

Producers

Macrophytes

The inner soft bottom parts of the archipelago north of the Simpevarp peninsula (around the Äspö island) are dominated by *Chara sp.* (Figure 4-10). West of Ävrö, a large area is covered by the Xanthophyceae *Vaucheria sp.* On corresponding bottoms in the southern area, the vegetation is dominated by vascular plant communities, dominated by *Potamogeton pectinatus* and *Zostera marina*. The sheltered inner coastal waters, particularly south of the Simpevarp peninsula, are

dominated by *P. pectinatus* (Figure 4-10). Further out towards more exposed areas *P. pectinatus* and *Z. marina* occurs together in a patchy appearance. On hard substrates, in shallow areas, the vegetation is dominated by *Fucus vesiculosus* and in deeper areas red algae covers the hard substrata /Fredriksson and Tobiasson 2003/. *Fucus sp.* in low abundance is recorded to approximately 10 m depth and red algae down to approximately 30 m /Tobiasson 2003/.

Phytoplankton

Phytoplankton in the Simpevarp area is dominated by diatoms, cryptophytes and dinoflagellates. The biomass varies greatly both intra- and inter-annually /Sundberg et al. 2004/.

Consumers

Benthic fauna

The benthic fauna is dominated by filter feeders (*Mytilus edulis*) and detritivores, often *Macoma baltica* or *Hydrobia sp.* In the coastal hard bottom areas, filter feeders constitute up to 95% of the biomass /Fredriksson 2005/ – detritivores on the other hand constitute 50–80% of the biomass in the inner areas e.g. Basin Borholmsfjärden.

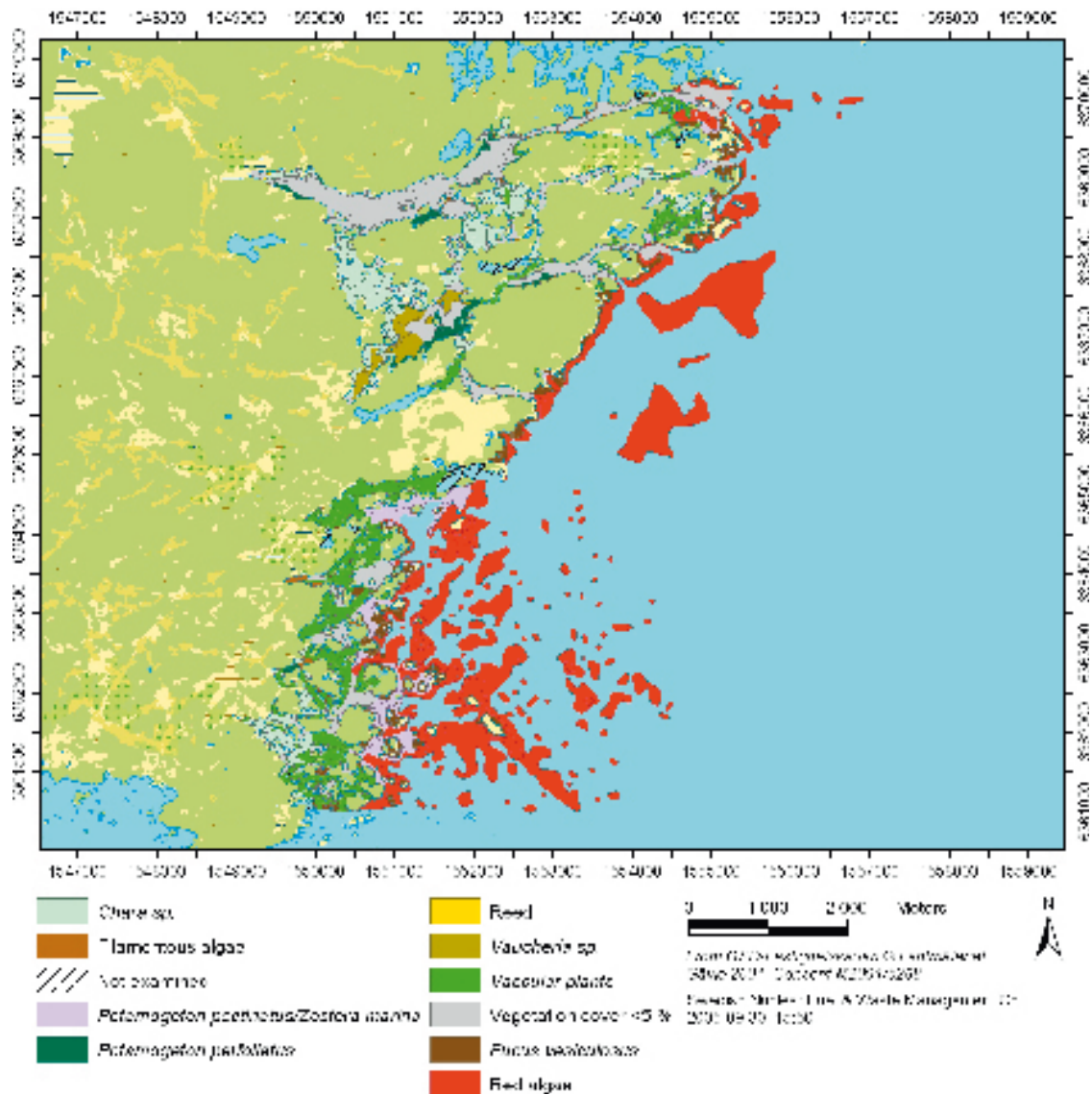


Figure 4-10. Vegetation map over Simpevarp. The map shows macrophyte communities identified by /Fredriksson and Tobiasson 2003/.

Epifauna

In the vegetation mapping study /Fredriksson and Tobiasson 2003/ also the fauna associated with vegetation was sampled. In total, 45 animal species associated to the vegetation occurred in the area around the Simpevarp peninsula. The *Fucus sp.* communities is the most diverse concerning associated fauna and harbour 31 species or higher taxa, while in the soft bottoms without vegetation only 14 species have been found.

Zooplankton

A survey of zooplankton was performed along the water sampling programme /Sundberg et al. 2004/. Zooplankton is more abundant in the inner bays than in the coastal areas. The fauna was dominated by copepods except in July when the cladocerans or rotifers dominated in the upper water column.

Conceptual model of the marine ecosystem

The organisms represented in the area were divided into different functional groups, which were then connected into a food-web. This classification scheme of which groups to use and how to divide the organisms among them is based on /Kumblad et al. 2003/ and is presented in /Lindborg 2006/.

A conceptual illustration describing the ecosystem in the Simpevarp area by habitat is shown in Figure 4-11, where the “phytobenthic habitat” is defined as the benthic habitat in the photic zone, “benthic” as the benthic habitat in the aphotic zone, and the “pelagic habitat” as the open water habitat, both photic and aphotic.

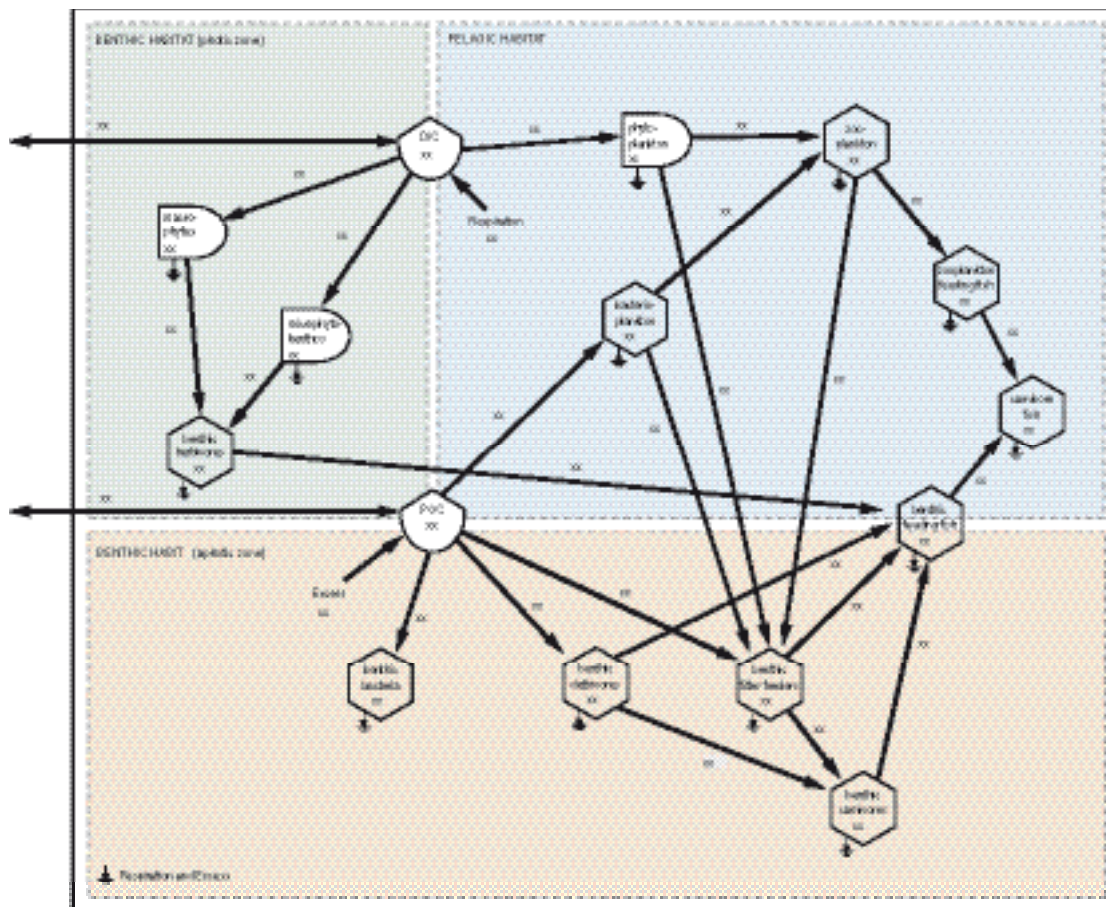


Figure 4-11. Conceptual illustration of the marine coastal ecosystem in the Simpevarp area including illustrations of the habitats (phytobenthic, soft benthic and pelagic).

4.7 Humans and land use

Input data sources and calculated numbers for the variables used to describe humans and land use in the Simpevarp area and its surroundings are shown in great detail in /Miliander et al. 2004/ and briefly in /Lindborg 2006/. The short description below illustrates the situation in the parish of Misterhult, since many of the data were available on the parish level. The parish of Misterhult is approximately 28 times larger than the Simpevarp area.

The assessment of the data acquired can be summarised as follows:

- The parish has a low density of population (6.6 individuals \times km⁻² in 2002) and the number of inhabitants has diminished slowly during the 1990s.
- The main employment sector is within electricity production. There is a clear net influx of commuting individuals to the region due the dominant employer (the OKG Power Company that operates the Oskarshamn nuclear power plant).
- Mining (decoration stone) and manufacturing are the main employment sectors among the inhabitants of the parish.
- There are proportionally more holiday-houses in the parish than in the Municipality of Oskarshamn and the County of Kalmar as a whole, which indicates that the region has a proportionally larger holiday population. The number of holiday houses has increased since 1996 (6%).
- The land use is dominated by forestry and the extraction of wood is the only significant human related outflow of biomass from the area.
- The hunting statistics show that the harvest of moose is more extensive in the parish than in the County of Kalmar, which indicates that hunting is an important out-door activity. Besides this, the coastal area is well used for leisure activities such as hiking, canoeing, fishing and boating. The entire coast is of national interest for outdoor life and nature conservation.
- The agriculture in the area is of limited extent. The arable land comprises 3.5% of the total land area, compared with 11.5% in the county as a whole. A wide spectrum of crops is cultivated, but the major crop is barley. Its significance has grown during the 1990s. The second most important crop, oats, is decreasing in importance.
- The flow of carbon to humans from the subareas within the Simpevarp area has been calculated according to the methodology described in /Lindborg 2006/. The result is presented in /Lindborg 2006/. The figures are used in the terrestrial ecosystem model that is described in Section 4.8.

4.8 Development of the ecosystem model

This section accounts for work done to describe and model the ecosystems of the Laxemar subarea. The description is divided into three subsystems, terrestrial, limnic and marine. Ongoing work aims at integrating these ecosystem models and linking the flow of matter between them, and further to identify ecosystems in the landscape that accumulate matter. This task is not completed yet, and in this report no effort has been made to link these systems into a landscape scale model. However, in /Lindborg 2006/ the models described here are used to build a first example of a spatially distributed model, describing the stocks and flows of carbon in the Laxemar subarea.

4.8.1 Terrestrial ecosystem description

The descriptive ecosystem model is applied at the landscape level covering 14 subcatchment areas making up the Laxemar subarea (Figure 4-12). Pools and fluxes for all functional groups are summed using GIS (see Section 4.6.1). The resulting budgets are presented in /Lindborg 2006/, where all the separate pools and fluxes, in accordance with the conceptual model, are used to quantify a number of ecosystem properties.

The dominating vegetation types within the Laxemar subarea are forests, primarily pine on acid rocks. The pine forest is of mesic (between dry and moist)-moist type.

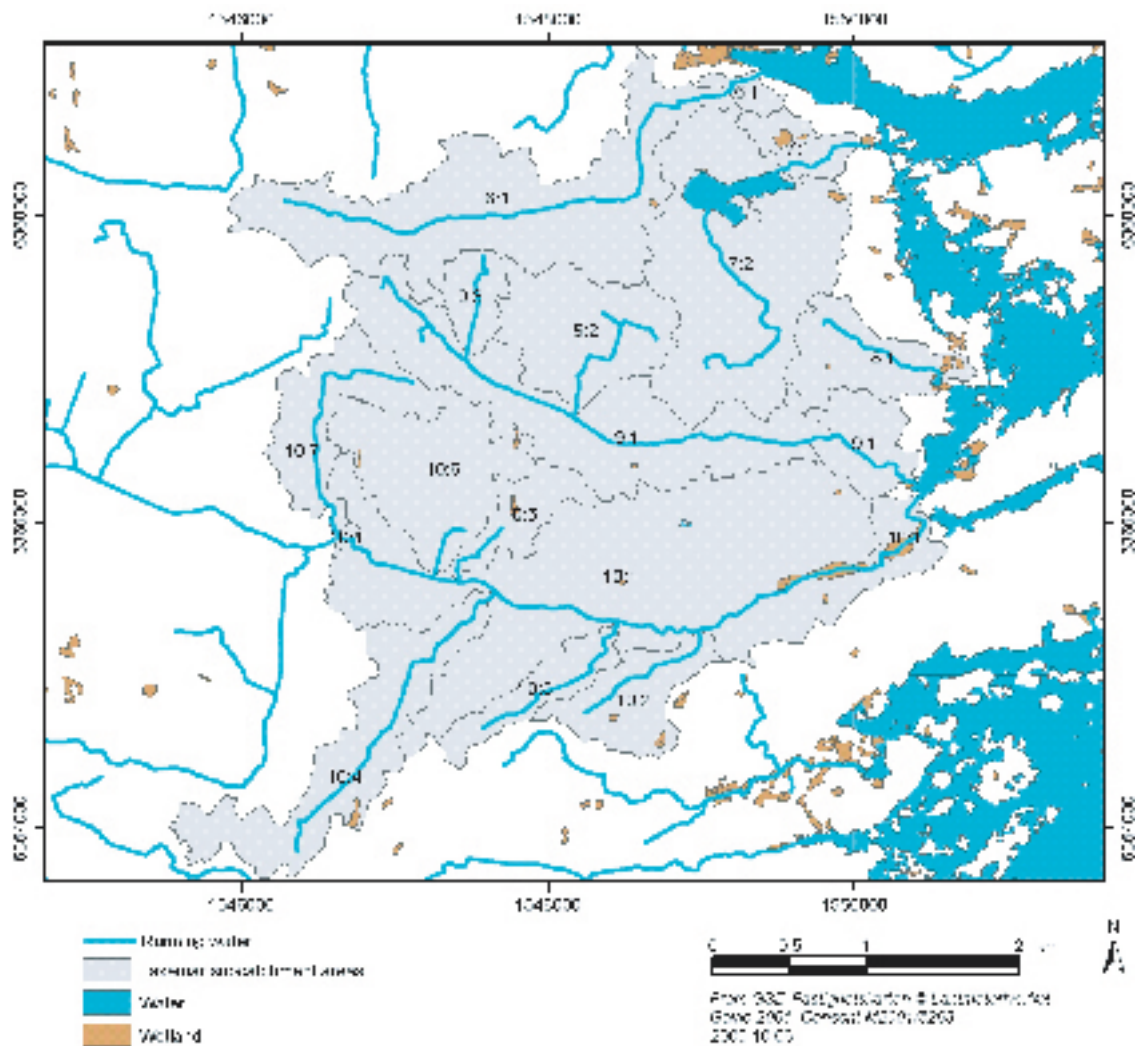


Figure 4-12. The subcatchment areas in the Laxemar subarea on which the descriptive ecosystem model was applied in order to construct large scale carbon budgets. Wetlands and running water are also shown.

Net ecosystem production

The net ecosystem production (NEP), which is the net accumulation of carbon in the discharge area during a time step, is highly variable between subcatchments /Lindborg 2006/. NEP, corrected for subcatchment area, ranged from 13 to 460 $\text{gC} \times \text{m}^{-2} \times \text{y}^{-1}$, indicating that there is an overall net yearly accumulation of carbon within all the modelled subcatchment areas of the Laxemar regional model area (Figure 4-11). This accumulation is found in both living biomass, mainly in the tree layer, and in the soil. Some of the variation in NEP may be explained by the land type coverage. A comparison using information about land type coverage (Table 4-9) and data for some specific vegetation types, suggests that the low NEP in subcatchment 10:5 is explained by the substantial coverage of clear-cuts, where the heterotrophic respiration in the soil layer is large. Similarly, the large NEP in subcatchment 8:1 may be explained by a very large proportion of older coniferous forests that accumulates carbon both in the soil and in biomass.

Table 4-9. The subcatchment areas within the Laxemar subarea characterised by their size and some land type coverage in terms of fraction of the total subcatchment area.

	Subcatchment area													
	6.1	7.1	7.2	8.1	9.1	9.2	9.3	10.1	10.2	10.3	10.4	10.5	10.6	10.7
Land area (km ²)	2.00	0.21	1.73	0.50	1.85	0.77	0.22	3.44	0.46	0.32	1.00	0.29	0.89	0.61
Wetlands	0	0.05	0	0.03	0	0	0	0.01	0.02	0	0.01	0.01	0	0
Conifer forest	0.52	0.27	0.58	0.85	0.56	0.53	0.68	0.49	0.46	0.71	0.57	0.22	0.49	0.57
Agriculture land	0.12	0	0.06	0	0.11	0.15	0.17	0.05	0.11	0.07	0.15	0.04	0.04	0.03
Young conifer forest	0.21	0.44	0.22	0.08	0.16	0.21	0.09	0.22	0.18	0.13	0.14	0.28	0.24	0.3
Clear cuts	0.06	0.11	0.03	0	0.08	0.1	0.02	0.09	0.14	0.05	0.04	0.39	0.14	0.09

Secondary and tertiary producers

The consumption of herbivores and carnivores is very similar over the landscape, which is an effect of a low resolution of their defined feeding habitats. Some are divided into field or forest feeding but the majority is evenly feeding in the landscape. A more precise definition of feeding habitat is only available for amphibians, but wetlands are rather scarce in the modelled area, and cattle, where the presence of agricultural land increases the secondary production due to the possibility of sustaining cattle.

Humans

The human consumption of products derived from the vegetation is of the same order as the herbivore consumption of vegetation in those cases in which the subcatchment area contain agriculture land and is thereby able to sustain cattle according to the premises presented in /Lindborg 2006/. The human consumption of meat and milk is one order of magnitude lower than the human consumption of vegetation and is similarly dependent on the subcatchment area's possibility of sustaining cattle.

Flow of matter

There are, so far, no site specific data from the area that can be used to confirm the estimated transport of carbon from the subcatchment areas. Calculations of the carbon budget for Lake Frisksjön in subcatchment 7:2 do indicate that the estimated transport of 6.9 ton C×y⁻¹ to the lake fits the carbon budget of the lake fairly well. However, observations from the lake indicate that the input of POC (Particulate Organic Carbon) should be fairly large and the estimates of input from land could therefore be somewhat low.

4.8.2 Limnic ecosystem description

Lake Frisksjön is the only lake in the selected drainage area. The lake has a total surface area of 0.13 km², a maximum depth of 2.8 m and a mean depth of 1.7 m. Similarly to most lakes in the region, the water colour is brown, and despite the relatively shallow water depth, large areas of the bottom are below the light penetration depth. The theoretical turnover time for the lake is 264 days. For a detailed description of the hydrological, chemical and biological characteristics of the lake, see /Lindborg 2006/.

Food web matrix for Lake Frisksjön

For the development of an ecosystem model, the major functional groups, producers and consumers, were further divided into a number of subgroups based on taxonomy, choice of habitat and food preferences. The consumption of different food sources for each functional group was obtained by first identifying the food-web relationships between all groups in the system. Consumers were assumed to eat in proportion to what is available of their food item/prey (in terms of biomass). The food-web relationships, together with food availability, were then used to calculate the food-web matrix for Lake Frisksjön (Table 4-10).

Table 4-10. Food web matrix for Lake Frisksjön, including estimated food proportions of different food sources (columns) for the different organism groups (rows). DOC = Dissolved Organic Carbon, POC = Particulate Organic Carbon, DIC = Dissolved Inorganic Carbon.

	Phytoplankton	Macrophytes	Epiphytic algae	Epiphytic bacteria	Epiphytic fauna	Bacterioplankton	Zooplankton	Z-fish	B-fish	C-fish	Benthic bacteria	Benthic fauna	DOC	POC	DIC
Phytoplankton						0.45					0.05				0.50
Macrophytes															0.00*
Epiphytic algae															1.00
Epiphytic bacteria													0.58	0.42	
Epiphytic fauna			0.50	0.50											
Bacterioplankton													0.58	0.42	
Zooplankton	0.59					0.21	0.19								
Z-fish (zooplanktivore)							1.00								
B-fish (benthivore)			0.03	0.03	0.00							0.94			
C-fish (carnivore)								0.01	0.11	0.10		0.79			
Benthic bacteria															1.00
Benthic fauna	0.01					0.01	0.01				0.03	0.04		0.91	

* Macrophytes use carbon from the atmosphere.

Primary producers obtain their carbon from the DIC (Dissolved Inorganic Carbon) pool. However, since phytoplankton partly consists of mixotrophic species, they can also use other carbon sources, mainly bacteria. Macrophytes use carbon from the atmosphere. Humans and birds are not included in the food web matrix, as quantitative data for these groups are lacking.

Carbon budget for Lake Frisksjön

The biomass of primary producers in Lake Frisksjön is dominated by macrophytes (Table 4-11). Also primary production is dominated by macrophytes, but phytoplankton contributes with a substantial part of total primary production, despite the low biomass of this functional group. Almost 80% of the secondary production occurs in the pelagial habitat, with mixotrophic phytoplankton, bacterioplankton and zooplankton being the most important contributors. Most of the remaining secondary production can be attributed benthic fauna and bacteria.

Taken on an annual basis, almost all groups of organisms show a carbon excess when subtracting respiration and grazing from production/consumption. Since there is no increase in biomass over time, this excess carbon is assumed to contribute to the POC pool (Particulate Organic Carbon).

The ecosystem model presented above indicates that the annual respiration in Lake Frisksjön is at the same level as the annual primary production, about 12 metric tonnes per year. Annual carbon input from the catchment area is estimated in the terrestrial ecosystem model at 6.9 tonnes. A rough estimate of carbon outflow, based on measured total organic carbon (TOC) in lake surface water and modelled discharge, indicates that the annual transport of organic carbon out of the lake is approximately 5 tonnes. Annual sedimentation has been estimated from the sedimentation rate ($1.2 \text{ mm} \times \text{y}^{-1}$) and sediment carbon content given in /Nilsson 2004/, at 1.9 tonnes carbon per year. Integrating the above, this gives an almost balanced overall carbon budget for Lake Frisksjön; the carbon deficit is c. 300 kg per year, which correspond to about 1% of the total annual carbon turnover in the lake (Figure 4-13).

Table 4-11. Total average biomass (gC), annual primary and secondary production (gC year⁻¹), and annual excess of functional organism groups in Lake Frisksjön, according to the carbon budget. Excess for a functional group denotes the difference between estimated annual supply (net primary/secondary production) and demand (grazing/predation). Note that phytoplankton includes both autotrophic and mixotrophic species and hence this group shows primary as well as secondary production.

Functional group	Biomass		Net primary production		Secondary production		Excess gC y ⁻¹
	gC	%	gC y ⁻¹	%	gC y ⁻¹	%	
<i>Pelagic habitat</i>	1.4E+5	0.49	4.3E+6	36.32	6.0E+6	78.83	
Phytoplankton	3.8E+4	0.13	4.3E+6	36.32	2.5E+6	33.29	5.6E+6
Bacterioplankton	1.4E+4	0.05			1.6E+6	21.33	-3.0E+6
Zooplankton	2.5E+4	0.09			1.3E+6	17.14	8.8E+5
Planktivore fish	1.5E+3	0.01			1.3E+4	0.18	1.0E+4
Benthivore fish	3.1E+4	0.11			2.7E+5	3.56	2.1E+5
Piscivore fish	2.9E+4	0.10			2.5E+5	3.33	1.9E+5
<i>Benthic habitat</i>	3.9E+5	0.00	0	0	1.5E+6	19.57	
Benthic bacteria	1.7E+5	0.58			4.5E+5	5.85	-1.4E+5
Benthic fauna	2.3E+5	0.80			1.0E+6	13.72	-1.4E+5
<i>Littoral habitat</i>	2.8E+7	98.13	7.5E+6	63.68	1.2E+5	1.60	
Macrophytes	2.8E+7	98.08	7.2E+6	60.79	0.0E+00		7.2E+6
Epiphytic algae	7.5E+3	0.03	3.4E+5	2.89	0.0E+00		1.8E+5
Epiphytic bacteria	7.5E+3	0.03			1.2E+5	1.57	9.8E+4
Epiphytic fauna	2.4E+2	0.00			2.3E+3	0.03	1.7E+3
<i>Lake total</i>	2.8E+7		1.2E+7		7.6E+6		

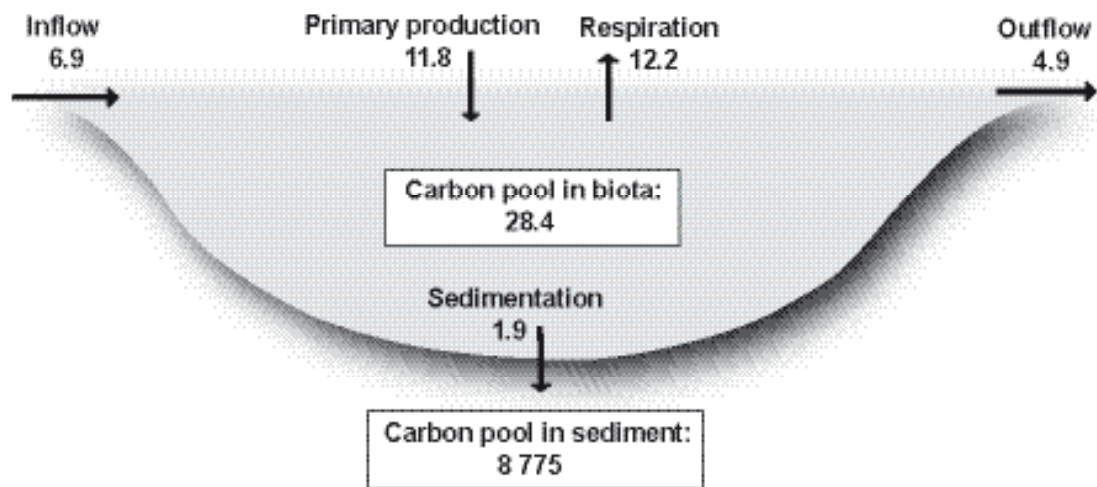


Figure 4-13. Major input and output pathways for carbon in Lake Frisksjön. Numbers denote annual carbon flow (metric tonnes of carbon per year). For comparison, the major carbon pools in the lake are shown within boxes (tonnes of carbon).

4.8.3 Marine ecosystem description

The Simpevarp marine ecosystem has been divided in fourteen basins (see Figure 4-14). The division is based on bathymetry and coincides with projected future drainage basins. The basins are treated as separate units, as would lakes be, based on the assumption that relevant flow of matter will be possible to quantify either from estimations of abiotic carbon flow (runoff and oceanographic flows) or biotic (migration of organisms).

The system is assumed to be in a steady, non seasonal, state and all input data are based on yearly averages. The parameters used in the calculations have been interpolated to a 10 m grid using different methods. All biomasses and production values are considered to be fixed and independent of each other and no fluxes between the grid-cells or to and from the system are quantified. The pool of particulate organic carbon in the sediments is not included. The results are presented per square metre or per basin.

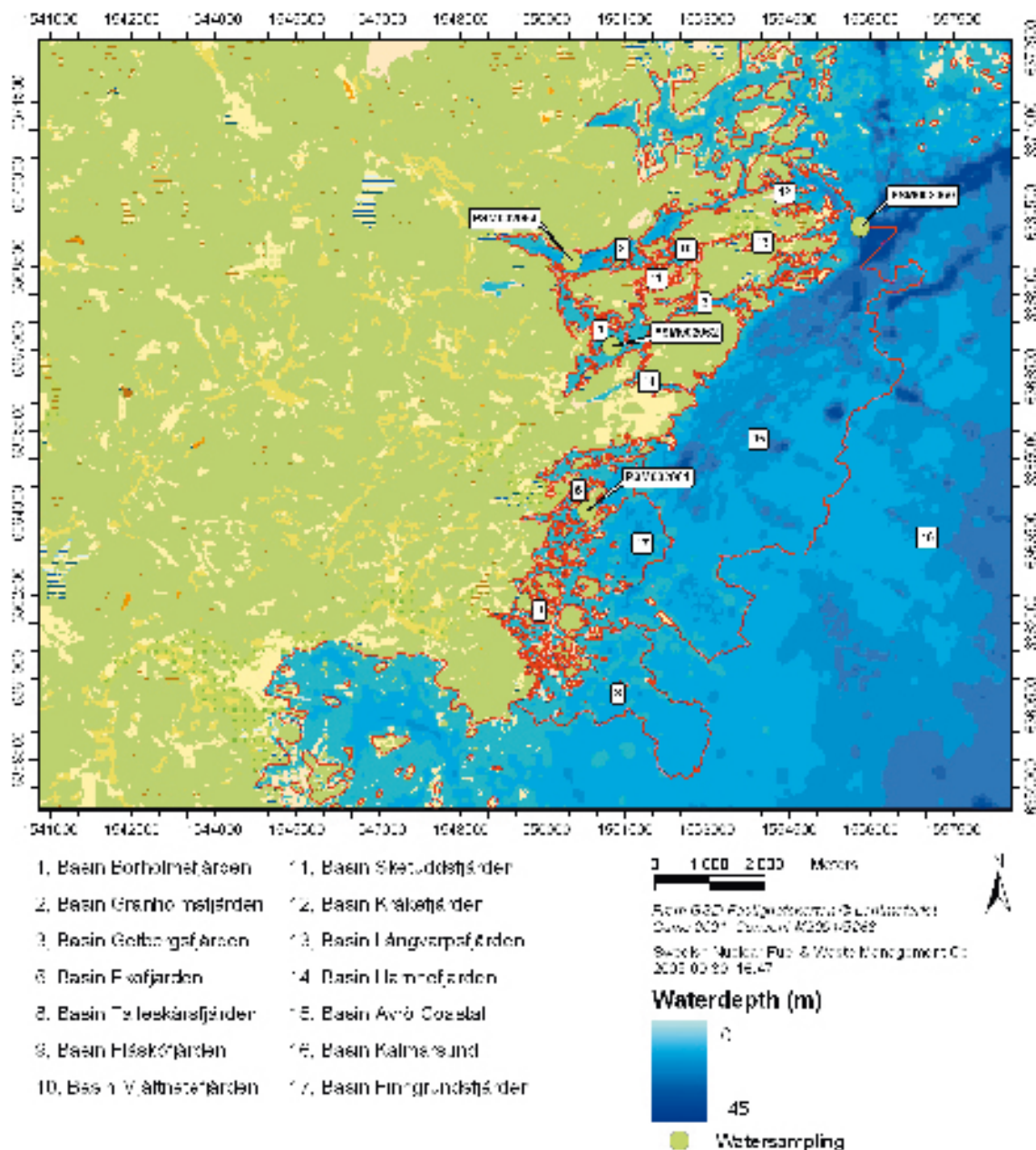


Figure 4-14. The basins in the Simpevarp area. The digital elevation model for the sea is displayed as increasing dark blue with depth.

Quantitative site specific model

The calculations of biomass, respiration, consumption and production for the different functional groups are described in /Lindborg 2006/ as well as the conversion factors used. The excess, defined as the excess of primary or secondary production subtracting the demand from consumers, has also been calculated.

Consumption proportions

The food matrix, presented in Table 4-12, shows the proportions of consumption of one functional group (vertical) of another functional group (horizontal). The proportions of food choice are similar to those calculated and assumed in an earlier study of the area /Lindborg 2005/. A large difference from previous calculations is found in benthic feeding organisms. Due to the large amount of filter feeders, this group contributes to a large part of the food source of benthic feeding fishes and birds. The matrix is an average of the whole area and there are large differences between and within the respective basins, due to variation in abiotic factors (e.g. hypsography, light penetration, substrate type etc.). Macrophytes and benthic fauna (especially filter feeders) dominate the biomass in all basins.

Primary producers

Primary production varies greatly between and within the basins. In some parts of the inner shallow areas, the calculated production exceeds $1,000 \text{ gC} \times \text{m}^{-2} \times \text{year}^{-1}$, whereas in pelagic areas with low or no benthic production the production ranges between 50 to $100 \text{ gC} \times \text{m}^{-2} \times \text{year}^{-1}$ (see Figure 4-15). On average for the whole area, the primary producing biomass and primary production are dominated by macrophytes and phytoplankton (see Table 4-13). In the inner, shallow areas the biomass and production of primary producers are dominated by macrophytes, whereas large areas in e.g. Basin Ävrö coastal are without benthic production, hence dominated by phytoplankton.

Table 4-12. Food web matrix with mean values of food proportions (estimated from the identified available biomass/production of their respective food source) in average of all basins.

	1	2	3	4	5	6	7	8	9	10	11	12	13	18	19
1. Phytoplankton														1.00	
2. Microphytes														1.00	
3. Macrophytes														1.00	
4. Bacterioplankton															1.00
5. Zooplankton	0.64			0.36											
6. Zooplankton feeding fish					1.00										
7. Benthic feeding fish									0.05	0.78	0.16	0.01			
8. Carnivorous fish						0.69	0.21	0.10							
9. Benthic herbivores			0.16	0.84											
10. Benthic filter feeders	0.22			0.12	0.03										0.63
11. Benthic detrivores													0.32		0.68
12. Benthic carnivores									0.05	0.78	0.16				
13. Benthic bacteria															1.00
14. Fish feeding birds						0.69	0.21	0.10							
15. Benthic feeding birds			0.21						0.04	0.61	0.13	0.01			
16. Seals						0.69	0.21	0.10							
17. Humans						0.69	0.21	0.10							
18. DIC															
19. POC															

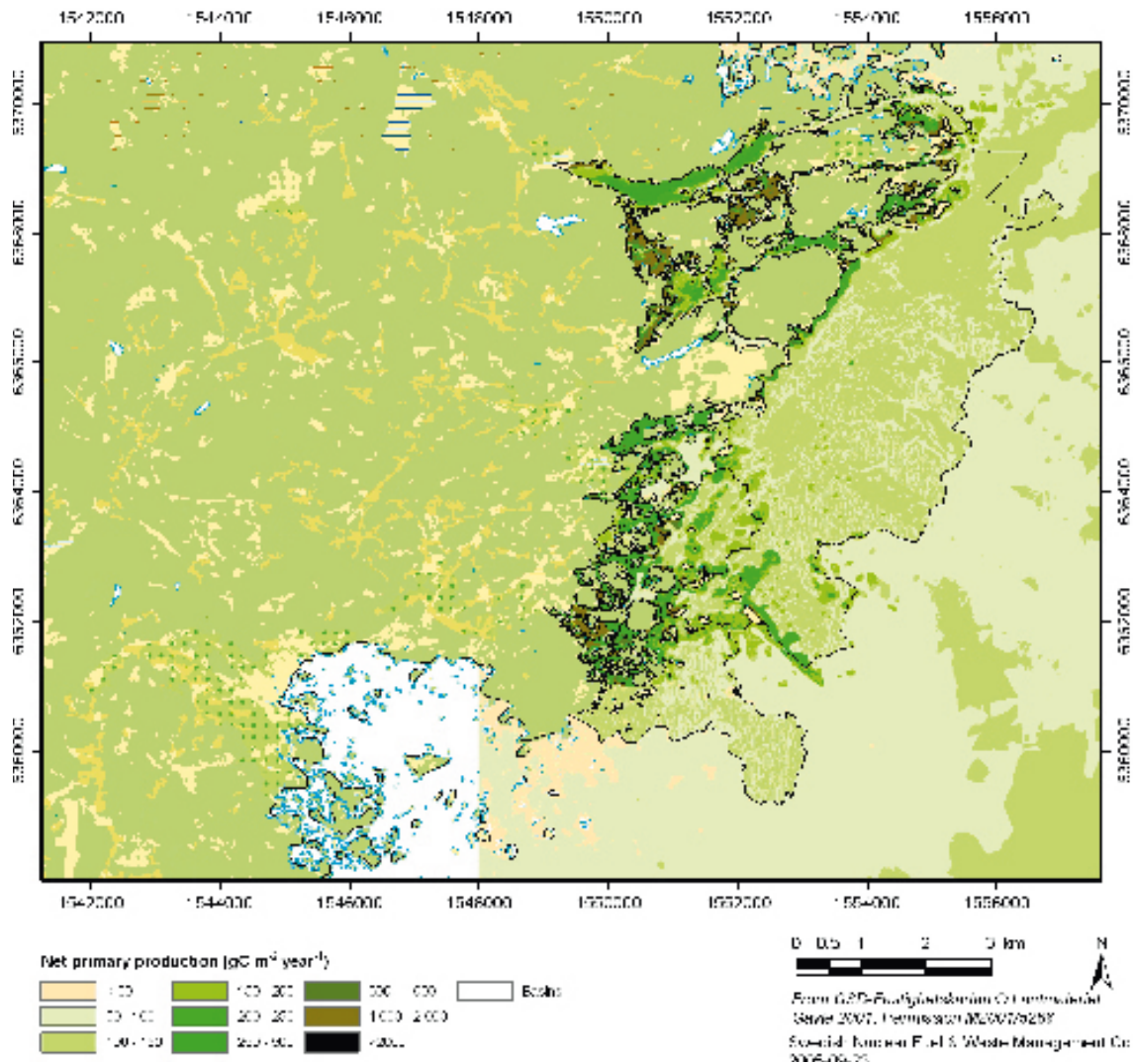


Figure 4-15. Total net primary production i.e. sum of phytoplankton, benthic micro- and macrophyte net production ($\text{gC} \times \text{m}^{-2} \times \text{year}^{-1}$).

Consumers

Among consumers filter feeders dominate the biomass, and the secondary production, in the whole area. As with primary producers there is a large variation within and between the basins, as very few filter feeders are found in the inshore areas where detritivores dominate. In the lower part of the phytobenthic community in the more exposed areas, the largest biomass of benthic filter feeders is found, up to $200 \text{ gC} \times \text{m}^{-2}$. In the soft bottom habitats in the inner basins there is a more modest biomass, not exceeding $25 \text{ gC} \times \text{m}^{-2}$ in benthic fauna in total.

Carbon balance

The average biomass, production and excess from each functional group is shown in Table 4-13. For all functional groups, except zooplankton and benthic bacteria, (Table 4-13) on average the secondary production is higher than the demand from their predators (net excess). This excess can either result in an accumulation in biomass or, as assumed in this steady state model, formation of POC (excretion from consumers and dead material from all functional groups). The fate of POC is either consumption by e.g. filter feeders and sedimentation (likely for some inner basins) or export for consumption in other basins.

Table 4-13. Average biomass ($\text{gC}\times\text{m}^{-2}$), primary or secondary production and excess ($\text{gC}\times\text{m}^{-2}\times\text{year}^{-1}$) for the functional groups in all basins. Nd denotes that no data is calculated.

	Biomass	Production	Excess
Phytoplankton	0.37	82.1	4.60
Microphytes	1.23	17.6	3.53
Macrophytes	11.9	94.01	81.6
Bacterioplankton	0.21	74.4	29.7
Zooplankton	0.05	1.49	-13.6
Zooplankton feeding fish	0.39	3.25	2.67
Benthic feeding fish	0.12	1.00	0.74
Carnivorous fish	0.06	0.48	0.27
Benthic herbivores	2.46	18.2	18.0
Benthic filter feeders	37.9	270	269.6
Benthic detritivores. meiofauna	6.91	56.4	55.0
Benthic carnivores	0.40	3.25	3.18
Benthic bacteria	0.52	4.54	-21.8
Fish feeding birds	0.008	Nd	Nd
Benthic feeding birds	0.003	Nd	Nd
Seals	0.006	Nd	Nd
DIC	135	Nd	-58.3
POC	1.09	Nd	-463
Sum Biota	61.3	627	433

A possible explanation for deficit associated with benthic bacteria is that there has been an overestimation of the predation by the large group benthic detritivores. It might also be due to an underestimation of the importance of POC as a food source for benthic detritivores. Table 4-13 also show a deficit of POC (negative excess) which is due to the fact that the influx of POC from terrestrial runoff and water exchange with other basins of the sea have not been included in the calculations.

The production, or inflow of POC and DIC is not calculated hence the negative excess values.

There are four sources of DIC to the basins; run-off from land, respiration, exchange with surrounding basins and the major: diffusion from the air. Diffusion and exchange with surrounding water were not calculated here, the run-off of DIC contributes with only a small part (see Table 4-14) but respiration contributes with a significant amount. Integrated over all basins, respiration supplies more carbon than is needed for primary production.

There are three sources of POC to the basins; run-off from land, excess from organisms and via exchange with surrounding basins. Exchanges with surrounding water are not calculated and the run-off of POC contributes only a small part (see Table 4-13). As reasoned earlier, some of the excess (secondary and primary production minus consumption) is in fact POC (dead organic matter, faeces etc.). This excess contributes in some of the basins with more POC than what is needed and is probably exported to the outer basins.

In Figure 4-16 a map of net primary production minus respiration in the area is presented. There is a pattern with net primary production in the inner areas and a net respiration in the outer (and deeper) areas. In /Lindborg 2006/ results for individual basins are presented (Basin Borholmsfjärden and Ävrö coastal, see Figure 4-14). Basin Borholmsfjärden, an example of shallow basin, produces more organic carbon, primarily as a result of primary production. The deeper phytobenthic areas, exemplified by Basin Ävrö coastal are net consumers of organic material, i.e. they consume the excess from the shallow, highly productive areas and runoff from land. Neglecting the exchange of organic carbon from the surrounding sea, the demand from the outer deep phytobenthos is much larger than the supply. This implies a large flow of organic matter from the shallow coastal habitat but also from the pelagic habitat.

Table 4-14. Net primary production, respiration (of consumers), drainage area and annual inflow of carbon (POC, DOC and DIC) for each basin.

Basin	Name	PP	Resp _{cons}	Drainage area size 10 ⁶ m ²	Annual inflow of carbon		
		10 ⁶ gC	10 ⁶ gC		POC 10 ⁶ gC	DOC 10 ⁶ gC	DIC 10 ⁶ gC
1	Basin Borholmsfjärden	757	54.2	46.3	14.3	153	26.7
2	Basin Granholmsfjärden	311	93.8	32.7	10.3	129	17.6
3	Basin Getbergsfjärden	80.0	21.0	1.26	0.39	4.42	0.69
6	Basin Eköfjärden	390	337	4.38	1.34	15.4	2.41
8	Basin Talleskärsfjärden	603	1,192	0.28	0.09	1.00	0.16
9	Basin Flåsköfjärden	495	108	4.28	1.31	15.0	2.35
10	Basin Mjältnatefjärden	197	8.56	0.98	0.30	3.46	0.54
11	Basin Sketudsfjärden	147	5.05	0.17	0.05	0.63	0.10
12	Basin Kråkefjärden	188	264	1.46	0.45	5.14	0.81
13	Basin Långvarpsfjärden	23.5	1.94	0.25	0.08	0.88	0.14
14	Basin Hamnefjärden	20.6	7.43	0.47	0.14	1.65	0.26
15	Basin Ävrö Coastal	2,900	5,750	2.19	0.67	7.67	1.20
17	Basin Finngrundsfjärden	422	775.28	0.49	0.15	1.73	0.27
	Sum	6,530	8,613	95.4	29.5	339	53.1

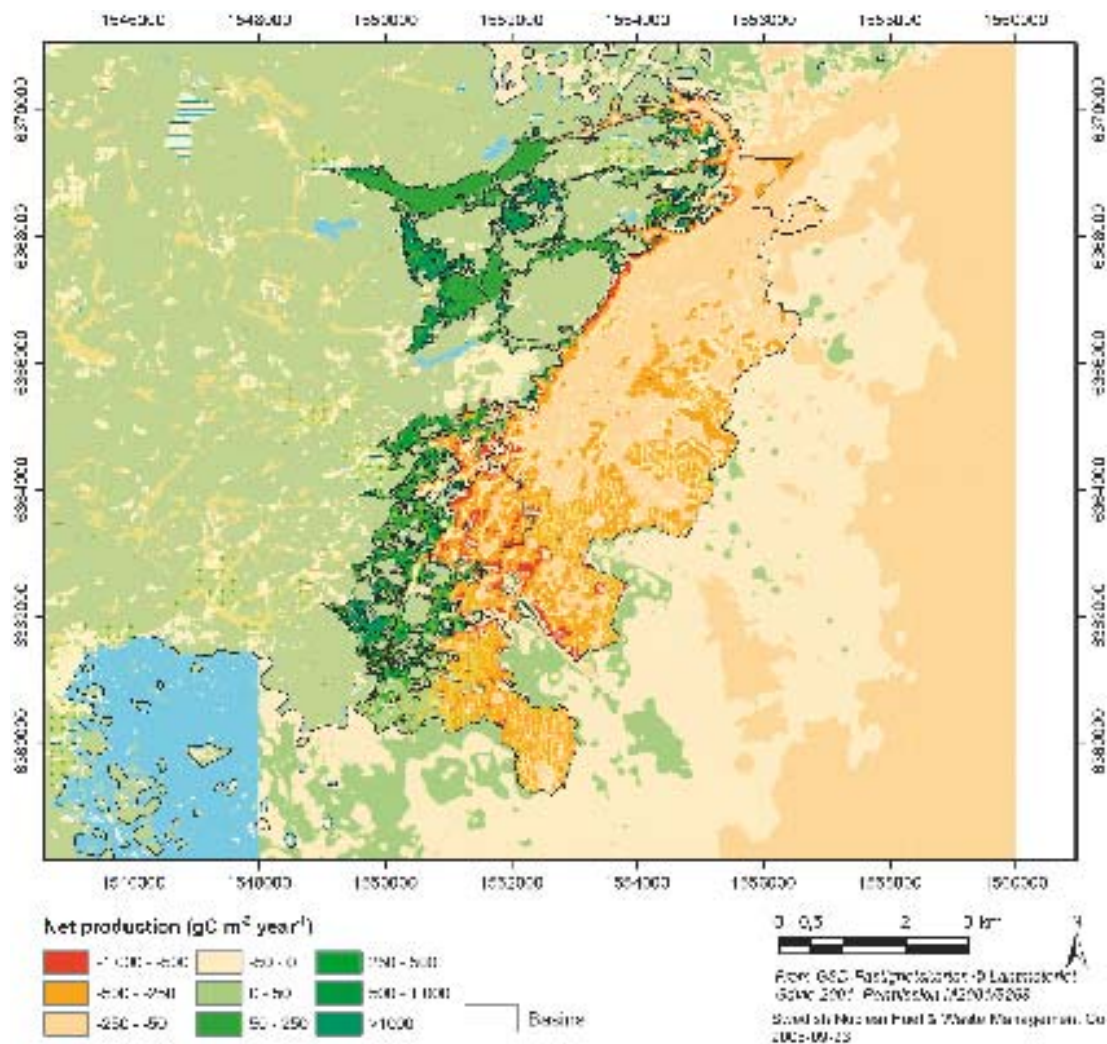


Figure 4-16. Net production, i.e. primary production minus respiration. Green indicate a positive value and red indicate a negative, i.e. net respiration.

4.9 Evaluation of uncertainties

This section discusses the uncertainties involved in the description of the surface systems. The uncertainties are also summarised in Chapter 12.

4.9.1 Abiotic descriptions

Uncertainties in the present descriptions of the climate, and the geology, hydrology, hydro-geology and oceanography as well as the chemistry of the surface system are discussed in /Lindborg 2006/. The main uncertainties are related to the limited availability of site data, especially for areas outside the Simpevarp and Laxemar subareas and for temporally variable parameters for which time series so far are short or non-existent. Most of the detailed investigations of the Quaternary deposits have been performed in the eastern part of the regional model area. Both the geological and hydrogeological descriptions are uncertain due to the limited information on the chemical and physical properties of Quaternary deposits currently available for the regional model area.

Important uncertainties identified in the modelling of surface hydrology and near-surface hydro-geology are associated with the limited data on the hydrogeological properties of site-specific materials, and the fact that only small amounts of time series data are available for assessing the temporal variations of the hydrological and hydrogeological processes (including the meteorological data describing the driving forces of these processes). Uncertainties also remain regarding the geometrical description of the system, i.e. the DEM, the Quaternary deposits and the description of the watercourses, although significant improvements to the database have been made. The next “data freeze” will contain data regarding the chemical and physical properties of the overburden and extended time series of meteorological and hydrological data. The next model version will also include new data from ditches, drainages, and “missing” watercourses that have been characterised. It is expected that these data will reduce the uncertainties associated with the abiotic descriptions.

4.9.2 Biotic description

Terrestrial ecosystem

There are several sources of uncertainties, 1) estimations of different properties have errors due to large variation and low sample sizes etc., 2) assigning these values to the different categories in the landscape assumes that these categories have been correctly identified, 3) pools and fluxes not accounted for.

The largest stocks and flows are associated with trees (except the soil organic carbon that is not treated here). This means that a low confidence in these entities would have a large impact on the overall confidence in the descriptive models. The estimates of tree properties are, however, the best we have (compared with all the categories of data used) in the sense of number of replicates, coverage of the region and the allometric functions used within the National Forest Inventory (NFI) to calculate biomass for the fractions above ground. There is a large variation depending on a number of factors such as nutrient status and wetness. Nutrient status is known to have a large effect on the biomass of roots /Persson 2002/. However these variations, depending on local factors, are considered to be evened out when viewing a larger area /Svensson 1984, see also Banfield et al. 2002/. The average error for the estimate of the tree biomass in NFI (for the area 217 km² forest) should be approximately 6% /Svensson 1984/. We have also introduced errors by discretizing continuous data into a number of categories, but these are on the other hand averages of a large sample covering most forest types.

Biomass expansion factors (BEFs) are used to distribute biomass and NPP properties among tree fractions (where such information has not been found in the NFI data). This does also introduce errors. BEFs are known to be sensitive to tree age /e.g. Lehtonen et al. 2004/ but here the same BEFs have been used irrespective of age i.e. in calculating below ground fractions from above ground fractions. This has certainly lead to an overestimation of the actual biomass and NPP below ground because the BEFs have been constructed from younger forests (~ 30 y) /Berggren et al. 2004/. This approach will be modified in later versions.

Some pools and fluxes have not been treated within this version e.g. NPP of tree branches leading to accumulation of biomass in the ground layer. These have been left out, so far, because they are small in comparison and therefore expected to have a small influence on the overall carbon budget. Overall, the total estimations may be somewhat higher than appropriate. This is caused by a rather high biomass and NPP of the mycelia, and an overestimation of biomass and NPP for the root fractions of mature conifer forests.

The calculated figures concerning consumption, production, respiration and egestion for the mammal species have been performed by /Truvé and Cederlund 2005/ using different established equations. The quality of the quantitative model has thereby been clearly improved since SDM Simpevarp 1.2 /SKB 2005a/. Furthermore, a more reputable elemental composition (e.g. carbon) of mammals has been made available.

Limnic ecosystem

The ecosystem model for Lake Frisksjön is an updated version of the model presented earlier for the the Simpevarp area in conjunction with SDM Simepvarp 1.2 /Lindborg 2005/. Compared with the previous model version, some of the assumptions on which the current model is based have been reconsidered, and a miscalculation concerning bacterial biomass has been corrected. As a result, the previously completely dominating role of bacteria in the lake ecosystem is reduced in the present model. In addition to the carbon budget for the limnic ecosystem, estimated inputs of carbon to the lake from external sources, as well as carbon outflow from the lake, have been used to produce an overall carbon budget for Lake Frisksjön.

The estimate of phytoplankton primary production is based on literature values from coloured lakes and can be assumed to be in the right order of magnitude, of actual production. Phytoplankton biomass was calculated from Chlorophyll a measurements in the lake. The ratio of Chl a:gC may vary with status of the algal community and this introduces some uncertainty into the estimated phytoplankton biomass.

Zooplankton biomass generally shows high seasonal variation, with the highest biomass during summer. The only site data on zooplankton biomass from the summer period were extremely high, and the values were not judged as representative for summer conditions in Lake Frisksjön. Instead, summer data from another humic lake in central Sweden were used in the model, but this use of generic data may add uncertainty to the model. Moreover, a potentially important component of the zooplankton community, the ciliates, has not been included in the model, mainly because of lack of quantitative data describing the role of ciliates in the limnic ecosystem. However, even if it is not possible to quantify the uncertainties connected to the zooplankton estimates, it does not seem likely that these uncertainties should be critical for confidence in the overall carbon budget for Lake Frisksjön.

Fish data are collected by standardised and generally accepted methods; however, the generated data is only semi-quantitative. The conversion of catch per unit effort (CPUE) data to an absolute estimate of biomass per unit area is associated with large uncertainties. There is no study which can be used to validate any conversion factor, and the proposed conversion factor used in this study may be regarded as an “expert guess”.

In conclusion, despite the fact that many of the parameters in the model are not measured in the lake, the carbon budget presented here is assumed to be close to reality. When site specific data were lacking, generic data have been assembled from lakes as similar to Lake Frisksjön as possible. The major uncertainties in the carbon budget are associated with assumptions concerning microbial organisms and processes, e.g. bacterial biomass and metabolism in all of the lake habitats, and the degree of heterotrophy in the phytoplankton community. These uncertainties are reflected in the carbon budget, in that both bacterioplankton and benthic bacteria show a carbon deficit on an annual basis, but the annual carbon excess for phytoplankton more than balances this deficit.

Marine ecosystem

The quality of data and how well data represents the site have been summarised in Table 4-16 and are discussed in general below and in more detail in /Lindborg 2006/. For several functional groups the quality of data has increased since Simpevarp 1.2.

The digital elevation model (DEM) that was used to estimate areas, volumes, depth, light penetration etc. originates from a combination of recent site-specific measurements and existing digital nautical charts and has a very high quality.

The estimation of solar radiation is based on the DEM (above) and averages of light penetration over several years for individual sites. The differences between various areas have been taken into account and the result can hence be regarded as reliable.

Primary production was estimated from actual radiation (PAR) during one year (2004) and associated conversion factors. The calculated primary production probably has a sufficiently good quality since the conversion factors used were species specific and mostly obtained from the Baltic Sea, and the insolation measurements used in the calculations were site specific.

The reasoning applicable to the estimates of the primary production also applies to the estimates of the respiration, i.e. that real measurements would have given a better estimate than the calculations used in this study. But, as for the primary production, species specific conversion factors contributed to the calculations being considered fairly correct.

Calculations of the modelled run-off from land are described in /Lindborg 2006/. Concentrations of DIC, DOC and POC were based on a 3 year monitoring sampling programme. The estimation of total carbon flow is probably of sufficient quality due to the long monitoring period.

Human population description

Most of the data in /Miliander et al. 2004/ were obtained from Statistics Sweden (SCB). When only a single object is found within a geographic area, SCB adjusts this single object to a “false” zero for reasons of personal privacy. If two objects are found, the count is adjusted to three /SCB 2003/. This can result in incoherence between the sum of values for different categories and the total number (as an example the total number of inhabitants and the sum of inhabitants per age class). Also, for sparsely populated areas the data become more statistically unreliable, irrespective of the above deliberate reporting bias.

Table 4-16. Estimations of the quality of input data and how representative the data are for the basins in the Simpevarp area. Higher figures indicate higher quality of data.

Functional group	Quality of data (1–4)	Representativity of data (1–4)
Areas and volumes	4	4
Light penetration	4	4
Bottom type (hard, soft)	3	4
Carbon transport from runoff	3	3
Concentration of carbon	3	4
Phytoplankton	3	4
Macrophytes	3	4
Bacterioplankton	3	2
Zooplankton	2	4
Zooplankton feeding fish	3	1
Benthic feeding fish	3	1
Carnivorous fish	3	1
Benthic herbivores	3	4
Benthic filter feeders	3	4
Benthic detritivores	3	4
Benthic carnivores	3	3
Benthic bacteria	3	2
Fish feeding birds	1	4
Benthic feeding birds	1	4
Humans	3	4

5 Bedrock geology

The bedrock geological model consists of three components; the rock domain model, the deterministic deformation zone model, and the statistical model of fractures and lineaments, the so-called discrete fracture network (DFN) model. The work has been carried out according to the strategy described in /Munier et al. 2003/. As in the case of model version Simpevarp 1.2, the rock domain and deterministic deformation zone models are presented for the whole regional model volume. The DFN model has utilised fracture data essentially from within the rock mass of the local model volume situated outside deformation zones. Alternative models are presented for the deformation zone model and the geological DFN model.

A geological model of the bedrock and deformation zones rely on two types of data; indirect and direct data. Indirect data, acquired through airborne and ground geophysical measurements together with elevation surveys and photography, provide essential information of the extent and location of deformation zones. Direct data, acquired through excavated trenches, field mapping or core observations, can determine their existence and geological character.

One rock domain model is presented. Only very minor changes have been made in the regional model domain compared to version Simpevarp 1.2. Since the investigations in connection with the complete site investigation are entirely focused on the local scale model domain, no major modifications are to be expected in future model versions. Accordingly, the rock domain model in the regional model domain is, and will in future model versions, only be based on bedrock information of reconnaissance character that existed prior to the site investigation and which formed the base for the compilation of the Simpevarp SDM version 0. Consequently, the uncertainties what relate to the occurrence and geometry, and also the characterisation of the rock domains in the regional model area will persist throughout the site investigation. However, a significant increase in the amount of data, especially from the Laxemar subarea, implies that major modifications and changes have been made in the Laxemar part of the local scale model domain. By consideration of the changes compared to model version Simpevarp 1.2, it is considered that the rock domain model is stabilising, although modifications of the rock domain boundaries in the local scale model domain are anticipated when new data become available, in particular from future cored boreholes.

Two alternative deformation zone models are presented; 1) the base case model, which consists of deformation zones of high, medium and low confidence of existence in the regional model area, and 2) an alternative model which consists of only the high and medium confidence deformation zones in the local model area. Relatively minor changes in the geometries of the modelled zones of the base case model have occurred since the previous model version, albeit most of the underlying primary data and lineaments have been reanalysed. Direct and indirect subsurface data together with better coverage of interpreted lineaments along the coast line has increased the knowledge of the geometries and the character of a number of regional and local major zones in the Laxemar subarea and on the Simpevarp peninsula. Several low confidence zones have been upgraded to high or medium confidence zones through confirmation by detailed indirect or by direct observations within the local model area. A few interpreted deformation zones in the Simpevarp 1.2 model have been rejected essentially through analyses of new subsurface data. One subhorizontal deformation zone, situated well below, repository depth has been identified by a strong seismic reflector in the central part of the Laxemar subarea.

The base case deformation zone model is stabilising with regards to the locations and geometries of regional, and, to a large extent, local major zones in the local model domain, although small adjustments are expected in future model versions with the access to more detailed surface and subsurface data.

The statistical fracture model (geological DFN) contains alternative interpretations for the Simpevarp and Laxemar subareas, respectively, as well as for different rock domains. The development of the geological DFN model involves major changes in the applied methodology and derivation of matching geometrical parameters for orientation, size and intensity. Large uncertainties remain for the subhorizontal fracture set.

One or more components of the bedrock geological model provide a foundation for the modelling work in rock mechanics, thermal properties, bedrock hydrogeology and, to lesser extent, bedrock hydrogeochemistry and bedrock transport properties. All components of the geological model have also a direct influence on the location and detailed design of the repository. The model also constitutes a significant input to the safety analysis work.

The geological descriptions provided in the following sections are focused on the Laxemar subarea, but it should be noted that the updating of the geological models relates to the entire regional model volume. The descriptions in Sections 5.3 and 5.4 are condensed versions of those provided in the comprehensive background report /Wahlgren et al. 2005b/ on the geological conditions, and evaluation of primary data related to the Laxemar 1.2 modelling of rock domains and deformation zones. Similarly, the account of the geological DFN modelling in Section 5.5 is a condensation of the comprehensive analysis presented by /Hermanson et al. 2005/. Where appropriate, direct comparison is made with the Simpevarp subarea. For a geological description of the Simpevarp subarea, the reader is referred to the SDM Simpevarp 1.2 report /SKB 2005a/.

5.1 State of knowledge at previous model version

The Simpevarp Site Descriptive Model version 1.2 related to the regional model area but the focus was on the eastern part of the local scale model area, i.e. principally the Simpevarp subarea /SKB 2005a/.

In model version Simpevarp 1.2, the surface geological information, i.e. the character and surface extension of dominant rock types, outside the Simpevarp subarea, were based on the SDM version 0. This variation in quality of the surface geological data and the limited subsurface information are the two most important factors that govern the uncertainties associated with the modelling of the rock domains in the Simpevarp SDM version 1.2. Consequently, the confidence of occurrence and geometry of the rock domains at the surface was judged to be medium to high in the part of the local model area making up the Simpevarp subarea, whereas it was judged to be low to medium outside the Simpevarp subarea. Due to the restricted subsurface information, the confidence of occurrence at depth was set to medium to low for most rock domains, except for the dominating rock domain RSMA01 (dominated by Ävrö granite) which forms the principal matrix in the local scale model volume. However, the geometrical relationships between rock domain RSMA01 and the other rock domains, in particular the major rock domains, were considered as highly uncertain.

The main uncertainties associated with the Simpevarp 1.2 rock domain model were:

- Nature of the bedrock below sea and on land outside the Simpevarp peninsula, Äspö and Ävrö in the regional model area (lower quality data in these areas).
- Spatial distribution of rock domains outside the Simpevarp subarea.
- Three-dimensional geometry of most rock domains.
- Proportion of rock types in domains (veins, patches, dykes, minor bodies; not evenly distributed at the 50–100 m scale and below). There could also be non-uniformity in their occurrence.
- Spatial distribution of compositional varieties of the Ävrö granite, i.e. granitic to granodioritic (“rich in quartz”) contra quartz monzodioritic (“poor in quartz”) varieties.
- Three-dimensional extent of “secondary red staining” (hydrothermal alteration).

A three-dimensional deformation zone model, which consists of 22 high confidence and 166 low confidence deformation zones in the whole regional model domain, was presented in the Simpevarp 1.2 site description. Deformation zones with a length of 1 km or more in the local model domain and zones with a length of 1.6 km or more in the regional model domain were addressed. The data coverage in the regional scale model domain did not allow the same high resolution as in the local scale model domain. Existing old structural models, a variety of new surface and sub-surface data, and new linked lineament data from a larger area were used in the modelling. The linked lineaments were further post-processed to better reflect geology and in order to minimise effects of differences in data coverage over land and sea.

The interpretation of high confidence zones were supported by a variety of geological and geophysical information in addition to the interpreted lineaments. Two important types of deformation zones were present within this group:

- Regional deformation zones with northeasterly strike, confirmed already in model version 0 or in other previous models established in the Simpevarp area such as the Äspö shear zone (ZSMNE005).
- Local major fracture zones, which have been confirmed either by new borehole information or in previous models in the Simpevarp area such as ZSMEW007A.
- Smaller zones and fractures, with a surface extent of less than 1 km were not included deterministically in the model, but handled in a stochastic way through the geological DFN model.

5.2 Evaluation of primary data

A full account of primary data used for the geological modelling for SDM Laxemar 1.2 is provided in Table 2-1. Below, the processing of these data is accounted for.

5.2.1 Surface geology

During the period between the data freezes for the model versions Simpevarp 1.2 and Laxemar 1.2, a considerable amount of new surface data have been generated from the Laxemar subarea. In contrast to the situation at the time of the Simpevarp 1.2 modelling, the Laxemar subarea is now covered by a detailed bedrock map compiled at the scale 1:10,000. As a complement to the outcrop database, generated during the bedrock mapping campaign, analytical work comprising modal, geochemical and petrophysical analyses has been carried out in order to characterise the various rock types. The results of this analytical work have subsequently been utilised in the characterisation of the identified rock domains in the geological modelling. The data from the surface is also complemented by new analytical data from cored boreholes.

The majority of the new primary data relate to the characterisation of the bedrock, mainly the various rock types, and not so much to the characterisation of the deformation zones. This is the explanation for the bias in the description below between the rock type related evaluation and description, and the evaluation of primary data related to the deformation zones.

In the Laxemar subarea and its immediate surroundings, the distribution, description and age of the various rock types have been documented with the help of the following information that to a major extent has been generated during recently performed site investigation activities:

- An outcrop database with numerical and descriptive data from 1,169 observation points /Persson Nilsson et al. 2004/, including repetitive measurements (commonly eight) of the magnetic susceptibility of the different rock types at every observation point.
- 51 modal analyses (mineral composition) of surface samples and 5 modal analyses from KLX03, recalculated and plotted in a QAPF diagram in order to classify the various rock types /Wahlgren et al. 2005a/.
- Chemical analyses of 30 surface samples and 5 samples from KLX03, which have been used to characterise the various rock types /Wahlgren et al. 2005a/.
- Petrophysical data, including density, magnetic and electric properties and porosity from laboratory measurements of 72 samples of different rock types, including scattered samples from the Simpevarp subarea and the remaining part of the regional model area /Mattsson et al. 2004c/.
- In situ gamma-ray spectrometry data from 171 locations, including locations in the Simpevarp subarea and the remaining part of the regional model area /Mattsson et al. 2004c/.
- Bedrock geological map compiled with the help of the outcrop database and magnetic data from airborne geophysical measurements /Wahlgren et al. 2005a/, (see Section 5.2.2).

- Bedrock geological map at the scale 1:50 of two sites where detailed fracture mapping has been carried out on cleaned outcrops, one of which is the drill site for KLX05 /Cronquist et al. 2004/ (see Section 5.2.7).

Attention is given to the mineralogical and chemical composition, grain size, texture, structure and petrophysical properties, including those derived from in situ gamma ray spectrometry, of the rock types in the Laxemar part of the local scale model area. For reference, a comparison is made to corresponding results from the Simpevarp subarea.

5.2.2 Outcrop mapping and complementary analytical studies

The character of the different rock types in the Laxemar and Simpevarp subareas is defined and characterised primarily on the basis of two data sets:

- Outcrop database from bedrock mapping.
- Complementary analytical results of representative samples from the surface.

These data form the basis for the compilation of the bedrock map (see Section 5.2.3). Furthermore, in combination with corresponding information from the cored boreholes they yield the properties of the rock types that are used to define the different rock domains in the rock domain model.

Outcrop mapping

The bedrock in the Laxemar subarea is well exposed except for a minor area in the southern part. Detailed bedrock mapping of the Laxemar subarea and its immediate surroundings was carried out during summer 2004 /Persson Nilsson et al. 2004/ in conjunction with the ongoing site investigation programme. In the remaining part of the regional model area, the bedrock mapping only related to selected target areas with the purpose of explaining geophysical anomalies. Consequently, the surface bedrock geological information in the regional model area is only based on the SDM version 0 bedrock map, and will continue to be so in the future.

Complementary analytical studies

In order to characterise the different rock types, modal and geochemical analyses as well as determinations of petrophysical properties, including density, magnetic and electric properties and porosity, have been performed on representative samples from the surface. Furthermore, in situ gamma-ray spectrometry measurements have been performed on selected outcrops. For the location of the sample sites for the different analytical studies and the locations of the in situ gamma-ray measurements, see /Wahlgren et al. 2005b/.

General classification of rock types in the Laxemar and Simpevarp subareas

As can be seen in the modal QAPF (Quartz-Alkali feldspar-Plagioclase-Feldspathoids) and geochemical classification diagrams in Figure 5-1, Figure 5-2 and Figure 5-3, the various rock types in the Simpevarp and Laxemar subareas display similar and overlapping compositional variations. Apart from the composition, the most important criteria employed in distinguishing between different rock types are texture and grain size.

The compositional alkali-calcic trend displayed in the QAPF (Figure 5-1) and geochemical classification diagrams (Figure 5-2 and Figure 5-3) for the studied rock types is characteristic for granite-syenitoid-dioritoid-gabbroid rocks in the Transscandinavian Igneous Belt /e.g. Högdahl et al. 2004/. The descriptions and characterisations of the individual rock types are presented below in conjunction with the description of the bedrock map.

According to the International Union of Geological Sciences /LeMaitre 2002/, the classification of rocks should be based on the modal composition. Thus, the geochemical classification diagrams, cf. Figure 5-2 and Figure 5-3, should not be used strictly for classification purposes, but merely as an indication of the compositional trends of the different rock types.

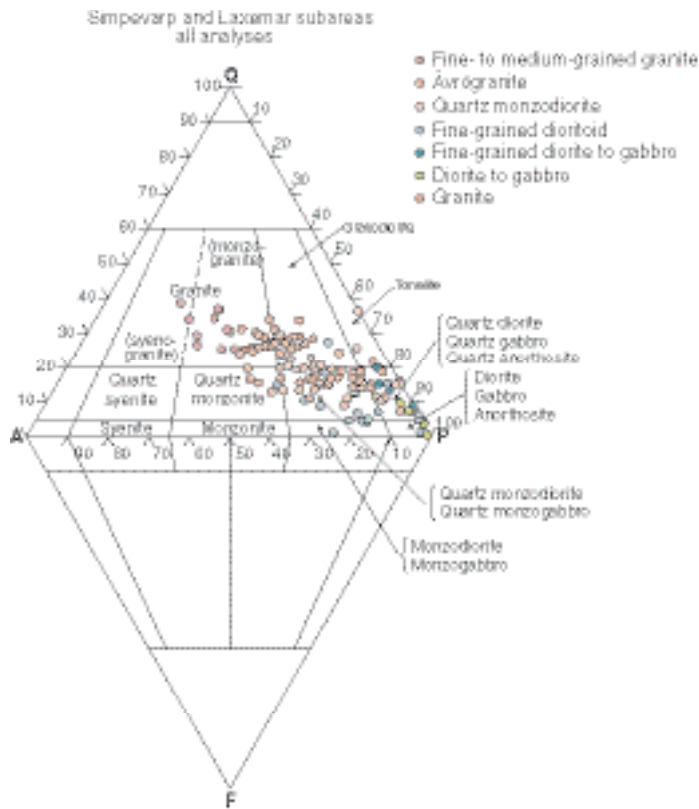


Figure 5-1. QAPF modal classification of rock types in the Simpevarp and Laxemar subareas according to /Strecheisen 1976/. All analysed samples are included.

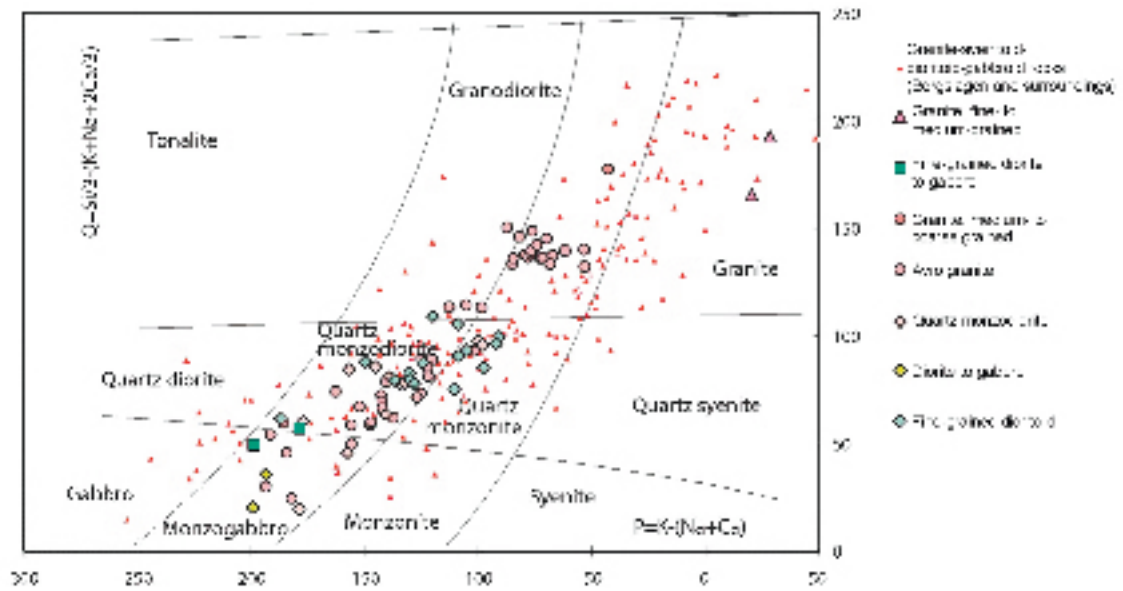


Figure 5-2. Geochemical classification of rocks from the Simpevarp and Laxemar subareas according to /Debon and LeFort 1983/. All analysed samples are included.

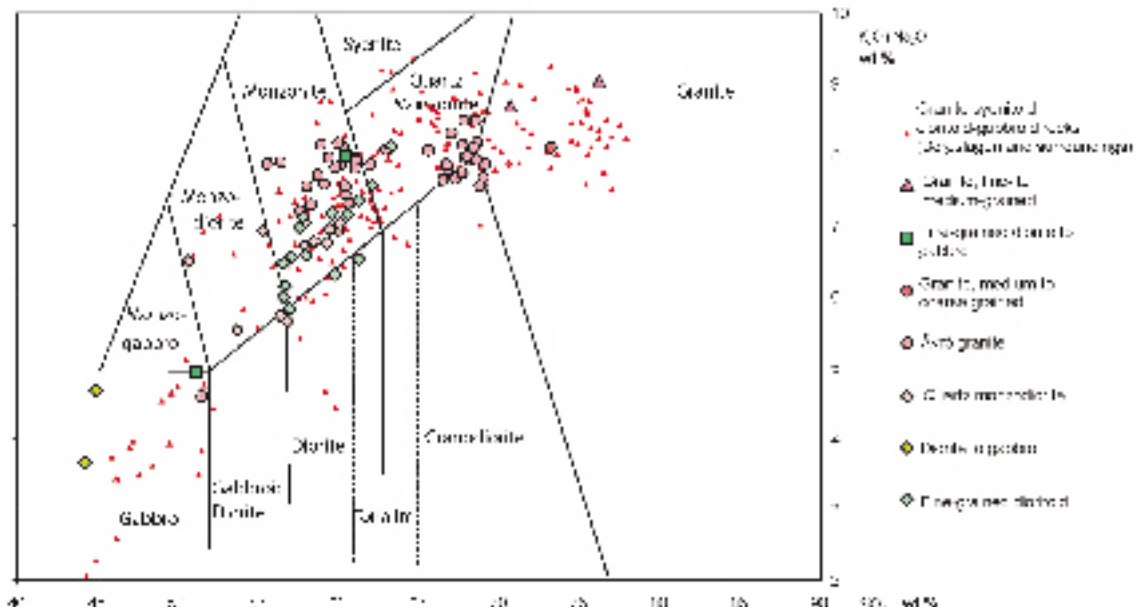


Figure 5-3. Geochemical classification of rocks from the Simpevarp and Laxemar subareas according to /Middlemost 1994/. All analysed samples are included.

5.2.3 Rock type distribution on the surface – bedrock map

The bedrock in the Simpevarp regional model area, as well as the major part of southeastern Sweden, is totally dominated by intrusive igneous rocks belonging to the approximately 1,810–1,760 Ma old generation of granite-syenitoid-dioritoid-gabbroid rocks in the 1,860–1,650 Ma old so-called Transscandinavian Igneous Belt (TIB). A characteristic feature is magma mingling and mixing relationships between the different rock types. The rocks are mostly well preserved and more or less undeformed, but a weak foliation is locally developed. However, low-grade ductile shear zones of mesoscopic to regional character do occur. A conspicuous rock type in the regional model area is c. 1,450 Ma old granites.

The nomenclature of the rock types and associated rock codes applied in the Oskarshamn site investigation is presented in Appendix 2 (which is identical to Appendix 1 in the Simpevarp 1.2 report /SKB 2005a/).

The bedrock in the Laxemar subarea and its immediate surroundings, which cover the western part of the local model area, is dominated by two rock types, namely:

- Ävrö granite (granite to quartz monzodiorite), medium-grained, generally porphyritic.
- Quartz monzodiorite, medium-grained, equigranular to weakly porphyritic.

The following rock types are subordinate in character, though they make up characteristic constituents in the bedrock and may be more or less frequently occurring:

- Granite, fine- to medium-grained.
- Pegmatite.
- Diorite to gabbro, fine-grained (mafic rock, fine-grained).
- Granite, medium- to coarse-grained.
- Diorite to gabbro, medium-grained.
- Dioritoid, fine-grained, unequigranular.

A new bedrock map at the scale 1:10,000 has been produced for the Laxemar subarea and its immediate surroundings /Wahlgren et al. 2005a/. This bedrock map has been combined with the bedrock map of the Simpevarp subarea /Wahlgren et al. 2004, SKB 2004b/. Furthermore, a digitised version of the bedrock map of Äspö /Kornfält and Wikman 1988/ is included. Thus, the major part of the local model areas is now covered with a detailed bedrock map at the scale 1:10,000 (Appendix 3). It should be noted that the Äspö island has not been re-mapped in conjunction with the ongoing site investigation. Due to this, the Äpö diorite and the greenstone at Äspö have been given separate rock codes and thereby colours on the bedrock map, partly because they cannot be directly transformed to the decided rock codes for the site investigation, and partly to keep traceability to the underground mapping in the Äspö HRL.

In order to visualise the differences between the detailed bedrock map of the Laxemar and Simpevarp subareas and the bedrock map from model version 0 in a simplified manner, these maps are merged in Figure 5-4. The difference in resolution and detail between the two maps is obvious.

The following text comprises a brief description of the rock types, particularly those found in the Laxemar subarea. For a more comprehensive description of the rock types, the reader is referred to /Wahlgren et al. 2005b/. The rock types in the Simpevarp subarea correspond to the rock types in the Laxemar subarea, but for a description, see the Simpevarp 1.2 report /SKB 2005a/.

Ävrö granite

Ävrö granite is the dominant rock type in the central and northern part of the Laxemar subarea, as well as in the regional model area (Appendix 3 and Figure 5-4). The Ävrö granite comprises a suite of commonly porphyritic rocks that vary in composition from quartz monzodiorite to granite, including granodioritic, tonalitic, quartz dioritic and quartz monzonitic varieties (Figure 5-5). The geochemical classification of the Ävrö granite is shown in Figure 5-6 and Figure 5-7. The compositional variation is very similar to that in the Simpevarp subarea /SKB 2005a, Wahlgren et al. 2005b/.

As can be seen in the QAPF classification diagram (Figure 5-5, left) and the geochemical classification diagrams (Figure 5-6 and Figure 5-7), it is indicated that the Ävrö granite in the Laxemar subarea constitute two populations, one richer in quartz (granodioritic to granitic) and one with a lower quartz content (quartz monzodioritic). This division in two populations is also supported by in situ gamma-ray spectrometry and density results /Mattsson et al. 2004c, Wahlgren et al. 2005b/.

In Figure 5-8 and Figure 5-9, quartz monzodioritic and granodioritic varieties of the Ävrö granite are displayed, respectively. The differences in mineralogical composition between the two varieties are shown in Figure 5-10, in which the Ävrö granite in the southern part of the Laxemar subarea represents the quartz monzodioritic variety.

The results of the modal and geochemical analyses indicate that the Ävrö granite in the central parts of the Laxemar subarea has a higher quartz content (granitic to granodioritic composition) compared with the peripheral parts which have a lower quartz content (quartz monzodioritic composition) that is similar to the quartz monzodiorite that dominates south of the Ävrö granite. This mineralogical variation has important implications for the thermal properties (see Section 7.2).

Quartz monzodiorite

The quartz monzodiorite dominates in the southern and southwestern part of the Laxemar subarea and neighbouring surroundings (Appendix 3). A typical appearance of the quartz monzodiorite can be seen in Figure 5-11. The quartz monzodiorite has a relatively restricted compositional range (Figure 5-6, Figure 5-7 and Figure 5-12). However, it should be pointed out that the 3 points that plot in the lower right-hand part in Figure 5-12 represents analyses from the quartz monzodiorite southeast of Lake Frisksjön (Appendix 3). The mineralogical composition of the quartz monzodiorite is displayed in Figure 5-10. It is indicated that the quartz monzodiorite in southern and southwestern Laxemar exhibits a slightly higher quartz content ($14.8 \pm 2.8\%$; N=7) compared with the quartz monzodiorite in the Simpevarp subarea ($10.5 \pm 2.5\%$; N=7), see also Figure 5-12.

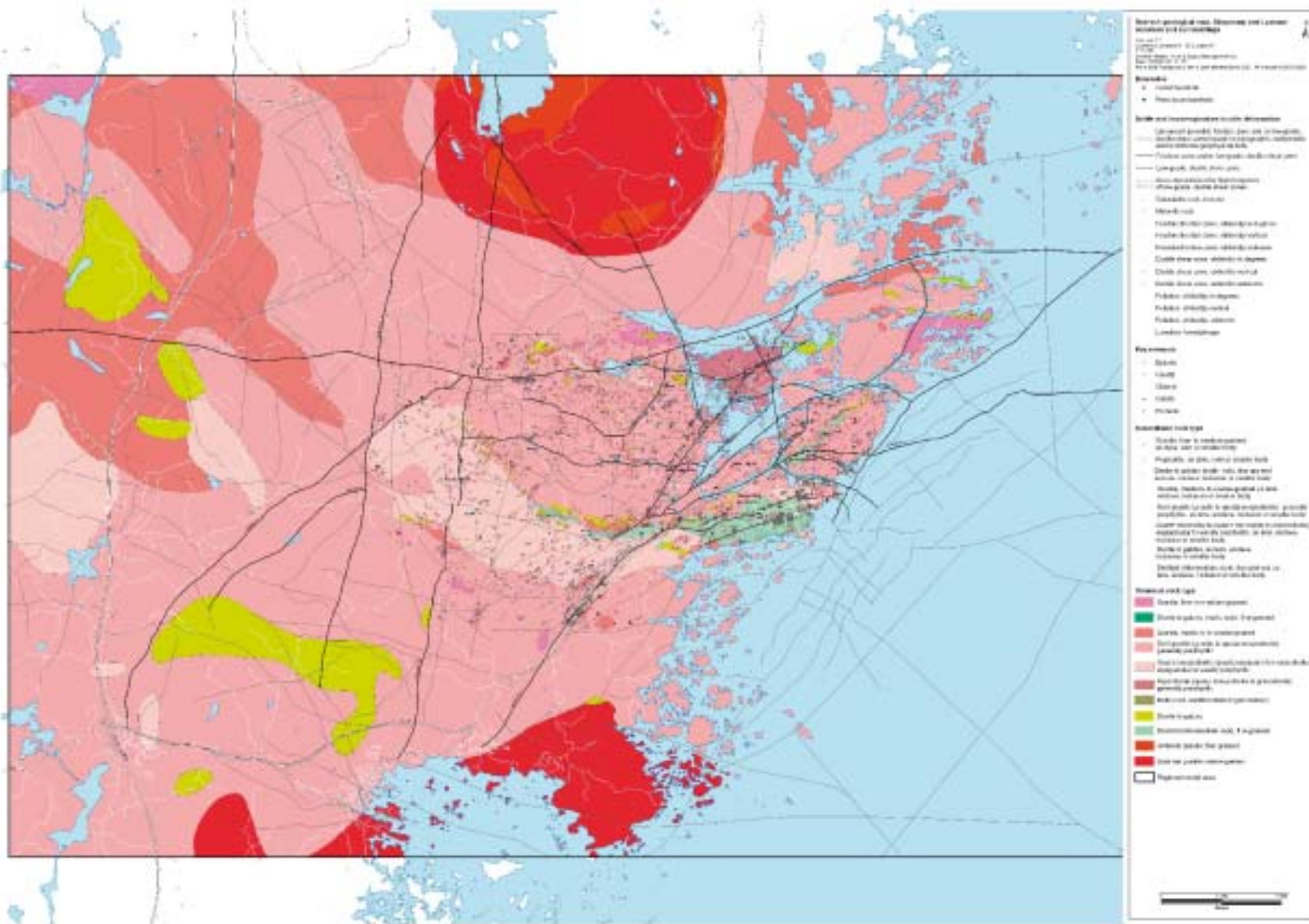


Figure 5-4. Combination of the bedrock map from the model version 0 in the regional model area and the bedrock map of the Laxemar and Simpevarp subareas.

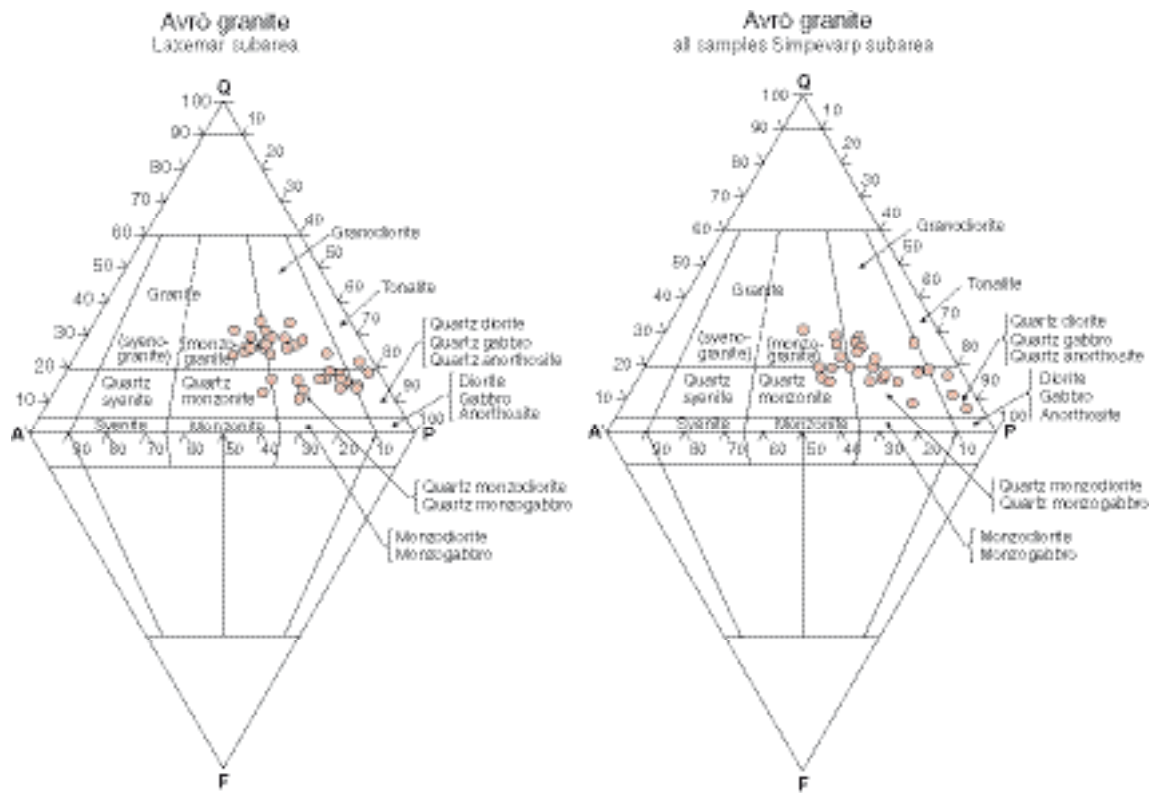


Figure 5-5. QAPF modal classification of Ävrö granite from the Laxemar subarea (left) and Simpevarp subarea (right) according to /Streckeisen 1976/.

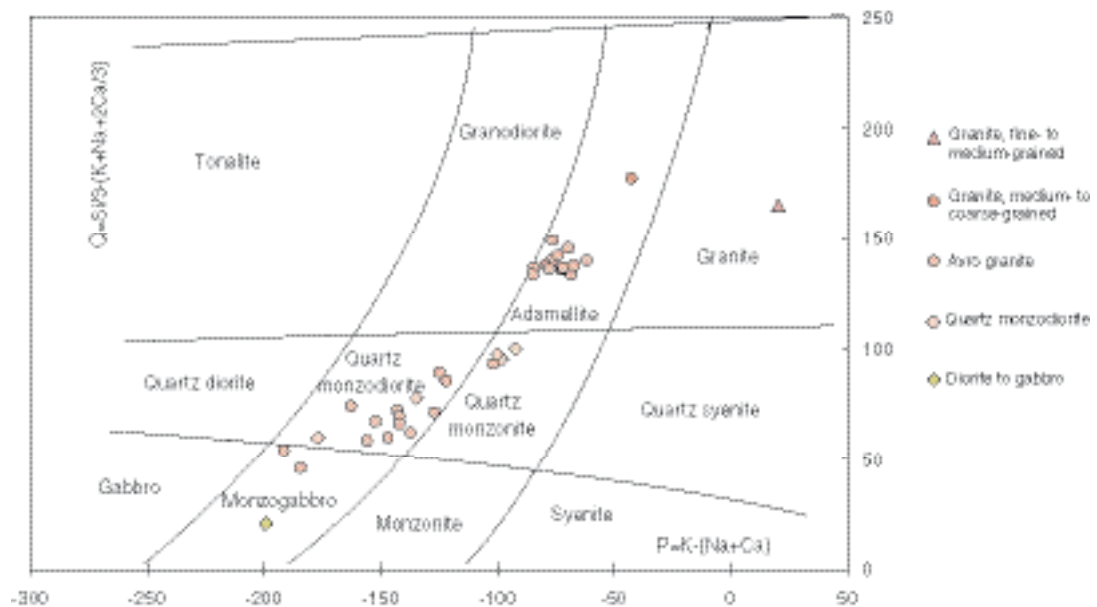


Figure 5-6. Geochemical classification of rocks from the Laxemar subarea according to /Debon and LeFort 1983/. Samples from KLX03 are included.

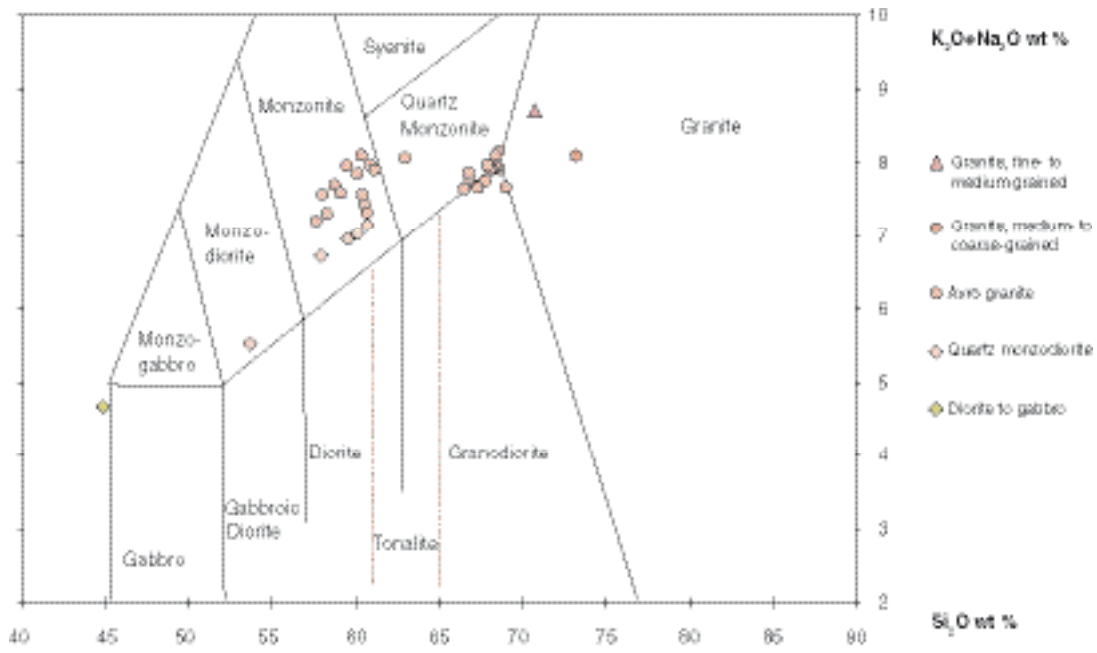


Figure 5-7. Geochemical classification of rocks from the Laxemar subarea according to /Middlemost 1994/. Samples from KLX03 are included.



Figure 5-8. Ävrö granite with quartz monzodioritic composition.



Figure 5-9. Ävrö granite with granodioritic composition. Note the intermediate to mafic enclave (dark in colour) in the right part of the picture.

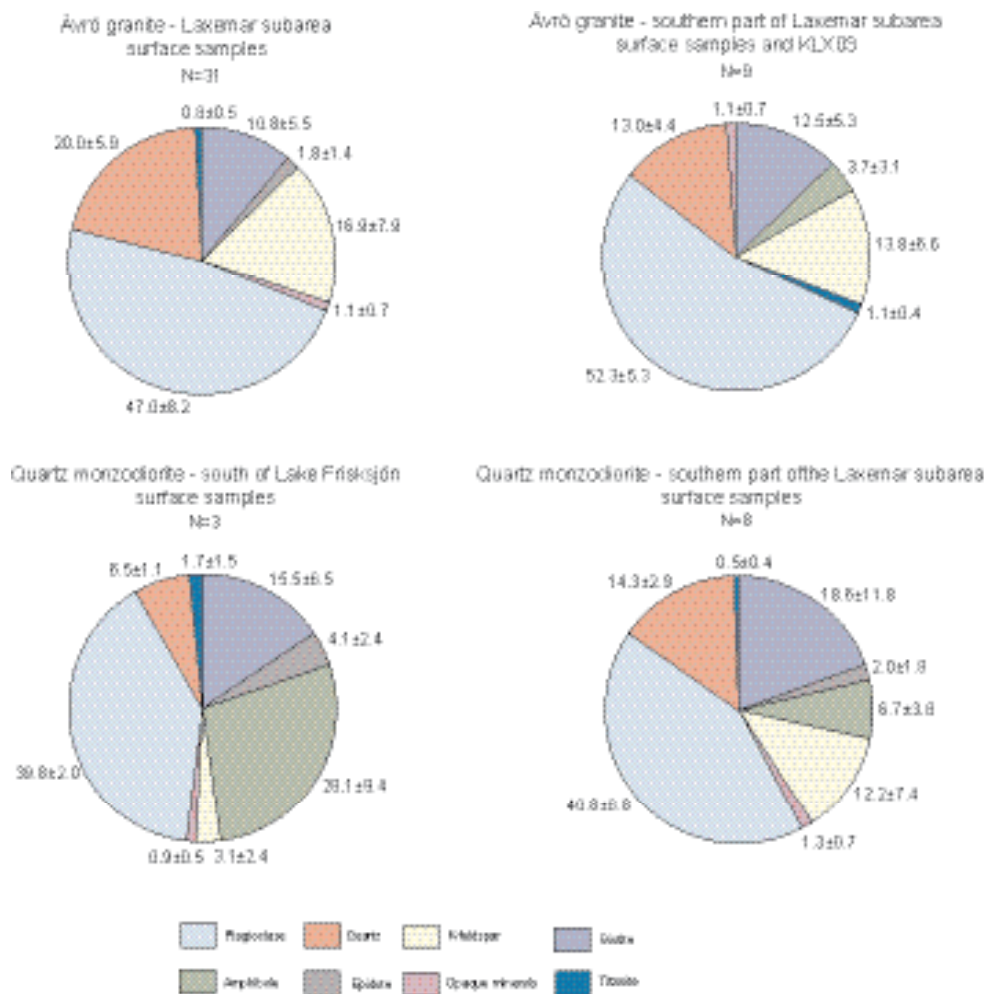


Figure 5-10. Diagrams showing the mineralogical composition (mean value and standard deviation) of Ävrö granite and quartz monzodiorite in different parts of the Laxemar subarea.



Figure 5-11. Characteristic appearance of equigranular quartz monzodiorite (PSM004115).

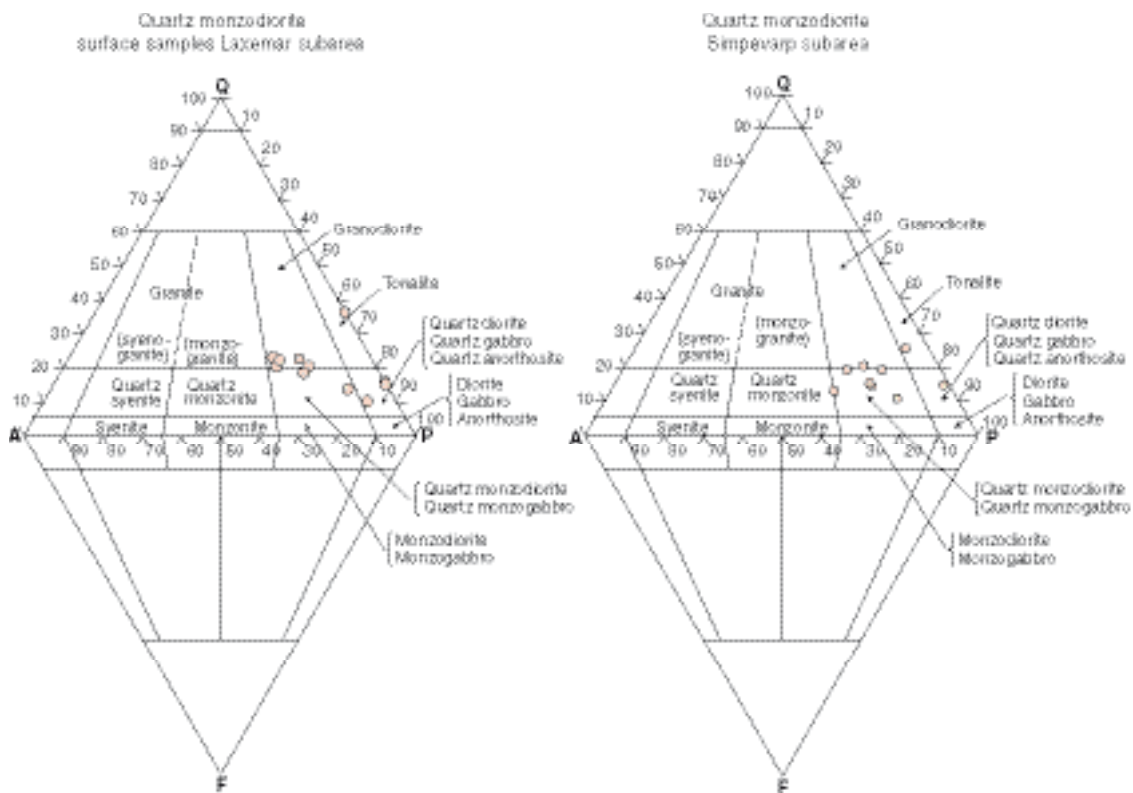


Figure 5-12. QAPF modal classification of quartz monzodiorite from surface samples in the Laxemar subarea (left) and Simpevarp subarea (right) according to /Streckeisen 1976/.

Fine-grained dioritoid

Fine-grained dioritoid occurs as minor bodies in the southern part of the Laxemar subarea, particularly along the contact zone between the Ävrö granite and the quartz monzodiorite (Appendix 3). It is inferred that these bodies originally formed parts of a coherent westward continuation of the large body of fine-grained dioritoid that covers the southern part of the Simpevarp peninsula (Appendix 3). Furthermore, the fine-grained dioritoid occurs as minor bodies or inclusions, especially in the Ävrö granite and the quartz monzodiorite.

Medium- to coarse-grained granite

Scattered minor bodies of red to greyish red, medium- to coarse-grained granite occur in the Laxemar subarea and its surroundings (Appendix 3), in particular immediately north of the subarea, north of the deformation zone ZSMEW002A (see Section 5.4). Along the boundary zone between the Ävrö granite and the quartz monzodiorite in the southern part of the subarea, granite occurs which is intimately mixed with diorite to gabbro. Furthermore, it occurs as mixed and mingled, diffusely delimited small occurrences in the Ävrö granite.

Diorite to gabbro

Diorite-gabbro occurs as scattered minor bodies and enclaves, particularly in the Ävrö granite in the Laxemar subarea and its immediate surroundings (Appendix 3). The most conspicuous occurrence of diorite to gabbro is the concentration along the contact zone between the Ävrö granite and the quartz monzodiorite in the southern part of the Laxemar subarea (Appendix 3; see also Figure 5-28). Furthermore, diorite to gabbro also frequently occurs as minor bodies in the northern part and north of the Laxemar subarea.

Fine- to medium-grained granite and pegmatite

Fine- to medium-grained granite is the most common and characteristic subordinate rock type in the Laxemar subarea (Appendix 3 and Figure 5-13). It occurs as dykes of various thickness (generally 0.1–1 m), but also as veins and minor, irregular bodies in the other rock types. Furthermore, fine- to medium-grained granite constitutes some larger bodies outside the Laxemar subarea in the eastern part of the regional model area (Figure 5-4). U-Pb zircon dating indicates that the fine- to medium-grained granite is coeval with the country rocks and belongs to the same magmatic generation /SKB 2005b, Wahlgren et al. 2005b/.



Figure 5-13. *Fine- to medium-grained granite (light red) in quartz monzodiorite.*

Pegmatite is also a frequently occurring subordinate rock type, though in much less amount than the fine- to medium-grained granite. The pegmatite dykes are generally less than 0.3 m thick.

During the bedrock mapping of the Laxemar subarea and its immediate surroundings, the orientation of a number of dykes of fine- to medium-grained granite and pegmatite was documented /Persson Nilsson et al. 2004/. As can be seen in Figure 5-14, both sets of dykes display a dominant ENE-WSW to NE-SW strike, but the dip varies from vertical to horizontal, although there is a slight dominance of a southeasterly dip /Wahlgren et al. 2005ab/. The dyke orientations obtained from the bedrock mapping of the Laxemar subarea are consistent with results obtained at the Äspö Hard Rock Laboratory /Jonsson 2004/.

Fine-grained diorite to gabbro

Fine-grained diorite to gabbro commonly occurs as minor composite intrusions, dykes or bodies, in association with fine- to medium-grained granite.

Götömar type granite

This conspicuous rock type in the regional model area constitutes two large bodies of approximately 1,450 Ma old granite, the so-called Götömar granite in the northern part and the so-called Uthammar granite in the southern part (Figure 5-4).

Age relations

Field relationships, such as mixing and mingling and diffuse contact relationships between the rock types in the Laxemar and Simpevarp subareas strongly support the interpretation that all rock types were formed more or less synchronously. This is confirmed by radiometric dating that consistently indicate that all rocks types, except for the Götömar type granites, were formed at c. 1,800 Ma /SKB 2005a, Wahlgren et al. 2005b/.

Petrophysical properties of rock types

A compilation of the petrophysical properties, including in situ gamma ray spectrometry, of the different rock types in the Laxemar subarea is presented in /Mattsson et al. 2004c/ and summarised in /Wahlgren et al. 2005b/. The petrophysical properties are also included in the property table associated with each of the rock domains (see Section 5.3.5 and Appendix 5). A brief description of the petrophysical properties follows below.

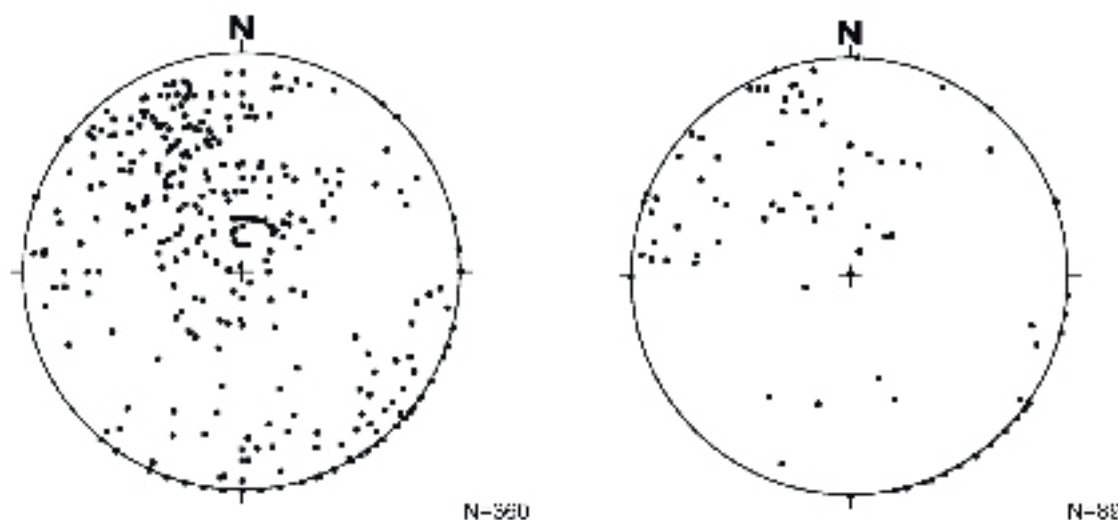


Figure 5-14. Orientation of dykes of fine- to medium-grained granite (left) and pegmatite (right) in the Laxemar subarea. Lower hemisphere of Schmidt equal area, stereographic plots.

Magnetic susceptibility and density

In Figure 5-15, the density and magnetic susceptibility of the various rock types in the Laxemar and Simpevarp subareas are displayed. The rock types display overlapping magnetic susceptibilities, and partly overlapping density values. Except for a slight overlap, it is indicated from the available samples in Figure 5-15 that the quartz monzodiorite has a higher density than the Ävrö granite, although the Ävrö granite comprises quartz monzodioritic varieties. This is presumably caused by the higher content of biotite and hornblende in the quartz monzodiorite compared to the quartz monzodioritic varieties of the Ävrö granite (see Figure 5-10).

Porosity and electrical resistivity

Porosities of the investigated rocks in the Laxemar and Simpevarp subareas are low, in general below 1%, which is normal for unaltered crystalline Swedish bedrock. The porosity values of the rock types overlap, but although the number of analyses is small, it is indicated that the fine-grained dioritoid and the diorite to gabbro have lower porosities than e.g. the Ävrö granite. Furthermore, the different rock types display overlapping resistivity values, and in consequence of the lower porosities, it is indicated that slightly higher resistivity is recorded for the fine-grained dioritoid and diorite to gabbro. From the distribution of the sample locations, it is revealed that the Ävrö granite in central and northern Laxemar displays higher porosity and lower resistivity values than the surrounding rock types.

In situ gamma ray spectrometry

The results of the in situ gamma ray spectrometry measurements show that the fine- to medium-grained granite has the highest content of potassium and thorium, which also has been observed in earlier studies /Mattsson et al. 2002/. Similarly to the mineralogical and chemical variation in the Ävrö granite, the latter also display variations in the gamma ray spectrometric data. The thorium content is generally higher in the granitic to granodioritic varieties of the Ävrö granite compared to the quartz monzodioritic ones.

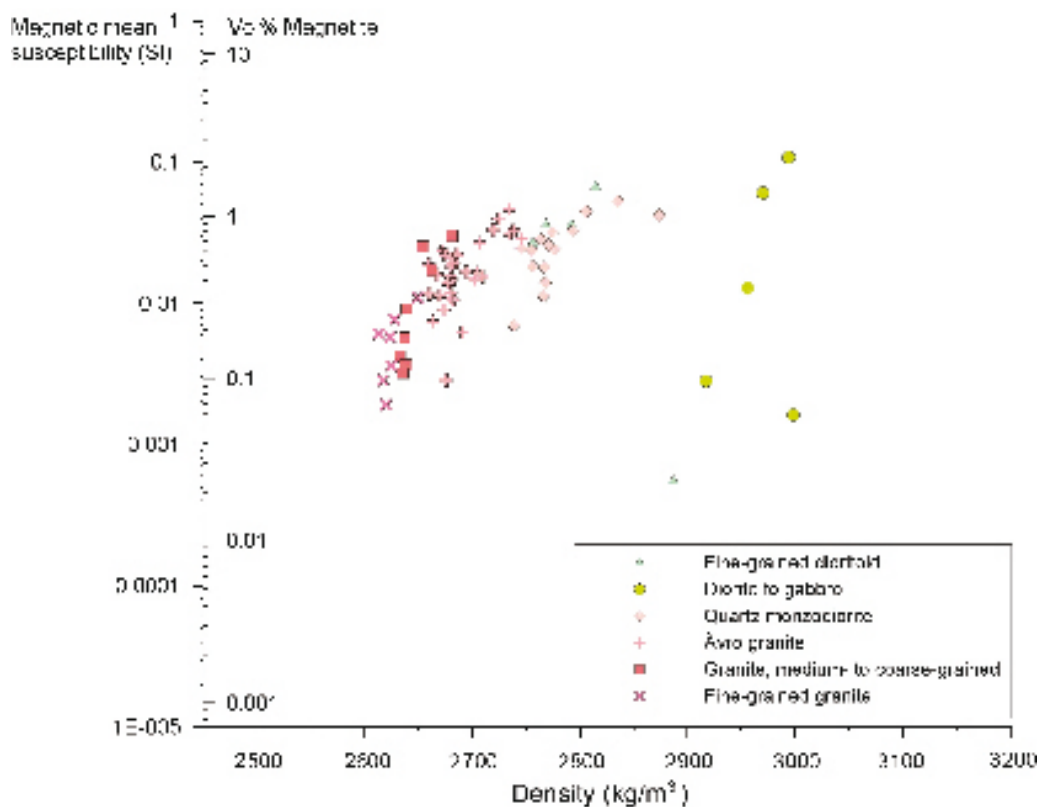


Figure 5-15. Diagram showing correlation between density and magnetic susceptibility of different rock types (surface samples) from the Simpevarp and Laxemar subareas /Mattsson et al. 2004c/.

All rock types in the Laxemar and Simpevarp subareas display low contents of uranium, except for pegmatite in which the uranium content locally exceeds 16 ppm.

Bedrock heterogeneity

Bedrock heterogeneity can be assessed at different scales. The most common factors to consider are:

- Occurrences of subordinate rock types, e.g. dykes, veins, patches, enclaves, inclusions or minor bodies, in a dominating rock type.
- A general mixture of various rock types with different composition and character.
- More or less large compositional variations within a dominating rock type.
- A combination of the above mentioned factors.

The subordinate rock types in the Laxemar subarea, as well as in the Simpevarp subarea, have been registered in the outcrop database /Wahlgren et al. 2004, Persson Nilsson et al. 2004/ at every observation point during the bedrock mapping. The bedrock map in Appendix 3 and the detailed bedrock maps of cleared outcrops /Wahlgren et al. 2005b/ reveal provisionally and approximately the contents of subordinate rock types. In particular, fine- to medium-grained granite, but also pegmatite and locally diorite to gabbro, are characteristic and constitute the most important factor contributing to heterogeneity.

As can be seen in the bedrock map in Appendix 3, the area along the contact between the Ävrö granite and the quartz monzodiorite in southern and southwestern Laxemar contains a large amount of diorite to gabbro. The latter occurs as minor enclaves up to more or less large bodies. In addition, fine- to medium-grained granite, pegmatite and fine-grained dioritoid occur. Consequently, this area is most heterogeneous when considering the implications of a mixture of different rock types.

Regarding compositional variations within a dominant rock type, this is represented by data on the Ävrö granite (cf. Figure 5-5, Figure 5-6 and Figure 5-28).

The degree of bedrock inhomogeneity is also evident from the variation of rock types in the cored boreholes (see Section 5.2.8).

5.2.4 Lineament identification

Primary data and types of inferred lineaments

Lineaments in the regional model area have been identified on the basis of a joint integrated interpretation of different sets of lineaments, each of which has been identified separately from the following data sets /Rønning et al. 2003, Triumph et al. 2003, Triumph 2004a, Wiklund 2002, Elhammer and Sandkvist 2005/:

- Helicopter-borne geophysical survey data, i.e. data on the total magnetic field, electromagnetic (EM) multifrequency data and very low frequency electromagnetic (VLF) data.
- Fixed-wing airborne, very low frequency electromagnetic (VLF) data.
- Detailed topographic data (terrain model).
- Terrain model of the sea bottom and bedrock surface in the sea area outside Simpevarp.

For a detailed description of the data sets used in the lineament identification, see /Wahlgren et al. 2005b/ and references therein/.

Evaluation

The process of joint interpretation of lineaments consists of the following major steps (cf. Figure 5-16):

- Construction of “coordinated lineaments” from “method-specific lineaments”.
- Parameterisation of the “coordinated lineaments”.
- Construction of “linked lineaments”.
- Parameterisation of “linked lineaments”.

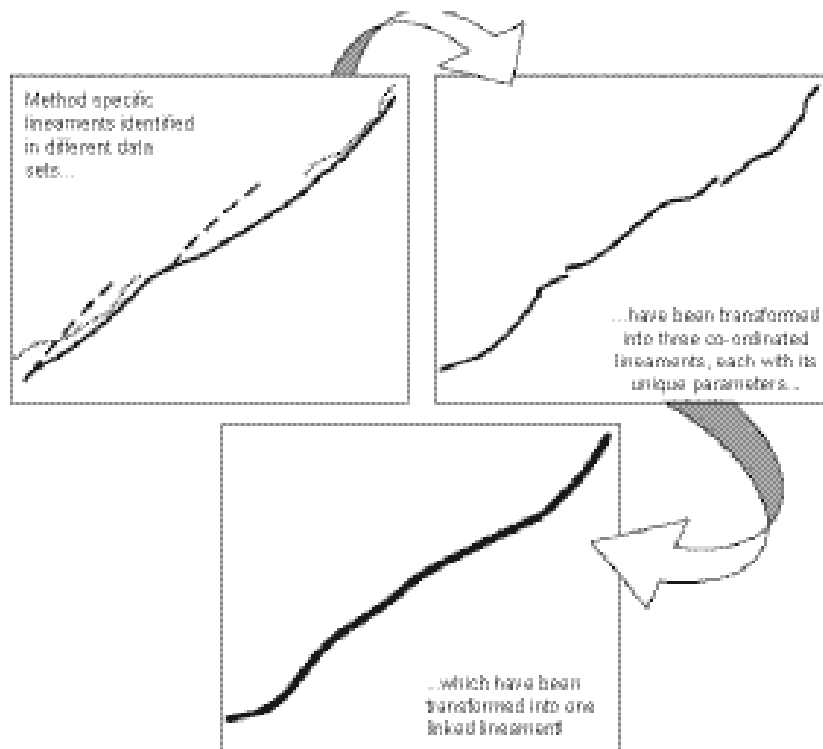


Figure 5-16. Schematic explanation of the joint lineament interpretation process.

For a more comprehensive description of the evaluation process, see /Wahlgren et al. 2005b, and references therein/.

The resulting lineament interpretation covers the land area covering the Simpevarp peninsula, Ävrö, Hälö, Äspö and Laxemar as seen in Figure 5-17. Lineaments of low resolution, originating from model version 0 /SKB 2005a/, cover the eastern part of the regional model area (sea area) and a minor rectangle in the north-west. Lineaments in the central part of the regional model area have not been changed since model version Simpevarp 1.2. New detailed bathymetric data along the coast line result in a more detailed coverage of lineaments further to the east.

The linking of lineaments between the low and high resolution areas has been performed by joining together lineament ends located sufficiently close using the underlying topographical and airborne geophysical data supported by expert judgement. Please note that the variable resolution of the background data imposes an artificial appearance of there being fewer lineaments at sea and in the north-west. The resulting lineament map is used in the deformation zone modelling (see Section 5.4).

5.2.5 Observation of ductile and brittle structures from the surface

Data that document the character and orientation of ductile and brittle structures at the surface in the Laxemar subarea and immediate surroundings originate from observations made in conjunction with the bedrock mapping of the Laxemar subarea and immediate surroundings during 2004. Available data comprise:

- 1,395 measurements of ductile and brittle structures and bedrock contacts at 1,350 observation points, including 181 observation points in the regional model area, that were documented during the bedrock mapping /Persson Nilsson et al. 2004/.
- Laboratory measurements of the anisotropy of the magnetic susceptibility (AMS) of samples from 66 outcrops /Mattsson et al. 2004c/, the majority of which is located in the Laxemar subarea and its immediate surroundings.
- Documentation of fracture fillings by visual inspection at 333 of the 1,350 observation points referred to above /Persson Nilsson et al. 2004/.

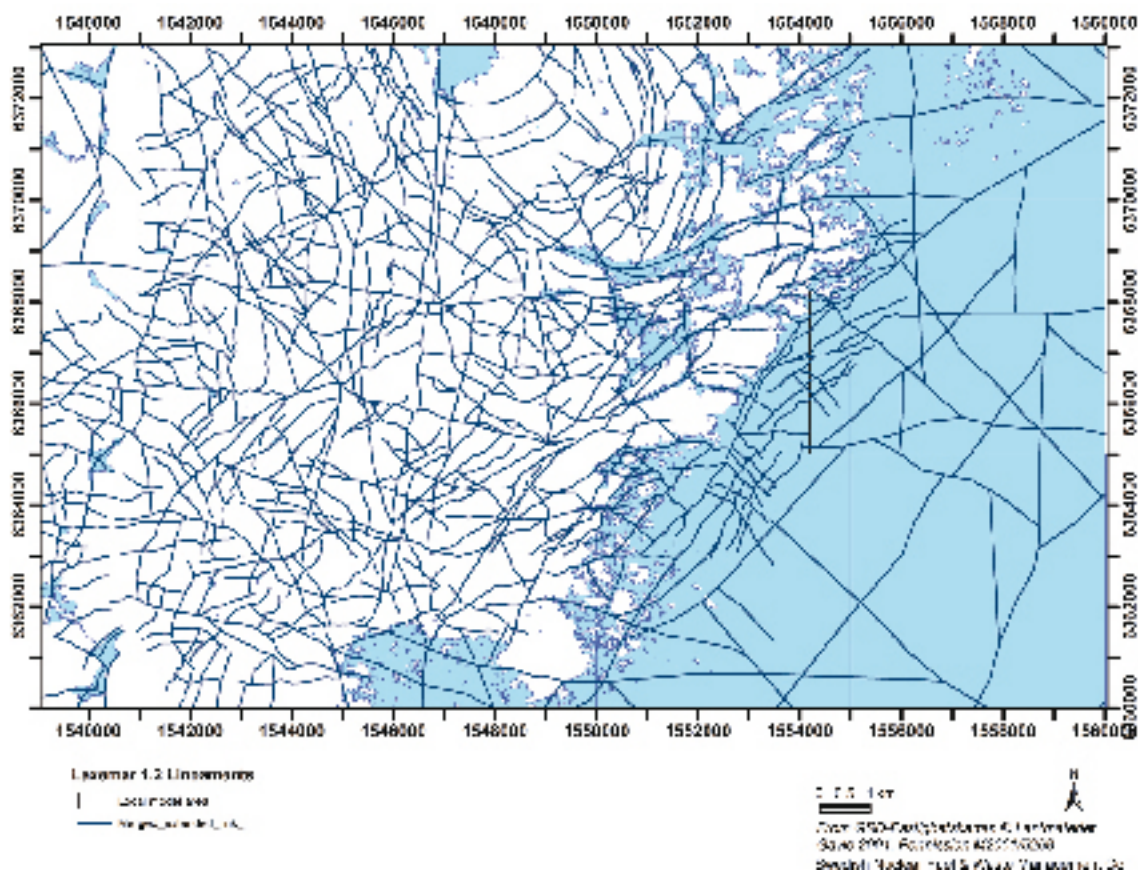


Figure 5-17. Resulting lineament map used as a basis for developing the deformation zone model as described in Section 5.4.

- Detailed mapping of fractures (including fracture fillings) longer than 50 cm at two cleaned outcrops in the Laxemar subarea /Cronquist et al. 2004/ and four in the Simpevarp subarea /Hermanson et al. 2004/.
- Scan-line mapping of frequency and orientation of fractures longer than 100 cm at 24 observation points in the Laxemar subarea and immediate surroundings /Berglund 2004/ and 16 in the Simpevarp subarea /Wahlgren et al. 2004/ – fracture fillings were also noted when identified.

Ductile structures

The rocks in the Laxemar as well as in the Simpevarp subarea are generally well-preserved and more or less undeformed (this is presumably valid also for the rocks in the remainder of the regional model area). However, locally a weak foliation is developed that is defined mainly by the preferred orientation of biotite.

The foliation in the Laxemar subarea and immediate surroundings has an east-west to northwesterly strike and a variable dip, whereas the foliation in the Simpevarp subarea displays an east-west to northeasterly strike and steep dip (Figure 5-18). Furthermore, the foliation is more or less concordant to the contacts between the dominant rock types which suggests a genetic relationship between the formation of the foliation and the formation of the rocks.

The most spectacular and characteristic ductile, structural features in the Laxemar and Simpevarp subareas are the occurrences of protomylonitic to mylonitic, low-grade ductile to brittle-ductile shear zones (Figure 5-19). The dotted pattern in the bedrock map in Appendix 3 defines two areas, or rather belts, with a high concentration of low-grade ductile to brittle-ductile shear zones. The regional scale shear zones within this belt have a northeast-southwest strike and a vertical to subvertical dip (Figure 5-20), which, on a local scale, can be seen as two branches, denoted zone ZSMNE005A (Äspö shear zone) and zone ZSMNE004A, of a larger regional structure that divides Laxemar from Simpevarp, see Section 5.4.4.

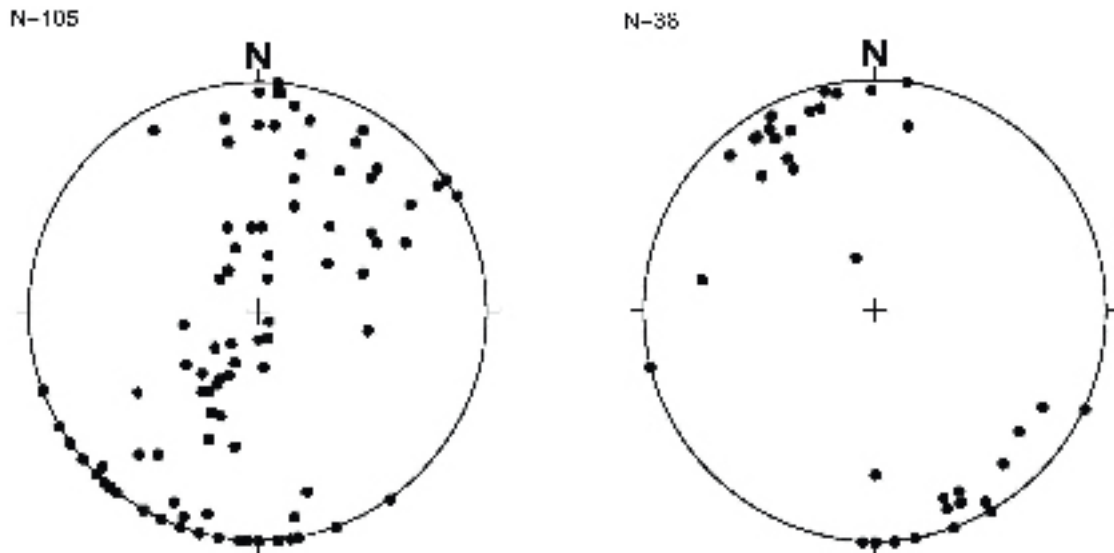


Figure 5-18. Poles to foliation in the Laxemar subarea and immediate surroundings (left) and Simpevarp subarea (right). Lower hemisphere of Schmidt equal area, stereographic plots.



Figure 5-19. Strongly deformed, protomylonitic Åvrö granite within ZSMNE004A.

Overprinting by ductile shear zones – division in structural domains

Available information from the bedrock mapping indicates that the Simpevarp subarea is more strongly affected by low-grade ductile shear zones than the Laxemar subarea. This is also strongly indicated in the magnetic anomaly map where the Simpevarp subarea, i.e. east of the Äspö shear zone, is characterised by a much more banded, anomaly pattern than the Laxemar subarea west of the Äspö shear zone (Figure 5-21). This difference is interpreted to be a result of overprinting of the ductile shear zones. Thus, the Simpevarp and Laxemar subareas may be considered as two different structural domains, and indicates that the Simpevarp subarea is situated in a spaced ductile shear belt, while the Laxemar subarea more or less have escaped this ductile shearing and in respect to the latter constitute a “tectonic lens”.

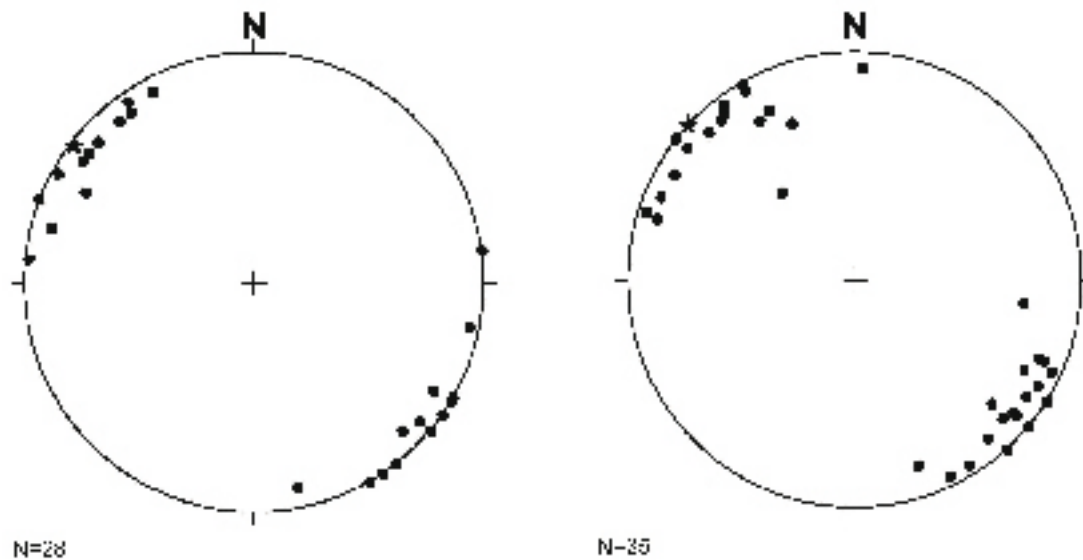


Figure 5-20. Poles to protomylonitic to mylonitic foliation in ductile shear zones in zone ZSMNE005 (Åspö shear zone) (left) and ZSMNE004A (right). Star marks the mean pole. Lower hemisphere of Schmidt equal area, stereographic plots.

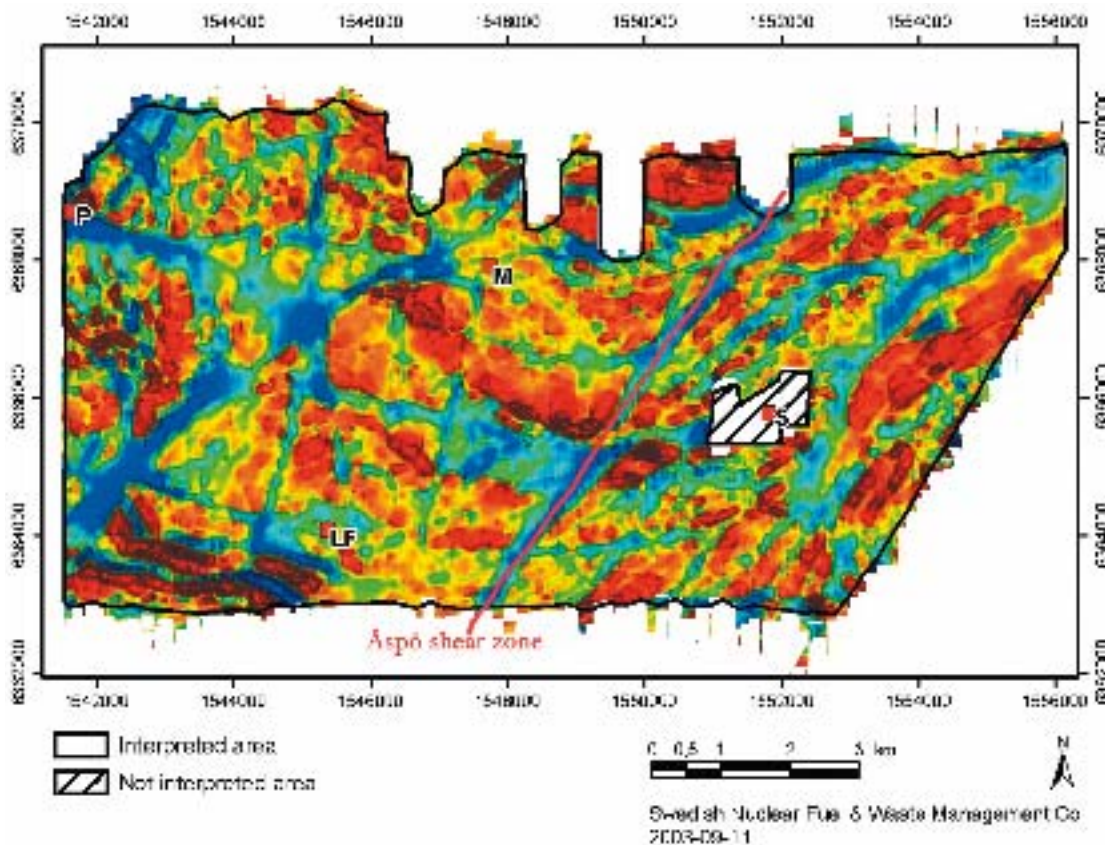


Figure 5-21. Map showing the total magnetic field from the helicopter survey. Reddish brown colour = strongly magnetic bedrock, blue colour = weakly magnetic bedrock.

A sinistral strike-slip component of movement has been suggested for the ductile deformation in the Äspö shear zone /Talbot and Munier 1989, Munier 1989/, and this is also indicated by the change in orientation of the magnetic anomaly pattern along both sides of the zone (Figure 5-21). Sinistral displacements along the NE-trending Äspö shear zone, may explain and is inferred to have caused the change in orientation of the lithological boundaries and the weakly developed foliation from northwesterly in the Laxemar subarea to northeasterly in the Simpevarp subarea. However, a special study will be carried out in order to try to assess the sense of movement (kinematics) of the ductile shear zones. The results of this study will have important implications for the future modelling work and understanding of the structural and tectonic evolution in the area.

Anisotropy of the magnetic susceptibility (AMS)

AMS data may be an important and useful tool in revealing an anisotropic fabric in rocks that appear well preserved and lack a clear visible tectonic fabric. The AMS-ellipsoids from samples from the Laxemar and Simpevarp subareas show a continuous variation in shapes from strongly prolate (“cigar-shape”) to strongly oblate (“disc-shape”) but the degree of anisotropy is below 1.3 for most of the samples. This indicates that a majority of the rocks within the site investigation area are well preserved and unaffected by any major deformation.

The orientation of the magnetic lineations (Kmax, corresponding to the long axis of the strain ellipsoid) and the poles to the magnetic foliation (Kmin, corresponding to the short axis of the strain ellipsoid) are shown separately for the Laxemar and Simpevarp subareas (Figures 5-22, 5-23, 5-24, 5-25).

The girdle distribution of the poles to the foliations indicates a folded geometry. However, the latter is only apparent since the spatial distribution of foliation is not in accordance with a folded geometry. It is inferred that the girdle distribution of the magnetic foliations in Figure 5-22 is caused by a mixture of the regional foliations and foliations related to, or disturbed by, the overprinting by low-grade ductile shear zones. The general east-west to westnorthwest orientation of the foliations coincides with the orientation of the lithological boundaries. This indicates that the magnetic fabric is related to the stress field that prevailed during the emplacement of the parent magma.

The magnetic lineation (maximum strain) directions show consistent northwesterly to westnorthwesterly orientations at both the Simpevarp and Laxemar subareas. Plunges are generally moderate to shallow, and though the foliation planes vary in orientation, the orientation of the lineation is fairly constant.

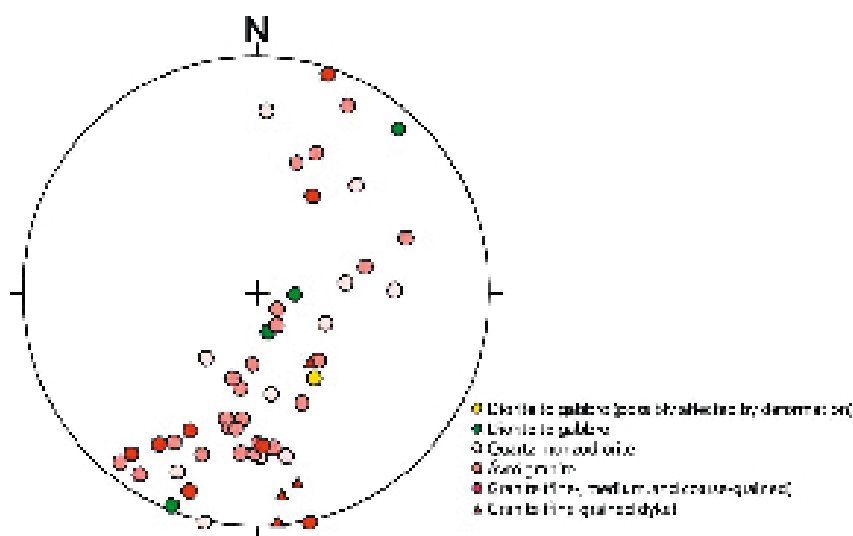


Figure 5-22. Equal area projection plots of minimum (poles to foliation) site mean anisotropy axes for rocks in the Laxemar subarea.

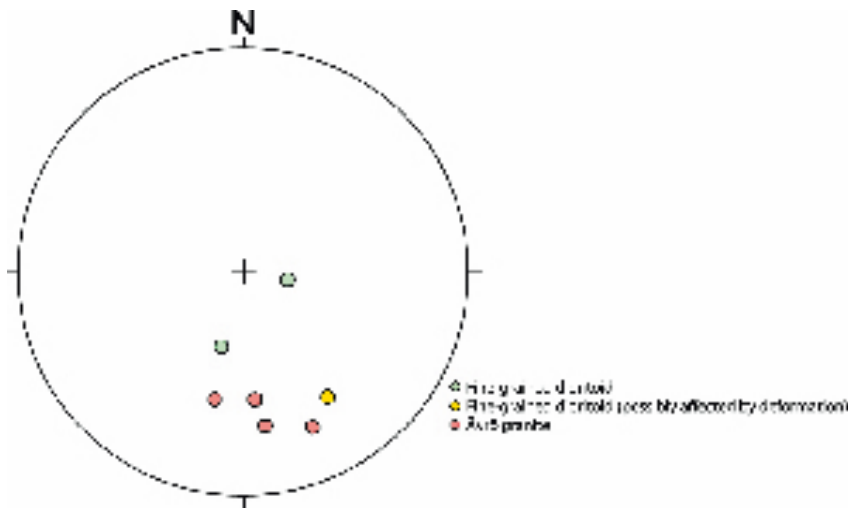


Figure 5-23. Equal area projection plots of minimum (poles to foliation) site mean anisotropy axes for rocks in the Simpevarp subarea.

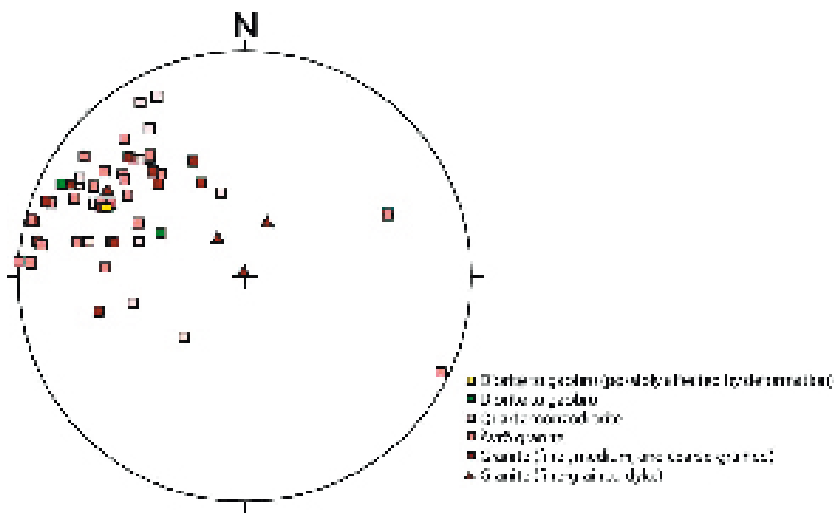


Figure 5-24. Equal area projection plots of maximum (lineation) site mean anisotropy axes for rocks in the Laxemar subarea.

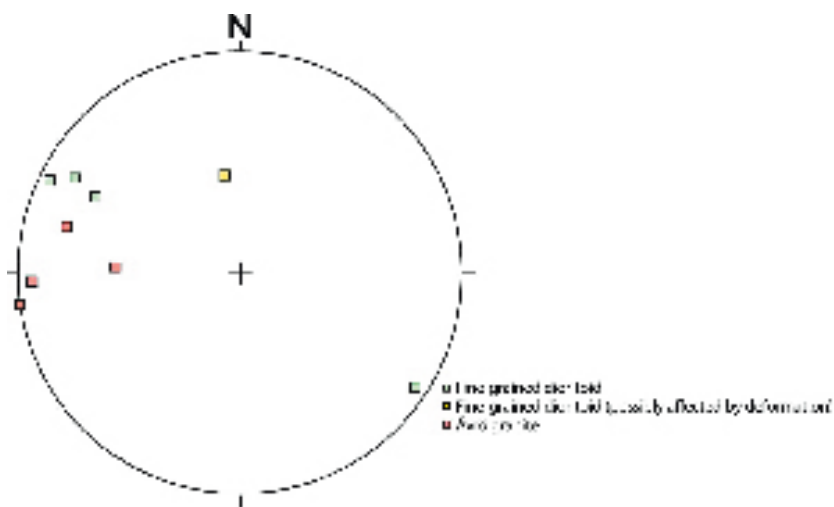


Figure 5-25. Equal area projection plots of maximum (lineation) site mean anisotropy axes for rocks in the Simpevarp subarea.

The orientation of the foliations revealed by the AMS-measurements /Mattsson et al. 2004c/ is similar to the strike of the commonly weakly developed foliations documented during the bedrock mapping of the Laxemar and Simpevarp subareas /Persson Nilsson et al. 2004, Wahlgren et al. 2004/. However, no lineations have been observed/measured during the bedrock mapping, so a comparison with the corresponding AMS results cannot be made.

Brittle structures

Detailed fracture mapping

Detailed fracture mapping has been performed on six outcrops in the Laxemar and Simpevarp subareas. Each outcrop covers an area between 250 to 600 m² and all visible fractures with trace lengths larger than 0.5 m are mapped with a total station. In total over 5,000 fractures have been mapped in both subareas. Fractures with a trace length > 0.2 m are mapped along two N-S and E-W scan-lines on each outcrop.

Description and evaluation of the detailed and scan-line fracture mapping in the Laxemar and Simpevarp subareas is reported in /Hermanson et al. 2005/. Two detailed outcrops are situated in the Laxemar subarea, cf. Figure 5-26 and provide input from the rock domain A01 and the Ävrö granite-dominated part of rock domain M01, cf. Section 5.3.2. In Figure 5-27, the cleaned outcrop ASM000209 in the southern part of the Laxemar subarea can be seen, and Figure 5-28 shows the fracture map from the same outcrop.

Brittle deformation and alteration

Brittle deformation has been documented during the bedrock mapping of the Laxemar subarea and immediate surroundings. In several places, rock exposures close to identified lineaments show signs of brittle deformation such as high frequency of open and/or sealed fractures, cataclastic deformation, alteration etc. which is an indication that the lineament represents a deformation zone (Figure 5-29).

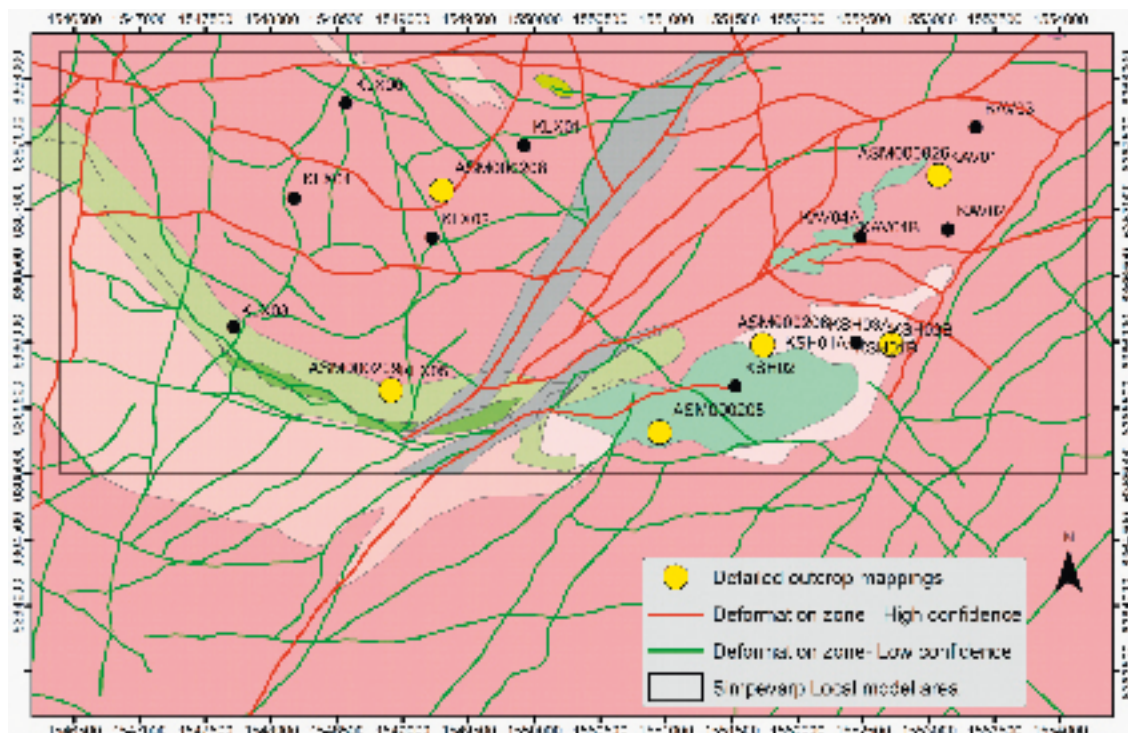


Figure 5-26. Detailed fracture mapping in Laxemar and Simpevarp subareas (new outcrops ASM000208 and ASM000209 in Laxemar).



Figure 5-27. Detailed fracture mapping on the cleaned outcrop ASM000209 in southern Laxemar. Drill site for cored borehole KLX05, cf. Figure 5-26.

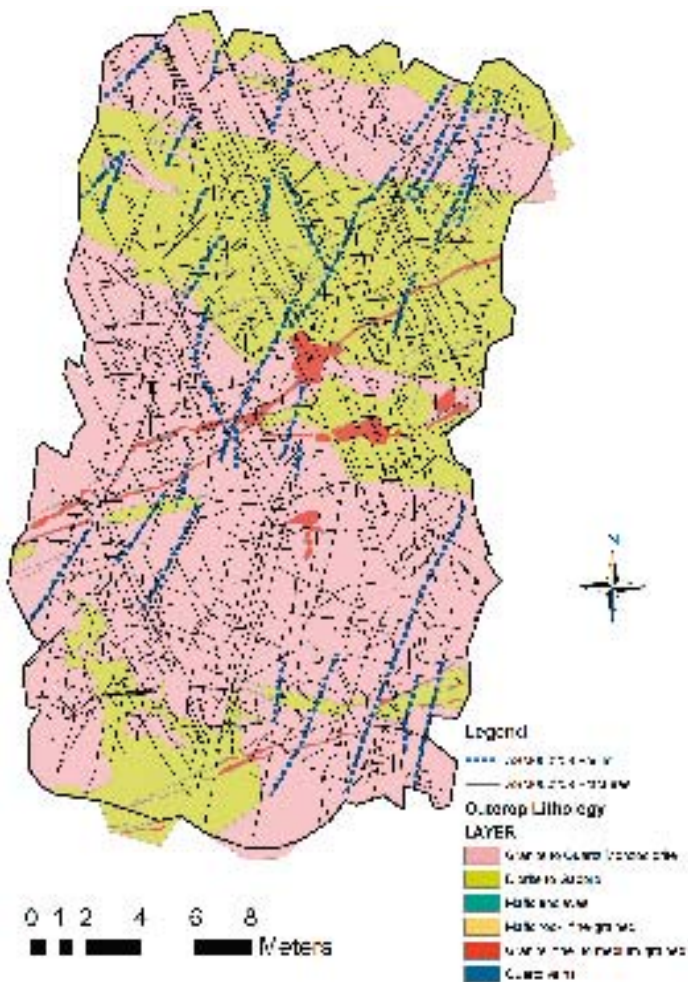


Figure 5-28. Detailed fracture mapping on outcrop ASM000209 (drill site of the forthcoming KLX05) in southern Laxemar (position indicated in Figure 5-26).

The extensive but inhomogeneous, red staining which is a characteristic phenomenon in the Simpevarp subarea was not observed to be of same extent in the Laxemar subarea and surroundings during the bedrock mapping. In the latter area, the red staining mainly occurs along and around fractures and interpreted deformation zones (Figure 5-29) in contrast to the Simpevarp subarea where the red staining also affected the interiors of rock volumes between prominent mesoscopic fractures.

As mentioned above, the Simpevarp and Laxemar subareas are inferred to have responded differently what relates to the overprinting of ductile shear zones, and the observed difference in the degree of red staining indicates that the Simpevarp subarea also responded differently than the Laxemar subarea during the brittle deformation/reactivation during the subsequent geological evolution. This may have great implications for the overall understanding of how the Simpevarp and Laxemar subareas are related, e.g. hydraulically and hydrogeochemically. This will be more closely considered and evaluated in the future modelling work.

The red staining alteration process is focussed on in an ongoing project /Drake and Tullborg 2004, Drake et al. 2004, SKB 2004b, cf. Eliasson 1993/. For further information about alteration and fracture fillings, see Section 5.2.8.

Similarly to the ductile shear zones, a special study is carried out on the kinematics in the brittle deformation zones. The latter includes studies both at the surface and in identified deformation zones in drill cores, and will generate important complementary information for the understanding of the structural evolution.

5.2.6 Surface geophysics

Various types of surface geophysical measurements have been carried out during the ongoing site investigation. These provide indirect information to study the occurrence of possible deformation zones or to help constrain the depth existence of rock types, rock units and rock domains, dependent of the kind of method applied. Independent data, e.g. outcrop and borehole data, are necessary to compare with the geophysical anomalies in order to confirm or refute the presence of e.g. a deformation zone.



Figure 5-29. Brittle deformation and red staining in Ävrö granite close to the deformation zone ZSMNW929A (see section Figure 5-72) in the northern part of the Laxemar subarea. Note the red staining (oxidation).

In Figure 5-30, surface geophysical measurements that have been used in the geological modelling are displayed, including measurements carried out in connection with the ongoing site investigation as well as older measurements. For further information about surface geophysical measurements, see /Wahlgren et al. 2005b/.

All the surface geophysical investigations in the Laxemar subarea, except for the gravity and magnetic total field measurements, have been focussed on an improved understanding of whether lineaments constitute deformation zones and to better verify and characterise these deformation zones. The evaluation of the results is described in conjunction with the description of the deformation zones (Section 5.4.4).

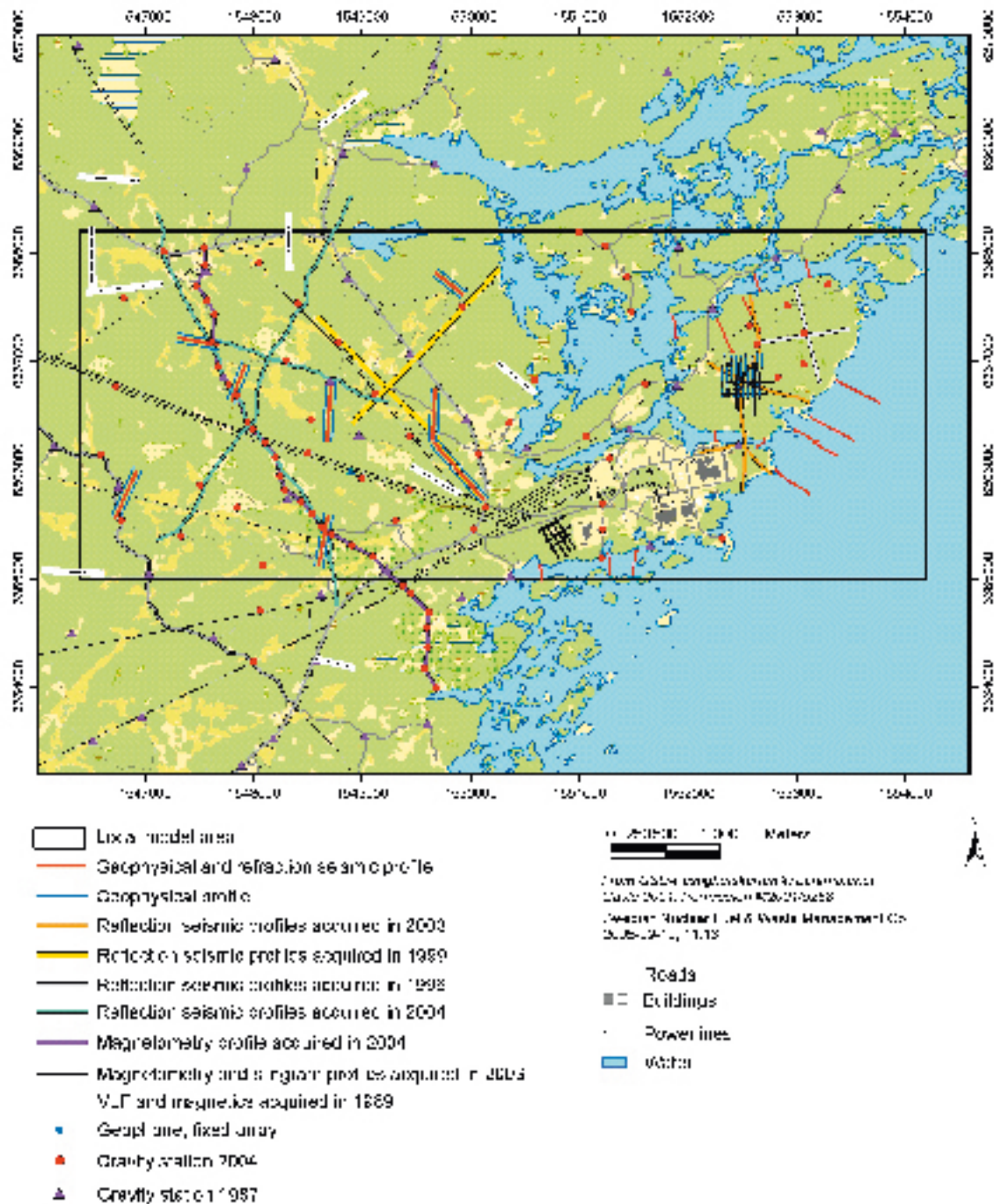


Figure 5-30. Location of surface geophysical measurements in the Laxemar and Simpevarp subareas utilised in the site descriptive modelling.

The gravity and accompanying total magnetic field measurements in the Laxemar subarea focussed on a better understanding of the geometry and extension at depth of the rock types. Of special interest is the rock volume containing a high frequency of diorite to gabbro in the southern part of the Laxemar subarea and also the contact relationship between the Göttemar granite and surrounding rocks north of the Laxemar subarea. The evaluation of the results of these measurements is described in conjunction with the description of the rock domain modelling, cf. Section 5.3.

5.2.7 Fracture statistics from borehole data

Data from approximately 6,800 m of cored boreholes in the Laxemar subarea, and c. 4,700 m of cored boreholes in the Simpevarp subarea have been used in the fracture statistical analysis. Boremap data for the Laxemar subarea exist for KLX02 (200–1,006 m), KLX03, KLX04A/B and in the Simpevarp subarea for KSH01A/B, KSH02, KSH03A/B, KAV01 and KAV04A/B. Preliminary and simplified mapping of KLX02 (200–1,006 m) in the Laxemar subarea have been utilised in the fracture statistical analysis.

The relatively steeply inclined cored boreholes, KLX01, KXL02, KLX03 and KLX04 provide the main input to the Laxemar-specific modelling with regards to fracture orientation, frequency and geological controls. Percussion boreholes, cf. Table 2-1, have been used to analyse surface near fracture statistics in the Laxemar subarea. A notable exception in the primary data usage for SDM Laxemar 1.2 is the use of data from boreholes KLX05 and KLX06 for the fracture mineralogical analyses, see subsection on Fracture mineralogy.

Below follows example statistics derived from boreholes drilled in the Laxemar subarea. A more extensive fracture statistical analysis from percussion and cored boreholes as well as from all previously cored boreholes in Laxemar and Simpevarp can be found in /Hermanson et al. 2005/.

Fracture orientations show a high variability as can be seen in Figure 5-31. In general, the same clusters of fracture orientations appear in all boreholes but have variable intensity in different directions which seems to be related mainly to intersections with brittle deformation zones of variable thickness. Changes in geological controls such as lithology or alteration of the host rock changes the general intensity of fracturing and regardless of orientation unless the borehole approaches a deformation zone (see further below).

Fracture orientation does not seem to have a specific orientation trend towards depth as is exemplified by an elevation/fracture pole trend plot for borehole KLX04 in Figure 5-32. However, fractures orthogonal to the borehole axis are over-represented as can be seen as a dense cloud of points along the borehole axis to the left in Figure 5-32. It turns out that these fracture orientations are related to fractures not visible in BIPS and whose orientations are not possible to infer from analysis of similar fractures close by in the drill core. At the time of the fracture analysis, such fractures were given a default orientation value in the Boremap system which was orthogonal to the borehole axis. Subsequent updates of database software implemented following the Laxemar 1.2 analysis now prevent this error by not attributing these fractures orientation values in the Boremap system.

Near surface fracture intensity has been evaluated through cumulative fracture intensity (CFI) plots both for shallow percussion boreholes, exemplified by data from percussion borehole HLX15, cf. Figure 5-33, and deep cored boreholes in the Laxemar subarea, cf. Figure 5-34. In the CFI plot, those portions of the plotted line that have constant slope indicate where the fracture intensity is constant. Shallower slopes indicate reduced intensity, while steeper slopes indicate increased intensity. The ranges of borehole depth over which the plotted line maintains a constant slope indicate domains of constant fracture intensity.

Surface stress-relief effects resulting in higher fracture intensities, for example, would manifest themselves as a distinct domain extending down from the surface to a few tens of metres. On a CFI plot, this domain would feature a slope that is much shallower than the slope found below in rock of similar geological character.

Fracture intensity does not increase dramatically close to the surface, which implies that surface observations on outcrops are comparable to borehole data from repository depth, /Hermanson et al. 2005/. Note, however, that fracture intensity from outcrops may not be directly comparable to

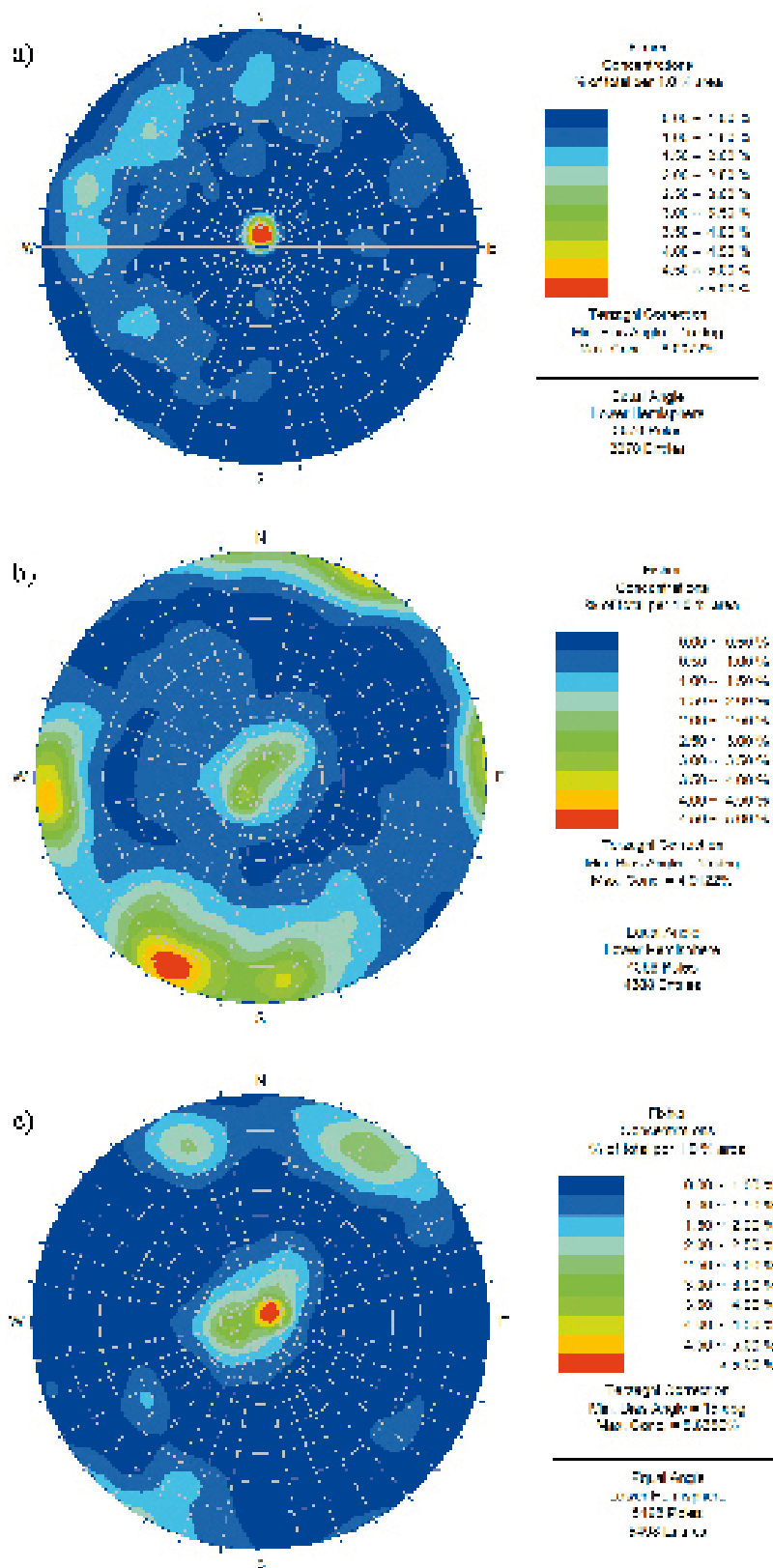


Figure 5-31. Fracture orientations in the cored boreholes A) KLX02, B) KLX03 and C) KLX04.

borehole intensity due to different mapping methods and the fact that surface erosion and outcrop quality limits the ability to distinguish fractures with no or very thin mineralisation in comparison with mapping cores. Furthermore, subvertical fractures are more prominent on horizontal outcrops than subhorizontal fractures (even after correction for orientation bias).

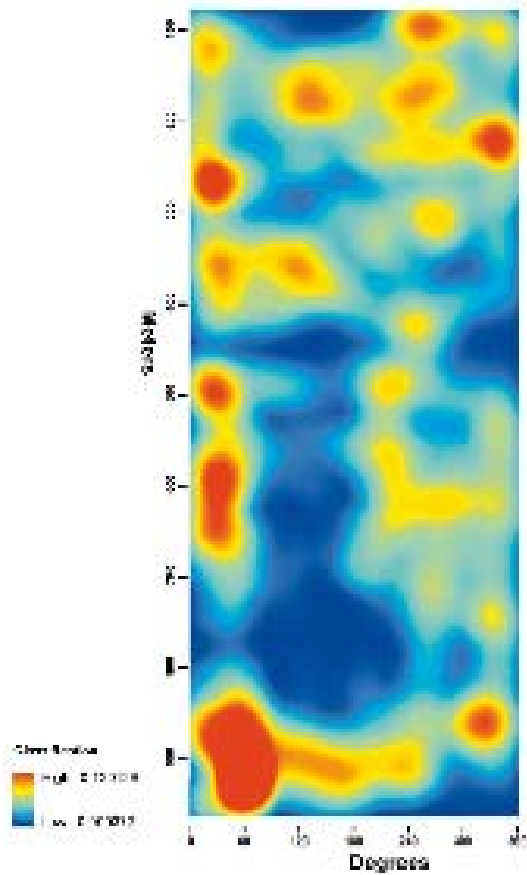


Figure 5-32. Fracture pole trend as a function of elevation, cored borehole KLX04, Laxemar subarea.

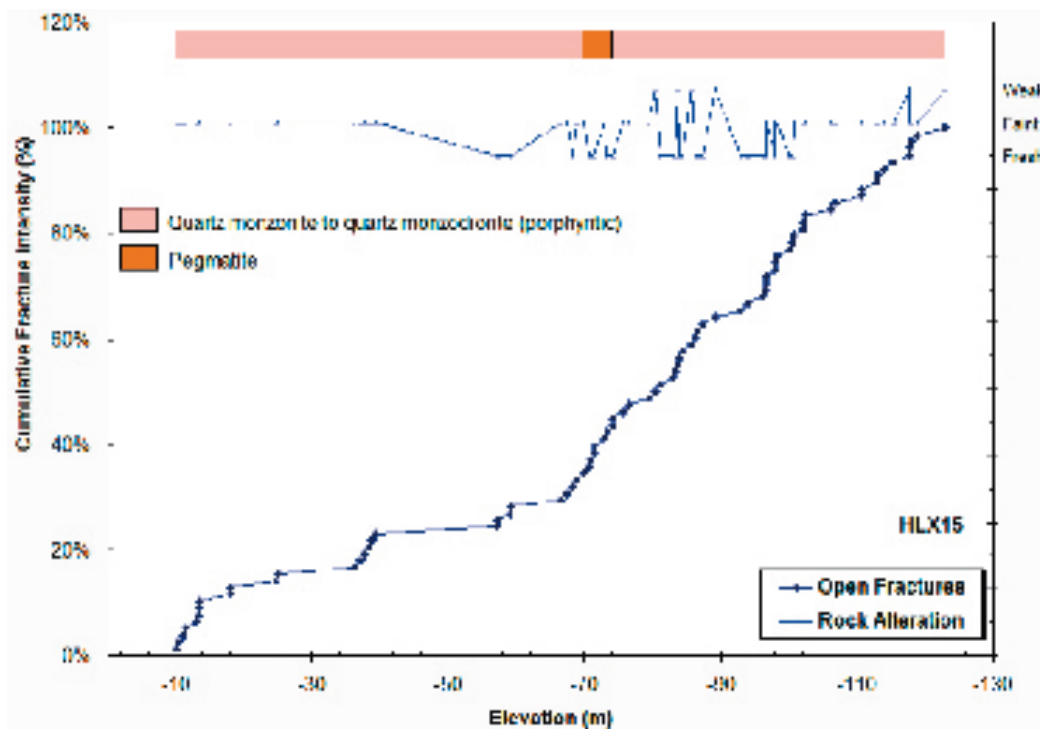


Figure 5-33. CFI plot for percussion borehole HLX15. Flat areas represent relatively low fracture frequency, while steeper slopes represent higher fracture intensity. Fracture data taken from BIPS log.

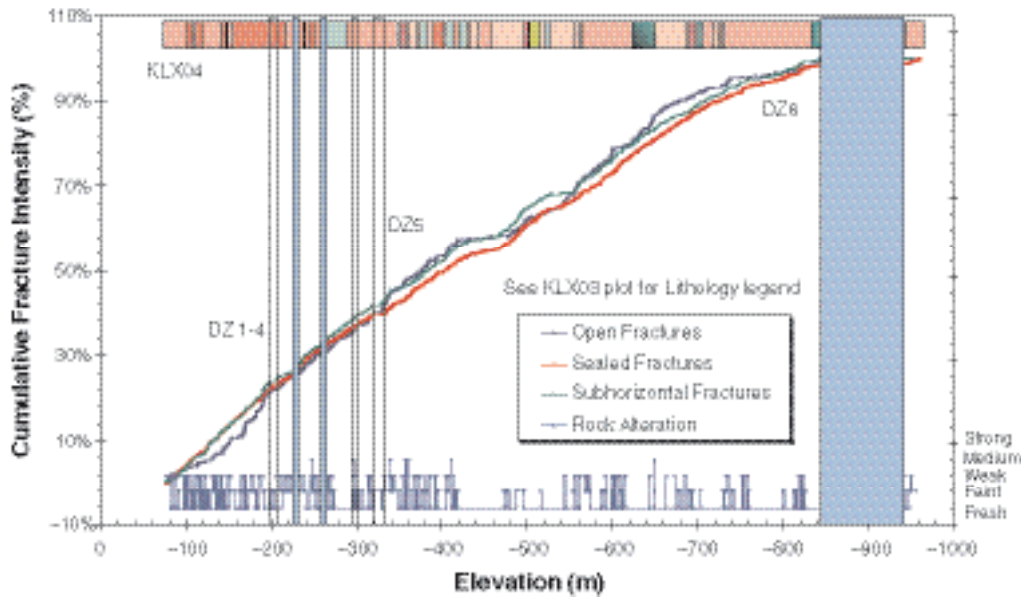


Figure 5-34. CFI plot for borehole KLX04. Flat areas represent relatively low fracture frequency, while steeper slopes represent higher fracture intensity. Fracture data taken from cored borehole and BIPS logs. Plot excludes data based on fractures contained within mapped deformation zones.

Various geological controls on fracture intensity have been evaluated. Fracture mineralogy, lithology and alteration may provide valuable information on how intensity varies within the rock mass. For example, fracture intensity in sections outside deformation zones in analysed cored boreholes in Laxemar has been correlated to host rock type in Figure 5-35 which illustrates five notable observations;

- Overall fracture intensity is lowest in pegmatite and sequentially increases in quartz monzonite – diorite – quartz monzodiorite – fine-grained dioritoid – granite, fine to medium grained – granite medium to coarse grained and is highest in the mafic rock.
- Open fractures dominate over sealed in mafic rock.
- Sealed fractures dominate over open in pegmatite, quartz monzonite and diorite.
- Open and sealed fracture intensity has a one to one relationship in quartz monzodiorite, fine-grained dioritoid and in the granites.
- The variation of fracture intensity to lithology within borehole sections identified as deformation zones differ compared to intensity observed outside deformation zones.

Figure 5-36 illustrates the change of frequency inside deformation zones as follows;

- Pegmatite and quartz monzonite appear to increase mostly in sealed fracture intensity whereas,
- the host rock of granite, monzodiorite and mafic rock shows an increase of open fracture intensity.

This implies that deformation zones associated with granite, monzodiorite and mafic rock are more likely to be permeable than zones in quartz monzonite and pegmatite.

5.2.8 Geologic interpretation of borehole data

The geological mapping and geophysical logging programmes for the boreholes has generated subsurface data that bear on the character of rock type (including alteration), and ductile and brittle deformation including fractures. These programmes are of vital importance for all three components in the geological modelling work, i.e. rock domain, deformation zone and DFN modelling. Due to the lack of a drill core, and thereby a somewhat more uncertain identification of rock types and deformation zones in the percussion boreholes, combined with the limited borehole length, the rock domain and deformation zone modelling work have focussed on data from the cored boreholes.

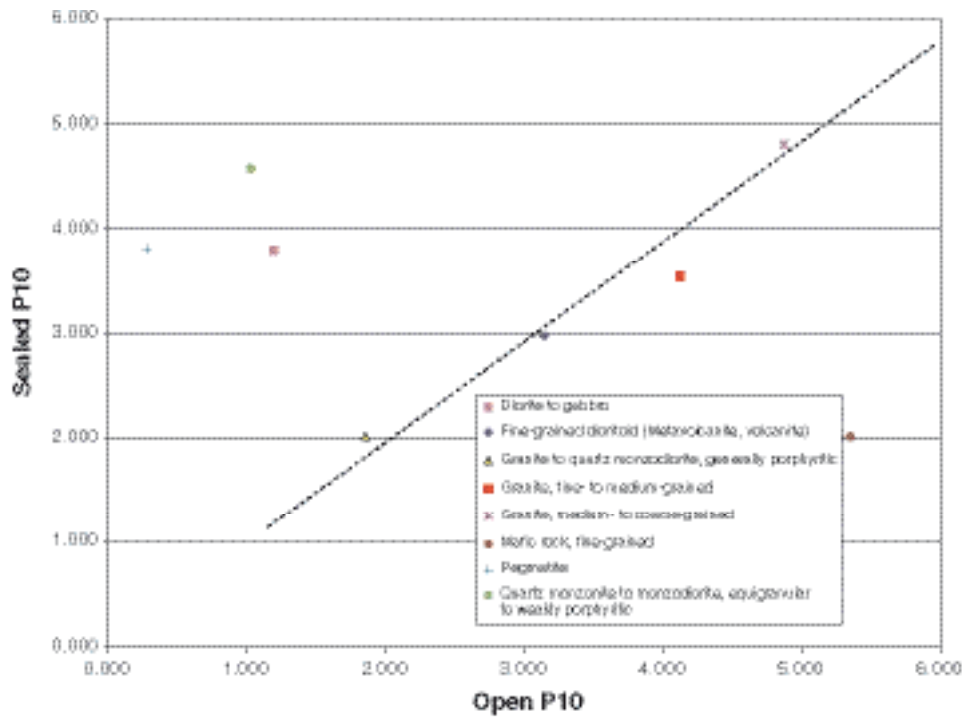


Figure 5-35. Cross plot of open fracture frequency (P_{10}) vs. sealed, mean values for lithologies in cored boreholes in the Laxemar subarea.

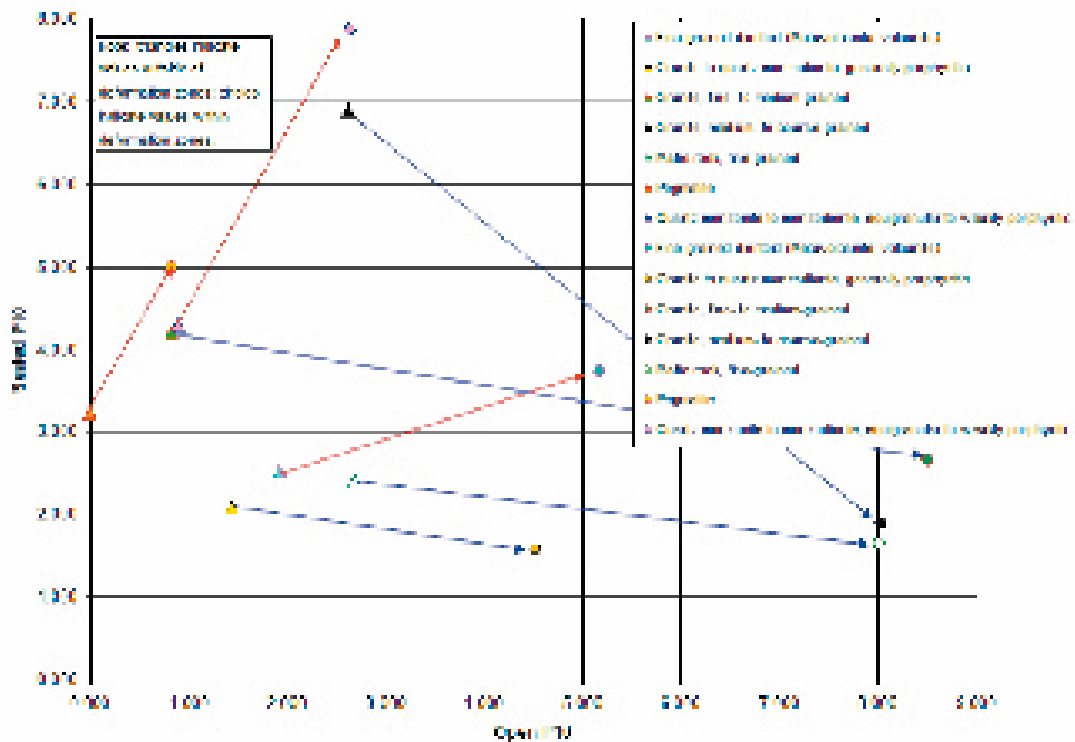


Figure 5-36. Cross plot of open fracture frequency (P_{10}) vs. sealed, mean values for lithologies in cored boreholes in the Laxemar subarea, adding also fracture data within deformation zones, compare with Figure 5-35. Arrows shows the change in intensity between fractures outside of deformation zones, to fractures inside of deformation zones. Red arrows indicate an increase in sealed fracture intensity whereas blue arrows indicate an increase in open fracture intensity.

Data from approximately 6,800 m of cored boreholes in the Laxemar subarea, and c. 4,700 m of cored boreholes in the Simpevarp subarea (see Figure 2-3), have been used in the rock domain and deformation zone modelling work in the Laxemar SDM model version 1.2. Boremap data exist for KLX02 (200–1,006 m), KLX03, KLX04A/B, KSH01A/B, KSH02, KSH03A/B, KAV01 and KAV04A/B. Preliminary and simplified mapping of KLX02 (1,006–1,700 m), KLX05 and KLX06 has been utilised in the rock domain modelling. The bedrock information from KLX01 has not been updated by new Boremap mapping in conjunction with the ongoing site investigation due to the lack of BIPS images. However, the rock nomenclature from the old mapping has been evaluated and translated to the nomenclature used in the site investigation.

Rock types in cored boreholes

The proportion of rock types, based on the Boremap mapping /Ehrenborg and Stejskal 2004abcde, 2005, Ehrenborg and Dahlin 2005ab/ in the cored boreholes KLX01 (not mapped by the Boremap system), KLX02, KLX03 and KLX04A and simplified mapping of KLX06 in the Laxemar subarea, and KSH01A, KSH02, KSH03A, KAV01 and KAV04A in the Simpevarp subarea is estimated by using the sum of the length of all sections of the rock type along each borehole /Wahlgren et al. 2005b/.

In Table 5-1, the proportion of rock types from the Boremap mapping between –400 and –600 m (envisaged repository depth interval) is compared to the proportion along the total borehole length for the cored boreholes KLX01, KLX02, KLX03 and KLX04.

As is evident from Table 5-1, the differences in the proportion of rock types in the cored boreholes at envisaged repository depth and the total borehole length clearly indicates the inhomogeneity in the bedrock from a lithological perspective. The differences in the proportions are partly explained by the actual distribution of the rock types along the boreholes. For example, in KLX02 and KLX03 the quartz monzodiorite is concentrated in and dominates the sections c. 1,450–1,700 m and c. 620–1,000 m, respectively, whereas the quartz monzodiorite in KLX04 makes up several more or less long sections in the interval c. 385–745 m.

In the forthcoming site descriptive modelling work, efforts will be made to try to analyse and present the variation in the distribution of subordinate rock types in the bedrock.

For further presentation and evaluation of the rock types in the cored boreholes, see /Wahlgren et al. 2005b/.

Table 5-1. Comparison of the proportion of rock types between total borehole length and envisaged repository depth interval (z = –400–600 m) in cored boreholes in the Laxemar subarea.

Rock type	KLX01		KLX02		KLX03		KLX04	
	Total borehole	Envisaged repository depth	Total borehole	Envisaged repository depth	Total borehole	Envisaged repository depth	Total borehole	Envisaged repository depth
Ävrö granite	82.27%	82.11%	67.24%	89.21%	56.70%	87.23%	62.15%	51.21%
Quartz monzodiorite	–	–	15.57%	–	35.74%	9.11%	13.45%	30.65%
Granite, medium- to coarse-grained	–	–	0.59%	–	–	–	11.74%	3.29%
Granite, fine- to medium-grained	3.25%	2.74%	1.38%	–	1.44%	–	5.50%	6.09%
Pegmatite	0.16%	0.62%	–	–	0.30%	–	–	–
Diorite to gabbro	4.17%	10.47%	–	–	0.95%	1.10%	0.59%	2.50%
Fine-grained diorite to gabbro	10.15%	4.07%	5.36%	0.88%	2.65%	–	2.85%	–
Fine-grained dioritoid	–	–	9.01%	7.20%	2.22%	2.56%	3.42%	5.90%
Various subordinate rock types	–	–	0.67%	2.69%	–	–	0.59%	–

Ductile structures in cored boreholes

As mentioned in Section 5.2.3, the rocks in the Laxemar subarea as in the Simpevarp subarea, generally are well-preserved and more or less isotropic, but locally a weak foliation is developed.

Foliated varieties of the rock types have also been documented in the Boremap mapping of the cored boreholes. In Figure 5-37 and Figure 5-38, orientation of all foliations documented in cored boreholes, excluding deformation zones, from the Laxemar and Simpevarp subareas is displayed, respectively. As can be seen in the figures, the majority of the foliations have been classified as weak to faint.

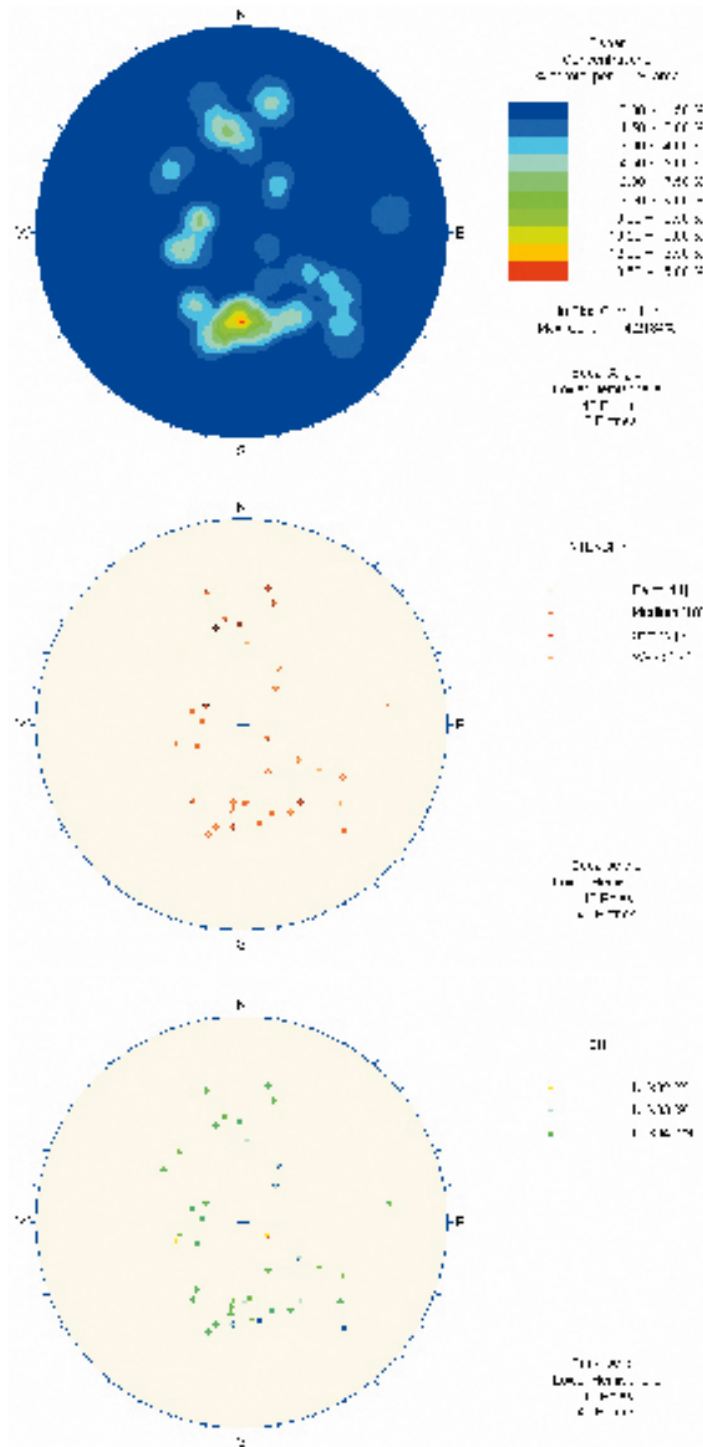


Figure 5-37. Orientation of foliations in the cored boreholes KLX02, KLX03 and KLX04 in the Laxemar subarea. Lower hemisphere of Schmidt equal area, stereographic plots.

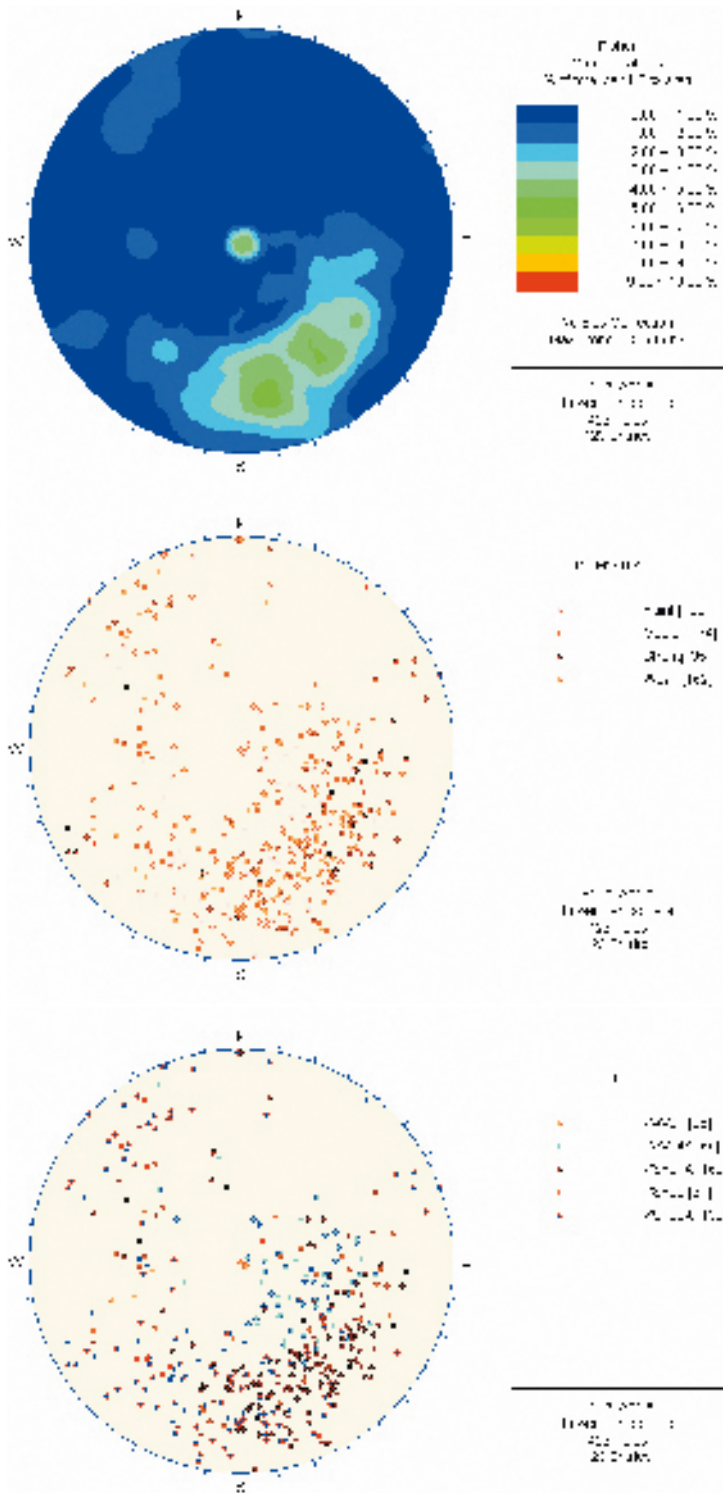


Figure 5-38. Orientation of foliations in the cored boreholes, KSH01A, KSH02, KSH03A, KAV01 and KAV04A in the Simpevarp subarea. Lower hemisphere of Schmidt equal area, stereographic plots.

It is evident from Figure 5-37, that the recorded foliations from the cored boreholes in the Laxemar subarea exhibit a great deal of scatter and deviates from the NW-SE orientation documented at the surface during the bedrock mapping campaign (cf. Figure 5-18), and neither do they correlate with magnetic foliations from the AMS study (Figure 5-22). It should be noted that the majority of the recorded foliations are from KLX04 and do not represent any geographical spread. In contrast, the orientation of the foliations recorded from the cored boreholes in the Simpevarp subarea coincides relatively well with those documented at the surface (Figure 5-18) and also with the few AMS measurements (Figure 5-23). However, the foliations documented at the surface are more steeply dipping.

The discrepancies between the orientations of the foliations documented at the surface, in the cored bore holes and the AMS study, especially for the Laxemar subarea are not fully understood and has to be evaluated in future work. A possible explanation for the deviating orientations between the surface and the borehole data may be that the foliations in the cored boreholes also include proto-mylonitic to mylonitic foliations related to shearing. The latter have been separated from the weakly developed foliations of more regional character during the bedrock mapping of the Laxemar and Simpevarp subareas /Wahlgren et al. 2004, Persson Nilsson et al. 2004/.

Geophysical logs including borehole radar

Besides production of an oriented image of the wall of each borehole with the help of the Borehole Image Processing System (BIPS) for use in the mapping work, borehole radar measurements and geophysical logs have been generated in all the boreholes. A combination of some of the geophysical data (e.g. density, natural gamma radiation) with the relevant petrophysical data provides a support to the mapping of the bedrock in the boreholes, especially in the percussion boreholes. The borehole radar measurements and geophysical logs also provide an important input to the geological single hole interpretation.

The following geophysical data have been generated in the logging procedure for each borehole:

- Density (gamma-gamma).
- Magnetic susceptibility.
- Natural gamma radiation.
- A variety of electrical measurements (e.g. focused guard resistivity, normal resistivity, single point resistance (SPR)).
- P-wave velocity (sonic) measurements.
- Caliper measurements.

Density, magnetic susceptibility and natural gamma radiation measurements have been combined to provide an independent control on the compositional interpretation of the rock types. The occurrences of larger individual fractures have been inferred from a combined analysis of the resistivity, SPR, P-wave velocity and mean caliper measurements.

Fracture mineralogy

Fracture minerals are mapped and determined macroscopically using the Boremap system. Many of the minerals are difficult to identify by eye and small crystals are easily overlooked. Therefore fracture mineral analyses have been carried out for identification, mainly comprising: 1) X-ray diffractometry; especially used for identification of clay minerals and composition of fault gouge materials, and 2) Microscopy of fracture fillings; thin sections and fracture surfaces have been studied by SEM, /Drake and Tullborg 2004, Drake and Tullborg in manuscript/.

The fracture mineral frequency plots (Figure 5-39 and Figure 5-40) are based on Boremap data from Sicada, although comments on suspected over/under representation of certain minerals are based on detailed fracture mineral studies carried out on thin sections and fracture mineral identification using X-ray diffractometry /Drake and Tullborg 2004, Drake and Tullborg in manuscript/.

The total number of fractures in boreholes KLX02, KLX03 and KLX04 is in the order of 3,000 to 6,000 fractures/1,000 m borehole. Only between 9 to 37% of these fractures are mapped as open in the respective borehole. This figure is notably and exceptionally higher for borehole KLX02 (68%), This borehole, existing before the onset of the site investigations, is drilled with a less sophisticated technique (double- instead of triple-tube barrel). Furthermore, the hole has not been logged with BIPS, instead the televiewer technique has been applied. These facts in combination means that the fracture mapping results from KLX02 may not be fully comparable with results from KLX03 and KLX04. Therefore the KLX02 results have not been included in the analysis. In order to compensate for this and obtain improved statistics Boremap data from KLX05 and KLX06 have been included in the fracture mineralogical analysis (Note that Boremap data from KLX05 and KLX06 are exclusively used only in the fracture mineralogical analysis).

The most common fracture minerals in the Laxemar subarea are chlorite and calcite (Figure 5-39 and Figure 5-40). Other common minerals are epidote, quartz, clay minerals, prehnite, laumontite, adularia (low-temperature K-feldspar), pyrite, hematite and fluorite. Fracture minerals that have been identified in small amounts include albite, gypsum, harmotome (Ba-zeolite), barite, muscovite, titanite, chalcopyrite, apatite, galena, sphalerite, Ti-oxide (probably anatase), REE-carbonate, U-silicate and apophyllite. Quartz and epidote are more common in sealed fractures than in open fractures and clay minerals and pyrite are more common in open fractures than in sealed fractures. Prehnite is underrepresented in the Boremap data for KLX03–06 while epidote and quartz are over-represented, since the present prehnite has been mapped as quartz or epidote.

The mineralogy in sealed and open fractures shows no significant variation with depth (Figure 5-41 and Figure 5-42). However, frequencies of calcite, pyrite and Fe-oxides in open fractures are expected to be variable in the upper 100 m due to interaction with recharge water but there are vary

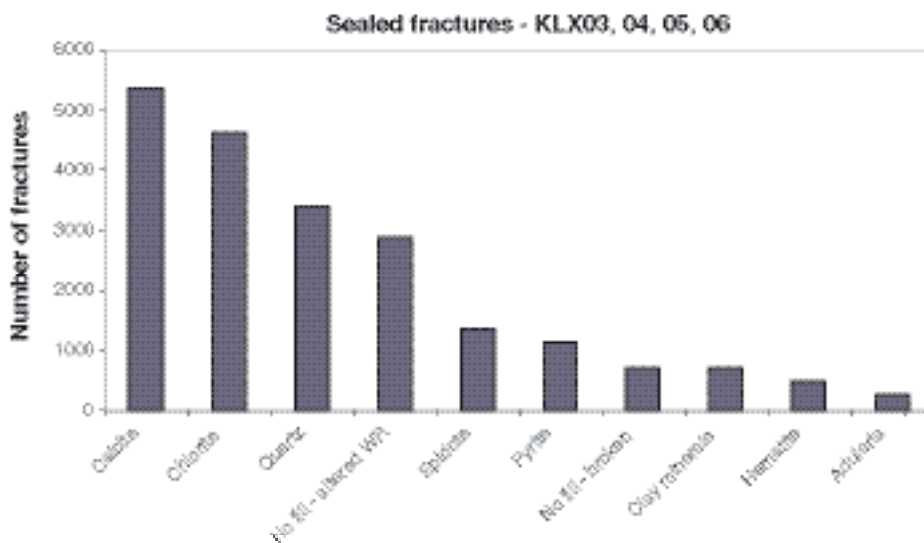


Figure 5-39. Number of observations of sealed fractures with a given mineral observed in boreholes KLX03 through KLX06. “No fill – altered WR” = extremely narrow, sealed fractures with altered wall rock and no visible fracture filling, “No fill – broken” = most certainly broken during drilling. The total number of sealed fractures is 14,585.

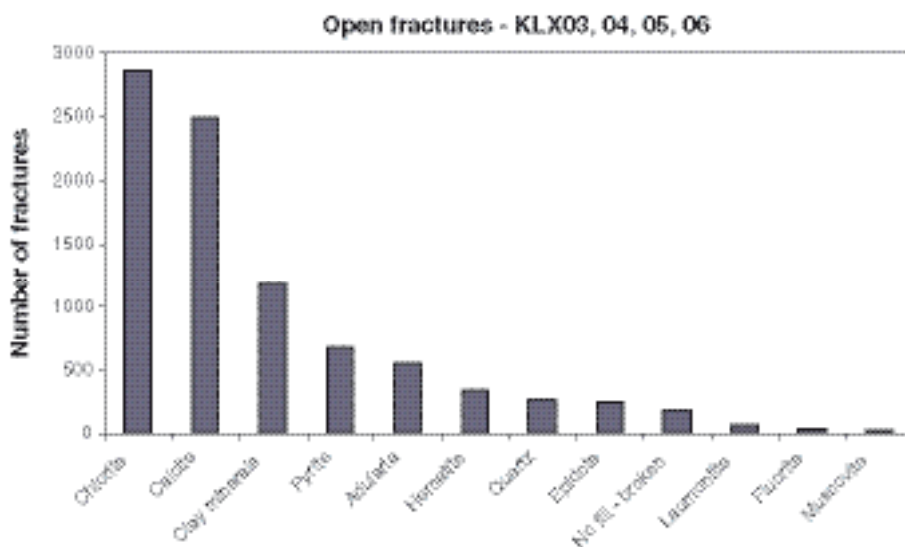


Figure 5-40. Number of observations of open fractures with a given mineral from observed in boreholes KLX03 through KLX06. “No fill – broken” = most certainly broken during drilling. The total number of open fractures is 4,049.

few observations in this near surface interval so far. More near surface data will be available in forthcoming model versions. Notable is that pyrite is most common in the depth interval 300–600 m and gypsum is commonly found in the interval 500–600 m (vertical depth). The mineralogy in the water conducting fractures is largely similar to that of the total group of fractures mapped as open (cf. Chapter 10). It should be noted that the fracture mineral frequencies shown in Figure 5-39, Figure 5-40, Figure 5-41 and Figure 5-42 can not be directly translated to amounts; e.g. pyrite is present in 5 to 30% of the fractures but the amount is still very limited.

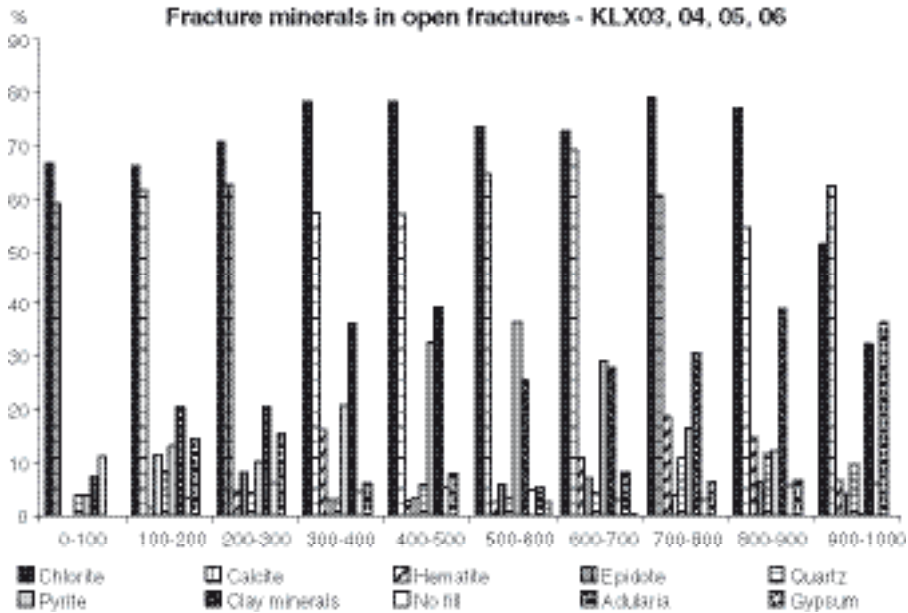


Figure 5-41. Variation in observations of fracture mineralogy in sealed fractures as a function of depth. “No fill” = narrow, sealed fractures with altered wall rock and no visible fracture filling. Depth is given as vertical depth. Note that the observations from 0–100 m depth are very few.

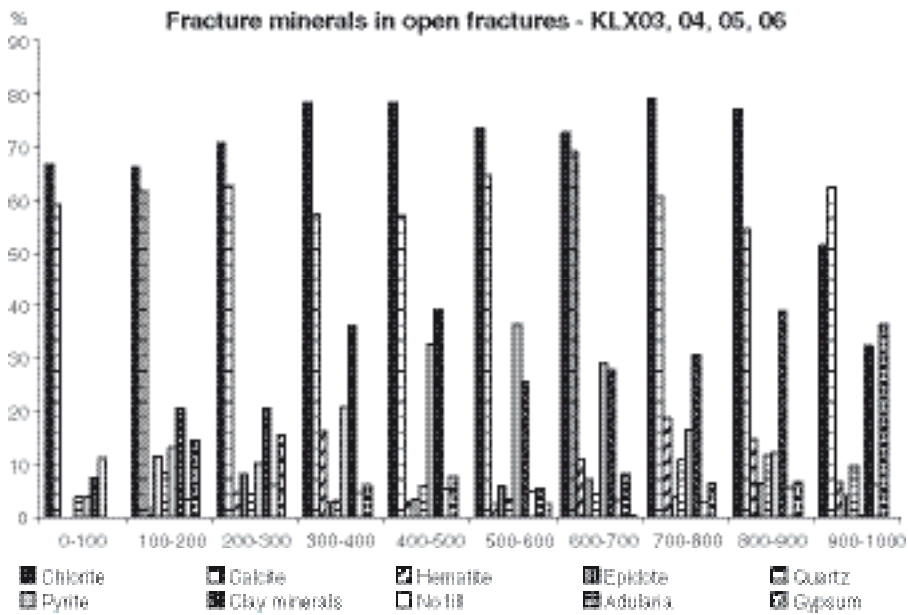


Figure 5-42. Variation in observations of fracture mineralogy in open fractures as a function of depth. “No fill” = most certainly broken during drilling. Depth is given as vertical depth. Note that the observations from 0–100 m depth are very few.

Clay minerals identified are, in addition to chlorite; corrensite (mixed layer chlorite/smectite or chlorite/vermiculite clay, the smectite or vermiculite layers are swelling, Figure 5-43), illite, mixed-layer illite/smectite (swelling) and a few occurrences of smectites.

Calcite has been analysed for its isotopic composition of $^{13}\text{C}/^{12}\text{C}$, $^{18}\text{O}/^{16}\text{O}$ and $^{87}\text{Sr}/^{86}\text{Sr}$ in order to sort out calcites of different generations, gain knowledge of formation conditions and to provide support for relative dating of different fracture filling generations.

A schematic fracture filling-sequence from the oldest (1) to the youngest (7) for Simpevarp/Laxemar/Äspö is as follows:

1. Quartz- and epidote-rich mylonite, occasionally including muscovite, titanite, Fe/Mg-chlorite, albite, (apatite), (calcite), (K-feldspar).
2. a. Epidote-rich cataclasite with quartz, titanite, Fe/Mg-chlorite, (K-feldspar), (albite).
b. Hematite-rich cataclasite with epidote, K-feldspar, quartz, albite, chlorite.
3. Euhedral quartz, epidote, Fe/Mg chlorite, calcite, pyrite, fluorite, muscovite, (K-feldspar).
4. Prehnite, (fluorite).
5. a. Calcite, (fluorite, hematite).
b. Dark red/brown filling – Adularia, Mg-chlorite (also as mixed layer clay (ML-clay) with illite), hematite (quartz), (apatite); sometimes cataclastic.
c. Calcite, adularia, laumontite, Mg-chlorite, quartz, illite (also as ML-clay with chlorite), hematite, (albite).
6. Calcite, adularia, Fe-chlorite, hematite, fluorite, pyrite, barite, harmotome, REE-carbonate, apophyllite, gypsum, illite/chlorite (ML-clay), corrensite, chalcopyrite, galena, sphalerite, Ti-oxide, U-silicate, laumontite.
7. Calcite, pyrite, FeOOH (near surface).

The overall fracture mineralogy observed in the Laxemar and Simpevarp subareas is very similar to earlier observations made at the Äspö HRL. The frequency of different fracture mineralisations do however vary between the different subareas and Äspö. The major differences between the fracture mineralogy of the Laxemar and Simpevarp subareas are essentially a matter of abundance and frequency of the different fracture minerals.

The red-staining of the wall rock around many fractures and deformation zones corresponds to hydrothermal alteration/oxidation, which has resulted in alteration of plagioclase to albite and K-feldspar, decomposition of biotite to chlorite and oxidation of Fe(II) to form hematite, mainly

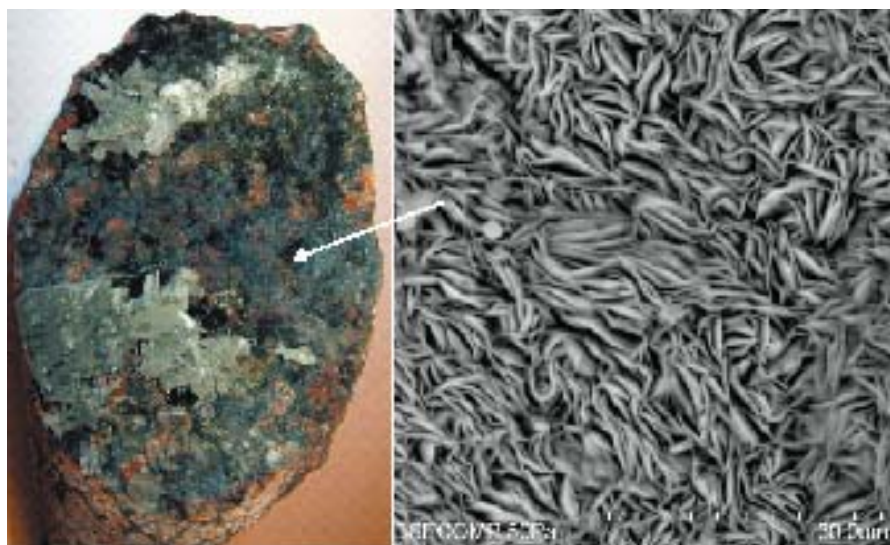


Figure 5-43. Typical example of corrensite coating (arrow) in open fracture from Laxemar. Right figure is a back-scattered electron image from Drake and Tullborg, in manuscript.

present as micrograins in secondary K-feldspar and albite in plagioclase pseudomorphs giving the red colour. However, there is not always a perfect correspondence between the extent of hydrothermal alteration and red staining. The red-staining is mainly found adjacent to early formed fractures filled with fillings of generation 1–4 (preferentially prehnite), and possibly generation 5.

Within the fractures several generations of hematite and pyrite are present. The findings of small pyrite grains in the outermost layers of the fracture coatings are in agreement with the present reducing groundwater chemistry /Laaksoharju et al. 2006/.

It has so far, not been possible to link different fracture minerals to different fracture orientations. This has previously also been proven difficult within the large data set from Äspö HRL /Munier 1993/ and /Mazurek et al. 1997/.

The sequence of minerals, going from greenschist (epidote) facies in combination with ductile deformation, to brittle deformation during prehnite facies and subsequent zeolite facies and further decreasing formation temperature series, indicates that the fractures were initiated relatively early in the geological history of the host rock and has been reactivated during several different periods of various physiochemical conditions.

Resulting single hole geological interpretation

The single-hole geological interpretation (SHI) provides a synthesis of all geological and geophysical data from a borehole. It forms an important link between all the detailed borehole data that are generated and the subsequent geological modelling work. It therefore has a similar role as the bedrock map that forms an important intermediate step between the detailed outcrop data generated during the bedrock mapping and the site descriptive modelling work. The SHI aims to document rock units with a minimum length of 5 m along the borehole as well as all deformation zones that intersect the borehole. Note that these geological features are unique for each borehole, i.e. rock unit 1 (RU1) in one borehole may not correspond to RU1 in another borehole. Correlation of the geological data from the SHI and the surface forms an important step in the 3D modelling work.

The following data have been used in all SHI:

- Geological mapping data using BIPS and the Boremap system.
- Borehole radar data and their interpretation.
- Geophysical logs and their interpretation.

Short descriptions of the interpreted rock units and deformation zones for the cored boreholes KSH01A/B, KSH02, KSH03A/B and KLX02, and the percussion boreholes HSH01, HSH02, HSH03, HAV09 and HAV10 are provided in /Mattsson et al. 2004ab, Hultgren et al. 2004/. The SHI of the cored boreholes KAV04A/B, KLX01 and KLX04, and the percussion boreholes HLX15, HLX21, HLX22, HLX23, HLX24 and HLX25 have also been utilised in the modelling although the P-reports presenting the results were not available at the time of the analysis. Sealed fractures are distinguished from open and partly open in the fracture orientation plots.

The confidence in the interpretation of the rock units and deformation zones has been assessed using the following encoding: 3=certain, 2=probable, 1=possible.

Rock units

Ävrö granite is the dominant rock type in the majority of the defined rock units in the different boreholes. However, although the Ävrö granite may constitute the dominant rock type, different rock units can be defined based on the amount and type of subordinate rock types in the borehole section (Figure 5-44). With the exception of the Ävrö granite, quartz monzodiorite is the only rock type that dominates larger sections in the boreholes. Certain rock units do not have rock types that are obviously dominant, but comprise a more or less complete mixture of two or more different rock types, for instance in the section 540–960 m in KLX02.

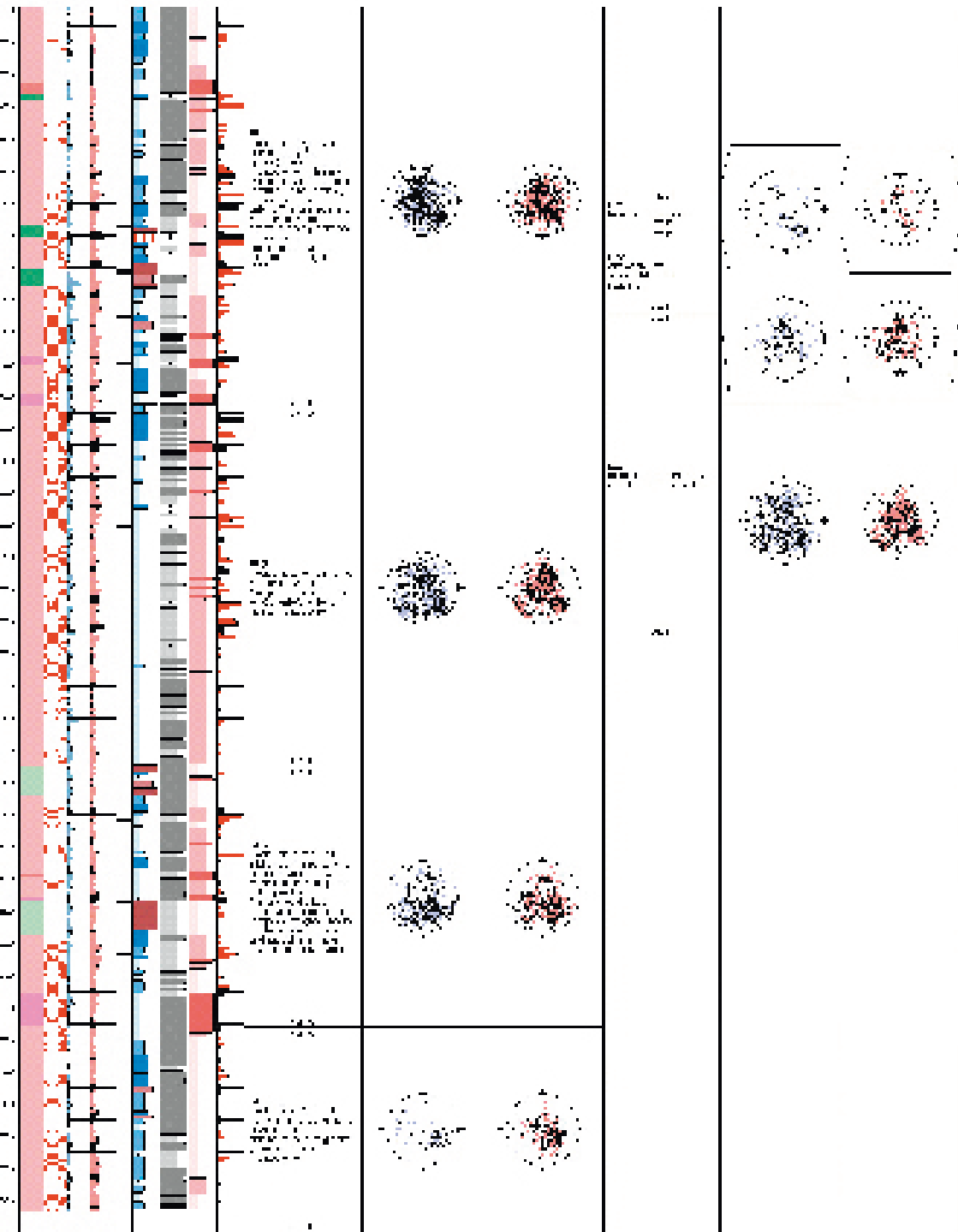


Figure 5-44. Single-hole geological interpretation of KAV01. Example of different rock units in which the Ävrö granite dominates, but the amount and type of subordinate rock types differ.

Deformation zones

The majority of the possible deformation zones identified in the SHI are brittle in character. These zones have been recognised primarily on the basis of the frequency of fractures (see Section 5.2.7), according to the recommendations in /Munier et al. 2003/. Both the transition zone and the core of the zone, if developed, have been included in the delineation of each interpreted zone (Figure 5-45). The presence of bedrock alteration, the occurrence of an inferred orientation of radar reflectors, resistivity, SPR, P-wave velocity, caliper and magnetic susceptibility logs have also played a significant role in the interpretation of the characteristics of the zones.

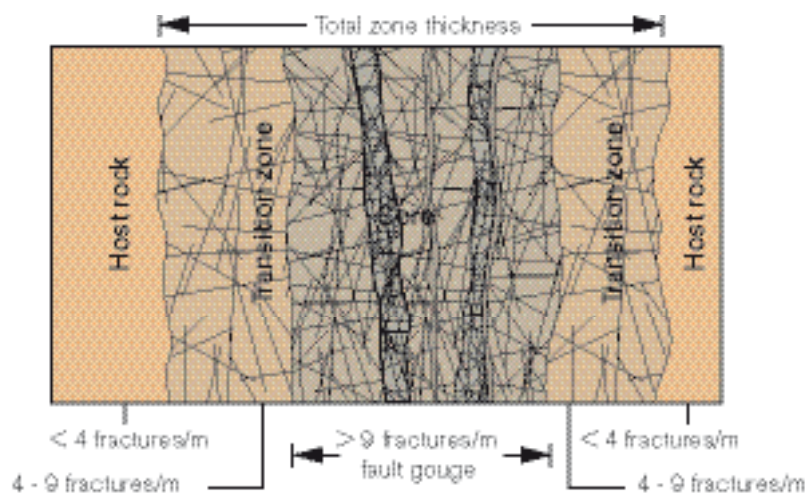


Figure 5-45. Terminology for characterisation of brittle deformation zones (modified after /Munier et al. 2003/).

Some deformation zones, or parts thereof, are characterised by ductile deformation under low-grade metamorphic conditions, as evidenced by protomylonitic to mylonitic or phyllonitic foliation. Purely ductile deformation zones are relatively thin, commonly a decimetre to a couple of metres in thickness, e.g. as seen in borehole KSH01A. Most of the thicker deformation zones are characterised by brittle deformation. However, a mixture of ductile and overprinting dominating brittle deformation is not uncommon, exemplified by the deformation zones between 162 and 275 m in KSH03A and 722.5 and 814 m in KLX03, cf. Appendix 4. This indicates the importance of reactivation of the zones, by one or several phases of brittle deformation, which is characteristic for virtually all identified deformation zones.

Simplified composite logs

Components of the SHI interpretation of the cored boreholes from the Laxemar and Simpevarp subareas have been combined with data and logs from other disciplines. The simplified composite logs are presented in Appendix 4.

5.3 Rock domain model

This section is a condensed description of the construction of the three-dimensional local scale and regional scale rock domain models for the Laxemar SDM 1.2, as presented by /Wahlgren et al. 2005b/. The Simpevarp 1.2 site descriptive rock domain model forms the basis for present modelling, which comprises the entire regional model domain.

5.3.1 Basis for modelling

The terms rock units and rock domains are used according to the terminological guidelines for geological site descriptive modelling given in /Munier et al. 2003/. Rock units are defined on the basis of the mineralogical composition, grain size, texture, structure and age of the dominant rock type, whereas rock domains are defined by integration of rock units taking into account these geological criteria. In addition, a complex and intimate mixing of rock units has also been used as a criterion in the definition of rock domains.

The construction of the rock domain model in the local scale model area is principally based on existing bedrock data from the surface, and information from available cored boreholes. In addition, modelling of gravity and magnetic data /Triumpf 2004b/ has also been used as important support for the geometric relationships between rock domains in the local scale model domain. Furthermore, modelling of gravity and magnetic data has been used for the geometrical modelling of the Göttemar and Uthammar granites /Nisca 1987, Triumpf et al. 2003, Triumpf 2004b/.

The following list is a summary of important data that have been utilised in the Laxemar 1.2 rock domain modelling:

- SDM Simpevarp version 1.2 /SKB 2005a/.
- Combined bedrock map of the Simpevarp and Laxemar subareas (1:10,000), including outcrop databases.
- Bedrock map version 0 (1:100,000).
- Boremap data and SHI for the cored boreholes KSH01A/B, KSH02, KSH03A/B, KAV01, KAV04A/B, KLX01, KLX02, KLX03, KLX04A/B and preliminary/simplified mapping of KLX05 and KLX06.
- Modal and geochemical analyses.
- Petrophysical rock parameters.
- In situ gamma-ray spectrometric data (surface measurements).
- Reflection seismic data.
- Geophysical modelling based on gravimetric and magnetic data.

Apart from the cored boreholes, information from a number of percussion boreholes (see Table 2-1 and Figure 2-3) in the local scale model area has been considered. However, due to the somewhat more uncertain recognition of rock types (lack of drill core) and the limited depth to which these boreholes were drilled, they were considered to be of less importance for the rock domain modelling.

5.3.2 Division into rock domains at the surface and in cored boreholes

Based on the Simpevarp 1.2 modelling, the following working stages have been followed during the Laxemar 1.2 rock domain modelling:

- Integration of the new combined bedrock map of the Laxemar and Simpevarp subareas with the bedrock map used in the version 0 report /SKB 2002b/, as well as the Simpevarp 1.2 2D rock domain model /SKB 2005a/.
- Definition of the areal extents of rock domains at the surface.
- Definition of rock domains in the cored boreholes.

Division of rock domains at the surface

This first stage in the modelling procedure includes identification of rock domains at the surface that involves a simplification of the bedrock map, this in order to enable correlation of data at the surface with that at depth in the modelling volume.

The simplification and integration procedures applied to the surface data have yielded a rock domain map that comprise 33 rock domains in the regional scale model area (Figure 5-46), 14 of which occur in the local scale model area (Figure 5-47 and Figure 5-48). Note the higher resolution in the local scale model area than in the remaining part of the model area.

The rock domains have been given different codes where domains denominated with the same capital letter are dominated by the same characteristics as displayed below:

- **RSMA**-domains: dominated by Ävrö granite.
- **RSMB**-domains: dominated by fine-grained dioritoid.
- **RSMB**A-domains: characterised by a mixture of Ävrö granite and fine-grained dioritoid.
- **RSMC**-domains: characterised by a mixture of Ävrö granite and quartz monzodiorite.
- **RSMD**-domains: dominated by quartz monzodiorite.
- **RSME**-domains: dominated by diorite to gabbro.

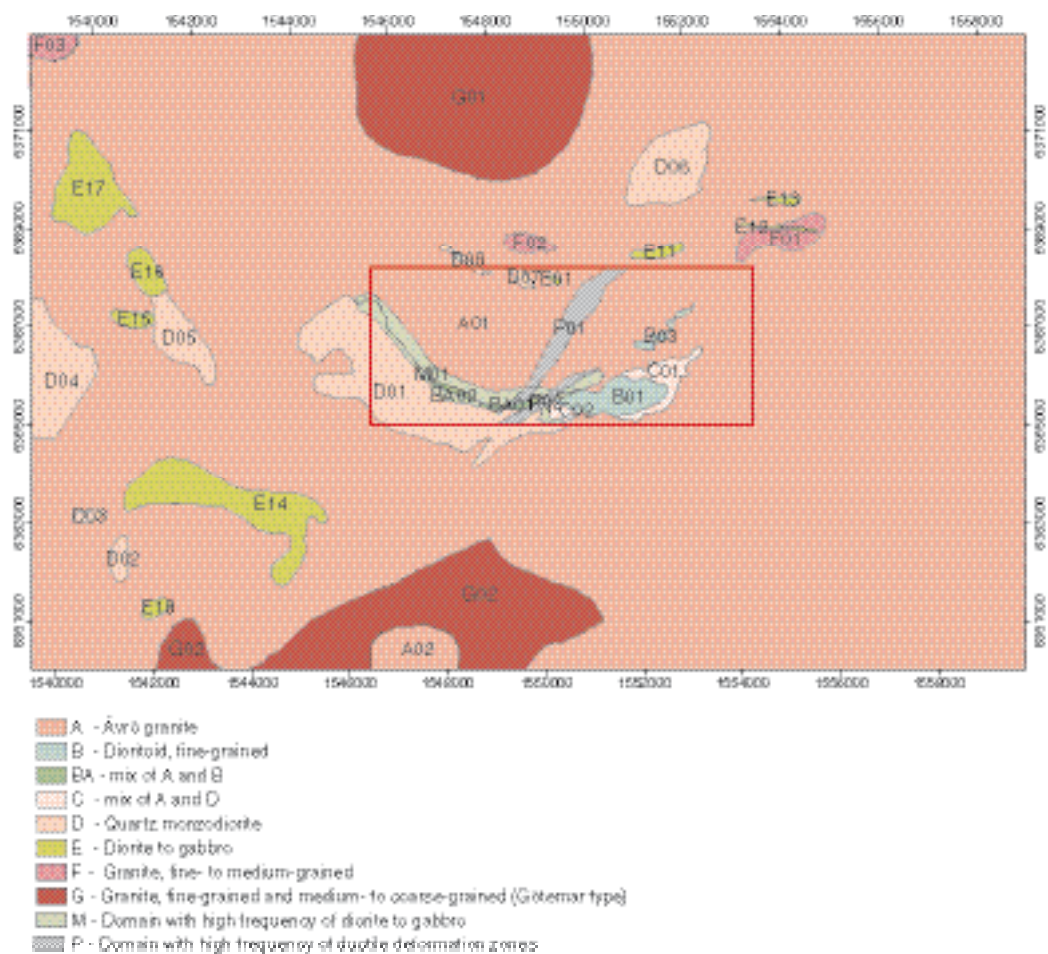


Figure 5-46. Surface view of the rock domains used in the regional model area ($N=33$), including the rock domains in the local scale model area. For reasons of simplicity the prefix RSM has been excluded from the map. Note that the legend only indicates the main characteristic for the rock domain.

- RSMF-domains: dominated by fine- to medium-grained granite.
- RSMG-domains: dominated by the Götömar type granite.
- RSMM-domains: characterised by a high frequency of minor bodies to small enclaves of diorite to gabbro in particularly Ävrö granite and quartz monzodiorite.
- RSMP-domains: characterised by a high frequency of low-grade ductile shear zones in the above mentioned rock types.

Rock domains of the same character that are physically separated are given different numbers, e.g. RSMC01 and RSMC02.

As can be seen in Figure 5-48, a number of domains overlap the boundaries of surrounding rock domains. This implies that the rock domains are in fact nested and partly inherit properties from the underlying domains (see Figure 5-48). The division of the RSMM01 domain into RSMM01a–d is caused by the cross-cutting RSMP01 and RSMP02 domains (see Figure 5-48). The black line in the western part of the RSMM01 domain (RSMM01a; Figure 5-47) marks the boundary between the Ävrö granite, M(A), in the northern to northeastern part and the quartz monzodiorite, M(D), in the southern to southwestern part (cf. Figure 5-47). Furthermore, this black line is used as a guide for modelling the boundary between Ävrö granite in the RSMA01 domain and the quartz monzodiorite in the RSMD01 domain in 3D, cf. Section 5.3. The black line in the RSMM01c domain marks the boundary between the Ävrö granite in the north and the fine-grained dioritoid (cf. Figure 5-47 and Figure 5-48).

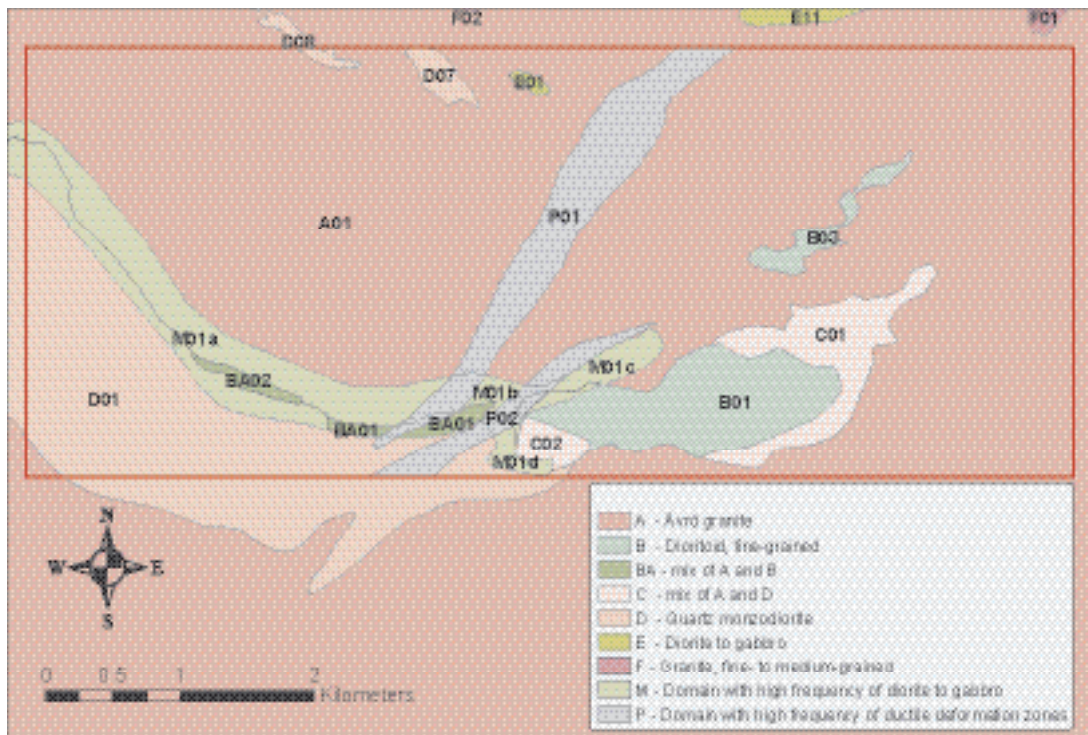


Figure 5-47. Surface view of the rock domains used in the local scale model area in the modelling procedure (N=14). For reasons of simplicity the prefix RSM has been excluded from the map. Note that the legend only indicates the main characteristic for the rock domain.

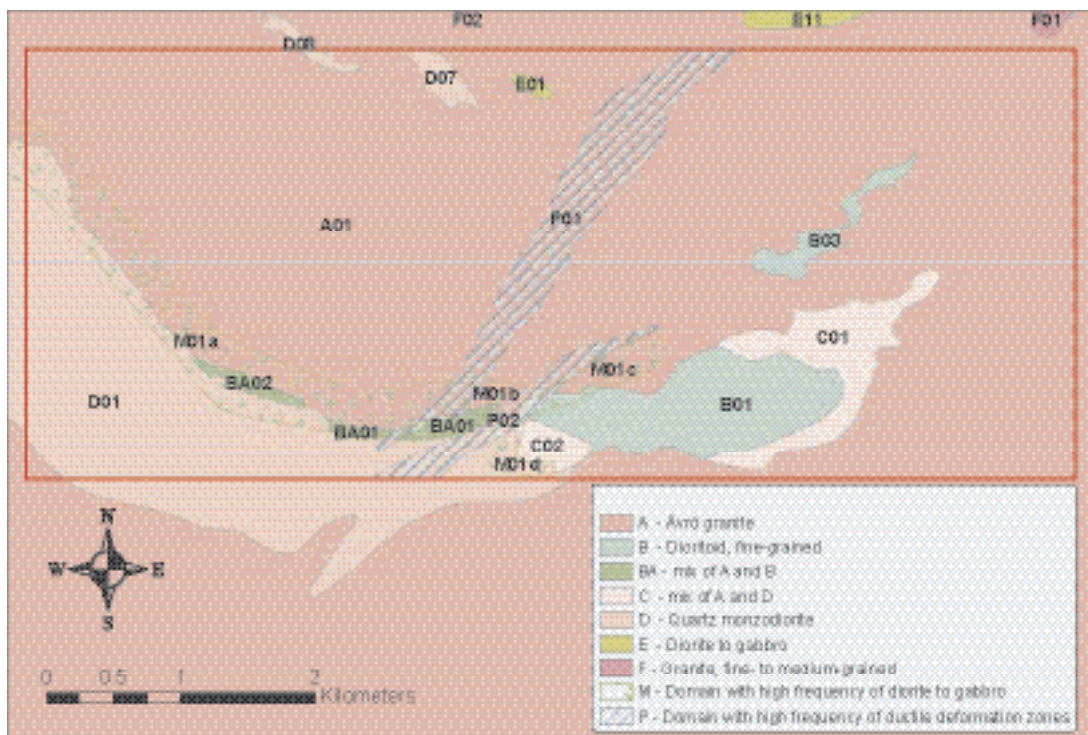


Figure 5-48. Surface view of the rock domains used in the local scale model area in the modelling procedure (N=14). The overlapping character of RSM and RSMP domains are displayed by transparent raster. For reasons of simplicity the prefix RSM has been excluded from the map. Note that the legend only indicates the main characteristic for the rock domain.

Definition of rock domains in cored boreholes

Rock domains have been defined in the cored boreholes, based on the Boremap mapping and single-hole interpretation, as well as preliminary mapping of the drill core from KLX05 and KLX06 (Table 5-2). The boundaries between the rock domains coincide with those reported in the SHI except for KLX05 and KLX06 since no SHI existed for these boreholes at the time of the data freeze.

Table 5-2. Definition of rock domains in cored boreholes. Entries in Sicada are rounded off to even metres.

Borehole	Sec up – Sec low (m)	Rock domain
KSH01A	100–322	RSMC01
KSH01A	322–631	RSMB01
KSH01A	631–1,001	RSMC01
KSH02	80–1,007	RSMB01
KSH03A	100–270	RSMC01
KSH03A	270–1,000	RSMA01
KAV01	20–750	RSMA01
KAV04A	101–289	RSMA01
KAV04A	289–690	RSMC01
KAV04A	690–1,003	RSMA01
KLX01	1–1,078	RSMA01
KLX02	200–540	RSMA01
KLX02	540–960	RSMB03
KLX02	960–1,450	RSMA01
KLX02	1,450–1,700	RSMD01
KLX03	101–798	RSMM01
KLX03	798–998	RSMD01
KLX04	101–991	RSMA01
KLX05 (Preliminary mapping)	100–400	RSMM01
KLX05 (Preliminary mapping)	400–465	RSMB01
KLX05 (Preliminary mapping)	465–649 (1,000)	RSMD01
KLX06 (Preliminary mapping)	100–995	RSMA01

5.3.3 Construction of the 3D rock domain model

The bedrock of both the local and regional model volumes employed for the Laxemar 1.2 rock domain model is dominated by more or less pristine igneous rocks. Hence, there are, with some exceptions, no ductile structural frameworks that can be adopted as guides for the three-dimensional geometric modelling of the domains (cf. the rock domain modelling in the Forsmark area /SKB 2005b/). The measured anisotropy of magnetic susceptibility indicates that the degree of anisotropy is only low to moderate (see Section 5.2.5). Thus, this anisotropy has not been considered an important guide in the construction of the geometry of the rock domains. However, the importance of the ductile structures for the geometric modelling will be more fully evaluated in future modelling work. Consequently, no real modelling concept has been applied in the downward projection of the rock domains defined at the surface. Accordingly, the shapes of the rock domains are mainly determined by the defined rock domain boundaries at the surface and as interpreted in the cored boreholes, cf. Table 5-2.

Arc geometry

The bedrock map of the Laxemar and Simpevarp subareas (Appendix 3) clearly demonstrates that the dominant rock types (except for the Ävrö granite) that form the matrix in the local scale model volume, are elongated and that the boundaries change orientation from northwest-southeast in the Laxemar subarea to northeast-southwest in the Simpevarp subarea. Consequently, the rock domains define an arc-shaped trend with its concave side towards the north (Figure 5-47).

Modelling of both gravity and magnetic data suggests that the whole arc-shaped complex is dipping to the north or northwest in the Laxemar subarea /Triumpf 2004b/. This is confirmed by the definitions of the rock domains RSMA01 and RSMD01 in the cored boreholes KLX02, KLX03, and KLX05. The intervening rock domain RSMM01 is not that well-defined in the boreholes. However, from the bedrock map, the concentration of diorite to gabbro along the contact between the Ävrö granite in the rock domain RSMA01 and quartz monzodiorite in the rock domain RSMD01 is evident. In conclusion, there are strong indications that the general extension at depth of the boundaries between the major rock domains RSMA01, RSMD01 and RSMM01 is to the north. The geometry in the 3D modelling is primarily based on the domain defined intercepts in the cored boreholes, but the modelled geometry is also strongly supported by the geophysical modelling, although the latter indicates a more shallow extension at depth than that obtained from the defined domain boundaries in the cored boreholes.

In absence of reliable information, the southern boundary of the rock domain RSMD01 is modelled vertically down to the bottom boundary of both the local and the regional model volumes.

Lens geometry

The lens geometry concept implies that the dioritoid dominated domains (RSMB and RSMBA) within the arc-shaped complex, have the shape of subvertical lenses oriented along the transitions between the above mentioned arc-shaped major rock domains. Apart from being visually appealing, this finding is supported by a number of borehole observations. For example, the segment between 322 and 631 m in the cored borehole KSH01, that is defined as part of RSMB01 (see Table 5-2), indicates an extension of the domain at depth that could be explained by the domain being lens-shaped with its centre located below ground surface. Apart from being lens-shaped, it is anticipated that these domains follow the same trend at depth as the surrounding major rock domains.

5.3.4 The 3D rock domain model

Most of the rock domains in the regional model volume have not been modified compared with model version Simpevarp 1.2. The exception is the geometries of the Götemar and Uthammar granites (RSMG01 and RSMG02), due to an updated geophysical modelling /Triumpf 2004b/. Furthermore, some domains in the immediate surroundings of the local model area have been modified, since new surface data have been made available from the detailed bedrock map. However, the new detailed bedrock map of the Laxemar subarea and surroundings, and additional information from new cored boreholes, have resulted in considerable modifications of the local scale rock domain model presented in SDM Simpevarp 1.2. The three-dimensional rock domain model of the regional model domain, with the local scale model domain inserted, is displayed in Figure 5-49.

34 principal rock domains have been identified in the regional model volume, 15 of which make up the local scale model volume. Note that the rock domain RSMBA03 only occurs at depth. However, in modelling terms the nesting of domains (see above) implies that, for example the RSMD01 domain is divided into 8 blocks. One block is pure RSMD01 whereas three blocks lie within the RSMM01 domain and 4 blocks within the RSMP01 and RSMP02 domains.

5.3.5 Property assignment

Each rock domain has been assigned a set of properties (Table 5-3), including, for example, the dominant and subordinate rock types in the domain. All property tables are presented in Appendix 5.

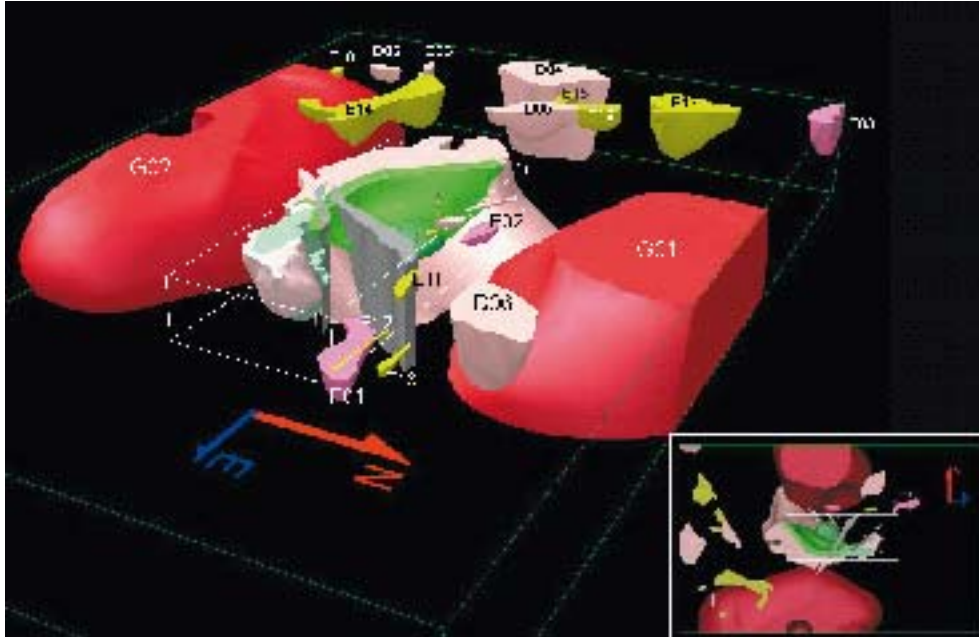


Figure 5-49. Regional rock domain model with the local scale model domain inserted. The Ävrö granite (RSM01) is transparent. View from the northeast.

For the rock domains situated within the Laxemar and Simpevarp subareas, the properties of the rock domains have been extracted from the outcrop databases and complementary mineralogical, geochemical and petrophysical data (see Section 5.2.2). Additional information is available in the data from the Boremap mapping as well as preliminary mapping of the cored boreholes. Only limited information is available for rock domains or those parts of rock domains that are situated outside the Laxemar and Simpevarp subareas.

Table 5-3. Properties assigned to each rock domain.

Rock domain ID (RSM***, according to the nomenclature recommended by SKB)
Property
Dominant rock type
Mineralogical composition
Grain size
Age (million years)
Structure
Texture
Density
Porosity
Magnetic susceptibility (SI units)
Electrical resistivity in fresh water (ohm m)
Uranium content based on gamma ray spectrometric data (ppm)
Natural exposure ($\mu\text{R/h}$)
Subordinate rock types
Degree of inhomogeneity
Metamorphism/alteration (%)
Mineral fabric (type/orientation)

Important properties for the construction of rock domains are composition, grain size and texture of the different rock types. In addition, structure, i.e. protomylonitic to mylonitic foliation and ductile shear zones, is of vital importance for the characterisation of the RSMP domains, see preceding section.

By using the information in the outcrop database from the bedrock mapping of the Laxemar subarea, it is possible to estimate qualitatively the relative amounts of the different rock types in each domain. For similar qualitative estimates for the Simpevarp subarea, see the Simpevarp SDM 1.2 /SKB 2005a/. For example, in rock domain RSMA01, the lithology that forms the dominant rock type is Ävrö granite, i.e. medium-grained, porphyritic granite to quartz monzodiorite (Figure 5-50). However, fine- to medium-grained granite, medium- to coarse-grained granite, pegmatite, fine-grained dioritoid, diorite to gabbro, fine-grained diorite to gabbro and quartz monzodiorite form subordinate rock types (Figure 5-50). Similar semi-quantitative information concerning the proportions of dominant and subordinate rock types in most of the remaining rock domains within the Laxemar subarea is presented in /Wahlgren et al. 2005b/.

Based on the mapping of rock types in the cored boreholes, an estimate of the proportions of different rock types in the rock domains has been performed by quantifying the total occurrence in terms of borehole length in metres and the percentage of the total length of the core for the different rock types. This is exemplified by rock domain RSMA01 in the Laxemar subarea in Figure 5-51. For further information about proportion of rock types in rock domains, see /Wahlgren et al. 2005b/.

Another property of the bedrock that is of importance and has great implications, in particular for the thermal modelling (cf. Section 7.3), is the compositional variation of the rock types, particularly the Ävrö granite (see Section 5.2.3). In Figure 5-52, the variation in quartz content in the quartz monzodiorite and the Ävrö granite in different domains is displayed. As can be seen, the quartz content is generally low and the variation between the domains is obvious. This has implications for the thermal conductivity and thereby thermal properties modelling (cf. Section 7.3).

Another factor of inhomogeneity that has to be considered is inhomogeneously distributed hydro-thermal alteration, e.g. red staining but also saussuritisation. An estimate for rock domain RSMA01 in the Laxemar subarea, excluding the interpreted deformation zones, by using Boremap data is displayed in Figure 5-53. As can be seen the alteration is generally non-existing to weak in character.

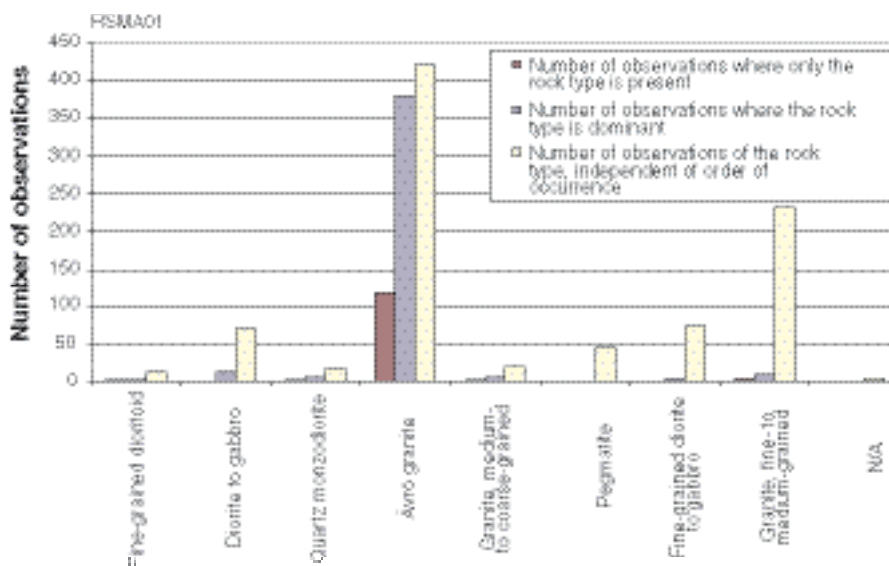


Figure 5-50. Qualitative assessment of dominant and subordinate rock types in rock domain RSMA01 (Ävrö granite) based on surface outcrop data from the bedrock mapping of the Laxemar subarea. Note that in the outcrop database, rocks are stored in relation to their order of occurrence at the observation point,

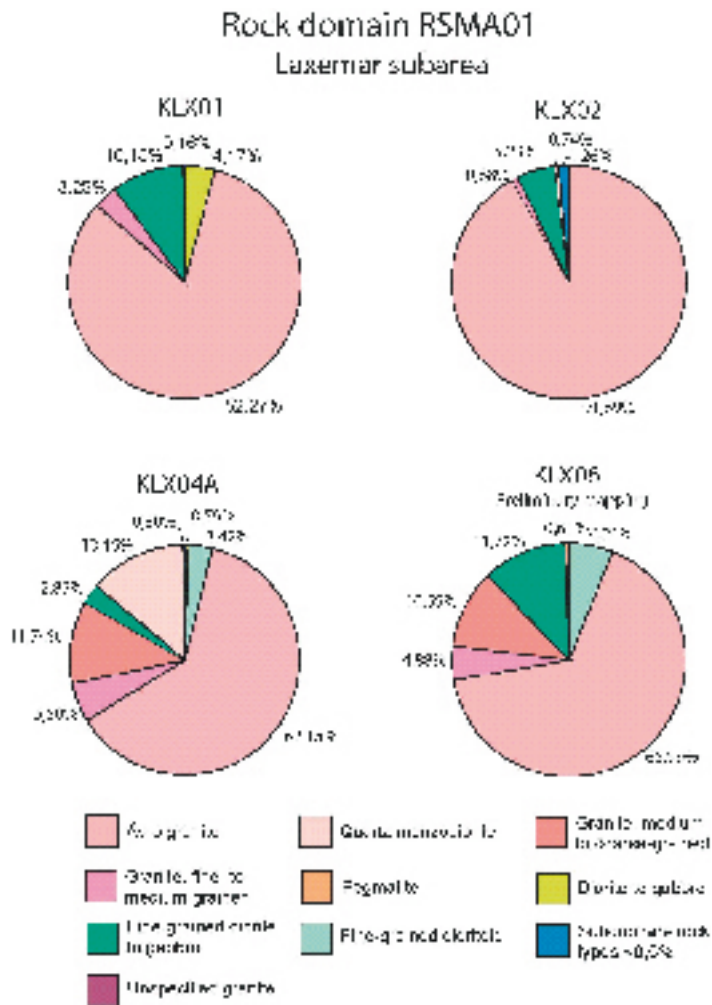


Figure 5-51. The proportion of different rock types in the rock domain RSMA01 in the Laxemar subarea, as interpreted in the cored boreholes KLX01, KLX02, KLX04 and KLX06.

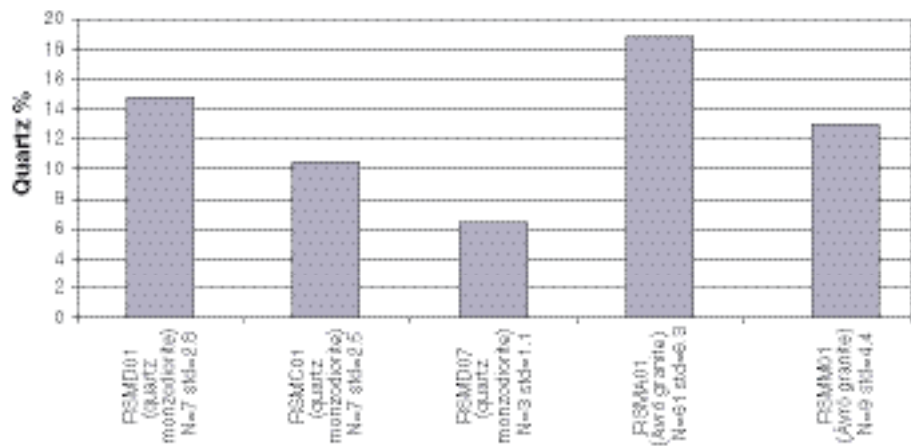


Figure 5-52. Quartz content (mean value) in quartz monzodiorite in RSMD01, RSMC01 and RSMD07, and in Ävrö granite in RSMA01 and RSMM01.

RSMA01 - alteration (mainly oxidation)
I axerrar subarea

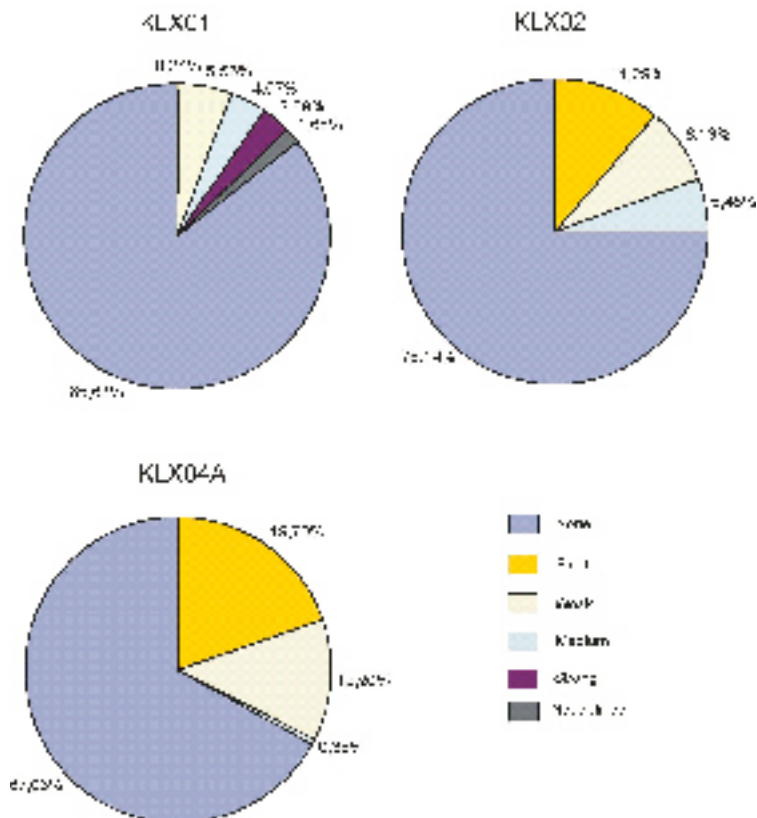


Figure 5-53. Estimate of alteration (mainly oxidation) in rock domain RSMA01, based on length of altered sections in the cored boreholes KLX01, KLX02 and KLX04A.

Ore potential

The Simpevarp regional model area may be considered as sterile with regard to ores and metallic mineralisations. Furthermore, there is no potential for industrial minerals. For a comprehensive description of the ore potential in the Simpevarp regional model area, see /Lindroos 2004/.

5.3.6 Evaluation of uncertainties

The uncertainties in the surface geological data in the regional model area are obvious since, 1) only a provisional bedrock map exist and, 2) there is almost a complete lack of subsurface information. Since all investigations during the complete site investigation will be focused to the local scale model area, these uncertainties will remain throughout the site investigation.

As there is a limited amount of subsurface data, there remain considerable uncertainties concerning the extension of the domains at depth apart from the following rock domains:

- The dominating rock domain RSMA01 (Ävrö granite), which constitutes the “matrix” of the rock domain model.
- The rock domain RSMB01 (fine-grained dioritoid) that has been verified between c. 320 and 630 m along the cored borehole KSH01A, and to a depth of 1,000 m in the cored borehole KSH02.

- The rock domain RSMC01 (mixture of Ävrö granite and quartz monzodiorite), which has been verified to a depth of 1,000 m in the cored borehole KSH01A, to a borehole length of c. 270 m in the cored borehole KSH03A and between 290 and 690 m in the cored borehole KAV04A.
- The rock domain RSMD01 (quartz monzodiorite) which is documented between c. 1,450 and 1,700 m in the cored borehole KLX02, between c. 800 and 1,000 m in the cored borehole KLX03 and between c. 465 and 1,000 m in the cored borehole KLX05A (preliminary mapping).
- The rock domains RSMP01 and RSMP02 which are based on consistent structural data and magnetic anomalies.

Even though rock domains, including the ones mentioned above, have been verified to a certain depth, the geometrical relationships in detail between most rock domains are considered uncertain. This problem will presumably persist throughout the site investigation programme for most of the rock domains, especially in the regional model area. The geometrical relationships between rock domains RSMP01 and RSMP02 and the surrounding rock domains are judged to be well constrained due to the consistency in the orientation of the mylonitic to protomylonitic foliation on which these domains are based. Furthermore, the general geometrical relationship between the two dominating rock domains RSMA01 and RSMD01, and the intervening RSMM01 rock domain in the Laxemar subarea is judged to be fairly well constrained. Thus, the uncertainty in the geometrical relationships between the rock domains primarily relates to the Simpevarp subarea and the remaining part of the regional model area.

A qualitative assessment of the confidence for the existence and geometry of interpreted rock domains is displayed in Table 5-4.

An important uncertainty is the insufficient information on the character of the inhomogeneity of the rock domains. In particular, this relates to the frequency and spatial distribution of subordinate rock types. The estimates of the proportion of subordinate rocks presented above indicate that the local variation may be high. This relates particularly to how much of a specific rock domain is occupied by subordinate rock types and, furthermore, are the subordinate rock types homogeneously distributed, or do they cluster in specific parts of the domain.

An uncertainty that is connected to the thermal modelling (see Chapter 7) is the spatial distribution of the compositional varieties of the Ävrö granite. In the forthcoming modelling work when more data from cored boreholes become available, the possibility to divide the RSMA01 domain into a quartz monzodioritic and a granitic to granodioritic variety will be evaluated. Another factor of uncertainty that is of importance for the thermal properties and thermal modelling is the degree and spatial distribution of hydrothermal alteration of the bedrock (see Chapter 7).

Table 5-4. Table of confidence for the existence and uncertainty in geometry of interpreted rock domains in the regional and local scale model volume employed for the Laxemar 1.2 site descriptive model.

Domain ID	Basis for interpretation	Confidence of existence at the surface	Confidence of existence at depth	Uncertainty of geometry at the surface	Uncertainty of geometry at depth	Comment
RSMA01	Bedrock geological map of the Simpevarp and Laxemar subareas and version 0 in the remaining area, KSH03A, KAV01, KAV04 A/B, KLX01, KLX02, KLX04, HAV09, HAV10, HLX21, HLX22, HLX23, HLX24, HLX25	High	High	Low	Medium	The uncertainty of geometry at both the surface and at depth is higher in the regional model area due lack of detailed information
RSMA02	Bedrock geological map, version 0	Medium	Medium	High	High	
RSMB01	Bedrock geological map the Simpevarp and Laxemar subareas, KSH01A, KSH02, HSH02	High	High	Low	Medium	
RSMB03	Bedrock geological map of the Simpevarp and Laxemar subareas	High	High	Low	High	

Domain ID	Basis for interpretation	Confidence of existence at the surface	Confidence of existence at depth	Uncertainty of geometry at the surface	Uncertainty of geometry at depth	Comment
RSMB01 (a-b)	Bedrock geological map of the Simpevarp and Laxemar subareas and KLX05 (preliminary mapping)	High	High	Medium	Medium	
RSMB02	Bedrock geological map of the Simpevarp and Laxemar subareas	High	High	Medium	Medium	
RSMB03	KLX02	–	High	–	Medium	This domain only occurs at depth
RSMC01	Bedrock geological map of the Simpevarp and Laxemar subareas, KSH01A, KSH01B, KSH03A, KSH03B, KAV04A, HSH01, HSH03	High	High	Low	Medium	
RSMC02	Bedrock geological map of the Simpevarp and Laxemar subareas	High	High	Medium	Medium	
RSMD01 (a–b)	Bedrock geological map of the Simpevarp and Laxemar subareas, KLX02, KLX03 and KLX05 (preliminary mapping), HLX15, HLX26, HLX28	High	High	Low	Medium	
RSMD02	Bedrock geological map, version 0	Medium	Medium	High	High	
RSMD03	Bedrock geological map, version 0	Medium	Medium	High	High	
RSMD04	Bedrock geological map, version 0	Medium	Medium	High	High	
RSMD05	Bedrock geological map, version 0	Medium	Medium	High	High	
RSMD06	Bedrock geological map, version 0	Medium	Medium	High	High	
RSMD07	Bedrock geological map of the Simpevarp and Laxemar subareas	High	High	Low	Medium	
RSMD08	Bedrock geological map of the Simpevarp and Laxemar subareas	High	High	Low	Medium	
RSME01	Bedrock geological map of the Simpevarp and Laxemar subareas	High	High	Low	Medium	
RSME11	Bedrock geological map, version 0	High	High	Medium	High	
RSME12	Bedrock geological map, version 0	High	High	Medium	High	
RSME13	Bedrock geological map, version 0	High	High	Medium	High	
RSME14	Bedrock geological map, version 0	High	High	Medium	High	
RSME15	Bedrock geological map, version 0	High	High	Medium	High	
RSME16	Bedrock geological map, version 0	High	High	Medium	High	
RSME17	Bedrock geological map, version 0	High	High	Medium	High	
RSME18	Bedrock geological map, version 0	High	High	Medium	High	
RSMF01	Bedrock geological map, version 0	High	High	Medium	High	
RSMF02	Bedrock geological map of the Simpevarp and Laxemar subareas	High	High	Low	Medium	
RSMF03	Bedrock geological map, version 0	High	High	Medium	High	
RSMG01	Bedrock geological map, version 0	High	High	Low	Medium	
RSMG02	Bedrock geological map, version 0	High	High	Low	Medium	
RSMM01 (a-d)	Bedrock geological map of the Simpevarp and Laxemar subareas, KLX03, KLX05 (preliminary mapping)	High	High	Low	Medium	
RSMP01	Bedrock geological map of the Simpevarp and Laxemar subareas, magnetic anomaly map, KAS04, KA1755A	High	High	Low	Low	
RSMP02	Bedrock geological map of the Simpevarp and Laxemar subareas, magnetic anomaly map	High	High	Low	Low	

5.4 Deterministic deformation zone modelling

5.4.1 Modelling assumptions and input from other disciplines

A set of fundamental assumptions underlying the deformation zone model are made.

It is assumed that:

- Deformation zones can be interpreted through both indirect sources of data such as geophysical maps (magnetics, VLF, slingram, gravimetric), topography, seismic reflections and refractions.
- Lineaments can provide the necessary detailed information about the location and extent at the surface of possible deformation zones.
- Deformation zones can further be interpreted through direct data in boreholes, tunnels and from surface field observations. The certitude in geological character and possible extent (length and thickness) of deformation zones inferred from indirect data sources is lower than for zones identified from direct observations.
- Different sources of data can complement each other and increase the confidence in the interpreted deformation zone. Several types of observations, both indirect and direct, also increase the degree of detail in which the zone can be described.
- Interpreted deformation zones can be interpolated between points of observation, if there are reasonable data to suggest the validity of such interpolation.
- Deformation zones are variable in their thickness and can be modeled honouring the inferred thickness, cf. Figure 5-45, or can be modelled as surfaces without thickness if no relevant data exist.
- Within the limits of the regional, or local model volumes, deformation zones interpreted at the ground surface can be extended toward depth with a depth extent equal to the interpreted length of the mapped surface trace. This means, for example, that deformation zones longer than 1 km at the surface are extended to the bottom of the local model volume (1,100 m).
- Each interpreted deformation zone has been ranked according to the confidence of its existence being high, medium or low. Zones that have high confidence ratings have, in addition to lineament indications, also supportive information from other sources of indirect data such as geophysics *and* from sources of direct data, such as boreholes or tunnels.
- Deformation zones ranked with medium confidence show clear topographic, magnetic and/or surface geophysical anomalies which cannot be disregarded as being other linear structures in the landscape, such as Quaternary deposits, ditches, power lines, roads, forest fire lanes, or other man-made constructions.
- Interpreted zones with assigned low confidence are only supported by indirect sources of information such as lineament indications of lesser strength, either from topography, magnetics or electromagnetic methods.

The local scale model of deformation zones has made use of:

- the deformation zone model presented in Simpevarp 1.2 site descriptive model /SKB 2005a/,
- the interpretation of lineaments completed during the ongoing site investigation programme (see Section 5.2.5),
- the regional structural model presented in version 0 of the site descriptive model /SKB 2002b/,
- the structural model of Äspö HRL (Äspö 96 model), /Rhén et al. 1997c/,
- GEOMOD structural model (updated structural model of the Äspö HRL) /Berglund et al. 2003/,
- Ävrö RVS model /Markström et al. 2001/,
- measurements of mainly ductile structures, as well as some brittle structures and bedrock contacts at 91 of the 353 observation points documented during the bedrock mapping carried out in the Simpevarp subarea during 2003 /Wahlgren et al. 2004/,

- measurements of mainly ductile structures, as well as some brittle structures and bedrock contacts deduced from the bedrock mapping carried out in the Laxemar subarea during 2004 /Persson Nilsson et al. 2004/,
- a variety of old structural geological data covering the Simpevarp peninsula and the islands of Hålö and Ävrö, as compiled by /Curtis et al. 2003ab/,
- data from cored boreholes KLX02 (200–1,006 m), KLX03, KLX04A/B, KSH01A/B, KSH02, KSH03A/B, KAV01 and KAV04A/B, cf. Figure 2-3,
- data from percussion boreholes HLX13, HLX15, HLX21–28, cf. Figure 2-3,
- seismic reflection data compiled in conjunction with the ongoing site investigation programme (see Section 5.2.8).

The lineament map used in the Simpevarp 1.2 modelling /SKB 2005a/ has been updated and forms the basis for the surface interpretation of deformation zones (see Section 5.2.5). Interpretations that are related to the new lineament map are always preferred, unless there is other additional supporting information from geophysics, boreholes or tunnels.

The Laxemar 1.2 deformation zone model addresses deformation zones in the regional and local model areas on the same basis to that employed for Simpevarp version 1.2 model /SKB 2005a/. The local scale model contains deformation zones that are inferred to be of length 1 km or longer, i.e. local major and regional deformation zones according to the terminology of /Andersson et al. 2000a/.

The surface data coverage has a lower resolution in the larger parts of the area outside the local model area. Parts of the offshore and a section in the north-west of the regional model area are covered only by the lineament map from the Simpevarp version 0 model, that is of a relatively low resolution /SKB 2002b/. Inferred deformation zones outside the local model area have, therefore, been limited to be of 1.6 km length or longer. This approach produces a model which has an increased level of resolution around the area of highest interest, i.e. the local model area. The consequences of variable data resolution inside the regional model volume are addressed in connection with the presentation of alternative models (see Section 5.4.3).

Structures that are considered to be shorter than the modeled deformation zones within the local and regional areas are handled through a statistical approach and are presented as part of the fracture statistical description in Section 5.5, and in more detail in /Hermanson et al. 2005/. Hence, all lineaments shorter than 1 km are treated as part of the stochastic fracture network.

In the cases where a deformation zone can be tied to both a lineament and a borehole, the strike of the zone is assumed to be the same as the trend of the matching lineament. The dip inferred from the borehole intercept is interpreted as the average dip angle of the zone, along its entire extent. Deformation zones observed only at the surface, which lack information on their subsurface extents, are assumed to be dipping vertical.

The steeply dipping zones are assumed to truncate, along their strike direction, against zones that have a higher order of significance. Generally, the order of significance is controlled by the classification of zones into regional and local major size classes or to best fit with the underlying data. The extension of deformation zones towards depth is assumed equal to the length of the associated surface lineaments. This assumption implies that the frequency of steeply dipping deterministically modelled deformation zones decreases with depth.

Gently dipping zones have been detected by integrating data from boreholes and interpretations from reflection seismics. The gently dipping zones are assumed to truncate, both along their strike and in the down-dip direction, against regional or local major, vertical and steeply dipping zones. In the working conceptual model, these zones are attributed a higher order of significance in the structural hierarchy.

5.4.2 Conceptual model of the kinematic evolution of deformation zones

The regional stress field at the time of formation of the deformation zones has had a major impact on the kinematics of deformation zones. The direction of the maximum compressive stress has shifted considerably during the geological evolution from being approximately N-S during the waning stages of the Svecokarelian orogeny, to approximately E-W during the Sveconorwegian orogeny, to approximately NW-SE during the Caledonian orogeny and the present day, see also Chapter 3.

Deformation zones that were formed in the ductile regime are inferred to be related to the waning stages of the Svecokarelian orogeny. Consequently, E-W oriented deformation zones that are ductile, or exhibit a ductile component, are inferred to have formed in response to compression, whereas zones oriented in NE-SW and NW-SE direction would be characterised by sinistral and dextral components of movement, respectively. However, the inferred E-W maximum compression during the Sveconorwegian orogeny imply that E-W oriented zones, if reactivated, were exposed to extensional forces, whereas the NE-SW and NW-SE oriented zones would reverse and be characterised by dextral and sinistral movements, respectively. The latter deformation zones subsequently were exposed to compressional forces during the Caledonian orogeny. A conceptual model for the sense of movement in deformation zones with different orientations is displayed in Figure 5-54.

In an attempt to unravel the kinematic history, and to test the model summarised above, there are ongoing studies, in conjunction with the complete site investigation phase, that aim to characterise both the ductile and brittle deformation zones kinematically. The results of these studies, both at the surface and in boreholes, will be evaluated in forthcoming site descriptive modelling

5.4.3 Conceptual deformation zone model with potential alternatives

The modelling procedure used for establishing the deformation zone model follows the methodology presented in /Munier et al. 2003/. An initial step in the modelling procedure made use of the Simpevarp 1.2 model, established with a special focus on the Simpevarp subarea /SKB 2005a/. Each deformation zone in this previous model was checked against the updated lineament map (see Section 5.2.5), topographic and magnetic background maps, and against new information from surface geophysics, seismics, as well as relative to new borehole data acquired for this model version.

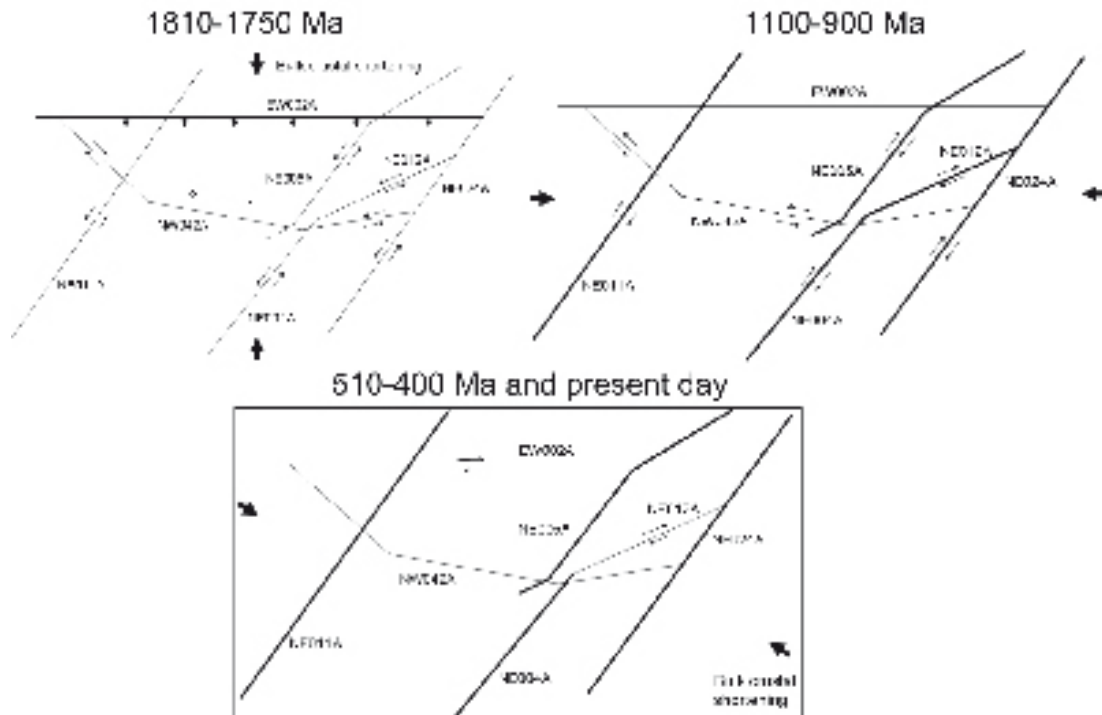


Figure 5-54. A conceptual model for the sense of movement in deformation zones with different orientations. Plan view with maximum compressive stress indicated by arrows.

To further enhance the classification of deformation zones, the ensuing modelling work includes introduction of the following groups of deformation zones in the regional model volume, in the order indicated below:

- Regional deformation zones which are supported by direct data observations through new boreholes, ground geophysics, seismics, lineament support, and which have been included in older existing structural models, *i.e. regional high confidence zones*.
- Regional deformation zones which have lineament support and have been included in older existing structural models, *i.e. regional medium confidence zones*.
- Local major deformation zones supported by direct data and observations in new boreholes, lineament support and which have been included in older structural models, or are supported by new ground geophysics, seismics or borehole data, *i.e. local major high confidence zones*.
- Local major deformation zones, which are supported by lineament data and have been included in older structural models, *i.e. local major medium confidence zones*.
- Low confidence deformation zones that have been inferred solely on the basis of the interpretation of lineaments (topographic, magnetic or EM), *i.e. local major low confidence zones*.
- The modelling procedure has made use of the key assumptions concerning relationships between dip and the along-strike and down-dip extents of individual deformation zones, as outlined in the previous section.

Base case deformation zone model

The base case deformation zone model consists of regional and local major high, medium and low confidence deformation zones. All deformation zones included in the base case model are interpreted to exist, although the degree of confidence (of existence) for zones that have no direct observations is lower.

Thirty-five deformation zones (modeled in 38 segments) have been interpreted with a high confidence in their existence. Each one of these zones is observed both indirectly, through lineament or geophysical data, and directly through field mapping, borehole or tunnel observations. Exceptions are the Mederhult zone (ZSMEW002A), and zones ZSMNS009, -10 and -11, which have not been observed in boreholes or tunnels but have been observed in field mapping, or has a major regional imprint in the topography, magnetic map or through clear anomalies in geophysical profiles that their existences are considered as being of high confidence. Also, a few high confidence zones have been based solely on indirect surface observations in combination with strong evidence from seismic refractions or reflections.

The high confidence deformation zones are illustrated in plan surface view (2D) in Figure 5-55 and Figure 5-56 and are summarised in Table 5-5 where each zone is classified based on its estimated length to either regional (> 10 km) or local major (> 1 km) deformation zones. The estimation of geological length is based on the surface impression from indirect data sources such as topography and magnetics. However, for regional deformation zones which substantially extend outside the regional model domain, length estimates are based on published geological material from the Swedish Geological Survey and on general geological understanding of south-eastern Sweden.

The average dips of the thirty-five high confidence zones have been estimated using existing observations from geophysical profiles, seismic refractions, seismic reflections, borehole or tunnel observations, where available. A vertical dip has been assumed for zones with no conditional information available on dip.

The observations are in several cases identical to observations used in the Simpevarp 1.2 modelling, but the redefined lineaments on the surface combined with new ground geophysics results, and new borehole data, have sometimes resulted in changes of the position and has therefore affected the attributed dip of a given deformation zone.

One hundred and fifty-five (N=155) medium and low confidence zones have also been included in the deformation zone model. Of these, sixty-two (N=62) are of medium confidence.

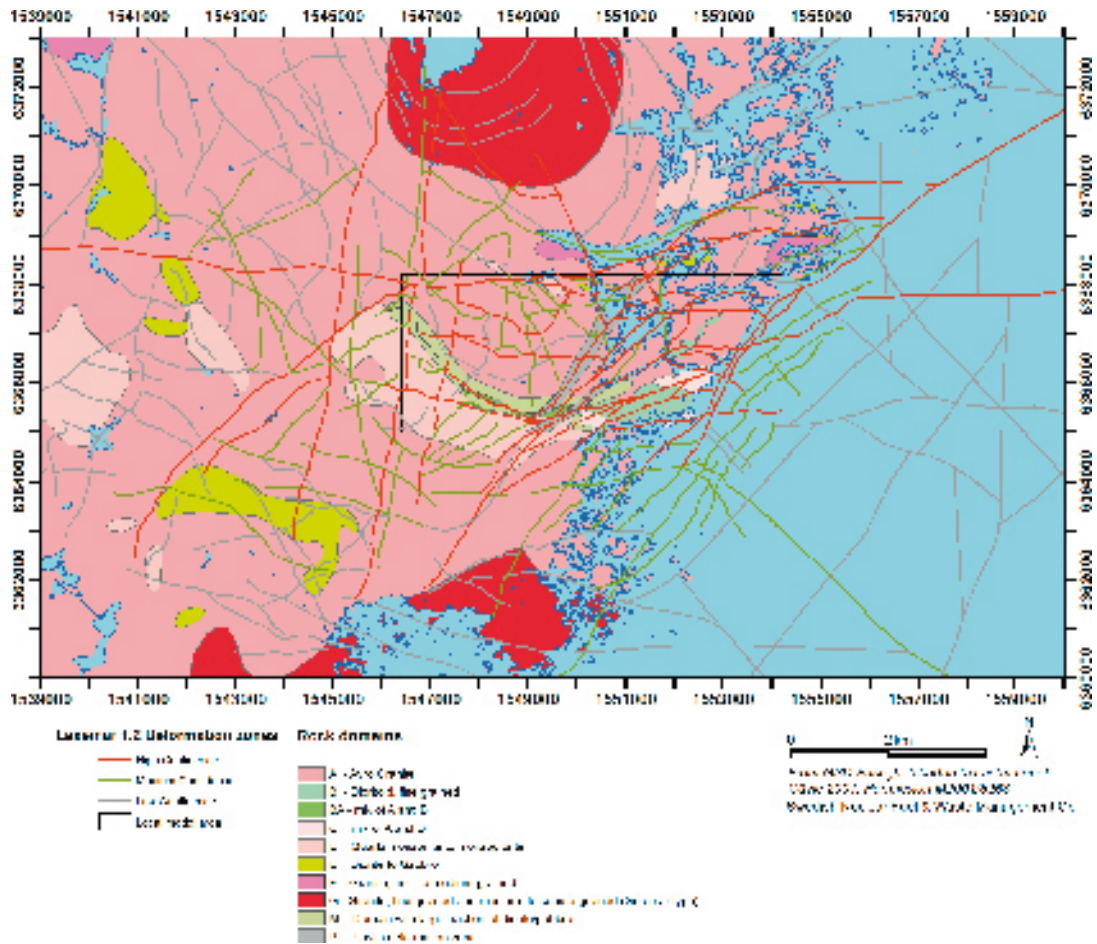


Figure 5-55. The interpreted thirty-five high confidence deformation zones in the Laxemar 1.2 regional model area (red) together with interpreted medium and low confidence deformation zones (green and grey respectively).

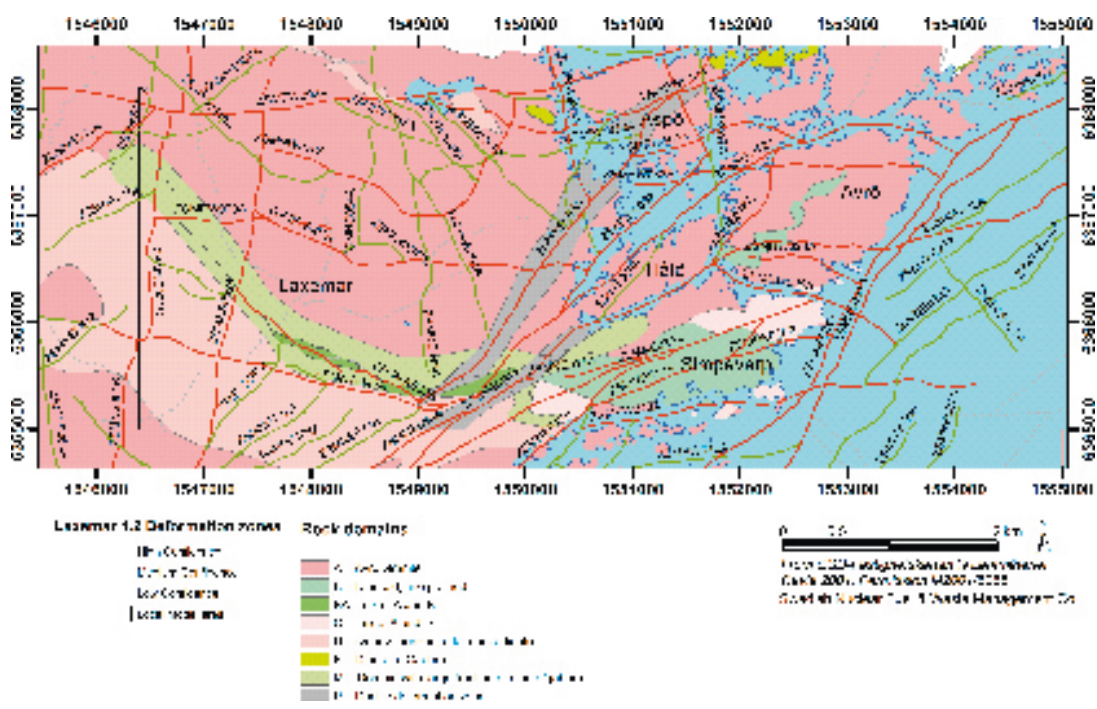


Figure 5-56. The interpreted high, medium and low confidence deformation zones in the Laxemar 1.2 local model area (red) including medium and low confidence zones (green and grey respectively).

Table 5-5. Summary of high confidence deformation zones (N=35) included in the Laxemar 1.2 deterministic deformation zone model. Detailed properties for each of these zones are given in Appendix 6.

Zone ID	Alternative name or common name	Occurrence in older models	Approximate length	Class	Basis for interpretation
ZSMEW002A	Mederhult zone	Simpevarp 1.2, v. 0, updated.	30 km	Regional	Airborne geophysics, topography, VLF, seismic refraction. Ground geology, boreholes.
ZSMEW007A		Simpevarp 1.2, updated.	3 km	Local Major	Airborne geophysics (magnetic 100% along the length, electrical data, low uncertainty), topography, borehole.
ZSMEW009A		Simpevarp 1.2, not updated.	2 km	Local Major	Topography, ground geology, tunnel, borehole.
ZSMEW013A	EW1A	Simpevarp 1.2, updated.	2–4 km	Local Major	Airborne geophysics (magnetic) 100% along the length, electrical data, low uncertainty), topography, boreholes.
ZSMEW023A		In Simpevarp 1.2 modelled as low confidence zones ZSMEW023A and ZSMEW026X, respectively. Updated.	4 km	Local Major	Airborne geophysics, topography, seismic refraction profiling; OKG tunnel intercept.
ZSMEW038A		New.	3 km	Local Major	Airborne geophysics, topography, tunnel mapping and BHs. Potentially involves a series of narrow mylonites in a number of BHs and the tunnel, with potential interference from other zones including ZSMNE006A. The current modeled geometry is an over simplification.
ZSMEW900		In Simpevarp 1.2 modelled as ZSMEW005A and ZSMEW007A. New.	2 km	Local Major	Airborne geophysics, topography, field mapping and geophysical ground survey.
ZSMNE004A		In Simpevarp 1.2 modelled as ZSMEW004A. Updated.	> 15 km	Regional	Airborne geophysics (magnetic 100% along the length, low uncertainty), tunnel.
ZSMNE005A	Äspö shear zone	Modelled in Simpevarp 1.2. Updated.	> 10 km	Local Major	Airborne geophysics (magnetic 100% along the length, low to medium uncertainty), ground geology, ground geophysics, borehole, Äspö HRL data.
ZSMNE006A	NE1	Simpevarp 1.2, updated.	2–4 km	Local Major	Airborne geophysics (magnetic 100% along the length, low to medium uncertainty), tunnel, boreholes, Äspö HRL data.
ZSMNE010A		Simpevarp 1.2, not updated.	3 km	Local Major	Airborne geophysics, topography, field control.
ZSMNE011A		Simpevarp 1.2, not updated.	8 to 12 km	Local Major	Airborne geophysics, topography, ground geophysics.
ZSMNE012A	NE4	In Simpevarp 1.2 modelled as ZSMNE012A and ZSMNW004A. Updated.	5 km	Local Major	Airborne geophysics, topography, seismic reflector, BH and tunnel (Äspö) intercepts
ZSMNE015A		New.	2 km	Local Major	Airborne geophysics, topography, field mapping, along with Clab 1, Clab 2 and OKG excavation mapping.
ZSMNE015B		New.	1 km	Local Major	Airborne geophysics, topography, field mapping, along with OKG excavation mapping.
ZSMNE016A		Simpevarp 1.2, updated.	1 km	Local Major	Linked lineaments, seismic refraction, BH and tunnel (Äspö) intercepts
ZSMNE018A		Simpevarp 1.2, updated.	1 km	Local Major	Airborne geophysics, extensive field mapping.

Zone ID	Alternative n name or common name	Occurrence in older models	Approximate length	Class	Basis for interpretation
ZSMNE019A		Simpevarp 1.2 ZSMNE019A and ZSMNE021A, northern part, updated.	4 km	Local Major	Airborne geophysics, topography, ground geophysical profiling.
ZSMNE024A		Simpevarp 1.2, not updated.	> 10 km	Regional	Airborne geophysics, seismic reflector, seismic refractor, BHs and OKG cold water intake tunnel. This zone should be considered together with ZSMNE031A. Together they define a broad complex structural belt of deformation off the coast of Ävrö.
ZSMNE031A		Simpevarp 1.2, updated.	5 km	Local Major	Airborne geophysics, seismic reflector, seismic refractor, BHs and OKG cold water intake tunnel. This zone should be considered together with ZSMNE024A. Together they define a broad complex structural belt of deformation off the coast of Ävrö.
ZSMNE040A		In Simpevarp 1.2 modelled as eastern part of ZSMNE040A. Updated.	> 1 km	Local Major	Airborne geophysics, resistivity and seismic refraction profiling.
ZSMNE050A		Simpevarp 1.2, updated.	2 km	Local Major	Airborne geophysics, topography, field mapping.
ZSMNE930A		New.	4 km	Local Major	Airborne geophysics, topography, extensive field mapping, excavation (OKG).
ZSMNS001A-D		Simpevarp 1.2, not updated.	10 to > 11 km	Regional (A–D)	Airborne geophysics, ground geophysics, topography, refraction seismics.
ZSMNS009A		Simpevarp 1.2, not updated.	10–12 km	Regional	Airborne geophysics, topography, ground magnetic and VLF.
ZSMNS017A-B NNW4		Simpevarp 1.2, updated.	3 km	Local Major	Topography, borehole and tunnel evidence.
ZSMNS059A		Simpevarp 1.2, updated.	5 km	Local Major	Airborne geophysics, topography, field mapping and geophysical ground survey, seismic reflector.
ZSMNW025A		Simpevarp 1.2, updated.	2 km	Local Major	Airborne geophysics, seismic refraction, borehole evidence.
ZSMNW028A		In Simpevarp 1.2 modelled as ZSMNW028A. Updated.	1 km	Local Major	Airborne geophysics and borehole evidence.
ZSMNW042A		Simpevarp 1.2, updated.	3 km	Local Major	Airborne geophysics, resistivity, magnetic and seismic refraction profiling.
ZSMNW928A		New.	1 km	Local Major	Seismic reflection and borehole evidence.
ZSMNW929A		In Simpevarp 1.2 modelled as western part of ZSMNE040A. Updated.	2 km	Local Major	Airborne geophysics, topography, boreholes.
ZSMNW931A		Simpevarp 1.2, updated.	4 km	Local Major	Airborne geophysics, topography, ground magnetic and VLF profiles.
ZSMNW932A		In Simpevarp 1.2 modelled as ZSMNW006A. Updated.	3 km	Local Major	Airborne geophysics, topography, ground magnetic and VLF profiles.
ZSMNW933A		New.	4 km	Regional	Airborne geophysics, topography, ground magnetic and VLF profiles.

Twenty-nine of the high confidence deformation zones were already identified in the Simpevarp 1.2 model /SKB 2005a/. In the current model version, five more high confidence deformation zones have been identified through geological field observations, borehole intersections in combination with ground geophysics or seismics, cf. Table 5-5. Most of the new material originates from Laxemar, although new submarine topography from the coast along Simpevarp and Ävrö has greatly improved the knowledge in the sea close to shore.

A few deformation zones from the Simpevarp 1.2 model have been removed on the basis of results from new data or new interpretations of existing topographic, bathymetric and airborne geophysical data, cf. Table 5-6.

Table 5-6. Deformation zones that have been removed from the Laxemar 1.2 deformation zone model since the last model version (Simpevarp 1.2).

Zone name	Reason for removal	Result
ZSMNW035A	New bathymetric data	Split into several shorter lineaments which are not possible to tie up to a deformation zone > 1 km
ZSMNW296A	New bathymetric data	Lack of evidence in the new data for a lineament
ZSMNE024A	New bathymetric data	Lack of evidence in the new data for a lineament
ZSMNE136	Length limitation	Lineament only 915 m (below truncation level of 1,000 m)
ZSMNW234A, B	Length limitation, offset between lineament segments to large	Segments 385 and 620 m each (below truncation level of 1,000 m)
ZSMNE138B	Length limitation, offset between lineament segments to large	Lineament segment 780 m (below truncation level of 1,000 m)
ZSMNE239A	Length limitation	Lineament only 971 m (below truncation level of 1,000 m)
ZSMNW016A	Length limitation	Lineament segment only 664 m (below truncation level of 1,000 m)
ZSMNE044A	Length limitation	Lineament only 411 m (below truncation level of 1,000 m)
ZSMEW013C	Length limitation, offset between lineament segments to large	Lineament segment only 647 m (below truncation level of 1,000 m)

Alternative deformation zone model

An alternative representation of the deformation zone model is to include only high and medium confidence deformation zones. These are deformation zones where evidence through direct observations, and strong seismic or geophysical profile anomalies certify their existence. Deformation zones of lower confidence may exist, but are in this case, not treated as part of the deterministic deformation zone model.

However, the high confidence deformation zones are almost all located inside the local model area, although several extend into the regional model area. Only three high confidence zones are defined completely within the regional model area and outside the local model area; NE010A, NE011A and NW933A. Therefore it is rather pointless and also misleading to present an alternative model in the regional model area.

The alternative deformation zone model consequently only exists in the local model domain as is shown in Figure 5-57, and consists of the thirty-two (N=32) high confidence zones that have at least some part originating from within the local model area together with thirty-four (N=34) medium confidence zones. This alternative model contains all the high confidence zones presented for the base case model with the exception of zones NE010A, NE011A and NW933A which fall outside the local model area.

The presented alternative deformation zone model is based on confidence levels. Other alternatives based on the geological characterisation, such as dividing zones into ductile and brittle, or on the basis of thickness or other geological means is preferable in future model versions. However, at the current level of understanding, data do not provide enough information for such alternatives. The vision is to provide better, geologically based, alternatives for model version 2.2.

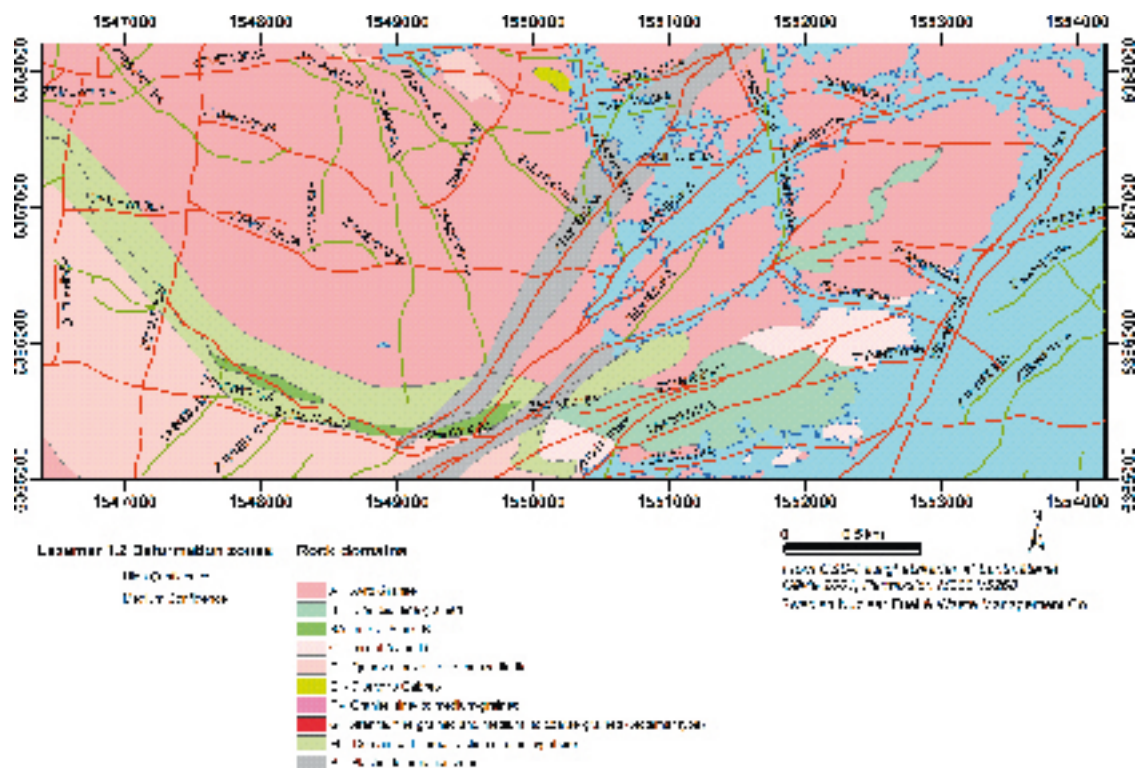


Figure 5-57. Alternative deformation zone model including high and medium confidence deformation zones within the local model area.

5.4.4 Property assignment to the base case model with specification of selected high confidence zones

Key properties, and numerical estimates of the uncertainty associated with some of these parameters, have been attributed to each of the base case high confidence deformation zones (N=35) that are based on a variety of geological and geophysical information, or deduced from older models. A summary of the properties of the deformation zones is presented below (Table 5-7) with complete tabular presentations in Appendix 6. A more comprehensive presentation of the high confidence deformation zones is given in /Wahlgren et al. 2005b/.

Table 5-7. Properties assigned to the high confidence deformation zones of the Laxemar 1.2 model, along which there are, to variable extents, supporting geological and geophysical data.

Property	Comment
Deformation zone ID	ZSM*****, in two places with additional letter A, B, C, D and E (according to the nomenclature recommended by SKB).
Position	With numerical estimate of uncertainty.
Strike and dip	With numerical estimate of uncertainty.
Thickness	With numerical estimate of uncertainty.
Length	With numerical estimate of uncertainty.
Ductile deformation	Indicated if present along the zone.
Brittle deformation	Indicated if present along the zone.
Alteration	Indicated if present along the zone.
Fracture orientation	In places, with numerical estimate of uncertainty.
Fracture frequency	With numerical estimate of uncertainty.
Fracture filling	Mineral composition.

There are few data available at present relating the properties (including numerical estimates of uncertainty) of the interpreted medium and low confidence deformation zones, which are based solely on the interpretation of linked lineaments.

Below follows a description of selected interpreted high confidence deformation zones, in order of their assumed importance, according to current understanding. A complete compilation of all descriptions can be found in /Wahlgren et al. 2005b/.

ZSMEW007A and ZSMEW900

The deformation zone ZSMEW007A (Figure 5-58) is based on a topographic and magnetic EW-lineament, seismics, ground geophysics and borehole intersections. The zone has been updated from Simpevarp version 1.2 with new borehole intersections as well as new ground geophysics. The previous interpretation extended from zone NS001C in the west to NE006A in the east. However, the western interpretation was not conclusive with regards to the dip. The eastern and central part of the zone was defined by the northerly dipping seismic reflector A /Juhlin et al. 2004a/ and an intersection in KLX02.

New interpretations in the west suggest a southerly dip based on a seismic reflector (L) /Juhlin et al. 2004a/, geophysical profiling /Lindqvist 2004a/ and from field observations /Persson Nilsson et al. 2004/. Also, HLX25 shows a low resistivity and low sonic section which corresponds with a southerly dip.

However, alternative interpretations are available through the new borehole KLX04 which together with resistivity profiles indicate also a northerly dip of the central and eastern part of EW007 as shown in Figure 5-59 and Figure 5-60. The magnetic anomaly also supports a division of EW007 into two separate structures (along its extent); one gently northerly dipping structure in the central/east and one steeply dipping towards the south (in the west).

In this model version it was therefore decided to terminate EW007 against NS059A in the west and create a new deformation zone, EW900 extending from NS001C to just south of KLX04. EW900 is interpreted to dip about 70 degrees to the south, whereas EW007 dips 43 degrees to the north as shown in Figure 5-61.

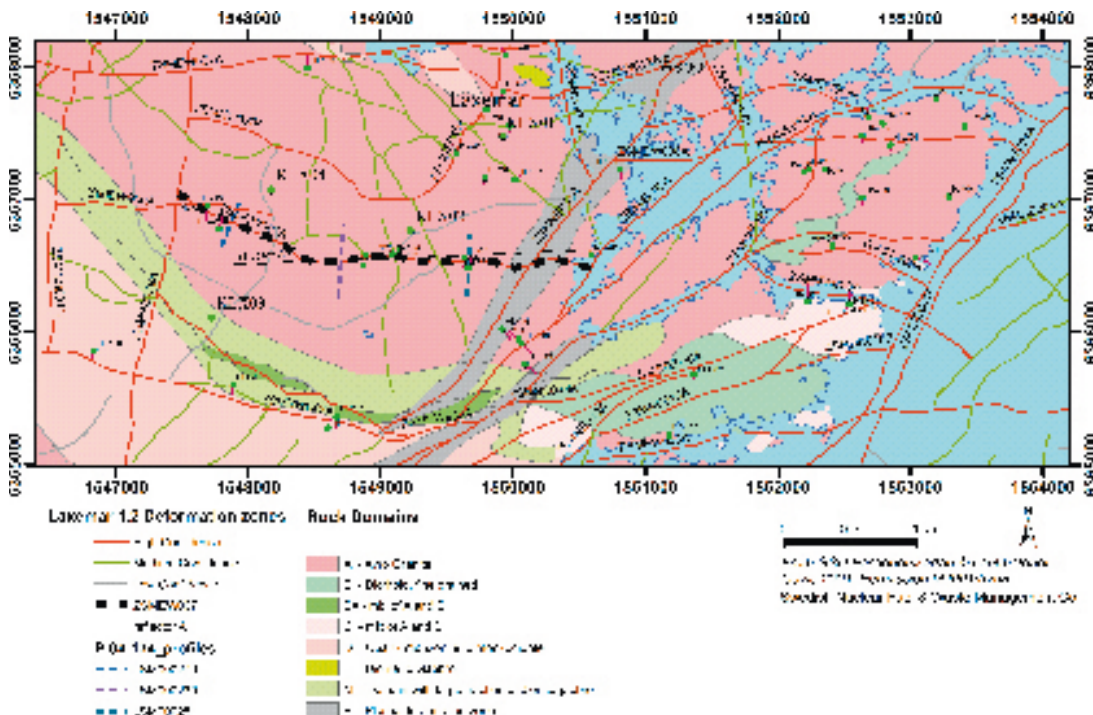


Figure 5-58. Illustration of EW007 together with all high, medium and low confidence zones identified in the local model domain. The surface intersection of seismic reflector A /Juhlin et al. 2004a/ crops out parallel to the central and eastern part of EW007.

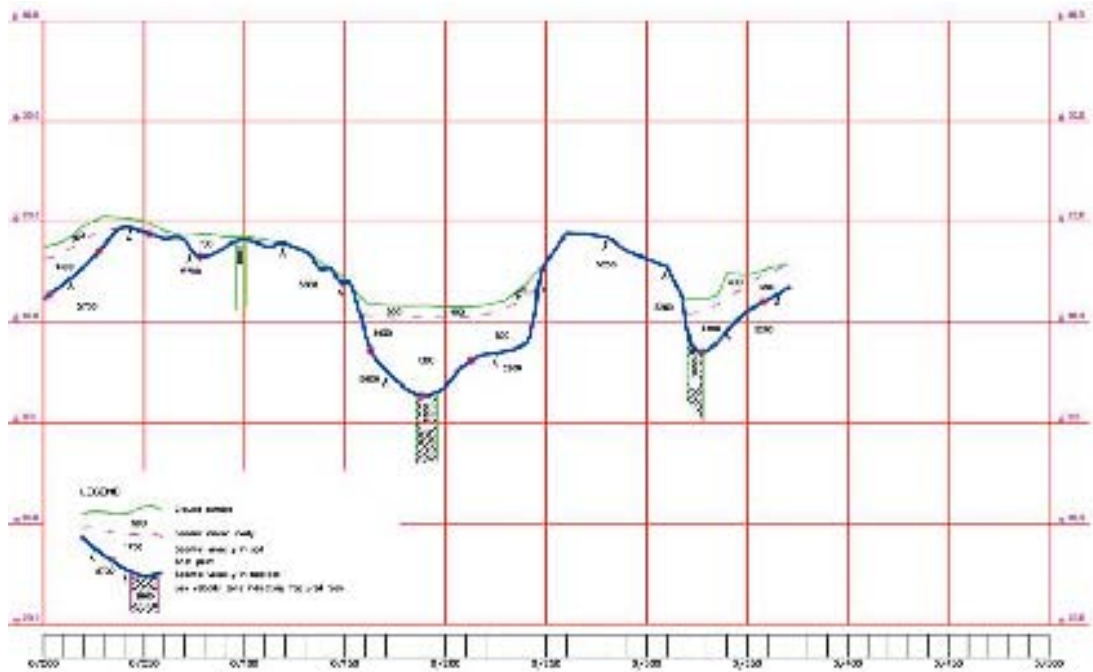


Figure 5-59. Refraction seismic along profile 279 (westernmost part of EW007) /Lindqvist 2004a/. See Figure 5-58 for location of the profile.

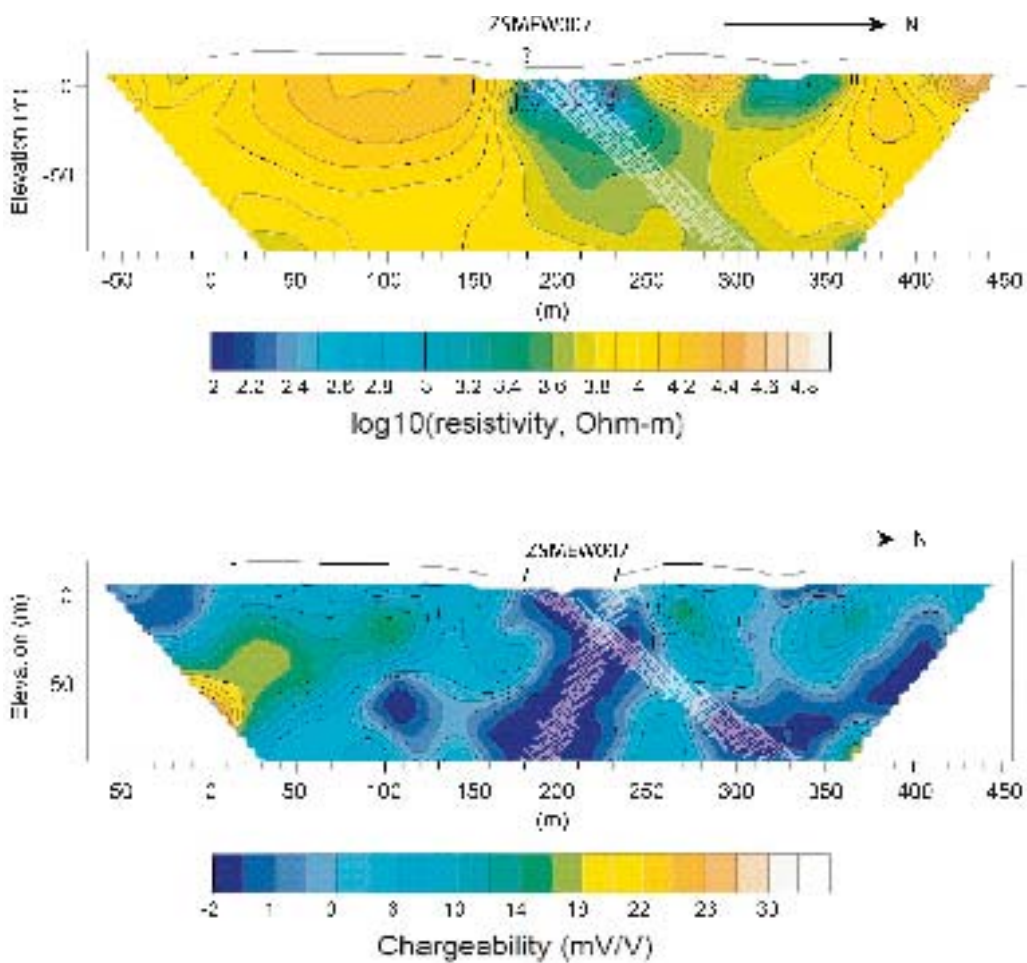


Figure 5-60. Vertical sections of resistivity and chargeability along profile 279 /Thunehed et al. 2004/. See Figure 5-58 for location of the profile.

Refraction seismic profiling across EW007 shows a zone with a thickness of at least 10 m, and possibly several neighbouring splay structures. Resistivity profiles across the central parts indicate a thickness of about 60 m and these profiles possibly show both the northerly dipping EW007 as well as the south dipping zone interpreted as EW900.

Figure 5-61 illustrates the interpreted northerly dip of EW007 and its interpreted intersections with boreholes KLX01, KLX02 and KLX04. At the intersection in KLX01 (972–1,044 m) the fracture frequency is increased and includes several crush sections and an increased alteration of the host rock. The interpreted intersection in KLX04 (314–391 m) shows an altered, highly fractured section where the foliation has an E-W orientation, i.e. parallel to EW007, which indicates not only a brittle component but also an older, ductile deformation along the zone.

ZSMNE005A (Äspö shear zone)

ZSMNE005A, the Äspö shear zone forms the boundary between the tectonically more deformed rock mass in the Simpevarp subarea and the comparatively less deformed Laxemar (see Section 5.2.5). The deformation zone is a complex and dominantly ductile zone with smaller sections of brittle deformation, cf. Figure 5-62.

At Äspö, where it is best known, /Rhén et al. 1997c/ describes its character as a primarily ductile shear zone with mylonites and epidotic anastomosing shear zones which are interpreted to control the orientation of later brittle deformation, evident in the form of increased fracturing and brecciation. Hydrothermal alteration and formation of different fracture filling minerals probably had an important sealing effect on the main core of the zone. The most hydraulically conductive parts appears to coincide with some narrow highly fractured sections, or single open fractures, which are probably not connected along the entire extent of the zone.

In the current model, an enveloping thickness of 250 m was attributed to the zone in order to contain all indicators from the geological field mapping, those inferred from the total magnetic field and the results from a reassessment of Äspö data including the Geomod model /Berglund et al. 2003/. The southern termination to the zone is based on the magnetic anomalies which are forming the basis for identifying the surface lineament for the Äspö shear zone.

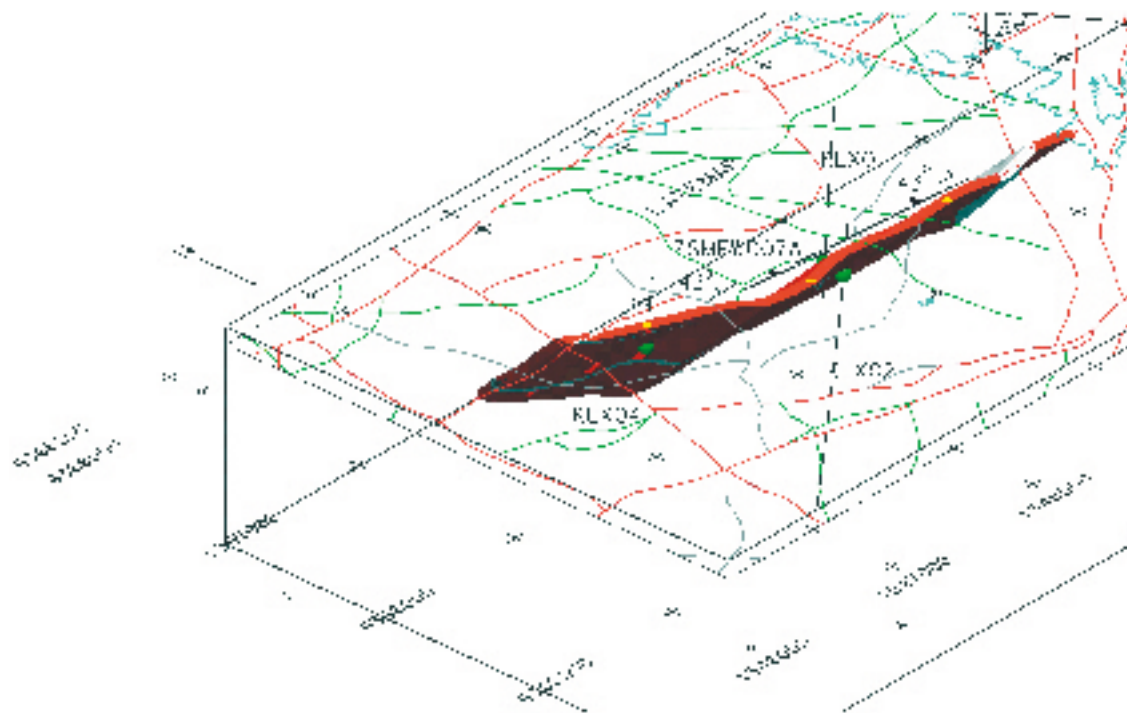


Figure 5-61. EW007 is interpreted to dip northwards (43°) and brittle deformation zones or increased fracturing are observed in KLX01, KLX02 and KLX04. The interpreted dip is parallel to seismic reflector A /Juhlin et al. 2004a/.

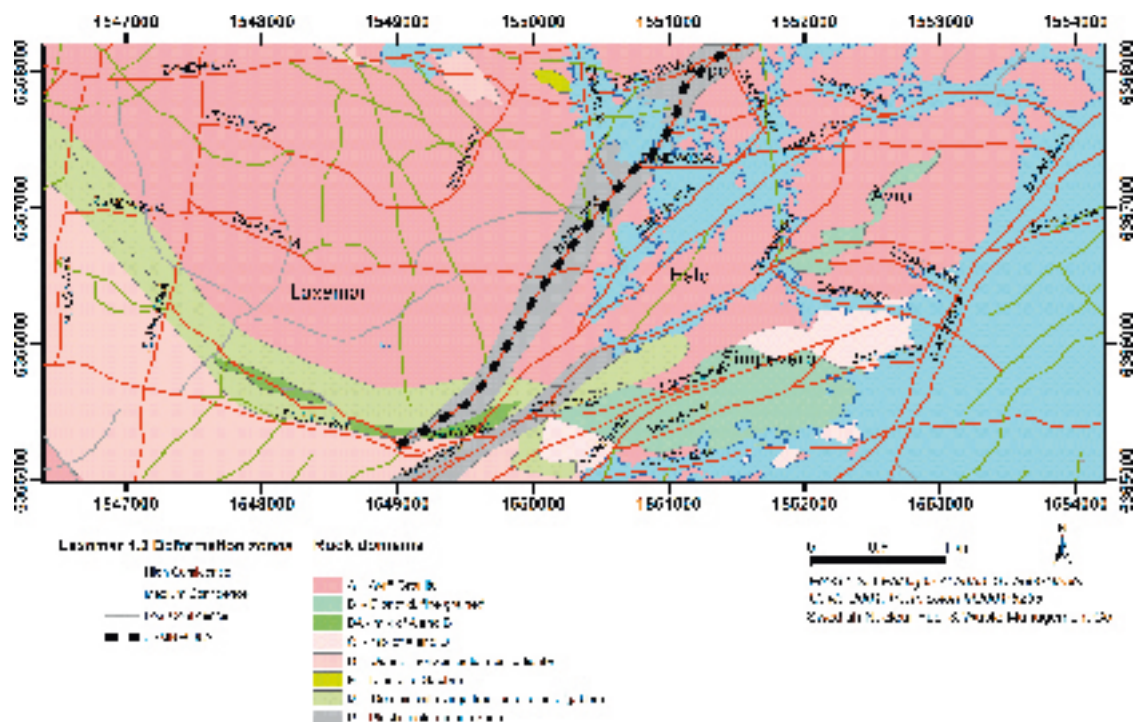


Figure 5-62. ZSMNE005A (Äspö shear zone).

The narrowing geometry of the zone in the south has been created to more closely conform to the ductile domain P in the rock domain model, cf. Figure 5-63. The northern extension of the zone has been developed in conjunction with a reassessment of the Mederhult zone (ZSMEW002A). Both zones have been reassessed on the basis of the tectonic patterns indicated by the data underlying the lineament map, particularly field mapping and the magnetic anomaly map, and also taking into consideration the indicated thickness and interpreted continuity of both zones.

The Äspö shear zone has been modelled vertical, as shown in Figure 5-63, rather than steeply dipping to the south as in the Simpevarp 1.2 model. The current stand is considered more reasonable considering the complexity and dominantly ductile nature of the zone, and the lack of well constrained data to support one certified dip direction for the whole deformation zone.

ZSMEW002A (Mederhult zone)

The regional Mederhult deformation zone, ZSMEW002A, follows, in the western part, the interpretation made in model version 0 and in the eastern part a topographic and magnetic lineament running along the northern coastline of Äspö (see Figure 5-64). The continuation of the zone along this alignment fits well with the trends indicated by seismic reflector projections /Juhlin et al. 2002, 2004a/, the resistivity measurements from the airborne geophysical surveys /Thunehed et al. 2004/, topographical map /Wiklund 2002/, ground geophysics /Stenberg and Sehlstedt 1989/ and the interpretation for the extension of Äspö shear zone (ZSMNE005A) /Berglund 2004/.

The shear zone has previously been verified by ground magnetic and VLF measurements /Stenberg and Sehlstedt 1989/, a refraction seismic survey /Rydström and Gereben 1989/, reflection seismics /Bergman et al. 2001/ and surface geology /Stanfors and Erlström 1995/. Results from the VLF measurements indicate that the zone has a steep southerly dip, whereas observations on the surface suggest a more gentle dip to the southeast.

The interpreted mean geometry in terms of strike and dip of the zone in the local model area is 90/65, cf. Figure 5-65. The conclusion in the version 0 model regarding dextral movements during the Phanerozoic has not been verified and remains an open issue, albeit the tectonic evolution suggests several episodes of alternate directions of movement (see Section 5.1.1). The Mederhult deformation zone is considered to be mainly a ductile regional scale shear zone.

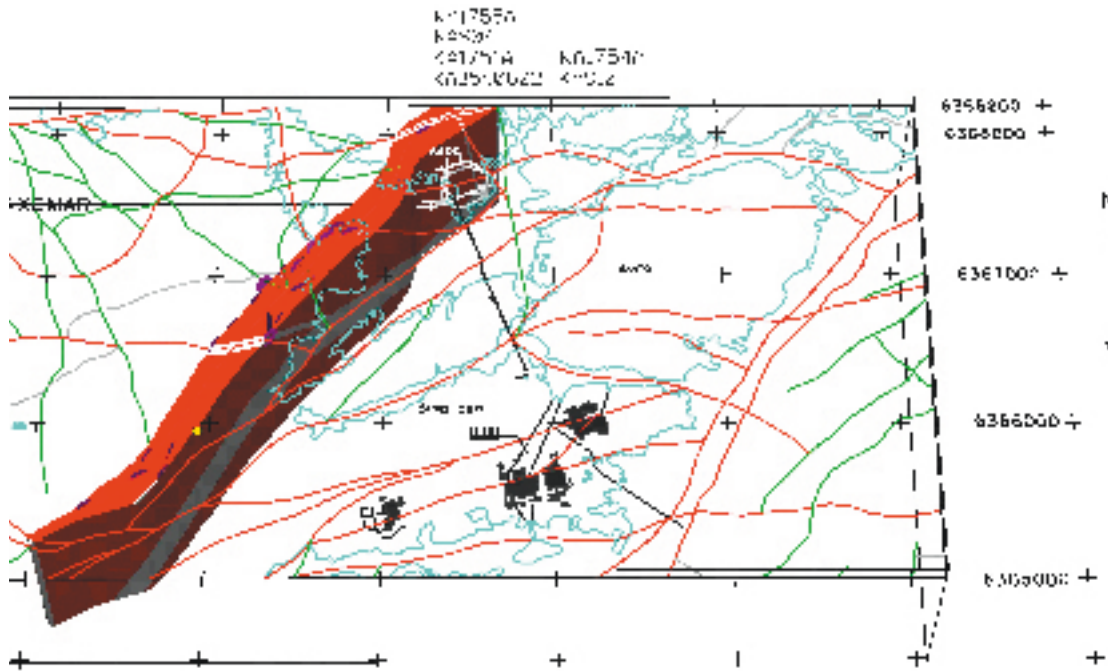


Figure 5-63. ZSMNE005A (Äspö shear zone) is modelled as a 250 m thick deformation zone with a vertical dip based on its complex and ductile nature. Discs at the surface intersection represent field observations. The list of boreholes (top) was used for direct observations of NE005 during modelling.

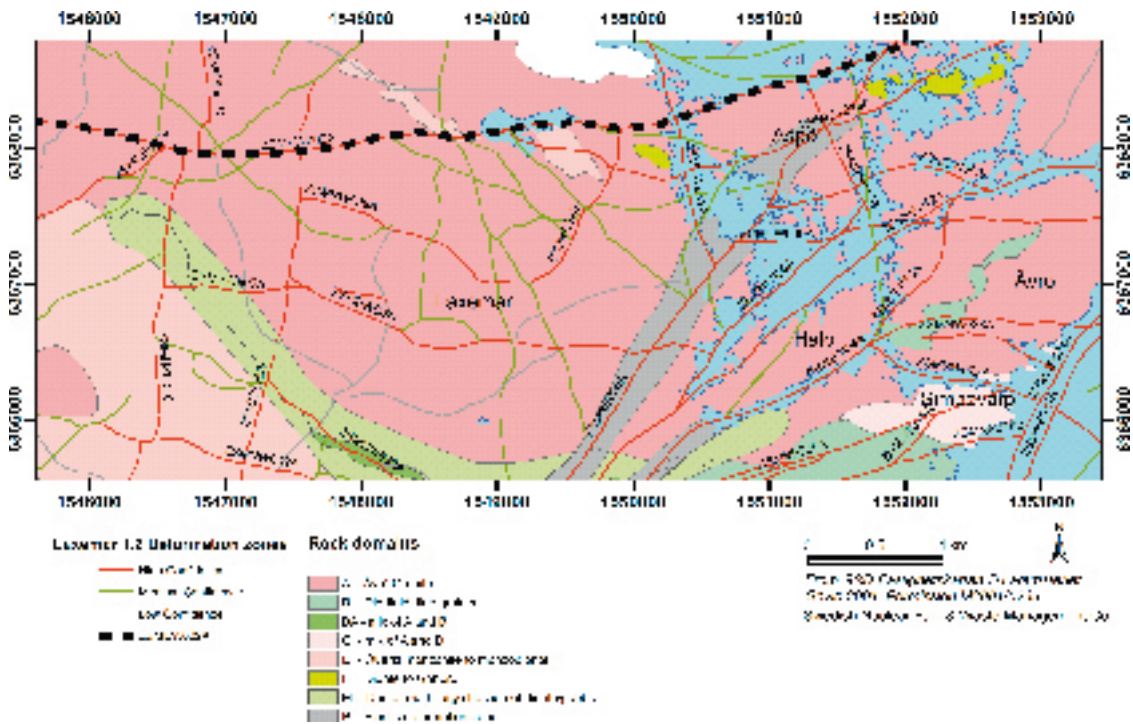


Figure 5-64. Location of the surface trace of ZSMEW002A (Mederhult zone).

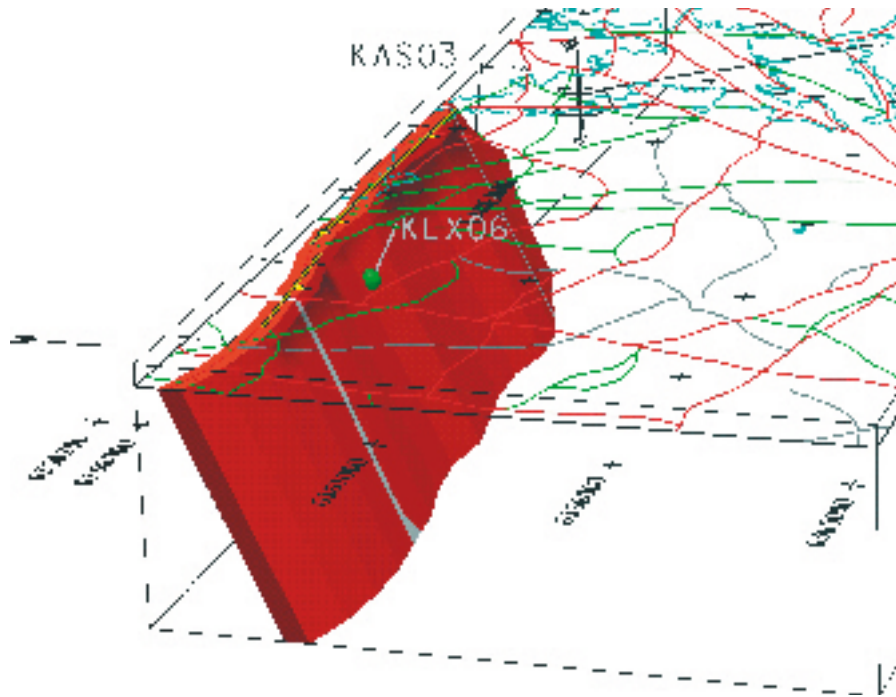


Figure 5-65. ZSMEW002A (Mederhult zone) is modelled as a 100 m thick shear zone with an orientation of 90/65. The intersection with KLX06 is indicated in green.

ZSMNE004A

ZSMNE004A is one of the larger NE trending regional deformation zones in the mainland area, and, together with the Äspö shear zone, forms the largest tectonic structure in the regional model area, cf. Figure 5-66. This is mainly a ductile deformation zone with a complex anastomosing geometry probably involving smaller subparallel deformation zones and splay structures, especially in the southern central part of the local model area close to the Äspö shear zone. However, the complexity is not well known with only a few detailed observations from field mapping /Wahlgren et al. 2004/ and from the Äspö tunnel.

The southern part of ZSMNE004A extends far beyond the regional model boundary and is observed in several outcrops /Persson Nilsson et al. 2004/. At the southern border of the local model the zone is interpreted to flex east and away from the southern termination of Äspö shear zone based mainly on the airborne magnetic map. The area is characterized by a mix of different rock types, intense ductile deformation and few surface outcrops. Two separate ductile rock domains enclosing ZSMNE004A and the Äspö shear zone are proposed for this area (see Section 5.3). The whole section where ZSMNE004A and the Äspö shear zone are in close proximity may be well connected, but information is not conclusive with regards to zone terminations and geological character. The northern part of ZSMNE004A turns eastwards across Ävrö and is interpreted (with lower confidence) to extend eastwards in the Baltic sea.

A 70 degree dip towards the southeast is observed in the Äspö HRL access tunnel at chainage 0/318 m which is also supported by seismic reflection and refraction studies at Ävrö /Juhlin et al. 2004b, Lindqvist 2004b/. Dip measurements from field mapping vary between 75N to 65S.

ZSMNE004A is modeled with a vertical dip in view of the variable dips from observations in the field, tunnel and from seismics. A 100 m geological thickness is suggested to describe the envelope of inferred minor splay structures and anticipated undulation of the zone. The current model of the three dimensional geometry is shown in Figure 5-67.

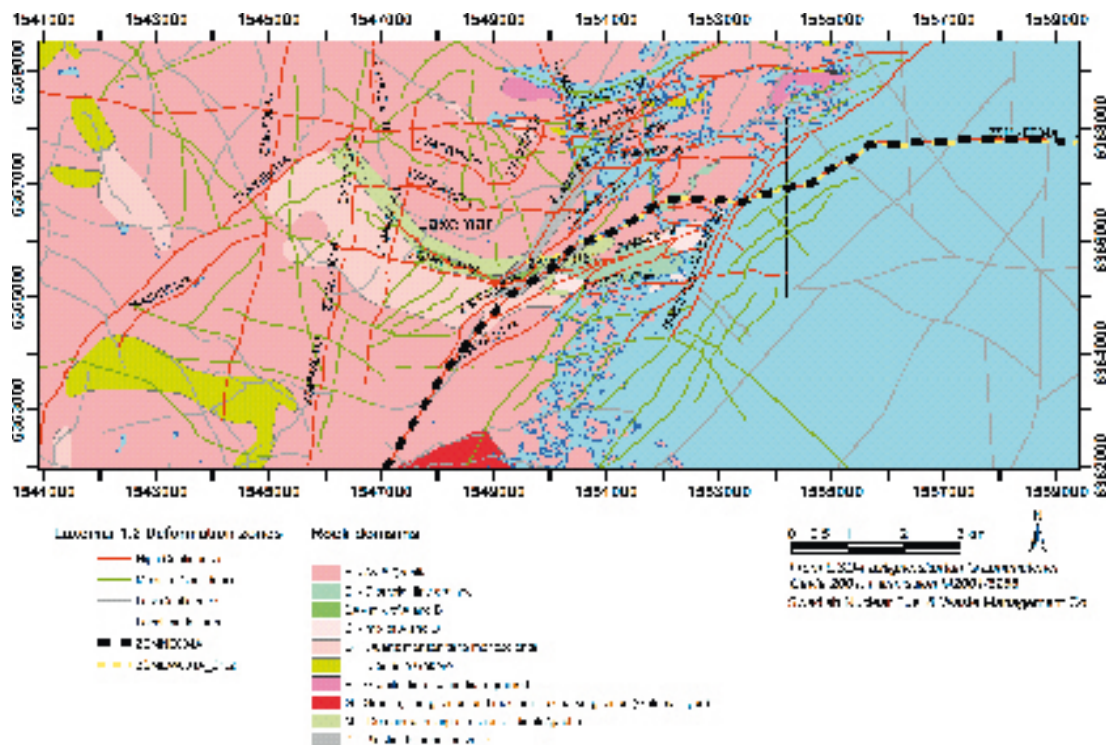


Figure 5-66. Location of ZSMNE004A (black) and the previous interpretation (yellow). The new interpretation extends the zone towards the south compared to the previous termination towards Åspö shear zone (ZSMNE005A).

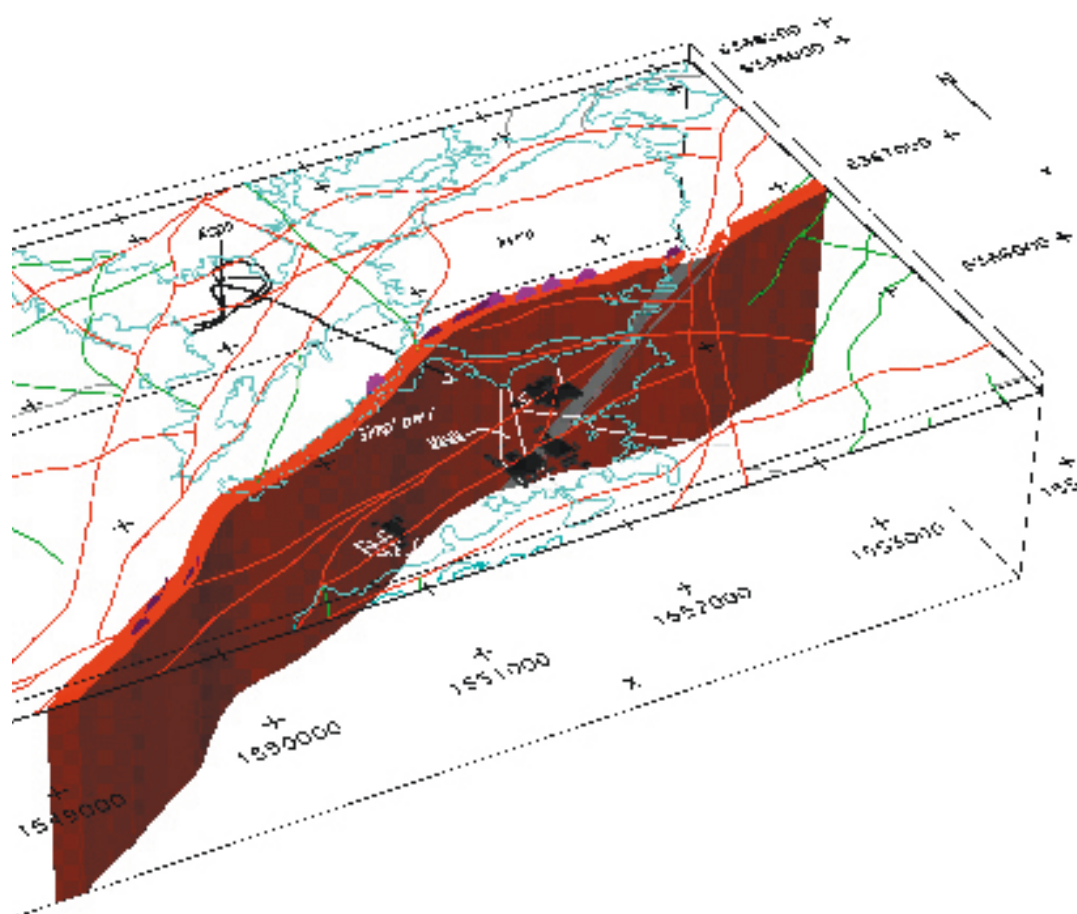


Figure 5-67. ZSMNE004A is modeled with a geometry of 050/90 and a geological thickness of 100 m including a proposed geological transition zone with related minor structures.

ZSMNW042A

The local major zone ZSMNW042A is located along the southern boundary of the local model area and extends between ZSMNE004A in the east to ZSMNE065A (a medium confidence zone) in the west, cf. Figure 5-68. The extent of the zone is well indicated in the topographical map as well as by a relatively strong magnetic anomaly. Three geophysical profiles indicate a subvertical deformation zone /Thunehed et al. 2004/ whereas seismic refractions indicates a 20 m thick core of more highly fractured rock dipping 75 degrees either to the north or to the south /Lindqvist 2004a/.

A series of percussion boreholes have been drilled on ZSMNW042A in conjunction with the geophysical profiles /Ask et al. 2004c/. However, the locations of these percussion holes are mostly completely within the zone limits and therefore are results from these holes inconclusive with regards to the geological character and thickness of the zone. Several intervals of increased fracturing are observed in HLX15 and HLX26, as can be seen in Figure 5-69 paired with significant water bearing structures in HLX27 and HLX28. This indicates that the hydraulic conductivity of the zone appears to be greater in the west than in the east. Results from the percussion drillings were only preliminary at the time of modelling and further data are necessary to confirm the character of this zone.

ZSMNS001A–D

The north-south trending regional deformation zone ZSMNS001A–D is divided into four segments which seem to be off set by E-W deformation zones in a right-lateral movement, cf. Figure 5-71. The segments are indicated both in topographic and airborne geophysical data and have been verified through ground magnetic measurements /Stenberg and Sehlstedt 1989/. Furthermore, the northern segment has also been verified in a refraction seismic survey /Rydström and Gereben 1989/ and by increased small-scale fracturing, locally sealed by epidote, and mesoscopic brittle-ductile shear zones along or close to the marked zone.

A steep to vertical dip is indicated by the results of the ground VLF measurements. The thickness of the zone core is estimated to be 5–10 m and the modelled geological thickness including a transition zone is 100 m. This deformation zone has not been studied since version 0 /SKB 2002b/ and needs further confirmation through drilling and possibly excavation.

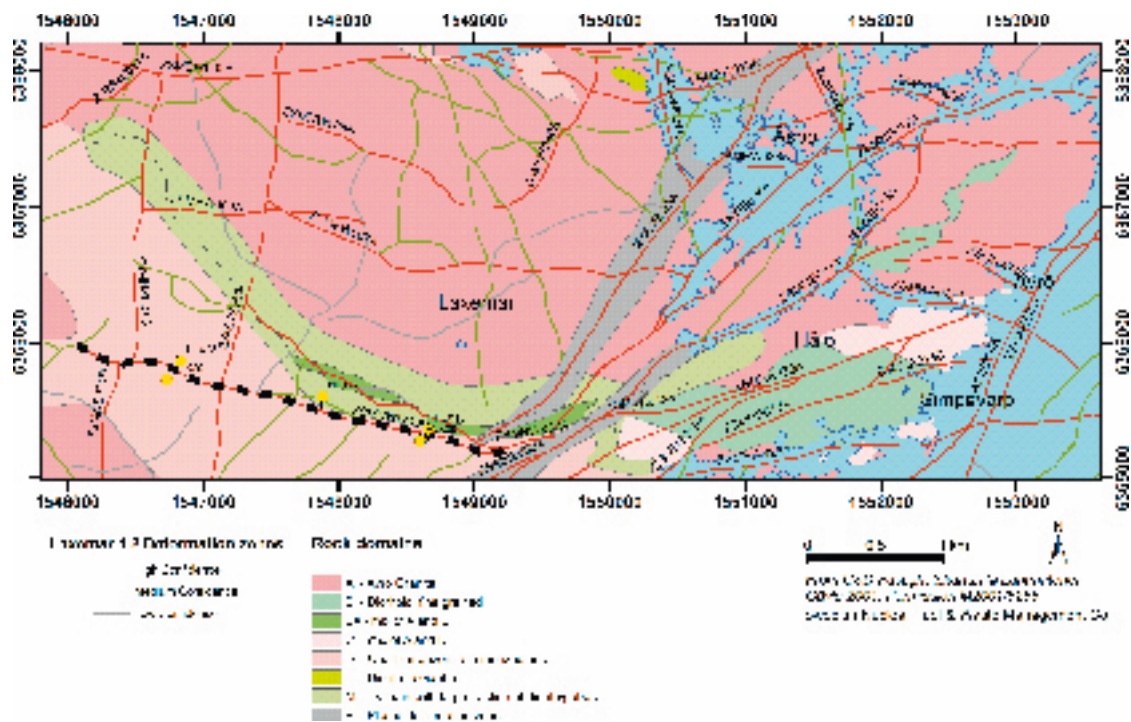


Figure 5-68. Location of ZSMNW042A.

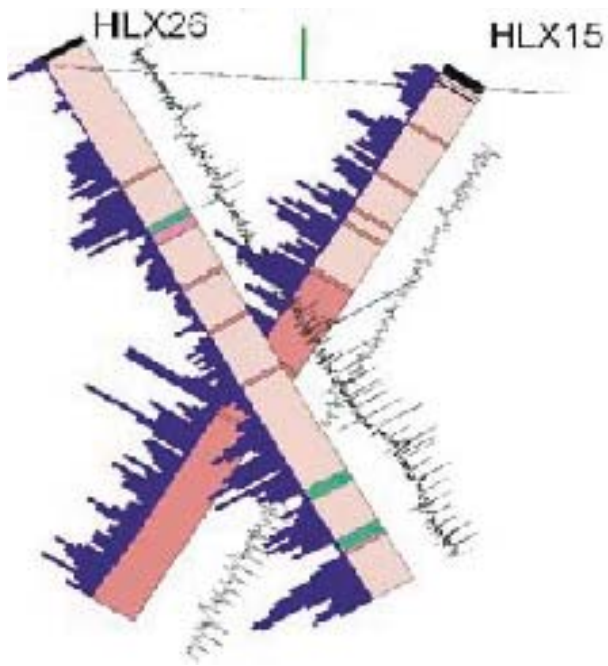


Figure 5-69. Percussion borehole log of HLX15 and HLX26 through ZSMNW042A /Ask et al. 2004c/.

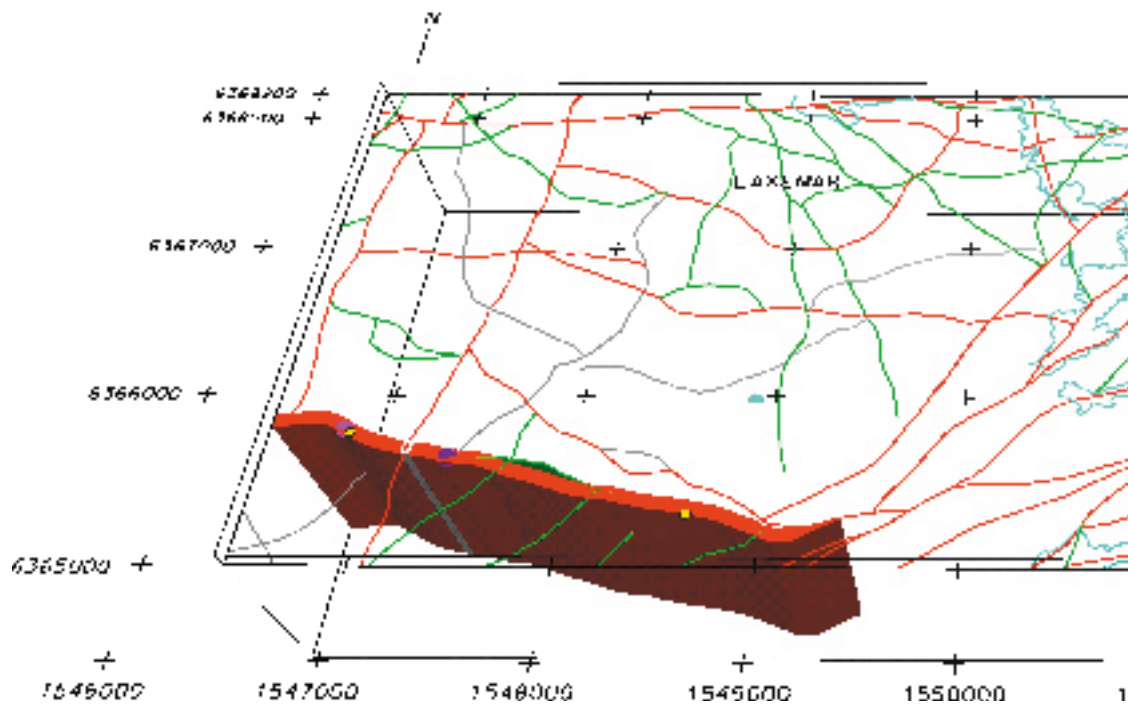


Figure 5-70. ZSMNW042A is modelled with a geometry of 105/90 and a geological thickness of 80 m including its transition zone.

ZSMNE040A and ZSMNW929A

The local major zones ZSMNE040A and ZSMNW929A have been modified since the Simpevarp 1.2 version in such a way that the original zone (ZSMNE040A) has been divided into two separate branches with ZSMNE040A in the east and ZSMNW929A in the west, cf. Figure 5-72.

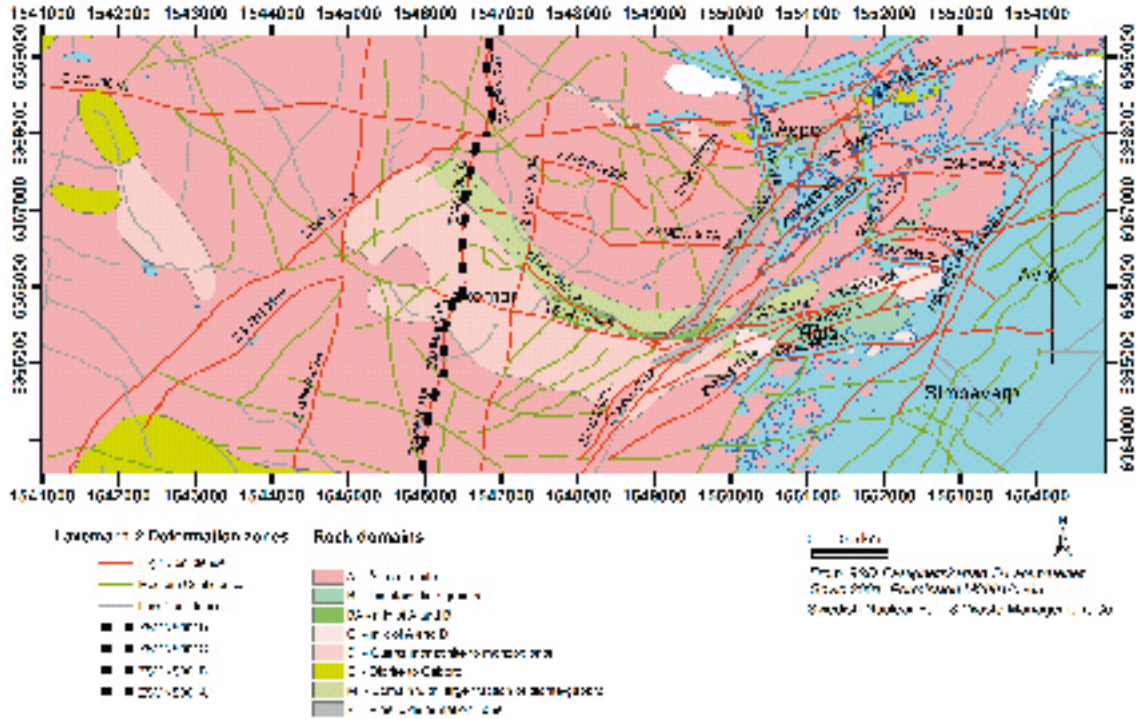


Figure 5-71. Location of ZSMNS001A–D.

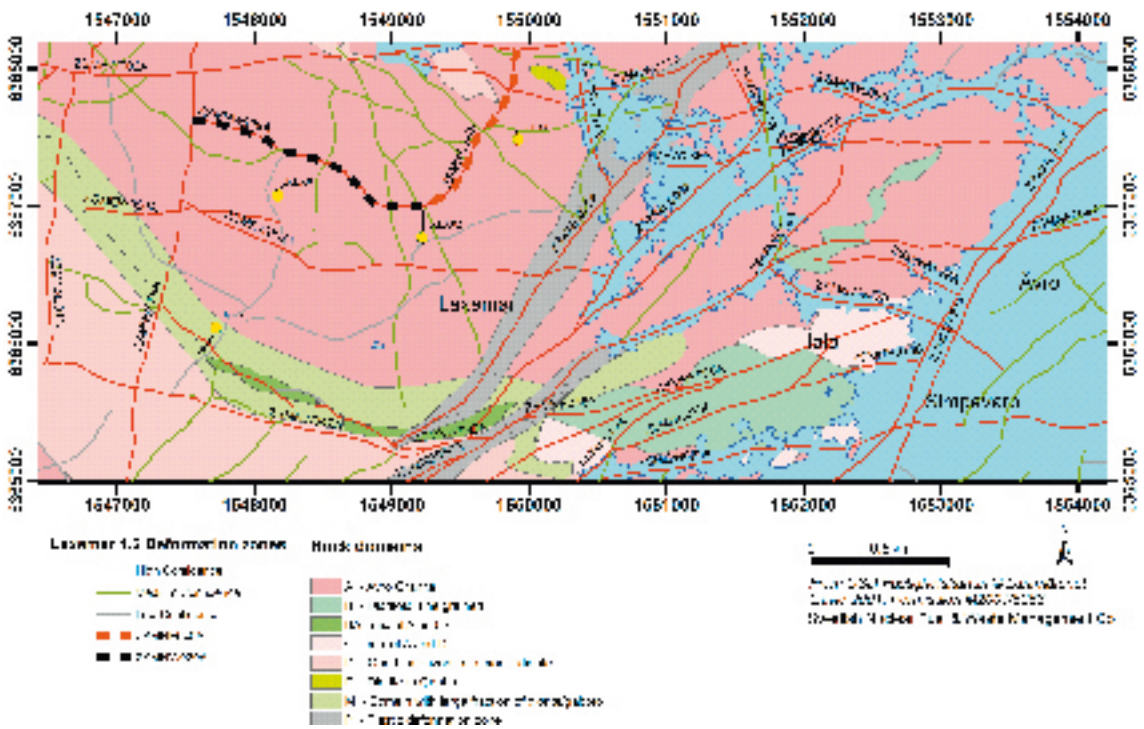


Figure 5-72. Location of ZSMNW929A and ZSMNE040A.

ZSMNW929A is indicated by field observations /Wahlgren et al. 2005b/, topographic and airborne geophysical lineaments and borehole intersections in KLX02A (at 845–880 m) and in KLX04 (at 870–970 m). The borehole intercepts are characterised by a general increase in the frequency of open fractures and a higher degree of oxidation. The zone is also characterised by distinctly low P-wave velocity and partly by a somewhat reduced resistivity. A number of borehole sections with increased fracturing, crush, sealed networks and altered host rock may indicate a more complex zone consisting of a number of minor deformation zones. This generally brittle zone has been modelled with a thickness of 50 m representing an envelope thickness containing smaller narrow inferred splays, illustrated in Figure 5-73.

ZSMNE040A is indicated through topographic and airborne geophysical lineaments, a borehole intersection in KLX01A (at 610 m) and is also weakly supported by anomalies in geophysical profiles /Thunehed et al. 2004/. A seismic reflection survey by /Bergman et al. 2001/ suggests a reflector with a matching surface intercept to the lineament but with weak indications for an intercept with KLX01A. The generally brittle zone has been modeled with a thickness of 20 m representing an envelope thickness inferred to contain discontinuous splays with thicknesses of c. 5 m of fractured rock as inferred from seismic refraction profiling, cf. Figure 5-74.

ZSMNW928A

ZSMNW928A is based on the interpreted subhorizontal seismic reflector N /Juhlin et al. 2004b/ and through possible intercepts with boreholes KLX02 and KLX04. The seismic reflector is strongly supported not to extend through the Mederhult zone in the north, which implies no surface intersection. Lateral extent in other directions is currently limited to the nearest high confidence regional or local major deformation zone but needs further evaluation through borehole data, hydraulic tests and/or seismics.

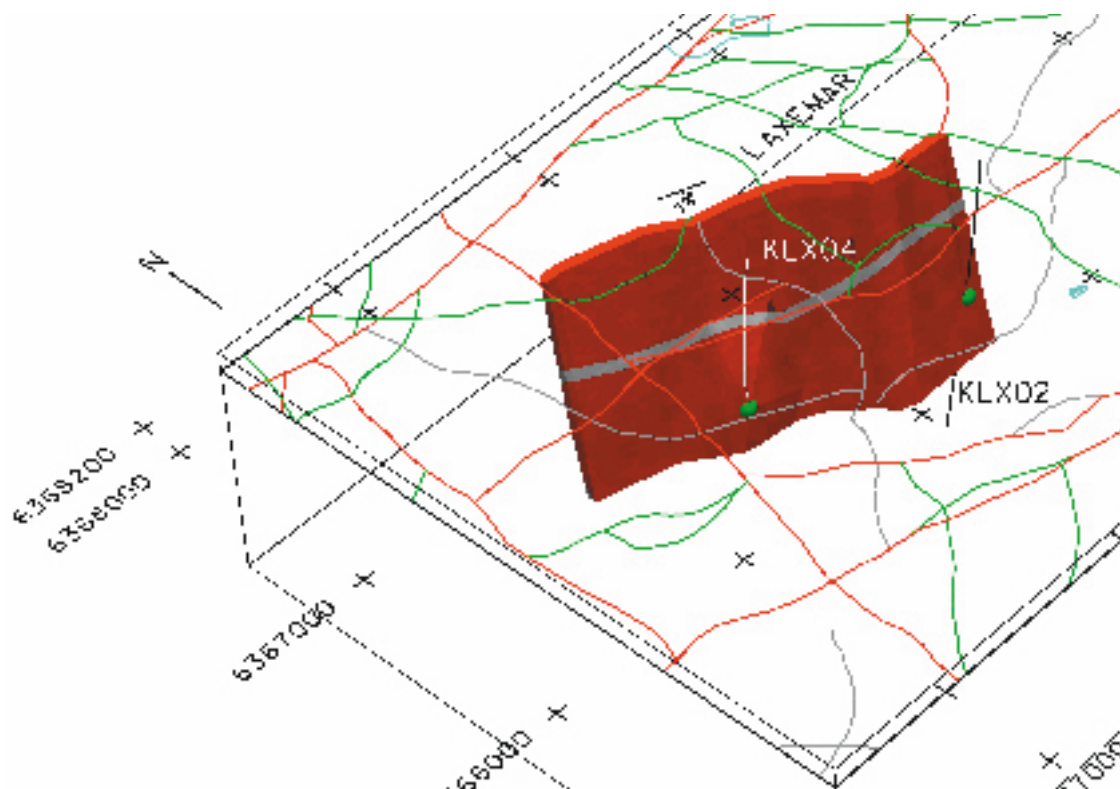


Figure 5-73. ZSMNW929A is modelled with a geometry of 113/79 and a geological thickness of 50 m including its transition zone.

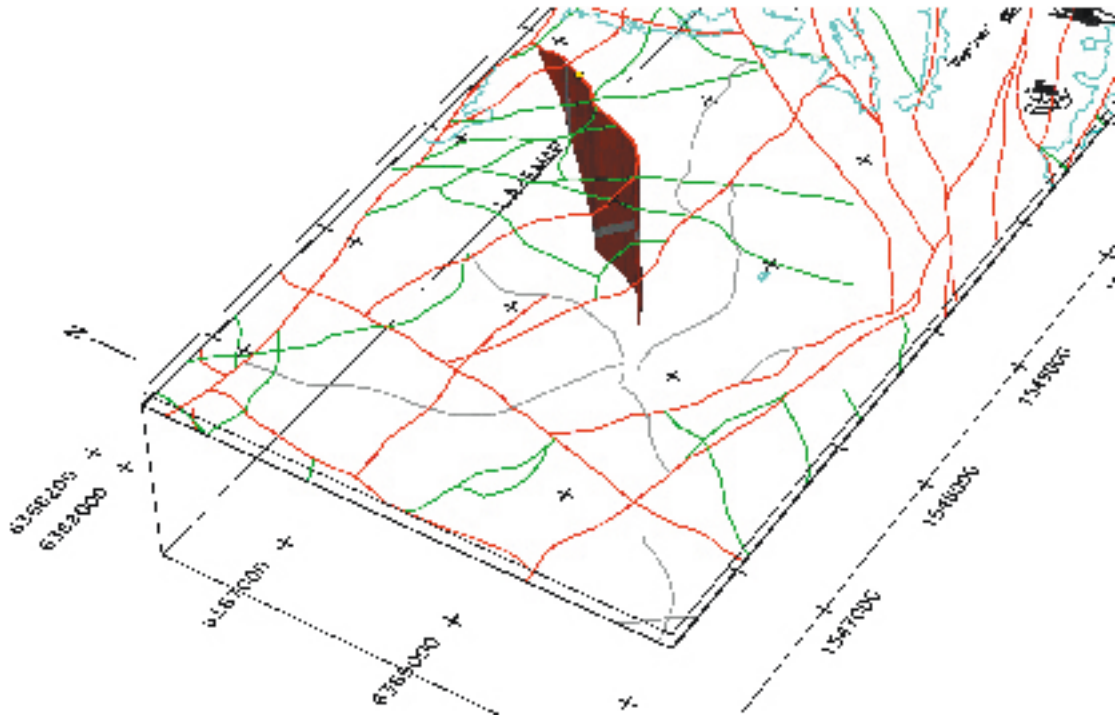


Figure 5-74. ZSMNE040A is modelled with a geometry of 030/90 and a geological thickness of 20 m including its transition zone.

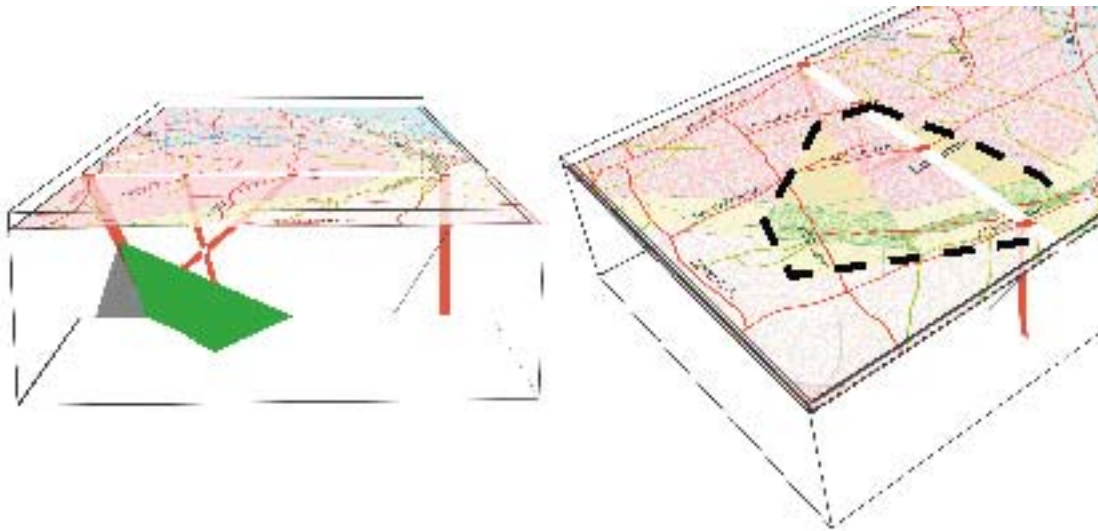


Figure 5-75. ZSMNW928 (green in the left illustration and hatched black line in the right) is modelled with a geometry of 120/28 and currently with no attributed geological thickness.

The possible intersection point in KLX02 (at 770–960 m) is indicated in the single-hole interpretation as a generally increased frequency of open fractures with increased oxidation. The most intensely fractured part of the zone is located between 845–880 m, cf. Figure 5-76, which is indicated by distinct low p-wave velocity and partly by a somewhat reduced resistivity. Nine radar reflectors from directional antenna have been attributed to the zone. The geometry of the reflectors is strike 94 to 133 degrees and dip 29 to 56 degrees. Most of them are dipping around 50°. A number of sections with increased fracturing may indicate associated minor deformation zones currently of unknown orientation.

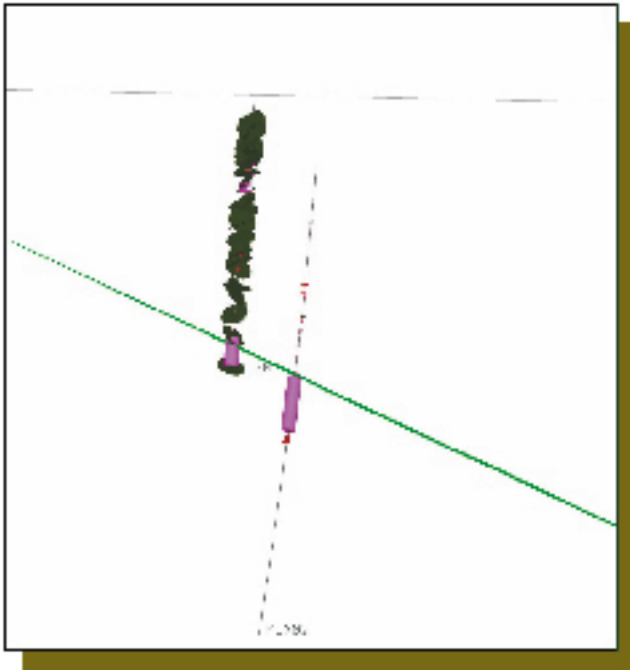


Figure 5-76. Possible intersection points with KLX04 (left) and KLX02 (right). ZSMNW928A is illustrated by the green line intersecting the boreholes.

The interpreted possible intersection point in KLX04 (at 873 to 973 m) is indicated in the single-hole interpretation as repetitive sections of crush and sealed networks. Alteration is evident in the upper part of the section.

The frequency of open fractures is relatively high, but variable throughout the section with a core zone characterised by strong inhomogeneous brittle deformation. The most intensely deformed part of the zone is found between c. 930 and 973 m. An intensely crushed part, between 936–946 m, correlates well with the seismic reflector N /Juhlin et al. 2004b/ at 940 m. Low resistivity, variable sonic, very low susceptibility and minor caliper anomalies are found in the sections 875–895 m and 935–971 m of KLX04.

Several radar reflectors are found within the zone, one at 877.5 m with the orientation 071/25, and one at 970.7 m with the orientation 046/20 or alternatively 270/07. Eleven radar reflectors have angles between 52–88° to the borehole axis, whereas one at 915.7 m has an angle of 31° to the borehole axis and one at 888.5 m has an angle of 21° to the borehole axis. The rock type is interpreted to be granite to quartz monzodiorite, generally porphyritic (Ävrö granite).

5.4.5 Evaluation of uncertainties

At present, thirty-five (N=35) deformation zones are attributed a high confidence of occurrence. One hundred and fifty-five (N=155) deformation zones are interpreted with medium or low confidence of occurrence, of which sixty-two (N=62) are of medium confidence.

The uncertainties in the deformation zone model in the regional model area are dependent on the lineament map, which gives the fundamental surface information regarding the zones. Since there is considerable uncertainty concerning the interpretation of the geological significance of the lineaments, the 155 deformation zones that are based solely on indirect interpretation of lineaments (and their underlying data) are judged to have a lower degree of confidence. The majority of the latter zones are found in the western part of the local model area and in the regional model area.

Uncertainties also depend on the almost complete lack of subsurface information outside the local model area. Since all investigations during the complete site investigation will be focused to the local model area, these uncertainties are likely to remain throughout the site investigation.

As there is a limited amount of subsurface data, there remain considerable uncertainties concerning the extension at depth of all zones. It is assumed that zones extend as deep as their interpreted surface length although there are limited possibilities to check this assumption at present. Borehole intersections are relatively few in each deformation zone and are used to confirm its existence and indicate the geometry and geological character of selected zones. Even though deformation zones have been verified at some specific depths, the detailed geometrical relationships such as termination and connectivity are still considered uncertain for most deformation zones. This uncertainty is likely to persist throughout the site investigation programme, especially in the regional model area.

Deformation zones interpreted with low and medium confidence are observed through indirect lineament interpretations at the surface and are modeled with a vertical dip. High confidence zones have dip angles according to information from boreholes, tunnels or through seismics.

Not all deformation zones identified with a high degree of confidence have direct observations. In fact, only twenty-four out of thirty-five high confidence zones have been identified in boreholes, tunnels and through seismics, as is shown in Table 5-8.

Four deformation zones; NE010A, EW900A, NE018A and NE050A have been identified through field observations in combination with several indirect data sources but generally lack confirmation from boreholes (EW900A may have indications from percussion boreholes, but the data are inconclusive).

Seven deformation zones; NE011A, NE019A, NE040A, NS009A, NW931A, NW932A and NW933A have been identified based only on strong support from geophysical profiles in combination with other sources of indirect data. The confidence that these deformation zones indeed exist is high, but confidence in their orientation, geological character and extent at depth is of course lower than for zones that have been penetrated by boreholes.

In addition, an alternative study of lineaments was conducted by an independent geological team using the same underlying topographic and airborne geophysical data /Korhonen et al. 2005/. A preliminary assessment of this independent analysis shows that there are few deviations from the lineament interpretations and the resulting lineament map used in the current model version. This preliminary assessment adds confidence that the lineament map in itself is rather stable, i.e. linear anomalies in the underlying data are interpreted in the same way by independent geological teams.

In summary, the confidence that all thirty-five high confidence deformation zones exist is high although the uncertainty with regards to extent at depth, dip angle and geological character is variable depending on the amount of available data.

Table 5-8. High confidence deformation zones (N=24) that have been verified by borehole, tunnel or through seismics at depth.

Zone ID	Alternative name	Class	Zone ID	Alternative name	Class
ZSMEW002A	Mederhult zone	Regional	ZSMNE015A		Local Major
ZSMEW007A		Local Major	ZSMNE015B		Local Major
ZSMEW009A		Local Major	ZSMNE016A		Local Major
ZSMEW013A	EW1A	Local Major	ZSMNE024A		Regional
ZSMEW023A		Local Major	ZSMNE031A		Local Major
ZSMEW038A		Local Major	ZSMNE930A		Local Major
ZSMNE004A		Regional	ZSMNS001A–D		Regional (A–D)
ZSMNE005A	Äspö shear zone	Local Major	ZSMNS017A–B	NNW4	Local Major
ZSMNE006A	NE1	Local Major	ZSMNS059A		Local Major
ZSMNE012A	NE4	Local Major	ZSMNW025A		Local Major
ZSMNW928A		Local Major	ZSMNW028A		Local Major
ZSMNW929A		Local Major	ZSMNW042A		Local Major

5.5 Statistical model of fractures and deformation zones

Discrete fracture network parameters are calculated through a series of steps, each of which depends on the results of the preceding steps. Fracture set identification and definition is the first necessary step in constructing the geological DFN model; each set may have a different ensemble of parameters that may be very different between sets. Fracture sets are defined for convenience in generating distributions of significant fractures in terms of properties such as orientation and size (and ultimately hydraulic parameters, cf. Chapter 8). Sets need neither be homogenous nor stationary, provided there is a consistent reason, backed by geologic evidence, for grouping the fractures together. In addition, the formation of a set or a group of sets reflect the mechanics of fracture formation, including stress state, strain, and rock strength of the lithologies surrounding the local model domain for a specific spatio-temporal situation.

Once fracture sets have been identified and specified, it is necessary to determine the geometrical description of each set. For a single fracture set, this description includes:

- Set orientation distribution, expressed as the trend and plunge of a mean pole calculated from all members of the set and the distribution function about this mean.
- Fracture set size expressed as a size-frequency radius distribution, honouring one or more of the following probability distribution functions: normal, lognormal, exponential, power law or uniform. Though not explicitly part of the radius distributions, suggested maximum and minimum size truncations are also included. These truncation values have an impact on fracture intensity in any DFN model implementation.
- Fracture set intensity. These are generally specified as P_{32} values, which represent the amount of fracture surface area (m^2) per unit volume (m^3) of rock.
- Fracture set spatial model. The spatial model controls the spatial distribution of fractures within the model volume.

5.5.1 Modelling assumptions and input from other disciplines

There are several assumptions that have been made in order to construct the DFN model for the Laxemar 1.2 model version. Each assumption is described below, along with its interpreted impact on the model, a rationale for why the assumption is reasonable, and recommendations for future re-evaluation of the assumption.

Assumption 1: The length of a deformation zone trace or a fracture in outcrop is an accurate and appropriate measure of a single fracture's trace length for the purpose of deriving the radius distribution of geologic structures.

This assumption contains two parts: that a deformation zone trace or a fracture in outcrop is a sufficiently accurate measure of a fracture's length; and that it is the appropriate one for computing size statistics. The purpose of using traces from the deformation zone model is to develop a DFN model that has fracture sizes and intensities that allow the adequate reproduction of flow and transport over large and small scales simultaneously.

The potential uncertainties in trace lengths at the outcrop scale are manifested (along with other uncertainties) as the variance among area-normalised frequency values for the outcrops.

Assumption 2: If a fracture set in outcrop represents a size-censored portion of a population of fractures that include a deformation zone-related trace set, then the fracture set in outcrop should have the same orientation as the deformation zone set. Conversely, the similarity in orientation is evidence in support of (however non-conclusive) combining the two separate groups of traces into a single set.

If both the fractures in outcrop and the fractures defining the deformation zones are part of a single population, then they are likely formed by the same geological and mechanical processes. As such, they should have similar orientations. While similar orientations could occur even if the two fracture sets were not part of the same parent population, it is less probable. If there is evidence to suggest

that the fractures in outcrop formed at a different time than the deformation zones, then this would be evidence that the two were not part of the same parent set. This assumption does not imply the existence or non-existence of fractures of intermediate size between outcrop and deformation zone scales.

Assumption 3: There is a ‘tectonic continuum’ between the outcrop-scale features (fractures) and the regional-scale structures (kilometre-scale deformation zones). Some of the outcrop fracture patterns constitute a small-scale expression of regional features. The size calculation for deformation zone-related sets is based upon fitting a power law curve to the combined data set of deformation zone and outcrop fracture trace lengths.

It is possible that most deformation zones are actually faults, while most outcrop fractures are mostly joints, which could be in different orientations and have different size characteristics. However, if the orientations are similar and the trace lengths appear to scale as a power law, then the simplest model to explain both these observations is that they are part of a tectonic continuum of fracturing extending from centimetre-scale fractures to kilometre scale fractures. Such a set of fractures can then be described by a single power-law size distribution.

Assumption 4: Variations in fracture intensity as a function of rock type, alteration zone or any other geological control can be extrapolated from sampled boreholes and outcrops to yet unsampled parts within the same rock domain.

Thus far, information on geological controls for fracture intensity variation suggests that lithology and alteration degree may constitute important controls. In order to specify fracture intensity throughout the model region, it is necessary to infer geologic similarity of unsampled rock domains to sampled ones, or to adjust model parameters for unsampled rock domains inferred from the presence of similar geologic or tectonic controls.

Assumption 5: For the Laxemar 1.2 geological DFN model, it is assumed that the fractures can be approximated as planar, circular discs possessing no thickness and whose orientations conform to the orientation statistics found through the methods described in Section 5.5.2. No statements are made regarding the aperture or hydraulic properties of the DFN fractures, for the latter properties see Chapter 8.

Although the fractures in the rock are probably neither circular nor planar, there are not sufficient data to mathematically characterise deviations from these two idealisations. In outcrop, deviations from planarity do not appear to be large. The major impact would be in the trace length computations, as the trace length will be equal to or longer than a straight line (or planar surface) connecting the fracture endpoints. The longer trace lengths will tend to promote higher fracture network connectivity. There are also mechanical reasons to presuppose that the actual fracture shapes may tend towards being equant (non-elongated), as the mechanical layering present in sedimentary rocks which promotes non-equant fracture shape is far less well-developed in the crystalline rocks of Laxemar and Simpevarp.

Assumption 6: The three-dimensional geometry of deformation zones is used as defined in the deformation zone model.

While assumption 5 stipulates that calculations in the DFN model are performed using a simple concept where fractures are planar discs regardless of their size, deterministic deformation zones from the deformation zone model are used as a direct input to the DFN model. Thus, assumptions underlying the deformation zone model apply also here, i.e. zones extend as deep as they are long.

Assumption 7: Since existing outcrop data are insufficient for making detailed studies of fracture size throughout the region of interest, it has been assumed that sizes may vary by subarea and rock domain, but that within each domain and subarea, sizes are assumed homogeneous.

It is not obvious as to what implications this assumption may have on hydrogeology and solute transport. Improved resolution will require a much greater amount of outcrop and borehole data.

The statistical model of fractures and deformation zones (geological DFN) has made use of the following information:

- 2D deformation zone traces from the Simpevarp 1.2 deformation zone model. Since the current DFN model was developed simultaneously with the Laxemar 1.2 deformation zone model, no input from the latter model was possible.
- Detailed fracture outcrop data from the Simpevarp outcrops ASM000025, ASM000026, ASM000205, ASM000206 /Hermanson et al. 2004/.
- Detailed fracture outcrop data from the Laxemar outcrops ASM000208 and ASM000209 /Cronquist et al. 2004/.
- Scan-line mapping from Simpevarp and Laxemar /Wahlgren et al. 2003, Berglund 2004/.
- 122 small outcrop mappings by /Ericsson 1987/.
- Fracture data from percussion boreholes HLX15, HLX25, HLX26, HLX27, HSH01, HSH02, HSH03 and cored boreholes KAV01, KAV04A, KAV04B, KLX01, KLX02, KLX04, KSH01A, KSH01B, KSH02, KSH03A, and KSH03B.
- A preliminary version of the rock domain model for Laxemar 1.2, dated 2005-01-10 (the delivery of the final model presented in Section 5.3). The difference between the preliminary delivery and the final rock domain model is considered minor with respect to the geological DFN analysis and consists mainly of slightly adjusted sections related to specific rock domains in the cored boreholes in the Laxemar subarea. Thus, the analysed fracture frequency has been assigned to these preliminary intersections in the cored boreholes and may not exactly reflect the same sections as given by the final rock domain model.

The Laxemar 1.2 DFN model essentially addresses deformation zones and fracture statistics in the local model domain that are equivalent to those used for the Simpevarp version 1.2 model /SKB 2005a/. The fracture analysis is extensive and is reported in full in /Hermanson et al. 2005/. Below follows a summary of the geological DFN model including alternative interpretations.

5.5.2 Conceptual model with potential alternatives

Orientation

Outcrop fracture sets were identified visually using the following qualitative properties and characteristics:

- Pole clustering on contoured stereonet plots.
- Similarity in orientation; i.e. representing consistent groups of common strikes.
- Fracture evolution (terminations, cross-cutting relationships, obvious steps or splays).
- Relationships to bedrock structures (orientations of foliation, bedding planes, igneous dykes).
- Characteristic lengths in outcrop (i.e. one grouping was consistently longer or shorter than another).

The fundamental assumption in the set classification process was that feature orientation, rather than size or host lithology, was the single-most important factor in determining membership of specific orientation sets.

Once the assignments on outcrop were completed, the sets were characterised either as regional or local in nature; this classification was based on the following criteria:

- Regional sets: Show consistent structural relationships to mapped deformation zones or to major geologic features (such as dykes, foliations, or bedding planes). Regional sets may also show consistent orientation or age relationships between outcrops. Regional fracture sets are an important components of the final DFN, as they most likely represent the second major control on rock-mass stability and groundwater flow (the deformation zones exerting the primary control).

- Local sets: Show changing orientations, sizes, or intensities from outcrop to outcrop. May be related to rock parameters or stress conditions that are spatially variable. May affect rock mass stability and groundwater flow on a local scale, but are most likely less important on a regional scale. Local sets may be confined to a single outcrop.

Additional cell mapping derived from regional bedrock mapping campaigns /Wahlgren et al. 2004, Berglund 2004, Ericsson 1987/ was qualitatively utilised to determine whether the models of fracture set orientations developed through detailed analysis of large-scale bedrock outcrops were visible on a regional scale, as well as, the general spatial relationships between identified sets, structural features, and rock domains.

The Laxemar 1.2 geological DFN model uses only univariate Fisher spherical probability distributions for the regional fracture set orientations, despite the fact that they are not always statistically significant, or the most statistically significant, (this was due to technical requirements of downstream model users on the distribution models used). Alternative spherical probability distributions (Bivariate Bingham, Bivariate Fisher) were also considered (but not implemented); at the local scale, these distributions tended to show better statistical fits to the observed data for some of the sets.

Table 5-9 and Table 5-10 show the chosen Laxemar 1.2 fracture orientation models for the Laxemar and Simpevarp subareas, respectively. These sets are based solely on univariate Fisher spherical probability distributions, and represent the ‘best fit’ to observed stereonet patterns.

Fracture sets S_A, S_B and S_C are all regional and are visible in outcrop and in the pattern of deformation zone traces. Fracture sets S_f and S_e are local variations of fracture sets which differ between subarea Laxemar and Simpevarp and are visible only in outcrop. Fracture set S_d is the subhorizontal fracture set which is rarely seen in outcrop, but is very common in the predominantly sub-vertical boreholes in both subareas.

Table 5-9. Fracture orientation set model (Laxemar subarea).

Laxemar subarea						
Set name	Probability distribution	Mean pole trend	plunge	Dispersion (k)	Goodness of fit K-S	% sig
S_A	Univ. Fisher	338.1	4.5	13.06	0.031	55.60%
S_B	Univ. Fisher	100.4	0.2	19.62	0.058	10.70%
S_C	Univ. Fisher	212.9	0.9	10.46	0.076	15.70%
S_d	Univ. Fisher	3.3	62.1	10.13	0.021	99.70%
S_f	Univ. Fisher	243.0	24.4	23.52	0.216	N/S

Table 5-10. Fracture orientation set model (Simpevarp subarea).

Simpevarp subarea						
Set name	Probability distribution	Mean pole trend	plunge	Dispersion (k)	Goodness of fit K-S	% sig
S_A	Univ. Fisher	330.3	6.1	16.80	0.091	N/S
S_B	Univ. Fisher	284.6	0.6	10.78	0.076	N/S
S_C	Univ. Fisher	201.8	3.7	14.60	0.043	5.20%
S_d	Univ. Fisher	84.6	81.8	6.98	0.053	6.90%
S_e	Univ. Fisher	67.1	15.5	11.73	0.105	N/S

Size

Fracture size analyses were performed on each fracture set identified by the preceding set identification analysis.

A non-linear optimisation process was used to calculate the parameters (e.g. mean, standard deviation) for a probability distribution model (e.g. lognormal, powerlaw, exponential) that best reproduced the observed trace length statistics for local fracture sets (S_d, S_e, S_f).

A second method, applied to regional (deformation zone-related) outcrop sets (S_A, S_B, S_C), was to calculate an area-normalised trace length frequency relationship. This was done by combining trace lengths from outcrop and deformation zones for the same set, and fitting a single scaling function to them as is shown in Figure 5-77.

The calculation of the fractal mass dimension is used to determine whether an Euclidean or Fractal function best characterises the scaling behavior of each individual deformation zone-related fracture set. The mass dimension exponent can vary from 2.0, which indicates Euclidean scaling, to lower values that imply that the traces scale in a fractal manner. The scaling behaviour is important to enable combination of data obtained over regions of very different area.

Intensity

Fracture intensity can be quantified by several measures, including the number of fractures per unit length (P_{10}), the number of fractures per unit area (P_{20}), the amount of trace length per unit area (P_{21}), and the amount of fracture surface area per unit volume of rock (P_{32}).

However, P_{32} is not measurable in the field; usually only values of P_{10} from boreholes or P_{21} from outcrop maps are available. Fortunately, it is possible to estimate P_{32} from either P_{10} or P_{21} through simulation. Thus, the procedure to calculate fracture intensity involves first determining geological controls on P_{10} and/or P_{21} , and then converting these values to values of P_{32} .

The determination of geological controls on fracture intensity relies upon comparing fracture intensity from boreholes with borehole geology, and subsequent evaluation of possible controls on intensity variations in outcrop. The boreholes form the primary source of data since:

- They provide a record of fracturing from the surface or near-surface to beyond the depth of the proposed repository.
- There are large amounts of fracture data from the boreholes, leading to better statistical power for hypothesis testing.
- The boreholes sample a wider variety of geological conditions than do the outcrops.

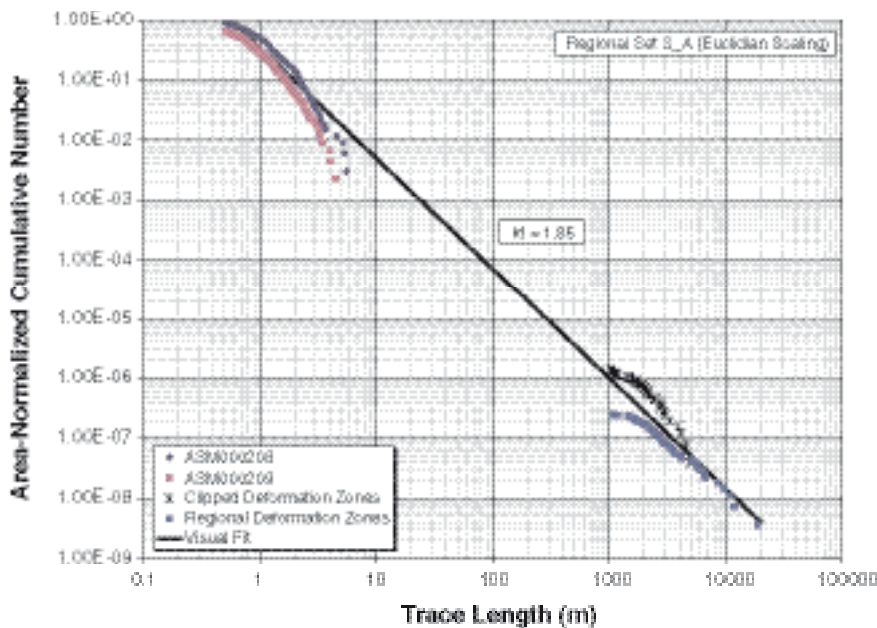


Figure 5-77. Euclidean trace length scaling plot for regional set S_A (Laxemar subarea).

- However, borehole data may be biased towards subhorizontal fracturing and may hence be better suited for investigating controls on subhorizontal fracture intensity.

Three approaches were used to evaluate spatial trends in fracture intensity: a) by plotting the moving average of a one-metre bin size fracture intensity data, over a five-metre window, b) by calculating the number of fractures per unit length (P_{10}) for varying interval sizes, and c) through Cumulative Fracture Intensity (CFI) plots.

The approach for calculating P_{32} from P_{10} or P_{21} requires simulation. The relation between P_{32} and the measurable fracture intensity quantities is given by:

$$P_{32} = C_1 P_{10} \text{ AND } P_{32} = C_2 P_{21} \quad \text{Equation 5-1}$$

where the constants C_1 and C_2 depend only upon the orientation of the borehole and the orientation distribution of the fracture set given that the borehole is simplified to a one-dimensional scan-line with zero radius. The goal of the simulations is to estimate C_1 if borehole data are being used and C_2 if outcrop data are used.

The form and parameter values of the size distribution model are important when the observed trace length distribution has been truncated. The amount of P_{21} that is removed by applying a threshold trace length size is sensitive to the form of the distribution (power law, lognormal, etc.), and hence the form of the distribution and its specific parameters become important. If there is no trace length sampling truncation applied, then the factor relating P_{32} to P_{21} does not depend either upon the form of the radius distribution or on its parameter values.

The workflow for calculating the conversion factor is as follows:

For any specified value of the power-law radius exponent (k_r), it is possible to find a combination of the minimum radius (x_{0r}) and P_{32} that will match exactly a value of P_{21} for which the measured and simulated traces have been excluded if they are shorter than the truncation length of traces on outcrop. In other words, the determination of P_{32} is not unique because there are two degrees of freedom, x_{0r} and P_{32} , and only one parameter to match, the truncated value of P_{21} .

However, it is possible to introduce a second constraint to make the solution unique. In this report, the second constraint is a value of P_{10} from boreholes in the same rock domain as the outcrop. A simultaneous match to the borehole P_{10} and the outcrop P_{21} does provide a unique set of values for x_{0r} and k_r as is schematically illustrated in Figure 5-78.

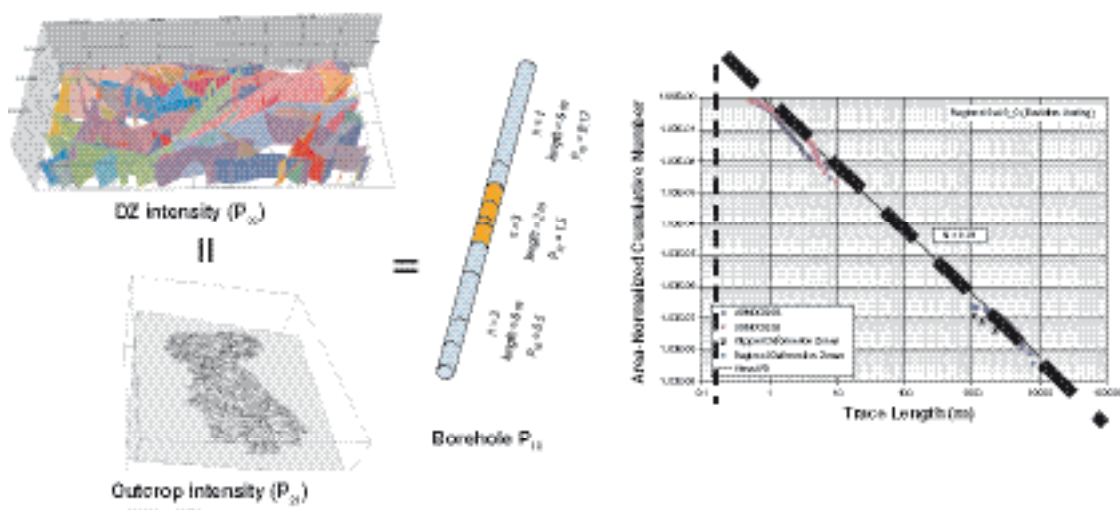


Figure 5-78. Schematic illustration of the procedure for obtaining a simultaneous match between deformation zone (P_{32}), outcrop (P_{21}) and borehole (P_{10}) intensity by finding a matching pair of the power-law radius exponent and the minimum radius.

Spatial model

The location of the fractures is specified by a combination of the intensity and spatial models. The spatial model describes how the location of fractures varies within spatial domains of stationary intensity. The spatial model is determined through the calculation of the mass dimension of the number of fractures per unit area (D_m) for outcrop trace data, and the number of fractures per unit length (P_{10}) for borehole data.

Outcrop trace data are used for calculating the spatial model for the subvertical fracture sets, as borehole data contain a bias that makes calculations for the subvertical sets in boreholes less reliable than the calculations based on outcrop data. The borehole data are used to determine the spatial model in the vertical direction for all of the sets in the domains where intensity is assumed stationary.

If the mass dimension has a value of 2.0 for trace data or 1.0 for borehole data, the fractures follow a Poisson distribution, i.e. the fractures are randomly positioned in space. Values less than 2.0 for trace data (less than 1.0 for borehole data) indicate a clustering process where there is some degree of spatial correlation among the locations of the fracturing. The failure of the data to approximate a straight line on the mass dimension plots indicates that the spatial model is something other than Poissonian or fractal. This would suggest that a further investigation of the spatial distribution of deformation zones and fracture sets is necessary, using a separate set of calculations and additional field data.

Alternative models

There are several Laxemar 1.2 DFN model alternatives:

- Different fracture orientation and size models are used for the subareas Simpevarp and Laxemar, based on the interpreted influence of the tectonic situation in the Simpevarp peninsula.
- Different fracture intensity models are employed for different rock domains. Currently there are stable fracture intensity models for rock domains A and B based on available borehole data.
- Different spatial models depending on the size of the model volume.

These three model alternatives can be combined in several ways to provide both local and regional scale DFN model input, in both subareas and for several types of rock domains. The models, as discussed above, are based on the same concept but exhibit different aspects of orientation, size and intensity. Should the downstream user require a DFN model in an area where no "hard" data are available, he or she has the option to combine the provided alternative models the way he/she thinks is most appropriate, see also Section 5.5.4.

5.5.3 Verification demonstration

A verification has been performed to evaluate if the geological DFN model for the Laxemar 1.2 local model domain is consistent with characteristics measured on outcrops and in boreholes from where it was derived, and if the model is consistent with a combination of selected core and outcrop data in the Laxemar and Simpevarp subareas.

The verification was limited to geometrical model parameters of the Laxemar 1.2 DFN model. More precisely, the consistency between the DFN model and field data was evaluated in terms of statistical distributions of the following four parameters:

- fracture frequency (P_{10} , m^{-1}) in boreholes,
- fracture intensity (P_{21} , m/m^2) in outcrops,
- trace lengths in outcrops, and
- fracture orientation in outcrops.

In the simulated borehole exploration, DFN realisations were sampled over 25 m borehole sections and on outcrops of similar sizes as the mapped outcrops.

General observations from the simulated exploration of the Laxemar 1.2 geological DFN model are:

- The general visual impression is that fracture orientations and spatial distribution of simulated outcrop fractures are similar to observed data as is illustrated in Figure 5-79 a and b.
- The total simulated fracture intensity (P_{21}) in outcrops is overestimated as can be seen in Figure 5-79 b and c.

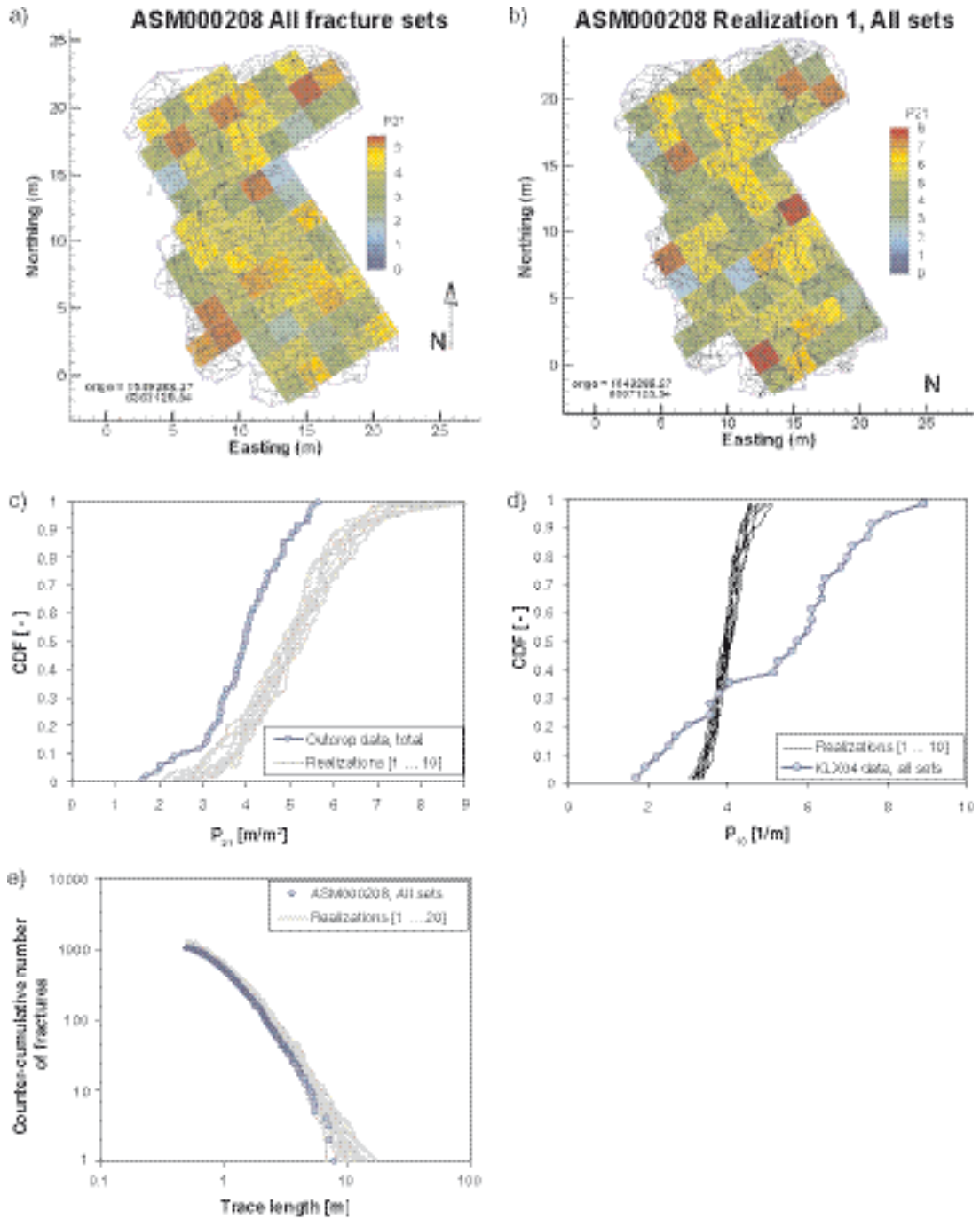


Figure 5-79. Evaluation of Laxemar subarea, RSMA, all fracture sets. Traces of outcrop ASM000208 compared to one realisation. Simulated fracture properties (10 realisations, grey lines) are compared to field data (blue), in terms of: c) fracture intensity, P_{21} , d) fracture frequency, P_{10} , and e) trace length distribution.

- The total simulated fracture frequency in 25 m-borehole sections (P_{10}) is underestimated, cf. Figure 5-79 d.
- The variability in simulated fracture frequency in 25 m-borehole sections (P_{10}) is underestimated, cf. Figure 5-79 d.
- The simulated trace orientations are similar to outcrop data, both in terms of mean pole and in dispersion around their mean poles. However, local sets (S_d , S_e , and S_f) are slightly different from observed fracture data as is shown in Figure 5-80.
- The simulated fracture trace length distribution fit outcrop data well, cf. Figure 5-79 e.

The total intensity (P_{21}) in outcrop is overestimated because the two local sets (S_d and S_f , or S_e) are based on borehole fracture frequency data, whereas the global sets are based on outcrop intensity. Likewise, fracture frequency is underestimated for the same reason. This emphasizes that there is a need for finding additional ways to constrain the local fracture set geometries. This is possible by either finding new subvertical outcrops for better sampling of subhorizontal fractures, or constraining the data better by using hydraulic injection test and flowlog information.

The variability of fracture frequency is underestimated because P_{32} has been included as a constant in the model according to the summary tables in Section 5.5.5. However, if P_{32} variability is included in the simulations, the necessary variability in observed data can be reproduced (P_{32} variability is described in /Hermanson et al. 2005/). The variability that is still visible in the simulations can be attributed to the variability in the orientation definitions (i.e. Fisher κ).

However, it is also evident that the global sets generally match outcrop data rather well, and the local sets match average fracture frequency in boreholes rather well. The main reason for this is that the global and local sets reflect different underlying types of data.

5.5.4 Discussion and guidelines for usage

The derivation of fracture orientations reveal five sets; three regional sets (S_A , S_B , S_C) observable on both outcrop and in deformation zone traces and two local sets in each subarea (S_d and S_f or S_e in Laxemar and Simpevarp respectively).

The variation in local fracture orientations suggests, together with results from the deformation zone model, that the Simpevarp subarea is located within a belt of shear zones and exhibits significantly different fracture behaviour from that of the Laxemar subarea which is set in a more tectonically stable environment.

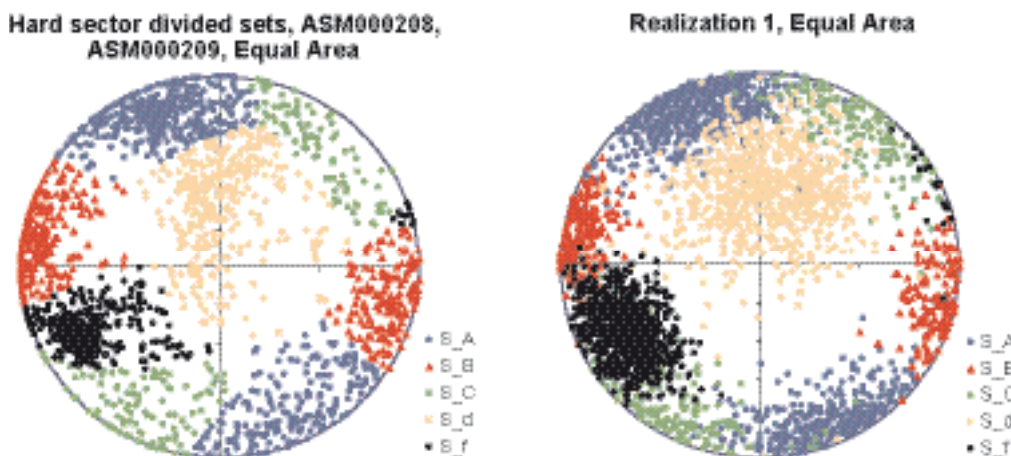


Figure 5-80. Stereoplots of simulated traces for the Laxemar subarea, RSMA: outcrop ASM000208 and ASM000209 data compared to one of five realisations.

The current DFN orientation distribution model may not be accurate enough for local-scale site studies. The five major aggregated fracture sets for each model subarea are likely a good enough match to regional fracture trends as to allow for reasonable regional groundwater flow and transport models. They can, however, be too simple for detailed shaft or tunnel stability analyses or canister failure evaluations. The presence of two or more additional subsets (visible in detailed outcrop trace maps) should be studied further; it may be necessary to further subdivide fracture sets, change set geometries, or change the set statistical distributions in subsequent model versions.

A limited analysis of borehole fracture orientation data suggests that, like intensity, fracture set orientations are not static functions and vary significantly with depth. The Laxemar 1.2 geological DFN orientation model is based solely on fracture patterns observed in outcrop, and it may not necessarily match conditions found at depth.

Fracture size analysis shows that regional fracture sets can be approximated by power-law size models. Local fracture sets are censored by the extents of the outcrops such that other size alternatives have better statistical fit. The local sets S_d , S_f and S_e are all censored by outcrop extents and also lack data for correlation with larger scale structures. A statistical fit to these sets better follow lognormal and exponential distributions as far as can be assessed at present. However, these size fits are very uncertain and will be necessary to re-evaluate in future model versions when more data are available.

Fracture intensity analyses shows that fracture intensity is:

- dependent on subarea,
- not dependent on surface stress relief,
- dependent on lithology,
- somewhat less dependent on rock domain.

Analysis of the fracture spatial distributions shows that fracturing is Poisson distributed on scales ranging from less than 30 to more than 100 m.

Fracture intensity for regional sets can be matched simultaneously to deformation zone, outcrop and borehole intensity by finding a unique pair of the power-law radius exponent and minimum radius for each regional fracture set.

Fracture intensity for local sets cannot be constrained in the same way and has to be derived from borehole P_{10} using outcrop size models. Validation exercises show that outcrop and borehole intensity cannot currently be matched simultaneously.

Fracture intensity is highly variable across both the Laxemar and Simpevarp subareas, and appears to be subject to a number of different geological controls. These appear to include host lithology, host rock domain, fracture age, degree of alteration, and presence of ductile or brittle deformation zones. The current level of understanding may be inadequate to characterise fracture intensity controls at either a regional scale or a local scale. Of particular concern are changes in intensity at depth, especially where anomalies in intensity are noted and no corresponding deformation zone has been identified.

For rock domain A in both the Laxemar and, especially for most regional sets, in domains A and B in the Simpevarp subarea, the P_{32} percentile derived from cored borehole fracture data, that allows for a match with the outcrop intensity, is typically below the median borehole fracture intensity value. In the case of the Simpevarp subarea, the percentile can be a very low value. This may be due to the spatial heterogeneity in fracture intensity (or perhaps in fracture size).

The outcrop intensity may represent something other than the mean or median fracture intensity, and so the resulting P_{32} and size model parameters for the regional sets incorporate this uncertainty.

Mapped outcrops may not contain a broad enough sample from which to estimate mean fracture intensity with much confidence. The boreholes, on the other hand, provide a much more comprehensive sample, and so the estimates of the mean intensity from borehole fracture data may provide more robust statistical characterisation of fracture intensity.

Below are given the parameter values necessary to implement the Laxemar 1.2 DFN model. The actual implementation is highly dependent on the study area chosen, the level of acceptable uncertainty for the model, and the software tools utilised to complete the simulation. A suggested set of modelling steps is presented below, however, it is strongly suggested that the reader refers to /Hermanson et al. 2005/ for a more detailed guideline.

Determine the location of the model volume within the Simpevarp area. If the model falls within either the Laxemar or Simpevarp subareas use the tables in Section 5.5.5 relevant to that subarea. The Laxemar 1.2 geological DFN model has not been developed with significant data from other locations (with the exception of several boreholes from Ävrö Island), and so it may not be valid for locations outside of the designated subareas.

- Determine several key factors: model scale, fracture size cut-offs, the location and extent of mapped rock domains within the desired modelling region, the subareas for each domain, and whether open, sealed or total fracturing is to be simulated.
- For each regional fracture set (S_A, S_B, or S_C), generate a fracture population within each rock domain model present within the model volume based on the parameters presented in Section 5.5.5. An example is presented below:
 - A model volume 2,000 m × 2,000 m by 2,000 m is chosen within the Laxemar subarea. The model volume contains two rock domains, A and D, of roughly equal size. Two separate iterations are required to generate a single realisation of regional set S_A.
 - Regional set S_A within Rock Domain A: Utilise the orientation model and dispersion for regional set S_A in the Laxemar subarea, the size model for regional set S_A in the Laxemar subarea, and the intensity model for regional set S_A within rock domain A. Orientations depend upon subarea and set.
 - Regional set S_A within Rock Domain B: Utilise the orientation model and dispersion for regional set S_A in the Laxemar subarea, the size model for regional set S_A in the Laxemar subarea, and the intensity model for regional set S_A within rock domain B. Orientations depend upon subarea and set.
- For regional fracture sets S_A, S_B and S_C in the Laxemar subarea and for regional set S_A in the Simpevarp subarea, specific values for x_{0r} and k_r and P_{32} are presented. Different minimum or maximum size cut-offs may be required for downstream modelling purposes, and if so, the P_{32} needs to be adjusted. It is up to individual modelling teams to choose values appropriate for their specific model volume from the parameters presented in /Hermanson et al. 2005, cf. Sections 6.2.1.1, 6.2.2.1 and 6.2.2.2 therein/. The size parameters depend upon subarea, rock domain and set.
- Specify an intensity value for each fracture set. This depends upon model scale, subarea, domain, set and any size cut-offs. Refer to the example of this calculation in /Hermanson et al. 2005, cf. Section 6.4 therein/.
- For each ‘local’ fracture set (S_d, S_e, S_f), generate a fracture population within each rock domain model present within the model volume based on the parameters presented in Section 5.5.5. The methodology is identical to that applied for the regional sets, except that a specific set of size model parameters is specified for each of the local fracture sets.
- “It is suggested that for simulation in the Laxemar subarea, rock domain A, DFN parameter values for regional sets are taken from Table 5-14 for all model sizes, except for extremely small models in the immediate vicinity of boreholes (i.e. metre to decametre scale). For simulating local fracture sets, Tables 5-14 and 5-15 should be used.”

If a different size truncation value for a specific orientation set or rock domain is desired, /Hermanson et al. 2005, cf. Equation 6-8 therein/, can be used to compute a new volumetric intensity based on a revised truncation threshold (P_{32t}). Additional model parameters, such as termination percentages, modifications of open-sealed fracture ratios, and fracture hydraulic parameters are left to the discretion of the individual modelling teams.

5.5.5 Summary of parameters of geological DFN models

Simpevarp subarea

Table 5-11. Orientation statistics for fracture sets in the Laxemar 1.2 DFN model (Simpevarp subarea).

Simpevarp subarea						
Set name	Probability distribution	Mean pole trend	plunge	Dispersion (k)	Goodness of fit K-S	% sig
S_A	Univ. Fisher	330.3	6.1	16.80	0.091	N/S
S_B	Univ. Fisher	284.6	0.6	10.78	0.076	N/S
S_C	Univ. Fisher	201.8	3.7	14.60	0.043	5.20%
S_d	Univ. Fisher	84.6	81.8	6.98	0.053	6.90%
S_e	Univ. Fisher	67.1	15.5	11.73	0.105	N/S

Table 5-12. Size statistics for fracture sets in the Laxemar 1.2 DFN model (Simpevarp subarea). P_{32} values are for all fractures (open and sealed). See Section 5.5.4 for explanations on how to use the data.

Simpevarp subarea					
Set name	Probability distribution	Mean radius or exponent (mass)	Mean radius or exponent (euclidian)	Standard deviation or min radius	Match point P_{32} (for regional sets only)
Domain A					
S_A	Power Law	2.72	2.76	0.864	0.320
S_B	Power Law	2.82	2.87	0.689	0.476
S_C	Power Law	2.92	3.00	0.596	1.312
S_d	Power Law	N/A	3.10	0.150	N/A
S_e	Lognormal	0.23	N/A	0.169	N/A
Domain B					
S_A	Power Law	2.72	2.93	0.367	2.152
S_B	Power Law	2.63	2.84	0.396	0.618
S_C	Power Law	2.66	2.88	0.372	0.868
S_d	Power Law	N/A	3.10	0.150	N/A
S_e	Lognormal	0.23	N/A	0.169	N/A

Table 5-13. Intensity (P_{32}) and spatial model for fracture sets in the Laxemar 1.2 DFN model (Simpevarp subarea). The intended scale of modelling for these intensity values is 30–100 m. See Section 5.5.4 for explanations on how to use the data.

Spatial Model: Poissonian for model discretisation regions of 30–100 m.

P_{32} ** intensity (m^{-1})	Set name	Mean P_{32} *	Open P_{32}	Sealed P_{32}	% Open fractures
Domain A	S_A	2.73	1.24	1.49	45.50%
	S_B	2.13	0.87	1.26	41.14%
	S_C	2.25	1.00	1.25	44.61%
	S_d	2.75	1.41	1.34	51.21%
	S_e	1.31	0.59	0.72	44.96%
Domain B	S_A	4.39	1.17	3.22	26.59%
	S_B	4.23	1.10	3.13	26.11%
	S_C	4.12	1.22	2.90	29.63%
	S_d	7.05	2.25	4.80	31.93%
	S_e	2.84	0.65	2.19	22.93%
Domain C	S_A	3.75	1.23	2.52	32.74%
	S_B	2.55	0.79	1.76	30.91%
	S_C	3.71	1.33	2.38	35.93%
	S_d	4.37	1.35	3.02	30.90%
	S_e	1.60	0.50	1.10	31.50%

* See Section 6.4 in /Hermanson et al. 2005/ for a more detailed explanation. If a coupled size/intensity alternative is preferred, the match point value of P_{32} shown in Table 5-12 should be substituted for the mean P_{32} for regional sets in Domains A and B. The open and sealed intensity values should also be adjusted accordingly by the ratio shown in this table.

** Note: Rock Domains BA, D, E, F, G, M(A), M(D), and P are not defined within the cored boreholes used to assign DFN intensities.

Laxemar subarea

Table 5-14. Orientation statistics for fracture sets in the Laxemar 1.2 DFN model (Laxemar subarea).

Laxemar subarea						
Set name	Probability distribution	Mean pole trend	plunge	Dispersion (k)	Goodness of fit K-S	% sig
S_A	Univ. Fisher	338.1	4.5	13.06	0.031	55.60%
S_B	Univ. Fisher	100.4	0.2	19.62	0.058	10.70%
S_C	Univ. Fisher	212.9	0.9	10.46	0.076	15.70%
S_d	Univ. Fisher	3.3	62.1	10.13	0.021	99.70%
S_f	Univ. Fisher	243.0	24.4	23.52	0.216	N/S

Table 5-15. Size statistics for fracture sets in the Laxemar 1.2 DFN model (Laxemar subarea). See Section 5.5.4 for explanations on how to use the data.

Laxemar subarea					
Set name	Probability distribution	Mean radius or exponent (mass)	Mean radius or exponent (euclidian)	Standard deviation or min radius	Match point P_{32} (for regional sets only)
Domain A					
S_A	Power Law	2.86	2.85	0.328	1.310
S_B	Power Law	2.92	3.04	0.977	1.026
S_C	Power Law	2.88	3.01	0.858	0.974
S_d	Exponential	N/A	0.25	0.250	N/A
S_f	Power Law	3.60	N/A	0.400	N/A

Table 5-16. Intensity (P_{32}) for fracture sets in the Laxemar 1.2 DFN model: Laxemar subarea. P_{32} values are for all fractures (open and sealed). The intended scale of modelling for these intensity values is 30–100 m. See Section 5.5.4 for explanations on how to use the data.

Spatial Model: Poissonian for model discretisation regions of 30–100 m.

P_{32}^{**} intensity (m^{-1})	Set name	Mean P_{32}^*	Open P_{32}	Sealed P_{32}	% Open fractures
Domain A	S_A	1.43	0.61	0.82	42.48%
	S_B	1.69	0.64	1.05	37.85%
	S_C	1.52	0.63	0.89	41.25%
	S_d	2.32	0.93	1.39	40.10%
	S_f	1.40	0.59	0.81	42.05%
Domain BA	S_A	1.20	0.81	0.39	67.44%
	S_B	1.51	1.11	0.40	73.74%
	S_C	1.05	0.64	0.41	60.67%
	S_d	1.16	0.97	0.20	83.06%
	S_f	1.26	1.01	0.25	79.78%
Domain D	S_A	2.00	0.13	1.87	6.41%
	S_B	1.45	0.02	1.43	1.06%
	S_C	0.71	0.12	0.59	16.13%
	S_d	3.14	0.13	3.01	3.96%
	S_f	0.53	0.01	0.52	2.44%
Domain M (A)	S_A	1.73	0.31	1.42	17.72%
	S_B	2.25	0.25	1.99	11.28%
	S_C	1.64	0.17	1.48	10.16%
	S_d	2.17	0.46	1.71	21.17%
	S_f	0.71	0.10	0.61	14.80%
Domain M (D)	S_A	3.60	0.55	3.05	15.24%
	S_B	2.27	0.33	1.94	14.56%
	S_C	3.81	0.60	3.21	15.68%
	S_d	4.12	1.11	3.01	27.04%
	S_f	2.08	0.37	1.71	17.83%

* See Section 6.4 in /Hermanson et al. 2005/ for a more detailed explanation. If a coupled size/intensity alternative is preferred, the match point value of P_{32} shown in Table 5-15 should be substituted for the Mean P_{32} for regional sets in Domains A and B. The open and sealed intensity values should also be adjusted accordingly by the ratio shown in this table.

** Note: Rock domains B, C, E, F, G, and P are not sampled in the Laxemar boreholes.

5.5.6 Evaluation of uncertainties

The use of spherical probability distributions with associated dispersions and goodness-of-fit statistics leads to a quantifiable level of dispersion uncertainty on fracture orientation. However, an evaluation of the chosen fracture set orientations indicates that none of the fitted fracture sets are statistically significant within a reasonable ($\alpha = 0.1$) confidence level. Whether the current model will accurately predict outcrop patterns at locations not already sampled is currently unknown.

Several outcrops (ASM000026, ASM000205, ASM000209) possess fractures, though identified as members of a single set through analysis of contoured polar stereonet, that may actually belong to separate sets. Because these sets overlap to a significant degree, they are difficult to distinguish through contouring. Since orientation set membership impacts both fracture size and intensity calculations, this conceptual model uncertainty in fracture orientations is inherent in the geological DFN model.

In addition, a limited evaluation of fracture orientation variation with depth suggests that set memberships (and perhaps set mean orientations) are not constant with depth. Since the DFN orientation model is based on fracture orientations in surface outcrops, this leads to an additional, non-quantifiable conceptual uncertainty: are the set divisions used producing a model whose fracture orientations are reasonable also at repository depth?

The most significant uncertainties overall are in fracture size and intensity. The analyses have shown that there are substantial variations in fracture intensity at a scale important for modelling. The uncertainty in intensity largely revolves around the issues of intensity extrapolation between scales, spatial variability (especially with depth), and with the presence of censored data. It is not known if the magnitude of these variations would have a significant impact on the groundwater flow or mechanical modelling, but since they span at least an order of magnitude and are not predictable, it is likely that they are significant for the downstream models.

The uncertainties in the intensity are the primary causes for the uncertainties in the size model for the regional sets. Currently, the range of possible size parameter values is a direct result of the uncertainty in the outcrop, borehole and deformation zone intensity uncertainties. This is due to both spatial variability in the size and intensity data, and also the lack of comprehensive fracture data in some of the rock domains. If it was possible to obtain accurate regional estimates of fracture intensity for all domains, then the uncertainty of the size models would be commensurately reduced for the regional sets. Moreover, if the uncertainty regarding local (borehole scale) variations in intensity were reduced, the local uncertainty of the size models would also be reduced accordingly.

Another uncertainty concerns the size of the horizontal sets. As it is unlikely that horizontal deformation zones, if they exist, will be easily detected through deformation zone analysis, it is uncertain at present as to whether the horizontal fracture sets found in outcrop and borehole are part of a parent subhorizontal fracture set that has some members with radii of hundreds or even thousands of metres, like the regional vertical sets. Since the horizontal fractures do not show mineralogical or morphological differences from the vertical sets, it seems more likely than not that these horizontal fractures do extend in size to hundreds or even thousands of metres.

6 Rock mechanics model

The rock mechanics model describes the properties of the intact rock and of the single fractures, as well as the properties of the bedrock on a larger scale, i.e. the rock mass between interpreted deformation zones and the rock within interpreted deformation zones. The rock mechanics model also includes a description of the in situ stress conditions in the area. These properties and state together are of importance, since they may affect the design and depth location of a possible geological repository. The starting point for the modelling work is an evaluation of the primary data, i.e. laboratory tests on core samples, measurements in boreholes and geological mapping of the drill cores. The estimation of rock mechanics properties for the rock mass is based both on empirical and theoretical approaches. The stress model is based on measurement observations, but is also supported by a numerical model of the site. The result of the modelling work is a list of predicted parameter values, for each rock domain defined within the local model area, including an estimation of variability and uncertainties. The presented rock mechanics model is developed in accordance with the strategy document for rock mechanics /Andersson et al. 2002a/.

6.1 State of knowledge at previous model version

The Simpevarp 1.2 description of the rock mechanics properties and the in situ state of stress consisted of estimates for deformation and strength parameters for both intact rock and the rock mass of defined (lithological) rock domains. The description was mainly based on data from five cored boreholes (KSH01A, KSH02, KSH03A, KAV01 and KLX02). Empirical characterisation schemes were used to estimate the mechanics properties of the rock mass. Furthermore, a theoretical approach was employed using the result from the geological DFN model and the estimates of intact rock and fracture properties to calculate the integrated rock mass properties. Old laboratory test data from the Äspö HRL were used together with the new results.

The rock mass in the Simpevarp subarea was described as having, on the average, normal (strong) mechanics properties typical of Swedish crystalline rocks, but being relatively inhomogeneous, with a large spread in fracturing characteristics, giving large spans for given parameter values. This was in accordance with the geological description showing that the defined rock domains were intersected by many smaller deformation zones. The stress model featured two different predictions resulting from dividing the local model volume into two different stress regions, with lower stresses below Ävrö and Simpevarp peninsula compared with the rest of the local model volume. The uncertainty within each region was lower than in the previous stress model (Simpevarp version 1.1), which showed quite large uncertainties, due to scarcity of data and a spread in the results from individual measurement points.

6.2 Evaluation of primary data

The primary data used for the rock mechanics modelling is briefly described in the following paragraphs. A list of the different data sources is given in Table 2-2.

6.2.1 Laboratory tests of intact core samples

To test the intact rock strength, uniaxial and triaxial loading tests were performed on samples from boreholes KSH01A, KSH02, KLX02 and KLX04. These tests are standard tests developed for drill core samples. The resulting load deformation curves have been interpreted to provide several standard parameters that have been put into the Sicada database. Some of the available test results from Sicada are shown in Table 6-1 and a more detailed compilation is given in /Lanaro et al. 2006/. It may be noted from Table 6-1 that the mean uniaxial compressive strength (UCS) is 192 MPa, 161 MPa and 205 MPa, respectively, for the three common rock types in the local scale model volume, respectively. The distributions of UCS and tensile strength data for the Ävrö granite are shown in Figure 6-1.

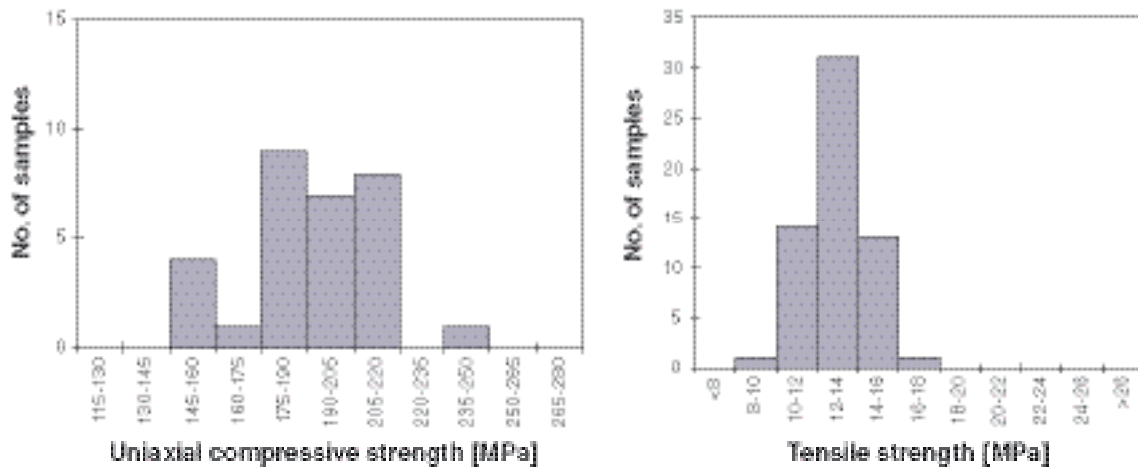


Figure 6-1. Histograms of a) the uniaxial compressive strength (UCS) and b) the tensile strength obtained from tests on core samples from KLX02 and KLX04. The rock type is granite to quartz monzodiorite (Ävrö granite), which is the most common rock type in the subarea.

Table 6-1. Laboratory test results on mechanics properties of intact rock samples. Mean values are provided. For further statistical details cf. /Lanaro et al. 2006/. See also the properties model in Table 6-5.

Laboratory test results	Granite to quartz monzodiorite (Ävrö granite)	Quartz-monzonite to monzodiorite	Finegrained dioritoid	Finegrained dioritoid including sealed fractures
Number of uniaxial tests	30	10	10	5
Number of triaxial tests	14	6	6	5
Mean UCS (uniaxial compressive strength), MPa	192	161	205	126
Mean σ_{ci} (crack initiation stress), from uniaxial tests, MPa	96	77	88	–
Mean E (Young's modulus) from uniaxial tests / triaxial tests, GPa	72 / 70	78 / 77	85 / 78	91 / 81
Mean ν (Poisson's ratio) from uniaxial tests / triaxial tests	0.20 / 0.18	0.27 / 0.22	0.26 / 0.21	0.24 / 0.18
Mean friction angle*	55.9°	59.5°	52.7°	49.3°
Mean apparent cohesion*, MPa	27.4	20.3	33.0	19.2
Number of indirect tensile strength tests (Modified Brazilian tests)	60	18	24	10
Mean tensile strength, MPa	13	18	19	14

*Best fitting Coulomb failure criterion based on both triaxial and uniaxial test results, but not based on the indirect tensile tests (see Figure 6-2). The confining stress levels were up to 20 MPa.

6.2.2 Laboratory tests on fracture samples

As a part of the standard testing program of drill core samples from the boreholes, normal stiffness tests and shear tests have been performed. Figure 6-3 shows a typical example of result from a normal loading test (a) and a shear tests (b) from one fracture, being sheared at three different normal stress levels and a good linear fit supports the use of the Mohr-Coulomb model, i.e. apparent cohesion and friction angle parameters. The difference between peak and residual strength values are in general small. The shear stiffness is defined as a secant stiffness from 0 MPa shear stress to half the peak shear stress.

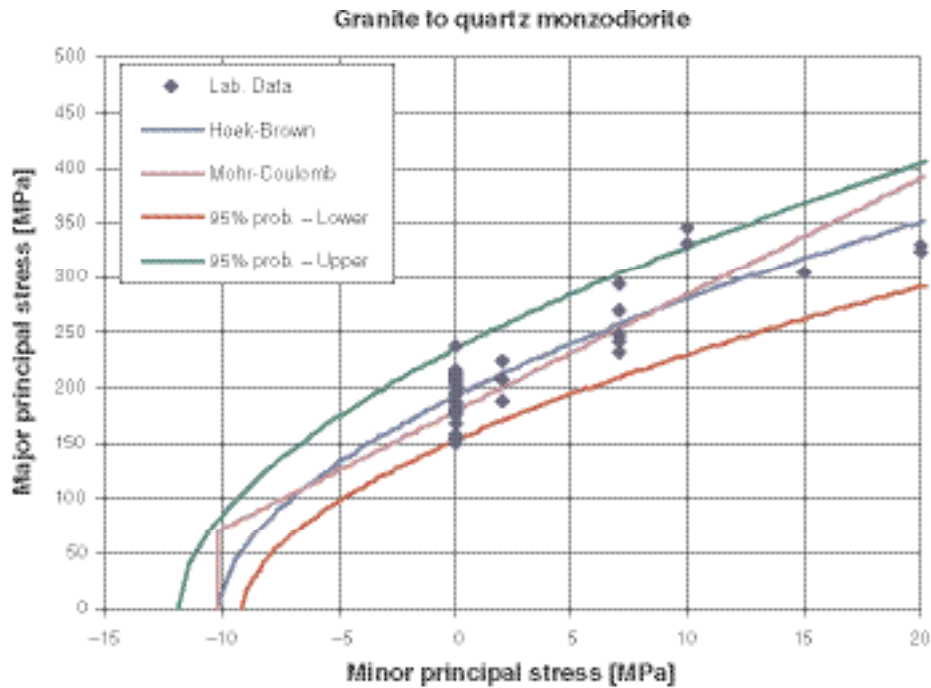


Figure 6-2. Major principal stress is plotted against minor principal stress at failure for each laboratory test on Ävrö granite (blue dots). The pink bilinear best fit model is the Coulomb model and this line has been used to determine the cohesion and friction angle parameters given in Table 6-1.

The shear testing methodology has been tested and improved during the course of the site investigation programme. In Table 6-2, the results from each of these test series are summarised and a significant difference between methods can be observed, in particular for the stiffness parameters. The results from the tests have also been studied separately for the different fracture sets. However, the results indicate fairly constant properties irrespective of the fracture set, i.e. no correlation between fracture properties and fracture orientation has been found so far. For further details on the fracture test results refer to the full compilation found in /Lanaro et al. 2006/.

Table 6-2. Normal and shear stiffness for the tested fracture samples. The tests were performed with different methodologies concerning sample preparation, casting materials and experimental set-up. Also the results obtained from tilt tests are given. /Lanaro et al. 2006/.

Method	Normal Stiffness		Shear Stiffness		Peak cohesion		Peak friction angle	
	k_n (MPa/mm)		k_s (MPa/mm)		c_p^{MC} (MPa)		Φ_p^{MC} (°)	
	Mean	St. Dev.	Mean	St. Dev.	Mean	St. Dev.	Mean	St. Dev.
Shear I	135	152	29	11	0.51	0.35	32	4.2
Shear II	237	79	41	12	0.82	0.37	36.6	3.0
Shear III	607	394	21	9	1.1	0.18	35.4	3.8
Tilt tests*	–	–	–	–	0.48	0.13	33.7	1.8

Shear I method: data from boreholes KAV01, KSH01A, and KSH02. 28 fracture samples.

Shear II method: data from boreholes KLX02 and KLX04. 19 fracture samples.

Shear III method: data from borehole KSH02. 7 fracture samples.

* From the Barton-Bandis' criterion for normal stresses between 0.5 and 20 MPa. 157 samples.

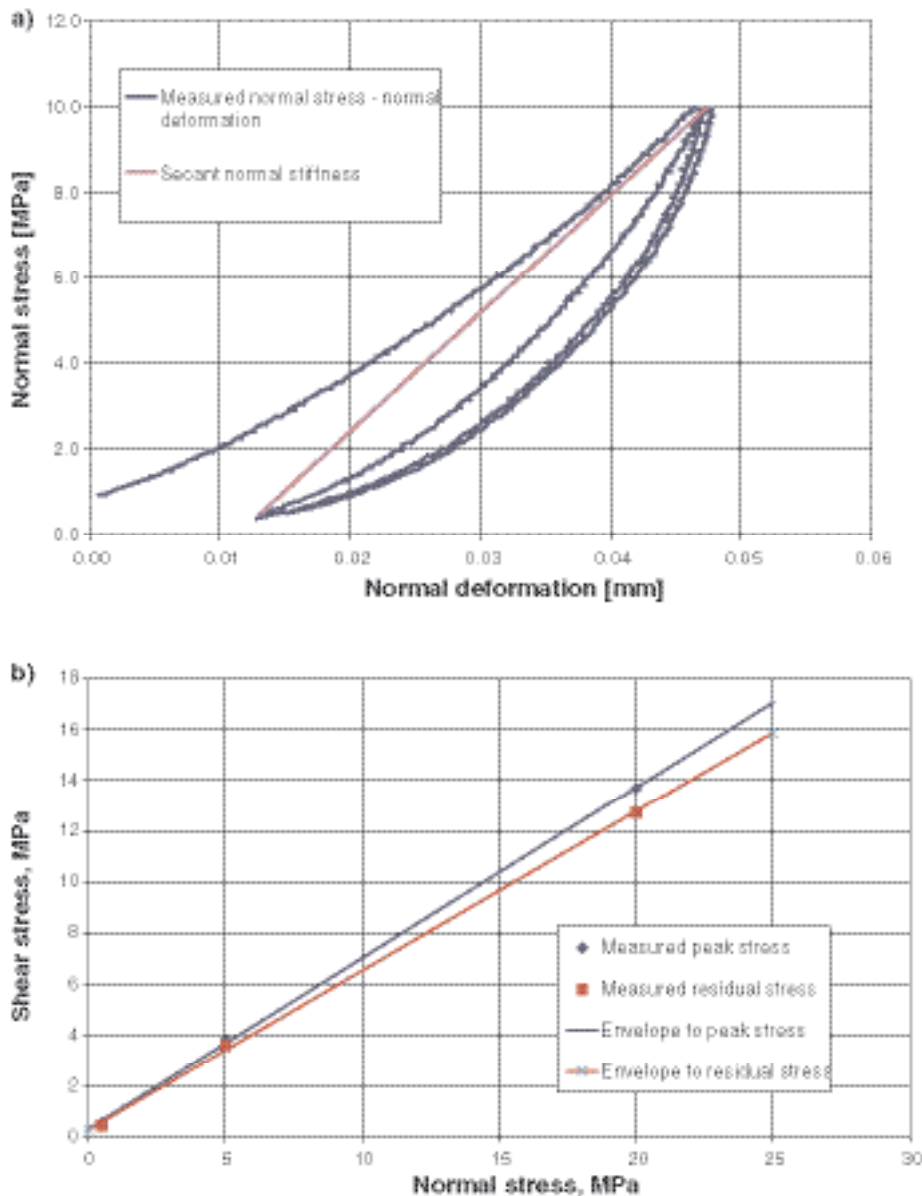


Figure 6-3. a). The definition of normal stiffness used: secant stiffness between 0.5 and 10 MPa normal stress on the second loading curve. b) Peak shear and residual shear strength according to the Coulomb's Criterion for one fracture sample (KLX02-117-1).

6.2.3 Rock mechanics interpretation of borehole data

Rock mechanics modelling employing empirical classification systems has been applied to the available borehole data. The primary data used are the Boremap logging data in the Sicada database. The methodology used is described by /Andersson et al. 2002a/. A compilation of the results from all boreholes which are part of the data freeze for the current model version, and a summary for the defined lithological rock domains, is provided by /Lanaro 2006/.

The empirical index Q is determined according to /Barton 2002/ and the empirical index RMR is determined according to /Bienawski 1989/. As an example, the results for Q along all additional studied boreholes for this model version are given in Figure 6-4. The mean value and the most frequent value of Q and the mean value of RMR for the different lithological domains are given in Table 6-3 and Table 6-4.

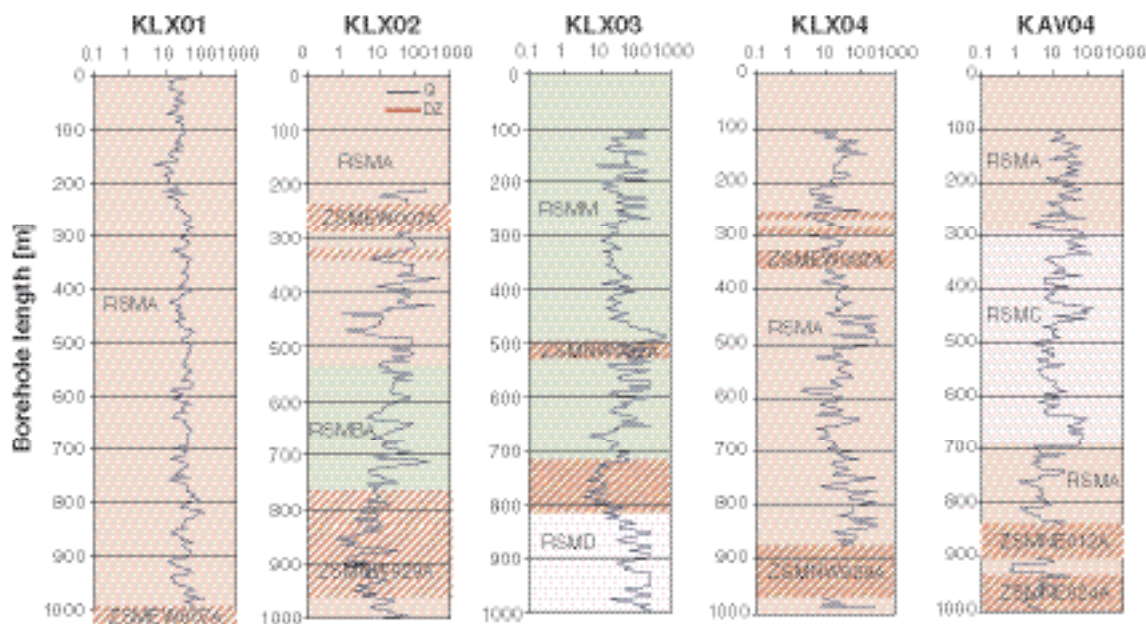


Figure 6-4. The empirical index Q for 5 m sections along the boreholes, shown by the blue curves. The division of boreholes into units is based on the geological single hole interpretation. The deformation zones are marked with red hatched stripes and the names of the deterministic zones are also given. Note that the axis for Q has a logarithmic scale.

Table 6-3. Empirical rock classification indices determined for the rock mass between deformation zones in the defined lithological rock domains.

Index	Domain A Subarea Laxemar	Domain A Subarea Simp. and Domain AB	Domain B	Domain C	Domain D	Domain M	Uncertainty in the mean estimation
Based on 5 m sections of drillcores	Mean value (Most freq.)	Mean value (Most freq.)	Mean value (Most freq.)	Mean value (Most freq.)	Mean value (Most freq.)	Mean value (Most freq.)	
Q (-)	45 (31)	35 (22)	23 (13)	27 (12)	155 (132)	82 (34)	± 3
RMR (-)	75	72	70	72	85	83	± 1

Table 6-4. Empirical rock classification indices determined for the rock inside the deformation zones, local major (deterministic) and local minor.

Index	Minor deformation zones and deterministic zones Domain A, Domain B, Domain AB and Domain C	Minor deformation zones and deterministic zones Domain D	Minor deformation zones and deterministic zones Domain M	Uncertainty in the mean estimation
Based on 5 m long sections of drillcores	Mean (Most freq.)	Mean (Most freq.)	Mean (Most freq.)	
Q (-)	5 (3)	31 (33)	11 (9)	$\pm 1-3$
RMR (-)	64	81	72	\pm Circa 10

6.2.4 Other data

Other data used are the analyses performed as part of the construction of the Clab II facility. The deformation modulus was, in this case, back-calculated from observed convergences and an estimated stress field /Fredriksson et al. 2001/. The most probable deformation modulus for the rock mass at Clab was estimated at 40 GPa.

Furthermore, results from back-analysis of the deformation modulus of the rock mass at the Äspö HRL have been used to compare with the results from the empirical and theoretical approaches. At the site of the Äspö HRL Pillar Strength Experiment (APSE) the deformation modulus has been estimated at 55 GPa, using results from tunnel convergence and stress measurements /Staub et al. 2004/.

6.2.5 Stress measurements

Rock stresses have been measured in 4 new cored boreholes as part of the site investigation programme at the Simpevarp and Laxemar subareas (KSH01, KSH02, KAV04 and KLX04, cf. Figure 2-3). All other existing measurement data from within the Simpevarp area have also been compiled jointly with the newer data. Figure 6-5 and shows the measurement results for the maximum and minimum principal stresses, respectively. Every point in the diagram represents one single measurement point and measurements in the same borehole are given the same symbol. Since the results show a large spread, a grouping of the data based on the geographical location of the borehole in relation to interpreted stress domain (cf. Section 6.4.2) was attempted and the red and blue symbols indicate these two groups.

The overall spread in the stress orientation data is large, but there is a clear concentration around the NW-SE orientation. For further details about the input data to the stress model see /Hakami and Min 2006/.

The scatter in stress magnitudes seen in Figure 6-5 may be explained either as a result of the uncertainty in the measurement method itself, or as a result of a true spread in the stresses. It is not possible, however, to determine how much each of the two factors influences the results obtained. In the modelling, it is assumed that the scatter in data represents a real stress variation and also that there are no systematic errors in the measurement data. How the measurement data were used to establish the final descriptive model is described in Section 6.4.

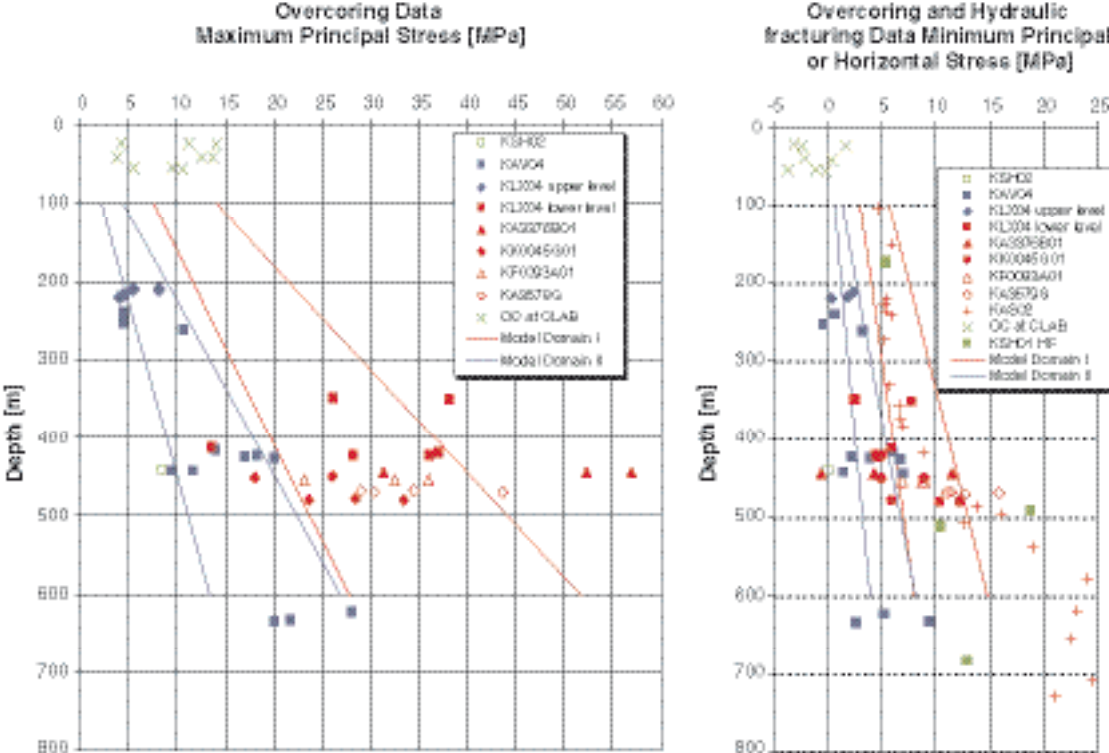


Figure 6-5. Results from stress measurements. a) Overcoring: maximum principal stress magnitudes. b) Overcoring: minimum principal stress magnitude, together with hydraulic fracturing measurements of minimum horizontal stress. The solid lines show the final model spans for the two different stress domains defined (see Section 6.4.4).

6.3 Rock mechanics property models

6.3.1 Assignment of properties for the intact rock

For the Laxemar 1.2 site descriptive model, laboratory data from the site investigation program are available for the three most dominant rock types.

The parameters are all described with truncated normal distribution functions as for SDM Simpevarp 1.2. The values were basically taken “as is” from the test results, but some deviations from this approach were made. The spread (the standard deviation) in the normal distribution was not always taken directly as the spread in the test results, because the number of tests was not sufficient. In such cases, the spread was judged also based on experience from spread on other rock types. The model values were also all selected as rounded off numbers, not to give a false impression of certainty in the parameter value assignments.

It is reasonable to believe also that the crack initiation stress should be higher in a sample where the maximum uniaxial stress at failure is high. In such cases, an uncorrelated distribution for each parameter would not be an appropriate description. Therefore, we studied the correlation between these two parameters and it was found to be confirmed for all rock types, see for example Figure 6-6. The crack initiation stress is modelled as a function of the UCS value. The crack initiation stress is about 50% of the UCS for Ävrö granite and 47% for the other rock types.

The assigned mechanics properties for three intact rock types are provided in Table 6-5. The rock type proportions in the defined rock domains are described in Section 5.3 (see also map in Figure 5-47).

To describe the uncertainty in the estimations, an estimated span is given within which the real mean value is considered to lie. This is regarded as an improvement compared to previous model versions. The uncertainty span was selected based on the statistical analysis of the data sample (the 95% confidence values around the mean). When the number of samples is large the uncertainty span naturally decreases. However, when selecting the uncertainty value the accuracy in the determination of the test parameter was also considered. The uncertainty description number was further, for simplicity, selected as a single symmetrical value and this value was finally chosen by expert judgement.

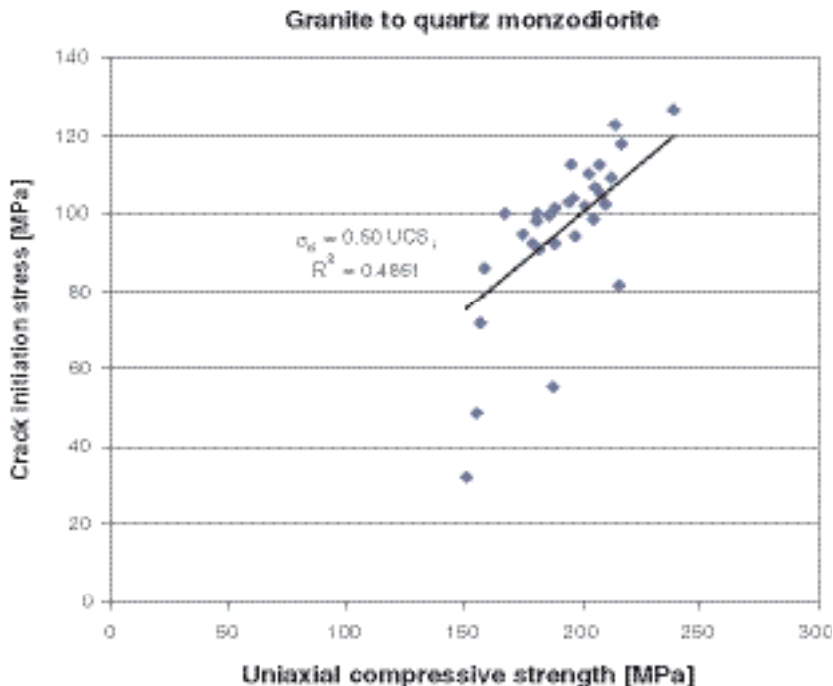


Figure 6-6. Crack initiation stress plotted against the uniaxial compressive strength for the Granite to quartz monzodiorite (Ävrö granite) samples. Since there is a correlation between the parameters, the model of the initiation stress is made as a linear function of the UCS. The model is shown as a solid line (cf. the histogram for the UCS values shown in Figure 6-1).

The main change in the description compared to the previous version is that the rock type Ävrö granite is now included, and we may note that this rock type has strength properties somewhere in between the Quartz monzonite to monzonite and the finegrained dioritoid. The total spread in the uniaxial compressive strength expected for the Ävrö granite is quite large, 150–240 MPa, probably reflecting the large variation in Ävrö granite mineralogy (cf. Figure 5-10).

Table 6-5. Estimated rock mechanics properties for intact rock (matrix) of the dominating rock types (i.e. small pieces of rock without any macroscopic fractures). All parameters are described as truncated normal distribution functions.

Parameter for intact rock (drill core scale)	Granite to Quartz monzodiorite (Ävrö granite)	Quartz- monzonite to monzodiorite	Finegrained dioritoid
	Mean / standard dev.	Mean / standard dev.	Mean / standard dev.
	Min – Max (trunc.)	Min – Max (trunc.)	Min – Max (trunc.)
	<i>Uncertainty in the mean</i>	<i>Uncertainty in the mean</i>	<i>Uncertainty in the mean</i>
Uniaxial compressive strength, UCS*	195 MPa / 20 MPa	165 MPa / 30 MPa	210 MPa / 50 MPa
	150–240 MPa	110–200 MPa	120–265 MPa
	± 5 MPa	± 8 MPa	± 10 MPa
Crack initiation stress, σ_{ci}	0.50 x UCS	0.47 x UCS	0.47 x UCS
	± 7 MPa	± 9 MPa	± 10 MPa
Young's modulus, E	70 GPa / 5 GPa	80 GPa / 10 GPa	85 GPa / 10 GPa
	60–90 GPa	70–90 GPa	70–110 GPa
	± 2 GPa	± 3 GPa	± 3 GPa
Poisson's ratio, ν	0.20 / 0.03	0.27 / 0.05	0.26 / 0.03
	0.15–0.26	0.18–0.33	0.19–0.31
	± 0.01	± 0.01	± 0.01
Tensile strength, T	13 MPa / 1.5 MPa	17 MPa / 4 MPa	20 MPa / 2 MPa
	9–17 MPa	12–24 MPa	14–24 MPa
	± 1 MPa	± 1 MPa	± 1 MPa
Mohr-Coulomb Friction angle, ϕ	56° / 2°	60° / 3°	55° / 6°
	53°–57°	57°–62°	35°–60°
	± 1°	± 1°	± 1°
Mohr-Coulomb Cohesion, c^*	27 MPa / 2.7 MPa	22 MPa / 3.2 MPa	32.5 MPa / 5.4 MPa
	23–32 MPa	14–29 MPa	20–40 MPa
	± 2 MPa	± 2 MPa	± 2 MPa

* The UCS should not be used as input to the Mohr-Coulomb model.

6.3.2 Assignment of properties to single fractures

The properties of single fractures are described by the parameters: normal and shear stiffness, and by friction angle and cohesion through Coulomb slip model, cf. Table 6-6. Note that an estimation of the dilation angle is also added in this model version. Because the accuracy and set-up for the Shear II stiffness measurements (see Section 6.2.2) were considered most reliable, it was judged that the model parameters (rounded-off numbers) should be based on these test results. The test results in /Lanaro et al. 2006/ show that the friction angle and the cohesion are correlated and therefore the model for the cohesion was chosen as a function of the friction angle. The values given for the friction angle and cohesion are applicable where normal stress is 0.5 MPa and above (see also the footnote to Table 6-6). Furthermore, all model parameters are assumed applicable for effective stress conditions, although laboratory results are not available to fully support this assumption (all fracture tests were performed without application of pore pressure).

In this model version, an estimation has been added of the uncertainty for the mean value of the parameter distributions. This value is not calculated, but chosen based solely on judgement. In particular concerning the stiffness values, the differences between methods makes the uncertainty large, and the uncertainty itself is difficult to quantify until the differences observed are understood in more detail.

Table 6-6. Estimated rock mechanics properties of single fractures. The prediction is the same for all fractures (independent of rock domain and/or fracture set).

Parameter for single rock fractures	All Domains, All fracture sets		
	Truncated normal distribution		
	Mean ; standard dev.	Min (trunc.) – Max (trunc.)	Uncertainty in the mean
Normal stiffness, MPa/mm ¹⁾	220 ; 43	150–310	20
Shear stiffness, MPa/mm ²⁾	40 ; 11	18–66	5
Peak friction angle, ϕ ³⁾	37° ; 3°	31°–41°	2°
Peak cohesion, c ¹⁾ , MPa	0.82 ; 0.37	0.26–1.56	0.15
Peak dilation angle, i	Bilinear model		
Stress dependent model:	$i_{\text{mean}} = 4^\circ$		
For $\sigma_n > 10$ MPa	$i_{\text{mean}} = 16 - 1.2\sigma_n$;	$i_{\text{min}} = 0.05 i_{\text{mean}}$	$u = 0.25 i_{\text{mean}}$
For $\sigma_n < 10$ MPa	SD = 0.5 i_{mean}	$i_{\text{max}} = 220 i_{\text{mean}}$	

1) See definition in Figure 6-3.

2) See definition in Section 6.2.2.

3) For normal stresses smaller than 0.5 MPa, a linear envelope should be assumed. This envelope should have zero cohesion and should equal the shear strength obtained from the properties in this table when the normal stress of 0.5 MPa is considered. A maximum friction angle of 70° should be adopted when higher values are obtained from the linear envelope for low normal stresses.

6.3.3 Conceptual models for rock mass characterisation

The actual behaviour of a rock mass under different loading conditions is very complicated. The rock mass is a composite of elements of many different kinds and scales, and the actual geometry of the different elements is not possible to know or describe in detail. A gross simplification of the rock mass and its behaviour is therefore needed. For the site-descriptive model, the aim is to describe the rock mass in sufficient detail that a preliminary repository design and safety analysis of the investigated site is possible. Following the strategy report /Andersson et al. 2002a/, a few parameters have been selected.

The selected parameters for the rock mass are: deformation modulus, Poisson's ratio, tensile strength and three parameters associated with the Mohr-Coulomb strength model; friction angle, cohesion and "apparent uniaxial compressive strength", UCS_m (where the subscript m is used to denote rock mass in contrast to the parameter for small scale intact rock). Note in particular that the UCS_m parameter for rock mass is not a standard parameter and it was chosen such that it fits a simplified linear model (Mohr-Coulomb) of the rock mass, and is not applicable to a real situation of zero confining stress. (This choice was made to facilitate selection of parameters for continuum modelling, as it would give a realistic strength at higher stress levels.) Also, note that these numbers will be dependent on the particular stress levels that are chosen to fit the linear Mohr-Coulomb model, in our case 10–30 MPa. More importantly, exactly the same definitions of parameters are employed for the site description of the Forsmark site. Hence, possibilities for comparison are facilitated.

6.3.4 Empirical approach to rock mass mechanics properties

One empirical index value was calculated for each 5 m section of a borehole, giving about 200 values in each borehole (see Figure 6-4). The data were sorted by borehole and also by lithological domain. Data associated with interpreted deformation zones, as provided by the single-hole interpretation, were also treated separately.

The use of two empirical systems enabled comparison of the outcome in terms of the estimated rock mechanics parameters. In the previous version /SKB 2005a/ the decision was made that only results from one of the systems should be retained and used in the further compilation and presentation of results. Consequently the values shown in the following tables are those determined from RMR /Lanaro 2006/. One example of results from the empirical approach is shown in Figure 6-7.

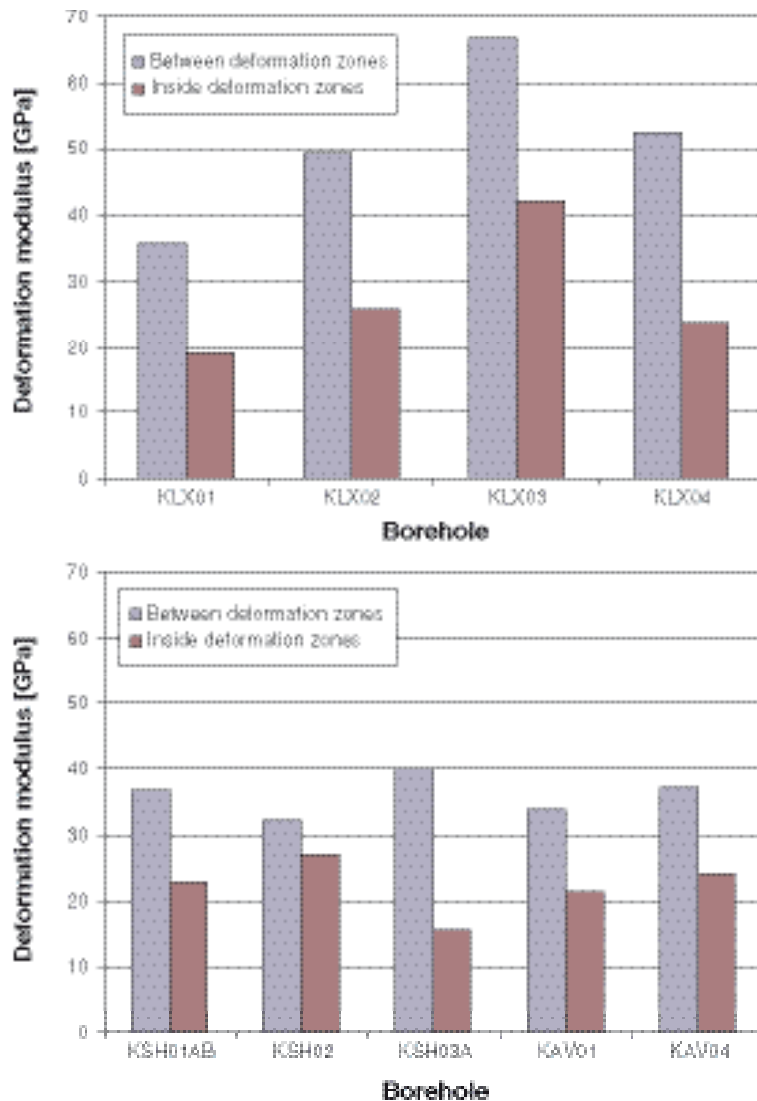


Figure 6-7. The deformation modulus determined from RMR values for the rock mass between deformation zones (blue) and the rock inside the deformation zones (i.e. zones modelled deterministically and zones defined in the geological single hole interpretation) (purple). Results shown separately for the boreholes in the a) Laxemar subarea and b) Simpevarp subarea. /Lanaro 2006/.

6.3.5 Theoretical approach to rock mass mechanics properties

The second approach used to estimate the mechanics property parameters for the rock mass was to calculate the composite behaviour based on knowledge about the respective properties of intact rock and fractures. This approach is denoted the “theoretical approach” and the underlying methodology is outlined in /Olofsson and Fredriksson 2005/.

The basic assumption here is that the developed geological DFN model may be used to simulate a fracture network that in turn may be used to create numerical models of the rock mass. A simulated fractured rock “slice” (20×20×1 m) is subsequently numerically loaded until it fails, upon which the stresses and strains in the block are determined (the same approach as used in Simpevarp 1.2, refer to /Fredriksson and Olofsson 2005/).

In the study performed for the site-descriptive model Simpevarp 1.2, only the influence from the variation in fracture properties was studied, whereas in the current version only the influence of differences in fracture intensity has been analysed. This decision was made since the geological

model (cf. Section 5.5) had shown that the intensity was fairly high and in particular that the variation in fracture intensity on a 25 m scale is significant. Also, the single fracture model has revealed no major differences between fracture sets. Therefore, the fracture intensity variation was considered to dominate the mechanics properties on this scale.

A total of 20 realisations of the fracture geometry were generated for three magnitudes of fracture intensity, corresponding to the P_{32} variation of the DFN model. Figure 6-8 shows examples of simulated networks at the three defined intensities.

Another improvement in the analysis in the current version is that the numerical loadings were performed at three confining stress levels, 0.5, 8 and 32 MPa (no pore pressure in fractures). The low confinement case has been added to give a possibility for direct comparison with the empirical approach. Since different confinements are used, the Mohr-Coulomb parameter may also be determined.

Examples of the result from the numerical modelling are given in Figure 6-9. Each point in the diagrams corresponds to one network realisation and the different colours reflect the fracture intensity. On the x-axis is the actual P_{10} value for the particular network of each 3DEC model. It can be noted that for all parameters there is a clear difference between the case with low intensity and the case with mean intensity. As expected, the deformation properties E_m and Poisson's ratio are found to be stress dependent.

The mean result from each intensity group was used as a base for the estimation of mean and standard deviation of the rock mass parameters for the theoretical modelling. A limitation of the theoretical approach, in the current version, is that the modelling has been performed only for one rock domain, namely Domain A in the Laxemar subarea. This limitation is due to time constraints. Furthermore, the properties of the deformation zones have not been directly assessed with the theoretical approach, apart from the likelihood that the high intensity cases can be assumed as being closer to those of the deformation zone situation.

For a complete summary of the results from the numerical modelling the reader is referred to the corresponding background report /Fredriksson and Olofsson 2006/, where all results and statistics are shown for deformation modulus, Poisson's ratio, apparent uniaxial strength UCS_m assuming a Mohr-Coulomb fit model, UCS_m assuming the Hoek and Brown model, the tensile strength determined using empirical relations to the Hoek and Brown model.

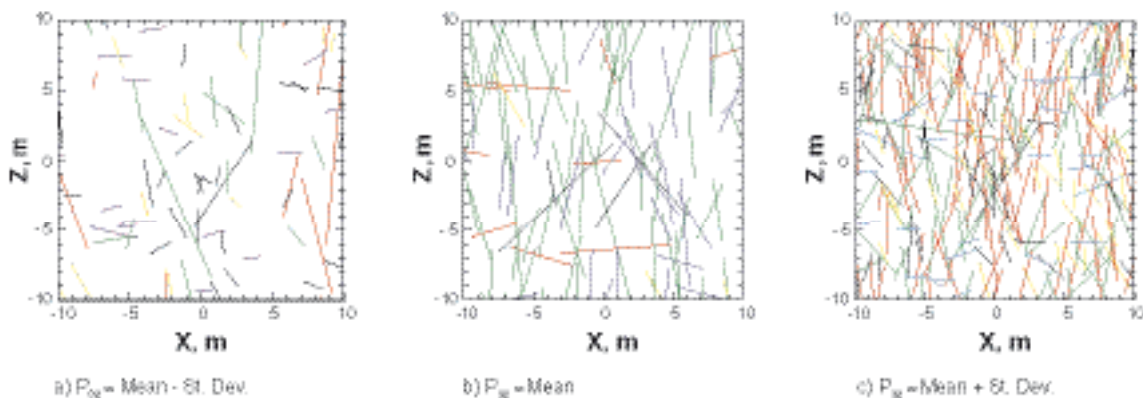


Figure 6-8. The theoretical approach consists of numerical simulation of a uniaxial loading of a rock block of 20×20 m size. Three different fracture intensities were analysed, a)–c), corresponding the P_{32} variation in the DFN model (see Section 5.5).

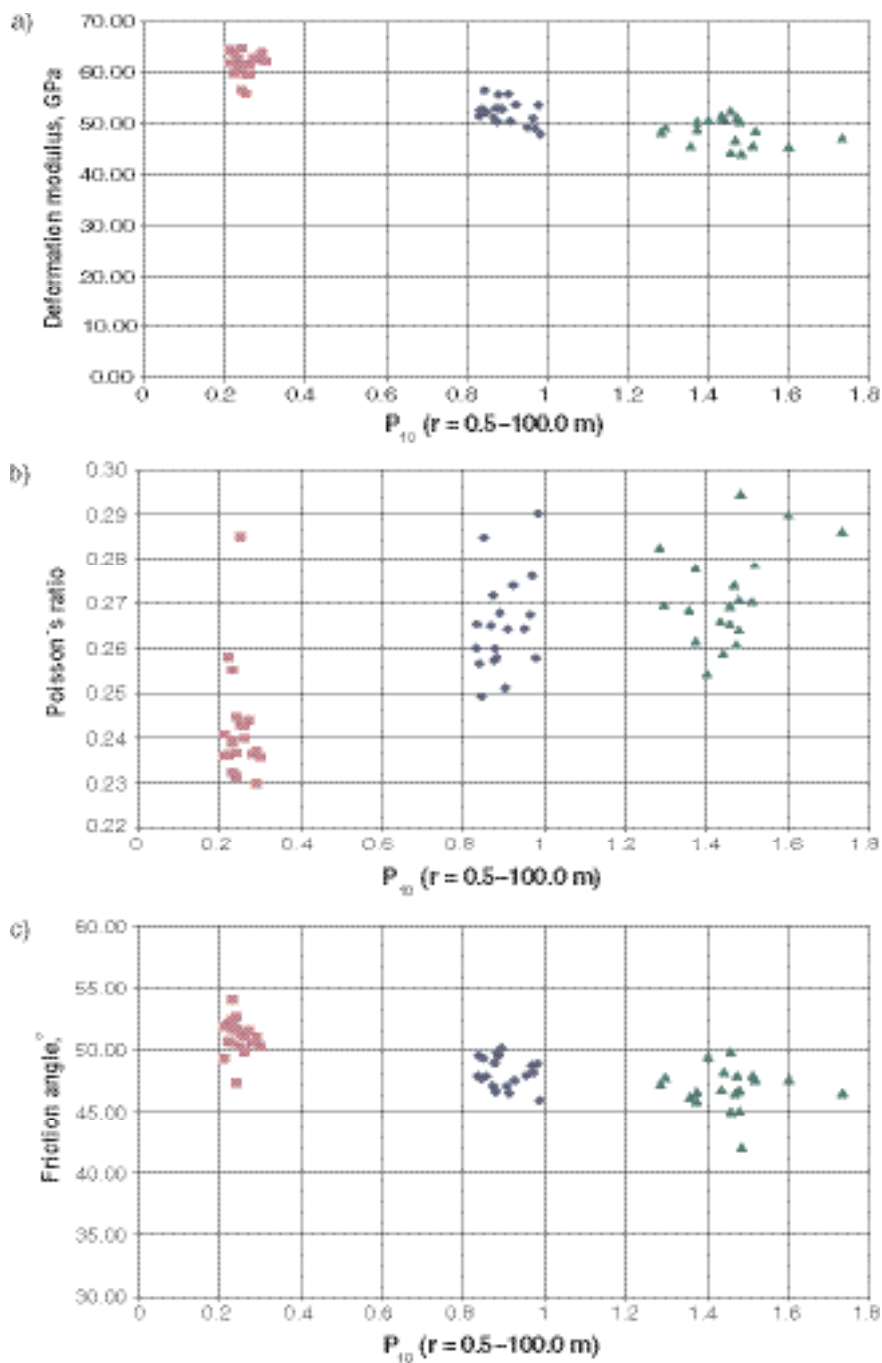


Figure 6-9. Example results from the 3DEC modelling of the rock mass, using the theoretical approach a) The variation in deformation modulus for rock mass in domain A, Laxemar subarea. b) The variation in Poisson's ratio. c) The variation of the friction angle according to Mohr-Coulomb. For all three diagrams the confining stress is 8 MPa and the values are plotted against the fracture intensity (P_{10}) of each analysed model.

6.3.6 Assignment of rock mass mechanics properties in the model volume

Each of the two approaches provides separate individual predictions (estimates) for the selected parameters. These estimates are fully independent from one another, and are clearly different, since the empirical approach utilises the borehole mapping data and the theoretical approach and subsequent numerical modelling use the laboratory fracture test data and the geological DFN model description. However, the intact rock test properties used as input are the same for both approaches.

To make the final assignment of properties to the rock mass model, the results from both approaches have been considered together. This has been done by making the following overall assumptions and steps.

- The empirical modelling provides only one value for the deformation modulus and the Poisson's ratio, i.e. the empirical relation includes no explicit stress dependence. It was assumed here that the E_m values were best estimates for the condition where the confining stresses are low, because it was believed that the empirical systems were built up based mostly on excavation cases from shallow depth. Therefore, the empirical results were assumed to correspond to a situation with a minor principal stress (confining effective stress) of 1.5 MPa, roughly corresponding to 50 m depth.
- The results from both approaches were co-plotted and compared. Model values (assuming a truncated normal distribution function) were selected based on these results, giving a good visual fit to the results. The model functions were selected such that the values were rounded off, not to give any false impression of certainty in the descriptive model. Symmetry in standard deviation and min-max truncation values was preferred, for reasons of simplicity.
- The spread due to the spatial variation was assumed contained in the standard deviation value and the min and max values, whereas the uncertainty was assumed to be covered by the uncertainty estimated for the mean value. This uncertainty was selected based on the differences seen in the approaches, such that mean results for both approaches would “come out true”, i.e. would fall within the uncertainty span. No weighting between the two approaches was consequently applied.
- In the cases where data were lacking from the theoretical approach (all but domain A in the Laxemar subarea), the actual numbers were selected based on the assumption that the results would be analogous to a similar case in Laxemar subarea, following the differences seen in the empirical approach results. In these cases, the uncertainty was assumed to be higher.

The diagrams in Figure 6-10 through Figure 6-13 show examples of obtained results following the modelling steps listed above. In the diagrams, the mean values are given with box symbols. The selected model is shown as solid red lines (cf. figure legends). As there are now theoretical results at low confining stress, it is interesting to note that the estimation of the deformation modulus is of the same magnitude for both approaches and fit well to the modelled curve. This means that the theoretical results support the choice of a bilinear representation for the deformation modulus made already in the previous version.

Also, the estimated model values for E_m compare well with the absolute magnitudes and relative difference between E_m at the shallow Clab excavations, and at the deeper Äspö HRL, 40 and 55 GPa (Section 6.2.4), respectively. These values were obtained by back analysis.

The “empirical” estimation of Poisson's ratio is based on the empirically determined deformation modulus, but using an analytical model for Poisson's ratio assuming a orthogonal fracture system with zero angle to the loading (e.g. /Priest 1993/). For this special case the ratio between E and ν for rock mass is the same as for the intact rock, therefore the estimated E -modulus became clearly low. The theoretical approach, on the other hand, calculates the Poisson's ratio in the quasi-2D numerical model for a stochastic (non-orthogonal) fracture network in a specific loading direction, the vertical. This case gives a higher value of the Poisson's ratio, increasing with decreasing confining stress. In reality the “equivalent Poisson's ratio” (and also the deformation modulus for that matter) is anisotropic in a fractured rock, and should ideally not be reduced to one single effective value, as was approximated here. The Poisson's ratio will be sensitive to the direction of the loading with respect to the fracture network geometry /Itasca 2003/, /Priest 1993/ or /Min 2004/. Also, the Poisson's ratio will change with the ratio between fracture normal and shear stiffness, at least during elastic deformation. This latter ratio is expected to decrease slightly at lower normal stresses. The theoretical approach employed here simulates only differences caused by fracture intensity and confinement, and the fracture properties in the models are not stress-dependent.

In conclusion, the main reason for the differences in the estimated Poisson's ratio, from empirical and theoretical approaches respectively, is that they include assumptions valid only for certain network geometry cases, and are not valid in general. The influence of anisotropy in the fracture network was not handled. However, the theoretical approach, using numerical modelling, should

be able to capture the real variation of Poisson's ratio of the fractured rock mass if the models were truly 3D, and if different loading directions were analysed. This was not done due to calculation limitations and time constraints. As a model assumption, it was chosen to keep the estimate for the "equivalent" Poisson's ratio constant and independent of stress, but to increase both the spread (reflecting the expected anisotropy) and the uncertainty span at lower stress. This parameter description is changed compared to version Simpevarp 1.2, and it may be further improved in future versions.

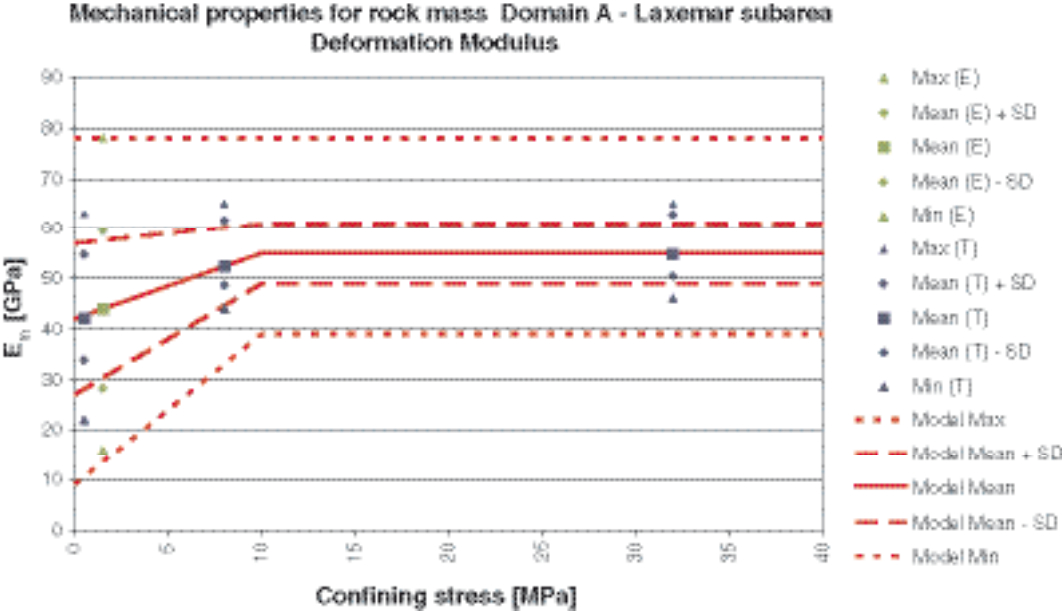


Figure 6-10. Diagrams showing deformation modulus in the lithological rock domain A in the Laxemar subarea as obtained from the empirical (E) and theoretical (T) approaches. For the theoretical approach the SD refers to standard deviation of the fracture intensity. The confining stress is here considered as the effective minor principal stress.

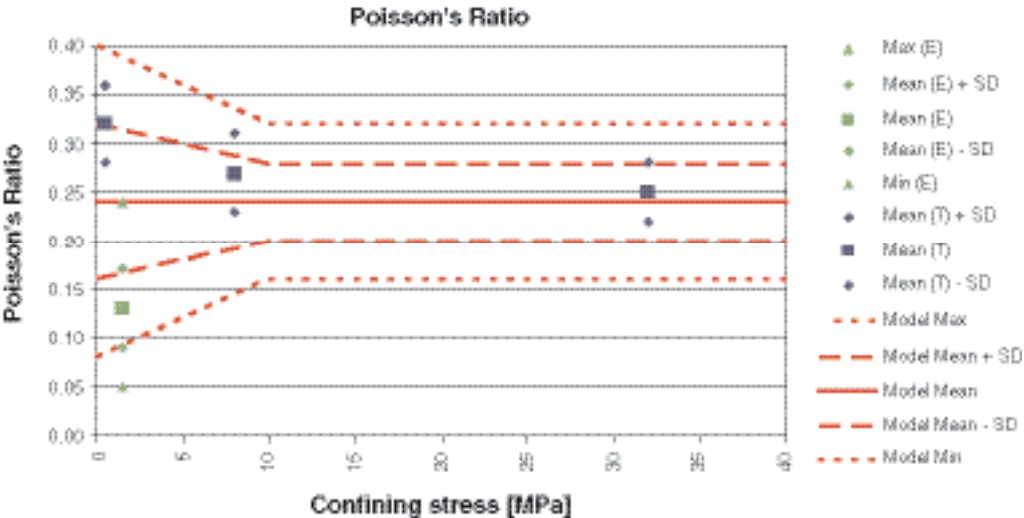


Figure 6-11. Diagrams showing the Poisson's ratio in lithological domain A, Laxemar subarea as obtained from the empirical (E) and theoretical (T) approach (vertical loading). The confining stress is here considered as the effective minor principal stress. See text.

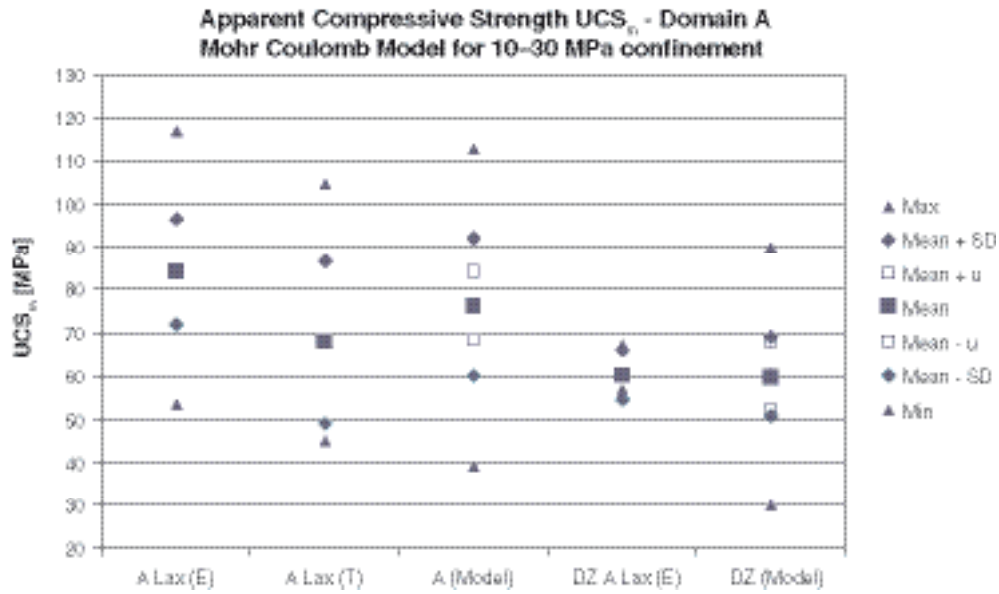


Figure 6-12. Uniaxial compressive strength for the rock mass and deformation zones in rock domain A, Laxemar subarea as obtained from the empirical and theoretical approaches. For the model the uncertainty (u) in the mean value is indicated as empty squares (the whole distribution would shift up or down with the mean value).

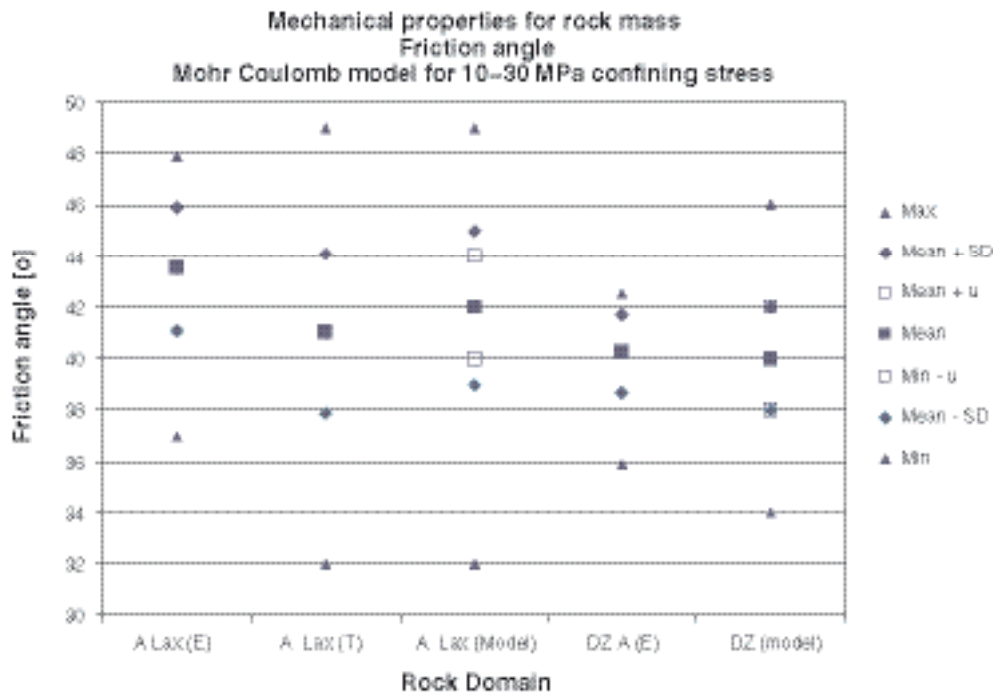


Figure 6-13. Friction angle for rock mass of rock domain A, Laxemar subarea, and Deformation zones in Domain A, as obtained from the empirical (E) and theoretical (T) approaches. The uncertainty (u) in the mean of model distribution is also indicated.

Evaluation of uncertainties

Table 6-8 includes a value to describe the uncertainty in the prediction (in italics). This value gives the expected possible difference between the given model mean and the real mean value of the actual distribution. The shape of the normal distribution is assumed unchanged if the mean value is increased or decreased, i.e. the standard deviation should be the same, whereas the min and the max truncation values should be adjusted by an amount equal to the adjustment of the mean value.

The uncertainty value is selected such that the span covers the results from both the empirical and the theoretical approaches. Also, the uncertainty value has been compared with the uncertainty value given for the empirical prediction (see also the following paragraph). The uncertainty is in most cases of the same order as the empirical uncertainty /Lanaro 2006/.

Table 6-7. Laxemar 1.2 – Estimated rock mechanics properties for the rock mass of defined rock domains.

Parameter for the rock mass (30×30×30 m scale)	Domain A (Laxemar) and Domain BA	Domain A (Simpevarp) and Domain C and Domain P	Domain B	Domain D	Domain M
	Mean; St. Dev. Min – Max truncation	Mean; St. Dev. Min – Max truncation	Mean; St. Dev. Min – Max truncation	Mean; St. Dev. Min – Max truncation	Mean; St. Dev. Min – Max truncation
	Uncertainty in Mean	Uncertainty in Mean	Uncertainty in Mean	Uncertainty in Mean	Uncertainty in Mean
Def Modulus $\sigma_3 > 10$ MPa ¹⁾	55 ; 6 39–78	49 ; 6 36–75	44 ; 7 26–75	61 ; 7 39–81	61 ; 7 39–81
$\sigma_3 < 10$ MPa ¹⁾ (GPa)	$E_{\text{mean}} = 42 + 1.3\sigma_3$; SD= 15-0.9 σ_3 $E_{\text{min}} = 9 + 3\sigma_3$ $E_{\text{max}} = 78$	$E_{\text{mean}} = 36 + 1.3\sigma_3$; SD= 15-0.9 σ_3 $E_{\text{min}} = 6 + 3\sigma_3$ $E_{\text{max}} = 75$	$E_{\text{mean}} = 30 + 3.1\sigma_3$ SD= 11-0.4 σ_3 $E_{\text{min}} = 6 + 2\sigma_3$ $E_{\text{max}} = 75$	$E_{\text{mean}} = 35 + 2.6\sigma_3$ SD= 11-0.4 σ_3 $E_{\text{min}} = 6 + 3\sigma_3$ $E_{\text{max}} = 70 + 1.1\sigma_3$	$E_{\text{mean}} = 35 + 2.6\sigma_3$ SD= 11-0.4 σ_3 $E_{\text{min}} = 6 + 3\sigma_3$ $E_{\text{max}} = 70 + 1.1\sigma_3$
	± 2	± 3	± 3	± 4	± 3
Poisson's ratio $\sigma_3 > 10$ MPa ¹⁾	0.24 ; 0.04 0.16–0.32	0.24 ; 0.04 0.16–0.32	0.24 ; 0.04 0.16–0.32	0.24 ; 0.04 0.16–0.32	0.24 ; 0.04 0.16–0.32
$\sigma_3 < 10$ MPa ¹⁾	$\nu_{\text{mean}} = 0.24$ SD= 0.08–0.004 σ_3 $\nu_{\text{min}} = 0.08 + 0.008\sigma_3$ $\nu_{\text{max}} = 0.40 - 0.008\sigma_3$	$\nu_{\text{mean}} = 0.24$ SD= 0.08–0.004 σ_3 $\nu_{\text{min}} = 0.08 + 0.008\sigma_3$ $\nu_{\text{max}} = 0.40 - 0.008\sigma_3$	$\nu_{\text{mean}} = 0.24$ SD= 0.08–0.004 σ_3 $\nu_{\text{min}} = 0.08 + 0.008\sigma_3$ $\nu_{\text{max}} = 0.40 - 0.008\sigma_3$	$\nu_{\text{mean}} = 0.24$ SD= 0.08–0.004 σ_3 $\nu_{\text{min}} = 0.08 + 0.008\sigma_3$ $\nu_{\text{max}} = 0.40 - 0.008\sigma_3$	$\nu_{\text{mean}} = 0.24$ SD= 0.08–0.004 σ_3 $\nu_{\text{min}} = 0.08 + 0.008\sigma_3$ $\nu_{\text{max}} = 0.40 - 0.008\sigma_3$
	± 0.03	± 0.03	± 0.03	± 0.03	± 0.03
Uniaxial compressive strength ²⁾³⁾	82 ; 12 38–128	77 ; 12 38–128	70 ; 12 31–118	109 ; 11 40–128	97 ; 12 40–128
(MPa)	± 3	± 6	± 4	± 6	± 6
Mohr-Coulomb, Friction angle, ϕ ³⁾	46 ; 3 35–49	42 ; 3 34–48	42 ; 3 35–49	47 ; 2 45–48	44 ; 2 37–49
	± 2.5	± 2.0	± 2.5	± 2.0	± 2.0
Mohr-Coulomb, Apparent cohesion, c ³⁾ (MPa)	16 ; 2 14–25	17 ; 1.7 12–23	16 ; 2 13–23	17 ; 2 10–24	17 ; 2 10–24
	± 2	± 2	± 2	± 2	± 2
Tensile strength (MPa)	0.9 ; 0.7 0.2–3.7	0.8 ; 0.5 0.1–2.2	1.0 ; 0.5 0.1–2.0	1.3 ; 0.3 0.7–1.6	2 ; 0.7 0.5–3.6
	± 0.15	± 0.15	± 0.15	± 0.15	± 0.15

¹⁾ Note that the model is a bilinear function. The first given constant values are expected for confining stress (σ_3) of 10 MPa or higher. The second group of values should be used for lower stress levels

²⁾ Assuming that a linear Mohr-Coulomb strength criterion is applied. The M-C model is fitted to confining stress levels 10–30 MPa, and the UCS_m-value is the intersection with the σ_1 axis in σ_1 - σ_3 space for this model.

³⁾ Uniaxial strength, friction angle and apparent cohesion are correlated parameters and should be selected to be mutually consistent in each case. If another material model is used the cohesion should be adjusted to the choice of model.

Table 6-8. Laxemar 1.2 – Estimated rock mechanics properties for the rock in deformation zones.

Parameter for the rock mass	Minor deformation zones in Domains A, B, BA and C.	Minor deformation zones in Domains D and M	All Deterministic deformation zones
(30×30×30 m scale)	Mean; St. Dev. Min – Max truncation	Mean; St. Dev. Min – Max truncation	Mean; St. Dev. Min – Max truncation
	Uncertainty in Mean	Uncertainty in Mean	Uncertainty in Mean
Def Modulus $\sigma_3 > 10 \text{ MPa}^{1)}$	38 ; 7 15–53	55 ; 6 39–78	26 ; 5 10–53
$\sigma_3 < 10 \text{ MPa}^{1)}$ (GPa)	$E_{\text{mean}} = 24 + 1.4\sigma_3$ SD= 7 $E_{\text{min}} = 5 + 1.5\sigma_3$ $E_{\text{max}} = 53$	$E_{\text{mean}} = 42 + 1.3\sigma_3$; SD= 15-0.9 σ_3 ; $E_{\text{min}} = 9 + 3\sigma_3$ $E_{\text{max}} = 78$	$E_{\text{mean}} = 16 + \sigma_3$ SD= 5 $E_{\text{min}} = 5 + \sigma_3$ $E_{\text{max}} = 53$
	± 4	± 4	± 6
Poisson's ratio $\sigma_3 > 10 \text{ MPa}^{1)}$	0.24 ; 0.04 0.16–0.32	0.24 ; 0.04 0.16–0.32	0.24 ; 0.04 0.16–0.32
$\sigma_3 < 10 \text{ MPa}^{1)}$	$\nu_{\text{mean}} = 0.24$ SD= 0.08–0.004 σ_3 $\nu_{\text{min}} = 0.08 + 0.008\sigma_3$ $\nu_{\text{max}} = 0.40 - 0.008\sigma_3$	$\nu_{\text{mean}} = 0.24$ SD= 0.08–0.004 σ_3 $\nu_{\text{min}} = 0.08 + 0.008\sigma_3$ $\nu_{\text{max}} = 0.40 - 0.008\sigma_3$	$\nu_{\text{mean}} = 0.24$ SD= 0.08–0.004 σ_3 $\nu_{\text{min}} = 0.08 + 0.008\sigma_3$ $\nu_{\text{max}} = 0.40 - 0.008\sigma_3$
	± 0.04	± 0.04	± 0.04
Uniaxial compressive strength ²⁾³⁾	60 ; 9 34–94	76 ; 12 38–128	55 ; 9 29–87
(MPa)	± 6	± 6	± 8
Mohr-Coulomb, Friction angle,	40 ; 2 34–46	44 ; 2 40–49	39 ; 3 33–45
$\phi^{3)}$	± 3.0	± 1.5	± 3.0
Mohr-Coulomb, Apparent cohesion,	14 ; 2 9–19	17 ; 2.5 10–24	13 ; 2 8–18
$c^{3)}$ (MPa)	± 3	± 1	± 3
Tensile strength (MPa)	0.55 ; 0.2 0.15–1.2	0.7 ; 0.4 0.1–2.0	0.15 ; 0.07 0.05–0.4
	± 0.15	± 0.15	± 0.15

¹⁾ Note that the model is a bilinear function. The first given constant values are expected for confining (effective) stress (σ_3) of 10 MPa or higher. The second group of values should be used for lower stress levels.

²⁾ Assuming that a linear Mohr-Coulomb strength criterion is applied. The M-C model is fitted to confining stress levels 10–30 MPa, and the UCS_m-value is the intersection with the σ_1 axis in σ_1 - σ_3 space for this model.

³⁾ Uniaxial strength, friction angle and apparent cohesion are correlated parameters and should be selected to be mutually consistent in each case. If another material model is used the cohesion should be adjusted to the choice of model.

There were no results from the theoretical approach from domains other than domain A in the Laxemar subarea. For the other domains, the uncertainty was based on the uncertainty estimation made from the empirical approach. This uncertainty is determined from the uncertainty in the input parameters of the empirical indices. For rock domains where the number of underlying data is small or in the cases for which no data are available, the uncertainty values are assumed to be larger. The uncertainties are given as absolute values in the same unit as the mean value. The main uncertainty factor associated with the theoretical approach is the uncertainty in the input data, such as the fracture intensity and the fracture properties. These uncertainties are discussed, by /Fredriksson and Olofsson 2004, 2005/ and /Olofsson and Fredriksson 2005/.

6.4 State of stress

6.4.1 Modelling assumptions and input from other disciplines

The stress modelling is mainly based on the stress measurement data presented in Section 6.2.5. As the measurement data show a large spread, the issue of finding a geological explanation for this condition is desirable. Following the developed methodology, the most probable explanation for the noted variation is expected to be associated with the existing structures (i.e. the modelled deformation zones). The deformation zone model, presented in Section 5.4, includes both the interpreted geometry and a description of the properties of the interpreted major deterministic deformation zones.

6.4.2 Conceptual model with potential alternatives

It is recognised that the essentially northeast trending deformation zones on either side of the Simpevarp peninsula-Hälö-Ävrö (i.e. zones ZSMNE012A and ZSMNE024A) can be interpreted to form a wedge-shaped body of rock that may represent a different stress regime from that prevailing at Äspö. Similarly, the rock volume above the zones ZSMEW007 and ZSMEW002 forms a wedge in the Laxemar subarea. When the measured stress data are sorted into two different groups representing these assumed geographical domains, it is noted that the spread within each group is significantly reduced compared with the combined spread of the two groups of data in combination. This fact lends some support for the posed hypothesis and the assumption was consequently made that the measurement data, although being associated with uncertainty, are sufficiently reliable to allow making the conjecture that the stress state the two suggested stress domains is dissimilar.

An alternative stress model would be that the stress domains have different shape, since there are uncertainties in the geometry of individual deformation zones, and this leads to a number of possible alternative models also for the stress situation. A radically different stress model alternative would be to assume no correlation between the stress state and interpreted deformation zones, but that the variation seen in the measurements is only caused by smaller scale structures (such as single fractures and mineral grain differences and their locations in relation to measurement points). This latter alternative hypothesis was considered less reasonable and has not been pursued further.

6.4.3 Modelling of stress distribution

The hypothesis of a structure-controlled explanation for the noted stress variation in the local scale model volume was evaluated using a numerical model. The underlying approach is further described in the strategy report /Hakami et al. 2002/ and the details of the current modelling are presented by /Hakami and Min 2006/. The three-dimensional mechanics block model includes the major interpreted deformation zones in the area, cf. Section 5.4. The zones are, for the purpose of the present analysis, simplified geometrically, whereby the deformation zones are simulated as ideal planes, as shown in Figure 6-14 and Figure 6-15.

When a given stress field is applied to the model, the orientation of the modelled zones in combination with the assigned strength properties define the displacements induced as some of the zones reach slip failure. The resulting stresses in the model are, at equilibrium, distributed in a way that is regarded as a plausible representation of the present stress distribution in the Laxemar and Simpevarp subareas. The applied stress boundary conditions, simulating tectonic compression in the direction NW-SE, are assumed to be those prevailing during the most recent evolutionary period, as described in Chapter 3 (cf. Table 3-2).

From the modelling results, it can be seen, as expected, that wedge-shaped rock masses surrounded by deformation zones with reduced strength properties, are not able to sustain high horizontal stresses, and the stress will consequently become lower inside the wedge and higher in areas outside (as illustrated in Figure 6-16). The results thus support a conceptual stress model describing the stress state in the modelled area as being made up of two different stress domains. Moreover, deformation zones that are subvertical may also influence the stress field, as can be seen in Figure 6-17 (e.g. the influence from ZSMNW042A in the south of Laxemar). Strike-slip movements on some modelled zones give rise to stress redistribution and the combined effects of all zones makes the resulting picture quite complex.

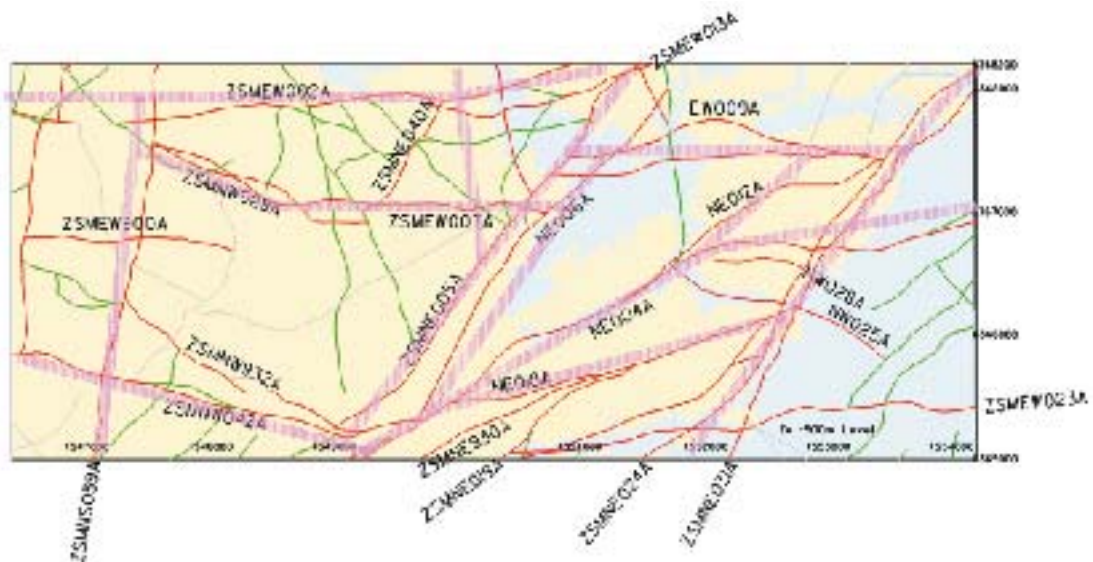


Figure 6-14. Deformation zone model Laxemar 1.2 at 500 m depth. The fracture zones in the 3DEC model are shown in pink.

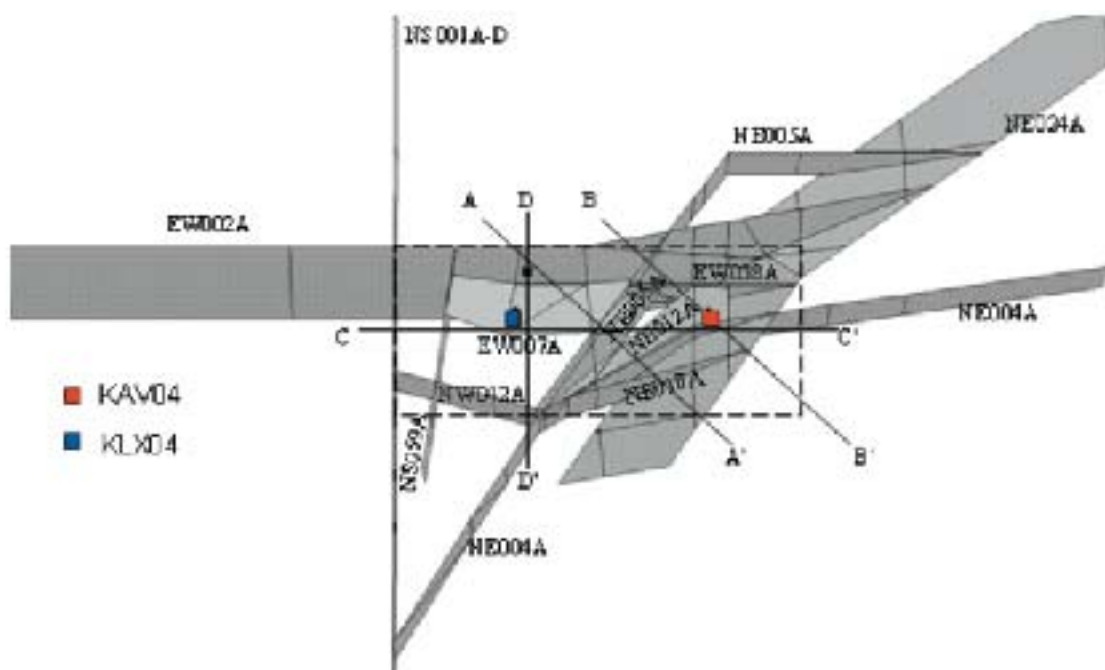


Figure 6-15. 2D plan view of the 3D numerical model including modelled deformation zones interpreted for Laxemar 1.2. Each zone is simplified and consists of one or two planar fractures in the model. The locations of vertical sections used for presenting the modelling results are indicated (A-A' through D-D'). /Hakami and Min 2006/.

The simplifications introduced, the crude meshing and uncertainties concerning the input parameters to the models may also introduce effects that may exaggerate the stress variation. Still, it is concluded that the modelling results provide useful support for the understanding of the potential effects of tectonically induced movements on the stress distribution in the Simpevarp area.

The modelled stresses are also directly compared with measurement data in Figure 6-18.

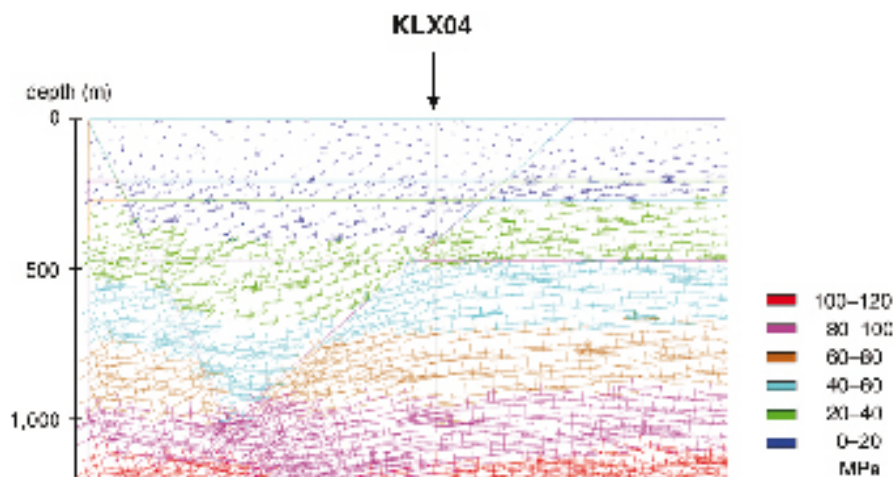


Figure 6-16. Modelled principal stress trajectories in the vertical section D-D' (cf. Figure 6-15 coloured by the major principal stress magnitude). The section includes borehole KLX04 where stress measurements have been performed. A clear influence on the stresses from the intersecting deformation zones is noted.



Figure 6-17. Modelled principal stress trajectories in a horizontal plane at 450 m depth. The colours indicate the magnitude of the major principal stress. It may be noted that the stresses differs quite substantially within the local area of this 3DEC model. Note that the colour code scales are not the same in the horizontal and vertical sections (see legends).

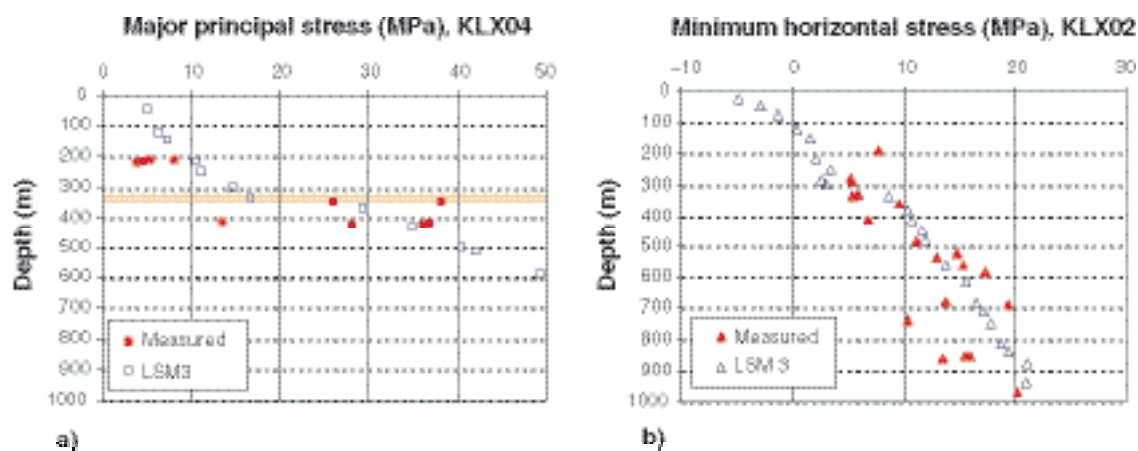


Figure 6-18. Comparison between stress measurement results and modelled stresses (Case LSM3), a) overcoring in KLX04 and b) hydraulic fracturing in KLX02. The borehole intersection with the deformation zone EW007A is indicated in Figure a). Figure 2-3 and Figure 6-15 show borehole location.

Resulting stress model

Table 6-9 through Table 6-12, the stress estimations are presented for the two defined stress domains included in the local scale model volume. The positions of the two stress domains are indicated in Figure 6-19. In this figure, the deformation zone model at ground surface is shown, and the defined stress domains are related to two major zones in this model.

Table 6-9. Model of in situ stress magnitudes in the Laxemar 1.2 stress domain I.

Parameter	σ_1 (MPa)	σ_2 (MPa)	σ_3 (MPa)
Mean stress magnitude, z = depth below ground surface (m)	0.058z+5 MPa	0.027z	0.014z+3
Uncertainty, 100–600 m	± 30%	± 30%	± 30%
Spatial variation in rock domains	± 20%	± 20%	± 20%
Spatial variation in or close to deformation zones	± 50%	± 50%	± 50%

Table 6-10. Predicted in situ stress orientations in the Laxemar 1.2 stress domain I.

Parameter	σ_1 , trend	σ_1 , dip	σ_2 , trend	σ_2 , dip	σ_3 , trend	σ_3 , dip
Mean stress orientation	132°	0°	90° **	90°	42°	0°
Uncertainty	± 15°	± 10°	± 90°	± 15–45° *	± 15°	± 15–45° *
Spatial variation, rock domains	± 15°	± 15°	± 15°	± 15°	± 15°	± 15°
Spatial variation inside or close to deformation zones	± 25°	± 30°	± 25°	± 30°	± 25°	± 30°

*At some level σ_2 and σ_3 may have similar magnitude and the dip can then be arbitrary. The three principal stresses are in each point oriented perpendicular to each other.

** Since the direction is expected to be subvertical, i.e. the dip 90, the trend of the tensor may therefore be arbitrary.

Table 6-11. Model of in situ stress magnitudes in the Laxemar 1.2 stress domain II.

Parameter	σ_1 (MPa)	σ_2 (MPa)	σ_3 (MPa)
Mean stress magnitude, z = depth below ground surface (m)	0.032z	0.027z	0.01z
Uncertainty, 100–600 m	30%	30%	30%
Spatial variation in rock domains	25%	25%	25%
Spatial variation in or close to deformation zones	50%	50%	50%

Table 6-12. Predicted in situ stress orientations in the Laxemar 1.2 stress domain II.

Parameter	σ_1 , trend	σ_1 , dip	σ_2 , trend	σ_2 , dip	σ_3 , trend	σ_3 , dip
Mean stress orientation	132°	0°	90°	90°	42°	0°
Uncertainty	± 20°	± 20°	± 90°**	± 15–45° *	± 20°	± 15–45° *
Spatial variation, rock domains	± 15°	± 15°	± 15°	± 15°	± 15°	± 15°
Spatial variation inside or close to deformation zones	± 25°	± 30°	± 25°	± 30°	± 25°	± 30°

*At some level σ_2 and σ_3 may have similar magnitude and the dip can then be arbitrary. The three principal stresses are in each point oriented perpendicular to each other.

** Since the direction is expected to be subvertical, i.e. the dip 90, the trend of the tensor may therefore be arbitrary.

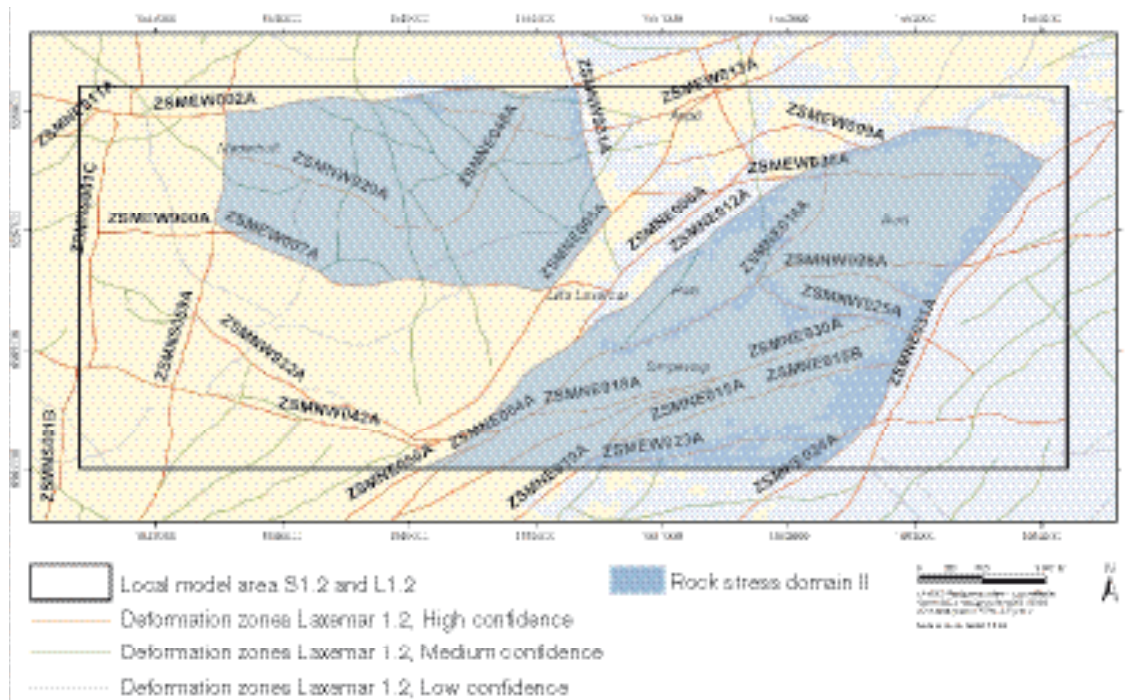


Figure 6-19. Stress domain II (blue) is the rock mass above the wedges formed by deformation zones below Ävrö and Hälö islands, and between ZSMEW002 (Mederhult zone) and ZSMEW007, respectively. In the area south of ZSMNE004A, below Simpevarp peninsula and southwards, it is more uncertain whether the rock belongs to Domain II or I. The stresses are expected to be higher in Domain I, as described in Table 6-9 through Table 6-12. This map is from ground level.

6.4.4 Evaluation of uncertainties in stress model

The reasons for uncertainty in the stress model are several. Firstly, the accuracy of the measurements themselves is limited. Secondly, the amount of data is not large, from a statistical viewpoint, and the fitted linear stress model functions have an inherent uncertainty due to this fact. Thirdly, the assumptions made regarding the stress domains and the need to extrapolate the available measurement results over large volumes also contribute to the uncertainty. The value selected for the total uncertainty thus encompasses different contribution and is based on an expert judgement for each contribution. The selected spans are shown graphically in Figure 6-5 and it can be seen that most of the observed data are enclosed within the model uncertainty spans.

The spatial variation is described with another percentage span, around the mean value, here implied as the local variation at a smaller scale (from data point to data point). In the rock mass well outside the major deformation zones the spatial variation of the stress is expected to be less than in the immediate vicinity of deformation zones.

7 Bedrock thermal model

The thermal model of the bedrock describes thermal properties at the rock domain level, which is of importance since the thermal properties of the rock mass affects the effective distance, both between canisters and deposition tunnels, and therefore places requirements on the necessary repository volume. Of particular interest is the thermal conductivity, since it directly influences the design of a repository. Measurements of thermal properties are performed at centimetre scale but values are required at the canister scale and therefore the spatial variability needs to be considered. Consequently, the thermal modelling includes elements of upscaling of thermal properties which is further described in /Sundberg et al. 2005a/. The work has been performed according to a strategy presented in /Sundberg 2003a/. A complete description of the thermal model for Laxemar 1.2 is made in /Sundberg et al. 2006/.

Thermal conductivity, λ (W/(m×K)), describes the ability of a material to transport heat. Heat capacity denotes the capacity for a material to store thermal energy. The volumetric heat capacity, C (J/(m³×K)), is the product of density, ρ , and specific heat capacity, c . (J/(kg×K)). The thermal diffusivity, κ (m²/s), describes a material's ability to level temperature differences. It is defined as the ratio between thermal conductivity and volumetric heat capacity. The geothermal gradient (°C/m) describes the temperature increase versus depth. The coefficient of thermal expansion (m/(m×K)) describes the linear expansion due to thermal influence.

7.1 State of knowledge at the previous model version

There is no previous model version specifically devoted to the Laxemar subarea. The Simpevarp site descriptive model version 1.2 describes the thermal properties of the adjacent Simpevarp subarea, and in doing so incorporates a limited amount of data from the Laxemar subarea. Thermal conductivity properties in SDM Simpevarp 1.2 /SKB 2005a/ were reported for four lithological domains, two of which are also present in the Laxemar subarea. Results indicated that the mean thermal conductivities of the different domains exhibit only a small variation, from 2.62 to 2.80 W/(m×K). Standard deviations vary according to the scale considered and for the canister scale were expected to range from 0.20 to 0.28 W/(m×K). A small temperature dependence was detected in thermal conductivity for the dominant rock types. A decrease of 1.1 to 3.4% per 100°C increase in temperature was found.

7.2 Evaluation of primary data

The evaluation of primary data includes analyses of measurements of thermal conductivity, heat capacity, temperature dependence of thermal properties, coefficient of thermal expansion and in situ temperatures. It also includes calculations of thermal conductivity from mineral composition and establishment of rock type distributions (PDF) of thermal conductivity. The spatial variation in thermal conductivity is also investigated by using density loggings. Table 2-3 summarises the available data on thermal properties used in the evaluation.

7.2.1 Thermal conductivity and diffusivity from measurements

Method

Laboratory measurements of thermal conductivity and thermal diffusivity have been performed with the Transient Plane Source method (TPS) /Gustafsson 1991/.

Compared TPS tests

As part of the quality assurance of thermal properties data, 10 samples from KSH01A were selected to compare TPS measurements at two different laboratories, Hot Disk AB /Dinges 2004/ and SP (Swedish National Testing and Research Institute) /Adl-Zarrabi 2004b/. For thermal conductivity,

a small but systematic bias is apparent; the SP values being on average 0.05 W/(m×K) lower than the Hot Disk values on the same samples. The differences in heat capacity measured on the same samples varied between –5.36% to 16.30% which expressed in heat capacity equates to –0.14 MJ/(m³×K) to 0.37 MJ/(m³×K).

Results

In Table 7-1 and Table 7-2 the results from all performed laboratory measurements of thermal conductivity and thermal diffusivity are summarised. Observe that samples from rock type Ävrö granite (501044) have been collected from the Simpevarp subarea /Adl-Zarrabi 2004abcd/, the Laxemar subarea /Adl-Zarrabi 2004ef/ and the Äspö HRL /Sundberg and Gabriellsson 1999, Sundberg 2002, Sundberg et al. 2005a/. Samples from rock type fine-grained dioritoid (501030) and quartz monzodiorite (501036), with the exception of two samples of 501036 from Äspö HRL, all come from the Simpevarp subarea /Adl-Zarrabi 2004abcd/.

Table 7-1. Measured thermal conductivity (W/(m×K)) of samples using the TPS method. Samples are from boreholes KAV01, KAV04A, KSH01A, and KSH02 (Simpevarp subarea), boreholes KLX02 and KLX04 (Laxemar subarea) together with borehole KA2599G01 (Äspö HRL) and the prototype repository tunnel (Äspö HRL).

Rock name	Name code	Sample location	Mean	St. dev.	Max	Min	Number of samples
Fine-grained dioritoid	501030	Boreholes KSH01A, KSH02.	2.79	0.16	3.16	2.51	26
Quartz monzodiorite	501036	Boreholes KSH01A, KAV04A.	2.74	0.16	2.95	2.43	15
Ävrö granite	501044	Boreholes KAV04A, KLX02, KLX04, KAV01, KA2599G01, Äspö HRL prototype tunnel.	2.90	0.35	3.76	2.16	71
Fine-grained granite	511058	Borehole KA2599G01.	3.63		3.68	3.58	2

Table 7-2. Measured thermal diffusivity (mm²/s) of samples using the TPS method. Samples are from boreholes KAV01, KAV04A, KSH01A, and KSH02 (Simpevarp subarea), and boreholes KLX02 and KLX04 (Laxemar subarea).

Rock name	Name code	Sample location	Mean	St. dev.	Number of samples
Fine-grained dioritoid	501030	Borehole KSH01A and KSH02.	1.28	0.16	26
Quartz monzodiorite	501036	Borehole KSH01A, KAV04A.	1.21	0.11	15
Ävrö granite	501044	Borehole KAV04A, KLX02, KLX04, KAV01.	1.38	0.14	39

Temperature dependence

Table 7-3 summarises the temperature dependence of thermal conductivity based on laboratory measurements of three separate rock types, namely fine-grained dioritoid (501030), quartz monzodiorite (501036), /Adl-Zarrabi 2004ab/, and Ävrö granite (501044), /Sundberg 2002/ and /Adl-Zarrabi 2004de/.

Table 7-3. Measured temperature dependence of thermal conductivity (per 100°C temperature increase) for different rock types from boreholes KSH01A, KSH02 (Simpevarp subarea), KA2599G01 (Äspö HRL), and KLX02 and KLX04 (Laxemar subarea). Mean value of temperature dependence calculated by linear regression.

Rock name	Name code	Sample location	Mean	St. dev.	Number of samples
Fine-grained dioritoid	501030	Boreholes KSH01A and KSH02.	–3.4%	1.6%	11
Quartz monzodiorite	501036	Borehole KSH01A.	–1.1%	1.1%	5
Ävrö granite	501044	Borehole KA2599G01.	–2.3%	3.7%	4
Ävrö granite	501044	Boreholes KLX02 and KLX04.	–5.3%	3.7%	9

7.2.2 Thermal conductivity from mineral composition

Method

Thermal conductivity of rock samples can be calculated with the SCA method (Self Consistent Approximation) /Dagan 1979, Sundberg 1988, 2003a/ using mineral compositions from modal analyses and reference values of thermal conductivity for different minerals taken from /Horai 1971, Horai and Baldrige 1972/. The calculations are performed at the millimetre scale. Although calculated values were earlier shown to be in good agreement with measured values /Sundberg 1988, 2002/, more recent studies in the Simpevarp subarea /Sundberg et al. 2005b/ reveal significant discrepancies, possible reasons for which are discussed below. Data and the calculations are further described in /Sundberg et al. 2006/.

Results

The results of the SCA calculations based on samples from both the Simpevarp and Laxemar subareas are presented in Table 7-4, subdivided according to rock type.

Table 7-4. Thermal conductivity (W/(m×K)) of samples from different rock types, calculated from the mineralogical compositions (SCA method).

Rock name	Name code	Mean	St. dev.	Number of samples
Fine-grained dioritoid	501030	2.43	0.33	31
Quartz monzodiorite	501036	2.41	0.14	23
Ävrö granite	501044	2.69	0.29	86
Fine-grained diorite-gabbro	505102	2.57	0.23	10
Diorite/Gabbro	501033	2.41	0.22	7
Fine-grained granite	511058	3.27	0.31	10
Granite	501058	2.97	0.59	5 ¹

¹ One sample taken from outside (west of) the Laxemar subarea.

SCA values (corrected for bias; see Table 7-5) for 31 surface samples of Ävrö granite within the Laxemar subarea are presented in Figure 7-1. High thermal conductivity values occur more commonly in the central parts of Laxemar, whereas lower values predominate in southern and north-eastern areas. The observed pattern of high and low thermal conductivities within the Ävrö granite mirrors the compositional variation observed in thin section analysis of this rock type, see Chapter 5. Quartz-rich varieties of Ävrö granite predominate in the central parts of the Laxemar subarea, whereas quartz-poor varieties occur predominantly along the southern flank, close to the contact with the quartz monzodiorite.

Evaluation of SCA results: comparison with measurements

In the site descriptive model Simpevarp version 1.2 it was found that calculated thermal conductivities using the SCA method were generally lower than thermal conductivities measured by the TPS method. Results from point-counting of fourteen new samples reinforce this pattern.

In Table 7-5, thermal conductivity values calculated using the SCA method are compared with measured values of proximal samples. The results indicate systematic deviations between measurements and calculations for all rock types.

The systematic bias observed in the SCA calculations as compared to the TPS measurements can be largely explained by the following factors:

- Alteration of plagioclase (sericitisation) and biotite (chloritisation) has been observed in samples throughout the Laxemar (see Chapter 5) and Simpevarp subareas /SKB 2005a/. The alteration products sericite and chlorite have higher thermal conductivities than their parent minerals. However, the proportion of these alteration products is underestimated by the method used in the modal analysis. This is considered to be the main source of uncertainty.

- Uncertainties exist regarding the reference values of thermal conductivity assigned to minerals, in particular for plagioclase, the thermal conductivity of which varies with its anorthite content.
- Errors associated with the point-counting method.

It is possible that the calculation method (SCA) also contributes to the bias. However, based on present knowledge this is assumed not to be significant since its basis is a 3D approximation /Dagan 1979, Sundberg 1988/.

Table 7-5. Comparison of thermal conductivity of different rock types calculated from mineralogical compositions by the SCA method and measured with the TPS method.

Method	Fine-grained dioritoid (n=5) samples Mean λ , (W/(m×K))	Quartz monzodiorite (n=3) Mean λ , (W/(m×K))	Ävrö granite – Äspö (n=18) Mean λ , (W/(m×K))	Ävrö granite – Laxemar/ Simpevarp (n=12) Mean λ , (W/(m×K))
Calculated (SCA)	2.56 ¹	2.34 ²	2.57 ²	2.82 ²
Measured (TPS)	2.85	2.62	2.68	3.06
Diff. (SCA – TPS)/TPS	-10.1%	-10.8%	-4.1%	-7.67%

¹ Corrected for sericitisation and chloritisation.

² No correction for sericitisation and chloritisation made.

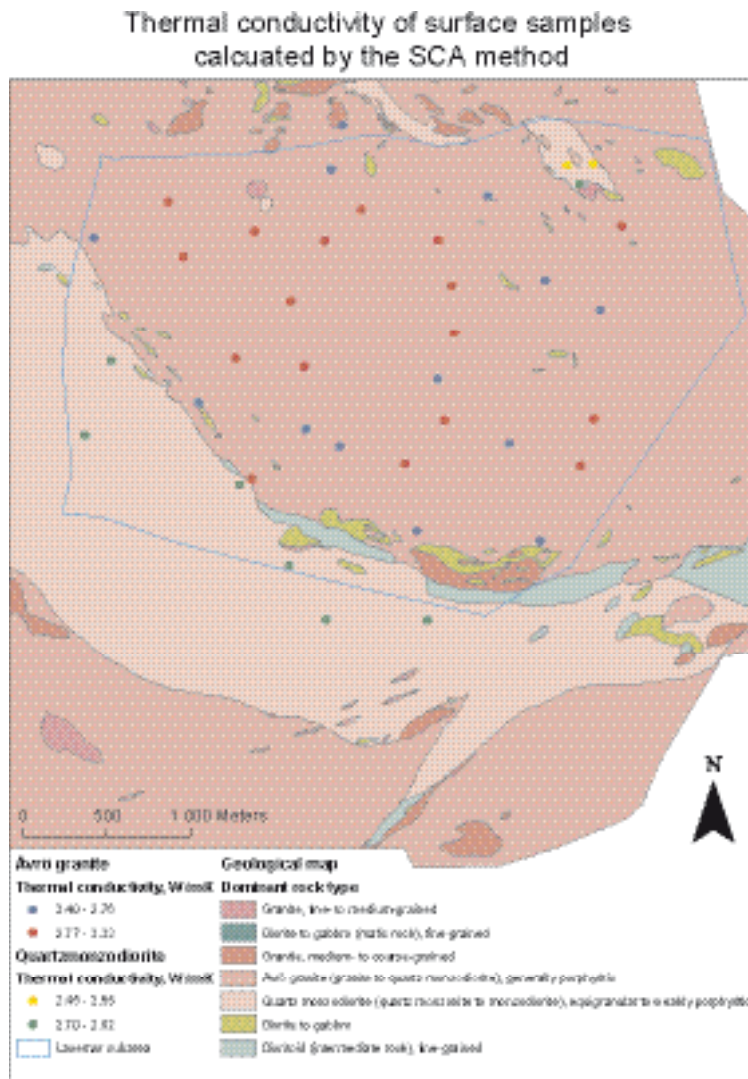


Figure 7-1. Thermal conductivity calculated from modal analysis (SCA method) for surface samples of Ävrö granite and, for comparison, quartz monzodiorite.

7.2.3 Thermal conductivity from density

A relationship between density and measured (TPS) thermal conductivity for Ävrö granite (501044), based on previous data /Sundberg 2003b, Sundberg et al. 2005b/ together with the results from 34 new measurements, has been developed, see Figure 7-2. No unequivocal relationship between thermal conductivity and density within other rock types for which data are available is apparent. In the case of fine-grained dioritoid, this is due to the restricted density range of the rock type.

Based on the relationship in Figure 7-2, the density values given by the density logging of boreholes were used to deterministically assign a thermal conductivity value to each logged decimetre section of Ävrö granite. Density logging data for boreholes KLX01, KLX02, KLX03 and KLX04 were re-sampled, calibrated and filtered /Mattsson 2004/ and /Mattsson et al. 2005/.

For the purposes of modelling thermal conductivity from density loggings, it is assumed that the established relationship is valid within the density interval 2,600–2,850 kg/m³, which corresponds to a thermal conductivity interval 1.84–3.74 W/(m×K), i.e. slightly outside the interval of measured data. The extreme, both high and low, values of thermal conductivity produced are purely an effect of the considerable random noise in the density loggings. It is still considered justified to extrapolate the density relationship within this interval since, firstly these extreme values tend to disappear as a consequence of upscaling, and secondly using a more restricted density range would produce a systematic bias in the results. When data from the four boreholes are combined in a frequency histogram (Figure 7-3), it appears that the distribution of thermal conductivity calculations for Ävrö granite contains two modes. This seemingly bimodal distribution is also evident in both the TPS and SCA data sets for Ävrö granite /Sundberg et al. 2006/.

In order to evaluate how well the thermal conductivity-density model (cf. Figure 7-2) reflects the actual thermal conductivity in the borehole, measured samples (TPS) were compared with values estimated from density logging. In relation to laboratory measurements, the density loggings underestimate the thermal conductivity by on average 1.78%, which is equivalent to 0.06 W/(m×K). However, samples with high conductivity values are strongly overrepresented in the comparison. Two samples of low thermal conductivity Ävrö granite indicate that the values estimated from density logging may be overestimating the true thermal conductivity in the low conductivity range for this rock type.

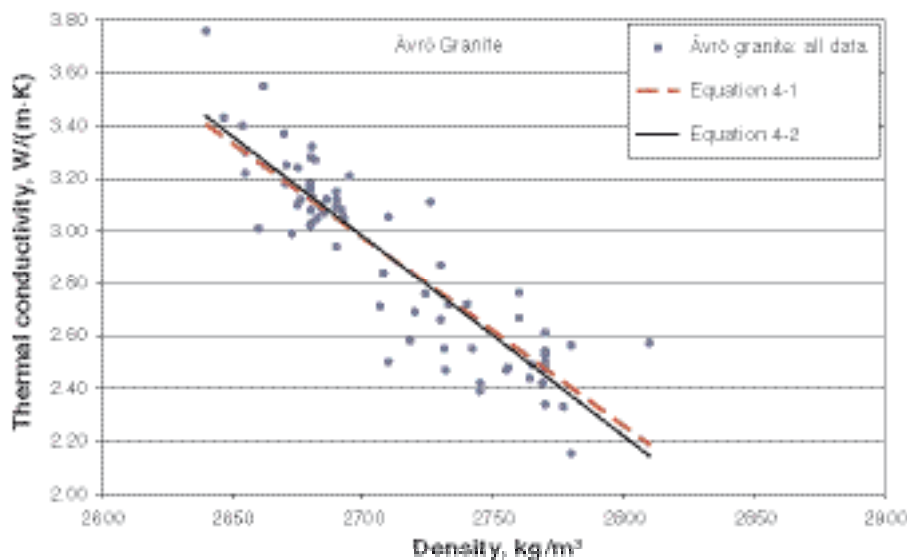


Figure 7-2. Relationships between density and thermal conductivity (TPS measurements), based on linear regressions limited to rock type Ävrö granite (501044). The black solid line is based on the relationship used in Laxemar 1.2 (red line: Simpevarp 1.2).

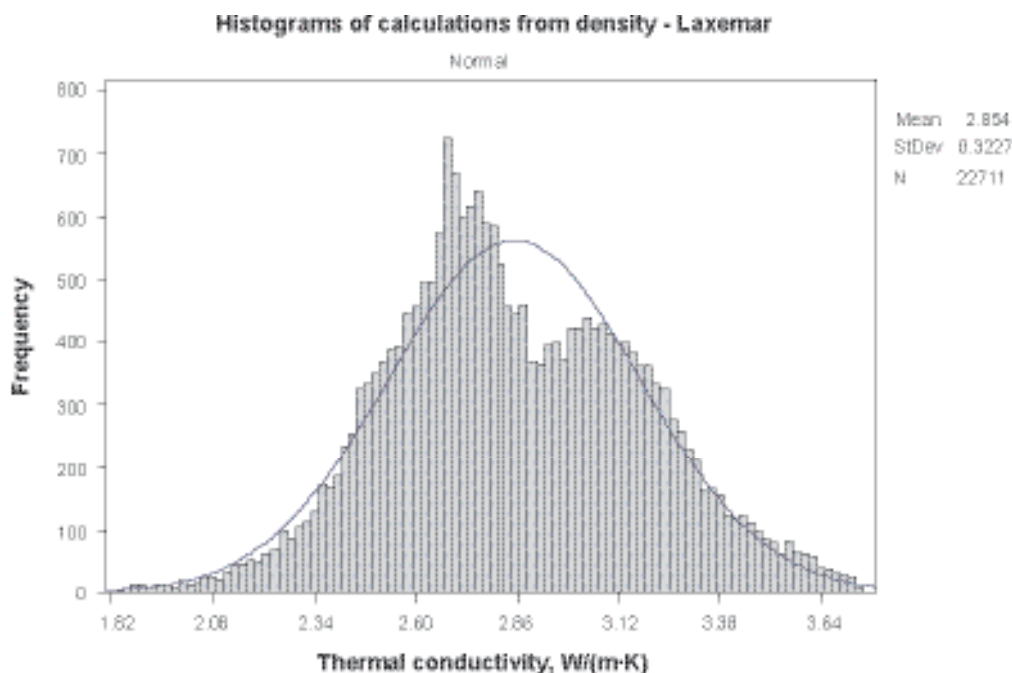


Figure 7-3. Histogram of thermal conductivities for Ävrö granite calculated from density loggings for boreholes KLX01, KLX02, KLX03, and KLX04. Normal distribution curve fitted.

7.2.4 Statistical rock type models of thermal conductivity

Method

Rock type models (Probability Density Functions, PDF:s) of thermal conductivity have been produced by using the available data from TPS measurements and SCA calculations from mineral composition. For some rock types, only SCA calculations are available. The most reliable data comes from TPS measurements, but these samples may not be representative of the rock type due to the limited number of samples and the sample selection procedure. Samples on which SCA calculations are based, it should be noted, have a larger spatial distribution in the rock mass.

Because of the availability of additional TPS measurements for Ävrö granite (501044), it has been decided to exclude the SCA data from the model for this rock type. The SCA calculations for rock types fine-grained dioritoid (501030) and quartz monzodiorite (501036) have been corrected in order to reduce the effect of a potential bias in the SCA calculations according to Table 7-5. For both rock types, a correction by a factor of 1.10 is applied.

The rock type models are used to model thermal properties for lithological domains, see Section 7.3. All rock types are assumed to be characterised by normal (gaussian) PDF:s. For Ävrö granite this assumption is unlikely to hold true. The available data for this rock type displays a bimodal distribution. However, this is only of minor importance in the modelling work which follows, since thermal conductivities for this rock type are generally calculated from the density loggings in order to include spatial variability. For domain RSMM, for which representative borehole data is lacking, a rock type model for Ävrö granite was based on thermal conductivity calculated from density loggings from KLX03 (see Section 7.3.4).

7.2.5 Heat capacity

Table 7-7 summarises the results from heat capacity determinations calculated from thermal conductivity and diffusivity measurements performed with the TPS method for different rock types. Determination of heat capacity has been performed on the same samples as used for measurements of thermal conductivity. Therefore the same problem concerning representativeness of the rock mass exists. Rock type models of heat capacity have been produced from the results. Heat capacity exhibits a large temperature dependence which is shown in Table 7-8.

Table 7-6. Model properties of thermal conductivity (W/(m×K)) from different methods and combinations divided by rock type. All rock type models (in bold) are based on normal (Gaussian) distributions (PDF:s).

Rock name (name code)	Samples	Mean	St. dev.	Max	Min	No. of samples	Simpevarp 1.2 – mean and St. dev. ²	Comment
Ävrö granite (501044)	Therm. cond. from density logging	2.85	0.32 ¹	3.74	1.84	22,711		Not used in model
	TPS	2.90	0.35	3.76	2.16	71		
	SCA	2.66	0.30	3.48	2.13	73		Not used in model
	Rock type model: TPS	2.90	0.35	3.76	2.16	71	2.79 (0.35)	
Quartz monzodiorite (501036)	TPS	2.74	0.16	2.95	2.43	15		
	SCA	2.41	0.11	2.55	2.23	20		Adjusted by factor 1.1 in model
	Rock type model: 1.1×SCA+TPS	2.69	0.14	2.95	2.43	35	2.62 (0.28)	
Fine-grained dioritoid (501030)	TPS	2.79	0.16	3.16	2.51	26		
	SCA	2.40	0.35	3.45	1.96	26		Adjusted by factor 1.1 in model
	Rock type model: 1.1×SCA+TPS	2.71	0.30	3.79	2.15	52	2.72 (0.30)	
Fine-grained granite (511058)	TPS	3.63		3.68	3.58	2		
	SCA	3.27	0.31	3.64	2.50	10		
	Rock type model: SCA+TPS	3.33	0.31	3.68	2.50	12	3.33 (0.34)	
Fine-grained diorite-gabbro (505102)	Rock type model: SCA	2.57	0.23	2.87	2.15	10	2.57 (0.23)	
Diorite/Gabbro (501033)	Rock type model: SCA	2.41	0.22	2.80	2.16	7	2.46 (0.21)	
Granite (501058)	Rock type model: SCA	2.97	0.59	3.79	2.12	5	2.59 (0.65)	
Pegmatite (501061)	Rock type model	3.31	0.48				–	Data from /Sundberg 1988/

¹ The st. dev. of thermal conductivity from density logging is partly a consequence of the restricted interval for the density vs. thermal conductivity relationship.

² Simpevarp site descriptive model, version 1.2 /SKB 2005a/.

Table 7-7. Determined heat capacity (MJ/(m³×K)) of samples from different rock types, using the TPS method. Samples are from boreholes KAV01, KSH01A, KSH02, KAV04a, KLX02 and KLX04 (Simpevarp and Laxemar subareas) together with borehole KA2599G01 (Äspö HRL) and boreholes from the prototype repository tunnel (Äspö HRL).

Rock name (sample location)	Mean	St. dev.	Number of samples
Fine-grained dioritoid, 501030 (borehole KSH01A and KSH02).	2.23	0.10	26
Quartz monzodiorite, 501036 (borehole KSH01A and KAV04A).	2.29	0.13	15
Ävrö granite, 501044 (borehole KAV01, KAV04A, KLX02, KLX04, KA2599G01 and Äspö HRL prototype tunnel).	2.24	0.13	68

Table 7-8. Determined temperature dependence of heat capacity (per 100°C temperature increase) on samples from different rock types in boreholes KSH01A and KSH02 (Simpevarp subarea), KLX02 and KLX04 (Laxemar subarea), and KA2599G01 (Äspö). The mean of the temperature dependence is estimated by linear regression.

Rock name (name code) (sample location)	Mean	St. dev.	Number of samples
Fine-grained dioritoid (501030) (boreholes KSH01A and KSH02).	25.6%	3.51%	11
Quartz monzodiorite (501036) (borehole KSH01A).	25.3%	3.30%	5
Ävrö granite (501044) (boreholes KA2599G01, KLX02 and KLX04).	25.1%	5.74%	13

7.2.6 Coefficient of thermal expansion

The coefficient of thermal expansion has been measured on borehole samples from the Simpevarp and Laxemar subareas /Åkesson 2004abcdef/. The results grouped according to rock type are presented in Table 7-9.

Table 7-9. Measured coefficient of thermal expansion (m/(m×K)) on samples with different rock types from boreholes KSH01A, KSH02, KAV01, KAV04A, KLX02 and KLX04 at the Simpevarp and Laxemar subareas (temperature interval: 20–80°C).

Rock type	Mean value	St. dev.	Min	Max	Number of samples
Fine-grained dioritoid (501030) (boreholes KSH1A and KSH02).	6.9×10^{-6}	1.5×10^{-6}	4.6×10^{-6}	9.9×10^{-6}	17
Quartz monzonite to monzodiorite (501036) (boreholes KSH01A and KAV04A).	8.2×10^{-6}	1.3×10^{-6}	5.8×10^{-6}	1.1×10^{-5}	14
Granite to quartz monzodiorite (501044) (boreholes KLX02, KLX04, KAV01 and KAV04A).	7.2×10^{-6}	1.8×10^{-6}	4.3×10^{-6}	1.1×10^{-5}	41

7.2.7 In situ temperature

Temperature and temperature gradient profiles have been investigated for boreholes KLX01, KLX02, KLX03, KLX04 and KAV04. Temperature was measured by fluid temperature logging. Temperature and temperature gradients plotted against elevation for each borehole are documented in /Sundberg et al. 2006/. Figure 7-4 summarises the results for all investigated boreholes. The filtered temperature seems to be almost linear with depth.

In Table 7-10 the temperatures at different depths are presented for the four investigated boreholes in the Laxemar subarea. There are errors associated with the loggings and this is indicated by the marked difference in temperature for the same borehole logged on different occasions. For some of the boreholes, difference flow loggings (PFL) have been performed. For borehole KLX03, the PFL without pumping gives temperatures that are about 1.5°C higher than the results from the fluid temperature logging.

Table 7-10. Temperature (°C) for the four investigated boreholes in the Laxemar subarea, at different depths below ground surface. The ground level (elevation) is between 10 and 25 m above sea level for all boreholes.

Borehole	Temperature at 400 m below ground level	Temperature at 500 m below ground level	Temperature at 600 m below ground level	Inclination (°)
KLX01	13.4	15.1	16.6	85–87
KLX02, 1993	12.3	13.8	15.3	82–85
KLX02, 2002	12.7	14.2	15.7	83–85
KLX02, 2003	13.1	14.5	16.1	83–85
KLX03	11.1	12.8	14.5	75–77
KLX04	11.4	13.2	15.1	82–85
Mean	12.3	13.9	15.6	(For calculation of mean temperature, only the latest value for KLX02 is used.)

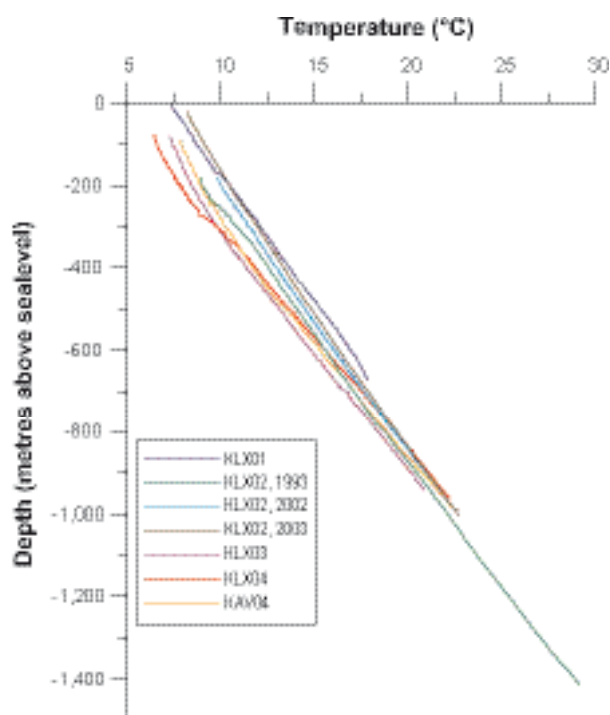


Figure 7-4. Temperature as a function of depth in four boreholes at Laxemar and one at Ävrö.

7.3 Thermal modelling of lithological domains

7.3.1 Modelling assumptions and input from other disciplines

Geological model

The rock domain model of the site descriptive model Laxemar version 1.2 forms the geometrical base for the thermal model and is described in Chapter 5. The focus of the thermal modelling is the Laxemar subarea west of the plastic deformation zones (i.e. west of ZSMNE005A (Äspö shear zone)), which is characterised by five lithological domains. Data from four boreholes, KLX01, KLX02, KLX03 and KLX04, are used in the modelling.

For the purposes of thermal modelling, the characterisation of rock domains by borehole intervals, as described in the rock domain model, has been modified so as to better represent the variability in thermal properties within domains RSMA and RSMD (Table 7-11 and /Sundberg et al. 2006/). The RSMM domain occurs in the south of Laxemar and is intersected by borehole KLX03. Since KLX03 does not adequately represent the lithological variability present in domain RSMM, modelling of this domain has had to rely on estimates of typical rock type composition derived primarily from surface geological mapping /Wahlgren et al. 2005b/. For domain RSME borehole data are not available, so in this case a rough estimate /Wahlgren et al. 2005b/ of rock type composition forms the basis for the thermal modelling.

Table 7-11. Data used for characterisation of rock domains for modelling of thermal properties.

Domain	Source of data for modelling
RSMA	KLX01 0–701 m. KLX02 200–540, 960–1,000 m. KLX04 100–990 m. KLX03 100–620 m.
RSMBA	KLX02 540–960 m.
RSMD	KLX03 620–1,000 m.
RSMM	Estimates of typical rock type compositions from geological mapping /Wahlgren et al. 2005b/.
RSME	Estimates of typical rock type compositions from geological mapping /Wahlgren et al. 2005b/.

7.3.2 Conceptual model of spatial variability

There are three main causes for the spatial variability of thermal conductivity at the domain level; (1) small scale variability between minerals, (2) spatial variability within each rock type, and (3) variability between the different rock types making up the domain. The first type entails variability in small samples (based on TPS measurements and modal analysis). At this scale, the variability can be substantial. However, the variability is rapidly reduced when the scale increases.

The second type is associated with variability in sample data from a rock type and cannot be explained by mineral scale variations. This is believed to be especially important for the rock type Ävrö granite. Variograms of thermal conductivity for different boreholes indicate variability at different scales. Although there are differences from one borehole to the other, at least 30% of the variability within Ävrö granite occurs at scales of less than about 2 m.

The third type of variability is due to the presence of different rock types in the lithological domain. This variability is more pronounced where the difference in thermal conductivity is large between the most common rock types of the domain. Large variability of this type can also be expected in a domain made up of many different rock types. It is believed that the variability between rock types is important for all defined domains. It is only reduced significantly when the scale becomes large compared to that of the spatial occurrence of the rock type.

Of importance at the domain level is the scale at which the thermal conductivity is relevant for the heat transfer from the canister. On the basis of present knowledge /Sundberg et al. 2005a/, variability below 1 m seems to have little or no relevance for the canister temperature. Therefore, the approach in the domain modelling is to use results mainly from 0.8 m scale so as not to underestimate the variability at the relevant scale, and to draw conclusions of representative thermal conductivity values based on this scale.

7.3.3 Modelling approach for domain properties

The methodology for thermal conductivity domain modelling and the modelling of scale dependency were developed for the Prototype Repository at the Äspö HRL /Sundberg et al. 2005a/. The methodology involves a base approach (see Figure 7-6) by which the mean thermal conductivity at domain level is modelled, and a number of complementary approaches which are applied in order to evaluate the spatial variability at domain level. The base approach differs slightly depending on whether borehole density loggings can, or cannot, be used. Rock domains RSMM and RSME are not represented by any boreholes and therefore Monte Carlo simulation is used as the base approach. For these domains, the base approach does not involve any upscaling. Anisotropy has not been considered in the domain modelling.

When evaluating the spatial variability at domain level, the four complementary approaches (Approaches 1–4) it is assumed that spatial variability for a domain can be estimated as the sum of the variance due to different rock types and the variance due to spatial variability within the dominating rock types:

$$V_{\text{tot}} = V_{\text{between rock types}} + V_{\text{within rock type}} \quad \text{Equation 7-1}$$

The “between rock type” variability is qualitatively different from, and therefore likely to be independent of, the “within rock type” variability. Therefore, adding the two types of variance is considered reasonable.

Table 7-12 summarises the different approaches applied to the respective domains. These approaches and the results are described in more detail below and in /Sundberg et al. 2006/.

Base approach

The main purpose of the base approach is to determine the mean thermal conductivity of each domain. The base approach using borehole data was applied to domains RSMA, RSMBA and RSMD. This approach is described in detail in /Sundberg et al. 2005a/ and /Sundberg et al. 2006/ and is summarised below.

Table 7-12. Modelling approaches used for different domains. For domains RSME and RSMM no representative borehole data are available.

Domain	Modelling approach		Approach 1	Approach 2	Approach 3	Approach 4
	Base approach Modelling from borehole data	Monte Carlo simulation				
RSMA	X			X	X	X
RSMBA	X			X	X	X
RSMD	X		X		X	X
RSMM		X				
RSME		X				

Each borehole belonging to a domain is divided into 0.1 m long sections and each section is assigned a thermal conductivity value according to the lithological classification of that section. The principle for assignment of thermal properties is illustrated in Figure 7-5. The next step is upscaling performed on a range of scales, from 0.1 m to approximately 60 m, and comprises the following main steps as illustrated in Figure 7-5:

1. The boreholes representing the domain are divided into a number of sections with a length according to the desired scale.
2. Thermal conductivity is calculated for each section as the geometric mean of the values at the 0.1 m scale. This gives the effective thermal conductivity at the desired scale.
3. The mean and the variance of all sections at the desired scale are calculated. For each scale, the calculations are repeated n times with different assignment of thermal conductivity values at the 0.1 m scale (stochastic simulation).

Above, the geometrical mean is used to produce an effective thermal conductivity in an appropriate scale from small scale determinations. The geometric mean is associated with transport in 2D and is often applied for estimation of effective transport properties /Dagan 1979, Sundberg 1988/. In reality the effective transport properties in 3D are influenced by the variance, which is not considered when the geometric mean is calculated. However, in this thermal application the variance is low and therefore the geometric mean is an adequate approximation. In /Sundberg et al. 2005a/ this is discussed further.

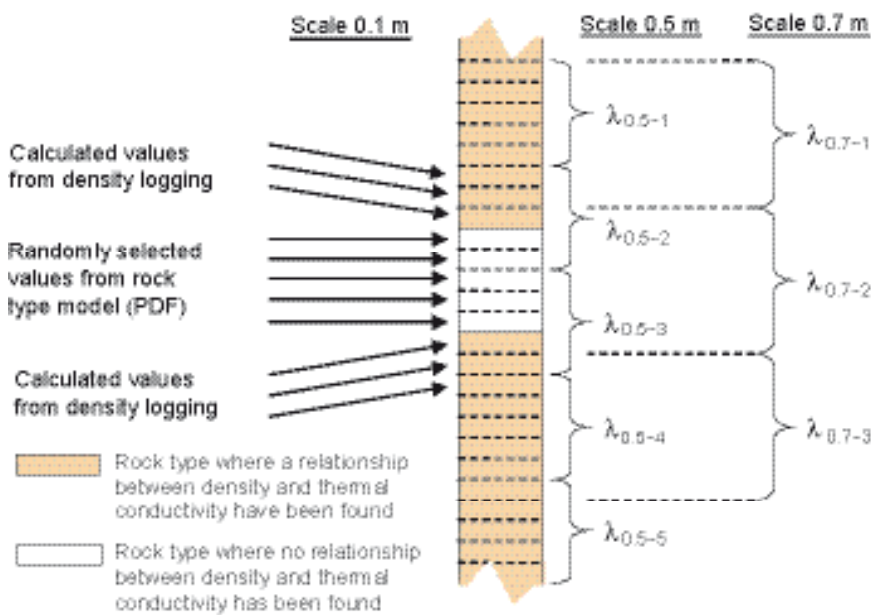


Figure 7-5. Thermal conductivity is assigned to 0.1 m sections by calculation from density loggings or randomly selected from the rock type models. Upscaling is performed by calculating geometric means for different scales, for example 0.5 and 0.7 m.

As illustrated in Figure 7-6, the base approach is slightly different between domains where density loggings can be used (domains RSMA and RSMBA, dominated by Ävrö granite) or cannot be used (domain RSMD). Density loggings of Ävrö granite can be used for domain RSMA and RSMBA to take into account spatial correlation within the dominating rock type. This is not possible for domain RSMD (quartz monzodiorite), which is dominated by other rock types for which no reliable “within rock type” relationship is presently available. Therefore, the variance for domain RSMD is underestimated in the base approach. The spatial variability within the dominating rock type needs to be added, see alternative approaches below.

Another type of base approach is applied to rock domains RSME (Diorite/gabbro) and RSMM (Mixed zone with large fraction of diorite/gabbro), which are not represented by any boreholes and must therefore be treated differently. For these domains, a simplified approach based on Monte Carlo simulation has been used. The PDF models for the rock types present in these domains (Table 7-6) are used to estimate the variability at the 0.1 m scale. No direct upscaling is possible due to lack of borehole data. Thus, spatial variability has not been taken into account for these domain.

Approach 1: Addition of within rock variability from domain RSMA

To estimate the spatial variability within the dominating rock types for which density loggings are unavailable, it was assumed that the variance caused by spatial variability within other dominant rock types is identical to spatial variability within rock type Ävrö granite in domain RSMA. The “within rock type” variance for Ävrö granite in domain RSMA was estimated and then added to the “between rock type” variance calculated for other domains /Sundberg et al. 2006/.

Approach 2: Extrapolation of spatial variability

When modelling domains RSMA and RSMBA according to the base approach, spatial distribution was only considered for 81.5% and 55.5% of the borehole lengths respectively, since not all 0.1 m

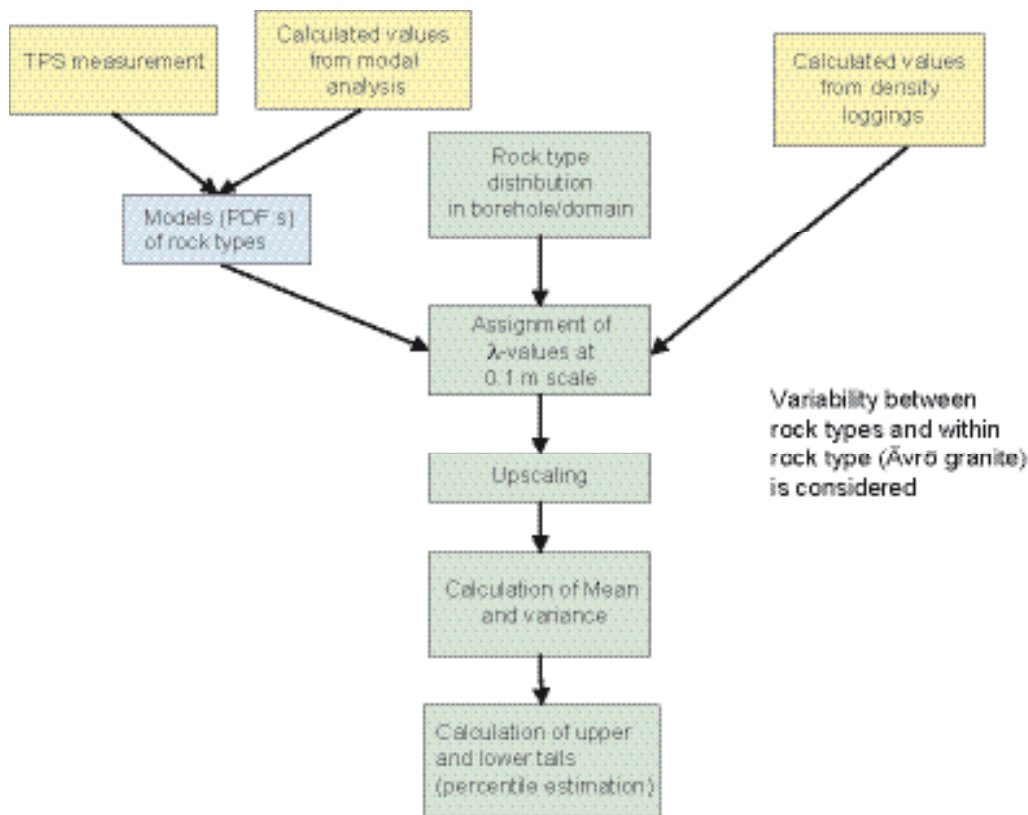


Figure 7-6. Base approach for estimation of thermal conductivity for domains RSMA (Ävrö granite) and domain RSMBA (Mixture of Ävrö granite and fine-grained dioritoid) and RSMD. Yellow indicates the data level, blue the rock type level, and green the domain level. The parameter λ refers to thermal conductivity.

sections of the domain were comprised of Ävrö granite, the only lithology for which density logging data could be used. For the remainder of the borehole length, thermal conductivity values were randomly assigned from the rock type models. Therefore, an approach was applied to correct for this. By randomly replacing thermal conductivity values estimated from density logging with random PDF values it is possible to study the effect of ignoring the “within rock type” spatial variability for parts of the borehole. By repeating this exercise for successively larger parts of the borehole, it is possible to construct a graph of how the variance is affected. This curve can be extrapolated to 100% in order to determine the total “within rock type” variance, see Figure 7-7. In this approach, it is implicitly assumed that the spatial variation of other rock types is similar to that of Ävrö granite. Since it is almost certainly the case that spatial variability in Ävrö granite is greater than for other rock types, the outcome of this approach overestimates the total “within rock type” variability.

Approach 3: Subtraction of small-scale variability

In the third approach, variograms based on density logging data are used to estimate the small scale variance of Ävrö granite in RSMA (Figure 7-8). In this approach, the small-scale variability for the scale of interest (0.8 m) within Ävrö granite is subtracted from the total variability of the same rock type (from PDF:s). This residual variability is assumed to be the variance after upscaling. The basis for the approach is that variability at scales smaller than the desired is evened out. A limitation of this approach is that data to construct variograms are available for Ävrö granite only. For domain RSMD, it was assumed that the small-scale variability within quartz monzodiorite is of the same relative magnitude as for Ävrö granite. This assumption is considered reasonable since both Ävrö granite and quartz monzodiorite are granitoid rocks with similar grain size.

Approach 4: Upscaling of “within rock type” variability

In this approach /Sundberg et al. 2005a/, the spatial variability within the dominant rock type is estimated based on TPS measurements or density loggings. Measurement data are classified in spatial groups depending on their location, and the geometric mean is calculated for each group.

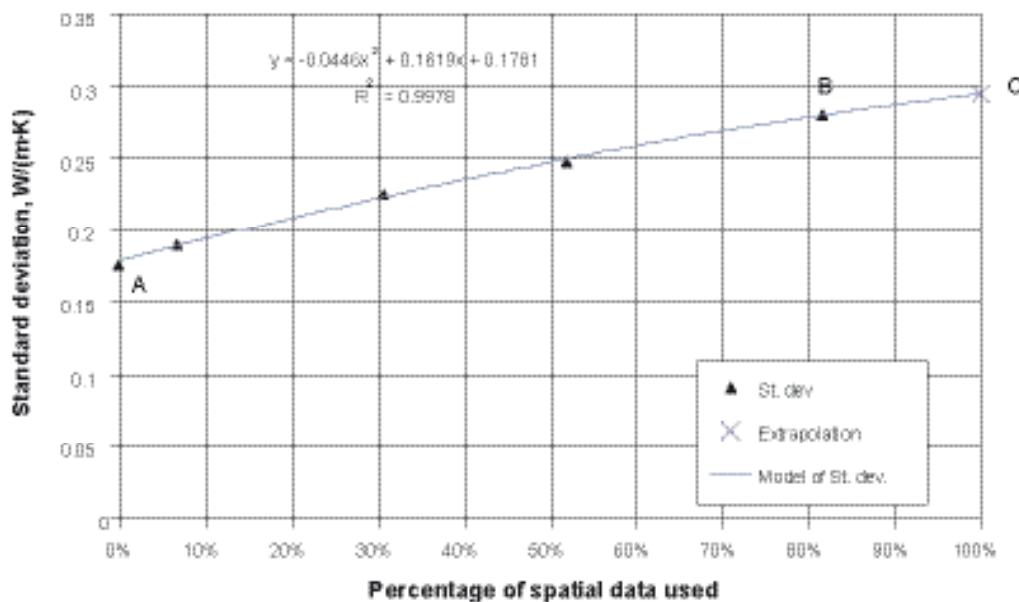


Figure 7-7. Extrapolation of standard deviation for thermal conductivity at scale 0.8 m as a function of the percentage of spatial data used in the modelling of domain RSMA. At point A, all data are randomly assigned from rock types PDF:s without consideration of spatial variability within the Ävrö granite. Point B corresponds to 81.5% of the values estimated from density loggings and thus considering spatial variability. Point C is extrapolated and corresponds to 100% spatial data values, assuming the same spatial variability within all rock types as in Ävrö granite.

This gives a set of data for the scale in question (based on the spatial groups). This procedure can be repeated for different scales and plotted on a graph (see Figure 7-9). The variance for the desired scale can be estimated from the graph and this “within rock type” variance is then added to the “between rock type” variance calculated in the base approach.

For domains with more than one dominant rock type, the total “within rock type” variance is estimated as the weighted sum of the spatial variance for the different dominant rock types, where the weighting factors are the fractions of the respective rock types in the domain. Although this approach only provides a rough estimate of the total variability it encompasses all the major types of variability within the domain.

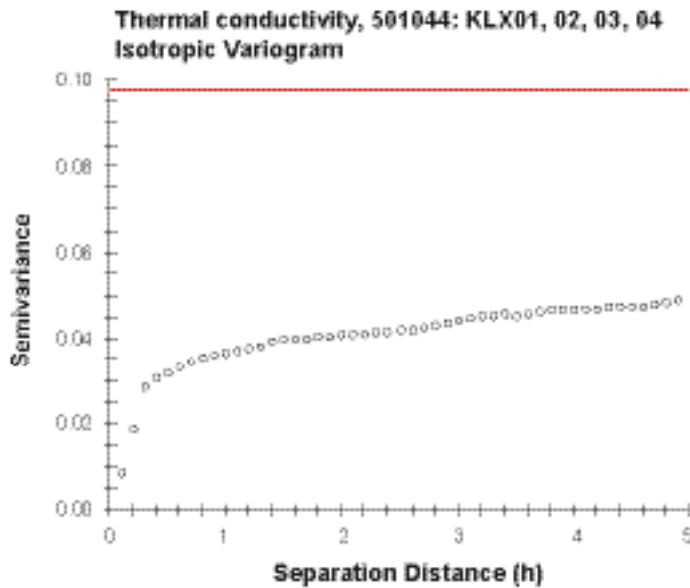


Figure 7-8. Variogram of thermal conductivity for Åvrö granite (501044) in domain RSMA in boreholes KLX01, KLX02, KLX03 and KLX04, estimated from density logging. Separation distance in metres. Unit of semivariance is $(W/(m \times K))^2$. The straight line indicates the total variance in the data.

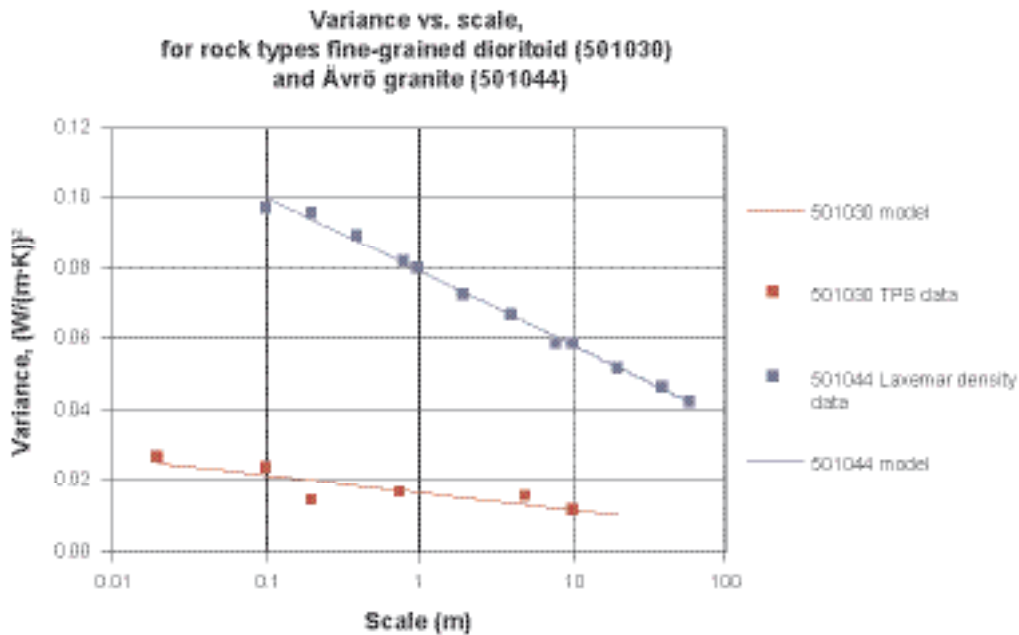


Figure 7-9. Comparison between “within rock type” variability for rock types fine-grained dioritoid (501030) and Åvrö granite (501044).

7.3.4 Domain modelling results

Borehole modelling

In /Sundberg et al. 2006/ thermal conductivity plotted against lithological logs and borehole length is shown for boreholes KLX01, KLX02, KLX03, KLX04 and KAV04A, (exemplified in Figure 7-10). The results are summarised in Table 7-13 for the 0.8 m scale. Borehole KAV04A is located in Simpevarp subarea (Ävrö island) and is not included in the modelling of Laxemar.

Table 7-13. Summary of thermal conductivity (W/(m×K)) modelling results at 0.8 m scale for boreholes KAV04A, KLX01, KLX02, KLX03 and KLX04.

Borehole	Scale, m	Mean	Standard deviation	Comment
KAV04A	0.8	2.951	0.284	Not included in Laxemar 1.2 model.
KLX01	0.8	2.751	0.233	
KLX02	0.8	2.927	0.258	
KLX03	0.8	2.627	0.171	
KLX04	0.8	2.946	0.254	

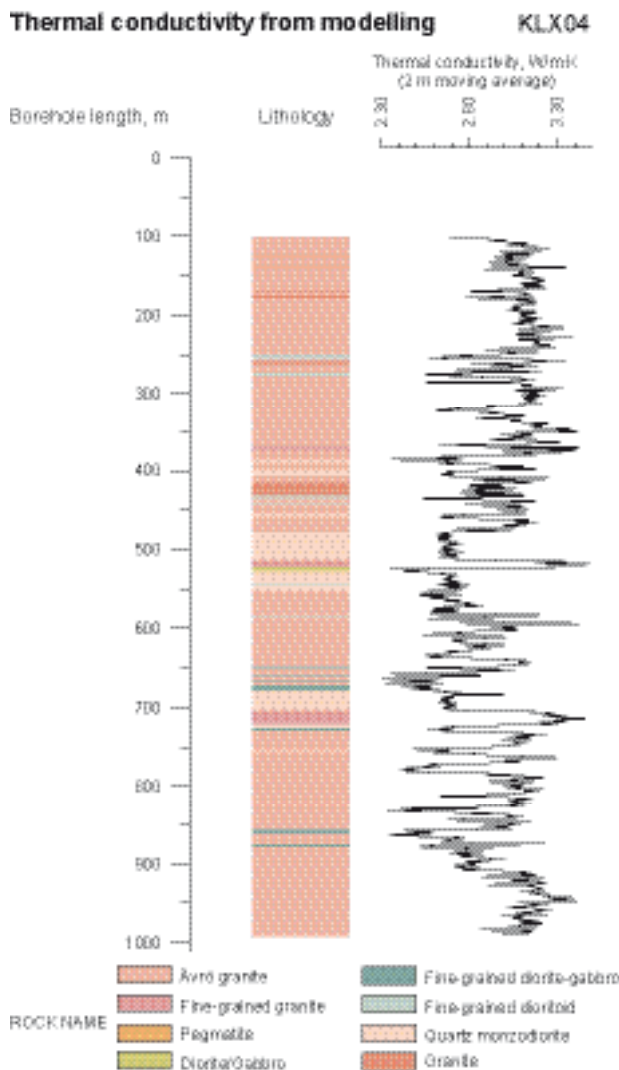


Figure 7-10. Exemplification of changes in thermal conductivity along borehole KLX04. Thermal conductivity is calculated as geometrical means over 2 m long sections (moving average) from 0.1 m data. The results originate from one realisation only, and are based on both deterministic (for Ävrö granite) and stochastic (for other rock types) computations.

Domain modelling: base approach

Modelling results for domains RSMA, RSMBA and RSMD at the 0.8 m scale are presented in Table 7-14 and Figure 7-11. Of particular interest is the large difference in thermal conductivity between boreholes making up domain RSMA. KLX03 displays the lowest thermal conductivity values whereas KLX02 and KLX04 have the highest values. The bimodal distribution and large variance at domain level (Figure 7-11) reflects the characteristic bimodal frequency distribution of the dominant rock type, i.e. Ävrö granite. For a more in-depth description of the variation in thermal conductivity within domain RSMA see /Sundberg et al. 2006/.

For domain RSMD the data distribution is characterised by a relatively low standard deviation and a long upper tail. Except for Ävrö granite, spatial variability within the rock types comprising this domain has not been taken into account. Thus the base modelling approach adopted for domain RSMD underestimates the variance at the 0.8 m scale.

The scale dependency in both the mean and standard deviation of thermal conductivity is illustrated for domain RSMA in Figure 7-12. As can be seen the differences are greatest at scales below 2 m.

Because of the lack of representative borehole data, the approach applied to the domains described above cannot be applied to domains RSME and RSMM. Therefore, a simplified approach based on Monte Carlo simulation is used in modelling these domains. The rock type model used for Ävrö granite in domain RSMM is based on results of density logging in KLX03, not on TPS measurements. This is justified by evidence of the low thermal conductivity nature of Ävrö granite in southern Laxemar indicated by density logging results from borehole KLX03 (Figure 7-3) and from surface samples of Ävrö granite in southern Laxemar (Figure 7-1).

The approach used for domains RSME and RSMM does not take account of any variance reduction due to upscaling. Therefore, the quoted standard deviation most certainly overestimates the dispersion at a larger scale

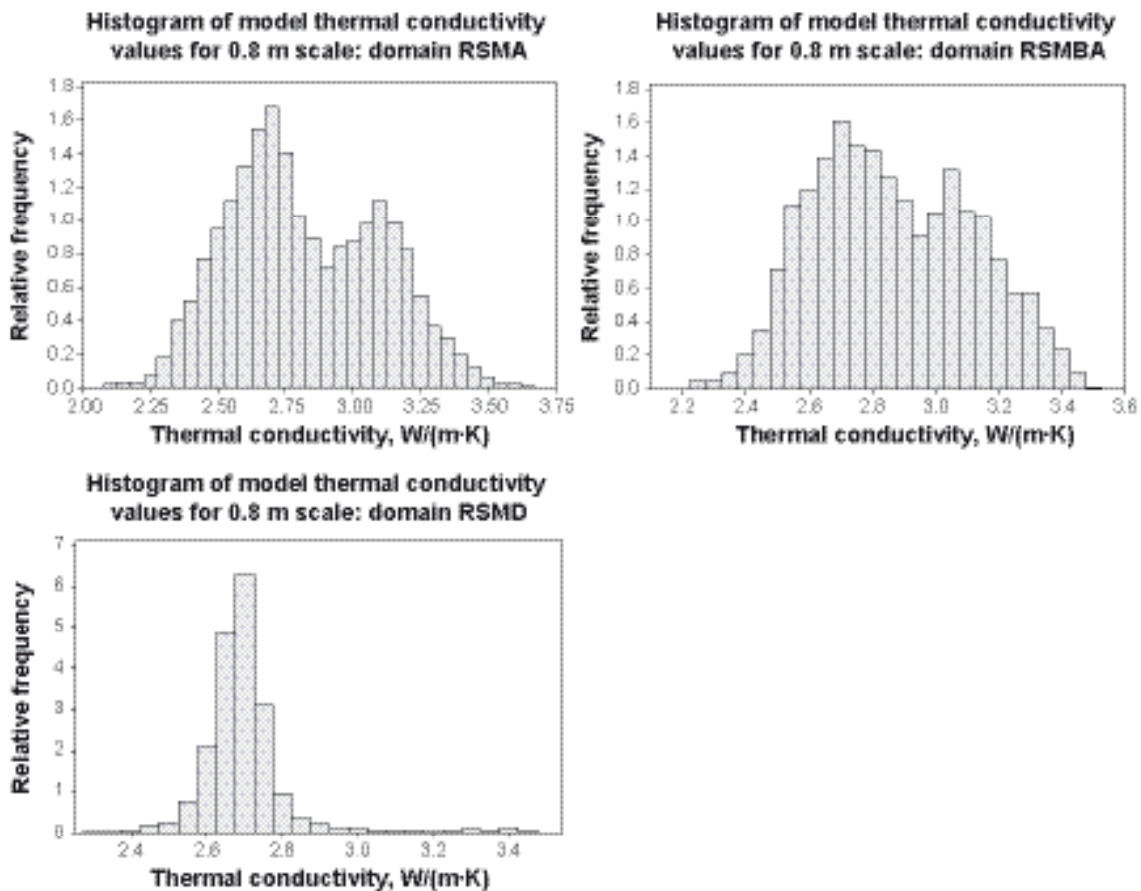


Figure 7-11. Histograms of thermal conductivities for domains RSMA, RSMBA and RSMD at the 0.8 m scale using the base approach.

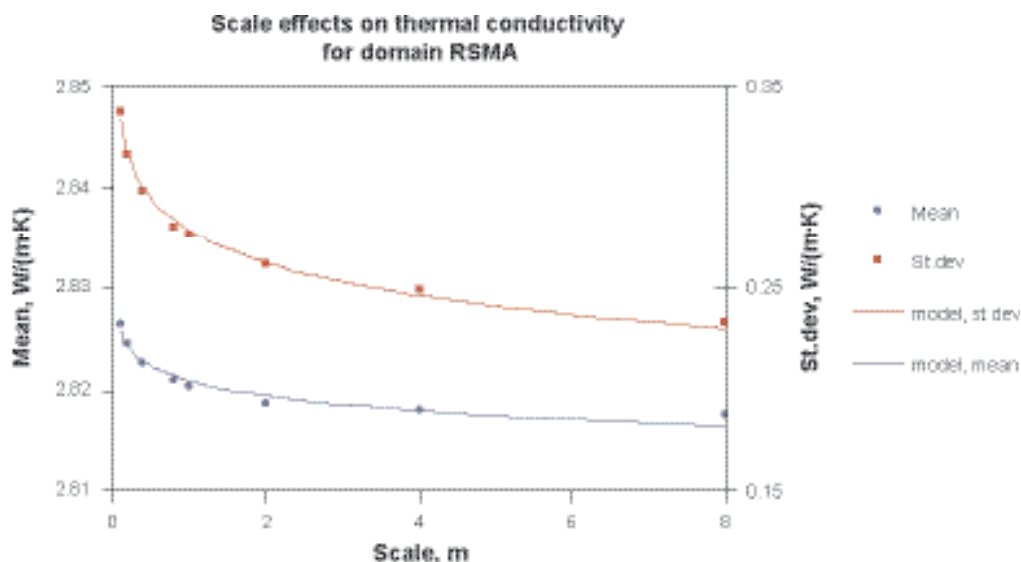


Figure 7-12. Modelling results of thermal conductivity for domain RSMA: scale dependence (0.1 to 8 m) of mean and standard deviation. Logarithmic curves fitted to data.

Table 7-14 presents the mean thermal conductivity together with standard deviations and upper and lower tails (defined as 0.5, 2.5 and 97.5 percentiles) for the modelled domains. It should be noted that the emphasis is placed on lower tail percentiles of the distributions as it is these that are critical for design purposes.

Table 7-14. Thermal conductivity (W/(m×K)) modelling results for domains. Upper and lower tails (percentiles) are calculated from the modelled data distribution according to the base approach. Note that the results at the 0.8 m scale apply to domains RSMA, RSMBA and RSMD only.

Scale (m)	Mean	St. dev.	0.5 percentile	2.5 percentile	97.5 percentile
RSMA (0.8 m)	2.821	0.281	2.238	2.352	3.365
RSMBA (0.8 m)	2.865	0.251	2.342	2.446	3.347
RSMD (0.8 m)	2.701	0.128	2.428	2.522	3.104
RSME (< 0.1 m)	2.45	0.29	1.85	1.98	3.22
RSMM (< 0.1 m)	2.58	0.22	1.98	2.13	2.98

Heat capacity

Frequency distributions of heat capacity have been produced by Monte Carlo simulation for four of the rock domains in the Laxemar subarea. The different rock types in the domains are weighted according to their relative abundance. Normal distribution models for rock types fine-grained dioritoid (501030), quartz monzodiorite (501036) and Ävrö granite (501044) are based on the data in Table 7-7. Other rock types have not been considered, due to the unavailability of measurements. From the simulations, the mean and standard deviation, in addition to 2.5 and 97.5 percentiles have been calculated for each domain, and are summarised in Table 7-15.

Table 7-15. Heat capacity MJ/(m³×K) of domains RSMA, RSMBA, RSMD and RSMM with 2.5 and 97.5 percentiles.

Domain	Mean value	St. dev.	2.5 percentile	97.5 percentile
RSMA	2.24	0.13	1.98	2.50
RSMBA	2.23	0.12	1.99	2.48
RSMD	2.29	0.12	2.06	2.52
RSMM	2.25	0.13	1.99	2.47

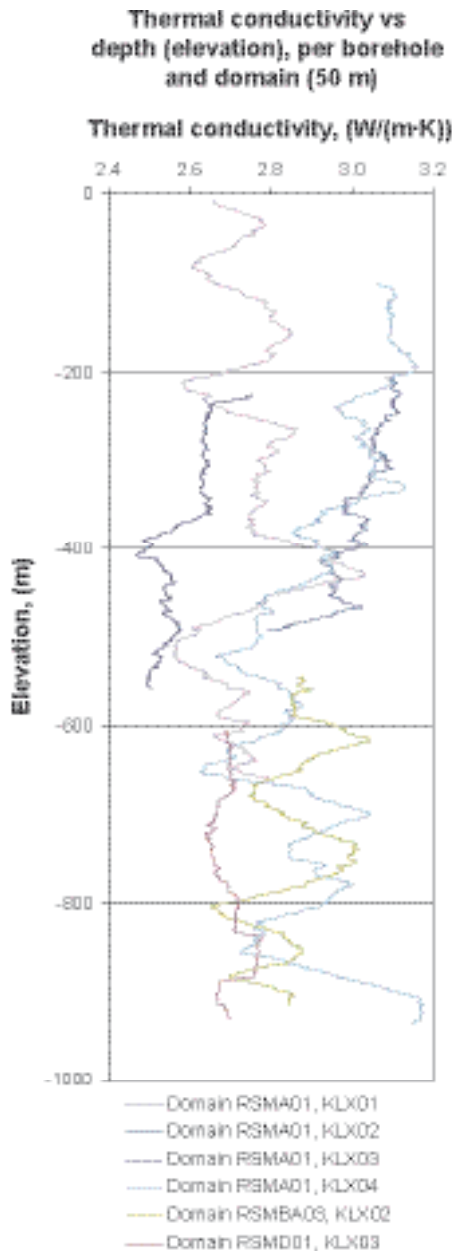


Figure 7-13. Visualisation of changes in thermal conductivity with depth for borehole sections for three domains (RSMA, RSMBA and RSMD). Thermal conductivity is expressed as moving geometrical mean calculations over 50 m long sections. Consequently the smaller-scale variability is not shown. The results are based on only one realisation.

Observe that the results in the above table are valid at 20°C. With increasing temperature the heat capacity increases considerably, see Table 7-8. The increase is approximately 25% per 100°C temperature increase for rock types Ävrö granite, quartz monzodiorite and fine-grained dioritoid.

In situ temperature

In the Laxemar model version 1.2 no modelling from temperature loggings has been done. The main reason for not modelling the temperature is that the temperature data are associated with a high degree of uncertainty for reasons discussed in Section 7.4.3.

7.3.5 Evaluation of domain modelling results

Variability of thermal conductivity

In order to evaluate the spatial variability at domain level, the base approach in addition to four complementary approaches have been used, as described above. The results from each approach are presented in Table 7-16. The base approach is believed to underestimate the standard deviation for domains RSMA and RSMBA, but particularly for RSMD, since the within rock variability is not fully accounted for (large difference between domains). As regards domains RSME and RSMM, the base approach overestimates the variability, since upscaling has not been possible.

Table 7-16. Summary of standard deviations (W/(m×K)) at the domain level from modelling results with the base approach compared with the four alternative/complementary approaches (Approaches 1–4). Numbers within brackets are calculated variances, (W/(m×K))², with the resulting standard deviations in bold.

Appr.	Scale (m)	RSMA (Ävrö granite)	RSMBA (Mixture of Ävrö granite and Fine-grained dioritoid)	RSMD (Quartz monzodiorite)	RSME (Dioite/gabbro)	RSMM (mix domain)	Comment
Base	0.8	0.28 (0.031+0.048=0.079) (between rock type + within rock type variance based on 81.5% spatial data)	0.25 (0.026+0.037=0.063) (between rock type + within rock type variance based on 55.5% spatial data)	0.13 Between rock type variance only (0.016)	0.29 Monte Carlo sim.	0.22 Monte Carlo sim.	Underestimation for RSMA RSMBA and RSMD. Overestimation for RSME and RSMM.
1	0.8			0.25 (0.017+0.048=0.065) (between rock type + within rock type variance from RSMA)			Strong overestimation for RSMD.
2	0.8	0.29 (0.031+0.056=0.087) (between rock type +100% within rock type variance)	0.29 (0.026+0.059=0.085) (between rock type +100% within rock type variance)	–	–		Overestimation
3	0.8	0.30 (0.031+0.062=0.093) between rock type variance + (total variance within dominating rock type – small scale variance)	0.30 (0.026+0.062=0.088) between rock type variance + (total variance within rock type – small scale variance from RSMA)	0.17 (0.017+0.012 ¹ =0.029) between rock type variance + (total variance within QMD – small-scale variance)			Overestimation for RSMA and RSMBA. For RSMD, st. dev. based on the assumption that the effect of upscaling in QMD is equivalent to that for Ävrö granite.
4	0.8	0.34 (0.031+0.082=0.113) (between rock type + within rock type variance)	0.29 (0.026+0.059 ² =0.085) (between rock type + within rock type variance)	0.22 (0.017+0.030 ³ =0.047) (between rock type + within rock type variance at 0.1 m scale)	–		Overestimation for RSMD: effects of upscaling within QMD not considered.

¹ “Within rock type” variance at 0.8 m scale for quartz monzodiorite (QMD) calculated by assuming that small-scale variance, i.e. 0–0.8 m, accounts for 37% of the total variance.

² Approximation of internal spatial variance within the rock types in the domain assuming a composition of 64% Ävrö granite and 36% fine-grained dioritoid (0.64×0.082+0.36×0.018=0.059).

³ Approximation of internal spatial variance within the rock types in the domain calculated assuming a composition of 84% quartz monzodiorite and 16% Ävrö granite (0.84×0.020+0.16×0.082=0.030). (See Approach 4 in Section 7.3.3)

Approach 1 almost certainly overestimates spatial variability for RSMD since the dominant rock type in this domain, quartz monzodiorite, is considered to display less "within rock type" variation than does Ävrö granite. The latter displays an unusually wide compositional variation /Wahlgren et al. 2005a/, a fact reflected in the large range of measured and calculated thermal conductivity values, see Table 7-6. As regards Approach 2, it is reasonable to assume that the total variance is overestimated, since the spatial variability within Ävrö granite is expected to be larger than for other rock types. Approach 3 should also overestimate the standard deviation, since the variance within the dominating rock type, i.e. Ävrö granite, is considered to represent the domain as a whole. It is not easy, generally speaking, to assess whether Approach 4 under- or overestimates the total variance for a domain. For domain RSMD, however, an upper limit for the standard deviation at the 0.8 m scale is provided by Approach 4, since variance reduction due to upscaling within quartz monzodiorite, the dominating rock type, is not considered.

Taking into account the outcomes of the different approaches, the following standard deviations for each domain are proposed.

- Both domain RSMA and RSMBA are attributed the value of 0.29 W/(m×K), which is the result from Approach 2 at the 0.8 m scale.
- For domain RSMD, the standard deviation given by Approach 3, 0.17 W/(m×K), is adopted. Since a variance reduction due to upscaling is to be expected, this approach is considered to provide a reasonable approximation of spatial variability for this domain.
- For domains RSME (Diorite/gabbro) and RSMM (mixed zone with large fraction of diorite/gabbro), no changes have been made in the standard deviation compared with the simulation results of the base approach.

Estimation of percentiles of thermal conductivity

Since the distributions of thermal conductivities at domain level cannot be shown to be normal, estimations of lower and upper tail percentiles based on the revised standard deviations cannot be calculated using parametric methods. To estimate lower and upper tail percentiles for the revised standard deviations, corrections were made to the percentile values calculated from the modelled distributions (Table 7-14). The correction method is described in /Sundberg et al. 2006/. As already mentioned, the lower tail percentiles are of most interest as it is these that are critical for design purposes.

The resulting values are suggested to be reasonable approximations of the respective percentiles for the 0.8 m scale, see Table 7-17. It should be mentioned that uncertainties associated with estimation of percentiles becomes larger at the extreme ends of the distributions. Because no scaling up has been performed for domains RSME and RSMM, the lower tails percentiles estimated from realisations based on Monte Carlo simulation, are conservatively low for larger scales. By taking into account the effect of upscaling on lower and upper tail percentiles observed in the other domains, which on average is about 0.2 W/(m×K) for the 0.8 m scale, corrected 0.5 and 2.5 and 97.5 percentiles can be approximated for domains RSME and RSMM, see Table 7-17. Obviously, these approximations are uncertain.

Table 7-17. Recommended mean, standard deviation, and lower and upper tail percentiles of thermal conductivity (W/(m×K)) per domain at 0.8 m scale. For RSME and RSMM, a rough correction has been applied to percentiles estimated from Monte Carlo simulated distributions, which are based on a < 0.1 m scale.

Domain	Mean	St. dev.	0.5 percentile	2.5 percentile	97.5 percentile
RSMA	2.82	0.29	2.20	2.32	3.39
RSMBA	2.87	0.29	2.24	2.37	3.43
RSMD	2.70	0.17	2.32	2.44	3.19
RSME	2.45		2.0	2.2	3.0
RSMM	2.58		2.2	2.3	2.8

Observe that the above table is valid at 20°C. The thermal conductivity decreases slightly at higher temperatures, 1–5% per 100°C temperature increase.

Comparison with previous model versions

A comparison of the thermal conductivity results at domain level presented in the Simpevarp 1.1 /SKB 2004b/, Simpevarp 1.2 /SKB 2005a/, and the current Laxemar 1.2 site descriptive model versions is provided in Table 7-18.

Table 7-18. Comparison of modelling results (the mean and the standard deviation) from the Simpevarp 1.1, Simpevarp 1.2 and Laxemar 1.2 site descriptive model versions.

Domain	Mean (W/(m×K))			Diff. (Laxemar 1.2– Simpevarp 1.2)/ Simpevarp 1.2	St. dev. (W/(m×K))		
	Version Simpevarp 1.1	Version Simpevarp 1.2	Version Laxemar 1.2		Version Simpevarp 1.1	Version Simpevarp 1.2	Version Laxemar 1.2
RSMA	2.67	2.80	2.82	0.7%	0.25	0.28	0.29
RSMD	2.38	2.62	2.70	3.1%	0.10	0.28	0.17

Observe that the above table is valid at 20°C. The thermal conductivity decreases slightly at higher temperatures, 1–5% per 100°C temperature increase.

7.3.6 Summary of domain properties

Thermal conductivity

Table 7-17 summarises the recommended mean, standard deviation and lower tail percentiles of thermal conductivity for each rock domain. For a discussion of these results, the reader is referred to the supporting document for thermal modelling, Laxemar version 1.2 /Sundberg et al. 2006/.

Heat capacity

Results of modelling of heat capacity on domain level, presented in Table 7-15 for four domains, indicate a small range (2.23–2.29 MJ/(m×K)) in mean heat capacity. Observe that these results are valid at 20°C. The heat capacity increases by approximately 25% per 100°C for the dominating rock types.

Coefficient of thermal expansion

No domain modelling has been made. It is suggested that the mean value for the dominant rock in each domain in Table 7-9 is considered representative for the whole domain.

In situ temperature

Domain modelling has not been performed. For all domains, mean in situ temperatures at 400, 500 and 600 m depth are estimated at 12.3, 13.9 and 15.6°C, respectively.

7.4 Evaluation of uncertainties

A more detailed description and discussion of uncertainties associated with thermal modelling are provided in /Sundberg et al. 2005a/ and the supporting document for thermal modelling Laxemar 1.2 /Sundberg et al. 2006/. An evaluation of the main uncertainties is however provided in this section.

Uncertainties are introduced at the following levels/stages:

- Data level.
- Rock type level.
- Domain level.

7.4.1 Thermal conductivity

Data level

The primary uncertainties at the data level apply to thermal conductivity calculations from mineralogy (SCA method), and calculations based on density measurements.

The uncertainty associated with SCA data is significantly larger than for TPS data (Section 7.2.2). For SCA data one of the most important sources of uncertainty is caused by alteration of minerals. Another uncertainty relates to the values of thermal conductivity assigned to the different minerals.

Thermal conductivities are calculated for Ävrö granite based on density loggings using the relationship in Figure 7-2. The major uncertainties associated with this procedure are:

- the high noise level in the density logging data (measurements),
- the statistical relationship between density and thermal conductivity.

Potential random errors due to noise might, for some of the boreholes, be as high as 50–60 kg/m³ /Mattsson and Thunehed 2004, Mattsson 2004/. There is also a potential bias in the values calculated from density measurement. This would be the case if the observed density vs. thermal conductivity relationship did not accurately represent the rock volume in the Laxemar subarea.

Rock type level

Uncertainty at the rock type level results in thermal conductivity estimates (PDF, mean and variance) that deviate from the true distribution for the rock type. The main causes of uncertainty are listed below.

The representativeness of samples selected for TPS measurements is less than satisfactory since samples were not taken with the purpose of statistically representing the rock mass. Consequently there is a potential for bias. As regards the calculated values based on modal analyses (SCA method) representativeness is considerably better for the major rock types, since sampling has been carried out at a greater number of locations. For subordinate rock types, representativity and the low number of samples contribute to uncertainty.

As evidence by the boremap mapping of the Laxemar boreholes, cf. Appendix 4, a significant volume, 10–15%, is comprised of weakly to strongly altered rocks. These altered rocks have not been sampled for measurement of thermal properties. This may have introduced a bias to the results.

Rock type models form an important input to the domain modelling. Several of the rock type models are based on small data sets as well as uncertain SCA data. In the case of fine-grained dioritoid and quartz monzodiorite, SCA data contributing to the models have been corrected by a factor derived from a comparison of SCA data with TPS data. Because the comparison is based on only a few samples, there is uncertainty in the accuracy of this correction. For the other rock types, for example diorite/gabbro, no correction was performed due to lack of TPS data, which of course leads to uncertain models.

Normal distribution models (PDF:s) were chosen to characterize the rock types. There is a slight deviation between data and models. Generally, the rock type models slightly overestimate the occurrence of low thermal conductivity values and underestimate the number of large values.

Another causes of uncertainty at the rock type level is the ambiguity in the geological classification of rock samples.

Domain level

Uncertainty at the domain level results in thermal conductivity estimates (mean, standard deviation and percentiles) that deviate from the true distribution of values at the scale of interest. The most important sources of uncertainty are the geological model, the related issue of representativeness of boreholes, the upscaling methodology in the modelling, and the estimation of spatial variability both within and between rock types.

In the base modelling approach, spatial variability within rock types other than Ävrö granite is ignored. This results in too large a variance reduction when the scale increases. To compensate for this, complementary approaches have been employed to take into account the variance due to spatial variability within other rock types. These approaches involve some uncertainties arising from the lack of knowledge of spatial variability within the rock types and within the domains. Apart from the need for more data, one way of overcoming this problem is to produce data sets by stochastic simulation that contains both variability within rock types and variability between rock types. This will eliminate the need for further adjustment of variances and percentiles, as described in Section 7.3.5.

Estimates of the proportion of rock types in domains not modelled using borehole data, namely RSME and RSMM, are associated with uncertainties. These uncertainties have not been accommodated in the modelling of thermal properties.

The recommended lower tail percentiles of thermal conductivity (0.5 and 2.5 percentiles) for each domain are partly based on differences observed between distributions that are assumed to be normally distributed. The performed adjustment of the percentiles is evidently associated with uncertainty. The percentiles are also uncertain due to the limited amount of data in the lower tails of the data distributions. For domain RSMA, 95% confidence intervals of the 0.5 and 2.5 percentiles have been estimated by a nonparametric method, according to /Mac Berthouex and Brown 2002/. The result indicates an uncertainty of approximately $\pm 0.05 \text{ W}/(\text{m}\times\text{K})$ for the 0.5 percentile and $\pm 0.02 \text{ W}/(\text{m}\times\text{K})$ for the 2.5 percentile. These uncertainties are considered to be lower than uncertainties associated with the estimation of percentiles.

Several stages in the modelling are based on addition of variances due to variability within rock types and variability between rock types. It should be noted that this methodology only produces rough estimates of the total variance.

The 3D geometry of most of the rock domains is uncertain (see Chapter 5), primarily because it is based on a only small number of boreholes.

With the exception of the rocks of the major deformation zones, the rocks in the Laxemar subarea generally appear to be texturally isotropic, although locally a weak foliation is visible /Nilsson et al. 2004/. Magnetic anisotropy data from laboratory measurements indicate a weak regional rock fabric striking west to west-northwest, parallel to the major lithological boundaries /Mattsson et al. 2004c/. Measurements to assess the anisotropy in thermal conductivity and thermal diffusivity have not been carried out as part of the current data freeze but should be considered for future investigations. Large-scale anisotropy produced by the preferential orientation of subordinate rock types should also be evaluated.

7.4.2 Heat capacity

A problem exists with the representativeness of measured values (TPS data). Samples are in several cases focused to certain limited parts of the rock mass. For quartz monzodiorite the number of samples is rather small. Subordinate rock types have not been considered when modelling the heat capacity.

No direct laboratory measurements of heat capacity have been performed. Instead, heat capacity has been determined through conductivity and diffusivity measurements performed with the TPS method.

7.4.3 In situ temperature

Temperature loggings from the same borehole at different times show a variation in temperature at specified depth which indicates an uncertainty in temperature loggings results. Errors associated with calibration of the temperature sensors have recently been recognized, so that accuracy is no better than $\pm 2^\circ\text{C}$.

Other possible sources of uncertainty are timing of the logging after drilling (drilling adds to temperature disturbance), water movements along the boreholes and uncertainty in the measured inclination of the boreholes.

7.4.4 Thermal expansion

There is a problem with the representativeness of the measurements, due to the availability of only a small number of samples concentrated to certain parts of the rock volume.

Pressure dependence on thermal expansion has not been investigated but may have a significant influence on the results.

7.5 Feedback to other disciplines

The basis for the division of the rock volume into rock domains relies partly on the needs expressed by the thermal modelling.

Cooperation with geology has been further developed during the work on the Laxemar model version 1.2. Mineralogical data and Boremap data have been used and interpreted during the thermal modelling. Where gaps have arisen in the understanding of properties relevant to thermal modelling, these have been communicated to geology to aid this discipline in its future investigations. One such issue is the mineralogy of alteration products. Potential anisotropies in thermal properties due to orientation and extension of dykes (large-scale anisotropy) and penetrative fabrics (small-scale anisotropy) have also been considered in the integration. These issues will be followed up in future investigations and modelling.

Temperature affects some hydraulic properties, the impact of which is assessed in the hydrogeological modelling. This issue is currently not being pursued as it is considered a second-order influence.

Repository design is the main receiver of the results from the thermal modelling. It is suggested that the design methodology is further developed to take into account the variability in thermal conductivity that has been identified and characterized.

8 Bedrock hydrogeology

This chapter covers the work within the Site Descriptive Modelling (SDM) for Laxemar 1.2 concerning bedrock hydrogeology. The hydrogeological descriptive model describes and justifies the assignment of hydraulic properties, boundary and initial conditions based on primary data and numerical simulations, useful for Repository Design, Safety Assessment, and Environmental Impact Assessment studies. Embedded in the above is an overall objective to provide a general conceptual “understanding of the investigated site”.

Section 8.1 briefly describes a few aspects on the previous model version, Simpevarp 1.2. Section 8.2 gives an overview of primary data, with details described in the supporting reports /Rhén et al. 2006ab/. The main concepts and strategies are outlined in Section 8.3. In Section 8.4 the properties of different domains are assessed. The bedrock hydrogeological model of Simpevarp regional model volume are divided into two principal types of domains; hydraulic rock domains (HRD) and hydraulic conductor domains (HCD). The geometries of the HRDs and HCDs coincide by and large with the geological rock domains and the deterministically modelled deformation zones, respectively. Some of the details of the assessment of hydrogeological properties to domains can be found in the supporting document by /Rhén et al. 2006c/. In Section 8.4 an overview is also given of the hydrogeologically DFN (Describe Fracture Network) models, with details described in the supporting documents accounting for the numerical hydrogeological modelling; /Hartley et al. 2006, Follin et al. 2006/.

Numerical simulation models are used to underpin the development of the bedrock hydrogeological model. The regional groundwater flow modelling performed is summarized in Section 8.5 with details reported in /Hartley et al. 2006/. The conclusions of the modelling are reported in Section 8.6 and uncertainties in the model and feedback to other disciplines are presented in Sections 8.7 and 8.8, respectively.

The development of the bedrock hydrogeological model is carried out according to the methodology described in /Rhén et al. 2003/.

One or more components of the bedrock hydrogeological model provide a foundation for the integration with, and modelling work in, other disciplines, primarily bedrock hydrogeochemistry and bedrock transport properties. All components of the bedrock hydrogeological model have a direct impact on the location and detailed design of the shafts and tunnels for the deep repository. They also provide a significant input for the Safety Assessment work in terms of hydraulic properties relevant for transport simulations.

The main product from hydrogeology is the hydraulic property and conceptual descriptions of the deformation zones and the rock mass inbetween the deterministically described deformation zones, aimed for calculating the flow through the bedrock. A main component in the property description is the Hydrogeological DFN models. A second product is the calibrated Regional groundwater flow model that is useful for testing the model parameters, mainly the deterministically described deformation zones to confirm geometrical interpretations, but also for further calculations by Repository Engineering, implementing a repository for studying drawdown and upconing of salt water during operation phase of the repository.

8.1 State of knowledge at previous model version

The hydrogeological model of the bedrock in Simpevarp model version 1.2 covered the entire regional area /SKB 2005a/ and the groundwater flow modelling performed for Simpevarp 1.2 is detailed in /Hartley et al. 2005, Follin et al. 2005/.

The Hydraulic Conductor Domains (HCDs) were based on the Simpevarp version 1.2 of the regional scale model of deformation zones. Some of the deformation zones in the regional scale model area were considered as high confidence deformation zones (concerning their existence) and several of

them had been tested hydraulically. However, most HCDs were attributed hydraulic properties based on other sources.

Based on data from the Simpevarp subarea, hydraulic DFN models were devised. These were calibrated using flow simulations comparing simulated inflow rates during flow logging with the actual in situ measured Posiva Flow Log (PFL) data.

The main uncertainties in the Simpevarp version 1.2 hydrogeological model concerned the following:

- The hydraulic DFN model and resulting connectivity were considered uncertain. The intensity of open fractures was considered uncertain. The models only represented a small domain within the regional area. Furthermore, three transmissivity models were tested and two of the models had an assumed correlation between transmissivity (T) and size. The T-model with T correlated to the size of the fractures provided the fit best. However, it was judged that the hydraulic DFN models/methodology had to be tested and developed further in future versions of the site-descriptive model.
- The current distribution of groundwater salinity was known at depth only from a few boreholes. This, in turn, made it difficult to test the importance of the hydrogeological initial condition with respect to present salinity. There was also an uncertainty associated with the conditions after the last glaciation that constituted this hydrogeological initial condition. The significance of this uncertainty was recommended to be explored through sensitivity analyses.
- The no-flow boundary conditions at the regional scale were regarded as uncertain, but their effects could be evaluated by sensitivity analyses in simulations.

The most important uncertainties are related to the alternative hydraulic DFN models and the deformation zone model (both in terms of the existence and properties of individual zones) as flow paths, transport times and construction issues are derived from, or conditioned by, these models and are primary considerations for both Safety Assessment and Repository Engineering.

8.2 Evaluation of primary data

Data from site investigations, here called primary data, available for the present model version are compiled and commented upon in this section. These primary data, used for the analysis and subsequent hydrogeological modelling, are listed in Table 2-4 in Chapter 2. Only new data obtained between the data freeze for Simpevarp model 1.2 and the data freeze for Laxemar 1.2 are discussed in this section. See also Table 2-4 and a more detailed description of the primary data given in /Rhén et al. 2006b/. The data used for model version Simpevarp model 1.2 /SKB 2005a/ are also described in more detail in /Rhén et al. 2006a/.

8.2.1 Hydraulic evaluation of of single hole tests

A number of hydraulic tests are used as essentially standardised methods in boreholes drilled during the site investigations. These are summarised in Table 8-1 and briefly described below.

The telescope drilling method, cf. Chapter 2, helps to minimise contamination of the rock with drilling fluid, enhancing the possibility of obtaining more representative water samples. This drilling scheme also makes it possible to pump at larger flow rates with a submersible pump (if needed) and allows monitoring of a fairly large amount of borehole sections using a multi-packer system. The draw back is that the upper 100 m, the wider part, can not be hydraulically tested in the same way as the rest of the borehole. However, an auxiliary 100 m long core borehole is sometimes drilled nearby from surface in order to sample geological and hydraulic data from the uppermost 100 m of the rock that is lost in the telescope borehole.

Table 8-1. Principal methods used during initial site investigations for measurement and evaluation of hydraulic parameters.

Measurement equipment	Acronym for method	Acronym for method variant	Type of test performed	Comments
Pipe String System	PSS		Pumping injection tests performed as constant rate tests. Injection tests performed as constant head test. Impulse test is an option.	Transient data collected. Evaluation based on transient or stationary conditions. Test in cored boreholes. Injection tests before the Site investigations were made with other equipment than PSS but are indicated in tables as "PSS".
Hydraulic test system percussion boreholes	HTHB		Pumping or injection tests performed as constant rate tests. Flow logging with impeller is an option.	Transient data collected. Evaluation based on transient or stationary conditions.
Wire Line Probe	WLP	WLP-pt	Pumping tests with WLP in cored boreholes.	Transient data collected. Evaluation based on transient or stationary conditions.
		WLP-ap	Absolute pressure measurement with WLP in cored bore holes.	Transient data collected.
Posiva Flow Log	PFL	PFL-s	Difference flow logging (section). Electrical conductivity (EC) and temperature of the borehole fluid as well as Single Point resistance (SP) is measured during different logging sequences.	Purpose is to estimate test section transmissivity and undisturbed pressure. Two logging sequences. Evaluation is based on stationary conditions.
		PFL-f	Difference flow logging (flow-anomaly).	Purpose is to estimate flow distribution and use PFL-s to estimate transmissivity for fractures/features. One single logging sequence.
Slug test			Slug or bail test.	Normally just performed in boreholes completed in the overburden.

Hydraulic tests during drilling

Hydraulic tests can be performed during the drilling with wire-line based equipment. The hydraulic tests include pumping tests and measurements of the absolute pressure and are generally performed for every 100 m of the drilled borehole. With this equipment, water sampling, pump tests and measurements of absolute pressure in a borehole section can be made without having to lift the drill stem. Hydraulic tests performed during drilling are generally affected to some degree by disturbances caused by the drilling operations. Transients from changes in pressure, temperature and salinity can affect the hydraulic response curves. However, these data are useful for a first, preliminary, assessment of hydraulic properties and serves also as back-up data if the PSS measurements fail. The test method is described in more detail in /Rhén et al. 2006ab/.

Posiva Flow Logg (PFL)

After completion of the drilling, the Posiva Flow Log (PFL³) is generally applied in the cored borehole. The section logging (PFL-s) is made with a test section length (length between rubber discs) of 5 m and a step length (distance between successive tests sections) of 0.5 m (5/0.5), with the purpose of measuring transmissivity in 5 m sections and indicating flowing sections with a resolution of 0.5 m, useful for planning of the hydrogeochemistry sampling and the flow-anomaly logging. The flow-anomaly logging (PFL-f) is made with a test section length of 1 m and a step length of 0.1 m (1/0.1) when moving the test tool along the borehole, with the purpose of identifying individual flowing fractures. PFL-s logging is performed in two sequences; with and without pumping. PFL-f logging is performed just with pumping.

³ In some earlier reports presenting PFL logging, a test employing the same test section length and step length as well as two different draw downs, was denoted "Sequential flow logging with PFL" and corresponds to PFL-s. Tests with a step length smaller than the test section length were denoted "overlapping flow logging with PFL", (PFL-o) and corresponds to PFL-f.

Thiem's equation /Thiem 1906/ or e.g. in /Kruseman and de Ridder 1991/ is used to calculate the transmissivity T_s for PFL-s representing a 5 m section and T_f for PFL-f representing a fracture, or hydraulic feature. The latter is often rather distinct, within a dm or so, in the borehole. Furthermore, the undisturbed hydraulic head (h) in the formation outside the test section (h_s for PFL-s and h_f for PFL-f) is measured. If no flow rate is possible to measure during PFL-s (without pumping), only the fracture (or hydraulic feature) transmissivity (T_f) is estimated. It is assumed that the influence radius divided by the borehole radius is can be approximated to a ratio of 500, corresponding to an influence radius of 19 m if the borehole diameter is 0.076 m. It is thus assumed that undisturbed formation pressure exists at a radial distance of c. 19 m. As a steady state solution is employed the evaluated transmissivity may be affected by a skin factor.

More details about the tests and field data can be found in e.g. /Rouhiainen and Sokolnicki 2005/ and /Rhén et al. 2006ab/.

Pipe String System (PSS)

Subsequently to PFL measurements, injection tests with the Pipe String System (PSS) are made starting with 100 m test sections, then 20 m sections within all 100 m sections with flow rates above the measurement limit and then 5 m sections in the borehole section 300–700 m in all 20 m sections with flow rates above measurement limit. The 20 and 5 m sections not measured for the above reason are assigned the value of the measurement limit of the specific capacity (Q/s) for the 100 m and 20 m sections, respectively. These Q/s values are then applied in the steady state solution by /Moye 1967/ to estimate a measurement limit in terms of a transmissivity value. The tests are evaluated as transient tests giving Transmissivity (T_T) and skin factor (assuming a storage coefficient $S=1E-6$). T_T is evaluated for the first seen radial flow period in a test. Steady state evaluation of transmissivity (T_M) based on /Moye 1967/ is also made. If it was not possible to evaluate T_T , the T_M values are used as “best choice” (BC) for the test section in question.

Overview of tests performed since Simpevarp model 1.2

Cored boreholes KLX02, KLX03, KLX04, KAV04A,B, and percussion boreholes HAV09–10 and 9 HLX10, -13, -14, -18, -20, -22, -24, -25, -32 boreholes have been tested during the early stages of the initial site investigations and were available for the Laxemar 1.2 modelling. In the cored boreholes, hydraulic tests with the wire-line probe (WLP), the Posiva flow logging tool (PFL) and the Pipe String System (PSS) were performed in most boreholes. In percussion holes HAV09–10 and HLX10, -13, -14, -18, -20, -22, -24, -25, -32 boreholes airlift tests or pumping tests were performed.

Single-hole hydraulic tests and interference tests conducted prior to the onset of the ongoing initial site investigations (historical data) were carried out at Äspö, Ävrö, Hälö, Mjälén, Laxemar and the Simpevarp peninsula /e.g. Rhén et al. 1997acd/. Some of these existing data are commented on in this section (KLX01, KLX02, KAV01, KAV02, KAV03), but test data have not been re-evaluated.

An overview of hydraulic tests results in the cored boreholes is provided in Figure 8-3. PSS tests performed in KLX03 were not available at the data freeze for model version Laxemar 1.2. A full account of new tests and the corresponding results is provided in /Rhén et al. 2006b/.

The hydraulic tests conducted in the percussion boreholes and some of the tests in cored boreholes were performed as open-hole pumping tests using a submersible pump or airlift pumping. The hydraulic tests performed in the cored boreholes were made during drilling as pumping tests and included measurements of absolute pressure using the SKB-developed Wire-Line Probe (WLP).

The single-hole hydraulic interpretation for Laxemar version 1.2 is presented in /Rhén et al. 2006b/. An overview of the drilling process is provided in Chapter 2 and detailed accounts including that of tests during drilling in cored boreholes are described by /Ask et al. 2005cd/. The drilling and some simple hydraulic tests in percussion boreholes are reported by /Ask and Samuelsson 2004c, Ask et al. 2004c, 2005ab, Ask and Zetterlund 2005/ and the PFL measurements by /Ludvigson et al. 2002, Rouhiainen 2000, Pöllänen and Sokolnick 2004, Rouhiainen et al. 2005, Rouhiainen and Sokolnicki 2005/. PSS tests are reported by /Rahm and Enachescu, 2004ef, 2005b/. A pumping test in KLX04

is reported in /Rahm and Enachescu 2005a/ and a combined interference and tracer test involving KLX02 and HLX10 is reported in /Gustafsson and Ludvigson 2005/. Evaluation methods and results are presented in the above reports.

No drilling report is available for HLX10, HLX11 and HLX12, but some data are found in /Ekman 2001, Andersson 1994/. Earlier data from KLX02 is compiled in /Ekman 2001, Andersson 1994/.

Overview of hydraulic tests performed during Initial Site Investigations

The modelling presented in the subsequent sections is based on more data than presented in the preceding section. The single-hole interpretations for model version Simpevarp version 1.2 and model version Laxemar 1.2, respectively, are presented in /Rhén et al. 2006ab/. The corresponding accounts of the drilling process and the tests during drilling in cored boreholes are described by /Ask et al. 2003, 2004ab/. The drilling and some simple hydraulic tests in percussion boreholes are reported by /Ask 2003/. Hydraulic tests after drilling of HSH02 and HSH03 are reported by /Ludvigson et al. 2003, Svensson 2004/ and the PFL measurements by /Rouhiainen 2000, Rouhiainen and Pöllänen 2003ab, 2004/. PSS tests are reported by /Rahm and Enachescu 2004bcd/ and /Ludvigson et al. 2004/. Evaluation methods and data are presented in those reports. A compilation of important Äspö data is found in /Rhén et al. 1997abc/.

Figure 8-1 shows an overview of the hydraulic tests in the main cored holes available for Laxemar version 1.2 modelling, displaying the elevation of the uppermost and lowermost test section for each borehole. (Data from cored boreholes on Äspö and Kråkemåla have been used to some extent.)

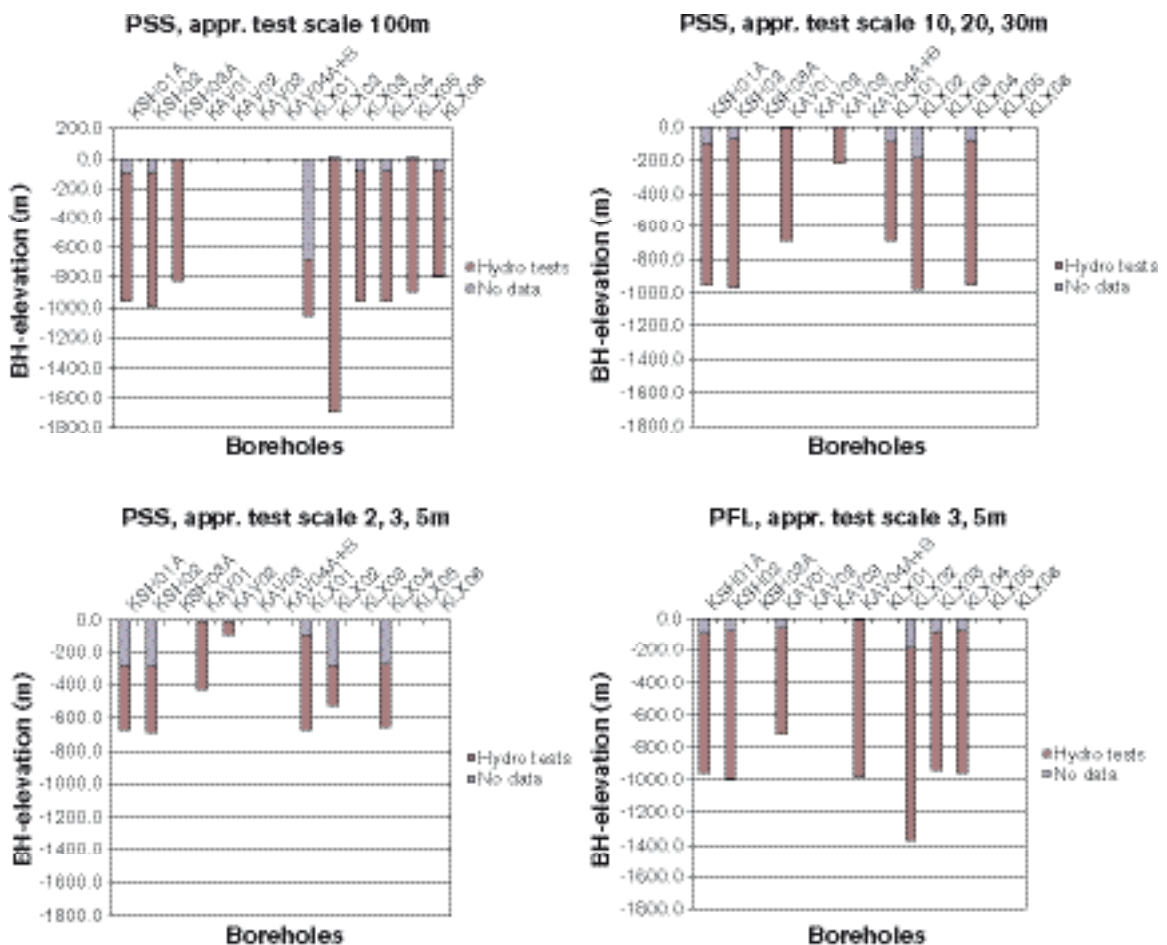


Figure 8-1. Overview of hydraulic tests with PSS at approximate test scale 100 m, test scale 10, 20 or 30 m, test scale 2, 3 or 5 m and hydraulic tests with PFL at approximate test scale 5 m, used for Laxemar model version 1.2.

Overview of results from hydraulic tests

Below the results from the hydraulic tests in new boreholes for Laxemar model version 1.2 are summarised. PLF-f and geological data are shown for all new boreholes for Laxemar model 1.2 (including KLX02) in Appendix 7 and are illustrated in Figure 8-3. In /Rhen et al. 2006ab/ all core holes are presented and treated in detail. A few explanations of the figures are provided below.

Boremap data

The geological mapping of the cores and the interpreted rock domains (related to model version Laxemar 1.2) by the geologists are important for the correlation studies.

Correlation of Boremap data and PFL flow anomalies

The measured flow anomalies with PFL have such good accuracy in position in the boreholes that they can generally be related to one or a few mapped open fractures using the Boremap data base and the BIPS images of the borehole wall. An example of the results from the PFL-f is shown together with Boremap data (open fractures, partly open fractures and crush zones) and the interpreted rock domains and deformations zones in Figure 8-2.

In the core mapping each fracture is classified as “Sealed”, “Open” or “Partly open” and with a judgement as to how certain the geologist is of this classification – expressed as “Certain”, “Probable” and “Possible”. “Partly open” refers to BIPS observations of the borehole wall indicating an aperture (channel) in an unbroken core – these observations are few. Measured PFL-f flow anomalies are classified as “Certain” or “Uncertain”. Both the core-mapped data and the flow anomalies are rigorously length corrected and it is expected that the positions of PFL-f objects along the boreholes normally can be correlated to mapped geological features within 0.2–0.3 m

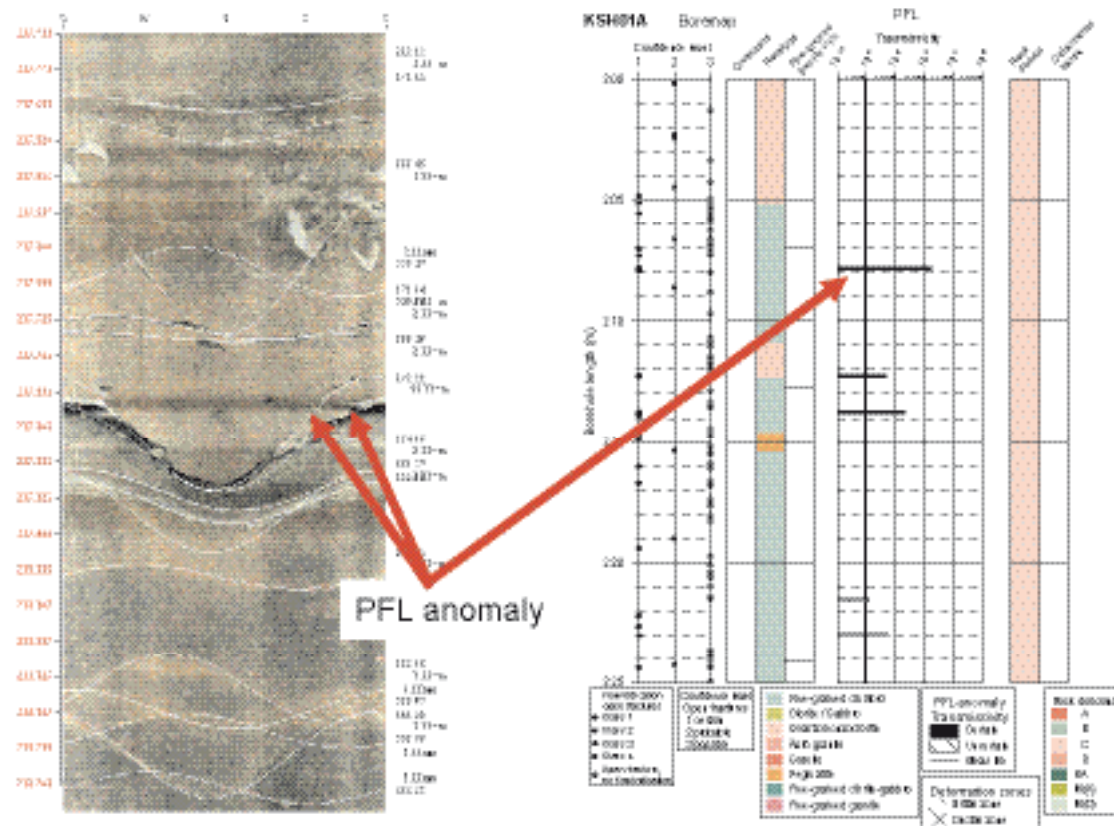


Figure 8-2. Close-up of BIPS image of a borehole section in borehole KSH01A and corresponding PFL accounting together with geological information. Shown object: $T (m^2/s) = 1.72E-7$. Generally open fractures cannot be seen in BIPS as clearly in the example above. White lines represents objects variously as open and sealed fractures, rock contacts etc. /Forsman et al. 2005a/.

As a first assumption when correlating core-mapped data and flow anomalies, all open and partly open fractures, as well as crush zones, are assumed to be possible flowing features. In most cases, one or several open fractures were identified within 0.2 m from a given flow anomaly. Only in a few cases were there no “open fractures”, “partly open fractures” or “crush zones” that could be linked to within 0.5 m of a flow anomaly, probably indicating that a fracture mapped as “sealed” should have been classified as “open”. In such cases one could generally find “sealed fractures” classified as “Probable” or “Possible” near the flow anomaly.

As the flow-anomalies in most cases could be correlated to individual open fractures, fracture properties, e.g. orientation can be coupled to the flow anomaly. The uncertainty classification of fractures and flow anomalies also provides a basis for sensitivity analysis. This is to be focus of future work. Details of this evaluation are presented in /Forsman et al. 2005b/. It is emphasised that the PFL-anomaly data have been the main input to the development of hydraulic DFN models. They have been used to obtain transmissivity information and as a calibration target for conductive fracture frequency. The DFN models were developed using assumptions of how fractures connect, are orientated, and whether they are open or closed etc.

An example of results is shown in Figure 8-3 and in Appendix 7 some explanations to the figure are given.

PFL-f data for KLX02 were not available for model version Simpevarp 1.2 but were made available for Laxemar 1.2. For KLX02, the core mapping was updated to the standard of the Site Investigations down to 1,000 m borehole depth. Below 1,000 m, the old core mapping in the Sicada data base has been translated to the current Site Investigation nomenclature.

Comparison of test methods and evaluation methodologies

Tests performed in KLX2, KLX03, KLX04 and KAV04 are commented on below. These tests and earlier tests are presented and discussed in more detail in /Rhén et al. 2006ab/.

PFL-s compared to PFL-f

The flow logging with PFL is performed using two different modes as described above. The evaluated transmissivities for the individual hydraulic features (PFL-f) were summed over the corresponding 5 m sections measured by PFL-s. The PFL-s results mostly compare well with the PFL-f summed-up transmissivities of individual hydraulic features. The simplified approach for PFL-f therefore appears to be reasonably accurate. Deviations observed in the KLX02 data are not surprising, due to the approximate evaluation of the flow anomalies from reports and the underlying data base. As mentioned before, PFL-f was not performed in KLX02 according to the methodology employed in the Site Investigations.

PSS steady state compared to PSS transient and sum PFL-f

Transmissivity evaluated using /Moye 1967/ (T_{Moye}) from PSS has been jointly compared with the evaluated transient transmissivities (T_T) from PSS and the summed-up transmissivities from the hydraulic features based on PFL-f, see example comparative plot for 20 m test scale in Figure 8-4. Despite the use of different test and evaluation methods, most of the transmissivities plot close to the 1:1 line within a range of 0.1 to 10 of the value on the x-axis. The transmissivity estimates therefore seem robust. However, one can notice that the transient evaluation of T seems to be systematically (although not always) a bit larger at all measured tests scales (5, 20 and 100 m). This means that there is generally a positive skin factor and that the transient evaluation of T (T_T) should be more representative for the formation than T_{Moye} . T_T is always used as the best choice value, as mentioned earlier.

PSS compared to summed up smaller section PSS

The PSS tests were also compared by summing up the 20 m tests sections to the corresponding 100 m section, /Rhén et al. 2006b/. Only the “best choice” values (BC) are compared. The sum of 20 m sections generally is found to compare well with the corresponding 100 m sections for all

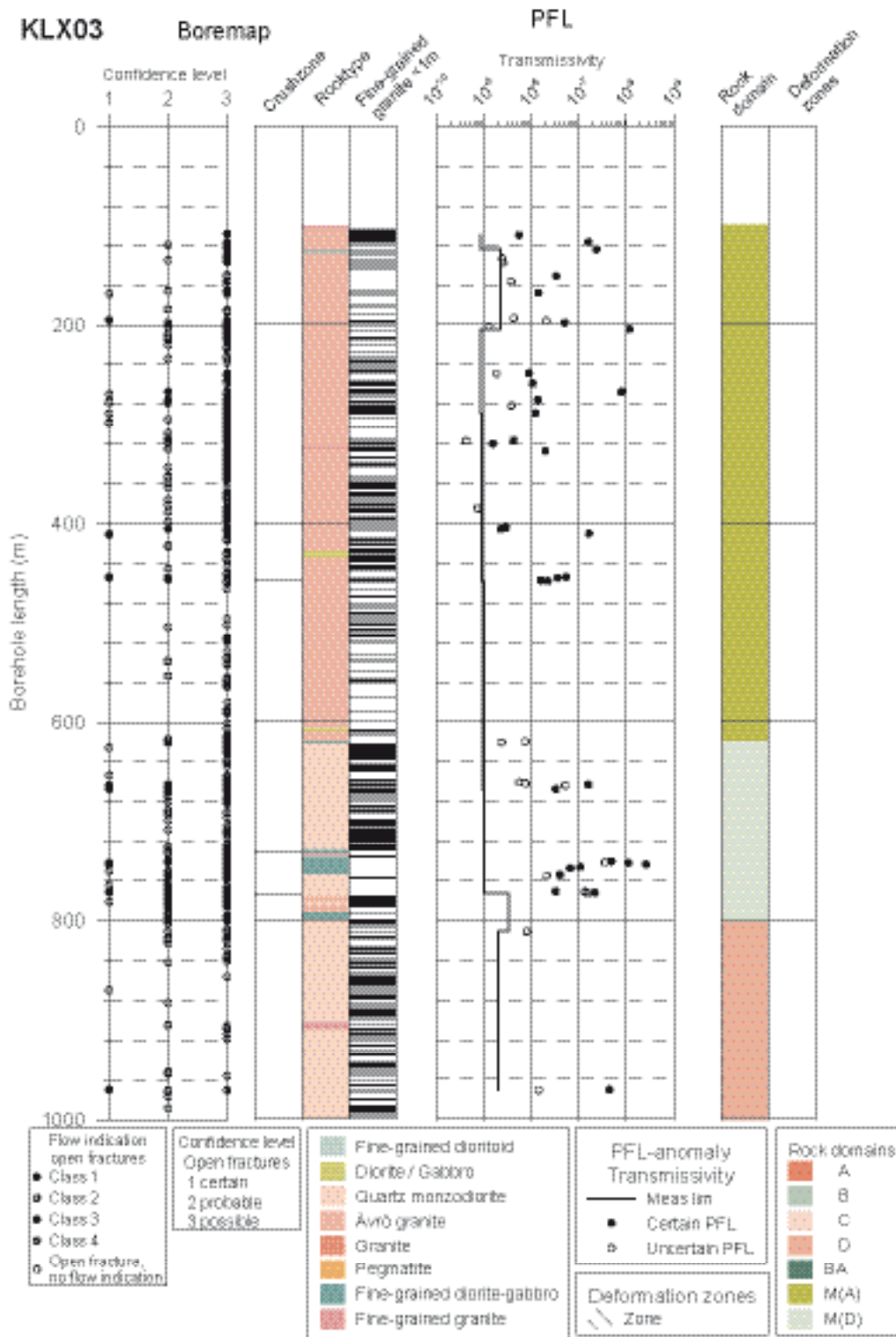


Figure 8-3. Transmissivity of hydraulic features of borehole KLX03 based on PFL-f data, Boremap data (open fractures, partly open fractures and crush zones, rock type and veins of fine-grained granite) and the interpreted rock domains and deformations zones /Forssman et al. 2005b/. The geological M domains is here subdivided in the part dominated by Ävrö granite M(A) and the one dominated by quartz monzodiorite M(D).

boreholes. However, there is a slight tendency for the sum of the values for the 20 m sections to be a bit higher than the corresponding 100 m section. This is in accord with experiences from the investigations for the Äspö Hard Rock Laboratory /Rhén et al. 1997c/.

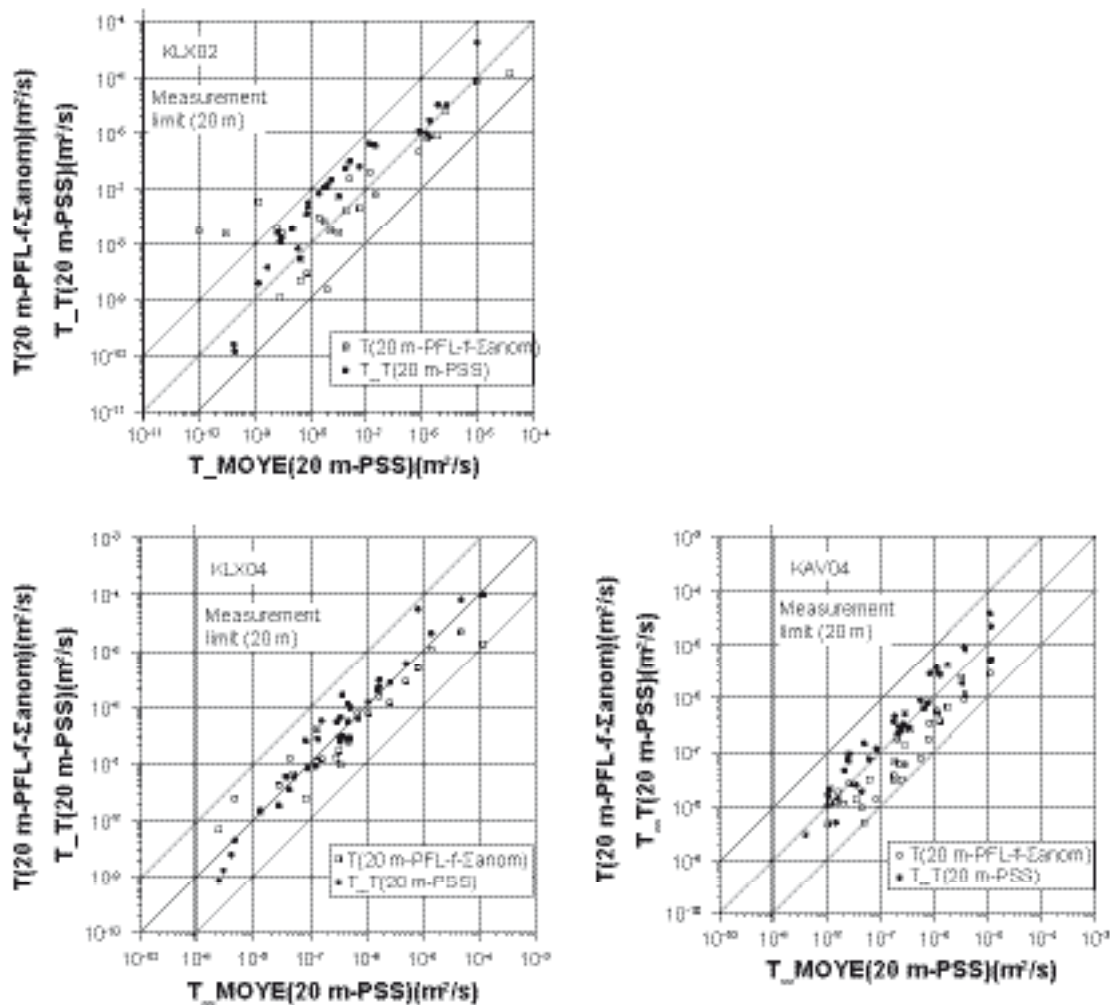


Figure 8-4. Cross plot of transmissivity PSS steady state vs. PSS transient and sum PFL-f: Transmissivities based on PSS data and steady state evaluation (T_{Moye}) versus transmissivities for the individual hydraulic features summed up to 20 m sections ($T(20\text{ m-PFL-}\Sigma\text{anom})$) in the plot and transmissivities based on PSS and transient evaluation ($T_T(20\text{ m-PSS})$) in the plot. (The bounding lines to the 1:1 line: 0.1 and 10 times 1:1 value.) /Rhen et al. 2006b/.

Statistics of single hole test results

Data from the hydraulic tests performed in the boreholes have been compiled and univariate statistics have been calculated and compared with data from other cored boreholes in the Simpevarp area, where similar tests have been conducted.

Hydraulic conductivity (or transmissivity) evaluated from hydraulic tests with the same test section length often fit rather well to a lognormal distribution. When the test section length decreases, the number of tests below the lower measurement limit of the equipment increases. The data set is hence “censored”, which has to be taken into account when choosing a statistical distribution that should describe the measured values above the measurement limit as well as possible. A data set is said to be truncated if the number of unmeasured values is unknown and it is censored if this number is known /Jensen et al. 2000/. For censored data below the measurement limit, the fitted distribution can be used to estimate the properties below the measurement limit, but these estimates are of course associated with uncertainty. When performing modelling based on the fitted distribution it has to be decided if extrapolation below the measurement limit is reasonable and whether there is a definite lower limit (below the lower measurement limit) for the property in question due to e.g. conceptual considerations. In crystalline rock, the matrix permeability sets the physical lower limit, cf. e.g. /Brace 1980/. The matrix hydraulic conductivity of crystalline rock is generally found to be c. $1\text{E-}14$ to $1\text{E-}13$ m/s.

The standard procedure for describing the hydraulic material properties from single-hole test data is to fit the logarithm of the data to a normal distribution, also taking the censored data into account. The associated statistics normally include the mean and standard deviation (std) of $Y, Y = \text{Log}_{10}(X)$, $X = \text{hydraulic conductivity (K) or transmissivity (T)}$, where the mean of $\text{Log}_{10}(X)$ corresponds to the geometric mean of X . Occasionally, the number of measurements below the lower measurement limit is greater than the number above the measurement limit, see Figure 8-5. However, it is here argued that the above methodology (the fitting of the statistical distribution to values above the lower

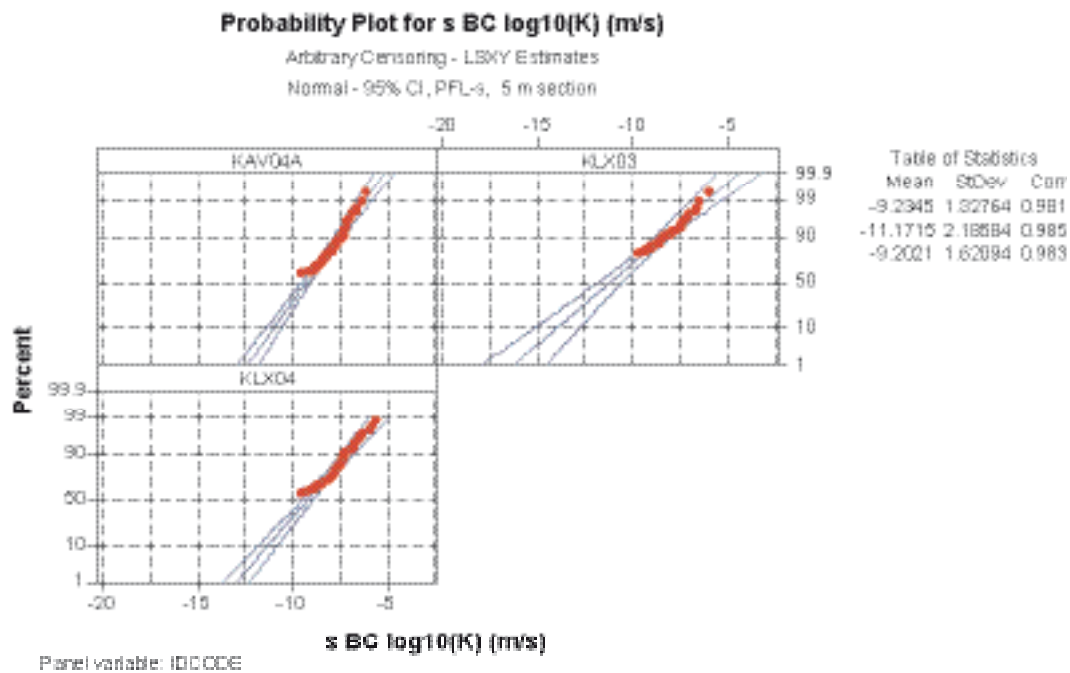
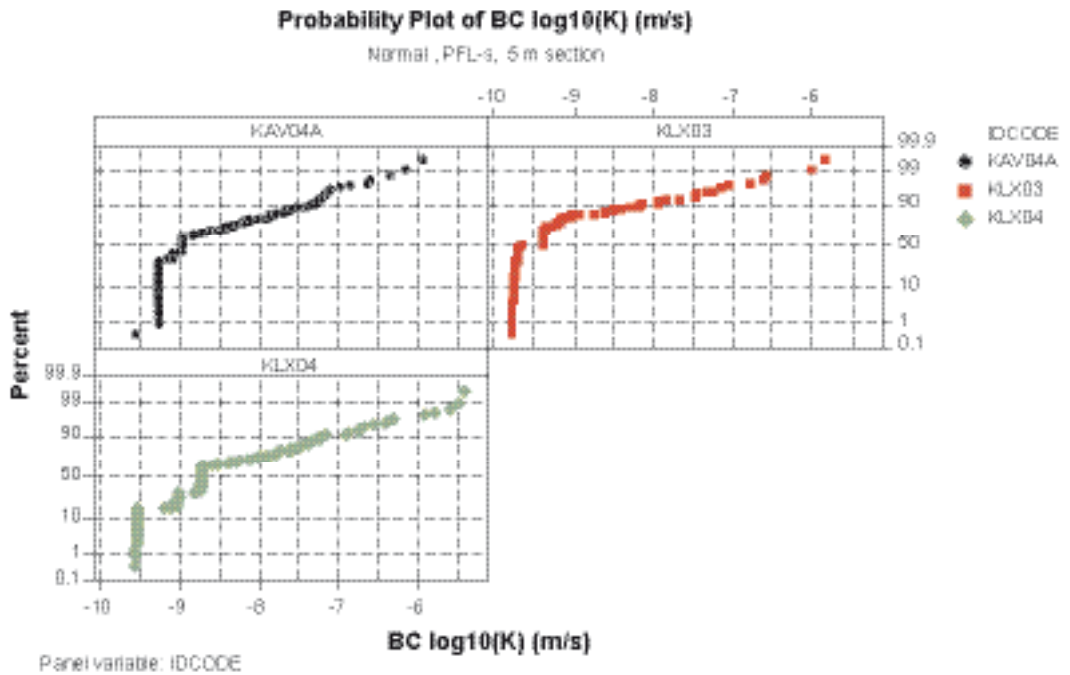


Figure 8-5. Example of statistical distributions plotted as Normal distributions. Top: All data including measurement limit values are plotted. Bottom: Statistical analysis of the values shown in the top figure, setting all measurement limit values as Censored values result in the matched mean and standard deviations shown in the caption.

measurement limit – the “known values”) is the appropriate way to describe a dataset with censored values. This while measured values above the measurement limit are fairly well reproduced by the distribution which also indirectly accounts for the values below the measurement limit. A power law distribution may work equally well, but this has not been tested here.

Statistics of single hole tests- sequential measurements

In Table 8-2 through Table 8-4 the univariate statistics are shown for the PFL-s and PSS tests for each borehole. In Table 8-5 data previously evaluated for Äspö HRL are shown for comparison. /Rhen et al. 2006b/ provides details of the statistical distributions shown.

The “Theoretical (lower) measurement limit” for PFL (under optimal conditions) is estimated at $c. T=1.7 E-10 \text{ m}^2/\text{s}$, based a minimum flow rate of 6 mL/h, 10 m drawdown and 19 m influence radius applied in Thiem’s equation. (Theoretical measurement limit, as outlined in /Rouhiainen and Sokolnicki 2005/). /Rouhiainen and Sokolnicki 2005/ describe the finding that due to a rough borehole wall, effects of fine particles in the borehole, high flow rates along the borehole, or gas in the water-filled borehole, the actual measurement limit adopted in the evaluation is in general higher than the Theoretical measurement limit, and may also vary along the borehole. Most likely gas is not a big problem as the pressure decrease in the borehole is very limited during the test. The actual, “Practical measurement limit” is evaluated from what is considered to be the noise level in the measurements. In some boreholes, one can see some PFL-f measurements below the measurement limit. The reason is that the Pratical measurement limit estimated from the measurement is approximate, and in a few cases it was judged that a flow anomaly was present and could be identified, even though the flow was lower than the PFL-s based Pratical measurement limit.

The lower measurement limit for PSS is more stable and generally lower than that for PFL-s. The tests using PSS are therefore essential, especially for confirming the conductivity of the rock in the lower transmissivity range.

/Rhen et al. 1997c/ estimated a geometric mean $K=1.3E-7 \text{ m/s}$ with a standard deviation ($\text{Log}_{10}K$) of 0.96 for well data obtained from the well archive of the Swedish Geological Survey (area approximately corresponding to the NE part of the municipality of Oskarshamn) and percussion holes located at Äspö, Ävrö, Mjälén. Hälö and Laxemar. The test scale was approximately 100 m, all borehole-test intervals with 0 to 200 m depth, and sample size 264. Subsequently, /Follin et al. 1998/ estimated a geometric mean $K=6.3E-8 \text{ m/s}$ for wells sunk in the bedrock within the municipality of Oskarshamn based on the well archive of the Geological Survey of Sweden (SGU). The test scale in this case varied between 10 and 100 m and the sample size was 149. Both analyses included wells intercepting fracture zones, if present.

Table 8-2. Univariate statistics for hydraulic tests performed in cored boreholes (Methods employed: PFL-s, Section Posiva Flow Logging) (K: m/s). (“Lower meas. Limit” in the table is the Practical measurement limit for PFL-s).

Borehole	Test type	Section upper (m)	Section lower (m)	Test scale (m)	Sample size, all	Sample size below the lower meas.lim values	Lower meas.limit ^{1,2} $\text{Log}_{10} K$ (m/s)	Mean $\text{Log}_{10} K$ (m/s)	Std $\text{Log}_{10} K$ (m/s)
KLX02	PFL-s	205.92	1,399.92	3	398	276	(-10) – (-8.3)	-9.8	1.27
KLX03	PFL-s	101.3	992.42	5	178	142	(-9.8) – (-8.2) ³	-11.2	2.19
KLX04	PFL-s	100.2	986.22	5	177	110	(-9.6) – (-8.7)	-9.2	1.62
KAV04A	PFL-s	100.16	996.17	5	179	110	(-9.6) – (-9.0)	-9.2	1.33

¹ Measurement limit estimated from in situ test results, “Practical measurement limit”. The measurement limit may vary along the borehole. Max and min values are shown in the table.

² PFL-s: Theoretical lower measurement limit (under optimal conditions) is $K = 3.3E-11 \text{ m/s}$ ($\text{Log}_{10}(K(\text{m/s})) = -10.5$) for test section length 5 m (or equivalently $T = 1.7E-10 \text{ m}^2/\text{s}$).

³ Only a few values near the upper range.

Table 8-3. Univariate statistics for hydraulic tests performed in cored boreholes. Method employed: PSS. (If only one test is available for a certain test scale, only a value is given in column “K”.)

Borehole	Test type	Section upper (m)	Section lower (m)	Test scale (m)	Sample size	Sample size below the lower meas.lim values	Lower meas. limit ¹ Log ₁₀ K (m/s)	K Log ₁₀ (K) (m/s)	Mean Log ₁₀ K (m/s)	Std Log ₁₀ K (m/s)
KLX02	PSS	300	545	5	49	33	(-11.7) – (-9.5)		-11.2	2.50
	PSS	204	1,004	20	48	15	(-11.3) – (-10.8)		-9.7	2.08
	PSS	204	1,004	100	8	0	(≈ -11.7)		-8.34	1.78
	PSS ²	3	1,700.5	100–300	11	0	(≈ -11)		-8.11	1.71
	Pump t. ³	202.95	1,700.5	≈1,000	1	–	–	-7.1		
KLX03	WLP	103	1,000.42	≈ 100	9	0	(-6)		-8.0	0.69
	Pump t.	11.65	1,000.42	1,000	1	–	–	-7.4		
KLX04	PSS	300.41	685.78	5	77	19	(-11.7) – (-9.7)		-9.2	2.0
	PSS	105.21	983.05	20	44	8	(-12.3) – (-10.7)		-8.7	1.99
	PSS	105.11	986.11	100	9	0	(≈ -12.6)		-8.1	1.92
	Pump t.	12.24	993.49	1,000	1	–	–	-6.8		
KLX05	WLP	0	1,000.2	≈ 100	10	0	(-6)		-8.1	0.85
KLX06	WLP	103	994.94	≈ 100	9	0	(-6)		-7.3	1.57
KAV04B	Pump t.	19.53	95.93	≈ 100	1	–	–	-6.4		
KAV04A	PSS	105.17	903.35	20	42	4	(-13.3) – (-10.8)		-8.2	1.44
	PSS	105.17	998.2	100	9	1	(≈ -12.6)		-7.9	1.64
	Pump t.	100	1,001.2	≈ 1,000	1	–	–	-7.6		

¹ Measurement limit estimated from in situ test data.

² Old test data made with similar equipment as PSS + new test data made with PSS.

³ Old test data.

Table 8-4. Univariate statistics for hydraulic tests performed in percussion-drilled boreholes. Methods used: Airlift tests, Pumping test (with submersible pump), HTHB-p: Pumping test or injections test, HTHB-f: flow logging. (If only one test is available for a certain test scale, only a value is given in column “K”.)

Borehole	Test type	Section upper (m)	Section lower (m)	Test scale (m)	Sample size	Sample size below the lower meas.lim values	Lower meas. limit ^{1,2} (m/s)	K Log ₁₀ (K) (m/s)	K Mean Log ₁₀ K (m/s)	K Std Log ₁₀ K (m/s)
BH in Table 5-3	Airlift/pump test	–	–	≈ 100	11	0	≈ -7.7	–	-6.9	1.19
HAV09	Airlift	14.9	200	≈ 100	1		≈ -7.7	-8.7		
HAV10	Airlift	11.9	100	≈ 100	1		≈ -7.7	-8.1		
HLX10	Pump test	0	85	≈ 100	1		≈ -7.7	-5.7		
HLX13	Airlift	11.87	200	≈ 100	1		≈ -7.7	-8.7		
HLX14	Airlift	11.9	115.9	≈ 100	1		≈ -7.7	-7.0		
HLX18	Pump test	15.12	181.2	≈ 100	1		≈ -7.7	-6.6		
HLX20	Pump test	9.12	202.2	≈ 100	1		≈ -7.7	-6.7		
HLX22	Pump test	9.1	163.2	≈ 100	1		≈ -7.7	-5.8		
HLX24	Pump test	9.1	175.2	≈ 100	1		≈ -7.7	-5.4		
HLX25	Pump test	6.12	202.5	≈ 100	1		≈ -7.7	-6.0		
HLX32	Pump test	12.3	162.6	≈ 100	1		≈ -7.7	-6.9		

¹ Mixed tests: airlift tests and pumping tests. Parameters evaluated from airlift tests are regarded as being uncertain as measured flow rates and drawdown/recovery curves generally are more uncertain than using submersible pump that gives more stable measurements.

² For a 100 m section with 50 m drawdown with HTHB. Airlift pumping may give lower values.

Table 8-5. Compilation of data from boreholes at Äspö HRL from /Rhén et al. 1997c/.

Borehole	Test type	Section upper (m)	Section lower (m)	Test scale (m)	Sample size	Lower meas. limit' Log ₁₀ (K) (m/s)	Mean Log ₁₀ (K) (m/s)	Std Log ₁₀ (K) (m/s)
KAS02–KAS08	Inj.test	c. 100	500–800	3	1,105	c. –11	–7.8 to –9.7	1.12 to 2.08

¹ Measurement limit estimated from field results.

Undisturbed formation pressure

During drilling of core holes, hydraulic tests are made generally for every drilled 100 m section with the SKB-developed Wire Line Probe (WLP), /see Rhén et al. 2006a/. One part of this hydraulic test program has been measurements of the formation pressure in selected test sections. As these tests are the first to be done in the borehole, they are to be expected to give estimates of the undisturbed formation pressure.

The methodology is as follows. The wireline probe is placed in position at the drill bit. The packer is inflated and the pressure build-up in the test section is recorded for a period of at least eight hours, typically this is done overnight.

The measured pressure is nearly hydrostatic, see /Rhén et al. 2006c/. No large differences can be seen that could indicate compartmentalisation or features giving confined conditions that generate different hydraulic regimes. The fracture system seems to be hydraulically well-connected on the scale tested.

8.2.2 Hydraulic evaluation of interference tests

The cross-hole interference test constitutes a good tool to confirm the presence and continuity of deformation zones. So far, only a limited number of interference tests have been made and consequently the present model of zone connectivity is mainly a product of geological interpretation. However, a number of deformation zones near Äspö HRL were studied by hydraulic testing /Rhén et al. 1997acd/ and hydraulic interference tests along the extent of zone ZSMEW007A (not yet reported) will be used to confirm the existence, near-surface geometry and extent of the zone in future model versions.

During the Initial Site Investigation a few interference tests have been reported, with pumping in HSH03 and observation in HSH01 /Ludvigsson et al. 2003/, as well as pumping in HLX10 and monitoring in KLX02 and a few other boreholes in the area /Gustafsson and Ludvigsson 2005/ to assess the connectivity through a potential deformation zone between HLX10 and KLX02. The response characteristics of the latter test can be seen in Figure 8-6. The deformation zone tested is suggested to intersect the upper parts of KLX02 (possibly in the more transmissive borehole section 200–400 m) but the intersection with HLX11 is considered uncertain. The zone tested probably corresponds to ZSMEW007A as modelled in the current model version Laxemar 1.2. The test seems to indicate that the conductive feature in HLX10 is well-connected to the upper part of KLX02, but less well to HLX11.

In the Laxemar subarea there exist data from two old interference tests where KLX02 is used as the pumped borehole /Ekman 2001/. These tests show fairly clear responses in the deeper sections in KLX01 (695–855, 856–1,078 m), indicating connected conductive structures between KLX01 and KLX02. The responses may be explained partly by the existence of deformation zone ZSMEW007. However, the pumping of section 805–1,103 m in KLX02 also indicates a fairly good connection to the lower part of KLX01 (695–855, 856–1,078 m), which currently lacks a plausible structural explanation

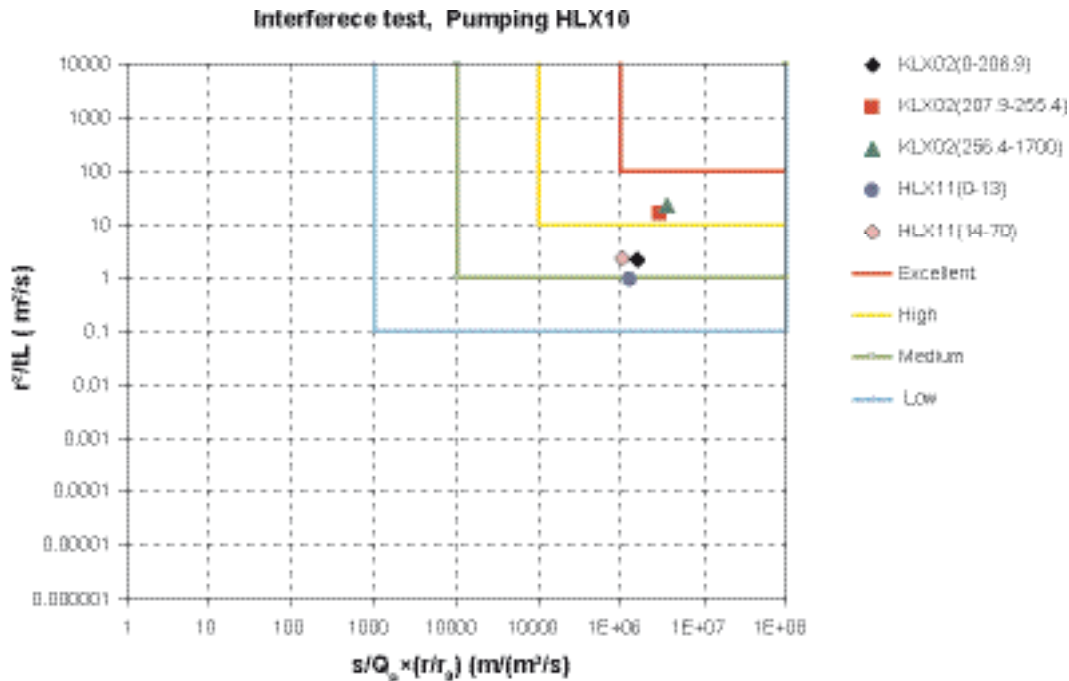


Figure 8-6. Response classification for interference tests. Pumping well: HLX10. The rectangles represents judgements of the responses: within Red: Excellent, within Yellow (outside red rect.): High, within Green (outside yellow rect.): Medium, within Blue (outside green rect.): Low, No response is plotted as $s=0.01$ m and $t_L=1E8$ s. s/Q_p : drawdown at the end of the pumping phase divided with the final pumping rate. r : The distance, r , between different borehole sections has been calculated as the spherical distance using coordinates for the mid-point for each test section or the point of application calculated from the hydraulic conductivity distribution in the observation or pump section. r_0 is set to 1. t_L : The time lag t_L is defined as the time after pumping stop when the pressure response in an observation section is greater than 0.1 m. /Rhén et al. 2006c/.

8.2.3 Joint hydrogeology and geology single hole interpretation

In /Rhén et al. 2006ab/ the PFL-f flow anomalies are evaluated for the different boreholes. A few observations are highlighted here. For details /see Rhén et al. 2006abc/.

It should be stressed that the statistics of the PFL-f flow anomalies are based on transmissivity values above a measurement limit. There are geological features (fractures and crush zones) that most likely have transmissivities below this limit.

Frequency of mapped fractures and PFL-f flow anomalies

The mapped frequencies of fractures; total, open total, partly open, sealed are cross-plotted against the PFL-f frequency in Figure 8-7. The number of fractures in crush zones was estimated as the borehole length of the crush zone in metres multiplied by 40 fractures/m (Standard procedure in the Sicada database for obtaining a rough estimate of the total fracture frequency including mapped fractures and crush zones. A core is mapped as “crush” if individual fractures cannot be mapped. Generally rock pieces in the core in a crush zone may be in the cm scale, as also found when mapping crush zones in tunnels. It is therefore reasonable to designate a frequency of 40 fractures/m in crush zones as a rough estimate.)

As indicated in Figure 8-7 there seems to be approximately a linear correlation between the frequencies of open fractures and the flow anomalies, except for KAV04B, which is the only borehole where data have been collected in the uppermost 100 m of the bedrock. All other data start at approximately 100 m depth below surface. The reason for this difference may be that near the surface there is a lower effective rock stress that affects the open fractures.

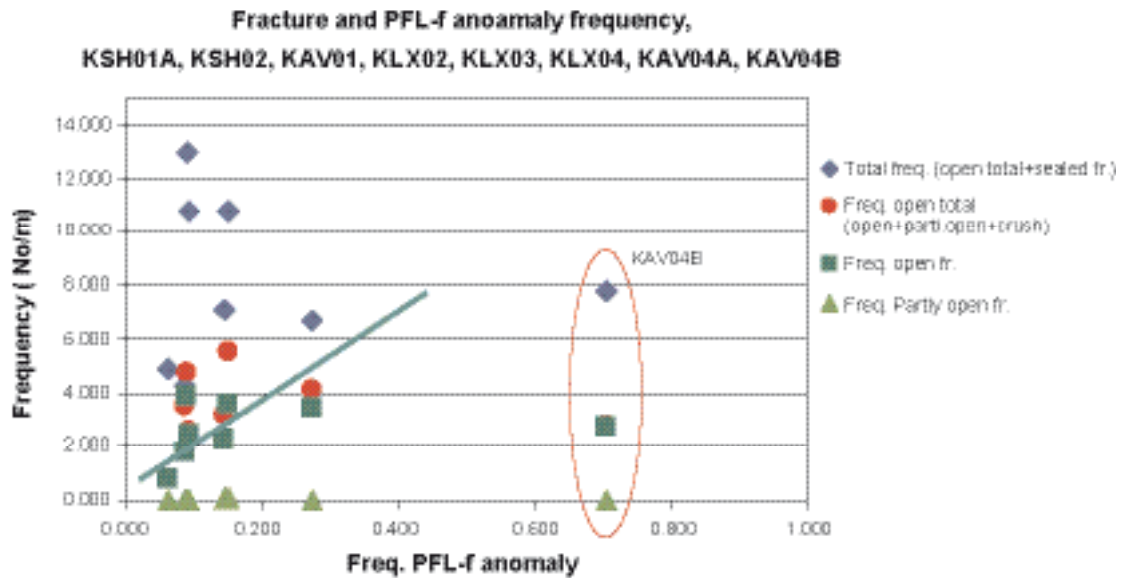


Figure 8-7. Cross plot of Frequency of fractures (open fractures, partly open fractures), open total fractures (open+ partly open+ estimated number of open fractures in crush) and total number of fractures (open total+ sealed) versus the frequency of PFL-f anomalies. All fractures mapped as “Certain”, “Probable” and “Possible” are included in each fracture category (borehole sections interpreted as deformation zones are included), see /Rhén et al. 2006ab/.

Transmissivity of PFL-f flow anomalies

According to /Rhén et al. 2006c/ the result indicates that one can expect 0.05–0.1 flow anomalies per mapped open fracture above a transmissivity about $1E-9$ m²/s (the approximate measurement limit for PFL-f) for rock between 100 to 1,000 m depth. In Table 8-6 and Table 8-7 statistics for PFL-f anomalies, excluding deformation zones (both deterministically modelled and the deformation zones in the geological single-hole interpretation), are shown for three elevation intervals. Transmissivity distributions and frequency of PFL-f anomalies are shown. As can be seen the transmissivity distributions are fairly similar. The major difference is in the frequency of conductive fractures (P_{10PFL}). In /Rhén et al. 2006abc/ similar tables are shown but also for all data, including the deformation zones. The transmissivity distributions are shown in Figure 8-8.

Table 8-6. Univariate statistics of hydraulic tests performed in cored boreholes in the Simpevarp subarea based on a lognormal distribution. Method employed: PFL-f. Sample size always refer to No. of anomalies. Data based on elevation reasonable for repository depth. (Confidence limits for mean $\text{Log}_{10}(T)$ is expressed as the deviation D from mean in the table; for confidence level of 0.95 the mean will be within value “Mean $\text{Log}_{10}(T)$ ” $\pm D$. Sample type “No DZ” means that PFL-f anomalies in deformation zones from geological single hole interpretation and deterministically defined deformation zones for Laxemar model 1.2 in RVS are excluded.) /Rhén et al. 2006c/.

Borehole	Test type	Upper elevation limit	Lower elevation limit	Bh length	Sample type	Sample size	P_{10PFL}	Lower meas. limit ¹	Mean $\text{Log}_{10} T$	Std $\text{Log}_{10}(T)$	D
		(m)	(m)	(m)	(m)		(m ⁻¹)	(m ² /s)	(m ² /s)	(m ² /s)	Conf.lim $\text{Log}_{10}(T)$: Mean $\pm D$, conf.level 0.95: (m ² /s)
KSH01A	PFL-f	-95	-300	139	No DZ	34	0.24	(-9.1) – (-9.0)	-8.25	0.86	0.30
	PFL-f	-300	-700	266	No DZ	6	0.023	(-9.1) – (-9.0)	-9.14	0.26	0.27
	PFL-f	-700	-957	270	No DZ	1	0.004	(-9.1) – (-9.0)	–	–	–
KSH02	PFL-f	-75	-300	155	No DZ	14	0.090	(-9.1) – (-8.7)	-7.02	0.76	0.44
	PFL-f	-300	-700	353	No DZ	50	0.14	(-9.1) – (-8.7)	-7.93	0.63	0.18
	PFL-f	-700	-989	282	No DZ	8	0.028	(-9.1) – (-8.7)	-7.06	0.57	0.48

Borehole	Test type	Upper elevation limit	Lower elevation limit	Bh length	Sample type	Sample size	P _{10PFL} PFL-f anom.	Lower meas. limit ¹ Log ₁₀ T	Mean Log ₁₀ (T)	Std Log ₁₀ (T)	D Conf.lim Log ₁₀ (T): Mean±D, conf.level 0.95: (m ² /s)
		(m)	(m)	(m)	(m)		(m ⁻¹)	(m ² /s)	(m ² /s)	(m ² /s)	(m ² /s)
KAV01	PFL-f	-57	-300	258	No DZ	106	0.41	(-9.6) – (-8.1)	-7.94	0.89	0.17
	PFL-f	-300	-700	185	No DZ	11	0.060	(-9.6) – (-8.1)	-8.52	0.70	0.47
	PFL-f	-700	-717	0	No DZ	0		(-9.6) – (-8.1)	-	-	-
KAV04A	PFL-f	-89	-300	211	No DZ	43	0.20	(-9.6) – (-9.0)	-7.59	0.66	0.20
	PFL-f	-300	-700	391	No DZ	52	0.13	(-9.6) – (-9.0)	-7.66	0.57	0.16
	PFL-f	-700	-982	160	No DZ	31	0.19	(-9.6) – (-9.0)	-7.25	0.78	0.29
KAV04B	PFL-f	-10	-85	76	No DZ	54	0.71	(-9.6) – (-9.0)	-7.21	1.04	0.28

Table 8-7. Univariate statistics of hydraulic tests performed in cored boreholes in the Laxemar subarea based on a lognormal distribution. Method employed: PFL-f. Sample size always refer to No. of anomalies. Data based on elevation reasonable for repository depth. (Confidence limits for mean Log₁₀(T) is expressed as the deviation D from mean in the table; for confidence level of 0.95 the mean will be within value “Mean Log₁₀(T)” ±D. Sample type “No DZ” means that PFL-f anomalies in deformation zones from geological single hole interpretation and deterministically defined deformation zones for Laxemar model 1.2 in RVS are excluded.) /Rhén et al. 2006ab/.

Borehole	Test type	Upper elevation limit	Lower elevation limit	Bh length	Sample type	Sample size	P _{10PFL} PFL-f anom.	Lower meas. limit ¹ Log ₁₀ T	Mean Log ₁₀ (T)	Std Log ₁₀ (T)	D Conf.lim Log ₁₀ (T): Mean±D, conf.level 0.95: (m ² /s)
		(m)	(m)	(m)	(m)		(m ⁻¹)	(m ² /s)	(m ² /s)	(m ² /s)	(m ² /s)
KLX02	PFL-f	-186	-300	104	No DZ	32	0.31	(-10) – (-8.3)	-7.23	0.95	0.34
	PFL-f	-300	-700	402	No DZ	21	0.052	(-10) – (-8.3)	-7.93	0.75	0.34
	PFL-f	-700	-1,372	488	No DZ	21	0.043	(-10) – (-8.3)	-7.77	0.89	0.41
KLX03	PFL-f	-79	-300	229	No DZ	25	0.11	(-9.8) – (-8.2) ¹	-7.81	1.05	0.43
	PFL-f	-300	-700	392	No DZ	15	0.038	(-9.8) – (-8.2) ¹	-7.87	0.70	0.39
	PFL-f	-700	-944	178	No DZ	3	0.017	(-9.8) – (-8.2) ¹	-7.44	0.94	2.3
KLX04	PFL-f	-75	-300	215	No DZ	44	0.20	(-9.6) – (-8.7)	-7.01	0.85	0.26
	PFL-f	-300	-700	393	No DZ	51	0.13	(-9.6) – (-8.7)	-7.34	0.77	0.22
	PFL-f	-700	-957	158	No DZ	1	0.0063	(-9.6) – (-8.7)	-	-	-

Transmissivity of crush zones

One or several flow anomalies have been observed in some, but not all, mapped crush zones. If several flow anomalies are observed in a borehole section mapped as crush, these transmissivities are summed up to represent the transmissivity of the crush zone. In two of the boreholes (KSH01A and KAV01) the geometric mean transmissivity is c. 10 times greater for crush zones (as individual features) than for individual flow anomalies outside the mapped crush zone, with a bit less difference noted for KLX04 and KSH02, and no difference in KLX02. However, the uncertainty is high for the mean value estimated for each borehole considering the confidence limits for the mean. The confidence interval for the mean of the KLX02 data is relatively small, but should still be considered highly uncertain while the data quality is lower than for the new boreholes, as mentioned earlier in this section.

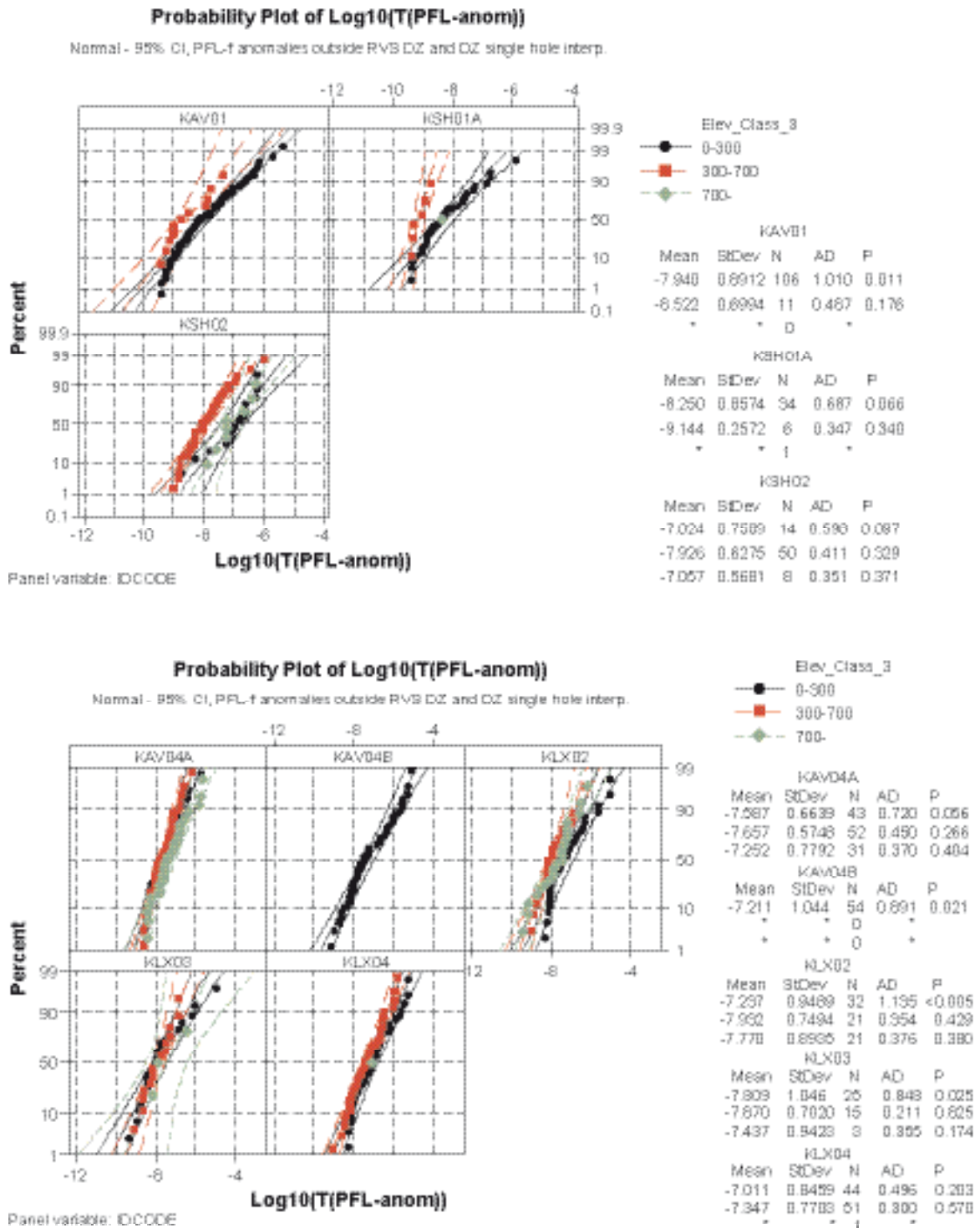


Figure 8-8. Statistics of PFL-f anomaly transmissivities. Data from the entire Simpevarp regional area. /Rhén et al. 2006ab/.

The frequency of crush zones with one or more PFL-f anomalies in relation to all mapped crush zones (number of crush zones with PFL-anomaly/number of all crush zones) is 0.23–0.43 for all boreholes (KLX02, KLX03, KLX04, KAV04A, KSH02A, KAV01) except two which have frequencies 0 and 1 (KSH01A, KAV04B respectively) /Rhén et al. 2006ab/. The total number of crush zones varies significantly between the boreholes, from 3 to 78, excluding the short borehole KAV04B. Thus, about 1/3 of the crush zones are conductive and about 2/3 are non-conductive, or rather below the measurement limit for PFL-f. For details see /Rhén et al. 2006abc/.

Some general observations based on the hydraulic test data

As can be seen in Table 8-2, there is a difference between boreholes; KLX03 is much less permeable than the KLX02, KLX04 and KAV04A boreholes. KLX03 is situated in rock domain M and D and the other boreholes sample geological rock domain A. The borehole data analysed for SDM Laxemar 1.2 also suggest that the defined geological rock domains exhibit distinct and significantly different hydraulic characteristics. PFL-s data from KSH01A and KSH01 also indicate that the geological rock domains B and C are less permeable than rock domain A, see /Rhén et al. 2006a/. The noted differences are further explored in Section 8.4.3.

If the PSS tests on a 100 m test scale are explored, see /Rhén et al. 2006ab/, there appears to exist a depth trend in hydraulic conductivity in boreholes KSH01, KSH03, KLX02, KLX03, KLX04, KLX05 and KLX06. In boreholes KAV04, KLX01 and KSH02 such a depth trend is not that obvious. However, the data suggest that further analysis of depth trends in the data is warranted to establish whether the depth trends are significant. This is done in Sections 8.4.3 and 8.4.4.

A few larger deformation zones have been intercepted by boreholes, and it appears that they, at least in some instances, are significantly more conductive than the surrounding rock mass. This is not surprising considering experience from mining and engineering in Swedish crystalline bedrock. The general engineering experience is that deformation zones are both important from a hydraulic and a rock mechanical point of view. It is thus rather obvious that the hydraulic properties of deformation zones should be examined in more detail. This is done in Section 8.4.2.

The PFL flow anomalies showed in Tables 8-6 and 8-7 show some interesting results. First, the transmissivity (T_f) distributions are fairly similar between the boreholes, and there appears not to be any consistent dependence with depth. The mean of $\text{Log}_{10}(T_f)$ value is around -7 to -8 , with a standard deviation of $\text{Log}_{10}(T_f)$ around 0.5 – 1 . Also the only borehole with observations in the uppermost 100 m (KAV04B) shows this characteristic. The exceptions being KSH01A and the deeper part of KAV01 that have mean of $\text{Log}_{10}(T_f)$ around -9 to -8.3 . The second observation is that the frequency of flow anomalies varies considerably. The frequency (anomalies/m) varies from 0.004 to 0.71 , the last figure representing the near surface data (0–100 m depth) in KAV04B. The highest frequency below 100 m depth is 0.41 . This may indicate that a hydraulic DFN model should be “intensity driven” rather than assuming that different transmissivity distributions are needed for matching data. However, hydraulic DFN models are complex, with a geometrical model that plays an important role in how the model matches in situ data. This is explored in more detail in Section 8.4.4.

8.3 Hydrogeological model – general conditions and concepts

This section describes the modelling strategy and conceptual models that form the basis for the hydrogeological modelling presented in the following sections.

8.3.1 Modelling objectives and premises

The hydrogeological descriptive model should provide a hydraulic parametrisation of interpreted deterministic deformation zones and the rock mass between the interpreted deformation zones. The Hydrogeological DFN models are in this context of particular importance. A key user of this information is Safety Assessment.

The hydrogeological descriptive model also provides data used for variable-density groundwater flow modelling. The flow models should be able to simulate groundwater flow within a given volume under natural (undisturbed) conditions, to provide a general understanding of the natural groundwater flow system, and disturbed system with a deep repository. The flow paths to the potential repository volume are of interest, as they provide a description of the rate at which potential corrodants are introduced. Likewise, the flow paths from the recharge areas of the potential repository volume within the modelled volume are important for estimation of the paleohydrogeological and hydrogeochemical evolution. Of importance in this context is the shoreline displacement which must be taken into account when modelling the long-time evolution of the groundwater flow (and

groundwater chemistry). The established flow paths from the repository volume to discharge areas are important for Safety Assessment.

The numerical groundwater flow modelling serves three main purposes:

- Model testing: Simulations of different major geometric alternatives or boundary conditions in order to disprove a given geometric interpretation, material property assignment, or boundary condition, and thus reduce the number of alternative conceptual models of the system.
- Calibration and sensitivity analysis: to explore the impact of different assumptions as to hydraulic properties, boundary and initial conditions.
- Description of flow paths and flow conditions: useful for the general understanding of the groundwater flow system (and hydrogeochemistry) at the site.

The numerical groundwater flow simulations are thus helpful for the assessing the interplay between geological structures (domains) and hydrogeological properties and conditions (hydraulic properties, boundary and initial conditions), as well as for improving the general understanding of the site. The close interaction between the geological and hydrogeological interpretations, together with the integration of the hydrochemical, transport and surface systems information, is critical to interpret the available hydrogeological data and also essential for obtaining consistent conceptual models that can be used in the numerical groundwater flow modelling

A given version of the site description, with its groundwater flow model, subsequently forms the basis for further analysis by Repository Design and Safety Assessment and for the planning of new investigations. Exploratory groundwater flow simulations are considered when planning field investigations or addressing specific Repository Engineering and Safety Assessment questions.

Overview of work done for Laxemar 1.2

The baseline data and models used in the hydrogeological descriptive modelling for model version Laxemar version 1.2, as presented in the following sections, are based on the current surface system and geological descriptive models as presented in Chapters 4 and 5, respectively. The modelling done for Laxemar 1.2 comprises estimates of hydraulic properties based on data from the Simpevarp and Laxemar subareas, including data from the Äspö HRL (Section 8.4), as well as numerical groundwater flow simulations (Sections 8.4 and 8.5). The flow simulations are also preceded by a hydraulic DFN analysis.

The hydraulic DFN analysis was conducted by two modelling teams /Hartley et al. 2006/ and /Follin et al. 2006/. The tasks for the teams were differentiated. /Hartley et al. 2006/ made a similar modelling effort for the hydrogeological DFN as employed previously in the Simpevarp 1.2 model description /Hartley et al. 2005/. The main task of /Follin et al. 2006/ was to conduct a sensitivity study to illustrate how reported uncertainties in the geological DFN propagate in, and affect, the hydrogeological modelling.

The construction of the final hydraulic DFN models used for numerical simulations was made in parallel with the finalisation of the geological DFN, i.e. the hydraulic DFN modelling was forced to adapt to a developing geological DFN, cf. Section 5.5. Details on the work conducted are described by /Hartley et al. 2006/ and /Follin et al. 2006/. A few comments are made later on in this section on the experiences gained.

The numerical groundwater flow modelling is made using the numerical codes DarcyTools /Svensson et al. 2004, Svensson and Ferry 2004, Svensson 2004/ and ConnectFlow /Hartley et al. 2003ab, Hartley and Holton 2003, Hoch and Hartley 2003, Hoch et al. 2003/, respectively.

It is noted that in the current regional scale flow modelling the underground openings of the Äspö HRL, which effectively constitute a large-diameter “well”, 450 m deep, and not included explicitly in the current modelling. The main motive for this simplification is the location of the Äspö HRL, which is below an island in the Baltic Sea. Hence, the radius of influence associated with Äspö HRL is deemed limited due to the vicinity of a significant positive hydraulic boundary. However, the sensitivity of the model to the non-inclusion of the Äspö HRL will be tested in future model versions.

8.3.2 General modelling assumptions and input from other disciplines

As described in Chapters 4 and 5, the Simpevarp area is dominated by a crystalline bedrock covered by a fairly thin overburden mainly consisting of till. The crystalline bedrock is fractured and it is interpreted that there are a number of major deformation zones within the area. The existence of these deformation zones have to some extent been confirmed by surface geophysics and drilling, see Chapter 5. Hydraulic tests have confirmed, in some cases, that the deformation zones are more conductive than the surrounding rock, as mentioned in Section 8.2 and as further elaborated in Section 8.4.2.

Different geological and geophysical investigations have resulted in a description of the spatial distribution of rock types, and interpreted larger geological entities (rock domains) consisting of rock types with similar geological properties, see Section 5.3. The deformation zone model developed for SDM Laxemar 1.2 is presented in Section 5.4 and is further detailed by /Wahlgren et al. 2005b/. Observations of the general character of the hydraulic tests, as pointed out in Section 8.2, indicate that the defined geological rock domains also exhibit distinct and significant hydraulic characteristics. In Section 8.4.3 it is shown that if the rock domains defined along each corehole is used for analysing the difference in hydraulic properties related to rock domain, there seems to be significant differences in hydraulic properties of the rock domains that should be taken into account in the hydrogeological description. However, it is also noted that the current database is sparse, and the conclusion that the geologically defined rock domains constitute a basis for defining hydraulic domains is uncertain.

The overburden consists mainly of till, but glacial sediments, peat and clay are also found. The hydraulic conductivity of these components is generally higher than for the crystalline bedrock. Depending on the modelling task, the hydrogeology of the overburden requires attention and quantification.

Based on the above deliberation, the conceptual model for the Simpevarp area, including the Laxemar subarea, can be illustrated as in Figure 8-9. The conceptual model consists of the following entities:

- The geometry of large, deterministically modelled deformation zones, here included as Hydraulic Conductor Domains (HCD) and the bedrock in between the deterministic zone (the rock mass), here included as Hydraulic Rock Domains (HRD).
- The distribution of Quaternary deposits (overburden), here included as Hydraulic Soil Domains (HSD) (including genesis, composition, material properties, stratification and thickness).

As the Simpevarp area is dominated by the fractured crystalline basement, the hydrogeological description of the HRDs, also used for flow modelling, may be either discrete (hydraulic DFN) or continuous (equivalent porous medium, EPM) depending on the DFN properties, the scale of

Hydrogeological description

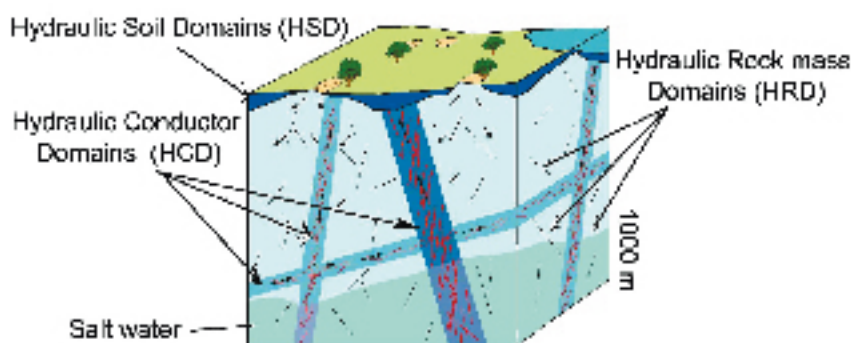


Figure 8-9. Division of the crystalline bedrock and the overburden (Quaternary deposits) into hydraulic domains representing the overburden, (HSD) and the rock mass volumes (HRD) between major fracture zones (conductors, HCD). Within each domain, the hydraulic properties are represented by mean values, or by spatially distributed statistical distributions /Rhén et al. 2003/.

resolution, and the modelling objectives. The basis for the assignment of hydraulic properties to the HSD model is the hydraulic testing conducted in the monitoring wells (soil pipes) in the Quaternary deposits. Details of the Quaternary deposits and the hydrogeological description of the overburden are provided in Chapter 4 and by /Lindborg 2006/.

Likewise, the investigations and documentation of the present-day meteorology, hydrology and near-surface hydrogeology (in terms of mapping of springs, wetlands and streams, surveying of land use (ditching and dam projects), resources for water supply, etc.), together with the shoreline displacement throughout the Holocene, also contribute an additional basis for the hydrological process modelling. This information provides input to:

- Interpretation of present-day drainage areas, as well as the distribution of recharge and discharge areas.
- Estimates of the average present-day precipitation and run-off, distribution of hydraulic head and flow in watercourses.
- Assessments of the evolution of boundary conditions since the last glaciation.

Present-day meteorology, hydrology and near-surface hydrogeology are described in Chapter 4 and are further detailed in /Lindborg 2005/ and /Werner et al. 2005/.

General assumptions regarding HCD, HRD, HSD, initial and boundary conditions

The primary hypotheses regarding the development of a hydrogeological descriptive model of the Simpevarp area, including the Laxemar subarea, are:

- The current hydrogeological and hydrogeochemical situation in the Simpevarp area is the result of natural transient processes that have evolved since the last glaciation;
- The present main component chemical composition can be modelled as a consequence of conservative (non-reactive) mixing between four end member water compositions. These are: Brine (reflecting the composition of high salinity fluids), Glacial, Littorina and Dilute groundwater (In /Hartley et al. 2006/ Dilute water is denoted "Meteoric water").
- The natural transient processes (land-rise, marine transgressions, dilution/mixing of sea water) can be modelled by appropriate choice of flow and reference water boundary conditions;
- The properties of the hydraulic rock domains (HRD) can be represented as EPM properties underpinned by a regional scale stochastic HydroDFN model.
- The spatial variability of hydraulic properties can be represented in an equivalent porous media (EPM, or equivalent continuum porous media, ECPM) model by appropriate upscaling of bedrock fracturing and downscaling of deformation zones using a suitable grid resolution;

Concepts for assignment of hydraulic properties to HRDs

The rock mass (domains) between the deterministically modelled deformations zones are modelled as fracture networks. The statistical fracture models are defined in Section 5.5 (geological DFN) and those models are the basis for constructing fracture network models of conductive fractures and features (hydraulic DFN). The main concepts for the construction of hydraulic DFN models are outlined below and details are presented in Appendix 8.

Conductive elements in terms of deformation zones and fractures

Potentially flowing minor deformation zones are simulated as stochastic single planar features, see Figure 8-10. This means that the fracturing within a given deformation zone is not studied in terms of its components, but is reduced to, and treated as one single object. Both minor (stochastic) and interpreted deterministic deformation zones are treated in the same way.



Figure 8-10. Potentially flowing stochastic deformation zones consisting of fracture swarms (clusters) are simulated as single planar features and are considered homogeneous with regards to their hydraulic properties /Follin et al. 2006/.

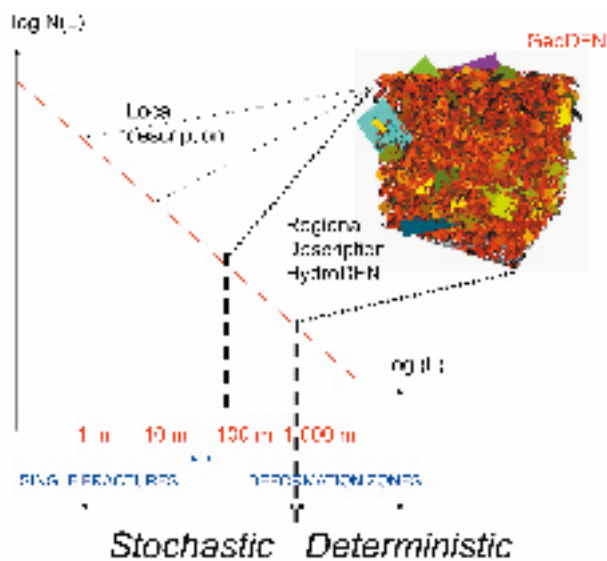


Figure 8-11. The frequencies of occurrence of single fractures and deformation zones are assumed to be power law distributed. The distinction between from single fractures and deformation zones is here semantic since the deformation zones are treated as single features /Follin et al. 2006/.

Distribution of size of conductive features

The sizes (L) of the potentially flowing fractures are assumed to follow a power law (base case, see Figure 8-11), or to be lognormally distributed.

When describing the intensity of a fracture set in terms of P_{10} (fractures/length along a scan line/or borehole), $(1/m)$, P_{21} (trace length/area, (m/m^2)) or P_{32} (fracture surface area/volume, (m^2/m^3)), it is always important to describe the size interval considered, as inclusion of the small sizes tends to affect the fracture intensity parameters. The DFN modelling presented in /Darcel et al. 2004/ indicates that fracture sizes down to 0.1 m may be relevant to include in the model.

Transmissivity distribution models

Three models for attribution of fracture transmissivity have been considered, see Figure 8-12 that all related transmissivity to size. Presently, it is not known which model is to be considered the most appropriate. However, when deformation zones are considered, they generally show an increased thickness when the size increases, implying the possibility that the also the number of flowing fractures increases with thickness. This would suggest that a positive correlation between fracture (structure) size and transmissivity is reasonable. The number of interconnected fractures in a deformation zone is probably highly variable, which should also make it more likely that the semi-correlated model is more reasonable than the correlated. For single fractures, the positive correlation between size and transmissivity is more uncertain.

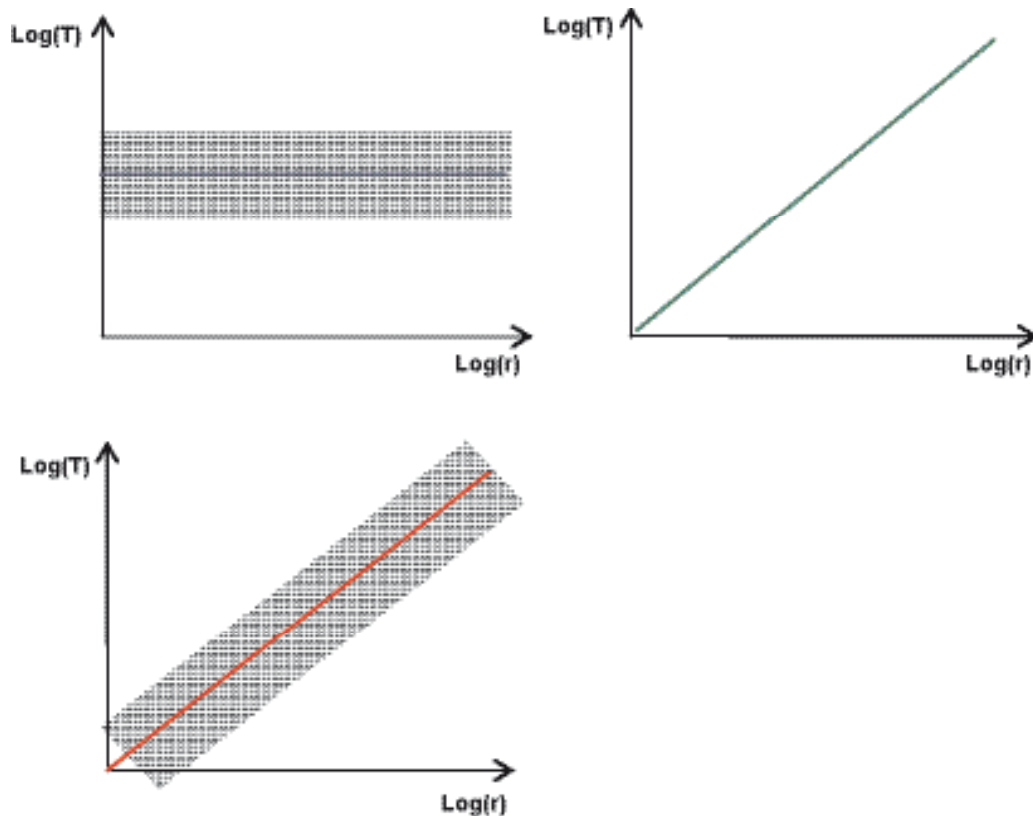


Figure 8-12. Schematic of transmissivity models: 1) Uncorrelated, 2) Correlated, and 3) Semi-correlated /Hartley et al. 2006/.

Identification of conductive fractures

Only the most transmissive of the potentially flowing open and partially open fractures are assumed to be detected by the Posiva Flow Log (PFL-f) due to the measurement limit. Figure 8-13 illustrates that the number of flowing fractures in a core-drilled borehole detected by the Posiva Flow Log, N_{PFL} , is regarded as a subset of the geometrically interconnected Open fractures, N_{CON} , which in turn is a subset of N_{CAL} , i.e.

$$N_{PFL} < N_{CON} < N_{CAL}$$

The implications of this deliberation for mapping transmissivity in a borehole are further discussed in Appendix 8.

8.3.3 General modelling strategy

The hydrogeological models representing the HRDs, the HCDs, and the HSDs are combined into a regional scale groundwater flow model, see Figure 8-14. The derivation of block scale parameters from hydraulic DFN is requested by Repository Engineering, but the underlying principle for the derivation, the equivalent porous medium (EPM) approach, is also used in the regional flow modelling.

The regional flow model is calibrated against hydraulic test data and hydrogeochemical data, e.g. chemical composition including; salinity, different water types and isotopic signatures. The calibrated regional flow model is used for sensitivity analysis of groundwater flow and advective transport of solutes using particle tracking. Conceptual models, assumptions and details on the modelling approaches used are presented in /Hartley et al. 2006/. Some of the key assumptions made in the hydraulic DFN modelling are discussed in /Follin et al. 2006/ who also scrutinise the impact of different uncertainties in the geological DFN modelling on the hydraulic DFN.

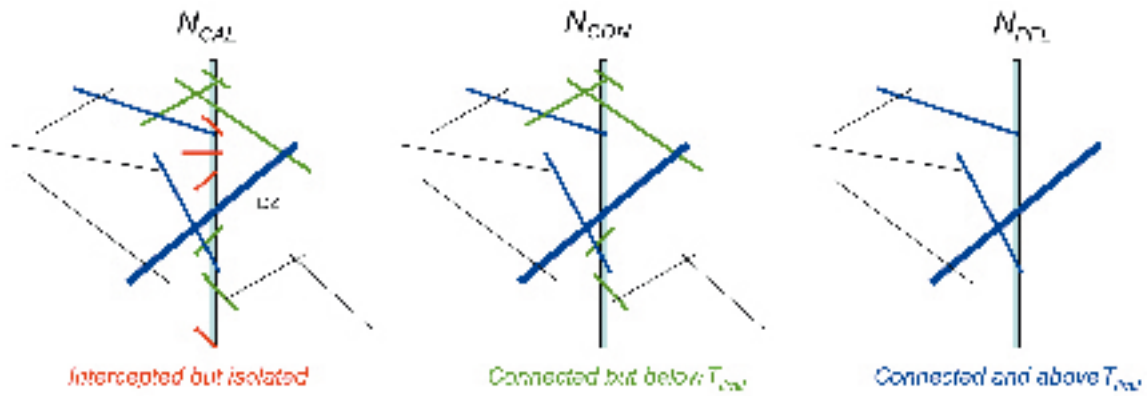


Figure 8-13. The definition of N_{CAL} , N_{CON} and N_{PFL} of Open fractures. T_{limit} denotes the lower measurement limit for transmissivity, which is typically $1 \times 10^{-9} \text{ m}^2/\text{s}$ for the Posiva Flow Log (PFL-f). /Follin et al. 2006/.

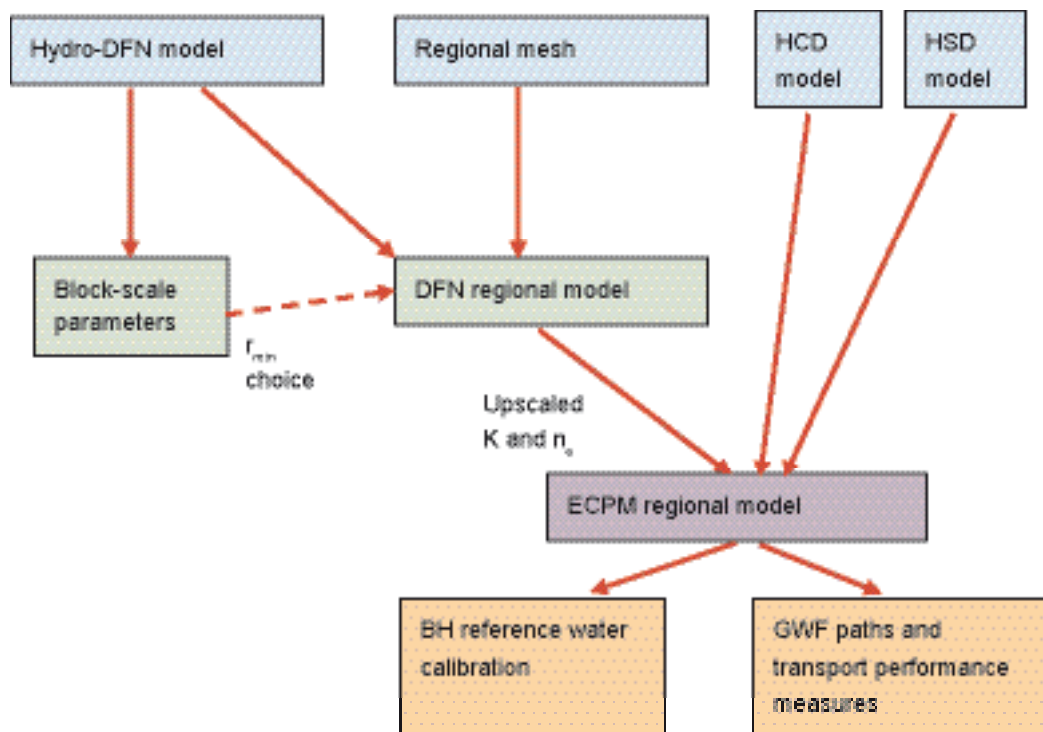


Figure 8-14. A schematic workflow for the modelling /Hartley et al. 2006/.

8.4 Assignment of hydraulic properties

In this section, the hydraulic properties of the overburden, the deterministically interpreted deformation zones and the rock domains are explored to establish if there are reasons to define separate hydraulic domains due to observed differences in hydraulic properties. Parameterisation of hydraulic domains is given on the basis of results of analysing hydraulic tests but also on the basis of results from numerical simulations, e.g. the Hydraulic DFN model. To some extent, parameters that come as a result from the regional groundwater flow modelling, presented in Section 8.5, are included and discussed in this section in order to provide a comprehensive picture of proposed hydraulic property assignment.

8.4.1 HSD – overburden

The investigations performed in the overburden and resulting models are reported in /Lindborg 2005, Werner et al. 2005, Nyman 2005/. In this section only a few results from these reports are highlighted that in turn have been input to the regional groundwater flow model presented in /Hartley et al. 2006/.

Generally, a thin cover of till is found across the entire rock surface, except for some areas where the rock is outcropping /Nyman 2005/. Precambrian bedrock covers 34.6% of the area according to Chapter 4. The standard Quaternary mapping does not consider very thin overburden layers, and therefore the bedrock surface that is free of overburden is less than the figure above. In the valleys the till is generally overlain by clay deposits. In some areas, peat is found on top of the clay layer (7.6% of the area, cf. Chapter 4). In a few places, glacial deposits are found and furthermore artificial fills associated with the nuclear power plants cover limited areas (0.13% of the area, cf. Chapter 4). The uppermost part of the overburden can be considered to be affected by surface processes, such as roots, biological activity and frost. This leads to a higher permeability and porosity compared with deeper strata in the overburden. For a more stratigraphic description and more details about the overburden, see Chapter 4.

For the regional modelling, see Section 8.5 and /Hartley et al. 2006/ the reference case consists of a simple three homogenous layer model of 3 m thick silty till, with the uppermost 1 m being more porous due to soil-forming processes. The model described in Chapter 4, with all its different layers of overburden, was also implemented in the regional groundwater flow model as an alternative model, but with a coarser grid (50 and 100 m) compared with the original overburden model (10 m grids), see /Hartley et al. 2006/.

HSD – properties

The hydraulic properties of the Hydraulic Soil Domains (HSD) are described by /Werner et al. 2005/ and are summarised in Table 8-8. It should be observed that the hydraulic conductivity values in Table 8-8 generally are higher than in the bedrock. This means that e.g. the clay layers will not significantly reduce the infiltration or have a large effect on the deep bedrock hydrogeology.

Table 8-8. HSD properties based on /Werner et al. 2005/. Hydraulic conductivity (K), Horizontal hydraulic conductivity (K_H), Vertical hydraulic conductivity (K_V).

HSD	Description	K_H (m/s)	K_H/K_V (–)	Specific yield, S_y (–)	Specific storage coefficient, S_s (1/m)
HSD (Z1-1)	Surface process affected layer, Clay	1E-6	1	0.03	6E-3
HSD (Z1-2)	Surface process affected layer, Till	4E-5	1	0.15	1E-3
HSD (Z1-3)	Surface process affected layer, Artificial fill	4E-5	1	0.15	1E-3
HSD (Z2)	Clay layer	1E-8	1	0.03	6E-3
HSD (Z3)	Till layer	4E-5	1	0.05	1E-3
HSD (M1)	Peat layer	1.5E-6	1	0.24	5E-2
HSD (M2)	Glaciofluvial sediment layer	1E-4	1	0.25	2.5E-2
HSD (M3)	Artificial fill layer	4E-5	1	0.05	1E-3

HSD – hydraulic properties inferred from the regional groundwater flow simulation.

No simulations or calibrations have been made to adjust the assigned hydraulic properties of the HSDs.

8.4.2 HCD – deterministic deformation zones

The basis for the interpretation of the HCD properties is the 3D deformation zone model in the RVS (Rock Visualisation System) and the intersections between boreholes and deformation zones in the RVS model. The judgement of the geologists as to where the deformation zones intersect the boreholes has guided the search for relevant hydraulic information. The hydrogeological properties extracted from transient pumping or injection tests have been used to estimate the HCD parameters. If a single hydraulic test section covers the entire part of a deformation zone defined in a borehole, the corresponding test results have been used, instead of summing up transmissivities for shorter test sections.

HCD – mean transmissivity

Table 8-9 presents mean and standard deviation for $\text{Log}_{10}(T)$ of the transmissivity (T) values that can be connected to each HCD (each deterministic deformation zones corresponds to a HCD), without taking any possible depth dependence in consideration. HCDs with no hydraulic test data have been assigned the geometric mean value based on all transmissivity data related to interpreted deterministic HCDs, and with an assumed geological thickness of 20 m.

It can be observed that the above mean value of T is higher than that measured at the intercepts of many of the high confidence deformation zones. It is important to observe that the confidence of existence (high, medium, low) is a judgement based on the available geological and geophysical observations that provide support of the existence of any given deformation zone. Hydrogeological observations may also contribute to confirming the existence. Furthermore, the hydraulic properties may vary over wide ranges, not necessarily transferable to judgement of confidence. Many of the low confidence zones in the local model area have shorter trace length on the surface compared to the high and medium confidence deformation zones. As described in the previous section, for the stochastic modelling of fractures and minor local deformation zones, a positive correlation between size and transmissivity is used in the attribution of material properties. If this is valid for the deterministically defined deformation zones, many of the low confidence zones would be less transmissive than the high and medium confidence deformation zones. This positive correlation between size and transmissivity remain to be tested as more data is obtained. Consequently the described assignment of the mean transmissivity of all HCD transmissivity data to non-tested HCDs of low confidence zones (possible minor local zones) may not be appropriate and justified. However, this route has been taken in the current modelling.

In the present model, the number of high, medium and low confidence deformation zones that have any measured T-value and the number zones that have no measured T-value is shown in Table 8-10. This table also reflects that drilling is important for the judgement of “confidence of existence”. When intercepted by drilling, hydraulic tests are generally performed that can be used for material property assignment.

Table 8-9. Univariate statistics for transmissivities associated with deterministically defined deformation zones in RVS model version Laxemar 1.2. (Confidence limits for mean $\text{Log}_{10}(T)$ is expressed as the deviation D from the mean in the table; for confidence level of 0.95 the mean of $\text{Log}_{10}(T)$ will be within value “Mean $\text{Log}_{10}(T)$ ” $\pm D$.)

Name of HCD, RVS ID, (Earlier name)	Geological confidence, High/Medium/Low	Geological thickness, b (m)	Sample elevation range (m.a.s.l.)	Sample mean elevation (m.a.s.l.)	Sample size	Mean $\text{Log}_{10}(T)$ (m ² /s)	Std $\text{Log}_{10}(T)$ (m ² /s)	D Conf.lim $\text{Log}_{10}(T)$: Mean $\pm D$, conf.level 0.95: (m ² /s)
ZSMEW002A (Mederhult zone)	High	100	-37 to -389	-194.7	5	-5.41	1.37	1.7
ZSMEW007A	High	50	-2 to -995	-178.4	8	-4.34	1.05	0.88
ZSMEW009A (EW3)	High	12	-22 to -490	-158.7	4	-4.92	0.35	0.56
ZSMEW013A (EW1A)	High	45	2 to -341.6	-116.1	5	-5.92	1.47	1.83

Name of HCD, RVS ID, (Earlier name)	Geological confidence, High/Medium/Low	Geological thickness, b (m)	Sample elevation range (m.a.s.l.)	Sample mean elevation (m.a.s.l.)	Sample size	Mean Log ₁₀ (T) (m ² /s)	Std Log ₁₀ (T) (m ² /s)	D Conf.lim Log ₁₀ (T): Mean ± D, conf.level 0.95: (m ² /s)
ZSMEW014A	Medium	20 ¹	4.5	4.5	1	-5.66		
ZSMEW038A (ZSMEW038A_B)	High	10	-17 to -193	-142.7	4	-3.92	1.40	2.23
ZSMEW039A	Medium	20 ¹	-5.3	-5.3	1	-6.26		
ZSMEW900A (ZSMEW005A 7A)	High	20	-1 to -135	-68	2	-4.29	0.90	-
ZSMNE004A (ZSMEW004A)	High	100	-43.7 to -151.6	-97.64	1	-5.55		
ZSMNE005A (Åspö shear zone; EW1b)	High	250	-32 to -849	-276.5	8	-4.66	1.02	0.85
ZSMNE006A (NE1)	High	130	-31 to -821	-244.6	12	-3.66	0.57	0.36
ZSMNE012A (includes NW004A (old names EW7-NE4))	High	120	-18 to -833	-193.3	9	-4.45	1.07	0.82
ZSMNE015A	High	10	-936	-936	1	-8.41		
ZSMNE016A	High	15	-49 to -129	-69.14	2	-5.60	1.06	
ZSMNE024A	High	80	-583 to -956	-386.4	4	-6.57	2.47	3.93
ZSMNE031A	High	15	-240 to -668	-454	2	-5.94	3.03	
ZSMNE040A	High	20	-4 to -38	-21	2	-6.14	2.96	
ZSMNS017B (NNW4)	High	20	-267 to -439	-300.3	9	-4.21	1.38	1.06
ZSMNW025A	High	10	-170	-170	1	-6.94		
ZSMNW028A (ZSMEW028A)	High	10	-81	-81	1	-6.45		
ZSMNW042A	High	80	-672	-672	1	-6.37		
ZSMNW048A	Medium	20 ¹	-30.3	-30.3	1	-4.52		
ZSMNW928A (Reflector N)	Medium	20 ¹	-746 to -869	-807.5	2	-6.12	0.05	
ZSMNW929A (ZSMNE040A)	High	50	-832 to -895	-863.5	2	-5.90	0.27	
ZSMNW932A (ZSMNW006A)	High	10	-470 to -549	-509.5	2	-6.06	0.78	
All other HCD		20 ¹				-4.92	1.48	

¹ Geological thickness assumed to be 20 m due to lack of data.

Table 8-10. Number of deformation zones (DZ) in the Laxemar 1.2 that have any measured T- value or do not have any measurement.

DZ classification	Number of DZ Total	Number of DZ With one or several T-values	Number of DZ No T-values
High confidence	32	20	12
Medium confidence	56	4	52
Low confidence	92	0	92
total	180	24	156

HCD – depth trends in transmissivity

In Figure 8-15 all transmissivity data for the HCDs representing each tested borehole section (one “best choice” (BC) T-value for each test section representing a HCD) are plotted. The dataset was divided into three subsets based on elevation (z) intervals; down to –300, –300 to –600 and below –600 m above sea level and univariate statistics were computed, see /Rhén et al. 2006c/. In

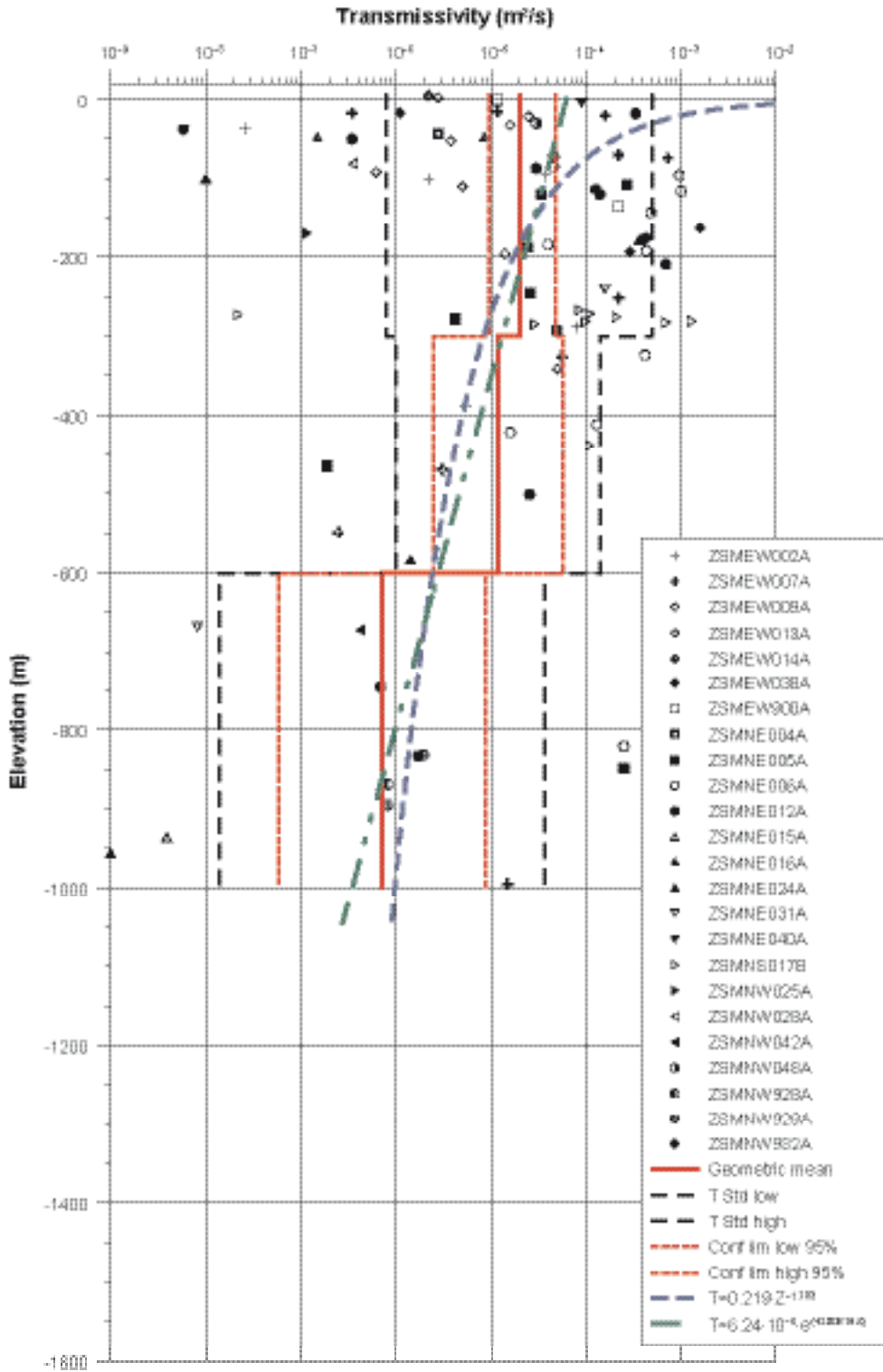


Figure 8-15. Depth trend of the transmissivity in HCDs. /Rhén et al. 2006c/.

Figure 8-15 the standard deviation, as well as the 95% confidence level for $\text{Log}_{10}(T)$ are shown. Two different functions have been fitted to the mean transmissivity values evaluated for the three elevation intervals, a power law dependence (Equation 8-1) and an exponential one (Equation 8-2):

$$T = a \times z^b \quad (\text{Equation 8-1})$$

$$T = a \times e^{(b \times z)} \quad (\text{Equation 8-2})$$

Table 8-11. Coefficients of depth trend models applied to transmissivity data in HCDs. Unit for transmissivity (T): m^2/s . Unit for elevation (z): metres above sea level. Note that the regression is equated using $-z$ as a parameter.

Depth trend model	Coefficient a	Coefficient B	Coeff. of determination, R-squared r^2
Power-law (Equation 8-1)	0.219	-1.783	0.72
Exponential (Equation 8-2)	6.24×10^{-5}	-0.00519	0.89

A linear trend function was also fitted to the standard deviation of $\text{Log}_{10}(T)$ of the three elevation data sets, see Figure 8-16, Equation 8-3 and Table 8-12:

$$\text{Std}(\text{Log}_{10}(T)) = a \times z + b \quad (\text{Equation 8-3})$$

As can be seen in Figure 8-15 the confidence limits for mean $\text{Log}_{10}(T)$ is wide for all three depth intervals. It can be concluded that the inferred depth trend of the transmissivity is very uncertain due to sparse data for the deformation zones. The inferred depth trend of the standard deviation is of course as well uncertain.

The above trend models described are possible alternatives that can be applied to the HCDs in the model version Laxemar 1.2. Using a stochastic approach and the depth trend functions to assign the transmissivity raises the question if there are any upper and lower limits of transmissivity in HCDs that should be honored. One can probably deduce a lower limit from the reasoning given in 8.4.3 for low-conductive (matrix) rock.

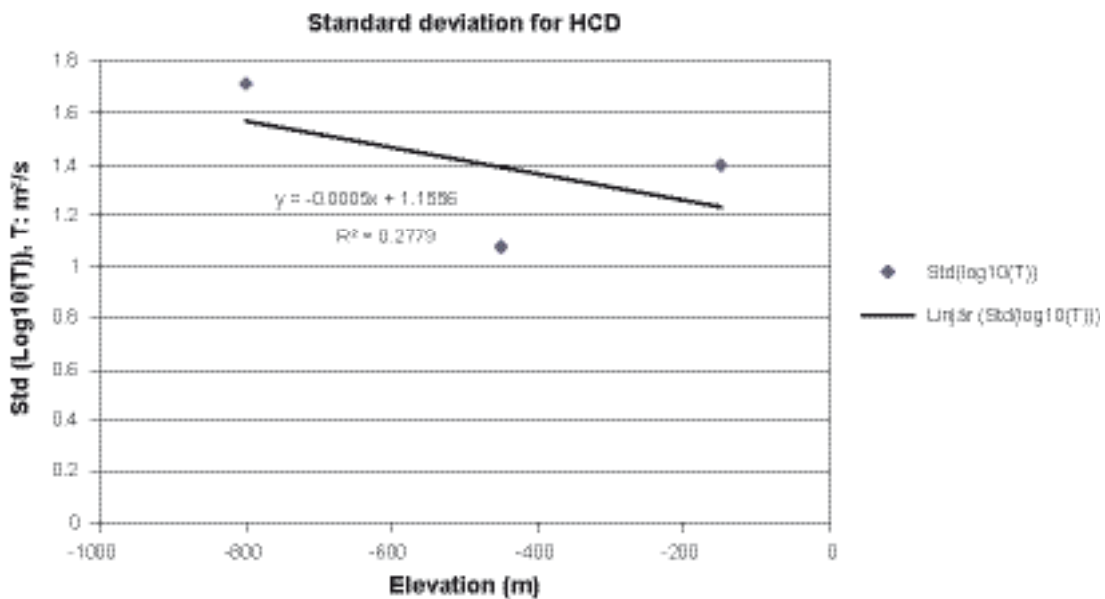


Figure 8-16. Depth trend of the standard deviation of transmissivity in HCDs, based on the evaluated standard deviations shown in Figure 8-15.

Table 8-12. Coefficient for depth trend model applied the standard deviation of $\text{Log}_{10}(T)$ in HCDs. Unit for transmissivity (T): m^2/s . Unit for elevation (z): metres above sea level. Note that the regression is equated using $-z$ as a parameter.

Depth trend model	Coefficient a	Coefficient b	Coeff. of determination, R-squared r^2
Std ($\text{Log}_{10}(T)$)	-0.0005	1.1556	0.28

The power-law function indicates very high transmissivity near the surface that is to be regarded as unrealistic. It is here proposed that the maximum transmissivity is set to $1\text{E}-3 \text{ m}^2/\text{s}$, which is close to the maximum value seen in Figure 8-15.

HCD – transmissivity inferred from the regional groundwater flow simulation

Several model cases, for HCD as formulated in /Hartley et al. 2006/ based on data in /Rhén et al. 2006c/, have been modelled and analysed. These cases have been analysed at a regional model scale, matching results of simulated hydrogeochemical evolution to measured hydrogeochemical data, /see Hartley et al. 2006/. No simulations or calibrations using hydraulic interference test data have been made to adjust the assigned hydraulic properties of the HCDs.

The reference case in /Hartley et al. 2006/ includes all HCDs (all deformation zones of high, medium and low confidence). A depth trend, as a step function in elevation (0 to -300 m above sea level, -300 to -600 m above sea level, deeper than -600 m above sea level) was also applied for the non-conditioned part of the HCD. To honour the measured values at the deformation zone intercepts, the depth trend curve was adjusted such it passes through the given mean T and the related “mean elevation”, see Table 8-9, and the mean transmissivity was then estimated for the three elevation intervals. If no tests were available for a HCD, the mean transmissivity for the three elevation intervals shown in Figure 8-15 were used.

The transmissivities of the HCDs were also conditioned to measured values (T values from PSS transient injection tests, 100 m test scale) in a horizontal band along the HCD at elevation corresponding to borehole intersection with the HCD. This conditioning band was superimposed and overruling the assignment given above. For more details concerning the reference case, see Section 8.5 and /Hartley et al. 2006/.

HCD – difference in properties compared to HRD

The hydraulic conductivity (K) of each HCD transmissivity value was calculated dividing the transmissivity value with the estimated geological thickness for each deformation zone, the latter given as a mean value in Table 8-9, In Section 8.4.3 the depth trend for the hydraulic conductivity of the rock mass, excluding test sections intersected by deformations zones (HCDs) is shown. In Figure 8-17 the geometric mean values of K for HCDs and HRD (representing the rock mass inbetween the HCDs) are plotted. As can be seen, the mean K of the HCDs is about an order of magnitude more conductive than the mean value of the HRDs. As can be seen in the geometric mean transmissivity values differ on a confidence level of 0.95 down to elevation -600 m. Below -600 m the samples in HCD are few, so the confidence band is wide for hydraulic conductivity in HCD, thus indicating that the confidence level is less than 0.95 that the geometric means differ. In combination, the results seem rather conclusive that it is meaningful to identify and model large deformation zones as separate domains as they have significantly higher hydraulic conductivity than the surrounding rock mass. However, the results also points out that some HCDs, as now interpreted in Laxemar 1.2, may have low transmissivity (and hydraulic conductivity). In the context of groundwater flow modelling, including or excluding such low-transmissive deformation zones is a matter of its location and hydraulic characteristics. If it may act as a hydraulic barrier, it should be included in the modelling. If it has the character of “normally fractured rock” (as can be the case for mainly ductile deformation zones) it may be justified to exclude those zones. It should be observed that in model version Laxemar 1.2 (cf. Figure 8-15), non of the geologically defined deformation zones have been excluded on the basis of the above discussion.

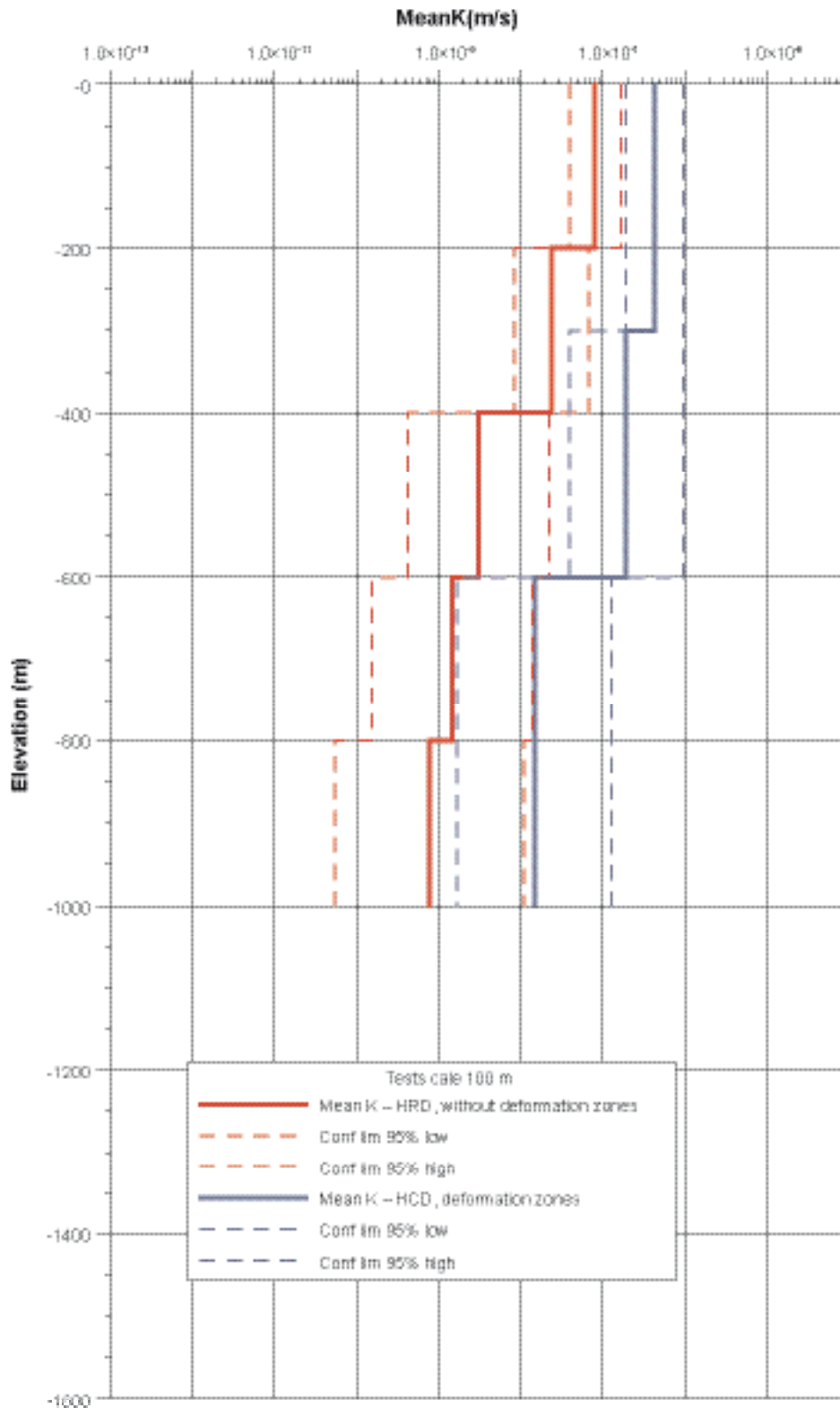


Figure 8-17. Comparison between the depth trend of the hydraulic conductivity in HCDs (equated from on geometric mean transmissivity from Figure 8-15 and geological thickness given in Table 8-9), and the depth trend of the geometric hydraulic conductivity of HRDs (excluding data from HCDs), as seen in Figure 8-19. /Rhén et al. 2006c/.

HCD – storage coefficient and transport aperture

Information on the storage coefficient is essential for estimating the influence radius of, and planning and interpreting, interference tests. In the regional groundwater flow modelling, the storage coefficient is of minor importance, unless the task is to test the model against interference tests.

Only one site-specific interpretation of the storage coefficient (S) has so far been made during the site investigations, but data from other investigations have been compiled. In /Rhén et al. 1997c/ the storage coefficient of deformation zones was estimated based on large-scale interference tests, and in /Rhén and Forsmark 2001/ the storage coefficient was estimated for larger and smaller deformation zones. In conjunction with the TRUE Block Scale experiment at Äspö HRL, a large number of hydraulic interference tests were made and the storage coefficient was estimated for larger and minor zones, e.g. /Andersson et al. 1998, 2000b/. Data were compiled from these projects and a relation was estimated for the correlation between T and S, see Table 8-13. The variation along the regression line can be expected to be within ± one order of magnitude for a value of S calculated with the formula in Table 8-13.

Likewise, the database for the kinematic porosity (n_e) (= mean transport aperture/hydraulic thickness of HCD (b_T)², the latter being the thickness of a HCD, to which the evaluated transmissivity for the corresponds

$$n_e = \frac{e_T}{b_T} \quad \text{(Equation 8-4)}$$

is also very limited. The equation given in Table 8-14 is based on the hydraulic aperture presented in /Dershowitz et al. 2003/. This equation gives similar values to those reported in /Rhén et al. 1997c/, with a=1.428 and b=0.523, based on a compilation of tracer tests in crystalline rock, ranging from tests of a single fracture up larger test scales with densely fractured rock and fracture zones. Kinematic porosity is considered as a calibration parameter, but Table 8-14 may be used for first estimates of the properties.

Table 8-13. Estimation of storage coefficient (S) for HCD from transmissivity (T). $S=aT^b$. T (m²/s), S (–).

Approximate test scale (m)	Coefficient a	Coefficient b	Reference
5–100	0.0007	0.5	/Rhén et al. 1997d/, /Rhén and Forsmark 2001/, /Andersson et al. 1998, 2000/.

Table 8-14. Estimation of mean transport aperture for HCD from transmissivity (T). $e_t=aT^b$. T (m²/s), e_t (m).

Approximate test scale (m)	Coefficient a	Coefficient b	Reference
5–100	0.46	0.5	/Dershowitz et al. 2003/.

8.4.3 HRD – bulk properties based on statistics of the hydraulic tests

This section explores assignment of hydraulic properties representative for the rock mass (HRD) between the deterministically defined deformation zones. Properties for the HRDs presented in this section are based on statistical analysis of borehole data. The assignment of HRD properties in the main cases of the groundwater modelling is based on the developed hydro DFN model, cf. further detailing and parameterisation of the models in Section 8.4.4.

The hydraulic tests performed at a 100 m test scale as presented in this section have the largest coverage in terms of area/volume. Test scales 20 m (actually 10, 20 and 30 m with 20 m dominating) and 5 m (actually 2, 3 and 5 m) show similar trends as test scale 100 m, but do not cover the area as well as at the test scale of 100 m. The results at smaller test scales are accounted for in /Rhén et al. 2006c/.

Observed difference in hydraulic conductivity between subareas

As a starting point for the analysis, data for the entire Simpevarp area was explored, not just the Laxemar subarea. Scrutiny of hydraulic data from the individual boreholes revealed that there seemed to be differences between the defined subareas Simpevarp and Laxemar, but also differences between subregions within the Simpevarp subarea. The Simpevarp subarea was consequently further subdivided as Ävrö seems to differ, being more permeable, compared with the Simpevarp peninsula.

100 m scale: As can be seen in Figure 8-18, the general tendency is that Simpevarp peninsula has the lowest hydraulic conductivity followed by the Laxemar subarea with Äspö and Ävrö as the most conductive units. It should however be remembered that the observations cover depth c. 0–1,000 m, with a slight dominance of observations in the depth interval 0–200 m. As will be seen in the next section, there is probably a depth dependence such that the representative hydraulic conductivity at repository depth is less than that indicated by Figure 8-18.

20 m scale: The median hydraulic conductivities are lower than those at the 100 m scale. The general tendency is that the Laxemar subarea shows the lowest hydraulic conductivity followed by the Simpevarp peninsula and then Äspö and Ävrö as the most conductive units. See /Rhén et al. 2006c/ for more details.

Depth trends in hydraulic conductivity (HRD)

Figure 8-19 and Figure 8-20 plot the HRD data (pure rock mass, with sections representing deformation zones excluded) at a test scale of 100 m, for a) the entire data set (Simpevarp peninsula, Laxemar subarea, Äspö, and Mjälén) with statistics given for the entire data set and b) for Laxemar subarea alone, respectively. The data sets were subdivided in subsets based on 200 m elevation intervals and the corresponding univariate statistics were computed, see /Rhén et al. 2006c/. In Figure 8-19 the standard deviations as well as the 95% confidence level for $\text{Log}_{10}(K)$ are shown for the entire data set. Two depth trend functions, a power law and an exponential model, cf. Equations 8-9 and 8-10, respectively, were also fitted to the mean values of the three elevation-stratified datasets, cf. Table 8-15.

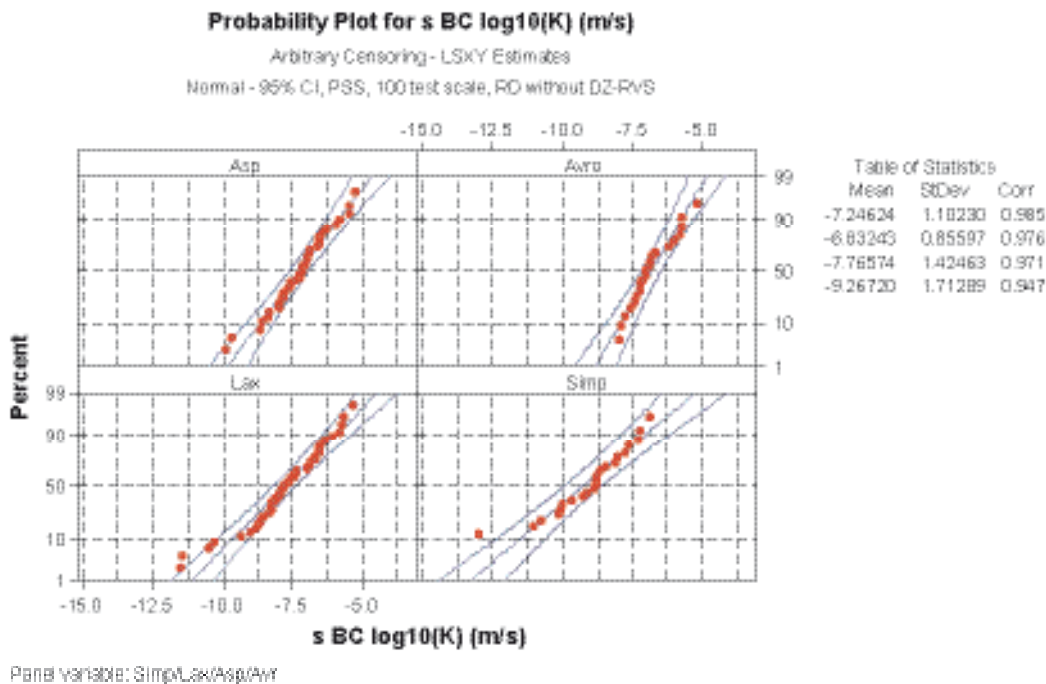


Figure 8-18. Hydraulic conductivity distribution of the rock mass by geographical area. Test scale 100 m. Data from the Laxemar subarea, Simpevarp peninsula, Äspö, Ävrö-Hälö-Mjälén. Data representing deterministically defined deformation zones in RVS model version Laxemar 1.2 are excluded. (Tabulated results follow read upper left to right corner followed by lower left to right corner.), cf. /Rhén et al. 2006c/.

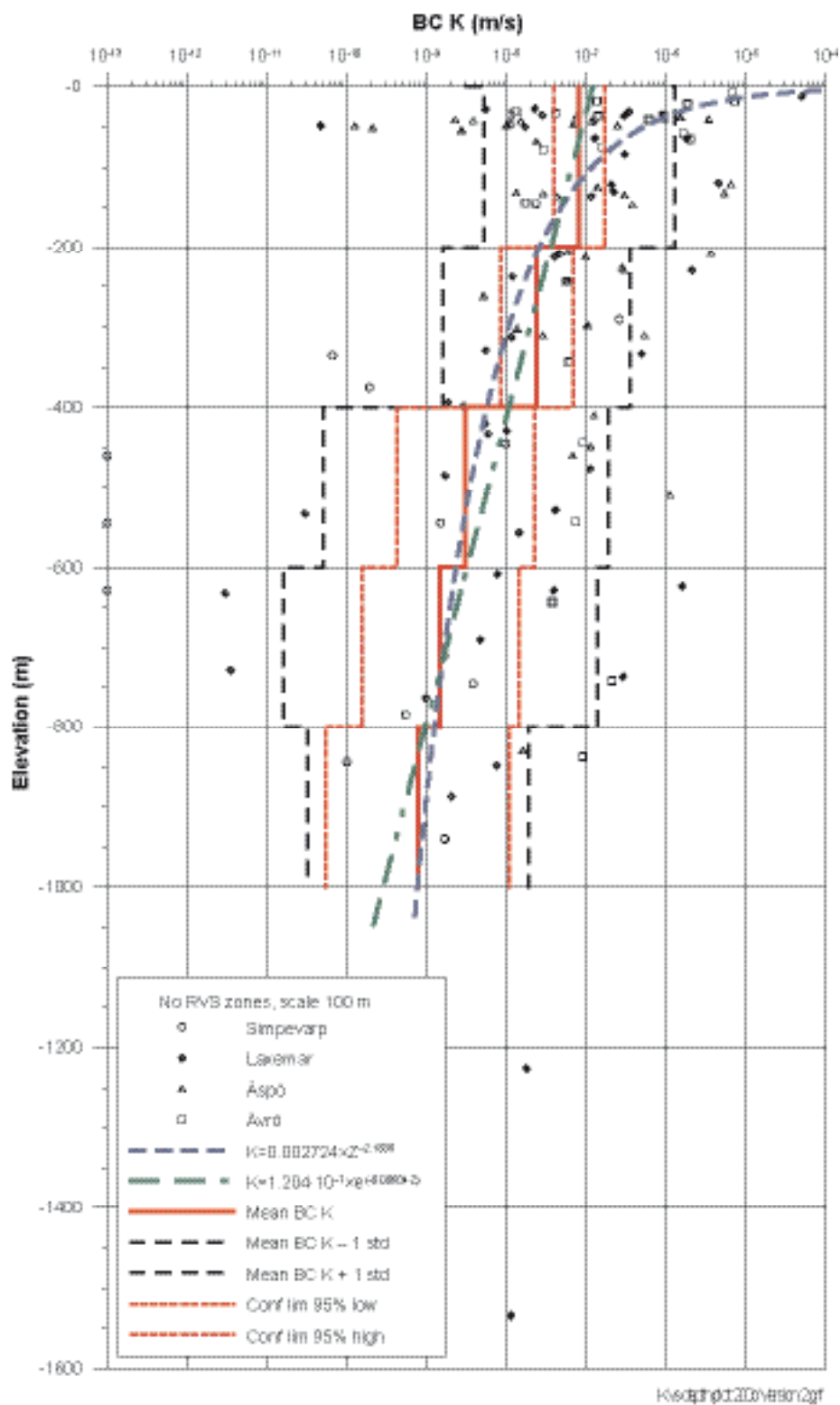


Figure 8-19. Depth trend of the hydraulic conductivity in HRDs. Test scale 100 m. Data from all areas (Laxemar subarea, Simpevarp peninsula, Äspö, Ävrö-Hälö-Mjälen) indicated. Depth trends and statistics given for a combined data set made up of data from the entire regional area. Data representing deterministically interpreted deformation zones in RVS model version Laxemar 1.2 are excluded. BC=Best choice value.

The fitting of these depth trend models was not considered reasonable for the Äspö and Ävrö data, but for data from Simpevarp peninsula. Visualisation and evaluation of by subarea is accounted for in more detail in /Rhén et al. 2006c/. However, a few remarks can be made in relation to the latter results. The 100 m results do not indicate any depth-dependence in the 0–500 m interval of the Äspö HRL data. In the data from the Laxemar subarea, see Figure 8-20, and the Simpevarp peninsula, see /Rhén et al. 2006c/, there seem to be a slight decrease in hydraulic conductivity with depth. There are hardly any data at depth from the Ävrö Island, but the few existing data indicate a depth trend such that values below 100 m are lower than that above 100 m. One should also observe that there are rather few observations in the elevation intervals 100–200 and 200–300 m in the Laxemar subarea, and some of the data may be directly or indirectly affected by the existence of fracture zones. The proposed “step-wise” change in hydraulic conductivity for the Laxemar subarea presented for the hydraulic DFN model in Section 8.4.5 and in detail in /Hartley et al. 2006/ may possibly depend on the fact that the few data in the few boreholes happened to intersect thick highly conductive sections that presently are not associated with any interpreted deformation zones. The increase in hydraulic conductivity from ground surface down to 300–400 m depth in both KLX02 and KLX04 may also possibly be related to the fact that the rock above, and bounded by ZSMEW007A and ZSMEW002A above ZSMEW007A, is subject to stress release that may have caused widening of fractures, and hence resulting in an increase in hydraulic conductivity, see also Section 6.4. In other boreholes the decrease of the hydraulic conductivity seems to commence at 100–300 m depth.

Table 8-15. Coefficients of depth trend models applied to hydraulic conductivity in HRDs. Test scale 100 m. Unit for hydraulic conductivity (K): m/s. Unit for elevation (z): metres above sea level. Note that the regression is equated using $-z$ as a parameter.

Area	Depth trend model*	Coefficient	Coefficient	Coeff. of determination, R-squared r^2
		a	b	
Regional model	Power-law (Equation 8-1)	0.002724	-2.1838	0.94
	Exponential (Equation 8-2)	1.204×10^{-7}	-0.00604	0.96
Laxemar subarea	Power-law (Equation 8-1)	0.00146	-2.0633	0.99
	Exponential (Equation 8-2)	1.0471×10^{-7}	-0.00557	0.95
Simpevarp peninsula	Power-law (Equation 8-1)	0.006332	-2.852	0.71
	Exponential (Equation 8-2)	9.495×10^{-9}	-0.00726	0.61

* Hydraulic conductivity K is used instead of T in the referred equations.

A linear trend function was also fitted to the standard deviation of $\text{Log}_{10}(K)$ of the elevation data-sets shown in Figure 8-16, see Equation 8-3, Figure 8-21 and Table 8-19:

Looking at the entire data set, see Figure 8-19, the confidence limits indicate that there is probably a depth trend. For the Laxemar subarea, see Figure 8-20, the depth trend must be considered uncertain, as the number of observations is rather few at depth. The trend of an increasing standard deviation with depth should be considered as uncertain.

Table 8-16. Coefficient for depth trend model applied the standard deviation of $\text{Log}_{10}(K)$ in HRDs. Test scale 100 m. Unit for hydraulic conductivity (K): m/s. Unit for elevation (z): metres above sea level. The regression is based on $-z$.

Area	Depth trend model	Coefficient a	Coefficient b	Coeff. of determination, R-squared r^2
Regional model	Std ($\text{Log}_{10}(K)$)	-0.0006	1.212	0.26

The above trend models are possible alternatives that can be applied to the HRDs in the model version Laxemar 1.2. Using a stochastic approach and the depth trend functions to assign the hydraulic conductivity raises the question if there are any upper and lower limits of hydraulic conductivity in HRDs that should be honored. Data from the SKB investigations, but also other projects /e.g. Juhlin et al. 1998, Smellie 2004/ suggest that the permeability (k) of the rockmass at great depth (6–8 km)

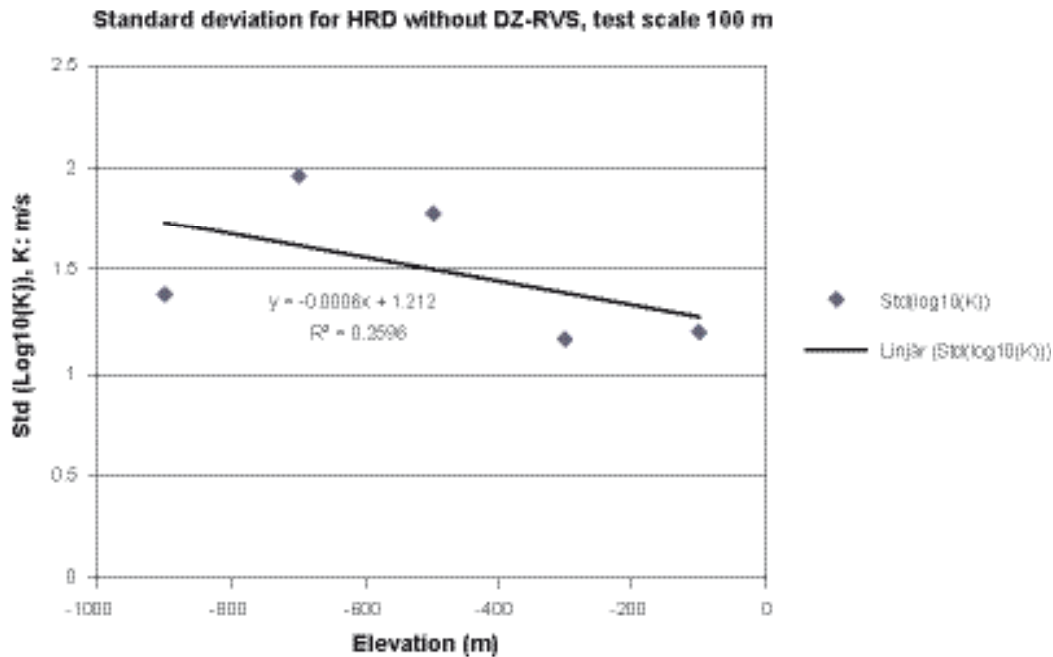


Figure 8-21. Depth trend of the standard deviation of hydraulic conductivity in HRDs, based on the evaluated standard deviations shown in Figure 8-19.

is $1\text{E}-18$ to $1\text{e}-20$ m^2 , which corresponds to a hydraulic conductivity of about $1\text{E}-11$ to $1\text{E}-13$ m/s . Laboratory measurements on intact core samples indicate similar ranges of permeability. It is not reasonable to assume that the hydraulic conductivity of a rock block can be lower than these values. It seems realistic to assume that the modelled rock blocks should at least exceed the permeability of the rock matrix, but probably a bit higher for grid sizes of 10 or 100 m in size.

Hydraulic properties of rock types

Rock types are mapped in outcrop and in boreholes and are an essential base for dividing the rock mass into geological rock domains with different properties relevant to the different types of modelling performed for the SDM Laxemar 1.2. Figure 5-4 and Appendix 3 shows the bedrock map indicating the distribution of rock types.

The information on rock types in boreholes is grouped into to classes: “Rock Type” in the Sicada data base for boreholes includes individual mapped objects longer than 1 m in the core. If the mapped length of an individual object is less than 1 m it is classified as a “Rock Occurrence”. The analysis of the hydraulic properties focus on both “Rock Type” and “Rock Occurrence” as defined above.

Statistics of hydraulic conductivity of different rock types

To determine if rock types have different hydraulic properties, it is necessary to use short test sections. The data set with the highest degree of spatial distribution, extensive both in terms of number of tests and tests of similar type is the PFL-s tests at 5 and 3 m test scale /Rhen et al. 2006c/. The dominant “Rock Type” (some test sections may include two or more rock types) has been used to label the individual test sections. Table 8-17 shows the statistics of the hydraulic conductivity related to “Rock type”.

There is a clear difference in mean hydraulic conductivity between rock types. As seen in Table 8-17 the Granite and Fine-grained granite (rock type codes 501058, 511058) are the most permeable. Ävrö granite (rock code 501044) has a lower hydraulic conductivity and the lowest hydraulic conductivity is found in the more basic rock types (rock type codes 501030, 501033, 501036, 505102). On the confidence level 0.95 these three groups have different geometric mean values, see Table 8-17.

Table 8-17. Hydraulic conductivity of different rock types based on PFL-s measurements. Test scale 5 m. Data from KAV01, KAV04A, KSH01, KSH02A, KLX02, KLX03 and KLX04. Data divided according to the Sicada code “Rock type”. Deformation zones in the geological single-hole interpretation and the deterministic deformation zones defined in RVS for version Laxemar 1.2 have not been excluded in the statistics presented. (Excluding the deformation zones would decrease the mean values, but the analysis have not yet been made). (Confidence limits for mean $\text{Log}_{10}(K)$ is expressed as the deviation D from mean in the table; for confidence level of 0.95 the mean of $\text{Log}_{10}(K)$ will be within value “Mean $\text{Log}_{10}(K)$ ” $\pm D$.)

Rock code	Rock type	Sample size	Mean $\text{Log}_{10}(K)$ (m/s)	Std $\text{Log}_{10}(K)$ (m/s)	D Conf.lim $\text{Log}_{10}(T)$: Mean $\pm D$, conf. level 0.95: (m/s)	Comments
All	All rock types	1,426	-10.01	1.72	0.09	
501033	Diorite/gabbro	5	-	-	-	Only one measurement above measlimit. Possibly similar to 501030 and 501036
501030	Fine-grained dioritoid	327	-10.33	1.58	0.17	
505102	Fine-grained diorite-gabbro	28	-11.30	2.99	1.16	
501036	Quartz monzodiorite	167	-10.76	2.05	0.31	
501044	Ävrö granite	827	-9.92	1.74	0.12	
501058	Granite	20	-8.82	1.74	0.81	
511058	Fine-grained granite	50	-8.74	1.29	0.37	
501061	Pegmatite	2	-	-	-	Only one measurement above measlimit: $K=1.1E-9$ m/s

As noted above, fine-grained granite mapped as “Rock Type” in Sicada represents core pieces > 1 m in the core. However, rock types shorter than 1 m in the core are mapped as “Rock Occurrence”. In parts of the core, there may be a large number of veins and smaller dykes intersecting the core, and a large number of them are fine-grained granites. The influence of the fine-grained granite has been studied by identifying all test sections with fine-grained granite mapped either as “Rock Type” or “Rock Occurrence” /Rhén et al. 2006c/. The result is that the presence of fine-grained granite veins does not seem to have a substantial impact on the hydraulic conductivity compared with the variation between different rock types as seen in Table 8-17. Fine-grained granite can, however, be expected to be more conductive than the dominant rock type when appearing in the form of thick dykes (thicker than 1 m).

Hydraulic properties of rock domains

Geological domains in 3D are defined in Section 5.3.5 and in /Wahlgren et al. 2005b/ and are shown in Figures 5-46 to 5-49. Each test section with hydraulic data has been classified according to the interpreted dominant geological rock domain, to explore if there is a difference in hydraulic properties between the geologically defined rock domains. However, rock domain M, which is a complex domain (see Section 5.3.2) was at an early stage of the modelling further divided into one domain dominated by Ävrö granite M(A) and one dominated by quartz monzodiorite M(D). This information was used to test if there is any hydraulic difference within the geological M domain.

Hydraulic tests with short test sections are the most suitable for the analysis of whether rock domains have different hydraulic properties, as there will not be many test sections that straddle a boundary between two geological rock domains. The PFL-s tests at 3 and 5 m test scale cover several boreholes and geographical areas and are considered the most suitable data set for this analysis. Figure 8-22 and Table 8-18 present the associated statistics for these measurements. On the confidence level 0.95 the rock domains have different geometric mean hydraulic conductivity when comparing groupings based on geological rock domains with similar K; (A and BA) ; (B, C and M(A)); (D and M(D)), see Table 8-17

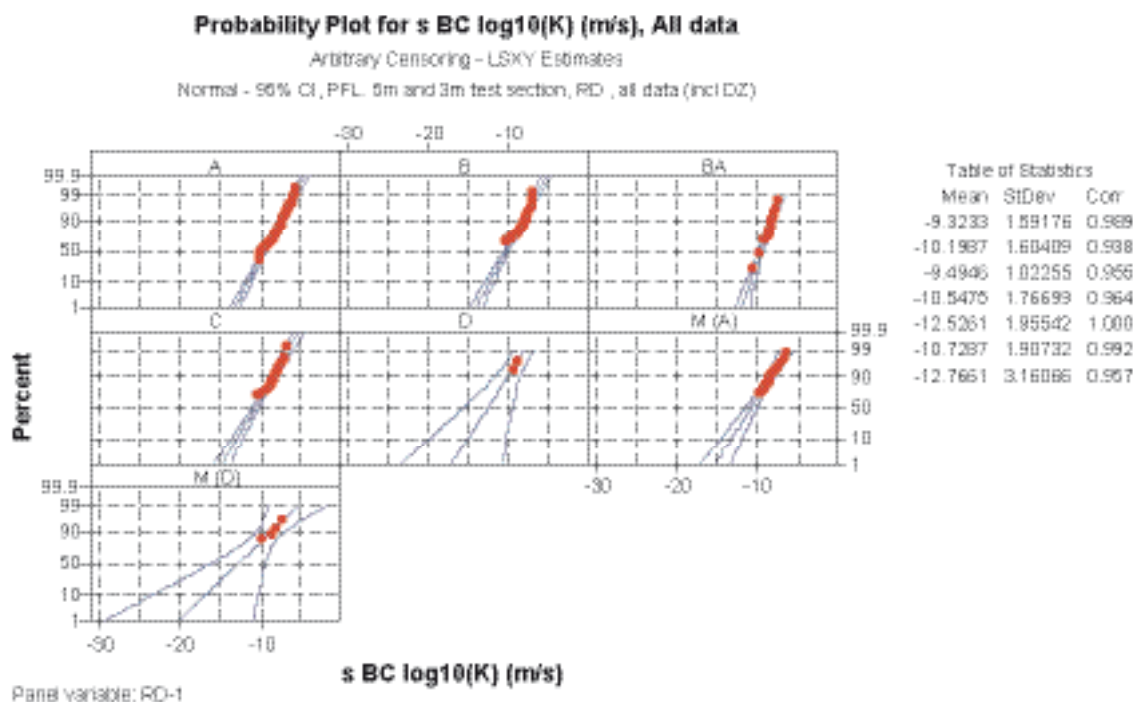


Figure 8-22. Statistics of hydraulic conductivity of different rock domains based on PFL-s measurements, cf. Table 8-18. Test scale 3 and 5 m. Top: Data from the entire Simpevarp regional area. Based on data from KAV01, KAV04A, KSH01A, KSH02, KLX02–04. Tabulated results follow plotted results top left to right followed by lower left to right.

Table 8-18. Hydraulic conductivity of different rock domains based on PFL-s measurements. Test scale 3 and 5 m. All data. Deformation zones in the geological single-hole interpretation and the deterministic deformation zones defined in RVS for version Laxemar 1.2 are not excluded. Based on data from KAV01, KAV04A, KSH01A, KSH02, KLX02–04 (Confidence limits for mean Log₁₀(K) is expressed as the deviation D from mean in the table; for confidence level of 0.95 the mean of Log₁₀(K) will be within value “Mean Log₁₀(K)” ±D.)

Rock domain	Sample size	Mean Log ₁₀ (K) (m/s)	Std Log ₁₀ (K) (m/s)	D Conf.lim Log ₁₀ (T): Mean±D, conf. level 0.95: (m/s)	Comments
All	1,426	-10.01	1.69	0.09	
A	666	-9.32	1.59	0.12	
B	245	-10.20	1.60	0.20	
BA	140	-9.49	1.02	0.17	
C	197	-10.55	1.77	0.25	
D	39	-12.53	1.96	0.64	Only 2 measurement above measlimit
M(A)	104	-10.73	1.91	0.37	
M(D)	35	-12.77	3.16	1.09	Only 4 measurement above measlimit

Hydraulic conductivities of different rock domains based on PSS measurements were also examined for the 100 m and “20 m” (10–20–30 m) test scales which also cover many boreholes and depth ranges, see /Rhén et al. 2006c/. PSS measurements with test scale 5 m were not examined, as these tests cover only a minor part of the rock mass. In /Rhén et al. 2006c/ data from the Laxemar subarea was also analysed stand-alone. The statistics give similar values. However, not all rock domains according to Table 8-18 are represented in the analysis.

Götemar and Uthammar granites

The Götemar and Uthammar granites are not represented above since no PFL-s measurements have been made in these rock domains, but there are other hydraulic data available for the Götemar granite. These data have been analysed, see /Rhén et al. 2006c/. The Götemar granite appears to be the most conductive domain in the regional area. The data from the Götemar Granite are difficult to interpret as these measurements are old, and less is known about the boreholes. However comparing the 20 m measurements in the Götemar granite with the statistics of 10–20–30 m PSS (for “all data”) shows that the geometric mean of the hydraulic conductivity is more than a magnitude higher than for rock domain A. The sample at test scale 2 and 3 m in the Götemar granite also have a higher hydraulic conductivity, and two boreholes, KKR01 and KKR02, indicate a geometric mean hydraulic conductivity of the Götemar granite that is more than a magnitude higher than for rock domain A – PFL-s (5 m scale). One borehole, KKR03 (in Kråkemåla), is sunk in a rock rather similar to rock domain A – PFL-s (5 m scale). The Uthammar granite is of similar origin and age as the Götemar granite and presumably has similar hydraulic properties.

Proposed Hydraulic Rock Domains (HRD)

Based on PFL (5 m scale) measurements, the fine-grained granite bodies (Sicada rock type code 511058) are an order of magnitude more conductive than the dominant rock type in the regional modelling area (Sicada code 501044, Ävrö granite), which is the main rock type in the geological Rock domain A. Possibly the fine-grained granite bodies modelled in the RVS can be assumed to be as conductive as the smaller fine-grained granites intersecting the boreholes.

Hydraulic properties of geological Rock domain A differs between the Laxemar subarea and the Äspö and Ävrö areas; the Laxemar area appearing to be less permeable. A reason for this may be that the rock mass east of the Äspö shear zone, including the southern part of Äspö and Ävrö as well as the Simpevarp peninsula, see the rhombohedral area indicated in Figure 8-23, may be part of a large-scale shear belt, cf. Section 5.2.5, that can explain the observed difference in hydraulic properties. The geological rock domain A is therefore suggested to be divided into two HRDs as defined below.

The following hydraulic rock domains (HRDs) are proposed, based on grouping of geological rock domains as defined in Section 5.3 (letters given within parantheses indicate the underlying geological rock domains):

HRD(F,G): (G01, (Götemar granite), G02 (Uthammar granites)). The most conductive domain. Assume 10* HRD(A) properties.

(F) (Granite, Fine- to medium-grained). One of the most conductive rock types. Assume 10* HRD(A) properties. The bodies are small and may probably be neglected in the regional model, but have been implemented.

HRD(A): (A+BA), Part of rock domain A outside rhombohedral area shown in Figure 8-23.) It is motivated due to the higher hydraulic conductivity in domain A in boreholes on Ävrö and southern Äspö compared to the Laxemar subarea.

HRD(A2): (A), Part of rock domain A within rhombohedral area shown in Figure 8-23). See comment on HRD (A) above.

HRD(B,C): (B+C). Low conductive domain.

HRD(D,E,M): (M(A)+M(D)+ D+E). The least conductive domain. Data corresponding to rock domains D and M(D) constitute small samples. M(A) is included in HRD(D, M) as it has a low hydraulic conductivity and is fairly small in size and is part of the M domain. There are no hydraulic data for rock domain E (diorite to gabbro), but as it is a basic rock type, the hydraulic conductivity is probably small according to the text above.

8.4.4 HRD – hydro DFN model

The hydrogeological modelling undertaken by /Hartley et al. 2006/ follows the scheme illustrated in Figure 8-14. A vital component of the scheme is the derivation of a hydraulic DFN. /Follin et al. 2006/ studied the key assumptions in the methodology in the underlying geological DFN model

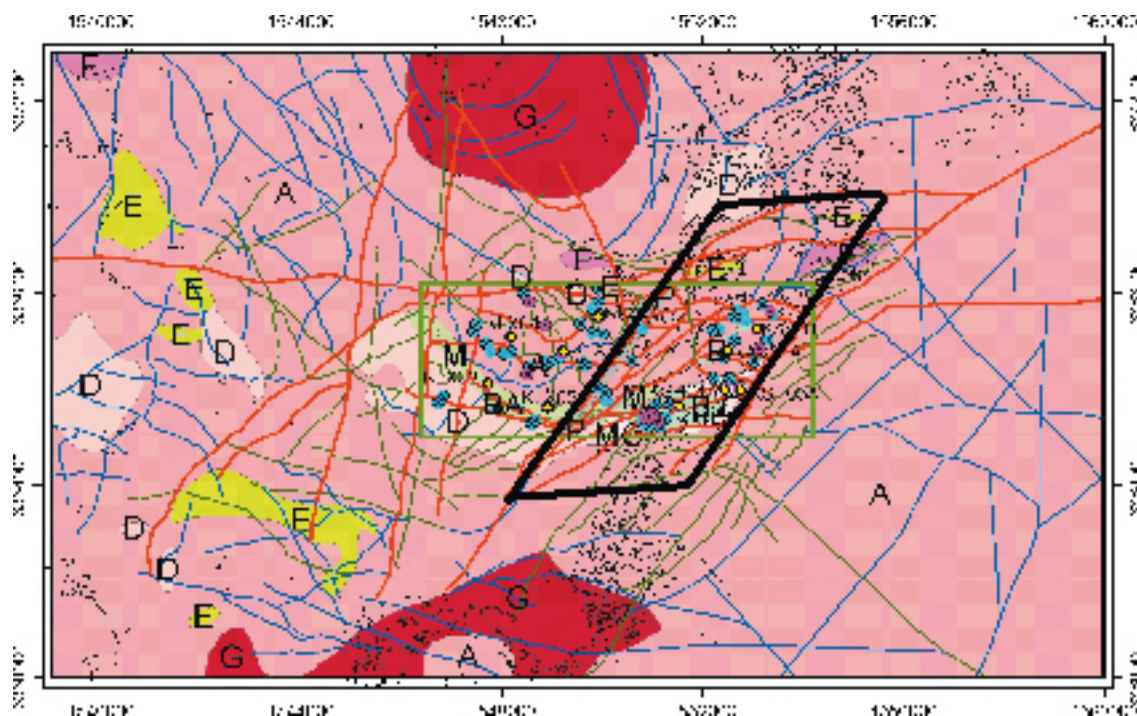


Figure 8-23. Rock domain model for Laxemar model version 1.2. The rhombohedral area indicates the area of HRD(A2), interpreted more strongly affected by low-grade ductile shear zones than the corresponding HRD(A) in the Laxemar subarea, see Section 5.2.5.

/Hermanson et al. 2005/ and addressed how these propagate into the hydraulic DFN modelling. The analysis of /Follin et al. 2006/ was limited to analysis of data from borehole, KLX04, situated in the main geological rock domain A, which dominates in the Laxemar subarea.

In /Hartley et al. 2006/ the **Hydro-DFN base case** is defined as the main output from the HydroDFN modelling. As result of the calibration of the regional model, cf. Section 8.5, a Hydro-DFN anisotropy variant, here called **Hydro-DFN regional case**, which is presented last in this section.

HRD- Fracture model and HydroDFN modelling steps

The HydroDFN modelling undertaken by /Hartley et al. 2006/ and /Follin et al. 2006/ include four main steps:

1. Assessment of geological data.
2. Assessment of hydraulic data.
3. Geological simulation and assessment of preliminary hydraulic fracture properties.
4. Hydraulic simulation.

Step 1 covers the division of borehole data into the entities: deformation zones and rock outside the deformation zones (rock mass), and subsequently into rock domains. This is followed by examination of the fracture properties (open or sealed) and intensities (P_{10}) as well as geometry of each deformation zone interpreted from the geological single hole interpretation.

Step 2 involves analysis of hydraulic data to obtain a representative value for each deformation zone treated as a part of the hydraulic DFN model. Deterministically defined deformation zones intersecting borehole are excluded from the analysis. A second component is to define the transmissivity distribution of hydraulic features, as defined in Section 8.3, along the borehole. A third component (only to some extent included in the Laxemar 1.2 modelling) is to test if the hydraulic features can be divided in to defined sets (orientation wise) with potentially significantly different hydraulic properties (distributions) and/or intensities, and whether this division differ from that of defined geological DFN sets.

Step 3 aims first at generation of a fracture model that compares with the mapped open and partly open fractures in boreholes (the geological DFN model provided was used, but, for the hydraulic DFN model fracture intensities etc. adjustments to better represent the specific boreholes studied was allowed). /Hartley et al. 2006/ used this fracture network for their flow simulations. /Follin et al. 2006/ excluded the non-connected fractures before the flow simulations for the Hydrogeological DFN model, see Figure 8-13.

Step 4. An important premise for the hydraulic simulation is the inferred relationship between T_f and L . Secondly, a sufficiently large model domain is constructed with appropriate boundary conditions for the hydraulic tests to be simulated. So far the inflow rate distribution along the boreholes, as obtained from the PFL measurements, has been used. These PFL measurements are conducted under pumping test conditions that last about a week. Simulated inflows to the modelled borehole are then cross-plotted against the measured inflows. The procedure is repeated for several realisations of each of the transmissivity models tested. Where available, PSS short interval (usually 5 m or 20 m) data are used to cross-validate the derived models, and reduce the uncertainty in the contribution to flow from low-transmissive fractures.

Main components from geological DFN used in hydraulic DFN

As pointed out earlier, the hydraulic DFN models were updated in several steps and the ConnectFlow and DarcyTools modelling teams were given more freedom to use the geological data and deviate from the exact formulations of the geological DFN models to fit both geometrical and hydraulic data. In /Hartley et al. 2006/ the following information was retained from the geological DFN model as defined by three regional subvertical sets (Set_A, Set_B and Set_C), one sub-horizontal set (Set_d), one local subvertical set for Simpevarp subarea (Set_e) and one local sub-vertical set for Laxemar subarea (Set_f). Sets A, B and C have roughly strikes; NE to E-W, NNW to NNE and W-E to NW respectively. Subsets f and e have roughly strike NW to NNW.

- The set classification based on orientation.
- Mean orientation and Fisher concentration for the Laxemar and Simpevarp subareas, respectively.
- The relative proportions between the sets r_0 , k_r for local sets Set_e and Set_f. The P_{32} of the open fractures of each rock domain is used to check P_{10} , in the borehole, but then the P_{32} for the open fractures are reduced to match flow.
- For boreholes including more than one domain, a length-weighted average of P_{32} is used.
- The following boreholes have defined the properties of the HRDs:
 - KLX04: Laxemar, HRD(A),
 - KLX03: Laxemar, HRD(D,E,M),
 - KSH01A: Simpevarp, HRD(B, C),
 - KAV04A: Simpevarp, HRD(A2).

HydroDFN base case for Laxemar 1.2

Typical results from the exploratory hydraulic DFN simulations by /Hartley et al. 2006/ are shown in Figure 8-24 through Figure 8-26.

The hydraulic DFN model parameters resulting from the analysis are:

- Fracture set geometry: orientation (mean trend and plunge of fractures poles, concentration (fracture pole dispersion parameter)).
- Length distribution model (power law).
- Intensity of conductive fractures for each set (P_{32c}).
- Transmissivity model (uncorrelated to fracture size (mean, standard deviation), correlated to fracture size (intercept, slope), semi-correlated to size (intercept, slope, standard deviation)).

The resulting hydraulic DFN base case models for defined HRDs of the Laxemar subarea are given in Table 8-19 and Table 8-20 and illustrated in Figure 8-27. The hydraulic DFN base cases for Simpevarp suparea are shown in /Hartley et al. 2006/.

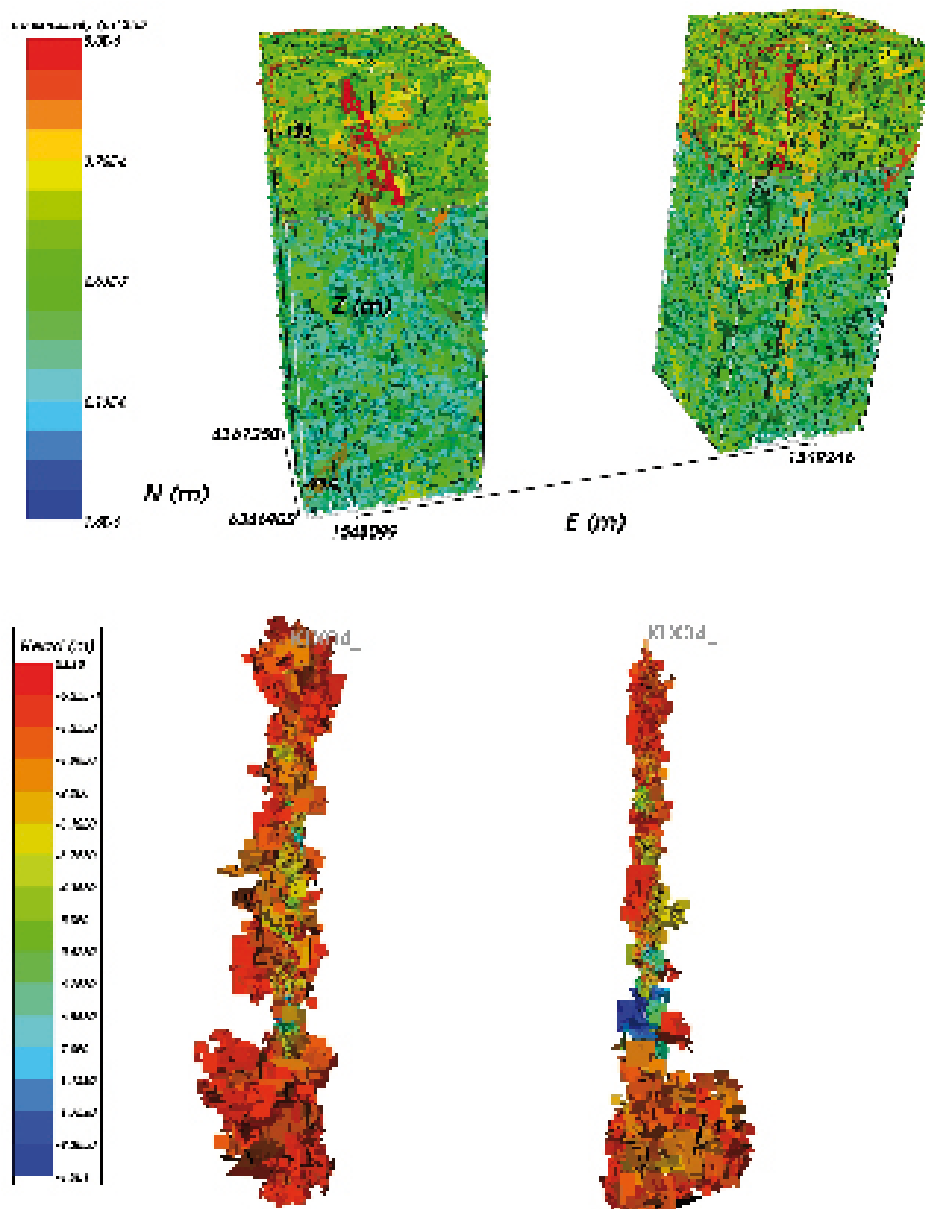


Figure 8-24. Top: Two realisations of the hydraulic DFN for a simulation domain of 400 m square cross-section and 1,088 m length around borehole KLX04. All fractures are shown and coloured by $\text{Log}(T)$, in this case T is semi-correlated to fracture radius (r) using a power law distribution. Bottom: Two hydraulic DFN realisations showing only the fractures around the borehole with a significant drawdown (> 1 m). /Hartley et al. 2006/.

One example of the difficulties faced when matching transmissivities and flow rates is shown in Figures 8-25 and 8-26 (left). As shown there are a number of high transmissivities and high flow rates that cannot be accounted for by the model. This may at first glance raise concern, but can to some extent be related to the definition of what parts of the borehole (KLX04) that should be considered as being a deformation zone, or not (i.e. where the transmissivities should be summed up to represent one feature). Possibly, some flow anomalies near defined deformation zones should actually be considered to be part of the very deformation zone. However, this can probably not be the sole explanation, and will be the subject of continued analysis in future modelling.

There is also a large number of low flow rates plotted in Figure 8-26. These values, many of which are below the measurement limit for the PFL, are interpreted to be a plausible representation of the actual conditions in KLX04.

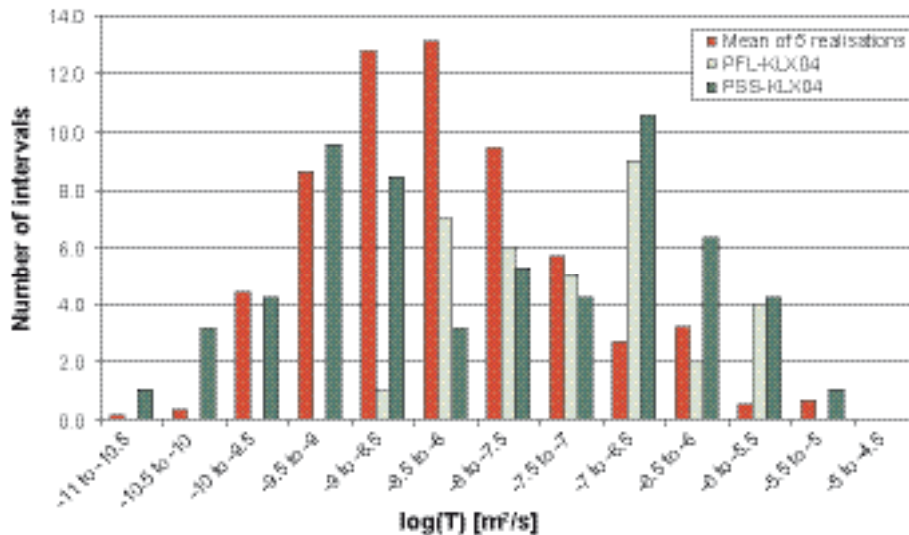


Figure 8-25. Comparison between simulated and measured transmissivity – results of best match, one example. Histogram of $\text{Log}(T)$ in 5 m intervals for the mean of 5 realisations of the correlated T distribution compared with measured PFL and PSS data for KLX04 below -300 m above sea level. This case is based on 35% of the P32 being open and partly-open fractures. /Hartley et al. 2006/.

Table 8-19. HydroDFN base case. Description of the hydraulic DFN input parameters using the ‘ k_r fit’ parameters for KLX04 matched to all hydraulic data (HRD(A)), with all other parameters taken from the geological DFN model. The P_{32} intensity of each set is given by the Relative intensity of P_{32} multiplied with the total Intensity P_{32} intensity given for the entire set of the selected elevation interval /Hartley et al. 2006/.

Fracture set name	Orientation set pole: (trend, plunge), concentration	Fracture radius model power-law (r_0 , k_r)	Intensity P_{32} (m^2/m^3); valid length interval (r_{\min} , r_{\max})	Relative intensity of P_{32}	Transmissivity model T (m^2/s)
Set_A	(338.1, 4.5) 13.06	(0.28, 2.73)	Above -300 m: 50% of open = 1.70	0.18	Correlated (above -300 m): (a,b) (3.2×10^{-8} , 1.2) Correlated (below -300 m): (a,b) (3.2×10^{-9} , 1.2)
Set_B	(100.4, 0.2) 19.62	(0.28, 2.83)	Below -300 m: 35% of open = 1.19	0.19	Uncorrelated (above -300 m): (μ , σ) (-6.0 , 0.9)
Set_C	(212.9, 0.9) 10.46	(0.28, 2.73)	(0.28, 564)	0.19	Uncorrelated (below -300 m): (μ , σ) (-6.7 , 0.9)
Set_d	(3.3, 62.1) 10.13	(0.28, 2.76)		0.27	Semi-correlated (above -300 m): (a,b, σ) (3.5×10^{-8} , 1.0, 0.9)
Set_f	(243, 24.4) 23.52	(0.40, 3.6)		0.17	Semi-correlated (below -300 m): (a,b, σ) (3.5×10^{-9} , 1.0, 0.9)

Table 8-20. HydroDFN base case. Description of the hydraulic DFN input parameters using the ‘ k_r fit’ parameters for KLX03 (HRD(D,E,M)), with all other parameters taken from the geological DFN model. The P_{32} intensity of each set is given by the Relative intensity of P_{32} multiplied with the total Intensity P_{32} intensity given for the entire set of the selected elevation interval /Hartley et al. 2006/.

Fracture set name	Orientation set pole: (trend, plunge), concentration	Fracture radius model power-law (r_0 , k_r)	Intensity P_{32} (m^2/m^3); valid length interval (r_{\min} , r_{\max})	Relative intensity of P_{32}	Transmissivity model T (m^2/s)
Set_A	(338.1, 4.5) 13.06	(0.28, 2.63)	Above -300 m: 60% of open = 0.84	0.22	Correlated (above -300 m): (a,b) (2.0×10^{-8} , 1.2) Correlated (below -300 m): (a,b) (2.0×10^{-9} , 1.0)
Set_B	(100.4, 0.2) 19.62	(0.28, 2.68)	Below -300 m: 30% of open = 0.42	0.15	Uncorrelated (above -300 m): (μ , σ) (-6.4 , 1.3)

Fracture set name	Orientation set pole: (trend, plunge), concentration	Fracture radius model power-law (r_0, k_r)	Intensity P_{32} (m^2/m^3); valid length interval (r_{min}, r_{max})	Relative intensity of P_{32}	Transmissivity model T (m^2/s)
Set_C	(212.9, 0.9) 10.46	(0.28, 2.59)	(0.28, 564)	0.17	Uncorrelated (below -300 m): (μ, σ) (-7.0, 1.3)
Set_d	(3.3, 62.1) 10.13	(0.28, 2.63)		0.36	Semi-correlated (above -300 m): (a, b, σ) ($1.8 \times 10^{-9}, 1.0, 0.9$)
Set_f	(243, 24.4) 23.52	(0.40, 3.6)		0.09	Semi-correlated (below -300 m): (a, b, σ) ($3.5 \times 10^{-9}, 1.0, 0.9$)

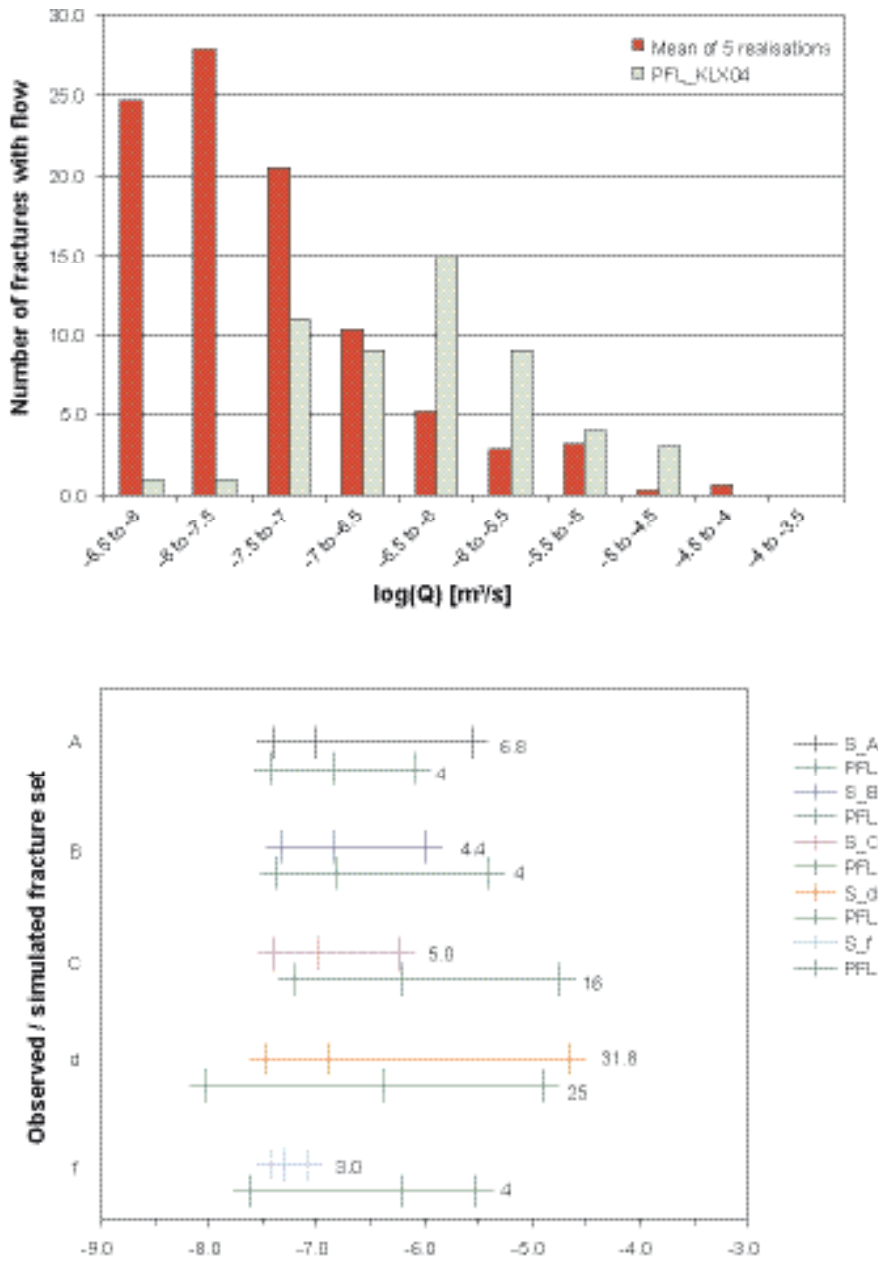


Figure 8-26. Comparison between simulated flow-rate and measured flow rate from PFL data- results for best match, one example from KLX04. Top: Histogram of Log(Q) flow rate to borehole, for the mean of five realisations compared with the PFL anomaly data for KLX04 below -300 m above sea level. Bottom: Plot of Log(Q) flow rate to borehole, for the mean of five realisations compared to the PFL anomaly data for KLX04 below -300 m above sea level. The flow in each fracture set is indicated, with vertical bars marking the minimum, median and maximum flow rates. In both cases, the correlated T distribution is used with 35 % of P_{32} taken to represent open and partly-open fractures /Hartley et al. 2006/.

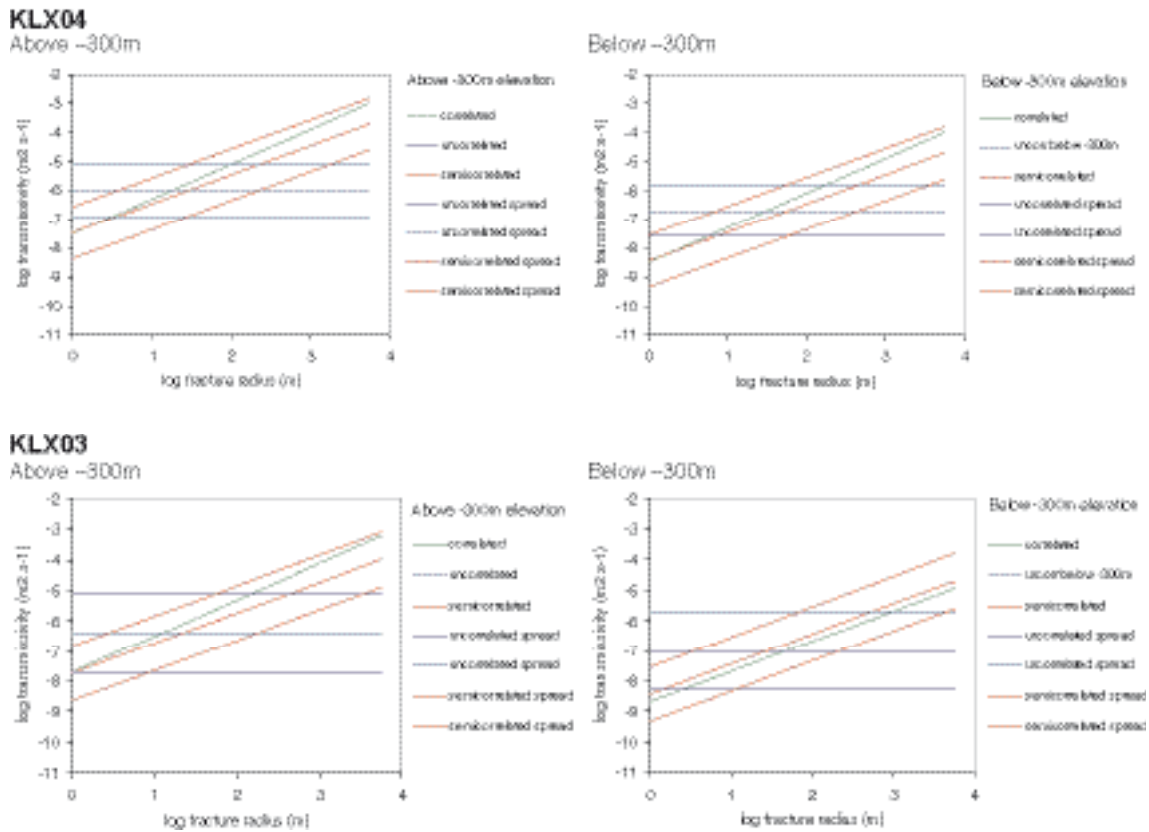


Figure 8-27. Transmissivity-size relationships for KLX03 and KLX04 /Hartley et al. 2006/.

Hydro-DFN regional case for Laxemar 1.2

A variant of the **Hydro DFN base case** was made during the calibration of the regional model, cf. Section 8.5. This variant is called: **Hydro DFN regional case**.

For the regional modelling reference case, the underlying hydraulic DFN model was initially based on the *Hydro DFN base case* with a semi-correlated T model. However, during the regional modelling studies, modifications were made to the hydraulic DFN prescription to achieve a better calibration against borehole hydrogeochemistry. The final hydraulic DFN parameters used for the *regional modelling reference case* are summarised in Table 8-21 to Table 8-24.

The use of homogeneous models for hydraulic conductivity using depth dependency trends based on the PSS data all resulted in a poor match against the hydrogeochemical data. For such models, a calibration could only be achieved using a hydraulic conductivity in the deep rock more than an order of magnitude less than measured values. Using the Hydro DFN base case gave interval conductivities consistent with the PSS 100 m interval data, and when anisotropy was introduced by reducing the transmissivity in the subvertical fracture sets Set_A and Set_B, a reasonable match with hydrogeochemistry was obtained. In this context it can be argued that the possible overestimation of the modelled transmissivity of low confidence deformation zones, as discussed in Section 8.4.2, could be a reason for the indicated need to reduce the hydraulic conductivity in the model corresponding to the deeper parts of the rock mass. However, it is noted that modelled low confidence zones are not associated with sections where hydrogeochemical data have been collected to the extent that it would influence calibration. Hence, the reduction made to rock mass conductivity, as discussed above, is deemed justified at the current level of understanding, although there may also be other changes of the model that could have improved the fit with the chemical data. However, given the currently limited amount of data it is not judged meaningful to explore yet other variants. More data are needed to better bound the uncertainty. The hydraulic DFN model gives a stochastic model of the HRD properties and there is uncertainty in the relationship between fracture transmissivity and size, though individual realisations and different T -models have a moderate effect on the simulated chemistry profiles in boreholes. The flow-wetted surface (a_v) of HRDs has a strong

effect on solute transport for variations in the range $a_r=1-2 \text{ m}^2/\text{m}^3$. This suggests that advective flow occurs in fractures with transmissivities below the detection limit of PFL anomalies that may have a significant effect on solute transport under natural flow conditions over periods of hundreds to thousands of years over what might be expected due to Rock Mass Diffusion (RMD).

Table 8-21. Hydro DFN regional case. Description of the hydraulic DFN input parameters using the 'kr fit' parameters for KLX04 matched to all hydraulic data (HRD(A)), with all other parameters taken from the geological DFN model. The P_{32} intensity of each set is given by the Relative intensity of P_{32} multiplied with the total Intensity P_{32} intensity given for the entire set of the selected elevation interval /Hartley et al. 2006/. Elevation (z) given in metres above sea level.

Fracture set name	Orientation set pole: (trend, plunge), concentration	Fracture radius model power-law (r_0, k_r)	Intensity P_{32} (m^2/m^3); valid length interval (r_{\min}, r_{\max})	Relative intensity of P_{32}	Semi-correlated transmissivity model parameters (a,b, σ)
Set_A	(338.1, 4.5) 13.06	(0.28, 2.73)	Above $z > -200$ m: 50% of open = 1.70	0.18	(3.5×10^{-9} , 1.0, 0.9) $z > -200$ (3.5×10^{-10} , 1.0, 0.9) $-200 > z > -600$
Set_B	(100.4, 0.2) 19.62	(0.28, 2.83)	Below $z < -200$ m: 35% of open = 1.19	0.19	(1.1×10^{-10} , 1.0, 0.9) $z < -600$
Set_C	(212.9, 0.9) 10.46	(0.28, 2.73)	(0.28, 564)	0.19	(3.5×10^{-8} , 1.0, 0.9) $z > -200$ (3.5×10^{-9} , 1.0, 0.9) $-200 > z > -600$
Set_d	(3.3, 62.1) 10.13	(0.28, 2.76)		0.27	(1.1×10^{-9} , 1.0, 0.9) $z < -600$
Set_f	(243, 24.4) 23.52	(0.40, 3.6)		0.17	

Table 8-22. Hydro DFN regional case. Description of the hydraulic DFN input parameters using the 'kr fit' parameters for KLX03 (HRD(D,E,M)), with all other parameters taken from the geological DFN model. The P_{32} intensity of each set is given by the Relative intensity of P_{32} multiplied with the total Intensity P_{32} intensity given for the entire set of the selected elevation interval /Hartley et al. 2006/. Elevation (z) given in metres above sea level.

Fracture set name	Orientation set pole: (trend, plunge), concentration	Fracture radius model power-law (r_0, k_r)	Intensity P_{32} (m^2/m^3); valid length interval (r_{\min}, r_{\max})	Relative intensity of P_{32}	Semi-correlated transmissivity model parameters (a,b, σ)
Set_A	(338.1, 4.5) 13.06	(0.28, 2.63)	Above $z > -200$ m: 60% of open = 0.84	0.22	(1.8×10^{-9} , 1.0, 0.9) $z > -200$ (3.5×10^{-10} , 1.0, 0.9) $-200 > z > -600$
Set_B	(100.4, 0.2) 19.62	(0.28, 2.68)	Below $z < -200$ m: 30% of open = 0.42	0.15	(1.1×10^{-10} , 1.0, 0.9) $z < -600$
Set_C	(212.9, 0.9) 10.46	(0.28, 2.59)	(0.28, 564)	0.17	(1.8×10^{-8} , 1.0, 0.9) $z > -200$ (3.5×10^{-9} , 1.0, 0.9) $-200 > z > -600$
Set_d	(3.3, 62.1) 10.13	(0.28, 2.63)		0.36	(1.1×10^{-9} , 1.0, 0.9) $z < -600$
Set_f	(243, 24.4) 23.52	(0.40, 3.6)		0.09	

Table 8-23. Hydro DFN regional case. Description of the hydraulic DFN input parameters using the 'kr fit' parameters for KSH01A (HRD(B,C)), with all other input parameters taken from the geological DFN model. P_{32} intensity of each set is given by the Relative intensity of P_{32} multiplied with the total Intensity P_{32} intensity given for the entire set of the selected elevation interval /Hartley et al. 2006/. Elevation (z) given in metres above sea level.

Fracture set name	Orientation set pole: (trend, plunge), concentration	Fracture radius model power-law (r_0, k_r)	Intensity P_{32} (m^2/m^3); valid length interval (r_{\min}, r_{\max})	Relative intensity of P_{32}	Semi-correlated transmissivity model parameters (a,b, σ)
Set_A	(330.3, 6.1) 16.80	(0.28, 2.77)	Above $z > -200$ m: 27% of open = 1.40	0.24	(1.4×10^{-9} , 1.2, 0.9) $z > -200$ (1.6×10^{-11} , 0.8, 0.9) $-200 > z > -600$
Set_B	(284.6, 0.6) 10.78	(0.28, 2.91)	Below $z < -200$ m: 27% of open = 1.40	0.15	(5.1×10^{-12} , 0.8, 0.9) $z < -600$
Set_C	(201.8, 3.7) 14.60	(0.28, 2.92)	(0.28, 564)	0.26	(1.4×10^{-8} , 1.2, 0.9) $z > -200$ (1.6×10^{-10} , 0.8, 0.9) $-200 > z > -600$
Set_d	(84.6, 81.8) 6.98	(0.28, 2.87)		0.26	(5.1×10^{-11} , 0.8, 0.9) $z < -600$
Set_f	(67.1, 15.5) 11.73	(0.21, 3.27)		0.10	

Table 8-24. Hydro DFN regional case. Description of the hydraulic DFN input parameters using the 'kr fit' parameters for KAV04A (HRD(A2)), with all other input parameters taken from the geological DFN model. The P32 intensity of each set is given by the Relative intensity of P32 multiplied with the total Intensity P32 intensity given for the entire set of the selected elevation interval /Hartley et al. 2006/. Elevation (z) given in metres above sea level.

Fracture set name	Orientation set pole: (trend, plunge), concentration	Fracture radius model power-law (r_0, k_r)	Intensity P_{32} (m^2/m^3); valid length interval (r_{min}, r_{max})	Relative intensity of P32	Semi-correlated transmissivity model parameters (a, b, σ)
Set_A	(330.3, 6.1) 16.80	(0.28, 2.78)	Above $z > -200$ m: 28% of open = 1.43	0.24	(4.5×10^{-9} , 0.7, 0.9) $z > -200$ (7.5×10^{-9} , 0.7, 0.9) $z < -200$
Set_B	(284.6, 0.6) 10.78	(0.28, 2.87)	Below $z < -200$ m: 22% of open = 1.13	0.16	
Set_C	(201.8, 3.7) 14.60	(0.28, 2.90)	(0.28, 564)	0.22	(4.5×10^{-8} , 0.7, 0.9) $z > -200$ (7.5×10^{-8} , 0.7, 0.9) $z < -200$
Set_d	(84.6, 81.8) 6.98	(0.28, 2.85)		0.27	
Set_f	(67.1, 15.5) 11.73	(0.21, 3.27)		0.11	

Conclusion from the HydroDFN modelling

The conclusions drawn by /Hartley et al. 2006/ from the results of the hydraulic DFN modelling were that:

- The fracture size distributions for open fractures were derived within the study of /Hartley et al. 2006/ due to problems of coordination with the final geological DFN model. Here, a minimum radius of 0.28 m was assumed and power-law shape parameters were derived for each set and each rock domain by matching the P_{32} values for open fractures in the boreholes with that of the deterministic deformation zones. The values derived are broadly consistent with the final values derived in the geological DFN, but the discrepancy leaves an uncertainty as to which is the most representative model for fracture size distribution. Although the nature of fracturing is strongly sensitive to the fracture size distribution, it is felt that ultimately the calculation of flow within the hydraulic DFN is less sensitive once all other parameters – open fracture intensity and transmissivity – have been constrained by conditioning on hydrogeological data.
- The methodology developed for integrating the PFL and PSS hydraulic data with the geological fracture interpretation as part of the Simpevarp 1.2 and Forsmark 1.2 modelling has been further developed here. The noteworthy improvements are to represent depth variations in fracture parameters, modelling larger domains, and improving the analysis of relative distributions of flow within individual fracture sets.
- Three different relationships between transmissivity and size have been considered, and all three can be made to give a reasonable match to the hydrogeological data. The semi-correlated model giving a slightly better match and more realistic relationship.
- Some problems were encountered with the hydrogeological data for KLX04 since the distribution of fracture transmissivity of the PSS 5 m interval data indicated a bi-modal nature. It is thought that this arises due to swarms of relatively high-transmissive fractures within single intervals. Such behaviour is difficult to reproduce in a model that assumes a Poisson spatial process and a single continuous relationship between fracture length and size. Such behaviour was not evident in the transmissivity distribution of individual fractures in the PFL anomaly data for any of the boreholes considered (KLX03, KSH01A and KAV04), and the other borehole with 5 m PSS interval data, KSH01A, did not show a bi-modal behaviour. This should be studied in future boreholes where short interval PSS data are provided.
- The spatial variability between boreholes implies that the uncertainty as to how representative it is to extrapolate a single borehole to an entire rock domain needs to be better explored and quantified.

The PFL data give some indication that the subvertical sets Set_A and Set_B are 0.5 to 1.0 orders of magnitude less transmissive than Set_C and Set_d. Furthermore, Set_C may have a transmissivity 0.5 to 1.0 order of magnitude higher than that of Set_d. At the moment these results are speculative being based on an analysis of KLX04 only. However, it is noted that the importance of anisotropy

may have been underestimated in opting for a simplified model with the same transmissivity relationships for all sets. It is recommended that more consideration be given to hydraulic anisotropy between fracture sets when analysing PFL data from new boreholes. Also the quantity of flow data from subvertical fractures is limited in vertical boreholes such as KLX04. The use of inclined boreholes with different orientations may provide more information on the hydraulic anisotropy of fracture sets.

/Follin et al. 2006/ conclude that the fracture intensity in the rock mass surrounding the KLX04 borehole is quite high down to c. –650 m above sea level. Because of the high intensity of open fractures, the correlated transmissivity-size model approach proposed by /Follin et al. 2006/ can be made to fit with a wide range of power-law distributed fracture size models. Below c. –650 m above sea level the conditions change drastically and the rock mass becomes very sparsely fractured and poorly connected. /Follin et al. 2006/ bring up the question whether borehole KLX04 is located in the vicinity of an unknown deformation zone of significance. Evidently, the uppermost c. 400 m of KLX04 includes at least four intervals with deformation zone-type properties. These are not incorporated in the current SDM Laxemar 1.2 deformation zone model, cf. Section 5.4 and Appendix 4.

8.4.5 HRD – hydroDFN base case – block modelling

The purpose of the Block modelling is to:

- Estimate hydraulic conductivity distributions at different scales (20 and 100 m) and under various anisotropy conditions (for Repository Engineering).
- Test implications of the truncation of the size distribution on the properties of the selected numerical grid.

An example of results is presented in Figure 8-28 and a summary of results for Laxemar subarea is given in Table 8-25 and Table 8-26. In /Hartley et al. 2006/ results for the Simpevarp subarea are also provided.

Table 8-25. Comparison of median hydraulic conductivity and anisotropy as established from KLX04 data (valid for HRD(A) below –300 m above sea level) for 20 m blocks and 100 m blocks in the k_r fit case.

T model	Scale (m)	Guard zone (m)	r_{min} (m)	Median $\text{Log}_{10}(K_x)$ (m/s)	Median $\text{Log}_{10}(K_y)$ (m/s)	Median $\text{Log}_{10}(K_z)$ (m/s)	Median ratio K_{hmax}/K_{hmin}	Median ratio K_{hmax}/K_z	Strike of K_{hmax} (by eye)
Corr	20	30	0.56	–7.97	–7.99	–8.09	4.71	1.53	100–130
Corr	100	100	5.64	–7.83	–8.05	–7.90	2.67	1.40	90–100, 120–130
Uncorr	20	30	1.13	–7.92	–8.00	–7.84	3.78	1.23	90–100
Uncorr	100	100	5.64	–8.20	–8.35	–8.12	2.54	1.12	80–100
Semi-corr	20	30	1.13	–8.35	–8.51	–8.27	5.00	1.19	90–110
Semi-corr	100	100	5.64	–8.22	–8.46	–8.12	3.42	1.18	80–110

Table 8-26. Comparison of median hydraulic conductivity and anisotropy established from KLX03 data (valid for HRD(D,E,M) below –300 m above sea level) for 20 m blocks and 100 m blocks in the k_r fit case.

T model	Scale (m)	Guard zone (m)	r_{min} (m)	Median $\text{Log}_{10}(K_x)$ (m/s)	Median $\text{Log}_{10}(K_y)$ (m/s)	Median $\text{Log}_{10}(K_z)$ (m/s)	Median ratio K_{hmax}/K_{hmin}	Median ratio K_{hmax}/K_z	Strike of K_{hmax} (by eye)
Corr	20	30	1.13	–9.19	–9.37	–9.25	8.60	1.25	50–30
Corr	100	100	5.64	–9.19	–9.25	–9.26	4.39	1.68	70–110
Uncorr	20	30	1.13	–10.20	–10.14	–10.31	6.06	1.48	70–90
Uncorr	100	100	5.64	–9.36	–9.52	–9.40	5.41	1.73	30–130
Semi-corr	20	30	1.13	–10.30	–10.37	–10.28	9.90	1.06	80–120
Semi-corr	100	100	5.64	–9.09	–9.21	–9.05	6.59	1.59	70–140

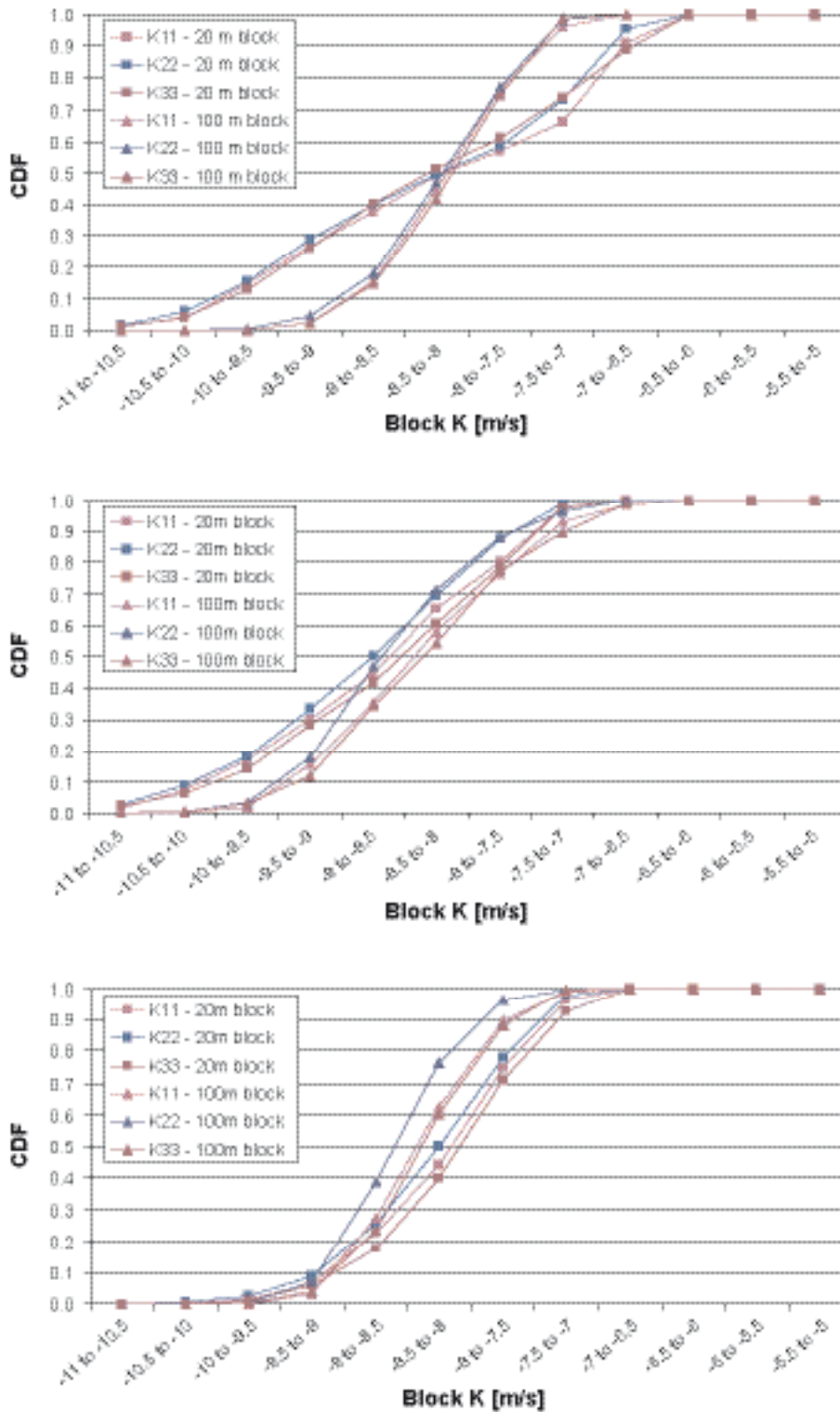


Figure 8-28. Hydraulic conductivity distribution for 'k,fit' case for hydraulic data below -300 m above sea level in KLX04 (valid for HRD(A)). Top: correlated transmissivity model. Middle: semi-correlated transmissivity model. Bottom: uncorrelated transmissivity model. K11, K22, K33 correspond to K_x (Easting), K_y (Northing) and K_z (vertical), respectively. Model input parameters are given in Table 8-25 and Table 8-26.

Conclusions from the block modelling

- Matching hydraulic data for all boreholes gives higher values for the median effective hydraulic conductivity, $\log(K_{eff})$ above -300 m above sea level, than below -300 m above sea level elevation. Median $\log(K_{eff})$ in the Ävrö granite HRD(A) is between -6.6 to -7.1 above -300 m above sea level, and -8.0 to -8.5 below -300 m above sea level elevation.
- Generally the 20 m block shows similar or lower median effective hydraulic conductivity, K_{eff} than the 100 m block. In all cases and all boreholes, the spread of the effective hydraulic conductivity is higher for the 20 m block scale than for the 100 m block-scale because there is a greater amount of averaging over individual fractures on the 100 m scale.
- An anisotropy with a major hydraulic conductivity oriented in NW-SE has been established for all cases for KLX04 (HRD(A)). For KLX03, the regional anisotropy exhibits aWNW-ESE orientation of the major hydraulic conductivity. For KSH01A, the major hydraulic conductivity is oriented W-E. For KAV04A the major hydraulic conductivity is oriented ENE-WSW. The established anisotropy is assumed valid on a regional scale.
- Sensitivity cases have considered the size of the guard zone (this is the difference between the length dimension of the volume in which fractures are generated and the length dimension of the smaller volume in which block properties are calculated). Simulation of smaller (20 m blocks) is more sensitive to the size of the guard zone. As a result of this investigation it was found that the 20 m block requires a 30 m guard zone and the 100 m block requires a 100 m guard zone.

The evaluated anisotropy is different from the experiences at the Äspö HRL. In the latter case, it was found that the highest conductivity in the horizontal direction is WNW-NW, but also N-S direction showed high conductivity /Rhén et al. 1997c/. The ratio between the maximum and the minimum hydraulic conductivity in the horizontal plane (based on probeholes sampling subvertical fractures) was c. 100, which is considerably higher than the corresponding ratios estimated for the boreholes in the Laxemar subarea.

Evaluation of hydraulic data from the Prototype Repository at Äspö HRL shows similar results, but also indicate that the most conductive fracture set is subvertical, with a strike about WNW /Rhén and Forsmark 2001/. It was also shown that the hydraulic conductivity was c. 100 times less in vertical boreholes compared to horizontal boreholes, indicating that subvertical fractures are the dominant conductive fractures.

An examination of the orientation of the fractures interpreted to correspond to PFL anomalies in the boreholes presented in Section 8.2 indicate, that steeply dipping fractures with a NW strike and subhorizontal fractures dominate. This circumstance will be looked into in more detail in the continued site modelling.

The geometric mean hydraulic conductivities from the PSS measurements are, in all cases but one, less for a test scale of 20 m than that for a scale of 100 m, see Section 8.2 and /Rhén et al. 2006ab/. The geometric mean hydraulic conductivity calculated from the block conductivities in some cases has a tendency to be lower for block scale 20 m compared with a block scale 100 m, but not all. It remains to be resolved why this is so.

8.5 Regional flow modelling

This section summarises the regional groundwater flow modelling made by /Hartley et al. 2006/ with focus on the flow field and parametrisation of the regional groundwater flow model. The regional groundwater flow modelling is largely based on data presented in Section 8.4, but also relate to data presented in Chapter 9. Conclusions from the flow modelling are presented in Section 8.6. The regional groundwater flow modelling results and conclusions coupled to hydrogeochemistry are presented in Section 9.7.

8.5.1 Initial and boundary conditions

Hydraulic boundary conditions have to be assessed when performing steady state groundwater flow simulations and the initial conditions need also be assessed for transient groundwater flow simulations. The initial and boundary conditions are equally important as the overall geometrical context (deformation zone model) and the hydraulic properties assignment, the latter presented in Section 8.4.

Boundary conditions

Top boundary

The applied boundary conditions are used to mimic the transient processes of shoreline displacement due to post-glacial rebound and the variations in the salinity of the Baltic Sea. The evolutions of these two quantities since the last glaciation are shown in Figure 8-29 and Figure 8-30. The modelling strategy was to keep the model domain fixed in size (i.e. retaining the same x, y and z coordinates), but vary the head and salinity on the top surface with time. Figure 8-30 illustrates the variability and associated uncertainty in the salinity of the Littorina sea with time. In the present modelling the short stages of Baltic ice lake and Yoldia sea (AD: Anno Domini. Baltic ice lake: -12,000 to -9,500 AD, Yoldia sea: -9,500 to -8,800 AD, Ancylus Lake: -8,800 to -7,500 AD, Littorina Sea: -7,500 AD to Present) were not modelled, as it was judged that these stages should have minor impact on the evolution of the area with time. There is also an uncertainty inherent in when the different stages of Baltic actually occurred. This will be analysed further in future modelling efforts.

The modelled shore displacement for Laxemar 1.2, cf. blue curve in Figure 8-29, follows the equation proposed by /Påsse 1997/. The more rapid changes according to some measurements as illustrated by the red curve in Figure 8-29, and also depicted in Figure 3-14, are consequently neglected. However, starting the modelling -8,000 AD, as indicated in Figure 8-29 (right blue-shaded area) also causes the highest parts of the Laxemar area never being covered by the sea or lake stages of the Baltic. As a consequence, the infiltration period over which water of Meteoric origin infiltrated the regional flow model is somewhat shorter than what is assumed the case after the last glaciation, and also did not cover the entire area at the start of the simulations. This is judged to have a minor influence on the results, but the effects should probably be studied more closely in future modelling.

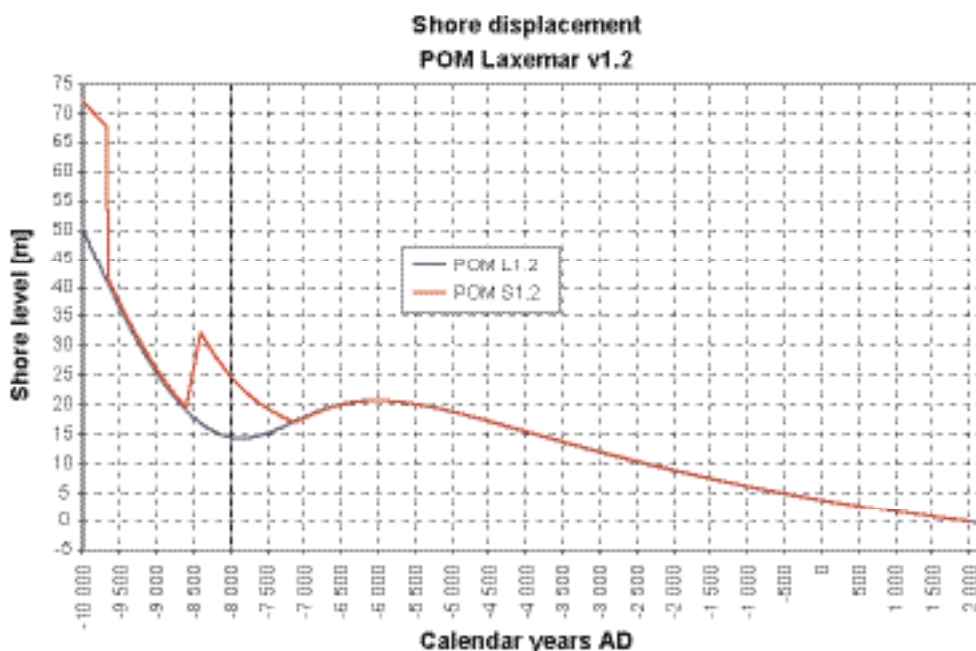


Figure 8-29. The shore-line displacement used for Laxemar v. 1.2 (blue). The relationship used for the Simpevarp v. 1.2 modelling is shown for comparison (red). Only data from -8,000 AD and onwards are used. (AD: Anno Domini), /Påsse 1997, Hartley et al. 2006/.

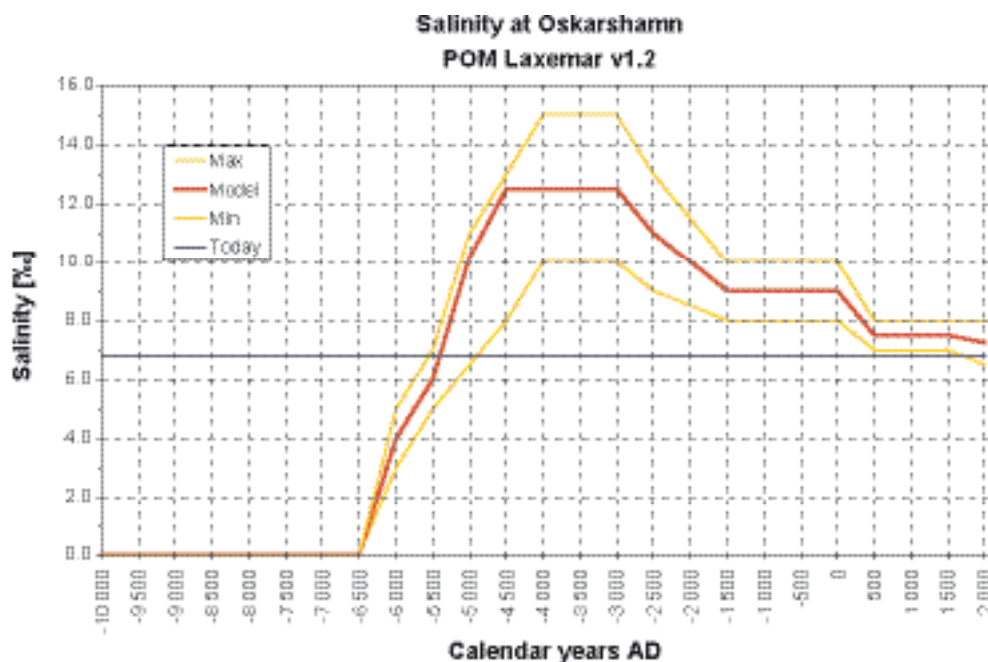


Figure 8-30. The salinity progression in the southern Baltic Sea from the start of the Littorina period. The red line shows the relationship used in the model and the yellow lines indicate the maximum and minimum of the ranges. The present-day salinity is indicated by the blue line. /Based on Westman et al. 1999 in Hartley et al. 2006/. (AD: Anno Domini) (Baltic ice lake: –12,000 to –9,500 AD, Yoldia sea: –9,500 to –8,800 AD, Ancylus Lake: –8,800 to –7,500 AD, Littorina Sea: –7,500 AD to Present).

Based on the surface hydrogeochemistry concept indicated in Section 3.3 and based on the analysis by Hydrogeochemistry, cf. Chapter 9 and /Laaksoharju et al. 2006/, groundwater compositions were defined using a simplified system of four reference waters, which have been used previously in M3 geochemical modelling /Hartley et al. 2006/:

- **Brine water** represents the sampled deep brine type of water (Cl=47,000 mg/L) found in KLX02. An old age for the Brine is suggested by the measured ³⁶Cl values indicating a minimum residence time of 1.5 Ma for the Cl component.
- **Glacial water** /Laaksoharju et al. 2006/ represents a possible melt-water composition from the younger than the last glaciation. Sampled modern glacial melt water from Norway is used for the major elements and the δ¹⁸O isotope value (–21‰ SMOW) is based on measured values of δ¹⁸O in surficial calcite coatings (subglacial CaCO₃ deposits precipitated on present rock surface on the Swedish west coast /Tullborg and Larson 1984/). The δD value (–158‰ SMOW) is a modelled value based on the equation (δD = 8×δ¹⁸O+10 for the meteoric water line /Craig 1961/).
- **Littorina water** represents modelled Littorina water, see Figure 8-30.
- **Metric water** (corresponding to the notation **Dilute Groundwater** used in Chapter 9) corresponds to a shallow groundwater sampled in percussion borehole HAS05 (sampled between –32 and –80 m above sea level) representing the shallow end member for the local hydrogeochemical model in Simpevarp area for SDM Laxemar 1.2.

The major ionic components and stable isotope compositions for the selected reference waters are given in Table 9-2 and /Hartley et al. 2006/. In the regional flow modelling, the mass fraction of each reference water is included as an initial condition or as part of a boundary condition. The transport of the reference waters is modelled using the the common basic equations for advection and diffusion, see /Hartley et al. 2006/.

As a main case, the head on the top surface was set to the topographic elevation, which evolves with time due to changes in the elevation relative to the shoreline (see Figure 8-29). Offshore, the pressure was set equal to the depth of the sea multiplied by the relative density of the Baltic Sea to freshwater.

Other variants considered were to use the developed Digital Elevation Model (DEM) as the water table, calculating the head on the top surface. The water table base-case is based on interpolation of elevation points of interpreted discharge areas; e.g. peat lands, water courses and lakes. Variants of a possible water table elevation were calculated based on the difference between the topography and the water table base case, multiplied by a factor 0–1, subsequently added to the water table base-case elevation /Rhen et al. 2006c/. The factors 0.3 and 0.6 were tested, with the corresponding cases called *Water table case-0.3* and *Water table case-0.6*. Hydraulic head given as as Water table case-0.3 became the reference case for the top surface, see text below and /Hartley et al. 2006/. The water table for past times was approximated as the present-day water table minus the shoreline displacement.

A third alternative was to use a flux type top surface boundary condition with a potential infiltration of 165 mm/year (mean of the present run-off, see Section 4.4.1). The potential infiltration may have varied after the last glaciation, but so far no estimates have been made for the regional groundwater flow modelling. Using a flux boundary conditions with this magnitude of potential infiltration, requires near surface conditions in the model that can transport water to discharge points, e.g. streams. The overburden generally has a high capacity for transporting water. The infiltration into the bedrock is consequently expected to be significantly lower than the 165 mm/year given above.

Vertical and bottom boundaries

The boundary conditions on the vertical sides are no-flow, and chemical zero flux of reference waters. At the bottom of the model at $z = -2,300$ m above sea level, there is a no-flow condition and chemically the groundwater is set to pure Brine, i.e Brine fraction = 1.0, all other fractions set to naught.

Initial conditions

The initial conditions for the reference waters assume a profile of Brine at depth and Glacial water at the surface, with a start time of –8,000 AD. The results from Simpevarp 1.2 suggested a piecewise linear initial condition defined as Initial Conditions (IC) and the present modelling suggests that initial condition IC1, see Figure 8-31, is chosen as the Reference Case, with full Glacial water down to 700 m depth, followed by a gradual increase in the Brine component to full Brine at 1,500 m depth. This profile, illustrated in Figure 8-31, is based on the present-day profile of Brine and Glacial water in KLX02, the only borehole deep enough to measure the Brine reference water.

An alternative initial condition (IC 2) was tried with full Glacial water to 300 m depth increasing to full Brine at 1,500 m depth, in an attempt to improve the calibration to measured Cl concentration in boreholes KLX01 and KSH01A, where saline water is found above 600 m depth.

The initial condition for flow was calculated by keeping the reference water fractions fixed, and calculating the flow field that is at hydrostatic equilibrium at the initial time of –8,000 AD.

8.5.2 Effects of model size and model resolution

To some extent the results from a numerical groundwater flow model depend on the model size and model resolution (discretisation). Therefore it is necessary to explore the effects of these factors and judge if they are small enough such that they do not affect the overall results and do not undermine the modelling objectives.

In Simpevarp 1.2 the appropriate size of the regional groundwater flow model was suggested to be the largest of the models presented by /Hartley et al. 2006/. However, in order to provide some cases for initial testing and calibration, a smaller model was also used for comparative studies in Laxemar 1.2, as described below. The larger model was, however, used for all cases considered to be relevant for Laxemar1.2.

Model domain size

New topographic and bathymetric data (DEM) are supplied for Laxemar 1.2 on a 10 m scale covering the entire regional-scale model. This high resolution data are used both to define the model area and to set boundary conditions on the top surface. In addition, a number of regional and local

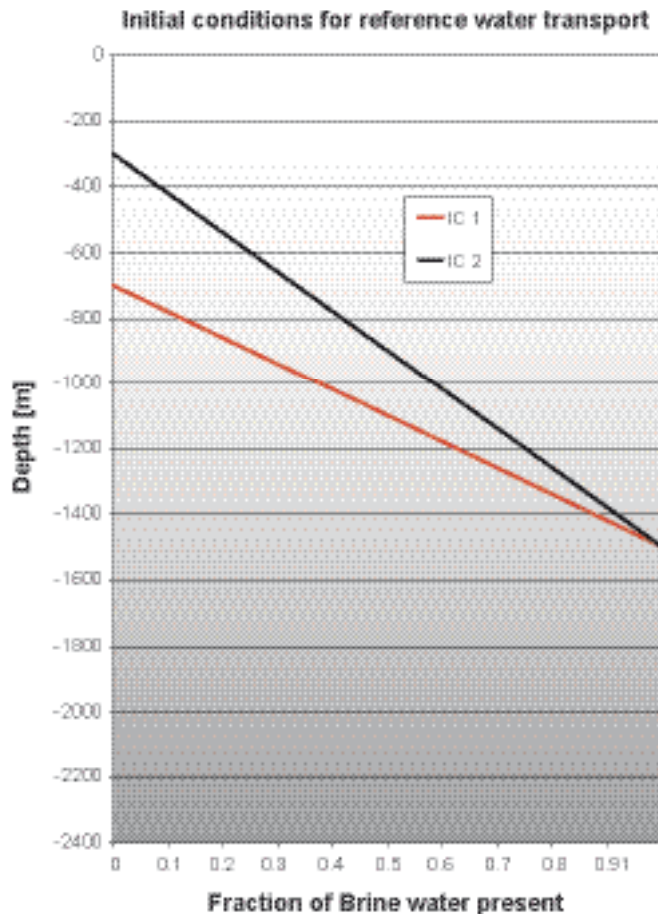


Figure 8-31. Initial conditions for reference water transport, at -8,000 AD. For Initial Condition IC1, the water is pure Glacial above -700 m above sea level followed by a linear transition between Glacial and Brine water towards pure Brine below -1,500 m above sea level. For IC2, the water is pure Glacial above -300 m above sea level, with a linear transition between Glacial and Brine water towards pure Brine below -1,500 m above sea level.

water divides have previously been identified and are also used here. In ConnectFlow it is possible to construct unstructured meshes with irregular boundaries, and hence it is possible to choose boundaries that follow water divides. Figure 8-32 shows the area coverage of the topographic data along with the regional model domain as used in the Laxemar 1.2 regional modelling. Also, the large regional model boundary (following water divides to the west and north) and the alternative smaller regional model area used for initial calibration modelling are given. The local scale model area (small rectangle in solid black) is also shown. A blow-up of areas with more refined resolution of the grid is shown in Figure 8-33, including the Laxemar and Simpevarp (particle) release areas.

Model resolution

The regional groundwater flow modelling performed by /Hartley et al. 2006/ is based on an equivalent porous media (EPM) representation by appropriate upscaling of bedrock fracturing and downscaling of deformation zones using a suitable grid resolution, cf. Figure 8-14. This means that the grid size determines the scale of the modelled heterogeneities, as the individual fractures or deformation zones are not explicitly modelled in the EPM model.

Based on the requirements of repository design, hydraulic properties are calculated in Section 8.4 on a 20 m and 100 m block scale support. Initially, for the regional-scale modelling 100 m grid resolution was specified. For practical reasons of model size, greater resolution over the whole regional model would be prohibitive for transient multi-component reference water transport problems. However, it is possible to increase the refinement in selected limited areas to get a better resolution of geological structures and simulated processes.

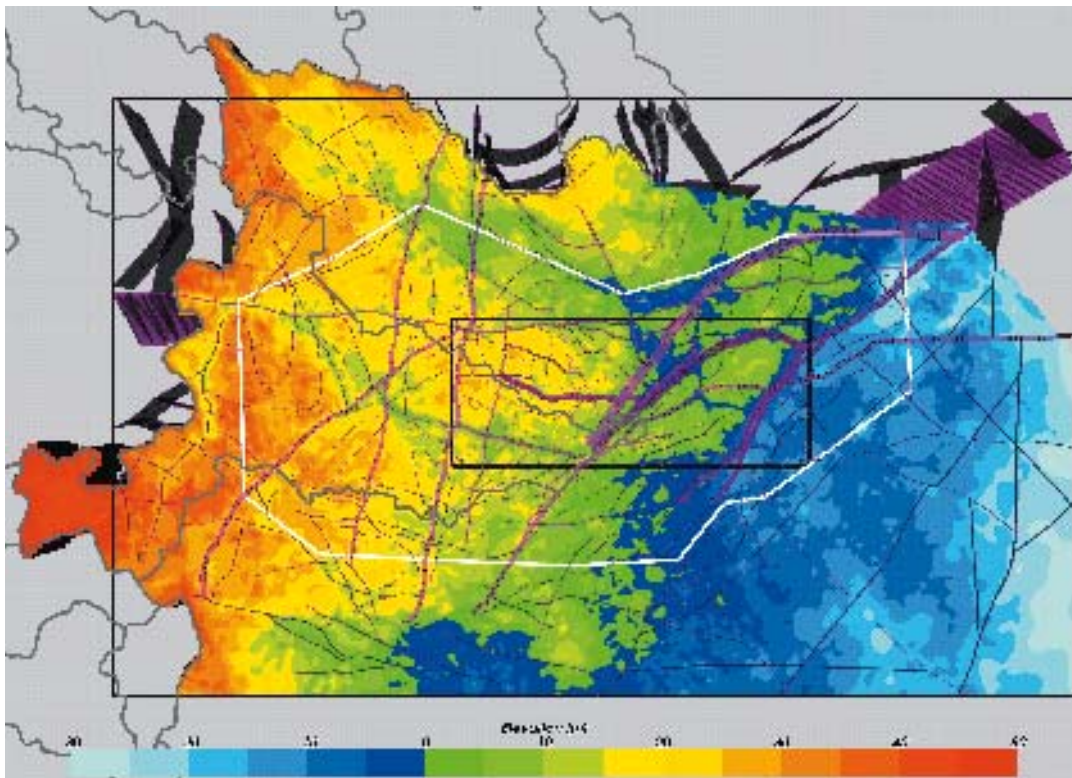


Figure 8-32. Map showing Topographic elevation (metres above sea level) of the Laxemar v. 1.2 regional model area. The definitions of the regional model (large black rectangle) and the local model (small black rectangle) areas, are superimposed together with the large regional model (grey lines following the water divides to the west and north) and the alternative smaller regional model used for calibration modelling (white). The water divides are shown as grey polygons and the HCD model is shown by superimposed purple objects. (Units: metres above sea level) /Hartley et al. 2006/.

The representation of the deformation zones with 100 m element size gives the potential for zones to be smeared out sufficiently to create artificial connections between them. For this reason, it was decided to add additional refinement down to 50 m locally within the so-called Laxemar and Simpevarp *release areas*, cf. Figure 8-33, extending vertically to an elevation of –1,000 m above sea level. At the interface between the two levels of refinement, internal boundary conditions are imposed to ensure continuity of calculated variables (pressure, and reference water fractions) and conservation of mass and flux of reference water. The improved refinement clearly gives a better representation of the deformation zones within the areas with refined meshing.

Figure 8-33 shows the location of refined areas around Laxemar, Simpevarp and Ävrö, as well as the alternative smaller regional model area. The refined areas have a grid resolution of 50 m, and everything outside of these areas has a grid resolution of 100 m. The Ävrö area is only refined in a few variants in order to investigate the impact on the chemistry calibration of the boreholes in this area.

Previous sensitivity studies (Simpevarp 1.2) using transport statistics as a performance measure suggested that the finer 50 m grid would reveal a bi-modal type behaviour caused by a better distinction between particles starting in a deformation zone and the surrounding rock, a distinction that is not apparent for a coarser 100 m grid.

8.5.3 Resulting groundwater flow model

In this section, the resulting groundwater flow model is presented together with some results from sensitivity studies. The model with the parameters that fit the hydrochemistry data best is called the “reference case”. The model parameters are largely as presented in Section 8.4, but due to

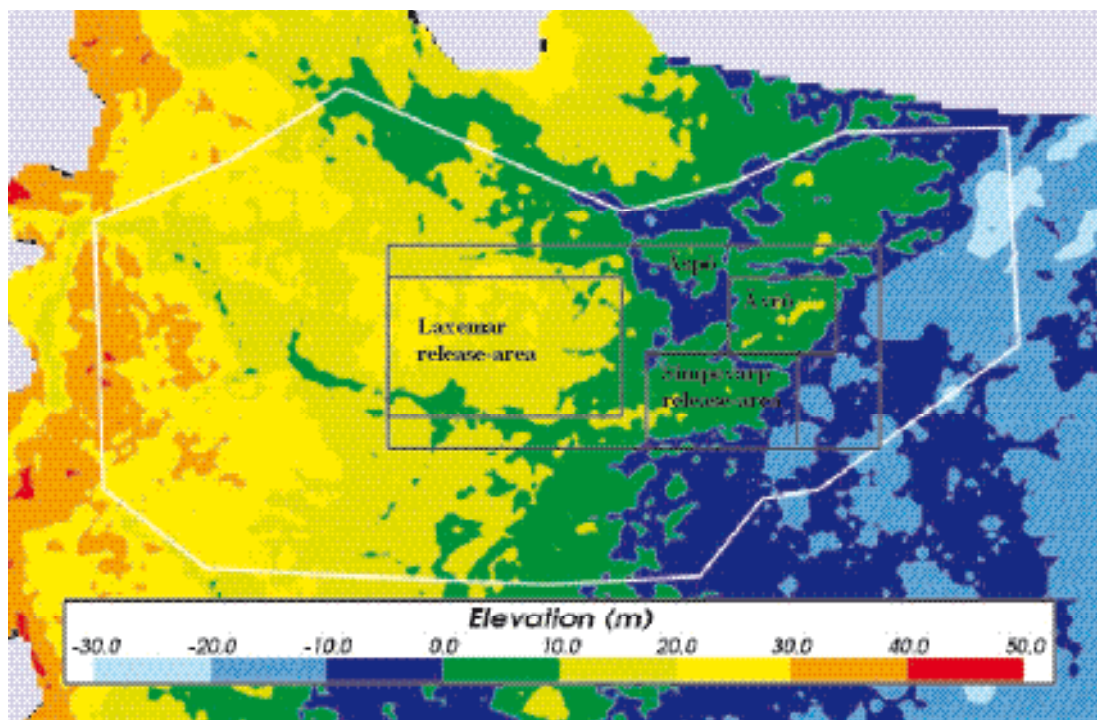


Figure 8-33. Close-up view of the Laxemar v. 1.2 of the local model area (largest black rectangle), refined areas (smaller black rectangles) and the alternative smaller regional model domain (white), Topography coloured according to elevation (units: metres above sea level). 50 m elements are used in the three refined areas Laxemar, Simpevarp and Ävrö. The indicated Laxemar and Simpevarp release areas are used for releasing particles when calculating flow paths and performance measures. The refined areas of Ävrö/Äspö are used in some variants to improve local calibration.

calibration some altered parameter settings have been judged to provide a better fit to the measured hydrochemistry data. The resulting variant of the Hydro DFN base case, is denoted the Hydro DFN regional case.

First, the reference case properties are presented together with a brief summary of how sensitive the model is to different applied properties/conditions. The modelled evolution of the groundwater flow system since the last glaciation is described in Section 9.7, including a comparison with measured present hydrogeochemistry. At the end of this section, an overview of the present groundwater flow conditions at the site is presented.

Reference case properties – and sensitivity to calibration targets

The model area used for the regional flow simulation is shown in Figure 8-32. Figure 8-34 through Figure 8-36 illustrate essential parts of the regional model that has been set up. Figure 8-34 presents the reference case HCDs (including high, medium and low confidence deformation zones) and an alternative case (including only high and medium confidence deformation zones).

As a reference-case in this Laxemar 1.2 modelling, it is assumed that the entire area is covered by 3 m thick silty till, with the uppermost 1 m more porous due to soil forming processes. This was represented explicitly in the model as three very thin layers of finite-elements of thickness 1 m at the top surface of the model. The HSD properties within each layer are uniform. More details about the overburden are found in Sections 4.3 and 8.4.1.

A heterogenous model for the distribution of Quaternary Deposits (QD) was also provided /Nyman, 2005/, and applied in the modelling as illustrated in Figure 8-36. This more detailed overburden model was only included in two of the modelled cases, and mainly demonstrates a capacity to include a fairly detailed description of the overburden model even in the regional model. This may potentially prove useful for future modelling.

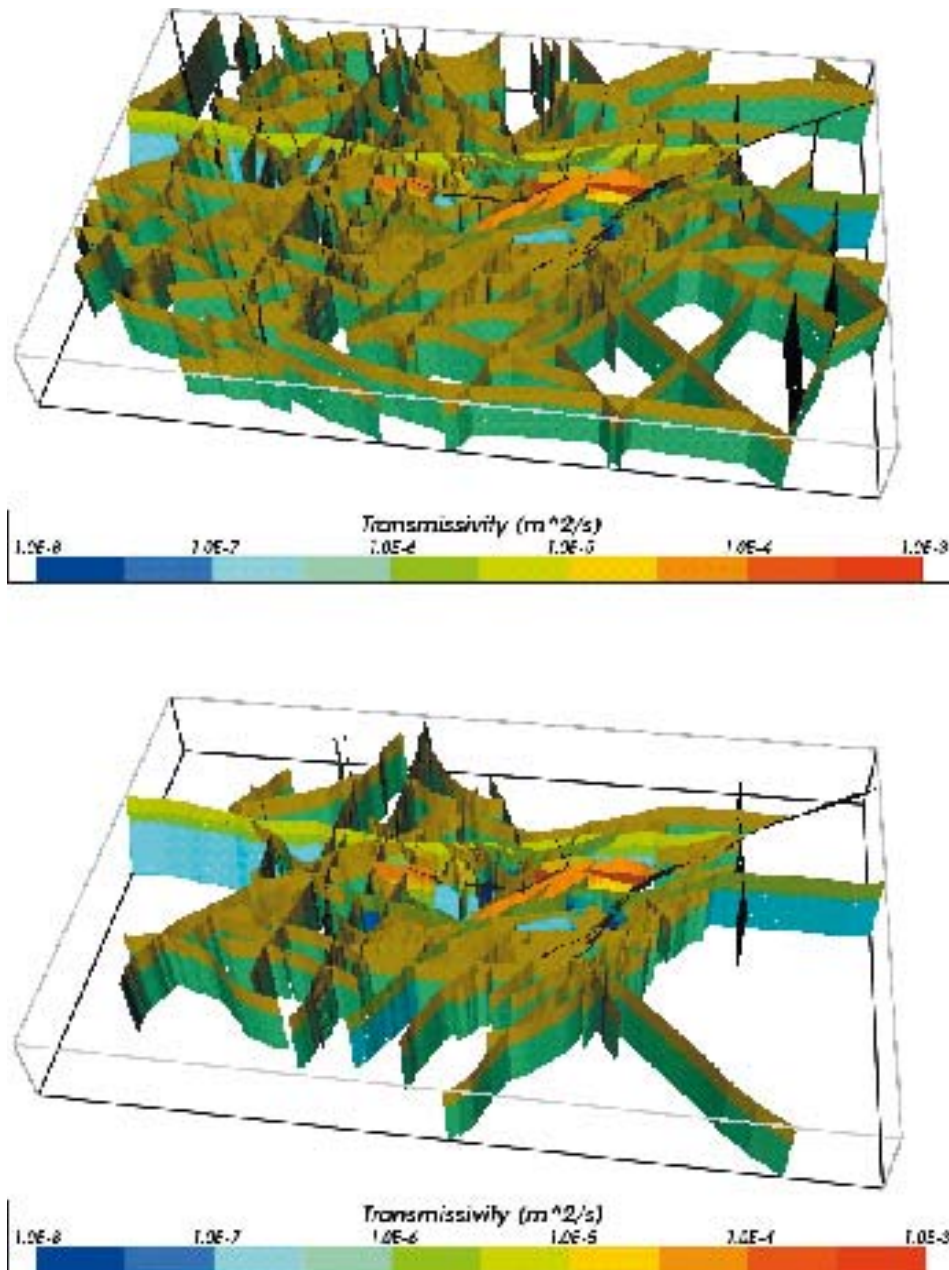


Figure 8-34. HCD with stepwise depth dependency in transmissivity for regional-scale modelling in 3D. The zones are coloured by transmissivity, where red is high and blue is low. Top: all HCDs (high, medium and low confidence), Bottom: Alternative model including HCDs corresponding to geological deformation zone confidence level high and medium.

The key variants of the regional model simulated using ConnectFlow were:

- Model domain size.
- Initial and boundary conditions for flow and reference water transport.
- Parameters of the hydraulic DFN.
- Hydraulic properties of HRD and HCD domains.
- Transport parameters for flow path calculations.

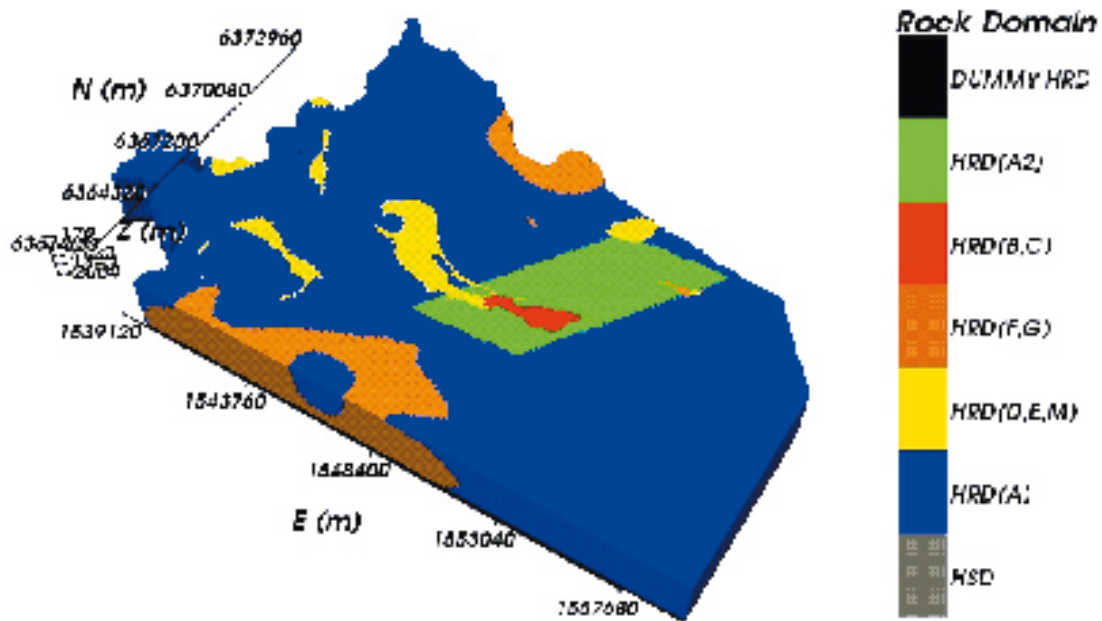


Figure 8-35. HRD model. The regional model domain is divided into : HRD(A), HRD(A2), HRD(B,C), HRD(D,E,M) and HRD(F,G), cf. Section 8.4.3. The HRD assigned in the depth interval $-2,100$ to $-2,300$ m above sea level constitutes a buffer between the bottom of the HCDs (not shown) and the bottom of the model. The HSD layers have been removed for reasons of readability of the figure.

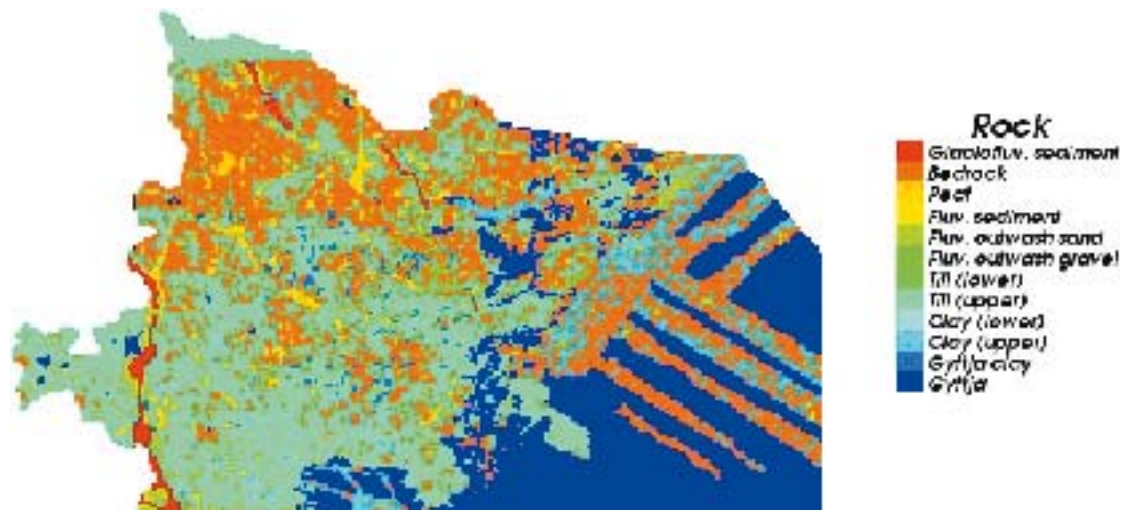


Figure 8-36. Implementation of the QD map for the extended regional model domain, cf. /Hartley et al. 2006/.

Several model cases were constructed to quantify and illustrate the effects of each of these variants. During the initial stages of the modelling, a significant number of other cases were created in order to gain an understanding of how individual model parameters affect the calibration, and ultimately what ranges of parameter values gave a reasonable match to the field-data. Instead, the approach was to define a reference case that gives a reasonable match, and then consider variants in relation to this to illustrate the sensitivity to the various.

The reference case properties and conditions are summarised in Table 8-27.

Table 8-27. Description of the Reference Case for Laxemar 1.2.

Property	Description	Uncertainties and parameter ranges
Domain	Extended regional model domain with 50 m element-size embedded grid in Laxemar, Simpevarp and Ävrö release areas, and 100 m element size elsewhere.	
Initial condition	Initial condition is set to full glacial melt water conditions between ground surface and an elevation of -700 m; then a linear gradient from Glacial to full Brine at -1,500 m above sea level. Between -700 m above sea level and -1,500 m above sea level, the Brine increases linearly from 0 to 100%. Below -1,500 m above sea level, a full Brine condition is applied.	Brine at shallower depths in Simpevarp subarea?
Top surface flow boundary condition	Top-surface head equal simulated water table base case +30% of the difference between the simulated water table base case and the topographic surface of the DEM.	Water table level or flux boundary condition.
Top surface waters	Top surface waters are: Brine water, Glacial water Littorina Water and Meteoric water (denoted "Dilute water" in Chapter 9).	
Density and viscosity	Density and viscosity are functions of salinity (transient), temperature (fixed), and total pressure (transient).	
Transmissivity model	Hydraulic properties are obtained from an upscaled regional-scale DFN that is based on the semi-correlated cases of the Hydro-DFN regional case models.	Alternative <i>T</i> models are correlated or uncorrelated.
Anisotropy	Anisotropy has been introduced by decreasing the transmissivity of fracture sets Set_A and Set_B by a factor of 10. (Sets A, B have roughly strikes; NE to E-W, NNW to NNE respectively.)	Anisotropy has not been fully investigated. Other possibilities include increasing transmissivity of Set_C.
HCD confidence	HCD included all zones (high, medium and low confidence deformation zones).	Alternative is exclusion of low confidence zones.
Depth dependency	HRD: The underlying DFN has a step change in properties according to the hydraulic DFN, although a transition at -200 m above sea level is used instead of one at -300 m above sea level. The upscaled conductivity is then reduced by half an order of magnitude below -600 m above sea level. HCDs: Implemented as a step function of elevation (0 to -300 m above sea level, -300 to -600 m above sea level, < -600 m above sea level), conditioned at boreholes against measured transmissivities.	Borehole data suggests that levels of the two step changes could within the ranges -200 to -350 m above sea level and -500 to -650 m above sea level
HSD	Homogeneous HSD of uniform thickness 3 m.	Overburden model.
Flow-wetted surface	Flow-wetted-surface (FWS) per unit volume of rock for transport calculations above -200 m above sea level: $a_r = 2.0 \text{ m}^2/\text{m}^3$ for HRD(A2), $a_r = 1.0 \text{ m}^2/\text{m}^3$ for HRD(D,E,M), $a_r = 1.5 \text{ m}^2/\text{m}^3$ elsewhere. For all rock domains below -200 m above sea level, $a_r = 1.0 \text{ m}^2/\text{m}^3$. Matrix diffusion length into matrix blocks above -200 m above sea level, $L_D = 0.5 \text{ m}$ for HRD(A2), $L_D = 1.0 \text{ m}$ for HRD(D,E,M), $L_D = 0.7 \text{ m}$ elsewhere, and $L_D = 1.0 \text{ m}$ for all rock domains below -200 m above sea level.	
Kinematic porosity	HRD kinematic porosity taken from upscaled hydraulic DFN, but using minima of $n_{etb} = 10^{-4}$ above -200 m above sea level, and $n_{etb} = 10^{-5}$ below -200 m above sea level. HCD porosity 10^{-3} for zone thickness $W < 100 \text{ m}$ and 10^{-2} for $W \geq 100 \text{ m}$.	
Diffusion accessible porosity	Diffusion accessible porosity from Byegård upper limit $n_m = 5.9 \times 10^{-3}$.	$1.3 \times 10^{-3} - 5.9 \times 10^{-3}$ /Byegård 2006/.
Diffusion coefficient	Intrinsic diffusion coefficient into matrix $D_e = 1.5 \times 10^{-13} \text{ m}^2/\text{s}$.	1.5×10^{-13} /Byegård 2006/ - 3.1×10^{-13} (ChemNet).

Selected results from the Paleo-hydrogeological calibration of the reference case are presented in Section 9.7, jointly with a comparison with measured chemical data.

In the previous study of approximately the same region /Hartley et al. 2005/, good matches were obtained between the measured concentration profiles and the calculated mixing fractions. In that study, the hydraulic properties were based on measurements made in boreholes near and around the Simpevarp peninsula. For the current Laxemar 1.2 modelling, borehole data from the Laxemar subarea are also taken into account, which has resulted in identification of areas of higher conductivity in the Laxemar 1.2 regional scale model, mainly in the dominating domain HRD(A), based on KLX04, as compared with the parameterisation made for the Simpevarp 1.2 model

As a consequence of this noted increase in hydraulic conductivity, it is more difficult to obtain reasonable matches between measured and calculated chemistry data. Numerous attempts have been made in order to obtain improved matches, including calibration of hydraulic properties, testing of alternative HCD, HRD and HSD model concepts and variations in transport parameters, but still a good match was difficult to obtain. To reconcile these difficulties in the more conductive parts of the Laxemar area (in HRD (A)), it was found necessary to reduce the hydraulic driving forces, i.e. consider alternative boundary conditions for groundwater flow. Hence, the key step in achieving a match is to lower the modelled water table below the topographic surface either by approximating a water table based on surface water elevations or using a specified flux type boundary condition with reduced infiltration to the deeper parts of the bedrock. The best match was obtained with the water table based on the Water table case-0.3, see Section 8.5.1. This model of the water table corresponds well with the measurements of the water level in boreholes drilled in the bedrock conducted during the site investigations for Äspö HRL /Rhén et al. 1997c/.

The use of a flux type boundary condition suggested that the former was equivalent to an infiltration to the bedrock of a few tens of mm/year. Other important steps in achieving a calibration using the hydraulic DFN derived for the Laxemar subarea were to introduce anisotropy (differences in transmissivity between the stochastic fracture sets) by reducing the transmissivity in the vertical sets orthogonal to the maximum in-situ horizontal stress, and to increase the flow-wetted surface (parameter a_r) above that suggested by the PFL anomaly data. Overall parameter sensitivity in relation to the modelled hydro-geochemistry profiles in site boreholes is summarised in Table 8-28 and discussed in 8.6.

Table 8-28. Summary of relative sensitivities based on modelled variants for parameter variations within probable ranges.

Variant	Relative sensitivity
Model Domain size	Low
Initial condition	Low
Top surface flow boundary condition	High
Hydraulic DFN realisation	Moderate
Transmissivity model	Moderate
Hydraulic anisotropy	High
HCD confidence	Low
Depth dependency (HRD,)	Moderate
Stochastic properties within HCD	High (Indicative results—more simulations needed)
Overburden (HSD)	Low
Flow-wetted surface	High
Diffusion accessible porosity	Low
Diffusion coefficient	Low

Calibration against past evolution of hydrogeochemistry

See Section 9.7.

8.5.4 Present-day flow conditions

This section presents the results for the reference case developed based on the calibration against the reference water mixing (as interpreted from borehole water samples) to give a reasonable match in the global sense. Hydraulic parameters, initial conditions and boundary conditions obtained for the regional reference case formed the basis for the sensitivity study.

Flow paths

To study the flow paths, particles are released from Laxemar release-area and Simpevarp release area, see Figure 8-33, at an elevation of –500 m above sea level.

In Figure 8-37 the exit locations of the particles released from Laxemar release area (coloured in blue) and Simpevarp release area (coloured in red) are shown for comparison of discharge from the two different release areas. The predominant exit locations of the particles released from the Laxemar release area are the valleys north and south of the Laxemar release area and along the shoreline between Äspö and Hålö. Compared to the Simpevarp release area, the particles released from Laxemar go more to the north. The main exit locations for the particles released from the Simpevarp release area are found around the Simpevarp peninsula and north of Hålö. A group of particles reaches further south along the shoreline.

Recharge and discharge

In Figure 8-38 and Figure 8-39 the vertical Darcy velocity distribution under present-day flow conditions is presented in horizontal slices. Close to the surface (at –10 m above sea level and at –100 m above sea level) the flow tends to be more downward (recharge) amounting to Darcy velocities of between 0.1 to 0.01 m/year in the rock mass. The points of discharge are located in the Baltic Sea, in the eastern part of the modelled area, and around modelled deformation zones (HCDs)

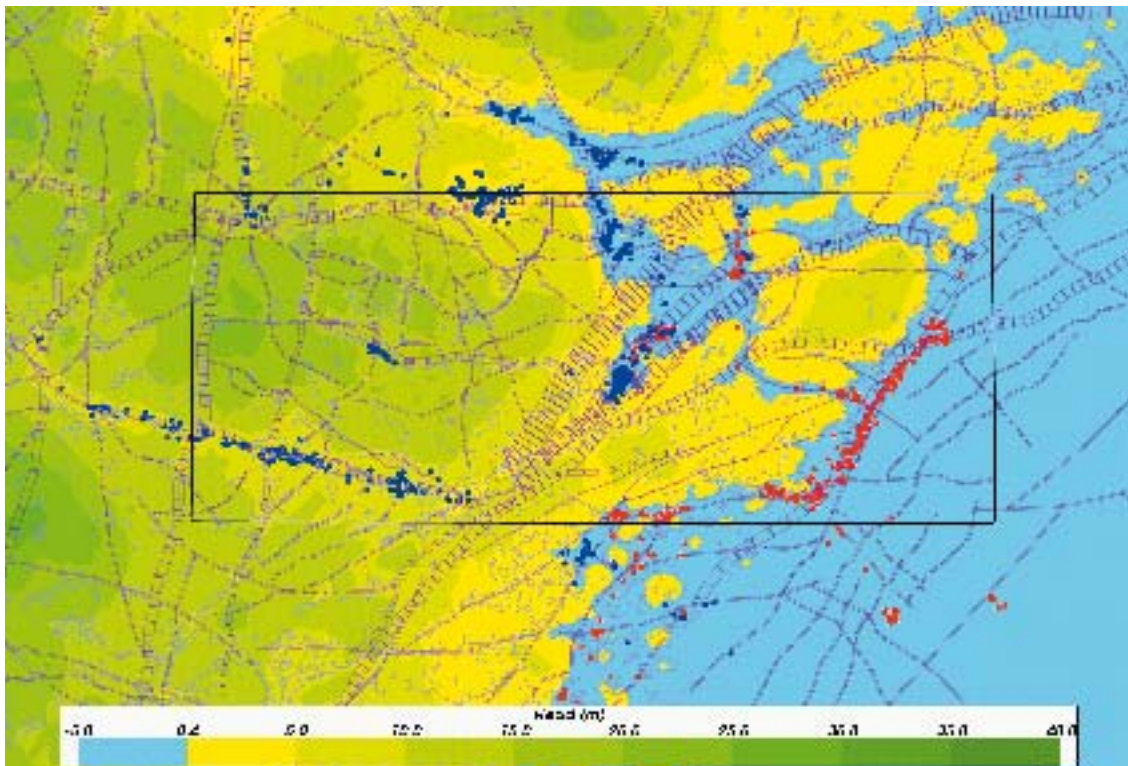


Figure 8-37. Close-up view of particle exit (discharge) locations in the local-scale release-area for the reference case. Particles released from the Laxemar release area are coloured in blue and particles from the Simpevarp release area are coloured in red. The local scale model area (black rectangle) and HCD (purple skeletons) are shown for reference. Because of the limited view, not all particles are shown in the picture, /Hartley et al. 2006/.

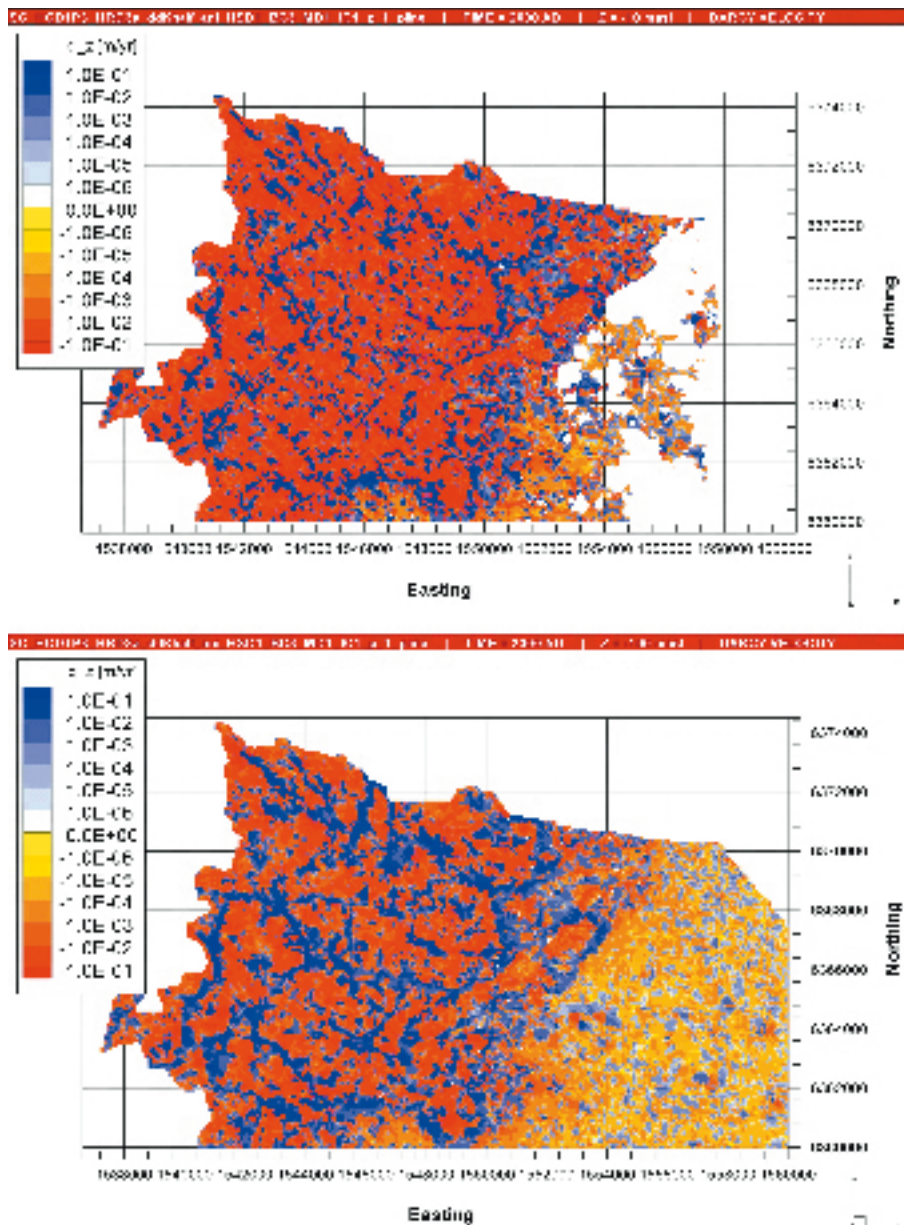


Figure 8-38. Present-day distribution of the vertical Darcy velocity, q_z , in horizontal slices at elevations -10 m above sea level (top), -100 m above sea level (bottom), for the reference case /Hartley et al. 2006/.

and valleys onshore. In the deformation zones, the vertical Darcy velocity is around 0.1 m/year. The flow field near the surface is very heterogeneous, indicating developed localised flow-cells. At -500 m above sea level, the Darcy velocity is generally around 0.01 – 0.0001 m/year, both in the recharge and discharge areas. This is one to two orders of magnitude lower than the flow rates above -100 m above sea level. The flow field also tends to be more homogeneous at this depth, so the areas of recharge and discharge for the deep hydrogeological system become more evident. For both the Laxemar and Simpevarp release areas, see Figure 8-33, flow is mainly downwards, which is promising from a Safety Assessment perspective. At $-1,000$ m above sea level, the vertical Darcy velocities are generally less than 0.0001 m/year.

In Figure 8-40 the recharge (red) and discharge (blue) for particles released within the local scale area are shown for the reference case. As discussed previously, the discharge areas are located along the shoreline and in a few valleys onshore. The recharge areas are calculated by back-tracking particles in the velocity field until they reach the surface. That is, path lines are calculated in the normal way, but by reversing the sign of the velocity vector a particle can be “started” at repository depth

and then tracked upstream to its eventual “point of recharge”. This method uses the variable-density velocity field calculated in the finite-element scheme to obtain a single pathline per particle. It does not consider the convergence or divergence of pathlines, although particles are released on a dense grid of points to give an indication of the heterogeneity of flow paths. The recharge areas are associated with several topographic highs both inside and outside the local scale release area. Generally, the recharge areas are found well inside the model domain, which lend some support (although not conclusive due to the boundary conditions chosen) that the regional water divides are an appropriate choice for the vertical boundaries of the regional model.

All the major islands (Äspö, Ävrö and Hålö) together with the Simpevarp peninsula act as recharge areas, as does the central parts of the Laxemar subarea. A few recharge areas that influence the Laxemar subarea are located at hills several kilometres to the west and southwest.

Discharge areas are mainly located in valleys to the south and north of Laxemar and along the shoreline, especially south of Äspö. There is also a minor discharge area associated with a small stream in the centre of the Laxemar subarea.

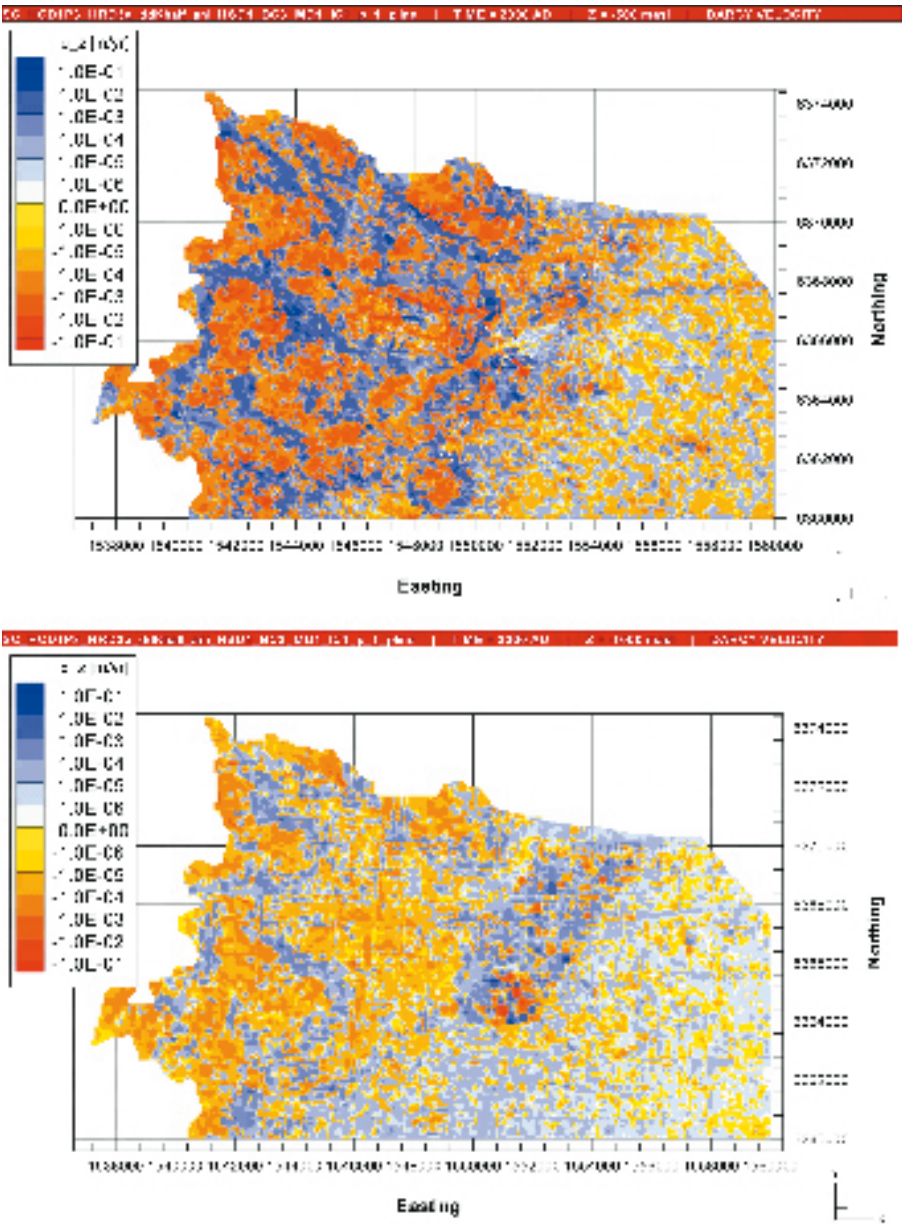


Figure 8-39. Present-day distribution of the vertical Darcy velocity, q_z , in horizontal slices at elevations -500 m above sea level (top) and $-1,000$ m above sea level (bottom), for the reference case /Hartley et al. 2006/.

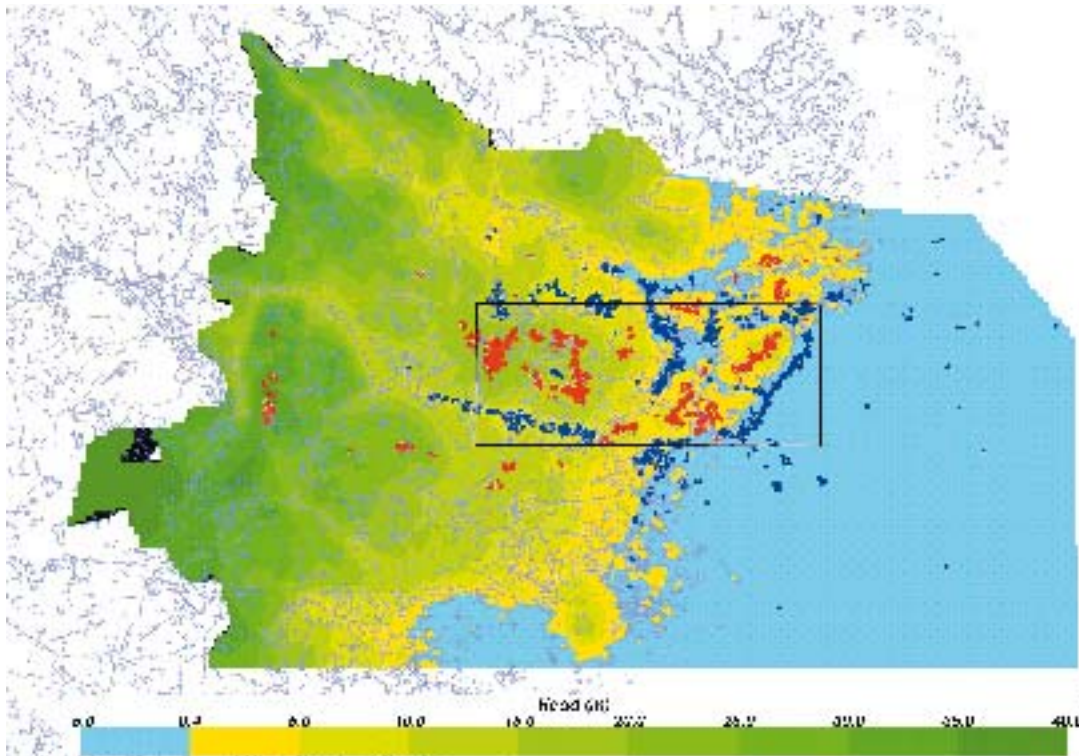


Figure 8-40. Recharge (red) and discharge (blue) locations for particles released in the local scale area for the reference case. The local scale release area (black rectangle) is shown for geographical reference. The recharge points are the upstream start points on the model surface for flow paths through the release area. The discharge points are the equivalent downstream exit points. /Hartley et al. 2006/.

8.6 Conclusions from the regional flow modelling

Suitable model domain

The enlarged regional-scale model based on several water catchments and the smaller model give similar modelling results for the concentration profiles in the boreholes. However, the larger model is necessary to study the recharge and discharge areas relevant to the Laxemar and Simpevarp release areas.

Initial and boundary conditions

The hydraulic boundary conditions on the top surface of the model have a considerable impact on the results, and with a water table often a several metres below the topographic surface gives the best calibration results relative to measured hydrogeochemistry. Within the tested range of initial conditions, the effect on the reference water concentration profiles is low.

HCD, HRD, HSD properties

The use of homogeneous models for hydraulic conductivity using depth dependency trends based on the PSS data all resulted in a poor match against the hydrogeochemical data. For such models an acceptable calibration could only be achieved using a hydraulic conductivity in the deep rock over order of magnitude less than the measured values.

Using the Hydro-DFN base case gives interval conductivities consistent with the PSS 100 m interval data, and when anisotropy is introduced by reducing the transmissivity in the subvertical fracture sets Set_A and Set_B, a reasonable match with hydrogeochemistry is obtained. The hydraulic DFN

model provides a stochastic model of the HRD properties and there is uncertainty in the relationship between fracture transmissivity and size. Model sensitivities related to the stochastic nature of the hydraulic DFN and the associated transmissivity model have moderate effects on the simulated chemistry profiles in boreholes.

The use of different depth dependencies on the HCD has a low to moderate effect on the results in terms of concentration profiles. By increasing the kinematic porosity values in HCD, a moderate effect on the results is obtained which in turn improved calibration results marginally. Removing low confidence zones from the model did not have a significant effect on the results. However, removal also the medium confidence zones was not tested.

The efforts to infer a rather complicated model of the overburden (HSD model) resulted in a low effect on the overall outcome. Only localised effects on recharge and discharge areas were experienced.

For the reference case, the underlying DFN model was initially based on the hydraulic DFN model with a semi-correlated T model. However, during the regional modelling studies, modifications were made to the DFN prescription to achieve a better calibration against borehole hydrogeochemistry. The final hydraulic DFN parameters used for the reference case are summarised in Table 8-21 through Table 8-24.

Flow paths

The path lengths of the released particles are generally quite short. Localised flows are present as a result of the topography and the heterogeneities of the bedrock. Most of the released particles exit inside, or very close to, the local scale model area. The exit locations are located close to the shoreline and in the valleys with lower topographic elevation. Due to the topography, most of the Laxemar release area is located beneath a recharge area.

There are only a few particles with long paths. A couple of particles reach the northern boundary close to the shoreline, suggesting that the boundary is possibly placed too close to the release area, and that the model domain size should be increased.

The case employing the lowest watertable (equal to *Water table case-0.3* Digital Elevation Model (DEM) as the water table, and *Water table case-0.6 a the other cases*) gives the best match to the hydrogeochemistry data in boreholes. However, in terms of flow path statistics and exit locations, there are only small differences in results between the three boundary conditions for the top surface of the model. The exit locations show similar locations for all three watertable cases, although the discharge locations are more dispersed for the case with the lowest watertable. The lack of sensitivity of the modelled exit locations is to be expected since all three cases are based on the same topographic surface (DEM), however different in smoothing of the watertable, so the positions of head maxima and minima are unchanged albeit the head gradients are modified.

8.7 Evaluation of uncertainties

The confidence in the geometry of the deformation zone model, hydraulic properties, boundary conditions and initial conditions to variable extent govern the overall confidence of results of the numerical groundwater flow simulations. Their identification further promotes the discussion of how and where uncertainty should be decreased, and why.

8.7.1 Overburden – HSD

The model suggested has low-medium confidence as the geological description of the overburden is simplified in Laxemar 1.2, although with considerable improvements from SDM Simpevarp 1.2.

8.7.2 Geometry of deformation zones and rock domains

Deformation zones (HCD)

The general confidence in the existence of interpreted deterministic deformation zones generally low, as most of the members of this category of deformation zones are only based on evidence of the existence of lineaments, and no hydraulic tests are available. However, a high confidence for existence has been judged for some of the deformation zones, particularly in the local model area, cf. Chapter 5 and /Wahlgren et al. 2005b/. For these zones, the confidence in some of the hydraulic properties and characteristics is judged in Table 8-29.

So far only a few hydraulic interference tests have been performed, and have been able also to hydraulically confirm, as supporting evidence to the geological evidences, the existence and geometry of a given deformation zone.

The confidence in the hydraulic thickness (essentially geological thickness incorporated from Chapter 5) is very low, based on one or a few intercepts of deformation zones by boreholes. Also, the hydraulic thickness may vary along the extent of the individual deformation zone “plane”. However, the thickness is judged to be of minor importance while transmissivity controls the capacity for flow in the deformation zones.

Rock domains (HRD)

Hydraulic tests cannot directly give information of rock domain geometry, but the hydraulic tests performed in rock domain volumes, interpreted with support from geological and geophysical data, can be used to assess if there are significant differences in hydraulic properties between the geologically defined rock domains, that should give rise to changes in the geometries of hydraulic rock domain geometries.

It was found that several of the rock domains had different hydraulic properties, thus indicating that rock domain geometry should be employed when devising hydraulic rock domains, subsequently used in flow models. The uncertainty in the geometries of interpreted geological rock domains is discussed in Chapter 5.

Table 8-29. Confidence in the hydraulic properties and characteristics (regional reference case) assigned to the HCDs in Laxemar 1.2. Hydraulic thickness (b) Transmissivity (T), Storage coefficient (S), Mean transport aperture (e_T).

Name of HCD, RVS ID, (Earlier name)	Geological confidence, High/Medium/Low	Geological thickness, b (m)	T (m^2/s)	S (-)	e_T (m)	Comment (intersection boreholes and other comments)
ZSMEW002A (Mederhult zone)	High	Low	Low-Medium	Low	Low	HAS10, HLX02, KAS03, KLX06, HLX20
ZSMEW007A	High	Low	Medium	Low	Low	KLX01, KLX02, KLX04, HLX10, HLX13, HLX14, HLX24, HLX22
ZSMEW009A (EW3)	High	Low	Low-Medium	Low	Low	HAS14, HAS21, KAS06, TASA(SA1420A,B, HA1405A,B)
ZSMEW013A (EW1A)	High	Low	Low-Medium	Low	Low	KA1755A, KAS04, HLX03, HAS18, HAS01
ZSMEW014A	Medium	Low	Low	Low	Low	HLX02
ZSMEW038A (ZSMEW038A_B)	High	Low	Medium	Low	Low	HAV05, KAS09, KBH02, TASA(SA-holes,chainage 1180)
ZSMEW039A	Medium	Low	Low	Low	Low	HLX05
ZSMEW900A (ZSMEW005A 7A)	High	Low	Low	Low	Low	HLX25, HLX14
ZSMNE004A (ZSMEW004A)	High	Low	Low	Low	Low	TASA(Sum SA0289A, SA0327A)

Name of HCD, RVS ID, (Earlier name)	Geological confidence, High/Medium/Low	Geological thickness, b (m)	T (m ² /s)	S (-)	e _r (m)	Comment (intersection boreholes and other comments)
ZSMNE005A (Åspö shear zone; EW1b)	High	Low	Medium	Low	Low	KA1755A, KA1754A, KA1751A, KAS04, KA3590G02, KAS02, KAS12, HLX09
ZSMNE006A (NE1)	High	Low	Medium	Low	Low	HLX18, KA1061, KA1131B, KAS07, KAS08, KAS09, KAS11, KAS14, KBH02, KAS02, KAS16, TASA(7 HA-probe-holes)
ZSMNE012A (includes NW004A (old names EW7-NE4)	High	Low	Medium	Low	Low	HAV02, HAV12, HAV13, HLX18, HMJ01, KAV01, KAV03, KAV04A, KBH02, TASA(chainage 867-Sum of pair, SA0792 more)
ZSMNE015A	High	Low	Low	Low	Low	KSH01A
ZSMNE016A	High	Low	Low	Low	Low	SA0344A, SA0344B
ZSMNE024A	High	Low	Low-Medium	Low	Low	KSH01A, KSH03A, KAV01A, KAV04A
ZSMNE031A	High	Low	Low	Low	Low	KSH01A, KSH03A
ZSMNE040A	High	Low	Low	Low	Low	HLX04, HLX01
ZSMNS017B (NNW4)	High	Low	Medium	Low	Low	HA1960A, SA1997A, SA2009A, SA2025B, SA2074B, SA2090B, SA2109B, KC0045F, KA2048B
ZSMNW025A	High	Low	Low	Low	Low	HSH01
ZSMNW028A (ZSMEW028A)	High	Low	Low	Low	Low	HAV09
ZSMNW042A	High	Low	Low	Low	Low	KLX05
ZSMNW048A	Medium	Low	Low	Low	Low	HLX07
ZSMNW928A (Reflector N)	Medium	Low	Low	Low	Low	KLX02, KLX04
ZSMNW929A (ZSMNE040A)	High	Low	Low	Low	Low	KLX02, KLX04
ZSMNW932A (ZSMNW006A)	High	Low	Low	Low	Low	KLX03, KLX05
All other HCD		Low	Low	Low	Low	-

8.7.3 Hydraulic properties of deformation zones and rock domains

Deformation zones (HCD)

The confidence in the transmissivity assigned to a particular deformation zone (HCD) is medium to low due to zero, one or a few borehole intercepts of individual deformation zones, see Table 8-29. Having 2–3 hydraulic test results in different boreholes in a deformation zone, the confidence is set to low to medium. Having 4 up to c. 10 hydraulic test results, the confidence is set to medium. The transmissivity can be expected to vary along the “plane” of the deformation zones, and since most zones are larger than 1 km one can expect that there will always be great difficulties to obtain a high confidence in the properties and heterogeneity by drilling and borehole testing. Several observations of a deformation zone transmissivity have been judged as low to medium, despite four or more borehole intercepts. The reason for this is that the borehole intercepts have to be examined in more detail, or that the observations are fairly local compared with the entire extent of the deformation zone.

The observations indicate that there may be a depth dependence of the transmissivity in deformation zones. The data are few and the depth dependency must be considered uncertain.

The confidence in the storage coefficient is low, and will be lower than the confidence in transmissivity, due to difficulties in making proper tests. However, it is judged that this is of minor importance, as it controls the transient responses on time scales of days-months when pumping, and during drawdown caused by tunnelling, which is deemed being of minor importance to long-term safety.

The variation of the storage coefficient is less than that of transmissivity, making it easier to analyse using sensitivity studies. However, the storage coefficient is important when the size of hydraulic features is to be assessed from hydraulic tests, and the size is an essential component when studying the transmissivity models suggested for the hydraulic DFN. The storage coefficient is also important when judging results from interference tests.

The confidence in the mean transport aperture (giving the flow porosity when used jointly with the hydraulic thickness) is low, and probably will be rather low for individual deformation zones. However, some new data will be collected and probably the confidence in transport aperture assigned will be increased during the continued site investigations. Still, the confidence will probably be low-medium, demanding sensitivity studies to investigate the implications of uncertainty in this property. The importance for Safety Assessment is also considered low.

The defined deformation zones (with high to low confidence) create a well-connected system, partly because of the geometrical definition (assumed to intersect or stop mutually or to be continuous over the plane) and partly because of the assigned hydraulic properties (assumed to be constant over the plane and to have a rather high transmissivity). The spatial distribution of properties within HCDs is difficult to assess (generally very few samples).

So far, only preliminary tests of assignment of a stochastic distribution of transmissivity within the HCDs have been assessed in flow models. These indicate a significant effect on the calibration of the regional groundwater flow model. This modelling concept of the large deformation zones will be tested more thoroughly in the future.

Rock domains (HRD)

A Hydraulic DFN model is the main alternative description for the rock domains in the current model strategy. It is a complex model including both a geometrical description of fractures (or rather hydraulic features, as the conceptual model describes it in Section 8.3 and Appendix 8) and the transmissivity distributions coupled to these fractures.

Different hydraulic DFN models are developed for different rock domains, but each DFN model, for a particular rock domain, was based on data from one single borehole. As there is really no spatial distribution of the borehole information, the models must be considered as uncertain.

The PFL measurements in boreholes in the Laxemar subarea indicate that there possibly exists an anisotropic condition. The data indicate a much less anisotropic conditions than found in the nearby Äsp HRL. An anisotropic model, which approximately complies with the PFL measurements, was tested and found to improve the regional model calibration. The magnitude (ratios) in the anisotropic conditions must be considered uncertain.

The hydraulic borehole data indicate that there may be a depth dependence in the hydraulic conductivity of the HRDs between the deterministically described deformation zones (HCDs). The data set test scale 100 m is rather large and seems to support that there is a depth dependency with some statistical significance. However, it may mainly be a difference between near-surface rock (0–200 m) and the rock below. The hydraulic DFN modelling also indicates depth dependence, but as data are sparse, the depth dependency observed in this modelling must be considered uncertain

The hydraulic conductivity (K) values from the block modelling at a 20 and 100 m scale, based on the Hydraulic DFN, compares rather well with measured values at the corresponding length scales. However, the geometric mean K for test scale 20 m and 100 m differs significantly considering the measured values,. This may indicate that the Hydraulic DFN model is not fully consistent with data and should be further tested.

A final comment can be made regarding the present Hydraulic DFN model/-s. According to the conceptual model, stating that there is a continuous distribution from small fractures up to large hydraulic features, equal to deformation zones, one should expect that the model predicts approximately the right the number of deterministically defined zones. This may not always be the case in the models provided, though rather close. It is partly a matter of data missing (not yet available, e.g statistics of minor deformation zones), but also conceptual issues and modelling methodology that should be further developed.

8.7.4 Boundary conditions and initial conditions

Model size

The size of the reference regional model seems to provide stable results in terms of flow paths and calibration of hydrochemical data.

Initial conditions

The initial conditions are highly uncertain, and can to some extent be tested by flow modelling and motivated through a believable conceptual model, as given in Section 3.3. The initial conditions tested are motivated from the conceptual model and the few cases tested in the regional groundwater flow modelling, indicate one case that complies somewhat better with the modelling results, compared with the present observed hydrochemistry. However, the results are not so sensitive to the cases tested. This may indicate that the initial conditions are properly chosen.

Boundary conditions

The hydraulic boundary conditions on the top surface of the model have a considerable impact on the results, with a water table often several metres below the topographic surface that gives the best calibration results against hydrogeochemistry. Using a lower water table below the topographic surface as a head boundary condition was found to be vital ingredient in achieving a calibrated model. Other ways of applying a lower water table were considered based on a specified flux type boundary condition. This suggested a maximum specified infiltration to the bedrock of a few tens of mm/year would give a reasonable match. It is suggested that this be compared with the infiltration to bedrock calculated by the SurfaceNet Group.

In the regional modelling time varying boundary conditions are applied both for shore displacement and water composition of the sea/lake stages of the Baltic. The shore displacement is probably rather well known, except for the time just after the glacial, retreat. The water composition and time periods are uncertain for the sea stages, but possibly the Littorina stage is less uncertain than previous stages. The implication of different time periods for the sea stages and different water composition have not been tested yet.

8.8 Feedback to other disciplines

Some of the observed uncertainties may be related to data (or lack of data) and results of models coming from other disciplines. Still, others are due to lack of hydrogeological field data. The first part is solved by communicating and discussing the model issues with other disciplines to identify the necessary actions to be taken. The second part is resolved by communicating with those responsible for the planning and execution of future site investigations. In this section the main issues are highlighted.

8.8.1 Important observations related to other disciplines

The hydraulic anisotropy and intensity of flowing fractures should be compared more closely with the overall rock stress field, but also with local changes of the stress field as shown by Figures 6-16 and 6-17. Possibly there is a correlation between the stress field and the distribution of the hydraulic properties that can be better substantiated when more data become available.

The reason for that the direction of major hydraulic conductivity (hydraulic anisotropy) may change spatially, as pointed out in Section 8.6.3 (although data are uncertain) could possibly also be explained by the fact that the fracture pattern changes spatially due to shapes of the rock domains, cf. e.g. the arc geometry discussed in Section 5.3.3. This can probably be analysed in more detail.

One key information for constructing the hydraulic DFN according to the concepts described in Section 8.3.2 and Appendix 8, is the identification of brittle deformation zones in boreholes and in outcrop. Further development of conceptual description of brittle deformation and the methodologies

for identification of brittle deformation zones is a main task for the disciplines geology, hydrogeology and rock mechanics during the Complete Site Investigation.

The further development of the methodology for constructing a hydraulic DFN model useful for Safety Assessment and Repository Engineering is partly depending on new data (that are planned for). What is perhaps more important is to obtain a better integration and consensus about useful concepts of how to integrate outcrop fracture data with borehole fracture data and, in doing so, motivate models that are consistent with near-surface rock as well as at that found at repository depth. The rock at repository depth is considered most important in this context, but essential data for the modelling comes from surface observations, and thus the “story” must be consistent going from surface and down into the bedrock. The latter issue is an important component of the integration of the disciplines geology and hydrogeology, but also in part, rock mechanics.

8.8.2 Can new boreholes resolve some of the issues raised?

The presence and distribution of Littorina and Glacial waters in the flow model are conditioned to the overall hydraulic conductivity and heterogeneity of the rock. Their distribution is seen as an essential part in confirming that reasonable assessments of the hydrogeological properties have been made in the hydrogeological descriptive model. The following activities are proposed:

- Based on the simulations, it should be determined if there are places where new boreholes could contribute significantly to the mapping of the spatial distribution of Littorina and Glacial waters. Improved understanding of whether “pockets” of Glacial water are present would be valuable for the modelling.
- In the context of the planned “hydrochemical borehole” KLX08 it should be considered if it is possible to make extensive sampling also in features with low transmissivities.
- It should be evaluated if it is possible and useful to revisit the boreholes to the east for complementary hydrochemical sampling to strengthen the dataset in terms of spatial distribution of different water types, especially Littorina and Glacial waters.

There is a weakness in the geological and hydraulic DFN modeling that, at least partly, is due to the lack of data from the near surface. At two locations in the Laxemar subarea, five 100 m long, cored boreholes, with different orientations, will be drilled at the beginning of the Complete Site Investigations (CSI) to collect data relevant for DFN modelling. The surface around the boreholes will be mapped in detail and there will also be a deep vertical cored borehole from the mapped surface. Hydraulic tests (PFL) will be made both as single hole measurement and interference tests. Furthermore, there is an ongoing project for estimating the character and frequency of minor deformation zones. It is expected that these data will be essential for further developing the concepts and methodology for geological and hydraulic DFN models.

As most boreholes have been more or less vertical, there exists a risk that the hydraulic anisotropy is not fully understood. Cored boreholes should be drilled in different directions to make sure that different fracture sets are captured. Possibly the boreholes drilled for improving DFN modelling, as stated above, will provide useful data in this context.

The data representation of some of the hydraulic rock domains is very weak. It is therefore essential to have more boreholes representing rock domains relevant for the deep repository (already in the present planning for CSI). This pertains in particular to hydraulic rock domain HRD(D,E,M).

8.8.3 What other data or tests can discriminate between models?

The results from the groundwater flow modelling suggest some issues on which to focus on further in the acquisition of site characterisation data:

- The use of boreholes with different inclinations would provide a better basis for studies of relative hydraulic anisotropy between fracture sets.
- Flow data from other boreholes with PFL and PSS data will help bound the variability of hydraulic properties within the main hydraulic rock domains and hence bound the uncertainty in extrapolating properties from boreholes to rock domains.

- PSS 5 m interval data from another borehole in the Laxemar subarea would help confirm whether the fracture transmissivity displays a bi-modal behaviour as partly suggested by the lower section of KLX04, or whether this was a unique feature of KLX04.
- The importance of the position of the watertable suggests the need more data should be acquired on surface hydrology in terms of groundwater levels and the infiltration of groundwater into the deep bedrock. This suggests a need for deeper co-operation between the HydroNet and SurfaceNet groups.
- The ChemNet group has started to provide information on the water chemistry in the matrix rock, to be compared with that measured in the fracture system. This is encouraged, and further work will help address uncertainties in the connection between the two types of porosity, and in other transport parameters.
- The use of these environmental isotopes than ^{18}O is considered important for the regional groundwater flow modelling as it defines more or less the old water type; Glacial water. Additional sampling to obtain both more spatially distributed data and data from low conductive features is valuable.

The hydraulic connectivity is a major issue where cross-hole interference tests may be helpful. The planned interference tests are on a large scale, mainly to indicate existence and connectivity of HCDs, in order to support in the modelling of the deterministically defined deformation zones, but also to provide hydraulic properties of some HCDs and useful data for testing groundwater flow models. Ideally, one would like to have a large number of observation sections and (especially as calibration data sets for numerical models) to have pseudo-steady state data, such that the storage component can be neglected. This may be difficult to achieve, but it is essential to consider the possibilities available. Boreholes within c. 1 km from an ongoing drilling, or ongoing pumping test, should be monitored. The responses measured may provide support for the interpretation of deformation zones, including orientation/position or indications of anisotropy. Longer pumping tests (days) should be made rather frequently as the number of observation points (boreholes) have increased.

Testing hydraulic connectivity at a smaller scale in the rock mass is more difficult. As outlined in the previous section, interference tests using the PFL to measure flow responses will be made within a “block” of c. $100 \times 100 \times 100$ m near the surface at two locations. The purpose is to test and develop both the methodology and concepts for geological and hydraulic DFN models. It is then assumed that it is possible to extend the DFN models to greater based on more sparsely spaced deep cored boreholes.

9 Bedrock hydrogeochemistry

There are relatively few new groundwater samples from boreholes in the Laxemar subarea that were not already evaluated during the Simpevarp 1.2 modelling phase. Therefore, this work has focused more on improving the methodology and tools used for evaluating the hydrochemistry combined with a sensitivity and uncertainty analysis of the available data. The major goal has been to consolidate groundwater geochemical understanding and the models used at the site.

Evaluation of the hydrogeochemical data has been carried out by considering not only the samples from Laxemar subarea, but also in relation to those from the Simpevarp subarea, Äspö and, in some cases, also related to the whole so-called “Fennoscandian hydrochemical dataset”. Information from hydrogeochemical model versions based on previously investigated sites in Sweden and elsewhere, and information from ongoing geological and hydrogeological modelling in the Simpevarp subarea, where included in the evaluation wherever possible.

The data evaluation and modelling of hydrogeochemical data consist of manual evaluation (Section 9.4), expert judgment (Section 9.4) and mathematical modelling (Sections 9.5 and 9.6), all of which must be combined when evaluating groundwater information. Visualisation techniques have been used to show the 3D geographical distribution of the different groundwater characteristics seen in the Simpevarp area and for supporting the conceptual model of the site (Section 9.6). Comparison and integration between hydrogeological and hydrogeochemical models is discussed in Section 9.7 and uncertainties in the hydrogeochemical model are discussed in Section 9.8.

The results of the detailed hydrogeochemical modelling described in this present chapter are used to produce an updated hydrogeochemical site descriptive model (Section 11.6). The background hydrogeochemical report /SKB 2006a/ describes in great detail the hydrogeochemical data evaluation and modelling carried out for the Laxemar subarea descriptive model version 1.2. The outcome of the hydrogeochemical modelling is used in, for example, the hydrogeological modelling, transport modelling and safety assessment modelling.

The results presented herein are the result of the collective effort made by the ChemNET analysis group and are presented in detail in /SKB 2006a/.

9.1 State of knowledge at the previous model version

The first model of the Simpevarp area was the Site Descriptive Hydrogeochemical Model version 0 /SKB 2002b/. Although there were few data from the Simpevarp regional model area to support a detailed hydrogeochemical site descriptive model, postglacial events believed to have affected the groundwater evolution and chemistry at Simpevarp were described in a conceptual model.

The model versions Simpevarp 1.1 /Laaksoharju et al. 2004/ and Simpevarp 1.2 /SKB 2004b/ represented the evaluation of the available groundwater analytical data from the Simpevarp area with special emphasis on the Simpevarp subarea. The complex groundwater evolution and patterns at Simpevarp are a result of many factors such as: a) the present-day topography and proximity to the Baltic Sea, b) past changes in hydrogeology related to glaciation/deglaciation, land uplift and repeated marine/lake water regressions/transgressions, and c) organic or inorganic alteration of the groundwater composition caused by microbial processes or water/rock interactions. The sampled groundwaters reflect to various degrees processes relating to modern or ancient water/rock interactions and mixing.

The groundwater flow regimes at the Laxemar and Simpevarp subareas are considered local and extend down to depths of around 600–1,000 m depending on local topography. Close to the Baltic Sea coastline, where topographical variation is small, groundwater flow penetration to greater depth will consequently be less marked. In contrast, the Laxemar subarea is characterised by higher topography resulting in a much more dynamic groundwater circulation which appears to extend to 1,000 m depth in the vicinity of borehole KLX02. The marked differences in the groundwater flow

regimes between the Laxemar and Simpevarp subareas are reflected in the groundwater chemistry where four major hydrochemical groups of groundwaters (types A–D) have been identified (further development and visualisation of this modelling is discussed in Section 9.7.2).

The redox state of groundwaters appears to be well described by sulphur redox pairs in agreement with some previous studies in this area and in other sites from the Fennoscandian Shield. Furthermore, the CH_4/CO_2 (of biogenic and possibly \pm abiogenic origin) is another important redox pair in determining the redox state.

A modelling approach was used to simulate the composition of the highly saline or brine groundwaters and, for the Simpevarp area, concluded that mixing is the main irreversible process. It controls chloride concentration that, in turn, determines the re-equilibrium path (water-rock interaction) triggered by mixing.

Coupled transport modelling was used to model the groundwater age, tritium content and calcite dissolution/precipitation processes at shallow groundwater depths at both the Laxemar and Simpevarp subareas. The modelled results provide additional support to hydrogeological models by using independent hydrochemical information and added support to the general hydrogeochemical understanding of the site.

The modelling also indicated that the groundwater composition at repository depths is such that the representative samples from KSH01A: 548–565 m and KSH02: 575–580 m can meet the SKB chemical stability criteria for Eh, pH, TDS, DOC and Ca+Mg.

9.2 Hydrogeochemical modelling

9.2.1 Modelling assumptions and input from other disciplines

The main modelling assumption is that the measured groundwater compositions are a result of mixing and reactions including different water types. The water types are a result of palaeohydrogeological events and recent hydrodynamic conditions (see Figure 3-15). A schematic presentation of how site evaluation/modelling is performed, its components and the interaction with other geoscientific disciplines, is shown in Figure 9-1. The methodology applied in this report is described in detail in the SKB strategy report for hydrogeochemical modelling /Smellie et al. 2002/.

Hydrogeochemical modelling involves the integration of different geoscientific disciplines such as geology and hydrogeology. This information is used as background information, supporting information or as independent information when models are constructed or compared.

Geological information is used in hydrogeochemical modelling as direct input in mass-balance modelling, but also to judge the feasibility of the results from, for example, saturation index modelling. For this particular modelling exercise, geological data were summarised, the information was reviewed and the relevant rock types, fracture minerals and mineral alterations were identified (cf. Appendix 1 in /SKB 2006a/).

The underlying geostructural model provides important information on water-conducting fractures used for the understanding and modelling of the hydrodynamics. The cross section used for visualisation of groundwater properties is generally selected with respect to the geological model and the hydrogeological simulations (cf. Section 9.7 and /SKB 2006a, and Appendix 1 and 5 therein/). The available hydrogeological information and the results of hydrogeological modelling are used in the coupled flow and transport modelling (cf. Appendix 5 in /SKB 2006a/). The measured values of Cl, ^{18}O , ^2H , ^{14}C and the results from the M3 mixing calculations were provided as input data for hydrodynamic modelling simulations (cf. Appendix 4 in /SKB 2006a/). In addition, a more comprehensive data table was provided to the hydromodellers where additional samples were indicated as useful for hydrogeological modelling purposes (Appendix 8 in /SKB 2006a/). The mixing models used are descriptive and do not include advection or diffusion processes. However, these models can indicate effects of transport processes or reactions in a simplified way.

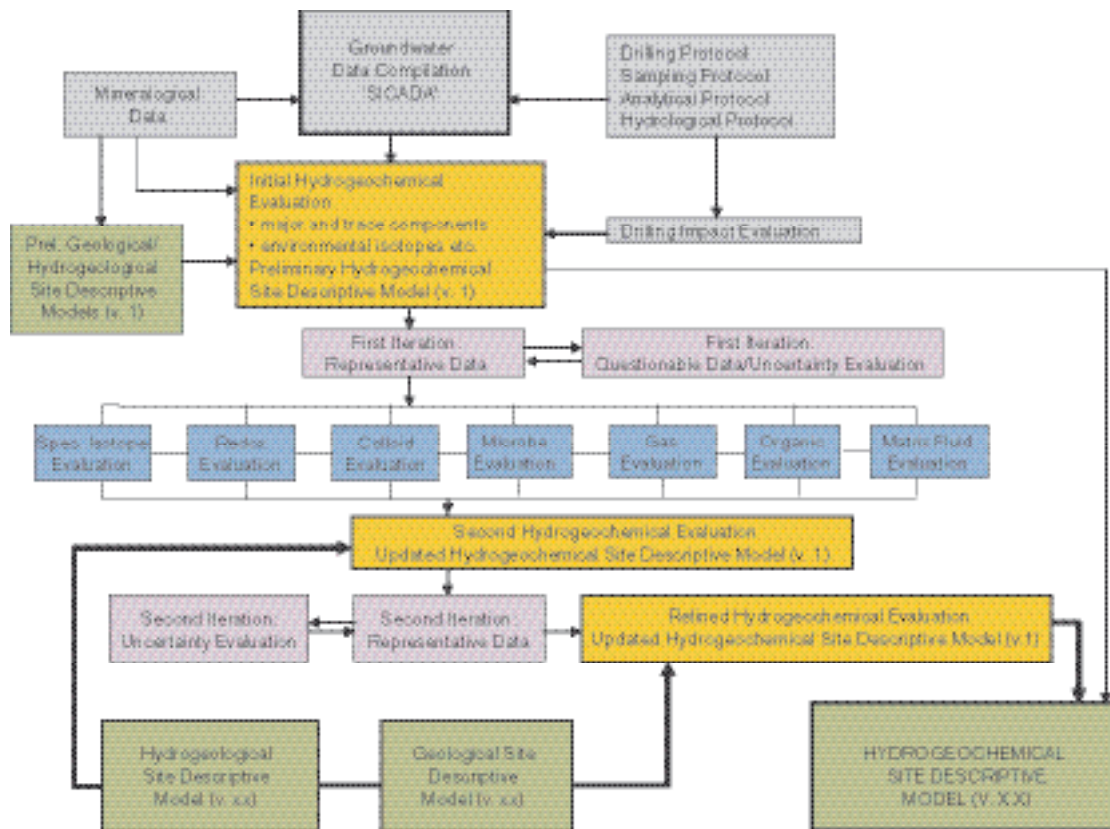


Figure 9-1. The evaluation and modelling steps used for Laxemar model version 1.2 (after /Smellie et al. 2002/).

9.2.2 Conceptual model with potential alternatives

The conceptual hydrogeochemical model for the Simpevarp area is the paleohydrogeological model shown in Figure 3-15. Much of the hydrogeochemical work focussed on tracing effects of the paleohydrogeological events, but also on assessing how mixing and reactions have altered the groundwater composition. The alternative conceptual models tested included different reference waters and local and regional models and different mathematical solutions to calculate the mixing proportions (cf. Appendix 3 and 4 in /SKB 2006a/); various modelling tools (associated with explorative analyses, PHREEQC, M3 and M4) and approaches were applied on the data set. The concept by which the water composition is modelled using PHREEQC and the M4 approach is discussed in Appendix 3 in /SKB 2006a/. M4 is a new method to calculate mixing proportions in the multivariate space. The uncertainties of the mixing models are evaluated and discussed in /SKB 2006a, see Appendix 3 and 4 therein/.

9.3 Hydrogeochemical data

Available hydrogeochemical data and their handling in Laxemar 1.2 are described in Table 2-5 (for further data details see Appendix 9 in /SKB 2006a/). The approach chosen has been to include all relevant data in the Simpevarp and Laxemar subareas together with the available information from the islands of Äspö (before the time of tunnel construction) and Ävrö.

The new samples in the version 1.2 “data freeze” for the Laxemar subarea (all collected in 2004) include:

30 samples from the Ävrö island:

- 8 samples from percussion boreholes (two samples from each of the following boreholes: HAV11, HAV12, HAV13 and HAV14).
- 22 samples from the cored borehole KAV04: 20 tube samples (from 0 to 1,000 m depth) and 2 packed-off samples (729–805 m and 729–819 m); 112 samples from the Laxemar subarea.
- 10 samples from percussion boreholes: 4 samples from borehole HLX14 (one of them selected as the representative sample for modelling purposes), two samples from HLX18, two from HLX20 (one of them of limited suitability; to be used with caution), one from HLX22 and one from HLX24.
- 102 samples from cored boreholes:
 - 26 samples from KLX03: 20 tube samples (from 0 to 990 m depth) and 6 packed-off samples (12–60 m, 12–100 m, 103–218 m [1 representative sample], 497–600 m, 600–695 m and 693–761 m),
 - 69 samples from KLX04: 21 tube samples (from 0 to 985 m depth) and 48 packed-off samples (104–109 [3], 103–213 [1 representative sample], 210–329 [1], 329–404 [1], 401–515 [1], 510–515 [25], 614–701 [1], 698–850 [1], 849–993 [1], 971–976 [13]m),
 - 7 packed-off samples from KLX06 (103–202 [1], 200–310 [1], 260–268 [2], 307–415 [1], 331–364 [1], 514–613 [1]m); 360 samples from Simpevarp.
- 44 groundwater samples:
 - 4 samples from percussion boreholes: 2 samples each from boreholes, HSH04 and HSH05,
 - one sample from KSH02 cored borehole (422.3–423.3 m),
 - 39 shallow groundwater (0–10 m depth) samples from soil pipes (one of them selected as limited suitability; to be used with caution for modelling).
- 296 surface water samples:
 - 92 sea water samples (56 selected as limited suitability; to be used with caution),
 - 64 lake water samples (48 selected as limited suitability; to be used with caution),
 - 140 stream water samples (65 selected as limited suitability; to be used with caution),
- 20 samples of precipitation (13 selected as limited suitability; to be used with caution).

Altogether, there are 502 new water samples, but not all of them with a complete chemical analysis at the time of the data Laxemar 1.2 freeze. Some of them have been considered representative for modelling purposes, see Appendix 6 in /SKB 2006a/. There are relatively few new samples from boreholes in the Laxemar subarea that were not already evaluated during the Simpevarp 1.2 phase.

9.3.1 Groundwater chemistry data sampled in boreholes

The Laxemar 1.2 hydrochemical evaluation involved data from five cored boreholes (KLX01–KLX04 and KLX06) and 14 percussion boreholes (HLX01–HLX08 and HLX10, 14, 18, 20, 22, 24) from the Laxemar subarea, three cored boreholes (KSH01A, KSH02 and KSH03A) and 4 percussion boreholes (HSH02–HSH05) from the Simpevarp peninsula, and two cored boreholes (KAV01 and KAV04A) and 10 percussion boreholes (HAV04–HAV07 and HAV09–HAV14) from Ävrö island. The borehole sampling locations are shown in Figure 2-3. The analytical programme included: major cations and anions (Na, K, Ca, Mg, Si, Cl, HCO_3^- , SO_4^{2-} , S^{2-}), trace elements (Br, F, Fe, Mn, Li, Sr, DOC, N, PO_4^{3-} , U, Th, Sc, Rb, In, Cs, Ba, Tl, Y and REEs) and stable (^{18}O , ^2H , ^{13}C , ^{37}Cl , ^{10}B , ^{34}S) and radioactive-radiogenic (^3H , ^{226}Ra , ^{228}Ra , ^{222}Rn , ^{238}U , ^{235}U , ^{234}U , ^{232}Th , ^{230}Th and ^{228}Th) isotopes, microbes, gases and colloids (cf. Appendix 6 in /SKB 2006a/).

The different analytical results obtained using contrasting analytical techniques for Fe and S have been confirmed with speciation-solubility calculations and checking their effects on the charge balance. The values selected for modelling were those obtained by ion chromatography (SO_4^{2-}) and spectrophotometry (Fe) assuming no colloidal contribution. The selected pH and Eh values correspond to available downhole data (cf. Appendix 6 in /SKB 2006a/).

9.3.2 Representativeness of the data

It has been considered, by some of the field staff and reviewers, that the evaluation approach employed for borehole groundwaters is too rigorous, determining that less than 20% of the total number of water samples are considered to be representative or suitable for the Laxemar v. 1.2 modelling, implying that there are a large number of water samples that are not used and correspondingly much information lost. This is a common and understandable misconception. In reality, all data provided by the Sicada database are available for use for all interested ChemNET analysis groups. However for each analysis group to familiarise themselves with all the data is not practical given the time constraints. Furthermore, because of the different modeling approaches, not all data are used by all the modelling groups. A comprehensive evaluation of the representativeness of samples is described in Appendix 1 in /SKB 2006a/.

The selection of 'representative' or 'suitable' values is, therefore, severalfold, for example as an aid to help provide a degree of confidence or support (or otherwise) when using or interpreting other data which may be less reliable for different reasons (e.g. incomplete analyses; lack of chemical stability during sampling; contamination etc.). It is important also to point out that to arrive at 'representative' or 'suitable' values requires using all the available hydrochemical data, and that these data are evaluated as much as possible with reference to known hydraulic conditions in: a) the borehole, b) the fracture zone sections being sampled, and c) the surrounding host bedrock. The reliability of these data is therefore judged as much as possible on prevailing hydraulic and geologic conditions during borehole drilling, monitoring and sampling.

Without the integration of hydrochemistry, geology, hydrogeology and borehole activities there would be a great danger that data could be misrepresented. An important example of this is the open hole tube sampling carried out in KLX02 in 1993 and 1997, where the hydrochemical and isotopic data collected along the borehole has been accepted and modelled as representing the evolution of formation groundwater with depth in the surrounding host rock, despite reservations related to open hole mixing as noted by /Laaksoharju et al. 1995/ and /Ekman 2001/, and more recently has been criticised during internal review. Other examples have included the use of tritium and radiocarbon data without considering closely enough: a) the possibility of induced mixing during borehole activities, b) natural dilution and radioactive decay of tritium with time when combining and comparing old and newly collected samples, c) the potential surface input of tritium from the nearby nuclear power facilities, and d) successive lowering of detection levels throughout the years.

The representativity check of the borehole groundwater samples from the Laxemar 1.2 data freeze revealed that there is only a very limited set of groundwater data suitable to be quality checked, and only very few of these available data are considered representative or suitable (highlighted in orange in Appendix 6 /SKB 2006a/), or of limited suitability but useable with caution (highlighted in green in Appendix 6 /SKB 2006a/). Most data have been deemed as unsuitable. Of course, data judged as being of limited suitability may still provide valuable information, for example: a) the use of some of the major ion analyses in hydrochemical plots, and b) observed compositional changes with time which may reflect groundwater mixing, either artificially induced by pumping and/or sampling or due to natural flow.

The absence of suitable data is attributed mainly to the very high portions of drilling fluid in many of the analysed groundwaters sampled during drilling, during pumping and injection tests, and during subsequent tube sampling. Furthermore, there are no complete sets of data comprising major elements, stable deuterium and ^{18}O , and tritium, which are the minimum requirement to evaluate the representativeness of the groundwaters in terms of, for example, charge balance and the inmixing of drilling water and near-surface groundwaters. However, even though no complete Class 5 data are available (because of some outstanding analyses), groundwaters that have major ions, TOC, D and ^{18}O , tritium and ^{14}C are rated as suitable if the charge balances are $< \pm 5\%$ and the drilling fluid $< 1\%$.

Table 9-1 refers to the Laxemar and Simpevarp subareas where the above criteria have been applied to establish the number of groundwater samples that fall into these categories. In conclusion, only seven groundwater samples from the Laxemar and Simpevarp subareas are considered suitable or of limited suitability and six of these are all from the upper part of the bedrock (0–218 m) and of dilute groundwater character. These shallow groundwaters mainly represent a recent meteoric/older

meteoric (tritium free) origin, except for KLX03: 103–218 m which is tritium free and shows inmixing of a cold climate recharge water component. One sample included is from greater depth (KAV04A; 245–293 m) and is of brackish character although it contains a substantial drilling water component (12.3%). It is suitable for major ion chemistry use but, for example, is not recommended for tritium analysis use, since the sample has been influenced by the drilling water.

All tube samples from KLX03 and KLX04 are lacking stable isotope data and tritium analyses, which means that even young dilute groundwaters with a relatively low percentage of drilling water (< 10%), can consist of modern meteoric, older meteoric or glacial water of unknown proportions.

Groundwaters with higher chloride contents are detected at depth in all the boreholes but these samples are characterised by: a) excessive amounts of drilling water, or b) an incomplete set of analyses, and c) mixing of different groundwater types along the borehole lengths (e.g. KAV04A).

In conclusion, the tube samples from all four sampled cored boreholes (KAV01, KAV04A, KLX03 and KLX04) are judged as unsuitable due to the reasons given above. In addition, the KLX03 and KLX04 tube samples, based on information from the differential flow measurements, show significant differences in the behaviour of the electrical conductivity profiles versus depth. The difference in values resulting from pumping compared to without pumping indicate generally higher electrical conductivity during pumping. The tube samples, which are collected under natural flow conditions (i.e. equivalent to without pumping) in the open borehole, therefore do not reflect the maximum salinity recorded during pumping. Instead, the tube samples indicate mixing of groundwaters of different origin, especially inmixing of near-surface groundwaters and, in many cases, extremely high portions of drilling water. It is therefore strongly recommended not to use the tube samples in the detailed modelling exercises, as they probably reflect a perturbed groundwater system and may give, for example, erroneous indications of near-surface groundwaters at great depth that do not reflect initial, undisturbed conditions. The tube samples are helpful when comparing open borehole chemistry and conditions, checking temporal variability and for reflecting the general geochemical depth trends.

The general uncertainty surrounding tube sampling has also been extended to borehole KLX02. Tube hydrochemical data from KLX02 have been consistently used over many years in several of the evaluation and modelling exercises. Even though there is a reasonably close correlation with some of the data from packed-off borehole sections, and a general absence of drilling water, there are some discrepancies (e.g. tritium; sulphate) which can be attributed to open hole mixing. Consequently, selected tube hydrochemical data have been highlighted green in the Laxemar 1.2 data freeze table indicating limited suitability and to be used with caution. For example, in the majority of the ion-ion plots and for much of the water/rock geochemical equilibrium modelling these data have been excluded altogether.

Table 9-1. Groundwater samples from the Laxemar and Simpevarp subareas rated with regards to suitability for analysis.

Water sample (metres depth)	Suitable	Limited suitability	Comment
HLX 10: 0–85	Yes		Class 3
HLX14: 0–115.90	Yes		Class 5
HLX20: 0–200.20		Yes	Class 5 No ² H and ¹⁸ O available
KLX03: 103–218	Yes		Class 3
KLX04: 103–213		Yes	Class 3 Drilling fluid 7.76%
KAV04: 0–100	Yes		Class 5
KAV04: 245.85–295.05		Yes	Class 3 Drilling fluid 12.37%

9.4 Explorative analysis

A commonly used approach in groundwater modelling is to commence evaluation by explorative analysis of different groundwater variables and properties. The degree of mixing, the type of reactions and the origin and evolution of the groundwater can be indicated by applying such analyses. Also of major importance is to relate, as far as possible, the groundwaters sampled to the near-vicinity geology and hydrogeology.

The results from drillcore mapping, BIPS measurements, differential flow measurements and electrical conductivities, together with groundwater quality and representativeness of the samples, are discussed in detail for all investigated boreholes in /SKB 2006a, cf. Appendix therein/. The major geological, hydrogeological and chemical borehole logs and measurements are presented in Appendix 4 and represent an important integration/comparison tool between chemistry and the other disciplines.

9.4.1 Examples of evaluation of scatter plots

The hydrochemical data have been expressed in several X-Y plots to derive trends that may facilitate interpretation. The hydrogeochemical evaluation presented below shows only a few examples of the chain of analysis employed in the systematic approach described in Appendix 1 in /SKB 2006a/ with traditional plots to group the main groundwater types characterising the Simpevarp area and to identify general evolution or reaction trends. A complete and very detailed evaluation of the major components and isotopes can be found in Appendices 1 and 3 in /SKB 2006a/. A discussion of many of the reactive elements is presented in the modelling part of this report and also in Appendix 3 in /SKB 2006a/.

Chloride depth trends

The Laxemar subarea data shows mostly dilute groundwaters (< 2,000 mg/L Cl) extending to at least 275 m in KLX01 and to around 500–600 m for boreholes KLX03 and KLX04 situated in the central part of the Laxemar subarea. In borehole KLX02, dilute groundwater was detected down to 800 m before a rapid increase in salinity to maximum values of around 47 g/L Cl at 1,700 m (Figure 9-2). The Simpevarp subarea data shows a higher level of salinity at shallow depths (brackish to around 5,000 mg/L Cl at approx. 300 m depth), more saline at intermediate depths (up to 10,000 mg/L Cl at 700 m) and also a more systematic increase to around 850 m (to a maximum of ~ 17,000 mg/L Cl) when compared with the Laxemar subarea.

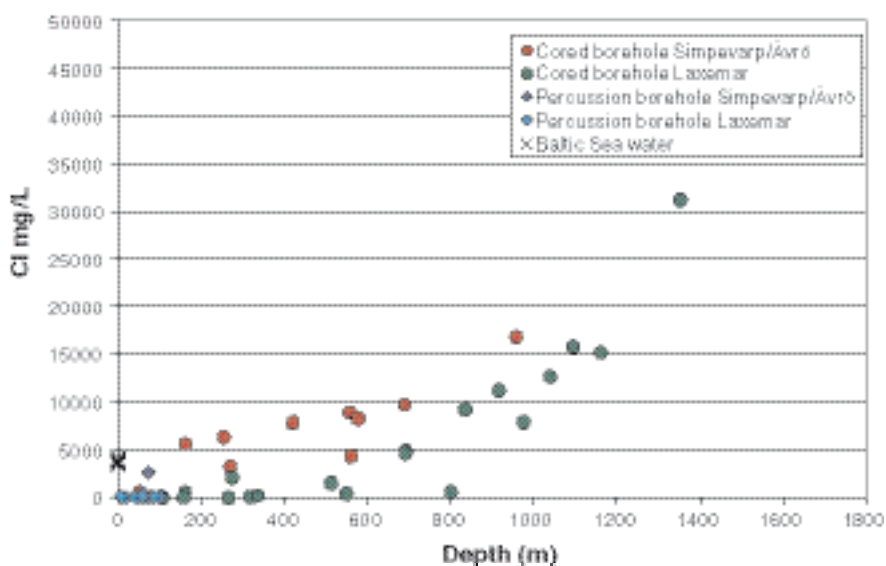


Figure 9-2. Depth (depth along boreholes) variation of chloride in the Simpevarp and Laxemar subareas.

Bicarbonate versus depth

Figure 9-3 plots bicarbonate concentration against depth. The plot shows the expected rapid decrease in bicarbonate from organic decomposition with increasing depth and correspondingly with increasing chloride. The small deviations or scatter in the depth trends associated with some of the cored boreholes in the Laxemar subarea may reflect on one hand the differing hydrogeology at the borehole locations sampled, and on the other hand possibly some effects of open hole mixing.

Magnesium versus chloride

Figure 9-4 shows the relationship of magnesium against chloride and underlines the generally higher magnesium contents in samples from the Simpevarp subarea (to ~ 70 mg/L) corresponding to more brackish conditions (3,000–7,000 mg/L Cl) and possibly suggesting a small Littorina Sea or older seawater component. Over the same range of salinity, the Laxemar groundwaters show generally very low Mg values (≤ 15 mg/L) except for a small magnesium increase to 30 mg/L Cl recorded in borehole KLX01, before decreasing to near zero values at higher salinities (~ 15,000 mg/L Cl).

Oxygen-18 versus deuterium and Cl

Figure 9-5 details the stable isotope data most of which plot on or close to the Global Meteoric Water Line (GMWL) indicating a meteoric origin. With respect to increasing depth (and therefore salinity) these stable isotope data indicate: a) shallow dilute groundwaters ranging from $\delta^{18}\text{O} = -10.9$ to -9.8‰ SMOW, $\delta\text{D} = -78.7$ to 67.1‰ SMOW, b) brackish to saline groundwaters ranging from $\delta^{18}\text{O} = -14.0$ to -11.7‰ SMOW, $\delta\text{D} = -100.0$ to -86.2‰ SMOW, and c) highly saline from $\delta^{18}\text{O} = -11.7$ to -8.9‰ SMOW, $\delta\text{D} = -78.6$ to -47.4‰ SMOW. There is a degree of overlap between a) and c) because of groundwater mixing and no obvious cold climate recharge signature. In contrast, the lighter $\delta^{18}\text{O}$ values of the brackish groundwater group (b) indicate the presence of a cold recharge meteoric component (glacial melt water inter-actions). This is further illustrated in Figure 9-6 by plotting $\delta^{18}\text{O}$ against chloride, especially the brackish nature of the groundwaters characterised by light isotope cold climate signatures. The limited data suggest there is no major Baltic Sea influence on the sampled groundwaters. One distinguishing feature is the characteristic deviation trend from the GMWL (i.e. the two highly saline groundwaters from -9.7 to -8.9‰ SMOW, $\delta\text{D} = -61.7$ to -47.4‰ SMOW) which appears to increase with increasing salinity. A similar deviation has been reported from the deep Canadian basement brines which has been discussed, among others, by /Frape and Fritz 1987/ who considered this as an indication of very intensive water/rock inter actions during long residence times.

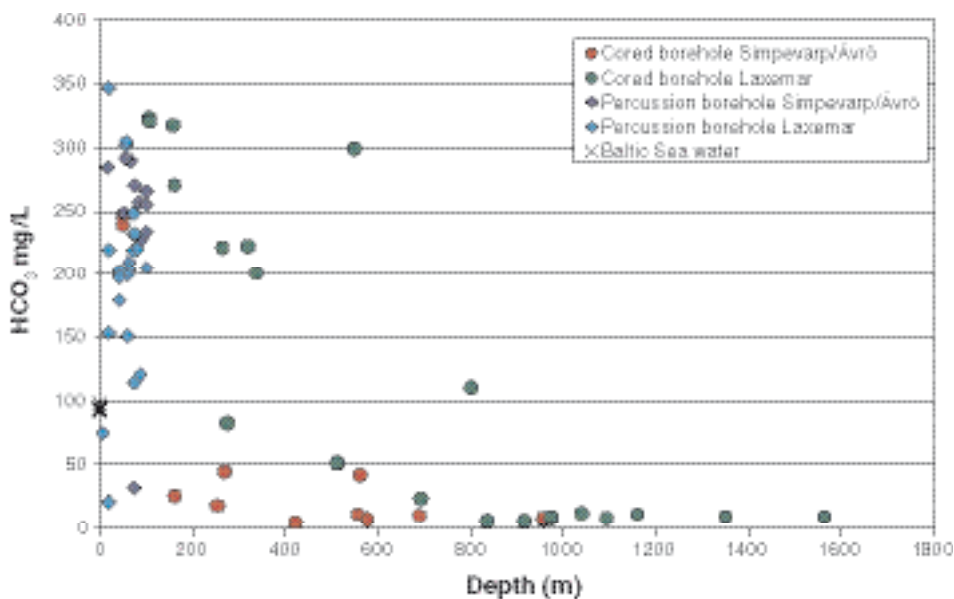


Figure 9-3. Plot of HCO_3^- vs depth (depth along boreholes) for the Simpevarp and Laxemar subareas.

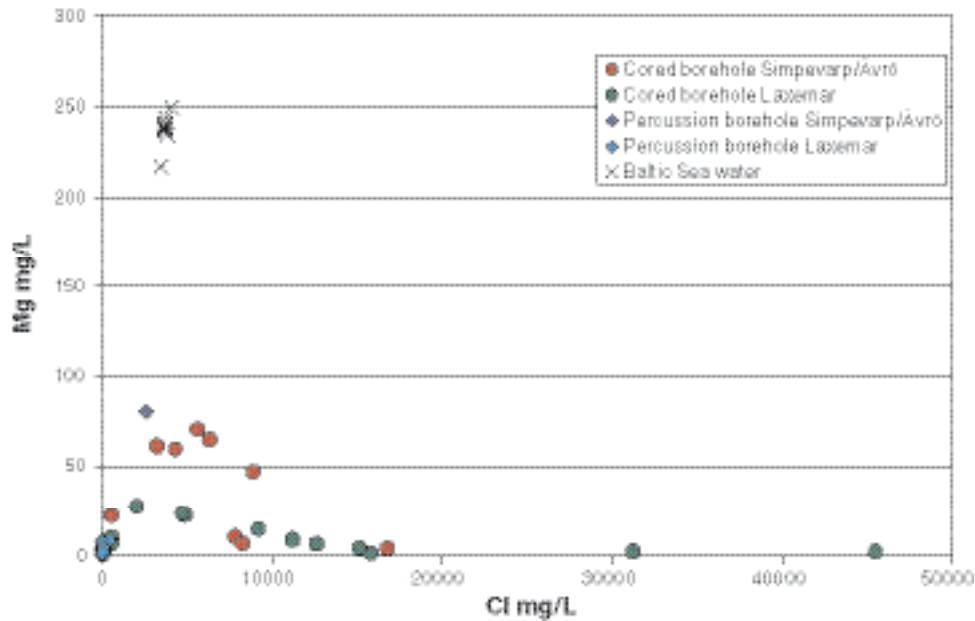


Figure 9-4. Plot of Mg vs Cl for the Simpevarp and Laxemar subareas.

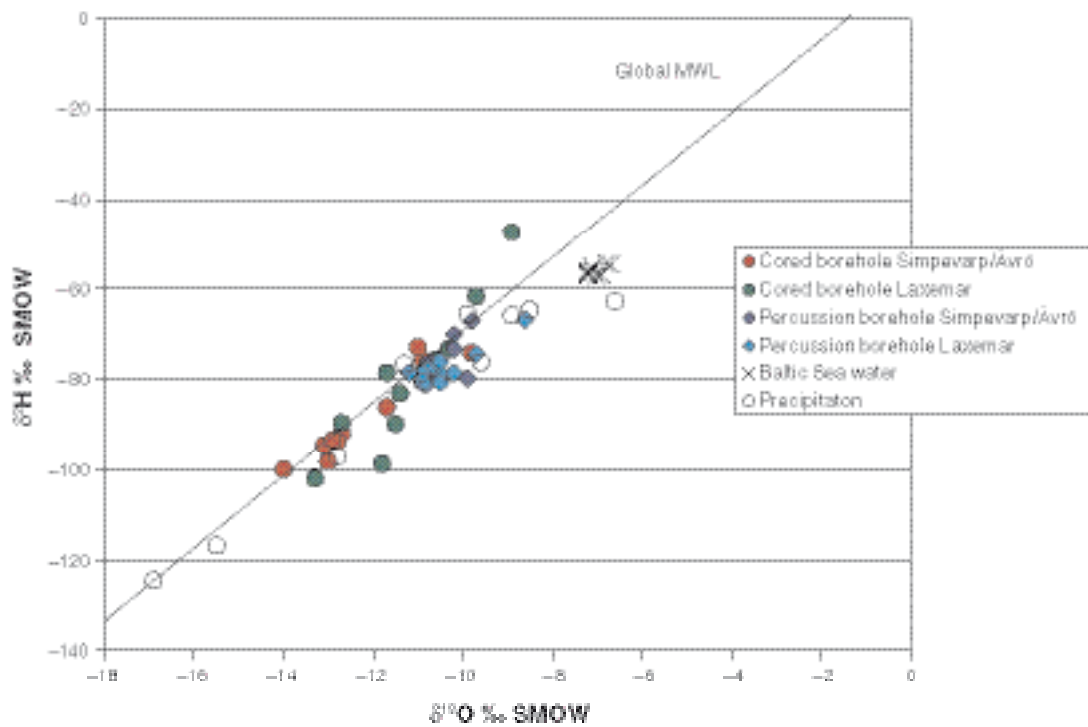


Figure 9-5. Plot of $\delta^{18}O$ vs δD for the Simpevarp and Laxemar subareas (Global Meteoric Water Line is indicated).

9.4.2 Descriptive observations – main elements

The site descriptive observations provided in this section are based on the detailed data evaluation presented in /SKB 2006a, cf. Appendix 1 therein/. The overall depth trends show increasing TDS with increasing depth. There are significant differences in “depth trends” between the two subareas; in Simpevarp, the upper fresh water regime (mostly Na-HCO₃) reaches only to approx. 150 m, whereas, in the central parts of the Laxemar subarea, fresh water is found down to 500 m and in some cases as deep as 800 m.

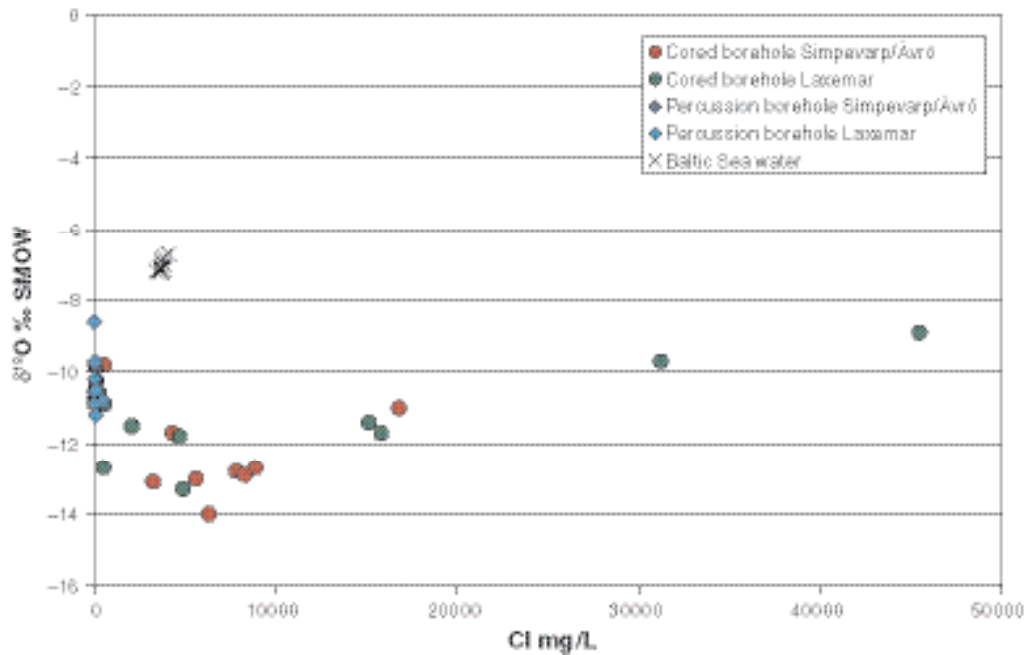


Figure 9-6. Plot of $\delta^{18}\text{O}$ vs Cl for the Simpevarp and Laxemar subareas

Ca/Na ratios increase markedly with depth and also illustrate differences between the two subareas down to around 1,000 m. The Simpevarp subarea saline groundwaters (~ 10,000–20,000 mg/L Cl) show a more Na-rich trend (Na-Ca-Cl dominant) compared with the Laxemar groundwaters which are more Ca-rich (Ca-Na-Cl dominant). Generally, at depths exceeding 1,000 m, higher saline Ca-Na-Cl groundwaters dominate in both areas.

At a more regional scale, deep groundwaters in the Simpevarp subarea and Äspö HRL (down to 1,000 m) are probably Na-Ca-Cl in type; for example, deep groundwaters at a borehole drilled in the town of Oskarshamn (KOV01; 1,000 m) and in the Laxemar subarea (1,300 to 1,700 m) are Ca-Na-Cl in type. Since Laxemar is inland and Oskarshamn is close to the coast, this should be an indication of discharging very deep groundwater at Oskarshamn. At greater depths below the Simpevarp subarea and Äspö HRL than presently sampled, Ca-Na-Cl groundwaters are expected to dominate.

Br/Cl ratios indicate an absence of marine signatures in the Laxemar subarea; all ratios are significantly higher than marine. Contrastingly, in the Simpevarp subarea, lower ratios indicate a weak but significant marine signature. Borehole KLX01 (the easternmost of the Laxemar boreholes) shows, however, a close to marine Br/Cl ratio at 272–277 m.

A clear marine signature (in terms of high Mg values, marine Br/Cl ratios and relatively high $\delta^{18}\text{O}$ values) is rare, but a small set of samples with a possible Littorina Sea signature do exist from 150–300 m depth sampled in fracture zones close to the Baltic Sea. In addition, there also seems to be a small marine input (Littorina or older), distinguished by slightly higher Mg values and lower Ca/Na ratios, in the Simpevarp subarea waters which is absent in the Laxemar subarea (with the exception of the upper 700 m in KLX01 which shares similarities to the Simpevarp samples).

The plot of $\delta^{18}\text{O}$ versus Cl indicates a contribution of cold climate or glacial melt waters to the brackish (i.e. 2,000–10,000 mg/L Cl) and deeper saline (i.e. 10,000–20,000 mg/L Cl) groundwater samples.

The SO_4 contents vary considerably within the brackish and saline groundwaters. Microbially mediated sulphate reduction, traced as high $\delta^{34}\text{S}$ (> 20‰ CDT or Cañon Diablo Troilite), is taking place not only in brackish waters but also in some fresh waters (i.e. those from KLX03 and HLX 14).

The SO_4 contents in the more highly saline groundwaters indicate in-mixing of SO_4 from deep brine waters, which in turn may have reached their high SO_4 content through leaching of sediments and/or dissolution of gypsum previously present in fractures. The presence of gypsum in sealed fractures in a few places within the site supports gypsum as a possible source for SO_4 in the deep groundwaters.

9.4.3 Descriptive observations – isotopes

The isotope data from borehole samples are still relatively few and not very much new information has been forthcoming since the Simpevarp 1.2 model version; see Appendix 1 in /SKB 2006a/. However, tritium has been given much attention together with ^{14}C since they represent isotopes of great interest for groundwater modelling. Furthermore, they also provide the possibility to assess potential contamination from the nearby power plants.

Tritium

Tritium data from precipitation, surface stream and lake waters, and sea water localities were studied with respect to their distribution, content and origin. It can be concluded that:

- Generally there is a spread in values between 8.5 to 19 TU for surface water localities which is almost equal to the variation in the precipitation (9–19 TU), i.e. the input term.
- The highest mean value is found in the Baltic Sea samples, with the highest contents (mean of 15.1 TU) in the samples from east of Kråkelund, north of Simpevarp.
- The highest values for the lake and stream waters are found in the eastern part of the Simpevarp area, but the mean values only deviate by 1–1.3 TU (11.4 compared with the highest value of 12.6 TU).

The question now to be addressed is how much of the tritium is due to fall-out contamination from the nuclear power plant? Present day contamination, although small, should be more apparent following the systematic decrease of global tritium values during the past five decades. Consequently, continued sampling of surface waters for tritium analyses is recommended with particular attention to surface water samples taken: a) close to the cooling water outlet of the nuclear power plant, b) close to the power plant, and c) some 100 km away, preferably down/upwind wind from the power plant.

The tritium values from the cored boreholes are few and only two values from the Laxemar subarea are available, representing relatively shallow sampling sections; KLX03: 103–218 m and KLX04: 103–213 m. The KLX04 sample shows values similar to HLX10; tritium close to 4 TU and $\delta^{18}\text{O}$ values around -11‰ SMOW. Both are dilute meteoric waters. The KLX03 sample, in contrast, shows tritium levels close to the detection limit (0.8 TU) and with a significantly lower $\delta^{18}\text{O}$ value (-12.7‰ SMOW) indicating a possible older cold climate meteoric water component. This water is less dilute, having a Cl content of 507 mg/L.

All the new samples analysed for tritium with chloride contents $> 5,000$ mg/L from the Simpevarp peninsula showed values below the detection limit when tube samples and samples with high contents of drilling fluid are excluded (cf. Figure 9-7). These samples are from depths of 150 m and deeper. This indicates that modern water (< 45 years) has reached a depth of about 150 m at the Simpevarp peninsula. Other analysed groundwaters (0–218 m) show low chloride contents and variable tritium contents. Old values analysed before year 2000 from Laxemar at depths > 200 m show tritium contents less than 10 TU which indicates that these values are lower than modern recharge values. However, the increased tritium in these samples is an indication of water portions from around 1960 (cf. Section 9.6).

Unfortunately, the number of new suitable groundwater samples analysed for tritium to date are very few and the possibility of evaluation is therefore highly restricted.

Tritium and Carbon-14

Tritium was also related to the regional distribution of carbon-14 in the analysis presented in /SKB 2006a, cf. Appendix 1 therein/. This indicated that Baltic Sea samples show the highest ^{14}C values (around 105 to 110 pmC or percentage modern carbon) which means that they have either some residual bomb test ^{14}C or, in common with the tritium values, contain a modern contribution from the nuclear power plant emissions resulting in higher than background values. Most of the lake and stream waters show values ranging from 60 to 100 pmC, accompanied by high tritium values (~ 8 –15 TU). With the exception of two samples (45 and 55 pmC), the soil pipes show values within the same interval as the surface waters. The percussion and cored boreholes show decreasing tritium contents with decreasing ^{14}C , i.e. waters with very low tritium reflect also the lowest ^{14}C values (around 30 pmC).

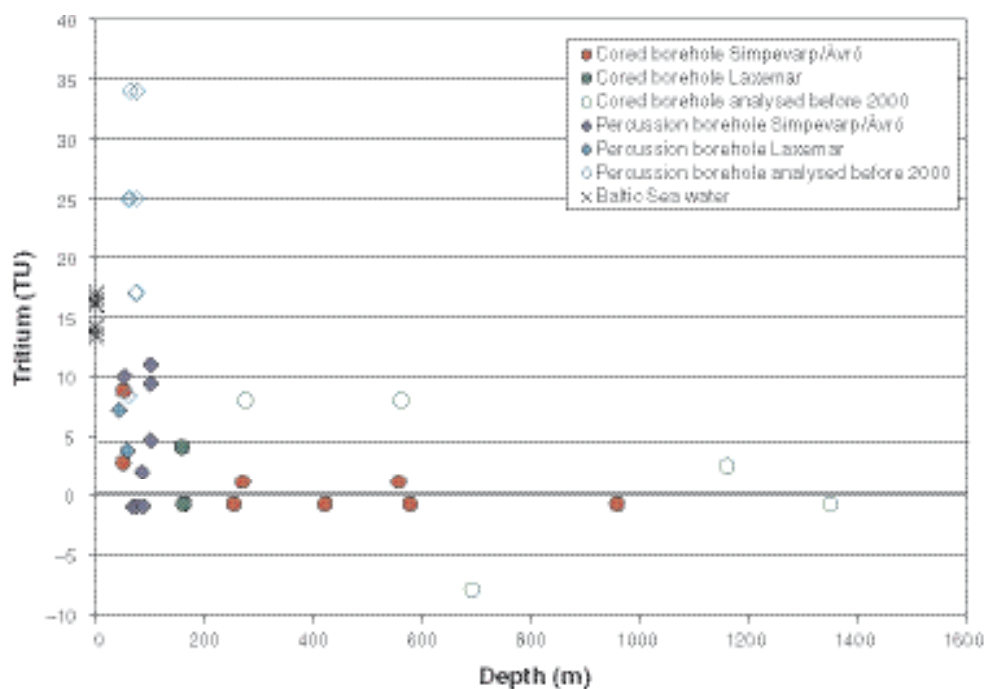


Figure 9-7. Tritium (TU) versus borehole depth (m) for surface waters and groundwaters from the Simpevarp and Laxemar subareas. Tritium values below detection limit (0.8 TU) are shown as negative values. Old analytical values from Laxemar with a detection limit of 8 TU are shown for comparison.

Carbon

All samples analysed for ^{14}C were also analysed for stable carbon isotope ratios (given as $\delta^{13}\text{C}$ ‰ PDB) (Appendix 1 in /SKB 2006a/). These $\delta^{13}\text{C}$ ratios, together with HCO_3^- contents, are commonly used to evaluate possible processes that have taken place resulting in ^{14}C changes in the groundwater.

Waters in equilibrium with atmospheric CO_2 show high $\delta^{13}\text{C}$ values (0 to -3 ‰ PDB); this is exemplified by the Baltic Sea samples.

Incorporation of biogenic CO_2 produced by breakdown of organic material of variable age, lowers the $\delta^{13}\text{C}$ values significantly; this is well illustrated by the surface waters which show significantly lower $\delta^{13}\text{C}$ values (-12 to -24 ‰).

The ^{14}C values of most of these waters are relatively high (although somewhat lower than the Baltic Sea values) and it is probable that the organic source for the CO_2 is young, although some dilution with ‘dead carbon’ (^{14}C free) has occurred. Some surface waters and most of the percussion and cored boreholes show similarly low $\delta^{13}\text{C}$ values but significantly lower ^{14}C values.

In particular, the shallow groundwaters from the percussion boreholes and the two samples from KLX03: 103–218 m and KLX04 103–213 m show high HCO_3^- contents (174 to 318 mg/L) and ^{14}C contents in the range of 70 to 40 pmC. Several explanations for the decrease of ^{14}C are possible: 1) dissolution of calcite has contributed ^{14}C -free carbon to the HCO_3^- , or 2) CO_2 has been produced from older organic material, or 3) these waters are old and very little ^{14}C has been contributed during a long period of time. The combination of all these factors is possible for the groundwater samples. The fracture calcites show no homogeneous $\delta^{13}\text{C}$ -values and it is therefore not possible to model calcite dissolution as a mixing of two end members.

Sulphur

Sulphur isotope ratios, expressed as $\delta^{34}\text{S}$ ‰ CDT, have been measured in dissolved sulphate in Baltic Sea waters, surface waters and groundwaters from the Simpevarp and Laxemar subareas (Appendix 1 in /SKB 2006a/). The recorded values were found to vary within a wide range (-1 to $+48$ ‰ CDT) indicating different sulphur sources for the dissolved SO_4^{2-} , for example:

- For the surface waters and most of the near-surface groundwaters (soil pipes) the SO_4^{2-} content is usually below 25 mg/L and the $\delta^{34}\text{S}$ is relatively low but variable (-7 to $+15\%$ CDT) with most of the samples in the range 0 – 10% CDT. These relatively low values indicate that atmospheric deposition and oxidation of sulphides in the overburden is the origin for the SO_4^{2-} . There is a tendency towards lower $\delta^{34}\text{S}\%$ CDT with higher SO_4^{2-} contents in these waters but the variation is large.
- The Baltic Sea waters cluster around the 20% CDT marine line but show a relatively large spread ($+16$ to $+23\%$ CDT). The reason for this is not fully understood but suggestions include: a) contribution from land discharge sources (e.g. streams) to various degrees (low values), and b) potential bacterial modification creating high values in the remaining SO_4^{2-} .
- The borehole groundwaters show $\delta^{34}\text{S}$ values between $+11.8$ to $+48.2\%$ CDT with most of the samples in the range $+15$ to $+25\%$ CDT. Values higher than marine ($> 20\%$ CDT) are found in samples with Cl contents $< 6,500$ mg/L Cl. These latter values are interpreted as a product of sulphate reduction taking place in situ. The two highest values ($+32$ and $+48\%$ CDT) are detected in waters where SO_4^{2-} contents are low (around 30 mg/L) and the Cl contents 70 and 503 mg/L, respectively. Such extreme $\delta^{34}\text{S}$ values as $+48\%$ CDT are strong indicators of closed, stagnant conditions.
- The groundwaters with higher salinities, all from the Simpevarp peninsula, share lower $\delta^{34}\text{S}$ but higher SO_4^{2-} contents. The reasons are uncertain and more information is needed. Possible explanations include dissolution of, for example, gypsum, or inmixing of very deep saline water which in turn has received contributions of sulphate from leaching of sediments etc. The deep and intermediate groundwaters are very reducing and non-corroded pyrite is present in the fractures so that oxidation of sulphides in these groundwaters seems not to be a plausible explanation.

Strontium

Available Sr isotope information from the Baltic Sea waters, near surface waters and groundwaters, show two or possibly three separate correlations between Sr isotopes and $1/\text{Sr}$ and Cl contents (Appendix 1 in /SKB 2006a/):

- Large variation in Sr ratios but relatively small variation in Sr content for the near-surface groundwaters indicating interaction (leaching) from overburden of different mineralogical compositions.
- Large variation in Sr content but small variation in Sr isotope ratios for the fresh groundwaters indicating homogenisation of the Sr isotope ratios due to mineral/water interactions along the flow paths (mainly ion exchange).
- Tendency towards higher Sr isotope ratios with increasing Sr content for the saline samples possibly as a result of more stagnant conditions.

Boron

Enhanced $\delta^{11}\text{B}$ has been used as an indicator of permafrost conditions as it appears to become isotopically enriched in the fluid phase during freeze-out conditions (Appendix 1 in /SKB 2006a/). For example, deep saline groundwaters characterised by negative $\delta^{18}\text{O}$ values tend to correlate with high ^{11}B values.

Since the boron isotope data are sporadic, initial scoping plots have been made using all data where both $\delta^{11}\text{B}$ and $\delta^{18}\text{O}$ have been analysed. Almost all of the $\delta^{11}\text{B}$ data in the Simpevarp area plot between 20 – 60% which is in agreement with earlier published data from Fennoscandia including the Äspö HRL. Of interest are three anomalously high $\delta^{11}\text{B}$ (80 – 110%) cored borehole outliers from the Simpevarp subarea (KSH01A: 556 m, KSH02: 422 m and KSH02: 578 m). Otherwise, the remaining borehole data fall within the same $\delta^{11}\text{B}$ range.

Plotting $\delta^{11}\text{B}$ against $\delta^{18}\text{O}$ couples these three Simpevarp cored borehole groundwaters with high $\delta^{11}\text{B}$ to somewhat lighter $\delta^{18}\text{O}$ values (-12.9 to -12.7% SMOW). According to the literature /e.g. Casanova et al. 2005/, this is consistent with the possibility that these groundwaters might reflect freeze-out processes which occurred under permafrost conditions.

9.4.4 Microbes

Microbes have been evaluated from the Simpevarp area (Appendix 2 in /SKB 2006a/). There are still rather few data from the Laxemar subarea and therefore the model reflects only the regional scale Simpevarp area. The model shows (Figure 9-8), that the dominating microbial process in ‘The anaerobic subsurface zone’ is heterotrophic sulphate reduction. This zone is found at depths from 100 to 500 m, ‘The deep sulphate reducing zone’ is found at about 600 to 900 m, and ‘The deep autotrophic zone’ is found from 1,000–1,400 m. There are indications of possible ongoing iron reduction and heterotrophic acetogenesis but this must be verified by thorough MPN-studies (most probable number of microorganisms is a statistical cultivation method for numbering the most probable number of different cultivable groups of microorganisms). The possible origin of carbon dioxide and hydrogen gas in this zone from ‘The deep chemosphere’ also requires to be verified with stable isotope studies of the gas in the groundwater.

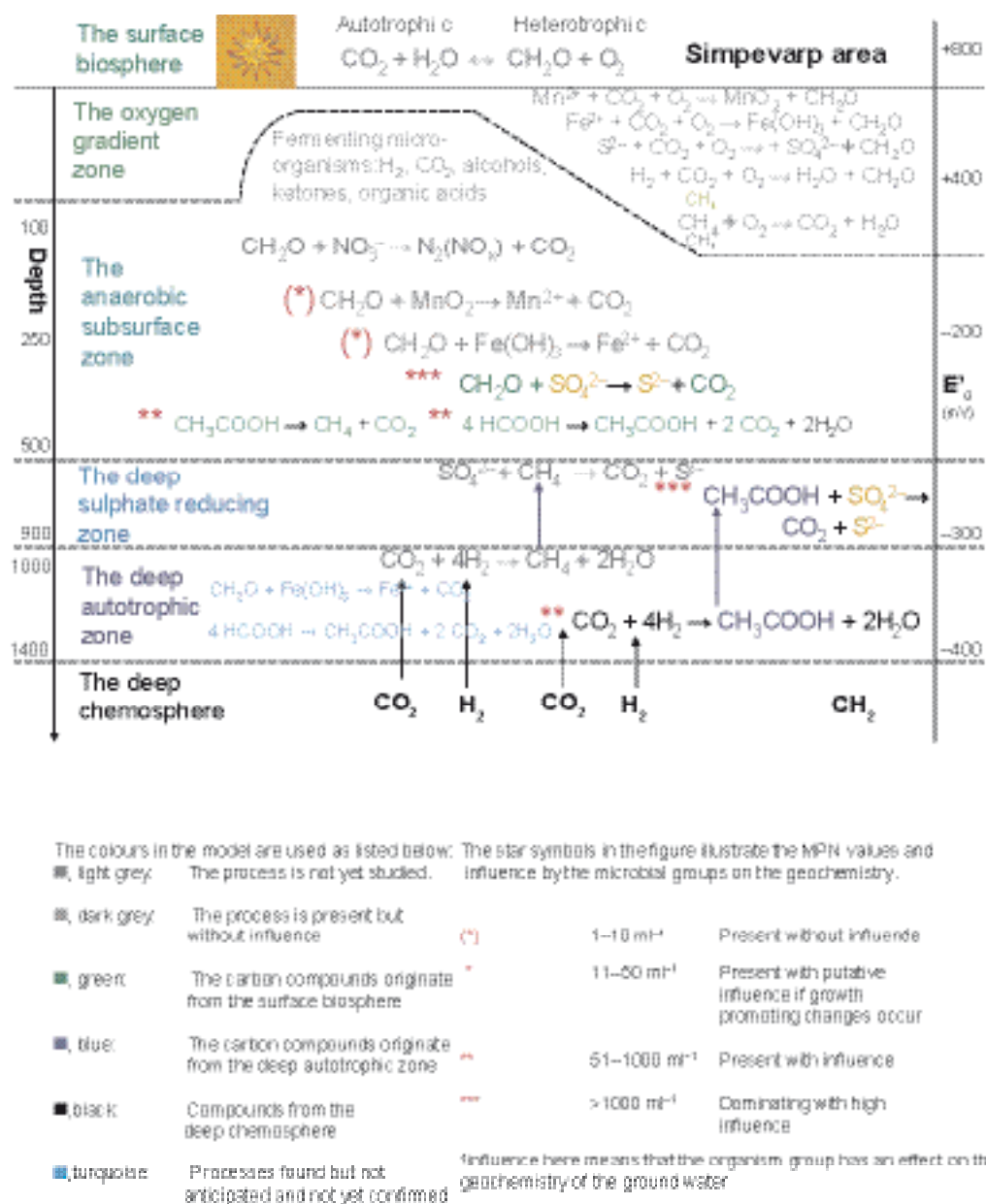


Figure 9-8. The microbial model of the Simpevarp area (regional scale) based on data available at the time of the Laxemar 1.2 data freeze. The star symbols before the reactions depict the significance of the reaction.

The following conclusions can be drawn.

- In the (regional scale) Simpevarp area three of the proposed zones in the subsurface microbial model have been identified: the anaerobic subsurface zone at least from 100 to 500 m, the deep sulphate-reducing zone between 600 and 900 m and the deep autotrophic zone from 1,000 to at least 1,400 m. The depths have to be seen as preliminary.
- In the anaerobic subsurface zone, sulphate-reducing bacteria, heterotrophic methanogens and heterotrophic acetogens are the dominating microorganisms.
- In the deep sulphate-reducing zone, acetate oxidation has been observed but no methane oxidation.
- In the deep autotrophic zone, autotrophic acetogens have been observed.
- The very few available data on microorganisms attached to the bedrock and production of hydrogen sulphide under optimal conditions indicate that the attached microorganisms in a 1 mm wide fracture can produce up to 1,000 times more hydrogen sulphide per day than unattached microorganisms.

9.4.5 Colloids

Colloid compositional data have been evaluated from the Simpevarp area (Appendix 2 in /SKB 2006a/). Particles in the size range 10^{-3} to 10^{-6} mm are regarded as colloids; their small size precludes them settling which renders them as a potential radionuclide transport mechanism in groundwater. The aim of the colloid study was to quantify and determine the composition of colloids in groundwater from boreholes, and to include the results in the hydrochemical modelling of the site.

In evaluating the background colloid values of the groundwaters, the amount of colloids versus depth was studied. It can be seen in Figure 9-9 that the amount of colloids was greatest in borehole KLX01: 458.5 m with $92.03 \mu\text{g l}^{-1}$, due to high amounts of aluminium colloids. The most plausible explanation is contamination from drilling activities when aluminium silicate colloids are released from the bedrock during the grinding and pumping. The other data range from around 13 to $33 \mu\text{g l}^{-1}$ with the most recent data from borehole KSH01A recording the lowest amounts. Since there are only two samples from this study, it is difficult to speculate on an explanation for this, but an improved sampling technique is a possible suggestion.

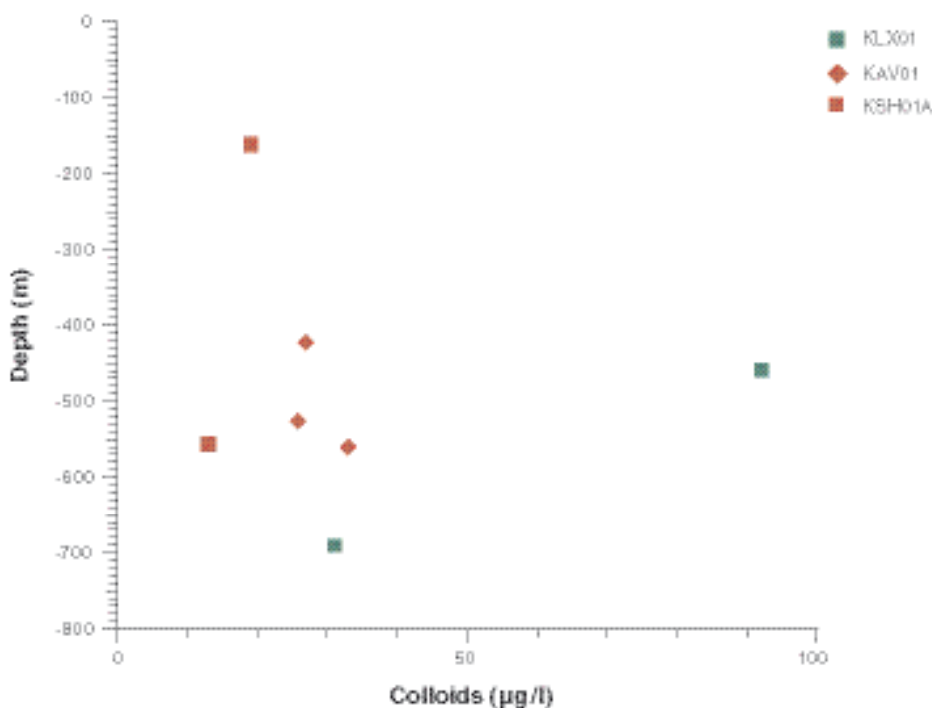


Figure 9-9. Colloids ($\mu\text{g l}^{-1}$) plotted versus depth in samples from boreholes KLX01, KAV01 and KSH01A in the Simpevarp area.

Generally, the average amount of colloids in this study was 23.1 with a standard deviation of $\pm 7.14 \mu\text{g l}^{-1}$ if the value from KLX01: 458.5 m is omitted. These values agree very well with data reported from colloid studies in Sweden (20–45 $\mu\text{g/l}$) and Switzerland (30 ± 10 and $10 \pm 5 \mu\text{g l}^{-1}$) /Laaksoharju et al. 1995, Degueldre 1994/ but about ten times lower than reported from Canada ($300 \pm 300 \mu\text{g l}^{-1}$) /Vilks et al. 1991/.

9.4.6 Gases

There were no new gas analyses available for version 1.2 except for data already reported in /SKB 2005a/.

9.4.7 Pore water composition in the rock matrix

In crystalline rocks, the pore water resides in the low-permeability zones (rock matrix) between principal water-conducting zones related to regional or local fracture networks. Depending on the residence time of water in these hydraulically active zones, interaction with water present in the pore space of the low-permeability zones might become significant. In addition, the pore water present in the low-permeability zones will be the first to interact with any artificial construction made in such zones (i.e. repository). It is therefore important to know the composition of such pore waters. An estimation of the evolution of this composition with time may be made by combining the information gained from pore water profiles determined over a low-permeability zone, with the chemical and isotopic data of water circulating in the fractures. The pore water studies are described in detail in /SKB 2006a, cf. Appendix 1 therein/.

In situ pore water that resides in the pore space between minerals and along grain boundaries in crystalline rocks of low permeability has been extracted successfully by laboratory out-diffusion methods using drillcore samples from borehole KLX03 from the Laxemar subarea. The obtained experimental solutions have been characterised chemically and isotopically and related to the in situ pore water composition of the rock, which, in turn, was related to the present and past formation groundwater evolution of the site. In addition, the method of extraction, together with associated measurements of interconnected porosity, provided the opportunity to derive diffusion coefficient values of potential use in predicting future rates of solute transport. Because of the very small volumes of pore water extracted, and the possibility of rock stress release occurring during drilling, which might lead to contamination by drilling fluid and also affect the derivation of rock porosity values, great care was taken to avoid such problems or, at least further understand their repercussions.

The results show that chloride concentrations in pore water and formation groundwater of the Ävrö granite are similar down to about 500 m depth suggesting steady state conditions between pore water and groundwater (Figure 9-10). This situation would change slightly at shallow levels when taking into account an assumed arbitrarily decreased water content due to stress release, in that the pore water at the most shallow levels would have higher chloride concentrations than the formation groundwater sampled at the same depth. Unfortunately, no formation groundwater could be sampled from the interval around 600 m where the pore water chloride concentrations are highest in the entire profile.

At increasing depth in the borehole (i.e. near the top of the quartz monzodiorite) the pore water becomes more dilute than the formation groundwaters in the fractures suggesting that the pore water retains an older signature. Interestingly, this dilute pore water is not associated with an isotopic composition of glacial melt water, which might initially be expected. Below about 800 m the chloride concentration of the pore water once again becomes similar to that of the formation groundwaters in the fractures (as does the overall chemical type), in common with the shallower levels described above and also in conjunction with an increase in transmissivity at around 750 m. The pore water differs significantly, however, in chloride content and chemical type from the deepest formation groundwater sampled. Chloride concentrations similar to this deep formation groundwater could be roughly reached if the already very low measured water content of the samples is arbitrarily decreased by 50% assuming stress release.

The characterisation of matrix rock pore water from the Laxemar borehole KLX03 resulted in the following main conclusions:

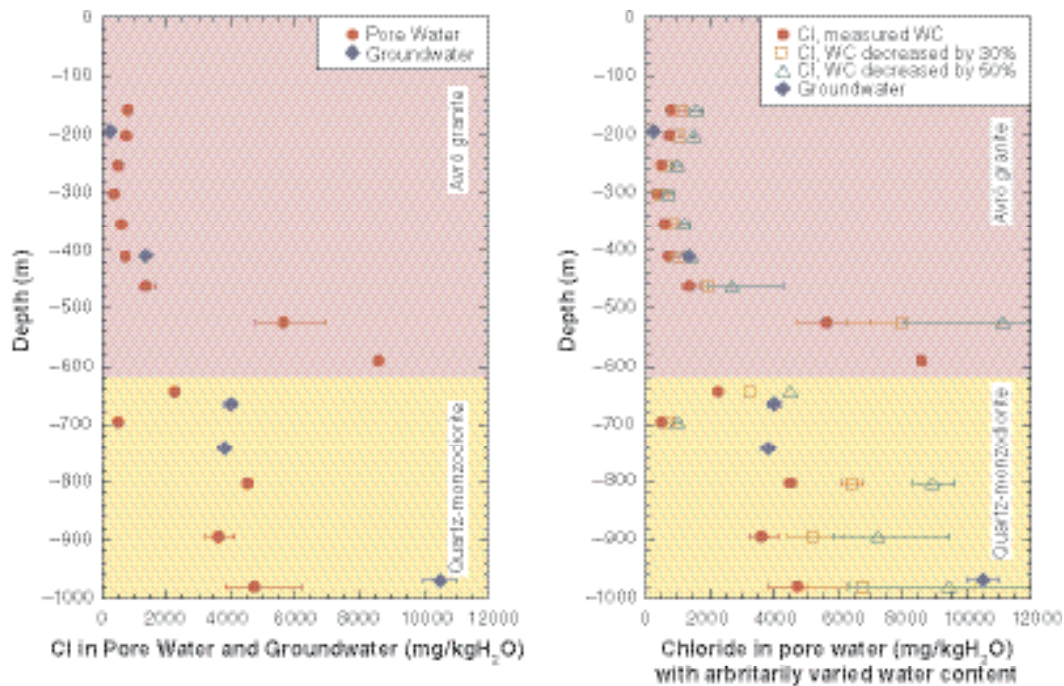


Figure 9-10. Chloride concentrations of matrix rock pore water from borehole KLX03 compared with groundwaters sampled from adjacent fractures as a function of sampling depth (left) and the same comparison with pore water chloride concentration calculated with arbitrarily decreased water contents to evaluate stress release effects (right; WC = water content).

- Independent derivation of water content (to calculate (water content) porosity) by drying and isotope diffusive exchange methods gave consistent results excluding artefacts such as desaturation of the samples.
- There is multiple evidence that stress release has occurred, however its potential effect on water content porosity values and related drilling water contamination does not appear to have significantly affected the rock samples.
- The uncertainties surrounding the possibility of stress release effects were addressed by calculating the hypothetical variation in water content using a change of 50% by stress release; this would essentially increase the pore water chloride by a factor of 2. It is shown that such an increase would be inconsistent with determined parameters independent of water content measurements.
- Diffusion between rock pore water and adjacent formation groundwater-bearing fractures and fracture zones, and *vice versa*, is identified as the dominant transport process; calculated diffusion coefficients agree well with present-day knowledge from the Laxemar site.
- Chemical and isotopic pore water signatures are characteristic and show a variation of groundwater composition with rock type and depth. In the Ävrö granite, shallow (< 450 m) and intermediate (450–600 m) zones can be distinguished. The pore water in the quartz monzodiorite indicates three zones (600–750 m, 750–850 m, and 850–1,000 m); this is in close agreement with the general trends in hydrochemistry of the adjacent formation groundwaters.
- There is little apparent evidence of a glacial melt signature in the pore waters; this could indicate that such waters had not diffused to the sampling location, or, they could have been subsequently removed, as suspected from the present steady state existing at shallower levels in the bedrock (to ~ 450 m).
- Pore waters at depth show an affinity with deep brine evolution.
- Steady state between pore water and formation groundwaters in the fractures is essentially only developed in the shallow zone of the Ävrö granite, whereas at depths greater than 450 m the chemical and isotopic composition of the pore water differs markedly from those of the formation groundwaters in fractures.

9.4.8 Fracture fillings

Available mineralogical information is based on Boremap data and more detailed investigations of cores from borehole KSH01A + B (cf. Appendix 1 in /SKB 2006a/). Even though most of the work reported so far has been carried out on core samples from the Simpevarp subarea, it can already be concluded that the sequences of minerals identified in the Simpevarp drillcores are recognised also in the Laxemar subarea boreholes and are very similar to earlier observations made at the Äspö HRL, cf e.g. /Landström and Tullborg 1995, Andersson et al. 2002c/.

In the perspective of groundwater chemistry, the presence of four minerals, calcite (CaCO_3), gypsum (CaSO_4), barite (BaSO_4) and fluorite (CaF_2), are worth attention as their solubility has an impact/control on the behaviour of some major ions.

Calcite is the most common of these minerals. It occurs frequently at all depths except in the upper tens of metres and below approx. 1,000 to 1,100 m where it is less common. A number of calcite generations have also been identified ranging from hydrothermal to possibly recent /Bath et al. 2000, Drake and Tullborg 2004/.

Barite occurs as very small grains but is relatively frequently observed (microscopically; not during the core logging) together with calcite, pyrite and the Ba-zeolite harmotome. In saline groundwater samples with very low SO_4 contents, anomalously high Ba contents have been identified. For example, this was the case for the deepest saline groundwater from the KOV01 borehole at Oskarshamn, pointing towards a possible barite solubility control on the Ba and SO_4 content in the water.

Fluorite occurs in several hydrothermal mineral associations together with epidote and later prehnite, but also together with the lower temperature (150°C) generation together with calcite, barite and pyrite. Fluorite can be assumed to partly control the fluorid content in the groundwaters.

Gypsum is identified only in relatively few fractures which in turn are usually situated in borehole sections showing a low degree of fracturing and low (or not measurable) transmissivity. Groundwater modelling /Laaksoharju et al. 2004/ suggest dissolution of gypsum as an explanation for the relatively high SO_4 contents in the saline Laxemar groundwaters, but until now in the fracture filling studies it has not been possible to identify any gypsum in fractures from the Simpevarp subarea. For example, gypsum has not been identified during the extensive work in the Äspö HRL. However, even though it can not be ruled out that it has been overlooked, a more probable explanation is that it is only present in some of the low-transmissive, relatively unfractured parts of the rock.

Other fracture fillings of particular interest for the hydrogeochemical interpretation are the redox sensitive minerals. These consist mainly of Fe-minerals which, in the fractures, are dominantly haematite and pyrite. Some goethite may be present, but is subordinate compared with haematite. In the very near-surface fractures, some less crystalline Fe-oxyhydroxides may be present, usually referred to as 'rust'. These are likely to be related to recent oxidation and are usually associated with calcite dissolution.

In the fractures, several generations of haematite and pyrite are present. The observation of small pyrite grains in the outermost layers of the fracture coatings is in agreement with the groundwater chemistry, indicating reducing conditions.

In a redox buffer perspective the main Fe-host in the fractures is, however, chlorite and clay minerals. Mössbauer analyses of fracture chlorites from Äspö HRL showed that 70–85% of the Fe present in fracture chlorites was Fe(II) /Puigdomenech et al. 2001/. In the bedrock, Fe is dominantly found in biotite, but also in magnetite, which is a common accessory mineral in the Ävrö granite and quartz monzodiorite.

Other redox sensitive phases may include Mn minerals but these are very rare and have not been identified in the area. However, Mn is present in the calcites (up to 1 or 2 weight %, although usually less than 0.5%) and also in some of the chlorites (less than 1 weight %).

9.4.9 Palaeorecord investigations of fracture filling minerals

Hydrogeological interpretations rely normally on borehole groundwater data and describe the present groundwater situation, which can also include the influence of perturbations such as groundwater short-circuiting in the surrounding bedrock and also along single boreholes under open hole conditions. Helping to unravel the influence of these perturbations (and other artefacts from borehole activities) to achieve an understanding of the 'undisturbed' formation groundwaters, and their palaeoevolution, is an integral part of the on-going hydrogeochemical evaluation process at the at the Laxemar/Simpevarp and Forsmark sites.

Insight into the palaeoevolution of the groundwater systems is greatly aided by the fracture mineralogy which, in the best of cases, can help to evaluate the hydrogeochemical stability over timescales of interest for repository safety and performance assessments. Calcite is the mineral most frequently used for palaeohydrogeological interpretations, as it can form during different temperature and pressure conditions including in present low temperature ambient groundwater environments. Stable isotope analyses (O, C and Sr) can provide information about the groundwater from which it precipitated and trace element compositions can add to this description. Under ideal conditions inclusions of formation groundwater are trapped within the developing calcite phases providing important information about the salinity and temperature of the in situ formation groundwaters. Moreover, many calcites show zonation and the character and succession of the different zones can provide information about changes in the groundwater chemistry with time.

Within the EU project PADAMOT /Milodowski et al. 2005/ a number of samples from borehole KLX01 have been analysed in detail for the purpose of palaeohydrogeological interpretation. This work has now been compiled and reported, and the analyses will be made available for the Laxemar 2.1 modelling. Furthermore, stable isotope analyses (including not only O and C but also Sr) and chemical analyses of calcites from KLX03 and KLX04 have been carried out, which also will be included in the forthcoming Laxemar 2.1 model version.

Uranium series analyses on fracture coatings from boreholes KSH01, KSH02 and KSH03 (in total 12 analyses) have been carried out and will be presented in the Laxemar 2.1 model version. Additional analyses from the Laxemar subarea are planned (samples are partly collected) and will be available for later model versions. The uranium series analyses provide very useful palaeohydrogeological information in that they not only provide information about changes in redox conditions and uranium transport, but may also provide time constraints on these processes.

9.4.10 Origin of brine water

The possible origin of brine is discussed in detail in /SKB 2006a, cf. Appendix 1 therein/. It was concluded that there are several sources of salts that may combine to form highly saline groundwaters and ultimately hypersaline brines at great depth. However, these deep saline groundwaters and brines are extremely old, have been subject to mixing, exist under near-stagnant hydraulic conditions and therefore have long residence times, and have undergone intensive water/rock interactions which have served to mask any evidence of their origin. Several hydrochemical and isotopic indicators are available to help unravel their hydrogeochemical evolution, but these have been applied with only limited success and there is still much debate.

A considerable amount of information has been published concerning the Canadian Shield brine occurrences (e.g. /Frape and Fritz 1982, Gascoyne et al. 1989, Herut et al. 1990, Bottomley et al. 1999/ and references therein) and although there is no dispute that the brine salinity is of marine basin origin, there is on-going debate as to the main mechanism responsible for concentrating the hypersaline brine; evidence exists for both evaporative and cryogenic processes.

In the Fennoscandian Shield the origin of the salinity is less clear; much evidence points to non-marine sources such as residual metamorphic/igneous fluids and fluid inclusions /Nordstrom et al. 1989/ accompanied by intensive meteoric water/rock interactions. The problem with these interactions is that they may mask any evidence of the possibility as to whether non-marine/old marine mixing has occurred at some period of time in the distant past. A marine origin for the brine salinity has been invoked by /Fontes et al. 1989/ and suggested also by /Louvart et al. 1999/ and /Casanova et al. 2005/. Therefore it is still an open question.

9.5 Mass balance, reaction path and mixing calculations

Hydrogeochemical modelling has been carried out with PHREEQC /Parkhurst and Appelo 1999/ using the WATEQ4F thermodynamic database. The main goal of the modelling was to investigate the processes that control water composition at the Simpevarp area based on a small subset of selected samples from the two main subareas (Laxemar and Simpevarp). The samples selected from boreholes KLX02 and KSH01A have a wide depth distribution and are representative of the depth evolution of the system (cf. Appendix 3 in /SKB 2006a/).

Modelling was carried out using the mass balance and mixing approach implemented in PHREEQC. The calculation procedure consists in assuming that each selected water is the result of: (a) mixing with the water immediately above the sampling location and with several end members (old waters already present in the rock system), and (b) reaction according to a preselected set of chemical reactions (only the simplest ones).

Once the samples have been selected, the next step involves the selection of the end members to be used in the calculations. The end members available for the modelling are Brine (B), Glacial (G), Littorina (L) and Precipitation. However, as in this specific modelling only groundwater samples are modelled, a new end member representative of a “Dilute Granitic Groundwater (DGW)”, representing shallow input into the system, was introduced (19.2 mg/l Na, 3 mg/l K, 38.5 mg/l Ca, 3.8 mg/l Mg, 162 mg/l HCO_3^- , 12 mg/l Cl, 21.5 SO_4^{2-} , -68.4‰ SMOW $\delta^2\text{H}$, -9.9‰ SMOW $\delta^{18}\text{O}$, 11.91 TU).

After the samples and the end members had been selected, the mass balance calculations following two evolution trends with depth were conducted, one in the Laxemar subarea (borehole KLX02) and the other in the Simpevarp subarea (borehole KSH01A). In both cases, the trend starts by “evolving” a precipitation water into a diluted granitic groundwater. In this case, the final solution is explained only by chemical reactions (no mixing) representative of the intense weathering in the overburden. The next step in both trends is the evolution from the representative diluted groundwater to the first real sample along the borehole. Now, apart from water-rock interactions, the potential mixing with “old” waters (B, G, L and DGW) is also taken into consideration in the balance. From this point on, all the subsequent steps include mixing of five end members (Previous Sample + DGW + G + L + B, as initial solution) and reactions involving calcite, silica, $\text{CO}_{2(g)}$, organic matter, cation exchange (+ eq. gypsum in Laxemar) to reproduce the chemical and isotopic composition of the new sample. Results are shown in Figure 9-11 and Figure 9-12.

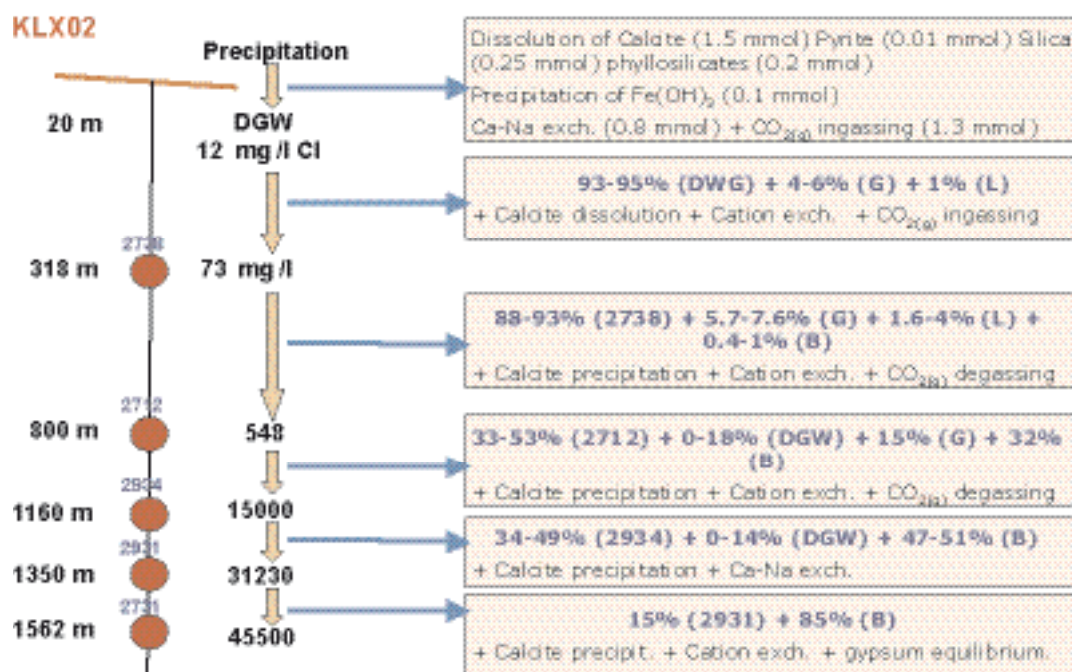


Figure 9-11. Mixing and mass balance calculations obtained in the depth evolution trend represented by KLX02 (Laxemar subarea). The numbers in blue indicate the number of the sample used as a reference water composition.

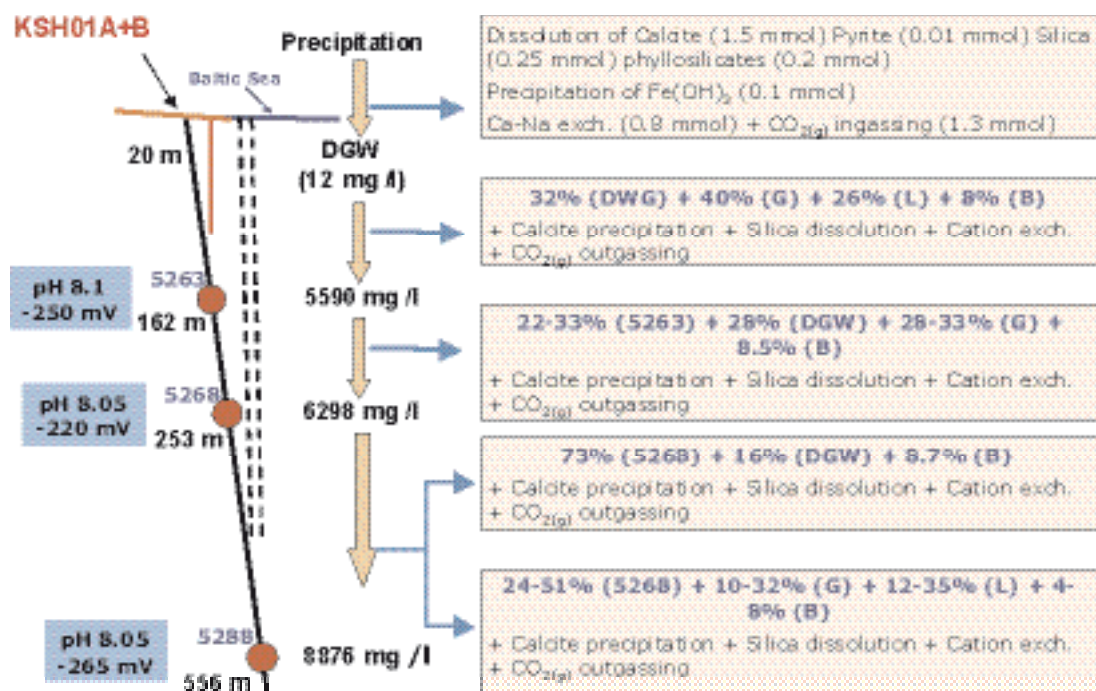


Figure 9-12. Mixing and mass balance calculations obtained in the depth evolution trend represented by KSH01A (Simpevarp subarea). The numbers in blue indicate the number of the sample used as a reference water composition.

In both cases, the mixing proportions evolve from dominant DGW proportions towards a more saline signature (Brine end member), more obvious in the Laxemar trend as the depth interval is three times greater than in the Simpevarp example.

Reactions are also similar although the amount of mass transfer is different. In general there is a clear dissolution process of the rock-forming minerals (except for iron oxyhydroxide precipitation and CO₂ ingassing in the overburden) in the shallow part of the system, and a trend towards equilibrium with the selected minerals as depth increases (precipitation with progressively lower mass transfers). Cation exchange can play an important role in the balance including Ca, Na, Mg and K (Figure 9-11 and Figure 9-12).

For this exercise, the considered reactions are the simplest ones. A better understanding of the actual chemical processes operating in the system should be obtained when more data about the fracture minerals dominating at each depth and when the modelled hydrogeological flow lines in the system become available.

9.5.1 Sensitivity and uncertainty analysis of the mixing models

A sensitivity and uncertainty analysis was performed using PHREEQC, M4 and M3 (cf. Appendix 3 and 4 in /SKB 2006a/). The analysis included three parts:

- Checking the inverse approach methodology implemented in PHREEQC by means of synthetic waters created with the PHREEQC built-in direct-approach capabilities.
- Checking the effects of the compositional variability of the end members on the mixing proportions calculated with M4 and M3.
- Using synthetic samples, to check the effects of chemical reactions on the mixing proportions calculated by M4.

Inverse approach

In order to check the inverse approach implemented in PHREEQC (and to cross-check M4) several synthetic waters have been composed representative of groundwaters affected by two broad geochemical processes: mixing with old waters and reaction with the rock-forming and fracture-filling minerals. This procedure was carried out with the direct approach implemented in PHREEQC. With the knowledge of the processes responsible for the chemical composition of these waters, the inverse approach has been used to account for the processes (cf. Appendix 3 in /SKB 2006a/).

The mixing and mass balance calculations performed with PHREEQC, give a reasonable estimate of the considered end members mixing proportions. The use of, at least, three conservative components (Cl, $\delta^2\text{H}$, $\delta^{18}\text{O}$) seems to provide extra robustness to the calculated proportions independently of the reactions (phases) included in the calculations.

All these results start with a selection of the end members to be used in the calculations. The effects of different selections were already checked elsewhere /Laaksoharju 1999, Luukonen 2001/ and can dramatically modify the obtained mixing proportions and mass transfers. Several calculations were made in the present work with two additional end members (Sea Sediment and Baltic) in the inverse modelling, not used in the direct calculations. The results indicate that Littorina proportions were the most affected, either lowering its proportion or producing the transfer of its proportion to one of the two new end members, Baltic or Sea Sediment. Therefore, end member selection is a fundamental component in this methodology and it requires a very careful hydrogeological and hydrogeochemical study of the system.

Sulphate-reduction in waters with high sulphate contents produces additional variations, mainly in the mixing proportions of the end members which supply this component to the waters (Brine and Littorina). Therefore, the presence of this process must be clearly established before the mass balance calculations are performed. Alternatively, the inclusion of a higher number of parameters in the model should be taken into account.

Finally, with the analytical data used in the mass balance calculations, the chemistry of groundwaters can be explained by invoking the action of different reactions, mainly ionic exchange and equilibrium with different mineral phases (mainly aluminosilicates and calcite). However, the lack of aluminium data in the studied groundwaters and of exchange capacity constants in the fracture filling minerals, are two important limitations, both in assessing the feasibility and extent of these processes before the balance calculation are carried out, and in the overall performance of the approach.

Compositional variability of end-members

A procedure has been developed to assess the impact of the compositional variability of water end members on the calculated mixing proportions (cf. Appendix 3 in /SKB 2006a/). This scheme is based on a PCA analysis performed with the M4 code.

The procedure starts from a pre-selected number of end members (i.e. no attempt is made here to define *which* end members to be use in the analysis) and has the following steps: (1) Define the compositional variability of the end-members; (2) Construct a probability density function (input probability) from the compositional ranges; (3) Generate, according to the chosen input probabilities, a large number of end member compositions; (4) For each run, compute the mixing proportions of selected samples; (5) Bin mixing proportions to construct the output probability distributions.

For the definition of the input probability density functions (pdfs) that characterise the compositional variation of each end member (step 2 above) the following two assumptions were adopted: (1) all compositional variables follow a *log-normal distribution* except those expressed as delta-values (^2H and ^{18}O), which follow a *normal distribution*; and (2) the input ranges are equated to the *99th percentile* of the chosen probability function, which means that, with a probability of 1%, end-member compositions outside the reported range are allowed. The ranges were defined by expert judgment, taking into account all the geochemical and hydrological knowledge of the system. Table 9-2 summarises the ranges used for the modelling for SDM Laxemar 1.2.

Table 9-2. Compositional ranges of the end members used in Laxemar 1.2 PCA mixing modelling.

End member	Na (mg/l)	K (mg/l)	Ca (mg/l)	Mg (mg/l)	HCO ₃ (mg/l)	Cl (mg/l)	SO ₄ (mg/l)	² H (dev)	³ H (TU)	¹⁸ O (dev)
Brine 1	8,500	45.5	19,300	2.12	14.1	47,200	906	-44.9	0	-8.9
Brine 2	9,540	28	18,000	130	8.2	45,200	8.4	-49.5	0	-9.3
Glacial 1	0.17	0.4	0.18	0.1	0.12	0.5	0.5	-158	0	-21
Glacial 2	0.17	0.4	0.18	0.1	0.12	0.5	0.5	-125	0	-17
Littorina 1	3,674	134	151	448	93	6,500	890	-38	0	-4.7
Littorina 2	1,960	95	93.7	234	90	3,760	325	-53.3	0	-5.9
Rain 1	0	0	0	0	0	0	0	-125	0	-17
Rain 2	0	0	0	0	0	0	0	-44	168	-6.9
DGW 1	19.2	3	38.5	3.8	162	12	21.5	-68.4	11.913	-9.9
DGW 2	237	4	25	6	370	119	118	-73.8	0.775	-9.9

Once a probability function has been chosen and the statistical meaning of the empirical compositional range is defined, the input probability functions are completely characterised. Figure 9-13 shows, as an example, the input pdfs for SO₄ (a lognormal distribution) and ²H (a normal distribution) for the five end-members used in the Laxemar 1.2 modelling (Brine, Glacial, Littorina, Rain and Dilute groundwater). The pdfs have been constructed by binning 10,000 values for each compositional variable and normalising to ensure that the area under each curve is equal to unity.

The output probabilities (the ones that give the uncertainty in the mixing proportions) are calculated by running the PCA-mixing step a large number of times, each one with a different composition of the end-members. The composition is chosen at random based on the input probability distributions. Each sample in the dataset has its own output pdf, reflecting the impact of the compositional variability of the end-members on the mixing proportions. Figure 9-14 shows the output pdfs for three selected samples from borehole KSH01A. The calculations were done using the 158 groundwater samples in Laxemar 1.2 dataset and the end-members Brine, Glacial, Littorina and Dilute groundwater. As can immediately be appreciated, the range of mixing proportions for each of the selected samples is quite narrow, considering the *a priori* compositional variability of the end members. This is a strong indication that the *computed mixing proportions are indeed robust estimators of the mixing behaviour of the waters.*

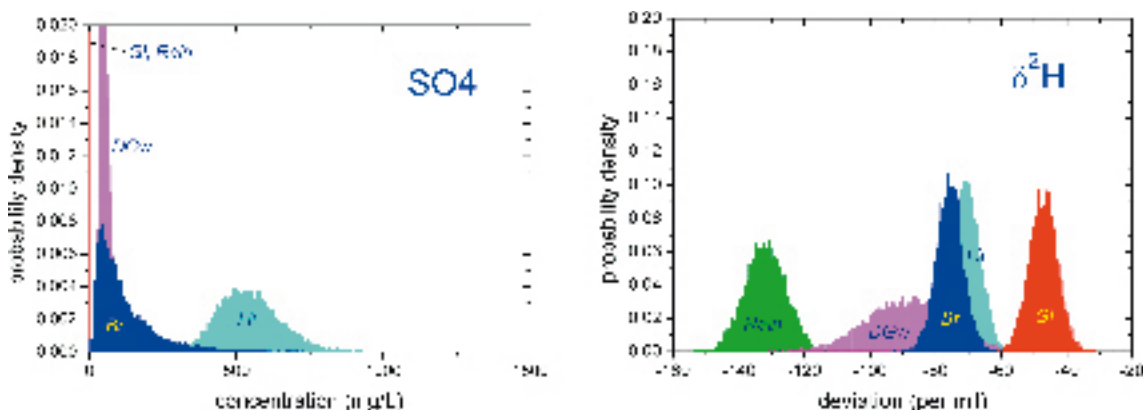


Figure 9-13. Input probability density functions for SO₄ and ²H, as constructed from the compositional ranges of the end-members Brine (blue), Glacial (red), Littorina (cyan), Rain (green) and Dilute Groundwater (magenta).

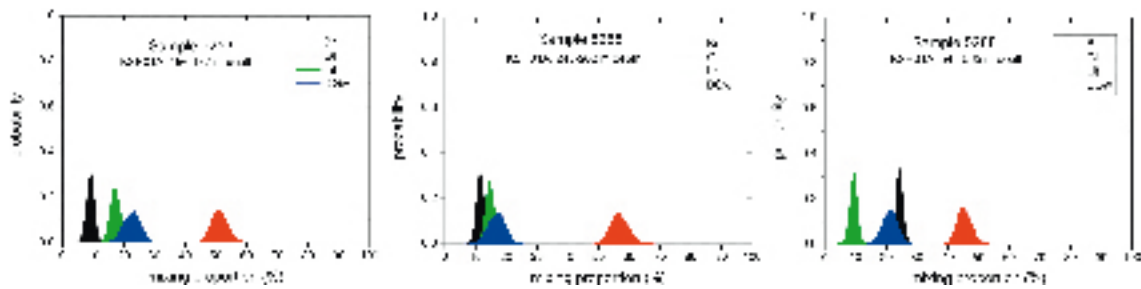


Figure 9-14. Mixing proportions for three samples from borehole KSH01A (Simpevarp area). End members used for the calculations are Brine + Glacial + Littorina + Dilute Groundwater. For the PCA analysis only groundwater samples from the Laxemar 1.2 iteration were used (158 samples).

The important conclusion that can be drawn from the above results is that, *once the number and type of end members are known*, the inclusion of the compositional variability of the reference waters in the PCA analysis gives a robust estimation of the mixing proportions, in the sense that the output probability functions are narrow, predicting mixing proportions tightly concentrated around a mean value. The bonus of this analysis, apart from the robustness itself, resides in the statistical bracketing of the variability of the mixing proportions, which is a fundamental issue when “exporting” these results as simulation targets for hydrogeological modelling.

Several M3 modelling concerns were identified during stages 1.1 and 1.2 of the site modelling project (cf. Appendix 4 /SKB 2006a/). The following concerns were addressed:

- *Can a better resolution be obtained by using only site specific data in the modelling?* In order to optimise the statistical modelling used in the M3 calculations, as many observations as possible are required. Therefore, data from as many Nordic sites as possible are analysed and the information is jointly compiled. The dataset is called “All Nordic Sites” containing data from the sites: Finnsjön, Fjällveden, Forsmark, Gideå, Karlshamn, Klipperås, Kråkemåla, Oskarshamn, Svartboberget, Taavinunnanen (all from Sweden), Olkiluoto, Kivetty and Romuvaara (from Finland).

Are all variables useful in the PCA? As many meaningful variables as possible are used in the M3 modelling. A fixed set of variables will, for example, allow comparisons between the groundwater characteristics of the Laxemar and Forsmark sites. The variables used are the major components (Na, K, Ca, Mg, Cl, HCO₃ and SO₄) and the isotopes ²H, ¹⁸O and ³H. However, the inclusion of all variables makes the model sensitive to effects from reactions (see, next section). An important concern was the use of tritium. Samples collected at different years are difficult to compare directly because of radioactive decay. The tritium values can also be affected by the nearby nuclear power plant. The tritium values for some of the analyses were time corrected in order to be more comparable. Subsequently, this approach has been questioned (see, Appendix 5 in /SKB 2006a/). The reason is that tritium is affected both by transport and decay and a simple time correction cannot be used on the obtained data.

- *Should samples from the surface and bedrock be analysed together in the same PCA?* There are no clear indications of direct flow connections between the surface and the bedrock system. Global models included all type of data and were analysed separately from other models containing only data from bedrock (bedrock models).

Based on the above concerns, five test runs were performed where the data and the variables were modified. The tests showed that, in most cases, the model is robust and is not affected to any large extent by changes in data set or removal of some variables or changes in the end-member selection in agreement with the M4 tests. The effects have anyhow to be tested carefully before accepting the changes in the final models to be used for site description. An example of the outcome is shown in Figure 9-15, where the removal of surface waters and tritium and changing the end-member from rain water to shallow groundwater did not change to any large extent the calculated mixing proportions.

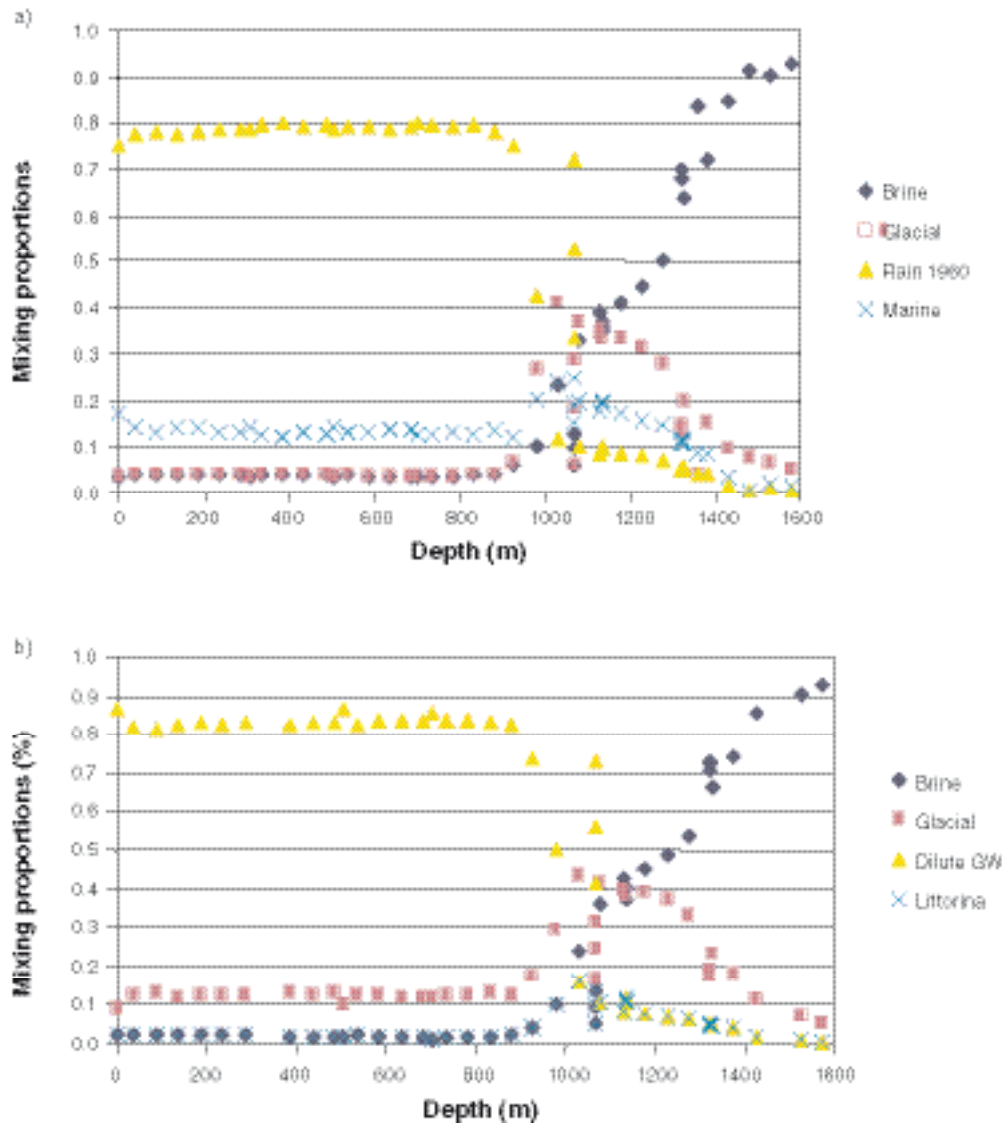


Figure 9-15. Mixing proportions along KLX02 calculated using: a) all data, and b) omitting surface samples and tritium and changing the end member from rain to shallow groundwater in the M3 analysis.

Effects of chemical reactions on mixing proportions

Synthetic waters created by PHREEQC with known mixing proportions and reaction processes have been used for verifying the M4 performance (cf. Appendix 3 in /SKB 2006a/).

Ideally, M4 should provide mixing proportions as close as possible to the synthetic ones, independently of the compositional variability introduced by reactions. Only then the chemical differences between the synthetic waters and the waters obtained from the M4-calculated mixing proportions can be used, via a mass balance step, for inferring the reactions that could have taken place in the system.

In order to verify this, several synthetic waters have been included in the Laxemar 1.2 dataset (Local Model, groundwaters only, 158 samples). Mixing proportions have been calculated considering Brine, Glacial, Littorina and Precipitation (=Rain) as end members. The variables used for these calculations were: Na, K, Ca, Mg, HCO₃, SO₄, Cl, δ²H, δ¹⁸O, ³H. The tests were performed on samples representing: pure mixing, mixing + ionic exchange, and mixing + sulphate reduction. A set of simulations was also run considering *only* conservative components (Cl, Br, δ²H, δ¹⁸O) to check the influence of non-conservative components on the mixing proportions.

The main results can be summarised as follows: When chemical reactions produce only minor compositional changes (lower than 2%) with respect to the chemical composition of samples created by conservative mixing, M4 gives mixing proportions in very good agreement with the measured ones.

When chemical reactions produce an important compositional change (higher than 10% for the studied samples), M4 mixing proportions do not, in general, reproduce the original values, and the amount of bias depends on both the chemical reaction and the type of water. For example, a simple reaction like sulphate-reduction (affecting only two of the components included as variables in the calculations, SO_4 and HCO_3) can be responsible of important deviations in the calculated mixing proportions. The reason for this is that the noise introduced by the non-conservative elements in this kind of statistical analysis readily propagates to the mixing proportions calculated by the code.

Preliminary tests carried out using only conservative elements suggest that mass balances are more robust than the ones computed using conservative *and* non-conservative elements. Further tests have to be conducted in order to see if the calculation in multidimensional space (M4) is more sensitive than calculations in 2D (M3).

Nevertheless, once the mixing proportions are calculated, mass balances provided by the code (with respect to the conservative elements, especially chloride), can easily detect those samples in which reactions have produced the biggest departure from the calculated mixing proportions (Figure 9-16). Waters with a high Cl imbalance are likely to be affected by reactions and should be checked independently because their mixing proportions are biased. An analysis of this sort should be considered a basic tool when assessing the reliability of the mass balance calculations and also of the calculated mixing proportions.

All the above uncertainties are taken into account in M3 in a lumped way when reporting that mixing proportions less than 10% are under the detection limit of the method and that the accuracy of the mixing proportion is $\pm 10\%$ from the reported values. The detection limit and accuracy values will be further checked in future calculations with M3 and M4.

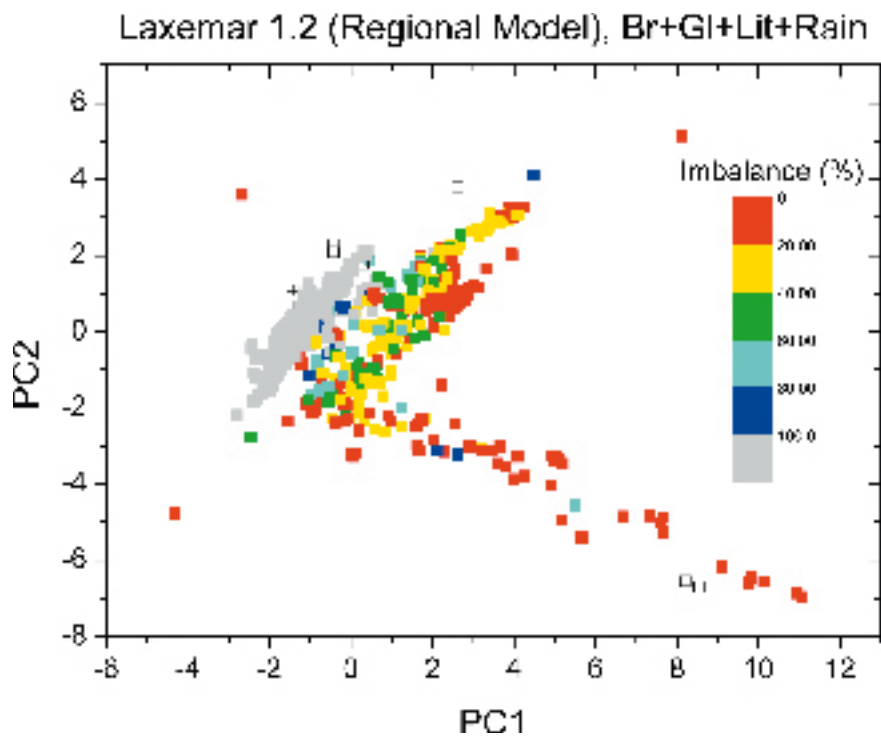


Figure 9-16. Chlorine imbalance (measured as an absolute percent deviation from the real Cl content) in the Laxemar 1.2 Regional Model based on 1,088 samples. Grey samples have Cl imbalance greater than 100% and mainly correspond to superficial waters with very low Cl content. Open squares are samples not explained by mixing (outside M4 hyper-tetrahedron).

As mentioned above, the alternative could be the use of M4 only with conservative components. The scooping calculations performed with this methodology indicate that the calculated mixing proportions agree very well with the synthetic ones and are not affected by the reduction in the number of compositional variables used as input data. The main drawback of this approach is that it cannot be implemented if the number of conservative components is low, specifically if it is lower than the number of end-members.

In other words, the applicability of the method depends on the number of end members to be considered, the availability of conservative components and, ultimately, the complexity of the groundwater system.

The uncertainty evaluations described above represent a major step forward in the uncertainty evaluation of the methods used and will help in judging the plausibility/reliability of the results calculated and will help future integration work with the hydrogeological modelling.

9.6 Conclusions used for the site descriptive model

The descriptive and modelled observations described in the preceding sections are used to derive the hydrogeochemical site descriptive model, summarised in Chapter 11. These observations are fundamental to the overall hydrochemical understanding of the site. The basic groundwater evolution and origin of the groundwater water is now fairly well established. The understanding of the groundwater system such as redox conditions have evolved both from a hydrochemical and microbial point of view. The uncertainty issues related to mixing modelling have been further detailed. Important features, summarised in previous sections and reported in detail in /SKB 2006a/ are described and visualised below.

An important tool for site understanding, i.e. constructing a conceptual model and integration of the results with hydrogeology, is the spatial representation and visualisation of available data. Hydrochemical modelling is usually made on a “water sample basis” with relatively little analysis on the spatial distribution of the information. Normally, the hydrochemical data are treated either by x-y plots (a given variable against chloride or depth, etc) or more sophisticated methods such as mass balance and statistical mixing models, but these kind of analyses often make it difficult to obtain an impression of information which corresponds to different hydrogeological and geographical settings, such as inland-coastal or recharge-discharge zones. This is why a specific visualisation application has been developed with the aim of representing “objectively” (i.e. without interpolation) the available hydrochemical information. The visualisation tool has been programmed using the IBM Open Visualisation environment, known as OpenDX (cf. Appendix 5 in /SKB 2006a/).

9.6.1 Modelling and visualisation of the near surface properties

The interaction between the surface and deep groundwaters were studied in great detail in /SKB 2006a, cf. Appendix 1 therein/. All original data used are stored in the primary databases (Sicada and/or GIS). The evaluation strategy was based on a large amount of background information which was systematically approached:

- Elevation maps showing the locations of the cored and percussion boreholes and soil pipes.
- Regional hydrological identification of recharge/discharge areas and their relation to the locations of cored and percussion boreholes.
- Hydrological characterisation of soil pipe locations in terms of potential recharge/discharge areas.
- Correlation of soil pipe groundwater hydrochemistry with the hydraulically identified recharge/discharge areas; selection of areas showing a positive correlation.

Based on geological and hydrological information and the distribution of soil types in the overburden, a preliminary classification of the soil pipe data in terms of recharge/discharge could be carried out. Prior to this, however, an initial classification was conducted based on the hydrogeological modelling (in turn based on topography).

Using the overburden soil pipe hydrochemical data a preliminary series of anomalous ('hot spot') chemical distribution maps were made (see Appendix 1 in /SKB 2006a/). The available data (most of the data points) at this initial stage included only chloride, sulphate, pH and alkalinity.

When available, the following background data were used when studying shallow groundwater from percussion drilled boreholes:

- Geophysical logs (BIPS, resistivity, fracturing).
- Recorded observations of hydraulic flow.
- Hydraulic tests and flow measurements.
- Hydraulic conductivity and transmissivity.

Using this information the hydrochemical data were, when possible, allocated to the following shallow depth intervals: 0–25 m, 25–50 m, 50–75 m, 75–100 m, 100–150 m, 150–200 m and 200–250 m. Selected ion and isotopic plots versus depth then were produced (see Appendix 1 in /SKB 2006a/). The data were plotted to identify any shallow groundwater trends that might, together with the Soil Pipe evaluation, give some indication of recharge/discharge features.

The conclusion is that this preliminary evaluation of groundwater data representing the geosphere/biosphere interface has shown promising results. This has involved overburden data from Soil Pipes and upper bedrock (0–200 m) data from percussion boreholes. Integration of these data has identified presumable areas of recharge/discharge which will be further investigated and quantified when more data become available. This will help to characterise the chemical and isotopic composition of the recharge water end member into the bedrock, and also the evolution of groundwaters at points of discharge from the bedrock into the overburden in future model versions.

The overall picture from the evaluation in presented in /SKB 2006a, cf. Appendix 1 therein/ is that discharge locations, at one location characterised by tritium free water, have been identified at the Simpevarp subarea (Åvrö), whereas near-surface groundwaters from Laxemar (only percussion borehole data available so far) are mainly characterised by recharge or shallow discharge (except for HLX20).

The soil pipe data described above were used for visualisation (cf. Appendix 5 in /SKB 2006a/) and Figure 9-17 shows the location of all the available soil pipes in the Laxemar and Simpevarp subareas (cf. Appendix 4 in /SKB 2006a/).

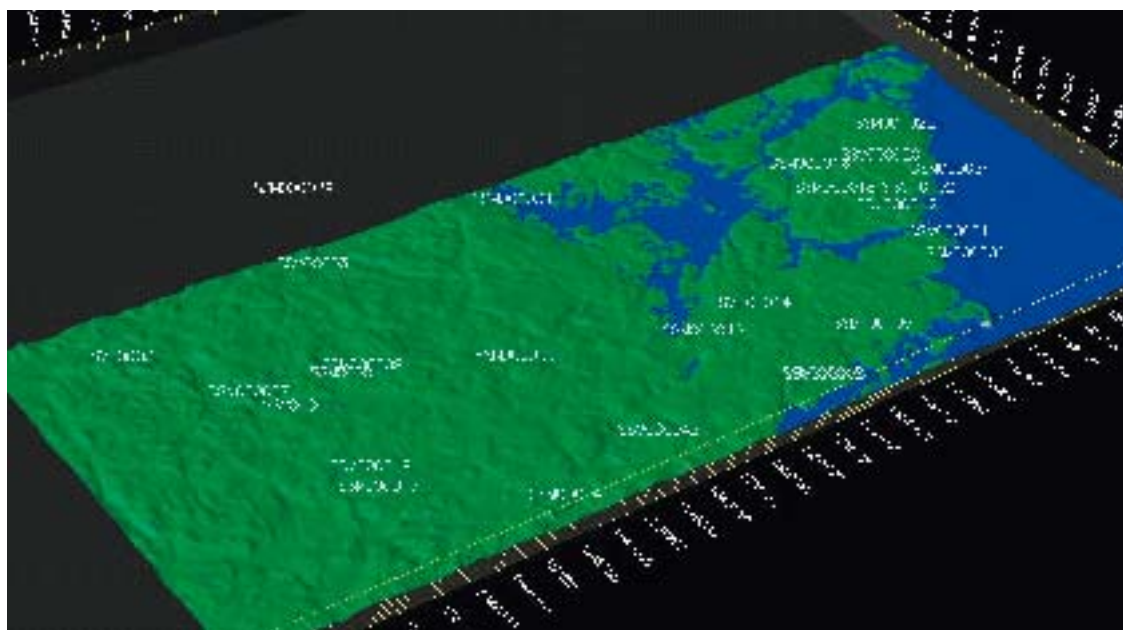


Figure 9-17. Spatial location of soil pipes included in the Laxemar v. 1.2 work.

Only those samples categorised as “representative samples” in the database have been included in the visualisation of near surface hydrochemistry. The amount of data is different depending on the type of element to be visualised (i.e. there are more representative samples with chloride or bicarbonate data than with tritium or ^{14}C data, for instance).

Figure 9-18 shows chloride concentrations in soil pipes. It can be seen that near surface groundwater samples are diluted, with chloride concentrations always lower than 150 mg/L. However, there is a clear influence of Baltic water in those soil pipes located close to the coast line (such as SSM00034 and SSM0040). An apparent anomaly to this general trend is observed in soil pipe SSM00022, located in Ävrö. This particular soil pipe is not located close to the coast line but inwards in the Ävrö Island. However it shows the highest chloride concentration of all the representative samples of soil pipes. This soil pipe also shows the highest concentrations of other solutes as strontium and sulphates, among others.

There are few representative samples in soil pipes having information on radioactive isotopes. Figure 9-19 shows the spatial distribution of available measurements of tritium. It can be recognised that soil pipe SSM00022 (Ävrö) shows clearly the lowest tritium activities, indicating that near surface groundwater in this point is of sub-modern age.

From the above analyses it can be seen that soil pipe SSM0022 on Ävrö shows hydrochemical signatures consistent with the influence of older and more saline groundwater than the rest of the representative samples from soil pipes. These hydrogeochemical signatures, typical of the near surface environment, could provide an indication of a groundwater discharge zone or stagnant older water that has been preserved under low permeable soil cover. It is worth noting that, at the present time, there is no available isotopic information for soil pipes at the Laxemar subarea.

9.6.2 Modelling and visualisation of the groundwater properties

Figure 9-20 shows a view for the location of the main cored boreholes (from the point of view of the number of representative samples) available in the Laxemar and Simpevarp subareas, as they are included in the Laxemar 1.2 data freeze (cf. Appendix 5 in /SKB 2006a/). These main available cored boreholes are KLX01, KLX02, KLX03 and KLX04 at the Laxemar subarea, and KSH01, KSH02, KSH03, KAV01, KAV04, KAS02, KAS03, KAS04 and KAS06 in the Simpevarp subarea, cf. Figure 2-3. It is worth noting that several percussion boreholes contribute to the hydrochemical

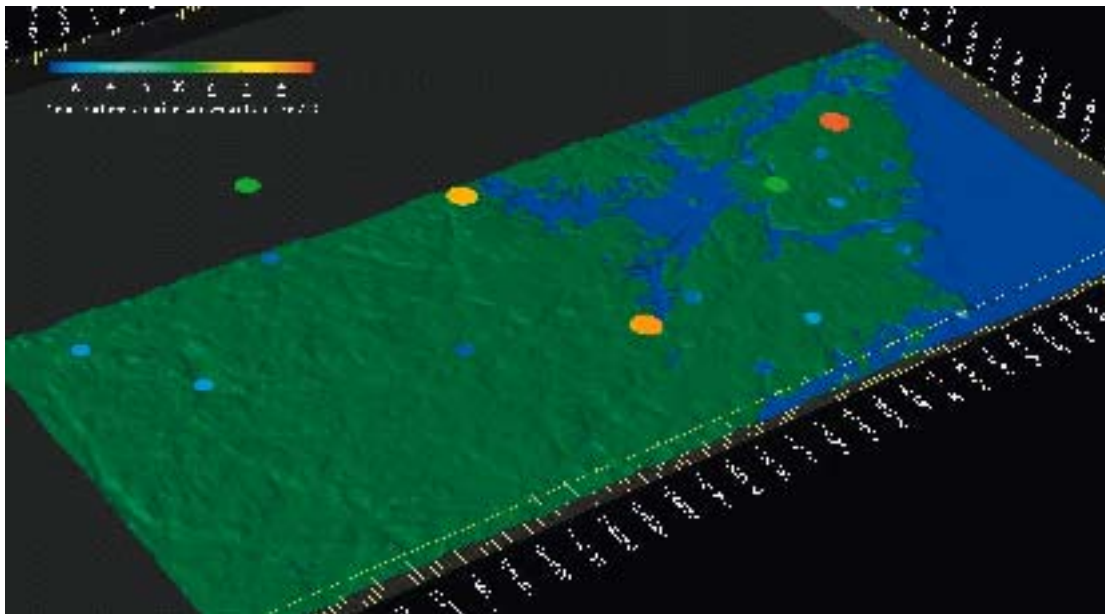


Figure 9-18. Spatial distribution of chloride concentration in soil pipes. The maximum value is located in soil pipe SSM00022 at Ävrö.

database with representative samples. The geometry of the percussion boreholes is not visualized for practical reasons, but all the representative samples available in the database, including percussion boreholes, have been taken into account in the hydrochemical visualisation.

Figure 9-20 shows a bottom view (from the southwest) of the Laxemar and Simpevarp subareas, including the geometry of the main cored boreholes and the Äspö tunnel. It is thought that both boreholes and tunnel are a very useful geographical reference for 3D visualisation of the bedrock hydrochemistry. It is worth noting that the geometry of the boreholes is not accurate but has been approximated from the coordinates of some water samples. This is the reason why Äspö boreholes do not reach the surface at the present version of the modelling. This aspect will be improved in the next stages of the site descriptive modelling.

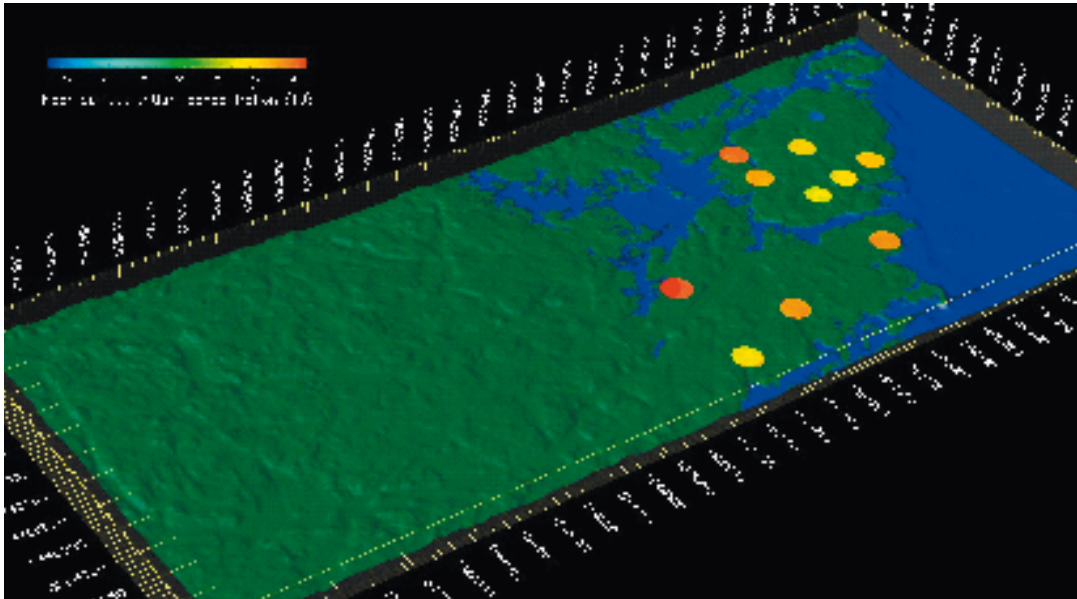


Figure 9-19. Spatial distribution of tritium (TU) in soil pipes. The minimum value is located in soil pipe SSM00022 at Ävrö.

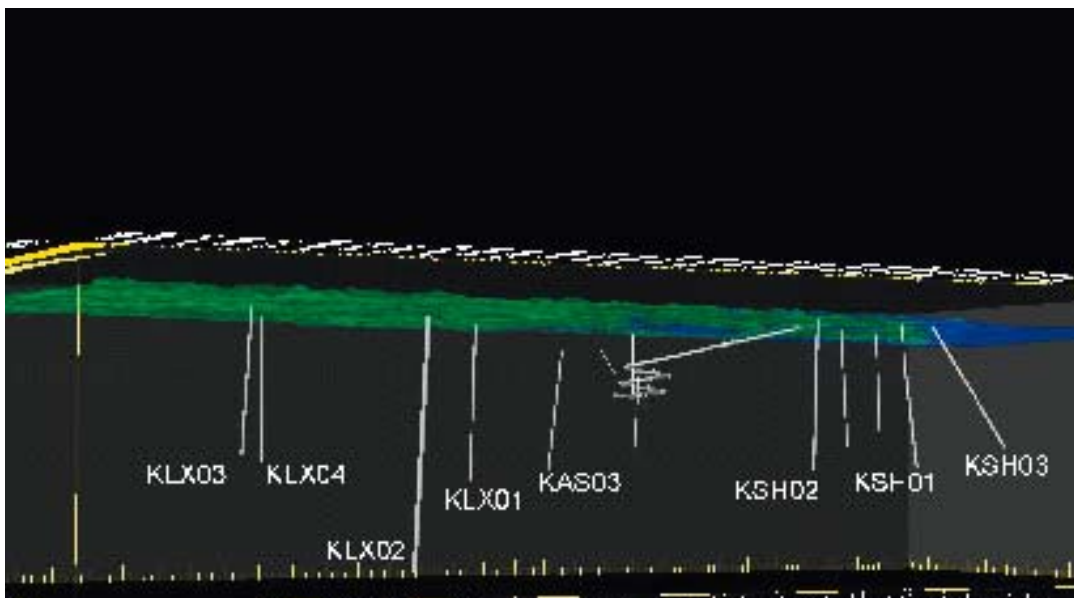


Figure 9-20. Bottom view (from the southwest) of the Laxemar and Simpevarp subareas. Main cored boreholes, as well as the Äspö tunnel, have been included as geographical references in the visualisation.

Figure 9-21 shows representative chloride data in the bedrock samples, except for boreholes KLX03 and KLX04, where all available samples (representative or not) have been included (only for chloride visualisation and some of them should be taken with caution).

The reason of including not representative dissolved chlorides in KLX03 and KLX04 is to have a “first guess” of the salinity distribution at Laxemar subarea (notice that all the “representative knowledge” available up to now comes from the “old” KLX01 and KLX02 boreholes). It is worth noting that the visualisation shown in Figure 9-21 does not include the deepest saline waters of KLX02 (the brine water samples). The reason for not including the brine samples into this visualisation is to enhance the contrast of salinity between the groundwater of the Laxemar and Simpevarp subareas. The Laxemar subarea represents a more continental (inland) hydrogeological framework with a thick fresh water body reaching maximum depths of nearly 1,000 m. However, the Simpevarp subarea represents a coastal hydrogeological framework where fresh water bodies are confined to the first 100–200 m of the bedrock.

According to the water classification used by /Laaksoharju et al. 2004/, 4 main hydrochemical water types have been identified in the Simpevarp area, namely type A to type D /Laaksoharju et al. 2004/.

Water Type A. This type comprises dilute groundwaters (< 2,000 mg/L Cl; 0.5–2.0 g/L TDS) of Na-HCO₃ type present at shallow (< 200 m) depths at the Simpevarp subarea, but at greater depths (0–900 m) at the Laxemar subarea. At both subareas the groundwaters are marginally oxidising close to the surface, but otherwise reducing. Figure 9-22 shows a visualisation of the spatial distribution of water type A (diluted). This type of water is interpreted as being related with a meteoric origin, and shows higher bicarbonate contents. Figure 9-23 shows the spatial distribution of bicarbonate concentrations. It can be seen that the higher values of bicarbonate concentrations coincides almost exactly with diluted groundwater (Type A). The high bicarbonate concentration can be mainly attributed to the occurrence of organic matter oxidation coming from the soil layers at emerging land.

Water Type B. This type comprises brackish groundwaters (2,000–6,000 mg/L Cl; 5–10 g/L TDS) present at shallow to intermediate (150–300 m) depths at the Simpevarp subarea, but at greater depths (approximately 900–1,100 m) at the Laxemar subarea. The origin of this water type could be different from one place to another. At the Simpevarp subarea there is potentially some residual Littorina Sea (old marine) influence. On the contrary, at the Laxemar subarea the saline component of this water type could mainly be attributed to the influence (dispersion/diffusion) of deep brine water. Figure 9-24 shows a visualisation of the spatial distribution of water type B (brackish).

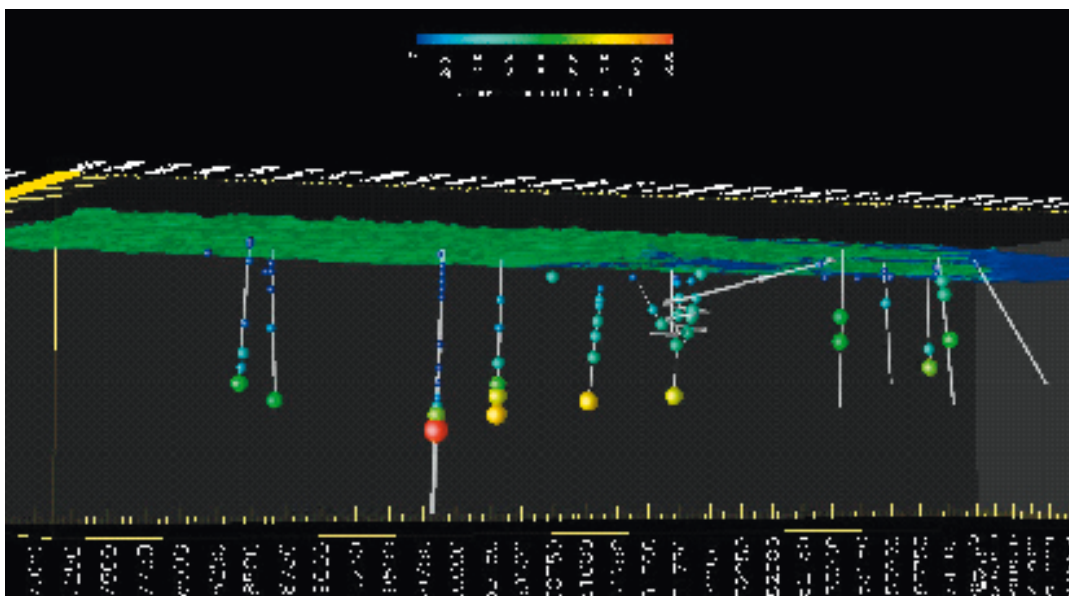


Figure 9-21. Distribution of chloride concentrations in the bedrock under the Laxemar and Simpevarp subareas above 1,100 m (excluding the most saline waters in KLX02). Symbol size is proportional to the chloride concentration value.

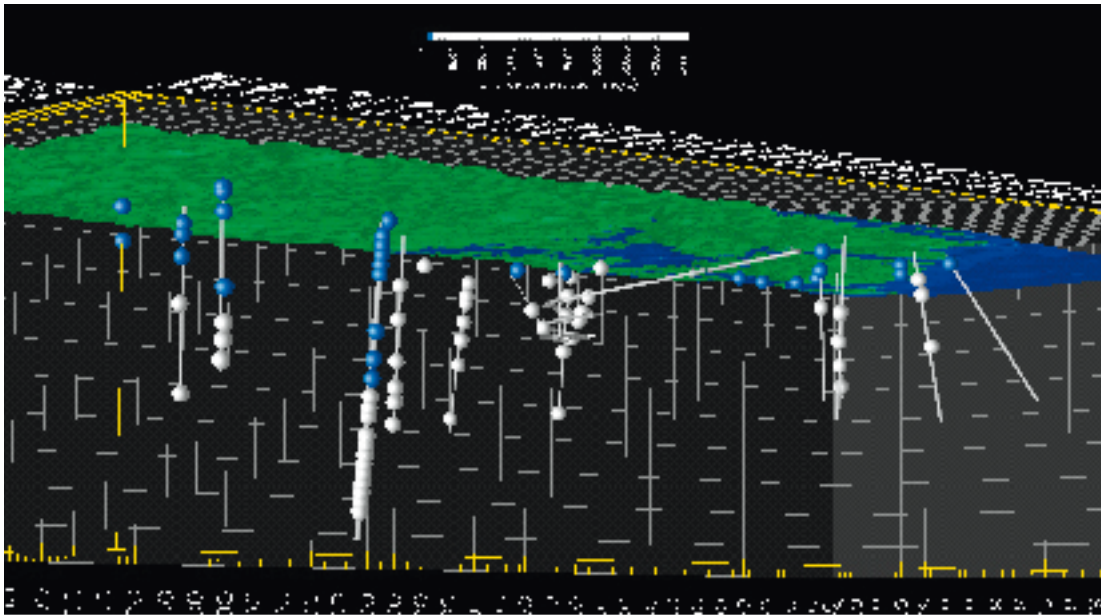


Figure 9-22. Spatial distribution of water type A (diluted), which can be related to a meteoric origin. Note that this type of water reaches much greater depths at the Laxemar subarea than at the Simpevarp subarea.

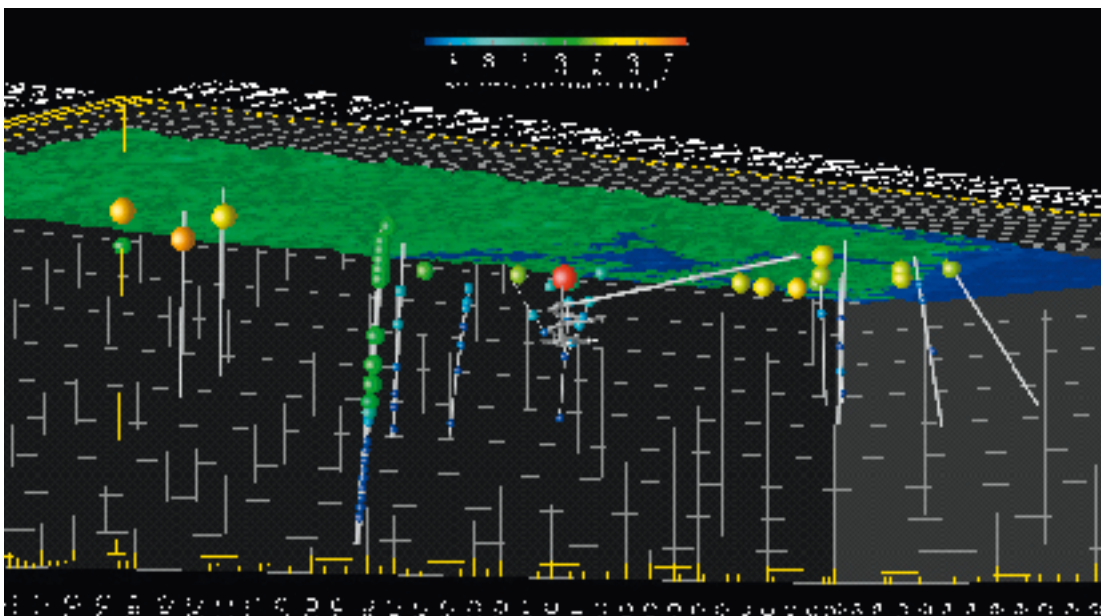


Figure 9-23. Spatial distribution of bicarbonate concentrations.

The complex origin of this water type B can be better understood by analysing other hydrochemical information. Figure 9-25 shows the spatial distribution of magnesium in groundwater. High magnesium concentrations are found in the Simpevarp subarea associated with the same waters corresponding to water type B (brackish). However, water type B at the Laxemar subarea shows low magnesium contents compared with the Simpevarp subarea. It is worth noting that magnesium is not a conservative element. On the contrary, it is well known that it can be involved in cation exchange processes, mainly in fractures and fracture zones with some clay content. However, according to /Laaksoharju 1999/ the average magnesium concentration in Baltic Sea water is 234 mg/L, while deep brine waters at KLX02 shows very low concentrations of magnesium (about 2 mg/L). This high

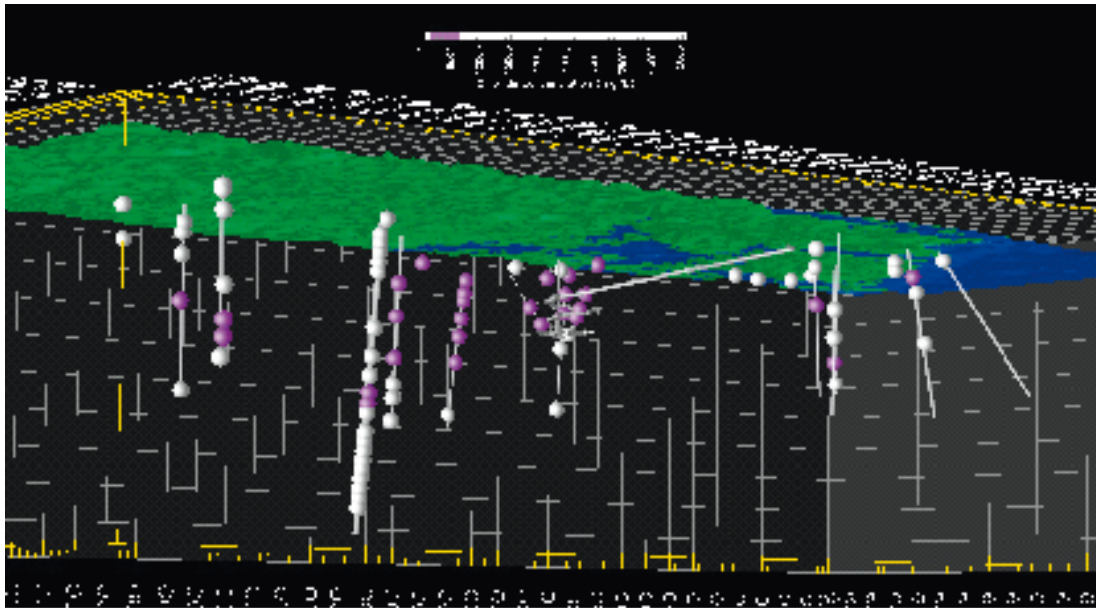


Figure 9-24. Spatial distribution of water type B (brackish). This type of water is found at relatively shallow depths in the Simpevarp subarea (mainly under Åspö), but also at Laxemar close to the coast (KLX01). Inland (KLX02-03-04) this type of water is found at greater depth, from 600 to 1,100 m.

contrast therefore could be qualitatively useful to establish a difference between the salinity of brackish waters at the Laxemar and Simpevarp subareas. According to the available data it can be stated that brackish waters at Laxemar are most likely related with the occurrence of a dispersion zone between deep saline waters and shallow diluted water of meteoric origin, while brackish waters of the Simpevarp subarea show an influence of marine waters. This is in accordance with /Laaksoharju et al. 2004/. These marine waters must be older than the Baltic Sea, since presently there is no driving force for marine water to penetrate in the bedrock. It has been postulated that this old marine water was introduced into the bedrock during the Littorina Sea stage, due to density driven flow caused by the presence of low density relict fresh glacial water deeper in the bedrock.

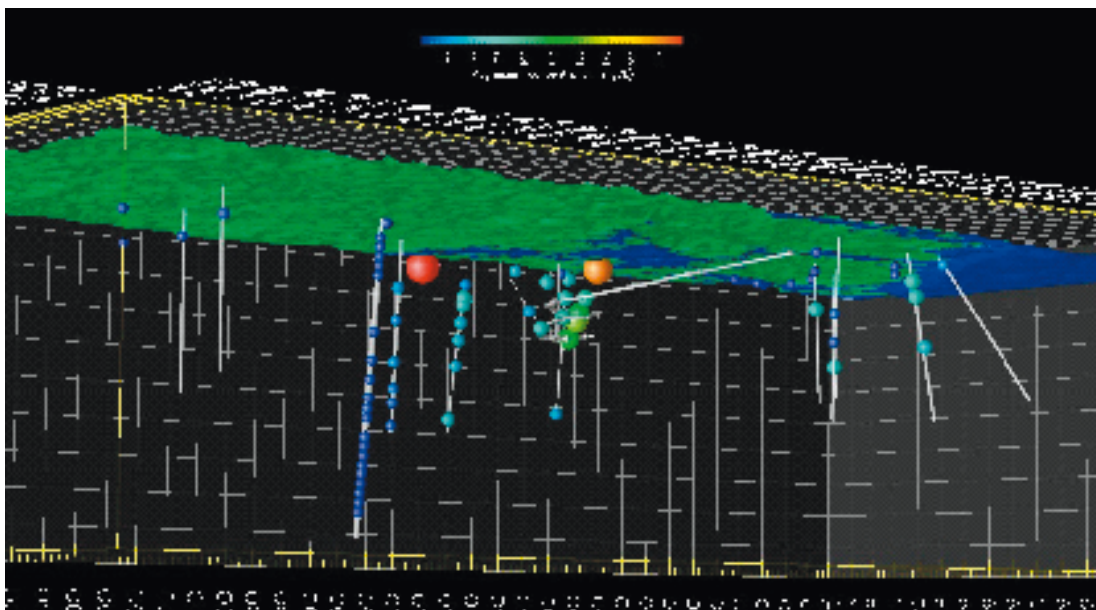


Figure 9-25. Spatial distribution of dissolved magnesium in groundwater. It can be seen that maximum magnesium concentrations are found in the Simpevarp subarea, indicating a possible influence of older marine waters.

Water Type C. This type comprises saline groundwaters (6,000–20,000 mg/L Cl; 25–30 g/L TDS) present at intermediate depths (> 200–300 m) at the Simpevarp subarea, and at greater depths (> 1,000 m) at the Laxemar subarea. Similarly to water type B, the type C water could show different hydrochemical signatures from one place to another. At the Simpevarp subarea (but also at coastal Laxemar locations; i.e. KLX01) signatures of old marine influence can be recognised (see magnesium in Figure 9-25), together with glacial signatures (as is shown in Figure 9-27). On the contrary, at the Laxemar subarea this water type could mainly be attributed to the influence (dispersion/diffusion) of deep brine water. Figure 9-26 shows a visualisation of the spatial distribution of water type C (saline).

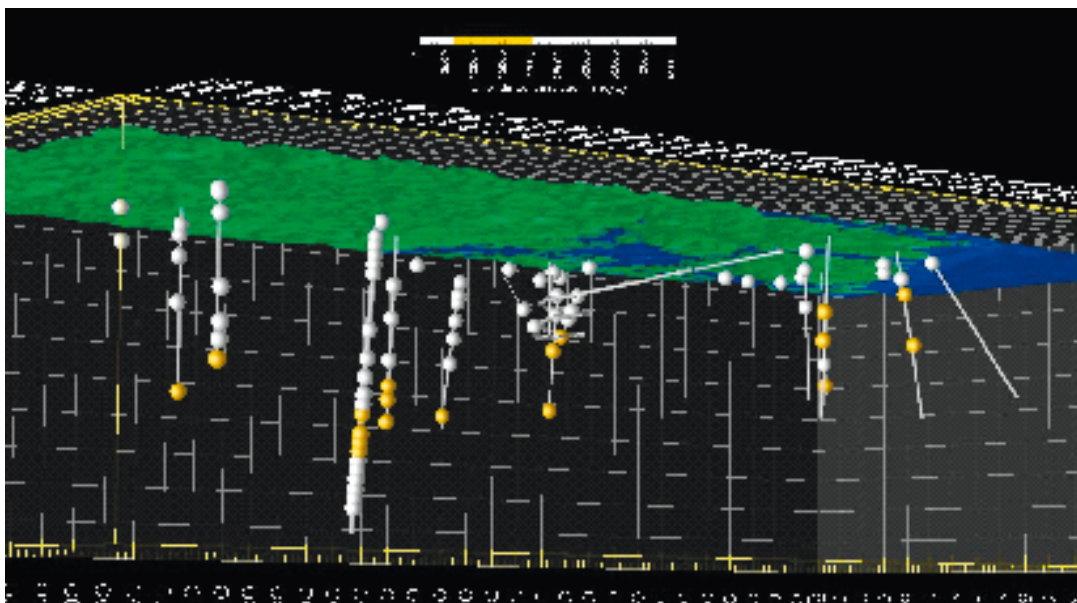


Figure 9-26. Spatial distribution of water type C (saline). This type of water is found at shallow to intermediate depths in the Simpevarp subarea, and at depth at Laxemar (800–1,200 m).

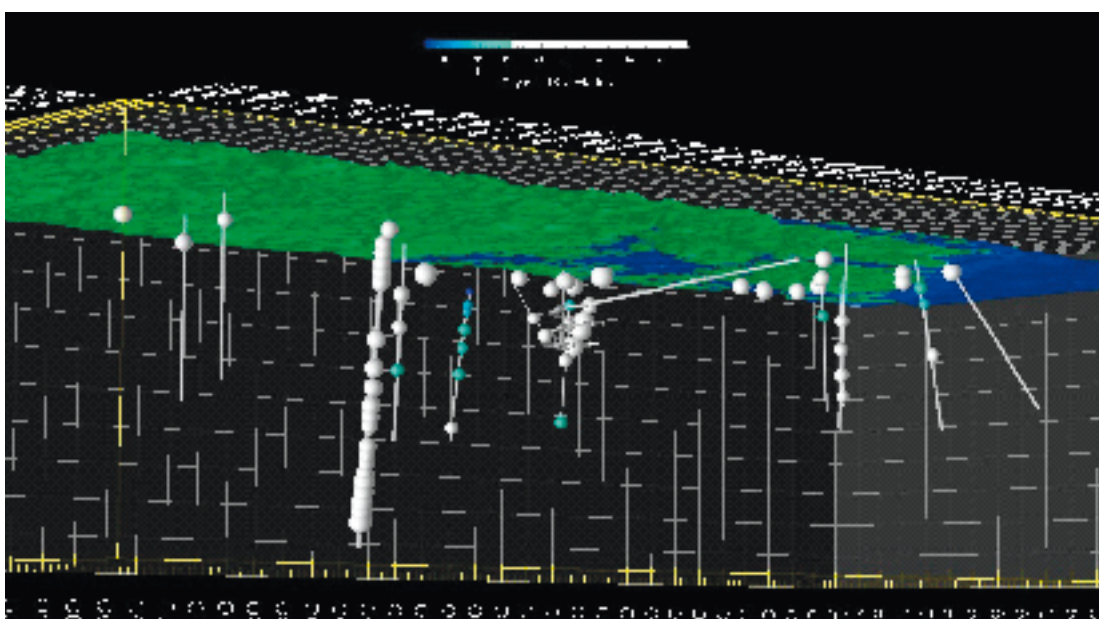


Figure 9-27. Spatial distribution of ^{18}O deviations lower than -13‰ SMOW. The rest of the measured values are marked in white.

Glacial isotopic signatures have been postulated to be present in groundwater at different places of Scandinavian bedrocks. According to /Laaksoharju 1999/, when the continental ice melted and retreated (about 13,000 years ago), glacial meltwater was hydraulically injected under considerable water pressure into the bedrock. The exact penetration depth of glacial water is uncertain but, according to /Svensson 1996/ and /Jaquet and Siegel 2003/, depths of several hundreds metres can be expected according to hydrodynamic models.

The best tracers for glacial water signatures are assumed to be the stable isotopes ^{18}O and ^2H . According to /Laaksoharju 1999/, the isotopic composition for a Glacial end-member water is -21‰ SMOW for ^{18}O , and -158‰ SMOW for ^2H . The clearest glacial signature at the Simpevarp area was found at depth on the Äspö island (KAS03) during the site characterisation process preceding construction of the access tunnel to the Äspö HRL.

Figure 9-27 and Figure 9-28 show the spatial distribution of water samples with ^{18}O lower than -13‰ SMOW and ^2H lower than -90‰ SMOW, respectively. These threshold values are arbitrarily assumed, but represent isotopic values that are judged to distinguish clear glacial signatures in brackish and saline groundwaters of the bedrock. This does not mean that water samples with higher isotopic values are free of glacial influences but simply represents an easy way to identify the available samples with a higher glacial influence.

According to Figure 9-27 and Figure 9-28, glacial isotopic signatures can be recognised clearly at the Simpevarp subarea, especially below the Äspö island and the Simpevarp peninsula. The clearest signature corresponds to borehole KAS03 at a shallow depth (about -120 m above sea level). At the Laxemar subarea, glacial signatures appear to be evident only close to the coast (KLX01) and at greater depth than in the Simpevarp subarea. It is worth noting that all glacial signatures are found in groundwater samples of types B and C (brackish or saline).

Water Type D. This water type comprises highly saline groundwaters ($> 20,000$ mg/L Cl; to a maximum of ~ 70 g/L TDS) and has only been identified in one borehole at the Laxemar subarea (KLX02) at depths exceeding 1,200 m. Figure 9-29 shows a visualisation of the spatial distribution of water type D (highly saline, also referred to as “brine”). Water samples of type D (highly saline) show the highest concentrations of most dissolved species (see Appendix 5 in /SKB 2006a/).

Water samples of type D (highly saline) show also the highest concentrations of sulphates in bedrock groundwaters, cf. Figure 9-30.

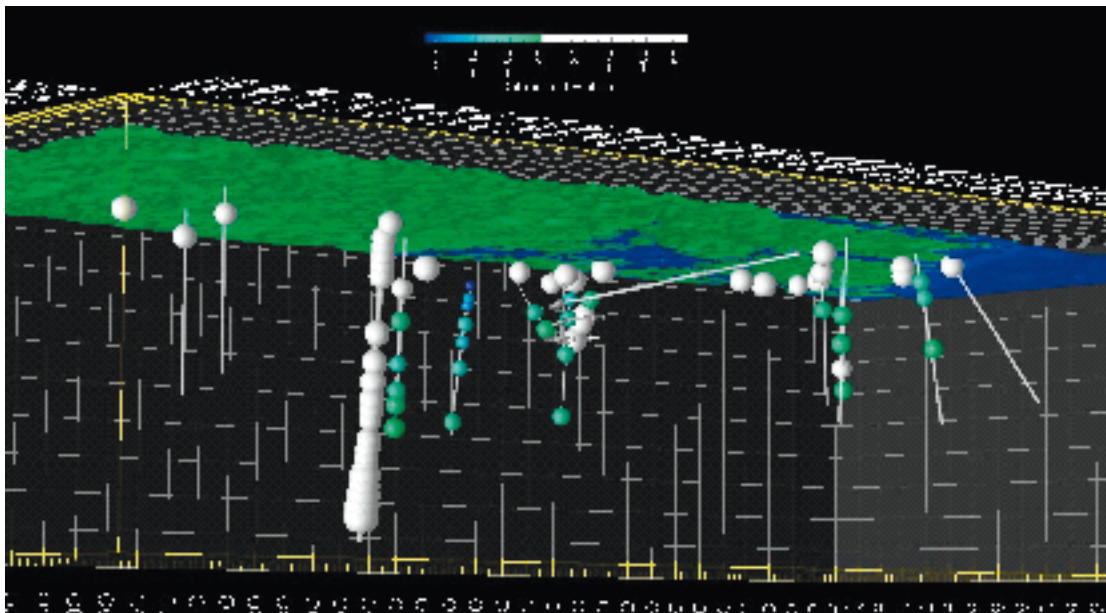


Figure 9-28. Spatial distribution of ^2H deviations lower than -90‰ SMOW. The rest of the measured values are marked in white.

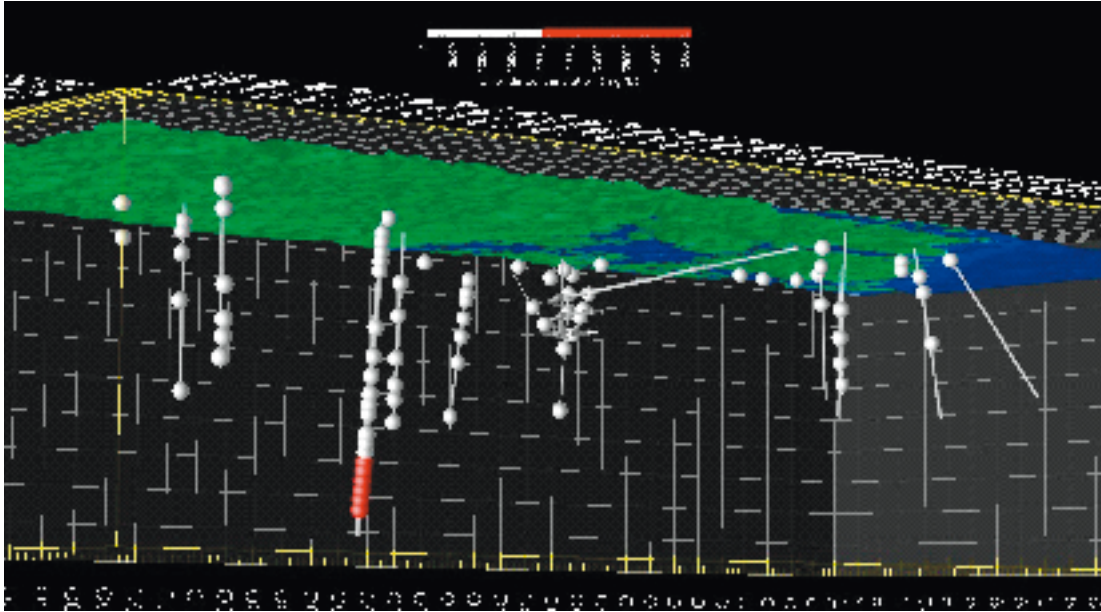


Figure 9-29. Spatial distribution of water type D (highly saline). This type of water has only been found in borehole KLX02 (Laxemar subarea), at depths from -1,200 to -1,600 m above sea level.

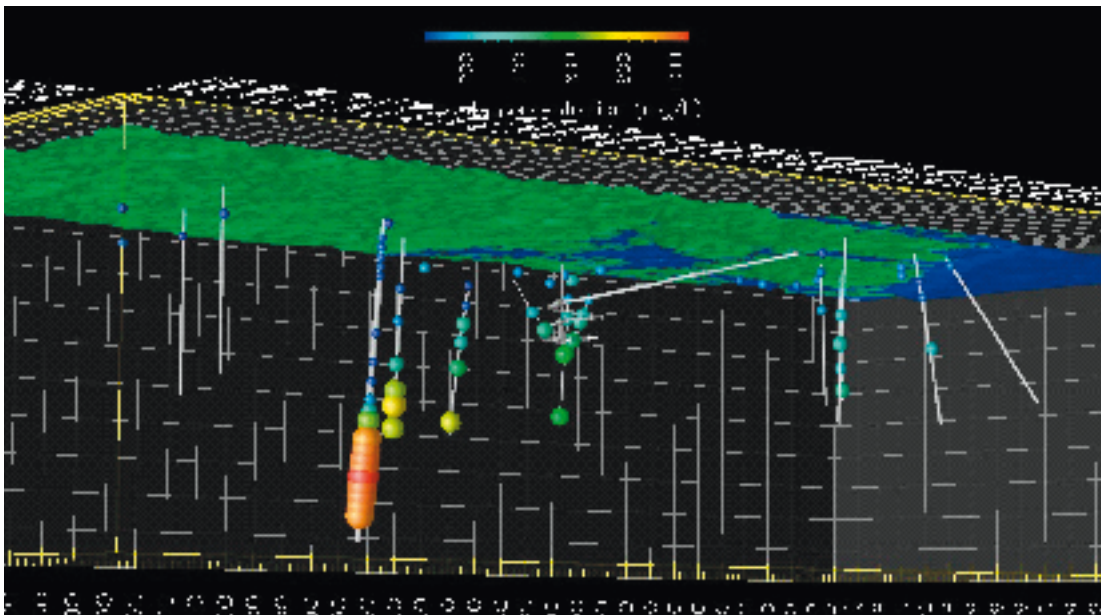


Figure 9-30. Spatial distribution of dissolved sulphates at the Laxemar and Simpevarp subareas.

Figure 9-31 show a summary visualisation of the spatial distribution of the four water types characterising the Laxemar and Simpevarp subareas. It can be seen that dilute water (type A) extends deeper at inland Laxemar locations compared to Laxemar coastal positions and the Simpevarp subarea in general, where dilute waters are only found at very shallow depths in the bedrock. On the contrary, brackish and saline waters (types B and C) are predominant at the Laxemar subarea coastal areas (KLX01) and at the Simpevarp subarea. Within the Simpevarp subarea, saline waters (type C) are found at much shallower depths under the Simpevarp peninsula than under the islands of Äspö and Ävrö.

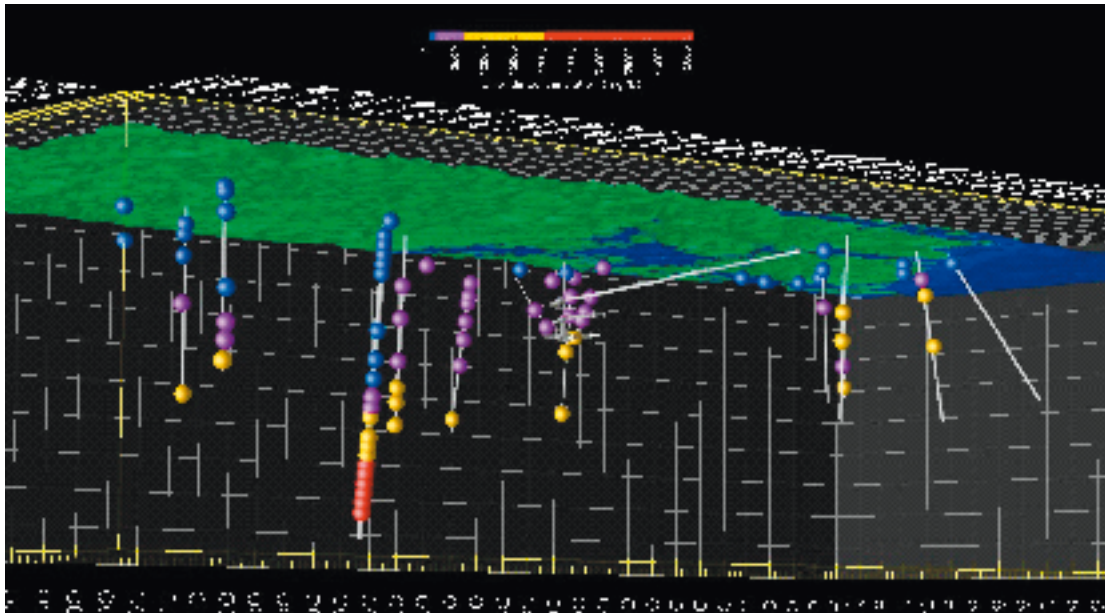


Figure 9-31. Bottom view from the southwest of the spatial distribution of water types in the Laxemar and Simpevarp subareas. Water type A (blue), B (purple), C (yellow) and D (red).

It is worth noting that water type classification based on chloride does not distinguish between the different origins of the B and C type of waters since the same chloride content in a water sample can have different origins (e.g. mixtures with marine or deep saline water). On the other hand, most of the dissolved species show qualitative trends very similar to chlorides. This could be taken as an indication of the important role of physical transport processes (e.g. dispersion-diffusion; i.e. mixing) in determining the hydrochemical nature of bedrock groundwater in the Laxemar and Simpevarp subareas. Even the concentrations of some of the hydrochemical components which are known to be clearly involved in geochemical processes (such as calcium) are obviously masked by the influence of the mixing between different waters. It is thought that the concentration contrast between highly saline waters and the rest is so large, that very little mixing involving this end-member water would produce mass transfers much higher than those involved in most geochemical processes. However, this is not always the case. Some dissolved components such as magnesium, bicarbonate, iron, silica and manganese (among some others) show a very different spatial distribution. The visualisation and spatial distribution analyses of all dissolved components can be found in the supporting document /SKB 2006a/.

As it was discussed above, it has been postulated that magnesium is a good tracer for the marine influence of groundwater samples (even though it is not a conservative solute), due to the fact that highly saline deep waters (type D) show very low concentrations compared with Baltic Sea waters.

It has been detected that maximum concentrations of dissolved iron has been measured at the shallowest positions in the bedrock, coinciding with those dilute water samples showing elevated concentrations of bicarbonates. Hydrogeochemical /Banwart et al. 1995, 1996/ and microbiological /Pedersen et al. 1995/ studies at the Äspö HRL provide significant evidence supporting Fe(III) reduction as a respiration pathway for the oxidation of organic carbon. This process could be mostly similar to what is happening at the shallower parts of the Laxemar and Simpevarp subareas following the emergence of the land during the last c. 2,000 years. Then, according to the observed concentrations of bicarbonate and iron in the dilute groundwater samples (Type A) of the Simpevarp subarea, microbially mediated oxidation of organic matter through the reduction of ferric minerals seems to be the most plausible hypothesis to explain the high bicarbonate concentrations of these groundwater samples. It is worth noting that both soil pipes and some shallow bedrock groundwater samples at Simpevarp are undersaturated with respect to calcite /cf. SKB 2004a and Appendices 4 and 6 therein/ and, therefore, dissolution of calcite would be also contributing to the observed bicarbonate concentrations in dilute groundwater.

9.6.3 Groundwater samples in relation to major deformation zones

The employed visualisation tool has also the capability of representing structural objects such as deformation zones. This capability is important for the construction of conceptual models in a bedrock environment which is affected by the presence of such features. The main deformation zones which have been studied in detail (in respect to the hydrochemical information available) are EW002A, EW007A, NE040A, NE005A and EW013A. The selection of these 5 structural features was made by considering the actual definition of the investigated area and the location of the boreholes in which representative hydrochemical information is available. In fact, for the case of the Laxemar subarea, deformation zones EW002A and EW007A are very important. NE040A is also a relevant structure due to the fact that it crosses the Laxemar subarea. The geometry of discrete features (deformation zones) corresponds to the structural model of Laxemar (version 1.2), cf. Section 5.4.

By including deformation zones in the visualisation tool allows analysing the possibility of “direct” hydrogeological connection between the different groundwater samples by way of the modelled deformation zones. Deformation zone EW002A is intercepted by borehole KAS03 below the Äspö Island and runs very close to the deeper saline water samples at KLX02 at Laxemar. Deformation zone EW007A is intersected by boreholes KLX02 and KLX04. However, chemical information at the intersection between KLX04 and EW007A is not considered representative and should be treated with a lot of caution.

Figure 9-32 illustrates an example of combined analysis of hydrochemical and the geological deformation zone model. Deformation zone NE040A is intersected by boreholes KLX02 and KLX01. It can be observed that both boreholes have a representative sample corresponding to the point of intersection with the deformation zone. The interesting observation is that borehole KLX02 intersects the deformation zone at a greater depth than in KLX01 and both representative samples are relatively dilute, so they can be assumed as being part of the current dynamic fresh water body at Laxemar. The geographical location of both boreholes, i.e. KLX02 (inland) and KLX01 (closer to the coast), is consistent with a topographically-driven flow from KLX02 towards KLX01. Consequently, it can be stated that these two representative groundwater samples fulfil the requisites to be further analysed by means of inverse geochemical models and reactive solute transport models.

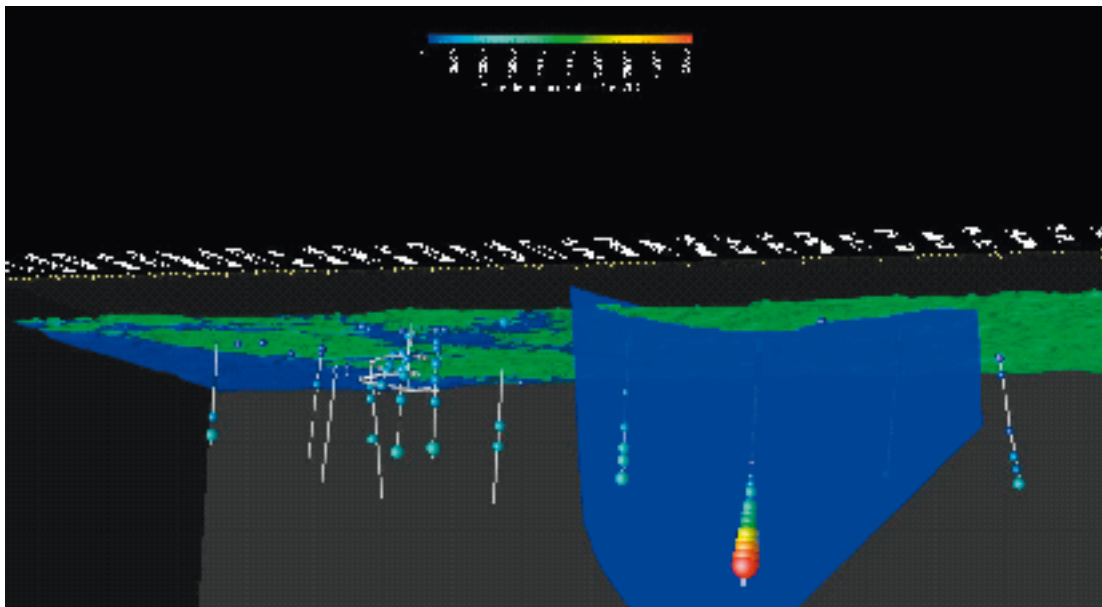


Figure 9-32. Bottom-north view of deformation zone NE040A and chloride concentrations in boreholes. This fracture zone intersects boreholes KLX02 (deeper and inland) and KLX01 (shallower and nearest to the coast).

9.6.4 Resulting conceptual model

The Laxemar subarea represents a continental (inland) hydrogeological framework with a thick fresh water body reaching maximum depths of nearly 1,000 m. However, the Simpevarp subarea represents a coastal hydrogeological framework where fresh water bodies are confined to the first 100–200 m of the bedrock. This dilute groundwater is predominantly of Na-HCO₃ type. The dilute groundwater can be marginally oxidising close to the surface but otherwise reducing. These dilute water bodies correspond to a hydrogeologically dynamic system that can be genetically linked with a meteoric origin. The high bicarbonate contents of this groundwater system can be mainly attributed to the occurrence of organic matter oxidation coming from the soil layers at emerging land, probably in most part due to the microbial activity of anaerobic microorganisms. Calcite dissolution can also be contributing to the alkalinity of dilute water, but it is thought that in a less extent than organic matter oxidation. Other important active hydrogeochemical processes are those related with silicates weathering, which have been conclusively detected by detailed geochemical modelling.

Consistently with the hydrogeological framework, brackish (2,000–6,000 mg/L Cl; 5–10 g/L TDS) and saline (6,000–20,000 mg/L Cl; 25–30 g/L TDS) groundwaters are present at shallow to intermediate (150–300 m) depths at the Simpevarp subarea, and at greater depths (approximately 900–1,100 m) at the Laxemar subarea. It is important to notice that the origin of these water types could be different from one place to another.

At the Simpevarp subarea some residual Littorina Sea (old marine) influence has been identified. On the contrary, at the Laxemar subarea there is no clear evidences of old marine signatures, due to the flushing and replacement of old marine groundwater by the fresh meteoric water circulation. At the Laxemar subarea, glacial signatures appear to be evident only close to the coast (KLX01) and deeper than in Simpevarp subarea. It is worth noting that all glacial signatures are found in groundwater samples brackish or saline with low tritium contents, and then the possibility of being cold modern waters infiltrated during winter seasons can be ruled out. On the other hand, the saline waters found in depth at Laxemar could mainly be attributed to the influence (dispersion/diffusion) of deepest high-salinity (brine) waters.

Brackish and saline waters located at the Simpevarp subarea and, in a less extent, at the coastal Laxemar locations show signatures of glacial influences. However, the glacial hydrochemical signatures are irregularly distributed and have been most clearly detected under the Äspö island and the Simpevarp peninsula. The highest glacial signature corresponds to borehole KAS03 at a shallow depth (about –120 m above sea level).

Finally, highly saline groundwaters (> 20,000 mg/L Cl; to a maximum of ~ 70 g/L TDS) and has only been identified in one borehole at the Laxemar subarea (KLX02) at depths exceeding 1,200 m. These waters show the highest concentrations of most dissolved species and then, even small amount of mixing between these deep highly-saline waters and other type of waters (meteoric, glacial or marine) produces mass transfers that can mask the effects of active geochemical processes in the bedrock. It is thought that deep and highly saline water corresponds to hydrogeological conditions virtually stagnant.

It is worth emphasising that the picture given by the current conceptual model represents the situation existing at the most conductive fractures of the bedrock, where it has been possible to collect groundwater samples. The hydrogeochemical conceptual model of the site is visualised in Section 11.6.

9.6.5 Revisitation of hydrogeochemical stability criteria

There are no new representative samples from repository depth from the Laxemar subarea so samples from earlier sampled boreholes were used to check if they can meet the SKB chemical suitability criteria for Eh, pH, TDS, DOC and Ca+Mg, see /Andersson et al. 2000a/. The samples from from KLX01 at 680–702 m (sampled in 1988) and KLX02 at 798–803 m (sampled in 1993) were selected for this purpose, despite the fact that they reflect conditions below repository depth.

Table 9-3 shows that these samples can meet the SKB suitability criteria for the analysed parameters.

Table 9-3. The hydrochemical composition of the analysed samples KLX01: 680–702 m and KLX02: 798–803 m.

Criterion	Eh (mV) No O ₂ present	pH (units) 6–10	TDS (g/L) < 100	DOC (mg/L) < 20	Colloids (mg/L) < 0.5	Ca+Mg (mg/L) > 40
KLX01: 680–702 m	–275	8.1	8.2	1.2	0.03	1,423
KLX02: 798–803 m	–125*	7.6	0.9	5	n.a.	134

* Measured during a sampling event in year 2002. Not analysed = n.a.

9.7 Integration between hydrogeological and hydrogeochemical models

Since hydrogeology and hydrogeochemistry deal with, and are affected by the same geological and hydrodynamic properties, these two disciplines should be able to complement each other when describing/modelling the groundwater system. Their integration and consolidation is therefore one of the most important tasks within the SDM work.

Testing such an integrated modelling approach was the focus of a SKB project (Äspö Task Force Task 5) based on data from Äspö HRL /Wikberg 1998, Rhén and Smellie 2003/. The advantages with such an approach were identified as follows.

- Hydrogeological models will be constrained by a new data set. If, as an example, the hydrogeological model, which treats advection and diffusion processes in highly heterogeneous media, cannot produce any Meteoric water at a certain depth and the hydrogeochemical data indicate that there is a certain fraction of this water type at this depth, then the hydrogeological model parameters and/or processes have to be revised.
- Hydrogeological models are fully three dimensional and transient processes such as shoreline displacement and variable-density flow can be treated, This means that the spatial variability of flow-related hydrogeochemical compositions can be modelled, visualised and communicated.
- Hydrogeochemical models generally focus on the effects on the obtained groundwater chemistry from reactions rather than on the effects from transport processes. An integrated modelling approach can describe flow directions and hence help to understand the origin of the groundwater. The turnover time of the groundwater system can indicate the age of the groundwater and, knowing the flow rate, can be used to indicate reaction rates. The obtained groundwater chemistry is a result of reactions and transport, and therefore only an integrated description enable plausible explanations of the measurements.
- By comparing two independent modelling approaches, a consistency check can be made. As a result greater confidence in active processes, geometrical description and material properties is achieved.

Within the framework of the SDM Laxemar 1.2 modelling comparison and integration between hydrochemistry and hydrogeology has been further further developed as exemplified in the following section.

The SDM Laxemar 1.2 regional groundwater flow model for groundwater flow described in Section 8.5 includes a double porosity description, with flow taking place in a connected network of fractures and deformation zones and with essentially immobile water in the rock mass between the modelled flowing fractures. Solutes can access the immobile water through diffusion into dead end fractures and by matrix diffusion in the rock matrix. The salinity of the water implies that density driven flow needs to be considered. Thus, the salt both affects the groundwater flow characteristics in the mobile water phase, and diffuses into the immobile water phase. Apart from solute tracer transport, also transport of water types has been modelled. Reactive transport has, however, not been considered in the hydrogeological modelling for Laxemar 1.2, see Chapter 8.

The developed hydrogeological regional flow model, cf. Section 8.5, has been used provide predictions of the groundwater components and isotopes, such as TDS and ¹⁸O, both in the rock matrix and in the flowing groundwater of the connected system of fractures, cf. Section 9.7.1. It has also

been used for dynamic predictions over time of different water types (Dilute groundwater (denoted Meteoric in /Hartley et al. 2006/), Littorina, Glacial and Brine). The groundwater flow model thus, independently from chemistry, provide predictions of the salinity features at selected points within the modelled rock volume, which can be compared with direct hydrogeochemical measurements or M3 calculations.

As described in Section 9.3.2 there were few new hydrogeochemical samples available from the Laxemar subarea at the time of the data freeze for SDM Laxemar 1.2. Thus, in order to facilitate and further develop this complex work of integration between hydrochemistry and hydrogeology data from earlier drilled boreholes (e.g. KLX01 and KLX02) were also used as calibration targets. The representativity of the data from borehole KLX02 has been discussed in various reports /e.g. Laaksoharju et al. 1995, SKB 2006a/. The effects of long-term pumping, open borehole effects and accuracy of tritium analyses have been of concern. The modellers have been aware of these effects and have taken this into account when evaluating the results. The models will be updated when new data become available in the next modelling versions and only then other boreholes can be selected for calibration and comparison purposes.

9.7.1 Paleo-hydrogeological calibration of the reference case

The reference case regional scale model transient coupled groundwater flow and transport model (extended regional model domain and calibrated reference case material properties) has been established through a calibration process relative to a set of hydrogeochemical calibration targets. The resulting reference case material properties are described in Section 8.5.

Even if a perfect match is not obtained, it is still possible to increase the level of knowledge on model response and influence of modelling approaches, by analysing the model variations performed. Furthermore, it is important to note that the calibration does not lead to a unique model that is consistent with observations. Rather it identifies combinations of hydraulic and transport characteristic features and values consistent with the site data and conversely, identifies combinations of settings which are unlikely to occur in reality.

In the text below examples of the calibrations are shown, based on /Hartley et al. 2006/.

Reference waters

Figure 9-33 through Figure 9-35 show the calibration of the reference case against the interpreted 4 reference water profiles for the calibration boreholes KLX01, KLX02 and KSH01A. These calculations were performed with matrix diffusion and the mixing fraction in both the fracture system and diffusion accessible porewater (matrix) are shown. It should be noted that the embedded grid has higher resolution of 50 m for the Laxemar, Simpevarp and Ävrö boreholes, but is coarser, 100 m, around Äspö.

For the Laxemar boreholes, Figure 9-33 shows that in KLX01 the model predicts the mixing zone to be too deep, suggesting that the model has either too high hydraulic conductivity at depth or too low at the surface, which would have the effect of forcing flow much more. The match for KLX02 in Figure 9-34: is more interesting, since the borehole is associated with many more data and is deeper. The transition from Brine to Dilute Groundwater occurs at approximately the correct depth and with a similarly steep slope. The spikes in Littorina and Glacial waters also occur at approximately the correct depths.

Complete results for the Simpevarp boreholes KSH01A, KSH02 and KSH03A are shown in /Hartley et al. 2006/, but here only the results for KSH01A are shown (Figure 9-35). For KSH01A, the mixing zone is located much higher, presumably because the borehole is located near the coast. The match for this borehole is generally good. The data point at about -550 m above sea level suggests more Glacial water than Littorina, which is opposite to the model prediction. The model suggests that the mixing fractions vary rapidly with depth due to the presence of zone ZSMNE024A and other deformation zones. Hence, results are quite sensitive at this depth and also, because several waters are present, the M3 analysis is likely to be more uncertain here. For KSH02, the model prediction for the transition from Glacial to Dilute Groundwater is located about 100 m too deep. KSH03A only has data points near the surface, but nevertheless is a good match.

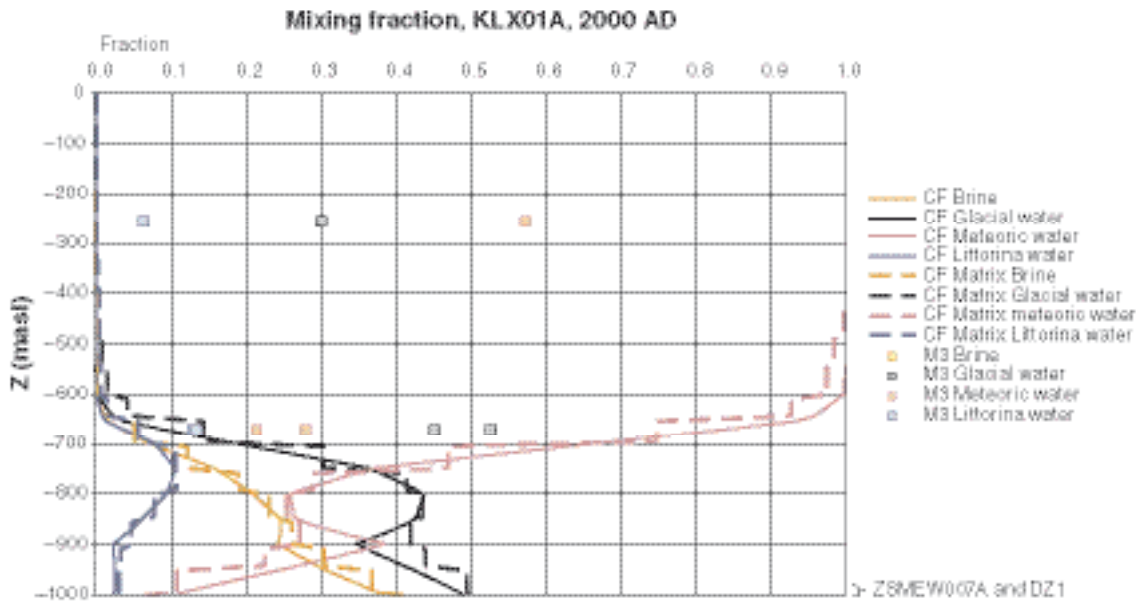


Figure 9-33. Comparison of 4 reference water fractions in KLX01 for the reference case. The mixing fractions in the fracture system are shown by solid lines, in the matrix by dashed lines, and the data are shown by points. Only representative data are shown /Hartley et al. 2006/.

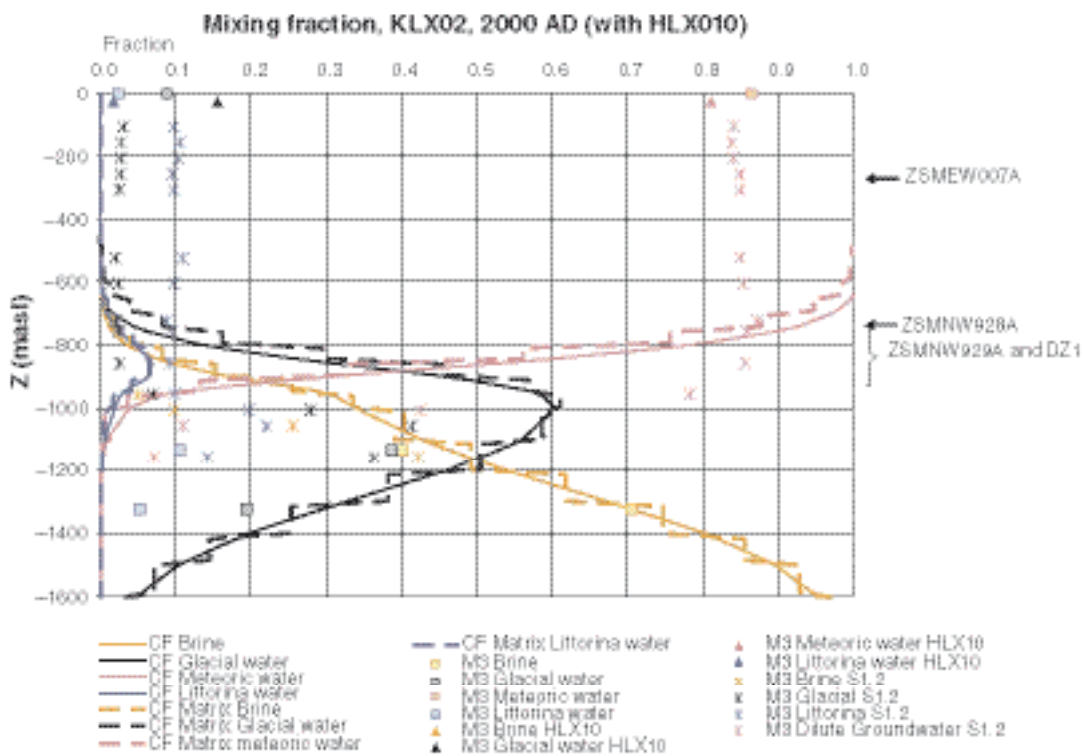


Figure 9-34. Comparison of 4 reference water fractions in KLX02 for the reference case. The mixing fractions in the fracture system are shown by solid lines, in the matrix by dashed lines, and the data are shown by points. The representative data are shown as filled points and some Simpevarp 1.2 data are included as asterix points /Hartley et al. 2006/.

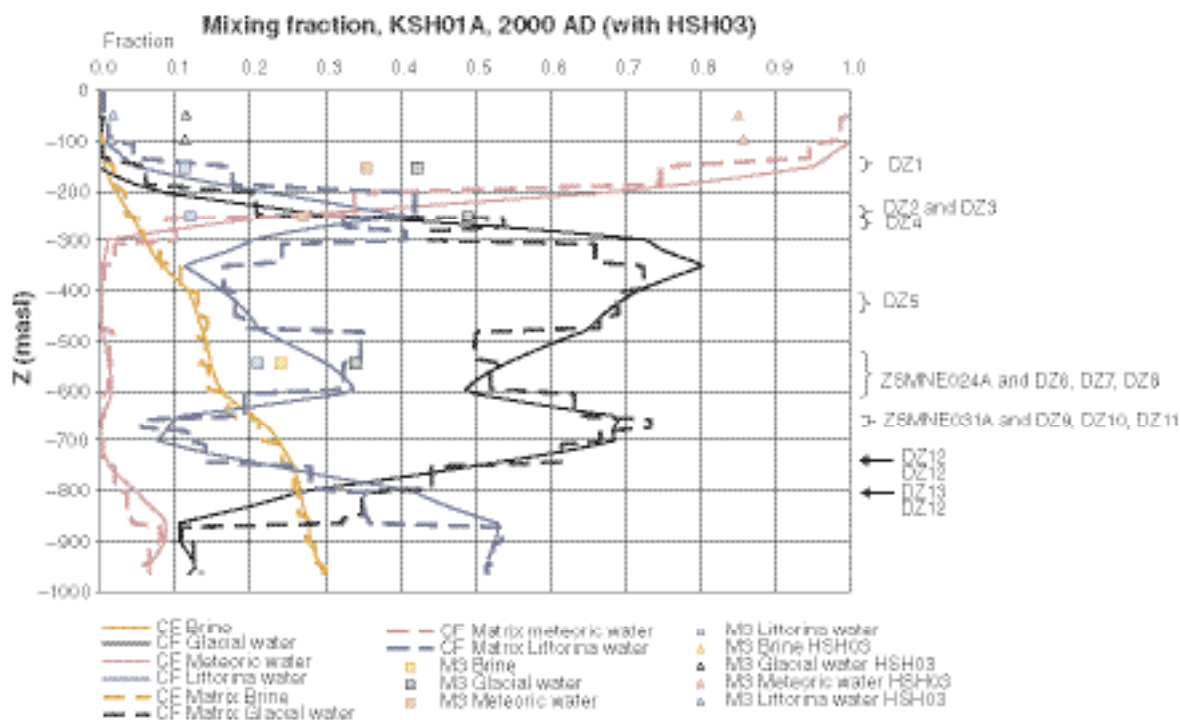


Figure 9-35. Comparison of 4 reference water fractions in KSH01A for the reference case. The mixing fractions in the fracture system are shown by solid lines, in the matrix by dashed lines, and the data are shown by points. Only representative data are shown /Hartley et al. 2006/.

For Ävrö, KAV01 has data points near the surface and at about -550 m (only shown in /Hartley et al. 2006/). The model predicts the mixing zone at about the right depth, but again suggests more Littorina than Glacial, though again this is within the M3 uncertainty magnitude. This location of the transition zone may be associated with the deformation zones ZSMNE012A, DZ1, DZ2 and DZ3, which the borehole intersects between about -400 and -580 m above sea level. If these deformation zones have too high a transmissivity, the model will predict too much flushing.

For KAS02 on Äspö, the model predicts the mixing zone at about the right depth but there is too little Glacial and too much Littorina compared to the M3 data (only shown in /Hartley et al. 2006/). A reasonable match is obtained for KAS03 although spikes in Glacial and Littorina fractions predicted by the model at depth are not seen in the M3 data. There is reasonable agreement between M3 data and the model for KAS04 and KAS06. In KAS04 the model predicts more Littorina than Glacial, as with KAS02.

Salinity

Salinity closely follows the profile of Brine, although there is also a contribution from the Littorina reference water. Figure 9-36 shows the comparison for salinity between the reference case simulation and the data for boreholes KLX01, KLX02, KLX03 and KLX04. In Figure 9-37 the modelling results are compared with the measured values for KSH01A, KSH02 and KSH03A. The boreholes mentioned could be used to illustrate the differences as you move from coastal (KSH01A, KSH02 and KSH03A) to inland (KLX01), and further inland (KLX02, KLX03 and KLX04) conditions. The relative depths of salinity for the series of boreholes are generally well modelled for the KLX and KSH boreholes, and they seem to have the right elements of change with depth.

For Äspö, the modelling results are compared to the measured values in Figure 9-38. A good match is obtained for KAS04 and KAS06. However, the model predicts a higher salinity due to Littorina than the measured data between about -400 and -900 m above sea level.

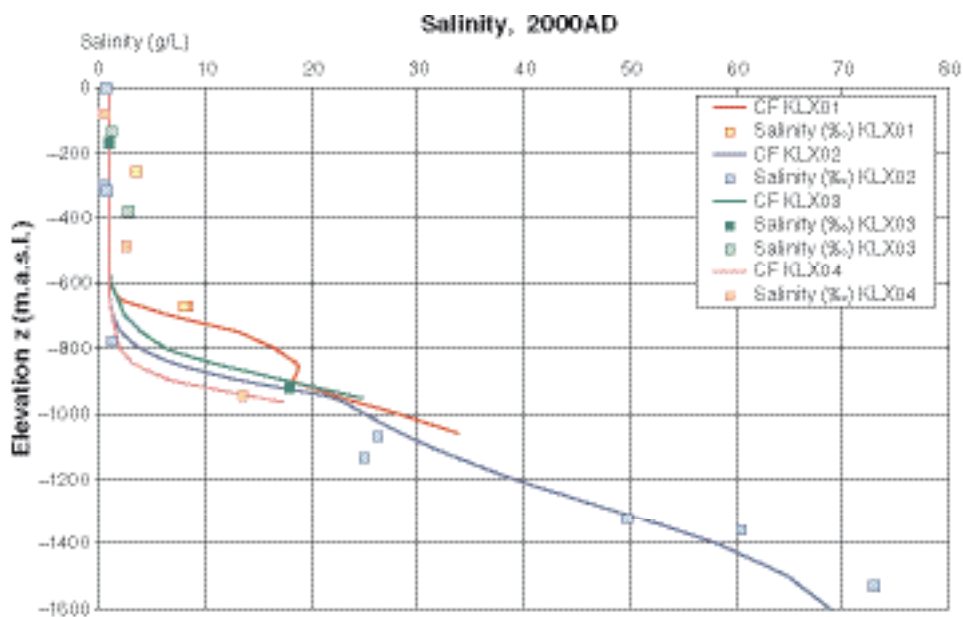


Figure 9-36. Comparison of salinity in KLX01, KLX02, KLX03 and KLX04 for the reference case. The salinity in the fracture system is shown by solid lines, and the data by points. Only representative data are shown, /Hartley et al. 2006/.

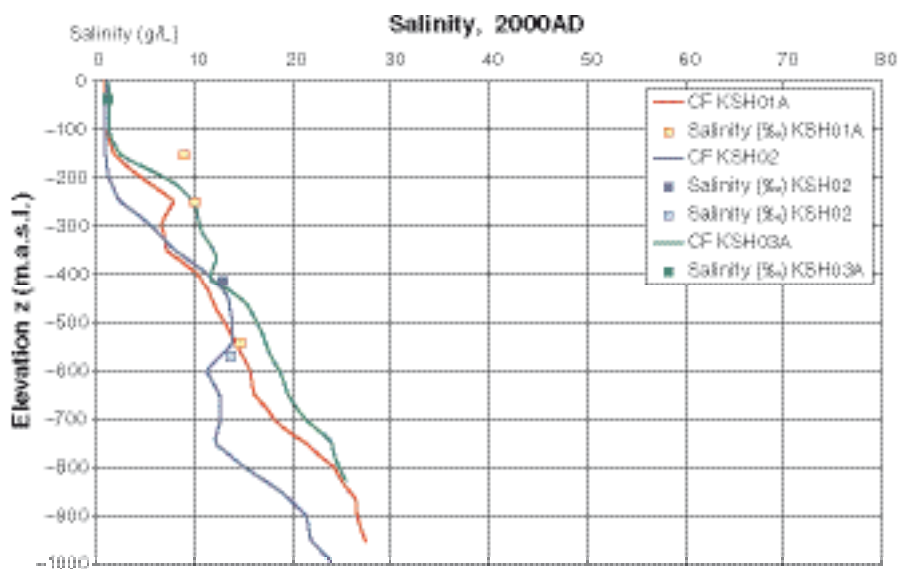


Figure 9-37. Comparison of salinity in KSH01A, KSH02 and KSH03A for the reference case. The salinity in the fracture system is shown by solid lines, and the data by points. Only representative data are shown, /Hartley et al. 2006/.

Environmental isotopes

In addition to comparing the interpreted hydrogeochemistry from the M3 approach, a comparison was made with the environmental isotopes, using them as conservative tracers. The Oxygen-18 isotope ratios are shown for boreholes KLX01, KLX02, KLX03 and KLX04 in Figure 9-39; KSH01A, KSH02 and KSH03A are shown in Figure 9-40, KAV01 and KAV04A in Figure 9-41; and KAS02, KAS03, KAS04 and KAS06 in Figure 9-42. High negative values of $\delta^{18}\text{O}$ are associated

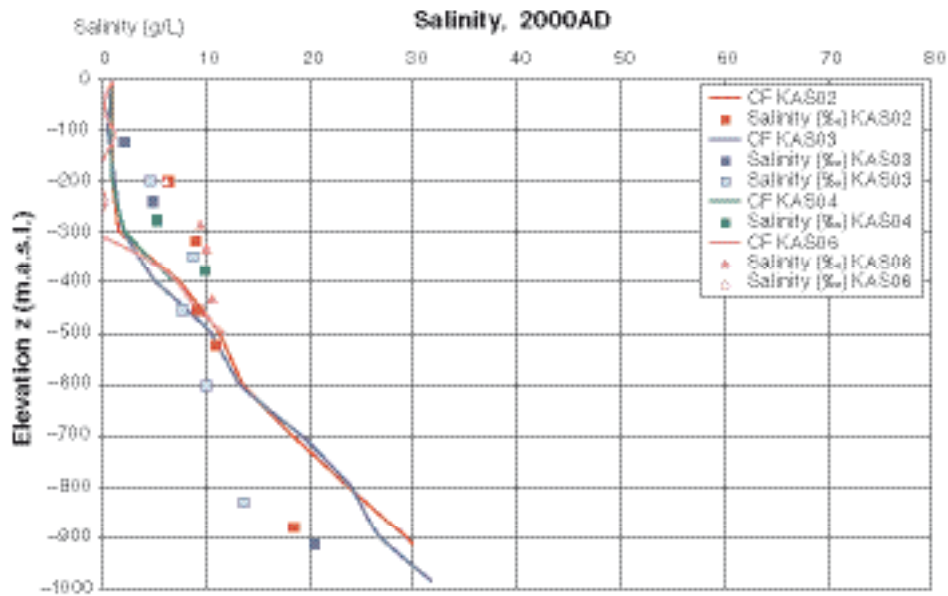


Figure 9-38. Comparison of salinity in KAS02, KAS03, KAS04 and KAS06 for the reference case. The salinity in the fracture system is shown by solid lines, and the data by points. Only representative data are shown, /Hartley et al. 2006/.

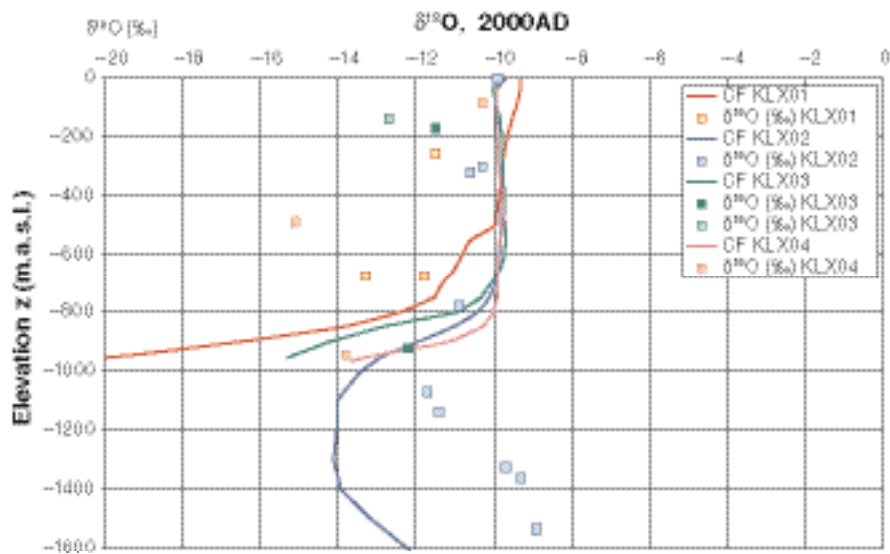


Figure 9-39. Comparison of Oxygen isotope ratio $\delta^{18}O$ in KLX01, KLX02, KLX03 and KLX04 for the reference case. $\delta^{18}O$ in the simulated fracture system is shown by solid lines, and the data by points. Only representative data are shown.

with Glacial water. For example, the model at KLX02 predicts the right sort of shape of profile, but there is a little too much Glacial water at depth, whereas the model is not predicting enough Glacial in the upper part of KLX01 due to too much mixing in the model near this borehole. Pockets of Glacial water in KAS02 and KAS04 do not seem to be reproduced in the model. Still, in general, the overall trends and shapes of the modelled profiles down the boreholes seem to mirror that of the measured chemical data.

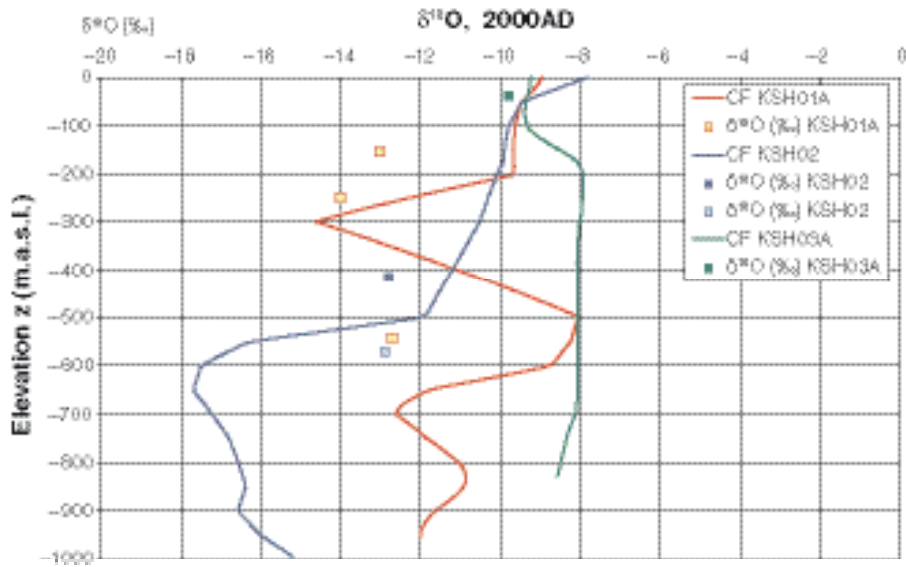


Figure 9-40. Comparison of Oxygen isotope ratio $\delta^{18}\text{O}$ in KSH01A, KSH02 and KSH03A for the reference case. $\delta^{18}\text{O}$ values in the simulated fracture system are shown by solid lines, and the data by points. Only representative data are shown.

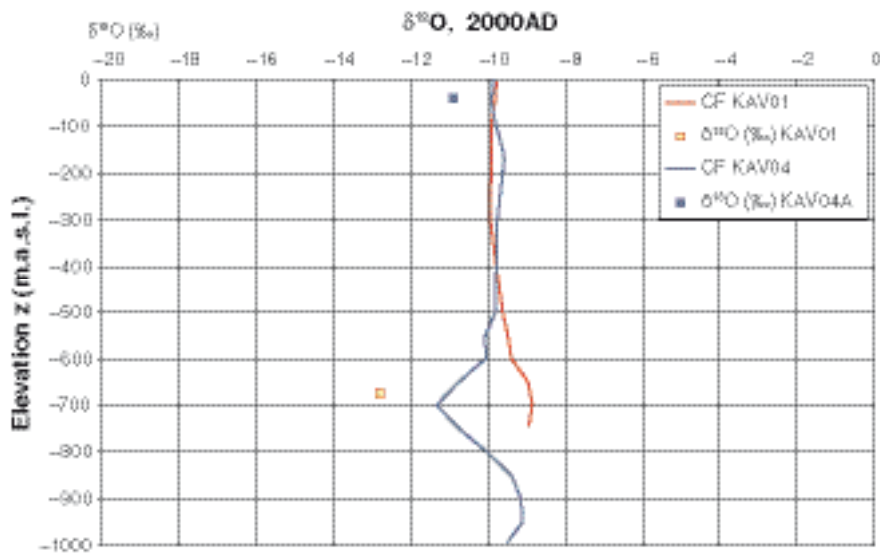


Figure 9-41. Comparison of Oxygen isotope ratio $\delta^{18}\text{O}$ in KAV01 and KAV04A for the reference case. $\delta^{18}\text{O}$ values in the simulated fracture system are shown by solid lines, and the data by points. Only representative data are shown.

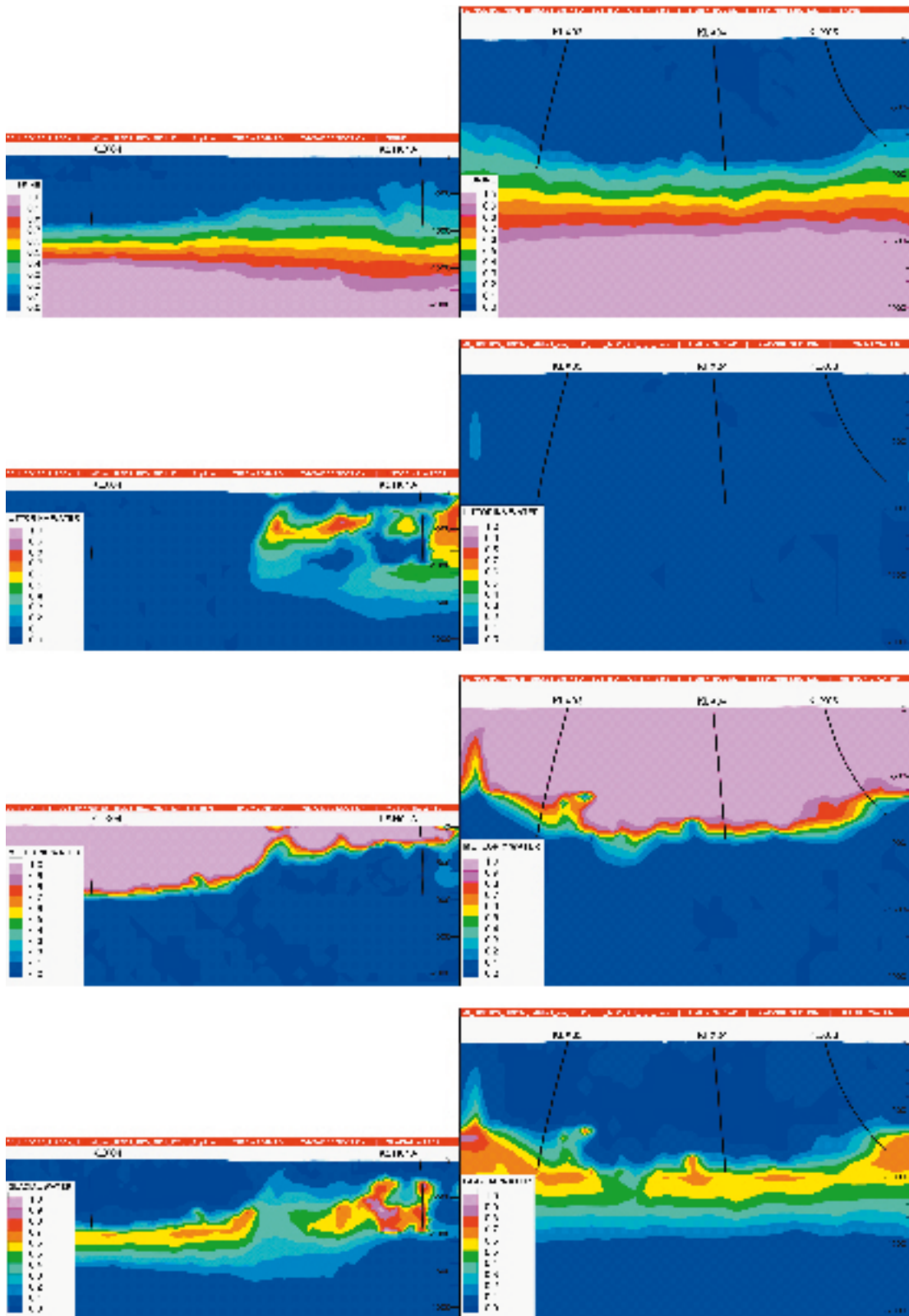


Figure 9-44. Vertical sections along the WNW-ESE (left column) and SSW-NNE (right column) transects, showing the present-day distribution of the reference waters (from top to bottom) Brine, Littorina, Meteoric water (Dilute Groundwater) and Glacial water; for the reference case.

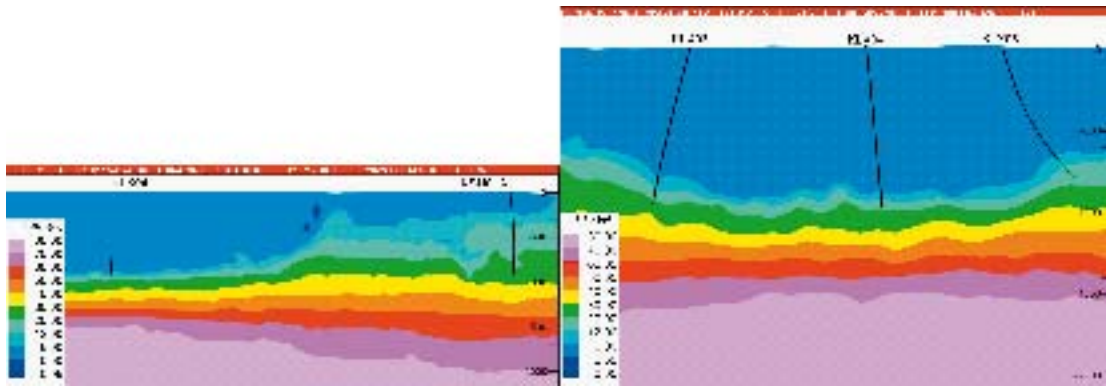


Figure 9-45. Cross-sections along the WNW-ESE (left column) and SSW-NNE (right column) transects, showing the present-day distribution of TDS, for the reference case.

9.7.3 Conclusions

The following conclusions are made.

- The hydrodynamic and hydrogeochemical descriptions support the fact that the site has been affected by the changing climate back in time since independent modelling can describe the occurrence of the water types; Dilute groundwaters (Meteoric), Littorina, Glacial and Brine. This while the chemical initial condition used in the flow modelling includes a well-defined definition of Glacial water, including that of stable isotopes.
- There is potentially too much flushing of Brine in the regional scale reference case suggesting that the calibration could benefit from decreasing hydraulic conductivities at depth. Results from a variant case suggests that reducing the underlying fracture transmissivity by half an order of magnitude below -600 m elevation is sufficient to significantly improve the representation of palaeo-hydrogeology at depth. This is well within the levels of uncertainty in hydraulic properties.
- The distribution of salinity (TDS) broadly corresponds with the conceptual hydrogeochemical sections presented in Section 11.6 of the distribution of brine and adds therefore credibility to the modelling results.
- Further integration is required where e.g. the salinity distribution is used to further explore the similarities/differences but also to be ultimately used for constructing a 3D hydrogeochemical conceptual model of the site and for describing the spatial variability in hydrogeochemical characteristics of the site.
- Calculated mixing proportions from the hydrogeological model can be used to calculate a water composition in the 3D bedrock volume. If process modelling is coupled to the predicted water composition, the spatial variability of important groundwater properties such as pH and Eh can be calculated for the whole rock volume and important questions concerning spatial variability can be addressed.

Compared with model version Simpevarp 1.2 /SKB 2005a/, great progress has been made in the integration work between hydrogeology and hydrochemistry. Hydrogeological modelling has shown that it is possible to simulate the observed water composition in the bedrock at Laxemar by assuming different initial conditions for Brine and Glacial end-members and boundary conditions of infiltration of Littorina and Sea water in accordance with the conceptual palaeohydrogeological model of the site (Figure 3-15). This provides support to the conceptual model used within the hydrogeochemical modelling work.

Integrated models will increase further the understanding of the origin, transport, mixing and reactions processes of the groundwater and will also provide a tool for predicting future chemical changes due to climate changes.

9.8 Evaluation of uncertainties

During every phase of the hydrogeochemical programme – drilling, sampling, analysis, evaluation, modelling – uncertainties are introduced which have to be accounted for, addressed and clearly documented to provide confidence in the end result, whether it is used in the site descriptive model, safety analysis or repository design /Smellie et al. 2002/. Handling of the uncertainties involved in constructing a site descriptive model has been documented in detail by /Andersson et al. 2002a/. The uncertainties can be conceptual uncertainties, data uncertainties, spatial variability of data, chosen scale, degree of confidence in the selected model, and error, precision, accuracy and bias in the model results. The main results of the different evaluations and modelling carried out within hydrogeochemistry are summarised in Chapter 11. Some of the identified uncertainties recognised during the modelling exercise are discussed below.

The following data/model uncertainties have been estimated, calculated or modelled for the Laxemar data based on models used for the 1.2 model versions and based on the Äspö modelling where similar uncertainties are believed to affect the present modelling (the values show the variability range in percent):

- temporal disturbances from drilling may be ± 10 –70%,
- effects from drilling during sampling is $< 5\%$,
- sampling; may be $\pm 10\%$,
- influence associated with the uplifting of water may be $\pm 10\%$,
- sample handling and preparation; may be $\pm 5\%$,
- analytical errors associated with laboratory measurements are $\pm 5\%$ (the effects on the modelling were tested in /SKB 2004a, cf. Appendix 4 therein/),
- mean groundwater variability during groundwater sampling (first/last sample) is about 25%,
- M3 model uncertainty is ± 0.1 units within 90% confidence interval (the effects on the modelling were tested in /SKB 2004a, cf. Appendix 4 therein/).

Conceptual uncertainties can occur in, for example, the palaeohydrogeological conceptual model. The occurrence and influence of old water end members in the bedrock can only be indicated by using certain component or isotopic signatures. The uncertainty therefore generally increases with the age of the end member. The relevance of an end member participating in groundwater formation can be tested by introducing alternative end member compositions or by using hydrodynamic modelling to test if old water types can reside in the bedrock during currently prevailing and throughout the relevant period of the past hydrogeological conditions. In this model version, a measure of validation is obtained by comparison with results of hydrogeological simulations.

Uncertainties in the PHREEQC code depend on which version of the code is being used. Generally the analytical uncertainties and uncertainties concerning the thermodynamic databases are of importance (in speciation-solubility calculations). Care is also required to select mineral phases that are realistic (even better if they have been positively identified) for the systems being modelled. Potential errors in these areas can be addressed by sensitivity analyses, alternative models and associated descriptions. A sensitivity analysis was performed concerning the calculations of activity coefficients in waters with high ionic strength. This analysis and also the uncertainties of the stability diagrams and redox modelling are discussed in /SKB 2004b, cf. Appendix 3/.

The uncertainties were evaluated using the inverse modelling approach included in PHREEQC, and by investigating the compositional variability of end-members and by checking the effects of chemical reactions on the mixing proportions calculated by M4. The test showed that PHREEQC is sensitive to the selection of end-member composition in contrast to M3 and M4, which are less sensitive. M4 showed sensitivity to effects resulting from reactions; such effects will have to be further tested for both M3 and M4.

The discrepancies between different hydrogeochemical modelling approaches can be due to differences in the boundary conditions used in the models or in the assumptions made. The discrepancies between models should be used as an important opportunity to guide further modelling, including validation efforts and confidence building. In this work, the use of different modelling approaches starting from manual evaluation to advanced coupled modelling can be seen as a combined tool for confidence building. Derivation of the same type of process descriptions, independently of modelling tool or approach, increases confidence in the modelling.

The comparison with hydrogeological analysis lends support for the post-glacial conceptual model used and for the concept where groundwaters are affected by changing climate. The evaluation of hydrochemistry needs to take transport aspects in consideration already in the early modelling phase.

10 Bedrock transport properties

The main objectives of the investigations and modelling of the transport properties of the bedrock are to provide parameter values for use in the radionuclide transport calculations performed by Safety Assessment, and to present a description of the site-specific transport conditions that can be used to support the selection of processes and parameters in radionuclide transport models developed by Safety Assessment and others. In relation to Safety Assessment, the role of the site modelling is to describe the site-specific parameters and conditions; Safety Assessment may use other parameters, depending on the scenarios investigated. In addition, the results of the transport properties modelling are used as qualitative and, where appropriate, quantitative input to transport modelling within site descriptive hydrogeological and hydrogeochemical modelling.

The site descriptive transport properties model presented in the current Laxemar 1.2 site descriptive model incorporates both retardation parameters and flow-related transport parameters. The integration of material property data and flow-related aspects of radionuclide transport was absent from the previous Simpevarp 1.2 model version.

In this chapter, material property aspects of the transport SDM are referred to as the *retention properties model* or simply the *retardation model*, whereas the synthesis of material property data with flow-related aspects is referred to as the *integrated transport properties model*. In this context, the terms *site modelling* and *transport properties modelling* refer to the methods and procedures used in developing these models for inclusion within the overall site description /Berglund and Selroos 2003/. The term *transport modelling* by itself, however, refers to the use of these models within the overall site description and for safety analysis.

The retardation model combines material properties data for the major rock types and their various alteration states with a description of various fracture sub-classes typical for the Laxemar site investigation area. This is intended to form a basis for the parameterisation of models used within Safety Assessment.

The major flow-related property of interest is the *flow-wetted surface to flow ratio*, which is also known as the *transport resistance* or simply, the *F-factor*. In certain situations the *water residence time* or *advective travel time*, t_w may also be important for the transport of poorly sorbing radionuclides and colloidal material. Scoping calculations have been used in an attempt to bound the limits of the F-factor for far-field solute transport in the current model version.

10.1 State of knowledge at the previous model version

Laxemar 1.2 represents the first iteration of a site descriptive model for the Laxemar subarea. Although new, the Laxemar 1.2 model version has inherited many features from the Simpevarp 1.2 /SKB 2005a, Byegård et al. 2005/ site descriptive model and related supporting documents from the previous model version for Simpevarp. The overall organisation and structure of the retardation model is essentially the same as that for Simpevarp 1.2, although altered to accommodate newly acquired site specific data for Laxemar.

The main uncertainty identified in both previous model versions (i.e. Simpevarp 1.1 and 1.2) was the lack of site specific transport data. Site specific formation factors based upon laboratory resistivity measurements for all major rock-types (i.e. Ävrö granite, quartz monzodiorite, and fine-grained dioritoid), as well as formation factors from in situ measurements were available for inclusion in Simpevarp 1.2. Data for sorption of Cs and Sr, however, were imported from Äspö Hard Rock Laboratory (Äspö HRL) investigation data, based upon geochemical analogy between Äspö diorite and all major Simpevarp rock types.

In the absence of data for altered site specific materials, specifically in association with fractures, all altered rock types were assumed to have the same diffusive and sorptive properties as that of altered Äspö diorite. A limitation of the imported Äspö HRL data was that different procedural methods

were used for the estimation of sorption coefficients (i.e. compared with the current experimental programme) and it was therefore necessary to use an extrapolation procedure to derive consistent K_d -values as described by /Byegård et al. 2005/. Owing to inconsistencies identified in the parameterisation of the previously established retention model within Simpevarp 1.2, no data was imported for the Laxemar 1.2 model version. Instead, a different extrapolation procedure was used, based upon assumed correlation of sorption properties with the measured surface area of mineral grains. The surface area was measured by way of the BET method using the sorption of gas molecules (typically N_2 or Ar) to a surface /Brunauer et al. 1938/. Although only semi-quantitative estimates can be made in this way, the concept is thought to be more representative of true sorption properties than the previous data import.

A decision was made early in the preparation of Simpevarp 1.2 to not integrate flow-related transport properties and material properties within the site descriptive model. This decision was based largely upon perceived difficulties in communicating the difference between the transport resistances and advective travel times obtained from large scale flow models used in the SDM to those obtained from high-resolution flow models including a repository layout developed by Safety Assessment. As a result of concerns raised during the review process of Simpevarp 1.2, the integration of these two different aspects of transport (i.e. flow-related properties and material properties) has been included in the Laxemar 1.2 SDM, although in a substantially modified form compared with that in Simpevarp 1.1 (i.e. not based on large scale hydrogeological simulations). It is noted here that this integration is only partially complete within the current site descriptive model and is meant to form a basis for further discussion and scrutiny within safety analysis.

10.2 Modelling methodology and input from other disciplines

The process of site descriptive modelling of transport properties is described by /Berglund and Selroos 2003/. Essentially, the description consists of three parts:

- Description of rock mass, fractures and deformation zones, including relevant processes and conditions affecting radionuclide transport; the description is required to express the understanding of the site and the evidence supporting the proposed model;
- Retardation model: Identification and description of “typical” rock-, fracture-, and deformation zone materials, including parameterisation;
- Integrated transport properties model: Synthesis of flow-related transport properties with material properties parameterisation of the 3D geological model and assessment of understanding, confidence and uncertainty.

The methods used within the transport programme produce primary data on the retardation parameters (i.e. the porosity, θ_m , the effective diffusivity, D_e , and the linear equilibrium sorption coefficient, K_d). These retardation parameters are evaluated, interpreted and presented in the form of a retardation model; the strategy for laboratory measurements, data evaluation and development of retardation models is described by /Widestrand et al. 2003/. In the three-dimensional modelling, the retardation model is used to parameterise the various geological “elements” in the site-descriptive geological model. These “elements” consist of the rock mass itself (described in terms of rock domains) containing varying proportions of different characteristic rock types, fracture types, and deformation zones. The integration of the material properties parameterisation with the flow-related properties (the F-factor) provides a basis for flow-path averaging and scale-up of flow path retention properties.

The site specific F-factor estimations in the present model version are obtained by “first-order” consideration of possible flow paths in the first 10–100 m surrounding a canister deposition location. It is assumed that the background networks of flowing fractures as identified from borehole investigations and characterised using hydraulic DFN models are representative of the flow paths likely to be encountered in this rock mass (i.e. Hydraulic Rock Domain, HRD). Although transmissivity data is available for many large-scale conductive features, cf. Chapter 8, there is a lack of supporting information required both for the parameterisation of suitable retardation models as well as for estimation of the flow-wetted surface of these features (e.g. the actual number of sub-parallel

fractures comprising the deformation zones, their geometry, and spatial distribution). For this reason, local minor and local major deformation zones (i.e. Hydraulic Conductor Domains, HCD) are not currently considered to provide substantial transport resistance for the retardation of radionuclide migration. This, of course, may be an overly conservative assumption, although given the current data set there is presently no well established scientific rationale for stating differently. In future versions of the site descriptive model it is anticipated that these HCD features will also be included within the integrated transport properties model.

As the estimation of the site specific transport resistance is strongly influenced by modelling assumptions that are not easily verifiable, we seek to make a prediction of this parameter from first principles using the minimum of essential assumptions. This is desirable not only for reducing uncertainties surrounding such calculations, but also for reasons of transparency and credibility. Where assumptions must be made that cannot be adequately quantified at this time, this fact is noted and alternative interpretations and supporting evidence are presented, where appropriate. This is particularly an issue for discussions concerning the distribution of transport resistance amongst different hydraulic conductors comprising the transport flow paths.

The development of retardation models relies to a large extent on interactions with other disciplines; primarily Geology and Hydrogeochemistry. Specifically, Geology provides lithological and structural models in which the rock types, fractures and deformation zones are described, as well as the mineralogical compositions of intact and altered materials. Hydrogeochemical information is used as a basis for the selection of water compositions in laboratory measurements of retardation parameters /Byegård et al. 2006/. Furthermore, hydrogeochemical data, together with results from mineralogical and geochemical analyses of fracture materials, are important inputs to the development of the retardation model and the description of the understanding of the retention processes at the site.

10.3 Conceptual model with potential alternatives

10.3.1 Basic conceptual model

The conceptual model underlying the present descriptive model is based on a description of solute transport in discretely fractured rock. Specifically, the fractured medium is viewed as consisting of mobile zones and immobile zones. The mobile zones are regions within fractures and deformation zones where groundwater flow and advective transport take place. The immobile zones include the rock mass itself as well as stagnant regions within or immediately adjacent to fractures and deformation zones where solutes can be retained (i.e. removed temporarily or permanently from the mobile water) /Berglund and Selroos 2003/. In the safety assessment framework that provides the basis for identification of retention parameters in the site descriptive models, retention is assumed to be caused by diffusion and equilibrium sorption. These processes are reversible and are here referred to as *retardation processes*. A schematic illustration of the mobile and immobile zones is depicted in Figure 10-1 below.

The conceptualisation outlined above implies that radionuclide transport takes place along flow paths consisting of connected “sub paths” in fractures and deformation zones of different sizes. The fractures and deformation zones reside in specific rock types comprising the various rock domains identified at the site (where the rock domains can contain one or more different rock types, as described in Chapter 5).

Four different, principal fracture types are currently considered within the retardation model. For the most part these differ only by type and depth of alteration, although provision is made in the conceptual model for inclusion of relations between material properties and transmissivity (or even fracture orientation) if these are subsequently shown to be operative. For the modelling of radionuclide transport retardation, larger complex fractures and minor deformation zones constitute the link between single fractures and larger-scale zones.

Fractures are considered to have layers of hydrothermal and sometimes tectonic alteration that extend from the fracture surface to some distance within the host rock. Although no retardation model has been developed for local minor deformation zones in this model version, it is implicitly assumed that each zone is comprised of one or several types of altered wall rock. The conductive

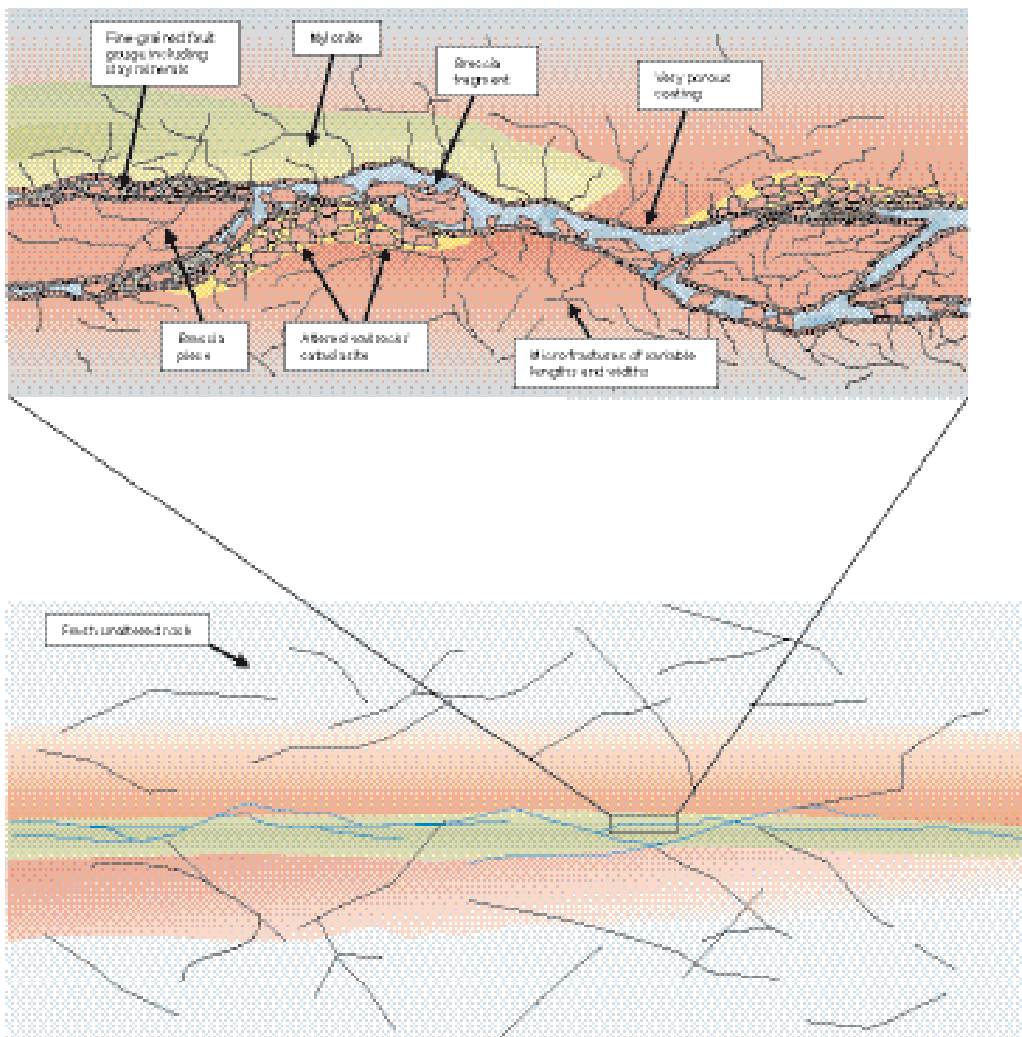


Figure 10-1. Schematic illustration of mobile and immobile volumes in a fracture. Based on conceptual model taken from /Andersson et al. 2002c/.

parts of the zones usually consist of multiple fractures and crush zones that can be classified as belonging to one or more of the four main fracture types mentioned above, or to a broader fault gouge classification. On the basis of this classification, four types of altered rocks have been selected for porosity, diffusion and batch-sorption measurements in the laboratory programme /Byegård et al. 2005/; these are fault gouge, chlorite, porous episyenetic wall rock, and cataclasite (with, or without mylonitic banding).

In the conceptual model, advection is the dominant process for moving the radionuclides in the transport direction, whereas the main role of diffusion is to remove the solutes from the mobile zone and transport them within the immobile zones.

It should be noted that this conceptual model, and the present methodology for site descriptive modelling in general, are to large extent based on previous experience from experiments at the Stripa mine /e.g. Birgersson et al. 1992/ as well as from the Äspö Hard Rock Laboratory (Äspö HRL). The conceptual model in its current form is derived primarily from the TRUE project /Winberg et al. 2000, Poteri et al. 2002/ carried out at the Äspö HRL, which may not necessarily be fully applicable to the transport conditions in the Simpevarp area including the Laxemar subarea. This means that the conceptual and methodological implications of the observations made during the site investigation must be considered. Presently, however, there are no indications that the established conceptual model is unrealistic or not applicable to the Laxemar subarea.

10.3.2 Alternative models

Alternative conceptual models could involve additional processes or more refined descriptions of the presently considered processes. Furthermore, different conceptualisations of the radionuclide transport paths could be considered. An example of this would be advective flow paths in accordance with the basic conceptual model described above in combination with, for instance, diffusive transport in the mobile zone. For radionuclide retention, consideration of more refined representations of sorption (process-based sorption models) and additional retention processes (e.g. precipitation and co-precipitation) are of particular interest. New modelling activities involving process-based sorption models were initiated during the Simpevarp 1.2 transport modelling and are ongoing. This modelling constitutes a first attempt at reactive-transport simulations in a single fracture, using data from the Äspö HRL /Dershowitz et al. 2003/. The aims were to gain experience of this type of modelling in a transport context, and to investigate whether the process-based sorption models show qualitative differences or specific features that cannot be reproduced with K_d -based models. Although such differences and features can be observed in the preliminary results of the study, it remains to be evaluated whether these effects occur under realistic conditions or are modelling artefacts. Hence, no conclusive results that could support, or provide alternatives to, the K_d -based model presented here are currently available. It is noted that models incorporating sophisticated process descriptions, with the aim of simulating more physically realistic conditions, should also be appropriate for the time scales considered.

10.4 Description of input data

The input data reports used in the site specific modelling are detailed in Chapter 2, Table 6-2. The Laxemar 1.2 data evaluation and retardation model are presented in a background report /Byegård et al. 2006/. For flow-related transport properties, data and models used for the estimation of the F-factor are given in the report by /Crawford 2006/. The background reports are summarised in this and the following sections; for further details the reader is referred to those reports.

10.4.1 Data and models from other disciplines

/Byegård et al. 2006/ have summarised and evaluated data from Geology and Hydrogeochemistry with the aim of identifying and describing relevant materials and conditions for transport analyses. The results provide a basis for the continued sample selection and laboratory investigations (primarily related to fractures and deformation zones), and for interpretations of experimental results and modelling. The background report by /Crawford 2006/ summarises and evaluates data primarily from Hydrogeology for the parameterisation of simplified models of transport within conductive features comprising the rock volume surrounding the repository.

Geology – rock types

As described in Chapter 5, the two rock types that dominate the Laxemar subarea are Ävrö granite and quartz monzodiorite. There are, however, strong variations in texture and composition and clear instances of magmatic mixing between different rock types. Minor rock types also occur as dykes, lenses and xenoliths.

Rock alteration, frequently indicated by red staining of the host rock along the fractures, is a common feature in the entire Simpevarp area, but most extensively widespread on the Simpevarp peninsula and in the northern part of the Laxemar subarea. Generally speaking, the altered parts of the rock can be assumed to have transport properties that differ from unaltered rock. This may be due to, for example, lower biotite content and, in some cases, higher content of sericite and illite that influences the sorption capacity. It should be noted that alteration can lead to an increase or a decrease in sorption K_d as compared with the host rock, depending upon the types of secondary minerals present and the solute concerned. Additionally, altered rock typically has a higher porosity and it is also possible for the changed structure of the porosity to influence the effective diffusivity of the rock. Depending on the nature of the alteration processes involved this could give rise to either increased or decreased effective diffusivity compared with the host rock.

Fractures and deformation zones

Crush zones have been excluded from the statistics of fractures and fracture mineralogy within this model version. The validity of this assumption needs to be further evaluated together with the geological and hydrogeological modelling teams within the scope of forthcoming model versions. For Laxemar and Simpevarp there seems to be some overlap in size and transmissivity between single fractures and crush zones (see Section 8.2 and also /Byegård et al. 2006/). This raises the question whether some, if not all, of these crush zones should be defined as minor zones from a transport modelling perspective.

A weakness in the current procedure for assigning transport properties to transmissive features, particularly fracture zones (HCD), is that the true flow-wetted surface of these features is unknown. More effort will be made in future versions of the site descriptive modelling to assess the flow-wetted surface in these features more accurately.

A particular problem for transport modelling and the parameterisation of the retardation model is how many substructures or parallel fractures are considered to comprise identified PFL flow anomalies. This is doubly important with respect to the fact that sealed as well as open, but non-flowing, fractures will contribute to the bulk material properties of the rock mass adjacent to flow paths (i.e. porosity and effective diffusivity). Previous investigations have found, for example, that the effective diffusivity (determined by in situ electrical resistivity measurements) in borehole sections containing sealed and non-flowing open fractures may be two to four times higher than that of rock lacking identifiable fractures /Löfgren and Neretnieks 2005a/. Potentially this could mean that the effective diffusivity (formation factor) of the rock mass containing sealed fractures is higher than that estimated from measurements made on non-fractured rock matrix pieces.

Presently, no significant mineralogical differences can be found between the open fractures identified from core logging and the open fractures identified with the PFL flow log /Byegård et al. 2006/. If such a difference were to exist this would have implications for the parameterisation of material properties of altered layers and surface rims for fractures where transport is likely to occur. Another aspect of this with implications for the flow distribution within fractures (i.e. channelling phenomena) is that accumulations of clay minerals and fault gouge could potentially hinder water flow if sufficiently large amounts are present. The water would then seek out paths where the transmissivity is locally higher. This could mean that fractures featuring large amounts of gouge and clay are also less transmissive than fractures with relatively small amounts of these infill materials.

Most of the open fractures contain chlorite and calcite. Other hydrothermal Al-silicates are common although subordinate and not expected to make significant contributions to the overall sorption capacity. Clay minerals and hematite, in contrast, are expected to have comparatively higher sorption capacities. Fractures sealed with porous and brittle minerals may constitute important diffusion pathways, although they may also be reactivated in the future and become advective flow paths.

Hydrogeology

Hydrogeology provides input for the calculation of flow-related transport properties in two ways. Firstly, the data obtained from hydraulic tests carried out in boreholes can be used to characterise the transmissivity distribution of individual flowing features as well as the average hydraulic conductivity of the rock over larger borehole intervals. The methods used for obtaining these data are many and are discussed in Chapter 8 and the associated background reports /e.g. Rhén et al. 2006c, Rahm and Enachescu 2004a–f, 2005ab/. Secondly, data obtained using the Posiva Flow Log (PFL) tool can be used to make estimates of conductive fracture frequencies (*CFF*) down to a very fine resolution (decimetre scale). Both the distribution of fracture transmissivities and the conductive fracture frequency are fundamental requirements for the estimation of realistic, site-specific F-factors. Hydrogeology also provides a hydraulic DFN model, cf. Section 8.4, for flow properties within the current SDM which is used for calculations made within SR-Can that include estimates of the F-factor. This section, however, attempts to make more robust estimates of the F-factor with simplified approaches that preserve the essential physics of the system while giving greater transparency.

In addition to the data that are used directly for the estimation of transport resistance, hydrogeology also provides qualitative information that can be used to identify the existence or non-existence of trends or correlations between fractures and specific rock types and alteration fabrics. Such

information may, in turn, provide a basis for identifying correlations between transport parameters and fracture types.

Hydrogeochemistry

The hydrogeochemical modelling of the Laxemar subarea is presented in Chapter 9 and only a brief overview of results with direct relevance for transport properties modelling is given here.

Compared with the groundwater chemistry of the Simpevarp sub area, two major differences can be noted. Firstly, fresh to diluted meteoric water dominates down to depth of 500–700 m in Laxemar whereas this groundwater type is only found in the upper 100–200 m in Simpevarp. Secondly, brackish to saline water with a marine component has not been identified in the Laxemar sub area although it was found within the Simpevarp sub area. The consequence of this is that the repository depth at Laxemar represents a mixing zone between fresh diluted water and old saline water typically in-mixed with a glacial component.

For the laboratory measurements of diffusivity and sorption capacity, the following groundwater types have been identified as representative for the present groundwater circumstances at the sites (I–III below) /Byegård et al. 2006/. In addition, a brine type water (IV) has been included in order to cover possible future changes in groundwater chemistry at repository depth. The water types are specific “simulants” of the more generalised groundwater categories A–D as described in Chapter 9 and are suggested for all sites under investigation:

- I. Fresh diluted Ca-HCO₃ water; groundwater now present in the upper 100–750 m of the bedrock, but also a water type that can be found at larger depths during late phases of glacial periods.
- II. Groundwater with marine character, Na-(Ca)-Mg-Cl (5,000 mg/L Cl); a possible transgression of the Baltic Sea may introduce this type of water to repository depth. (Thought to be less important for the Laxemar subarea than for the Simpevarp subarea.)
- III. Groundwater of Na-Ca-Cl type (8,800 mg/L Cl); present groundwater at repository level in the Simpevarp peninsula.
- IV. Brine type water of very high salinity, Ca-Na-Cl type water with Cl content of 45,000 mg/L; during a glacial period, brine type waters can be forced to more shallow levels than at present /e.g. Puigdomenech 2001/.

The detailed compositions of these water types are given in the background report to this chapter /Byegård et al. 2006/.

For the Laxemar samples, water of salinity close to type III above has been used for the diffusivity measurements, however, only the major components (i.e. Ca²⁺, Na⁺, Cl⁻ and SO₄²⁻) were included as the exact ion composition is not expected to influence the diffusion experiments.

For the batch sorption experiments, the groundwater composition is considered to be more important, and three different groundwater compositions have been selected (types I, III and IV). In a smaller subset, owing to limited available sample quantities (e.g. for fracture materials), only two water types have been selected. In these cases, water types I and III have been given priority.

10.4.2 Transport data

Available data

The data available for Laxemar 1.2 modelling are summarised in Chapter 2, cf. Table 2-6. The data set consists of laboratory and in situ measurements of material properties as well as supporting information from other disciplines.

Many of the experiments are still in progress and thus the dataset available for use in the transport modelling is somewhat limited. The available site investigation data on transport properties at the data freeze for Laxemar 1.2 are summarised in /Börjesson and Gustavsson 2005/, /Thunehed 2005/, and /Löfgren and Neretnieks 2005b/. This largely consists of numerical data from the water saturation porosity measurements, a small number of through-diffusion data, and formation factors

obtained from laboratory as well as in situ electrical resistivity measurements. All reported transport data not included in the above references lie outside the data freeze.

Supporting descriptive data from the combined geological/hydrogeochemical interpretations of fracture mineralogy and wall rock alteration data are provided by /Drake and Tullborg 2005/. Other geological, hydrogeological, and hydrogeochemical inputs were obtained from the SDM report, (i.e. from draft versions of the relevant chapters) and the hydrogeochemical modelling background reports from Simpevarp 1.2 /SKB 2004c/ and Laxemar 1.2 /SKB 2006a/.

No surface area or sorption data were available for the Laxemar 1.2 data freeze, although a small number of preliminary data have been included in this report based upon the data presented in the background report by /Byegård et al. 2006/. No PMMA porosity measurements are presented in this model version (polymethylmethacrylate; an impregnation method for studying the pore system, see /Hellmuth et al. 1993, 1994, Byegård et al. 1998/).

Application of Äspö HRL data to Laxemar

In the previous Simpevarp 1.2 model version, data was imported from Äspö HRL data for analogue rock types /for details see Byegård et al. 2005/. No such data import has been used in Laxemar 1.2.

Owing to differences between the evaluation procedures as well as the properties of the analogue rock types, the altered layers within the Simpevarp 1.2 retardation model were parameterised with weaker retention properties than the unaltered rock matrix. Although possible, it is now thought that this is an artefact of the previous data import and a new procedure has been adopted in Laxemar 1.2 in order to obtain data estimates for rock types and alteration forms where there are no available sorption measurement data (see Section 10.5.4).

10.5 Evaluation of transport data

Only a brief account of the Laxemar 1.2 data evaluation is given in the following sections. This consists primarily of summary tables of the available data. The details of the data evaluation procedure are described in the background report by /Byegård et al. 2006/ where additional comments and references are given. Data concerning the distribution of transmissivities in the rock volumes characterising the Laxemar subarea are detailed in Chapter 8 and are not repeated here. Some data, however, are presented in this section concerning the estimated specific flow-wetted surface of flowing features within the rock. Details concerning these calculations are given in the background report by /Crawford 2006/.

10.5.1 Methods and parameters

The main laboratory methods used within the Transport programme are through-diffusion tests on slices of rock samples for determining the effective matrix diffusivity, D_e , and batch sorption tests on crushed rock and fracture-filling materials for determining the equilibrium sorption distribution coefficient, K_d . Most of the through-diffusion tests are performed with HTO (tritiated water) as a tracer. The formation factor, F_f , which is related to the diffusivity as $F_f = D_e/D_w$ (D_w is the free diffusivity in water), is evaluated from the measured diffusivities, and is then used to calculate the diffusivities of all tracers or nuclides of interest, see /Widestrand et al. 2003/.

Electrical resistivity measurements are also used to determine the formation factor. This is a relatively fast method, which enables testing of large numbers of samples. Thus, the majority of the laboratory formation factor data are from resistivity measurements. In addition, the laboratory programme includes measurements of the porosity, θ_m , by the water saturation technique, and for some samples also by PMMA measurements. The through-diffusion tests also provide estimates of the porosity by means of the “capacity factor” calculated from the experimental results.

The in situ methods within the Transport programme include borehole electrical resistivity measurements (in situ formation factor logging), as well as tracer tests of various kinds. The aim of these tracer experiments is the demonstration of field-scale retardation through tracer tests carried out

in situ. At the present time, a small number of single well injection-withdrawal (SWIW) tests involving both sorbing and non-sorbing tracers have been carried out in the Laxemar subarea /Gustafsson and Nordqvist 2005/. More of these tests are underway or in the planning stage. Other field tracer tests include the in situ K_d experiment currently underway at the Äspö HRL within the LTDE (long term diffusion experiment) project as well as planned tracer tests in multi-well configurations. These field experiments are also considered to be sources of primary data for the SDM.

10.5.2 Porosity

The results of porosity measurements on samples from the boreholes in Laxemar are summarised in Table 3-1 in the background report /Byegård et al. 2006/. The large standard deviations of some of the data, with sample mean minus the standard deviation (σ) showing negative values in some cases, indicate that log-normal distributions are more appropriate than, for example, normal or rectangular distributions for describing the data. It is noted that the porosities are low and remarkably consistent amongst the various rock types represented in the Laxemar subarea.

The geological characterisation under binocular microscope shows a great number of small cracks that are 3–15 mm in length and with a width of ≤ 0.5 mm in both fresh and altered rock samples. These cracks are larger than intragranular micro cracks /Strähle 2001/, and cut right through mineral grains. A comparison of results where the samples with alteration or cracks have been excluded indicates that cracks may increase the porosity. Alteration of the rock is thought to influence porosity /e.g. Eliasson 1993/ although there are currently not enough data to quantify this effect. Making allowances for differences in sample support amongst the various rock types, it appears that all major rock types have similar porosities in the range 0.14–0.4% when based upon the data for rock without cracks.

Stress release effects during sampling and damage induced during sawing and sample preparation also are thought to result in overestimation of the measured porosity and diffusivity of the samples. Damage acquired during sawing may include additional microfractures in the samples, which thus may increase the porosity in the rock closest to the edges of the sampled rock. It follows that this effect should be more pronounced in shorter rock samples. The effect of the sample length is illustrated in Table 3-2 in the background report /Byegård et al. 2006/, which indicates that the measurement method gives an increase in porosity values with shorter sample lengths. This is supported by earlier porosity measurements in connection with diffusion experiments /Johansson et al. 1997/ and is consistent with expectations based upon consideration of pore-connectivity over different length scales (i.e. it is expected that fewer pores will be connected over longer length scales). It should be noted, however, that the statistical significance of some of the data in both Table 3-1 and Table 3-2 is questionable owing to too few samples being available to make rigorous comparisons.

10.5.3 Diffusion

For the Laxemar 1.2 modelling, diffusivity values are available from through-diffusion tests in the laboratory /Börjesson and Gustafsson 2005, Byegård et al. 2006/, as well as from resistivity measurements both in situ and in the laboratory /Löfgren and Neretnieks 2005b/.

Through-diffusion studies

Results from through-diffusion experiments are given in Table 3-3 in the background report /Byegård et al. 2006/. The through-diffusion results from the site investigation should be considered preliminary, because steady state conditions, necessary for final evaluation, have not been reached in most samples.

For the Ävrö granite samples that are considered to have reached steady state conditions, formation factors in the range 5.2×10^{-5} – 7.5×10^{-5} have been obtained for three closely spaced, 10 mm long core samples taken from KLX02 plus a single measurement of 3.1×10^{-4} for a 30 mm long sample from a different part of the same borehole. These are slightly lower than the values obtained for the corresponding laboratory resistivity measurements, but are similar to the values obtained for the resistivity measurements performed in situ (cf. Table 3-4 in /Byegård et al. 2006/). The other steady-state data in the background report, Table 3-3 /Byegård et al. 2006/ relate to three 30 mm samples of

porphyritic and coarse-grained Ävrö granite, for which approximately five times higher formation factors were obtained. This is not unexpected as the presence of larger grains in these samples is suspected to be associated with larger intergranular voids and consequently higher effective diffusivities. A systematic deviation, however, between the porosity determined by water saturation and the α -factor (which, for tritiated water, can be assumed to be identical to the effective transport porosity of the rock) can be observed for these three samples. The reason for this is not clear and will need to be addressed in future model versions.

A large number of samples where steady state conditions have not been obtained are (for comparative purposes) also included in the results given in the background report, Table 3-3 /Byegård et al. 2006/. These preliminary results indicate a general consistency with the laboratory resistivity measurements, possibly with through-diffusion results giving somewhat lower formation factors than those obtained using laboratory resistivity measurements.

Electrical resistivity measurements

A summary of the results of the electrical resistivity measurements reported by /Löfgren and Neretnieks 2005b/ is provided in Table 10-1 below. The results are expressed in terms of formation factors, both in non-log and \log_{10} units. The data suggest formation factors approximately in the range 10^{-5} – 10^{-4} with Ävrö granite having the highest formation factor by a factor of 2–4 compared to other rock types. Similarly to the porosity data discussed above, standard deviations are in many cases of the same order of magnitude as the mean values.

Table 10-1. Summary of formation factors for the rock types of the Laxemar subarea. The values are given as mean value $\pm \sigma$ of the considered datasets. Non-log (N) and \log_{10} values (LN) are specified for each category where appropriate (number of samples is given as N_s).

Rock Type	Method:	Electrical resistivity (lab)	N_s	Electrical resistivity (in situ)	N_s
Ävrö granite	N	$(1.4 \pm 1.0) \times 10^{-4}$	114	$(6.2 \pm 2.9) \times 10^{-5}$	43
	LN	-3.98 ± 0.35		-4.27 ± 0.27	
Quartz monzodiorite	N	$(3.6 \pm 3.5) \times 10^{-5}$	3	$(2.14 \pm 0.09) \times 10^{-5}$	6
	LN	-4.56 ± 0.39		-4.67 ± 0.02	
Fine-grained dioritoid	N	9.2×10^{-6}	1		
	LN	-5.04			
Fine-grained diorite-gabbro	N	$(6.4 \pm 4.2) \times 10^{-5}$	7	$(3.4 \pm 1.7) \times 10^{-5}$	2
	LN	-4.30 ± 0.33		-4.49 ± 0.22	
Granite	N	7.5×10^{-5}	1		
	LN	-4.13			

Detailed discussions concerning the distribution of formation factors as well as possible correlations with porosity and borehole length can be found in the background data report /Byegård et al. 2006/. Some general observations, however, concerning the electrical resistivity data are made below.

Laboratory resistivity versus porosity

A tendency of increased formation factor with increasing porosity can be observed in the results. The results appear very scattered when plotted on a linear scale although seem to be better behaved when plotted on logarithmic axes. Quantification of the formation factor correlation with porosity is tenuous, however, and there is only a very vague suggestion of correspondence with a power law relation such as Archie's law. There is a weak suggestion of a log-normal distribution of porosities in some of the porosity data sets. The distribution of formation factors, however, does not appear to follow any well defined distribution.

In situ versus laboratory-obtained data

Formation factors measured in situ are generally lower than those obtained using electrical resistivity measurements in the laboratory. The difference is as much as a factor of 2–4 for boreholes KLX03 and KLX04. The difference indicates either the effect of in situ compression or that the laboratory samples have been mechanically damaged when brought to the laboratory /Löfgren and Neretnieks 2005b/. Due to large scatter in the dataset, it is difficult to identify any particular depth trend in the laboratory data and there is no unequivocal statistical evidence for a significant decrease in diffusivity in samples from larger depths. Likewise, there is no statistical evidence for such a decrease in the in situ data. If present, such a trend could indicate an increased effect of stress release on these samples owing to the greater mass of overburden at larger depths. The effect of stress release on formation factor has been observed in the laboratory with samples recompressed to formation stress levels /Skagius and Neretnieks 1985/. It should be noted, however, that in situ stresses are multi-axial in nature and the effect of stress release is not only related to overburden, but also complicated by formation stresses acting along horizontal axes (see Chapter 6).

The data variation in the in situ measurements is typically less than that found in resistivity measurements made in the laboratory. The most probable reason for the difference in data variance is likely to be a scaling effect relating to the larger effective sampling volume of the in situ measured data as compared to the laboratory measured resistivity values. This issue is discussed in more detail by /Liu et al. 2005/.

10.5.4 Sorption

The notion of sorption in the context of the site descriptive model relates to the adsorptive interaction of radionuclides with the surfaces of geological materials. This occurs principally by way of the association of ionic solutes with charged mineral surfaces. In the simplified approach to sorption modelling adopted within the SDM, sorption processes are considered to be linear (no concentration dependency) as well as being fast and reversible (chemical kinetics are not considered). The concept is the same as that described in the strategy report by /Widestrand et al. 2003/.

BET measurements

Given that the adsorption of radionuclides takes place on the surfaces of geological materials, the quantification of available surface areas is an important predictor of the sorption capacity of the rock material. Various ferric oxides, for example, have very large specific surface areas and have been shown to be strongly adsorbing minerals for cations that associate with surfaces by way of surface complexation /e.g. Jakobsson 1999/. Furthermore, the presence of clay minerals (as a group identified as a significant potential sink for Cs⁺) also gives rise to increased surface areas in the measurements on rock samples. Although at this stage no method is available for establishing a quantitative relationship between specific surface areas and sorption parameters, results of BET surface area measurements are included in the retardation model as qualitative data important for the understanding of the sorption processes. The results of the measurements on the Laxemar site rock types are given in the background report /Byegård et al. 2006, cf. Table 3-5 and Table 3-6/.

The BET measurements indicate that crushing of the rock material results in the formation of new surfaces that are non-representative for the intact rock. From the results of the samples for major rock types, the 63–125 µm size fraction shows 5–50 times higher BET surface than that for the 2–4 mm size fraction. The measured BET surface area of the particles (A_{BET}) is the sum of the external surface area (A_{EXT}) and a contribution from internal surfaces (A_{INT}). Only the internal surface area of the rock is of relevance for sorption within the rock matrix in situ. In order to estimate the internal surface area of the rock, an extrapolation procedure is used based upon the BET surface measured for the two distinct particle size fractions (see background report by /Byegård et al. 2006/ for details). Extrapolating the results to obtain an inner BET surface (assuming constant particle sphericity) gives values in the range of 0.018–0.079 m²/g.

It should be noted that the formation of large amounts of additional surface area during crushing that are non-representative for intact rock introduces considerable uncertainty concerning the use of crushed rock material for the determination of sorption coefficients. Even the large particle size

fraction, 2–4 mm can be expected to be mechanically damaged (in terms of additional internal microfracturing caused by crushing) as compared with undisturbed in situ rock.

This means that surface areas estimated on the basis of extrapolations using crushed rock are likely to be overestimated with respect to the undisturbed rock matrix. These are biases that will need to be addressed further in forthcoming versions of the site description when more detailed, site-specific sorption data becomes available.

Material carefully sampled from natural fractures (see Table 3-6 in the background report /Byegård et al. 2006/) exhibits higher BET surface areas relative to the crushed major rock types by 2–3 orders of magnitude. A possible explanation for this is the presence of, for example, clay minerals and ferric oxides close to the fracture surfaces (i.e. materials that in different alteration processes have become very porous and acquired large surface areas). The large disparity between the surface areas measured for these materials and non-altered rock types indicates that the altered materials may be significant sinks for radionuclides.

Sorption data

For the Laxemar 1.2 SDM, some preliminary results from laboratory sorption measurements are reported from the site investigation programme. The sorption data have been evaluated in accordance with the proposed strategy for laboratory measurements /Widestrand et al. 2003/ and a detailed description is given in the background report by /Byegård et al. 2006/.

Only preliminary experimental data for Ävrö granite sampled from KLX03A (522.61–523.00 m) are available at this time. The experiments have been performed using the crushed rock in contact with both fresh groundwater and present day groundwater from repository depth (GW Type I and III, respectively). The data for different size fractions have been evaluated according to Equation 7-4 in /Widestrand et al. 2003/ in order to extrapolate an estimate of the sorption coefficient for the internal surfaces of the crushed rock material (K_d) as well as an estimate of external surface sorption parameter (K_a).

Using this method and measured solute partitioning ratios for the 63–125 μm and 2–4 mm particle size fractions, sorption coefficients (K_d) for Cs(I), Sr(II), Ni(II), Ra(II), and Am(III) have been estimated and are given in Table 10-2 below.

The data obtained for most of the solutes are in line with expected values as given in recommendations by /Carbol and Engkvist 1997/ with the exception of Am(III), the measured K_d for which is some 2–4 orders of magnitude lower than batch-measurement data found in the literature. If the data are correct, this could have non-trivial consequences for safety analysis. Based upon the known sorption characteristics of Am(III) from other sources it is possible that the low values could be an experimental artefact. As the sorption measurements are preliminary and additional control measurements (e.g. measurement of solid phase activity) have not been possible to perform, the results for Am(III) should be considered as provisional in the current retardation model (see the background report by /Crawford 2006/ for a more detailed discussion). More work will need to be done to clarify this issue in forthcoming SDM versions.

A considerable problem associated with the current sorption data set is that data are only available for the interaction with Ävrö granite. For the other major rock types and for the fracture specific materials, no site-specific experimental sorption data exist. Sorption data have been estimated for these rock types using an extrapolation procedure, assuming that the sorption K_d is linearly proportional to the BET surface area. The extrapolation procedure was based upon sorption and BET surface area data for the 63–125 μm size fraction of Ävrö granite as a reference material, scaled with respect to the BET surface area of the target rock type. Details of the extrapolation procedure are given in the background report /Byegård et al. 2006/.

It should be noted that the BET surface area for the different rock types was preferentially obtained from the extrapolation of inner BET surface area where possible (see Table 3-5 and Table 3-6 in the background report /Byegård et al. 2006/). For some rock materials (particularly fracture specific materials) only the small size fraction has been measured (i.e. 63–125 μm or $< 125 \mu\text{m}$). In these cases the measured BET surface area for the small size fraction has been used directly.

Table 10-2. Experimentally determined sorption coefficients for various radionuclides in contact with Ävrö granite sampled from KLX03A (522.61–523.00 m) with fresh (GW Type I) and repository level (GW Type III) groundwater. The values are preliminary and are obtained for contact times of one month, with the exception of Am(II) where a contact time of 3 months has been applied. The final values will be measured (cf. /Widestrand et al. 2003/) after 6 months contact time. Values are given as mean $\pm \sigma$ for the considered data set where available.

Tracer	Fresh groundwater (type I)		Saline groundwater (type III)	
	K_d (m ³ /kg)	K_a (m)	K_d (m ³ /kg)	K_a (m)
Cs(I)	$(4.2\pm 3.5)\times 10^{-2}$	$(2.8\pm 0.3)\times 10^{-2}$	$< 2\times 10^{-2}$	$(9.5\pm 1.4)\times 10^{-3}$
Sr(II)	$(5.8\pm 1.4)\times 10^{-3}$	$(8.0\pm 1.3)\times 10^{-4}$	$< 4\times 10^{-4}$	$< 2\times 10^{-5}$
Ra(II)	$(1.4\pm 1.1)\times 10^{-1}$	$(1.9\pm 1.0)\times 10^{-2}$	$(4.0\pm 3.6)\times 10^{-3}$	$(9.7\pm 3.3)\times 10^{-4}$
Ni(II)	$(1.3\pm 0.8)\times 10^{-1}$	$(1.8\pm 0.8)\times 10^{-2}$	$< 2\times 10^{-2}$	$(3.5\pm 0.8)\times 10^{-3}$
Am(III)	$(1.0\pm 0.5)\times 10^{-2}$	$(2.8\pm 0.5)\times 10^{-3}$	$(1.9\pm 1.5)\times 10^{-2}$	$(2.4\pm 1.4)\times 10^{-3}$

The results from these BET surface area based extrapolations of K_d -values are given in Table 3-8 in the background report /Byegård et al. 2006/. Very similar values are found for the different major rock types. For the fracture and fracture zone materials, however, significantly higher K_d -values are reported. This is a direct consequence of the high BET surface areas measured for these samples.

It should be emphasized that this extrapolation is only an approximate method for assigning K_d -values to rock materials where measurement data is unavailable (Incidentally, this is also why the extrapolated data given for Ävrö granite in Table 3-7 are numerically different to the actual measurement data given in Table 3-8 in the background report /Byegård et al. 2006/). In /Allard et al. 1983/, for example, a far from perfect correlation was obtained for the cation exchange capacity (CEC) relative to the BET surface area, indicating a more complex and mineral-dependent relationship between the sorption capacity and the BET surface area. More recent studies /e.g. Bertetti et al. 1996, Jenne 1998, Prikryl et al. 2001, Davis et al. 2004/ lend strong support to the concept of BET surface area normalisation, although there do appear to be intrinsic differences between the sorption properties of specific minerals, in terms of both the density of sorption sites relative to BET surface areas, as well as different mechanisms of sorption on, for example, clay mineral edges sites as compared to basal crystal planes. Nevertheless, in the absence of sorption measurements for most of the site specific rock types in the Laxemar subarea, this concept is considered to be the best available method of assigning sorption coefficients to the various rock types. In forthcoming versions of the site description, additional sorption measurement and CEC data will be available and the possibility will exist for a more rigorous evaluation of the K_d -prediction concept.

For solutes not included in Table 3-8 in the background report /Byegård et al. 2006/, K_d values from /Carbol and Engkvist 1997/ are recommended for use in transport modelling. Although not adjusted for BET surface areas of site specific materials, these data should still give order of magnitude estimates of sorption strength for different species under both non-saline and saline conditions.

10.5.5 Specific flow-wetted surface

In the background report by /Crawford 2006/, the specific flow-wetted surface is estimated for rock volumes characteristic of those sampled by boreholes in the Laxemar subarea.

The specific flow-wetted surface or a_R (m²/m³) is the estimated surface area of flowing features per unit volume of rock and is calculated from geometrical-statistical treatment of the frequency of flow anomalies in boreholes as identified by Posiva Flow Log (PFL) measurements (for details, see /Crawford 2006/).

The approximated specific flow-wetted surface, a_R and two-sided, 95% binomial confidence intervals for the statistical uncertainty in a_R are given in Table 10-3 for various boreholes in the Laxemar subarea.

The actual specific flow-wetted surface is sensitive to the average width of flow channels residing within fractures. The width of these channels is unknown although speculated to be in the range 0.1–0.5 m /e.g. Abelin et al. 1994, Birgersson et al. 1992, Moreno and Neretnieks 1989, Neretnieks and Moreno 2005/. If the unknown flow channels are very narrow, on the order of 0.1 m, the actual flow-wetted surface may be as little as half of those values given in Table 10-3.

Table 10-3. Mean specific flow-wetted surface, a_R (m^2/m^3) estimated from PFL measurements for different boreholes in the Laxemar sub-region (deterministic deformation zones excluded). Data is given for upper 450 m of rock as well as for entire borehole as indicated by the upper (secup) and lower (seclow) bounds of the tested section. Two-sided, 95% binomial confidence intervals are also given for the specified borehole data.

Borehole ID	Secup (m)	Seclow (m)	Test Scale (m)	Sample Size	\bar{a}_R (m^2/m^3)	95% conf. int.
KLX02	204.42	405.42	3	68	1.33	0.94–1.83
KLX03	101.3	992.42	5	161	0.16	0.11–0.23
	101.3	450	5	70	0.32	0.21–0.50
KLX04	100.2	986.22	5	148	0.33	0.25–0.45
	100.2	450	5	60	0.58	0.41–0.87
KAV04A	100.16	996.17	5	168	0.38	0.29–0.48
	100.16	450	5	70	0.34	0.23–0.52

It is important to note that the confidence intervals given in the table only consider uncertainty related to the estimated value of the fracture frequency and do not have any relation to additional uncertainties relating to channelling effects as described above or measurement errors and bias.

The specific flow-wetted surface is a parameter of central importance for the estimation of transport resistance in fractured rock. Although this is only strictly true for a porous medium representation of flow and transport, we note that in systems where diffusive exchange with the rock matrix dominates the solute residence time distribution, the magnitude of the surface area over which matrix diffusion takes place is a key entity governing transport. In flow and transport models based upon concepts other than a porous medium approach, the specific flow-wetted surface is not used directly as a model parameter. In DFN-modelling concepts, for example, the specific flow-wetted surface still appears implicitly in terms of the conductive fracture intensity, or P_{32c} (actually, $a_R = 2 \times P_{32c}$). For the same input data set and making allowances for basic differences in modelling assumptions, however, the various modelling approaches should reproduce the same average flow-wetted surface to flow ratio (F-factor) for the system as a whole, although not necessarily distributed the same way /e.g. SKB 2004d/. The magnitude of the specific flow-wetted surface is therefore an indicator of the potential for solute-rock matrix interaction for a given flow system and has a strong qualitative significance for site understanding in this respect.

10.5.6 Field scale tracer tests

An important element of the site descriptive modelling is the demonstration of retention processes in situ and the partial validation of laboratory data by means of different kinds of field-scale tracer tests. This section gives a brief overview of the tests that have been performed thus far within the site investigations of the Simpevarp area. For further details the reader is referred to the relevant data reports.

Groundwater flow established from tracer dilution tests

The tracer dilution technique is a highly sensitive method for measuring very small groundwater flow rates in fractures and fracture zones. Tracer dilution as a means of flow detection is roughly 1–2 orders of magnitude more sensitive than flow measurements made using the Posiva Flow Log (PFL) tool.

The method consists of filling a packed-off borehole section with a non-sorbing tracer and measuring the rate at which groundwater flowing through the test section dilutes the initial tracer charge. Using a simple mixing model, incorporating a correction for flow-field convergence in the vicinity of the borehole, the flow rate of water through the fracture or fracture zone intersecting the borehole section can be estimated by a curve fitting technique.

Tests have been carried out within a number of sections in boreholes KLX02 (2 borehole sections) and KSH02 (5 borehole sections) /Gustafsson and Nordqvist 2005/. Two of the tests in KSH02 were made in conjunction with SWIW tests (described below). In the tests that have been performed, uranine has generally been used as a non-sorbing tracer, although salt (NaCl) at a concentration higher than the background level has also been used in some instances where high turbidity in the groundwater made fluorometric measurements of uranine concentration impractical. Although the tests are to a certain extent influenced by “noise” of various kinds (tidal effects, etc.), the estimated flow rates agree, by and large, with previous experiences at other sites.

Single well injection withdrawal (SWIW) tests

Currently, two single well injection withdrawal (SWIW) tests have been performed in KSH02 in the Simpevarp subarea. One test was made in a single fracture at 422 m depth (with a transmissivity of 10^{-6} m²/s), whereas the other was made in an interpreted fracture zone at a depth of 576 m (with a transmissivity of 5.2×10^{-7} m²/s). The procedure used for making a SWIW test is described in detail in /Gustafsson and Nordqvist 2005/ as well as in the background feasibility study reports /Nordqvist and Gustafsson 2002, 2004/. It comprises the following phases and typical timescales:

- 1) Pumping and storage of groundwater from the selected fracture for subsequent injection.
- 2) Pre-injection of accumulated water to establish steady state hydraulic conditions (2–3 h).
- 3) Active injection of one or more tracers within the packed-off borehole section (1 h).
- 4) Injection of groundwater (chaser fluid) after cessation of tracer injection (12–14 h).
- 5) Waiting phase (< 1 h).
- 6) Tracer recovery phase (withdrawal of water under active pumping, 100–200 h).

In both of the experiments carried out in KSH02 a mixture of uranine (non-sorbing) and cesium (sorbing) were used as tracer substances. From the recovery data, clear and unambiguous indications of cesium retention were obtained. In the data report, a numerical model (SUTRA /Voss 1984/) simulating radial advective flow and transport with equilibrium sorption was used in a preliminary evaluation of the data.

Using the tracer recovery data for both solutes, the longitudinal dispersivity (α_L) and linear retardation factor (R) were simultaneously fitted using a least squares approach for a range of fixed flow porosities (i.e. fracture apertures). The linear retardation factor, although not a physically meaningful entity in the presence of matrix diffusion, is operationally defined as the ratio of the delayed tracer breakthrough time relative to the water residence time. The analysis gave a retardation factor on the order of 1,000 for the borehole section at 422 m and a factor of 90 for the borehole section at 576 m.

Multiple well tracer tests

A combined multiple well, pumping and tracer test has been carried out between boreholes KLX02 and HLX10 at Laxemar /Gustafsson and Ludvigson 2005/. Although the principal objectives of this investigation were to assess the connectivity of KLX02 and HLX10 through potential fracture zones intersecting both boreholes and to determine their hydraulic properties, a tracer test using a non-sorbing tracer (Rhodamine) was also performed with the aim of assessing the transport properties of any flow paths connecting these boreholes. The boreholes are roughly 260 m apart as measured at the surface. Although clear hydraulic responses were observed in the monitoring borehole KLX02 during pumping in HLX10, no tracer breakthrough was observed in this test. In the data report, the non-recovery of tracer was ascribed to equipment failure during the pumping test.

10.6 Transport properties of rock domains

10.6.1 Methodology

The parameterisation of the retardation model is based on the following considerations and parameters:

- **Rock matrix porosity, θ_m (-):** The results from the water saturation porosity measurements on site-specific rock materials have been selected in this work. A lognormal distribution has been considered to describe the system somewhat better (although not perfectly) than a normal distribution, and has therefore been selected for the representation.
- **Rock matrix formation factor, F_m (-):** This parameter is used to multiply literature values of the radionuclide-specific free diffusivities in water (D_w (m²/s); tabulated by e.g. /Ohlsson and Neretnieks 1997/) to obtain the effective diffusivities, D_e (m²/s), for the different radionuclides. Since the results of the laboratory electrical resistivity measurements are based on a larger number of samples and have been found not to deviate significantly from the through-diffusion results, they have been selected for the retardation model. Detailed in situ measurements of formation factors are, however, forthcoming and are thought to be more relevant for model parameterisation owing to that they are obtained under prevailing formation stresses. It is anticipated that these will be used in future versions of the retardation model parameterisation. For consistency with the closely related porosity parameter, a lognormal distribution has been selected also for the formation factor representation.
- **Rock matrix sorption coefficient, K_d (m³/kg):** All available site data are imported for use in the retardation model. Site-specific data on the BET surface areas of the different rock types are used as supporting data and are used to extrapolate K_d -values where measurement results are unavailable.

10.6.2 Description of rock domains

The geological model in the Laxemar 1.2 SDM is based on the concept of rock domains, cf. Chapter 5, whereas the sampling for the transport programme is based on rock types and mainly focused on the two major rock types (Ävrö granite and quartz monzodiorite). The samples selected for laboratory investigation represent both fresh and altered forms of these rock types. Minor rock types have also been sampled, although no data for these are currently available. There are some indications that fine-grained granite may be of greater importance for transport owing to its frequent association with open fractures as well as its distinctive material and hydraulic properties /e.g. Mazurek et al. 1997, Landström and Tullborg 1993/. This, however, has not been addressed in the present work.

As discussed in previous chapters, large parts of the rock are hydrothermally altered, which is expected to affect the transport properties. Hydrothermal alteration occurs both in Ävrö granite and quartz monzodiorite as well as in subordinate rock types.

Table 10-4 presents selected transport parameters for the fresh and altered major rock types. The percentages quantify the portions of the rock types that are altered and are estimated from data in the Laxemar 1.2 geological description, see Chapter 5, and boremap classifications, where only the classes referred to as weak, medium and strong alteration have been considered. The alteration generally seems to be weaker at Laxemar when compared to the Simpevarp subarea. It has not yet been fully established, however, how to translate degrees of alteration between the two subareas, mainly due to differences in rock types and some uncertainties in the classifications used.

The parameterisation of the major rock types can be used to parameterise the different rock domains. Several rock domains constitute the rock volume of the Laxemar subarea. The rock domains consist of mixtures of the different rock types according to Table 10-5, which is based on borehole data relating to the proportions of different rock types from KLX02–KLX06 and represent five of the primary rock domains.

Table 10-4. Suggested transport parameters for the major rock types in the Laxemar subarea. Parameter values in italics refer to K_d -values that have not been measured for that particular rock type, but instead have been obtained by extrapolation from the results for the BET surface area measurements (cf. Table 3-8 in /Byegård et al. 2006/). Values are given as mean $\pm \sigma$ for the considered data set where available.

Rock Type	Porosity (vol%)	Formation factor (-)	Water type	K_d (m ³ /kg) Cs(I)	Sr(II)	Ni(II)	Ra(II)	Am(III)
Ävrö granite	0.27±0.09	(1.4±1.0)×10 ⁻⁴	III	< 2×10 ⁻²	< 4×10 ⁻⁴	(1.1±0.6)×10 ⁻²	(4.0±3.6)×10 ⁻³	(1.0±0.5)×10 ⁻²
			I	(4.2±3.5)×10 ⁻²	(5.8±1.4)×10 ⁻³	(1.3±0.8)×10 ⁻¹	(1.4±1.1)×10 ⁻¹	(1.0±0.5)×10 ⁻²
Quartz monzodiorite	0.17±0.08	(3.6±3.5)×10 ⁻⁵	III	< 9×10 ⁻²	< 4×10 ⁻⁵	< 1.5×10 ⁻²	< 5×10 ⁻³	< 1.4×10 ⁻²
			I	< 0.11	< 4×10 ⁻³	< 0.1	< 0.1	< 1.3×10 ⁻²
Fine-grained dioritoid	0.14±0.14	1.0×10 ⁻⁵ ^A	III	(1.0±0.9)×10 ⁻¹	< 10 ⁻⁴	(1.8±0.9)×10 ⁻²	(5±3)×10 ⁻³	(1.7±1.0)×10 ⁻²
			I	(1.4±0.7)×10 ⁻¹	(5±3)×10 ⁻³	(1.2±0.7)×10 ⁻¹	(1.2±0.6)×10 ⁻¹	(1.7±1.0)×10 ⁻²
Fine-grained diorite-gabbro	0.22±0.08	(6.4±4.2)×10 ⁻⁵	III	(1.0±0.8)×10 ⁻¹	< 10 ⁻⁴	(1.8±0.6)×10 ⁻²	(5±2)×10 ⁻³	(1.6±0.6)×10 ⁻²
			I	(1.4±0.4)×10 ⁻¹	(5±2)×10 ⁻³	(1.1±0.6)×10 ⁻¹	(1.1±0.3)×10 ⁻¹	(1.6±0.5)×10 ⁻²
Fine-grained granite	0.22±0.0002	No data	III	No data	No data	No data	No data	No data
			I	No data	No data	No data	No data	No data
Granite	0.38	8.0×10 ⁻⁵ ^A	III	No data	No data	No data	No data	No data
			I	No data	No data	No data	No data	No data
Diorite to gabbro	No data	No data	III	(7±6)×10 ⁻²	< 6×10 ⁻⁵	(1.2±0.3)×10 ⁻²	(3.6±0.8)×10 ⁻³	(1.1±0.3)×10 ⁻²
			I	(9±2)×10 ⁻²	(3.5±0.8)×10 ⁻³	(8±4)×10 ⁻²	(8±2)×10 ⁻²	(1.1±0.3)×10 ⁻²
Altered Ävrö granite (selected to represent all altered wall rock)	No data	No data	III	(1.4±1.1)×10 ⁻¹	< 10 ⁻⁴	(2.5±0.7)×10 ⁻²	(7±2)×10 ⁻³	(2.2±0.7)×10 ⁻²
			I	(1.9±0.4)×10 ⁻¹	(7±2)×10 ⁻³	(1.6±0.7)×10 ⁻¹	(1.6±0.4)×10 ⁻¹	(2.2±0.6)×10 ⁻²

^A. Data is based upon a single measurement therefore no uncertainty interval is given.

Table 10-5. Estimated percentages of different rock types in the rock domains of the Laxemar subarea (see Figure 5-51 and /Wahlgren et al. 2005b/ for details).

	Rock Domain:				
	RSMA01	RSMD01	RSMBA01	RSMBA03	RSM01
Ävrö granite	73%	–	47%	57%	38–73%
Quartz monzodiorite	3%	95%	–	–	0–27%
Fine-grained dioritoid	2%	–	27%	32%	–
Fine- to medium-grained granite	4%	4%	–	1%	1–16%
Pegmatite	0.2%	0.3%	2%	1%	0–0.3%
Diorite to Gabbro	1%	–	–	–	1–36%
Fine-grained diorite to gabbro	8%	–	23%	8%	–
Granite	0–5%	–	–	1%	0–26%

10.7 Transport properties of fractures and deformation zones

10.7.1 Methodology

According to the retardation model concept proposed by /Widstrand et al. 2003/, the aim is to prepare retardation models for the identified fractures and deformation zone types by describing and quantifying retardation parameters for the different layers of geological materials present in (and adjacent to) the fractures and deformation zones. The geological materials in the fractures or deformation zones could consist of, for example, fault gouge, fracture coatings, mylonite and altered wall rock. Additional parameters in the retardation model include the thickness of each layer and the hydraulic properties and preferential directions of each fracture type.

It should be noted that the present Safety Assessment transport modelling uses retardation parameters for fresh (non-altered) rock as it is the parameterisation of the unaltered rock that can be shown to be of overwhelming importance for radionuclide transport retardation at such timescales /e.g. Crawford 2006/. The Safety Assessment modelling at this present time is therefore not directly dependent on the availability of parameter values for fault gouge, fracture coatings and altered rock.

In the Laxemar 1.2 retention properties model, an identification and quantitative description of different fracture types is presented. Given the current state of knowledge, no identification of deformation zone types can be made owing to the limited data available. The limited availability of data also implies that some parameter values are missing in the tables for the identified fracture types. The on-going site investigation programme will improve the basis for parameterisation of fractures and deformation zones.

10.7.2 Description of fractures

The following simplifications and quantitative estimates are used as a basis for the identification and parameterisation of different fracture types:

The chlorite/calcite combination is the overall dominating coating type in the identified open fractures. Hematite is also present in about 10% of the open fractures, while clay minerals are present in 30% of all open fractures.

According to the presently available data, the presence of different fracture coatings cannot be related to specific rock types. This is important for the application of the identified fracture types in transport models. If such relations exist, they could provide a basis for assigning different fracture types to the various rock domains.

For the rock hosting fractures, it is suggested that a significant fraction of the fractures are situated within altered parts of the rock, although there is some uncertainty concerning the actual fracture frequency in altered zones /Byegård et al. 2006/.

Based on the core mapping only, the following quantification and description of different fracture types is suggested (fracture coatings and alteration rims are considered to be symmetrically represented on opposing fracture faces):

- A. 40% have chlorite and calcite as a fracture coating (≤ 0.5 mm thick) and fresh wall rock.
- B. 20% have chlorite and calcite as a fracture coating \pm prehnite, epidote, etc. (≤ 1 mm thick) and altered wall rock ≤ 2 cm thick.
- C. 10% have a chlorite/calcite/hematite mixture as a fracture coating (≤ 1 mm thick); all of these fractures have altered wall rock ≤ 5 cm.
- D. 30% have a chlorite/calcite/clay mineral mixture as a fracture coating (≤ 2 mm thick); all of these fractures have altered wall rock ≤ 5 cm.

The quantitative descriptions of the identified fracture types, including the available retardation parameters, are given in Table 10-6 to Table 10-9.

The notation “pending” used frequently in the tables indicates that the transport parameter for the given geological unit is not available for this version of the site description. These gaps are intended to be filled in later versions of the site description.

Table 10-6. Retardation model for Fracture Type A.

		Fracture coating	Fresh host rock
Distance		Max 0.5 mm	≥ 0.5 mm
Porosity		pending	According to Table 10-4
Formation factor		pending	According to Table 10-4
Cs, K_d (m ³ /kg)	GW type I	pending	According to Table 10-4
	GW type III	pending	According to Table 10-4
Sr, K_d (m ³ /kg)	GW type I	pending	According to Table 10-4
	GW type III	pending	According to Table 10-4
Ni, K_d (m ³ /kg)	GW type I	pending	According to Table 10-4
	GW type III	pending	According to Table 10-4
Ra, K_d (m ³ /kg)	GW type I	pending	According to Table 10-4
	GW type III	pending	According to Table 10-4
Am, K_d (m ³ /kg)	GW type I	pending	According to Table 10-4
	GW type III	pending	According to Table 10-4
Mineral content		Chlorite, calcite	See geological description
Grain size		Pending	Pending
Proportion of conducting structures		40%	
Transmissivity interval		Pending	
Direction		Pending	

Table 10-7. Retardation model for Fracture Type B. Values given in italics represent extrapolations based upon BET surface area measurements.

		Fracture coating	Altered wall rock	Fresh host rock
Distance		0.5–1.0 mm	< 2 cm	≥ 2 cm
Porosity		pending	According to Table 10-4	According to Table 10-4
Formation factor		pending	According to Table 10-4	According to Table 10-4
Cs, K_d (m ³ /kg)	GW type I	<i>7±1</i>	According to Table 10-4	According to Table 10-4
	GW type III	<i>5±4</i>	According to to Table 10-4	According to Table 10-4
Sr, K_d (m ³ /kg)	GW type I	<i>0.24±0.05</i>	According to Table 10-4	According to Table 10-4
	GW type III	<i>< 0.004</i>	According to Table 10-4	According to Table 10-4
Ni, K_d (m ³ /kg)	GW type I	<i>5±2</i>	According to Table 10-4	According to Table 10-4
	GW type III	<i>0.9±0.2</i>	According to Table 10-4	According to Table 10-4
Ra, K_d (m ³ /kg)	GW type I	<i>5±1</i>	According to Table 10-4	According to Table 10-4
	GW type III	<i>0.25±0.05</i>	According to Table 10-4	According to Table 10-4
Am, K_d (m ³ /kg)	GW type I	<i>0.7±0.2</i>	According to Table 10-4	According to Table 10-4
	GW type III	<i>0.8±0.2</i>	According to Table 10-4	According to Table 10-4
Mineral content		Chlorite, calcite ± (prehnite, epidote, etc.)	See geological description	See geological description
Grain size		Pending	Pending	Pending
Proportion of conducting structures		20%		
Transmissivity interval		Pending		
Direction		Pending		

Table 10-8. Retardation model for Fracture Type C. Values given in italics represent extrapolations based upon BET surface area measurements.

		Fracture coating	Altered wall rock	Fresh host rock
Distance		0.5–1.0 mm	< 5 cm	≥ 5 cm
Porosity		pending	According to Table 10-4	According to Table 10-4
Formation factor		pending	According to Table 10-4	According to Table 10-4
Cs, K_d (m ³ /kg)	GW type I	<i>8±2</i>	According to Table 10-4	According to Table 10-4
	GW type III	<i>6±5</i>	According to Table 10-4	According to Table 10-4
Sr, K_d (m ³ /kg)	GW type I	<i>0.30±0.06</i>	According to Table 10-4	According to Table 10-4
	GW type III	<i>< 0.005</i>	According to Table 10-4	According to Table 10-4
Ni, K_d (m ³ /kg)	GW type I	<i>7±3</i>	According to Table 10-4	According to Table 10-4
	GW type III	<i>1.0±0.3</i>	According to Table 10-4	According to Table 10-4
Ra, K_d (m ³ /kg)	GW type I	<i>7±1</i>	According to Table 10-4	According to Table 10-4
	GW type III	<i>0.30±0.06</i>	According to Table 10-4	According to Table 10-4
Am, K_d (m ³ /kg)	GW type I	<i>0.9±0.3</i>	According to Table 10-4	According to Table 10-4
	GW type III	<i>0.9±0.3</i>	According to Table 10-4	According to Table 10-4
Mineral content		Chlorite, calcite, hematite	See geological description	See geological description
Grain size		Pending	Pending	Pending
Proportion of conducting structures		10%		
Transmissivity interval		Pending		
Direction		Pending		

Table 10-9. Retardation model for Fracture Type D. Values given in italics represent extrapolations based upon BET surface area measurements.

		Fracture coating	Altered wall rock	Fresh host rock
Distance		1–2 mm	< 5 cm	≥ 5 cm
Porosity		pending	According to Table 10-4	According to Table 10-4
Formation factor		pending	According to Table 10-4	According to Table 10-4
Cs, K_d (m ³ /kg)	GW type I	<i>60±10</i>	According to Table 10-4	According to Table 10-4
	GW type III	<i>40±30</i>	According to Table 10-4	According to Table 10-4
Sr, K_d (m ³ /kg)	GW type I	<i>2.1±0.4</i>	According to Table 10-4	According to Table 10-4
	GW type III	<i>< 0.04</i>	According to Table 10-4	According to Table 10-4
Ni, K_d (m ³ /kg)	GW type I	<i>50±20</i>	According to Table 10-4	According to Table 10-4
	GW type III	<i>8±2</i>	According to Table 10-4	According to Table 10-4
Ra, K_d (m ³ /kg)	GW type I	<i>50±9</i>	According to Table 10-4	According to Table 10-4
	GW type III	<i>2.1±0.4</i>	According to Table 10-4	According to Table 10-4
Am, K_d (m ³ /kg)	GW type I	<i>7±2</i>	According to Table 10-4	According to Table 10-4
	GW type III	<i>7±2</i>	According to Table 10-4	According to Table 10-4
Mineral content		Chlorite, calcite, clay minerals	See geological description	See geological description
Grain size		Pending	Pending	Pending
Proportion of conducting structures		30%		
Transmissivity interval		Pending		
Direction		Pending		

10.7.3 Description of deformation zones

Based on the information available at this stage in the site investigation, it is not possible to provide a retardation model for the local minor and local major deformation zones. This is due partly to the lack of transport data, but also due to uncertainties in the classification of deformation zones. The only data available thus far are BET surface area measurements. Porosity- (PMMA), diffusion- and sorption measurements are still in progress.

A few general aspects can, however, be indicated at this stage:

- The local minor deformation zones are hosted in altered rock. Fault gouge and cataclasite are common.
- Chlorite- and clay-rich zones (on the order of < 1 cm), hosted in altered wall rock (dm-wide), are also found.
- The available data are too limited to allow conclusions on the abundances of different types of deformation zones.

10.7.4 Application of the retardation model

Table 10-4 and Table 10-5 provide a basis for parameterisation of the rock domains RSMA01, RSMB01 and RSMC01. The parameterisation of each rock domain could range from a simple selection of a single parameter value for the dominant rock type in that domain to, for instance, volume averaging using data for fresh or altered rock, or both. For the diffusion parameters of the major rock types, statistical distributions are given that can be used as a basis for stochastic parameterisation of transport models.

No specific recommendations, however, are given here on the selection of data from the retardation model. This implies that the present model does not provide detailed guidelines on how to “dress” the geological model with transport parameters using the tabulated retardation parameters. At this stage of model development, the retardation model should be viewed as a presentation of the interpreted site-specific information on retardation parameters, intended to provide a basis for the formulation of alternative parameterisations within the Safety Assessment modelling.

The quantitative descriptions of the identified fracture types, including the available retardation parameters, are given in Table 10-6 to Table 10-9. The fracture types in the present retardation model could be used as a basis for modelling radionuclide transport along flow paths in the fractured medium. However, the model could also be viewed as primarily proposing a basic structure for discussion and further development which, from the viewpoint of numerical transport modelling, will become more useful when more data are at hand.

Concerning the parameterisation of flow paths in transport models, it should also be noted that at present there are no data supporting, for instance, quantitative correlations between fracture types and hydraulic properties. Furthermore, there is currently no data support to relate different fracture coatings to specific rock types.

No identification or description of deformation zone types is given in the present model. The available information and indications related to deformation zones, however, are described in Section 10.7.3.

10.7.5 Supporting evidence from process-based modelling

As discussed in Section 10.3.2, alternative retention processes and process models are considered within the site descriptive transport modelling, thus far mainly in the form of process-based sorption models. It is expected that the results of this modelling will be useful for supporting, or for providing alternatives to, the K_d -based sorption model regarding actual parameter values as well as for the understanding of the site-specific sorption processes in general. No results that can be used for these purposes, however, are presently available.

10.8 Transport properties of flow paths

In the event of deposition canister failure, radionuclides may escape and migrate to the surrounding rock through the bentonite buffer or backfilling material surrounding the canister emplacement. The radionuclides may then be transported into fractures intersecting the deposition hole, into the disturbed zone around the excavated volume, and into fractures intersecting the tunnels.

Large scale deformation zones with relatively fast water flows are not currently considered to provide substantial transport resistance. For transport modelling, single fractures or fracture clusters constituting potential transport pathways from a canister position to the nearest major deformation zone are therefore likely to be of overwhelming importance for the solute transport retardation. A central problem in establishing a retention property model is how to identify these fractures, which are well connected and large enough to have a dominating impact on transport, but which are small enough to not be identified as substantial deformation zones.

In the current model, the bulk of the transport resistance is conceptualised to reside in the network of background fractures and minor deformation zones comprising the first 10–100 m of rock surrounding the repository. To distinguish this from transport through major deformation zones to the surface and other regional scale transport processes, this zone is referred to as the *immediate far-field* as shown schematically in Figure 10-2. Major deformation zones and large-scale conducting structures are, however, included in the hydraulic DFN model as described in Chapter 8.

10.8.1 Generic, first order estimation of the F-factor

Given that the estimation of the site specific transport resistance is strongly influenced by modelling assumptions that are not easily verifiable, we seek to make a prediction of this parameter from first principles using only absolutely necessary assumptions. Here we consider what the theoretical transport resistance would be if the flow path sampled in a borehole were to extend from a deposition hole to a more distant major fracture zone in a straight line.



Figure 10-2. Schematic representation of flow and transport in the “immediate far-field” conceptualised to be the first 10–100 m between any given canister hole and the nearest large scale deformation zone.

The transport resistance, or F-factor, for a flow path is the ratio of the fracture surface area in contact with flowing water (fws), and the flow rate of the water along that path (q), or simply fws/q . For a single flow path, the F-factor can be shown to be:

$$F = \frac{2L_p}{T i} \quad \text{Equation 10-1}$$

Where L_p (m) is the length of the transport path, T (m^2/y) is the transmissivity and i (m/m) is the hydraulic gradient.

As can be seen from Equation 10-1 the estimate of F is, in theory, independent of the width of the migration path. This, however, is dependent upon the transmissivities being correctly estimated from hydraulic test data and also does not make any consideration of the interconnectivity of different conducting features that make up the network of flow paths in the rock. It should be noted, however, that there are a number of uncertainties embedded in the estimation of flow path transmissivities and Equation 10-1 may be sufficient given that reported transmissivities from PFL data are typically only accurate as an order of magnitude estimate /e.g. Ludvigson et al. 2002/. It should also be pointed out that F-factors estimated using other approaches (such as DFN-modelling) contain essentially the same uncertainties. The advantage of using the very simple approaches described in this and the following sections is that the models are based upon very simple principles and are fundamentally transparent unlike the more complex models of flow and transport typically used in safety analysis.

The representative hydraulic gradient required to give a reasonable estimate of F is also uncertain. It is influenced by surface hydraulic boundary conditions as well as strongly transmissive conductors in the far-field that influence the distribution of hydraulic head at depth. In the following discussion we therefore consider a range of gradients that are likely to be representative of the hydraulic conditions at repository depth.

Assuming a path length of 100 m and a hydraulic gradient ranging from 0.1–1.0%, Equation 10-1 can be used to make generic estimates of the value of F . These data are given in Table 10-10.

The form of Equation 10-1 implies that the F-factor scales linearly with distance and the generic estimates given in Table 10-10 can therefore be easily scaled to any other transport distance through multiplying by an appropriate factor. Note that a similar table to Table 10-10 was provided in the Preliminary Safety Evaluation of the Forsmark site /SKB 2005d/.

Table 10-10. Generic transport resistance (F-factor) estimated for different fracture transmissivities, a path length of 100 m, and some representative hydraulic gradients (data is given in log₁₀ units).

Transmissivity (m ² /s)	Log ₁₀ (F) (y/m)		
	0.1% (0.001 m/m)	0.5% (0.005 m/m)	1% (0.01 m/m)
10 ⁻⁴	1.8	1.1	0.8
10 ⁻⁵	2.8	2.1	1.8
10 ⁻⁶	3.8	3.1	2.8
10 ⁻⁷	4.8	4.1	3.8
10 ⁻⁸	5.8	5.1	4.8
10 ⁻⁹	6.8	6.1	5.8
10 ⁻¹⁰	7.8	7.1	6.8

Generally speaking, larger F-factors correspond to longer travel times for transported solutes. It is also noted here that the F-factor approach is not strictly applicable for situations where the solute (typically non-sorbing) penetrates the entire depth of the rock matrix. In such situations, it is the equilibrium storage capacity of the rock matrix that determines the solute retardation and the F-factor is not a significant entity.

Generic simulation results /Crawford 2006/ indicate clearly that peak arrival time scales approximately with the square of the F-factor for solutes over a wide range of sorption strengths, provided the transport time is negligible relative to the water residence time. Owing to this quadratic relation, the uncertainty of the peak arrival time is highly sensitive to the uncertainty in the estimated F-factor thus illustrating the importance of correctly estimating this variable for safety assessment applications.

10.8.2 Estimations of the F-factor using site specific data

The F-factor is dependent not only on the hydraulic characteristics of individual flowing features comprising a flow path, but also their interconnectivity in the extended network of fractures surrounding the repository. For migration from the repository within the immediate far-field, radionuclides may be transported over a number of independent flow paths. The effective F-factor for such an ensemble of possible flow paths therefore is best described in terms of a statistical distribution of F-factors.

Although the network of flow channels and potential migration paths is complex, it is possible to make estimates of the F-factor distribution from site specific data according to different conceptual models that represent extremes of possible behaviour. While not altogether physically realistic, they nonetheless can provide approximate bounds for the likely distribution of transport resistance to be found in the repository target volume. Moreover, they can also be used to provide a “reality check” on more sophisticated models where underlying concepts and assumptions may not be as transparent.

Results obtained using flow channelling models

In this section, two different conceptual models are used to make estimates of the mean F-factor and its distribution. These are the Channel Network Model (CNM) /Moreno and Neretnieks 1993, Gylling 1997/ and the Stochastic Multi Channel Model (MCM) /Neretnieks 2002/. These models represent extremes of flow channel interconnectivity and are described in some detail in the background report by /Crawford 2006/. Simulations have been made with both model concepts to evaluate the transport resistance distribution of the rock surrounding the repository:

- In the CNM concept it is assumed that fluid flow and solute transport take place in a network of interconnected flow channels. The channels within the network are short and highly interconnected with transmissivities sampled randomly from a lognormal distribution. Using a particle tracking technique, the F-factor distribution for an ensemble of transport paths can be calculated for different flow network realisations. Apart from the distribution of flow, the main assumption in this representation of transport is that full mixing is assumed at channel intersections.

- The MCM concept is essentially an extension of the first order approximation discussed in the previous section. In this case, however, solutes are assumed to be released simultaneously within a cluster of independent non-mixing flow channels. The individual flow channels have transmissivities reflecting the measured transmissivity distribution obtained from borehole data. This is the same as estimating the F-factor using Equation 10-1, although extending the calculation to the entire transmissivity distribution. In this case, the main assumption for transport is that there is no mixing between channels which results in the initial variability between channels to persist along the entire transport path length.

If the measured transmissivity distribution is assumed to be representative of individual flow channels, then the magnitude of the F-factor calculated using either the CNM or MCM approaches can be shown to be formally insensitive to flow channel width for any specified channel length. Owing to the short and highly interconnected nature of the flow paths in the CNM, the calculated F-factor distribution tends to reflect the average flow properties of channel members making up the flow path ensemble within the rock volume. The variance of the F-factor distribution is therefore dependent upon the number of channels and mixing nodes separating the release and recovery locations. This is contingent upon the choice of channel length, although it can be considered to be a secondary effect of flow path discretisation. To illustrate the impact of different assumptions of average channel length, CNM simulations have been made using a range of channel lengths varying between 1–10 m. Calculation results for both MCM and CNM approaches are detailed in the background report by /Crawford 2006/ and only a brief overview is given here.

Overall, the CNM predicts mean F-factors approximately in the range 10^5 – 10^8 (y/m) depending upon which borehole data are used as a basis for the calculation. Using the MCM approach, F-factors in the range 10^3 – 10^5 (y/m) are predicted. In individual cases (i.e. for specific borehole calculations), the mean F-factor calculated using the CNM is slightly higher than that calculated using the MCM approach. Although counteracted to a certain degree by network channelling effects that give locally high flow rates along preferential flow paths, this is at least partly due to the circuitous nature of particle transport paths in the CNM simulations.

A significant difference between calculations made with the CNM and MCM approaches is the magnitude of the estimated variance for the F-factor distribution and consequently, also the calculated $F_{U10\%}$ and $F_{U1\%}$ values (The $F_{U10\%}$ and $F_{U1\%}$ correspond to the F-factors where at most 10% and 1%, respectively, of flow channels have a lower F-factor, assuming a lognormal distribution). The variance of the F-factor calculated using the CNM is reduced considerably by the interconnectedness of the channel network whereas the MCM model has an F-factor variance that is identical to the original transmissivity distribution. If there is a strong positive correlation between transmissivity and fracture characteristic length, then we would expect the F-factor distribution to approach that of the MCM model for the fast flow paths. If there is no such correlation, on the other hand, we would expect the F-factor distribution to be more reminiscent of the results obtained using the CNM approach.

It should be remembered that the actual F-factor distribution for a given radionuclide release scenario is strongly dependent upon the connectivity of flow paths leading from the deposition hole through the immediate far-field and is particularly sensitive to the number and transmissivity of the fractures initially encountered in the vicinity of a leaking canister. The “actual” F-factor for transport from a leaking canister is therefore subject to a large degree of variation depending upon the probability of channels with various transmissivities intersecting a deposition hole and their connectivity with the wider fracture network. The simulation results presented here are based upon average properties of the rock volume and do not consider these stochastic aspects that are more of a safety assessment character.

Results obtained using a stream tube model

An alternative for making estimates of the F-factor is to use a stream tube model such as that commonly used in safety assessment studies (e.g. FARF31 /Norman and Kjellbert 1990, SKB 1999/). The F-factor for a stream tube is given by:

$$F = \frac{L_p \alpha_R}{K i}$$

Equation 10-2

Where L_p (m) is the transport path length, a_R (m^2/m^3) is the specific flow-wetted surface, and q (m^3/y) is the flow rate. As previously defined in Equation 10-1, T (m^2/y) is the transmissivity and i (m/m) is the hydraulic gradient. For the simplified case where the stream tube is conceptualised as being made up of a “bundle” of independent flow paths, it can be shown rigorously that Equation 10-1 and 10-2 and give identical results.

Estimates of the site specific F-factor can be made using Equation 10-2 with the specific flow-wetted surface data given in Table 10-3 and hydraulic conductivity data from Table 8-8 and Table 8-9. These data have been used to make estimates of the F-factor and are detailed in the background report by /Crawford 2006/.

The stream tube approach predicts mean F-factors in the range 10^3 – 10^8 (y/m), although the results obtained are strongly dependent upon the scale of measurement for the hydraulic conductivity, the method used for the hydraulic conductivity measurement, as well as the estimated value of the specific flow-wetted surface. Generally, a larger measurement interval gives a higher hydraulic conductivity and consequently lower estimates of the F-factor. An additional uncertainty in this analysis is that Posiva Flow Log (PFL) data is used to obtain the specific flow-wetted surface, whereas the hydraulic conductivities are obtained using different methods. As methods such as the Pipe String System (PSS) and pump tests (PT) typically have higher sensitivities than the PFL method, there is a potential disparity between the data values used as a basis for the calculations.

The combination of PFL-derived flow-wetted surface estimates with more sensitive measurements of hydraulic conductivity gives F-factors that could be considered too low when taken at face value. Given that fast flow paths will tend to dominate solute transport processes, however, this is not a major consideration as the hydraulic conductivity measured over larger scales (e.g. 20–100 m) will be mostly dominated by the major conducting flow paths which are also the basis of the PFL data estimates of the specific flow-wetted surface.

10.9 Evaluation of uncertainties

General discussions on the uncertainties related to the site-descriptive transport model are given in the transport modelling guidelines /Berglund and Selroos 2003/ and in Chapter 12. Similar to the other geoscientific disciplines, spatial variability is considered an important potential source of uncertainty in the modelling of transport properties. In previous investigations of rock samples from Äspö and Laxemar, spatial variability has been observed in the form of differences between different rock materials, as well as variability among samples taken from the same (based on geological classification) materials /Byegård et al. 1998, 2001, Löfgren and Neretnieks 2003, Xu and Wörman 1998/. Furthermore, studies at Äspö have indicated large differences in retardation properties for materials at different stages of alteration in the vicinity of fractures /Byegård et al. 1998, 2001/. These results show that significant (order of magnitude) spatial variability in retardation parameters can be expected over all scales and types of variability.

The impact that these uncertainties have upon radionuclide transport calculations depends upon the types of uncertainty and the way in which they are handled in safety assessment. Uncertainties relating to the parameterisation of the various rock types and their alteration forms in the retardation model arise partly due to artefacts of sample size, the number of samples used to obtain data, as well as the representativity of those samples selected for the laboratory programme in comparison with the in situ rock properties. In the case of sorption properties, this extends also to the water composition used for sorption measurements.

For spatial variability in retention properties (i.e. D_e , θ_m , and K_d), which are potentially describable as Gaussian random variables along a transport path, the variance of the effective mean value for a specific rock type is expected to decrease on increasing length scales /e.g. Lake and Srinivasan 2004/. Additional uncertainties relate to the kinds of rock and alteration types likely to be encountered by solutes along transport paths, their relation to the overall rock volume, as well as the parameterisation of alteration layers in the rock matrix. There is evidence to suggest, for example, that there may be significant uncertainties in the retention properties of the altered rock forms relative to unaltered rock matrix in the Simpevarp 1.2 SDM /SKB 2005a/ owing to the amalgamation of site specific data with imported data from Äspö HRL investigations. This is discussed in more detail in the background report by /Crawford 2006/. In the present model version, such artefacts are

largely unavoidable owing to a lack of available (and internally consistent) experimental data for the different rock types and their alteration forms. The disparity, however, may have only limited importance on safety assessment timescales owing to the overwhelming importance of the relatively thicker unaltered rock matrix for the retardation of radionuclide transport.

It is difficult to give a definitive estimation of relative diffusive properties in the current SDM for Laxemar as there is a considerable inequality in sample support amongst the different rock types and measurement methods. Based upon the recommended transport parameters in Table 10-4, however, Ävrö granite appears to have the highest effective diffusivity (associated with higher retention) with a formation factor on the order of $F_f \geq 10^{-4}$. Other reported rock types appear to have essentially similar diffusive properties to each other (although with formation factors slightly lower than Ävrö granite) and any relative differences are speculative owing to the inherent data uncertainty. There appear to be no significant differences between the diffusion properties data obtained for Simpevarp rock types and those from the Laxemar subarea.

Similarly to the diffusive properties of the rock, the currently available sorption measurement data indicates only very small differences between the major rock types. Provided sorption properties can be reasonably well correlated with BET surface area, the differences between different rock types should be less than the estimated uncertainty in the sorption data itself.

Given the provisional nature of the retention properties data and the fact that a large proportion of the data are extrapolated on a tentative basis, it is not currently possible to rigorously compare the retention properties of different rock domains, nor draw specific conclusions concerning the differences between rock domains in the Laxemar subarea and those within the Simpevarp subarea. The rock types found in both the Laxemar and Simpevarp subareas, however, appear to have broadly similar retention properties based upon the current level of understanding.

In general, the main uncertainties identified in the Laxemar 1.2 modelling are related to the absence of site-specific transport data for both the retardation model as well as the integrated transport properties model incorporating estimations of the F-factor. Furthermore, the available data are currently insufficient for establishing quantitative relations between transport parameters and other properties such as lengths, orientations and hydraulic properties of fractures and deformation zones. Despite these difficulties, it is still possible to provide bounding estimates of the variability of the F-factor for individual migration paths.

The data detailed in the background report /Crawford 2006/ suggest a mean value on the order of about 10^6 (y/m) for a mean path length of 100 m and typical in situ conditions, but based on the extreme assumptions of channel length and flow channel interdependence investigated, up to 10% of the migration paths could have an F-factor less than 10^4 (y/m). It can also be stated that, for safety assessment, the relevant issue is the spatial distribution of migration paths related to the scale of individual deposition holes. The percentile of deposition holes with a low F-factor would not exactly equal the percentile of individual flow paths with this low F-factor in the rock volume as a whole, as a deposition hole could be intersected by a varying number of migration paths (varying from zero to several for each hole). Moreover, the F-factor for a deposition hole would be dominated by the path with lowest F-factor value intersecting the hole. Therefore, upscaling using various assumptions in the DFN-model is needed to provide more quantified uncertainty ranges for application within Safety Assessment.

Channelling effects are not very well understood and the current generation of hydraulic DFN models do not capture all relevant aspects of the phenomenon. Some attempts have been made, for example, to investigate the influence of flow heterogeneity arising due to variable aperture within fracture planes /e.g. Outters 2003, Painter 2006/. Thus far, however, no assessments have been made of the potential impact of flow “wormholes” formed at the boundaries of fracture plane intersections. It is noted that we do not currently have good means for observing and assessing channelling phenomena with the aim of identifying fast and persistent flow paths by the methods used today. Any flow wormholes present in the rock are not readily found by boreholes owing to their narrow width.

The uncertainties relevant for the present description of transport properties can be categorised as follows:

- Uncertainties in the data and models obtained from other disciplines; primarily geology and hydrogeochemistry for the retention model, but also Hydrogeology for estimations of the transport resistance.

- Uncertainties in the interpretations and use of data and models from other disciplines, i.e. in interpretations of the relations between transport properties and various underlying properties, and the simplifications made when identifying and parameterising “typical” materials and fractures.
- Data uncertainties related to measurements and spatial variability of transport parameters, including the “extrapolation” of small-scale measurements to relevant model scales.
- Conceptual uncertainties related to transport-specific processes and process models (see Section 10.3.2 and 10.8.2).

This model provides quantitative information on transport data uncertainties only. Uncertainty ranges are given in the data tables above and, in most cases, are taken directly from the experimental data. Essentially, these ranges incorporate both random measurement errors and the spatial variability associated with the particular dataset. The uncertainties introduced by the inputs from other disciplines and by the “expert judgement” utilised to interpret and use these data have not been addressed in the transport description. Whereas the uncertainties in the description devised by geology and hydrogeochemistry are discussed in Chapter 5 and Chapter 9, respectively, no attempt has been made to formulate alternative interpretations or otherwise address the “expert judgment” aspects of the work. None of the quantifications of uncertainty currently consider the possibility of measurement bias in more than a cursory fashion. This issue will need to be dealt with more rigorously in forthcoming versions of the SDM.

Regarding the uncertainties related to spatial variability and scale, it may be noted that all measurements providing data to the retardation model have been obtained in the laboratory, on a millimetre- to centimetre-scale. The proper means of “upscaling” these parameters is by integrating them along flow paths in groundwater flow models, implying that the scale of the flow model is the relevant model scale. The approach is here to present the data on the measurement scale, thereby providing a basis for further analysis in conjunction with numerical flow and transport modelling.

The lack of representative measurement data for subordinate rock types as well as for transitional forms of indeterminate taxonomy (i.e. rock having characteristics of more than one rock type) is an uncertainty within the current site descriptive model. A situation in which this could be of importance for safety assessment is if extensive, preferential flow paths exist within these rock types. This could have an impact on transport calculations if the effective proportions of the types of rock encountered by transported radionuclides were appreciably biased in favour of the subordinate rock types (i.e. increased) relative to the mix of rock types currently considered to make up the bulk of the rock volume. As the effective retention experienced by a transported solute is related to the integrated value of the material properties parameter along a flow path, the subordinate rock types would need to comprise a very large proportion of the flow path, or have very different material properties to the main rock types identified to have a perceptible impact.

Amongst the subordinate rock types discussed in Chapter 5, the rock types of main concern based upon their relative occurrence (varying between 1–15% for the various boreholes, cf. Figure 5-42) would be fine- to medium, as well as coarse-grained granite. There is some evidence in the PFL data (cf. Table 8-14) that these rock types are associated with slightly higher hydraulic conductivities which, although largely speculative, may suggest the presence of preferential flow paths. Based upon the available information, other subordinate rock types are present in only relatively small quantities and generally seem to have lower hydraulic conductivities than the main rock types.

From the available transport data, it appears that the subordinate granites have roughly the same diffusive properties as the main rock types. It is noted, however, that porphyritic, coarse-grained granite may have an effective diffusivity up to five times higher than that of the main rock-types. Although no sorption or BET surface area data are available for the subordinate rock-types in the Laxemar subarea, data from Äspö HRL /Byegård et al. 1998/ indicates that fine-grained granite may have weaker sorption properties (by a factor of between 4 and 14) than Äspö diorite. On the assumption that Äspö diorite can be considered to be an approximate analogue for Ävrö granite or quartz monzodiorite (the most abundant rock types in Laxemar) /Byegård et al. 2005, SKB 2005a/, this could be a potential uncertainty in transport calculations made within safety assessment and should be considered.

11 Resulting description of the Laxemar subarea

This chapter provides condensed accounts of the version 1.2 site-descriptive models of the Laxemar subarea. The presentation follows the consecutive order of the discipline-wise presentation in preceding chapters. Examples of intra-disciplinary integration and corroboration of results and models are provided as part of the discussion in Chapter 13.

11.1 Surface properties and ecosystems

11.1.1 Quaternary deposits and other regoliths

Four main types of overburden environments have been distinguished in the regional model area based on the present knowledge of Quaternary deposits (QD). These environments occur both on the present land and sea floor.

- I) The highest topographic areas, which are dominated by exposed bedrock, till and numerous small peatlands, classified as bogs or fens. The overburden in these areas is generally one or a few metres thick. It is possible that small pockets with thicker QD occur, e.g. in the small wetlands. This environment is completely dominated by forest.
- II) Narrow valleys dominated by clay gyttja, peat and/or wave washed material. Glacial clay and till underlie these deposits. The total thickness of QD is several meters in these environments. The floors of the valleys have often been ditched and are used as arable land. At the sea floor, the valleys close to the coast are dominated by clay gyttja, which is currently being deposited. Glacial clay and sand dominate the valley floors outside the archipelago. These bottoms are characterised by erosion and transportation of sediment.
- III) Areas with moraine and a low frequency of bedrock exposures occur in the south-western part of the model area, but also in the central part of the Laxemar subarea. The till in this environment is generally thicker than the till in overburden environment (I).
- IV) The areas constituting glaciofluvial deposits of which Tunaåsen esker in the western part of the regional model area is the most prominent. These deposits are well drained and are often covered with forest.

11.1.2 Climate, hydrology, hydrogeology and oceanography

The present knowledge of the climate, surface hydrology and near-surface hydrogeology in the Simpevarp area (including the Laxemar subarea) can be summarised as follows:

- The annual (corrected) precipitation in the Simpevarp area is on the order of 600–700 mm. The long-term (1961–1990) average precipitation at the SMHI station in Oskarshamn is 633 mm. During 2004, the precipitation on Äspö was 660 mm. The long-term average “regional” specific discharge has previously been estimated to be in the range 150–180 mm /Larsson-McCann et al. 2002/. The Laxemar 1.2 modelling shows that there are large differences in the specific discharge between seasons, years and catchment areas. This is due to seasonal and inter-annual variability of the meteorological conditions, and also differences in land use, fraction of open water and so forth between catchment areas. Hence, these results indicate that water balance and the specific discharge most properly is calculated and reported on a catchment-by-catchment area basis, rather than applying one “average” value for the whole Simpevarp area.
- The topography of the Simpevarp area is characterised by a relatively small-scale undulation. The area consists of a large number of catchment areas and small water courses. Most water courses have a low discharge or are dry during large parts of the year. There are relatively short periods with large discharge, associated with heavy precipitation events and/or snow melt. In many areas, the surface hydrology is affected by human activities, primarily in the form of ditches and other drainage systems.

- The groundwater level in QD is generally shallow, on the order of 0.5–1.5 m below the ground surface. The amplitude (the difference between the maximum and minimum levels) is also generally small, c. 0.5–1 m. Near-surface groundwater in QD implies that the boundaries of the 26 catchment areas (areas contributing to the discharge to surface waters) can be assumed to coincide with the corresponding near-surface groundwater divides.
- Investigations on the QD stratigraphy below some lakes, wetlands, and peat areas indicate that the QD in the bottom of such areas typically consists of low-permeable layers, limiting the contact between groundwater and surface water. A better characterization of such potential discharge areas requires measurements of groundwater levels in QD below lakes, wetlands and peat areas. Such data are not yet available.
- The whole near-surface groundwater flow system is transient, due to temporally variable meteorological conditions. Groundwater recharge from precipitation (snow melt) is considered to be the dominant source of groundwater recharge. There are more and also larger discharge areas during dry periods, compared with wet periods. Hence, the spatial distribution of recharge and discharge varies with time, due to (seasonally) variable meteorological conditions. Areas in the vicinity of the main water courses and Lake Frisksjön are considered to be permanent discharge areas, whereas the high-altitude areas are permanent recharge areas. Even though there is yet no field evidence, the Laxemar 1.2 modelling indicates that lakes in the Simpevarp area contribute to groundwater recharge during dry periods, when groundwater levels are low.

11.1.3 Chemistry

Surface water

The freshwater systems in the Simpevarp area can generally be classified as mesotrophic, brown-water types. Most freshwaters are markedly coloured due to a high content of humic substances, and show very high levels of dissolved organic carbon. Both streams and lakes are also relatively rich in nitrogen and phosphorus. Most freshwater sampling sites show almost neutral or moderately acid pH values and an alkalinity corresponding to a relatively good buffering capacity. There are, however, a few sampling sites in streams which show very acid pH values and no or negligible buffering capacity, indicating the occurrence of acidified surface waters in the Simpevarp area.

The sampling sites in the sea can be divided into two different types; those representing the open sea and outer archipelago, and those representing the relatively confined bays close to the mainland. The first type shows a relatively stable chemical composition, whereas the confined bays show strong variation in most parameters, due to varying mixing conditions between sea water and the runoff from adjacent terrestrial areas. The confined bays generally show lower concentrations of ions than the open sea sites, whereas the concentrations of organic compounds and nutrients, especially the nitrogen fractions, are considerably higher.

Shallow groundwater

Shallow groundwater in the Simpevarp area is characterised by neutral or slightly acid pH values, an alkalinity ranging from high to very low, and a normal or slightly elevated content of major constituents in a national context. However, several parameters show large deviations from normal conditions in Sweden. Iron and manganese show markedly elevated concentrations, and also fluoride, iodide, strontium, and some trace elements, show higher concentrations in the area, compared with Swedish reference data from shallow groundwater and surface waters.

Overburden

When the chemical composition of till, sediment and soil from the Simpevarp area are compared with regional and national data, only minor differences are revealed, indicating that the overburden in the Simpevarp area is relatively usual in a Swedish context.

11.1.4 Ecosystem description

The surface ecosystem is described using a large number of properties which, when combined, will constitute the ecosystem site descriptive model /cf. Löfgren and Lindborg 2003/. The surface ecosystem is divided into different subsystems based on the presence of system-specific processes and properties, and also on the collection, measurement and calculation of data that may differ between different subsystems. Accordingly, three different subsystems are characterised: (1) the *terrestrial* system, which includes all land and wetland areas, (2) the *limnic* system, i.e. lakes and rivers, and (3) the *marine* system. The amount of data collected from the site describing both the abiotic and the biotic parts of the ecosystems has increased considerably since SDM Simpevarp 1.2 /SKB 2005a/, and the data are presented in detail in /Lindborg 2006/. A brief summary of our present knowledge of the different ecosystems is given below. Detailed carbon budgets have been developed for each of the three ecosystems and these are presented in Section 4.8. Data from all three ecosystems are also combined into an integrated ecosystem model in order to describe fluxes of water and carbon between the ecosystems /Lindborg 2006/.

Terrestrial system

Generally, the vegetation is strongly influenced by the type of bedrock, Quaternary deposits and human land management present. The bedrock in the area mainly consists of granites, and the Quaternary deposits are mainly till, though silt and clay have been deposited in the valleys. This is manifested in the vegetation, where pine forests dominate on till, and all the arable land and pastures are found in the valleys. The wetlands are characterised by mires poor in nutrients. The land management is today mainly restricted to forestry activities that are, among other things, seen as numerous clear-cuts in different successional stages. Many traces of a more intensive management are seen in the landscape. This is particularly illustrated by the dominant woodland key habitat type of old semi-natural grasslands or meadows with old pruned deciduous trees in close proximity to old settlements.

The most common mammal species in the Simpevarp regional model area and adjacent areas is roe deer (5 deer \times km⁻²). Moose is also fairly common (0.7 moose \times km⁻²), but unevenly distributed, which is normal for this part of Sweden due to variations in hunting pressure, snow depth and distribution of food. European and mountain hare are fairly low in abundance, compared with other regions (see Table 4-5). However a significant number of the mammals in the Simpevarp area are domestic animals and there are 4.3 cows and calves per km² in the area. In total, 126 species of birds were found in the regional model area in 2003, and 28 of these are noted in the Red List of endangered bird species in Sweden. The most common species on land are Chaffinch (*Bofink*).

The soil fauna represents the largest carbon pool amongst the terrestrial fauna. In those parts of the Simpevarp area where there is some agricultural activity, domestic animals (cattle) represent the second largest carbon pool. The uptake of vegetation by humans and herbivores (including cattle) represent the largest carbon flows.

Limnic system

The lakes and streams in the Simpevarp regional model area are, as most surface waters in the northern parts of the County of Kalmar, rich in organic matter, mainly humic compounds that give the water a brownish colour. The catchment areas within the regional model area are generally small, which means that some of the streams periodically show very low discharge or are even ephemeral. Most of the streams in the area are more or less affected by human activities, such as straightening or ditching, and many of the present lakes have been lowered in order to reclaim more land for agriculture.

Streams

Generally, the chemical composition of stream water in the regional model area shows only minor differences from typical stream sites in the County of Kalmar. Mean values for major ions and electrical conductivity are somewhat lower for sites in the regional model area, whereas mean values for C/N/P-fractions, and especially for total nitrogen, are somewhat higher for sites in the regional

model area. This is partly due to high nutrient concentrations at some sampling points situated in farming areas. Mean values of alkalinity and pH for stream sites in the Simpevarp area are low, especially for upstream sites with small sub-catchment areas.

Lakes

Only a few, relatively small and shallow lakes are situated within the regional model area. The concentrations of nutrients in these lakes are moderate and they can be characterised as mesotrophic with brown water. One larger lake in the northern part of the area, Lake Götemar, shows considerably lower concentrations of nutrients and can be classified as an oligotrophic clearwater lake. Compared with typical values for lakes in the County of Kalmar, the lakes in the Simpevarp area show higher concentrations of ions associated with marine water and of total nitrogen. The buffering capacity of the investigated lakes, measured as HCO_3^- -concentration, is generally good and the pH values are close to neutral and stable over the season. Accordingly, there are no signs of anthropogenic acidification affecting the lakes.

All lakes develop a thermal stratification during summer, and the oxygen levels in the bottom water become low during stagnant conditions, both in summer and in winter. Despite the relative shallowness, the brown water prevents light from penetrating down to the bottom in the deeper parts, and substantial parts of the bottom in all lakes are free from vegetation. This means that primary production by phytoplankton and submerged macrophytes in the lakes is low, and the limnic food web is to a large extent sustained by energy (i.e. organic carbon) from the terrestrial system.

The fish community of the investigated lakes can be regarded as typical for small brownwater lakes in the area; it is dominated by perch both in number and biomass. Pike and roach occur in all investigated lakes, and the total number of species in a lake varies between 3 and 7.

Marine system

Most of the surface water from the regional model area drains into a few, relatively confined, coastal basins, and the water chemistry of these basins differs considerably from the water chemistry of the outer parts of the archipelago. The marine system in the area can therefore be divided into two different types, the first type representing the open sea and outer archipelago (two sub types), and the second type the relatively confined bays close to the mainland. The bays show lower concentrations of ions than the open sea, whereas the concentrations of organic compounds and nutrients, especially the nitrogen fractions, are considerably higher. As a consequence of the relatively high concentration of organic compounds (humus) in the bays, water transparency is rather low throughout the year in the confined areas as opposed to the open sea. Despite low transparency, due to the shallow water column and large phytoplankton concentrations, the confined bays have high primary production, both in the pelagic and the benthic communities. The results show that the highest benthic net production is found in shallow *Chara* sp. communities. The benthic filter feeders (dominated by *Mytilus edulis*) dominate the biomass and respiration in the outer parts of the area. The highest benthic net respiration is found in the lower parts of the phytobenthic community. Net community production in the pelagic zone is found down to a depth of approximately 10 to 20 m, varying with measured water transparency and chlorophyll content in the sub basins.

Overall, the preliminary figures show a net production in the semi-enclosed shallow basins, whereas the deeper open coastal basins show net respiration. This relationship reflects a similar pattern in organic carbon; a net production of organic carbon (a result of the high primary production) is found in the confined basins and a net demand (consumption by filter feeders) is found in the outer areas. This pattern suggests a large flow of organic carbon from the inner basins and from the pelagic to the filter feeder-dominated coastal benthic community.

11.1.5 Humans and land use

The Simpevarp area is a sparsely populated area located in a relatively lightly populated county. In 2002, the population density was 7.4 inhabitants \times km⁻², three times lower than in the County of Kalmar as a whole. The demographic statistics show no upward trend, instead there is a slow downward trend in Simpevarp area as well as in the Municipality of Oskarshamn and the County

of Kalmar. Most (83.6%) of the people that work within Simpevarp area (employed day-time population) are occupied within the sectors of electricity-, gas- and water supply, sewage and refuse disposal. This dominance is due to the Oskarshamn nuclear power plant (OKG) /Miliander et al. 2004/.

The forests are influenced by active and ongoing forestry; approximately one third of the forests within the regional model area are younger than 30 years. The average age of the productive forest is approximately 53 years. About 25% of the logging products are used for pulp production, and the rest as timber. The Simpevarp area is a frequently visited area for outdoor activities, such as hunting, fishing, hiking as well as picking of wild berries and mushrooms /Miliander et al. 2004/.

11.2 Bedrock geological description

The bedrock geological model consists of three components; the rock domain model, the deterministic deformation zone model, and the statistical analysis of fractures and deformation zone traces, i.e. the discrete fracture network (DFN) model. One or more components of the bedrock geological model provide a foundation for the modelling work in rock mechanics, thermal properties, hydrogeology (bedrock) and, to lesser extent, hydrogeochemistry (bedrock) and transport properties (bedrock). All components of the geological model have a direct impact on the location and detailed design of the repository. They also provide a significant input for the Safety Assessment.

The Laxemar 1.2 modelling work is focused on the Laxemar subarea, which makes up a part of the local scale model volume. However, the rock domain and deformation zone modelling work also comprises an update of the model of the Simpevarp subarea, as well as of the whole regional model volume. The modelled rock domains are identified by the three letters RSM, followed by one or two letters and two digits, e.g. RSMA01. Domains denominated with the same capital letters are characterised by similar properties.

In a similar manner, the deformation zones are identified by the three letters ZSM followed by a code that consists of a combination of letters and digits. The first two letters indicate to which orientation set the deformation zone belongs, for example NE, EW etc. The property tables for each rock domain and deformation zone is presented in Appendices 5 and 6, respectively. Confidence assessments of the rock domains and deformation zones are presented in Sections 5.3 and 5.4, respectively.

The DFN model has utilised fractures from essentially the local scale model volume and surface traces from the already existing Simpevarp 1.2 regional deformation zone model. The DFN model describes the geometrical properties of fractures in the rock mass in between deformation zones and different DFN models have been developed for a) the Laxemar and Simpevarp subareas b) rock domains RSMA and RSMB. Fracture set orientations, sizes, intensities, geological controls and spatial distributions are characterised and summarised in table format for input to downstream model users.

11.2.1 Rock domain model

The detailed bedrock map of the Simpevarp and Laxemar subareas and complementary analytical data from the surface, together with data from approximately 6,800 m of cored boreholes in the Laxemar subarea, and c. 4,700 m of cored boreholes in the Simpevarp subarea constitute the basis for the establishment of the rock domain model in SDM Laxemar 1.2. The cored borehole data at depth confirm the character of the bedrock at the surface. Hence, the more abundant data from the surface are of great importance for the characterisation of the identified rock domains. In comparison to the rock domain model in the SDM Simpevarp 1.2 /SKB 2005a/, the rock domain model in the Laxemar part of the local scale model domain has been considerably modified. This is principally due to the new detailed bedrock map of the Laxemar subarea, but also to information from cored boreholes that were not available in the previous model version.

The three-dimensional rock domain model of the regional model domain, with the local scale model domain indicated, is displayed in Figure 11-1.

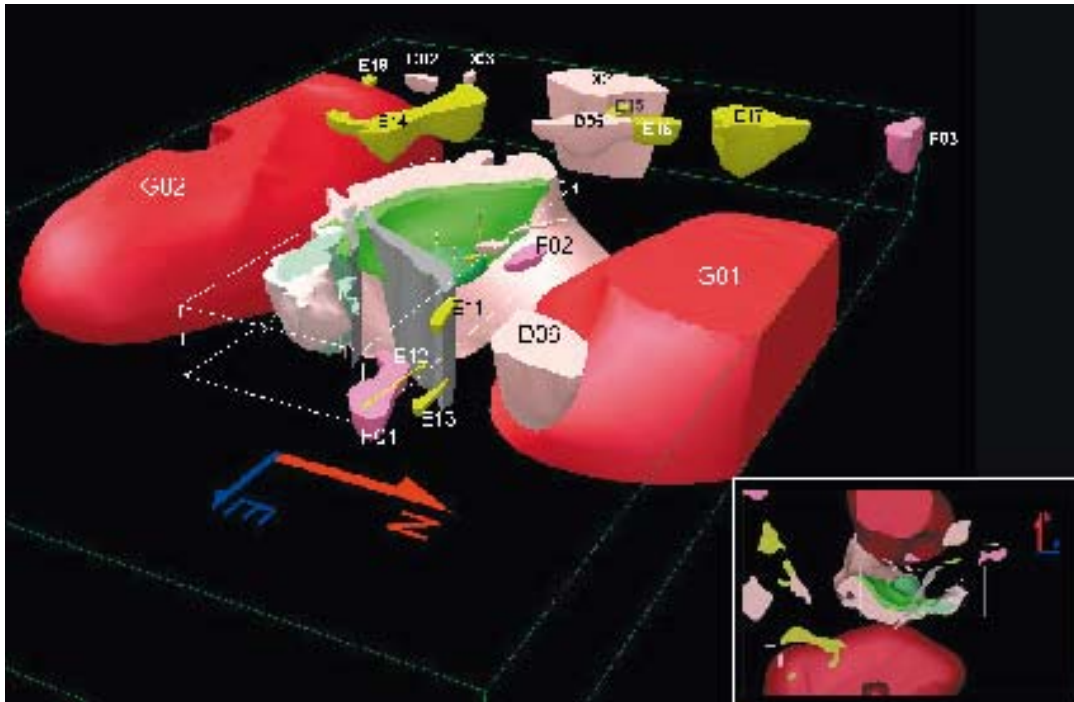


Figure 11-1. Regional rock domain model with the local scale model domain inserted. The Ävrö granite (RSMA01) is transparent. View from the northeast.

In the regional model volume, modifications are mainly restricted to the rock domains RSMG01 (Götemar granite) and RSMG02 (Uthammar granite). In the SDM Simpevarp 1.2, the Götemar granite intersected the bottom of the northern part of the local scale model volume. However, based on new geophysical modelling, the Götemar granite does not enter at depth in the SDM Laxemar 1.2 local scale model volume.

As can be seen in Figure 11-2, the rock domains RSMA01 and RSMD01 dominate the local scale model volume. Focussing only at the Laxemar part of the local scale model volume, the RSMA01 and RSMD01 domains dominate the northern to northeastern and the southern to southwestern part, respectively. The northward extension at depth of the RSMD01 domain is confirmed by intercepts in the cored boreholes KLX02, KLX03 and KLX05, and is also supported by geophysical modelling based on gravimetric and magnetic data. It is indicated in the cored boreholes KLX03 and KLX05, and in the modelling of the gravity and magnetic data, that the extension at depth of the rock domain RSMM01, which is characterised by the abundant occurrence of diorite to gabbro, does not follow the domain boundary between RSMA01 and RSMD01, but rather enters the RSMA01 domain with increasing depth.

As mentioned in Section 5.3.3, the domains that are characterised by fine-grained dioritoid (domains RSMB and RSMBBA), form elongated lens-shaped bodies along, or close to, the contact between the Ävrö granite in the RSMA01 domain and the quartz monzodiorite in the RSMD01 domain, and between the RSMC01 and RSMC02 domains. The RSMB and RSMBBA domains have northerly extension at depth similar to RSMM01 (see Figure 11-3). An exception is the RSMBBA03 domain which is modelled horizontally. The orientation and spatial extent of this lens shaped domain is based on a subhorizontal seismic reflector that is interpreted to be caused by the lithological variations /Juhlin et al. 2002/. Note that this domain only occurs at depth (Figure 11-2 and Figure 11-3).

The modelling of the RSMP01 and RSMP02 domains, which correspond to the deformation zones ZSMNE005A (Äspö shear zone) and ZSMNE004A, respectively (cf. Section 5.2.4), have been restricted to the local scale model volume due to their uncertain continuation outside the local scale model area. These domains and their geometry are based on a high frequency of subvertically to vertically dipping, low-grade ductile shear zones.

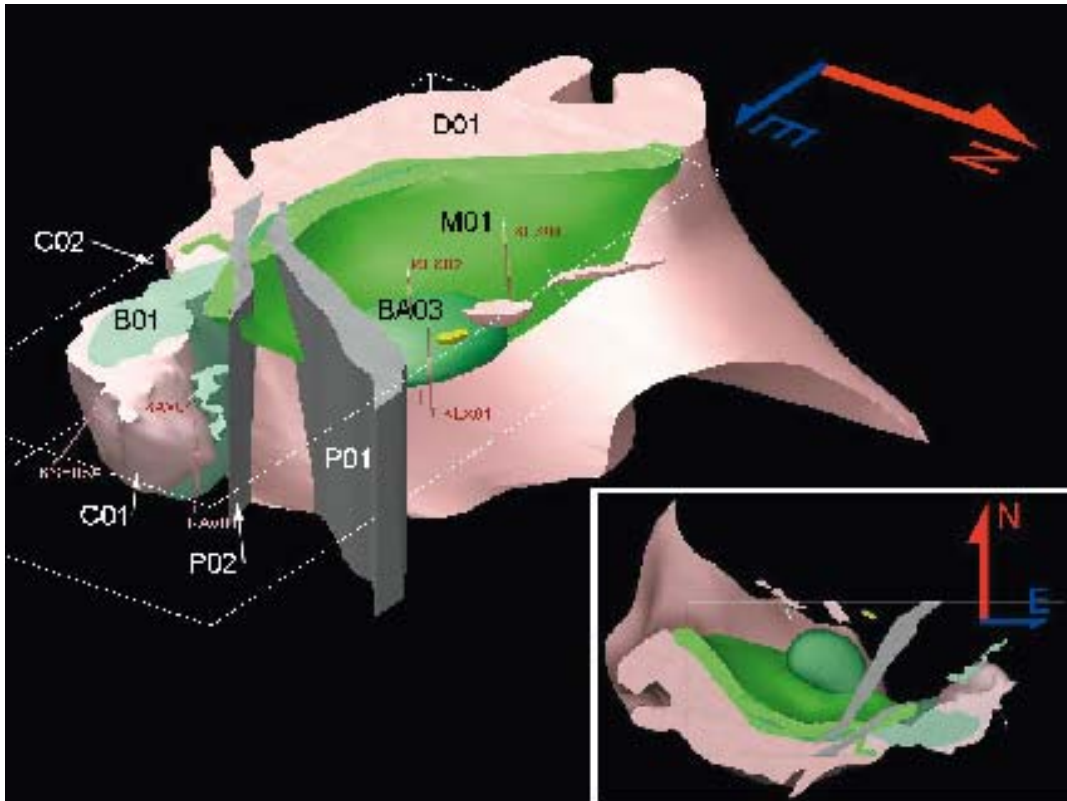


Figure 11-2. Close up of the rock domains in the local scale model volume. Note the northward extension at depth of the RSMD01 and RSMM01 domains. The RSMA01 domain is transparent. View from the northeast.

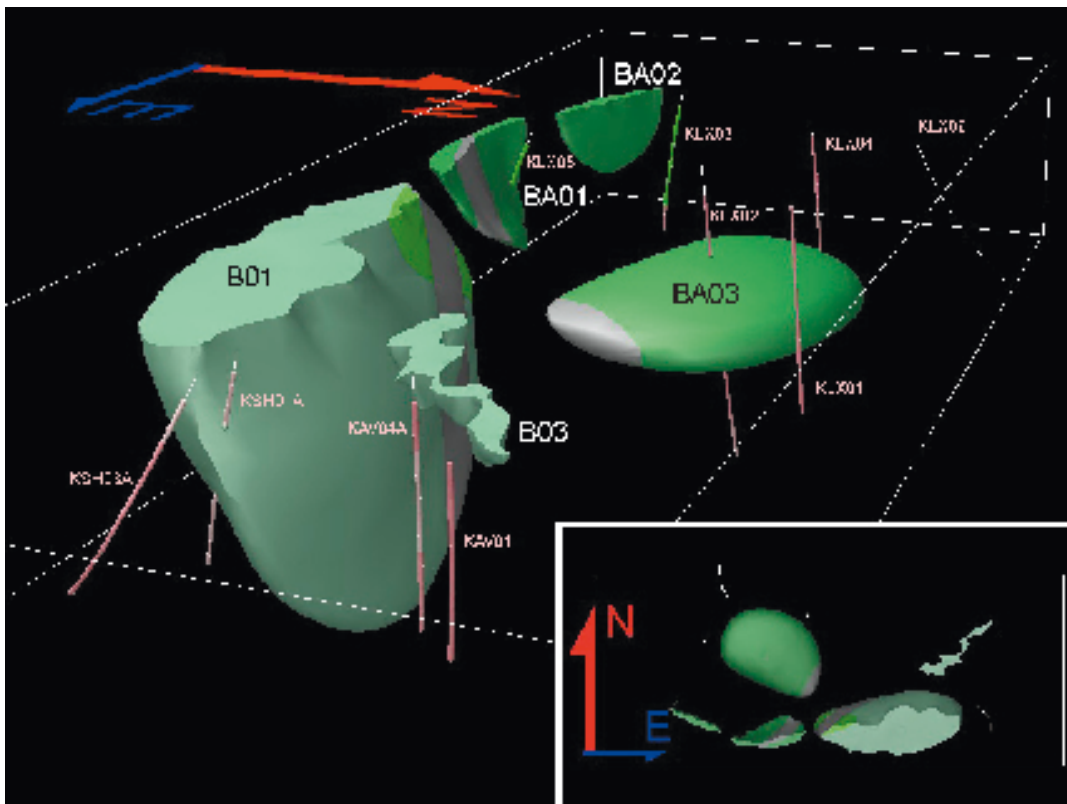


Figure 11-3. RSMB and RSMBA rock domains in the local scale model volume.

In the Simpevarp subarea, the geometry of rock domains has only been slightly modified, and is very similar to the SDM Simpevarp 1.2 /SKB 2005a/.

The geometrical relationships in detail between most rock domains are considered uncertain. However, the geometrical relationships between rock domains RSMP01 and RSMP02 and the surrounding rock domains are judged to be well constrained due to the consistency in the orientation of the mylonitic to protomylonitic foliation on which these domains are based. Furthermore, the general geometrical relationship between the two dominating rock domains RSMA01 and RSMD01, and the intervening RSMM01 rock domain in the Laxemar subarea is judged to be fairly well constrained. Thus, the rock domain model is judged to be stabilising in the Laxemar subarea, and the uncertainty in the geometrical relationships between the rock domains primarily relates to the Simpevarp subarea and the remaining part of the regional scale model area.

The degree of inhomogeneity in the rock domains, i.e. the proportion of subordinate rock types in relation to the dominant rock type in the domain, is estimated from the Boremap data. Based on data from different cored boreholes in the Ävrö granite-dominated RSMA01 domain, the proportion of Ävrö granite varies between c. 62 and 92%. Among the subordinate rock types, e.g. fine-grained diorite to gabbro varies between c. 3 and 12%, fine- to medium-grained granite between c. 1 and 6%. This actualises the uncertainty that relates to the proportion, distribution and orientation of subordinate rock types in the rock domains.

An important property and also uncertainty is the compositional variation of the Ävrö granite. This relates especially to the quartz content which has major implications for the thermal conductivity and, thus, for the thermal modelling. Based on modal analyses of samples from both the surface and drill cores, the quartz content in the Ävrö granite in the RSMA01 domain is $18.8 \pm 6.3\%$ (N=61), while it is $13.0 \pm 4.4\%$ (N=9) for the Ävrö granite in the RSMM01 domain. The quartz content in the quartz monzodiorite in RSMD01 domain is $14.8 \pm 2.8\%$ (N=7), that is very similar to the quartz content in the Ävrö granite in the RSMM01 domain. Thus, from a compositional point of view, the Ävrö granite in the RSMM01 domain and the quartz monzodiorite in the RSMD01 domain may be considered as uniform.

The three-dimensional distribution and characterisation of hydrothermal alteration is uncertain due to limited information. Hydrothermal alteration may affect both the thermal and transport properties. What concerns the thermal conductivity, this is usually increased by increasing alteration. Based on Boremap data, c. 67 to 86% of drill cores, excluding the identified deformation zones, in the RSMA01 domain is not affected by alteration. When alteration is observed, it is generally faint to weak in character.

11.2.2 Deterministic deformation zone model

The base case deformation zone model covers the whole regional model area and consists of deformation zones of high, medium and low confidence of existence. The surface intersections of the deformation zones within the local scale model area are illustrated in Figure 11-4. The deformation zone model is illustrated below in a 3D perspective view within the regional (Figure 11-5) and local (Figure 11-6) scale model volumes. All deformation zones included in the base case model are considered to exist, although the degree of confidence for zones that have no direct observations is lower.

Thirty-five high confidence deformation zones are identified within the regional model area. Each one of these interpreted zones are observed both indirectly, through lineament or geophysical data, and directly through field mapping, borehole or tunnel observations. Exceptions are the Mederhult zone (ZSMEW002A), and zones ZSMNS009A, -10A and -11A, which have only been observed in field mapping, through major regional imprints in the airborne geophysics or through clear anomalies in ground geophysical profiles. However, a few high confidence zones are based solely on indirect surface observations through seismic refractions or reflections.

The average dips of the thirty-five (N=35) high confidence zones have been estimated using existing observations from geophysical profiles, seismic refractions, seismic reflections, borehole or tunnel observations, where available. A vertical dip has been assumed for zones where no conditional information on dip exists.

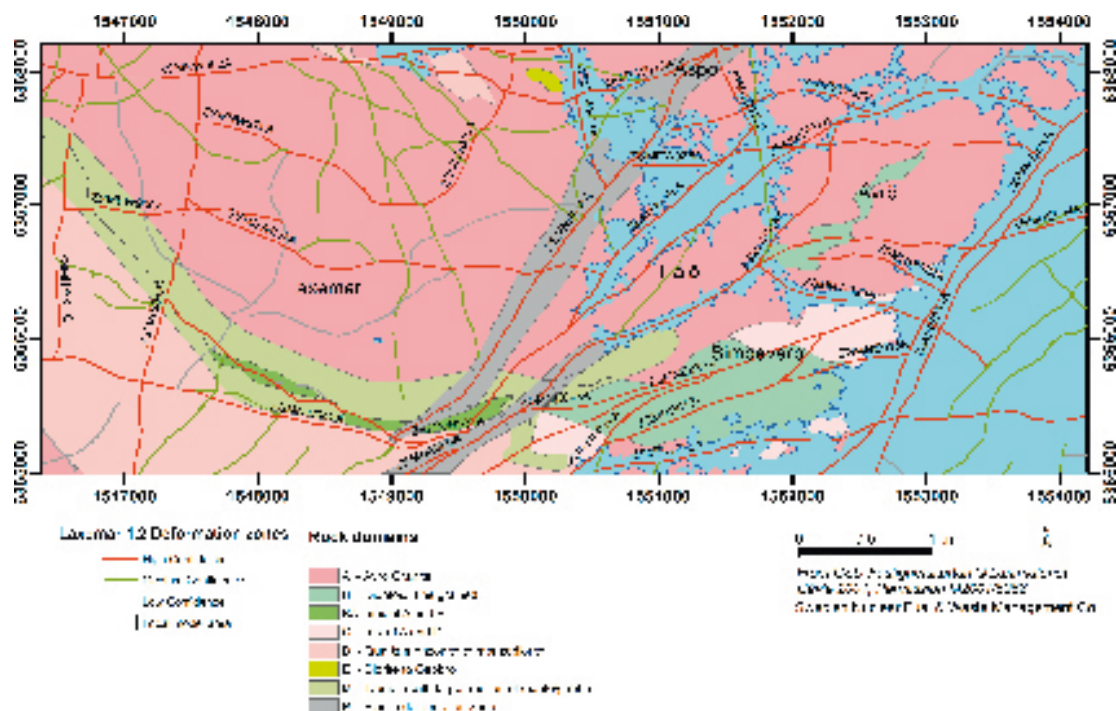


Figure 11-4. Illustration of the base case deformation zone model with high (red), medium, (green) and low (grey) confidence zones within the local scale model area. The alternative deformation zone model consists only of the high and medium confidence (red+green) deformation zones.

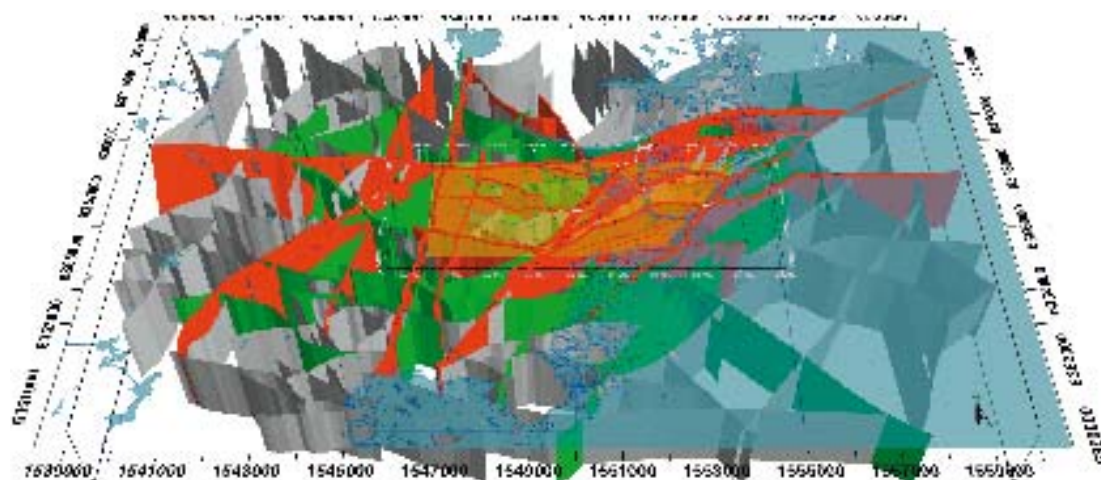


Figure 11-5. Regional scale model of deformation zones. Red, green and grey indicates high, medium and low confidence zones respectively. Area of local scale model indicated for reference (see Figure 11-6).

One hundred and fifty-five (N=155) medium and low confidence zones have also been included in the deformation zone model. Of these, sixty-two (N=62) are of medium confidence.

Twenty-nine of the high confidence deformation zones were already identified in the Simpevarp 1.2 model /SKB 2005a/. In this model version, five more high confidence deformation zones have been identified through geological field observations, borehole intersections in combination with ground geophysics or seismics.

A few deformation zones from the Simpevarp 1.2 model have been possible to remove through confirmatory drillings, field observations and geophysical profiles.

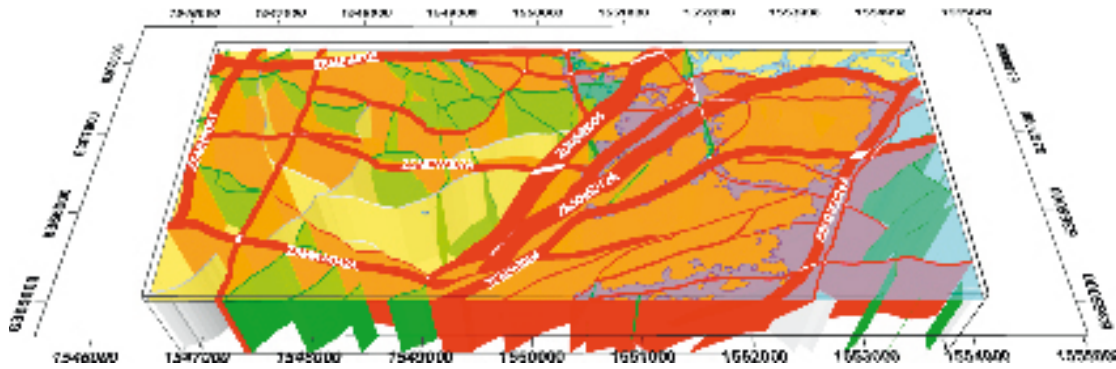


Figure 11-6. Local scale model of deformation zones. Red, green and grey indicates high, medium and low confidence zones respectively, cf. Figure 11-4.

An alternative representation of the deformation zone model is to include only high and medium confidence deformation zones that exist within the local model area, cf. Figure 11-4. These are deformation zones where evidence through direct observations, strong seismic or geophysical profile anomalies emphasise their existence. Deformation zones with lower confidence may exist, but are in this case not treated as part of the deterministic deformation zone model.

The alternative local scale deformation zone model includes thirty-two (N=32) high confidence zones which have at least some part originating from within the local model area and the corresponding intermediate confidence zones. This alternative model contains all high confidence zones presented for the base case model with the exception of zones ZSMNE010A, ZSMNE011A and ZSMNW933A, which all fall outside the local scale model area. In addition, the alternative model contains thirty-four (N=34) medium confidence zones.

A description of deformation zones, in order of their assumed importance and according to the current understanding, is found in Section 5.4.

The dominant zones ZSMNE005A and ZSMNE004A form the tectonic belt between the Laxemar subarea in the west and Simpevarp subarea in the east. The Simpevarp peninsula is dominated by these NE trending shear zones which also can be found along the shorelines of the Simpevarp peninsula and the Ävrö island.

The Laxemar subarea, on the other hand, is more dominated by E-W trending zones, intersected by several N-S trending deformation zones. ZSMNE007A and ZSMNW042A are dominant approximately E-W trending zones in the central and southernmost part of Laxemar, respectively. Both zones are clearly indicated as topographic depressions, through magnetic anomalies and in the results of geophysical profile measurements. Available data indicate that the zones show a complex internal character and are dominated by brittle deformation. Borehole intercepts support their existence, albeit divided into several minor branches. Their internal geometry is inferred to consist of smaller segments which may be interconnected throughout the length of the zones.

Most of the N-S trending zones are currently assumed to exhibit more brittle components, but there is no borehole evidence to support this interpretation at this point.

There are seismic reflections in the Laxemar subarea suggesting at least one gently dipping deformation zone towards the south (ZSMNW928A). A planar geometric model of the strongest reflector results in an intersection in KLX02 which coincides with an identified deformation zone section in the single-hole geological interpretation. However, a more thorough analysis remains with regards to the extent and character of this zone. There are also additional gently dipping reflections of lesser strength in the Laxemar subarea that require additional analysis in the next model version.

A preliminary assessment of the tectonic history suggests that there may have been at least three major events which may have inflicted variation in the state of stress on the zones, and, thus, different sense of movement along the NE, E-W and N-S trending zones.

The uncertainty in the regional deformation zone model is governed by the lineament interpretation, which gives the fundamental surface information for the interpretation of the zones. Since there is considerable uncertainty concerning the interpretation of the geological significance of the lineaments, the 155 deformation zones that are based solely on indirect interpretation of lineaments (and their underlying data) are judged to have a medium to low degree of confidence. The majority of the latter zones are found in the western part of the local model area and in the regional scale model area.

An alternative study of lineaments has been conducted by an independent team using the same underlying topographic and airborne geophysical data /Korhonen et al. 2005/ which shows that there are few deviations from this lineament interpretation and the resulting lineament map used in the current model version. This preliminary assessment adds confidence that the lineament map in itself is rather stable, i.e. linear anomalies in the underlying data have been interpreted in a similar way by two independent teams.

Uncertainties also depend on the almost complete lack of subsurface information outside the local scale model area. Since all investigations during the complete site investigation will be focused to the local model area, these uncertainties are likely to remain throughout the site investigation.

As there are limited amounts of subsurface data, there remain considerable uncertainties concerning the extension at depth of all interpreted deformation zones. It is assumed that zones extend as deep as their interpreted surface extension, although there are limited possibilities to check this assumption at present. Borehole intersections are relatively few in each deformation zone and are mainly used to confirm the existence and indicate the orientation and geological character of selected zones. Even though deformation zones have been verified at a certain depth, the detailed geometrical relationships such as termination and connectivity are still considered uncertain for most deformation zones. This uncertainty is likely to persist throughout the site investigation programme, especially in the regional scale model area.

11.2.3 Statistical model of fractures and deformation zones

Discrete fracture network parameters are calculated through a series of steps, each of which depend on the results of the preceding steps. Fracture set identification and definition is the first necessary step in constructing the geological DFN model; each set may have a different ensemble of parameters that may be highly variable between sets. In addition, the formation of a set or a group of sets reflect the mechanics of fracture formation, including stress state, strain, and rock strength of the lithologies in the local scale model area.

The geometrical description of each set includes:

- Set orientation distribution, expressed as the trend and plunge of a mean pole calculated from all members of the set and its dispersion around the mean.
- Fracture set size expressed as a size-frequency radius distribution, honouring one or more of the following probability distribution functions: lognormal, exponential or power law. Though not explicitly part of the radius distributions, suggested maximum and minimum size truncations are also included. These truncation values have an impact on fracture intensity in any DFN model implementation.
- Fracture set intensity. These are generally specified as P_{32} values, which represent the amount of fracture surface area (m^2) per unit volume (m^3) of rock.
- Fracture spatial model. The spatial model controls the spatial distribution of fractures within the model volume.

The derivation of fracture orientations reveals five sets; three regional sets (S_A, S_B, S_C) observable both in outcrop and in deformation zone traces, and two local sets in each subarea (S_d and S_f or S_e in Laxemar and Simpevarp subareas, respectively).

The variation in local fracture orientations suggests, together with results from the deformation zone model, that the Simpevarp subarea is located within a belt of shear zones and exhibits significantly different fracture behaviour from that of the Laxemar subarea which is set in a more

tectonically stable environment. A limited analysis of borehole fracture orientation data suggests that, like intensity, fracture set orientations are not static functions and vary significantly with depth.

Fracture size analysis shows that regional fracture sets can be approximated by power-law size models. Local fracture sets are censored by the outcrop size such that lognormal and exponential size distribution models have better statistical fit.

Fracture intensity is highly variable across both the Laxemar and Simpevarp subareas, and appears to be subject to a number of different geological controls. These appear to include lithology, rock domain, fracture age, degree of alteration, and presence of ductile or brittle deformation zones. The current level of understanding may be inadequate to characterise fracture intensity controls at either a regional scale or a local scale. Of particular concern are changes in intensity at depth, especially where anomalies in intensity are noted and no corresponding deformation zone has been identified.

Analysis of the fracture spatial distributions show that fracturing is distributed homogeneously in space at scales ranging from around 30 to at least 100 m.

Fracture intensity can be matched simultaneously to deformation zone, outcrop and borehole intensity by finding a unique pair of the power-law radius exponent and minimum radius for each regional fracture set (see Section 5.5.2).

Fracture intensity for local sets cannot be constrained the same way and has to be derived from borehole P_{10} using outcrop size models. Verification exercises show that outcrop and borehole intensity of local fracture sets cannot currently be matched simultaneously (see Section 5.5.3).

There are several alternative geological DFN models embedded in the overall Laxemar 1.2 geological DFN model;

- Different fracture orientation and size models are used for the subareas Simpevarp and Laxemar, based on the interpreted influence of the tectonic situation in the Simpevarp peninsula.
- Different fracture intensity models are employed for different rock domains. Currently there are stable fracture intensity models for rock domains A and B based on available borehole data.
- Different spatial models depending on the size of the model volume.

These three model alternatives can be combined in several ways to provide both local and regional scale DFN model input, in both subareas and for several types of rock domains. The models, as discussed above, are based on the same concept but show different aspects of orientation, size and intensity. Should the downstream user require a DFN model in an area where no “hard” data are available, he or she has the option to combine the provided alternative models in different ways depending on the usage, see also Section 5.5.4.

11.3 Rock mechanics description

11.3.1 Mechanical properties

The mechanical properties are described separately for intact rock, single fractures and for rock mass in the different lithological domains and in deformation zones. A detailed description is found in Chapter 6 and a summary is given in the following sections.

Intact rock

The description for each parameter is provided as a truncated normal distribution function for the three main rock types occurring in the local model area. The mean uniaxial compressive strength (UCS) is expected to be 195 MPa for the Ävrö granite (i.e. granite to quartz monzodiorite), 165 MPa for quartz-monzonite to monzodiorite, and 210 MPa for the fine-grained dioritoid. The spread in the compressive strength is fairly large. The standard deviation is 20, 30 and 50 MPa, respectively, for these three rock types. The crack initiation strength is about 47–50% of the UCS.

The mean value for the Young’s modulus varies slightly between rock types, from 70 GPa for the Ävrö granite to 85 GPa for the fine-grained dioritoid. The standard deviation for Young’s modulus is 5–10 GPa.

For the Poisson's ratio, tensile strength and estimated Mohr-Coulomb strength parameters refer to Table 6-5.

Single fractures

The single fracture mechanical properties are described by the Mohr-Coulomb fracture model, using the parameters peak friction angle and cohesion. The available data have not revealed any clear differences between different sets of fractures, and the current description therefore applies to all fractures. The mean friction angle is estimated to be 37° with a standard deviation of 3°. The cohesion is described as a function of the friction angle, giving a mean value of 0.8 MPa. The dilation angle of single fractures is estimated as 4° at depth.

The fracture samples tested show high normal stiffness, in the range from 150 to 310 MPa/mm with a mean value of 220 MPa/mm (defined as a secant stiffness between 0.5 and 10 MPa normal stress). The shear stiffness is about 40 MPa/mm (for more details cf. Table 6-6). However, the uncertainty in the stiffness determination is regarded fairly large since laboratory tests on fractures are difficult to perform.

Rock mass equivalent properties

For repository design and safety assessment it will be necessary to study the rock mechanics effects at both large and small scales. On the large scale, the bedrock is commonly regarded as a continuous material, even though it consists of intact rock and fractures. Equivalent continuum material properties were estimated as a part of the description of the rock mass and the rock in deformation zones.

The resulting model parameters are given as truncated normal distributions, as for the intact rock. Both the deformation modulus and the Poisson's ratio should be estimated with respect to the stress conditions, as they are stress-dependent parameters. However, above 10 MPa confining stress (σ_3), the parameters are considered constant in this descriptive model.

The mean for the deformation modulus, at depth, is 55–61 GPa in the Laxemar Subarea (rock mass in domains A, D and M). The spread in all rock mass model parameters is fairly large, due to the expected variation in fracturing, and the total range (min and max truncations) for the deformation modulus, at depth, range from 36 to 81 GPa (rock mass in domains A, D and M). In the deformation zones, the deformation modulus is expected to be lower, having a mean of 26–55 GPa.

The uncertainty in the model is quantified by providing a span within which the actual mean value for each parameter is expected to lie. The uncertainty for the deformation modulus is ± 2 –4 GPa in the rock mass outside deformation zones.

The commonly used Mohr-Coulomb material model was chosen for the strength description. (Refer to Section 6.3.2 for the definition of parameters used). The mean friction angle is fairly similar in rock mass in all domains, 42°–47°, and lower, 39°–42° in the deformation zones. The estimated apparent mean cohesion varies from 13 to 17 MPa.

Further details of all the model parameters are given in Table 6-7 and 6-8.

11.3.2 In situ stress conditions

For the description of the stresses the local model area has been divided into two “stress domains”. In Domain II, which consists of two wedge shaped volumes at Ävrö in the Simpevarp subarea and one in the northern part of the Laxemar subarea (see Figure 6-19), the maximum principal stress is expected to be lower than in the surrounding rock mass, attributed to an interpreted stress relief related to wedge-formed rock volumes formed by intersecting deformation zones, allowing the wedged block to move freely upwards.

The stress magnitude is described as a linear function with depth. At 500 m depth, the stress model in Domain I gives a mean value for the maximum principal stress in the span 24–44 MPa. In Domain II, the mean is expected in the span 11–21 MPa. The uncertainty is mainly explained by lack of measurement data.

The modelled mean orientation of the maximum horizontal stress is 132° (i.e. NW-SE), in the whole local model volume, which corresponds to the expected global stress direction from plate movements. However, both the trend and dip of stresses may vary locally, in particular in the vicinity of deformation zones.

The complete set of stress model parameters, including qualitative estimations of uncertainty and local variation, are given in Tables 6-9 to 6-12.

11.4 Bedrock thermal properties

In situ temperature

In situ temperature has been measured in five boreholes. The temperature has been logged on different occasions in one of them. The mean of all temperature loggings at 500 m depth is 13.9°C, see Table 7-10. Temperature vs. depth is presented in Table 7-10. Temperature loggings from different boreholes show a variation in temperature at a specified depth which indicates an uncertainty in temperature logging results. Possible sources of uncertainty are errors in logging procedure, timing of the logging after drilling and water movements along the boreholes.

Thermal properties

Thermal conductivity was modelled for five rock domains with different modelling approaches. Results indicate that the mean thermal conductivity is expected to exhibit variation between the different domains, from 2.45 W/(m×K) to 2.87 W/(m×K) (Table 7-17). The standard deviation varies according to the scale considered. The lower 2.5 percentile is within the range 2.2–2.44 W/(m×K) for all five domains (Table 7-17). The spatial variation is considered to be large, especially for domains RSMA and RSMBA.

The temperature dependence is rather small with a mean decrease in thermal conductivity of 1–5% per 100°C increase in temperature for dominant rock types. The dominant rock types are assumed to have isotropic thermal properties, but this has not been investigated. There is also possibly anisotropy in a larger scale caused by the orientations of subordinate rock types.

There are a number of important uncertainties associated with these results. The primary uncertainties at the data level apply to thermal conductivity calculations from mineralogy (SCA method), and calculations based on density measurements. In addition, the representativeness of rock samples is uncertain, as is the representativeness of the boreholes for the domains. Further, there are uncertainties associated with the methodology of upscaling the thermal conductivity.

In general, there are no large differences between the modelled thermal conductivity for the two domains common to both Laxemar 1.2 and Simpevarp 1.2 (Table 7-18). However, for domain RSMD, the variability is estimated to be smaller in Laxemar 1.2.

The mean heat capacity for the different domains ranges between 2.23–2.29 MJ/(m×K) with the 2.5 and 97.5 percentiles at 2 and 2.5 MJ/(m×K) respectively (Table 7-15). Heat capacity exhibits rather large temperature dependence. For the dominating rock types the increase in heat capacity is approximately 25% per 100°C temperature increase (Table 7-8).

The mean coefficient of thermal expansion was determined between 6×10^{-6} – 8×10^{-6} m/(m×K) for three dominating rock types (Table 7-9)

11.5 Bedrock hydrogeological description

The geometrical entities of the bedrock hydrogeological model consist of deformation zones (Hydraulic Conductor Domains) and the rock mass between deformation zones (Hydraulic Rock Domains). Properties of these entities and the overburden (Hydraulic Soil Domains) are essential parts of the site-descriptive model and constitute the basis for the regional groundwater flow model-

ling that, in turn, provides important information for the interpretation of evolving hydrogeochemistry and assessment of transport paths to and from a potential repository site. The parameterisation of the hydrogeological model is also important for assessment of bedrock transport properties and for subsequent analysis by Repository Engineering and Safety Assessment.

The geological models provide important information (rock domains, deformation zones and geological DFN) for the hydrogeological description and modelling. Measured hydrogeochemical data are essential for testing the regional scale groundwater flow models.

The current model version model is mainly focussed on the Laxemar subarea, but since the regional groundwater flow model is important for the hydrogeological description, substantial work has been invested to parameterise the entire regional model volume, although primary data mainly cover the local scale model domain. Chapter 8 and Section 9.7 provide an extensive review of the hydrogeological borehole data, identification and parameterisation of hydrogeological domains, and a resulting regional groundwater flow model, and the modelled present-day spatial distributions of important hydrogeochemical constituents. Information on overburden, hydrological and meteorological characteristics used in the modelling is discussed in Chapter 4.

11.5.1 Hydraulic properties

The properties of the hydraulic rock domains are treated in an implicit fashion by transferring a stochastic (fracture) network simulation of fractures and minor deformation zones to an equivalent porous medium representation (EPM). The hydraulic conductor domains are based on the deterministically defined deformation zones in the geological model. Hydraulic rock domains are largely based on rock domains defined in the geological model, but some geological rock domains have been merged into a unified single hydraulic rock domain, on the basis of similarities in hydraulic material properties.

Hydraulic conductor domains

General description

The hydraulic conductor domains in the hydrogeological model are based on the version Laxemar 1.2 regional scale structural model, see Figure 11-4 (The deformation zone model is presented in Section 5.4). Some of the zones in the regional scale model are interpreted as high-confidence zones (concerning their existence) and several of them have been also hydraulically tested. However, most hydraulic conductor domains have been attributed hydraulic properties which are to be regarded as uncertain.

Intersections with boreholes are identified for 25 of all the deformation zones, where also hydraulic test data are available. Some of these deformation zones have more than one borehole intercepts, providing several transmissivity estimates for a single deformation zone. The range of the interpreted geometric mean transmissivity (T) for these hydraulic conductor domains is $4E-9$ to $2.2E-4$ m^2/s . The geometric mean transmissivity based on all tested hydraulic conductor domains is $T=1.2E-5$ m^2/s . For individual hydraulic conductor domains with several hydraulic tests the standard deviation $\text{Log}_{10}T$ is generally between 1 and 3. The calculated geometric mean T for all hydraulic conductor domains was assigned to all remaining hydraulic rock domains in the regional scale model, regardless of their size, geological genesis and assigned confidence level. This may have overestimated the significance, in terms of transmissivity, of certain deformation zones, particularly those attributed low confidence of existence

Analysis of the data from individual measurements of transmissivity of the hydraulic conductor domains indicates that there is an indication of a decreasing transmissivity with depth. However, the observations below 300 m depth are few and confidence ranges for calculated geometric mean transmissivity indicate that the depth trend may be insignificant, cf. Figure 8-15.

The hydraulic thickness of the hydraulic conductor domains is based on the geological interpretation of zone thickness made for the regional scale structural model version Laxemar 1.2.

Reference case properties of the regional groundwater flow model

The reference case in the regional modelling /Hartley et al. 2006/ incorporated the depth dependence as a step function with elevation intervals (0 to –300 m above sea level, –300 m to –600 m above sea level and –600 m above sea level to model bottom). The calibration of the regional groundwater flow model entailed modification of the transmissivity of the hydraulic conductor domains where the measured transmissivities based on 100 m PSS data in KLX01 through KLX006, KSH01A through KSH03A, KAV04A, and KAV01 (KAV01: based on sum of 10 m tests to 100 m), were used to assign transmissivity values representative of at the corresponding depth interval as horizontal bands in the hydraulic conductor domains. The latter values were superimposed on the depth trend.

An alternative model representation, where deformation zones with low confidence are excluded, was also modelled. Removal of the latter zones was shown to have small impact on the calibration of hydrogeochemistry, when compared with the reference case with all deformation zones included.

Hydraulic rock domains

General description

A comparison shows that the evaluated geometric mean hydraulic conductivity (K) in hydraulic conductor domains is about 10 times higher than the corresponding mean of hydraulic rock domains, see Figure 8-17.

There seem to be a significant depth trend in the hydraulic conductivity of hydraulic rock domains, at least between 0–200 m depth and below 400 m depth, see Figure 8-17.

PFL-f data indicates anisotropic conditions, with the highest conductivity in the direction c. NW in the Laxemar subarea.

The hydraulic conductivity (K) of the rock domains differs. Rock domain A at Ävrö and southern part of Äspö appears more conductive than the corresponding domain A in the Laxemar subarea. The hydraulic rock domains with more basic rock types, B, C, D, (and probably E – not data available), and M are less conductive than domain A (5–20 times lower), but some samples from a single rock domain are in the latter small and sometimes just from one borehole, see Table 8-18. The Göttemar granite, and possibly also the Uthammar granite (no data available), the latter with the same origin as the Göttemar granite, as well as large bodies of fine-grained granite (no data of the modelled rock domain but data from smaller volumes of fine-grained granite) are probably an order of magnitude more conductive than the Ävrö granite (rock domain A), see Section 8.4.3.

Hydraulic DFN model

The hydraulic DFN model employed in the current analysis is based on a version of the developed version Laxemar 1.2 geological DFN model that has been modified to match both fracture data (open fractures) and the hydraulic test data.

The working hypothesis embedded in the hydraulic DFN model employed for SDM Laxemar 1.2 is that it relates an inferred power-law fracture size distribution (up to the size of local minor fracture zones) to hydraulic properties by assuming that transmissivity is dependent size through a power-law relationship (correlated and semi-correlated, and uncorrelated).

Alternative geometric models and different transmissivity models for fractures (hydraulic features) resulted in a number of alternative hydraulic DFN models that all match the measured data, see Tables 8-19 through 8-24, representing the *Hydro DFN base case* and the variant; *HydroDFN regional case*. The semi-correlated model appears to fit the data slightly better than the other models according to /Hartley et al. 2006/. DarcyTools team only examined the correlated model.

Mean properties of rock blocks

The *Hydro DFN base case* was used to estimate the hydraulic conductivity distribution of 20 and 100 m blocks, see Section 8.4.5. The mean $\text{Log}_{10}(K)$ for blocks of size of 20 and 100 m, excluding deterministic deformation zones and below elevation –300 m above sea level, were estimated at: $\text{Log}_{10}(K (20 \text{ m})) = -10.3$ to -7.9 and $\text{Log}_{10}(K (100 \text{ m})) = -9.4$ to -7.8 , depending on rock domain, see Tables 8-25 and 8-26.

Reference case properties of the regional groundwater flow model

Generally, the hydraulic feature sizes in hydraulic DFN model implemented in the regional groundwater flow simulations are within the range 25–1,000 m.

The regional flow modelling made by /Hartley et al. 2006/, using measured hydrochemistry data for calibration, suggests that some parameter settings related to the hydraulic rock domains are more reasonable when matching to measured data, than others. This case is denoted the Reference case. Hydraulic DFN models were also developed for different smaller regions representing four different hydraulic rock domains for the reference case, all incorporating a depth dependency as a step function of elevation (0 to –200 m above sea level, –200 to –600 m above sea level and –600 m above sea level to the model bottom). The *Hydro DFN base case*, with semi-correlated model, was modified to what is called the *Hydro DFN regional case* by decreasing the transmissivity of fractures sets A and B (steeply dipping fractures with strike ENE to NNE) by a factor 10. The kinematic porosity of the hydraulic rock domains is based on upscaled values from the hydraulic DFN model using minima of $1E-4$ above elevation –200 m above sea level and $1E-5$ below elevation –200 m above sea level.

11.5.2 Groundwater flow pattern

Flow distribution

The level of the top boundary conditions, as a head boundary, appears to control much of the flow pattern and the amount of hydrochemical components earlier intruded and still present (according to measurements) in the upper part of the rock mass.

At depth, the salinity field decreases the magnitude of the flow rates considerably and hence groundwater fluxes near the ground surface are much higher than those at depth. At –1,000 m above sea level, flow rates are of very low magnitude. Near the surface, at –10 m above sea level and –100 m above sea level, the vertical flow component is mainly oriented downwards (recharge) amounting to around 0.1 to 0.01 m/year. The flow field near the surface is very heterogeneous indicating development of local flow cells. At –500 m above sea level, the flow rates are generally around 0.01–0.0001 m/year, both in recharge and discharge areas. At –1,000 m above sea level the flow rates are generally less than 0.0001 m/year.

Discharge areas are located in the extreme east, associated with the Baltic Sea and onshore discharge areas, the latter mainly in conjunction with deformation zones. The Darcy velocity in the deformation zones is around 0.1 m/year.

The results of the groundwater flow simulations undertaken suggest that the Laxemar subarea and Simpevarp subarea are predominantly subjected to recharging flow conditions at –500 m above sea level. However, the Darcy flow rates at –500 m above sea level at the Simpevarp subarea are lower than for Laxemar subarea at corresponding elevation. However, it should be remembered that these inferences are based on modelling employing present-day boundary conditions, not a transient simulation with an assumed future shore displacement function and releasing particles at present.

Flow paths

Based on the present day boundary conditions, the flow paths from release areas located within the Laxemar and Simpevarp subareas at –500 m above sea level were simulated. It was found that the released particles rapidly reach a deformation zone and subsequently follow the system of deformation zones to discharge points below the Baltic Sea, or the large valleys. The discharge points for release in the Laxemar subarea are located mainly in the large valleys in the northern and southern parts of Laxemar and around the shoreline, especially south of Äspö island. The discharge points for particles released in the Simpevarp subarea are, as expected, found north of the island of Hälö and mainly along the shore of the Simpevarp peninsula.

11.6 Bedrock hydrogeochemical description

The results of the hydrogeochemical modelling, as described in Chapter 9, have been used to produce a hydrogeochemical site descriptive model. This conceptual hydrochemical model of the site incorporates and summarises most of the important findings relevant to the distribution of chemical elements. The approach to construct the conceptual model is described in /SKB 2006a and Appendix 1 therein/. Based on existing geological and hydrogeological information and in collaboration with the site hydrogeologists and geologists, schematic manual versions of transects were produced to facilitate illustration of the most important structures/deformation zones and their potential hydraulic impact on the groundwater flow. This hydraulic information was then integrated with the results of the hydrogeochemical evaluation and modelling results to show the vertical and lateral changes in the groundwater chemistry.

The marked differences in the groundwater flow regimes between the Laxemar and Simpevarp subareas are reflected in the groundwater chemistry. Figure 11-7 shows, along the main WNW-ESE transect, the four major recognised groups of groundwaters and their interpreted spatial extents, denoted by A–D. The ‘B’ type groundwaters are subdivided into ‘B_L’ and ‘B_S’ types referring to Laxemar and Simpevarp, respectively.

Figure 11-8 is oriented perpendicular to the main groundwater flow direction which is indicated by the encircled black dots. Only KLX03 has sufficient data (with some data from KLX04) to give a good estimation of the depth extent of the various groundwater types A–D, and only B_L groundwaters are present where the transect is contained within the Laxemar subarea.

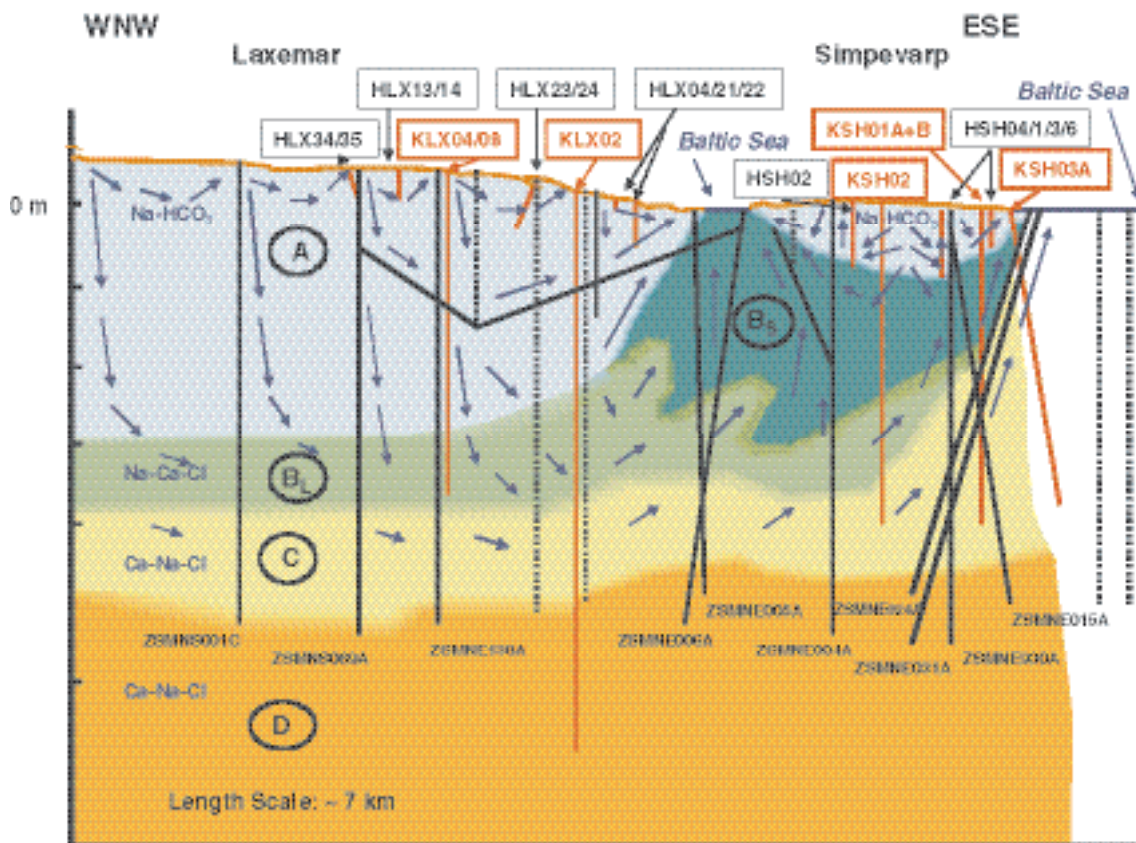


Figure 11-7. Schematic 2-D visualisation along the WNW-ESE transect integrating the major structures, the major groundwater flow directions and the variation in groundwater chemistry from the sampled boreholes. Sampled borehole sections are indicated in red, major structures are indicated in black (full lines = confident; dashed lines = less confident), and the major groundwater types A–D are also indicated. The blue arrows are estimated groundwater flow directions.

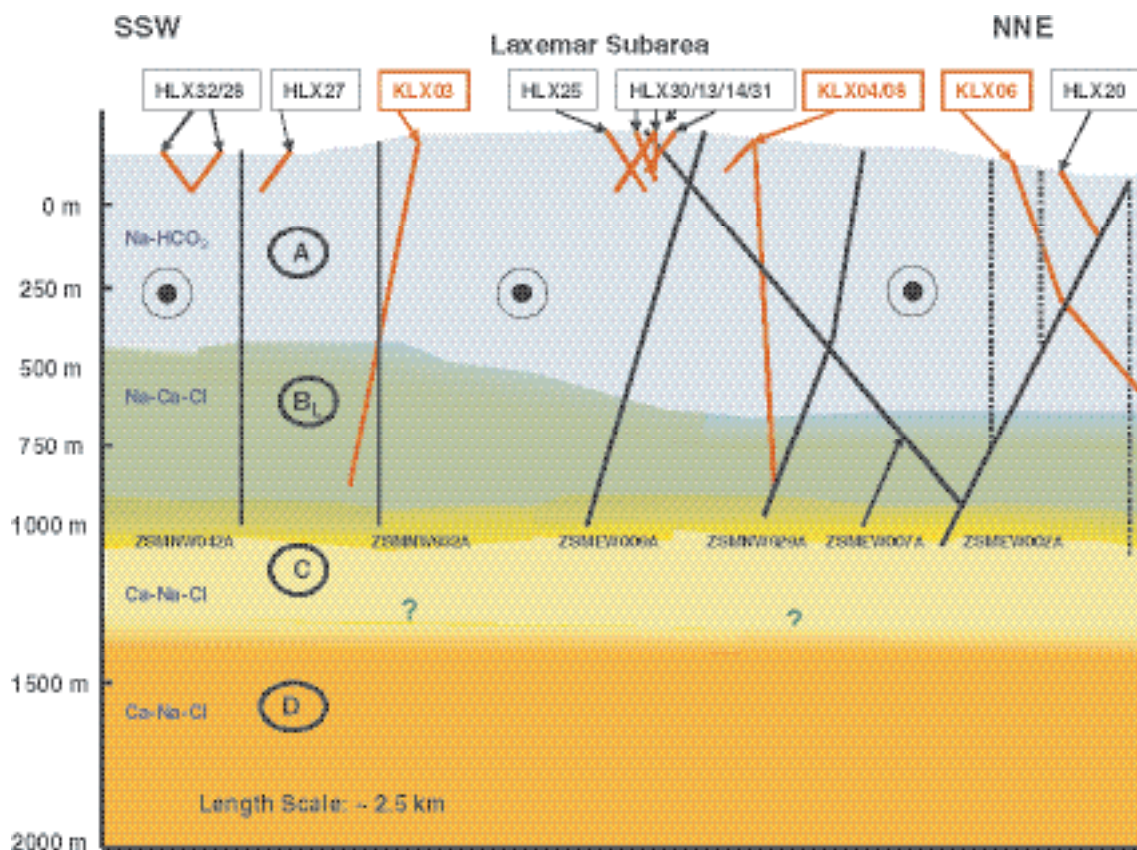


Figure 11-8. Schematic 2-D model along the SSW-NNE transect integrating the major structures, the major groundwater flow directions and the variation in groundwater chemistry from the sampled boreholes. Sampled borehole sections are indicated in red, major structures are indicated in black (full lines = confident; dashed lines = less confident), and the major groundwater types A–D are also indicated. The encircled black dot symbol indicates the dominant horizontal to subhorizontal groundwater flow direction is out from the page, that is in a easterly direction.

11.6.1 Summary of groundwater types

The general features of the four identified groundwater types, in terms of approximate depth, chemistry, major reactions and main mixing processes, are summarised below.

Type A – shallow (< 200 m) at Simpevarp but deeper (down to ~ 800 m) in the Laxemar subarea

Dilute groundwater (< 2,000 mg/L Cl; 0.5–3.5 g/L TDS); $\delta = -11$ to -8% SMOW.

Mainly meteoric and Na-HCO₃ in type.

Redox: Marginally oxidising close to the surface, otherwise reducing.

Main reactions: Weathering; ion exchange (Ca, Mg); dissolution/precipitation of calcite; redox reactions (e.g. precipitation of Fe-oxyhydroxides); microbially mediated reactions (SRB) which may lead to formation of pyrite.

Mixing processes: Mainly meteoric recharge water in the Laxemar subarea; potential mixing of recharge meteoric water and a modern sea component at Simpevarp subarea; localised mixing of meteoric water with deeper saline groundwaters in the Laxemar and Simpevarp subareas.

Type B – shallow to intermediate (150–600 m) at Simpevarp but deeper (down to ~ 500–950 m) in the Laxemar subarea

Brackish groundwater (2,000–10,000 mg/L Cl; 3.5–18.5 g/L TDS); $\delta = -14$ to -11% SMOW.

B_L – Laxemar subarea: Meteoric, mainly Na-Ca-Cl in type; Glacial/Deep saline components.

B_S – Simpevarp subarea: Meteoric mainly Na-Ca-Cl in type but some Na-Ca(Mg)-Cl(Br) types (\pm marine, e.g. Littorina); Glacial/Deep saline components.

Redox: Reducing.

Main reactions: Ion exchange (Ca, Mg); precipitation of calcite; redox reactions (e.g. precipitation of pyrite).

Mixing processes: Potential residual Littorina Sea (old marine) component at Simpevarp, more evident in some fracture zones close to or under the Baltic Sea; potential glacial component in Simpevarp and Laxemar subareas; potential deep saline (non-marine) component in Simpevarp and Laxemar subareas.

Type C – intermediate to deep (~ 600–1,200 m) at Simpevarp but deeper (900–1,200 m) at Laxemar subarea

Saline (10,000–20,000 mg/L Cl; 18.5–30 g/L TDS); $\delta = \sim -13\%$ SMOW (NB. few data).

Dominantly Ca-Na-Cl in type at Laxemar but Na-Ca-Cl changing to Ca-Na-Cl only at the highest salinity levels in the Simpevarp subarea; increasingly enhanced Br/Cl ratio and SO₄ content with depth in both Simpevarp and Laxemar subareas; Glacial/Deep saline mixtures.

Redox: Reducing.

Main reactions: Ion exchange (Ca).

Mixing processes: Potential glacial component in the Simpevarp and Laxemar subareas; potential deep saline (i.e. non-marine) and an old marine component (Littorina?) at shallower levels in the Simpevarp subarea; Deep saline (non-marine) component in the Laxemar subarea.

Type D – deep (> 1,200 m) only identified in the Laxemar subarea

Highly saline (> 20 000 mg/L Cl; to a maximum of ~ 70 g/L TDS); $\delta = > -10\%$ SMOW.

Dominantly Ca-Na-Cl with higher Br: Cl ratios and a stable isotope composition that deviates from the GMWL when compared to Type C groundwaters; Deep saline/brine mixture; Diffusion dominant transport process.

Redox: Reducing.

Main reactions: Water/rock reactions under long residence times.

Mixing processes: Probably long term mixing of deeper, non-marine saline component driven by diffusion.

Compared with the Simpevarp 1.2 visualisation /Laaksoharju 2005/ one of the major differences is the extent of the brackish 'B' type groundwaters, especially in the Simpevarp subarea. This is in part due to the absence of borehole KLX01, omitted because: a) it is located too far from the transects to be satisfactorily projected, and b) it has a marine component which makes it more representative for the NE 'close to the Baltic Sea' part of the Laxemar subarea but anomalous in the 'total' Laxemar subarea context. The 'B' type groundwaters in the Laxemar subarea therefore become meteoric and brackish, containing a mixture of glacial/deep saline groundwaters but devoid of an old marine (i.e. Littorina) component. They are referred to as 'B_L' type groundwaters. In the Simpevarp subarea the 'B' type groundwaters differ in that there is a weak but significant component of Littorina present,

and these are referred to as ‘B_S’ type groundwaters. As indicated in Figure 11-7, the B_L groundwaters are continuously fed into the Simpevarp subarea at depth, mixing with the B_S groundwaters and gradually discharging to shallower levels.

11.6.2 Comparison between modelled and measured geochemistry

The regional groundwater flow modelling reported in Section 8.5 and summarised in Section 11.5.2 also involved modelling of water types, as reported in Section 9.7. This section highlights some main results.

The modelled distribution of salinity (TDS) shown in Section 9.7 corresponds well with the general patterns indicated in Figure 11-7 and Figure 11-8 the characteristics of water types A–D measured in boreholes. However, there is potentially too much flushing of Brine in the regional scale reference case, suggesting that the calibration could benefit from a decreased hydraulic conductivity at depth.

The reference waters were also modelled, and the modelled distribution of Glacial water and Littorina water is of special interest. The modelling results suggest the possibility that the Littorina water type may be present near the coast and below the Baltic Sea, mainly in the depth range –100 to –600 m above sea level and, furthermore, that the water chemistry may be quite heterogeneous, see Figure 11-9. Possibly, the Glacial water type may be found in “pockets” and in larger quantities near and below the Baltic sea, mainly in the depth range –300 to –1,200 m above sea level, cf. Figure 11-9. This heterogeneity in distribution of water types is attributed to an underlying heterogeneity in the distribution of the hydraulic properties.

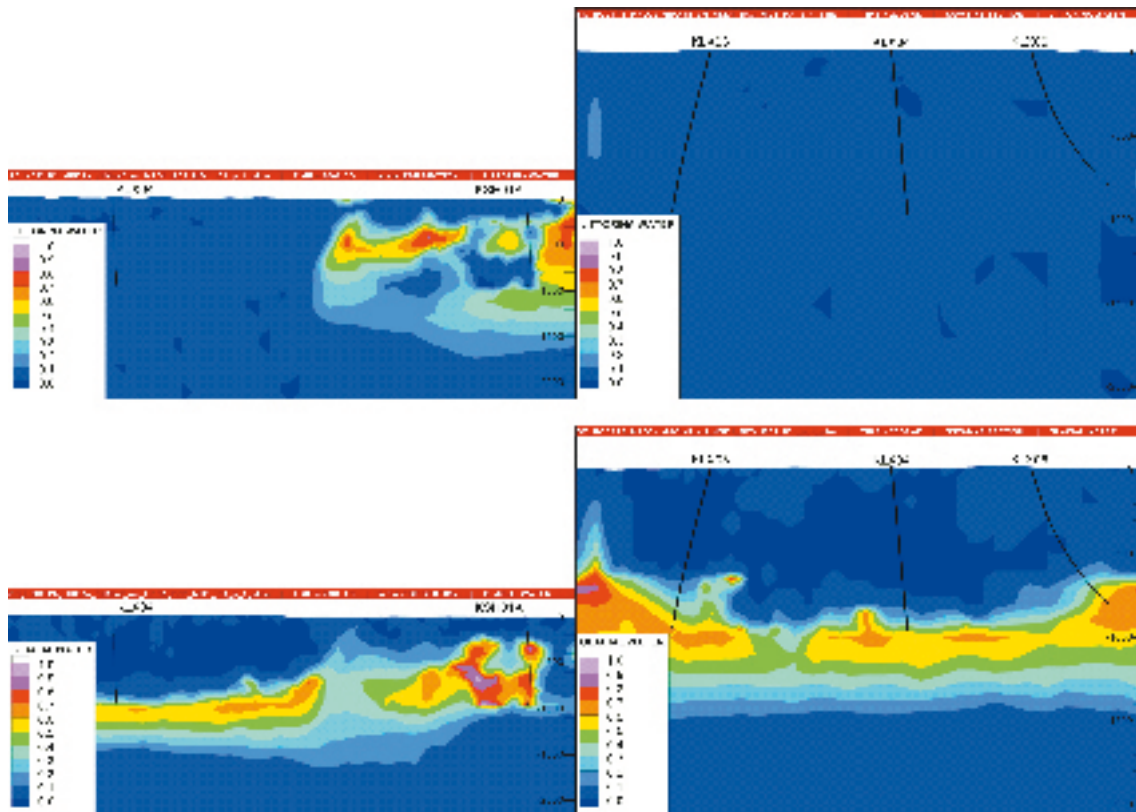


Figure 11-9. Vertical sections along the WNW-ESE (left column) and SSW-NNE (right column) transects (corresponding to those shown in Figure 11-7 and Figure 11-8, respectively), showing the present-day distribution of the reference waters Littorina (top) and Glacial water (bottom), for the regional reference case (see Section 9.7).

11.7 Bedrock transport properties

As described in Chapter 10, measurement data from the laboratory programme have been used to parameterise a *retardation model* that considers the transport properties of the major rock domains, as well as the properties of defined fracture types, with focus on the Laxemar subarea. The retardation model for rock domains considers the properties of the unaltered intact rock matrix, whereas that for fracture types additionally considers the material properties of alteration zones of various kinds and extents within the wall rock adjacent to fracture flow paths. No attempt has been made to parameterise local minor and local major deformation zones owing to a lack of hard data for these structures. These, however, are not currently considered to contribute substantially to the overall transport resistance. A major improvement in the current site descriptive model is the inclusion of sorption data for a larger set of nuclides, representing a wider range of sorption properties, than was available for the previous model version.

At present preliminary sorption measurement data exists only for Ävrö granite taken from a single location in borehole KLX03A. Many of these data are of a provisional nature owing to the long times required for laboratory characterisation of the samples. The preliminary sorption data are based on a rock-solute contact time of one month for the radionuclides of Cs(I), Sr(II), Ni(II), Ra(II), and three months for Am(III). Final sorption measurements will not be made until after six months contact time. Depending on the thickness of the sample, through-diffusion experiments also typically require three to six months contact time in order to obtain useful estimates of effective diffusivity using a non-sorbing tracer (tritiated water).

Owing to the long lag time between drill core sampling and final laboratory determination of sorption and diffusion properties and the initial lack of hard data for materials property parameterisation, it has therefore not been possible to strictly adhere to the data freeze for model version 1.2. Additionally, site specific measurement data for rock types and alteration forms other than Ävrö granite are not presently available.

In the previous model version for Simpevarp 1.2 /SKB 2005a/, data were imported from Äspö HRL studies for analogue rock types. Due to a lack of internal consistency between the measurement data used for unaltered rock and those imported for the altered rock types, the altered layers in the previous model were parameterised with weaker retention properties than those for the unaltered rock matrix. This, however, is now believed to be an artefact of the previous data import. To account for the lack of data for rock types other than Ävrö granite and those for altered rock in the current retention model, data have been extrapolated by assuming the sorptive strength of the rock is linearly correlated with BET-surface area. This is thought to be a more accurate means of extrapolating data for the altered rock layers, and based upon the available data and previous experience from the Äspö HRL it is thought that the alteration layers do, indeed, have stronger retention properties than the unaltered rock matrix.

11.7.1 Effective diffusivities of major rock types

The effective diffusivity assigned to the various rock types in the retardation model is currently based largely upon electrical resistivity measurements carried out in the laboratory. These measurements give effective diffusivities that are larger than those obtained by in situ measurement of electrical resistivity. The differences, however, between in situ and laboratory measurements are not unequivocal when considering the data variance and overall measurement uncertainty. Although in situ measurement data have some uncertainty due to lack of knowledge concerning the true salinity of matrix porewater, at least part of the difference (if a difference indeed exists) could result from effects of tangential stress concentrations around the borehole paired with effects of stress unloading of rock samples in the case of measurements on core specimens.

It is difficult to give a definitive estimation of relative diffusive properties in the current SDM for Laxemar 1.2 as there is a considerable inequality in sample support amongst the different rock types and measurement methods. Based upon the recommended transport parameters in Table 10-4, however, Ävrö granite appears to have the highest effective diffusivity (associated with higher retention) with a formation factor on the order of $F_f \geq 10^{-4}$. Other reported rock types appear to have essentially similar diffusive properties to each other (although with slightly lower formation factors than Ävrö granite) and any relative differences are speculative owing to the inherent data uncertainty. These

observations are both quantitatively and qualitatively consistent with the data previously reported for SDM Simpevarp 1.2 /Byegård et al. 2005, SKB 2005a/.

A particular uncertainty in the current model version is the unknown effective diffusivity of altered Ävrö granite which is assumed to be representative of all altered rock forms in the Laxemar subarea.

11.7.2 Sorption properties of major rock types

Although there are no laboratory determined sorption measurements for other major rock types available at this time, BET surface area measurements indicate that relative sorption strengths (strongest to weakest sorption) should approximately follow the order Fine-grained dioritoid/Fine grained diorite-gabbro > Ävrö granite/diorite to gabbro > quartz monzodiorite. Altered Ävrö granite has a BET-surface area about twice that of the unaltered Ävrö granite. It is difficult to determine an accurate order of relative sorption strengths as it is not strictly robust to compare measured sorption data for Ävrö granite with extrapolated data for the other rock types. Additionally, the order of relative sorption strengths as identified from Table 10-4 (recommended data values) are not the same for different sorbing species. It is noted, for example, that Ävrö granite in contact with non-saline groundwater (GW type I) exhibits the strongest relative sorption for Ni(II) and Ra(II), although the weakest for Cs(I) and Am(III), with Sr(II) appearing somewhere in the middle of the relative order. For saline groundwater (GW type III) Ävrö granite exhibits consistently the weakest sorption for all species except for Sr(II) for which it exhibits the strongest sorption (i.e., if the comparison is based purely upon BET surface area extrapolation).

The relative order of sorptive strength for the various solutes on Ävrö granite in contact with non-saline groundwater (GW Type I) are, in order; Ra(II) > Ni(II) > Cs(I) > Am(III) > Sr(II). The corresponding order for saline groundwater (GW Type III) is, Cs(I) > Ni(II) > Am(III) > Ra(II) > Sr(II).

Although the particular ordering of sorption strengths is somewhat unexpected if only based on cation charge grounds, the results can be rationalised in terms of the relative abundance of $\text{HCO}_3^-/\text{SO}_4^{2-}$ in the Type I and Type III groundwater categories and are therefore in overall agreement with expectations.

While there is much uncertainty in establishing a relative order of sorption strengths amongst the various rock types, it is clear that most solutes sorb more strongly under non-saline conditions than under saline conditions, at least for the groundwater water compositions used in the laboratory measurements. The main exception is Am(III) which appears to be unaffected by different groundwater salinities. It is noted here that this effect is expected on the basis of the known sorption mechanisms for this radionuclide (i.e., it sorbs by way of a surface complexation mechanism which renders it less sensitive to ionic strength variations). The measured sorption K_d for Am(III) is significantly lower than expected. Possible reasons for this are discussed in the background reports /Byegård et al. 2006, Crawford 2006/.

From the recommended data, Cs(I) appears to exhibit the smallest dependency upon salinity with only a very modest increase in sorption strength (a factor of roughly ≤ 2) for K_d in non-saline groundwater relative to saline groundwater. This is also an expected result which is in line with the known sorption characteristics of this radionuclide.

For the other solutes, Sr(II) exhibits the largest increase (a factor of roughly 10–100), whereas Ni(II) and Ra(II) show more modest increases with factors of 6–12 and 20–35, respectively. These differences as mentioned above may be partly due to solution speciation effects involving $\text{HCO}_3^-/\text{SO}_4^{2-}$, although for Sr(II) and Ra(II) they are also related to ionic strength (specifically competition for ion-exchange sorption sites with other cations in solution).

It should be noted that the differences between the rock types are typically very small and, based upon the presently available BET data, are often less than the estimated uncertainty in the sorption data itself. Furthermore, the results for Ävrö granite clearly indicate a strong influence of solution composition. It is noted here that in the ongoing site investigations, this has the potential to mask the possibly smaller differences between the data obtained for different rock types. The proposed order of sorption strengths for different rock types should therefore be treated with utmost caution.

11.7.3 Overall retention properties and migration of solutes along potential flow paths

The previous discussion on diffusion and sorption notwithstanding, given the provisional nature of the retention properties data and the fact that a large proportion of the data are extrapolated on a tentative basis, it is not currently possible to rigorously compare the retention properties of different rock domains, nor draw specific conclusions concerning the differences between rock domains in the Laxemar subarea and those within the Simpevarp subarea.

As described in Chapter 10, the proper means of upscaling parameters for safety assessment purposes is the integration of material properties along a flowpath. For spatial variability in material properties it is expected that the mean parameter variability over large spatial scales will be smaller than that present in the original data (which relates to measurements made on mm- to dm-scale in the laboratory). A large uncertainty in the parameterisation is, of course, related to measurement bias of various kinds. Many of the biases are, however, well known and the experimental programme takes these into account as far as is practically possible at the present time.

As discussed in Chapter 10, the parameterisation of the retardation model for rock types other than Ävrö granite and for all altered rock types is subject to large uncertainties. Based upon scoping calculations presented in the background report by /Crawford 2006/, however, it is expected these uncertainties overall will give a much smaller uncertainty for solute transport than the F-factor owing to its non-linear impact upon solute transport times.

12 Overall confidence assessment

The Site Descriptive Modelling involves uncertainties and it is necessary to assess the confidence in the modelling. Based on the SKB integrated strategy report /Andersson 2003/, and experience gained in version 1.1, procedures (protocols) have been further developed for assessing the overall confidence in the modelling. These protocols concern whether all data are considered and understood, uncertainties and the potential for alternative interpretations, consistency between disciplines, and consistency with understanding of past evolution, as well as comparisons with previous model versions. These protocols have been used in a technical auditing exercise as a part of the overall modelling work. This chapter reports the conclusions reached after that audit.

12.1 How much uncertainty is acceptable?

A site descriptive model will always contain uncertainties, but a complete understanding of the site is not needed. As set out in the geoscientific programme for investigation and evaluation of sites /SKB 2000/, the site investigations should continue until the reliability of the site description has reached such a level that the body of data for safety assessment and repository engineering is sufficient, or until the body of data shows that the site does not satisfy the requirements. Even if the Construction and Detailed Investigation Phase does not imply potential radiological hazards, it would still be required that no essential safety issues remain that could not be solved by local adaptation of layout and design.

12.1.1 Safety assessment needs

The Safety Assessment planning suggests that only certain site properties are really important for assessing safety. These are:

- the intensity and size distribution of deformation zones and fractures within the potential repository volume,
- whether there is ore potential,
- the intact rock strength relative to the in situ stress state and coefficient of thermal expansion within the potential repository volume,
- the rock thermal conductivity within the potential repository volume,
- the distribution of hydraulic conductivity (or the transmissivity distribution of the DFN-model) in the repository volume,
- the spatial distribution of the hydraulically connected features to the extent that it allows assessment of the transport resistance along potential migration paths,
- the chemical composition of the groundwater, especially absence of dissolved oxygen and TDS levels below 100 g/L, at repository depth,
- the distribution of transport resistance, and
- the porosity, diffusivity and sorption properties of the rock matrix.

Generally, these properties are connected to the preferences and requirements already stated in /Andersson et al. 2000a/. Consequently, there is a need to ensure that the site modelling is able to produce qualified uncertainty estimates of these properties.

Furthermore, it is necessary to develop sufficient *understanding* of the processes and mechanisms governing the general evolution of the site. Such understanding would aid in addressing questions such as whether there can be fast flow paths due to channelling, what is the source of the brine at depth, what is the impact of rock stresses on available sorption surfaces in the rock, do we understand the impact of the mixing processes during the chemical sampling etc. However, full

understanding of all aspects of a site is neither attainable nor needed. For example, some properties, like thermal conductivity or rock matrix diffusivity, could show a high variability on the local scale, but the impact on performance, i.e. heat flow or resulting retention, depends on larger scale averages. Thus, seemingly large variability will not have much impact in such cases and it is not necessary to determine the details of the small scale variation.

12.1.2 Repository engineering needs

For Repository Engineering, there are essentially three design issues to be addressed during the Site Investigation phase:

- Is there enough space?
- How could the layout be adapted with respect to mechanical stability and water inflow and how would such adaptation affect the degree of utilisation?
- Are critical tunnel locations (e.g. of problematic deformation zones) properly assessed?

The overriding issue of whether there is enough space for the repository may be divided into determining the generally available space and the degree of utilisation within that generally available space. The factors controlling the generally available space are the position and geometry of regional and local major deformation zones. Deposition tunnels must not be placed closer than a certain respect distance from such zones. Working definitions of respect distances exist, but some refinement work is still going on regarding what should be appropriate respect distances, see e.g. /SKB 2004e/.

The repository layout is not only controlled by the regional and local major deformation zones. For example, deposition hole positions connected to large fractures or high inflows will not be used and the thermal rock properties affect the minimum allowable distances between deposition tunnels and deposition holes. During site investigations, this is handled in the design by estimating a “degree of utilisation” for the deposition panels already adjusted to the regional and local major deformation zones. Final selection of deposition holes and tunnels will be made locally, underground, during the construction and detailed investigation phase. Distribution of inflow to the deposition tunnels is an important aspect of the degree of utilisation. Apart from water, other factors affect the degree of utilisation. These include heat conductivity, as noted above, and rock mechanics properties affecting bedrock stability and the potential for rock spalling.

For the engineering planning and selection of the surface access point, it is necessary to identify and characterise potentially difficult tunnel locations (i.e. where the tunnel would pass close to or through deformation zones) in the rock. The information needed will be quite detailed, which means that the site description will be used only to identify potential access locations. At these locations there will later be a need to drill some additional exploration boreholes in order to assess the actual critical passages.

12.1.3 Assessing the importance of the uncertainties

As further discussed by e.g. /Andersson et al. 2004/ there are several planned occasions during the Site Investigation when Safety Assessment will be able to provide organised feedback as regards the sufficiency of the site investigations. The SR-Can project delivered its first interim report in mid 2004 /SKB 2004e/, but the actual assessment will be published in 2006. Preliminary Safety Evaluations of the investigated sites have been made for Simpevarp /SKB 2005a/ and for Forsmark /SKB 2005b/, and will also be made for Laxemar using this site descriptive model as input. Quantitative feedback from Safety Assessment can not be obtained before the Laxemar PSE or SR-Can are completed, but the type of feedback that will be obtained can be assessed in relation to its potential impact on decisions related to the site investigation programme.

The Overall Confidence Assessment presented in this chapter concerns i) whether all data are considered, understood, and what is the accuracy of, and biases in, the data, ii) what are the uncertainties in the models, their causes, potential for alternative interpretations and what further characterisation would reduce uncertainty, iii) consistency between disciplines, iv) consistency with understanding of past evolution, and v) comparison with previous model versions, Figure 12-1.

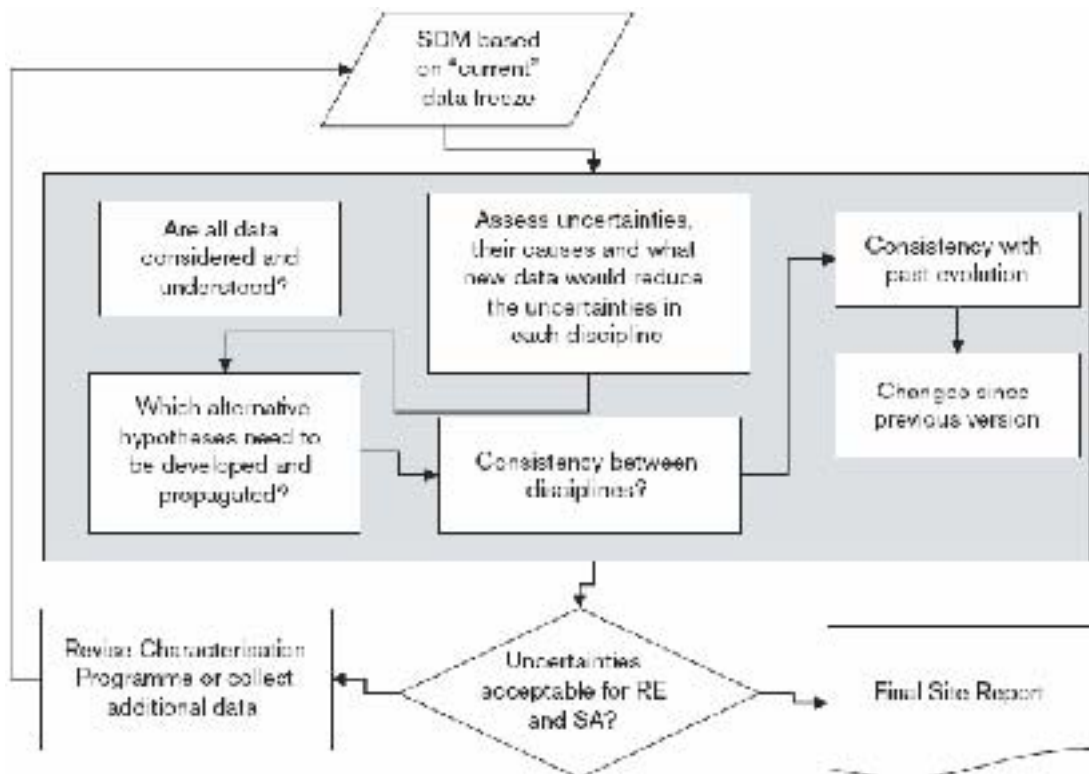


Figure 12-1. The Overall Confidence Assessment presented in this chapter concerns the various aspects inside the blue box in the flow chart above.

Less emphasis is put on the importance of the uncertainties. Such an assessment could strictly only be done by the users and is a planned part of the design and safety assessment activities where the Site Descriptive Model is input. Still, some general remarks based on the overall list of important issues as listed above can be made. A more comprehensive discussion on implications for further work is presented in Chapter 13. That discussion is based on the assessment presented in this chapter.

12.2 Are all data considered and understood?

Checking whether all data are considered and understood is the first step in the Overall Uncertainty and Confidence Assessment (see Figure 12-1). A similar and unbiased treatment of all data and interpretations that explain several different observations enhances confidence.

12.2.1 Answers to auditing protocol

A protocol has been developed for checking the use of available data sources. It concerns:

- Data that have been used for the current model version (by referring to tables in Chapter 2).
- Available data that have not been used and the reason for their omission (e.g. not relevant, poor quality, ...).
- If applicable – What would have been the impact of considering the non-used data?
- How accuracy is established (e.g. using QA procedures) for the different data (essentially by reference to tables in Chapter 2).
- For data (types) where accuracy is judged low – whether accuracy is quantified (with reference to applicable sections of this report or supporting documents).
- If biased data are being produced, can the bias be corrected?

The filled in auditing protocols are provided in Appendix 9. It should be noted that the questions sometimes produce long answers, but this does not necessarily mean grave impacts on the uncertainty for key features of the Laxemar site.

12.2.2 Overall judgement

In general most available data have been analysed and treated according to good practices. The database for the modelling is well defined and is accounted for in the tables of Chapter 2. The following overall conclusions are drawn.

- Generally, all data available at the time of the data freeze 1.2 and as listed in the tables of Chapter 2 have been considered in the modelling. There are some exceptions, mainly concerning the use of old data from Äspö HRL and especially the experience and observations made underground. These could be much more used for verifying the resulting geological as well as the hydrogeological discrete fracture model. However, it needs also be considered the Äspö HRL, although located in the same general area, may not have exactly the same properties as those within the Laxemar subarea.
- Inaccuracy in the field data is, with some important exceptions, judged to be a minor source of uncertainty in the resulting model description.
- There are some biases of different kinds in the data. A possible systematic bias is the predominance of vertical boreholes. The limited number of gently dipping boreholes makes corrections of fracture orientation biases very difficult and also raises concerns about the possibility of predicting the anisotropy of the transmissive features. There is also “bias” due to lack of data from important parts of the rock mass which raises questions about the representativity of the rock mechanics, thermal, hydrogeological and hydrogeochemical samples. There are generally few data at depth from the rock domains where the potential repository might be located. These biases are hard to account for. More representative data would be needed.

12.3 Uncertainties and potential for alternative interpretations?

The next step in the Overall Uncertainty and Confidence Assessment, see Figure 12-1, is to assess the uncertainties in the different discipline-specific analyses and modelling. Small estimated uncertainties and inability to produce many different alternative interpretations from the same database are indications of confidence – although not a strict proof. A related issue is whether new measurements or other tests could resolve uncertainties or distinguish between alternatives and thereby further enhance confidence.

12.3.1 Auditing protocol

The site descriptive model represents an integrated characterisation of a natural rock mass. Uncertainties are an inherent aspect of any such characterisation and thus also of the site descriptive model. There are different types or origins of the uncertainties. Some are conceptual and may depend on unresolved scientific issues or on inadequate understanding (and/or modelling) of the geological, physical or chemical properties or behaviour of the rock mass. Other uncertainties have to do with limitations in the available database due to spatial variations, temporal variations, measurement accuracy, quality of data or the lack of some data. Uncertainties cannot be avoided. It must be kept in mind that some uncertainties are more important than others, see Section 12.1. All main uncertainties should be identified, but efforts on quantifying and reducing uncertainty should primarily be focused on the important uncertainties. A more thorough general discussion on these issues are given in previous Site Descriptive Model reports (see e.g. /SKB 2005a).

A common philosophy is required for addressing uncertainty and the implementation needs to be audited. There is a need to consider how uncertainties can be identified through uncertainty elicitation. A protocol has been developed for checking this. It concerns:

- Listing the main uncertainties in the different disciplines.

- Identifying the causes of each uncertainty (e.g. data inaccuracy, information density, uncertainty in other discipline model or process understanding), also indications from new data not yet fully analysed is a valid cause.
- Whether the uncertainty has been assessed considering information from more than one data source or through a calibration or validation exercise (a positive answer would be an argument in support of the adequacy of quantification of the uncertainty)
- Assessing the impact on other uncertainties (in all disciplines).
- Quantification of the uncertainty (with reference to the applicable section of the Site Descriptive Model report).
- Whether there is a potential for an alternative representation and whether an alternative actually has been developed.
- Whether there are unused data that could be used to reduce the uncertainty.
- What new data would potentially help resolve the uncertainty and are these new data already considered in the plans for the Complete Site Investigations at Laxemar?

The filled-in auditing protocols are provided in Appendix 9. It should be noted that only some of the listed uncertainties would be of concern for Safety Assessment or Repository Engineering. As already explained, assessing the importance of these uncertainties lies outside the scope of the current report, but a general comment on this issue is made below.

12.3.2 Main uncertainties

Bedrock geological model

As already identified and discussed in Chapter 5, and as listed in Table A9-3 of Appendix 9, the main uncertainties in the version 1.2 *Bedrock Geological* model of *Rock Domains* concern details of the spatial distribution of the different rock types in the model volume. These uncertainties also affect the geometry of the rock domains.

- The spatial distribution of Rock Domains in the regional model area is uncertain, since only reconnaissance data are available. However, the geometrical relationships between RSMA01, RSMD01, RSMM01, RSMP01 and RSMP02 in the local model volume are considered less uncertain. The uncertainty is due to restricted subsurface information in a pristine igneous bedrock terrain with little structural control (i.e. guidance for modelling).
- Heterogeneity and proportion of subordinate rock types in the domains, i.e. veins, patches, dykes, minor bodies, frequency of minor deformation zones, is uncertain due to limited information. It is difficult to estimate both the proportion and spatial distribution, although there are various inputs in the local volume such as the outcrop database for the Simpevarp and Laxemar subareas, the cored boreholes, cleaned outcrops and the bedrock map.
- The orientation of subordinate rock types, particularly fine- to medium-grained granite and pegmatite, is uncertain, again due to limited information.
- The spatial distribution of compositional variations of rock types – for example the Ävrö granite that are “rich” (granite to granodiorite) contra “poor” (quartz monzodiorite) in quartz is also uncertain. There are limited data at depth, but a rough separation is can be carried out at the surface for the Ävrö granite. However, more or less rapid changes in composition do occur locally, due to mixing and mingling phenomena during formation of the igneous rocks.
- The three dimensional distribution and characterization of secondary alteration, e.g. oxidation (red staining), saussuritization, sericitization and chloritization (hydrothermal alteration) is uncertain. There is limited information and it is difficult to estimate the proportion, spatial distribution and not the least the degree (“strength”) of alteration. However, the alterations usually imply increased thermal conductivity, i.e. ignoring this result in underestimates of the thermal conductivity.

None of the uncertainties in the regional domain are of significant importance for Safety or Repository Engineering. However, even though the uncertainty is lower in the Laxemar subarea, it is still important for the thermal model and thus also of importance for safety and engineering.

A more detailed bedrock map in the regional model area, boreholes in the regional domain and a detailed marine geological survey would reduce the uncertainties in the regional domain, but these matters are not included in the CSI programme. Due to the detailed needs of the thermal model, more subsurface data are needed in the Laxemar subarea volume from cored boreholes. These data include detailed geophysical information and documentation of the orientation of subordinate rock types. Detailed investigation of cleaned outcrops to get information on the amount, proportion, distribution and character of subordinate rock types, would also reduce uncertainty inside the Laxemar subarea. An increased number of modal and chemical analyses and density data both from the surface and cored boreholes would reduce the uncertainty in the spatial distribution of compositional variations, especially within the Ävrö granite. The uncertainty in secondary alteration would partly be reduced by very detailed microscopy study of thin-sections both from surface and from drill cores sampled. This would provide information on the extent and a semi-quantitative estimate of the degree of alteration.

As already identified and discussed in Chapter 5 and as listed in Table A9-3 of Appendix 9, the main uncertainties in the version 1.2 of the *Bedrock Geological model of Deformation Zones* are the following:

- The existence of deformation zones is uncertain due to lack of complete coverage of supporting subsurface data, but the number of high confidence zones has increased with targeted subsurface investigations. Furthermore, targeted drilling campaigns together with geophysical profiles and seismics have confirmed most of the proposed deformation zones that were suggested based on surface lineaments. Seismic data appear to support the assertion that there are no regional gently dipping deformation zones.
- Potentially there are deformation zones not included in the model. This would mainly concern sub-horizontal zones as these are harder to detect. However, it is clear that gently dipping regional zones do not exist within the local model domain, but there is generally lack of ability to secure data from local major and local minor gently dipping deformation zones.
- The continuity along strike and dip at depth and the termination of the deformation zones are uncertain. This in turn makes the resulting size (length) of the deformation zone uncertain. Furthermore, there is good evidence that some lineaments are the surface expression of curved subsurface structures, which results in additional uncertainty in projecting the surface expression to depth. However, provided the surface expression of lineaments means something about the lengths and terminations at depth, then good data is already at hand and are being used. It should be noted that this hypothesis exaggerates the sizes of the zones.
- The character and properties of the zones are uncertain, even for the well established high confidence) zones. There is a strong spatial variation of properties (width, internal structure, fracturing, also hydraulic properties ...) seen in the few cases where there are multiple borehole intercepts in a zone.

The deformation zone geometry, but to a lesser extent the properties, of the deformation zones within the Laxemar subarea are important for Repository Engineering as this will determine the repository layout. However, more exact orientation and positions of the deformation zones are only needed when planning making a detailed layout and planning the underground excavation work. The already existing understanding may be sufficient for judging the space needed for the repository. Provided the repository layout fulfils the stated respect distances and that there is a low probability of undetected deformation zones, the remaining uncertainty in deformation zones is of less importance for safety.

There are several ongoing and planned activities that should reduce the deformation zone uncertainties. An alternative producer has revisited the underlying basis for the linked lineament map. The two alternatives show great similarities. A future targeted borehole campaign will increase confidence in selected local major zones around areas of interest. The detailed laser map, detailed magnetic map and field controls in selected 400 m squares will increase confidence in existence of local minor zones. However, it is hard to identify any new data that would further increase confidence in the existence (non-existence) of the gently dipping deformation zones apart from already planned verification efforts on seismic reflectors using vertical seismic profiling, drilling and hydraulic tests. To increase confidence in extent of zones, several boreholes are needed in the same structure including interference tests, seismics etc. Some such tests are included already in the ongoing plans.

As already identified and discussed in Chapter 5 and as listed in Table A9-3 of Appendix 9 the main uncertainties in the version 1.2 *Bedrock Geological Discrete Fracture Network* model are the following:

- The fracture orientation distribution, and the associated set identification, is uncertain since outcrops are sub-horizontal and boreholes sub-vertical, and are also mapped with different resolution. The uncertainties are quantified. Different conceptual assumptions regarding tools and possible modelling “style” could be made.
- The fracture size distribution is uncertain, since it is based on interpolation between lineament and mapped outcrop data and for some sets only local information is available. The uncertainty is even larger for the sub-horizontal since there is very little data on subhorizontal fracture traces. Uncertainty is assessed through possible variability in size fits (upper, lower bounds and best fit).
- The fracture intensity and its variability is uncertain. The current assumption is that fracture intensity is different in the different Rock Domains, but there is a high variability in borehole fracture intensity, also in sections not identified as deformation zones. There is a need for better understanding the difference between volumes in the rock having anomalously high fracture intensity in contrast to the increased intensity inside local minor deformation zones. A possible alternative is a fractal spatial model for background fractures and system for identifying local minor deformation zones in boreholes.
- The thickness-size correlation and the coupling to the deformation zone model is uncertain. There is currently not a sufficiently well established basis for establishing such relation. Within this study some verification exercises for intensity measures have been performed for conceptual model alternatives 1 and 2. The issue will be further assessed within the separate SKB Expect project /Cosgrove et al. 2006/.

These uncertainties, especially the uncertainty in size and intensity, have direct Safety and Engineering implications. Further analysis and characterisation efforts for reducing these uncertainties include making better use of results in the Äspö tunnel mapping system for verification and various exercises, analysing the independent alternative lineament interpretation, focusing on lineament data falling into the scale between outcrop and 1,000 m zones (i.e. as derived from the detailed laser map, detailed magnetic map and field controls in selected 400 m squares), refined analysis with respect to alteration (suaritisation, oxidation) and refined rock domain/fracture intensity analyses. However, above all more data are needed from boreholes penetrating the potential repository volume.

Rock mechanics

As already identified in Chapter 6 and Table A9-4 of Appendix 9, the main uncertainties in the version 1.2 *rock mechanics stress* model are the following:

- Rock stress magnitudes and distribution within the Laxemar subarea are uncertain due to sparse data and scatter in data. However, different measurements have been used and compared, and experiences from excavations at depth in the Äspö HRL (down to 450 m) also confirm that stress magnitudes high enough to exceed the elastic response of the rock mass to tunnelling do not exist in the Äspö HRL area, since major stability problems have not been observed.
- The geometry of the division of local model area into different stress domains is uncertain, due to scarcity of data in the local model area and uncertainties in the deformation zone model. In particular differences in the extent, the termination and dip of deformation zones are considered important.

Uncertainty in stress has importance for Repository Engineering because a high stress magnitude affects the assessment of potential for spalling and other rock stability issues. Stress is also important for safety assessment as it affects the potential for thermal spalling.

More stress measurements in the Laxemar subarea, will become available for model version Laxemar 2.2. This will reduce uncertainty. Possibly additional inference could be made from the fact that core diskings is not observed in available drill cores from deep cored boreholes, as this would indicate some upper bound to the stress levels.

As already identified in Chapter 6 and Table A9-4 of Appendix 9, the main uncertainties in the version 1.2 *rock mechanics properties* are the following:

- Rock mechanics properties for the intact rock of rock type Quartz monzodiorite and the Ävrö granite in the southern part of Laxemar subarea are possibly biased, since only laboratory tests from the Simpevarp subarea and the northern part of the Laxemar subarea are available.
- The occurrence, extent and characteristics of statistically represented minor deformation zones is uncertain, due to the uncertainties in the geological DFN model, the uncertainty in the thickness-size correlation and the uncertainty in the deformation zone model.
- Currently there is not an established approach to assess the effects of pore pressure on rock mass strength properties in the theoretical approach. The process is understood but parameters are uncertain. The uncertainty is not quantified, but the effect is probably negligible.
- For deformation zones only the empirical approach is used, and the description is uncertain. The bedrock material inside deformation zones is not easily sampled, nor suitable, for laboratory testing.

Uncertainty in intact rock properties has importance for Repository Engineering as it affects the assessment of potential for spalling and other rock stability issues. The intact rock properties are also important for safety assessment as it affects the potential for thermal spalling.

There is a need to obtain representative data from all important rock types in the potential repository volume. Uncertainty in intact rock properties will be reduced by additional laboratory tests data on intact rock, especially from the Ävrö granite and Quartz monzodiorite in southern Laxemar. Uncertainties in rock mass and deformation zone properties would possibly be reduced by use of old data (observations on length, width and property relation) from Äspö HRL, and by improved deformation zone and DFN models. Comparison of drillhole empirical classification with actual experiences from excavations at Äspö HRL is also important.

Thermal model

As identified in Chapter 7 and Table A9-4 of Appendix 9, the main uncertainties in the version 1.2 *thermal model* are the following:

- The spatial distribution of thermal conductivity is uncertain, due to uncertainties due to uncertain representativity of SCA (estimates based on mineralogical composition of sample) and of TPS (direct laboratory measurement on small scale sample) data, uncertainties in the density logging of the Ävrö granite and uncertainty in scale transformation.
- The determination of the in situ temperature is uncertain, due to uncertainty in temperature data, possibly due to calibration error or convection in the boreholes. There are differences between boreholes.
- Thermal expansion data are uncertain, possibly due to data inaccuracy. Comparison between methods and laboratories is done but so far not reported.

The uncertainties have few direct implications for Safety Assessment, but are important for Repository Engineering. Further reduction of the uncertainty related to the variability of thermal conductivity and also on the initial temperature would enable a more efficient use of the rock volume.

Representative direct measurements of thermal conductivity (TPS) for all rock types including some altered rock samples, together with data from geology on abundance and nature of alteration, will reduce uncertainty in thermal conductivity and its scaling. A further development is to establish a relationship between rock mapped as altered rock in Boremap and measured thermal conductivity. Extensive sampling of other rock types is needed to produce variograms to describe spatial variability. For Ävrö granite, more samples with both density and thermal conductivity measurements are needed. These samples should be collected in the Laxemar subarea and should ideally include both high and low conductivity varieties. Additional measurements (verification data set) in density logged boreholes are required for verification of the density – thermal conductivity model. There is also a need for improved quality of density logging data. It may also be possible to

use temperature loggings to evaluate variability in thermal conductivity, but there would then also be a need to better characterise the domains in the geological modelling so that the observed variations in thermal conductivity could be matched to the appropriate domains.

Uncertainty in in situ temperature would be reduced by more high quality temperature logs in combination with optimal timing of measurement. Uncertainty in thermal expansion could be assessed by the use of existing data from the APSE experiment at Äspö HRL. Laboratory test method development is also underway.

Hydrogeology

As already identified in Chapter 8 and in Table A9-5 of Appendix 9, the main uncertainties in the version 1.2 *hydrogeological* model are the following:

- The geometry and connectivity of the deformation zones is uncertain. There are only few interference tests in the Laxemar subarea. In principle, this uncertainty affects transport paths and the integrated evaluation together with hydrogeochemistry, but the actual importance is tested by analysing cases with and without the low confidence zones.
- Spatial variability of transmissivity in the deformation zones is uncertain. Only few deformation zones have been subject to more than one hydraulic test. Nevertheless, the combined data from many zones suggest a depth trend, although not fully verified, where transmissivity decreases with depth.
- There are various uncertainties in the hydraulic properties between the deterministically modelled deformation zones, modelled by the hydraulic discrete fracture network, mainly due to few data in representative volumes and the high variability found in the existing data. These uncertainties include the not fully verified depth dependence, uncertainties in the underlying DFN model, the conceptual models for and coupling transmissivity as a function of fracture size. There is probably also an anisotropy bias introduced by the steeply dipping boreholes overestimating the importance of the subhorizontal set.
- Also the difference in hydraulic properties as a function of rock domain is uncertain, partly due to uncertainty in the geometry of the rock domains, but more importantly due to lack of data. Only rock domain A, dominated by Ävrö granite, is intersected by more than one borehole, and there the different boreholes show rather great differences. It is thus not fully established whether the rock domains have different properties or if the properties simply vary strongly in space.
- A unified elevation model, covering topography and bathymetry including a well specified shoreline, is available. However, the overburden model is still under development and the position of the bedrock surface and the overburden stratigraphy, especially below the sea, must be considered uncertain.
- Regional scale boundary and initial conditions are also uncertain. However, various hypotheses on the water type distribution at the end of the last glaciation were assessed already in Simpevarp 1.2 by exploring various locations of, and conditions at, the regional boundary and by exploring various initial conditions. These analyses suggest that the conditions at depth are reasonably well defined for the palaeohydrogeology simulations.

Uncertainties in the hydraulic DFN model, its anisotropy and potential function of rock domain, within the potential repository volume are of high importance both for Safety Assessment and Repository Engineering. Uncertainties in the geometry, connectivity and properties of the deformation zones are much less important. Uncertainties in the digital elevation model or in palaeohydrology initial and boundary conditions affect understanding, but have very limited direct importance for Safety Assessment or Repository Engineering.

More data from the rock mass of the potential repository volume is needed before it is meaningful to more elaborately try to bound the uncertainties and spatial variability of the rock mass hydraulic properties of the Laxemar subarea. The uncertainties in the rock mass properties would be reduced by new hydraulic tests using inclined boreholes and by boreholes (with tests) in rock outside the deformation zones within in the hydraulic rock domain D, M(A) and M(D), that have only been tested to a limited degree to date. Detailed hydraulic tests 0–100 m below surface and interference

tests between these boreholes may to some extent be used to test the model, but would be of limited value for characterising the rock within the potential repository volume. Interference tests at greater depth would in theory be very valuable, but are in practice very difficult to carry out due to the generally long distances that need to be studied in the a sparsely fractured rock involved. Single-hole interference tests (one section for injection and several pressure monitoring sections) could potentially be used to test connectivity, but no tools are presently available and the usefulness of the methodology is not known. PSS data can possibly be used more to test the hydraulic DFN models by simulating existing tests performed at various scales and the anisotropy could be better assessed using PFL data together with information on the orientation of the flowing features.

Hydrogeochemistry

As identified in Chapter 9 and in Table A9-5 of Appendix 9, the main uncertainties in the version 1.2 *hydrogeochemical* model are the following:

- The spatial variability of groundwater composition at depth is uncertain. The information density concerning borehole groundwater chemistry is low. The samples are mixed and represent an average composition. There is a lack of data on water composition in the low conductivity fractures and in the rock matrix. Also the “mixing” proportions of “water types” have uncertainties greater than those of the individual chemical components and may therefore not necessarily indicate a unique origin of the water. The basic model is the interpolated distribution from the data. An alternative hypothesis is that there exist lenses of “deviating” groundwater composition (glacial water) in the low conductive fractures and in the matrix. Both hypotheses are partly assessed in the hydrogeological flow modelling and will also be studied in the context of future geochemical sampling and interpretation. A validation test has been conducted where representative/non-representative samples have been used as a basis for interpretation. The regional groundwater flow modelling has also applied different initial conditions following the last glaciation to reproduce present chemistry at depth. It is likely, but not yet tested, that a high resolution flow model would show under what is conditions lenses with different water composition could occur.
- Groundwater composition in the rock matrix is uncertain, since there are few measurements and there are uncertainties in interpretation associated with the sampling. There are only small extractable volumes available for analysis, and there is possibility of contamination, together with modelling uncertainties and assumptions. However, a carefully conducted chemical analytical programme is under way and stress release impacts are assessed using rock mechanics information.
- The identification of end-member waters has been improved upon, but there is still some uncertainty. Some is due to the judgemental aspect of the M3 (principal components) analysis.
- Uncertainties in important chemical reactions, i.e. those controlling redox and pH, relate to model uncertainties, inaccurate pH measurements, inaccuracy in the thermodynamic databases, potential errors in mineral phase selections and potential errors in end-members selection. Probably, the important chemical reactions that control the redox are known, but the uncertainty is in where the reducing agent (methane) emanates and how it gets there.
- Temporal averaging implies uncertainties in the seasonal variability in surface water chemistry, which ultimately impacts the groundwater in the bedrock. The sampling may not describe the seasonal variation and samples may be taken at different time intervals from the surface versus the shallow boreholes.

There are no direct Safety or Engineering implications stemming from the uncertainties in the hydrogeochemical model. The listed groundwater compositions are well within the bounds of the preferred conditions, see Chapters 9 and 11. Still, reducing the uncertainties would enhance understanding and thus the capability of predicting the future evolution.

Representative data from repository depth at the Laxemar subarea are needed. The uncertainties in groundwater composition would be reduced by more observations from deep boreholes, analyses of rock matrix samples and electromagnetic data for regional characterisation. Data from extreme

end-member waters would also be useful, but it should be clear there may not exist samples of pure end members, e.g. it would be difficult to find a pure Littorina Sea water. Samples for rock matrix determination have already been collected and the results will be available for model version 2.1. In situ pH measurements, more data on fracture mineralogy and data on rock matrix mineralogy (including Fe^{2+}) will reduce the uncertainty in redox processes. Enhanced sampling reflecting seasonal variation from selected surface and borehole locations in identified recharge/discharge areas will reduce uncertainty in seasonal variation of the surface waters.

Bedrock transport properties

As already identified in Chapter 10 and Table A9-5 of Appendix 9, the main uncertainties in the version 1.2 model of the *bedrock transport properties* are the following:

- Sorption and diffusion parameters for site-specific materials as well as data imported from other sources (e.g. Simpevarp subarea, Äspö HRL, etc.) are uncertain, especially the sorption data. There is only a small amount of site investigation data available for the Laxemar subarea and values vary in space. Stress release effects on core samples may affect measured diffusivities. The conceptual model of sorption may also be incorrect if other geochemical processes are active. These uncertainties are general and apply to all data used, both site-specific and imported. The uncertainty in diffusion is assessed with electrical resistivity data analysed both in the laboratory and in the field combined with through diffusion experiment. There are multiple samples and sample lengths for all laboratory experiments.
- Sorption properties, diffusivities and porosities of the geologic material representative to the fractures (e.g. fracture rim zone, fault gouge material and fracture filling) are uncertain due to shortage of relevant material thus far and possible discrepancy with data obtained at Äspö HRL within TRUE program. However, a larger uncertainty is the accessibility of the fault gouge material.
- The spatial variability and correlation between matrix transport properties and flow paths is uncertain. Lack of site-specific transport data impedes the establishment of quantitative correlations. There is also general uncertainty in matrix retention properties, as already discussed. However, generally, there is an expectation of low correlation between matrix and flow path properties, but a higher correlation between fracture surface and flow path properties.
- The distribution of transport resistance (F) at Safety Assessment timescales is uncertain. As a derived parameter, the estimation of F and its distribution are strongly influenced both by uncertainties in models used to interpret primary borehole data (i.e. to give transmissivity distributions from PFL and other hydrological investigations) as well as models used to estimate the derived parameter itself (F). This also includes assumptions, (both stated and implicit) used in data derivation (e.g. flow dimension, flow geometry, etc.). Transmissivity distributions must be at the resolution of individual water conductors to be reliable for F distribution estimations. Scoping calculations to establish an envelope of possible behaviour using different channel network representations bound the uncertainty.

The uncertainty in sorption and diffusion parameters is related to uncertainties in salt transport and reactive (hydrogeochemical) transport modelling, but uncertainty in transport resistance F and its distribution under Safety Assessment conditions is far more important than (possibly) smaller uncertainties in material property data. Retention properties of fractures are of limited importance for Safety Assessment, since this retention is conservatively discarded. All these uncertainties are of limited importance for Repository Engineering.

Representative data from repository depth at the Laxemar subarea are needed. Further reduction in the uncertainty in the transport resistance F, would rely on re-interpretation of primary data using alternative models as well as use of multiple independent modelling concepts for parameter estimation as well as additional detailed hydraulic tests (PFL-data) from more boreholes. More site specific data on diffusion and sorption parameters from rock domains of interests would reduce uncertainty in these properties. Measurements on large intact pieces of rock would reduce uncertainty in scaling. Potentially, more borehole data can establish a relation between matrix properties and flow paths, but the expectations for this should be low, since it such a correlation is expected to be weak, if it exists at all.

Surface and near surface

As already identified in Chapter 4 and in Table A9-6 of Appendix 9 the main uncertainties in the version Laxemar 1.2 model of *the surface system* are related to the lack of some types of data. Specifically, the most important gaps in the present database concern:

- Composition, spatial distribution, depth and thickness of individual strata of Quaternary deposits: there is low information density in the Laxemar subarea. However, there is now a model describing the data density of overburden depth and stratigraphy that allows the degree of uncertainty to be quantified.
- Chemical and physical properties of Quaternary deposits: there is low information density in the Laxemar subarea.
- Hydraulic properties in Quaternary deposits and near surface bedrock: there are insufficient data and models/descriptions of hydraulic properties and flow conditions in the overburden and uppermost rock.
- Water discharge in the surface system – spatial and temporal variability in runoff: There are no data from discharge stations in the Laxemar subarea and there are generally short time series in the regional model area.
- No calibration or validation has been made on the surface hydrology model: there is a lack of time series of surface water and groundwater levels. However, a sensitivity analysis for the properties of the Quaternary deposits has been performed.
- Quantification of water balance components (evapotranspiration, distribution of runoff between surface water and groundwater): there are limited site and generic data.
- Temporal and spatial variation in water composition of groundwater: no site sampling to describe the seasonal variation is available.
- Chemical description of Quaternary deposits and soils: there is a lack of descriptive data.
- Transport of matter in the terrestrial system: there are limited data on discharge combined with measurements of concentrations of dissolved and suspended matter.
- Chemical composition of biota: there are no data.
- Upscaling of spot sampling of biota: sample representativity and classification are uncertain.
- Properties of terrestrial vegetation: there is a lack of data.

These uncertainties will be reduced as additional data becomes available. Furthermore, uncertainties related to the understanding of site-specific processes will be analysed in future model versions. It is also worth remembering that there is a general conceptual uncertainty in that what is observed in the surface system at the present day may not be representative of the future, even if climate conditions should not evolve, and that it may be desirable to adopt a modified description (e.g. more cautious) or alternative descriptions for Safety Assessment.

12.3.3 Alternatives

Alternative model generation should be seen as an aspect of model development in general and as a mean of exploring confidence. At least in early stages, when there is little information, it is evident that there will be several different possible interpretations of the data, but this may not necessitate that all possible alternatives are propagated through the entire analysis chain including Safety Assessment (SA). Combining all potential alternatives with all its permutations leads to an exponential growth of calculation cases – variant explosion – and a structured and motivated approach for omitting alternatives at early stages is therefore a necessity.

As can be seen from the uncertainty tables in Appendix 9, some alternative hypotheses have actually been developed into alternative models. Furthermore, the alternative hypotheses are all assessed in order to decide on their treatment. This assessment is based on addressing the following set of questions for each potential alternative identified:

- Is the alternative “resolved in version Laxemar 1.2? (Only concerns hypotheses raised in version Simpevarp 1.1 and Simpevarp 1.2).
- Will the alternative affect other SDM models (or aspects of those models)?
- What are judged to be the important implications for Repository Engineering in phase D1?
- What are judged to be the important implications for Safety Assessment analyses in PSE (Preliminary Safety Evaluation) and SR-Can?
- What are judged to be the implications for investigations to “resolve” alternatives?

Finally, based on the answers to these questions a recommendation is made whether the alternative should be developed and propagated, be discarded or be put “on hold”, by applying the following criteria:

- Reasons to *develop/propagate now* include: potentially large impact on Safety Analysis or Repository Engineering, potentially very expensive to resolve by further data collection or just issue judged to be good to put “at rest” early.
- Reasons *not to propagate/develop* include: “old hypothesis” which is now resolved, shown to have little impact on Safety Assessment or Repository Engineering (can be directly discarded), or alternative that could be factored into quantified uncertainty.
- Reasons to *wait with development/propagation* include: issue judged to have limited impact on Safety Assessment or Repository Engineering (RE), issue will be resolved through expected investigations producing data for later data freezes.

Alternative hypotheses not explored or discarded will be “kept on the list” for further scrutiny.

The judgements made for the different alternative hypotheses are summarised in Table 12-1. The judgements regarding importance for Safety Assessment and Engineering are preliminary, but have been reviewed by experts within the Safety Assessment and Repository Engineering teams.

Bedrock geological model

As further explained in Table A9-3 in Appendix 9, identified hypotheses for alternative models of the bedrock geology concern:

- Geometry of rock domains in the Laxemar subarea.
- Alternative lineament interpretation.
- Changes of existence or geometry of deformation zones (geometry and extent) in the Laxemar subarea.
- Character and properties – also in the well established zones.
- Alternative (geological) DFN model.
- Width of minor deformation zones in the DFN model.

Some of these alternatives hypotheses have been further assessed, whereas others are discarded or kept, as summarised in Table 12-1.

Rock mechanics

As further explained in Table A9-4 in Appendix 9, identified hypotheses for alternative models of the rock mechanics concern:

- Rock Mass Mechanics Properties – due to alternative DFN-models.
- Alternative Stress Model.

Some of these alternatives hypotheses have been further assessed, whereas others are discarded or kept, as summarised in Table 12-1.

Table 12-1. Assessment of alternatives.

Potential “Primary” alternatives in SDM (see Tables A9-3 to A9-5) of Appendix 9	Is the need for alternative resolved in Laxemar 1.2? (Only concerns non resolved issues in Simpevarp version 1.2)	Impact on other discipline models (or aspects of these models)?	Implications for Repository for Engineering in phase D1	Implications for analyses in PSE and Safety Assessment	Implications for investigations to “resolve” alternative	Handling in Laxemar version 1.2
Bedrock geology						
Geometry of Rock Domains in the Laxemar subarea.	No. Subdivision of the Ävrö granite in a quartz-rich and quartz-poor variety is a natural step for upcoming model versions. A possible future alternative concept for division of rock domains in the Laxemar subarea (within the local scale model volume) could be introduced based primarily on the composition of rock types. This applies primarily to the compositional variation of the Ävrö granite.	Affects thermal, rock mechanics and hydrogeological models. Work implication minor (since 3D extrapolation anyway made in geological model). However, uncertainty is (if needed) already now described as a wider uncertainty range – and not necessarily as alternative models.	May affect space and degree of utilisation.	Changed repository volume. Revised thermal analyses.	The available subsurface information does not allow construction of any alternative models for this model version. More subsurface data are needed in the local scale model volume – cored boreholes, detailed geophysical information (modelling). Additional subsurface data from the regional model volume is not motivated bearing in mind the great needs to better understand the bedrock in the local scale model volume.	Uncertainty is acknowledged, but no need for an alternative model at this point. <i>Not necessary</i> to propagate at this point. Implications are straightforward.
Alternative lineament interpretation.	Partly. An independent lineament interpretation has now been performed.	May affect deformation zone model (if alternative lineament interpretation is really different compared to “original” lineament interpretation). See also next row.	See next row.	See next row.		Have been made for Laxemar 1.2, but implications not yet fully assessed. A preliminary assessment suggest good resemblance between the two alternatives, thus reducing the need to develop separate Deformation Zone models in future versions.
Changes of existence or geometry of deformation zones (extent and directions) in Laxemar subarea.	No, see Table A9-3. Two alternatives exist; One model containing only high and medium confidence deformation zones and one alternative containing also low confidence deformation zones based only on one source of surface lineaments. There are also specific questions regarding some of the zones as well as the size distribution and existence of sub-horizontal zones, but it seems clear that there are no regional sub-horizontal deformation zones in the area.	Would require update of the rock stress modelling and the groundwater flow modelling.	Yes, new design – changed repository volume.	Yes, new set of migration calculations (due to new hydrogeological model).	See Table A9-3, i.e. more boreholes and a targeted borehole drilling campaign to increase confidence in selected local major zones around areas of interest. Detailed Laser map, Detailed magnetic map and field control in selected 400 m squares, will increase confidence in existence (and occurrence) of local minor zones. Hard to see any new data that would further increase confidence in the existence (non-existence) of the gently dipping deformation zones.	Potentially important to propagate. Alternatives considered in sensitivity analysis of RE. Implications for SA are relatively straightforward and it could be less cost effective for full analysis in 1.2. The issue will anyway be resolved later in the investigations.

Potential “Primary” alternatives in SDM (see Tables A9-3 to A9-5) of Appendix 9	Is the need for alternative resolved in Laxemar 1.2? (Only concerns non resolved issues in Simpevarp version 1.2)	Impact on other discipline models (or aspects of these models)?	Implications for Repository Engineering in phase D1	Implications for analyses in PSE and Safety Assessment	Implications for investigations to “resolve” alternative	Handling in Laxemar version 1.2
Character and properties – also of the well established zones.	No, there remains potential for alternatives. Impact is partly assessed in hydrogeology.	Affects assignment of hydraulic and mechanical properties of these zones.	See hydrogeology and rock mechanics rows below.	See hydrogeology and rock mechanics row.	See Table A9-3.	Not done yet – but there remains potential for alternatives. Impact is partly assessed in hydrogeology.
Alternative (geological) DFN-model.	No. Different conceptual assumptions regarding tools and possible modelling “style”. However, alternatives are now presented for each main rock domain.	Rock Mass Mechanics, Hydrogeology, Transport.	May affect space and degree of utilisation. (Amount of key blocks may be affected by alternative DFN-models.)	Yes, new set of calculations for RN-transport. Affects probability of identifying critical (too large) deformation zones or fractures in deposition holes).	See Table A9-3.	Implications on probability of canister intersection for the different alternatives presented will be assessed within SR-Can.
Width of minor deformation zones in the DFN-model.	No. However, the uncertainties in the relation are not fully explored within SDM Laxemar 1.2, but should be within the SKB “Expect” project.	Rock Mass Mechanics model, Hydrogeology, Transport.	Affects degree of utilisation.	Affects probability of identifying critical (too large) deformation zones in deposition holes).	See Table A9-3.	Analysed within the special Expect Project run by SKB /Cosgrove et al. 2006/. Implications to be assessed within SR-Can.
Rock Mechanics						
Rock Mechanics Properties – due to alternative DFN-models.	No. The DFN-model is input to the “theoretical approach” and there are alternative DFN-models.	No.	Impact depends on change of properties.	No – or minor impact expected.	Potentially carry out sensitivity analyses on the SDM-level using the different DFN models as input.	The quantification of uncertainty using different methods, see Table A9-4, is judged sufficient. However, should possibly be reconsidered depending on handling of minor deformation zones in the DFN.
Alternative Stress Model.	The stress model based on the updated deformation zone model for Laxemar 1.2 may be compared with the one produced for Simpevarp 1.2. In particular the differences in the extent, termination and dip of deformation zones are considered important.	No (but stress modelling may provide feedback to deformation zone model and possibly hydrogeology).	Affects degree of utilisation, spalling, and thus possibly overall layout).	Elevated stress levels may imply potential for thermal spalling.	More stress measurements in the Laxemar subarea (will become available for Laxemar 2.2). See Table A9-4.	The current model with two stress domains is considered likely. The uncertainty is expected to be resolved by the additional data to be obtained during the CSI.
Thermal properties						
Thermal properties.	There is no alternative model. Uncertainty handled by uncertainty range.	No.	Would affect canister spacing.	Would affect certainty in temperature calculations.	An upscaling validation test is currently carried out using the prototype repository data.	There is no quartz monzodioritenative model. Uncertainty handled by uncertainty range.

Potential “Primary” alternatives in SDM (see Tables A9-3 to A9-5) of Appendix 9	Is the need for alternative resolved in Laxemar 1.2? (Only concerns non resolved issues in Simpevarp version 1.2)	Impact on other discipline models (or aspects of these models)?	Implications for Repository for Engineering in phase D1	Implications for analyses in PSE and Safety Assessment	Implications for investigations to “resolve” alternative	Handling in Laxemar version 1.2
Hydrogeology						
Alternative in the geological model of geometry of deformation zones and their connectivity.	No (see Table A9-5).	New regional hydrogeologic model – affects palaeohydrogeological model.	Possibly minor – would affect construction consequence analysis and impact of “open repository”.	Possibly minor for radionuclide migration (small transport resistance in zone). Impact of “open repository”. Potentially important for evolution of groundwater chemistry, but not very dramatic.	See Table A9-5.	The impact of this uncertainty on regional flow and evolution of groundwater composition is assessed in the numerical regional flow modelling by exploring cases with only high and medium confidence deformation zones and one alternative containing only high confidence deformation zones. Alternatives considered in the risk analysis of Design D1 for Laxemar.
Change of hydraulic properties (“transmissivity” and connectivity) of deformation zones in Laxemar subarea. (Depth dependence, T correlation to orientation.)	New	New regional hydrogeologic model – affects palaeohydrogeological model.	Possibly minor – would affect construction consequence analysis and impact of “open repository”.	Possibly minor for radionuclide migration (little transport resistance in zone). Impact of “open repository”. Potentially important for evolution of groundwater chemistry and thus on retardation properties and parameters.	See Table A9-5 in Appendix 9.	The need to further resolving this issue essentially depends on how it affects the understanding of regional groundwater flow and the evolution of water composition. Some different cases of the transmissivity distribution are explored in the regional flow modelling, see Chapter 8.
Alternative hydraulic DFN, including alternative T vs. Size correlation. Depth dependence, correlation to rock domain, T correlation to orientation.	Alternative is kept since Simpevarp 1.1.	Affects hydrogeology model (need to remake calibration efforts – but possibly only on smaller scale). Potentially – no need to e.g. update palaeohydrogeology and regional scale descriptions.	May perhaps affect space and degree of utilisation.	Potentially large impact on transport. New set of calculations for RN-transport.	See Table A9-5 in Appendix 9.	Several hydraulic DFN models with different T-models (T correlated/un-correlated) fractures have been calibrated to the data. The alternatives are propagated to the regional flow modelling and will be propagated to Safety Assessment. Potential for more alternatives, especially regarding anisotropy and rock domain dependence, but these are not developed. Judged more efficient to await more data in subsequent data freezes to potentially resolve these issues.

Potential "Primary" alternatives in SDM (see Tables A9-3 to A9-5) of Appendix 9	Is the need for alternative resolved in Laxemar 1.2? (Only concerns non resolved issues in Simpevarp version 1.2)	Impact on other discipline models (or aspects of these models)?	Implications for Repository Engineering in phase D1	Implications for analyses in PSE and Safety Assessment	Implications for investigations to "resolve" alternative	Handling in Laxemar version 1.2
Hydrogeochemistry						
Spatial variability in 3D at depth.	New. The basic model is the interpolated distribution from the data. An alternative hypotheses is that there are lenses of "deviating" groundwater composition (glacial water) in the low conductive fractures and in the matrix.	Both hypotheses are partly assessed in the hydraulic modelling and also in future geochemical sampling and interpretation.	Limited impact.	Affects understanding and also the predictions of future groundwater chemistry.	Table A9-5 in Appendix 9.	In version Laxemar 1.2 both hypotheses are partly assessed in the hydraulic modelling and also in future geochemical sampling and interpretation. There is currently no need to propagate to SR-Can, since the issue rather affects the understanding of the direct predictions. This viewpoint will, however, be re-assessed in SR-Site.
Alternative hypotheses in groundwater composition and processes.	Possibly, but potential for alternatives should still be considered in future versions.	May affect "palaeo-hydrogeological" simulations.	No impact.	Predictions of future groundwater composition (and thus resulting migration data).	Table A9-5 in Appendix 9.	In version Laxemar 1.2 different modelling approaches are applied to the same data set to describe the same processes. Thereby, the most realistic descriptions can be identified and the less realistic discarded.
Transport						
Understanding of retention/retardation processes as a basis for selection of parameters in models.	New.	Could impact hydrogeochemistry model.	No impact.	Affects retention and understanding.	Table A9-5 in Appendix 9. However, this issue is not readily resolved by more site specific data.	Uncertainty in sorption process as such assessed within Safety Assessment, SR-Can (see SR-Can Process and Data Reports).
Understanding the distribution of transport resistance (F) at PA timescales.	New.	Impacts the coupled hydrogeochemistry and hydrogeology modelling.	No.	Key impact on migration modelling.	Table A9-5 in Appendix 9.	Alternative models, of varying complexity are used for derivation of this parameter and for interpretation of primary data, see Chapter 10. The uncertainty will be more fully explored in SR-Can also using upscaling based on the hydraulic DFN-modelling.

Thermal model

As further explained in Table A9-4 in Appendix 9, there is no need for alternative models in the thermal modelling. Uncertainty is handled by uncertainty range.

Hydrogeological model

As further explained in Table A9-5 in Appendix 9, identified hypotheses for alternative models of the bedrock hydrogeology concern:

- Alternative in the geological model of geometry of deformation zones and their connectivity.
- Change of hydraulic properties (“transmissivity” and connectivity) of deformation zones in Laxemar subarea. (Depth dependence, T correlation to orientation.).
- Alternative hydraulic DFN models representing the hydraulic rock domains, including alternative T vs. Size correlation, depth dependence, T correlation to orientation and correlation to rock domains.

Some of these alternatives hypotheses have been further assessed, whereas others are discarded or kept, as summarised in Table 12-1.

Hydrogeochemical model

As further explained in Table A9-5 in Appendix 9, identified hypotheses for alternative models of the hydrogeochemical model concern:

- Spatial variability in 3D at depth.
- Alternative hypotheses in groundwater composition and processes.

Some of these alternatives hypotheses have been further assessed, whereas others are discarded or kept, as summarised in Table 12-1.

Bedrock transport properties

As further explained in Table A9-5 in Appendix 9, identified hypotheses for alternative models of the transport properties concern:

- Understanding of retention/retardation processes as a basis for developing the migration concept.
- Understanding the distribution of transport resistance (F) at PA timescales.

Some of these alternatives hypotheses have been further assessed, whereas others are discarded or kept, as summarised in Table 12-1.

Surface system

Formulation and analyses of alternative models is not judged a necessary or useful approach at the present stage of surface and near-surface systems modelling. Due to the relatively rapid development of the surface system compared to the bedrock, Safety Assessment applies a more stylised approach. Also, as the surface system is much more accessible than the subsurface, there is less room for overall conceptual uncertainty and most uncertainty can be mapped onto parameter variation.

12.3.4 Overall assessment

Compared with version Simpevarp 1.2, more of the uncertainties are now quantified or explored as alternatives. Only some of the uncertainties have direct implications for Safety Assessment or Repository Engineering. Notably, these uncertainties mainly concern the thermal, rock mechanics and hydraulic properties of the rock between the deformation zones in the potential repository volumes. These uncertainties appear hard to resolve without borehole investigations in these

volumes. Remaining uncertainties in the deformation zones are of less concern comparatively. One should also note that when going underground the possibilities to make relevant observations of the repository increases dramatically. There is no need to fully resolve the spatial variability before the underground exploration phase.

12.4 Consistency between disciplines

Another prerequisite for confidence is consistency (i.e. no conflicts) between the different discipline model interpretations. This is checked in the next step of the Overall Uncertainty and Confidence Assessment (see Figure 12-1). A protocol has been developed using an interdisciplinary interaction matrix for documentation. For each interaction, the following questions have been addressed.

- Which aspects of the “source” discipline would it be valuable to consider in developing the “target” SDM? The answer should be based on overall process understanding and the answers to the questions on impacts on uncertainties and alternatives provided in Tables A9-3 to A9-6 in Appendix 9 and in Table 12-1.
- Which aspects of the “source” discipline have actually been used when developing the “target” SDM?
- Are there any discrepancies between answers to the first and second question, and if so why?

Discrepancies between what it would be valuable to consider and what actually is considered affects confidence in the model. Again, it is primarily for the users to determine whether these discrepancies are grave or acceptable. However, an overview of this issue is provided at the conclusion of this section.

12.4.1 Important and actually considered interactions

Table 12-2 provides an overview of the interactions judged to be important (green) and to what extent these were actually considered (black) in Laxemar version 1.2. Table A9-7 in Appendix 9 lists them in full. In addressing the questions, the efforts is spent primarily on issues judged to be important and not in explaining why unimportant interactions indeed are so.

Impacts on Bedrock Geology

As can be seen from Table A9-7 in Appendix 9, many disciplines are judged to provide important feedback to the geological modelling.

Feedback from *rock mechanics* on stress orientations in relation to fracture sets could give additional confidence in the deformation zone and DFN model. The analysis of rock mechanics properties could affect the division of rock domains and deformation zones (e.g. less reason to split between domains or reason to split an existing domain). These couplings have also been considered in Laxemar 1.2. The stress modelling of Stress domain II gave further confidence on the deformation zones in the Ävrö region and northern Laxemar, and also implied more focus on this area due to its importance for the stress modelling. The rock mechanics modelling group also assessed differences in mechanical properties in different rock domains. The analysis suggests that division into rock domains (together with the additional fracturing domains) appear appropriate for the rock mechanics modelling needs, but also points out the need for further division of the Ävrö granite in southern Laxemar based on the quartz content.

Also the *thermal modelling* could provide feedback on the description of rock domains. The geological modelling could enhance the utility of its own predictions by considering what is really used and shown to be critical for the thermal modelling. This coupling has been considered. In fact, an important basis for the rock domain divisions is based on the needs expressed by the thermal modelling. The thermal modelling needs have also initiated the suggested alternative rock domain model (see Table A9-3 in Appendix 9) and also a future further division of the Ävrö granite in southern Laxemar based on quartz content.

Table 12-2. Summary of interactions judged to be important (green) and to what extent these were actually considered (black) in v1.2. (There is a clockwise interaction convention in the matrix, e.g. influence of geology on rock mechanics is located in Box 1,2, whereas the influence of rock mechanics on geology is located in Box 2,1). Table A9-7 in Appendix 9 provides the full version of this table.

Bedrock Geology	Yes/Yes	Yes/Mostly	Yes/Yes	Yes/Yes	Yes/Yes	Yes/Yes	No need	Yes/Yes	No need
Yes/Yes	Rock Mechanics (in the bedrock)	No need	Yes/Mostly	Yes/Yes	Yes/Yes	No need	No need	No need	No need
Yes/Yes	No need	Thermal (in the bedrock)	Yes/Insignificant influence.	No need	No need	No need	No need	No need	No need
Yes/Mostly	Yes/ Yes	Yes/Yes	Hydrogeology in the bedrock	Yes/Yes, but more work needed	Yes/Yes.	Yes/No	Yes/Partly	No need	No need
No need	No need	No need	Yes/Yes, but more work needed.	Hydrogeo-chemistry in the bedrock	Yes/ Yes, but not fully assessed	Yes/Yes, but no detailed modelling.	No need	No need	No need
No need	No need	No need	Yes/Yes, but not fully assessed.	Yes/ Yes, but not fully assessed	Transport Properties in Bedrock and QD	No need	No need	No need	No need
No need	No need	No need	Yes/Yes	Yes/Mostly	Yes/Yes	Chemistry in surface systems (QD, water biota)	Yes/Limited	Yes/Limited	Yes/Yes
No need	No need	No need	Yes/ Yes	Yes/Partly	Yes/Yes	Yes/Yes	Surface hydrology, near surface hydrogeology and oceanography	Yes/Yes	Yes/Yes
Yes/Yes	No need	No need	Yes/Yes	Yes/Partly	Yes/Yes	Yes/ Not yet	Yes/Yes	Quaternary Deposits, Topography and bathymetry	Yes/Yes
No need	No need	No need	No need	Yes/ Mostly	Yes/Yes	Yes/Partly	Yes/Yes	Yes/Yes	Biota in surface systems

Hydrogeology could provide confirmation of and indications of the existence and the properties of deformation zones (i.e. are there hydraulic contacts or not) as well as to control of the hydraulic applicability of the DFN-model. Hydrogeology should also provide feedback on the significance of the rock domain divisions. However, data available for Laxemar 1.2 do not really allow for hydraulic assessment of most of the deformation zones. An updated characterisation of the zones (e.g. ductile/brittle) is needed before such data could be used for classifying zones into different transmissivity classes. Still, there are some indications on the large-scale connectivity of EW007 in the near surface (first 200 m from percussion holes), but there is lack of data for other zones in the Laxemar subarea. Much feedback on the hydraulic applicability of the geological DFN-model has been given during the development of this model, which led to an updated size distribution for features larger than 500 m. There is still lacking a complete understanding of the local fracture sets – especially the subhorizontal set and some modifications to the size distribution are judged necessary in the hydraulic DFN model. Hydraulic differences between rock domains are assessed, and partly also between rock types. There seem to be significant differences between the rock domains (see Table A9-5 in Appendix 9), but hydraulic data are missing in some domains. Nevertheless, the hydraulic assessment lends further support the rock domain modelling.

Surface data on post-glacial tectonics are used in the descriptive model, but there is only a small amount of data available. These data show no indication of such movement.

Impacts on rock mechanics model

As can be seen from Table A9-7 in Appendix 9, it is mainly the *bedrock geology* model that impacts the rock mechanics model through the rock domains, deformation zones and DFN model. This input is used within the rock mechanics modelling. It is especially noted that stress domain II could be explained by the deformation zone geometry. Also the large differences in stiffness between different rock domains will affect the local stress field. However, the variation in rock domain stiffness in Laxemar is judged too low to be of importance.

In principle also *Hydrogeology* would impact the rock mechanics description, since water pressures reduce the rock stress to effective stress. However, this coupling has little effect on the parameters predicted, but is of course considered by Repository Engineering. The coupling is considered in the descriptive text, see Section 6.3.

Impacts on thermal model

As can be seen from Table A9-7 in Appendix 9, it is mainly the *bedrock geology* model that impacts the thermal model through the rock domain and rock type descriptions including data on alteration mineralogy (type and abundance) and nature of anisotropy (e.g. foliations). This input is used within the thermal modelling. However, it is noted that the alteration data are yet only partly used and that indicator variograms for subordinate rock types are not fully used for the upscaling. It would possibly be valuable to assess the potential larger scale anisotropy of the thermal properties considering orientations of dykes. Even the potential anisotropy related to foliation could be evaluated with a few direct thermal measurements in the laboratory.

Thermally driven hydraulic convection in boreholes affects uncertainty in measurement of initial temperature. This is considered when assessing uncertainty in in situ temperature.

Impacts on hydrogeology model

As can be seen from Table A9-7 in Appendix 9, many disciplines should inform the hydrogeological modelling and most of this input is considered.

Bedrock geology provides the geometrical framework in terms of rock domains, Deformation zones and DFN-geometry for the hydrogeological models. Most of this input is considered and the differences between rock domains is now assessed. Descriptions of deformation zones not are fully used in the property assignment, currently only the width and the positions. Potentially, a more detailed property description could be used for assessing the variability within the deformation zones, but an updated zone characterisation (e.g. ductile/brittle) is needed before such data could be used for classifying zones into different transmissivity classes.

Stress orientation, i.e. a *rock mechanics* input, is expected to affect hydraulic anisotropy. There is an attempt to assess anisotropy from the borehole data (using the detailed PFL-data), but the issue is not yet fully resolved. However, since strong anisotropy and correlation with the stress field is found at Äspö HRL – this hypothesis is retained despite unclear evidence in data from the Simpevarp and Laxemar subareas.

Temperature affects water density and viscosity. In version Simpevarp 1.2, the impact was assessed in the regional hydrogeological modelling. The impact is insignificant.

There is a strong coupling between hydrogeology and *hydrogeochemistry*, since it is suggested that advection with the groundwater flow is a main process for groundwater evolution. Furthermore, density differences created by varying salinity affect the flow regime. These couplings are considered in the modelling work. The regional hydrogeological simulations adopt density-dependent flow and use present-day salinity and water type distribution as “calibration targets”. However, it should also be noted that mixing is not the only important process controlling the groundwater composition, especially for less conservative species than chlorine. Other parameters, like redox, pH, sulphate and carbonate, are controlled by local and/or global geochemical reactions. These species, however, would not affect the flow. Model predictions of the depth of the redox front have not yet been made. If such predictions are made, they can be compared with the current hydrogeochemical data. Hydrogeochemistry could also lend support for modelled discharge/recharge areas, by assessing whether there are indications of discharge of deep groundwaters where the model predicts this should occur. However, existing data have not yet been fully interpreted and such comparisons are not yet made.

The regional simulations of past groundwater evolution involves modelling of salt migration. The migration properties should be consistent with assessed migration properties of the *transport model*. As discussed in Section 8.5, the models can match total dissolved solids (TDS) in boreholes for the present situation by adjusting flow and matrix parameters, but clearly there are uncertainties in the parameterisation of the models. Feedback on the importance of DFN and channelling representations are not produced within SDM Laxemar 1.2, but will partly be addressed within SR-Can.

There are also important *surface system* inputs to the hydrogeological modelling. Chemistry in surface systems provides input of surface water types considered in the modelling. Surface hydrology, near surface hydrogeology and oceanography provide the upper boundary conditions, although a simplified description is used in the deep rock model. Topography and the description of the overburden provide input to the description of the bedrock surface.

Impacts on hydrogeochemistry model

As can be seen from Table A9-7 in Appendix 9, many disciplines are judged to provide important feedback to the hydrogeochemical modelling and most of this input is considered.

Fracture mineralogy and the chemical composition of the bedrock, as provided by the geological model, require consideration. Fracture mineralogy is considered and the chemical composition is used in the modelling of the palaeo effects. The bedrock geochemistry (mineralogy) is used in deriving the matrix pore water composition.

Stress release of core samples could affect the interpretation of matrix pore water composition. These impacts are considered, but the conclusions are not yet final.

Groundwater flow (advection/mixing) and matrix diffusion are considered as main mechanisms for the distribution and evolution of groundwater composition. Simulation of the evolution of salinity and distribution of proportions of different end-member waters enables comparison between predictions and measured data. The simulated position of the fresh water and the occurrence of Littorina water (including “pockets” of glacial waters in low conductivity regions, surrounded by more modern water) agrees fair with measured data, although there are uncertainties (see Table A9-6 in Appendix 9). There is however a need for additional hydrogeological inputs. Additional analyses, not yet done, include, predictions of discharge and recharge areas as regards the hydrogeochemical implications (could be used to assess reasonableness of near-surface chemical data and vice versa), using the flow model as input for simulations of depth of the redox front, or hydraulic simulation of the sampling procedure as this could cause additional mixing.

Modelling salt migration etc. should be consistent with assessed migration properties. Differences in water composition between matrix and high conductive fractures need to be consistent with matrix data used in transport model. Coupled modelling is indeed undertaken, but the transport model implications of the matrix pore water data are currently not fully assessed.

There are also interactions with the *surface system*. Surface and near-surface hydrogeochemistry and hydrology and hydrogeology influence the waters in the bedrock. Some data are used in a simplified coupled/integrated model and the measured near-surface data are used as reference water in mixing calculations. Also the description of the Quaternary deposits provides input to selection of water types and input to coupled modelling. Surface biogeochemical processes are identified, but not quantified.

Impacts on transport model

As can be seen from Table A9-7 in Appendix 9, many disciplines are judged to provide important feedback to the transport modelling and most of this input is considered.

Geology provides the spatial distribution of properties based on the identified rock types in the rock domain model. Porosity measurements on surface and borehole samples as well as fracture mineralogy and hydrothermal alteration, are also important input data to the transport modelling. However, the lack of measured transport property data in the different rock domains limits the degree to which correlations with these variables can be established.

Consideration of the stress impact on “intact” rock samples for laboratory measurements of e.g. matrix porosity and formation factors is part of the data evaluation. A qualitative comparison is made between the laboratory and in situ data together with the in situ stress data. However, the comparison with the stress data is not straight-forward. There are also many other potential reasons for deviations between laboratory and in situ data.

Hydrogeology should provide essential input to the transport modelling. It identifies potential flow paths where description is needed and it constitutes a key input to the flow related transport properties, i.e. the transport resistance (F). Flow logs are indeed considered in identification of “type structures”, but only for fractures – not for deformation zones at this time. Input for transport resistance F, considered in Laxemar 1.2, is mainly from the transmissivity distribution using various assumptions. More elaborate estimates of F, using the hydraulic DFN model, will be made in SR-Can.

Groundwater composition affects sorption parameters and to some extent also the matrix diffusion. This is input to process-based retention modelling. Differences in water composition between the matrix and highly conductive fractures need to be consistent with matrix data used in transport model. Groundwater composition (identified water types) is used to set up laboratory tests and in parameterisation of the retardation model. However, the transport model implications of the matrix pore water data are currently not yet fully assessed.

Surface system

As shown in Table A9-7 in Appendix 9, many interactions take place among the different surface disciplines, which is why an integrated modelling approach is adopted for the surface system. However, the table also indicates that some of these interactions are only partially performed in this model version.

A full modelling of the *chemistry of the surface systems* would require input from several sources. Hydrogeology in the bedrock should be part of a coupled hydrogeological/ hydrogeochemical model of the surface system. However, no such modelling has been done. Hydrogeochemistry in the bedrock should provide boundary condition to the surface system models. Some comparisons are made, but no detailed modelling has been undertaken. The type of Quaternary deposits and processes models of them could provide input to potential correlation between chemistry and type of deposits. However, such modelling is not yet made. Biogeochemical processes (primary production and respiration) impact the chemistry in the surface system, but no detailed modelling is performed.

Modelling the *surface hydrology* and *near surface hydrogeology*, requires input of hydraulic properties and boundary conditions in the rock. However, the current modelling uses the bedrock hydrogeology model developed for Simpevarp 1.2, since the corresponding updated model for the Laxemar subarea was not available at the time of the modelling.

12.4.2 Overall assessment

Table A9-7 in Appendix 9 demonstrates the integrated character of the Site Descriptive Modelling. Different disciplines depend on the outcome of other disciplines and provide important feedbacks to those disciplines. Furthermore, to a large extent the interactions judged to be important are also considered in the modelling, and the current discrepancies between the needed interactions and the interactions considered is not assessed as a major problem for confidence in the SDM version 1.2 of the Laxemar subarea. Still, some further improvements are identified as being useful:

- There are possibly hydraulic differences between the rock domains. This lends further support to the rock domain modelling, but hydraulic data are missing in some domains. Furthermore, data available for Laxemar 1.2 do not really allow for hydraulic assessment of most of the deformation zones. An updated characterisation of the zones (e.g. ductile/brittle) is needed before such data could be used for classifying zones into different transmissivity classes. There is still lacking a complete understanding of the local fracture sets – especially the subhorizontal set and some adjustments to the size distribution are judged necessary in the hydraulic DFN model.
- The thermal modelling could make more use of the alteration data and indicator variograms for subordinate rock for the upscaling. It would possibly be valuable to assess the potential large-scale anisotropy of the thermal properties considering orientations of dykes. Even the potential anisotropy related to foliation could be evaluated with a few direct thermal measurements.
- Model predictions, using the hydrogeological model as input, of the depth of the redox front have not yet been made. If such predictions are made, they can be compared with the current hydrogeochemical data. Hydrogeochemistry could also lend support for modelled discharge/recharge areas, by assessing whether there are indications of discharge of deep groundwaters where the models predicts this should occur. However, existing data have not yet been fully interpreted and such comparisons are not yet made.
- Stress release of cores could affect the interpretation of matrix pore water composition. These impacts are considered, but the conclusions are not yet final. There is also a need for additional hydrogeological inputs to the hydrogeochemical modelling. Additional analyses not yet done include, predictions of discharge and recharge areas as regards the hydrogeochemical implications (could be used to assess reasonableness of near-surface chemical data and vice versa), using the flow model as input for simulations of depth of the redox front, or hydraulic simulation of the sampling procedure that could cause additional mixing.
- Lack of measured transport property data in the different rock domains makes the correlation between properties and rock domains weak. Transport model implications of the matrix pore water data are currently not yet fully assessed. More elaborate estimates of F, using the hydraulic DFN model, will be made in SR-Can.
- A full modelling of the *chemistry of the surface systems* and the *surface hydrology* and *near surface hydrogeology*, requires more input of hydraulic properties and hydrogeological and hydrogeochemical boundary conditions in the rock.

12.5 Consistency with understanding of past evolution

For confidence, it is essential that the understanding of naturally ongoing processes considered being important can explain – or at least does not contradict – the model descriptions. The distribution of the groundwater compositions should, for example, be reasonable in relation to rock type distribution, fracture minerals, current and past groundwater flow and other past changes. Such ‘palaeohydrogeologic’ arguments may provide important contributions to confidence even if they may not be developed into firm ‘proofs’.

Table A9-8 in Appendix 9 lists how the current model is judged to be consistent with the overall understanding of the past evolution of the site, as outlined in Chapter 3. The following is noted.

The geological model is consistent with the regional geological evolutionary model for the past 1,900 million years to the Quaternary. It would be potentially interesting, to couple the geologic evolution and the formation of the different fracture sets (if the order of formation could be determined) with hydrogeochemical indications (e.g. fracture minerals) of age. However, such studies performed at Äspö HRL were rather inconclusive, but could nevertheless provide some insights into the validity of the conceptual model for groundwater flow and hydrogeochemical development. There are no new data in Laxemar 1.2 that would necessitate an update of this evolutionary model. Also the stress model is consistent with the regional geological evolutionary model during this time period, concerning the general stress direction in the latest period. But no attempt to mechanically explain the creations of the deformations zones during previous periods has been performed.

Regarding the Quaternary period there is no information in support of potential “syn- to post-glacial” movements. Near surface boulder “caves” and “assemblies” are an effect of glacial erosion and are not indications of post glacial seismic events /Lagerbäck et al. 2005/. There is no reason to change the current view of the conceptual model of stress. Implications from up-lift could possibly be assessed, but are not judged important in the Laxemar subarea. The thermal development is not assessed. There is also a lack of historical development data.

Groundwater flow and salinity transport simulations cover the period from the melting of the last glaciation, but not alterations before that. Instead, the simulations have explored the impact of various assumptions on initial conditions, properties, events and boundary conditions since the latest deglaciation (approximately 14,000 years ago). In general, analysing the impact of potential changes after the glaciation on the current day groundwater flow and distribution of groundwater composition will affect and support the conceptual groundwater flow model. The interaction between the evolution of the surface water composition and the evolution of the groundwater composition is described concerning processes and origins of various water types (e.g. meteoric water, glacial melt water, Littorina water, brine). However, there are large uncertainties in initial conditions and the time evolution of boundary conditions: What is the time period for existence of the Littorina sea? Should the meteoric boundary conditions be divided into several time periods? What is the most appropriate origin of the water type “Marine sediments”, etc? These uncertainties set a bound for how far it is meaningful to carry out palaeohydrogeological simulations.

There is a fairly good understanding of the last 14,000 years of development of the surface system, and the description of this historical development is consistent with the description of the present system.

12.6 Comparison with previous model versions

The final evaluation of confidence envisaged in the flow chart of Figure 12-1 concerns to what extent measurement results from later stages of the investigation compare with previous predictions. This is important for discussing the potential benefit of additional measurements. Clearly, if new data compare well with a previous prediction, the need for yet additional data may even further diminish.

12.6.1 Auditing protocol

Again, a protocol has been developed for checking this. It concerns:

- changes compared with the previous model version (i.e. version Simpevarp 1.2 /SKB 2005a/),
- whether there were any “surprises” associated to these changes, and
- whether changes are significant or only concern details, i.e. is the model “stabilising”.

Table A9-9 in Appendix 9 lists the answers to these questions.

12.6.2 Assessment

As can be seen from Table A9-9 in Appendix 9 there are significant changes in version Laxemar 1.2 compared with version Simpevarp 1.2 /SKB 2005a/, but there are no substantial surprises.

Geological model

There is an updated *rock domain model*, with increased understanding and confidence in the three-dimensional geometry and properties of the rock domains in the local scale model volume. Apart from updating and refinement, the most conspicuous change compared to the Simpevarp 1.2 model is the definition of the two domains RSMP01 and RSMP02 (encompassing two branches of the Äspö shear zone). These are based on structural criteria (high frequency of ductile to brittle-ductile shear zones) and, at least geographically, separate the Laxemar and Simpevarp subareas. The updating and refinement of the rock domain models was based on:

- Increased understanding of and confidence in the surface distribution of rock domains in the local scale model area and updating and refinement of the two-dimensional rock domain model, due to the new detailed bedrock map of the Laxemar subarea and surroundings.
- New information from additional cored boreholes.
- New outcrop database for the Laxemar subarea and an increased number of modal, chemical and petrophysical analyses of rock types.

There are no surprises in the rock domain model. Changes of the rock domains are significant in the local scale model volume, particularly in Laxemar subarea and in the area in between the latter and the Simpevarp subarea. The rock domain model is definitely stabilising, but will certainly be refined further by use of forthcoming data from cored boreholes.

There is also an updated *deformation zone model*, with an increased number of high confidence zones in Laxemar subarea, although many medium confidence zones still are left. A new medium confidence zone is added. Assessment of existence is now made in three confidence classes: high, medium and low. Subhorizontal zones are also assessed within the Laxemar subarea. The updating and refinement was based on:

- Verification of some zones by targeted drillings.
- Increased confidence in the surface expression of deformation zones along the coastline of Ävrö and Simpevarp, due to new bathymetric data and an alternative lineament interpretation increases confidence in the previously identified lineaments that were based on land information.
- Evaluation modelling of the geological thickness of the high-confidence zones.

The changes of the deformation zones in the Laxemar subarea mostly concern details, but there are still important uncertainties, since there are several medium and low confidence zones inside the Laxemar subarea.

There is also an *updated geological DFN model*, divided into the different rock domains and subareas. The model is verified against available outcrops, and there seems to be a good correlation between fracture intensity and rock type. The DFN model is now judged better adapted to other user's needs, but there are still many uncertainties and hypotheses left to explore.

Rock mechanics

The *rock mechanics property model* is updated, with quantified uncertainties for all aspects of the rock mechanics model and with increase confidence due to:

- Better data for rock mechanics properties increase confidence in intact rock mechanics properties description.
- Higher confidence in laboratory data from fracture tests.
- Better support for the empirical rock classification.
- The theoretical approach is improved due to the rock domain specific geological DFN model input.

- Dilation angle is included in the model.

There is no real surprise in the modelling and the overall description is considered rather stable.

The *rock stress model* is also updated. By considering additional deformation zones also the Laxemar subarea is divided in to two stress domains. However, there are no new stress data. The stress model is updated based on evaluation of modelling results. There is no real surprise in the modelling and the overall description is rather stable. However, the stress model is still uncertain, mainly due to lack of data.

Thermal model

Compared with version Simpevarp 1.2 the main changes in the *thermal model* are:

- Higher confidence in thermal conductivity rock type models.
- Better understanding of spatial variability within domain RSMA, but no significant change in mean thermal conductivity.
- Mean thermal conductivity for domain RSMD is somewhat higher (2.70 W/m×K) in Laxemar 1.2 than in Simpevarp 1.2 (2.62 W/m×K)
- Model results are reported for domains RSMBA and RSMM, not modelled in Simpevarp 1.2 and there is potentially low thermal conductivity in domain M.
- In Simpevarp 1.2 modelling results for domain RSMA were adjusted to take account of suspected bias (overestimation) in thermal conductivity values calculated from density. Results from Laxemar 1.2 require no such correction, even if, contrary to what was found in Simpevarp 1.2, a slight underestimation of thermal conductivity is indicated by the density logging data. However, there are large uncertainties concerning calculated values for Ävrö granite with low thermal conductivity.

There are no real surprises in the modelling results. However, uncertainties remain and there is still potential for improving the model.

Hydrogeology

Compared with version Simpevarp 1.2 the main changes in the *hydrogeological model* are:

- A clearer picture of the definition of hydraulic rock domains (HRD) and that they mainly coincide with the geological rock domains, even if there still are some data lacking to support this.
- Assessed data from different scales, and also old data, show a clear tendency for depth dependence in hydraulic properties both in deformation zones and in the rock mass outside the deformation zones.
- More data from the Laxemar subarea were available for the development of the hydraulic DFN model of Laxemar subarea.

The depth dependence was a surprise in the sense that such dependence is not found at Äspö HRL, but the finding is consistent with knowledge from most other sites. The depth trends and the difference in properties between the rock domains is a major change compared with Simpevarp 1.2, but the significance of these trends still remains to be verified. There is strong spatial variability and few data. Uncertainties remain and there is still much potential for improving the model.

Hydrogeochemistry

Compared with version Simpevarp 1.2 the main changes in the *hydrogeochemical model* are:

- Only a few more water samples are available for the Laxemar subarea. The sharp depth trend in salinity suggested by KLX02 is not fully supported by the new data. There seems to be a more gradual increase.

- There are a few samples of matrix pore water.
- Improved understanding of the system, from recharge to discharge, but still some key data on the recharge are missing.
- Improvement of the methodology and tools used in water/rock reaction modelling by conducting an analysis of sensitivity and uncertainty: ^3H data evaluation has shown the limitations and possibilities in using such data for further modelling.
- Development of M3 modelling including an assessment of its uncertainties.
- Microbial evaluation assessing importance for redox conditions (but the model is still uncertain due to limited data).
- Re-assessing the data still suggests no evidence of Littorina water in the Laxemar subarea (only some evidence in KLX01 which is located close to a Baltic Sea inlet).

There are no real surprises in the overall chemistry. This is also in agreement with the preliminary results that there is no difference in salinity between matrix and flowing water down to about 500 m, whereas below that the matrix is in some cases more saline (i.e. further evidence for non-marine waters in the Laxemar subarea). The conceptual model appears stable and changes concern details. The updated data on ^3H could be a significant source of information in further modelling of the hydrogeological and hydrogeochemical evolution.

Transport model

Compared with model version Simpevarp 1.2 the main changes in the *bedrock transport* model are:

- Flow related transport parameters are included in the analysis.
- Scale-up effects are considered by flow path averaging over different rock types.

Results are broadly consistent with previous system knowledge. For material property analysis it is a question of details. The inclusion of flow related parameters is significant from a perspective of site knowledge and understanding. (previously included only in the Safety Assessment rather than in the SDM). There are still significant uncertainties in the flow related parameters.

Surface system

Compared with version Simpevarp 1.2 the main changes in the *surface system* model are inclusion of the following:

- Soil model (GeoEditor).
- Quaternary Deposit depth, stratigraphy and mapping.
- Bathymetric model (part of DEM improved).
- Hydrology model over local model area (larger model domains and use of more site data).
- Meteorological data from local stations.
- Geometric data on watercourses.
- Ecosystem models over local model area.
- Additional data on marine biota allow an improved ecosystem description.

There are no surprises, but there are significant changes in all sub-disciplines that constitute the surface system. The overall model is still under construction and areas not previously described have now been modelled. The description has by this version started to stabilise at the information level given from the Site Investigation. However, not all geographical areas are covered.

13 Conclusions

This chapter summarises the essence of the preliminary descriptive model, Laxemar subarea version 1.2. Firstly an account of important achievements in the current version of the descriptive model is given. This is followed by a resume of the current understanding related to the Laxemar subarea which emphasises the consistency in the understanding as achieved by the integration of the various disciplines. After this comes a condensed account of the handling of uncertainties and model alternatives detailed in the discussion of uncertainty and confidence in Chapter 12. This sets the context for a discussion of the implications for future modelling in order to improve the site-descriptive model and further reduce uncertainty. Finally, the implications for the concluding stages of the complete site investigations are discussed. This latter part addresses what additional data or measurements are required to further reduce existing uncertainties and facilitate additional improvement in the site descriptive models.

13.1 Major developments since the previous model version

Important developments have been made in the Laxemar 1.2 descriptive model compared with that presented in the Simpevarp 1.2 model. Some of these are applicable to the whole of the Simpevarp area. However, most developments are related to the Laxemar subarea. The principal achievements and developments since the Simpevarp 1.2 model are summarised below.

- The surface system models feature an improved soil model. This model takes into account new data on depth and stratigraphy of Quaternary deposits. Furthermore, the model area considered in the process-based hydrological modelling has been enlarged compared to that in Simpevarp 1.2. The GIS-based hydrological model, which covers the whole regional model area, has not been updated since the previous model version.
- An increased understanding and confidence in the surface distribution of rock domains in the local scale model area has been achieved, including an updated and refined two-dimensional rock domain model. This is primarily attributable to the new detailed bedrock map of the Laxemar subarea and surroundings. Considering only the Laxemar part of the local scale rock domain model, the RSMA01 and RSMD01 domains dominate the northern to northeastern and the southern to southwestern part, respectively.
- The updated deformation zone model includes an increased number of high confidence zones in the Laxemar subarea compared to Simpevarp 1.2. Most medium confidence zones, however, are still without verification. Increased confidence in the surface expression of deformation zones along the coastline of Ävrö and Simpevarp has been achieved by introducing new bathymetric data in the digital elevation model (DEM). The geological thickness has been assessed for the high confidence zones. The model includes a subhorizontal zone in the Laxemar subarea, although at great depth. There is a high degree of confidence that no sub-horizontal zones of regional significance exist at shallow depth in the Laxemar subarea although possible subhorizontal zones of local major character (or smaller) cannot be ruled out at present and will be further investigated. An alternative deformation zone model has been developed from which low confidence deformation zones are excluded.
- An alternative lineament interpretation performed by an independent team increases confidence in the lineament map used as a basis for the deformation zone model.
- The developed geological DFN-model, which introduces new data from boreholes KLX03 and KLX04, provides parameterisation for different rock domains and also for the Laxemar and Simpevarp subareas. The model is verified against available outcrops, but does not fit borehole data very well.
- The rock mechanics property model is updated, with quantified uncertainties for parameters included in the model. The increased confidence and the basis for quantification are due to better rock mechanics property data which increase confidence in the intact rock mechanics properties description. Likewise the confidence in laboratory data on fracture mechanical properties

has improved. These two improvements provide a better support for the empirical rock mass classification. Similarly, the theoretical approach to rock mass properties is improved due to use of the rock domain-specific DFN-model and the observed relation between fracture intensity and rock type.

- The rock stress model has been updated by considering additional deformation zones and changes in geometry of existing zones, whereby also the Laxemar subarea is divided into two stress domains.
- The thermal model features an improved understanding of the spatial variability in thermal conductivity within domain RSMA (dominated by Ävrö granite), cf. Figure 13-1. No significant changes in mean thermal conductivity relative to SDM Simpevarp 1.2 are observed. The average thermal conductivity for domain RSMD (dominated by quartz monzodiorite) is somewhat higher (2.70 W/m×K) in Laxemar 1.2 than in Simpevarp 1.2 (2.62 W/m×K). Modelling results are reported for rock domains RSMBA and RSMM, which were not modelled in Simpevarp 1.2. Results suggest potentially low thermal conductivity in domain M, which constitutes a mixed domain with a high fraction of diorite and gabbro.
- Collected hydraulic data provide a clearer definition of hydraulic rock domains (HRD) and the fact that they mainly coincide with defined geological rock domains (RD). Assessed data (including old data) from different test scales show a tendency for a decreasing hydraulic conductivity with depth, both in deformation zones (DZ) and in the rock mass between the DZs.
- A strong coupling between hydrogeology and hydrogeochemistry is acknowledged, and this coupling is also honoured in the modelling work. In the hydrogeological modelling, density effects introduced by variable salt content are accounted for and simulation results are compared with the present distributions of salinity and water type. It was found that it is non-trivial to match the hydrogeological model to the measured chemical data. Although most efforts were directed towards elucidating noted differences using altered parameterisations of the underlying HRD properties, it was found that assigned hydraulic boundary conditions at the upper horizontal surface were equally, or even more important.
- Only a few additional representative water samples are available for the Laxemar subarea. The sharp depth trend in salinity suggested by KLX02 is not fully substantiated by the new data. Evaluation of tritium data has shown the limitations and possibilities in using such data for further modelling. The importance of microbial activity for redox conditions has been evaluated (but the model is still uncertain due to limited data).
- Improvement has been achieved in the methods and tools used to model the chemical changes associated with water mixing and water/rock interactions by the application of sensitivity analyses of the mixing models and expanding the reactive transport capabilities including the actual information of fracture filling minerals.
- The current bedrock transport model provides site specific data from the Laxemar subarea on porosity, diffusivity and sorption. Furthermore, flow-related transport parameters are quantified from the analysis.

13.2 Current understanding of the site

In this section a condensed description is provided of the current understanding of the Simpevarp area, with special emphasis on the Laxemar subarea. Special attention is given to integrated understanding and conjectures made using evidences from one or more disciplines in combination.

The description and account given here should be regarded as a short and portable compilation of the collective understanding of the Simpevarp area as of model version Laxemar 1.2.

13.2.1 General understanding of the Laxemar subarea

In the execution programme for the Simpevarp area /SKB 2002b/, a number of important site specific questions were formulated. They concerned; *”size and locations of rock volumes with suitable properties, location and importance of fine-grained granite bodies and deformation zones,*

high rock stresses, thermal conductivity of the bedrock, rock mechanics properties of rock mass, and ore potential”.

In the following, condensed resumes are given of current understanding partly addressing the above issues, but also related to other important issues and aspects of the Laxemar subarea, as inferred from the Laxemar 1.2 modelling.

Topography and the surface system

The Laxemar subarea is characterised by a relatively flat topography (c. 0.4% overall topographical gradient), which largely reflects that of the underlying bedrock surface, and is characterised by a high degree of bedrock outcrop (38%). However flat, the landscape is interrupted by occasional narrow valleys, often associated with fracture zones in the bedrock. Till is the dominant Quaternary deposit which covers about 45% of the subarea. A 3D stratigraphical model of the overburden with Quaternary and other sediments and deposits has been developed. This model has been used to improve the description of the surface hydrology and near-surface hydrogeology, and has also been considered in the hydrogeological modelling of the deep rock.

The *modelling of ecosystems* (terrestrial and aquatic) in terms of pools and fluxes introduced in SDM Simpevarp 1.2 has been further developed using data from an enlarged model area covering most of the Laxemar subarea. Furthermore, the marine ecosystem model now covers a series of sub-basins along the coast from Uthammar to Kråkelund. Thus, knowledge of the functional aspects of the ecosystems at the regional scale has improved. Also, with the enlargement of the studied drainage area, site-specific knowledge of the Laxemar subarea has been gained. The *major pools of carbon* in the ecosystem are found in the soils and sediments, where also the longest turnover times for carbon are found. The model places new and stronger constraints on potential variations in the future states of ecosystems in the landscape. This in turn reduces the uncertainties in estimating radionuclide transport and related consequences to man and the environment that are of importance in subsequent Safety Assessment.

Rock domains, thermal and mechanic properties

Four main *lithological domains* have been defined in the Laxemar subarea, a domain RSMA which is composed mainly of Ävrö granite and which dominates the northern and central parts of the subarea, a domain RSMD consisting mainly of quartz monzodiorite, which together with a mixed domain RSMM (diorite to gabbro) dominate on the surface in the southwest and dip in an arc-shaped fashion to the north with the concave side to the north, cf. Figure 13-1. Embedded in the RSMM domain are found smaller bodies of rock domain RSMBA (constituting a mix of Ävrö granite and fine-grained dioritoid). Furthermore, a conspicuous rock domain (RSMP) is related to the north-easterly oriented set of shear zones which make up the eastern boundary of the subarea. The latter domain is characterised by a high frequency of low-grade ductile to brittle-ductile shear zones in the rock types transected by the low-grade ductile shear belts making up the domain.

Lithological heterogeneity in the bedrock is introduced in the Laxemar subarea in the form of subordinate rock types (dykes, enclaves or minor bodies in the dominant rock type, mainly fine-grained granite and pegmatite). An additional contribution to heterogeneity is provided by a general mixture of different rock types of different composition and character, compositional variations within a dominant rock type, and combinations of the mentioned contributions.

A conspicuous characteristic of the gabbroid-dioritoid-syenitoid-granite rocks of the Simpevarp area is their *low quartz content*. The higher the quartz content the higher the thermal conductivity. The quartz content also shows a large variability as evidenced by Figure 13-1 which indicates that the diorite to gabbro and quartz monzodiorite domains (RSMBA and RSMD) have the lowest quartz content. The results of the modelling of thermal conductivity, cf. Figure 13-1, show mean values of the thermal conductivity on the 0.8 m scale in the order of 2.7 to 2.9 W/mK and also show a high variability. The bimodal distribution of thermal conductivity suggested by the resulting distributions for domains RSMA and RSMBA, suggest that these domains can be further divided in a quartz-rich and a quartz-poor variety. Such further subdivision will be pursued in future modelling.

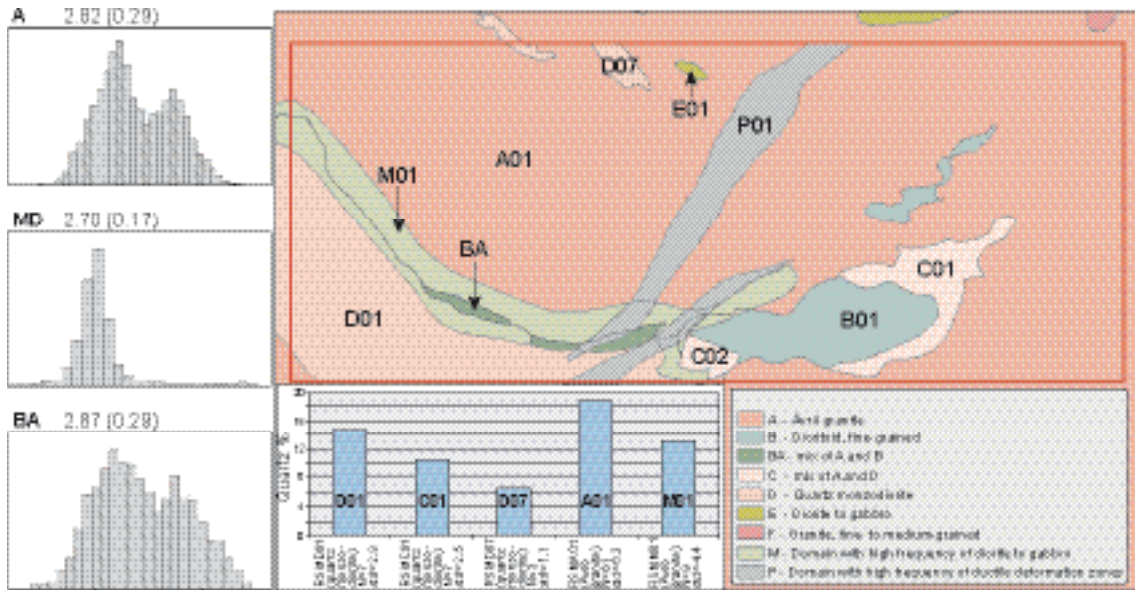


Figure 13-1. Composite showing rock domain model (upper right), variability in quartz content of rock domains (as inferred from surface samples) (lower central) and modelled distributions and recommended mean and standard deviation by rock domain of thermal conductivity for 0.8 m scale (left).

The rock mechanics properties of the intact rock are estimated from new laboratory tests on drill cores. Especially, the uniaxial strength depends on rock type, with the lowest strength in quartz monzonite to monzodiorite, i.e. a rock type found in the RSMD domain of the Laxemar subarea. Quantification of mechanical properties of the naturally fractured rock mass and rock associated with interpreted deformation zones is supported by new data on intact rock, underpinned by empirical and theoretical relationships. The former makes use of the Q-index whereas the latter approach makes use of large scale numerical loading tests of simulated fractured rock blocks under confining stress. The modelled results for the Laxemar subarea indicates a deformation modulus E_m for a rock mass at repository depth and at high confining stress of about 55 GPa. Correspondingly, a shallow deformation zone at low confining stress shows a deformation modulus of about 38 GPa. These model values for the deformation modulus E_m compare well with the absolute magnitude and relative difference for E_m estimated at the shallow Clab excavations and at the deeper Äspö HRL, 40 and 55 GPa (Section 6.3.6), respectively.

Deformation zones and fracturing

The model of deformation zones is primarily based on the updated lineament map, cf. Figure 13-2. Of the 35 zones attributed a high confidence of existence, five zones have been added since SDM Simpevarp 1.2. For the most part, the SDM Simpevarp 1.2 interpretations of deformation zones in the Simpevarp subarea are retained. Most changes to the model have been made to zones in the central parts of the Laxemar subarea, involving geometry (dip and extent) and degree of confidence. Additional support for the underlying lineament map is provided by an independent alternative lineament interpretation. A new entity in Laxemar 1.2, however, is the subhorizontal zone (ZSMNW928A) interpreted from reflection seismics and borehole data, and shown to be located well below typical repository depth (> 770 m, compared with 500 m) in the central parts of the Laxemar subarea.

The bedrock in the Simpevarp area, which generally is well preserved and undeformed, has been exposed to a series of tectonic events which have involved shifts in the direction and magnitude of compressional forces exerted on the rock mass, as discussed in Section 5.4.2. Characteristic ductile features in the Simpevarp area are the occurrences of low-grade brittle-ductile shear zones made up of the northeasterly belt of zones associated with deformation zones ZSMNE005A (Äspö shear zone) and ZSMNE004A, which also make up the rock domain RSMP discussed above, cf. Figure 13-1.

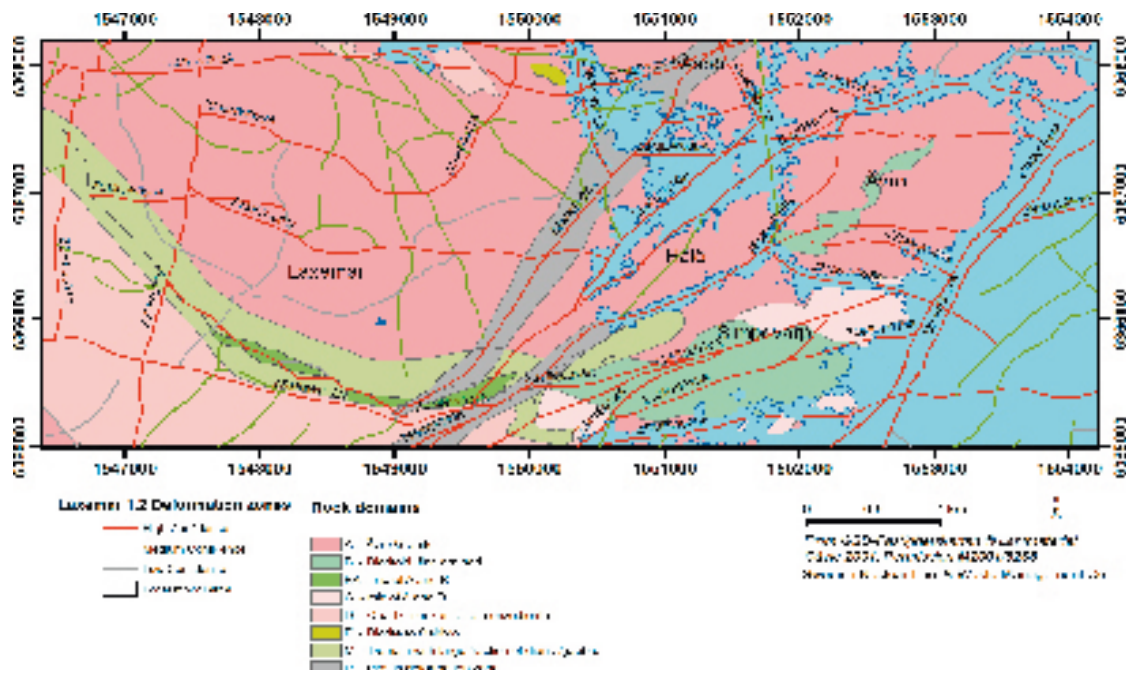


Figure 13-2. Illustration of the base case deformation zone model with high (red), medium, (green) and low (grey) confidence zones within the local scale model area. The alternative deformation zone model consists only of the high and medium confidence (red+green) deformation zones.

In the Simpevarp subarea the distributional pattern of deformation zones largely align with the belt of shear zones in the western part of the Simpevarp subarea. In the Laxemar subarea, north of zone ZSMNW42 and the contact between the Ävrö granite and the quartz monzodiorite, the geometrical pattern of interpreted deformation zones is more irregular, although the principal orientations deformation zones are NS and EW. Currently ongoing kinematic and fracture mineralogical studies are expected to shed more light on the evolution of the deformations in the area, and why the current differences exist. Current understanding, however, indicates that the Simpevarp subarea is more strongly affected by the occurrence of the above shear zones than the Laxemar subarea, supported by a more banded pattern in the magnetic anomaly map of the Simpevarp subarea, and suggesting that the two subareas may be considered as two different structural domains, at least in respect of the frequency in ductile overprinting.

Also the analysis of the fracturing in the rock mass between interpreted larger deformation zones, and the variation in local fracture orientations suggests, together with results from the deformation zone model, that the Simpevarp subarea is located within a belt of shear zones and exhibits significantly different fracture behaviour from that of the Laxemar subarea which is located outside of this belt.

The analysis and display of fracture orientations reveal five sets; three regional sets (S_A, S_B, S_C) observable in both outcrop and in deformation zone traces in the two subareas and two local sets typical to their respective subareas (S_d and S_f/S_e, respectively), where S_d represents the subhorizontal set in each subarea.

The Laxemar 1.2 geological DFN orientation model is based solely on fracture patterns observed in outcrop, and may not necessarily match conditions found at depth. Fracture size analysis shows that regional fracture sets can be approximated by power-law size models. Local fracture sets are censored by the outcrop sizes such that alternate size models have a better statistical fit, but this would not necessarily be the case if the spatial extent of the exposures was larger.

Fracture intensity is shown to be dependent on subarea, somewhat dependent on the rock domain, and locally dependent on host rock lithology, fracture ages, degree of alteration, and presence of ductile or brittle deformation zones. This is indicated by intensities (P_{32} of all fractures) of the

regional sets in the domain RSMA of the Laxemar subarea varying between 1.4 to 1.7 m⁻¹, and the corresponding intensities in the Simpevarp subarea being some 30–100% higher.

Verification exercises on the average show a fair show correspondence in outcrop, but also show that outcrop and borehole intensity cannot be matched simultaneously at present, cf. Section 5.5.3.

Relationship between deformation zones and rock stress distribution

Modelling for SDM Simpevarp 1.2 indicated that rock stresses could be defined in two different stress domains, where stress Domain II showed relatively low stress levels. This situation, supported by numerical stress modelling, was attributed to unloading of a wedge-shaped rock volume underneath the Simpevarp peninsula and Hälö and Ävrö islands, as delineated by the intersecting deformation zones ZSMNE012A and ZSM024A. For the Laxemar subarea and SDM Laxemar 1.2, and in analogy with the situation at Simpevarp, lower stresses (Domain II) are also attributed to the wedge-shaped rock delineated by deformation zones ZSMEW002A and ZSMEW007A. In Domain II with lower stresses the magnitude of the maximum principal stress (σ_1) at 500 m in the Simpevarp subarea is estimated at 11 to 21 MPa, and between 25 to 42 MPa in the remainder of the modelled area (Domain I), cf. Figure 13-3. However, at least for potential repository depths, most of the local model volume in Laxemar subarea appears to lie within stress Domain I, i.e. the domain with the relatively higher stress levels.

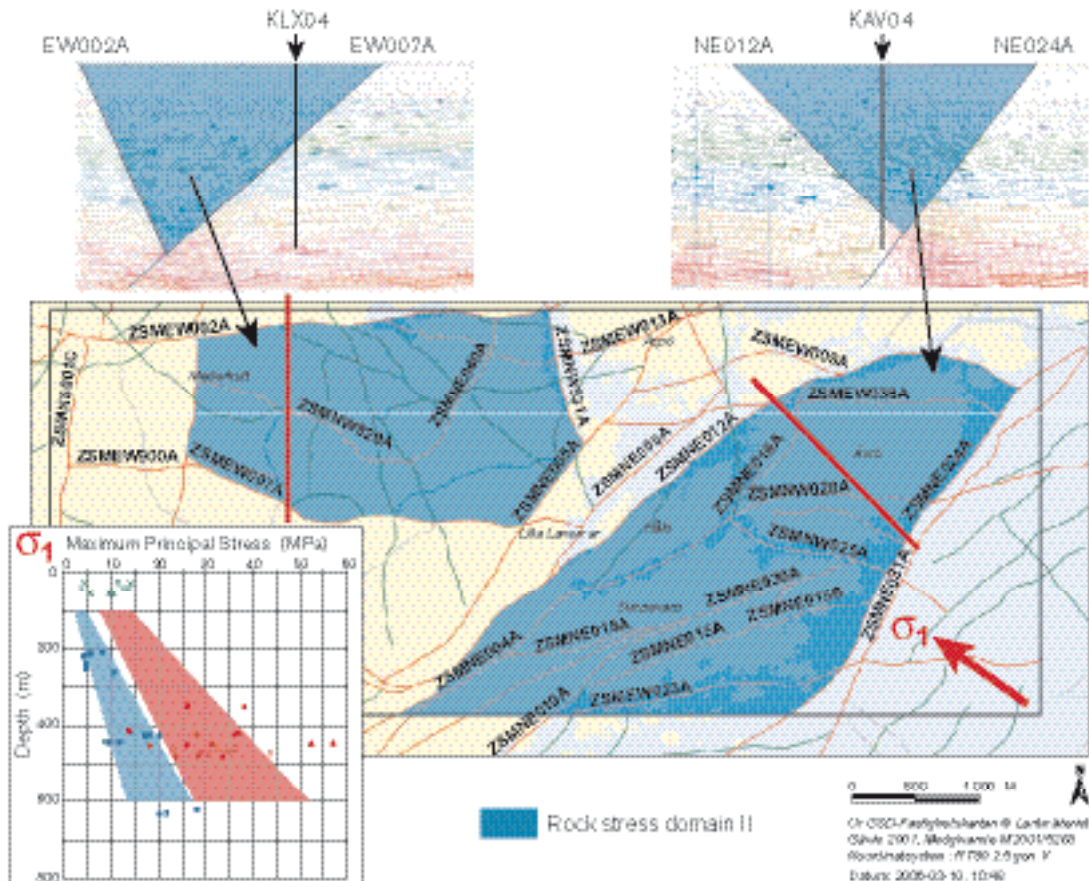


Figure 13-3. Composite showing map of deterministic deformation zones in the background with stress domains indicated by colour; measured rock stresses mapped by stress domain (lower left, Domain I=red, Domain II=blue), and sections through the 3D stress model showing effects on the stress field induced by wedge-shaped block unloading (upper left and upper right). Current maximum principal stress indicated at lower left.

Hydraulic properties and their geological controls

Analysis of the hydraulic test data from deformation zones and intervening rock mass shows indications of hydraulic properties decreasing with depth. This is unlike the situation at Äspö HRL where no such dependence has been noted. Hydraulic properties have been assigned to hydraulic rock domains (HRDs) defined based on the underlying rock domains defined by geology. The tectonic and structural differences between the Simpevarp and Laxemar subareas are also reflected in the model description of the hydraulic rock domains where e.g. HRD(A) (Ävrö granite) is subdivided in one prismatic body covering the Simpevarp subarea which has been attributed increased hydraulic conductivities compared with the remainder of the Ävrö granite in the Laxemar subarea. Young granitic intrusions (Götemar and Uthammar) and fine-grained granites are assigned an increased hydraulic conductivity compared with Ävrö granite. Rock domains including quartz monzodiorite and diorite (HRD(D), HRD(M) and HRD(B,C)) are all assigned values significantly lower than HRD(A). The relative magnitudes of the identified hydraulic rock domains are shown in Figure 13-4. It should be pointed out that the low hydraulic conductivity of the quartz monzodiorite at present is only supported by a small number of data above the measurement limit.

The analysis using the developed hydraulic DFN model indicates that the intensity of flowing fractures does not vary significantly between rock domains apart from a lower intensity estimated for the domain D and the mixed domains M. This is in conformity with the variation in hydraulic properties between hydraulic rock domains as discussed above. However, the few borehole data and the strong variability in hydraulic properties found in and between boreholes does not allow for a firm affirmation of the representativity of neither the depth dependence nor in the domain-related differences. Furthermore, the use of one single transmissivity model for all fracture sets is questionable while PFL flow log data from the Laxemar subarea (KLX04) indicates Sets A (NE) and B (NNE) having 0.5–1 order of magnitude lower transmissivity than Set d (Subhorizontal), where furthermore Set C (WNW) have up to 0.5 to 1 orders of magnitude higher mean transmissivity than Set d. However, the current analysis is essentially based on data from borehole KLX04, and can at this time be regarded as indicative only. The noted anisotropy, with a higher hydraulic conductivity in the WNW(-NW) fracture set, is in accord with the principal horizontal stress direction, and also corroborates earlier findings on hydraulic anisotropy from the Äspö HRL, although much less pronounced.

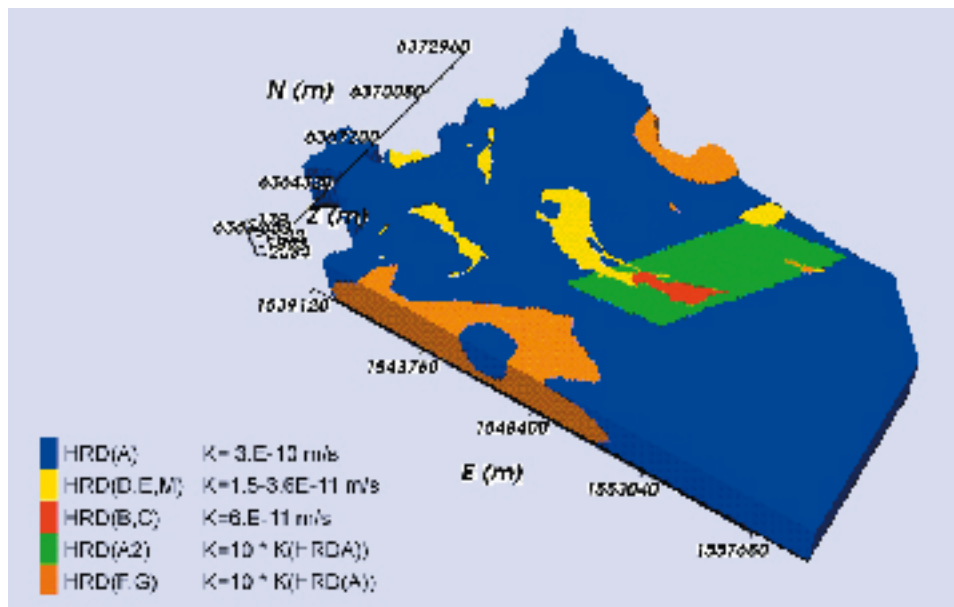


Figure 13-4. Overview of hydraulic properties of hydraulic rock domains (HRDs). Mean values of PFL-measurements (3 m/5) in hydraulic domains (HRDs) in the Simpevarp area. The green rhombohedral area corresponds to increased hydraulic conductivity in the part of HRD(A) (Ävrö granite) which is located in the Simpevarp subarea.

Groundwater flow and hydrogeochemistry

The general flow direction through the modelled area is determined by the overall topographical gradient towards the Baltic sea. The controls of the flow are apart from the hydraulic gradient also the geometry and properties of the hydraulic rock domains (rock mass) and the hydraulic conductor domains, as discussed above. The marked difference in groundwater circulation between the Simpevarp and Laxemar subareas, with deeper developed circulation cells at Laxemar, also affects the distribution of groundwater chemical characteristics. The hydrogeochemical conceptual model has been developed in close collaboration with hydrogeology. The conceptual hydrogeochemical model is shown in Figure 13-5 together with a corresponding WNW section through the base case hydrogeological flow model mapping total dissolved solids (TDS).

Four groundwater types have been identified in the Simpevarp area, cf. Figure 13-5; the Type A (dilute and mainly of Na-HCO₃) is found at shallow depths (< 100 m), Type B (brackish, mainly Na-Ca-Cl) at shallow to intermediate depths (150–300 m), Type C (saline (6,000–20,000 mg/l Cl, 25–30 g/L TDS), mainly Na-Ca-Cl) at intermediate to deep levels (> 300 m). Type D (highly saline, > 20,000 mg/l, max TDS ~ 70 mg/l), only seen in KLX02 at depths > 1,200 m.

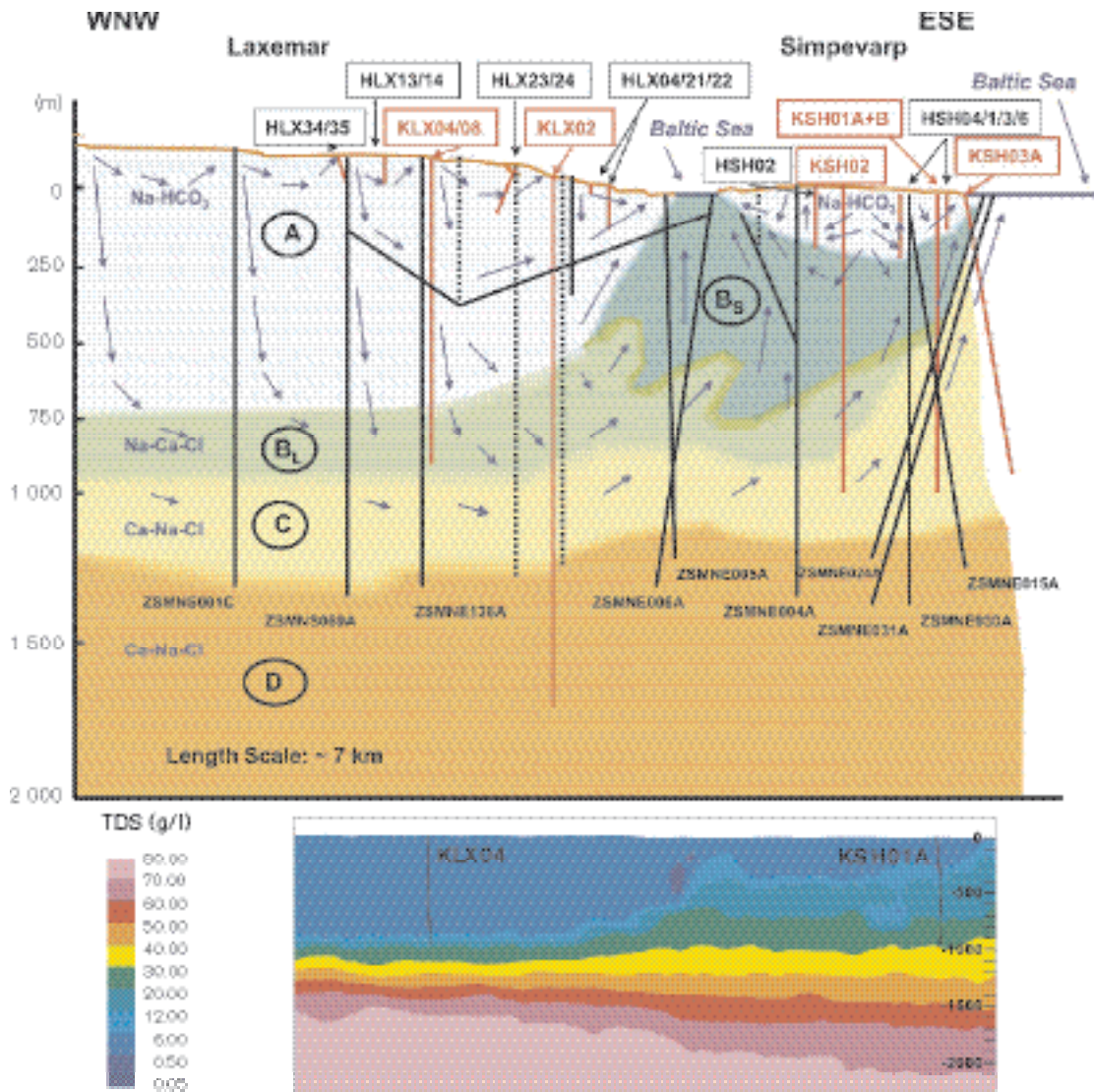


Figure 13-5. Composite showing a comparison between the conceptual hydrogeochemical WNW section (top) and the corresponding section through the regional scale base case hydrogeological model showing the distribution of total dissolved solids (TDS) (bottom).

Bedrock transport properties

BET surface area measurements (see Chapter 10) on intact rock samples indicate that relative sorption strengths (strongest to weakest retention) should approximately follow the order: Fine-grained dioritoid/Fine grained diorite-gabbro > Ävrö granite > diorite to gabbro > quartz monzodiorite although the differences between the various rock types are likely to be very small.

From the available data, Ävrö granite appears to have a higher formation factor (associated with higher retention, see Chapter 10) than the other rock types. Although this could be an artefact of sampling bias, the trend appears to be consistent for data obtained from both the Laxemar and Simpevarp subareas, with Ävrö granite having roughly a factor four times higher formation factor than the other rock types, which appear to have formation factors of roughly the same magnitude.

The single largest uncertainty is currently related to the estimation of the transport resistance (F-factor). It can be shown quantitatively that the uncertainty in arrival time for a given solute is directly proportional to the uncertainty in individual retardation parameter (i.e., specifically K_d and D_e , although more commonly the product of these two entities). For the transport resistance (F-factor), however, the arrival time is quadratically related to the value of the F-factor and the uncertainty in this parameter therefore has a strong impact upon model predictions. The F-factor is simultaneously the least well understood parameter as well as the most important parameter uncertainty for predicting radionuclide residence times in safety assessment modelling of radionuclide transport. This uncertainty in the F-factor will be reduced by a combination of modelling and additional transmissivity data from PFL-logging during the coming stages of the site investigations.

13.2.2 Uncertainties, alternatives and integration of models

As discussed in Chapter 12, the available primary data have been analysed and treated according to acceptable practices. Furthermore, inaccuracies and biases are understood and accounted for in the subsequent modelling. However, the biases introduced by the absence of more gently dipping boreholes makes corrections of fracture orientation biases very difficult and also raises concerns about the possibility to predict the anisotropy of the transmissive features. There are also questions about the representativity of the rock mechanics, thermal, hydrogeological and hydrogeochemical samples. There are generally few data at depth from rock domains where the potential repository might be located. These biases are hard to account for without getting access to more representative data.

More of the uncertainties are now quantified, or explored as alternatives. Notwithstanding, several hypotheses remain to be tested and some uncertainties remain to be quantified. Some uncertainties are related solely to the overall understanding of the site and do not have direct implications for safety assessment or repository engineering, whereas others have more significant implications. Those important uncertainties that have direct and quantitative implications for safety assessment are as follows.

- The sizes, intensity and transmissivities of fractures in the rock mass between interpreted deterministic deformation zones are uncertain. Strong arguments cannot be made at present that data from individual boreholes in the Laxemar subarea can be regarded as representative for the hydraulic properties of the rock domains they sample. Inherent in this statement is that (lateral) spatial variability is considered not to be captured adequately. Furthermore, there is very little hydraulic conductivity information for the quartz monzodiorite (RSMD) and gabbro/diorite (RSME) in the southwestern part of the Laxemar subarea.
- Uncertainties in stress and intact rock strength affect the potential risk of thermally induced spalling in deposition holes.
- The uncertainty in the estimation of flow-related transport parameters (i.e. the F-distribution), is partly due to uncertainties in the underlying hydraulic DFN model but also due to uncertainties in the conceptual model for migration (i.e. how the F-distribution is calculated).

Some of these uncertainties are important also for repository engineering

Clearly, also the uncertainty in the occurrence, geometry (dip, thickness and extent) of deformation zones and to a lesser extent the uncertainty in the transmissivity (including heterogeneity) and hydraulic connectivity of these zones is important for safety and for engineering. Some zones in the Laxemar subarea have not yet been probed by boreholes.

Uncertainties related to magnitudes and spatial variability, possible anisotropy and up-scaling of thermal conductivity have direct implications for repository engineering, given the relatively low thermal conductivity of the rocks in the Simpevarp area. The established groundwater compositions in the Simpevarp area fulfil the present suitability criteria by margin. However, there is only a limited number of new representative chemical data from the Laxemar subarea in the current data freeze. However, given that these uncertainties are of importance for the understanding of the past hydrogeochemical evolution, they are also relevant as an independent control of hydrogeological models, and underlying material property models, used to predict past and future evolution of groundwater chemistry in the Simpevarp area.

Uncertainties in rock mechanics properties, rock stresses and thermal properties are quantified. Uncertainties in the occurrence and geometry of deterministically modelled deformation zones have been illustrated by providing two different models, the consequences of which have been explored in the hydrogeological modelling. The hydrogeological modelling has also involved a large number of sensitivity cases which have been used to illustrate various effects related to boundary conditions, hydraulic properties of deformation zones (including depth dependence), hydraulic properties of fractures between deterministic deformation zones (including assumptions related to the underlying DFN model). Uncertainties in the hydrogeochemical model have been addressed by using alternative modelling approaches to the same data set. A novelty in the Laxemar 1.2 work has been to analyse the sensitivity in the M3 calculations of water composition by allowing for an inherent uncertainty in the definitions of the different extreme water types making up the end members of the model.

As demonstrated in Section 12.4, there are many important interactions between the various disciplines, many of which have in fact been considered in the development of the SDM Laxemar 1.2. Overall, the current discrepancies between the needed interactions and the interactions actually considered are not considered a major problem for confidence in the SDM version 1.2 of the Laxemar subarea.

The Laxemar 1.2 site-descriptive model is in also in overall agreement with the current understanding of past evolution as described in Chapter 3 and partly in Section 5.4 (deformation history) as discussed in Section 12.5. Furthermore, the hydrogeological modelling of groundwater chemical evolution arrives at reasonable present day groundwater compositions when compared with borehole data.

The understanding of the Simpevarp area, and specifically the Laxemar subarea, has overall been confirmed by the outcome of the Laxemar 1.2 modelling. No major surprises have arisen in the modelling in relation to what was known by Simpevarp 1.2. Changes of the rock domains are significant in the local scale model volume, particularly in the Laxemar subarea. The rock domain model is definitely stabilising, but will certainly be refined by use of forthcoming new data from cored boreholes. The changes to the deformation zones in the Laxemar subarea mostly concern details, but there are still important uncertainties, since there are several medium and low confidence zones inside the Laxemar subarea. Partial support for the deformation zone model is provided by the alternative lineament interpretation made by an independent team. In contrast, the modelling of the fracturing, thermal and hydraulic properties of the rock volumes between deformation zones in the rock mass (in potential deposition areas) is still not stable, due to few representative data.

In summary, more quantitative data and in particular more subsurface data have been produced for the Laxemar 1.2 modelling. Despite this, there are still uncertainties in the deformation zone model in the local scale model area, where a number of zones still require direct confirmation through drilling. This implies both uncertainties in geometry and material properties. These uncertainties are propagated to the hydrogeological model. In the case of the latter, there are also uncertainties related to the hydraulic properties of the fracture network within the rock mass. A partial support for the current hydrogeological model is provided by comparing predicted hydrogeochemistry with that measured. Although important steps have been taken with regards to structural controls

(deformation zones and fracturing) on hydraulic properties, there is a need to further improve the understanding of the hydraulic properties of the rock mass (in potential deposition areas) and important deformation zones, and in this order of priority.

13.3 Implications for future modelling

The model version Laxemar 1.2 presented in this report concludes the site-descriptive modelling using data collected during the Initial Site Investigation phase at Oskarshamn. The subsequent modelling associated with the Complete Site Investigation phase (CSI) will be made in three steps. The first step (Laxemar 2.1) is limited in scope and is primarily directed towards providing feedback to the site. The subsequent steps Laxemar 2.2 and Laxemar 2.3 are mainly to resolve, on a continuous basis, the remaining uncertainties which are important for repository engineering and safety assessment. The following sections address important aspects related to further modelling, in the perspective of the principal objective and scope of the first modelling step (Laxemar 2.1) during CSI.

A decision in principle has already been taken to proceed with investigations in the Laxemar subarea, the final decision pending the Laxemar version 1.2 SDM results presented in this report and the results of the associated preliminary safety evaluation. It is in this context worth pointing out that the preliminary safety evaluation of the Simpevarp subarea, based on the SDM Simpevarp 1.2, showed that, even considering remaining uncertainties, the Simpevarp subarea meets all safety requirements and most of the safety preferences /SKB 2005e/. However, the available space for potential deposition areas is limited at the Simpevarp subarea.

13.3.1 Technical aspects and scope of the Laxemar 2.1 modelling

The modelling step Laxemar 2.1 will make use of all data available as of June 30 2005, which constitutes the data freeze Laxemar 2.1. Laxemar 2.1 modelling work has been started up during 2005 with support from the modelling team in relation to the selection and argumentation of understanding for the focussed area in the Laxemar subarea /SKB 2005f/ and in helping to devise a site investigation programme for the CSI /SKB 2005c/.

One important aspect of the Laxemar 2.1 modelling concerns the size of the local model volume. For SDM Simpevarp 1.2 and SDM Laxemar 1.2 a local scale model volume hosting both subareas has been employed. However, for Laxemar 2.1 a need was identified to reduce the local model area in order to enable increase in resolution and to reduce the overall uncertainty in the description. This will also improve the handling of 3D models in RVS and will also enable representation of variability in the geological, rock mechanics and thermal descriptions, with special emphasis on the area prioritised for a potential repository. Updated regional geological models of rock domains and deformation zones, the latter partly based on a revised lineament interpretation, are foreseen for Laxemar 2.1, plus an interim local scale geological model.

Additional important geological aspects to be considered in the future modelling concern:

- Taking into account relevant aspects of the alternative lineament model.
- Inclusion of new high-resolution airborne laser scanning (LIDAR) and corresponding new improved surface geophysical data (in particular expected to further inform size distribution of structures (in the interval 30–500 m) and the characteristics of local minor deformation zones).
- Taking into account new information from new deep cored boreholes targeting deformation zone ZSMEW007A.
- Quantitative address of uncertainties in the geological DFN model. Further study of the representativeness of developed models for rock domains.

It is important that identified feedbacks from other disciplines are incorporated in the development of the next version of the geological model. This concerns for example the following aspects:

- Feedback from bedrock hydrogeology that can confirm both existence and extent (from hydraulic connectivity) of interpreted deformation zones. However, for the most part this information relates to superficial parts of zones sampled with percussion boreholes.

- What fracture mineralogy can tell about formation and reactivation of fractures and deformation zones. This includes studies of calcite generations (relative datings) and preferred locations and orientation of fractures.

Examples of other aspects to consider for future modelling include:

- Current redox conditions and projection of future development. Controls (incl. microbes), analysis of depth, extent and spatial and temporal variation of the redox front (calcites, uranium series), investigation of oxidation state ("Red staining" and FeII/FeIII ratios in altered and unaltered rock)
- Matching of near-surface and deeper hydrogeology, and correspondingly for hydrogeochemistry.

13.3.2 Modelling procedures and organisation of work

Further experience has been gained on procedures and organisation of the modelling work during the Laxemar 1.2 modelling. Interdisciplinary modelling is a continuous learning process which will continue to develop throughout the site descriptive modelling.

The capture and evaluation of primary data is a very demanding effort. In the Simpevarp area, with descriptive models produced both for the Simpevarp and Laxemar subareas, this has with time become more burdensome as the amount of data increase for each successive model version. A challenge for the future work is to safeguard that data collected from the data bases are not processed repeatedly, such that the major effort can be put on the analysis and modelling.

Already during the work on the Laxemar version 1.2, and perhaps more during the early round of Laxemar 2.1 work, the interaction between the site modelling team and site investigation, as well as between the site modelling team and the principal clients of the site-descriptive modelling has increased and improved. The establishment of discipline-specific NET groups, cf. Section 1.4.3, has further facilitated this interplay since for the most part representatives of all three producer and client categories are represented in these groups. In addition, representatives from the site investigations and repository engineering actively follow the progress of the modelling work by participating in project group meetings and related seminars.

Significant improvements have also been made in the integration between disciplines in the modelling work. Since the NET-groups handle most of the discipline-specific questions, it has been possible for the project group to focus on integration issues.

Another important component supporting integration and information exchange has been the workshops held for assessing uncertainty and confidence. These types of workshops will continue, but with objectives and participation adapted to the focus of the current modelling. For example, a workshop during modelling step 2.1 will focus on identifying remaining uncertainties that require additional field data, with participation from the modelling project, the site investigation team and also from repository engineering and safety assessment. The prime aim of such a workshop would be to capture relevant feedbacks from the results of the design work and safety assessments based on Laxemar model version 1.2.

13.4 Implications for the ongoing investigation programme

The recommendations arising from the work with model version Laxemar 1.2 are divided firstly into recommendations or feedback that have been given to the site investigation organisation during the course of the modelling work, and secondly, recommendations that have emerged predominantly from the uncertainties in model version Laxemar 1.2.

A complication, or rather a sorting problem, arises from the fact that the modelling team has been engaged in Laxemar 1.2 and Laxemar 2.1 activities simultaneously. It is not the intention here to give an account in detail of the preliminary Laxemar 2.1 work, discussed briefly in Section 13.3.1. Instead an account is given as to the direct feedback given during the process. It goes without saying that the boundaries between a clear-cut distinction between a recommendation based on Laxemar 1.2 modelling alone, and a recommendation informed by subsequent work, in some instances is very difficult to assure.

13.4.1 Recommendations provided during the modelling work

During the work with model version 1.2, the project group has had continuous information exchanges with the site investigation team, e.g. concerning questions related to the location of drilling sites, location and orientation of cored boreholes, programme for verification of lineaments in the Laxemar subarea and of a more detailed character (e.g. sampling procedures and methods for various tests).

The recommendations related to borehole positions and geometries, primarily of cored boreholes, have not been formally documented in decision papers established by the modelling team. Rather, the recommendations are recorded in minutes from meetings with site investigations, e-mailed recommendations, and ultimately in decision memoranda established by site investigations.

Recommendations concerning drilling of new boreholes

Given SKB's decision in principle to prioritise the Laxemar subarea to the Simpevarp subarea, the recommendations made concerning new cored boreholes are entirely directed to the Laxemar subarea.

During the course of Laxemar 1.2 modelling, the modelling team has provided multi-disciplinary input to four cored boreholes; KLX07, KLX08, KLX09 and KLX10.

The objectives of boreholes KLX07 and KLX08 are to obtain information on the geometry and thickness of deformation zone ZSMEW007A in the central parts of the Laxemar subarea. The separation of the boreholes is approximately 1 km. The geometry of the boreholes was selected in order to penetrate the zone in the case that it is vertical or is dipping north. Furthermore, the collar positions were selected such that the boreholes could act as pumping boreholes in conjunction with interference tests with observations in neighbouring percussion boreholes along the extent of the penetrated zone.

The objective of borehole KLX09 is to investigate the rock mass including minor local deformation zones at depth north of deformation zone ZSMEW007A. The collar position is about 1 km north of the surface expression of the zone in the central parts of the Laxemar subarea.

The objective of borehole KLX10 is to investigate the rock mass including minor local deformation zones at depth south of deformation zone ZSMEW007A. The collar position is about 1 km south of the surface expression of the zone in the central parts of the Laxemar subarea.

13.4.2 Recommendations based on uncertainties in the current site descriptive model Laxemar 1.2

Progress has been made on the site-specific issues raised in the complementary program for research and development (FUD-K) /SKB 2001a/ and subsequently in the planning document for the site investigations in the Simpevarp area /SKB 2002c/, but uncertainties in the site description still remain. The main noted uncertainties are listed and discussed in Section 12.3. Compared with version Simpevarp 1.2, more of the uncertainties are now quantified or explored as alternatives. Only some of the uncertainties have direct implications for Safety Assessment or Repository Engineering. These uncertainties mainly concern the thermal, rock mechanics and hydraulic properties of the rock mass between the deformation zones in the potential repository volumes. These uncertainties are difficult to resolve without borehole investigations targeted on these volumes. Remaining uncertainties in the geometry and properties of deformation zones are comparatively of less concern. Using these uncertainties as a starting point, the site modelling team has made an effort to assess whether the identified uncertainties can be reduced by additional data, and if so, what are those data, and how can they be collected?

In the assessments, the assumption is made that the SKB decision in principle to prioritise the Laxemar subarea in favour of the Simpevarp subarea will be fully implemented in early 2006.

Location of new boreholes

Given that much of the noted uncertainty is associated with lack of data at depth, a continued drilling programme and new borehole information (during and after completion of drilling) is expected to contribute to an improved description of the bedrock. Since the noted uncertainties foremost are associated with properties of the rock mass making up potential deposition volumes between interpreted deformation zones, proposed drilling activities are directed to such rock volumes. Such drilling is discussed in outline in this section and is detailed in subsequent sections.

As pointed out above, boreholes KLX07 and KLX08 are expected to provide the necessary platform to unveil the geometry of zone ZSMEW007A, whereas the two boreholes KLX09 and KLX10 will provide information on the rock mass north and south of ZSMEW007A in central Laxemar. Additional deep cored boreholes should be targeted in the southwestern parts of Laxemar to better characterise the rock mass made up of quartz monzodiorite, the mixed rock domains and their contacts with the Ävrö granite.

Second order priorities for deep cored boreholes are verification drilling on selected interpreted deformation zones. Furthermore, a program of shorter boreholes (< 100 m) with variable geometries (orientation and inclination) should be carried out to facilitate improved information for DFN modelling. These boreholes should also be subject to hydraulic tests and possibly also hydrogeochemical characterisation.

Characteristics and properties of potential deposition volumes

Drilling and investigation of potential deposition volumes is a prioritised undertaking, and is also expected to provide important information on rock types (domains) that have as yet been sampled only to a low degree. It is envisaged that some 4 deep cored boreholes will be required in the designated focussed area. These boreholes should be subject to the full investigation programme, and one borehole is expected to be a borehole dedicated to rock stress measurements. These boreholes are expected to provide valuable data in the fields of geology (rock types, lithological heterogeneity, fracture minerals, fracturing, minor deformation zones). Similarly the boreholes will furnish data on thermal properties and their variation, rock mechanics properties and rock stresses. Furthermore, the hydraulic test data will provide important additional data that will help assess representativity of boreholes and variability within interpreted hydraulic rock domains.

Heterogeneity of lithological domains

The heterogeneity of the interpreted lithological domains (and rock units making up the domains) could potentially affect the distribution of thermal conductivity which in turn may have implications for the positioning and layout of a possible repository. The heterogeneity is mainly induced by subordinate rock types (dykes, enclaves or minor bodies in the dominant rock type, mainly fine-grained granite and pegmatite) and gradational variation in mineralogical composition within a given domain. The effect of lithological heterogeneity on positioning and layout is deemed manageable. Likewise, the impact of lithology, and lithological variability on the actual construction of a geological repository is deemed minor or negligible. This implies that no specific action to further inform on lithological heterogeneity in the Laxemar subarea is required. The information can be collected from the boreholes drilled for other purposes.

Occurrence, geometry and properties of deformation zones

Borehole information provided for the Laxemar 1.2 modelling has furnished improved constraints of deformation zones in the Laxemar subarea; ZSMEW007A (KLX04), ZSMNW932A (KLX03) and in part (preliminary mapping available only); ZSMNW042A (KLX05), ZSMEW002A (Mederhult zone, KLX06). However, both the occurrence and geometry of interpreted deformation zones are still associated with uncertainty. This applies in particular to zones of intermediate and low confidence within the local scale model volume. In contrast to the Simpevarp 1.2 model, a sub-horizontal zone (ZSMNW928A) has been interpreted on the basis of reflection seismics and is also interpreted to intercept KLX02 and KLX04 at great depth. It is expected that the possible existence of major subhorizontal zones is largely covered by the array of seismic profiles in combination with available deep cored boreholes. However, a close scrutiny in search of the possible existence of such

zones will be required also in the future site investigations and modelling work. This is particularly true for local subhorizontal zones of minor extent. This implies that there may still be yet undetected zones which are not part of the current models. Similarly, there may be zones in the current model which are in fact not deformation zones. For obvious reasons, changes in the interpretation will primarily occur within the local scale model area.

It is expected that the new remote sensing data that will become available for Laxemar 2.1 (airborne laser scanning data (LIDAR) and new ortophoto) in combination with detailed high-resolution surface geophysics and associated field control in the central parts of the Laxemar subarea will provide a good surface platform for an improved deformation zone model. Additional support from surface data can be obtained from planned detailed ground geophysics to be performed in the western part of the Laxemar subarea.

Suggested field activities in order to eliminate or reduce uncertainties related to existence and geometry of important deformation zones are:

- Targeted drilling using cored boreholes on selected deformation zones. This applies to drilling on high confidence zones ZSMNW042A, ZSMNS001A, ZSMNS059A and ZSMEW900A and some zones of intermediate level of confidence. Notwithstanding the importance of obtaining verification of the existence and properties of the above mentioned deformation zones it is again emphasised that these boreholes come second in priority to those cored boreholes targeted on potential deposition volumes.
- Targeted percussion drilling (or short cored boreholes) and excavation of trenches on selected interpreted deformation zones of low and medium confidence.
- Cross-hole hydraulic interference tests between boreholes (where applicable, and possibly supplemented by injections of solute tracers) may provide information on the connectivity (extent) of interpreted deformation zones.

Fracture statistics and DFN modelling

An important step taken in the current model version is the verification exercise where the geological DFN model has been used to verify the P_{21} intensity of the surface outcrop and the corresponding P_{10} intensity in a borehole. The results show difficulties in obtaining simultaneous good fits of the resulting intensities in outcrop and in the borehole. This is partly attributed to the sampling problem involved and the fact that essentially only vertical boreholes are available and few measured data in the depth interval 0–100 m, but is also related to conceptual difficulties.

The airborne LIDAR and new ortophoto data available for Laxemar 2.1 are expected to fill in data in the power law size distribution model in the size range 30–500 m. Similarly, a series of short inclined cored boreholes drilled in various directions in conjunction with the KLX09 drill site (associated with detailed fracture mapping of the cleared drill site) is expected to provide useful data which will improve the DFN model. The array of boreholes will also be used for hydraulic tests (including interference tests).

The main challenge for the DFN modelling is to come up with models consistent with all underlying sampling domains and which honour correlations with rock domains. Furthermore, to undertake a closer integration between the geological and hydraulic DFN modelling, and also to assess effects of propagation of uncertainties in the DFN modelling chain.

Rock stress distribution – rock mechanics properties

The understanding of the rock stress situation in the Laxemar subarea is considered satisfactory. The explanation for low rock stresses in the Simpevarp subarea, supported by stress modelling, has been expanded with an analogous situation in the northern part of the Laxemar subarea where a wedge-shaped assumed unloaded rock block is formed by the intersecting zones ZSMEW002A (Mederhult zone) and ZSMEW007A). Additional stress measurements are planned in a borehole in south central Laxemar. The results of stress measurements in this borehole may be put in the context of interpreted deformation zones and differences in the patterns of their interpreted existence and orientation north and south of zone ZSMNW042A.

Similarly, understanding of the existence and properties of minor (stochastic) deformation zones will be improved through incorporation of the new detailed ground geophysics and the new airborne laser scanning data (LIDAR) in the geological DFN model. Efforts should be made to improve understanding of mechanical properties of deformation zones, making use of drill core material and material collected from dug trenches. It is, however, debatable whether mechanical properties of the deeper part of the deformation zone can be inferred from material collected in the dug trenches. More site-specific test results on mechanical properties of rock at depth will become available for Laxemar 2.1.

Bedrock thermal conductivity

In order to reduce uncertainties in thermal conductivity and its scaling, more representative direct measurements of thermal conductivity (TPS) are required for all rock types including samples of altered rock supplemented by data from geology on abundance and nature of alteration. Additional sampling of rock types is also needed to produce variograms to inform on spatial variability. For Ävrö granite in the Laxemar subarea more samples with both density and thermal conductivity measurements are needed including both high and low conductivity varieties. The current model suggests that the Ävrö granite is bimodal in thermal conductivity. In order to explore further this bimodality, attributed to differences in quartz content, an attempt will be made for Laxemar 2.2 to update the lithological map and divide the Ävrö granite accordingly. This would serve as a basis to further model thermal properties in 3D.

Transmissivity distribution – hydraulic tests

New hydraulic test data from the rock mass of potential deposition volumes are required in order to ascertain variability and representativeness of borehole data for given hydraulic rock domains. Of particular interest are additional flow log and injection test data from potential deposition volumes in rock domains RSMA 01 (western part), RSMD01 and RSMM01. Furthermore, the expected targeted drilling on selected deformation zones will constrain the geometry of the zones, and will also provide transmissivity data. It is however acknowledged that very few deformation zones will be sampled with more than one borehole. Hence, the understanding of variability within a given zone will remain difficult to assess. The site-specific database on HCDs is growing and allows for a attribution of a “global” statistic to describe variability. Results of ongoing kinematic studies may provide the necessary tools by which to group HCD data in a more appropriate manner.

As a complement to the geological efforts described above, any new short inclined cored boreholes with the purpose of obtaining fracture statistics should also be subject to detailed hydraulic tests to facilitate the hydraulic DFN modelling. Detailed hydraulic tests 0–100 m below surface and interference tests between these boreholes at the array of short cored boreholes at the site of KLX09 may to some extent be used to test the developed hydraulic DFN model. Similar tests in additional short coreholes are also planned for the site of KLX11. The value of this analysis for strengthening the model for the rock within the potential repository volume is limited. Interference tests at greater depth would in theory be highly valuable, but are in practice very difficult to carry out due to the generally long distances involved in the current borehole array. Even with boreholes targeted at a given network of structures, the deviations in end coordinates involved with deep boreholes produce a low degree of geometrical precision. This lack of geometrical control of boreholes, paired with the sparsely fractured nature of the rock in which the tests are conducted, may render the tests difficult to conduct and interpret. Opportunities for these types of tests are however considered on a continuous basis

Groundwater composition – pore water in intact rock matrix

There are no direct Safety or Engineering implications stemming from the uncertainties in the hydrogeochemical model. However, a further reduction of the uncertainties would enhance understanding and predictive capability. The uncertainties in groundwater composition would be reduced by more data observations from deep boreholes, analyses of rock matrix samples and data from extreme end-member waters. It is expected that the data freeze for Laxemar 2.1 will substantially increase the database of representative waters at depth at Laxemar. Similarly, samples

for rock matrix determination have already been collected and the results will be available for model version 2.1. Further constraints would exist if end-member water compositions could be obtained by additional data on extreme waters. In-situ pH measurements, more data on fracture mineralogy and data on rock matrix mineralogy (including Fe^{2+}) will reduce the uncertainty in redox processes. Finally, sampling reflecting seasonal variation from selected surface and borehole locations in identified recharge/discharge areas will reduce uncertainty in seasonal variation of chemical composition of the surface waters.

Bedrock transport properties

A major step taken in Laxemar 1.2 is inclusion of an analysis of flow-related transport parameters, which was not included in SDM Simpevarp 1.2. Uncertainties in sorption and diffusion parameters are reflected in subsequent uncertainties in salt transport and reactive (hydrogeochemical) transport modelling. However, the uncertainty in transport resistance F and its distribution under Safety Assessment conditions is far more important than the assumed smaller uncertainties in material property data. Retention properties of fractures similarly are of limited importance for Safety Assessment.

Field data that can help further reduce the uncertainty in the transport resistance F , are additional detailed hydraulic tests (PFL-data) from more boreholes in potential deposition volumes. More site specific data on diffusion and sorption parameters from rock domains of interest would reduce uncertainty in these properties. Measurements, of e.g. diffusion characteristics, on larger intact pieces of rock would possibly reduce uncertainty in scaling. Potentially, more borehole data can establish a relation between matrix properties and flow paths, but expectations for this should be set low because of the statistical nature of the knowledge of the developed flow paths.

Surface system

The main current uncertainties in the surface system model stem from lack of data on some components and in some areas, and lack of time series data. An additional aspect that is given special attention in the Laxemar 2.1 modelling is the integration of the models focusing on the deep rock and the surface/near-surface systems, respectively, especially hydrogeological and hydrogeochemical models. The associated uncertainties cf. Section 12.3, will be reduced as additional data become available. Furthermore, uncertainties related to the understanding of site-specific processes will be analysed in future model versions.

13.5 General conclusions

In revisiting the specific objectives stated for the version 1.2 modelling of the Laxemar subarea as given in Chapter 1 the following conclusions are drawn;

- The available new primary data have been adequately analysed as part of the Laxemar 1.2 modelling.
- The three-dimensional descriptive models of lithological domains and deformation zones have been updated, covering defined local and regional scale model volumes. In addition, the geological DFN model includes a verification exercise incorporating a visual comparison between the model and measured entities. The geological models have formed the basis for the parameterisation of other discipline models and have also formed the geometrical and structural basis for subsequent hydrogeological flow modelling.
- Confidence in the developed models has been treated in a systematic way as presented in Chapter 12, including assessment of uncertainties, and interactions and feedback between disciplines. The results overall show a stabilisation in developed models.
- Possible alternative models have been screened and prioritised in relation to the needs of repository engineering and safety assessment. In the current approach the alternative modelling propagated in hydrogeological flow modelling is related to alternative models relating transmissivity to feature size and the effects of not including deformation zones of low degree of confidence in existence in the flow model.

- Site-specific issues have been addressed and understanding has developed as part of the performed Laxemar 1.2 modelling as demonstrated in the preceding sections. No new important site-specific issues have been raised.
- Modelling results and identified uncertainties have been used to propose complementary investigations to further increase understanding and reduce uncertainties. A cornerstone in the recommendations is to collect data for characterising and parameterising the rock mass of potential deposition volumes in the Laxemar subarea.

14 References

- Abelin H, Birgersson L, Widén H, Ågren T, Moreno L, Neretnieks I, 1994.** Channeling experiments in crystalline fractured rocks, *J. Contam. Hydrol.*, 15(3), pp. 129–158.
- Adl-Zarrabi B, 2004a.** Drill hole KSH01A: Thermal properties: heat conductivity and heat capacity determined using the TPS method and mineralogical composition by modal analysis. SKB P-04-53, Svensk Kärnbränslehantering AB.
- Adl-Zarrabi B, 2004b.** Drill hole KSH02: Thermal properties: heat conductivity and heat capacity determined using the TPS method and mineralogical composition by modal analysis. SKB P-04-54, Svensk Kärnbränslehantering AB.
- Adl-Zarrabi B, 2004c.** Drill hole KAV01: Thermal properties: heat conductivity and heat capacity determined using the TPS method and mineralogical composition by modal analysis. SKB P-04-55, Svensk Kärnbränslehantering AB.
- Adl-Zarrabi B, 2004d.** Drill hole KAV04A: Thermal properties: heat conductivity and heat capacity determined using the TPS method and mineralogical composition by modal analysis. SKB P-04-270, Svensk Kärnbränslehantering AB.
- Adl-Zarrabi B, 2004e.** Drill hole KLX02: Thermal properties: heat conductivity and heat capacity determined using the TPS method and mineralogical composition by modal analysis. SKB P-04-258, Svensk Kärnbränslehantering AB.
- Adl-Zarrabi B, 2004f.** Drill hole KLX04: Thermal properties: heat conductivity and heat capacity determined using the TPS method and mineralogical composition by modal analysis. SKB P-04-267, Svensk Kärnbränslehantering AB.
- Agrell H, 1976.** The highest coastline in south-eastern Sweden. *Boreas* 5, 143–154.
- Agrell H, Friberg N, Oppgård R, 1976.** The Vimmerby Line – An ice-margin zone in north-eastern Småland. *Svensk geografisk årsbok* 52, 71–91.
- Allard B, Karlsson M, Tullborg E-L, Larson S-Å, 1983.** Ion exchange capacities and surface areas of some major components and common fracture filling materials of igneous rocks, SKBF Technical Report 83-64, Svensk Kärnbränslehantering AB.
- Alling V, Andersson P, Fridriksson G, Rubio Lind C, 2004.** Biomass production of Common reed (*Phragmites australis*), infauna, epiphytes, sessile epifauna and mobile epifaunal, Common reed biotopes in Oskarshamn's model area. Svensk Kärnbränslehantering AB (in prep)
- Alm E, Sundblad K, 2002.** Fluorite-calcite-galena-bearing fractures in the counties of Kalmar and Blekinge, Sweden. SKB R-02-42, Svensk Kärnbränslehantering AB.
- Ambrosiani Garcia K, 1990.** Macrofossils from the till-covered sediments at Öje, central Sweden. In: *Late Quaternary Stratigraphy in the Nordic Countries 150,000–15,000 B.P.* (Andersen B.G. & Königsson L.-K. Eds). *Striae* 34, 1–10
- Andersson O, 1994.** Deep drilling and documentation of a 1700m deep borehole at Laxemar, Sweden, SKB TR-94-02, Svensk Kärnbränslehantering AB.
- Andersson P, Ludvigsson J-E, Wass E, 1998.** Äspö Hard Rock Laboratory, True Block Scale Project, Preliminary characterisation. Combined interference tests and tracer tests, SKB IPR-01-44, Svensk Kärnbränslehantering AB.
- Andersson J, Ström A, Svemar C, Almén K-E, Ericsson L O, 2000a.** What requirements does the KBS-3 repository make on the host rock? Geoscientific suitability indicators and criteria for siting and site evaluation. SKB TR-00-12, Svensk kärnbränslehantering AB.

- Andersson P, Ludvigsson J-E, Wass E, Holmqvist M, 2000b.** Äspö Hard Rock Laboratory, True Block Scale Project, Tracer test stage. Interference tests, dilution tests and tracer tests, SKB IPR-00-28, Svensk Kärnbränslehantering AB.
- Andersson J, Christiansson R, Hudson J, 2002a.** Site Investigations Strategy for Rock Mechanics Site Descriptive Model. SKB TR-02-01, Svensk Kärnbränslehantering AB.
- Andersson J, Berglund J, Follin S, Hakami E, Halvarson J, Hermanson J, Laaksoharju M, Rhén I, Wahlgren C-H, 2002b.** Testing the methodology for site descriptive modelling. Application for the Laxemar area, SKB TR-02-19, Svensk Kärnbränslehantering AB.
- Andersson P, Byegård J, Dershowitz B, Doe T, Hermanson J, Meier P, Tullborg E-L, Winberg A, 2002c.** TRUE Block Scale Project. Final report. 1. Characterisation and model development. SKB TR-02-13, Svensk Kärnbränslehantering AB.
- Andersson J, 2003.** Site descriptive modelling – strategy for integrated evaluation. SKB R-03-05, Svensk Kärnbränslehantering AB.
- Andersson J, Munier R, Ström A, Söderbäck B, Almén K-E, Olsson L, 2004.** When is there sufficient information from the Site Investigations? R-04-23, Svensk kärnbränslehantering AB.
- Andersson J (ed), 2004.** T-H-M in Safety Assessments. Findings of DECOVALEX III, SKI Report (in progress).
- Andrejev O, Sokolov A, 1989.** Numerical modelling of the water dynamics and passive pollutant transport in the Neva inlet. *Meteorologia i Hydrologia*, 12, 78–85, (in Russian).
- Andrejev O, Sokolov A, 1990.** 3D baroclinic hydrodynamic model and its applications to Skagerrak circulation modelling. 17th Conf. of the Baltic Oceanographers, Proc., 38–46, 23, 280–287.
- Andrejev O, Sokolov A, 1997.** The data assimilation system for data analysis in the Baltic Sea. *System Ecology contributions* No. 3. 66 pp.
- Andrejev O, Myrberg K, Lundberg P, 2004a.** Age and renewal time of water masses in a semi-enclosed basin – application to the Gulf of Finland, *Tellus*, 56A, 548–558.
- Andrejev O, Myrberg K, Alenius P, Lundberg P, 2004b.** Mean circulation and water exchange in the Gulf of Finland – a study based on three-dimensional modelling. *Boreal Env. Res.*, 9, 1–16.
- Andrén T, Björck J, Johnsen S, 1999.** Correlation of the Swedish glacial varves with the Greenland (GRIP) oxygen isotope stratigraphy. *Journal of Quaternary Science* 14, 361–371.
- Andrén E, Andrén Th, Sohlenius G, 2000.** The Holocene history of the southwestern Baltic Sea as reflected in a sediment core from the Bornholm Basin. *Boreas* 29, 233-250.
- Andrén C, 2004a.** Oskarshamn site investigation, Amphibians and reptiles in SKB special area of investigation at Simpevarp. SKB P-04-36. Svensk Kärnbränslehantering AB.
- Andrén C, 2004b.** Underlag till Energiflöden i ekosystem med grod- och kräldjur. Nature – Artbevarande & Foto (in Swedish).
- Aquilonius A, 2005.** Vegetation in Lake Frisksjön. Oskarshamn site investigation. SKB P-05-173, Svensk Kärnbränslehantering AB.
- Aronsson M, Persson Th.** Pollen diagrams from Lake Höckhultesjön and Lake Malghults göl. Unpublished data from department of Quaternary Geology, Lund University.
- Ask H, 2003.** Oskarshamn site investigation – Drilling of three flushing water wells, HSH01, HSH02 and HSH03. SKB P-03-114, Svensk Kärnbränslehantering AB.
- Ask H, Morosini M, Samuelsson L-E, Stridsman H, 2003.** Oskarshamn site investigation – Drilling of cored borehole KSH01. SKB P-03-113, Svensk Kärnbränslehantering AB.

- Ask H, Samuelsson L-E, 2004a.** Oskarshamn site investigation. Drilling of two flushing water wells, HAV09 and HAV10. SKB P-04-150, Svensk Kärnbränslehantering AB.
- Ask H, Samuelsson L-E, 2004b.** Oskarshamn site investigation. Drilling of two percussion boreholes, HLX 13 and HLX14. SKB P-04-234, Svensk Kärnbränslehantering AB.
- Ask H, Samuelsson L-E, 2004c.** Oskarshamn site investigation. Percussion drilling of borehole HLX20 for investigation of lineament EW002. SKB P-04-236, Svensk Kärnbränslehantering AB.
- Ask H, Morosini M, Ekström L, 2004a.** Oskarshamn site investigation. Drilling of cored borehole KSH02. SKB P-04-151, Svensk Kärnbränslehantering AB.
- Ask H, Morosini M, Samuelsson L-E, Stridsman H, 2004b.** Oskarshamn site investigation – Drilling of cored borehole KSH03. SKB P-04-233, Svensk Kärnbränslehantering AB.
- Ask H, Samuelsson L-E, Zetterlund M, 2004c** Oskarshamn site investigation. Percussion drilling of boreholes HLX15, HLX26, HLX27, HLX28, HLX29 and HLX32 for investigation of lineament NW042. SKB P-04-235, Svensk Kärnbränslehantering AB.
- Ask H, Zetterlund M, 2005.** Oskarshamn site investigation. Percussion drilling of boreholes HLX16, HLX17, HLX18 and HLX19. SKB P-05-190, Svensk Kärnbränslehantering AB.
- Ask H, Samuelsson L-E, Zetterlund M, 2005a.** Oskarshamn site investigation. Percussion drilling of boreholes HLX21, HLX22, HLX23, HLX24, HLX25, HLX30, HLX31 and HLX33 for investigation of lineament EW007. SKB P-05-55, Svensk Kärnbränslehantering AB.
- Ask H, Morosini M, Samuelsson L-E, Ekström L, Håkansson N, 2005b.** Oskarshamn site investigation. Drilling of cored borehole KLX03. SKB P-05-167, Svensk Kärnbränslehantering AB.
- Ask H, Morosini M, Samuelsson L-E, Ekström L, Håkansson N, 2005c.** Oskarshamn site investigation. Drilling of cored borehole KLX04. SKB P-05-111, Svensk Kärnbränslehantering AB.
- Ask H, Morosini M, Samuelsson L-E, Ekström L, Håkansson N, 2005d.** Drilling of cored borehole KAV04. Oskarshamn site investigation. SKB P-05-25, Svensk Kärnbränslehantering AB.
- Banfield G E, Bhatti J S, Jiang H, Apps M J, 2002.** Variability in regional scale estimates of carbon stocks in boreal forest ecosystems: results from West-Central Alberta. *Forest Ecology and Management* 169:15-27.
- Banwart S (ed.), Laaksoharju M, Skårman C, Gustafsson E, Pitkänen P, Snellman M, Landström O, Aggeryd I, Mathiasson L, Sundblad B, Tullborg E-L, Wallin B, Pettersson C, Peder-sen K, Arlinger J, Jahromi N, Ekendahl S, Hallbeck L, Degueldre C, Malmström M, 1995.** Äspö Hard Rock Laboratory. The Redox Experiment in Block Scale. Final reporting of results from the three year project. SKB Progress Report PR 25-95-06, Stockholm, Sweden.
- Banwart S, Tullborg E-L, Pedersen K, Gustafsson E, Laaksoharju M, Nilsson A-C, Wallin B, Wikberg P, 1996.** Organic carbon oxidation induced by large-scale shallow water intrusion into a vertical fracture zone at the Äspö Hard Rock Laboratory (Sweden). *Journal of Contaminant Hydrology*, 21, 115–125.
- Barton N, 2002.** Some new Q-value correlations to assist in site characterisation and tunnel design. *I.J. Rock Mech. & Min. Eng.*, Vol. 39, p. 185–216.
- Bein A, Arad A, 1992.** Formation of saline groundwaters in the Baltic region through freezing of seawater during glacial periods. *Journal of Hydrology*, 140, Elsevier Science B.V. pp 75–87.
- Berggren J, Kyläkorpi L, 2002.** Ekosystemen i Simpevarpsområdet – Sammanställning av befintlig information. SKB R-02-10, Svensk Kärnbränslehantering AB.
- Berggren D, Bergkvist B, Johansson M-B, et al. 2004.** A description of LUSTRA's common field sites. Department of Forest Soils, Swedish University of Agriculture Sciences, Uppsala, Report 87.
- Berglund B, 1966.** Late-Quaternary vegetation in southeastern Sweden. A pollen-analytical study. II. Post-Glacial time. *Opera Botanica* 12:1, 190 pp.

- Berglund B, 1971.** Littorina transgressions in Blekinge, South Sweden. A preliminary survey, Geologiska Föreningens i Stockholm Förhandlingar 93, 625–652.
- Berglund B E, Digerfeldt G, Engelmark R, Gaillard M-J, Karlsson S, Miller U, Risberg J, 1996.** Palaeoecological events during the last 15000 years, Regional syntheses of palaeoecological studies of lakes and mires in Europe. – Sweden. In Berglund, B.E., Birks, H.J.B., Ralska-Jasiewiczowa, M. and Wright, H.E. (eds): IGCP Project 158B 233–280.
- Berglund J, Curtis P, Eliasson T, Ohlsson T, Starzec P, Tullborg E-L, 2003.** Äspö Hard Rock Laboratory – Update of the geological model 2002. SKB IPR-03-34, Svensk Kärnbränslehantering AB.
- Berglund S, Selroos J-O, 2003.** Transport properties site descriptive model – Guidelines for evaluation and modelling. SKB R-03-09, Svensk Kärnbränslehantering AB.
- Berglund J, 2004.** Oskarshamn site investigation. Scan line fracture mapping. Subarea Laxemar and passage for tunnel. SKB P-04-244, Svensk Kärnbränslehantering AB.
- Berglund B, Sandgren P, Barnekow L, Hannon G, Jiang H, Skog G, Yu S-Y, 2005.** Early Holocene history of the Baltic Sea, as reflected in coastal sediments in Blekinge, southeastern Sweden. Quaternary International 130, 111-139.
- Bergman T, Isaksson H, Johansson R, Lindén A H, Lindgren J, Lindroos H, Rudmark L, Wahlgren C-H, 1998.** Förstudie Oskarshamn. Jordarter, bergarter och deformationszoner. SKB R-98-56, Svensk Kärnbränslehantering AB.
- Bergman T, Follin S, Isaksson H, Johansson R, Lindén A H, Lindroos H, Rudmark L, Stanfors R, Wahlgren C-H, 1999.** Förstudie Oskarshamn. Erfarenheter från geovetenskapliga undersökningar i nordöstra delen av kommunen. SKB R-99-04, Svensk Kärnbränslehantering AB.
- Bergman T, Isaksson H, Rudmark L, Stanfors R, Wahlgren C-H, Johansson R, 2000.** Förstudie Oskarshamn. Kompletterande geologiska studier. SKB R-00-45, Svensk Kärnbränslehantering AB.
- Bergman B, Juhlin C, Palm H, 2001.** Reflektionsseismiska studier inom Laxemarområdet. SKB R-01-07, Svensk Kärnbränslehantering AB.
- Bertetti F, Pabalan R, Turner D, Almendarez M, 1996.** Neptunium(V) sorption behaviour on clinoptilolite, quartz and montmorillonite. Mat. Res. Soc. Symp. Proc. Vol. 412, pp 631–638.
- Beunk F F, Page L M, 2001.** Structural evolution of the accretional continental margin of the Paleoproterozoic Svecofennian orogen in southern Sweden. Tectonophysics 339, 67–92.
- Bienawski Z T, 1989.** Engineering rock mass classifications. John Wiley & Sons.
- Birgersson L, Widén H, Ågren T, Neretnieks I, 1992.** Tracer migration experiments in the Stripa Mine 1980–1991, SKB Stripa Project 92-25, Svensk Kärnbränslehantering AB.
- Björck S, 1995.** A review of the history of the Baltic Sea, 13.0–8.0 ka BP. Quaternary International 27, 19–40.
- Björck S, Kromer B, Johnsen S, Bennike O, Hammarlund D, Lemdahl G, Possnert G, Lander Rasmussen T, Wohlfarth B, Hammer C H, Spurk M, 1996.** Synchronized Terrestrial-atmospheric deglacial records around the North Atlantic. Science 274, 1155–1160.
- Björck J, 1999.** The Alleröd-younger Dryas pollen zone in an 800-years varve chronology from southeastern Sweden. GFF 121, 287–292.
- Bolin B, Rodhe H, 1973.** A note on the concepts of age distribution and transit term in natural reservoirs. Tellus, 25, 58–62.
- Boresjö Bronge L, Wester K, 2003.** Vegetation mapping with satellite data of the Forsmark, Tierp and Oskarshamn regions. SKB P-03-83, Svensk Kärnbränslehantering AB.

- Bossart P, Hermanson J, Mazurek M, 2001.** Analysis of fracture networks based on the integration of structural and hydrogeological observations at different scales. SKB TR-01-21, Svensk Kärnbränslehantering AB.
- Bottomley D J, Katz A, Chan L H, Starinsky A, Douglas M, Clark I D, Raven K G, 1999.** The origin and evolution of Canadian Shield brines: evaporation or freezing of seawater? New lithium isotope and geochemical evidence from the Slave craton. *Chem. Geol.*, 155, 295–320.
- Brace W F, 1980.** Permeability of Crystalline and Argillaceous Rocks. *Int. J. Rock. Mech. & Geomech. Abstr.* Vol. 17, pp 241–251.
- Brunauer S, Emmet P H, Teller E, 1938.** Adsorption of gases in multimolecular layers. *J. Am. Chem. Soc.*, 60: 309–319.
- Brunnberg L, 1995.** Clay-varve chronology and deglaciation during the Younger Dryas and Pre-boreal in the easternmost part of the Middle Swedish Ice Marginal Zone. Stockholm university, Quaternaria A2, 94 pp.
- Brunberg A-K, Carlsson T, Brydsten L, Strömgren M, 2004.** Oskarshamn Site investigation, Identification of catchments, lake-related drainage parameters and lake habitats. SKB P-04-242, Svensk Kärnbränslehantering AB.
- Brydsten L, 2004.** Method for construction of digital elevation models for site investigation program in Forsmark and Simpevarp. SKB P-04-03, Svensk kärnbränslehantering AB
- Brydsten L, Strömgren M, 2005.** Digital elevation models for site investigation programme in Oskarshamn. SKB R-05-38. Svensk Kärnbränslehantering AB.
- Byegård J, Johansson H, Skålberg M, Tullborg E-L, 1998.** The interaction of sorbing and non-sorbing tracers with different Äspö rock types – Sorption and diffusion experiments in the laboratory scale. SKB TR-98-18, Svensk Kärnbränslehantering AB.
- Byegård J, Widestrand H, Skålberg M, Tullborg E-L, Siitari-Kauppi M, 2001.** Complementary investigation of diffusivity, porosity and sorptivity of Feature A-site specific geological material. SKB ICR-01-04, Svensk Kärnbränslehantering AB.
- Byegård J, Gustavsson E, Tullborg E-L, Berglund S, 2005.** Site descriptive modelling of transport properties. Retardation model Simpevarp 1.2. SKB R-05-05, Svensk Kärnbränslehantering AB.
- Byegård J, Gustavsson E, Tullborg E-L, 2006.** Bedrock transport properties: Preliminary site description Laxemar subarea – version 1.2, SKB R-06-27, Svensk Kärnbränslehantering AB.
- Bödvarsson R, 2003.** Swedish National Seismic Network (SNSN). A short report on recorded earthquakes during the fourth quarter of the year 2002. SKB P-03-02, Svensk Kärnbränslehantering AB.
- Börjesson S, Gustavsson E, 2005.** Oskarshamn site investigation: Laboratory data from the site investigation programme for the transport properties of the rock. Data delivery for data freeze Laxemar 2.1. SKB P-05-106, Svensk Kärnbränslehantering AB.
- Carbol P, Engkvist I, 1997.** Compilation of radionuclide sorption coefficients for performance assessment. SKB R-97-13, Svensk Kärnbränslehantering AB.
- Carlsson T, Brunberg A-K, Brydsten L, Strömgren M, 2005.** Oskarshamn site investigation. Characterisation of running waters, including vegetation, substrate and technical encroachments. SKB P-05-40. Svensk Kärnbränslehantering AB.
- Casanova J, Négrel P, Blomqvist R, 2005.** Boron isotope fractionation in groundwaters as an indicator of past permafrost conditions in the fractured crystalline bedrock of the fennoscandian shield. *Water Res.*, 39, 362-370.
- Chapin III F S, Matson P A, Mooney H A, 2002.** Principles of Terrestrial Ecosystem Ecology. Springer Verlag New York, Inc. ISBN 0-387-95439-2.

- Clark D A, Brown S, Kicklighter D W, et al. 2001.** Measuring net primary production in forests: concepts and field methods. *Ecological applications* 11(2):356–370.
- Cosgrove J W, Stanfors R, Röshoff K, Andersson J, 2006.** Geological characteristics of large fractures and minor deformation zones and strategy for their detection in a repository. SKB R-06-39, Svensk Kärnbränslehantering AB (in prep).
- Craig H, 1961.** Isotope variations in meteoric waters. *Science*, 133: 1702-1703.
- Crawford J, 2006.** Modelling in Support of Bedrock Transport Property Assessment, Preliminary site description Laxemar subarea – version 1.2. SKB R-06-28, Svensk Kärnbränslehantering AB.
- Cronquist T, Forssberg O, Hansen L, Jonsson A, Koyi S, Leiner P, Sävås J, Vestgård J, 2004.** Oskarshamn site investigation. Detailed fracture mapping of two outcrops at Laxemar. SKB P-04-274, Svensk Kärnbränslehantering AB.
- Curtis P, Elfström M, Stanfors R, 2003a.** Oskarshamn site investigation – Compilation of structural geological data covering the Simpevarp peninsula, Ävrö and Hälö. SKB P-03-07. Svensk Kärnbränslehantering AB.
- Curtis P, Elfström M, Stanfors R, 2003b.** Oskarshamn site investigation. Visualization of structural geological data covering the Simpevarp peninsula, Ävrö and Hälö. SKB P-03-86. Svensk Kärnbränslehantering AB.
- Dagan, 1979.** Models of groundwater flow in statistically homogenous porous formations. *Water resources res.*, 15 (1), 47–63.
- Darcel C, Davy P, Bour O, Dreuzy J-R de, 2004.** Alternative DFN model based on initial site investigations at Simpevarp. SKB R-04-76, Svensk Kärnbränslehantering AB.
- Davis J, Meece D, Kohler M, Curtis G, 2004.** Approaches to surface complexation modelling of Uranium(VI) adsorption on aquifer sediments. *Geochim. et Cosmochim. Acta*, 68(18), pp 3621–3641.
- Debon F, Le Fort P, 1983.** A chemical-mineralogical classification of common plutonic rocks and associations. *Transactions of Royal Society of Edinburgh, Earth Sciences* 73, 135–149.
- Degueldre C, 1994.** Colloid properties in groundwater from crystalline formation. Paul Scherrer Institute, Villigen, Switzerland.
- Dershowitz W, Winberg A, Hermanson J, Byegård J, Tullborg E-L, Andersson P, Mazurek M, 2003.** Äspö Hard Rock Laboratory. Äspö Task Force on modelling of groundwater flow and transport of solutes – Task 6C – A semi-synthetic model of block scale conductive structures at the Äspö HRL. SKB IPR-03-13, Svensk Kärnbränslehantering AB.
- DHI Software, 2004.** MIKE SHE User's Guide.
- DHI Water&Environment, 2001.** GeoEditor - User Manual. DHI Water&Environment, Hörsholm, Denmark.
- Dinges C, 2004.** Drill hole KSH01A. Thermal properties: thermal conductivity and specific heat capacity determined using the Hot Disk thermal constants analyser (the TPS technique) – Compared test. SKB P-04-160, Svensk Kärnbränslehantering AB.
- Domenico P-A, Schwartz F W, 1998.** Physical and chemical hydrogeology (2nd ed.). John Wiley & Sons Inc, New York.
- Drake H, Tullborg E-L, 2004.** Oskarshamn site investigation. Fracture mineralogy and wall rock alteration. Results from drill core KSH01A+B. SKB P-04-250, Svensk Kärnbränslehantering AB.
- Drake H, Savolainen M, Tullborg E-L, 2004.** Fracture filling and wall rock alteration – results from borehole KSH01, Simpevarp and KFM01, Forsmark. *GFF* 126, 170.

- Drake H, Tullborg E-L, 2005.** Oskarshamn site investigation. Fracture mineralogy and wall rock alteration. Results from drill cores KAS04, KA1755A and KLX02, SKB P-05-174, Svensk Kärnbränslehantering AB.
- Drake H, Tullborg E-L, in manuscript.** Fracture mineralogy, results from drill cores KLX03, KLX04, KLX05, KLX06, KLX07A+B, KLX08 and KLX10A. SKB P-XX-XX. Svensk Kärnbränslehantering AB.
- Ehrenborg J, Stejskal V, 2004a.** Oskarshamn site investigation. Boremap mapping of core drilled boreholes KSH01A and KSH01B. SKB P-04-01, Svensk Kärnbränslehantering AB.
- Ehrenborg J, Stejskal V, 2004b.** Oskarshamn site investigation. Boremap mapping of core drilled borehole KLX02. SKB P-04-129, Svensk Kärnbränslehantering AB.
- Ehrenborg J, Stejskal V, 2004c.** Oskarshamn site investigation. Boremap mapping of core drilled borehole KAV01. SKB P-04-130, Svensk Kärnbränslehantering AB.
- Ehrenborg J, Stejskal V, 2004d.** Oskarshamn site investigation. Boremap mapping of core drilled borehole KSH02. SKB P-04-131, Svensk Kärnbränslehantering AB.
- Ehrenborg J, Stejskal V, 2004e.** Oskarshamn site investigation. Boremap mapping of core drilled boreholes KSH03A and KSH03B. SKB P-04-132, Svensk Kärnbränslehantering AB.
- Ehrenborg J, Dahlin P, 2005a.** Oskarshamn site investigation. Boremap mapping of core drilled borehole KLX04. SKB P-05-23 (in press), Svensk Kärnbränslehantering AB.
- Ehrenborg J, Dahlin P, 2005b.** Oskarshamn site investigation. Boremap mapping of core drilled borehole KLX03. SKB P-05-24, Svensk Kärnbränslehantering AB.
- Ekman M, 1996.** A consistent map of the postglacial uplift of Fennoscandia. *Terra-Nova* 8/2, 158–165.
- Ekman L, 2001.** Project deep drilling KLX02 – Phase 2, Methods, scope of activities and results. Summary report. SKB TR-01-11, Svensk Kärnbränslehantering AB.
- Elhammer A, Sandkvist Å, 2005.** Oskarshamn site investigation. Detailed marine geological survey of the sea bottom outside Simpevarp. SKB P-05-35, Svensk Kärnbränslehantering AB. In press.
- Eliasson T, 1993.** Mineralogy, geochemistry and petrophysics of red coloured granite adjacent to fractures. SKB TR-93-06, Svensk Kärnbränslehantering AB.
- England M H, 1995.** The age of water and ventilation timescales in a global ocean model. *J. Phys. Oceanogr.*, 25, 2756-2777.
- Engqvist A, Omstedt A, 1992.** Water exchange and density structure in a multi-basin estuary. *Continental Shelf Res.*, 12, 1003–1026.
- Engqvist A, 1996.** Long-term nutrient balances in the eutrophication of the Himmerfjärden estuary. *Estuarine, Coastal & Shelf Sci.*, 42: 483–507.
- Engqvist A, 1997.** Water exchange estimates derived from forcing for the hydraulically coupled basins surrounding Äspö island and adjacent coastal water. SKB TR-97-14, Svensk Kärnbränslehantering AB.
- Engqvist A, 1999.** Estimated retention times for a selection of coupled coastal embayments on the Swedish west, east and north coasts. Swedish EPA (NV) report 4910. ISBN 91-620-4910-0. 47 pp.
- Engqvist A, Andrejev O, 2003.** Water exchange of the Stockholm archipelago – A cascade framework modelling approach. *J. Sea Res.*, 49, 275–294.
- Ericsson L O, 1987.** Fracture mapping on outcrops. Äspölaboratoriet. SKB PR 25-87-05, Svensk Kärnbränslehantering AB.

- Ericsson U, Engdahl A, 2004.** Surface water sampling at Simpevarp 2002–2003. SKB P-04-13, Svensk Kärnbränslehantering AB.
- Fairbanks R, 1989.** A 17,000-year glacio-eustatic sea level record: influence of glacial melting rates on the Younger Dryas event and deep-ocean circulation. *Nature* 342, 637–642.
- Follin S, Årebäck M, Axelsson C-A, Stigsson M, Jacks G, 1998.** Förstudie Oskarshamn, Grundvattnets långsiktiga förändringar. SKB R-98-55, Svensk Kärnbränslehantering AB.
- Follin S, Stigsson M, Svensson U, 2005.** Variable-density groundwater flow simulations and particle tracking – Numerical modelling using DarcyTools. Preliminary site description Simpevarp subarea – version 1.2. SKB R-05-11, Svensk Kärnbränslehantering AB.
- Follin S, Stigsson M, Svensson U, 2006 (in press).** Hydrogeological DFN modelling using structural and hydraulic data from KLX04, Preliminary site description, Laxemar subarea – version 1.2. SKB R-06-24, Svensk Kärnbränslehantering AB.
- Fontes J-Ch, Louvat D, Michelot J-L, 1989.** Some constraints on geochemistry and environmental isotopes for the study of low fracture flows in crystalline rocks – The Stripa case. In: International Atomic Energy Agency (Eds.) *Isotopes techniques in the study of the Hydrology of Fractured and Fissured Rocks*. IAEA, Vienna, Austria.
- Forsman I, Zetterlund M, Forsmark T, Rhén I, 2005a.** Oskarshamn site investigation. Correlation of Posiva Flow Log anomalies to core mapped features in KSH01A, KSH02A and KAV01. SKB P-05-65, Svensk Kärnbränslehantering AB.
- Forsman I, Zetterlund M, Forsmark T, Rhén I, 2005b.** Oskarshamn site investigation. Correlation of Posiva Flow Log anomalies to core mapped features in KLX02, KLX03, KLX04, KAV04A and KAV04b. SKB P-05-241, Svensk Kärnbränslehantering AB.
- Frape S K, Fritz P, 1982.** The chemistry and isotopic composition of saline groundwaters from the Sudbury Basin, Ontario. *Canad. J. Earth Sci.*, 19, 645–661.
- Frape S K, Fritz P, 1987.** Geochemical trends from groundwaters from the Ca-nadian Shield. In: (Eds.) P. Fritz and S.K. Frappe. *Saline waters and gases in crystalline rocks*. Geol. Assoc. Canada Spec. Paper 33, 19–38.
- Fredén C, 2002.** Berg och Jord, Sveriges Nationalatlas. 208 pp (in Swedish).
- Fredriksson A, Hässler L, Söderberg L, 2001.** Extension of Clab – Numerical modelling, deformation measurements and comparison of forecast with outcome. Proceedings of the ISRM Reg Symp EUROCK 2001, Espoo, Finland 4–7, June 2001.
- Fredriksson R, Tobiasson S, 2003.** Simpevarp site investigation. Inventory of macrophyte communities at Simpevarp nuclear power plant. Area of distribution and biomass determination. SKB P-03-69, Svensk Kärnbränslehantering AB.
- Fredriksson R, 2004.** Inventory of the soft-bottom macrozoobenthos community in the area around Simpevarp nuclear power plant. Oskarshamn site investigation, SKB P-04-17, Svensk Kärnbränslehantering AB.
- Fredriksson R, 2005.** Inventory of the marine fauna attached to hard substrates in the Simpevarp area. Oskarshamn site investigation. SKB P-05-45, Svensk Kärnbränslehantering AB.
- Fredriksson A, Olofsson I, 2005.** Rock mechanics characterisation of the rock mass – Theoretical approach. Preliminary site description Simpevarp subarea – version 1.2. SKB R-05-87, Svensk Kärnbränslehantering AB.
- Fredriksson A, Olofsson I, 2006.** Rock mechanics modelling of rock mass properties – Theoretical approach, Preliminary site description, Laxemar subarea -version 1.2. SKB R-06-16, Svensk Kärnbränslehantering AB.

- Gascoyne M, Ross J D, Purdy A, Frape S K, Drimmie R J, Fritz P, Betcher R N, 1989.** Evidence for penetration of sedimentary basin brines into an Archean granite of the Canadian Shield. WRI, (Ed.) Miles. Balkema, Rotterdam.
- Gower S T, Kucharik C J, Norman J M, 1999.** Direct and indirect estimations of Leaf Area Index, fAPAR, and Net Primary Production of terrestrial ecosystems. *Remote Sensing of Environment* 70:29–51.
- Green M, 2004.** Bird surveys in Simpevarp 2003. Oskarshamn site investigation, SKB P-04-21, Svensk Kärnbränslehantering AB.
- Green M, 2005.** Bird monitoring in Simpevarp 2002-2004. Oskarshamn site investigations, SKB P-05-42, Svensk Kärnbränslehantering AB.
- Gregersen S, Korhonen H, Husebye E S, 1991.** Fennoscandian dynamics: Present-day earthquake activity. *Tectonophysics* 189, 333–344.
- Gregersen S, 1992.** Crustal stress regime in Fennoscandia from focal mechanisms. *Journal of Geophysical Research* 97, B8, 11821–1827.
- Gustafsson G, Stanfors R, Wikberg P, 1989.** Swedish Hard Rock Laboratory. First evaluation of 1988 year pre-investigations and description of the target area, the island of Åspö. SKB TR-89-16, Svensk Kärnbränslehantering AB.
- Gustafsson S, 1991.** Transient plane source techniques for thermal conductivity and thermal diffusivity of solid materials. *Rev. Sci. Instrum.* 62, p 797–804. American Institute of Physics, USA.
- Gustafsson E, Ludvigson J-E, 2005.** Oskarshamn site investigation. Combined interference test and tracer test between KLX02 och HLX10. SKB P-05-20, Svensk Kärnbränslehantering AB.
- Gustafsson E, Nordqvist R, 2005.** Oskarshamn site investigation: Groundwater flow measurements and SWIW tests in boreholes KLX02 and KSH02, SKB P-05-28, Svensk Kärnbränslehantering AB.
- Gylling B, 1997.** Development and applications of the channel network model for simulations of flow and solute transport in fractured rock. Ph.D. thesis, Dept. Chemical Engineering and Technology, Royal Inst. of Technology, Stockholm.
- Hakami E, Hakami H, Cosgrove J, 2002.** Strategy for a Rock Mechanics Site Descriptive Model. Development and testing of an approach to modelling the state of stress. SKB R-02-03, Svensk Kärnbränslehantering AB.
- Hakami E, Min K-B, 2006.** Modelling of the state of stress, Preliminary site description, Laxemar subarea – version 1.2. SKB R-06-17, Svensk Kärnbränslehantering AB.
- Hartley L J, Holton D, 2003.** ConnectFlow (Release 2.0) Technical Summary Document. SERCO/ERRA-C/TSD02V1.
- Hartley L J, Hoch A R, Cliffe K A C, Jackson C P, Holton D, 2003a.** NAMMU (Release 7.2) Technical Summary Document. SERCO/ERRA-NM/TSD02V1.
- Hartley L J, Holton D, Hoch A R, 2003b.** NAPSAC (Release 4.4) Technical Summary Document. SERCO/ERRA-N/TSD02V1.
- Hartley L, Hoch A, Hunter F and N Marsic 2005.** Regional hydrogeological simulations – Numerical modelling using ConnectFlow. Preliminary site description Simpevarp subarea – version 1.2. SKB R-05-12, Svensk Kärnbränslehantering AB.
- Hartley L, Hunter F, Jackson P, McCarthy R, Gylling B, Marsic N, 2006 (in prep).** Regional hydrogeological simulations – Numerical modelling using ConnectFlow. Preliminary site description, Laxemar subarea – version 1.2. SKB R-06-23, Svensk Kärnbränslehantering AB.
- Haveman S A, Pedersen K, Ruotsalainen P, 1998.** Geomicrobial investigations of groundwaters from Olkilouto, Hästholmen, Kivetty and Romuvaara, Finland. POSIVA Report 98-09, Helsinki, Finland, 40 p.

- Hellmuth K H, Siitari-Kauppi M, Lindberg A, 1993.** Study of porosity and migration pathways in crystalline rock by impregnation with ¹⁴C-polymethylmethacrylate. *J. of Contaminant Hydrology*, 13: 403–418.
- Hellmuth K H, Lukkarinen S, Siitari-Kauppi M, 1994.** Rock matrix studies with carbon-14-polymethylmethacrylate (PMMA). Method, development and applications. *Isotopenpraxis Environ. Health Stud.*, 30: 47–60.
- Hermanson J, Hansen L, Wikholm M, Cronquist T, Leiner P, Vestgård J, Sandahl K-A, 2004.** Detailed fracture mapping of four outcrops at the Simpevarp peninsula and Ävrö. SKB P-04-35, Svensk Kärnbränslehantering AB.
- Hermanson J, Forsberg O, Fox A, La Pointe P, 2005.** Statistical model of fractures and deformation zones. Preliminary site description, Laxemar subarea, version 1.2. SKB R-05-45, Svensk Kärnbränslehantering AB.
- Herut B, Starinsky A, Katz A, Bein A, 1990.** The role of seawater freezing in the formation of subsurface brines. *Geochim. et Cosmochim. Acta*, 33, 1321–1349.
- Hoch A R, Hartley L J, 2003.** NAMMU (Release 7.2) Verification Document. SERCO/ERRA-NM/VD02V2
- Hoch A R, Hartley L J, Holton D, 2003.** NAPSAC (Release 4.3) Verification Document. SERCO/ERRA-NM/VD02V1.
- Horai K, 1971.** Thermal conductivity of rock-forming minerals. *J. Geophys. Res.* 76, p 1278–1308.
- Horai K, Baldrige S, 1972.** Thermal conductivity of nineteen igneous rocks, Application of the needle probe method to the measurement of the thermal conductivity of rock. Estimation of the thermal conductivity of rock from the mineral and chemical compositions. *Phys. Earth Planet. Interiors* 5, p 151. Mac Berthouex, P and Brown, L C, 2002. *Statistics for environmental engineers*, 2nd edition. Lewis Publishers.
- Hultgren P, Stanfors R, Wahlgren C-H, Carlsten S, Mattsson H, 2004.** Oskarshamn site investigation. Geological single-hole interpretation of KSH03A, KSH03B, KLX02, HAV09 and HAV10. SKB P-04-231, Svensk Kärnbränslehantering AB.
- Hättstrand C, Stroeven A, 2002.** A preglacial landscape in the centre of Fennoscandian glaciation: geomorphological evidence of minimal Quaternary glacial erosion. *Geomorphology* 44, 127–143.
- Högdahl K, Andersson U B, Eklund O, (Editors) 2004.** The Transscandinavian Igneous Belt (TIB) in Sweden: a review of its character and evolution. Geological Survey of Finland, Special Paper 37, 1–125.
- Hökmark H, Fälth B, 2003.** Thermal dimensioning of the deep repository. Influence of canister spacing, canister power, rock thermal properties and nearfield design on the maximum canister surface temperature. SKB TR-03-09, Svensk Kärnbränslehantering AB.
- Ingvarson N H, Palmeby A S L F, Svensson L O, Nilsson K O, Ekfeldt T C I, 2004.** Oskarshamn site investigation – Marine survey in shallow coastal waters, Bathymetric and geophysical investigation 2004. SKB P-04-254, Svensk Kärnbränslehantering AB.
- Itasca, 2003.** 3DEC User's Guide. Itasca Consulting Group Inc., Minneapolis, Minnesota.
- Jansson U, Berg J, Björklund A, 2004.** A study on landscape and the historical geography of two areas – Oskarshamn and Forsmark, June 2004. SKB R-04-67, Svensk Kärnbränslehantering AB.
- Jakobsson, 1999.** Measurement and modelling using surface complexation of cation (II to IV) sorption onto mineral oxides. Ph.D. Thesis. Chalmers University of Technology, Department of Nuclear Chemistry, Göteborg, Sweden.
- Jaquet O, Siegel P, 2003.** Groundwater flow and transport modelling during a glaciation period. SKB R-03-04. Svensk Kärnbränslehantering AB.

- Jarsjö J, Shibuo Y, Prieto C, Destouni G, 2005.** GIS-based modelling of coupled groundwater-surface water hydrology in the Forsmark and Simpevarp areas. Svensk Kärnbränslehantering AB (report to be published).
- Jenne E, 1998.** Adsorption of metals by geomedial – Variables, mechanisms, and model applications, Academic Press.
- Jensen J L, Lake L W, Corbett P W M, Goggin D J, 2000.** Statistics for petroleum engineers and geoscientists, Handbook of Petroleum Exploration and Production, 2, Second ed, Elsevier, Amsterdam.
- Johansson L, Johansson Å, 1990.** Isotope geochemistry and age relationships of mafic intrusions along the Protogine Zone, southern Sweden. Precambrian Research 48, 395–414.
- Johansson H, Byegård J, Skarnemark G, Skålberg M, 1997.** Matrix diffusion of some alkali and alkaline earth metals in granitic rock. Mat. Res. Soc. Symp. Proc. 465: 871–878.
- Johansson T, Adestam L, 2004a.** Oskarshamn site investigation, Drilling and sampling in soil-Installation of ground water monitoring wells. SKB P-04-121, Svensk kärnbränslehantering AB.
- Johansson T, Adestam L, 2004b.** Oskarshamn site investigation. Slug tests in groundwater monitoring wells in soil in the Simpevarp area. SKB P-04-122. Svensk Kärnbränslehantering AB.
- Johansson T, Adestam L, 2004c.** Drilling and sampling in soil. Installation of groundwater monitoring wells in the Laxemar area. SKB P-04-317. Svensk Kärnbränslehantering AB.
- Johansson T, Adestam L, 2004d.** Slug tests in groundwater monitoring wells in soil in the Laxemar area. SKB P-04-318. Svensk Kärnbränslehantering AB.
- Johansson P-O, Werner K, Bosson E, Berglund S, Juston J, 2005.** Forsmark 1.2 – Background report for climate, surface hydrology and near-surface hydrogeology. SKB R-05-06, Svensk Kärnbränslehantering AB.
- Jonsson S, 2004.** Djupförvarsteknik. Relation between fine-grained granitic dykes and structures at the Äspö Hard Rock Laboratory, north of Oskarshamn, Sweden. SKB TD-04-11, Svensk Kärnbränslehantering AB.
- Juhlin C, Wallroth T, Smellie J, Eliasson T, Ljunggren C, Leijon B, Beswick J, 1998.** The very deep hole concept – Geoscientific appraisal of conditions at great depth, SKB TR-98-05, Svensk Kärnbränslehantering AB.
- Juhlin C, Bergman B, Cosma C, Keskinen J, Enescu N, 2002.** Vertical seismic profiling and integration with reflection seismic studies at Laxemar, 2000. SKB TR-02-04, Svensk Kärnbränslehantering AB.
- Juhlin C, Bergman B, Palm H, Tryggvason A, 2004a.** Oskarshamn site investigation. Reflection seismic studies on Ävrö and Simpevarpshalvön, 2003. SKB P-04-52, Svensk Kärnbränslehantering AB.
- Juhlin C, Bergman B, Palm H, 2004b.** Oskarshamn site investigation. Reflection seismic studies performed in the Laxemar area during 2004. SKB P-04-215, Svensk Kärnbränslehantering AB.
- Kautsky U, 1995.** Ecosystem processes in coastal areas of the Baltic Sea. Doctoral Thesis, Department of Zoology, Stockholm University, Sweden.
- Kellner E, 2003.** Wetlands – different types, their properties and functions. SKB TR-04-08. Svensk Kärnbränslehantering AB.
- Knutsson G, Morfeldt C-O, 1993.** Grundvatten – teori och tillämpning. Svensk Byggtjänst AB (in Swedish).
- Koistinen T, Stephens M B, Bogatchev V, Nordgulen O, Wennerström M, Korhonen J, 2001.** Geological map of the Fennoscandian Shield, scale 1:2 000 000. Geological Surveys of Finland, Norway and Sweden and the North-West Department of Natural Resources of Russia.

- Korhonen K, Kuivamäki A, Ruotoistenmäki T, Paananen M, 2005.** Interpretation of lineaments from airborne geophysical and topographic data. An alternative model within version Laxemar 1.2 of the Oskarshamn modelling project. SKB P-05-247, Svensk Kärnbränslehantering AB.
- Kornfält K-A, Wikman H, 1987.** Description of the map of solid rocks around Simpevarp. SKB PR 25-87-02, Svensk Kärnbränslehantering AB.
- Kornfält K-A, Wikman H, 1988.** The rocks of the Äspö island. Description to the detailed maps of solid rocks including maps of 3 uncovered trenches. SKB PR-25-88-12, Svensk Kärnbränslehantering AB.
- Kornfält K-A, Persson P-O, Wikman H, 1997.** Granitoids from the Äspö area, southeastern Sweden – geochemical and geochronological data. GFF 119, 109–114.
- Kresten P, Chyssler J, 1976.** The Götömar massif in south-eastern Sweden: A reconnaissance survey. Geologiska Föreningens i Stockholm Förhandlingar 98, 155–161.
- Kristiansson J, 1986.** The ice recession in the south-eastern part of Sweden. University of Stockholm. Department of Quaternary Research 7, 132 pp.
- Kruseman G P, de Ridder N A, 1991.** Analysis and evaluation of pumping test data, ILRI publication 47, Wageningen.
- Kumblad L, Gilek M, Naeslund B, Kautsky U, 2003.** An ecosystem model of the environmental transport and fate of carbon-14 in a bay of the Baltic Sea, Sweden. Ecological modelling 166:193–210.
- Kyläkorpi L, 2005.** Tillgänglighetskartan. SKB report, in press.
- Laaksoharju M, Smellie J, Nilsson A-C, Skårman C, 1995.** Groundwater sampling and chemical characterisation of the Laxemar deep borehole KLX02. SKB TR-95-05, Svensk Kärnbränslehantering AB.
- Laaksoharju M, Wallin B (eds), 1997.** Evolution of the groundwater chemistry at the Äspö Hard Rock Laboratory. Proceedings of the second Äspö International Geochemistry Workshop, June 6–7, 1995. SKB International Co-operation Report ISRN SKB-ICR-91/04-SE. ISSN 1104-3210 Stockholm, Sweden.
- Laaksoharju M, 1999.** Groundwater Characterisation and Modelling: Problems, Facts and Possibilities. Dissertation TRITA-AMI-PHD 1031; ISSN 1400-1284; ISRN KTH/AMI/PHD 1031-SE; ISBN 91-7170-. Royal Institute of Technology, Stockholm, Sweden. Also as SKB TR-99-42, Svensk Kärnbränslehantering AB.
- Laaksoharju M (ed), Smellie J, Gimeno M, Auqué L, Gómez J, Tullborg E-L, Gurban I, 2004.** Hydrogeochemical evaluation of the Simpevarp area, model version 1.1. SKB R-04-16, Svensk Kärnbränslehantering AB.
- Laaksoharju (ed), 2005.** Hydrogeochemical evaluation of the Simpevarp area, model version 1.2. SKB R-04-74, Svensk Kärnbränslehantering AB.
- Laaksoharju M (ed), Smellie J, Tullborg E-L, Waber N and Morales T, 2006.** Hydrogeochemical Evaluation, Preliminary site description, Laxemar subarea – version 1.2, SKB R-06-12, Svensk Kärnbränslehantering AB.
- Lagerbäck R, Robertsson A-M, 1988.** Kettle holes – stratigraphical archives for Weichselian geology and palaeoenvironment in northernmost Sweden. Boreas 17, 439–468.
- Lake L W, Srinivasan S, 2004.** Statistical scale-up of reservoir properties: concepts and applications, J. Petrol. Sci. Eng., 44, pp 27–39.
- Lanaro F, 2006.** Rock mechanics modelling of rock mass properties – Empirical approach, Preliminary site description, Laxemar subarea – version 1.2. SKB R-06-14, Svensk Kärnbränslehantering AB.

- Lanaro F, Öhman J, Fredriksson A, 2006.** Rock mechanics modelling of rock mass properties – Summary of primary data, Preliminary site description, Laxemar subarea – version 1.2. SKB R-06-15, Svensk Kärnbränslehantering AB.
- Landström O, Tullborg E-L, 1993.** Results from a geochemical study of zone NE-1, based on samples from the Äspö tunnel and drillcore KAS 16 (395 to 451 m). SKB Progress Report 25-93-01, Svensk Kärnbränslehantering AB.
- Landström O, Tullborg E-L, 1995.** Interactions of trace elements with fracture filling minerals from the Äspö Hars Rock laboratory. SKB TR-95-13. ISSN 0284-3757. 65 pp. Svensk Kärnbränslehantering AB.
- Larson S Å, Tullborg E-L, 1993.** Tectonic regimes in the Baltic Shield during the last 1200 Ma – A review. SKB TR-94-05, Svensk Kärnbränslehantering AB.
- Larson S Å, Tullborg E-L, Cederbom C, Stiberg J-A, 1999.** Sveconorwegian and Caledonian foreland basins in the Baltic Shield revealed by fission-track thermochronology. *Terra Nova* 11, 210–215.
- Larsson-McCann S, Karlsson A, Nord M, Sjögren J, Johansson L, Ivarsson M, Kindell S, 2002.** Meteorological, hydrological and oceanographical information and data for the site investigation program in the community of Oskarshamn. SKB TR-02-03, Svensk Kärnbränslehantering AB.
- Lehtonen A, Mäkipää R, Heikkinen J, Sievänen R, Liski J, 2004.** Biomass expansion factors (BEFs) for Scots pine, Norway spruce and birch according to stand age for boreal forests. *Forest Ecology and Management* 188:211–224.
- LeMaitre R W (Editor), 2002.** A classification of igneous rocks and glossary of terms: Recommendations of the International Union of Geological Sciences, Subcommittee on the Systematics of Igneous Rocks, 2nd edition, Blackwell, Oxford.
- Lidmar-Bergström K, 1991.** Phanerozoic tectonics in southern Sweden. *Zeitschrift für Geomorphologie N.F.* 82, 1–16.
- Lidmar-Bergström K, Olsson S, Olvmo M, 1997.** Paleosurfaces and associated saprolites in southern Sweden. *Geological Society* 120, 95–124.
- Lindborg T (ed), 2005.** Description of surface systems, Preliminary site description Simpevarp subarea – version 1.2. SKB R-05-01, Svensk Kärnbränslehantering AB.
- Lindborg T (ed), 2006.** Description of surface systems, Preliminary site description Laxemar subarea – version 1.2. SKB R-06-11, Svensk Kärnbränslehantering AB.
- Lindén A, 1984.** Some ice-marginal deposits in the east-central part of the South Swedish Upland. *Sveriges Geologiska Undersökning C* 805, 35 pp.
- Lindqvist G, 2004a.** Oskarshamn site investigation. Refraction seismic measurements in Laxemar. SKB P-04-134, Svensk Kärnbränslehantering AB.
- Lindqvist G, 2004b.** Oskarshamn site investigation. Refraction seismic measurements in the water outside Simpevarp and Ävrö and on land on Ävrö. SKB P-04-201, Svensk Kärnbränslehantering AB.
- Lindroos H, 2004.** The potential for ore, industrial minerals and commercial stones in the Simpevarp area. SKB R-04-72, Svensk Kärnbränslehantering AB.
- Liu J, Löfgren M, Neretnieks I, 2005 (in preparation).** SR-Can, Data and uncertainty assessment, Matrix diffusivity and porosity in-situ, SKB R-XX-YY, Svensk Kärnbränslehantering AB.
- Lohm U, Persson T, 1979.** *Levande Jord. Aktuell biologi* 3. Esselte studium.
- Louvat D, Michelot J L, Aranyossy J-F, 1999.** Origin and residence time of salinity in the Äspö groundwater system. *Appl. Geochem.*, 14, 917–925.

- Ludvigson J-E, Hansson K, Rouhiainen P, 2002.** Methodology study of Posiva difference flowmeter in borehole KLX02 at Laxemar, SKB R-01-52, Svensk Kärnbränslehantering AB.
- Ludvigson J-E, Levén J, Jönsson S, 2003.** Oskarshamn site investigation. Hydraulic tests and flow logging in borehole HSH03. SKB P-03-56, Svensk Kärnbränslehantering AB.
- Ludvigson J-E, Levén J, Källgården J, Jönsson S, 2004.** Oskarshamn site investigation. Single-hole injection tests in borehole KSH02. SKB P-04-247, Svensk Kärnbränslehantering AB.
- Lundin L, Lode E, Stendahl J, Björkvald L, Hansson J, (in press).** Soils and site types in the Oskarshamn area. Svensk kärnbränslehantering AB.
- Lundin L, Lode E, Stendahl J, et al, 2004.** Soils and site types in the Forsmark area. SKB R-04-08, Svensk Kärnbränslehantering AB.
- Lundqvist J, 1985.** Deep-weathering in Sweden. *Fennia* 163, 287–292.
- Lundqvist J, 1992.** Glacial stratigraphy in Sweden. Geological Survey of Finland Special paper 15. 43–59.
- Lundqvist J, Wohlfarth B, 2001.** Timing and east-west correlation of south Swedish ice marginal lines during the Late Weichselian. *Quaternary Science Reviews* 20, 1127–1148.
- Luukkonen A, 2001.** Groundwaters mixing and geochemical reactions. An inverse-modelling approach. In: A. Luukkonen and E. Kattilakoski (eds.), Äspö hard-rock laboratory. Groundwater flow, mixing and geochemical reactions at Äspö HRL. Task 5. Äspö Task Force on groundwater flow and transport of solutes. SKB IPR-02-041, Svensk Kärnbränslehantering AB.
- Löfgren A, Lindborg T, 2003.** A descriptive ecosystem model – a strategy for model development during site investigations. SKB R-03-06, Svensk Kärnbränslehantering AB.
- Löfgren M, Neretnieks I, 2003.** Formation factor logging by electrical methods. Comparison of formation factor logs obtained in situ and in the laboratory. *J. Contam. Hydrol.* 61: 107–115.
- Löfgren M, Neretnieks I, 2005a.** Oskarshamn site investigation. Formation factor logging in-situ and in the laboratory by electrical methods in KSH01A and KSH02. Measurements and evaluation of methodology. SKB P-05-27, Svensk Kärnbränslehantering AB.
- Löfgren M, Neretnieks I, 2005b.** Oskarshamn site investigation. Formation factor logging in-situ and in the laboratory by electrical methods in KLX03 and KLX04. SKB P-05-105, Svensk Kärnbränslehantering AB.
- Mac Berthouex P, Brown L C, 2002.** Statistics for environmental engineers, 2nd edition. Lewis Publishers.
- Maddock R H, Hailwood E A, Rhodes E J, Muir Wood R, 1993.** Direct fault dating trials at the Äspö Hard Rock Laboratory. SKB TR-93-24, Svensk Kärnbränslehantering AB.
- Mansfeld J, 1996.** Geological, geochemical and geochronological evidence for a new Paleoproterozoic terrane in southeastern Sweden. *Precambrian Research* 77, 91–103.
- Markström I, Stanfors R, Juhlin C, 2001.** Äspölaboratoriet – RVS-modellering, Ävrö – Slutrapport. SKB R-01-06, Svensk Kärnbränslehantering AB.
- Mattsson H, Triumf C-A, Wahlgren C-H, 2002.** Prediktering av förekomst av finkorniga granitgångar i Simpevarpsområdet. SKB P-02-05, Svensk Kärnbränslehantering AB.
- Mattsson H, 2004.** Interpretation of geophysical borehole data and compilation of petrophysical data from KSH03A (100–1,000 m), KSH03B, HAV09, HAV10 and KLX02 (200–1,000 m). Oskarshamn site investigation. SKB P-04-214, Svensk Kärnbränslehantering AB.
- Mattsson H, Thunehed H, 2004.** Interpretation of geophysical borehole data and compilation of petrophysical data from KSH02 (80–1000 m) and KAV01. SKB P-04-77, Svensk Kärnbränslehantering AB.

- Mattsson H, Stanfors R, Wahlgren C-H, Carlsten S, Hultgren P, 2004a.** Oskarshamn site investigation. Geological single-hole interpretation of KSH01A, KSH01B, HSH01, HSH02 and HSH03. SKB P-04-32, Svensk Kärnbränslehantering AB.
- Mattsson H, Stanfors R, Wahlgren C-H, Carlsten S, Hultgren P, 2004b.** Oskarshamn site investigation. Geological single-hole interpretation of KSH02 and KAV01. SKB P-04-133, Svensk Kärnbränslehantering AB.
- Mattsson H, Thunehed H, Triumf C-A, 2004c.** Oskarshamn site investigation. Compilation of petrophysical data from rock samples and in situ gamma-ray spectrometry measurements. Stage 2 – 2004 (including 2002). SKB P-04-294, Svensk Kärnbränslehantering AB.
- Mattsson H, Thunehed H, Keisu, M, 2005.** Interpretation of geophysical borehole measurements and compilation of petrophysical data from KLX01, KLX03, KLX04, HLX21, HLX22, HLX23, HLX24, HLX25, HLX26, HLX27 and HLX28. Oskarshamn site investigation. SKB P-05-34, Svensk Kärnbränslehantering AB.
- Mazurek M, Bossart P, Eliasson T, 1997.** Classification and characterization of water-conducting features at Äspö: Results of investigations on the outcrop scale. SKB International Cooperation Report ICR 97-01.
- Middlemost E A K, 1994.** Naming materials in the magma/igneous rock system. *Earth-Science Reviews* 37, 215–224.
- Miliander S, Punakivi M, Kyläkorpi L, Rydgren B, 2004.** Simpevarp site description: Human population and human activities. SKB R-04-11, Svensk Kärnbränslehantering AB.
- Milnes A G, Gee D G, 1992.** Bedrock stability in southeastern Sweden. Evidence from fracturing in the ordovician limestones of northern Öland. SKB TR-92-23, Svensk Kärnbränslehantering AB.
- Milnes A G, Gee D G, Lund C-E, 1998.** Crustal structure and regional tectonics of SE Sweden and the Baltic Sea. SKB TR-98-21, Svensk Kärnbränslehantering AB.
- Milodowski A E, Tullborg E-L, Buil B, Gómez P, Turrero M-J, Haszeldine S, England G, Gillespie M R, Torres T, Ortiz J E, Zacharias J, Silar J, Chvátal M, Strnad L, Še-bek O, Bouch J E, Chenery S R, Chenery C, Shepherd T J, McKervey J A, 2005.** Application of mineralogical petrological and geochemical tools for evaluating the palaeohydro-geological evolution of the PADAMOT Study sites. PADAMOT PROJECT Technical Report WP2. EU FP5 Contract nr FIKW-CT2001-20129.
- Min K-B, 2004.** Fractured Rock Masses as Equivalent Continua – A numerical study. Doctoral thesis. Royal Institute of Technology, Stockholm, Sweden. ISBN 91-7283-757-8.
- Morén L, Pässe T, 2001.** Climate and shoreline in Sweden during Weichsel and the next 150,000 years. SKB TR-01-19, 67 pp. Svensk Kärnbränslehantering AB.
- Moreno L, Neretnieks I, 1989.** Channelling in fractured zones and its potential impact on the transport of radionuclides, In: Lutze W., and Ewing, R. C. (eds.), *Mat. Res. Soc. Symp. Proc., Scientific Basis for Nuclear Waste Management XII*, Vol. 127, pp. 779–786.
- Moreno L, Neretnieks I, 1993.** Fluid flow and solute transport in a network of fractures, *J. Contam. Hydrol.*, 14(3-4), pp. 163–192.
- Morosini M, Hultgren H 2003.** Inventering av privata brunnar i Simpevarpsområdet, 2001–2002. SKB P-03-05, Svensk Kärnbränslehantering AB.
- Moye D G, 1967.** Diamond drilling for foundation exploration. *Civil Eng. Trans., Inst. Eng. Australia*, p95–100.
- Muir-Wood R, 1993.** A review of the seismotectonics of Sweden. SKB TR-93-13, Svensk Kärnbränslehantering AB.

- Munier R, 1989.** Brittle tectonics on Äspö, SE Sweden. SKB PR 25-89-15, Svensk Kärnbränslehantering AB.
- Munier R, 1993.** Segmentation, fragmentation and jostling of the Baltic shield with time. Thesis, Acta Universitatis Upsaliensis 37.
- Munier R, 1995.** Studies of geological structures at Äspö. Comprehensive summary of results. SKB PR 25-95-21, Svensk Kärnbränslehantering AB.
- Munier R, Stenberg L, Stanfors R, Milnes A G, Hermanson J, Triumf C-A, 2003.** Geological Site Descriptive Model. A strategy for the model development during site investigations. SKB R-03-07, Svensk Kärnbränslehantering AB.
- Munier R, 2004.** Statistical analysis of fracture data, adapted for modelling Discrete Fracture Networks – version 2. SKB R-04-66. Svensk Kärnbränslehantering AB.
- Mörner N-A, 1989.** Postglacial faults and fractures on Äspö. SKB PR 25-89-24, Svensk Kärnbränslehantering AB.
- Naturvårdsverket, 2000.** Environmental Quality Criteria – Lakes and water courses. Swedish Environmental Protection Agency Report 5050.
- Neretnieks I, 2002.** A stochastic multi channel model for solute transport – analysis of tracer tests in fractured rock, *J. Contam. Hydrol.*, 55(3–4), pp. 175–211.
- Nilsson G, 2004.** Oskarshamn site investigation. Investigation of sediments, peat lands and wetlands. Stratigraphical and analytical data. SKB P-04-273. Svensk Kärnbränslehantering AB.
- Nilsson K P, Bergman T, Eliasson, T, 2004.** Bedrock mapping 2004 – Laxemar subarea and regional model area. Outcrop data and description of rock types. Oskarshamn site investigation. SKB P-04-221, Svensk Kärnbränslehantering AB.
- Nisca D, 1987.** Aerogeophysical interpretation. Bedrock and tectonic analysis. SKB PR 25-87-04, Svensk Kärnbränslehantering AB.
- Nitare J, Norén M, 1992.** Nyckelbiotoper kartläggs i nytt projekt vid Skogsstyrelsen. Svensk botanisk tidskrift volym 86: 219–226.
- Nordenskjöld C E, 1944.** Morfologiska studier inom övergångsområdet mellan Kalmarslätten och Tjust. *Medd. Lunds Geog. Inst. Avd. VIII*, (in Swedish).
- Nordqvist R, Gustavsson E, 2002.** Single-well injection-withdrawal tests (SWIW). Literature review and scoping calculations for homogeneous crystalline bedrock conditions. SKB R-02-34, Svensk Kärnbränslehantering AB.
- Nordqvist R, Gustafsson E, 2004.** Single-well injection-withdrawal tests (SWIW). Investigation of evaluation aspects under heterogeneous crystalline bedrock conditions, SKB TR-04-57, Svensk Kärnbränslehantering AB.
- Nordstrom D K, Lindblom S, Donahoe R J, Barton CC, 1989.** Fluid inclusions in the Stripa granite and their possible influence on the groundwater chemistry. *Geochimica Cosmochimica Acta*, 53, 1741-1755.
- Norman S, Kjellbert N, 1990.** FARF31 – A far field radionuclide migration code for use with the PROPER package, SKB TR-90-01, Svensk Kärnbränslehantering AB.
- Nyborg M, Vestin E, Wilén P, 2004.** Oskarshamn site investigation. Hydrogeological inventory in the Oskarshamn area. SKB P-04-277. Svensk Kärnbränslehantering AB.
- Nyman H, 2005.** Depth and stratigraphy of Quaternary deposits. Preliminary site description Laxemar subarea – version 1.2. SKB R-05-54, Svensk Kärnbränslehantering AB.

- Näslund J O, Rodhe L, Fastook J L, Holmlund P, 2003.** New ways of studying ice sheet flow directions and glacial erosion by computer modelling-examples from Fennoscandia. *Quaternary Sciences Reviews* 22, 245–258.
- Olofsson I, Fredriksson A, 2005.** Strategy for a numerical Rock Mechanics Site Descriptive Model. Further development of the theoretical/numerical approach. SKB R-05-43, Svensk Kärnbränslehantering AB.
- Olsen L, Mejdahl V, Selvik S, 1996.** Middle and Late Pleistocene stratigraphy, Finnmark, north Norway. *NGU Bulletin* 429, 111p.
- Ohlsson Y, Neretnieks I, 1997.** Diffusion data in granite – Recommended values. SKB TR-97-20, Svensk Kärnbränslehantering AB.
- Outters N, 2003.** A generic study of discrete fracture network transport properties using FracMan/MAFIC, SKB R-03-13, Svensk Kärnbränslehantering AB.
- Painter S, 2006.** Effect of single-fracture aperture variability on field-scale transport, SKB R-06-25, Svensk Kärnbränslehantering AB.
- Parkhurst D L, Appelo C A J, 1999.** User's Guide to PHREEQC (Version 2), a computer program for speciation, batch-reaction, one-dimensional transport, and inverse geochemical calculations. U.S. Geological Survey Water-Resources Investigations Report 99-4259, 312 p.
- Pedersen K, Arlinger J, Jahromi N, Ekendahl S, Hallbeck L, 1995.** "Microbiological investigations". In: *The Redox Experiment in Block Scale. Final Reporting of Results from the Three year Project. Chapter 7.* Steven Banwart (Ed). SKB Progress Report 25-95-06. Svensk Kärnbränslehantering AB.
- Persson H, 2002.** Root systems of arboreal plants. In Waisel, Y., Eshel, A. and Kafkafi, U. (ed.) *Plant roots – The hidden half.* 3rd. ed. Marcel Dekker, Inc. New York, Basel.
- Persson Nilsson K, Bergman T, Eliasson T, 2004.** Oskarshamn site investigation. Bedrock mapping 2004 – Laxemar subarea and regional model area. Outcrop data and description of rock types. SKB P-04-221, Svensk Kärnbränslehantering AB.
- Pitkänen P, Luukkonen A, Ruotsalainen P, Leino-Forsman H, Vuorinen U, 1998.** Geochemical modelling of groundwater evolution and residence time at the Kivetty site. POSIVA Report 98-07, Helsinki, Finland, 139 p.
- Poteri A, Billaux D, Cvetkovic V, Dershowitz B, Gómez-Hernández J-J, Hautojärvi A, Holton D, Medina A, Winberg A, 2002.** TRUE Block Scale Project. Final Report – 3. Modelling of flow and transport. SKB TR-02-15, Svensk Kärnbränslehantering AB.
- Priest S D, 1993.** Discontinuity analysis for rock engineering. Chapman & Hall, London, ISBN 0-412-47600, 473 p.
- Prikryl J, Jain A, Turner D, Pabalan R, 2001.** Uranium(VI) sorption behaviour on silicate minerals mixtures. *J. Cont. Hydrol.*, 47, pp 241–253.
- Puigdomenech I (ed), 2001.** Hydrochemical stability of groundwaters surrounding a spent nuclear fuel repository in a 100,000 year perspective. SKB TR-01-28, Svensk Kärnbränslehantering AB, 83 p.
- Puigdomenech I, Ambrosi J-P, Eisenlohr L, Lartigue J-E, Banwart S, Bate-man K, Milodowski A E, West J M, Griffault L, Gustafsson E, Hama K, Yoshida H, Kotelnikova S, Pedersen K, Michaud V, Trotignon L, Morosini M, Rivas Perez J, Tullborg E-L, 2001.** O₂ depletion in granitic media. SKB Tech.Rep. (TR-01-05), SKB, Stockholm, Sweden.
- Påsse T, 1997.** A mathematical model of past, present and future shore level displacement in Fennoscandia. SKB TR-97-28, 55 pp. Svensk Kärnbränslehantering AB.

- Påsse T, 2001.** An empirical model of glacio-isostatic movements and shore-level displacement in Fennoscandia. SKB R-01-41, 59 pp. Svensk Kärnbränslehantering AB.
- Påsse T, 2004.** The amount of glacial erosion of the bedrock. SKB TR-04-25, Svensk kärnbränslehantering AB.
- Pöllänen J, Sokolnicki M, 2004.** Oskarshamn site investigation – Difference flow measurements in borehole KAV04A and KAV04B. SKB P-04-216, Svensk Kärnbränslehantering AB.
- Rahm N, Enachescu C, 2004a.** Oskarshamn site investigation: Hydraulic testing of percussion drilled lineament boreholes on Ävrö and Simpevarp, 2004, SKB P-04-287, Svensk Kärnbränslehantering AB.
- Rahm N, Enachescu C, 2004b.** Oskarshamn site investigation: Hydraulic injection tests in borehole KLX02, 2003, SKB P-04-288, Svensk Kärnbränslehantering AB.
- Rahm N, Enachescu C, 2004c.** Hydraulic injection tests in borehole KSH01A, 2003/2004, Simpevarp, SKB P-04-289, Svensk Kärnbränslehantering AB.
- Rahm N, Enachescu C, 2004d.** Hydraulic injection tests in borehole KSH03A, 2004, Simpevarp. SKB P-04-290, Svensk Kärnbränslehantering AB.
- Rahm N, Enachescu C, 2004e.** Oskarshamn site investigation. Hydraulic injection tests in borehole KAV04A, 2004. Subarea Simpevarp. SKB P-04-291, Svensk Kärnbränslehantering AB.
- Rahm N, Enachescu C, 2004f.** Oskarshamn site investigation: Hydraulic injection tests in borehole KLX04, 2004, SKB P-04-292, Svensk Kärnbränslehantering AB.
- Rahm N, Enachescu C, 2005a.** Oskarshamn site investigation. Pumping tests and water sampling in borehole KLX04, 2004. Subarea Laxemar. SKB P-05-16, Svensk Kärnbränslehantering AB.
- Rahm N, Enachescu C, 2005b.** Oskarshamn site investigation. Pumping tests and hydraulic injection tests in borehole KLX06, 2005. Subarea Laxemar. SKB P-05-184. Svensk Kärnbränslehantering AB.
- Rhén I, Bäckblom G, Gustafsson G, Stanfors R, Wikberg P, 1997a.** Äspö HRL – Geoscientific evaluation 1997/2. Results from pre-investigations and detailed characterization. SKB TR-97-03, Svensk Kärnbränslehantering AB.
- Rhén I, Gustafsson G, Wikberg P, 1997b.** Äspö HRL – Geoscientific evaluation 1997/5. Models based on site characterization 1986–1995. SKB TR-97-03, Svensk Kärnbränslehantering AB.
- Rhén I, Gustafsson G, Wikberg P, 1997c.** Äspö HRL – Geoscientific evaluation 1997/5. Models based on site characterization 1986–1995. SKB TR-97-06, Svensk Kärnbränslehantering AB.
- Rhén I, Gustafsson G, Wikberg P, 1997d.** Äspö HRL – Geoscientific evaluation 1997/4. Results from pre-investigations and detailed site characterization. Comparisons of predictions and observations. Hydrogeology, groundwater chemistry and transport of solutes. SKB TR-97-05. Svensk Kärnbränslehantering AB.
- Rhén I, Forsmark T, 2001.** Äspö Hard Rock Laboratory, Prototype repository, Hydrogeology, Summary report of investigations before the operation phase. SKB IPR-01-65, Svensk Kärnbränslehantering AB.
- Rhén I, Smellie J (eds), 2003.** Task force on modelling of groundwater flow and transport of solutes. Task 5 summary report. SKB TR-03-01, Svensk Kärnbränslehantering AB.
- Rhén I, Follin S, Hermanson J, 2003.** Hydrological Site Descriptive Model – a strategy for its development during site investigations. SKB R-03-08, Svensk Kärnbränslehantering AB.
- Rhén I, Forsmark T, Forsman I, Zetterlund M, 2006a (in prep).** Hydrogeological single-hole interpretation of KSH01, KSH02, KSH03, KAV01 and HSH01–03, Preliminary site description, Simpevarp subarea – version 1.2, SKB R-06-20, Svensk Kärnbränslehantering AB.

- Rhén I, Forsmark T, Forsman I, Zetterlund M, 2006b (in prep).** Hydrogeological single-hole interpretation of KLX02, KLX03, KLX04, KAV04A and KAV04b, Preliminary site description, Laxemar subarea – version 1.2, SKB R-06-21, Svensk Kärnbränslehantering AB.
- Rhén I, Forsmark T, Forsman I, Zetterlund M, 2006c (in prep).** Evaluation of hydrogeological properties for Hydraulic Conductor Domains (HCD) and Hydraulic Rock Domains (HRD), Preliminary site description, Laxemar subarea – version 1.2, SKB R-06-23, Svensk Kärnbränslehantering AB.
- Ringberg B, Hang T, Kristiansson J, 2002.** Local clay-varve chronology in the Karlskrona-Hultsfred region, southeast Sweden. *GFF* 124, 79–86.
- Risberg J, Miller U, Brunnberg L, 1991.** Deglaciation, Holocene shore displacement and coastal settlements in eastern Svealand, Sweden. *Quaternary International* 9, 33–39.
- Robertsson A-M, Svedlund J-O, Andrén T, Sundh M, 1997.** Pleistocene stratigraphy in the Dellen region, central Sweden. *Boreas* 26, 237–260.
- Rodhe A, 1987.** Depositional environment and lithostratigraphy of the middle Proterozoic Almesåkra Group, southern Sweden. *Sveriges geologiska undersökning Ca* 69.
- Rouhiainen P, 2000.** Äspö Hard Rock Laboratory – Difference flow measurements in borehole KLX02 at Laxemar. IPR-01-06, Svensk Kärnbränslehantering AB.
- Rouhiainen P, Pöllänen J, 2003a.** Oskarshamn site investigation – Difference flow measurements in borehole KSH01A at Simpevarp. P-03-70, Svensk Kärnbränslehantering AB.
- Rouhiainen P, Pöllänen J, 2003b.** Oskarshamn site investigation – Difference flow measurements in borehole KSH02 at Simpevarp. P-03-110, Svensk Kärnbränslehantering AB.
- Rouhiainen P, Pöllänen J, 2004.** Oskarshamn site investigation – Difference flow measurements in borehole KAV01 at Ävrö. P-04-213, Svensk Kärnbränslehantering AB.
- Rouhiainen P, Sokolnicki M, 2005.** Oskarshamn site investigation: Difference flow logging of borehole KLX04 – Subarea Laxemar, SKB P-05-68, Svensk Kärnbränslehantering AB.
- Rouhiainen P, Pöllänen J, Sokolnicki M, 2005.** Oskarshamn site investigation: Difference flow logging of borehole KLX03 – Subarea Laxemar, SKB P-05-67, Svensk Kärnbränslehantering AB.
- Rudmark L, 2000.** Beskrivning till jordartskartan 5G Oskarshamn NO. SGU Ae 94. 64 pp.
- Rudmark L, 2004.** Oskarshamn site investigation, Investigation of Quaternary deposits at Simpevarp peninsula and the islands of Ävrö and Hälö. SKB P-04-22, 19 pp. Svensk Kärnbränslehantering AB.
- Rudmark L, Malmberg-Persson K, Mikko M, 2005.** Oskarshamn site investigation. Investigation of Quaternary deposits 2003–2004. SKB P-05-49. Svensk Kärnbränslehantering AB.
- Rühling Å, 1997.** Floran i Oskarshamns kommun. Svensk Botanisk Förening, Lund.
- Rydström H, Gereben L, 1989.** Regional geological study. Seismic refraction survey. SKB PR 25-89-23, Svensk Kärnbränslehantering AB.
- Rønning H J S, Kihle O, Mogaard J O, Walker P, 2003.** Simpevarp site investigation – Helicopter borne geophysics at Simpevarp, Oskarshamn, Sweden. SKB P-03-25, Svensk Kärnbränslehantering AB.
- Röshoff K, Cosgrove J, 2002.** Sedimentary dykes in the Oskarshamn-Västervik area. A study of the mechanism of formation. SKB R-02-37, Svensk Kärnbränslehantering AB.
- SBF, 1999.** Nyckelbiotopsinventeringen 1993–1998 – Slutrapport. Swedish Board of Forestry, Jönköping.
- SCB, 2003.** SCB:s Marknadsprofiler, produktkatalog mars 2003-februari 2004, Statistics Sweden.

Schmelzbach C, Juhlin C, 2004. 3D processing of reflection seismic data acquired within and near the array close to KAV04A on Ävrö, 2003. SKB P-04-204. Svensk Kärnbränslehantering AB.

Schoning K, Klingberg F, Wastegård S, 2001. Marine conditions in central Sweden during the early Preboreal as inferred from a stable oxygen gradient. *Journal of Quaternary Science* 16, 785–784.

Shackelton N J, Berger A, Peltier W R, 1990. An alternative astronomical calibration of the lower Pleistocene timescale based on ODP Site 677. *Transactions of the Royal Society of Edinburgh: Earth Sciences* 81, 251–261.

Shackelton N J, 1997. The deep-sea sediment record and the Pliocene-Pleistocene boundary. *Quaternary International* 40, 33–35.

Šibrava V, 1992. Should the Pliocene-Pleistocene boundary be lowered? *Sveriges Geologiska Undersökning, Ca* 81, 327–332.

Skagius K, Neretnieks I, 1985. Diffusivity measurements and electrical resistivity measurements in rock samples under mechanical stress, TR-85-25, Svensk Kärnbränslehantering AB.

SKB, 1990. Granskning av Nils-Axels Mörnars arbete avseende postglaciala strukturer på Äspö. SKB AR 90-18 (in Swedish), Svensk Kärnbränslehantering AB.

SKB, 1999. Deep repository for spent nuclear fuel, SR 97 – Post-closure safety, SKB TR-99-06, Svensk Kärnbränslehantering AB.

SKB, 2000. Geoscientific programme for investigation and evaluation of sites for the deep repository. SKB TR-00-20, Svensk Kärnbränslehantering AB.

SKB, 2001a. Site investigations – Investigation methods and general execution programme. SKB TR-01-29, Svensk Kärnbränslehantering AB.

SKB, 2001b. Geovetenskapligt program för platsundersökning vid Simpevarp SKB R-01-44. Svensk Kärnbränslehantering AB.

SKB, 2002a. Preliminary safety evaluation, based on initial site investigation data. Planning document, SKB TR-02-28, Svensk Kärnbränslehantering AB.

SKB, 2002b. Simpevarp – site descriptive model version 0. SKB R-02-35, Svensk Kärnbränslehantering AB.

SKB, 2002c. Execution programme for the initial site investigations at Simpevarp. SKB P-02-06, Svensk Kärnbränslehantering AB.

SKB, 2003. Prioritering av områden för platsundersökningen i Oskarshamn. SKB R-03-12. Svensk Kärnbränslehantering AB.

SKB, 2004a. Hydrogeochemical evaluation for Simpevarp model version 1.2. Preliminary site description of the Simpevarp area. SKB R-04-74, Svensk Kärnbränslehantering AB.

SKB, 2004b. Preliminary site description Simpevarp area – version 1.1. SKB R-04-25, Svensk Kärnbränslehantering AB.

SKB, 2004d. RETROCK project. Treatment of geosphere retention phenomena in safety assessments. Scientific basis of retention processes and their implementation in safety assessment models (WP2), Work Package 2 report of the RETROCK Concerted Action. SKB R-04-48, Svensk Kärnbränslehantering AB.

SKB, 2004e. Interim main report of the safety assessment SR-Can. SKB TR-04-11. Svensk Kärnbränslehantering AB.

SKB, 2005a. Preliminary site description. Simpevarp subarea – version 1.2. SKB R-05-08, Svensk Kärnbränslehantering AB.

- SKB, 2005b.** Preliminary site description. Forsmark area – version 1.2. SKB R-05-18, Svensk Kärnbränslehantering AB.
- SKB, 2005c.** Program för fortsatta undersökningar av berggrund, mark, vatten och miljö inom delområde Laxemar. Platsundersökning Oskarshamn. SKB R-05-37 Svensk Kärnbränslehantering AB.
- SKB, 2005d.** Preliminary safety evaluation for the Forsmark area. Based on data and site descriptions after the initial site investigation stage. SKB TR-05-16. Svensk Kärnbränslehantering AB.
- SKB, 2005e.** Preliminary safety evaluation for the Simpevarp subarea. Based on data and site descriptions after the initial site investigation stage. SKB TR-05-12. Svensk Kärnbränslehantering AB.
- SKB 2005f.** Utvärdering av platsdata inför fokusering av de fortsatta undersökningarna inom delområde Laxemar. Platsundersökning Oskarshamn. SKB P-05-264. Svensk Kärnbränslehantering AB
- SKB, 2006a.** Hydrogeochemical evaluation. Preliminary site description, Laxemar subarea – version 1.2. (2006), SKB R-06-12, Svensk Kärnbränslehantering AB.
- SKB, 2006b.** Description of surface systems. Preliminary site description, Laxemar subarea – version 1.2. (2006), SKB R-06-11. Svensk Kärnbränslehantering AB.
- SNV, 1984.** Våtmarksinventering inom fastlandsdelen av Kalmar Län: Del 1 Allmän beskrivning och katalog över särskilt värdefulla objekt. Statens Naturvårdsverk, Solna, Rapport PM 1787.
- Slunga R, Norrman P, Glans A-C, 1984.** Baltic shield seismicity, the results of a regional network. Geophysical research letters 11, 1247–1250.
- Slunga R, 1989.** Analysis of the earthquake mechanisms in the Norrbotten area. In Bäckblom and Stanfors (Eds.), Interdisciplinary study of post-glacial faulting in the Lansjärv area northern Sweden. 1986–1988. SKB TR-89-31, Svensk Kärnbränslehantering AB.
- Slunga R, Nordgren L, 1990.** Earthquake measurements in southern Sweden APR 1 1987–NOV 30 1988. SKB AR 90-19, Svensk Kärnbränslehantering AB.
- Smellie J, Laaksoharju M, Tullborg E-L, 2002.** Hydrogeochemical site descriptive model – a strategy for the model development during site investigations. SKB R-02-49, Svensk Kärnbränslehantering AB.
- Smellie J, 2004.** Recent geoscientific information relating to deep crustal studies, SKB R-04-09, Svensk Kärnbränslehantering AB.
- Stanfors R, Rhén I, Forsmark T, Wikberg P 1994.** Evaluation of the fracture zone EW-1, based on the cored boreholes KA1755A, KA1751, KA1754A and KAS04. SKB PR-25-94-39. Svensk Kärnbränslehantering AB.
- Stanfors R, Erlström M, 1995.** SKB Palaeohydrogeological programme. Extended geological models of the Äspö area. SKB AR 95-20, Svensk Kärnbränslehantering AB.
- Staub I, Andersson C, Magnor B, 2004.** Äspö Hard Rock Laboratory – Äspö Pillar Stability Experiment, Geology and mechanical properties of the rock mass in TASQ. SKB R-04-01. Svensk Kärnbränslehantering AB.
- Stenberg L, Sehlstedt S, 1989.** Geophysical profile measurements on interpreted regional aeromagnetic lineaments in the Simpevarp area. SKB PR 25-89-13, Svensk Kärnbränslehantering AB.
- Stephansson O, Dahlström L-O, Bergström K, Sarkka P, Vitinen A, Myrvang A, Fjeld O, Hansen T H, 1987.** Fennoscandian Rock Stress Database – FRSDDB. Research report TULEA 1987:06, Luleå University of Technology, Luleå.

- Stephens M B, Wahlgren C-H, Weihed P, 1994.** Geological Map of Sweden, scale 1:3 000 000. SGU series Ba 52, Sveriges Geologiska Undersökning.
- Stephens M B, Wahlgren C-H, 1996.** Post-1.85 Ga tectonic evolution of the Svecokarelian orogen with special reference to central and SE Sweden. GFF 118, Jubilee Issue, A26–27.
- Stigebrandt A, 1985.** A model for the seasonal pycnocline rotating system with application to the Baltic proper. *J. Phys. Oceanogr.*, 15, 1392–1402.
- Stigebrandt A, 1990.** On the response of horizontal mean vertical density distribution in a fjord to low-frequency density fluctuations in the coastal water. *Tellus*, 42A, 605–614.
- Streckeisen A, 1976.** To each plutonic rock its proper name. *Earth Science Reviews* 12, 1–33.
- Stråhle A, 2001.** Definition och beskrivning av parametrar för geologisk, geofysisk och bergmekanisk kartering av berget. SKB R-01-19, Svensk Kärnbränslehantering AB.
- Strömberg B, 1989.** Late Weichselian deglaciation and clay varve chronology in east-central Sweden. *Sveriges geologiska undersökning*, Ca 73.
- Strömberg M, 2005.** Oskarshamn site investigation. Surveying of water courses in catchment areas 6, 7 and 9. Svensk Kärnbränslehantering AB (in prep).
- Sturesson E, 2003.** Platsundersökning Oskarshamn – Nyckelbiotopsinventering I Simpevarpsområdet. SKB P-03-78, Svensk Kärnbränslehantering AB.
- Sultan L, Claesson S, Plink-Björklund P, Björklund L, 2004.** Proterozoic and Archaean detrital zircon ages from the Palaeoproterozoic Västervik Basin, southern Fennoscandian Shield. *GFF* 126, 39.
- Sundberg J, 1988.** Thermal properties of soils and rocks, Publ. A 57 Dissertation, Doctoral thesis, Geologiska institutionen, Chalmers University of Technology and University of Göteborg.
- Sundberg J, Gabrielsson A, 1999.** Laboratory and field measurements of thermal properties of the rock in the prototype repository at Äspö HRL. SKB IPR-99-17, Svensk Kärnbränslehantering AB.
- Sundberg J, 2002.** Determination of thermal properties at Äspö HRL, Comparison and evaluation of methods and methodologies for borehole KA2599G01, SKB R-02-27, Svensk Kärnbränslehantering AB.
- Sundberg J, 2003a.** Thermal Site Descriptive Model, A Strategy for the Model Development during Site Investigations, SKB R-03-10, Svensk Kärnbränslehantering AB.
- Sundberg J, 2003b.** Thermal Properties at Äspö HRL, Analysis of Distribution and Scale Factors, SKB R-03-17, Svensk Kärnbränslehantering AB.
- Sundberg J, Ericsson U, Engdahl A and Svensson J-E, 2004.** Phytoplankton and zooplankton. Results from sampling in the Simpevarp area 2003-2004. Oskarshamn site investigation, SKB P-04-253, Svensk Kärnbränslehantering AB.
- Sundberg J, Back P-E, Hellström G, 2005a.** Development of Methodology for Rock Thermal Conductivity Estimation at Canister Scale with the Äspö HRL Prototype Repository as an Example. Analysis of uncertainty and scale dependence by measurement, inverse thermal modelling and value of information analysis. SKB R-05-82, Svensk Kärnbränslehantering AB. Report in progress.
- Sundberg J, Back P, Bengtsson A, 2005b.** Thermal modelling. Preliminary site description Simpevarp subarea – version 1.2. SKB R-05-24, Svensk Kärnbränslehantering AB.
- Sundberg J, Wrafter J, Back P-E, Ländell M, 2006.** Oskarshamn site investigation. Thermal modelling. Preliminary site description Laxemar subarea – version 1.2. Svensk Kärnbränslehantering AB. Report in progress.
- Svantesson S, 1999.** Beskrivning till jordartskartan 7G Västervik SO/ 7H Loftahammar SV. SGU Ae 124. 109 pp.

- Svensson S A, 1984.** Hur säker är riksskogstaxeringen? Swedish University of Agricultural Sciences, Garpenberg, Skogsfakta (inventering och ekonomi) nr. 5.
- Svensson N-O, 1989.** Late Weichselian and early Holocene shore displacement in the central Baltic, based on stratigraphical and morphological records from eastern Småland and Gotland, Sweden. LUNDQUA 25, 181 pp.
- Svensson U, 1996.** SKB Palaeohydrogeological programme. Regional groundwater flow due to advancing and retreating glacier-scoping calculations. In: SKB Project Report U 96-35, Svensk Kärnbränslehantering AB.
- Svensson U, 2004.** DarcyTools, Vesrion 2.1. Verification and validation. SKB R-04-21, Svensk Kärnbränslehantering AB.
- Svensson U, Ferry M, 2004.** DarcyTools, Version 2.1. User's guide. SKB R-04-20, Svensk Kärnbränslehantering AB.
- Svensson U, Kuylenstierna H-O, Ferry M, 2004.** DarcyTools, Version 2.1. Concepts, methods, equations and demo simulations. SKB R-04-19, Svensk Kärnbränslehantering AB.
- Svensson J, 2005.** Fältundersökning av diskrepanser gällande vattendrag i GIS-modellen. Svensk Kärnbränslehantering AB (in Swedish).
- Söderlund U, Patchett P J, Isachsen C, Vervoort J, Bylund G, 2004.** Baddeleyite U-Pb dates and Hf-Nd isotope compositions of mafic dyke swarms in Sweden and Finland. GFF 126, 38.
- Söderlund P, Juez-Larré J, Page L, Dunai T, 2005.** Extending the time range of apatite (U-Th/He) thermochronometry in slowly cooled terranes: Palaeozoic to Cenozoic exhumation history of south-east Sweden. Earth and Planetary Science Letters 239, 266–275.
- Talbot C, Munier R, 1989.** Faults and fracture zones in Äspö. SKB PR 25-89-11, Svensk Kärnbränslehantering AB.
- Talbot C, Ramberg H, 1990.** Some clarification of the tectonics of Äspö and its surroundings. SKB PR 25-90-15, Svensk Kärnbränslehantering AB.
- Thiem G, 1906.** Hydrologische Methoden. Gebhardt, Leipzig, 56 pp.
- Thunehed H, Triumf C-A, Pitkänen T, 2004.** Oskarshamn site investigation. Geophysical profile measurements over interpreted lineaments in the Laxemar area. SKB P-04-211, Svensk Kärnbränslehantering AB.
- Thunehed H, 2005.** Oskarshamn site investigation: resistivity measurements and determination of formation factors on samples from KLX04 and KSH02, SKB P-05-75, Svensk Kärnbränslehantering AB.
- Tirén S A, Beckholmen M, Isaksson H, 1987.** Structural analysis of digital terrain models, Simpevarp area, southeastern Sweden. Method study EBBA II. SKB PR 25-87-21, Svensk Kärnbränslehantering AB.
- Tobiasson S, 2003.** Tolkning av undervattensfilm från Forsmark och Simpevarp. SKB P-03-68, Svensk Kärnbränslehantering AB.
- Triumf C-A, 2003.** Oskarshamn site investigation – Identification of lineaments in the Simpevarp area by the interpretation of topographical data. SKB P-03-99, Svensk Kärnbränslehantering AB.
- Triumf C-A, Thunehed H, Kero L, Persson L, 2003.** Oskarshamn site investigation. Interpretation of airborne geophysical survey data. Helicopter borne survey data of gamma ray spectrometry, magnetics and EM from 2002 and fixed wing airborne survey data of the VLF-field from 1986. SKB P-03-100, Svensk Kärnbränslehantering AB.
- Triumf C-A, 2004a.** Oskarshamn site investigation. Joint interpretation of lineaments. SKB P-04-49, Svensk Kärnbränslehantering AB.

- Triumf C-A, 2004b.** Oskarshamn site investigation. Gravity measurements in the Laxemar model area with surroundings. SKB P-04-128, Svensk Kärnbränslehantering AB.
- Truvé J, Cederlund G, 2005.** Mammals in the areas adjacent to Forsmark and Oskarshamn. Population density, ecological data and carbon budget. SKB R-05-36, Svensk Kärnbränslehantering AB.
- Tröjbom M, Söderbäck B, 2006.** Chemical characteristics of surface systems in the Simpevarp area. Visualisation and statistical evaluation of data from surface water, precipitation, shallow groundwater, and regolith. SKB R-06-18, Svensk Kärnbränslehantering AB.
- Tullborg E-L, Larson S Å, 1984.** $\delta^{18}\text{O}$ and $\delta^{13}\text{C}$ for limestones, calcite fissure infillings and calcite precipitates from Sweden. Geologiska föreningens i Stockholm förhandlingar 106, 127–130.
- Tullborg E-L, Larson S Å, Björklund L, Samuelsson L, Stigh J, 1995.** Thermal evidence of Caledonide foreland, molasse sedimentation in Fennoscandia. SKB TR-95-18, Svensk Kärnbränslehantering AB.
- Tullborg E-L, Larson S Å, Stiberg J-A, 1996.** Subsidence and uplift of the present land surface in the southeastern part of the Fennoscandian Shield. GFF 118, 126–128.
- Ukkonen P, Lunkka J P, Jungner H, Donner J, 1999.** New radiocarbon dates from Finnish mammoths indicating large ice-free areas in Fennoscandia during the Middle Weichselian. Journal of Quaternary Science 14, 711–714.
- Vilks P, Miller H, Doern D, 1991.** Natural colloids and suspended particles in Whiteshell Research area, Manitoba, Canada, and their potential effect on radiocolloid formation. Applied Geochemistry 8, 565-574.
- Vogt K A, Grier C C, Meier C E, Edmonds R L, 1982.** Mycorrhizal role in net primary production and nutrient cycling in *Abies amabilis* ecosystems in western Washington. Ecology 63(2): 370–380.
- Voss C I, 1984.** SUTRA – Saturated-Unsaturated Transport. A finite element simulation model for saturated-unsaturated fluid-density-dependent ground-water flow with energy transport or chemically-reactive single-species solute transport. U.S: Geological Survey Water-Resources Investigations Report 84-4369.
- Wahlgren C-H, Persson L, Danielsson P, Berglund J, Triumf C-A, Mattsson H, Thunehed H, 2003.** Geologiskt underlag för val av prioriterad plats inom området väster om Simpevarp. Delrapport 1–4. SKB P-03-06, Svensk Kärnbränslehantering AB.
- Wahlgren C-H, Ahl M, Sandahl K-A, Berglund J, Petersson J, Ekström M, Persson P-O, 2004.** Oskarshamn site investigation. Bedrock mapping 2003 – Simpevarp subarea. Outcrop data, fracture data, modal and geochemical classification of rock types, bedrock map, radiometric dating. SKB P-04-102, Svensk Kärnbränslehantering AB.
- Wahlgren C-H, Bergman T, Persson Nilsson K, Eliasson T, Ahl M, Ekström M, 2005a.** Oskarshamn site investigation. Bedrock map of the Laxemar subarea and surroundings. Description of rock types, modal and geochemical analyses. SKB P-05-180, Svensk Kärnbränslehantering AB.
- Wahlgren C-H, Hermanson J, Curtis P, Forssberg O, Triumf C-A, Drake H, Tullborg E-L, 2005b.** Geological description of rock domains and deformation zones in the Simpevarp and Laxemar subareas. Preliminary site description, Laxemar subarea, version 1.2. SKB R-05-69, Svensk Kärnbränslehantering AB.
- Werner K, Bosson E, Berglund S, 2005.** Description of climate, surface hydrology, and near-surface hydrogeology. Preliminary site description Laxemar subarea – version 1.2. SKB R-05-61, Svensk Kärnbränslehantering AB.
- Westman P, Wastegård S, Schoning K, Gustafsson B, 1999.** Salinity change in the Baltic Sea during the last 8,500 years: evidence causes and models. SKB TR-99-38. 52 pp. Svensk Kärnbränslehantering AB.

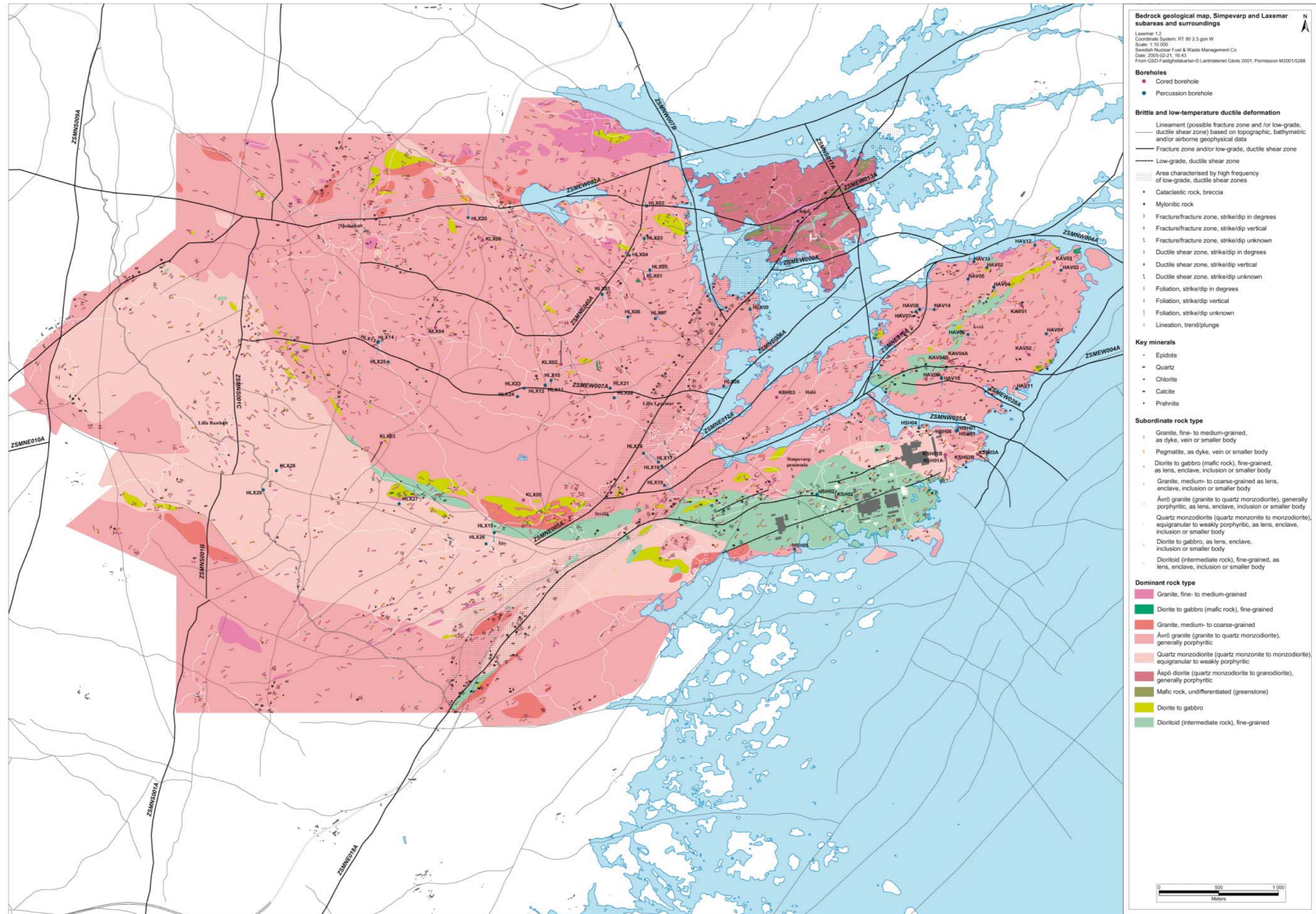
- Widestrand H, Byegård J, Ohlsson Y, Tullborg E-L, 2003.** Strategy for the use of laboratory methods in the site investigations programme for the transport properties of the rock. SKB R-03-20, Svensk Kärnbränslehantering AB.
- Wikberg P, 1998.** Äspö Task Force on modelling of groundwater flow and transport of solutes. SKB progress report HRL-98-07, Svensk Kärnbränslehantering AB.
- Wiklund S, 2002.** Digitala ortofoton och höjdm modeller. Redovisning av metodik för platsundersökningsområdena Oskarshamn och Forsmark samt förstudieområdet Tierp Norra. SKB P-02-02, Svensk Kärnbränslehantering AB.
- Wikman H, Kornfält K-A, 1995.** Updating of a lithological model of the bedrock of the Äspö area. SKB PR 25-95-04, Svensk Kärnbränslehantering AB.
- Winberg A, Andersson P, Hermansson J, Byegård J, Cvetkovic V, Birgersson L, 2000.** Äspö Hard Rock Laboratory. Final report of the first stage of the Tracer Retention Understanding Experiments, SKB TR-00-07, Svensk Kärnbränslehantering AB. ISSN 1404-0344.
- Wu P, Johnston P, Lambeck K, 1999.** Postglacial rebound and fault instability in Fennoscandia. *Geophysical Journal International* 139, 657–670.
- Xu S, Wörman A, 1998.** Statistical patterns of geochemistry in crystalline rock and effect of sorption kinetics on radionuclide migration. SKI Technical Report 98:41. Statens kärnkraftsinspektion.
- Åberg G, 1978.** Precambrian geochronology of south-eastern Sweden. *Geologiska Föreningens i Stockholm Förhandlingar* 100, 125–154.
- Åhäll K-I, 2001.** Åldersbestämning av svårdaterade bergarter i sydöstra Sverige. SKB R-01-60, Svensk Kärnbränslehantering AB (in Swedish).
- Åhäll K-I, Connelly J, Brewer T, 2002.** Transitioning from Svecofennian to Transscandinavian Igneous Belt (TIB) magmatism in SE Sweden: Implications from the 1.82 Ga Eksjö tonalite. *GFF* 124, 217–224.
- Åkesson U, 2004a.** Drill hole KSH01A Extensometer measurements of the coefficient of thermal expansion of rock. SKB P-04-59, Svensk Kärnbränslehantering AB.
- Åkesson U, 2004b.** Drill hole KSH02 Extensometer measurements of the coefficient of thermal expansion of rock. SKB P-04-60, Svensk Kärnbränslehantering AB.
- Åkesson U, 2004c.** Drill hole KAV01 Extensometer measurements of the coefficient of thermal expansion of rock. SKB P-04-61, Svensk Kärnbränslehantering AB.
- Åkesson U, 2004d.** Drill hole KLX02 Extensometer measurements of the coefficient of thermal expansion of rock. SKB P-04-260, Svensk Kärnbränslehantering AB.
- Åkesson U, 2004e.** Drill hole KLX04 Extensometer measurements of the coefficient of thermal expansion of rock. SKB P-04-269, Svensk Kärnbränslehantering AB.
- Åkesson U, 2004f.** Drill hole KAV04 Extensometer measurements of the coefficient of thermal expansion of rock. SKB P-04-272, Svensk Kärnbränslehantering AB.



Nomenclature of rock types (in English and Swedish), including rock codes applied in the site investigation at Oskarshamn

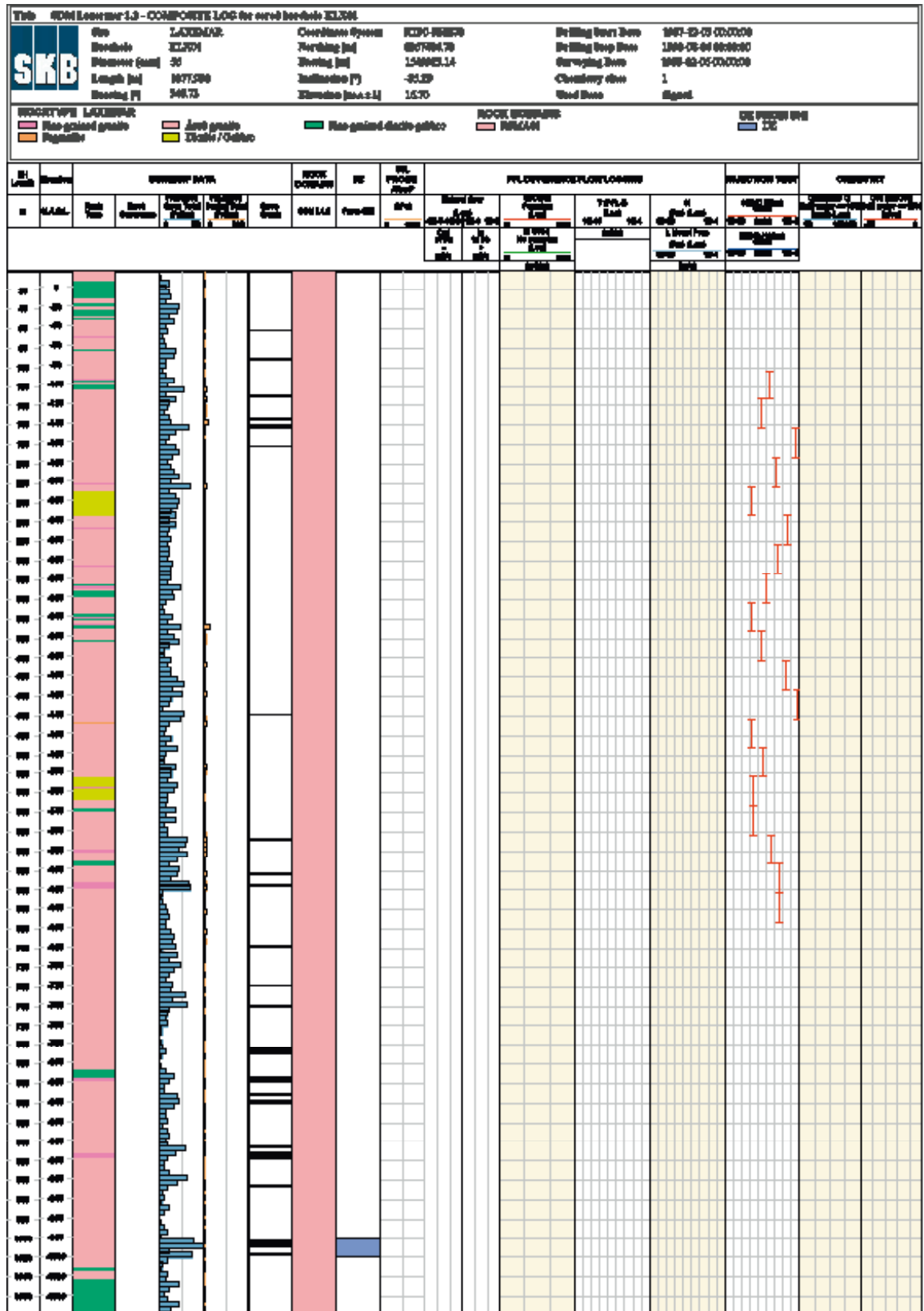
Nomenclature of rock types applied in the site investigation in Oskarshamn.

Rock code	Rock nomenclature (names within parenthesis refer to nomenclature used in the the Äspö Hard Rock Laboratory and related studies)	Descriptive nomenclature of rock type	R	G	B
501027	Dolerite Diabas	Dolerite Diabas	152	83	161
531058	Fine-grained Götemar granite Finkornig Götemargranit	Granite, fine- to medium-grained, ("Götemar granite") Granit, fin- till medelkornig, ("Götemargranit")	255	0	0
521058	Coarse-grained Götemar granite Grovkornig Götemargranit	Granite, coarse-grained, ("Götemar granite") Granit, grovkornig, ("Götemargranit")	200	24	56
511058	Fine-grained granite Finkornig granit	Granite, fine- to medium-grained Granit, fin- till medelkornig	235	122	179
501061	Pegmatite Pegmatit	Pegmatite Pegmatit	241	157	86
501058	Granite Granit	Granite, medium- to coarse-grained Granit, medel- till grovkornig	237	113	116
501044	Ävrö granite (<i>Småland-Ävrö granite</i>) Ävrögranit (<i>Småland-Ävrögranit</i>)	Granite to quartz monzodiorite, generally porphyritic Granit till kvartsmonzodiorit, vanligtvis porfyrisk	246	162	168
501036	Quartz monzodiorite (<i>Äspö diorite, tonalite</i>) Kvartsmonzodiorit (<i>Äspödiorit, tonalit</i>)	Quartz monzonite to monzodiorite, equigranular to weakly porphyritic Kvartsmonzonit till monzodiorit, jämnkornig till glest porfyrisk	250	199	193
501033	Diorite/gabbro Diorit/Gabbro	Diorite to gabbro Diorit till gabbro	193	221	53
501030	Fine-grained dioritoid (<i>Metavolcanite, volcanite</i>) Finkornig dioritoid (<i>Metavulkanit, vulkanit</i>)	Intermediate magmatic rock Intermediär magmatisk bergart	168	216	183
505102	Fine-grained diorite-gabbro (<i>Greenstone</i>) Finkornig diorit-gabbro (<i>Grönsten</i>)	Mafic rock, fine-grained Mafisk bergart, finkornig	69	185	124
509010	Sulphide mineralization Sulfidmineralisering	Sulphide mineralization Sulfidmineralisering	204	204	204
506007	Sandstone Sandsten	Sandstone Sandsten	217	192	106

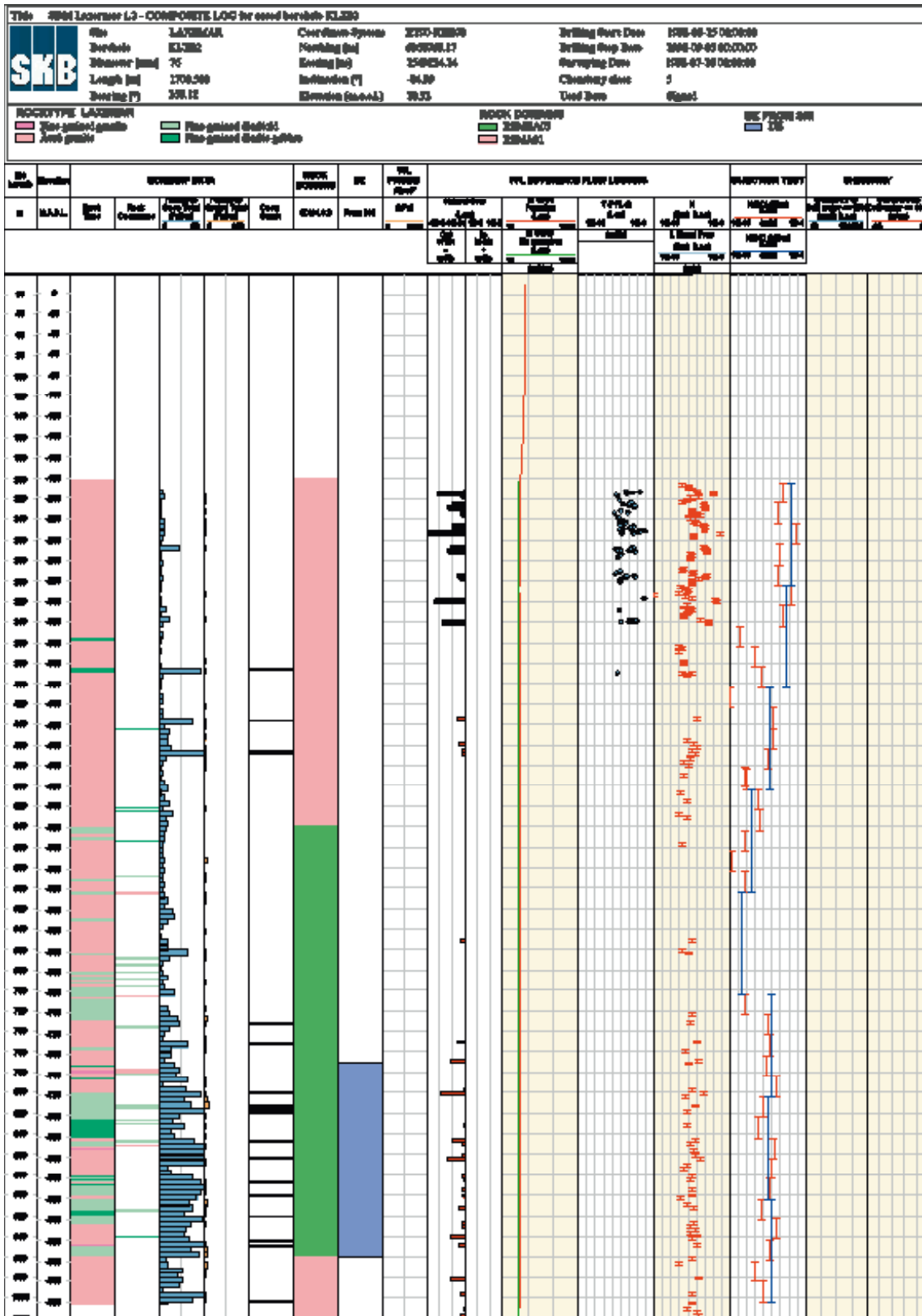


Composites of geological, hydrogeological and hydrogeochemical borehole logs

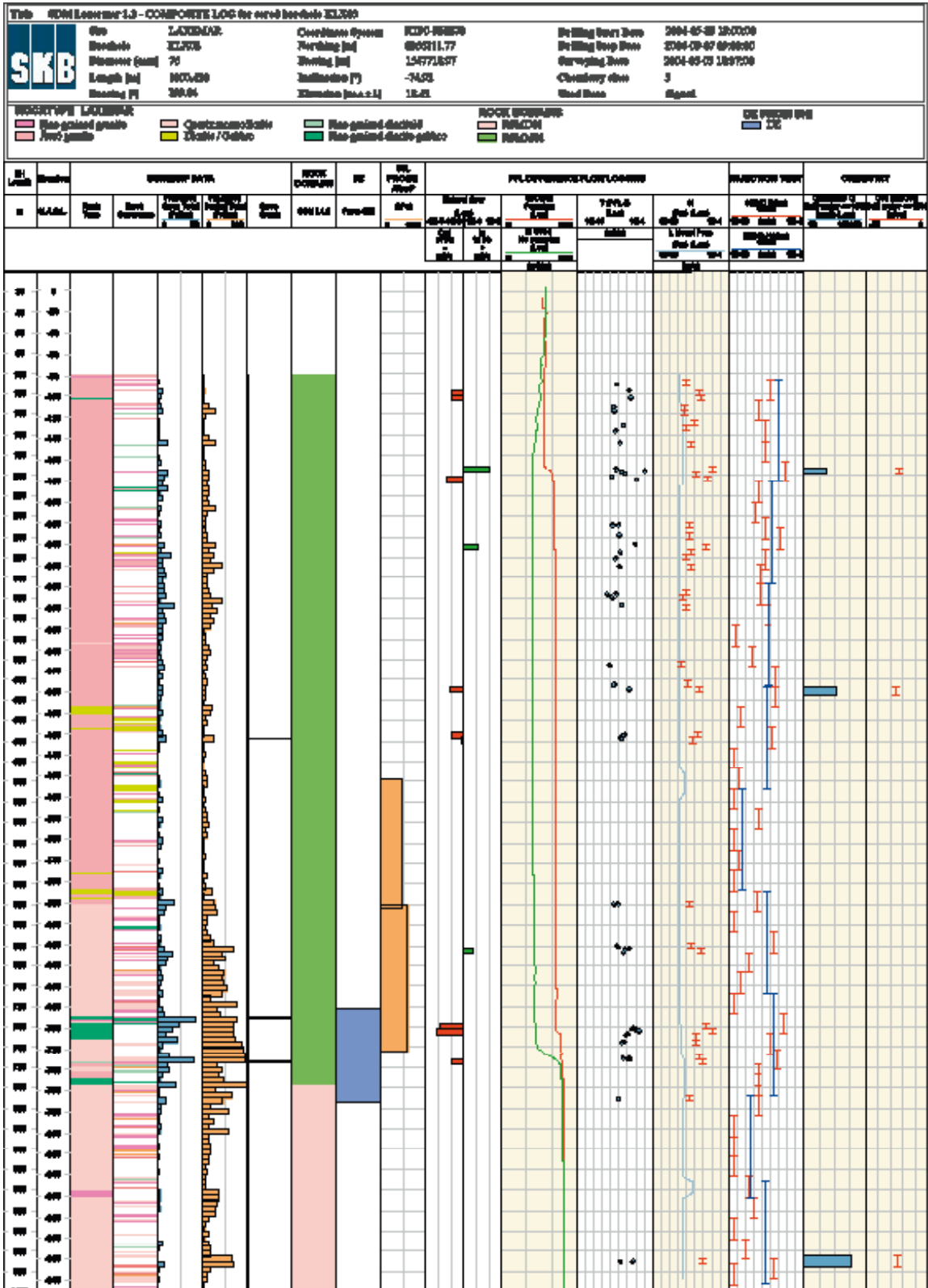
Cored borehole KLX01



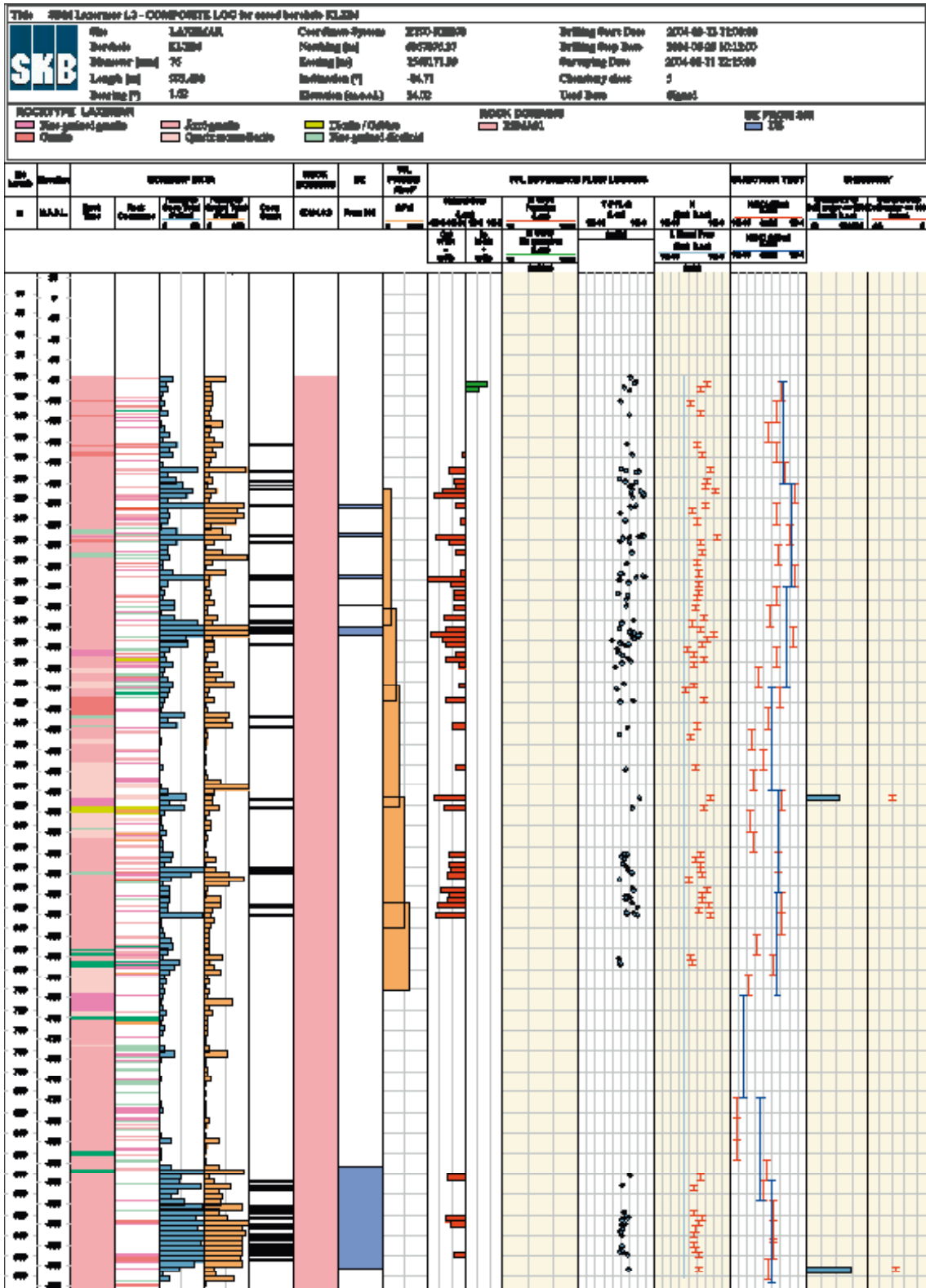
Cored borehole KLX02



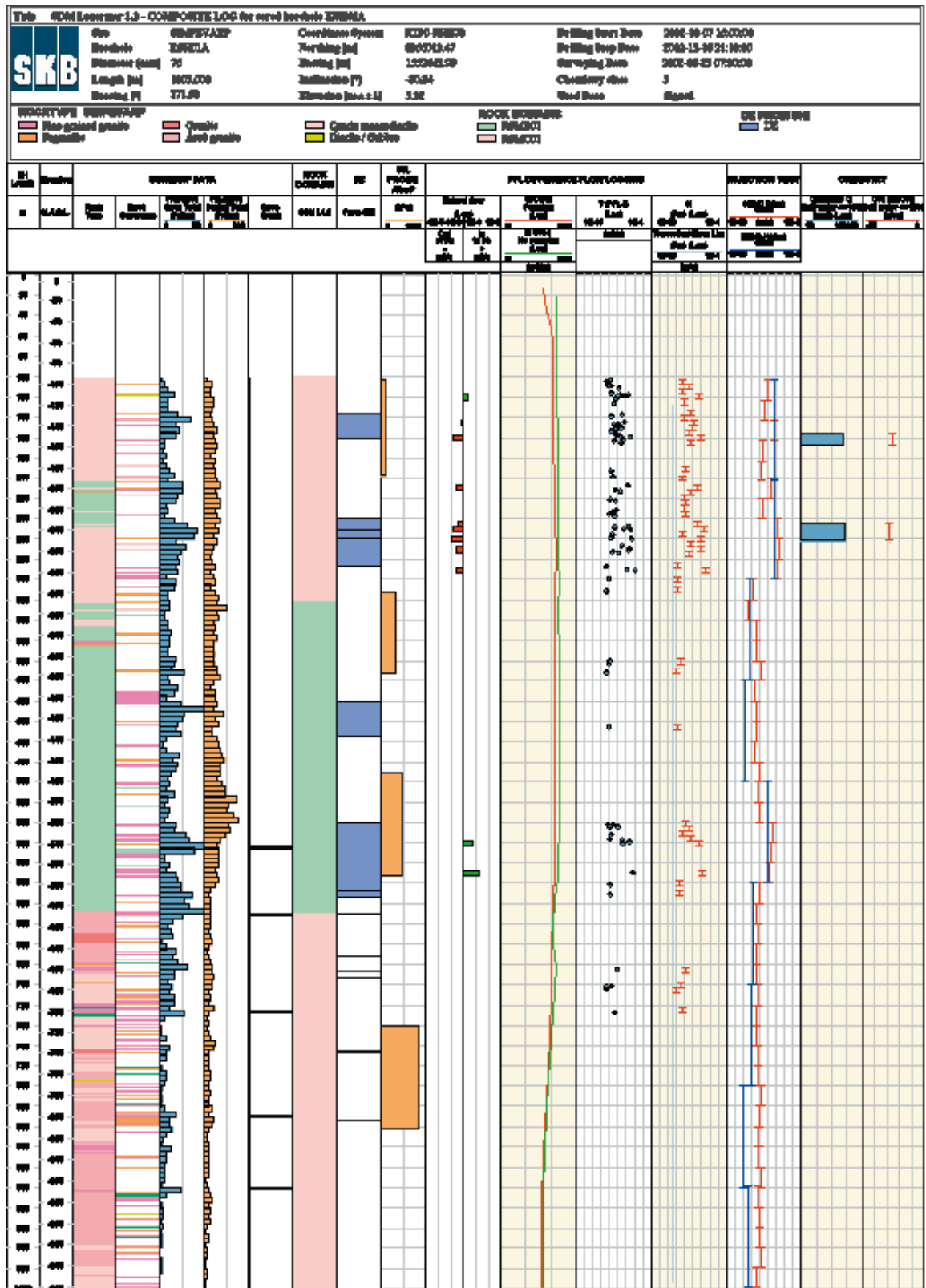
Cored borehole KLX03



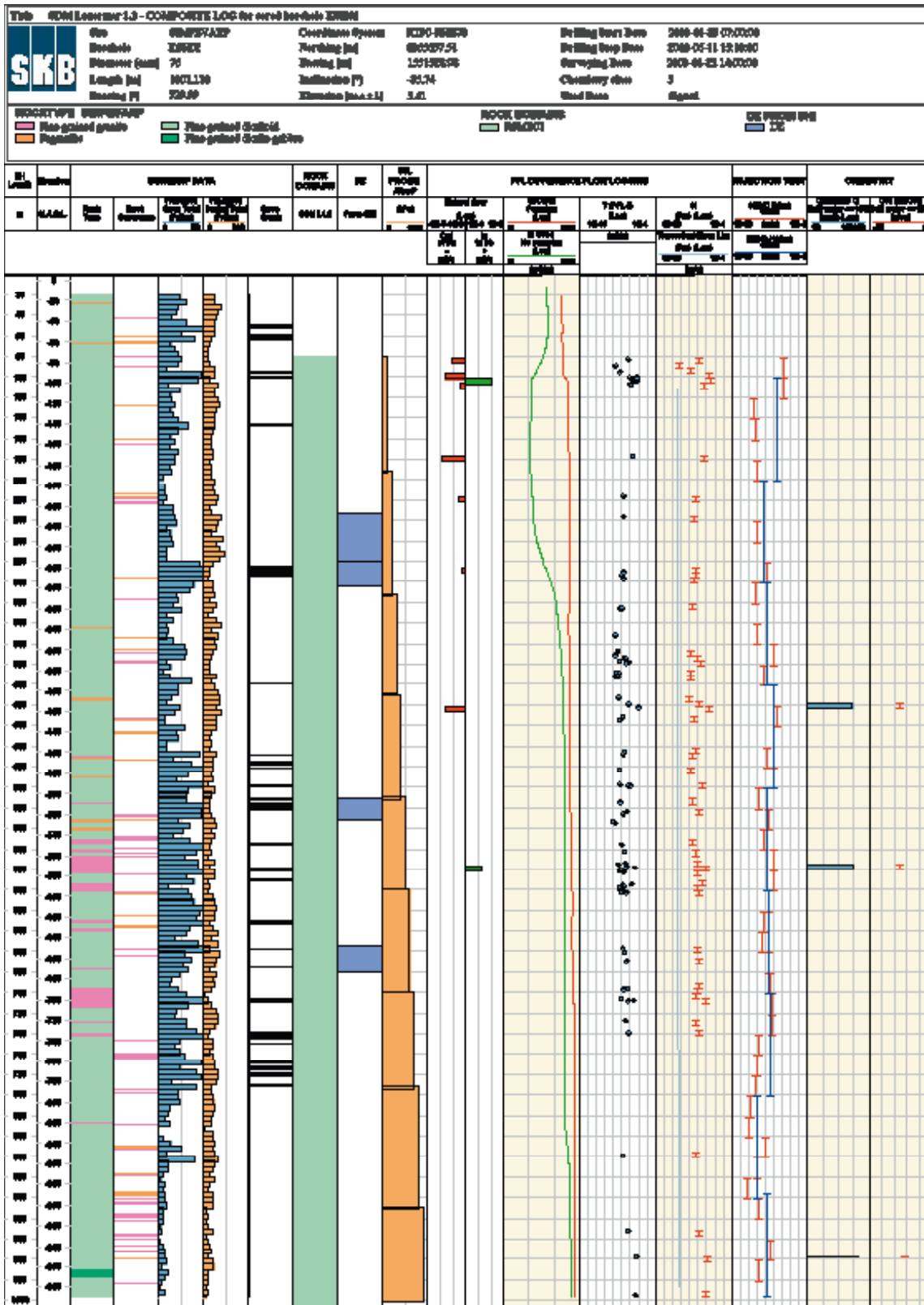
Cored borehole KLX04



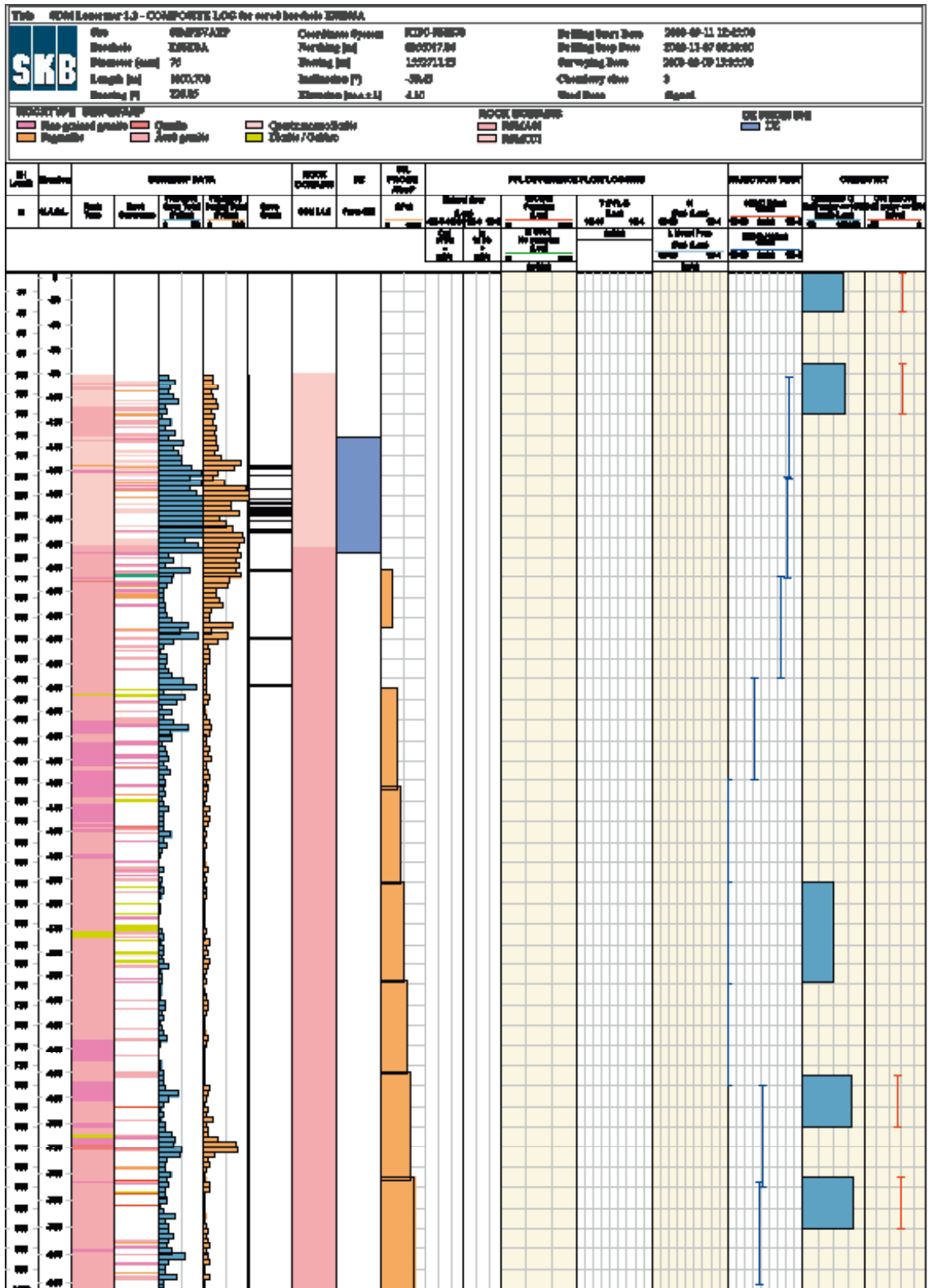
Cored borehole KSM01A



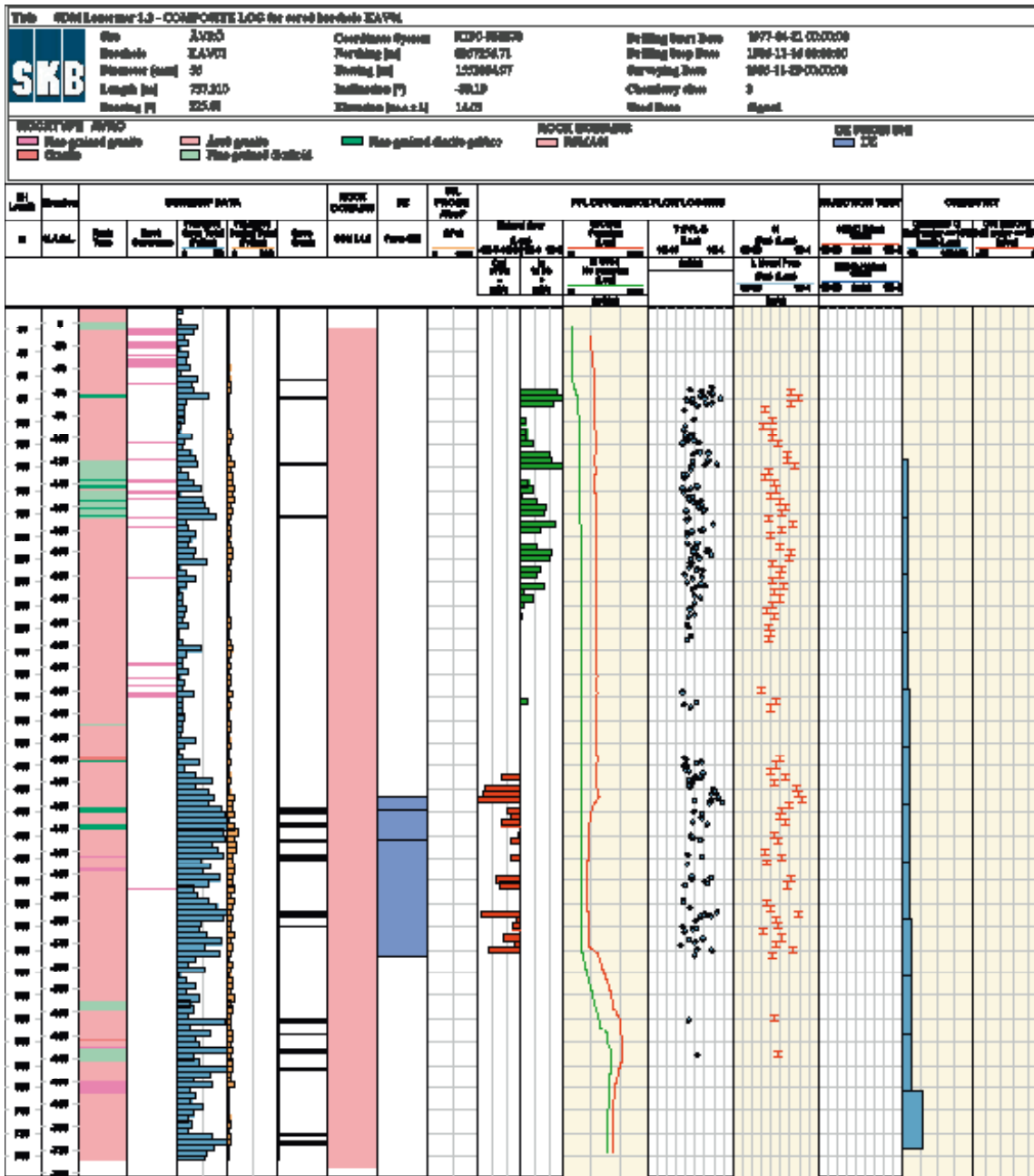
Cored borehole KSM02



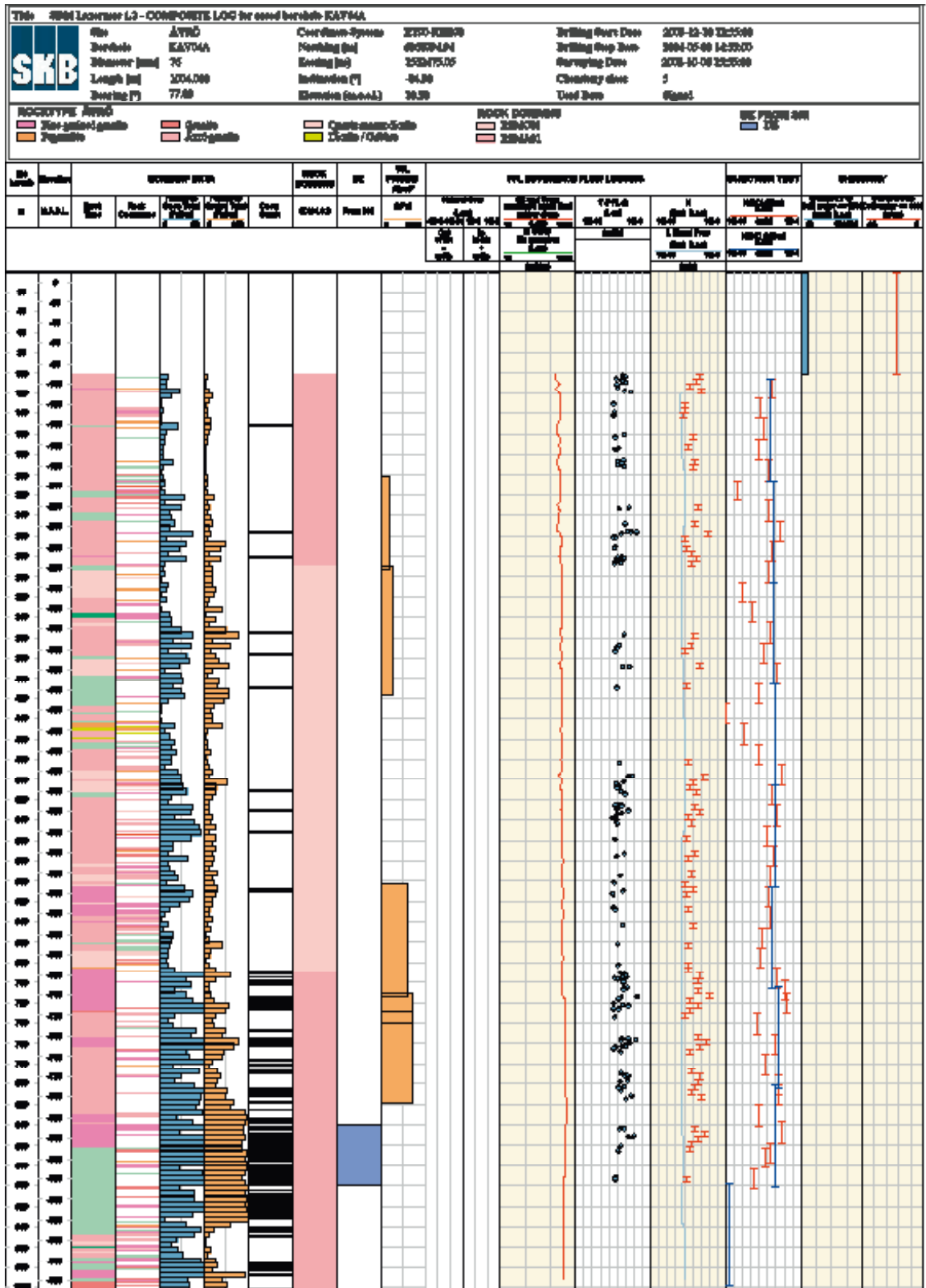
Cored borehole KSM03A



Cored borehole KAV01



Cored borehole KAV04A







Property tables for rock domains

Average values for Magnetic susceptibility and Electric resistivity are given in logarithmic scale \pm std (base 10).

RSMA01				
Property	Character	Quantitative estimate	Confidence	Comment
Dominant rock type (%)	Ävrö granite (501044)	54–92	High	The quantitative estimate is based on occurrence in KSH03A, KAV01, KAV04A/B, KLX02, KLX04 and the Äspö tunnel (section 2,265–2,874 m).
Mineralogical composition (%) (dominant minerals)	Quartz	18.8 \pm 6.3	High	N=61. The quantitative estimate is based on modal analyses of surface samples from the Simpevarp and Laxemar subareas and samples from KSH01A, KSH03A, KAV01. Mean value \pm std.
	K-feldspar	17.6 \pm 8.5		
	Plagioclase	46.5 \pm 8.4		
	Biotite	10.5 \pm 4.9		
Grain size	Medium-grained		High	Based on outcrop database for the Simpevarp and Laxemar subareas and its immediate surroundings.
Age (million years)		1,800 \pm 4	High	U-Pb zircon-titanite dating of Ävrö granite.
Structure	Isotropic to weakly foliated. Scattered mesoscopic, ductile shear zones		High	Based on outcrop database for the Simpevarp and Laxemar subareas and its immediate surroundings.
Texture	Unequigranular to porphyritic		High	Based on outcrop database for the Simpevarp and Laxemar subareas and its immediate surroundings.
Density (kg/m ³)		2,716 \pm 40	High	N=81. The quantitative estimate is based on surface samples from the Simpevarp and Laxemar subareas and samples from KAV01, KAV04A and KLX01. Mean value \pm std.
Porosity (%)		0.44 \pm 0.19	High	N=79. The quantitative estimate is based on surface samples from the Simpevarp and Laxemar subareas and samples from KAV01, KAV04A and KLX01. Mean value \pm std.
Magnetic susceptibility (SI units)		3.390 \pm 0.29	High	N=81. The quantitative estimate is based on surface samples from the Simpevarp and Laxemar subareas and samples from KAV01, KAV04A and KLX01. Average value in logarithmic scale \pm std.
Electric resistivity in fresh water (ohm m)		3.98 \pm 0.20	High	N=79. The quantitative estimate is based on surface samples from the Simpevarp and Laxemar subareas and samples from KAV01, KAV04A and KLX01. Average value in logarithmic scale \pm std.

RSMA01

Property	Character	Quantitative estimate	Confidence	Comment
Uranium content based on gamma ray spectrometric data (ppm)		4.0±1.4	High	N=67. The quantitative estimate is based on measurements on outcrops from the Simpevarp and Laxemar subareas, and a few measurements from the remaining part of the regional model area. Mean value ± std.
Natural exposure (microR/h)		11.4±2.2	High	N=67. The quantitative estimate is based on measurements on outcrops from the Simpevarp and Laxemar subareas, and a few measurements from the remaining part of the regional model area. Mean value ± std.
Subordinate rock types (%)	Fine- to medium-grained granite (511058) Pegmatite (501061) Fine-grained dioritoid (501030) Diorite to gabbro (501033) Fine-grained diorite to gabbro (505102) Quartz monzodiorite (501036)	1–22 0–1 2–21 0–12 0–5 1–14	High	The quantitative estimate is based on occurrence in KSH03A, KAV01, KAV04A, KLX02, KLX04, outcrop ASM000208 and the Äspö tunnel (section 2,265–2,874 m).
Dykes of fine- to medium-grained granite (511058)	Orientation	Mean pole=338/12 K=1.5 	High	N=72. Measurements from the local model area west of RSMP01 and RSMP02 and north of ZSMEW007A. Based on outcrop database for the Laxemar subarea and immediate surroundings. Mean pole is marked with a star.
		Mean pole=336/7 K=4.6 	High	N=8. Measurements from the local model area west of RSMP01 and RSMP02 and south of ZSMEW007A. Based on outcrop database for the Laxemar subarea and immediate surroundings. Mean pole is marked with a star.
Pegmatite (501061)	Orientation	Mean pole=325/12 K=0.8 	High	N=20. Measurements from the local model area west of RSMP01 and RSMP02 and north of ZSMEW007A. Based on outcrop database for the Laxemar subarea and immediate surroundings. Mean pole is marked with a star.
		Mean pole=297/9 K=0.4 	High	N=5. Measurements from the local model area west of RSMP01 and RSMP02 and south of ZSMEW007A. Based on outcrop database for the Laxemar subarea and immediate surroundings. Mean pole is marked with a star.

RSMA01				
Property	Character	Quantitative estimate	Confidence	Comment
Degree of inhomogeneity	Low		High	Based on outcrop database for the Simpevarp and Laxemar subareas and KSH03A, KAV01, KAV04A/B, KLX01, KLX02 and KLX04. The degree of inhomogeneity may locally be higher.
Metamorphism/alteration (%)	Inhomogeneous hydrothermal alteration (secondary red staining)	14–59	High	The quantitative estimate is based on faint to weak, including subordinate medium and strong, oxidation in KSH03A, KAV01, KAV04A, KLX01, KLX02 and KLX04 outside interpreted deformation zones in the single-hole interpretation. Epidotization, saussuritization, sericitization and chloritization also occur in subordinate amounts, varying between 0 and 3%.
Mineral fabric (type/orientation)	Weak magmatic to tectonic foliation	Mean pole=337/3 K= 3.6	High	N=41. Measurements from the local model area <i>east of</i> rock domains RSMP01 and RSMP02. Based on outcrop database for the Simpevarp and Laxemar subareas and immediate surroundings The stereogram includes poles to all foliation measurements irrespective of rock domain. Mean pole is marked with a star.
		Mean pole=24/3 K= 0.8	High	N=105. Measurements from the local model area <i>west of</i> rock domain RSMP01 and RSMP02. Based on outcrop databases for the Laxemar subarea and immediate surroundings The stereogram includes poles to all foliation measurements irrespective of rock domain. Mean pole is marked with a star.

RSMA02				
Property	Character	Quantitative estimate	Confidence	Comment
Dominant rock type (%)	Ävrö granite (501044)		Medium	
Mineralogical composition (%) (dominant minerals)				No data; inferred to be comparable to RSMA01.
Grain size				No data; inferred to be comparable to RSMA01.
Age (million years)		c. 1,800	High	No data; inferred to be comparable to RSMA01.
Structure				No data; inferred to be comparable to RSMA01.
Texture				No data; inferred to be comparable to RSMA01.
Density (kg/m ³)				No data; inferred to be comparable to RSMA01.
Porosity (%)				No data; inferred to be comparable to RSMA01.
Magnetic susceptibility (SI units)				No data; inferred to be comparable to RSMA01.
Electric resistivity in fresh water (ohm m)				No data; inferred to be comparable to RSMA01.
Uranium content based on gamma ray spectrometric data (ppm)				No data; inferred to be comparable to RSMA01.
Natural exposure (microR/h)				No data; inferred to be comparable to RSMA01.
Subordinate rock types (%)				No data; inferred to be comparable to RSMA01.
Degree of inhomogeneity				No data; inferred to be comparable to RSMA01.
Metamorphism/alteration (%)				No data; inferred to be comparable to RSMA01.
Mineral fabric (type/ orientation)				No data; inferred to be comparable to RSMA01.

RSMB01				
Property	Character	Quantitative estimate	Confidence	Comment
Dominant rock type (%)	Fine-grained dioritoid (501030)	89–91	High	The quantitative estimate is based on occurrence in KSH01A and KSH02.
Mineralogical composition (%) (dominant minerals)	Quartz	7.4±5.0	High	N=21. The quantitative estimate is based on modal analyses of surface samples from the Simpevarp subarea, KSH01A and KSH02. Mean value ± std.
	K-feldspar	11.3±6.4		
	Plagioclase	51.4±8.7		
	Biotite	14.7±7.6		
	Amphibole	0–14		
	Pyroxene	0–22		
Grain size	Fine-grained		High	Based on outcrop database for the Simpevarp and Laxemar subareas and its immediate surroundings.
Age (million years)		c. 1,800	High	Not dated. Based on U-Pb zircon age of the Ävrö granite (cf. RSMA01) and the quartz monzodiorite (cf. RSMC01). Field relationships strongly indicate that the fine-grained dioritoid is formed during the same magmatic event.
Structure	Isotropic to weakly foliated. Scattered mesoscopic, ductile shear zones		High	Based on outcrop database for the Simpevarp and Laxemar subareas and its immediate surroundings.
Texture	Equigranular to unequigranular		High	Based on outcrop database for the Simpevarp and Laxemar subareas and its immediate surroundings.
Density (kg/m ³)		2,786±20	High	N=9. The quantitative estimate is based on surface samples and KSH02. Mean value ± std.
Porosity (%)		0.33±0.08	High	N=9. The quantitative estimate is based on surface samples and KSH02. Mean value ± std.
Magnetic susceptibility (SI units)		3.39±0.55	High	N=9. The quantitative estimate is based on surface samples and KSH02. Average value in logarithmic scale ± std.
Electric resistivity in fresh water (ohm m)		4.54±0.37	High	N=9. The quantitative estimate is based on surface samples and KSH02. Average value in logarithmic scale ± std.
Uranium content based on gamma ray spectrometric data (ppm)		4.0±1.7	High	N=9. The quantitative estimate is based on measurements on outcrops. Mean value ± std.
Natural exposure (microR/h)		11.6±3.4	High	N=9. The quantitative estimate is based on measurements on outcrops. Mean value ± std.
Subordinate rock types (%)	Quartz monzodiorite (501036)	0–3	High	Quantitative estimate based on occurrence in KSH01A and KSH02.
	Fine-to medium-grained granite (511058)	3–8		
	Pegmatite (501061)	2–3		
	Fine-grained mafic rock (505102)	0–1		
	Ävrö granite (501044)	0–1		
Degree of inhomogeneity	Low		High	Based on outcrop database for the Simpevarp subarea, KSH01A and KSH02.
Metamorphism/alteration (%)	Inhomogeneous hydrothermal alteration (secondary red staining)	10–38	High	The quantitative estimate is based on faint to weak, including subordinate medium and strong, oxidation in KSH01A and KSH02 outside interpreted deformation zones in the single-hole interpretation.
Mineral fabric (type/ orientation)				No data

RSMB03				
Property	Character	Quantitative estimate	Confidence	Comment
Dominant rock type (%)	Fine-grained dioritoid (501030)	90.6–94.2	High	The quantitative estimate refers to RSMB01.
Mineralogical composition (%) (dominant minerals)	Quartz	7.4±5.0	High	N=21. The quantitative estimate is based on modal analyses of surface samples from the Simpevarp subarea, KSH01A and KSH02. Mean value ± std.
	K-feldspar	11.3±6.4		
	Plagioclase	51.4±8.7		
	Biotite	14.7±7.6		
	Amphibole	0–14		
	Pyroxene	0–22		
Grain size	Fine-grained		High	Based on outcrop database for the Simpevarp subarea.
Age (million years)		c. 1,800	High	Cf. RSMB01.
Structure	Isotropic to weakly foliated. Scattered mesoscopic, ductile shear zones		High	Based on outcrop database for the Simpevarp subarea.
Texture	Unequigranular		High	Based on outcrop database for the Simpevarp subarea.
Density (kg/m ³)		2,786±20	High	N=9. The quantitative estimate refers to RSMB01. Mean value ± std.
Porosity (%)		0.33±0.08	High	N=9. The quantitative estimate refers to RSMB01. Mean value ± std.
Magnetic susceptibility (SI units)		3.39±0.55	High	N=9. The quantitative estimate refers to RSMB01. Average value in logarithmic scale ± std.
Electric resistivity in fresh water (ohm m)		4.54±0.37	High	N=9. The quantitative estimate refers to RSMB01. Average value in logarithmic scale ± std.
Uranium content based on gamma ray spectrometric data (ppm)		4.0±1.7	High	N=9. The quantitative estimate refers to RSMB01. Mean value ± std.
Natural exposure (microR/h)		11.6±3.4	High	N=9. The quantitative estimate refers to RSMB01. Mean value ± std.
Subordinate rock types (%)	Fine- to medium-grained granite (511058) Pegmatite (501061) Diorite to gabbro (501033) Ävrö granite (501044)		High	Based on outcrop database for the Simpevarp subarea. No quantitative estimate is available.
Degree of inhomogeneity	Low		High	Based on outcrop database for the Simpevarp subarea.
Metamorphism/alteration (%)	Inhomogeneous hydrothermal alteration (secondary red staining)		High	Based on outcrop database for the Simpevarp subarea.
Mineral fabric (type/orientation)				No data

RSMBA01(a-b)				
Property	Character	Quantitative estimate	Confidence	Comment
Dominant rock type (%)	Fine-grained dioritoid (501030) Ävrö granite (501044)	27 47	Medium	Mixture of fine-grained dioritoid (501030) and Ävrö granite (501044). Assumption of mixture based on sections in KLX02 and KLX05. The quantitative estimate is based on KLX05 (preliminary mapping).
Mineralogical composition (%) – (dominant minerals)				Cf. data for RSMA01 and RSMB01.
Grain size				Cf. data for RSMA01 and RSMB01.
Age (million years)		c. 1,800	High	Cf. data for RSMA01 and RSMB01.
Structure				Cf. data for RSMA01 and RSMB01.
Texture				Cf. data for RSMA01 and RSMB01.
Density (kg/m ³)				Cf. data for RSMA01 and RSMB01.
Porosity (%)				Cf. data for RSMA01 and RSMB01.
Magnetic susceptibility (SI units)				Cf. data for RSMA01 and RSMB01.
Electric resistivity in fresh water (ohm m)				Cf. data for RSMA01 and RSMB01.
Uranium content based on gamma ray spectrometric data (ppm)		3.8±0.8		N=2 The quantitative estimate is based on measurements on outcrops. Mean value ± std.
Natural exposure (microR/h)		10.3±1.0		N=2. The quantitative estimate is based on measurements on outcrops. Mean value ± std.
Subordinate rock types (%)	Fine- to medium-grained granite (511058) Fine-grained diorite to gabbro (505102) Quartz monzodiorite (501036) Pegmatite (501061)	23 2	High	Based on outcrop database for the Laxemar subarea and KLX05. The quantitative estimate is based on KLX05. Only existence but no quantitative estimate is available for fine- to medium-grained granite (511058) and quartz monzodiorite (501036).
Degree of inhomogeneity	Medium		Medium	Based on outcrop database for the Laxemar subarea.
Metamorphism/alteration (%)	Inhomogeneous hydrothermal alteration (secondary red staining)		Medium	Based on outcrop database for the Laxemar subarea. Alteration intensity unknown.
Mineral fabric (type/ orientation)				No data

RSMBA02



Property	Character	Quantitative estimate	Confidence	Comment
Dominant rock type (%)	Fine-grained dioritoid (501030) Ävrö granite (501044)		Medium	Mixture of fine-grained dioritoid (501030) and Ävrö granite (501044). Assumption of mixture based on sections in KLX02 and KLX05.
Mineralogical composition (%) (dominant minerals)				Cf. data for RSMA01 and RSMB01.
Grain size				Cf. data for RSMA01 and RSMB01.
Age (million years)		c. 1,800	High	Cf. data for RSMA01 and RSMB01.
Structure				Cf. data for RSMA01 and RSMB01.
Texture				Cf. data for RSMA01 and RSMB01.
Density (kg/m ³)				Cf. data for RSMA01 and RSMB01.
Porosity (%)				Cf. data for RSMA01 and RSMB01.
Magnetic susceptibility (SI units)				Cf. data for RSMA01 and RSMB01.
Electric resistivity in fresh water (ohm m)				Cf. data for RSMA01 and RSMB01.
Uranium content based on gamma ray spectrometric data (ppm)		3.6		N=1 The quantitative estimate is based on measurement on outcrop.
Natural exposure (microR/h)		11.1		N=1 The quantitative estimate is based on measurement on outcrop.
Subordinate rock types (%)	Fine- to medium-grained granite (511058) Pegmatite (501061) Fine-grained diorite to gabbro (505102) Diorite to gabbro (501033)			Existence is based on outcrop database for the Laxemar subarea. No quantitative estimate is available.
Degree of inhomogeneity	Medium		Medium	Based on outcrop database for the Laxemar subarea.
Metamorphism/alteration (%)				No data
Mineral fabric (type/orientation)				No data

RSMBA03 (only occurs at depth)				
Property	Character	Quantitative estimate	Confidence	Comment
Dominant rock type (%)	Fine-grained dioritoid (501030)	32	High	Mixture of fine-grained dioritoid (501030) and Ävrö granite (501044). The quantitative estimate is based on K LX02.
	Ävrö granite (501044)	57		
Mineralogical composition (%) (dominant minerals)				Cf. data for RSMA01 and RSMB01.
Grain size				Cf. data for RSMA01 and RSMB01.
Age (million years)		c. 1,800	Medium	Cf. data for RSMA01 and RSMB01.
Structure				Cf. data for RSMA01 and RSMB01.
Texture				Cf. data for RSMA01 and RSMB01.
Density (kg/m ³)				Cf. data for RSMA01 and RSMB01.
Porosity (%)				Cf. data for RSMA01 and RSMB01.
Magnetic susceptibility (SI units)				Cf. data for RSMA01 and RSMB01.
Electric resistivity in fresh water (ohm m)				Cf. data for RSMA01 and RSMB01.
Uranium content based on gamma ray spectrometric data (ppm)				Cf. data for RSMA01 and RSMB01.
Natural exposure (microR/h)				Cf. data for RSMA01 and RSMB01.
Subordinate rock types (%)	Fine-grained diorite to gabbro (505102)	8	High	The quantitative estimate is based on K LX02.
	Fine- to medium-grained granite (511058)	1		
	Granite (501058)	1		
	Pegmatite (501061)	1		
Degree of inhomogeneity	High		High	Based on K LX02.
Metamorphism/alteration (%)	Inhomogeneous hydrothermal alteration (secondary red staining)	22	High	The quantitative estimate is based on faint to weak oxidation in K LX02 outside interpreted deformation zones in the single-hole interpretation.
Mineral fabric (type/ orientation)				No data

RSMC01				
Property	Character	Quantitative estimate	Confidence	Comment
Dominant rock type (%)	Quartz monzodiorite (501036)	24–72	High	Mixture of quartz monzodiorite (501036) and Ävrö granite (501044). Quantitative estimate based on occurrence in KSH01A, KSH03A and KAV04A.
	Ävrö granite (501044)	23–45		
Mineralogical composition (%) (dominant minerals)	Quartz (501036)	10.5±2.5	High	N=7. The quantitative estimate refers to the quartz monzodiorite and is based on modal analyses of surface samples from the Simpevarp subarea and KSH01A, B. For the composition of the Ävrö granite, cf. RSMA01.
	K-feldspar (501036)	12.3±5.4		
	Plagioclase (501036)	45.5±3.6		
	Biotite (501036)	16.3±5.2		
	Amphibole (501036)	6.7±4.5		
	Pyroxene (501036)	0–8.2		
Grain size	Medium-grained		High	Based on outcrop database for the Simpevarp subarea.
Age (million years)		1,802±4	High	U-Pb zircon dating of quartz monzodiorite. For the radiometric age of Ävrö granite, cf. RSMA01.
Structure	Isotropic to weakly foliated. Scattered mesoscopic, ductile shear zones		High	Based on outcrop database for the Simpevarp subarea.
Texture	Equigranular (501036) Unequigranular to porphyritic (501044)		High	Based on outcrop database for the Simpevarp subarea.
Density (kg/m ³)	Quartz monzodiorite (501036)	2,837±57	High	N=13. Quantitative estimate based on data from KSH01A/B and KSH03A.
	Ävrö granite (501044)	2,724±72	High	
Porosity (%)	Quartz monzodiorite (501036)	0.44±0.14	High	N=13. Quantitative estimate based on data from KSH01A/B and KSH03A.
	Ävrö granite (501044)	0.64±0.42	High	
Magnetic susceptibility (SI units)	Quartz monzodiorite (501036)	3.171±0.758	High	N=13. Quantitative estimate based on data from KSH01A/B and KSH03A.
	Ävrö granite (501044)	3.153±0.295	High	
Electric resistivity in fresh water (ohm m)	Quartz monzodiorite (501036)	4.13±0.31	High	N=13. Quantitative estimate based on data from KSH01A/B and KSH03A.
	Ävrö granite (501044)	3.62±0.39	High	
Uranium content based on gamma ray spectrometric data (ppm)				Cf. RSMA01 and RSMD01.
Natural exposure(microR/h)				Cf. RSMA01 and RSMD01.
Subordinate rock types (%)	Fine-grained dioritoid (501030)	0–15	High	The quantitative estimate is based on occurrence in KSH01A, KSH03A and KAV04A.
	Fine- to medium-grained granite (511058)	2–10		
	Granite (501058)	0–2		
	Fine-grained mafic rock (505102)	0–1		
	Pegmatite (501061)	2–3		
	Diorite to gabbro (501033)	0–1		
Degree of inhomogeneity	High		High	Based on outcrop database for the Simpevarp subarea, KSH01A, B, KSH03A, B and KAV04A.
Metamorphism/ alteration (%)	Inhomogeneous hydrothermal alteration (secondary red staining)	13–86	High	Based on outcrop database for the Simpevarp subarea, KSH01A, B, KSH03A, B and KAV04A. The quantitative estimate is based on faint to weak, including subordinate medium and strong, oxidation in KSH01A, KSH03A and KAV04A outside interpreted deformation zones in the single-hole interpretation.

RSMC01				
Property	Character	Quantitative estimate	Confidence	Comment
Mineral fabric (type/orientation)				No data
RSMC02				
Property	Character	Quantitative estimate	Confidence	Comment
Dominant rock type (%)	Quartz monzodiorite (501036) Ävrö granite (501044)		High	Cf. RSMC01.
Mineralogical composition (%) (dominant minerals)				Cf. RSMC01.
Grain size				Cf. RSMC01.
Age (million years)		c. 1,800	High	Cf. RSMC01.
Structure				Cf. RSMC01.
Texture				Cf. RSMC01.
Density (kg/m ³)	Quartz monzodiorite (501036) Ävrö granite (501044)			Cf. RSMC01.
Porosity (%)	Quartz monzodiorite (501036) Ävrö granite (501044)			Cf. RSMC01.
Magnetic susceptibility (SI units)	Quartz monzodiorite (501036) Ävrö granite (501044)			Cf. RSMC01.
Electric resistivity in fresh water (ohm m)	Quartz monzodiorite (501036) Ävrö granite (501044)			Cf. RSMC01.
Uranium content based on gamma ray spectrometric data (ppm)				Cf. RSMA01 and RSMD01.
Natural exposure (microR/h)				Cf. RSMA01 and RSMD01.
Subordinate rock types (%)	Fine-grained dioritoid (501030) Fine- to medium-grained granite (511058) Granite (501058) Fine-grained mafic rock (505102) Pegmatite (501061) Diorite to gabbro (501033)		High	Based on outcrop database for the Laxemar subarea and its immediate surroundings. No quantitative estimate available.
Degree of inhomogeneity	High		High	Based on outcrop database for the Laxemar subarea and its immediate surroundings.
Metamorphism/alteration (%)	Inhomogeneous hydrothermal alteration (secondary red staining)		Medium	Based on outcrop database for the Laxemar subarea and its immediate surroundings. Alteration frequency and intensity unknown.
Mineral fabric (type/orientation)				Very few data. Cf. stereogram in RSMA01 east of RSMP01.

RSMD01(a-b)				
Property	Character	Quantitative estimate	Confidence	Comment
Dominant rock type (%)	Quartz monzodiorite (501036)	95	High	The quantitative estimate is based on KLX03.
Mineralogical composition (%) (dominant minerals)	Quartz	14.8±2.8	High	N=7. The quantitative estimate is based on modal analyses of surface samples from the Laxemar subarea and its immediate surroundings.
	K-feldspar	13.9±6.2		
	Plagioclase	43.8±3.6		
	Biotite	14.3±2.9		
	Amphibole	7.6±3.0		
Grain size	Medium-grained		High	Based on outcrop database for the Laxemar subarea and its immediate surroundings.
Age (million years)		1,802±4	High	Based on U-Pb zircon dating of sample from RSMC01.
Structure	Isotropic to weakly foliated. Scattered mesoscopic, ductile shear zones		High	Based on outcrop database for the Laxemar subarea and its immediate surroundings.
Texture	Equigranular		High	Based on outcrop database for the Laxemar subarea and its immediate surroundings.
Density (kg/m ³)		2,767±19	High	N=12. The quantitative estimate is based on surface samples from the Laxemar subarea and its immediate surroundings. Mean value ± std.
Porosity (%)		0.54±0.11	High	N=12. The quantitative estimate is based on surface samples from the Laxemar subarea and its immediate surroundings. Mean value ± std.
Magnetic susceptibility (SI units)		3.33±0.22	High	N=12. The quantitative estimate is based on surface samples from the Laxemar subarea and its immediate surroundings. Average value in logarithmic scale ± std.
Electric resistivity in fresh water (ohm m)		4.12±0.14	High	N=12. The quantitative estimate is based on surface samples from the Laxemar subarea and its immediate surroundings. Average value in logarithmic scale ± std.
Uranium content based on gamma ray spectrometric data (ppm)		3.1±0.6	High	N=34. The quantitative estimate is based on measurements on outcrops in the Laxemar subarea and its immediate surroundings. Mean value ± std.
Natural exposure (microR/h)		9.5±1.2	High	N=34. The quantitative estimate is based on measurements on outcrops in the Laxemar subarea and its immediate surroundings. Mean value ± std.
Subordinate rock types (%)	Fine- to medium-grained granite (511058)	4	High	The existence is based on outcrop database for the Laxemar subarea and its immediate surroundings and KLX03. Quantitative estimate based on KLX03. No quantitative estimate is available for fine-grained diorite to gabbro (505102), Ävrö granite (501044) and fine-grained dioritoid (501030).
	Pegmatite (501061)	0.3		
	Fine-grained diorite to gabbro (505102)			
	Ävrö granite (501044)			
	Fine-grained dioritoid (501030)			

RSMD01(a-b)				
Property	Character	Quantitative estimate	Confidence	Comment
Dykes of fine- to medium-grained granite (511058)	Orientation	Mean pole=357/54 K=1.3 	High	N=31. Measurements from the local model area. Based on outcrop database for the Laxemar subarea and immediate surroundings. Mean pole is marked with a star.
Pegmatite (501061)	Orientation	Mean pole=341/31 K=1.4 	High	N=10. Measurements from the local model area. Based on outcrop database for the Laxemar subarea and immediate surroundings. Mean pole is marked with a star.
Degree of inhomogeneity	Low		High	Based on outcrop database for the Laxemar subarea and its immediate surroundings and KLX03.
Metamorphism/alteration (%)	Inhomogeneous hydrothermal alteration (saussuritization) Inhomogeneous hydrothermal alteration (secondary red staining)	25 7	High	The quantitative estimate is based on faint to weak and subordinate medium, saussuritization and oxidation in KLX03 outside interpreted deformation zones in the single-hole interpretation. The saussuritization is based on a slight greenish colouring of the plagioclase.
Mineral fabric (type/ orientation)	Weak magmatic to tectonic foliation			Cf. RSMA01 west of RSMP01 and RSMP02

RSM02				
Property	Character	Quantitative estimate	Confidence	Comment
Dominant rock type (%)	Quartz monzodiorite (501036)		Medium	Based on Simpevarp SDM v. 0.
Mineralogical composition (%) (dominant minerals)				No data
Grain size				No data
Age (million years)		c. 1,800	High	No data; inferred to be comparable to U-Pb zircon age of quartz monzodiorite in RSMC01.
Structure				No data
Texture				No data
Density (kg/m ³)				No data
Porosity (%)				No data
Magnetic susceptibility (SI units)				No data
Electric resistivity in fresh water (ohm m)				No data
Uranium content based on gamma ray spectrometric data (ppm)				No data
Natural exposure (microR/h)				No data
Subordinate rock types (%)				No data
Degree of inhomogeneity				No data
Metamorphism/alteration (%)				No data
Mineral fabric (type/orientation)				No data

RSM03				
Property	Character	Quantitative estimate	Confidence	Comment
Dominant rock type (%)	Quartz monzodiorite (501036)		Medium	Based on Simpevarp SDM v. 0.
Mineralogical composition (%) (dominant minerals)				No data
Grain size				No data
Age (million years)		c. 1,800	High	No data; inferred to be comparable to U-Pb zircon age of quartz monzodiorite in RSMC01.
Structure				No data
Texture				No data
Density (kg/m ³)				No data
Porosity (%)				No data
Magnetic susceptibility (SI units)				No data
Electric resistivity in fresh water (ohm m)				No data
Uranium content based on gamma ray spectrometric data (ppm)				No data
Natural exposure (microR/h)				No data
Subordinate rock types (%)				No data
Degree of inhomogeneity				No data
Metamorphism/alteration (%)				No data
Mineral fabric (type/orientation)				No data

RSMD04				
Property	Character	Quantitative estimate	Confidence	Comment
Dominant rock type (%)	Quartz monzodiorite (501036)		Medium	Based on Simpevarp SDM v. 0.
Mineralogical composition (%) (dominant minerals)				No data
Grain size				No data
Age (million years)		c. 1,800	High	No data; inferred to be comparable to U-Pb zircon age of quartz monzodiorite in RSMC01.
Structure				No data
Texture				No data
Density (kg/m ³)				No data
Porosity (%)				No data
Magnetic susceptibility (SI units)				No data
Electric resistivity in fresh water (ohm m)				No data
Uranium content based on gamma ray spectrometric data (ppm)				No data
Natural exposure (microR/h)				No data
Subordinate rock types (%)				No data
Degree of inhomogeneity				No data
Metamorphism/alteration (%)				No data
Mineral fabric (type/orientation)				No data

RSMD05				
Property	Character	Quantitative estimate	Confidence	Comment
Dominant rock type (%)	Quartz monzodiorite (501036)		Medium	Based on Simpevarp SDM v. 0.
Mineralogical composition (%) (dominant minerals)				No data
Grain size				No data
Age (million years)		c. 1,800	High	No data; inferred to be comparable to U-Pb zircon age of quartz monzodiorite in RSMC01.
Structure				No data
Texture				No data
Density (kg/m ³)				No data
Porosity (%)				No data
Magnetic susceptibility (SI units)				No data
Electric resistivity in fresh water (ohm m)				No data
Uranium content based on gamma ray spectrometric data (ppm)				No data
Natural exposure (microR/h)				No data
Subordinate rock type(s)				No data
Degree of inhomogeneity				No data
Metamorphism/alteration				No data
Mineral fabric (type/orientation)				No data

RSM06				
Property	Character	Quantitative estimate	Confidence	Comment
Dominant rock type (%)	Quartz monzodiorite (501036)		Medium	Based on Simpevarp SDM v. 0.
Mineralogical composition (%) (dominant minerals)				No data
Grain size				No data
Age (million years)		c. 1,800	High	No data; inferred to be comparable to U-Pb zircon age of quartz monzodiorite in RSMC01.
Structure				No data
Texture				No data
Density (kg/m ³)				No data
Porosity (%)				No data
Magnetic susceptibility (SI units)				No data
Electric resistivity in fresh water (ohm m)				No data
Uranium content based on gamma ray spectrometric data (ppm)				No data
Natural exposure (microR/h)				No data
Subordinate rock types (%)				No data
Degree of inhomogeneity				No data
Metamorphism/alteration (%)				No data
Mineral fabric (type/orientation)				No data

RSMD07				
Property	Character	Quantitative estimate	Confidence	Comment
Dominant rock type (%)	Quartz monzodiorite (501036)		High	
Mineralogical composition (%) (dominant minerals)	Quartz	6.5±1.1	High	N=3. The quantitative estimate is based on modal analyses of surface samples.
	K-feldspar	3.1±2.4		
	Plagioclase	39.8±2.0		
	Biotite	15.5±6.5		
	Amphibole	28.1±9.4		
Grain size	Medium-grained		High	Based on outcrop database for the Laxemar subarea, and its immediate surroundings.
Age (million years)		c. 1,800	High	No data; inferred to be comparable to U-Pb zircon age of quartz monzodiorite in RSMC01.
Structure	Isotropic to weakly foliated.		High	Based on outcrop database for the Laxemar subarea and its immediate surroundings.
Texture	Equigranular		High	Based on outcrop database for the Laxemar subarea and its immediate surroundings.
Density (kg/m ³)				No data
Porosity (%)				No data
Magnetic susceptibility (SI units)				No data
Electric resistivity in fresh water (ohm m)				No data
Uranium content based on gamma ray spectrometric data (ppm)				No data
Natural exposure (microR/h)				No data
Subordinate rock types (%)	Fine- to medium-grained granite (511058) Pegmatite (501061) Ävrö granite (501044) Diorite to gabbro (501033)		High	Based on outcrop database for the Laxemar subarea and its immediate surroundings. No quantitative estimate is available.
Degree of inhomogeneity	Medium		High	Based on outcrop database for the Laxemar subarea and its immediate surroundings.
Metamorphism/alteration (%)				No data
Mineral fabric (type/orientation)				Cf. RSMA01 west of RSMP01 and RSMP02.

RSMD08				
Property	Character	Quantitative estimate	Confidence	Comment
Dominant rock type (%)	Quartz monzodiorite (501036)		High	
Mineralogical composition (%) (dominant minerals)	Quartz K-feldspar Plagioclase Biotite Amphibole			No data from this domain. Cf. quantitative estimate in RSMD07.
Grain size	Medium-grained		High	Based on outcrop database for the Laxemar subarea. and its immediate surroundings.
Age (million years)		c. 1,800	High	No data; inferred to be comparable to U-Pb zircon age of quartz monzodiorite in RSMC01.
Structure	Isotropic to foliated.		High	Based on outcrop database for the Laxemar subarea and its immediate surroundings.
Texture	Equigranular		High	Based on outcrop database for the Laxemar subarea and its immediate surroundings.
Density (kg/m ³)				No data
Porosity (%)				No data
Magnetic susceptibility (SI units)				No data
Electric resistivity in fresh water (ohm m)				No data
Uranium content based on gamma ray spectrometric data (ppm)		1.7		N=1. The quantitative estimate is based on measurement on outcrop.
Natural exposure (microR/h)		7.1		N=1. The quantitative estimate is based on measurement on outcrop.
Subordinate rock types (%)	Fine- to medium-grained granite (511058) Pegmatite (501061) Granite (501058) Ävrö granite (501044) Diorite to gabbro (501033)		High	Based on outcrop database for the Laxemar subarea and its immediate surroundings. No quantitative estimate is available.
Degree of inhomogeneity	Medium		High	Based on outcrop database for the Laxemar subarea and its immediate surroundings.
Metamorphism/alteration (%)				
Mineral fabric (type/orientation)				Cf. RSMA01 west of RSMP01 and RSMP02.

RSME01				
Property	Character	Quantitative estimate	Confidence	Comment
Dominant rock type (%)	Diorite to gabbro (501033)		High	
Mineralogical composition (%) (dominant minerals)	Quartz Plagioclase Biotite Amphibole	4±0.6 47.4±4.5 10.8±3.8 29.4±5.3	Medium	N=4. The quantitative estimate is based on modal analyses of surface samples from corresponding rock types in the Simpevarp subarea. No data from this domain. Mean value ± std.
Grain size	Medium-grained		High	Based on outcrop database for the Laxemar subarea and its immediate surroundings.
Age (million years)		c. 1,800	High	Not dated. Based on U-Pb zircon age of the Ävrö granite (cf. RSMA01) and the quartz monzodiorite (RSMC01). Field relationships strongly indicate that the diorite to gabbro is formed during the same magmatic event.
Structure	Isotropic to weakly foliated		High	Based on outcrop database for the Laxemar subarea and its immediate surroundings.
Texture	Equigranular		High	Based on outcrop database for the Laxemar subarea and its immediate surroundings.
Density (kg/m ³)		2,960±43	High	N=11. The quantitative estimate is based on surface samples from corresponding rock types in the Laxemar subarea, KLX01 and KLX03. No data from this domain. Mean value ± std.
Porosity (%)		0.19±0.14	High	N=11. The quantitative estimate is based on surface samples from corresponding rock types in the Laxemar subarea, KLX01 and KLX03. No data from this domain. Mean value ± std.
Magnetic susceptibility (SI units)		2.694±0.733	High	N=11. The quantitative estimate is based on surface samples from corresponding rock types in the Laxemar subarea, KLX01 and KLX03. No data from this domain. Average value in logarithmic scale ± std.
Electric resistivity in fresh water (ohm m)		4.38±0.24	High	N=11. The quantitative estimate is based on surface samples from corresponding rock types in the Laxemar subarea, KLX01 and KLX03. No data from this domain. Average value in logarithmic scale ± std.
Uranium content based on gamma ray spectrometric data (ppm)		1.9±0.8	High	N=5. The quantitative estimate is based on surface samples from corresponding rock types in the Laxemar subarea. No data from this domain. Mean value ± std.
Natural exposure (microR/h)		5.7±1.2	High	N=5. The quantitative estimate is based on surface samples from corresponding rock types in the Laxemar subarea. No data from this domain. Mean value ± std.
Subordinate rock types (%)	Fine- to medium-grained granite (511058)		High	Based on outcrop database for the Laxemar subarea and its immediate surroundings. No quantitative estimate is available.
Degree of inhomogeneity	Medium		High	Based on outcrop database for the Laxemar subarea and its immediate surroundings.
Metamorphism/alteration (%)				No data
Mineral fabric (type/orientation)				Cf. RSMA01 west of RSMP01 and RSMP02.

RSME11				
Property	Character	Quantitative estimate	Confidence	Comment
Dominant rock type (%)	Diorite to gabbro (501033)		High	
Mineralogical composition (%) (dominant minerals)				No data
Grain size				No data
Age (million years)		c. 1,800	High	Not dated. Based on U-Pb zircon age of the Ävrö granite (cf. RSMA01) and the quartz monzodiorite (RSMC01). Field relationships strongly indicate that the diorite to gabbro is formed during the same magmatic event.
Structure				No data
Texture				No data
Density (kg/m ³)				No data
Porosity (%)				No data
Magnetic susceptibility (SI units)				No data
Electric resistivity in fresh water (ohm m)				No data
Uranium content based on gamma ray spectrometric data (ppm)				No data
Natural exposure (microR/h)				No data
Subordinate rock types (%)				No data
Degree of inhomogeneity				No data
Metamorphism/alteration (%)				No data
Mineral fabric (type/ orientation)				No data

RSME12				
Property	Character	Quantitative estimate	Confidence	Comment
Dominant rock type (%)	Diorite to gabbro (501033)		High	
Mineralogical composition (%) (dominant minerals)				No data
Grain size				No data
Age (million years)		c. 1,800	High	Not dated. Based on U-Pb zircon age of the Ävrö granite (cf. RSMA01) and the quartz monzodiorite (RSMC01). Field relationships strongly indicate that the diorite to gabbro is formed during the same magmatic event.
Structure				No data
Texture				No data
Density (kg/m ³)				No data
Porosity (%)				No data
Magnetic susceptibility (SI units)				No data
Electric resistivity in fresh water (ohm m)				No data
Uranium content based on gamma ray spectrometric data (ppm)				No data
Natural exposure (microR/h)				No data
Subordinate rock types (%)				No data
Degree of inhomogeneity				No data
Metamorphism/alteration (%)				No data
Mineral fabric (type/ orientation)				No data

RSME13

Property	Character	Quantitative estimate	Confidence	Comment
Dominant rock type (%)	Diorite to gabbro (501033)		High	
Mineralogical composition (%) (dominant minerals)				No data
Grain size				No data
Age (million years)		c. 1,800	High	Not dated. Based on U-Pb zircon age of the Ävrö granite (cf. RSMA01) and the quartz monzodiorite (RSMC01). Field relationships strongly indicate that the diorite to gabbro is formed during the same magmatic event.
Structure				No data
Texture				No data
Density (kg/m ³)				No data
Porosity (%)				No data
Magnetic susceptibility (SI units)				No data
Electric resistivity in fresh water (ohm m)				No data
Uranium content based on gamma ray spectrometric data (ppm)				No data
Natural exposure (microR/h)				No data
Subordinate rock types (%)				No data
Degree of inhomogeneity				No data
Metamorphism/alteration (%)				No data
Mineral fabric (type/orientation)				No data

RSME14				
Property	Character	Quantitative estimate	Confidence	Comment
Dominant rock type (%)	Diorite to gabbro (501033)		High	
Mineralogical composition (%) (dominant minerals)				No data
Grain size				No data
Age (million years)		c. 1,800	High	Not dated. Based on U-Pb zircon age of the Ävrö granite (cf. RSMA01) and the quartz monzodiorite (RSMC01). Field relationships strongly indicate that the diorite to gabbro is formed during the same magmatic event.
Structure				No data
Texture				No data
Density (kg/m ³)				No data
Porosity (%)				No data
Magnetic susceptibility (SI units)				No data
Electric resistivity in fresh water (ohm m)				No data
Uranium content based on gamma ray spectrometric data (ppm)				No data
Natural exposure (microR/h)				No data
Subordinate rock types (%)				No data
Degree of inhomogeneity				No data
Metamorphism/alteration (%)				No data
Mineral fabric (type/ orientation)				No data

RSME15

Property	Character	Quantitative estimate	Confidence	Comment
Dominant rock type (%)	Diorite to gabbro (501033)		High	
Mineralogical composition (%) (dominant minerals)				No data
Grain size				No data
Age (million years)		c. 1,800	High	Not dated. Based on U-Pb zircon age of the Ävrö granite (cf. RSMA01) and the quartz monzodiorite (RSMC01). Field relationships strongly indicate that the diorite to gabbro is formed during the same magmatic event.
Structure				No data
Texture				No data
Density (kg/m ³)				No data
Porosity (%)				No data
Magnetic susceptibility (SI units)				No data
Electric resistivity in fresh water (ohm m)				No data
Uranium content based on gamma ray spectrometric data (ppm)				No data
Natural exposure (microR/h)				No data
Subordinate rock types (%)				No data
Degree of inhomogeneity				No data
Metamorphism/alteration (%)				No data
Mineral fabric (type/ orientation)				No data

RSME16				
Property	Character	Quantitative estimate	Confidence	Comment
Dominant rock type (%)	Diorite to gabbro (501033)		High	
Mineralogical composition (%) (dominant minerals)				No data
Grain size				No data
Age (million years)		c. 1,800	High	Not dated. Based on U-Pb zircon age of the Ävrö granite (cf. RSMA01) and the quartz monzodiorite (RSMC01). Field relationships strongly indicate that the diorite to gabbro is formed during the same magmatic event.
Structure				No data
Texture				No data
Density (kg/m ³)				No data
Porosity (%)				No data
Magnetic susceptibility (SI units)				No data
Electric resistivity in fresh water (ohm m)				No data
Uranium content based on gamma ray spectrometric data (ppm)				No data
Natural exposure (microR/h)				No data
Subordinate rock types (%)				No data
Degree of inhomogeneity				No data
Metamorphism/alteration (%)				No data
Mineral fabric (type/ orientation)				No data

RSME17

Property	Character	Quantitative estimate	Confidence	Comment
Dominant rock type (%)	Diorite to gabbro (501033)		High	
Mineralogical composition (%) (dominant minerals)				No data
Grain size				No data
Age (million years)		c. 1,800	High	Not dated. Based on U-Pb zircon age of the Ävrö granite (cf. RSMA01) and the quartz monzodiorite (RSMC01). Field relationships strongly indicate that the diorite to gabbro is formed during the same magmatic event.
Structure				No data
Texture				No data
Density (kg/m ³)				No data
Porosity (%)				No data
Magnetic susceptibility (SI units)				No data
Electric resistivity in fresh water (ohm m)				No data
Uranium content based on gamma ray spectrometric data (ppm)				No data
Natural exposure (microR/h)				No data
Subordinate rock types (%)				No data
Degree of inhomogeneity				No data
Metamorphism/alteration (%)				No data
Mineral fabric (type/ orientation)				No data

RSME18				
Property	Character	Quantitative estimate	Confidence	Comment
Dominant rock type (%)	Diorite to gabbro (501033)		High	
Mineralogical composition (%) (dominant minerals)				No data
Grain size				No data
Age (million years)		c. 1,800	High	Not dated. Based on U-Pb zircon age of the Ävrö granite (cf. RSMA01) and the quartz monzodiorite (RSMC01). Field relationships strongly indicate that the diorite to gabbro is formed during the same magmatic event.
Structure				No data
Texture				No data
Density (kg/m ³)				No data
Porosity (%)				No data
Magnetic susceptibility (SI units)				No data
Electric resistivity in fresh water (ohm m)				No data
Uranium content based on gamma ray spectrometric data (ppm)				No data
Natural exposure (microR/h)				No data
Subordinate rock types (%)				No data
Degree of inhomogeneity				No data
Metamorphism/alteration (%)				No data
Mineral fabric (type/ orientation)				No data

RSMF01				
Property	Character	Quantitative estimate	Confidence	Comment
Dominant rock type (%)	Fine- to medium-grained granite (511058)		Medium	
Mineralogical composition (%) (dominant minerals)	Quartz	25.8±4.2	Medium	N=5. The quantitative estimate is based on samples from the Laxemar subarea and KSH03. No data from this domain.
	K-feldspar	33.8±3.3		
	Plagioclase	29.8±3.3		
Grain size				No data
Age (million years)		c. 1,800	High	Based on /Wikman and Kornfält 1995/; U-Pb zircon dating of fine-grained granite in the access tunnel to ÅHRL.
Structure				No data
Texture				No data
Density (kg/m ³)				No data
Porosity (%)				No data
Magnetic susceptibility (SI units)				No data
Electric resistivity in fresh water (ohm m)				No data
Uranium content based on gamma ray spectrometric data (ppm)				No data
Natural exposure (microR/h)				No data
Subordinate rock types (%)				No data
Degree of inhomogeneity				No data
Metamorphism/alteration (%)				No data
Mineral fabric (type/orientation)				No data

RSMF02				
Property	Character	Quantitative estimate	Confidence	Comment
Dominant rock type (%)	Fine- to medium-grained granite (511058)		High	
Mineralogical composition (%) (dominant minerals)				Cf. RSMF01.
Grain size	Fine- to medium-grained			Based on outcrop database for the Laxemar subarea and its immediate surroundings.
Age (million years)		c. 1,800	High	Based on /Wikman and Kornfält 1995/; U-Pb zircon dating of fine-grained granite in the access tunnel to ÄHRL.
Structure	Isotropic to weakly foliated			Based on outcrop database for the Laxemar subarea and its immediate surroundings.
Texture	Equigranular			Based on outcrop database for the Laxemar subarea and its immediate surroundings.
Density (kg/m ³)				No data
Porosity (%)				No data
Magnetic susceptibility (SI units)				No data
Electric resistivity in fresh water (ohm m)				No data
Uranium content based on gamma ray spectrometric data (ppm)				No data
Natural exposure (microR/h)				No data
Subordinate rock types (%)	Diorite to gabbro (501033) Ävrö granite (501044) Pegmatite (501061) Fine-grained diorite to gabbro (505102)		High	Based on outcrop database for the Laxemar subarea and its immediate surroundings. No quantitative estimate is available.
Degree of inhomogeneity	Medium		Medium	Based on outcrop database for the Laxemar subarea and its immediate surroundings.
Metamorphism/alteration (%)				No data
Mineral fabric (type/ orientation)				No data


RSMF03				
Property	Character	Quantitative estimate	Confidence	Comment
Dominant rock type (%)	Fine- to medium-grained granite (511058)		Medium	
Mineralogical composition (%) (dominant minerals)				Cf. RSMF01.
Grain size				No data
Age (million years)		c. 1,800	High	Based on /Wikman and Kornfält 1995/; U-Pb zircon dating of fine-grained granite in the access tunnel to ÅHRL.
Structure				No data
Texture				No data
Density (kg/m ³)				No data
Porosity (%)				No data
Magnetic susceptibility (SI units)				No data
Electric resistivity in fresh water (ohm m)				No data
Uranium content based on gamma ray spectrometric data (ppm)				No data
Natural exposure (microR/h)				No data
Subordinate rock types (%)				No data
Degree of inhomogeneity				No data
Metamorphism/alteration (%)				No data
Mineral fabric (type/ orientation)				No data

RSMG01				
Property	Character	Quantitative estimate	Confidence	Comment
Dominant rock type (%)	Granite (521058) Fine-grained granite (531058)		High	
Mineralogical composition (%) (dominant minerals)	Quartz K-feldspar Plagioclase	31.3±5.6 36.7±7.1 24.1±6.3	High	N=10. Quantitative estimate based on modal analyses in /Wikman and Kornfält 1995/. Mean value ± std.
Grain size	Fine- to medium- and coarse-grained		High	Based on /Wikman and Kornfält 1995/.
Age (million years)		1,452±11/-9	High	U-Pb zircon dating. Based on /Åhäll 2001/.
Structure	Isotropic		High	Based on /Kresten and Chyssler 1976/ and /Wikman and Kornfält 1995/.
Texture	Equigranular and porphyritic		High	Based on /Kresten and Chyssler 1976/ and /Wikman and Kornfält 1995/.
Density (kg/m ³)		2620±20	High	N=14. Based on /Nisca 1987/.
Porosity (%)				No data
Magnetic susceptibility (SI units)		1.80±0.90	High	N=14. Based on /Nisca 1987/. Average value in logarithmic scale ± std.
Electric resistivity in fresh water (ohm m)				No data
Uranium content based on gamma ray spectrometric data (ppm)		14.6±8.2	High	N=7. Based on geochemical analyses /Wikman and Kornfält 1995/.
Natural exposure (microR/h)				No data
Subordinate rock types (%)				Not assessed
Degree of inhomogeneity	Low		High	
Metamorphism/alteration (%)				Not assessed
Mineral fabric (type/ orientation)				

RSMG02				
Property	Character	Quantitative estimate	Confidence	Comment
Dominant rock type (%)	Granite (521058)		High	
Mineralogical composition (%) (dominant minerals)	Quartz	34.6±5.5	High	N=5. Quantitative estimate based on modal analyses in /Wikman and Kornfält 1995/. Mean value ± std.
	K-feldspar	37.4±7.2		
	Plagioclase	21.6±3.8		
Grain size	Coarse-grained			
Age (million years)		1,441+5/-3	High	U-Pb zircon dating. Based on /Ahäll 2001/.
Structure	Isotropic		High	
Texture				
Density (kg/m ³)		2,620±10	High	N=10. Based on /Nisca 1987/.
Porosity (%)				No data
Magnetic susceptibility (SI units)		2.35±0.64	High	N=10. Based on /Nisca 1987/. Average value in logarithmic scale ± std.
Electric resistivity in fresh water (ohm m)				No data
Uranium content based on gamma ray spectrometric data (ppm)				No data
Natural exposure (microR/h)				No data
Subordinate rock type(s)				No data
Degree of inhomogeneity	Low		High	
Metamorphism/alteration				No data
Mineral fabric (type/orientation)				

RSMM01 (a–d)				
Property	Character	Quantitative estimate	Confidence	Comment
Dominant rock type (%)	Ävrö granite (501044)	38–73	High	The rock domain is characterized by the high amount of diorite to gabbro (501033) mainly in the contact zone between the Ävrö granite (501044) and the quartz monzodiorite (501036) in RSMA01 and RSMD01, respectively. The quantitative estimate is based on KLX03, KLX05 (preliminary mapping), outcrop ASM000209 and the bedrock map of the Laxemar and Simpevarp subareas.
	Quartz monzodiorite (501036)	0–27		
	Diorite to gabbro (501033)	1–36		
Mineralogical composition (%) (dominant minerals)	Quartz (501044)	13.0±4.4	High	N=9. The quantitative estimate refers to Ävrö granite and is based on modal analyses of surface samples from the Laxemar subarea and KLX03. For the composition of the quartz monzodiorite and the diorite to gabbro, cf. RSMD01 and RSME01, respectively.
	K-feldspar (501044)	13.8±6.6		
	Plagioclase (501044)	52.3±5.3		
	Biotite (501044)	12.5±5.3		
	Amphibole (501044)	3.7±3.1		
Grain size				Cf. RSMA01, RSMD01 and RSME01.
Age (million years)		c. 1,800	High	Cf. RSMA01 and RSMC01.
Structure	Isotropic to weakly foliated. Scattered mesoscopic, ductile shear zones			Based on outcrop database for the Laxemar subarea and immediate surroundings.
Texture				Cf. RSMA01, RSMD01 and RSME01.
Density (kg/m ³)				Cf. RSMA01, RSMD01 and RSME01.
Porosity (%)				Cf. RSMA01, RSMD01 and RSME01.
Magnetic susceptibility (SI units)				Cf. RSMA01, RSMD01 and RSME01.
Electric resistivity in fresh water (ohm m)				Cf. RSMA01, RSMD01 and RSME01.
Uranium content based on gamma ray spectrometric data (ppm)				Cf. RSMA01, RSMD01 and RSME01.
Natural exposure (microR/h)				Cf. RSMA01, RSMD01 and RSME01.
Subordinate rock types (%)	Fine- to medium-grained granite (511058)	1–16	High	Based on outcrop database for the Laxemar subarea and immediate surroundings, KLX03, KLX05 and outcrop ASM000209. The quantitative estimate is based on KLX03, KLX05 (preliminary mapping), outcrop ASM000209 and the bedrock map of the Laxemar and Simpevarp subareas.
	Pegmatite (501061)	0–0.3		
	Fine-grained diorite to gabbro (505102)	0–3		
	Granite (501058)	0–26		
	Fine-grained dioritoid	1–3		
Dykes of fine- to medium-grained granite (511058)	Orientation	Mean pole=335/29 K=0.8	High	N=28. Measurements from the local model area. Based on outcrop database for the Laxemar subarea and immediate surroundings. Mean pole is marked with a star.



RSMM01 (a–d)				
Property	Character	Quantitative estimate	Confidence	Comment
Pegmatite	Orientation	Mean pole=331/8 K=1.1	High	N=14. Measurements from the local model area. Based on outcrop database for the Laxemar subarea and immediate surroundings. Mean pole is marked with a star.
				
Degree of inhomogeneity	High		High	Based on outcrop database for the Laxemar subarea and immediate surroundings, bedrock map, KLX03, KLX05 and outcrop ASM000209. The degree of inhomogeneity varies and may be low locally.
Metamorphism/ alteration (%)	Hydrothermal alteration (saussuritization in Ävrö granite (501044))	3	High	The quantitative estimate is based on faint to weak and subordinate medium, saussuritization and oxidation in KLX03 outside interpreted deformation zones in the single-hole interpretation. The saussuritization is based on a slight greenish colouring of the plagioclase.
	Hydrothermal alteration (saussuritization in quartz monzodiorite (501036))	43		
	Hydrothermal alteration (red staining in Ävrö granite(501044))	9		
	Hydrothermal alteration (red staining in quartz monzodiorite (501036))	17		
Mineral fabric (type/ orientation)	Weak magmatic to tectonic foliation			Cf. RSMA01 west and east of RSMP01 and RSMP02.

RSMP01				
Property	Character	Quantitative estimate	Confidence	Comment
Dominant rock type (%)	Ävrö granite (501044)		High	Based on outcrop databases for the Laxemar subarea and immediate surroundings.
Mineralogical composition (%) (dominant minerals)				Cf. RSMA01 what concerns undeformed to weakly deformed varieties of the Ävrö granite. No quantitative data for mylonitic varieties.
Grain size	Fine- to medium-grained		High	Based on outcrop databases for the Laxemar subarea and immediate surroundings.
Age (million years)		c. 1,800	High	Age refers to rock types. Cf. RSMA01. Age of low-grade deformation is unknown, but is inferred to be close in time (c. 1,800–1,750 Ma) to the age of intrusion of the rock types.

RSMP01				
Property	Character	Quantitative estimate	Confidence	Comment
Structure	Isotropic to mylonitic			Based on outcrop databases for the Laxemar subarea and immediate surroundings.
Texture	Unequigranular to porphyritic to porphyroclastic		High	Based on outcrop databases for the Laxemar subarea and immediate surroundings.
Density (kg/m ³)				Cf. RSMA01 for undeformed varieties. No data for mylonitic varieties.
Porosity (%)				Cf. RSMA01 for undeformed varieties. No data for mylonitic varieties.
Magnetic susceptibility (SI units)				Cf. RSMA01 for undeformed varieties. No data for mylonitic varieties.
Electric resistivity in fresh water (ohm m)				Cf. RSMA01 for undeformed varieties. No data for mylonitic varieties.
Uranium content based on gamma ray spectrometric data (ppm)				Cf. RSMA01 for undeformed varieties. No data for mylonitic varieties.
Natural exposure (microR/h)				Cf. RSMA01 for undeformed varieties. No data for mylonitic varieties.
Subordinate rock types (%)	Fine- to medium-grained granite (511058) Pegmatite (501061) Diorite to gabbro (501033) Fine-grained dioritoid (501030) Fine-grained diorite to gabbro (505102)		High	Existence is based on outcrop database for the Laxemar subarea. No quantitative estimate is available. The fine-grained dioritoid is predominantly occurring in the southernmost part of the domain. Otherwise the amount of subordinate rock types is presumably comparable to RSMA01.
Degree of inhomogeneity	Low		High	Based on outcrop databases for the Laxemar subarea and immediate surroundings. The degree of inhomogeneity based on subordinate rock types are judged to be comparable to RSMA01, but the degree of inhomogeneity what relates to the degree of ductile shear deformation is high.
Metamorphism/ alteration (%)	Low-grade metamorphic alteration		High	Based on outcrop databases for the Laxemar subarea and immediate surroundings.
Mineral fabric (type/ orientation)	Protomylonitic to mylonitic foliation	Mean pole=307/2 K=1.3	High	N=28. Based on outcrop databases for the Laxemar subarea and immediate surroundings. The foliation has a northeasterly orientation and a subvertical to vertical dip. The stereogram includes poles to all measurements of mylonitic foliation from RSMP01. Mean pole is marked with a star.



RSMP02				
Property	Character	Quantitative estimate	Confidence	Comment
Dominant rock type (%)	Ävrö granite (501044) Quartz monzodiorite (501036)		Medium	Ävrö granite (501044) dominates in the northeastern and southwestern part of the domain, and quartz monzodiorite (501036) in the central part.
Mineralogical composition (%) (dominant minerals)				Cf. RSMA01 and RSMD01a for undeformed varieties. No data for mylonitic varieties.
Grain size				Cf. RSMA01 and RSMD01a for undeformed varieties. No data for mylonitic varieties.
Age (million years)		c. 1,800	High	Age refers to rock types. Cf. RSMA01 and RSMC01. Age of low-grade deformation is unknown, but is inferred to be close in time (c. 1,800–1,750 Ma) to the age of intrusion of the rock types.
Structure				Cf. RSMA01 and RSMD01a for undeformed varieties. No data for mylonitic varieties.
Texture				Cf. RSMA01 and RSMD01a for undeformed varieties. No data for mylonitic varieties.
Density (kg/m ³)				Cf. RSMA01 and RSMD01a for undeformed varieties. No data for mylonitic varieties.
Porosity (%)				Cf. RSMA01 and RSMD01a for undeformed varieties. No data for mylonitic varieties.
Magnetic susceptibility (SI units)				Cf. RSMA01 and RSMD01a for undeformed varieties. No data for mylonitic varieties.
Electric resistivity in fresh water (ohm m)				Cf. RSMA01 and RSMD01a for undeformed varieties. No data for mylonitic varieties.
Uranium content based on gamma ray spectrometric data (ppm)				Cf. RSMA01 and RSMD01a for undeformed varieties. No data for mylonitic varieties.
Natural exposure (microR/h)				Cf. RSMA01 and RSMD01a for undeformed varieties. No data for mylonitic varieties.
Subordinate rock types (%)	Fine-grained dioritoid (501030) Diorite to gabbro (501033) Granite (501058) Fine- to medium-grained granite (511058) Pegmatite (501061) Fine-grained diorite to gabbro (505102)		High	Existence is based on outcrop database for the Laxemar subarea. No quantitative estimate is available. The amount of subordinate rock types is presumably comparable to RSMA01 and RSMD01.
Degree of inhomogeneity	Medium		High	Based on outcrop databases for the Laxemar subarea and immediate surroundings.
Metamorphism/alteration (%)	Low-grade metamorphic alteration		High	Based on outcrop databases for the Laxemar subarea and immediate surroundings.
Mineral fabric (type/orientation)		Mean pole=313/0 K=2.8	High	N=35. Based on outcrop databases for the Laxemar subarea and immediate surroundings. The foliation has a northeasterly orientation and a subvertical to vertical dip. The stereogram includes poles to all measurements of mylonitic foliation from RSMP02. Mean pole is marked with a star.



Property tables for deformation zones

ZSMEW002A				
Property	Estimate	Span	Basis for interpretation	Comments
Confidence in existence	High		Linked lineament, BH and geophysical ground survey	
Strike (regional scale)	090	± 20	Strong magnetic and topographic lineament	
Dip (regional scale)	65	± 10	Seismic relector and BH incators	
Thickness, (including transition zones, regional scale)	100 m	20 to 200 m	Lineament, BH and geophysical ground survey	Complex zone, inferred anastomosing geometry.
Length (regional scale)	17.8 km	± 5 km	Linked lineaments	30 km, including extension outside the regional model area
Rock type	Ävrö granite dominates, with fine grained diorite gabbro		KAS03 and KLX06	
Ductile deformation	Yes		Mylonite KAS17. Field mapping	Brittle-ductile zone. Dominantly brittle.
Brittle deformation	Yes		Field indicators. Multiple crush zones KLX06 v. 1 only preliminary mapping available). Breccia and crush zones KAS03	Brittle-ductile zone. Dominantly brittle.
Alteration	Oxidation			
Water				
Fracture orientation	Not yet assessed			
Fracture frequency m ⁻¹	9		KAS03	Frac' frq'incl' crush (= 20 frac/m) (m ⁻¹)
Fracture filling	Ca 66%, Chl 67%, Ep 6%, He 46% Qtz 5%		KAS03	

BH	Geometrical intercept	Target intercept	Comment
KAS03	307–495	280–480	Brittle and ductile indicators.
KAS17	249–360		Only incomplete preliminary mapping available.
KLX06	300–430	300–400	Only preliminary mapping available.
HLX20	60–185		No results available.

ZSMEW007A

Property	Estimate	Span	Basis for interpretation	Comments
Confidence in existence	High		Linked lineament, BH and geophysical ground survey	
Strike (regional scale)	278	± 20	Strong magnetic and topographic lineament	
Dip (regional scale)	43	± 10	Seismic reflector and BH indicators	Seismic reflector survey (P-04-215) reflector A, good agreement with strike and dip 43° N. Geophysical profiling; resistivity, magnetic; all suggest northern dip 40–55°.
Thickness, (including transition zones, regional scale)	50 m	20 to 60 m	Lineament, BH and geophysical ground survey	Complex zone. 50 m, based on inclusion of estimated likely transition zones. 10 m wide 'core' of more highly fractured rock based on general ref: geophysical profiling -refraction (P-04-134)
Length (regional scale)	3.3 km	± 200 m	Linked lineaments	
Ductile deformation	–			Brittle deformation zone
Brittle deformation	Yes		Rare field indicators, high fracture frequency in BH's	Brittle deformation zone
Alteration	Oxidation		BH's	Red colouration
Water	Water bearing		BH's	No analysis available
Fracture orientation	Not yet assessed			
Fracture frequency m ⁻¹	10		KLX01, KLX02, KLX04	Frac' frq'incl' crush (= 20 frac/m) (m ⁻¹)
Fracture filling	Ca 41%, Chl 64%, Ep 23%, He 10% Qtz 1%		KLX01, KLX02, KLX04	

BH	Geometrical intercept	Target intercept	Comment
KLX01	972–1,044	1,000–1,020	Oxidation, high fracture frequency, narrow sections with crushed rock, several chlorite or calcite sealed fractures. Uncertainty = 3
KLX02	234–311	265–275	Orientated open fracture sets between BH length 260–280 m show good agreement.
KLX04	314–391	346–355	Brittle deformation with brecciation (sealed network). Low resistivity, variable sonic, very low susceptibility and small caliper anomaly. Radar reflectors at 350.7 m with the angle 70° to borehole axis and at 352.1 m with the angle 20° to borehole axis. Uncertainty: 3
HLX23	0–39		No results available- will require remodelling at a higher resolution with local lineament adjustment to include results
HLX24			No results available- will require remodelling at a higher resolution with local lineament adjustment to include results
HLX21	1–52		No results available- will require remodelling at a higher resolution with local lineament adjustment to include results
HLX22			No results available- will require remodelling at a higher resolution with local lineament adjustment to include results

ZSMEW009A

Property	Estimate	Span	Basis for interpretation	Comments
Confidence in existence	High		Linked lineaments; Surface mapping; BHs; TASA (Äspö) tunnel intercept.	
Strike (regional scale)	085	± 15	Linked lineaments	
Dip (regional scale)	76	± 10	linked lineaments, TASA	
Thickness, (including transition zones, regional scale)	12 m	5 to 20 m	Linked lineaments; BHs; TASA (Äspö) tunnel intercept.	
Length (regional scale)	1.7 km	± 100 m	Linked lineaments	
Ductile deformation	Yes		KAS06 (66 m) mylonitic	Ductile-brittle zone
Brittle deformation	Yes		TASA (Äspö)	Ductile-brittle zone
Alteration	1.5 to 2 m thick central clay zone.		TASA (Äspö)	
Water	90 l/min		Inflow into TASA	Ref: PR 25-95-20
	$1.7 \times 10^{-5} \text{ m}^2/\text{s}$		Inflow into TASA	Ref: PR HRL96-19
Fracture orientation	Not analysed			
Fracture frequency m^{-1}	14		KAS06	Frac' frq'incl' crush (= 20 frac/m) (m^{-1})
Fracture filling	Ca 65%, Chl 79%, Ep 6%, He 21% Qtz 1%		KAS06	

BH	Geometrical intercept	Target intercept	Comment
HAS14	0.2–49		Await results
HAS21	25–57		Await results
KAS06	59–76	60–75	Strong tectonization and several sections of crushed core. 1 m thick mylonitic section.
KAS07	562–604 (Base)		Not used in the current model to define geometry. (tectonization recorded -Ref: Geomod)
TASA		1,407–1,421	Ref: PR HRL96-19
Surface trench (Äspö)		x = 6367638 y = 1551412 z = 2.5	1.5 m thick mylonite

ZSMEW013A (EW1a)

Property	Estimate	Span	Basis for interpretation	Comments
Confidence in existence	High		Linked lineaments, field mapping and BHs.	
Strike (regional scale)	85	105 to 065	Linked lineaments	105 in west curving round to 065
Dip (regional scale)	90	± 10	Linked lineaments and BHs.	Ref: Geomod EW1a
Thickness, (including transition zones, regional scale)	45 m	20 to 50 m	Linked lineaments and BHs.	
Length (regional scale)	4.4 km	2.5 to 4.4 km	Linked lineaments.	An alternative interpretation is to terminate the zone against ZSMNE005A
Ductile deformation	Yes		Field mapping and BH (mylonite)	Brittle-ductile zone
Brittle deformation	Yes		BH breccia and crush zones.	Brittle-ductile zone
Alteration	Epidotized			
Water				
Fracture orientation	Not yet assessed			
Fracture frequency m ⁻¹	5		KA1755A, KAS04	Frac' frq'incl' crush (= 20 frac/m) (m ⁻¹)
Fracture filling	Ca 57%, Chl 46%, Ep 23%, He 1%, Qtz 3%		KA1755A, KAS04	

BH	Geometrical intercept	Target intercept	Comment
KA1755A	188–234	180–230	A crush zone, with enhanced fracture frequency. A thin breccia/mylonite and a c. 5–7 m wide zone of tectonization have been recorded. The area as interpreted as EW-1a in /Stanfors et al. 1994/.
KAS04	100–185	87–158	Five thin mylonites at depths: 87, 140, 147, 153 and 158 m. Intense tectonization around the mylonite at 147 m. Ref: Geomod.
HLX03	0–19	–	Awaiting results
HAS01	4–100	–	No information

ZSMEW023A

Property	Estimate	Span	Basis for interpretation	Comments
Confidence in existence	High		Linked lineaments; seismic refraction profiling; OKG tunnel intercept.	
Strike (regional scale)	275	± 15	Linked lineaments	
Dip (regional scale)	90	± 20	OKG	
Thickness, (including transition zones, regional scale)	20 m	5 to 50 m	Linked lineaments, seismic refraction profiling and field mapping	The upper 50 m limit is based on indications from OKG that suggest locally a more diffuse zone consisting of increased fracturing and only minor shears.
Length (regional scale)	3.8 km	± 200 m	Linked lineaments	
Ductile deformation	–		No indicators	Brittle zone
Brittle deformation	Yes		OKG	Brittle zone
Alteration	Chlorite and clay			Clay may be depth dependent and be associated with the weathering profile considering the relatively shallow intercept position.
Water	Low transmissivity		Local 'dripping' reported in OKG excavation mapping.	
Fracture orientation	Not analysed			
Fracture frequency	Not analysed			
Fracture filling	CHI, Ca, Clay		OKG	

BH	Geometrical intercept	Target intercept	Comment
OKG		Cold water intake ch. 065–110 m	OKG cold water intake ch 065–110 m increased fracturing with up to 1 m wide chlorite and clay filled shear zone.
HSH05	191–200 (Base)	–	Await results

ZSMEW038A

Property	Estimate	Span	Basis for interpretation	Comments
Confidence in existence	High		Linked lineaments, tunnel mapping and BHs.	Considered a minor structure.
Strike (regional scale)	090	± 10	Linked lineaments and tunnel	Complex split geometry. Potentially involves a series of narrow mylonites in a number of BHs and the tunnel, with potential interference from other zones including ZSMNE006A. The current modelled geometry is an over simplification.
Dip (regional scale)	90	± 15	Linked lineaments, BHs and tunnel intercepts	
Thickness, (including transition zones, regional scale)	10 m	1 to 15 m	Linked lineaments, BHs and tunnel intercepts.	1 m thick in TASA; 10 m represents an envelope thickness.
Length (regional scale)	3.2 km	± 100 m	Linked lineaments.	
Ductile deformation	Yes		Tunnel mapping (mylonite) TASA ch. 1180 A minor mylonite, alternative intercepts exist.	Dominantly ductile zone. Possible brittle reactivation. Requires further review of Äspö data.
Brittle deformation	Yes		Inferred from tunnel mapping, transmissivity and seismic refraction profiling. Requires further study. Tunnel brittle evidence maybe associated with the development of other zones.	Dominantly ductile zone. Possible brittle reactivation. Requires further review of Äspö data.
Alteration				
Water	T = 1.3×10 ⁻⁶ m ² /s		TASA ch. 1180	
Fracture orientation	Not yet assessed			
Fracture frequency m ⁻¹	13		KA1131B	Frac' frq'incl' crush (= 20 frac/m) (m ⁻¹)
Fracture filling	Ca 95%, Chl 70%, Ep 20%, He 0%, Qtz 0%		KA1131B	

BH	Geometrical intercept	Target intercept	Comment
HAV05	20–38	–	Awaiting results.
KAS09	220–239	249–253	Possible associated mylonite.
KBH02	538–547		
KA1131B	35–44	34–36	Mylonite
KA1061	100–109	74–75	Possible associated mylonite
TASA		1,180	(0.5–1 m thick)

ZSMEW900A				
Property	Estimate	Span	Basis for interpretation	Comments
Confidence in existence	High		Linked lineament, field mapping and geophysical ground survey	
Strike (regional scale)	100	± 20	Magnetic and topographic lineaments	Lineament interpretation needs further review.
Dip (regional scale)	70	± 20	Seismic reflector, field mapping and geophysical profiling.	Based generally on field measurements, seismic reflector L (P-04-215), geophysical profiling (P-04-134)
Thickness, (including transition zones, regional scale)	20 m	± 10	Lineament, geophysical ground survey	Based on inclusion of estimated likely transition zones. 10 m wide 'core' of more highly fractured rock based on general ref: geophysical profiling –refraction (P-04-134)
Length (regional scale)	1.7 km	1 to 2 km	Linked lineaments	Clear alternative lineament tie-ups are possible.
Ductile deformation	Yes		Single field indicator	Ductile-brittle deformation zone
Brittle deformation	Yes		Field indicators, inferred from seismic refraction survey	Ductile-brittle deformation zone
Alteration	–		Await results	
Water	–		Await results	
Fracture orientation			Await results	
Fracture frequency			Await results	
Fracture filling			Await results	

BH	Geometrical intercept	Target intercept	Comment
HLX25	169–182	166–185	Low resistivity, low sonic, variable density and low susceptibility.
HLX14	11–29	–	Await results

ZSMNE004A

Property	Estimate	Span	Basis for interpretation	Comments
Confidence in existence	High		Linked lineament, Extensive field mapping and tunnel (Åspö) intercept. Seismic refraction.	
Strike (regional scale)	050	generally 030–070	Strong magnetic and topographic lineament; extensive field mapping	Curving geometry. However, the 090 trending eastwards extension has high uncertainty.
Dip (regional scale)	90	± 20	Extensive field mapping and tunnel (Åspö) intercept.	The vertical dip has been modified from Simp V 1.2 (70°S) to vertical ± 20° to allow for variations along entire zonelength. It may be preferable to model the zone with a steep dip to the S in the N and a vertical to N dip in the south with a smooth change over.
Thickness, (including transition zones, regional scale)	100 m	20 to 120 m	Linked lineament, tunnel and field mapping.	A ductile complex zone, inferred anastomosing geometry. The 100 m thickness is an envelope thickness containing the inferred splays.
Length (regional scale)	15.6 km	8 to > 15 km	Linked lineaments	Possible termination at ZSMNE024A or NE extension outside the regional model area. Limited data.
Ductile deformation	Yes		Extensive field mapping evidence.	Ductile-brittle zone.
Brittle deformation	–		TASA- highly fractured rock:see engineering comment below. Possible general association with KAV04 raised fracture frequency, though this is not clearly supported by fracture orientations.	Ductile-brittle zone.
Alteration				
Water	2.8×10 ⁻⁶ m ² /s		TASA ch. 300	
Fracture orientation	Not yet assessed			
Fracture frequency	Not yet assessed			
Fracture filling	Chl, Ca, Cy, Fe, Qz; clay		TASA ch.302–334	

BH	Geometrical intercept	Target intercept	Comment
HLX19	174–202	–	Awaiting results
KAV04	–	–	No geometrical intersection but the BH lies on the border of the modelled transition zone and may be responsible for the relatively high fracture frequency and degree of alteration throughout much of the BH though this is not clearly supported by fracture orientations.
TASA		302–334	

ZSMNE005A (Äspö shear zone)				
Property	Estimate	Span	Basis for interpretation	Comments
Confidence in existence	High		Linked lineaments – particularly magnetic. Field mapping results. BHs	
Strike (regional scale)	060	030 to 90	Linked lineaments	030 within the local model area, curving to 090 further north.
Dip (regional scale)	90	± 10	Field mapping	Modelled as vertical to allow for local variations. However, a dip of 90 to 80 SE is considered most probable.
Thickness, (including transition zones, regional scale)	250 m	50 to 300 m	Aerial magnetic survey, topography and field mapping	Complex zone, inferred anastomosing geometry.
Length (regional scale)	10.5 km	± 200 m	Linked lineaments	
Ductile deformation	Yes		Frequent evidence from field mapping	Ductile-brittle zone. Ductile clearly dominates but there has been clear brittle reactivation.
Brittle deformation	Yes		Weak evidence from field mapping. However, BHs show increased fracturing and brecciation.	Ductile clearly dominates but there has been clear brittle reactivation.
Alteration				
Water				/Rhén et al. 1997c/: report the most conductive parts coincide with some narrow highly fractured sections or single open fractures which are probably not connected along the entire zone.
Fracture orientation	Not yet assessed			
Fracture frequency m ⁻¹	9		KA1755A, KA1754A, KA1751A, KAS04, KA3590G02, KAS02, KAS12	Frac' frq'incl' crush (= 20 frac/m) (m ⁻¹)
Fracture filling	Ca 45%, Chl 69%, Ep 14%, He 14%, Qtz 3%		KA1755A, KA1754A, KA1751A, KAS04, KA3590G02, KAS02, KAS12	

BH	Geometrical intercept	Target intercept	Comment
KA1755A	22–288	95–140	At core length 95–140 m generally > 10 fract./m, at nine sites > 20 fract./m. This wide zone coincides geometrically with EW-1b. Most of the zone is developed in fine-grained granite and partly in granodiorite. Only a thin zone of true mylonite, with a medium tectonized area of 2–4 m around it. RQD is less than 25 at several locations in the zone. At core length 203–213 m c. 10 fract./m except for a 1–2 m wide zone (ref: Geomod)
KA1754A	26–160 (Base)	90–115	A crush zone and surrounding tectonization at c. 90–115 m fits geometrically with EW-1b. The area has a very high fracture frequency and the rock is fine grained granite, granodiorite and “greenstone” (ref: Geomod)
KA1751A	45–150 (Base)	110–114	The rock is fine grained granite, granodiorite and greenstone. No major indications of deformation in the database. However, in /Stanfors et al. 1994/ a section between core length 140 and 150 m coincides with this area and is mapped as a fracture zone and as tectonized. At approximately 110 m there is a crush zone and a tectonized area developed in fine-grained granite and “greenstone” (ref: Geomod)
KAS04	2–464	131–437	Two mylonites. Also four areas with weak to intermediate tectonization. The rock is granodiorite and fine-grained granite (ref: Geomod)
KA3590G02	20–30 (Base)	19–30	Intermediate tectonization. The rock is granodiorite. (ref: Geomod)

KAS02	–	795–924	No longer geometrical intercept but keep indicator for review
KAS12	0 (Top)–269	19–286	
HLX09	99–151 (Base)	–	Awaiting BH results
HLX16	0–83	–	Awaiting BH results
KAS17	86–360	–	Only summary preliminary mapping available. Awaiting results

ZSMNE006A

Property	Estimate	Span	Basis for interpretation	Comments
Confidence in existence	High		Linked lineaments, BH and tunnel (Åspö) intercepts	
Strike (regional scale)	215	± 10	Linked lineaments	
Dip (regional scale)	65	± 20	Linked lineaments, BH and tunnel (Åspö) intercepts	
Thickness, (including transition zones, regional scale)	130 m	60 to 130 m	Linked lineaments, BH and tunnel (Åspö) intercepts	Model thickness of 130 m represents an envelope thickness containing narrower inferred splays. At Åspö NE1 is considered to consist of 3 main branches totaling 85 m as intercepted in the tunnel.
Length (regional scale)	2.1 km	2 to 4 km	Linked lineaments	An alternative interpretation allows the zone to continue further north eastwards.
Ductile deformation	Yes		Multiple 1cm thick Mylonite bands, tunnel mapping.	Dominantly brittle zone with minor ductile indicators
Brittle deformation	Yes		Breccia and fault gauge	Dominantly brittle zone with minor ductile indicators
Alteration	1 m wide central completely altered clay core			5–8 m wide partially clay altered.
Water				All 3 branches are water bearing
Fracture orientation	230/35, 341/45, 284/90, 045/30, 050/60, 094/60, 120/35, 310/38, 310/75			The first two sets are water bearing. The analysis did not include the 933 fractures in the 1 m core. See text for details.
Fracture frequency m ⁻¹	11		KA1131B, KAS07, KAS08, KAS11, KAS14, KBH02, KAS02	Frac' frq'incl' crush (= 20 frac/m) (m ⁻¹)
Fracture filling	Ca 60%, Chl 49%, Ep 27%, He 23%, Qtz 1%		KA1131B, KAS07, KAS08, KAS11, KAS14, KBH02, KAS02	

BH	Geometrical intercept	Target intercept	Comment
KA1061	94–209 (Base)	198–209	Ref: Geomod
KA1131B	47–203 (Base)	173–203	Ref: Geomod
KAS07	402–602 (Base)	497–602	Ref: Geomod
KAS08	440–590 (Base)	537–601	Ref: Geomod
KAS09	53–225	50–112	Ref: Geomod
KAS11	115–249	156–220	Ref: Geomod
KAS14	38–194	51–91	Ref: Geomod
KBH02	543–706 (Base)	667–706	Ref: Geomod
KAS02	740–924 (Base)	806–914	Ref: Geomod
KAS16	228–439	380–430	Ref: Geomod
TASA		1,240–1,325	Ref: Geomod

ZSMNE010A

Property	Estimate	Span	Basis for interpretation	Comments
Confidence in existence	High		Linked lineaments. Ref: v. 0. Verified by field control- epidote healed fractures	This zone has not been reviewed in Laxemar v. 1.2.
Strike (regional scale)	055	± 15	Linked lineaments	
Dip (regional scale)	90		Assumed. No information	
Thickness, (including transition zones, regional scale)	10 m	2 to 10 m	Ref: v. 0. Verified by field control- epidote healed fractures	
Length (regional scale)	3.4 km	± 200	Linked lineaments	
Ductile deformation	–		No data	Brittle zone.
Brittle deformation	Yes		Field control. Ref: v. 0.	Brittle zone.
Alteration			No data	
Water				
Fracture orientation				
Fracture frequency				
Fracture filling	Ep		Field control. Ref: v. 0.	

BH	Geometrical intercept	Target intercept	Comment
n.a	n.a	n.a	

ZSMNE011A

Property	Estimate	Span	Basis for interpretation	Comments
Confidence in existence	High		Linked lineaments. Ref: v. 0. Verified by field control- ground magnetic and VLF measurements.	This zone has not been reviewed in Laxemar v. 1.2.
Strike (regional scale)	055	± 15	Linked lineaments	
Dip (regional scale)	90		Assumed. No information	
Thickness, (including transition zones, regional scale)	100 m	± 50	Linked lineaments	Ref: v. 0, 5–10 m 'cores' of highly fractured rock. 50–150 m wide transition envelope.
Length (regional scale)	8.5 km	8 to 12 km	Linked lineaments	Possible extension to SW.
Ductile deformation	Yes		Field evidence, Ref: v. 0.	Ductile-brittle zone.
Brittle deformation	Yes		Field control. Ref: v. 0. increased small scale fracturing, mesoscopic brittle and ductile-brittle deformation zones and epidote healed fractures	Ductile-brittle zone.
Alteration			No data	
Water			No data	
Fracture orientation			No data	
Fracture frequency			No data	
Fracture filling	Ep		Field control. Ref: v. 0.	

BH	Geometrical intercept	Target intercept	Comment
n.a	n.a	n.a	

ZSMNE012A (EW7-NE4)

Property	Estimate	Span	Basis for interpretation	Comments
Confidence in existence	High		Linked lineaments, seismic reflector, BH and tunnel (Åspö) intercepts	
Strike (regional scale)	060	050 to 110	Linked lineaments	
Dip (regional scale)	45	± 10	Linked lineaments, BH and tunnel (Åspö) intercepts	
Thickness, (including transition zones, regional scale)	120 m	60 to 120 m	Linked lineaments, BH and tunnel (Åspö) intercepts	Model thickness of 120 m represents an envelope thickness containing narrower inferred splays. At Åspö this zone potentially incorporates both EW7 and NE4. Seismic refraction profiling indicate cores of fractured or altered rock with thicknesses of 15 to 20 m and velocities of 2,500–3,300 m/s
Length (regional scale)	5.5 km	± 200 m	Linked lineaments	
Ductile deformation	Yes		Mylonite on northern boundary (TASA)	Ductile-brittle zone
Brittle deformation	Yes		Breccia and crushed mylonite.	Ductile-brittle zone
Alteration	Clay. Fracture fillingschlorite and epidote		TASA	
Water	Transmissivity 10 ⁻⁴ to 10 ⁻⁵ m ² /s		TASA	
Fracture orientation	Not yet assessed			
Fracture frequency m ⁻¹	9		KAV01, KAV04A, KBH02	Frac' frq'incl' crush (= 20 frac/m) (m ⁻¹)
Fracture filling	Ca 64%, Chl 48%, Ep 20%, He 14%, Qtz 3%		KAV01, KAV04A, KBH02	

BH	Geometrical intercept	Target intercept	Comment
HAV02	90–163 (Base)	90–150	Penetration rate indicates fractured or weak rock from c. 89–149 m depth.
HAV12	18–136	51–127	Penetration rate and BIPS indicate fractured or weak rock from c. 51–76 m with possible extension to 93 m. Low permeability. Between c. 100–127 m is water bearing. (only preliminary results available)
HAV13	0–121		Await results
HXL018	0–181 (Base)	16–181	Penetration rate indicates fractured or weak rock between 16–115 m, c. 147–151 m and c. 160–181 m. Water inflows at c. 53 m (1.5 l/min), c. 57 m (20 l/min), c. 67 m (21 l/min), c. 110 m (37–70 l/min) and c. 150 m (> 130 l/min). (only preliminary results available)
HMJ01	0–46 (Base)		No information
KAV01	401–630	400–580	Increased fracturing; alteration; low susceptibility and resistivity; low density. Mapped minor shear zones, breccias and mylonites.
KAV03	188–248	164–232	Sicada: 183–185 m brittle-ductile shear zone.
KAV04A	745–947	840–900	Increased number of crush zones. The deformation zone is characterized by an inhomogeneous brittle-cataclastic deformation. The focused resistivity (300) is markedly low along the section c. 860–900 m, but no other geophysical logging methods indicate significant anomalies.
KBH02	107–245	140–194	Sicada; 140.18 m–194.01 m code 42 = Brittle-ductile shear zone
TASA		779–858	

ZSMNE015A

Property	Estimate	Span	Basis for interpretation	Comments
Confidence in existence	High		Linked lineament, field mapping, along with Clab 1, Clab 2 and OKG excavation mapping.	
Strike (regional scale)	050	± 20	Field and excavation mapping	070 in west curving to 035 eastwards
Dip (regional scale)	70	± 10	Clab 1, Clab 2 and OKG excavation mapping.	
Thickness, (including transition zones, regional scale)	10 m	3 to 15 m	Clab 1, Clab 2 and OKG excavation mapping.	Clab: 2–3 m thick breccia and 2–3 m thick schistose section. OKG: 5–7 m thick breccia.
Length (regional scale)	1.9 km	± 200	Linked lineaments	ZSMNE015A and B = 2.9 km
Ductile deformation	Yes		Field mapping; schistose banding in Clab	Ductile-brittle zone
Brittle deformation	Yes		Breccia in Clab 1 and 2	Ductile-brittle zone
Alteration	Cm wide clay bands		Clab 1 and Clab 2 excavation mapping.	May be depth/weathering dependent. Clab intercept is relatively shallow.
Water	Max' tunnel inflow recorded as 11 l/min		Clab 1 and Clab 2 excavation mapping.	
Fracture orientation				
Fracture frequency				
Fracture filling	Clay and chl		Clab 1 and Clab 2 excavation.	

BH	Geometrical intercept	Target intercept	Comment
Clab 1 access tunnel			Ref P-03-07 and P-03-86
Clab 2 access tunnel			Ref P-03-07 and P-03-86
OKG3 intake tunnel			Ref P-03-07 and P-03-86

ZSMNE015B

Property	Estimate	Span	Basis for interpretation	Comments
Confidence in existence	High		Linked lineament, field mapping, along with OKG excavation mapping.	
Strike (regional scale)	080	± 10	Field and excavation mapping	
Dip (regional scale)	90	± 10	OKG excavation mapping.	
Thickness, (including transition zones, regional scale)	5 m	1 to 5 m	OKG excavation mapping.	OKG: irregular thickness 0.5–5 m thick breccia.
Length (regional scale)	1.0 km	± 100	Linked lineaments	ZSMNE015A and B = 2.9 km
Ductile deformation	–		No info'	Ductile-brittle zone (by association with ZSMNE015A)
Brittle deformation	Yes		'Crush zones' and Chlorite gouge reported on boundaries (OKG)	Ductile-brittle zone (by association with ZSMNE015A)
Alteration	Clay		OKG excavation mapping.	May be depth/weathering dependent. Clab intercept is relatively shallow.
Water	'Dry'		Nothing noted in OKG excavation mapping.	
Fracture orientation				
Fracture frequency				
Fracture filling	Clay and chl		OKG excavation.	

BH	Geometrical intercept	Target intercept	Comment
OKG cold water intake tunnel			Ref P-03-07 and P-03-86

ZSMNE016A

Property	Estimate	Span	Basis for interpretation	Comments
Confidence in existence	High		Linked lineaments, seismic refraction, BH and tunnel (Äspö) intercepts	
Strike (regional scale)	030	± 20	Linked lineaments	
Dip (regional scale)	90	± 10	Linked lineaments, BH and tunnel (Äspö) intercepts	
Thickness, (including transition zones, regional scale)	15 m	± 10	Linked lineaments, BH and tunnel (Äspö) intercepts, seismic refraction profile	
Length (regional scale)	1.3 km	± 100 m	Linked lineaments	
Ductile deformation	–			Brittle deformation zone
Brittle deformation	Yes		TASA ch 350–370. Inferred from BH penetration rates and seismic refraction survey, 5–10 m wide low velocity zone 3,000 m/sec.	Brittle deformation zone
Alteration				
Water	Transmissivity 10 ⁻⁶ m ² /s		TASA ch. 350	
Fracture orientation				
Fracture frequency				
Fracture filling	Chlorite, calcite, epidote and clay.		Tunnel mapping	

BH	Geometrical intercept	Target intercept	Comment
HAV14	143–172	130–175	Penetration rate indicates fractured or weak rock (weakness zone) from c. 130–175 m,. Water bearing between 164–169 m (85 l/min). (only preliminary results available)
HAV07	–	–	No intercept but in close proximity. Penetration rate indicates fractured or weak rock from c. 16–95 m.
TASA		350–370	

ZSMNE018A

Property	Estimate	Span	Basis for interpretation	Comments
Confidence in existence	High		Linked lineament, Extensive field mapping evidence.	
Strike (regional scale)	080	± 10	Linked lineament, Extensive field mapping evidence.	
Dip (regional scale)	90	± 10	Field mapping	
Thickness, (including transition zones, regional scale)	50 m	± 25	Linked lineament and field mapping.	A ductile complex zone, inferred anastomosing geometry. The 50 m thickness is an envelope thickness containing the inferred splays.
Length (regional scale)	1.3 km	± 100	Linked lineaments	
Ductile deformation	Yes		Extensive field mapping evidence.	Ductile zone with weak evidence of brittle reactivation.
Brittle deformation	Yes		One clear brittle indicator. One other indicator associated with an inferred splay.	Ductile zone with weak evidence of brittle reactivation.
Alteration				
Water				No information
Fracture orientation	Not yet assessed			
Fracture frequency	Not yet assessed			
Fracture filling				

BH	Geometrical intercept	Target intercept	Comment
–	–	–	–

ZSMNE019A

Property	Estimate	Span	Basis for interpretation	Comments
Confidence in existence	High		Linked lineament, ground geophysical profiling	
Strike (regional scale)	060	± 15	Linked lineament.	
Dip (regional scale)	90	± 20	None	Simple assumption
Thickness, (including transition zones, regional scale)	5 m	1 to 10 m	Linked lineament, ground geophysical profiling	
Length (regional scale)	3.7 km	± 200	Linked lineaments	
Ductile deformation	–			No information
Brittle deformation	–			No information
Alteration				No information
Water				No information
Fracture orientation				No information
Fracture frequency				No information
Fracture filling				No information

BH	Geometrical intercept	Target intercept	Comment
–	–	–	No intercepts

ZSMNE024A

Property	Estimate	Span	Basis for interpretation	Comments
Confidence in existence	High		Linked lineaments, seismic reflector, seismic refractor, BHs and OKG cold water intake tunnel.	This zone should be viewed together with ZSMNE031A. Together they define a broad complex structural belt of deformation off the coast of Ävrö
Strike (regional scale)	225	215 to 235	Linked lineaments	
Dip (regional scale)	52	± 10	Linked lineaments, seismic reflector, and BHs. Reflector and KSH03A are the primary constraints	
Thickness, (including transition zones, regional scale)	80 m	± 20	Linked lineaments and BH	Model thickness of 80 m represents an envelope thickness containing narrower inferred splays. OKG suggests fractured cores 2 to 10 m thick. Seismic refraction profiling indicates cores of fractured or altered rock with thicknesses of up to 30 m and velocities of 3,400–4,200 m/s. This zone should be seen as contributing to a broader tectonic belt.
Length (regional scale)	11.6 km	10 to 15++km	Linked lineaments	Lineament data for ZSMNE024A and ZSMNE031A suggests this deformation belt extends beyond the boundaries of the regional model area.
Ductile deformation	–		BHs	Ductile-brittle zone. Major brittle element.
Brittle deformation	Yes		BHs and tunnel evidence	Ductile-brittle zone. Major brittle element.
Alteration Water	Chlorite		OKG	Noted as 'highly weathered' -OKG 'moderately water bearing' -OKG
Fracture orientation	Not yet assessed			
Fracture frequency m ⁻¹	13		KSH01A, KSH03A, KAV01A, KAV04A	Frac' frq'incl' crush (= 20 frac/m) (m ⁻¹)
Fracture filling	Ca 51%, Chl 45%, Ep 18%, He 25%, Qtz 15%		KSH01A, KSH03A, KAV01A, KAV04A	

BH	Geometrical intercept	Target intercept	Comment
OKG			Moderately water bearing, highly weathered,
HAV11	95–178	124–180	Only preliminary results available. Penetration rate and BIPS figs' indicate fractured or weaker rock from c. 124–180 m; water bearing measured at 145 m c. 32 l/min and judged to originate from c. 129–142 m
KSH01A	542–669	540–631	DZ6, 540–609 m Partly increased fracturing. Partly heavy alteration. Indication: Low susceptibility, low resistivity. DZ7 609–614 m, Low-Grade, ductile shear-zone. DZ8, 614–631 m, Partly increased fracturing. Partly heavy alteration. Indication: Low susceptibility, low resistivity.

KSH03A	175–258	162–275	Inhomogeneous, low-grade, ductile deformation. High frequency of open and sealed fractures and crush zones. Brecciation between 220–235 m and mylonitization between 270–275 m. Marked low resistivity and, where available, lower sonic. Sonic data are missing between 203.5–255.2 m). Distinct, major caliper anomaly. Generally low magnetic susceptibility. A number of sections with increased fracturing may indicate minor deformation zones.
KAV01A	674–757 (Base)	660–757	Single hole interpretation includes no clear DZ in this location. However, examination of the log suggests that it is not unreasonable to suggest indicators are present.
KAV04A	937–1,004 (Base)	940–1,004	Single hole interpretation gives DZ1 840–900 m with the description: Increased number of crush zones. The deformation zone is characterized by an inhomogeneous brittle-cataclastic deformation. The focused resistivity (300) is markedly low along the section c. 860–900 m, but no other geophysical logging methods indicate significant anomalies. Note that ZSMNE012A is modelled with an interception from 840–900 m. Examination of the log suggests that it is not unreasonable to suggest deformation indicators continue below 900 m of KAV04A

ZSMNE031A

Property	Estimate	Span	Basis for interpretation	Comments
Confidence in existence	High		Linked lineaments, seismic reflector, seismic refractor, BHs and OKG cold water intake tunnel.	This zone should be viewed together with ZSMNE024A. Together they define a broad complex structural belt of deformation off the coast of Ävrö
Strike (regional scale)	215	± 20	Linked lineaments	
Dip (regional scale)	52	± 20		Based on the assumption that this zone is intimately associated with ZSMNE024A. OKG intake tunnel suggests a shallower 40° dip
Thickness, (including transition zones, regional scale)	15 m	2 to 20 m	Linked lineaments and BH	Seismic refraction profiling indicates cores of fractured or altered rock with thicknesses of up to 15 m and velocities of 3,300–3,400 m/s. This zone should be seen as contributing to a broader tectonic belt.
Length (regional scale)	4.4 km	4.0 to 15++km	Linked lineaments	Lineament data for ZSMNE024A and ZSMNE031A suggests this deformation belt extends beyond the boundaries of the regional model area.
Ductile deformation	–			Brittle zone. Major brittle element.
Brittle deformation	Yes		BHs and tunnel evidence	Brittle zone. Major brittle element.
Alteration	Chl and clay		OKG	
Water	'Dry'		OKG	No inflow recorded in OKG
Fracture orientation	Not yet assessed			
Fracture frequency m ⁻¹	11		KSH01A, KSH03A,	Frac' frq'incl' crush (= 20 frac/m) (m ⁻¹)
Fracture filling	Ca 57%, Chl 52%, Ep 10%, He 29%, Qtz 15%		KSH01A, KSH03A,	

BH	Geometrical intercept	Target intercept	Comment
OKG			Brecciated zone with 2 m (apparent) thickness. Chlorite and clay on SE boundary with associated wedge failure in the roof.
KSH01A	682–704	687–693	Single hole interpretation: DZ10 686.5–692.5 m, Low-Grade, ductile shear-zone. DZ11 692.5–693 m, Increased fracturing. Indication: Low susceptibility, and density.
KSH03A	282–297	287–292	Note: Single hole interpretation: 162–275 m. However, indicators of deformation occur below this depth. eg 286.5–292 m Breccia.

ZSMNE040A

Property	Estimate	Span	Basis for interpretation	Comments
Confidence in existence	High		Linked lineaments; magnetic, resistivity and seismic refraction profiling-	
Strike (regional scale)	030	± 10	Linked lineaments	
Dip (regional scale)	90	± 10	Magnetic and resistivity profiling.	Modelled as vertical to allow for local variations. However, resistivity profiling weakly indicates a steep (80°) dip to SE
Thickness, (including transition zones, regional scale)	20 m	5 to 20 m	Magnetic, resistivity and seismic refraction profiling	20 m represents an envelope width, inferred to contain discontinuous splays with widths of c. 5 m of fractured rock as inferred from seismic refraction profiling.
Length (regional scale)	1.4 km	± 100 m	Linked lineaments	
Ductile deformation	–			Brittle zone (preliminary assessment- but based on extremely weak evidence)
Brittle deformation	Yes		Inferred from seismic refraction low velocity. Possible associated field mapping indicators.	Brittle zone (preliminary assessment- but based on extremely weak evidence)
Alteration				
Water				
Fracture orientation				
Fracture frequency				
Fracture filling				

BH	Geometrical intercept	Target intercept	Comment
HLX01	0–30		Awaiting BH results
HLX04	21–82		Awaiting BH results

ZSMNE050A

Property	Estimate	Span	Basis for interpretation	Comments
Confidence in existence	High		Linked lineaments. Field mapping (5 locations)	
Strike (regional scale)	045	035 to 065	Linked lineaments	
Dip (regional scale)	90	± 15	Field mapping	
Thickness, (including transition zones, regional scale)	50 m	20 to 70 m	Linked lineaments and field mapping	An envelope width containing transition zones and inferred splays.
Length (regional scale)	2.2 km	2.0 to 3.0 km	Linked lineaments	
Ductile deformation	Yes		Field mapping	Ductile zone
Brittle deformation	–		No data	Ductile zone
Alteration			No data	
Water			No data	
Fracture orientation			No data	
Fracture frequency			No data	
Fracture filling			No data	

BH	Geometrical intercept	Target intercept	Comment
n.a	n.a	n.a	

ZSMNE930A				
Property	Estimate	Span	Basis for interpretation	Comments
Confidence in existence	High		Linked lineament, Extensive field mapping evidence. Excavation evidence (OKG)	
Strike (regional scale)	065	± 10	Linked lineament, Extensive field mapping evidence.	
Dip (regional scale)	90	± 10	Field mapping and excavation evidence (OKG)	
Thickness, (including transition zones, regional scale)	5 m	1 to 30 m	Linked lineament, Extensive field mapping evidence. Excavation evidence (OKG)	A ductile complex zone, anastomosing geometry visible in the OKG excavations. The 30 m upper limit thickness is an envelope thickness containing the inferred splays with individual widths of 0.5 to 3 m.
Length (regional scale)	4.2 km	± 200 m	Linked lineaments	
Ductile deformation	Yes		Extensive field mapping evidence.	Ductile zone with weak evidence of brittle reactivation.
Brittle deformation	–		Weak indications probably associated with the weathering profile. The presence of well developed schistosity indicates deformation at depth.	Ductile zone with weak evidence of brittle reactivation.
Alteration	Clay			Note: the evidence of clay comes from the OKG excavations located at a shallow depth ie this may be related to a shallow weathering effect.
Water	Low transmissivity		No inflow indications marked on OKG excavation mapping	The clay is more likely to indicate a hydraulic barrier rather than a conductor.
Fracture orientation	Not yet assessed			Strongly developed schistosity (OKG excavation mapping)
Fracture frequency	Not yet assessed			
Fracture filling	Chlorite			

BH	Geometrical intercept	Target intercept	Comment
OKG	–	–	OKG 3 "turbine building shear zone"

ZSMNS001A-D

Property	Estimate	Span	Basis for interpretation	Comments
Confidence in existence	High		Linked lineaments. Ref: v. 0. Verified by field control- ground magnetic and VLF measurements. The northern segment has also been verified by a refraction seismic survey /Rydström and Gereben 1989/	This zone has not been reviewed in Laxemar v. 1.2. Eastern side down thrown. Ref: /Kresten and Chyssler 1976/.
Strike (regional scale)	010	± 15	Linked lineaments	
Dip (regional scale)	90	± 15	Steep to vertical dip -VLF	
Thickness, (including transition zones, regional scale)	100 m	± 50 m	Linked lineaments	Ref: v. 0, 10 m 'cores' of highly fractured rock. 50–150 m wide transition envelope.
Length (regional scale)	A_3.4 km B_1.1 km C_2.2 km D_4.4 km	10 to > 11 km	Linked lineaments	Possible southward and northward extension beyond the regional model boundary
Ductile deformation	Yes		Field evidence, Ref: v. 0.	Ductile-brittle zone.
Brittle deformation	Yes		Field control. Ref: v. 0. Mesoscopic brittle-ductile shear zones along or close to the marked fracture zone	Ductile-brittle zone.
Alteration			No data	
Water			No data	
Fracture orientation			No data	
Fracture frequency			No data	
Fracture filling	Ep		Field control. Ref: v. 0.	

BH	Geometrical intercept	Target intercept	Comment
n.a	n.a	n.a	

ZSMNS009A

Property	Estimate	Span	Basis for interpretation	Comments
Confidence in existence	High		Linked lineaments. Ref: v. 0. Verified by field control- ground magnetic and VLF measurements.	
Strike (regional scale)	010	± 10	Linked lineaments	
Dip (regional scale)	90	± 15	Steep to vertical dip -VLF	
Thickness, (including transition zones, regional scale)	80 m	± 40 m	Linked lineaments	Ref. v. 0. 5–50 m thickness has been inferred to represent the upper estimate of a highly fractured 'core' value. An 80 m width has been used in the model, including transition zones.
Length (regional scale)	9.8 km	10 to > 12 km	Linked lineaments	Possible southward extension beyond the regional model boundary
Ductile deformation	Yes		Field evidence, Ref: v. 0. increased small scale fracturing, mesoscopic brittle and brittle-ductile deformation zones and epidote-healed fractures	Ductile-brittle zone.
Brittle deformation	Yes		Field control. Ref: v. 0.	Ductile-brittle zone.
Alteration			No data	
Water			No data	
Fracture orientation			No data	
Fracture frequency			No data	
Fracture filling	Ep		Field control. Ref: v. 0.	

BH	Geometrical intercept	Target intercept	Comment
n.a	n.a	n.a	

ZSMNS017A and B (NNW4)

Property	Estimate	Span	Basis for interpretation	Comments
Confidence in existence	High		Linked lineaments, tunnel mapping and BHs.	One of a number of parallel steep structures present in this area, ref: NNW4 Geomod.
Strike (regional scale)	335	± 10	Linked lineaments and tunnel	
Dip (regional scale)	83	± 10	Linked lineaments, BHs and tunnel intercepts	Ref: Geomod NNW4. The dip is a 'best fit' geometrical result, it should be treated as generally subvertical.
Thickness, (including transition zones, regional scale)	20 m	20 to 100 m	Tunnel mapping	The upper limit does not represent a single discrete structure but rather an envelope width containing an associated group of structures.
Length (regional scale)	17A 2.1 km 17B 1.1 km	± 100 m ± 100 m	Linked lineaments.	
Ductile deformation	Yes		Tunnel mapping (mylonite) TASA ch. 2015, 2120, 2920	Ductile-brittle zone. Important brittle component as indicated by high transmissivities.
Brittle deformation	Yes		Increased fracturing and crush zones KA2048B	Ductile-brittle zone. Important brittle component as indicated by high transmissivities.
Alteration	Weak to medium, Clay, Chl, Ca and Ep.			
Water	T = 2.1×10^{-4} m ² /s		TASA ch. 2020	
Fracture orientation	Not yet assessed			
Fracture frequency m ⁻¹	11		KA2048B	Frac' frq'incl' crush (= 20 frac/m) (m ⁻¹)
Fracture filling	Ca 74%, Chl 38%, Ep 9%, He 28%, Qtz 0%		KA2048B	

BH	Geometrical intercept	Target intercept	Comment
KA2048B	6–67	28–46	8 fractures per m and crushed core c. 1 m total
TASA		2,010–2,020	Ref: Geomod and PR HRL-96-19
TASA		2,115–2,125	Ref: Geomod and PR HRL-96-19
TASA		2,910–2,930	Ref: Geomod and PR HRL-96-19

ZSMNS059A

Property	Estimate	Span	Basis for interpretation	Comments
Confidence in existence	High		Linked lineament, field mapping and geophysical ground survey	
Strike (regional scale)	000	± 10	Strong magnetic and topographic lineament	
Dip (regional scale)	90	± 10	Seismic relector, field mapping incators and geophysical ground survey.	A seismic reflector interpreted as representing a splay of this zone has been identified as dipping 80° to the west field mapping results further south suggest 80–85° to the east. The zone will be modelled as being vertical with a ± 10° uncertainty.
Thickness, (including transition zones, regional scale)	50 m	20 to 60 m	Geophysical ground survey	Geophysical profiling indicates a complex zone; a width of 50 m has been used in the model as being representative of the zone over its entire length and covers inferred multiple splays and transition zones. Individual splays are inferred to have cores of more highly fractured rock that have widths varying between 5 m to 15 m, based on seismic refraction profiling results.
Length (regional scale)	5.3 km	± 200 m	Linked lineaments	Southern termination most uncertain.
Ductile deformation	Yes		Five field indicators	Brittle-ductile zone. No subsurface investigations yet to substantiate a brittle component.
Brittle deformation	Yes		Inferred from seismic refraction profiling results	Brittle-ductile zone. No subsurface investigations yet to substantiate a brittle component.
Alteration				No anylsls available
Water				No anylsls available
Fracture orientation				No anylsls available
Fracture frequency				No anylsls available
Fracture filling				No anylsls available

BH	Geometrical intercept	Target intercept	Comment

ZSMNW025A

Property	Estimate	Span	Basis for interpretation	Comments
Confidence in existence	High		Linked lineament, seismic refraction profiling	A minor structure
Strike (regional scale)	110	± 10	Linked lineament	
Dip (regional scale)	90	± 10	HSH01A	A dip of 88 gives a best fit with HSH01A. However, it seems unjustified to define such a specific dip based on such local evidence when surrounding investigations provide weak or no supporting indications.
Thickness, (including transition zones, regional scale)	10 m	1 to 15 m	Linked lineament and seismic refraction profiling	Variable width, considered discontinuous.
Length (regional scale)	1.9 km	± 100 m	Linked lineaments	Considered discontinuous
Ductile deformation	–		No info'	Brittle zone
Brittle deformation	Yes		increased fracturing c. 15/m	Brittle zone
Alteration				Await BH results
Water				Await BH results
Fracture orientation	Not yet assessed			
Fracture frequency m ⁻¹	7		HSH01A	Frac' frq'incl' crush (= 20 frac/m) (m ⁻¹)
Fracture filling	Ca 1%, Chl 83%, Ep 1%, He 0%, Qtz 14%		HSH01A	

BH	Geometrical intercept	Target intercept	Comment
HSH01A	170–197	160–171	Increased fracturing indicated by high penetration rate, low susceptibility and low resistivity. Alteration indicated by drill cuttings.
HSH04A	132–151		Await results
HSH06A	115–132		Await results

ZSMNW028A

Property	Estimate	Span	Basis for interpretation	Comments
Confidence in existence	High		Linked lineaments; detailed topographic and magnetic study (ref: P-03-66) and BH.	
Strike (regional scale)	105	± 15	Linked lineaments	
Dip (regional scale)	90	± 10	Linked lineaments and BH	A dip of 83° gives a best fit with HAV09. However, oriented fractures in the hole suggest 250/88°. The zone is considered subvertical and it seems unjustified to define a more specific dip.
Thickness, (including transition zones, regional scale)	10 m	± 5 m	Linked lineaments and BH	
Length (regional scale)	1.1 km	± 100 m	Linked lineaments	
Ductile deformation	–		No information	Brittle zone
Brittle deformation	Yes		Increased fracturing in BH	Brittle zone
Alteration			Await results	
Water			Await results	
Fracture orientation	Not yet assessed			
Fracture frequency m ⁻¹	1		HAV09	Frac' frq'incl' crush (= 20 frac/m) (m ⁻¹)
Fracture filling	Ca 0%, Chl 0%, Ep 0%, He 0%, Qtz 0%		HAV09	-needs review and consensus with single hole interpretation.

BH	Geometrical intercept	Target intercept	Comment
HAV09	72–96	75–105	The zone is indicated by increased fracture frequency, high drill penetration rate, low resistivity, low magnetic susceptibility, low density, low p-wave velocity and distinct, marked caliper anomalies.

ZSMNW042A

Property	Estimate	Span	Basis for interpretation	Comments
Confidence in existence	High		Linked lineaments, magnetic, resistivity and seismic refraction profiling	
Strike (regional scale)	105	± 10	Linked lineaments	
Dip (regional scale)	90	± 20	Linked lineaments. Dip- field mapping suggests dip to south, HLX15 orientated fractures suggest 75° to S or N. Surface geophysics suggest subvertical.	
Thickness, (including transition zones, regional scale)	80 m	30 to 80 m	Magnetic and topographic lineament widths.	Model width of 80 m represents an envelope width containing narrower inferred splays. Seismic refraction results indicate a narrower, 20 m wide fractured core.
Length (regional scale)	3.3 km	± 100 m	Linked lineaments	ZSMNW042A,B,C together = 8.3 km
Ductile deformation	Yes		Weak field indicators	Await BH results. current weak evidence suggests a ductile-brittle zone.
Brittle deformation	Yes		Weak field indicators	Await BH results. current weak evidence suggests a ductile-brittle zone.
Alteration				
Water				
Fracture orientation				
Fracture frequency				
Fracture filling				

BH	Geometrical intercept	Target intercept	Comment
HLX15	0–143		Await results
HLX26	40–151 (Base)		Await results
HLX27	136–165 (Base)		Await results
HLX28	72–154 (Base)		Await results
HLX29			Await results- no current geometrical intercept
KLX05			Await results- no current geometrical intercept

ZSMNW928A

Property	Estimate	Span	Basis for interpretation	Comments
Confidence in existence	Medium		Seismic reflector and coincidence with BH deformation indicators	Based on seismic reflector N geometry /Juhlin et al. 2004b/. Relevant BH data has not been fully evaluated yet.
Strike (regional scale)	120	± 20	Seismic reflector 'N' /Juhlin et al. 2004b/	No surface expression. Based on seismic reflector N geometry /Juhlin et al. 2004b/
Dip (regional scale)	28	± 5	Seismic reflector 'N' /Juhlin et al. 2004b/	Based on seismic reflector N geometry /Juhlin et al. 2004b/
Thickness, (including transition zones, regional scale)	–	–	Seismic reflector 'N' /Juhlin et al. 2004b/	Modelled with zero thickness. Relevant BH data has not been fully evaluated yet.
Length (regional scale)	2.2 km	2 to 5 km	Seismic reflector survey	Length estimate limited by the extent of the survey coverage.
Rock type	Ävrö granite dominates, with fine grained diorite gabbro		KLX02 and KLX04	Preliminary- relevant BH data has not been fully evaluated yet.
Ductile deformation	Not yet assessed			Relevant BH data has not been evaluated yet.
Brittle deformation	Not yet assessed			
Alteration	Not yet assessed			
Water	Not yet assessed			
Fracture orientation	Not yet assessed			
Fracture frequency m ⁻¹	Not yet assessed			
Fracture filling	Not yet assessed			

BH	Geometrical intercept	Target intercept	Comment
KLX02	764	–	Not yet assessed
KLX04	898	–	Not yet assessed.

ZSMNW929A

Property	Estimate	Span	Basis for interpretation	Comments
Confidence in existence	High		Linked lineament and BH intercepts.	
Strike (regional scale)	113	± 10	Magnetic and topographic lineaments	Lineament interpretation needs further review.
Dip (regional scale)	79	± 10	Lineament trace coupled with KLX02 and KLX04 single hole interpretations and orientated fractures in KLX04 between 870–970 Bhl.	
Thickness, (including transition zones, regional scale)	50 m	20 to 50 m	Magnetic and topographic lineaments	Model width of 50 m represents an envelope width containing narrower inferred splays.
Length (regional scale)	1.9 km	± 100 m	Linked lineaments	
Ductile deformation	–		No indicators	Brittle deformation zone
Brittle deformation	Yes		BHs, increased fracture frequency and crush zones	Brittle deformation zone
Alteration	Oxidation			
Water	–			Not yet analysed
Fracture orientation	Not yet assessed			
Fracture frequency m ⁻¹	10		KLX02, KLX04	Frac' frq'incl' crush (= 20 frac/m) (m ⁻¹)
Fracture filling	Ca 51%, Chl 57%, Ep 13%, He 7%, Qtz 10%		KLX02, KLX04	.

BH	Geometrical intercept	Target intercept	Comment
KLX02	778–935	770–960	Generally increased frequency of open fractures and higher oxidation. The most intensive part of the zone is located between 845–880 m, which is indicated by distinct low p-wave velocity and partly somewhat lower resistivity. A number of sections with increased fracturing may indicate minor deformation zones.
KLX04	861–986	873–973	Repeated crush and sealed network. Alteration in upper part, but missing in the central part. High frequency of open fractures. Zone centre with strong inhomogeneous brittle deformation. The most intensely deformed part in this section is between c. 930 and 973 m. A radar reflector at 915.7 m has an angle of 31° to borehole axis and one reflector at 888.5 m has the angle 21° to borehole axis. Rock type is interpreted to be granite to quartz monzodiorite, generally porphyritic (Ävrö granite). Note: An intensely crushed part at 936–946 m may correlate with a seismic reflector (ZSMNE928A) with the orientation 120/30.

ZSMNW931A

Property	Estimate	Span	Basis for interpretation	Comments
Confidence in existence	High		Linked lineaments. Ref: v. 0. Verified by field control- ground magnetic and VLF measurements.	Ground geophysics Ref: /Stanfors and Erlström 1995/
Strike (regional scale)	165	± 10	Linked lineaments	
Dip (regional scale)	90	± 15	Assumed	
Thickness, (including transition zones, regional scale)	50 m	50 to 100 m	Linked lineaments. Ref v. 0. ground geophysics	An envelope width containing transition zones and inferred splays.
Length (regional scale)	3.9 km	± 200 m	Linked lineaments	ZSMNW931A + B = 4.3 km
Ductile deformation	–		No data	Brittle zone.
Brittle deformation	Yes		Inferred from VLF	Brittle zone.
Alteration			No data	
Water			No data	
Fracture orientation			No data	
Fracture frequency			No data	
Fracture filling	Ep		No data	

BH	Geometrical intercept	Target intercept	Comment
n.a	n.a	n.a	

ZSMNW932A (formerly ZSMNW006A)

Property	Estimate	Span	Basis for interpretation	Comments
Confidence in existence	High		Linked lineament and geophysical ground survey	Seismic refraction profiling did not identify any corresponding low velocity zone.
Strike (regional scale)	120	120 to 90	Linked lineaments	
Dip (regional scale)	90	± 20	geophysical ground survey identified no clear indicators.	
Thickness, (including transition zones, regional scale)	0 m	0 to 20 m	geophysical ground survey identified no clear indicators.	
Length (regional scale)	2.8 km	± 200 m	Linked lineaments	ZSMNW932A,B,C,D combined length 4.9 km
Ductile deformation	–		No evidence from field mapping	Awaiting BH results
Brittle deformation	–		No evidence from field mapping	Awaiting BH results
Alteration				Awaiting BH results
Water				Awaiting BH results
Fracture orientation				Awaiting BH results
Fracture frequency				Awaiting BH results
Fracture filling				Awaiting BH results

BH	Geometrical intercept	Target intercept	Comment
KLX03	505	–	Only summary preliminary mapping available. No strong indicators. Awaiting results
KLX05	624	–	Only summary preliminary mapping available. No strong indicators. Awaiting results

ZSMNW933A

Property	Estimate	Span	Basis for interpretation	Comments
Confidence in existence	High		Linked lineaments. Ref: v. 0. Verified by field control- ground magnetic and VLF measurements.	Ground geophysics Ref: /Stenberg and Sehlstedt 1989/
Strike (regional scale)	150	150 to 090 eastwards	Linked lineaments	
Dip (regional scale)	90	± 15	Assumed	
Thickness, (including transition zones, regional scale)	40 m	± 20	Linked lineaments. Ref v.0. ground geophysics VLF	Ref v. 0. ground geophysics VLF
Length (regional scale)	3.8 km	± 200	Linked lineaments	
Ductile deformation	–		No data	Brittle zone
Brittle deformation	Yes		Inferred from VLF	Brittle zone
Alteration			No data	
Water			No data	
Fracture orientation			No data	
Fracture frequency			No data	
Fracture filling	Ep		No data	

BH	Geometrical intercept	Target intercept	Comment
n.a	n.a	n.a	

Correlation of flow anomalies (PFL-f) with Boremap data from new boreholes analysed for model version Laxemar version 1.2

Flow indication confidence levels for open fractures (PFL confidence)

The classification of “level of confidence in flow indication”, or the PFL confidence, is based on the distance between the anomaly and the interpreted fracture. That is, if the anomaly has a flow indication of Class 1, the interpreted fracture is within 0.1 m away from the anomaly. Correspondingly, the anomaly is of flow indication Class 2, if the interpreted fracture is within 0.2 m of the anomaly. Four classes have been defined according to;

Class 1	0–0.1 m
Class 2	0.1–0.2 m
Class 3	0.2–0.3 m
Class 4	0.3–0.4 m

Features with PFL confidence > 4 are rare and considered to be non-significant. Therefore, they are not plotted in the diagrams presented in this appendix.

Confidence level open fractures

The confidence level for open fractures accounts for the certainty with which the fracture is interpreted. In this model version, three levels of confidence in the Sicada database are introduced;

Level 1	Certain
Level 2	Probable
Level 3	Possible

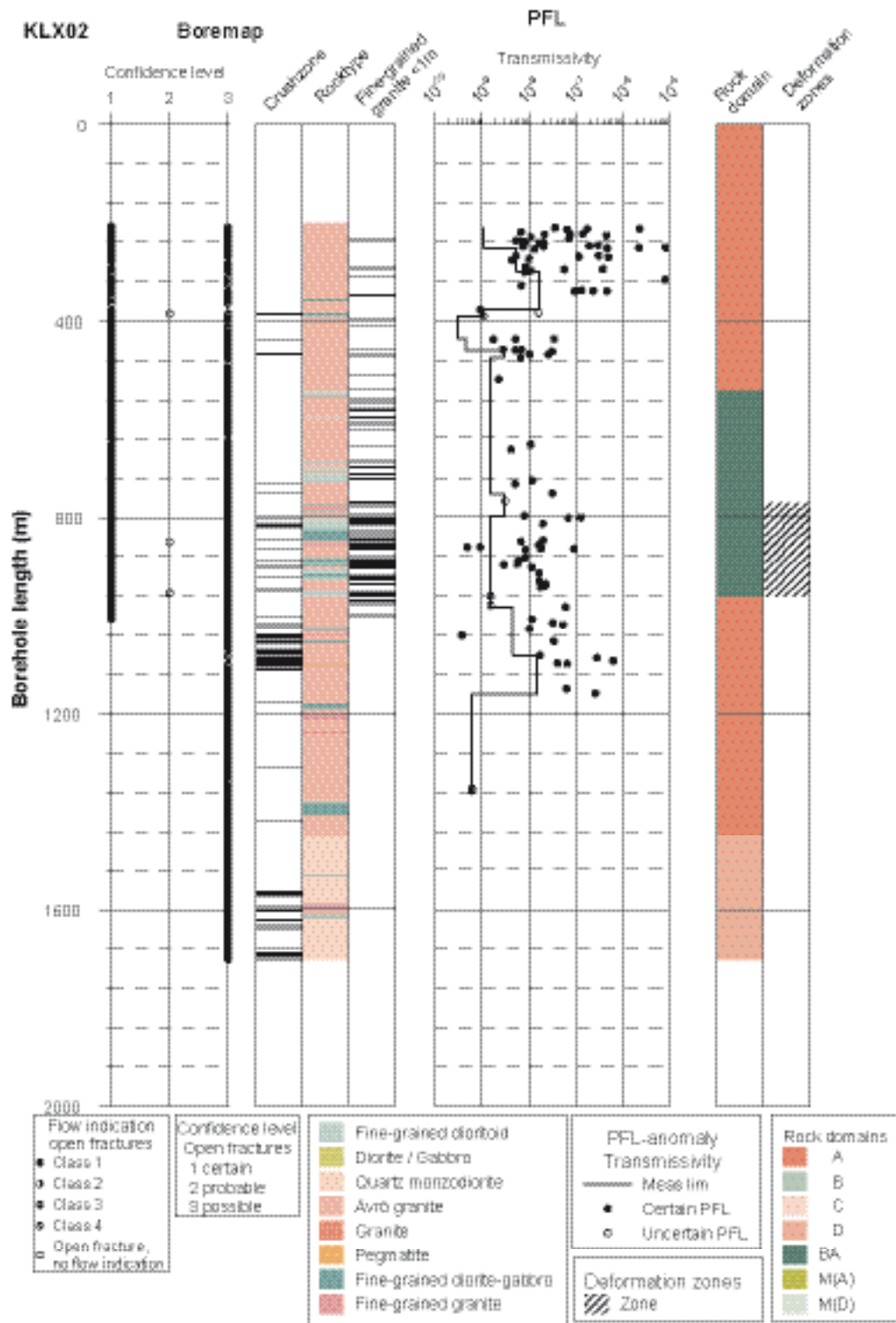


Figure A7-1. Transmissivity of hydraulic features in borehole KLX02 based on PFL-f data, Boremap data (open fractures, partly open fractures and crush zones, rock type and veins of fine-grained granite) and the interpreted geological rock domains and deformation zones /Forssman et al. 2005b/.

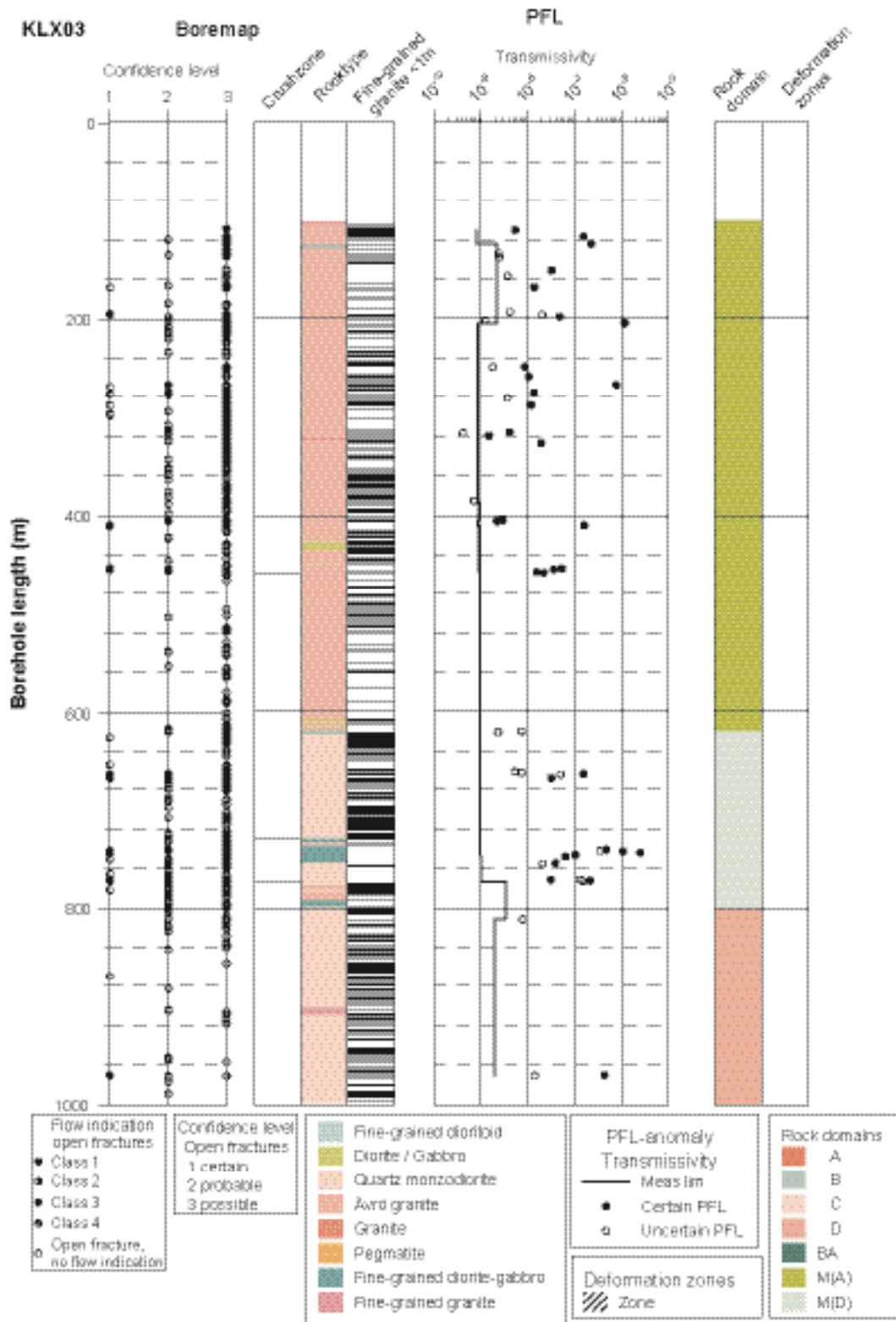


Figure A7-2. Transmissivity of hydraulic features of borehole KLX03 based on PFL-f data, Boremap data (open fractures, partly open fractures and crush zones, rock type and veins of fine-grained granite) and the interpreted geological rock domains and deformation zones /Forssman et al. 2005b/.

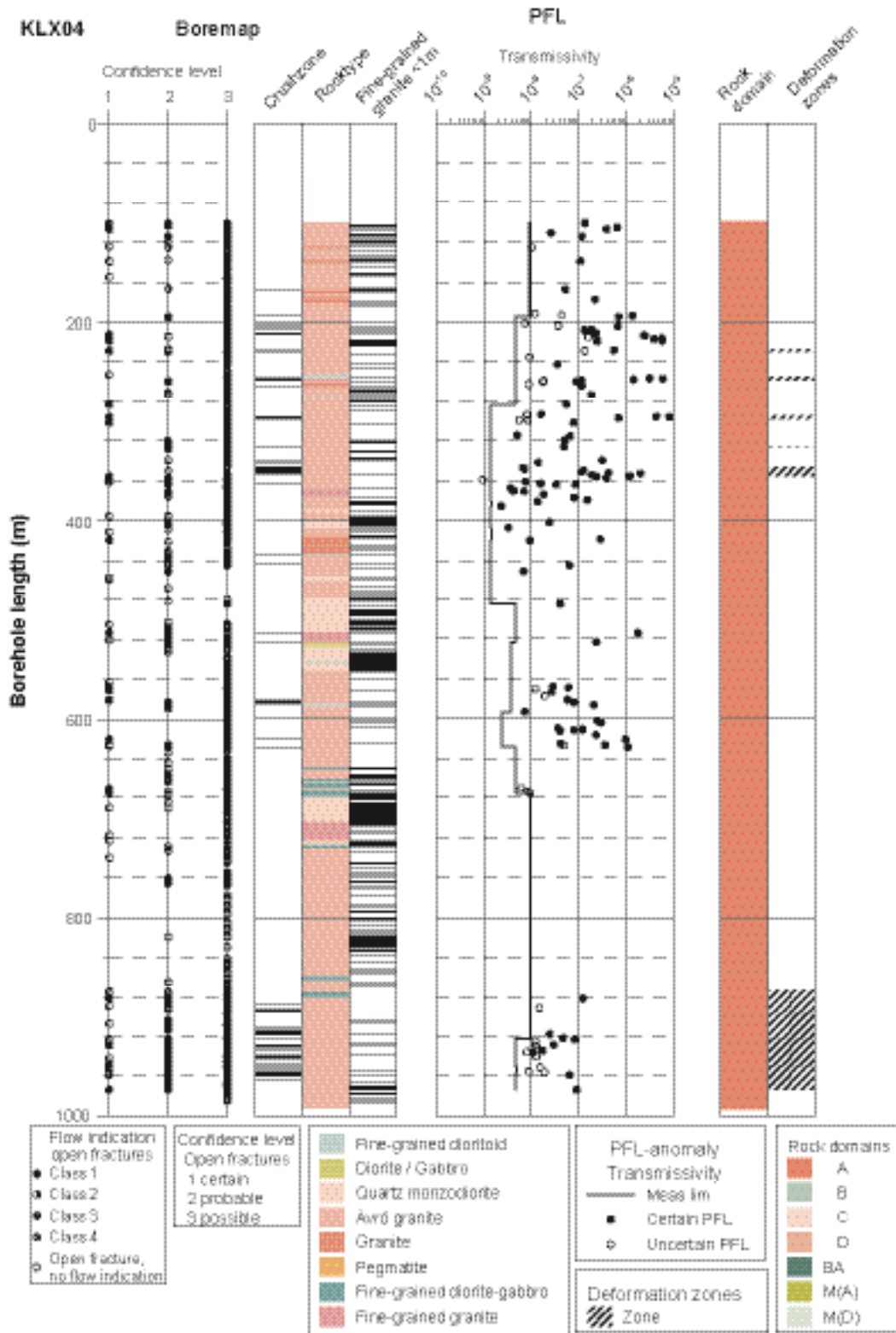


Figure A7-3. Transmissivity of hydraulic features of borehole KLX04 based on PFL-f data, Boremap data (open fractures, partly open fractures and crush zones, rock type and veins of fine-grained granite) and the interpreted geological rock domains and deformation zones /Forssman et al. 2005b/.

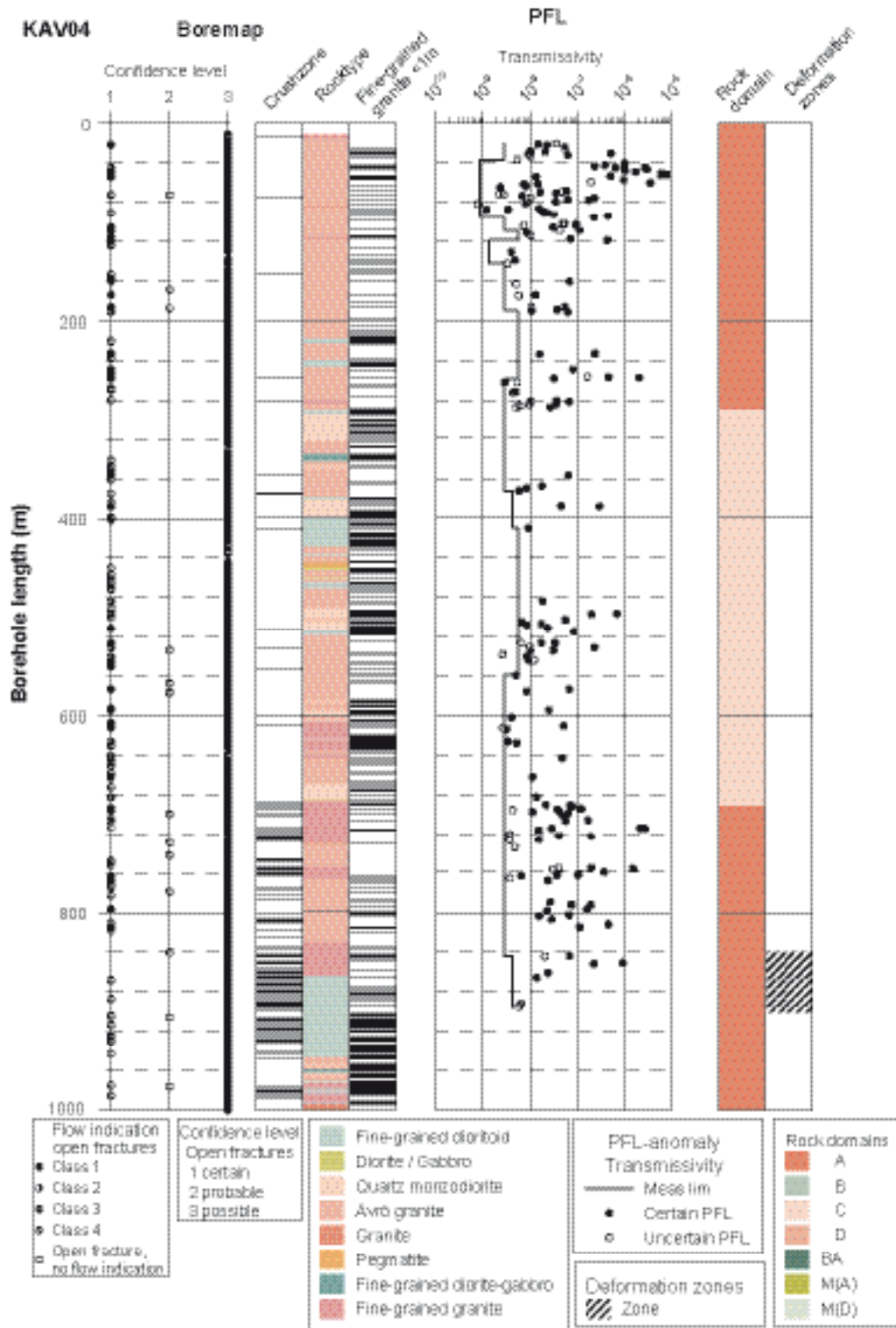


Figure A7-4. Transmissivity of hydraulic features of borehole KAV04(A+B) based on PFL-f data, Boremap data (open fractures, partly open fractures and crush zones, rock type and veins of fine-grained granite) and the interpreted geological rock domains and deformation zones /Forssman et al. 2005b/.

Concepts for assignment of hydraulic properties to the hydraulic rock domains (HRD)

The hydraulic rock (domains) between the deterministically modelled deformations zones are modelled as fracture networks, cf. Chapter 8. The statistical fracture models are defined in Chapter 5 (geological DFN) and those models are the basis for constructing fracture network models of conductive fractures and features (hydraulic DFN). The basic concepts for the construction of hydraulic DFN models are outlined below.

1. Potential conductive fractures: Open and partly open fractures

All naturally open and partially open fractures seen in a cored borehole are considered potential candidates for flow. Sealed fractures, on the other hand, are considered impervious. The site characterisation of open and partially open fractures allows for three levels of geological confidence – “Certain”, “Probable” and “Possible”. All naturally open and partially open fractures or a subset based on “Certain” and “Probable”, have been used as alternative base for analysis.

2. Conductive features: Deformation zones and conductive fractures

Potentially flowing minor deformation zones are simulated as stochastic single planar features, see Figure A8-1. This means that the fracturing within a given deformation zone is not studied in terms of its components, but treated as a single object. Both minor (stochastic) and interpreted deterministic deformation zones are treated in the same way.

If N_{TOT} is the total number of potentially flowing fractures in a borehole and N_{DZ} is the number of potentially flowing fractures in an intercepted deformation zone, the remaining number of potentially flowing fractures in the borehole (“the geological fracture intensity” N_{CAL}) to be matched in the modelling process may be written as,

$$N_{CAL} = N_{TOT} - \sum_{DZ} (N_{DZ} - 1) \quad \text{(Equation A8-1)}$$

In Equation (A8-1) the factor 1 is subtracted from the number of fractures in a deformation zone, as the zone it self is one feature to be included in the modelling process. The transmissivity of a potentially flowing stochastic deformation zone is considered equal to its geological thickness-hydraulic conductivity product and the storativity is equal to its geological thickness-specific storativity product. This implies that the transmissivity of a deformation zone, as determined by its intersection with a borehole, is equal to the sum of the transmissivities of the flowing fractures,

$$T_{DZ} = \sum_f (T_f) \quad \text{(Equation A8-2)}$$



Figure A8-1. Potentially flowing stochastic deformation zones consisting of fracture swarms (clusters) are simulated as single planar features and are considered homogeneous with regards to their hydraulic properties /Follin et al. 2006/.

3. Conductive fractures are assumed planar and homogenous

Potentially flowing single fractures between deterministically modelled deformation zones are simulated as stochastic planar features and are considered homogeneous with regards to their hydraulic properties, i.e. transmissivity T_f , storativity S_f . In case of heterogeneous fracture properties, equivalent homogeneous (effective) values are considered. However, large deformation zones may be modelled heterogenous, but then equivalent properties for subdomains within the deformation zone at a scale c. 10–100 m are employed. The fracture in-plane heterogeneity cannot be modelled at regional and site scale due to the computational efforts required. It can also be pointed out that there is limited data on fracture aperture and it cannot be obtained in practice in field investigations. Even if one has a conceptual understanding, approximations are needed in case the heterogeneity in any scale is to be included in the modelling.

In reality, the flow is through channels distributed across the fracture plane. Possibly, also intersections between fractures (fracture intersection zones, FIZ) can be considered as potential channels, see e.g. /Poteri et al. 2002/. The physical channels are formed by the undulating, sometimes mutually displaced, fracture surfaces (spatial distribution of the fracture asperity) that do not exactly match, thus creating channels. The distribution of flow channels is, however, also governed by the acting boundary conditions. The flow channels in the fracture plane occupy only a minor part of the fracture volume, and parts of the fracture surface is not accessible for flow due to the undulating fracture surfaces may isolate parts of the fracture from one another. Exchange of solutes to stagnant pools of water, outside the flow channels, is by diffusion, which is faster than the diffusional exchange between the flowing water and the rock matrix. It can also be expected that parts of the fracture are filled with fault gouge material, i.e. fine-grained, clayey material. All these characteristics cannot, and need not always, be modelled in detail, but must be approximated in some way. Details on how these processes are treated in ConnectFlow and DarcyTools can be found in /Hartley et al. 2006/.

4. Conductive fractures – a subset of all fractures mapped as open or partly open

It is assumed that the conductive and connected fracture network may be characterised as a subset of all open and partly open fractures. Fractures mapped as sealed are not considered.

5. Distribution of size of conductive features

The sizes (L) of the potentially flowing fractures are assumed to follow a power law (base case, see Figure A8-2), or lognormally distributed.

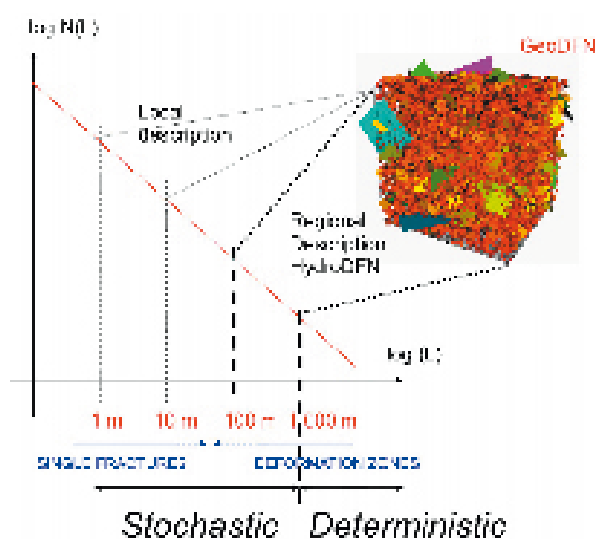


Figure A8-2. The frequencies of occurrence of single fractures and deformation zones are assumed to be power law distributed. The distinction between single fractures and deformation zones is here semantic since the deformation zones are treated as singular objects (cf. Item 1 above) /Follin et al. 2006/.

Fracture shapes are modelled as squares with side length L . This is what is meant by “size” in this context. (Assuming circular shape the corresponding radius r is

$$r = \sqrt{L^2 / \pi} \quad \text{(Equation A8-3)}$$

When describing the intensity of a fracture set in terms of P_{10} (fractures/length along a scan line/or borehole), $(1/m)$, P_{21} (trace length/area, (m/m^2)) or P_{32} (fracture surface area/volume, (m^2/m^3)), it is always important to describe the size interval considered, as inclusion of the small sizes tends to affect the fracture intensity parameters.

6. Minimum fracture size

The assignment of a minimum size of open fractures is a difficult issue. Observations of fracture traces on outcrops down to 0.5 m can be made and shorter lengths can be observed, but it is clear that it is difficult to map these fractures in a comprehensive way. Probably, one cannot observe all small fractures in outcrop but, if present, they can be seen in a borehole core. Therefore, one should test different assumptions and see what implications they may have. This has an effect on the length distributions that are estimated in the DFN analysis. Two assumptions have been tested:

1. The number of potentially flowing fractures seen in a cored borehole (the geological fracture intensity) is assumed to be dependent on the borehole diameter, which is 0.076 m.
2. Due to practical reasons, generally the lower trace length threshold on outcrops is around 0.5 m. Smaller fractures can be observed, but they are difficult to map. One assumption is that the minimum size corresponds to about 0.5 m. Trace length on outcrops depends on several geometrical parameters that describes the spatial distribution of fractures. However, assuming Poisson distributed fractures in space, circular shape with radius r generates mean trace length $= r \times \pi/2$ for fractures with radius r . (That is, a trace length of 0.5 m should approximately correspond to a fracture with a radius $r_0=0.32$ m.)

/Darcel et al. 2004/ made an alternative DFN model based on the initial site investigations at Simpevarp. They found that the (mean global model) radius $r_0 \leq 0.1$ m. This supports assumption 1 above.

/Follin et al. 2006/ examined the sensitivity of the hydrological DFN model to the minimum fracture size by treating two quite different geometrical models (A and B):

$$A. k_r = 2.90 \text{ and } r_0 = 0.282 \text{ m} \qquad B. k_r = 2.56 \text{ and } r_0 = 0.038 \text{ m}$$

The key parameters of a power-law size population providing the number of fractures of different sizes are the shape parameter k_r and the location parameter r_0 , where $k_r > 2$ and $r_0 > 0$ m /Follin et al. 2006/, i.e.

$$f(r) = \frac{k_r r_0^k}{r^{k+1}} \text{ , } r_0 \leq r < \infty \quad \text{(Equation A8-4)}$$

The details behind these settings are discussed in /Follin et al. 2006/. In brief, parameter combination A resembles the geological DFN settings reported by /Hermanson et al. 2005/. However, the parameter combination A does not match the intensity of large lineaments greater than 1,000 m observed within the local model domain. For this reason, /Follin et al. 2006/ also tested parameter combination B, which renders a greater number of large features and a sparser (less connected) network than parameter combination A. /Follin et al. 2006/ concluded, that both parameter combinations render hydraulic DFN models that compare well with the 5 m test section transmissivities determined by the PSS method (double packer injection tests). /Follin et al. 2006/ noted that a plausible explanation for this result is the high fracture intensity observed in the borehole used in the analysis (KLX04) in combination with the assumption of correlated transmissivity-size model, cf. item 8 below.

The major difference between the two parameter combinations, according to /Follin et al. 2006/ is in the lower end of the size distribution where the number of connected fractures differs depending on the assumed values of k_r and r_0 . The contribution of flow from small fractures is difficult to appreciate hydraulically, however, because of the magnitude of lower measurement limit of the PFL-f method, which is c. $(1-2) \times 10^{-9} \text{ m}^2/\text{s}$.

In conclusion, if the magnitude of the lower measurement limit of the PFL-f method is sufficient, e.g. from a Safety Assessment point of view, the spacing of the PFL-f anomalies is already a good indicator of the hydrogeological DFN connectivity. If the magnitude of the lower measurement limit of the PFL-f method is too high, however, e.g. an order of magnitude or so, the spacing between the hydrogeologically connected fractures is smaller than the spacing between the PFL-f anomalies, which means that the connectivity of important features increases. In such case the spacing between the features of interest is probably better represented by $P_{10,CON}^{-1}$, which is the mean spacing of the connected Open and Partly open fractures, see point 9 below. However, $P_{10,CON}^{-1}$ depends on the values of r_0 , hence an uncertain model parameter.

7. Spatial distribution of fractures and deformation zones: Poisson distribution

The spatial pattern of potentially flowing fractures and minor deformation zones modelled as stochastic entities in the rock mass between the deterministically modelled deformation zones is assumed to be Poissonian.. However, the resulting connected conductive feature network may be non-Poissonian, due to the fact that groups of non-connected fractures (but “potentially flowing” in terms of that they are part of all “open or partly open” fractures) are excluded.

8. Transmissivity distribution models

Several models for the fracture transmissivity have been considered, see Figure A8-3 and below:

- 1. The fracture transmissivity T is assumed to be uncorrelated to the fracture size L, with a log-normal distribution of T. ($N(0,1)$ represents a stochastic standard normal distribution.)

$$T_f = 10^{[\mu + \sigma N(0,1)]} \tag{Equation A8-5}$$

- 2. The fracture transmissivity Tf is assumed to be positively and fully correlated to the fracture size L.

$$T_f = a L^b \tag{Equation A8-6}$$

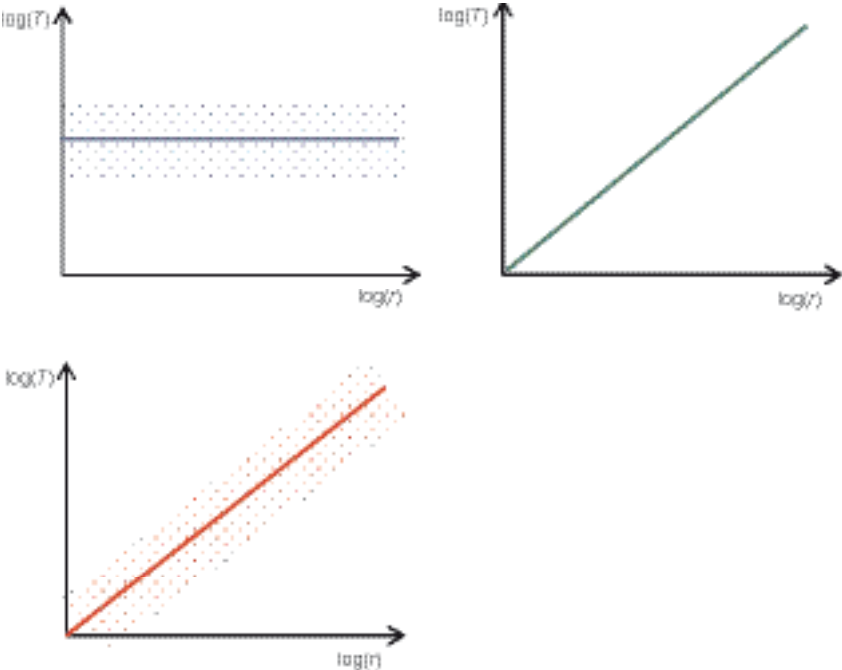


Figure A8-3. Schematic of transmissivity models: 1) Uncorrelated, 2) Correlated, and 3) Semi-correlated /Hartley et al. 2006/.

3. The fracture transmissivity T_f is assumed to be positively correlated to the fracture size L , with a superimposed random log-normal spread.

$$T_f = 10^{\lceil \log_{10}(aL^b) + \sigma N(0.1) \rceil} \quad \text{(Equation A8-7)}$$

where:

μ : Mean of $\log_{10}(T_f)$ distribution.

σ : Standard deviation of $\log_{10}(T_f)$ distribution.

a, b : Factor and exponent describing the power-law relation between transmissivity T_f and size L .

$N(0.1)$: Standard normal distribution.

The last two assumptions imply that the fracture transmissivities are power-law distributed, provided that the length distribution is a power-law distribution. In addition, it can be assumed that the geologically inferred size distribution can be used to estimate the transmissivity distribution and that the measured transmissivities interpreted are free of boundary effects.

9. Transmissivity range of hydraulic features versus observations

Only the most transmissive of the potentially flowing open and partially open fractures are assumed to be detected by the Posiva Flow Log (PFL-f) due to the measurement limit. Figure A8-4 illustrates schematically that the number of flowing fractures in a core-drilled borehole detected by the Posiva Flow Log, N_{PFL} , is regarded as a subset of the geometrically interconnected Open fractures, N_{CON} , which in turn is a subset of N_{CAL} , i.e.

$$N_{PFL} < N_{CON} < N_{CAL} \quad \text{(Equation A8-8)}$$

As pointed out in Section 8.2 the magnitude of the lower measurement limit of the PFL is sensitive to various disturbances such as drilling debris or dissolved gases in the borehole fluid. The PSS has a somewhat lower measurement threshold than the PFL and is also less sensitive to disturbances.

Another concern related to the PFL is that large flow anomalies are occasionally not detected. This problem can occur if the flow anomalies coincide with “cavities” in the borehole, creating by-pass over the PFL packer. This type of problem is less frequent with the PSS. In conclusion, the two methods should be run in parallel as they provide significantly different and partly complementary approaches.

Sums of T_f values (ΣT_f), for the generated model, over the same test section length as the PSS data are used when comparing model to measured PSS data. Again, one must expect that the model can produce test sections with transmissivities below the measurement limit.

More details of the assumptions made for the HydroDFN modelling can be found in /Hartley et al. 2006/ and /Follin et al. 2006/.

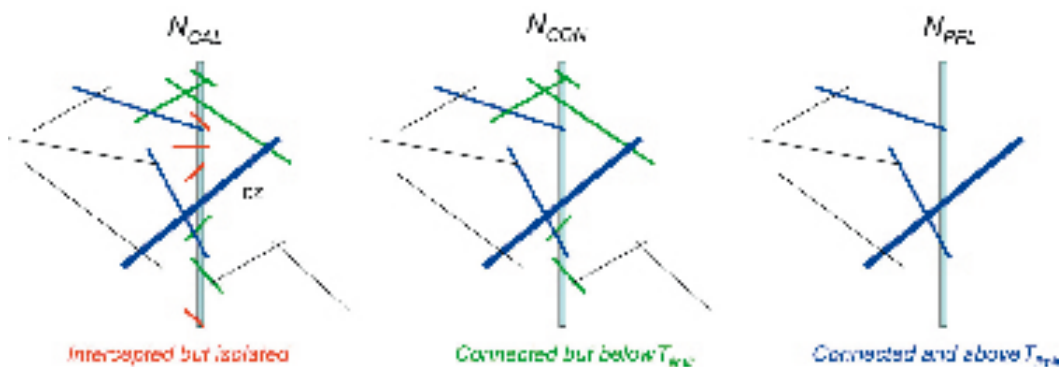


Figure A8-4. The definition of N_{CAL} , N_{CON} and N_{PFL} of Open fractures. T_{limit} denotes the lower measurement limit for transmissivity, which is typically $1 \times 10^{-9} \text{ m}^2/\text{s}$ for the Posiva Flow Log (PFL-f). /Follin et al. 2006/

Overall confidence assessment

Table A9-1. Protocol for use of available data and potential biases in the bedrock description.

Question	Geology	Rock Mechanics	Thermal	Hydrogeology	Hydrogeochemistry	Transport
Which data have been used for the current model version (refer to tables in Chapter 2 of the report).	<p>See Table 2-1.</p> <p>Preliminary mapping of the cored boreholes KLX05 and KLX06 have been utilized in the rock domain modelling. Note, also previous models of Äspö, Ävrö and Laxemar as well as earlier model versions of Simpevarp have been used as input for the modelling of deformation zones.</p> <p>The DFN-model is divided into two subareas; Simpevarp and Laxemar. Specifically data from the following sources have been utilised:</p> <p>Laxemar subarea DFN: ASM000208 (outcrop) ASM000209 (outcrop) Borehole data (KLX03,04 HLX25,26,27,15) Simpevarp subarea DFN; ASM000025, 026, 205, 206 (outcrops) KSH01A, KSH02A, KSH03, KAV01, KAV04 Surface based geophysics bathymetry data See further Table 2-1.</p>	<p>See Table 2-2.</p> <p><i>Non-primary data from the geological modelling:</i></p> <ul style="list-style-type: none"> – DFN-model – Deformation zone model – Lithological model – Geological single hole interpretation. 	See Table 2-3.	<p>Listed in Table 2-4.</p> <p>Hydraulic tests in all boreholes, but especially KLX03, KLX04, KSH01A, KSH02 and KAV04 important.</p> <p>Much of the old data used (boreholes from the surface, Äspö, Ävrö, Mjälén, Hälö, Laxemar and Kråkemåla).</p>	<p>Listed in Table 2-5.</p> <p>Based on Simpevarp 1.2 data complemented with water samples from KLX03, 04, 06. HLX 10, 14, 18, 20, 22, 24. KAV01, KAV04A, HAV09, HAV10, 11, 12, 13, 14. HSH02, 03,04, 05. (Pecussion drilled holes 0–200 m). Porewater data from KLX03. Also surface water data: Baltic sea, Lakes, streams and shallow soil pipes (about 0–5 m deep).</p>	<p>Listed in Table 2-6</p> <p>Data from Transport programme: Most data originate from Simpevarp subarea, with some additions, as listed below. These data are of a preliminary nature.</p> <ol style="list-style-type: none"> 1. Resistivity lab KLX02, KLX04 ?? + Simpevarp data to fill gaps. 2. In situ formation factor KLX02, KLX04 + Simpevarp subarea data to fill gaps. 3. BET-area, crushed material KLX02, KLX04 + Simpevarp subarea data to fill gaps. 4. Through diffusion KLX02, KLX04 + Simpevarp subarea data to fill gaps. <p>Data from other disciplines</p> <p>Porosity (matrix) (geology/mechanics?)</p> <p>Lithological data (geology)</p> <p>Mineralogical data (geology)</p> <p>Water chemical composition (groundwater chemistry)</p> <p>Fracture orientation (geology)</p> <p>Fracture transmissivity (hydrogeology)</p> <p>Fracture frequency (bore hole log, geology)</p> <p>Frequency of hydraulically conductive features from PFL data.</p> <p>Sorption, diffusivity and porosity from Simpevarp subarea investigations.</p>

Question	Geology	Rock Mechanics	Thermal	Hydrogeology	Hydrogeochemistry	Transport
If available data have not been used –what is the reason for their omission (e.g. not relevant, poor quality, lack of time, ...)	<p>A) Rock domain modelling: Boremap mapping of available percussion boreholes have not been fully evaluated because 1) lack of drill core and thereby a more uncertain identification of rock types and 2) limited borehole length.</p> <p>B) Rock type properties: Modal and geochemical analyses from KLX01 and KLX02 that are generated prior to site investigation have not been used due to old rock nomenclature in Sicada. Not full use of Äspö HRL data for the geological models due to variable quality.</p> <p>C) DZ model makes use of a few KAS boreholes and a variety of Äspö HRL data</p> <p>D) For DFN-model: Only verification of DFN-model using KBH02.</p> <p>Note that there are potentially interesting data for “verification of DFN-model – like mapping of shafts, TBM tunnel etc. These have not been used in Laxemar 1.2.</p>	<p>A) Percussion drill hole data have not been used. Reasons: – The empirical approach is built up around drill core interpretation. – The theoretical approach builds directly on the DFN-model for fracture sets, sizes and intensity. – The percussion holes give information only from shallow depths.</p> <p>B) Old drill core raw data. Reasons: – The quality and format is different from current – The vast amount of data from Äspö HRL could not have been analysed within the time frame. – Some Äspö data has already been used during the development of the methodology (See R-02-04).</p>	<p>Old modal analyses from surface samples excluded due to different rock classification.</p> <p>Modal analyses in the thermal program from KAV01, KSH01A KSH02 excluded because the results were judged uncertain/less reliable. These samples have been reanalyzed. Some of this data were not delivered to Sicada in time for the data freeze, and have therefore not been used.</p> <p>Seven modal analyses of surface samples collected outside the local model boundary were excluded.</p> <p>Temperature loggings have not been fully used for modeling of thermal conductivity. This is because of poor quality data and lack of historical temperature data.</p>	<p>Old data from Äspö, Hälö, Ävrö, Mjälén have been used for the surface based boreholes.</p> <p>Äspö HRL holes drilled from tunnel have been only used for assessing properties of deformation zones due to lack of time. But there is potential for more use of the Äspö HRL data.</p> <p>Clab data not used at all! Some of the available data are likely relevant to the Simpevarp subarea, but were not assessed in time.</p>	<p>Äspö HRL data not used, (partly due to some of the current data being disturbed by the HRL).</p> <p>Old Äspö HRL-data are part of the overall Nordic database, used as a basis for conceptual modelling and comparisons.</p> <p>Many observations judged to be unrepresentative have been excluded from the detailed modelling.</p>	<p>Some Äspö data excluded already in SDM Simpevarp 1.2 due to methodological differences from established site investigation methods and/or incomplete supporting geological or hydrochemical information.</p>

Question	Geology	Rock Mechanics	Thermal	Hydrogeology	Hydrogeochemistry	Transport
(If applicable) What would have been the impact of considering the non-used data?	<p>A) Considered to have no impact. Only confirming information from the cored boreholes.</p> <p>B) Considered to have no impact. Only confirming the utilized analyses from the site investigation.</p> <p>C–D) Better understanding of Äspö in relation to Simpevarp/Laxemar subareas.</p> <p>D) One of the few possibilities of “verifying” the size distribution of the subhorizontal set and to minimise introduced orientation bias from the subvertical boreholes and subhorizontal outcrops.</p>	<p>A) The description of spatial variation in fracture intensity and description of occurrence, thickness and crude characterisation of fracture zones may have resulted in a more detailed description of the near-surface rock mass.</p> <p>B) More certain description of the rock mass and the deformation zones in the area around the Äspö HRL.</p>	<p>Old modal analyses: Larger material for calculation of thermal rock type models (more accurate models).</p> <p>Modal analyses in thermal program: More samples to enable calibration with TPS measurements.</p> <p>Surface samples outside local model boundary: All except one are of Ävrö granite. No improvement achieved by using this data.</p> <p>Temperature loggings: Possibly better understanding of variations in thermal conductivity.</p>	<p>The neglect of Clab data has minor impact since they cover a small area and a depth down to about 50 m below surface. However, the data may contribute to the understanding of near-surface conditions, in at least rock domain B (i.e. outside the Laxemar subarea).</p> <p>The description of Äspö (i.e. outside the Laxemar subarea) could have been better based also on Äspö HRL data.</p> <p>The hydraulic DFN model could have been tested more thoroughly. Alternatives for possible anisotropic conditions, similar to what has been seen in Äspö HRL could have been tested. The integrated hydrogeological and geologic interpretation of the model could have benefited. (Verification and parameterisation of deformation zones).</p>	<p>Omission of Äspö data is judged to have limited impact on the overall modelling of the Laxemar area.</p> <p>All data could be used for an overall qualitative assessment of distribution of water types etc.</p> <p>When possible, the non-representative data have been used for checking the impact on the visualisation and the overall understanding of the site. The results indicate that locally the difference can be $\pm 50\%$, at site scale in the order $\pm 10\%$.</p>	<p>Some of the Äspö HRL data (from TRUE Block Scale) are of high quality. However, unclear whether Äspö HRL data are representative for the Laxemar subarea. (There are differences in the importance of altered/unaltered parts of the rock matrix). It would be of interest for the process understanding to compare the TRUE-data with the data from the Laxemar subarea and to assess the reasons for the different impacts of alteration.</p> <p>Other omitted data too uncertain to be of real value.</p>

Question	Geology	Rock Mechanics	Thermal	Hydrogeology	Hydrogeochemistry	Transport
How is data accuracy established (e.g. using QA procedures) for the different data? (Essentially just refer to tables in Chapter 2).	<p>Data from Sicada qualified in accordance with method descriptions. See Table 2-1 and referenced P-reports.</p> <p>Modellers have had contact with, for example, the Boremap mapping team and have also made their own inspection of the drill core. Furthermore, the modellers have been involved in the sampling both at the surface and of the drill core and also in the geological single-hole interpretation.</p> <p>The modelling team has performed a qualitative check of modal analyses by comparison with corresponding geochemical analyses.</p> <p>The modelling team has also performed several quality checks of fracture data from BOREMAP and from the outcrops.</p>	<p>Data from Sicada qualified in accordance with method descriptions. In addition the following tests have been made:</p> <p>Boremap data: QA according to methodology document. Used as is, but simple checks – like “double values for same depth” are found and corrected for.</p> <p>Shear tests and normal loading tests: Detailed analysis of every single test result. Improvement of test procedure and interpretation has been performed.</p> <p>Uniaxial and triaxial tests: QA according to methodology document</p> <p>Tilt tests: Used as is.</p> <p>– P-wave: Used as is.</p> <p>Stress measurements: Inherent uncertainty in different measurement techniques applied are discussed and considered (by judgement) in the modelling.</p>	<p>For details about data collection and accuracy refer to the individual P-reports.</p> <p>In addition to the quality assurance mentioned in P-reports, the thermal modelling team made their own reasonableness check while working with data. For example, modal analyses have been compared with TPS measurements to evaluate their validity.</p>	<p>The interpretation of new hydraulic tests presented in the data reports listed in Chapter 2 follows standard QA procedures (Method descriptions).</p> <p>Data are also checked when stored in Sicada and when used in the modelling. The hydraulic tests focus mainly on the transmissivity.</p> <p>Old data (Äspö HRL and Ävrö), are generally of good quality but some tests are of less good quality due to different methodology employed.</p> <p>Data from old investigations on Simpevarp are judged to be of lower quality than the PLU investigations and Äspö investigations – more “standard engineering investigations”.</p>	<p>Surface water data: QA established. Measurement errors in the order of (± 5–10% in analyses), see Chapter 4.</p> <p>GW data: QA established, see Chapter 3 in Chemical Background Modelling report /SKB 2006a/. Measurement errors in the chemical analysis of the gw-samples in order of (± 5–10%), see Section 9.2.</p> <p>To what extent a given sample actually represents the groundwater where it was sampled is assessed by a complete chemical analysis, checking contamination of drilling fluids and assessing stability in time series, see Chemical modelling report /SKB 2006a/ and Section 9.2.</p>	<p>Data: QA according to Method Descriptions.</p> <p>QA of data from other disciplines as described in Chapter 2 and references cited therein. (However, to a large extent the input from other disciplines are from models rather than direct data – as will be discussed in the uncertainty Table A9-5 below).</p> <p>Accuracy in other data established by evaluation of the raw data according to the Method descriptions.</p>

Question	Geology	Rock Mechanics	Thermal	Hydrogeology	Hydrogeochemistry	Transport
List data (types) where accuracy precision is judged low – and answer whether inaccuracy is quantified (with reference to applicable sections of this report or supporting documents).	<p>The identification of rock type and fracture filling in percussion boreholes are considered to be of significantly lower quality than corresponding data from the cored boreholes. Furthermore, the identification of fractures in the percussion boreholes is solely based on BIPS images, and accordingly the fracture intensity in these boreholes is judged to be too low. These inaccuracies have not been quantified but point to the difference in the data quality from the percussion boreholes compared to cored boreholes.</p> <p>Some inaccuracies in the coding of the Boremap data presumably exist, e.g. coding of some rock types. Not possible to quantify inaccuracy. These potential minor mistakes are judged to be of subordinate importance and have no effect on the modelling work.</p> <p>Errors in the deviation measurements of the cored boreholes are quantified.</p> <p>Orientation of radar reflectors in the cored boreholes are judged to be of low accuracy. The accuracy is not quantified.</p> <p>There are judgements made, i.e. no real data, in connection with the interpretation work to produce co-ordinated and linked lineaments. This has a fundamental effect on the lineament length and therefore also on the length of deformation zones. Not possible to quantify – personal judgement. Addressed by traceable, quantitative stepwise interpretation from indirect surface maps of topography and geophysics to final lineament map and by utilising different lineament interpretation groups.</p>	<p>Normal stiffness – A new experimental set up has been used. Methodology report updated. Accuracy of experimental setup and methodology not quantified, but by comparing results from different methods it is judged that currently achieved accuracy is acceptable.</p> <p>Shear stiffness – New setup used. Methodology report updated. Accuracy of experimental setup and methodology not quantified but by comparing results from different methods it is judged that currently achieved accuracy is acceptable.</p> <p>Large scatter in results from tilt test – laboratory shear tests are given more weight in the modelling.</p> <p>Maximum (horizontal) principal stress from hydraulic (HF or HTPF) measurement methods. – Not quantified- although other stress measurements (OC) provide estimates of these stresses. (See Section 6.4).</p>	<p>Modal analyses where the extent of alterations in minerals have not been fully evaluated. These inaccuracies have meant that direct measurements of thermal properties are favoured instead of calculation from the mineral content.</p> <p>Temperature loggings from different boreholes show a variation in temperature at canister level. The difference is not large but even small differences influence the repository design. The explanation is primarily errors in the temperature logging, timing of the logging, water movements in the boreholes, and the inclination measurements of borehole inclinations.</p>	<p>Results from WL-tests or airlift-pumping generally have less accuracy than other hydraulic tests but are still useful if no other tests are available. In most cases these data are not used in the modelling as injection tests in 100 m scale have been available.</p> <p>Some old data from the Simpevarp peninsula made for engineering purposes are judged to be of low quality. These data have so far not been used in the modelling.</p> <p>No quantification of inaccuracy available at present.</p>	<p>With few exceptions there are very few examples of poor accuracy in the representative data set.</p> <p>Major components, stable isotopes ($\pm 5-10\%$). The effect of these errors on the interpretation is checked by the explorative analyses, outlined in Chapter 9.</p>	<p>General uncertainties included in the evaluation concept for sorption coefficients and diffusivities are addressed and discussed in the supporting report /Byegård et al. 2005/.</p> <p>Accuracy of in situ resistivity measurement depends on assumed water composition of the pore liquid. This composition is uncertain.</p> <p>Low accuracy/precision in correlation between through diffusion experiment results and data from resistivity measurements.</p> <p>Issues related to upscaling from small sample sizes used in lab measurements to REV scale. This may be important for assigning physically meaningful distributions of uncertainty for sorption and diffusion parameters.</p>

Question	Geology	Rock Mechanics	Thermal	Hydrogeology	Hydrogeochemistry	Transport
	<p>Process of linking lineaments is uncertain – especially since real deformation zones (DZ) often consist of “non”-continuous parts (i.e. EW007). This means that detailed data (like dip, size) from an individual segment may have little relevance for the entire structure. This is considered in the subsequent uncertainty assessment of DZ properties, but this scale issue implies severe communication difficulties – there is a need to make a more realistic description of a zone in different scales.</p> <p>DFN model does not use the lineaments but instead a 2D section of deformation zones from Simpevarp 1.2 DZ model. Uncertainty of zone size in the DZ model for high confidence zones given in DZ property tables. Trace lengths have impact on DFN, but precision is low. This uncertainty is currently not propagated into the DFN analysis in Laxemar 1.2.</p> <p>No or very limited data on size of subH fractures. Uncertainty addressed as different size models for each set. May be improved by verification exercises using tunnel data from Äspö.</p> <p>Orientation of fractures in core mapping usually has high accuracy, but there is a limited subset where the orientation is more uncertain.</p> <p>Identification of DZ in single hole interpretation. It is judged that the zones identified in the Single Hole interpretations are indeed zones. However, there are probably additional DZ that could be “distilled” from the rock mass fracturing and thus assess the understanding of the clustering, but there are also fracturing in the rock mass which are not connected to DZ. These limitations in the Single Hole interpretation are considered in evaluating the uncertainty in the DFN-model.</p>					

Question	Geology	Rock Mechanics	Thermal	Hydrogeology	Hydrogeochemistry	Transport
	<p>Orientation of Deformation Zones in single-hole interpretation not given, but directions of fractures in these zones have high accuracy – improved since Simpevarp 1.2</p> <p>Interpretation of open/sealed fractures in boreholes has quite high accuracy as combined BIPS and core mapping have been utilized. It is a relatively small part of all fractures (10–20% of the sealed fractures could be potentially open), but open/sealed interpretation on outcrops is of poor accuracy.</p> <p>Interpretation and combination of borehole and outcrop fracture data are uncertain since different mapping techniques have different resolutions (cut-off).</p>					

Question	Geology	Rock Mechanics	Thermal	Hydrogeology	Hydrogeochemistry	Transport
If biased data are being produced, can these be corrected for the bias?	<p>A) No bias in data coverage (surface and boreholes) is considered to exist for the local scale rock domain.</p> <p>B) Few data from areas covered by the sea and, thus, the location and extension of the sedimentary cover rocks in the sea area is uncertain. However, the sedimentary rocks do not extend west of the deformation zone ZSMNE024A.</p> <p>C) The bedrock information in the regional model area on land is only of reconnaissance character. This will not be corrected for during the CSI.</p> <p>Reflection seismic data from the surface focus on gently dipping structures. VSP data from KLX02 have been utilised for corrections.</p> <p>Fracture intensity in cored boreholes overemphasizes sub-horizontal fracturing – can be corrected, but subH size comes from outcrop and implies great uncertainties.</p> <p>NW and SE corners in regional model have lower resolution in the surface based geophysics (these are also corners of less concern in the model).</p> <p>Note, the new bathymetry data increase the detail along the coast line – i.e. the previous bias noted in e.g. Simpevarp 1.2 is not as much any concern any more.</p> <p>There is a bias introduced by the data gap between lineaments (lower cutoff > 500 m) and outcrop fracture mapping (window < 30 m).</p> <p>Steeply inclined boreholes predominate and, therefore, overemphasizes orientation bias of subhorizontal fractures.</p>	<p>Potential directional bias as essentially only sub-vertical boreholes are used.</p> <p>Spatial coverage in the Laxemar subarea is scarce. However, the lithological model indicates homogeneity within the sampled rock domain (Domain A).</p> <p>Geographical bias (lack of representativity) while the data used for describing quartz monzodiorite in the Laxemar subarea are imported from boreholes in the Simpevarp subarea.</p>	<p>Generally poor representativity in TPS data due to possible biased sample selection. This applies also to modal analyses data for subordinate rock types. Sample selection (TPS) has not been fully randomized. Samples (TPS) were taken rather to characterise the rock type – not to find varieties. See Chapter 7 for in depth discussion of these problems.</p> <p>Poor representativity of samples measured with TPS in subarea Laxemar has been reduced by including data from Simpevarp and Äspö HRL. On the other hand, a bias may have been introduced by using data from outside the Laxemar subarea (given number of data in subarea Laxemar is limited).</p> <p>Bias resulting from using modal data in the SCA method: SCA data is judged to be more uncertain than direct measurements (when available). SCA data has been compared with TPS data and where possible, a correction of SCA data has been made. (Does not apply to Ävrö granite for which TPS data only has been used)</p> <p>Bias may be present in thermal conductivity values calculated from density logging. More data required to quantify bias. With more data the density – thermal conductivity relationship can be refined, which should lead to a reduction in bias.</p>	<p>The core holes are more or less sub-vertical and may introduce a window effect in the borehole transmissive feature statistics (similar to problem with fracture statistics – see Geology) due to their vertical orientation. Hence, the structural model of the rock between the fracture zones may be biased. (Importance of anisotropy.) This effect can be addressed by incorporating more boreholes with other orientations.</p> <p>Few data in the near-surface rock system (hardly any data in detailed scale in the first 100 m). Implies uncertainties in describing the connections between the surficial and deeper groundwater flow system.</p> <p>Spatial coverage is judged fair within the Laxemar subarea- but there are very few data in some of the minor Rock Domains, i.e. D, MA, (as well as in the Simpevarp subarea domain B and A). These possible biases could only be corrected by obtaining data from these Rock Domains).</p>	<p>Only few data from depth are part of the representative data set. This means that most of the deep data assessment originates from KLX02. (This bias could only be handled by obtaining more representative data from other locations at depth).</p> <p>Few samples from the low transmissive parts of the fractures and minor zones. Some data from the rock matrix (KLX03). Too few data presently available to assess bias.</p> <p>Potential sources of bias include contamination from drilling fluid. Such biased data have been corrected by using back-calculations, but the representativity may be still be questioned.</p>	<p>Uncertain – depends upon parameter.</p> <p>Difficult to reinterpret primary borehole hydrological data in any detail to perform QA on transmissivity distributions.</p> <p>Transmissivity distributions must be on the resolution of individual water conductors to be reliable for FWS/q distribution estimations. (Also if T-distribution taken from the hydraulic DFN model, all assumptions made on e.g. correlation between size and T, could result in a bias in the transport property assessment).</p> <p>Potential impact from disturbed (stress release) of laboratory samples. This would imply too high diffusivities etc. in the lab. samples compared to in situ. There is possibly some indications of degree of bias by comparing in situ and laboratory formation factor data. This difference can be used to correct the bias, but accuracy in in situ data needs also be considered, see above.</p> <p>Poor coverage of transport property data – only a few rock domains tested, but matrix properties do not vary too much between rock domains (uncertainty in transport is dominated by uncertainty and variability of FWS/q).</p>

Table A9-2. Protocol for use of available data and potential biases in the description of the near surface.

Question	Chemistry in surface systems	Oceanography, hydrology and near surface hydrogeology	Quaternary deposits (Overburden)	Biota
Which data have been used for the current model version (refer to tables in Chapter 2 of the SDM report).	Water Environmental monitoring boreholes SSM – Class 3 + isotopes Surface water sampling – Class 3–5 + biosupplements + sonde measurements Precipitation – Class 3 + isotopes Regolith C/N/P-analyses on soil QD Biota No data	Regional and local oceanographic data Regional and local meteorological data Regional and local discharge data Topography on land and bathymetry of the Baltic sea; Geometric data on catchment areas, lakes and water courses Surface water levels Groundwater levels Hydraulic properties of Quaternary deposits	Detailed map of QD (terrestrial and coastal areas) Soil type (soil classification) Stratigraphical distribution of till and sediments Textural composition of till and sediments Mineral composition of till and sediments Total depth of QD along geophysical profiles	Terrestrial producer model: Vegetation map Vegetation inventory National Forest Inventory Primary production and biomass Key biotopes Dead wood Soil type (soil and site type classification) Leaf area index Terrestrial consumer model: Bird inventory Mammal inventory Inventory of amphibians and reptiles Aquatic producer model: Classification of lake habitats Producer biomass and production Marine and limnic vegetation Aquatic consumer model: Fish sampling Consumer biomass and production Marine fauna
If available data have not been used – what is the reason for their omission (e.g. not relevant, poor quality, lack of time, ...)	Chemical data have not been used for modelling of processes – lack of time	Hydrogeological model for Laxemar 1.2 has not been used in near surface hydrological models, Simpevarp 1.2 used instead – model input not available in time		
(If applicable) What would have been the impact of considering the non-used data?	Better description and understanding of temporal and spatial chemical processes, e.g. transport processes between the rock – surface systems	Integrated models		
How is data accuracy established (e.g. using QA procedures) for the different data? (Essentially just refer to tables in Chapter 2).	Consistency checks of data by e.g. plotting, control of charge balance (± 5 –10%) and comparisons between laboratories and between methods	Consistency checks of data by water balance calculations and comparisons between local and regional data	Consistency checks of different data sets by e.g. comparison of soil map and QD map, comparison of results from different methods (e.g. marine sediments)	Data accuracy evaluated by statistical description, and by comparison with generic values of parameters in each model

Question	Chemistry in surface systems	Oceanography, hydrology and near surface hydrogeology	Quaternary deposits (Overburden)	Biota
List data (types) where accuracy is judged low – and answer whether accuracy is quantified (with reference to applicable sections of this report or supporting documents).	Chemical data from near surface groundwater, QD and biota – no data or low temporal/spatial resolution	Simple discharge measurements – accuracy is not quantified Groundwater levels and hydraulic conductivity data have low spatial resolution and/or short time series – accuracy is not quantified	Low accuracy of QD map outside the River Laxemarån catchment area and outside the local model area Low spatial resolution of data on QD stratigraphy, depth and physical properties No information on artificial filling in the model area	Production of biomass and standing stocks of biomass in the aquatic systems – accuracy is not quantified
If biased data are being used, can these be corrected for the bias?		Meteorology: Precipitation data is corrected for measurement errors by standard procedure – local conditions have not been considered Measurements of hydraulic conductivities are underrepresented in clay, gyttja and peat – generic data are used for these QD types	Mean depth of QD in marine areas is used to predict QD depth in the terrestrial areas where information is lacking	

Table A9-3. Protocol for assessing uncertainty in the bedrock Geology aspects of the SDM.

Aspect of SDM	Uncertainty	Cause (e.g. data inaccuracy, information density, uncertainty in other discipline models or process understanding)	Has uncertainty been assessed considering information from more than one data source or through a calibration or validation exercise?	Impact on other uncertainties (in all disciplines)	Quantification (provide reference to applicable section of the SDM report)	Potential Alternative representation. (Is there reason for this and has one been developed)	Are there unused data which could be used to reduce uncertainty	What new data would potentially help resolve uncertainty? (Are they considered in L2.1 investigation)
Geology – rock domain model	Spatial distribution of Rock Domains in the regional model area.	Only reconnaissance data available – lack of detailed bedrock map.	No, there is only one data source (version 0 bedrock map).	No	Difficult to quantify. Not relevant.	No alternative exists.	No	New and more detailed bedrock map in the regional model area.
	Bedrock relationships in the sea area.	No data – bedrock not exposed.	No, there is no data source (except bedrock map version 0).	No	Difficult (impossible) to quantify.	No alternative exists.	No	New bedrock map needed. Drilling and detailed marine geological survey (possible documentation of sedimentary cover rocks).
	3D geometry of the rock domains, except for the geometrical relationships between RSMA01, RSMD01, RSMM01, RSMP01 and RSMP02 in the local model volume that are considered less uncertain. The uncertainty applies particularly for the regional model volume.	Restricted subsurface information. Pristine igneous bedrock terrain with little structural control (i.e. guidance for modelling).	No, very restricted subsurface information.	3D extent of rock domains and distribution of mechanical and thermal properties that depend on rock domains.	Difficult to quantify.	The available subsurface information does not allow construction of any alternative models for this model version. Subdivision of the Ävrö granite in a quartz-rich and quartz-poor variety is a natural step for upcoming model versions. Rock domain model: A possible future alternative concept for division of rock domains in the Laxemar subarea (within the local scale model volume) could be introduced based primarily on the composition of rock types. This applies primarily to the compositional variation of the Ävrö granite.	No	More subsurface data are needed in the local scale model volume – cored boreholes, detailed geophysical information (modelling). Additional subsurface data from the regional model volume is not motivated bearing in mind the great needs to better understand the bedrock in the local scale model volume.

Aspect of SDM	Uncertainty	Cause (e.g. data inaccuracy, information density, uncertainty in other discipline models or process understanding)	Has uncertainty been assessed considering information from more than one data source or through a calibration or validation exercise?	Impact on other uncertainties (in all disciplines)	Quantification (provide reference to applicable section of the SDM report)	Potential Alternative representation. (Is there reason for this and has one been developed)	Are there unused data which could be used to reduce uncertainty	What new data would potentially help resolve uncertainty? (Are they considered in L2.1 investigation)
	Heterogeneity – Proportion of rock types in domains: veins, patches, dykes, minor bodies, frequency of minor deformation zones. (Statistical anisotropy?)	Restricted information – difficult to estimate both the proportion and spatial distribution. Proportion of subordinate rock types in rock domains in the local scale model volume is considered, i.e. inhomogeneities.	Yes, 1) outcrop database for the Simpevarp and Laxemar subareas, 2) cored boreholes, 3) cleaned outcrops, 4) bedrock map.	Spatial distribution of mechanical, thermal and transport properties that depend on rock types.	Proportions given –uncertainty expressed as ranges in the property table, see Chapter 5. No description of “size” distribution of heterogeneity. (Although indicator variograms from rock types have been assessed in the thermal modelling).	No – is better expressed as uncertainty range.	No, but indicator variograms could be used.	1) Information from new boreholes, 2) detailed investigation of cleaned outcrops concerning the amount, proportion, distribution and character of subordinate rock types.
	Orientation of subordinate rock types, particularly fine- to medium-grained granite and pegmatite.	Restricted information. A great number of the documented fine- to medium-grained granites and pegmatites are not dykes <i>sensu stricto</i> , but display irregular shapes with no or only weak preferred orientation.	No, only based on outcrop database for the Laxemar subarea.	Thermal modelling	Stereograms included in property tables. Uncertainty expressed using the Fisher distribution parameters (mean pole and k-value, i.e. shape parameter).	No	Documentation of the orientation of subordinate rock types in cored boreholes (Boremap data).	

Aspect of SDM	Uncertainty	Cause (e.g. data inaccuracy, information density, uncertainty in other discipline models or process understanding)	Has uncertainty been assessed considering information from more than one data source or through a calibration or validation exercise?	Impact on other uncertainties (in all disciplines)	Quantification (provide reference to applicable section of the SDM report)	Potential Alternative representation. (Is there reason for this and has one been developed)	Are there unused data which could be used to reduce uncertainty	What new data would potentially help resolve uncertainty? (Are they considered in L2.1 investigation)
	Spatial distribution of compositional variations of rock types – for example the Ävrö granite that are “rich” (granite to granodiorite) contra “poor” (quartz monzodiorite) in quartz.	Restricted data at depth– a rough separation is possible to carry out at the surface for the Ävrö granite. However, more or less rapid changes in composition do locally occur, due to mixing and mingling phenomena during formation of the igneous rocks.	Yes, qualitatively from both modal and chemical composition, density data and also gamma-ray spectrometry.	Spatial distribution of thermal domain modelling especially within the Ävrö granite.	Difficult to quantify but is discussed in Chapter 5.	No – is better expressed as uncertainty range.	No	Increased number of modal and chemical analyses and density data both from the surface and cored boreholes.
	3D distribution and characterisation of secondary alteration, e.g. oxidation (red staining), saussuritisation, sericitisation and chloritisation (hydrothermal alteration) in the rock domains between the deformation zones.	Restricted information – difficult to estimate both the proportion, spatial distribution and not the least the degree (“strength”) of alteration.	Yes, documentation in connection with the Boremap mapping of drillcores (used for estimates), and qualitatively treated in connection with the microscope study of thin-sections.	Thermal and transport properties of altered rocks are possibly different compared to unaltered (fresh) rocks. Spatial extent of the altered volumes could be in the order of tens of m. However, the alterations usually imply increased thermal conductivity, i.e. ignoring this results in incorrect estimates (underestimates) of the thermal conductivity.	Quantified as proportions, see Chapter 5.	No – is better expressed as uncertainty range.	No	Very detailed microscopy study of thin-sections both from the surface and from drill cores, including a semi-quantitative estimate of the degree of alteration. The latter should comprise separate estimates for the various kinds of alterations.

Aspect of SDM	Uncertainty	Cause (e.g. data inaccuracy, information density, uncertainty in other discipline models or process understanding)	Has uncertainty been assessed considering information from more than one data source or through a calibration or validation exercise?	Impact on other uncertainties (in all disciplines)	Quantification (provide reference to applicable section of the SDM report)	Potential Alternative representation. (Is there reason for this and has one been developed)	Are there unused data which could be used to reduce uncertainty	What new data would potentially help resolve uncertainty? (Are they considered in L2.1 investigation)
Geology – structural model	Existence of deformation zones (only some interpreted with high confidence) – are all lineaments really deformation zones?	Lack of complete coverage of supporting subsurface data. The number of high confidence zones increases with targeted subsurface investigations.	Targeted drilling campaigns together with geophysical profiles and seismics confirm most of the proposed deformation zones that have been suggested based on surface lineaments. The number of high confidence zones reflects increased confidence. Seismic data appear to support the assertion that there are no regional gently dipping deformation zones. (A few local major gently dipping deformation zones are in the model).	Hydrogeology and rock mechanics are directly affected by this uncertainty. The deformation zone model provides the geometrical framework for the hydrogeological modelling.	Quantification through high, medium, low confidence. The additional high confidence and medium confidence zones are mainly in the local model domain. These additions are mainly in the Laxemar subarea.	Yes, potentially multiple alternatives could be produced. Two alternatives exist; One model containing only high (confirmed) and medium confidence deformation zones and one alternative containing also low confidence deformation zones based only on one source of data on surface lineaments. Size distribution of SubH DZ is uncertain (see below), but it seems clear that there are no regional gently dipping deformation zones in the area, i.e. this would not be a reason to form alternative models.	The underlying basis for the linked lineament map has been revisited by an alternative independent producer. Results will be utilised in L2.1. These investigations can increase knowledge at scales 100 m and up.	BH intercepts part of ongoing PLU. Seismic survey results. Targeted BH campaign increase confidence in selected local major zones around areas of interest. L2.1 data (Detailed Laser map, Detailed magnetic map, Field control in selected 400 m squares). Will increase confidence in existence (and occurrence) of local minor zones. Hard to see any new data that would, further increase confidence in the existence (non-existence) of the gently dipping deformation zones.
	Potentially there are non-included zones (mainly subhorizontal) (e.g. the Nordenskjöld hypothesis, /Nordenskjöld 1944/.	Non-included zones: the Clab-OKG 'hole effect'. SubH Regional zones does not exist within the local model domain Generally lack of large scale abilities to secure data from subH Local major and local minor DZ.	No No	Hydrogeology and rock mechanics are directly affected by this uncertainty. The deformation zone model provides the geometrical framework for the hydrogeological modelling.	No A few subhorizontal DZ have been proposed and included in the geometric framework based on seismics.	A few subhorizontal has been proposed and included in the geometric framework based on seismics, but this may not be necessary to handle in a totally alternative model. (See also previous line)	No	Ongoing PLU verification. Verification efforts on seismic reflectors. VSP/ Drilling/Hydraulic tests. Hard to see any new data that would, further increase confidence in the existence (non-existence) of regional gently dipping deformation zones.

Aspect of SDM	Uncertainty	Cause (e.g. data inaccuracy, information density, uncertainty in other discipline models or process understanding)	Has uncertainty been assessed considering information from more than one data source or through a calibration or validation exercise?	Impact on other uncertainties (in all disciplines)	Quantification (provide reference to applicable section of the SDM report)	Potential Alternative representation. (Is there reason for this and has one been developed)	Are there unused data which could be used to reduce uncertainty	What new data would potentially help resolve uncertainty? (Are they considered in L2.1 investigation)
	Continuity along strike and at depth, dip and termination., i.e. the resulting size (length) of the deformation zone.	<p>It is intrinsic to the modelling process and questions of scale.</p> <p>Extent of interpreted DZ uncertain – especially since real DZ often consist of “non”-continuous parts (i.e. EW007). This means that detailed data (like dip, size) from an individual segment may have little relevance for the entire structure. (This is considered in the subsequent uncertainty assessment of DZ properties. But this scale issue implies severe communication difficulties – there is a need to make a more realistic description of the zones in different scales).</p>	<p>Yes, but more can be done.</p> <p>25 of the deformation zone extensions have been verified by boreholes. This does not give full evidences for the size. It is very difficult to assess length and extension at depth – progress unlikely within 2.1–2.3.</p> <p>However, provided the surface expression of lineaments means something about the lengths and terminations at depth, then good data is already at hand and are being used. It should be noted that this hypothesis exaggerates the sizes of the zones.</p>	Hydrogeology and rock mechanics are affected by this uncertainty.	<p>Size range given for the high – and some of the medium confidence deformations zones.</p> <p>There are some specific questions regarding some of the zones – see also next column.</p>	<p>There are specific questions regarding the following DZ.</p> <p>Southern termination of ZSMNE005A. For example: is there justification for an alternative interpretation that the zone continues to the SW, with or without an offset across NW932A or NW042A. The complex local rock body geometries make this difficult and maybe the magnetic map show a combination of lithology and DZ?</p> <p>Eastern extension of NW042A or NW932A. Can it continue and play a similar roll to EW002A in the north?</p> <p>NE terminations of NE094, NE108, NE107, NE063. This clear set of interpreted zones all terminate at or near NW042A. Check terminations to assist with assessment of structural relationships. How many have indications of existence on the northern side of NW042, how many fall short?– or are all current terminations clear and without alternatives?</p> <p>NW extension of EW007A. This could be an alternative looked at for L 1.2. The zone does not terminate against NS059 but continues. Watercourse indicates extension of the zone towards the west.</p>	No	<p>To increase confidence in extent of zones several boreholes are needed in the same structure including interference tests, seismics etc. Such tests (for some of the zones) are included already in L2.1.</p> <p>However, detailed data must not be misused to suggest shorter zones than motivated from a larger scale perspective.</p>

Aspect of SDM	Uncertainty	Cause (e.g. data inaccuracy, information density, uncertainty in other discipline models or process understanding)	Has uncertainty been assessed considering information from more than one data source or through a calibration or validation exercise?	Impact on other uncertainties (in all disciplines)	Quantification (provide reference to applicable section of the SDM report)	Potential Alternative representation. (Is there reason for this and has one been developed)	Are there unused data which could be used to reduce uncertainty	What new data would potentially help resolve uncertainty? (Are they considered in L2.1 investigation)
						<p>Connection- degree of continuity along EW900 as it crosses over NS059A. ie should it be modelled in different segments?</p> <p>NW extension of NW932. The lineament follows the rock type boundary. Possible continuation to the west of NS059?</p> <p>Degree of continuity of NW170, NE138 and NE043. Superficially each of these geometries appears to be combinations of different structures. Review the position as to whether or not they are continuous or should be broken up. (At the regional, 1,600 m, scale)</p>		
	Character and properties – also in the well established zones (e.g. from Åspö). Strong spatial variation of properties (width, internal structure, fracturing, also hydraulic properties...) as seen in multiple intercepts.	Information density and spread of data. Inherent concentrations of data.	Partly. Zones rated as high confidence includes uncertainty description based on all supporting data.	Hydrogeology and rock mechanics are directly affected by this uncertainty – and this in turn causes uncertainty in the distribution of e.g. hydraulic properties in the “plane” of structures.	Partly. See property tables for high confidence deformation zones.	Not done yet – but there remains potential for alternatives. Impact is partly assessed in hydrogeology.	No	Additional boreholes.

Aspect of SDM	Uncertainty	Cause (e.g. data inaccuracy, information density, uncertainty in other discipline models or process understanding)	Has uncertainty been assessed considering information from more than one data source or through a calibration or validation exercise?	Impact on other uncertainties (in all disciplines)	Quantification (provide reference to applicable section of the SDM report)	Potential Alternative representation. (Is there reason for this and has one been developed)	Are there unused data which could be used to reduce uncertainty	What new data would potentially help resolve uncertainty? (Are they considered in L2.1 investigation)
Geology – DFN model	Fracture set (orientation) identification.	Subhorizontal outcrops and subvertical boreholes which are also mapped with different resolution.	Yes, implicit in methodology and illustrated in verification example.	Hydrogeology is affected by these uncertainties and to some extent also rock mechanics.	See Section 5.5.	Section 5.5. Different conceptual assumptions regarding tools and possible modelling "style". Alternatives presented for each main rock domain.	Yes, mainly Äspö (tunnel mapping, 3D) and Clab data.	Inclined BHs in close proximity to detailed fracture outcrops.
	Fracture size distribution – interpolation between lineament and mapped outcrop data and for some sets only local information (extrapolation to larger sizes).	Uncertainty in the relevance of deformation zone extents. What do they represent, length, continuity etc. Lack of size data between deformation zones lower end and outcrop higher end. Highly uncertain size data for subhorizontal fractures.	Uncertainty assessed through possible variability in size fits (upper, lower bounds and best fit).	Hydrogeology (hydraulic DFN modelling), especially the size range 10–500 m – Affects intensity of minor stochastic conducting zones.	See Section 5.5.	Different alternatives, see above and Section 5.5.	Äspö TBM tunnel TMS mapping could be better used for verification and exercises.	Confirmation of the extents of zones. Alternative lineament interpretations. Lineament interpretation on data which falls into the scale between outcrop and 1,000 m zones.

Aspect of SDM	Uncertainty	Cause (e.g. data inaccuracy, information density, uncertainty in other discipline models or process understanding)	Has uncertainty been assessed considering information from more than one data source or through a calibration or validation exercise?	Impact on other uncertainties (in all disciplines)	Quantification (provide reference to applicable section of the SDM report)	Potential Alternative representation. (Is there reason for this and has one been developed)	Are there unused data which could be used to reduce uncertainty	What new data would potentially help resolve uncertainty? (Are they considered in L2.1 investigation)
	Uncertainty in the thickness-size correlation. Coupling to DZmodel.	“Stochastic” deformation zones in single hole interpretation are quite thick. Uncertainty in Size Correlation not analysed.	Some verification exercises for intensity measures have been performed for DFN conceptual model alternatives 1 and 2.	Hydrogeology is critically affected by these uncertainties and to some extent also rock mechanics.	Yes, see Section 5.5.	No, but the issue is assessed within the separate SKB Expect project.	Yes, mainly Äspö and Clab data. Possibly old data (observations on length, width and property relation) from Clab etc. could be used to observe extent of some of these minor zones.	Inclined BHs, alternative orientations, in different rock domains. Preferably in conjunction with surface area mapping. Use Äspö tunnel mapping data to assess coupling of intensity to lineament proxy!
	Fracture intensity –variability in rock mass outside identified deformation zones. Assumption of fracture intensity coupled to Rock Domains.	High variability in borehole fracture intensity, not identified as zones. Intensity can be a function of rock type instead of rock domains.	Verification exercises for intensity measures have been performed. Intensity anomalies tested against geological parameters rock type, rock domain, alteration – no clear answer.	Hydrogeology is critically affected by these uncertainties and to some extent also rock mechanics.	Yes, partly see the DFN background report /Hermanson et al. 2005/, but analyses show no clear dependence.	Systematic variability with depth has been tested and rejected, see Section 5.5. Need for understanding difference between potential volumes in the rock which have anomalously high fracture intensity in contrast to the increased intensity inside local minor deformation zones. Possible alternative is fractal spatial model for background fractures and system for identifying local minor DZ in boreholes. (Assessed in a separate project).	Data in conjunction with field observations and refined single hole interpretations. Refined analysis with respect to alteration (sasuaritisation, oxidation) and refined rock domain/fracture intensity model. Inclined boreholes, in different rock domains.	

Table A9-4. Protocol for assessing uncertainty in the rock mechanics and thermal property aspects of the SDM.

Aspect of SDM	Uncertainty	Cause (e.g. data inaccuracy, information density, uncertainty in other discipline model or process understanding)	Has uncertainty been assessed considering information from more than one data source or through a calibration or validation exercise?	Impact on other uncertainties (in all disciplines)	Quantification (provide reference to applicable section of the SDM report)	Potential Alternative representation. (Is there reason for this and has one been developed)	Are there unused data which could be used to reduce uncertainty	What new data would potentially help resolve uncertainty? (Are they considered in L2.1 investigation)
Bedrock in situ stress state	Rock stress magnitudes and distribution within the Laxemar subarea.	Data inaccuracy (see Table 12-1) and scarcity of data.	Different measurements have been used and compared, see discussion in Section 6.4. Experiences from excavations at depth in Äspö HRL also confirm that extremely high stress magnitudes do not exist in the Äspö HRL area, since major stability problems have not been observed.	Low – although note that some Rock Mechanics Parameters are stress dependent (relations are given explicitly in Chapter 6).	Uncertainty in stress magnitude is described as a span of potential values for the mean. See Table 6-11 and 6-12.	No alternative representation has been developed. (Better expressed as an uncertainty interval.)	The fact that core diskings is not observed in available cored boreholes is not used as soft input in the modelling.	More stress measurements in the Laxemar subarea (will become available in L2.2).
	Uncertainty in the division of local model area into different stress domains.	Scarcity of data in the local model area. Uncertainties in the deformation zone model.	Stress data exists from the two domains in the current model. Numerical stress modelling using the deformation zones as input, confirms the existence of two different stress domains.	Possible impact on (explaining) possible differences in transmissivity anisotropy between Äspö HRL and the hydrogeological model description in the local scale.	See Table 6-11 and 6-12.	Yes. The stress model based on the updated deformation zone model for Laxemar 1.2 may be compared with the one produced for Simpevarp 1.2. In particular the differences in the extent, termination and dip of deformation zones are considered important.	No	More stress measurements in the Laxemar subarea (will become available in L2.2).

Aspect of SDM	Uncertainty	Cause (e.g. data inaccuracy, information density, uncertainty in other discipline model or process understanding)	Has uncertainty been assessed considering information from more than one data source or through a calibration or validation exercise?	Impact on other uncertainties (in all disciplines)	Quantification (provide reference to applicable section of the SDM report)	Potential Alternative representation. (Is there reason for this and has one been developed)	Are there unused data which could be used to reduce uncertainty	What new data would potentially help resolve uncertainty? (Are they considered in L2.1 investigation)
Bedrock mechanical properties	Extent/ occurrence of stochastic (minor) deformation zones, having different mechanical properties, inside the domains between deterministic zones.	Number of drill holes is limited and biased to vertical holes. Uncertainty in the deformation zone model. Uncertainty in the thickness-size correlation.	Both single hole interpretation results and DFN-modelling results have been used. The empirical classification has been used to estimate the occurrence of minor def zones.	The description should be compatible with the description of geology (and hydrogeology).	Not quantified.	Not developed. (Should possibly be considered in the DZ model and/or DFN-model.)	Possibly old data (observations on length, width and property relation) from Äspö HRL etc. could be used to observe extent of some of these minor zones (see Table 12-1),.	Improved DZ and DFN models. Comparison of drillhole empirical classification with actual experiences from excavations at Äspö HRL.
	Effects of pore pressure on rock mass strength properties.	No established approach to assess this effect. Uncertainty in parameter/process understanding. See Section 6.3.	Pore pressure is part of empirical approach but not part of theoretical approach.	Low	The process is understood but parameters are uncertain. The uncertainty is not quantified, but effect is probably negligible. See Section 6.3.	No need	No	Theoretical approach extended to include impact of pore pressure.
	Rock mechanical properties for intact rock of rock type Quartz monzodiorite and Ävrö granite in southern Laxemar.	No laboratory tests of Quartz monzodiorite from Simpevarp subarea are available. Ävrö granite in southern Laxemar is judged to have lower quartz content than in the samples from Simpevarp	No	Minor effect on the rock mass properties.	See Section 6.3.	No reason. Better expressed as uncertainty.	No	New data available for L2.1. Additional laboratory tests data on intact rock, especially from the Ävrö granite and Quartz monzodiorite in southern Laxemar.
	Mechanical properties – deformation zones.	For deformation zones only the empirical approach is used. The bedrock material inside zones is not easily sampled for lab. testing.	No	No	See Section 6.3.	No reason. Uncertainty is now better expressed as the ranges given in Table 6-3.	Possibly data from Äspö HRL tunnel intersection with deformation zones in the model.	More geological information on the DZ properties (e.g. from trenches and drill core data from boreholes intersection with large deformation zones).

Aspect of SDM	Uncertainty	Cause (e.g. data inaccuracy, information density, uncertainty in other discipline model or process understanding)	Has uncertainty been assessed considering information from more than one data source or through a calibration or validation exercise?	Impact on other uncertainties (in all disciplines)	Quantification (provide reference to applicable section of the SDM report)	Potential Alternative representation. (Is there reason for this and has one been developed)	Are there unused data which could be used to reduce uncertainty	What new data would potentially help resolve uncertainty? (Are they considered in L2.1 investigation)
Bedrock thermal properties	Thermal rock type models.	Uncertain representativity for SCA and TPS data. SCA calculations from modal analysis (thermal conductivity of mineral, alteration, modal composition), see Table 12-1. Altered rock has not been analysed.	For major rock types uncertainty in SCA data has been evaluated by comparison with TPS data and by sensitivity studies. Correction factors have been applied, for QMD and fine-grained dioritoid based on small no. of samples. No such assessment has been performed for subordinate rock types. It is thought that altered rock has higher thermal conductivities than unaltered rock.	No	Spatial variability is quantified, see below. Uncertainty in spatial variability is discussed, see Chapter 7.	No, uncertainty captured as distribution.	No	Representative direct measurements (TPS) of thermal conductivity for all rock types including some altered rock samples. Data from geology on abundance and nature of alteration (part of L2.1). A further development is to establish a relationship between rock mapped as altered rock in Boremap and measured thermal conductivity. Extensive sampling of other rock types to produce variograms of spatial variability.
	Thermal conductivity of Ävrö granite from density logging.	Uncertainty in calculation of thermal conductivity from density loggings.	Validity in using density to calculate thermal conductivity in rock type Ävrö granite (501044) is demonstrated. Measurements (TPS) have been made in order to verify the use of density loggings to calculate thermal conductivity. Most measurements are made on samples with high thermal conductivities. Scarcity of data for samples with low conductivities.	No	Bias partly evaluated by comparison with TPS data.	None	No	For Ävrö granite more samples with both density and thermal conductivity measurements. These samples should be collected in the Laxemar subarea and should ideally include both high and low conductivity varieties (partly in L2.1). Additional measurements (verification data set) in density logged boreholes required for verification of density – thermal conductivity model. Improved quality of density logging data.

Aspect of SDM	Uncertainty	Cause (e.g. data inaccuracy, information density, uncertainty in other discipline model or process understanding)	Has uncertainty been assessed considering information from more than one data source or through a calibration or validation exercise?	Impact on other uncertainties (in all disciplines)	Quantification (provide reference to applicable section of the SDM report)	Potential Alternative representation. (Is there reason for this and has one been developed)	Are there unused data which could be used to reduce uncertainty	What new data would potentially help resolve uncertainty? (Are they considered in L2.1 investigation)
	Thermal conductivity – scale transformation.	Uncertainties in transformation between different scales e.g. measurement scale to canister scale.	Rock type models and density loggings have been used to analyse the effect of up-scaling the spatial variability in Ävrö granite.	No	Spatial variability is quantified. Uncertainty in spatial variability is discussed, see Chapter 7.		No	Measurements at relevant scale.
	Thermal conductivity – rock domains.	<p>Uncertainties in large scale variations within domains with medium or low presence of Ävrö granite (See geology).</p> <p>Small number of boreholes used to characterise domains.</p> <p>Uncertainties in rock type abundances for domains where borehole information is lacking.</p> <p>3D geometry of most of the rock domains is also uncertain.</p> <p>Uncertainties in the modelling approach.</p>	Different approaches are used to evaluate the variability in thermal conductivity.	No	Spatial variability is quantified. Uncertainty in spatial variability is discussed, see Chapter 7.		<p>No, but range is estimated by considering different approaches, see Chapter 7.</p> <p>Possible to use temperature loggings to evaluate variability in thermal conductivity, see Table 12-1.</p>	<p>Need for more data to evaluate the spatial variability with higher confidence (partly in L2.1)</p> <p>Better characterisation of domains can be achieved with more boreholes (partly in L2.1).</p> <p>Improved confidence in Rock Domain model would help.</p>
	Thermal properties in DZ.	No thermal data from the DZ.	No	Uncertainty judged to be of limited importance. Peak canister temperature only depends on local thermal properties around the canister, see /Hökmark and Fälth 2003/.	A range could be set.	No reason.	No	No need

Aspect of SDM	Uncertainty	Cause (e.g. data inaccuracy, information density, uncertainty in other discipline model or process understanding)	Has uncertainty been assessed considering information from more than one data source or through a calibration or validation exercise?	Impact on other uncertainties (in all disciplines)	Quantification (provide reference to applicable section of the SDM report)	Potential Alternative representation. (Is there reason for this and has one been developed)	Are there unused data which could be used to reduce uncertainty	What new data would potentially help resolve uncertainty? (Are they considered in L2.1 investigation)
	In situ temperature.	Uncertainty in temperature data, possibly due to calibration error, convection in the boreholes, etc.	Difference between boreholes.	No (the differences are small – but are important for Engineering and layout).	A range is provided (see Chapter 7).	No reason.	No	More high quality temperature logs in combination with optimal timing of measurement.
	Thermal expansion.	Possible data inaccuracy.	Not yet – but comparison between methods and laboratories is done but not reported. Comparison with Äspö HRL APSE data could be useful.	No, but affects Rock mechanics evolution due to heating.	A range is provided (see Chapter 7).	Not yet. It could be discussed whether the expansion is linear with T or not.	Data from the APSE experiment at Äspö HRL.	Laboratory test method development (is already underway).

Table A9-5. Protocol for assessing uncertainty in the hydrogeology, hydrogeochemistry and transport property aspects of the SDM.

Aspect of SDM	Uncertainty	Cause (e.g. data inaccuracy, information density, uncertainty in other discipline models or process understanding)	Has uncertainty been assessed considering information from more than one data source or through a calibration or validation exercise?	Impact on other uncertainties (in all disciplines)	Quantification (provide reference to applicable section of the SDM report)	Potential Alternative representation. (Is there reason for this and has one been developed)	Are there unused data which could be used to reduce uncertainty	What new data would potentially help resolve uncertainty? ((Are they considered in L2.1 investigation)
Bedrock hydro-geology	Geometry of deformation zones and their connectivity.	See geology table. More integration with geology can decrease uncertainty in connectivity. However, there are only few interference tests in Laxemar subarea.	Modelled a decreased number of DZ and tested in numerical gw-modelling.	Has impact on the flow model and then transport paths and the integrated evaluation together with hydro-geochemistry.	Discussed in Chapter 8. Uncertainty in connectivity of the zones is less than in Simpevarp 1.2 (but still significant) in Laxemar subarea.	Yes, and a few cases have been tested in the regional flow modelling.	A few (Äspö data, local coverage), but cannot reduce overall uncertainty much. Conceptual gain?!	New borehole data and reflection seismics (much a integration with geology). Interference data –drilling and cross-hole tests!
	Transmissivity distribution in zones (spatial variability).	Spatial variability: Sparse data in zones (need multiple data points in each zone).	In a few DZ there are more than one hydraulic test. The complete set of data suggests a depth trend (decrease with depth).	Flow field and connectivity within and between deterministic DZ.	The overall depth trend is given as the basic model- There are also alternative descriptions (see next column). The spatial variability is estimated based on the overall spatial variability in data as measured in different zones, but the main case analysed in the flow simulations assume no spatial variability apart from the depth trend.	Yes. Planned for some different cases of T-distribution explored in regional flow modelling for next model version. In principle DZ can be modelled as HydroDFN and effective values as well as correlation models can be estimated and used in continuum models – this has not yet been tested or established.	No! Potentially, existing correlation structure established using Äspö data could be used!	Boremap+BIPS+PFL data for a number of zones and some interference tests within these zones.

Aspect of SDM	Uncertainty	Cause (e.g. data inaccuracy, information density, uncertainty in other discipline models or process understanding)	Has uncertainty been assessed considering information from more than one data source or through a calibration or validation exercise?	Impact on other uncertainties (in all disciplines)	Quantification (provide reference to applicable section of the SDM report)	Potential Alternative representation. (Is there reason for this and has one been developed)	Are there unused data which could be used to reduce uncertainty	What new data would potentially help resolve uncertainty? ((Are they considered in L2.1 investigation)
	Hydraulic DFN model. Fracture transmissivity distribution. Anisotropy	<p>Uncertainty in DFN-models. Uncertain conceptual models for coupling transmissivity as a function of fracture size.</p> <p>Larger features of the DFN-model usually are made up of many small fractures, and do not represent individual fractures.</p> <p>Variable measurement limit for PFL, that is higher than PSS, and affects PFL-anomaly estimates of fracture transmissivity. Also dependent on the lower measurement limit of PSS. Lack of detailed hydraulic tests in Boremap logged cored boreholes 0–100 m below surface.</p> <p>There are also uncertainties in how to estimate size and intensity models for the conductive features.</p> <p>Anisotropy bias by steeply dipping boreholes (overestimating importance of subhorizontal set – this also means that the hydraulic anisotropy found at Äspö HRL is hard to detect.</p>	Yes. Calibration using inflow measurements from PFL in individual boreholes.	Yes. The heterogeneity of the flow field and its implications for transport paths and expected distribution of ground waters with different composition. Inflow estimates to the open repository.	Yes.	Several hydraulic DFN models with different T-models (T correlated/ un-correlated) fractures have been tested.	PSS data can be used more to test the hydraulic DFN models by simulating existing tests performed at various scales. PFL data with the oriented flowing features.	<p>Data to resolve the geometry of fractures using inclined coreholes. Detailed hydraulic tests 0–100 m below surface. Interference tests between bore holes may to some extent (generally long distances in a sparsely fractured rock) be used to test model.</p> <p>Single-hole interference tests (one section for injection and several pressure monitoring sections) is a possibility to tests connectivity but no tools are present available and the usefulness of the methodology is not known.</p>

Aspect of SDM	Uncertainty	Cause (e.g. data inaccuracy, information density, uncertainty in other discipline models or process understanding)	Has uncertainty been assessed considering information from more than one data source or through a calibration or validation exercise?	Impact on other uncertainties (in all disciplines)	Quantification (provide reference to applicable section of the SDM report)	Potential Alternative representation. (Is there reason for this and has one been developed)	Are there unused data which could be used to reduce uncertainty	What new data would potentially help resolve uncertainty? ((Are they considered in L2.1 investigation)
	Hydraulic properties as a function of rock domain.	<p>Different geological DFN in the different rock domains.</p> <p>Uncertainty in geometry of some of the rock domains (cf. the Götemar and Uthammar intrusions that could possibly extend at depth in the Laxemar subarea).</p> <p>Only hydraulic data from some of the different rock domains.</p> <p>Only more than one hole in domain A.</p>	There are data already from the main rock domain A in the Laxemar subarea.		The main assumption is a rock domain specific hydraulic DFN. Only properties in rock domain A is based on several boreholes. Properties of the rock domains D, M(A) and M(D) in the Laxemar subarea are only based on one corehole, KLX03A. It is not really possible to estimate the spatial variability on a larger scale.	The uncertainty not quantified. The main assumption is a rock domain specific hydrogeology-DFN, but there are of course potential for alternative interpretations (i.e. no rock domain specific variability). However, these alternatives are not analysed.	No	More hydraulic tests in the different rock domains in the Laxemar subarea. It is planned to drill one more corehole into rock domain D, M(A) and M(D).
	Digital elevation model.	<p>Unified elevation model (topography and bathymetry) (including well specified shoreline) is available.</p> <p>However, the overburden model is still under development and the position of the bedrock surface and the overburden stratigraphy, especially below the sea, must be considered uncertain.</p>	Yes (An approximate position of the water table have been estimated as an alternative to use topography as prescribed head on top-surface in the regional modelling.)	<p>Affects distribution of modelled discharge areas.</p> <p>Point of departure for palaeohydro simulations and establishment of near surface conditions for description and modelling of recharge and discharge areas.</p>	Yes (Projection to results of modelling in regional scale).	No reason to test more alternatives than presently used.	No	New drillings and refraction seismics will decrease the uncertainties in the overburden model and of the bedrock surface position (bed rock topography), but not the topography and bathymetry.

Aspect of SDM	Uncertainty	Cause (e.g. data inaccuracy, information density, uncertainty in other discipline models or process understanding)	Has uncertainty been assessed considering information from more than one data source or through a calibration or validation exercise?	Impact on other uncertainties (in all disciplines)	Quantification (provide reference to applicable section of the SDM report)	Potential Alternative representation. (Is there reason for this and has one been developed)	Are there unused data which could be used to reduce uncertainty	What new data would potentially help resolve uncertainty? ((Are they considered in L2.1 investigation)
	Regional scale initial and boundary conditions.	Boundary conditions are uncertain since there are no well defined boundaries. One main uncertainty in modelling the palaeohydrology is the uncertainty in the initial conditions for the modelling period that also will be more or less unknown and can possibly be assessed by modelling. Other uncertainties are the Littorina water characteristics and time frame (see also next row).	Yes. Transient simulation of transport (TDS, water types) not accounting for chemical reactions, and comparing with present-day water chemistry.	Joint hydrogeochemical and hydrogeological conditions Transport description. Open repository (initial condition).	Yes (Results are presented in Chapter 8.)	Different initial and boundary conditions have been tested.	No. Possibly isotopes can be used more in the testing of models.	New boreholes and new sampling points will improve description of present day salinity distribution (incl. additional matrix data) and distribution of isotopes that may help. However, there is more need for matrix porewater data from the potential repository levels at the Laxemar subarea (see below).
Hydrogeo-chemistry	Spatial variability in 3D at depth.	The information density concerning borehole groundwater chemistry is low. The samples are mixed and represent an average composition. Uncertainty in water composition in the low conductive fractures and in the matrix due to lack of data. Also the "mixing" proportions of "Water types" have uncertainties greater than the individual chemical components but individual components can have several sources and may therefore not necessarily indicate a unique origin of the water.	A validation test has been conducted where representative/non-representative samples have been used as a basis for interpretation. The regional groundwater flow modelling has also applied different initial conditions after the last glaciation to reproduce measured values at depth.	This may cause uncertainties concerning the salinity interface in e.g. hydrogeological modelling and transport modelling. Causes uncertainties in overall hydrochemical understanding of the site.	Yes, see Chapter 9. Uncertainty in water composition in the low conductive fractures and in the matrix is still unclear – but data from Äspö HRL suggest different composition in high and low conductivity fractures.	The basic model is the interpolated distribution from the data. An alternative hypotheses is that there are lenses of "deviating" groundwater composition (glacial water) in the low conductive fractures and in the matrix. Both hypotheses are partly assessed in the hydraulic modelling and also in future geochemical sampling and interpretation.	Comparison with hydrogeological description.	More data observations from deep boreholes. Rock matrix samples, especially from the rock volumes from the potential repository levels at the Laxemar subarea

Aspect of SDM	Uncertainty	Cause (e.g. data inaccuracy, information density, uncertainty in other discipline models or process understanding)	Has uncertainty been assessed considering information from more than one data source or through a calibration or validation exercise?	Impact on other uncertainties (in all disciplines)	Quantification (provide reference to applicable section of the SDM report)	Potential Alternative representation. (Is there reason for this and has one been developed)	Are there unused data which could be used to reduce uncertainty	What new data would potentially help resolve uncertainty? ((Are they considered in L2.1 investigation)
	Groundwater composition in the rock matrix. (See also first line)	Few measurements and uncertainties in interpretation. The uncertainties are associated with sampling, the small extractable volumes available for analysis, and the possibility of contamination, together with modelling uncertainties and assumptions.	A carefully conducted chemical analytical programme. Stress release impacts assessed using rock mechanics information.	May affect the hydrogeological modelling and transport modelling. The description of the interaction between groundwaters in the highly permeable and low permeable systems will be uncertain.	Yes, see Chapter 9	Yes, see (spatial distribution above).	No	Additional samples for rock matrix determination will be collected.
	Identification and selection of end-member waters.	The identification of end-member waters has been improved upon, but there is still some uncertainty. Some is due to the judgemental aspect of the M3 (principal components) analysis.	Integration with hydrogeology to identify and use same end-members.	May cause uncertainties in the chemical process description and in the integration with hydrogeology. Causes uncertainties in overall hydrochemical understanding of the site. However, the proper interpretation of the M3 analyses results for hydrogeology should be done with understanding of the method uncertainties, together with independent modelling of individual species.	Different end-members have been selected in the regional/local models, no quantification has been conducted, see Section 9.5 and 9.6	Different modelling approaches are applied on the same data set to describe the same processes for confidence building.	No	Data from extreme waters.
	Important chemical reactions (i.e. controlling redox etc. Model uncertainties (e.g. equilibrium calculations, migration and mixing).	Inaccurate pH measurements, inaccuracy in the thermodynamic databases, potential errors in mineral phase selections and potential errors in end-members selection, model uncertainties.	For validation different modelling approaches are applied to the same data set.	May cause uncertainties in transport modelling and hydrogeological modelling. Causes uncertainties in overall hydrochemical understanding of the site.	Yes, see Chapter 9.	Different modelling approaches are applied to the same data set to describe the same processes thereby confidence is built into the description.	No	In situ pH measurements and more data on fracture mineralogy. Data on Rock matrix mineralogy (including Fe ²⁺) are already part of L2.1.

Aspect of SDM	Uncertainty	Cause (e.g. data inaccuracy, information density, uncertainty in other discipline models or process understanding)	Has uncertainty been assessed considering information from more than one data source or through a calibration or validation exercise?	Impact on other uncertainties (in all disciplines)	Quantification (provide reference to applicable section of the SDM report)	Potential Alternative representation. (Is there reason for this and has one been developed)	Are there unused data which could be used to reduce uncertainty	What new data would potentially help resolve uncertainty? ((Are they considered in L2.1 investigation)
	Temporal (seasonal) variability in surface water chemistry, which ultimately impacts the groundwater in the bedrock. Temporal averaging follows from processes being slow.	The sampling may not describe the seasonal variation and samples may be taken at different time intervals from the surface versus the shallow boreholes.	No this has not been done, but a detailed surface hydrogeological modelling may be helpful for this type of exercise.	Can cause uncertainty concerning the interaction between surface and groundwaters and may affect transport modelling. The amount of reactions taking place at the surface may not be properly described.	The effects of seasonal variation have not been quantified but the effects have been identified, see Section 9.3.	Different modelling approaches are applied to the same data set to describe the same processes.	No	Sampling reflecting seasonal variation from selected surface and borehole locations in identified recharge/discharge areas.
Transport properties	Sorption and diffusion parameters for site-specific materials as well as data imported from other sources (e.g. Simpevarp, Äspö, etc.)	<p>Only small amount of site investigation data available for the Laxemar subarea.</p> <p>There is uncertainty in matrix retention properties, especially concerning the sorption properties.</p> <p>Reasons are spatial variability, limited data set (no site specific sorption data).</p> <p>Impact of stress release on core samples.</p> <p>Conceptual model of sorption may be incorrect if other geochemical processes are active.</p> <p>These uncertainties are general and apply to all data used, both site-specific and imported.</p>	<p>Identification of data from other sources based on geological comparison. Same uncertainties also apply to data taken from other sources as outlined below.</p> <p>Diffusion assessed with electrical resistivity in both lab and field combined with through diffusion experiment</p> <p>Multiple samples and sample lengths for all lab experiments.</p> <p>Impact of stress release on core samples assessed qualitatively by comparing lab. and in situ tests.</p>	<p>Related to uncertainties in salt transport and reactive (hydrogeochemical) transport modelling.</p> <p>However, uncertainty in F and its distribution under PA conditions is far more important than (possibly) smaller uncertainties in material property data for overall uncertainty in transport properties of first 10–100 m in far-field.</p>	By means of distributions (resistivity), intervals and/or quantifications of uncertainty observed in the measurements. Stress release effects can at present only be estimated semi-quantitatively.	Not relevant (uncertainty in sorption process as such assessed within Safety Assessment, SR-Can).	No	Yes, more site specific data on transport parameters

Aspect of SDM	Uncertainty	Cause (e.g. data inaccuracy, information density, uncertainty in other discipline models or process understanding)	Has uncertainty been assessed considering information from more than one data source or through a calibration or validation exercise?	Impact on other uncertainties (in all disciplines)	Quantification (provide reference to applicable section of the SDM report)	Potential Alternative representation. (Is there reason for this and has one been developed)	Are there unused data which could be used to reduce uncertainty	What new data would potentially help resolve uncertainty? ((Are they considered in L2.1 investigation)
	Sorption properties, diffusivities and porosities of the geologic material representative of the fractures (e.g. fracture rim zone, gouge material and fracture filling).	Shortage of relevant material thus far and possible discrepancy with data obtained at Äspö HRL within the TRUE program.		Related to uncertainties in salt transport and reactive (hydrogeochemical) transport modelling. Limited importance for Safety Assessment.	Scoping calculations to ascertain impact of alteration on transport properties.		Possibly, if one would allow import from other sites (e.g. Äspö data).	Yes, more site specific data on transport parameters.
	Assignment of uncertainty distributions for sorption, diffusion, and porosity data. When scaled up from measurement scale to REV scale for PA.	Between samples variation based upon small sample sizes used in lab measurements may not give appropriately scaled estimates of material property variation at REV scale.	Not at this time	May influence ranges of retention times predicted in PA analyses.	Not at this time. The uncertainties presented in Laxemar 1.2 are on the lab scale. (Further discussion on the upscaling are needed within the Safety Assessment, see the SR-Can Data Report.)	No	No	Sorption and diffusion measurements on large, intact pieces of rock. Not currently considered.
	Assignment of parameter values to the "elements" in the geological description (rock domains and deformation zones).	All relevant materials and structures are not represented in the site-specific database. Parameterisation to a large extent based on expert judgement.	Use of data from other sources and "extrapolation" of database according to modelling methodology.	Related to uncertainties in salt transport and reactive (hydrogeochemical) transport modelling.	Uncertainties are given for each rock domain. The implications for the upscaling are not quantified (see discussion above).	Alternatives could follow from alternative geological models. No alternative developed at this stage.	Possibly – potential for further import of Äspö data will be assessed.	Site data on transport and geological parameters from rock domains of interest.
	Understanding of retention or retardation processes as a basis for selection of parameters in models.	Limited site-specific input to development of process understanding available.	A study, presently based on Äspö data, of "alternative" processes and process models has been performed.	Coupled to hydro-geochemical description (process modelling).	None (to be addressed within SR-Can).	Potential for development of alternative retention models. No alternative developed at this stage.	Possibly – all hydrogeochemical site data not considered in present model version.	Transport data and incorporation on hydrogeochemical data in the analysis. However, this issue is not readily resolved by more site specific data.

Aspect of SDM	Uncertainty	Cause (e.g. data inaccuracy, information density, uncertainty in other discipline models or process understanding)	Has uncertainty been assessed considering information from more than one data source or through a calibration or validation exercise?	Impact on other uncertainties (in all disciplines)	Quantification (provide reference to applicable section of the SDM report)	Potential Alternative representation. (Is there reason for this and has one been developed)	Are there unused data which could be used to reduce uncertainty	What new data would potentially help resolve uncertainty? ((Are they considered in L2.1 investigation)
	Spatial variability and correlation between matrix transport properties and flow paths	Lack of site-specific transport data impedes the establishment of quantitative correlations. There is also general uncertainty in matrix retention properties. Reason: spatial variability, limited data set, and transfer of information from lab to field. Generally expectation of low correlation between matrix and flow path properties; higher correlation between fracture surface and flow path properties.	A first attempt is made to associate "typical fractures" with hydraulic properties. This was done for Simpevarp 1.2 and is used here also.	Coupled to hydro-geological description (properties of structures in flow models).	A range of properties for each different rock type are given, see section. Correlation hard to establish.	Quantitative coupling between retardation and flow paths is handled by Safety Assessment.	Possibly – only a limited evaluation of available hydrogeological data performed at this stage.	Potentially, more borehole data can establish a relation (however, low expectations).
	Distribution of transport resistance (F) at Safety Assessment timescales.	As a derived parameter, the estimation of F and its distribution are strongly influenced both by uncertainties in models used to interpret primary borehole data (i.e. to give transmissivity distributions from PFL and other hydrological investigations) as well as models used to estimate the derived parameter itself (F). This also includes assumptions, (both stated and implicit) used in data derivation (e.g. flow dimension, flow geometry, etc.) Transmissivity distributions must be on the resolution of individual water conductors to be reliable for F distribution estimations. Lack of transparency concerning underlying assumptions implicit in data obtained from other disciplines (i.e. Bedrock Hydrogeology).		Related to uncertainties in salt transport and reactive (hydrogeochemical) transport modelling. Potentially a more important source of uncertainty than matrix material properties (sorption, diffusion, porosity).	Yes, partly by scoping calculations to establish an envelope of possible behaviour using a channel network representation. Estimates are, however, model dependent and can vary between alternative model concepts. This has not been investigated in detail. The uncertainty will be more fully explored in SR-Can also using upscaling based on the hydrogeological DFN-modelling.	Alternative models, of varying complexity are used for derivation of this parameter and for interpretation of primary data, see Chapter 10.	No	Reinterpretation of primary data using alternative models as well as use of multiple independent modelling concepts for parameter estimation. PFL-data from more boreholes.

Table A9-6. Protocol for assessing uncertainty in the near surface aspects of the SDM.

Aspect of SDM	Uncertainty	Cause (e.g. data inaccuracy, information density, uncertainty in other discipline models or process understanding)	Has uncertainty been assessed considering information from more than one data source or through a calibration or validation exercise?	Impact on other uncertainties (in all disciplines),	Quantification (provide reference to applicable section of the SDM report)	Potential Alternative representation. (Is there reason for this and has one been developed).	Are there unused data which could be used to reduce uncertainty	What new data would potentially help resolve uncertainty? (Are they considered in L2.1 investigation).
Surface system – Quaternary deposits (QD)	Terrestrial: composition, spatial distribution, depth and thickness of individual strata.	Low information density in the Laxemar subarea.	Yes, different data sources has been used in modelling.	Hydrological and transport modelling (flow of matter). Bedrock surface mapping. Hydrogeological modelling of deep rock. Hydrogeochemistry modelling. Ecosystem descriptions and models. Transport models of bedrock/surface interaction.	Model describing the data density of QD-depth and stratigraphy.	No	No	Measurements of composition, spatial distribution, depth and thickness of individual strata.
	Chemical and physical properties of QD.	Low information density in the Laxemar subarea.	No	Hydrological and transport modelling (flow of matter). Bedrock surface mapping. Hydrogeological modelling of deep rock. Hydrogeochemistry modelling. Ecosystem descriptions and models. Transport models of bedrock/surface interaction.	No	No	No	Measurement data of Chemical – and physical properties.
Surface system – Surface hydrology, near-surface hydrogeology and oceanography	Hydraulic properties. In QD and near surface bedrock.	Insufficient data and models/ descriptions of hydraulic properties and flow conditions in overburden and uppermost rock.	Temporal variability (spatial, to some extent): Evaluation of data from different SMHI stations in the region (performed in v. 0; TR-02-03).	Hydrogeological models (recharge to rock, effects of repository drawdown). Transport/flow of matter (incl. radionuclide transport models). Ecosystem models.	No	No	No	Geologic (e.g. stratigraphy) and hydrogeologic (e.g. hydraulic properties, ground-water levels) data.

Aspect of SDM	Uncertainty	Cause (e.g. data inaccuracy, information density, uncertainty in other discipline models or process understanding)	Has uncertainty been assessed considering information from more than one data source or through a calibration or validation exercise?	Impact on other uncertainties (in all disciplines),	Quantification (provide reference to applicable section of the SDM report)	Potential Alternative representation. (Is there reason for this and has one been developed).	Are there unused data which could be used to reduce uncertainty	What new data would potentially help resolve uncertainty? (Are they considered in L2.1 investigation).
	Water discharge in the surface system – spatial and temporal variability in runoff.	No data from discharge stations in Laxemar local model area. Generally short time series in regional model area.	No	Hydrological models (comparison/calibration). Hydrogeological models (basis for setting boundary conditions). Transport/flow of matter. Ecosystem models.	No	No	Measurements from Laxemarån and surrounding water courses (OKG measurements 1970 to 2005).	Site specific data – measurements initiated 2004, but time series is not available in Laxemar 1.2.
	No calibration/validation has been made on the surface hydrology model.	Lack of time series of surface water and groundwater levels.	No	Hydrological models (basic description, comparison/calibration). Hydrogeological models (basis for setting BCs). Transport/flow of matter. Ecosystem models.	Sensitivity analysis for the properties of the QD has been performed.	No	No	Site specific data – monitoring has been initiated in some soil tubes and surface waters; Important to NOT interrupt measurements during CSI.
	Quantification of water balance components (evapotranspiration, distribution of runoff on surface water and groundwater).	Limited site and generic data.	No	Hydrological models (basic description, comparison/calibration). Hydrogeological models (basis for setting BCs). Transport/flow of matter. Ecosystem models.	No	No	No	Runoff and evapotranspiration measurements.
Surface system – Chemistry	Temporal and spatial variation in water composition in groundwater.	No site sampling to describe the seasonal variation available.	No	Impacts the transport modelling, and the description of rock/surface system.	No	No	No	Sampling reflecting temporal/spatial variation at the site.
	Uncertainty in chemical description of QD/soils.	Lack of descriptive data.	No.	Causes uncertainties in overall hydrochemical model and in the understanding of the transfer of matter between and in rock/surface systems.	No	No.	No	Sampling reflecting spatial variation at the site.

Aspect of SDM	Uncertainty	Cause (e.g. data inaccuracy, information density, uncertainty in other discipline models or process understanding)	Has uncertainty been assessed considering information from more than one data source or through a calibration or validation exercise?	Impact on other uncertainties (in all disciplines),	Quantification (provide reference to applicable section of the SDM report)	Potential Alternative representation. (Is there reason for this and has one been developed).	Are there unused data which could be used to reduce uncertainty	What new data would potentially help resolve uncertainty? (Are they considered in L2.1 investigation).
	Transport of matter in the terrestrial system.	Limited data on discharge measurements combined with concentrations of dissolved and suspended matter.	No	Ecosystem models and the integrated ecosystem model. Safety assessment.	No	No	No	Always measure discharge when sampling chemistry.
	Chemical composition of biota.	No data	No	Impact on safety analysis.	No	No	No	Chemical composition of biota.
Ecosystems – biotic	Upscaling of spot sampling of biota.	Sample representativity and classification.	No	Surface hydrology modelling. Description of the site. Impact on safety analysis.	No	No	No	Further sampling.
	Properties of terrestrial vegetation (eg. root depth and LAI).	Lack of data.	No	Surface hydrology modelling. Terrestrial ecosystem modelling. Impact on safety analysis.	No	No	No	Field measurements (initated).

Table A9-7. Interactions judged to be important (green) and to what extent these were actually considered (black).

<p>Bedrock Geology</p>	<p>Spatial distribution of rock mechanics properties based on rock domain properties, including the fracturing and deformation zone geometry and properties.</p> <p>Deformation zone geometry influences the stress field. Also large differences in stiffness between different rock domains could possibly affect the local stress field.</p> <p>Rock domains used for selecting mechanical properties. DFN model is used to infer mechanical properties in the theoretical approach.</p> <p>Deformation zone geometry influences the stress field. It is noted that stress domain II could be explained by the deformation zone geometry. Also large differences in stiffness between different rock domains could possibly affect the local stress field. However, the variation in rock domain stiffness in Laxemar subarea is judged too low to be of importance.</p>	<p>Spatial distribution of properties based on rock domains.</p> <p>Modal analyses is used as (one) input.</p> <p>Data on alteration mineralogy (type and abundance).</p> <p>Nature of anisotropy (e.g. foliations).</p> <p>First two aspects considered, but the alteration data only partly so.</p> <p>Indicator variograms for subordinate rock types etc. not fully used for the upscaling.</p> <p>It would possibly be valuable to assess the potential larger scale anisotropy of the thermal properties considering orientations of dykes.</p> <p>Even potential anisotropy related to foliation could be evaluated with a few direct thermal measurements of anisotropy.</p>	<p>Rock Domains, Deformation zones and DFN-geometry is the geometrical framework.</p> <p>Geometry is considered (i.e. key input to the hydrogeological modelling).</p> <p>Significance of differences between RDs assessed.</p> <p>Description of deformation zones not fully used in the property assignment. (Currently only the width and the positions in the boreholes are used). Potentially, the more detailed property description given could be used for assessing the variability within the deformation zones.</p> <p>Need an updated zone characteristics (e.g. ductile/brittle) before such data could be used for testing classifying zones into different transmissivity classes.</p>	<p>Fracture mineralogy and Chemical composition of Bedrock should be considered.</p> <p>Fracture mineralogy is considered and the chemical composition is used in the modelling of the palaeo effects.</p> <p>Bedrock geochemistry (mineralogy) is used in deriving the matrix pore water composition.</p>	<p>Spatial distribution of properties based on rock domains (identified rock types in rock domain model).</p> <p>Porosity measurements on surface and borehole samples.</p> <p>Fracture mineralogy and hydrothermal alteration.</p> <p>Is done, but lack of transport property data in the different RD makes correlation study weak.</p>	<p>Data on mineralogy and geochemistry.</p> <p>Are used</p>	<p>No need</p>	<p>Data on fracture zones.</p> <p>Are used</p>	<p>No need</p>
-------------------------------	---	--	---	--	---	---	----------------	--	----------------

<p>Stress orientations in relation to fracture sets could give additional confidence i DZ and DFN model.</p> <p>Reason for division of RD and DZ could be re-assed (less reason to split between domains or reason to split existing domain).</p> <p>Stress modelling of Stress domain II gave further confidence on the Deformation zones in the Ävrö region (also more focus on this area due to its importance for the stress modelling).</p> <p>Rock Mechanics modelling group has assessed differences in mech. prop. in different RD. The analysis suggests that division into rock domains (together with the additional fracturing domains) appear appropriate for the rock mechanics modelling needs.</p>	<p>Rock Mechanics (in the bedrock)</p>	<p>No need</p>	<p>Stress orientation expected to affect hydraulic anisotropy field.</p> <p>Hypothesis of anisotropy in T assessed – not yet fully resolved. (Since strong correlation found at ÅHRL – the hypothesis is kept despite unclear evidence in data from Simpevarp and Laxemar subareas.)</p>	<p>Stress release of cores could affect the interpretation of matrix porewater composition.</p> <p>These impacts are considered, but the conclusions are not yet final.</p>	<p>Consider stress impact on “intact” rock samples for laboratory measurements of e.g. matrix porosity and formation factors.</p> <p>Part of the data evaluation. A qualitative comparison is made between the laboratory and in situ data together with the in situ stress data. (However, the comparison with the stress data is not straight-forward. There are also many other potential reasons for deviations between laboratory and in situ data.)</p>	<p>No need</p>	<p>No need</p>	<p>No need</p>	<p>No need</p>
<p>Could affect description of RD.</p> <p>The basis for the rock domain divisions is based on the needs expressed by the thermal modelling. The thermal modelling has also suggested an alternative Rock Domain model (see Table A9-3).</p>	<p>No need (thermal expansion analysis is outside SDM see Table 12-4).</p>	<p>Thermal (in the bedrock)</p>	<p>Temperature affects some hydraulic properties.</p> <p>Impact is assessed in the hydrogeological modelling. May later be discarded as an insignificant influence.</p>	<p>No need</p>	<p>No need</p>	<p>No need</p>	<p>No need</p>	<p>No need</p>	<p>No need</p>

<p>Confirmation and indications of deformation zones (i.e. are there hydraulic contacts or not).</p> <p>Feedback on the significance of the rock domain divisions.</p> <p>Control of the hydraulic applicability of the DFN-model.</p> <p>Significance of differences between RD assessed, and there seem to be some significant differences but hydraulic data missing in some domains.</p> <p>Hydraulic differences between rock types also partly assessed.</p> <p>Need updated DZ characterisation (e.g. ductile/brittle) before such data could be used for testing classifying zones into different transmissivity classes.</p> <p>There are some indications on the large scale connectivity of EW007 in the near surface (first 200 m from percussion holes). Lack of data for other zones in the Laxemar subarea.</p> <p>Much feedback in the hydraulic applicability of the DFN-model given during the development of these</p>	<p>Water pressure reduces the rock stress to effective stress.</p> <p>Not directly used in the modelling, but is considered in the descriptive text, see Section 6.3.</p>	<p>Thermal convection in boreholes affects uncertainty in measurement of initial temperature.</p> <p>Is considered when assessing uncertainty in in situ temperature.</p>	<p>Hydrogeology in the bedrock</p>	<p>Groundwater flow (advective mixing and matrix diffusion) is considered a main mechanism for distribution and evolution of groundwater composition.</p> <p>Simulation of past salinity and, distribution of end-member waters, evolution, predicted salinity distribution and possibility to compare predicted and measured. The simulated position of the fresh water and the occurrence of Littorina water (including "pockets" of glacial waters in low conductive parts, surrounded by more modern water) agrees fair with measured data, although there are uncertainties (see Table A9-6).</p> <p>There is however need for additional hydrogeological inputs e.g.</p> <p>Predictions of discharge and recharge areas have not yet been fully interpreted as regards the hydrogeochemical implications (could be used to assess reasonableness</p>	<p>Identification of potential flow paths where description is needed.</p> <p>Correlation between transport and hydrogeological parameters.</p> <p>Input to the F-factor (transport resistance) estimates.</p> <p>Flow logs considered in identification of "type structures" only for fractures – not for deformation zones at this time.</p> <p>Input for F considered in Laxemar 1.2 is mainly from the T-distribution using various assumptions. More elaborate estimates of F, using the hydraulic DFN model will be made in SR-Can.</p>	<p>Input to coupled hydrogeological/hydrogeochemical modelling of the surface system.</p> <p>No such modelling has been done.</p>	<p>Input of hydraulic properties and BC in rock.</p> <p>Parameterisation from Simpevarp 1.2 only used in Laxemar 1.2 surface hydrology modelling.</p>	<p>No need</p>	<p>No need</p>
---	---	---	---	--	---	---	---	----------------	----------------

<p>models, leading to an updated the size distribution for sizes larger than 500 m. There is still lacking a complete understanding of local fracture sets – especially the subhorizontal set.</p> <p>Some differences in the size distribution judged necessary in the Hydrogeological DFN.</p>				<p>of near-surface chemical data and vice versa).</p> <p>Using the flow model as input for simulations of depth of the redox front.</p> <p>Simulating the sampling procedure (water budget), that could cause additional mixing, has so far not yet been analysed hydraulically.</p>					
<p>No need (current hydrogeochemistry has very little impact on mineralogy). The rates are extremely small.</p>	No need	No need	<p>Hypothesis of palaeo-evolution. Density affects flow.</p> <p>Support for modelled discharge/recharge areas.</p> <p>Support for redox model.</p> <p>Present day salinity and water type distribution are “calibration targets” for simulation. Models consider density effects.</p> <p>Predictions of discharge and recharge areas have not yet been fully interpreted as regards to the hydrogeochemical data to assess reasonableness of predicted recharge-discharge areas.</p> <p>Not yet model predictions of depth of the redox front to compare with hydrogeochemical data.</p>	<p>Hydrogeo-chemistry in the bedrock</p>	<p>Groundwater composition affects diffusion and sorption parameters.</p> <p>Input to process-based retention modelling.</p> <p>Differences in water composition between matrix and high conductive fractures need to be consistent with matrix data used in transport model.</p> <p>Groundwater composition (identified water types) used to set up laboratory tests and in parameterisation of Retardation model.</p> <p>The transport model implications of the matrix pore water data are currently not fully assessed.</p>	<p>Boundary condition in surface system models.</p> <p>Some comparisons are made, but no detailed modelling.</p>	No need	No need	No need

No need	No need	No need	<p>Modelling salt migration should be consistent with assessed migration properties.</p> <p>Feedback on what aspects of the Hydrogeological DFN that is of importance for the transport resistance estimates. Feedback on importance of channelling in the fractures.</p> <p>Consistency check as regards porosities and mass transfer parameters used in palaeo-simulations.</p> <p>Feedback on importance of DFN and channelling not produced within SDM Laxemar 1.2, but will partly be addressed within SR-Can.</p>	<p>Modelling salt migration etc. should be consistent with assessed migration properties.</p> <p>Differences in water composition between matrix and high conductive fractures need to be consistent with matrix data used in transport model.</p> <p>The transport model implications of the matrix pore water data are currently not fully assessed.</p>	Transport Properties in Bedrock and QD	No need	No need	No need	No need
No need	No need	No need	<p>Identification of water types and boundary conditions.</p> <p>Input of surface water type considered in the modelling.</p>	<p>Identification of water types and boundary conditions.</p> <p>Some data used in simplified coupled/integrated model.</p>	Biogeochemical properties of QD (e.g sorption, solubility).	Chemistry in surface systems (QD, water biota)	<p>Supporting analyses, evaluation of chemical data to identify discharge areas of deep groundwater.</p> <p>Limited by lack of chemical data from the groundwater.</p>	<p>Data on specific processes, e.g. precipitation-dissolution.</p> <p>Data on chemical characteristics of QD.</p> <p>Limited by lack of chemical data from the groundwater and QD.</p>	<p>Chemical composition of soil, waters and biota.</p> <p>Used in modelling and validation of flow of matter in ecosystem descriptions.</p>

No need	No need	No need	Upper boundary conditions. GIS-modelled water courses. Simplified description used in deep rock model.	Input to deep rock model (e.g. GW recharge to rock). Hydraulic properties and boundary conditions in coupled models. Some data (e.g. groundwater levels) used in simplified coupled/ integrated model.	Flow field and evapotranspiration components. Done	Flow pattern, input to mass balance and mass transport modelling. Done	Surface hydrology, near surface hydrogeology and oceanography	Hydrogeological properties (comparison/ consistency check). Accumulation and erosion. Done	Flow rates, volumes of surface waters and groundwater, groundwater levels, water balances, physical properties of the water. Done: Used in turnover calculations for water and biomass transport modelling.
Syn- and post glacial tectonics. Only small amount of data available.	No need	No need	Bedrock surface. Used	Description of Quaternary deposits (QD) and soils provide input to selection of water types and input to coupled modelling. Some data used in simplified coupled model.	Geological model (QD map, DEM and stratigraphic model) used as a basis for numerical model. Physical properties of QD. Done	Type of QD, solid phases (description, process models). QD/water chemistry correlation. Not yet	Geological model (QD map, DEM and stratigraphic model) used as a basis for numerical model. Physical properties of QD. Done	Quaternary Deposits, Topography and bathymetry	Geological model (QD map and stratigraphic model) and soil map used as modelling inputs. Done
No need	No need	No need	No need	Biogeochemical processes. Processes identified, but not quantified.	Bioturbation	Biogeochemical processes (primary production and respiration). No detailed modelling performed.	Input data to water balance modelling.	Turbation, soil type and accumulation processes. Done	Biota in surface systems

Table A9-8. Consistency with past evolution.

Site Descriptive Model (SDM) Technical Audit: Consistency with past evolution		
Time period and subject	Is SDM consistent with evolution in this time period?	Are there findings from the modelling suggesting a need to update the Evolutionary model?
1,900 million years to the Quaternary		
Bedrock Geology	The Geological model is consistent with the regional geological evolutionary model. It would be potentially interesting, i.e. not done in Laxemar 1.2, to couple the geologic evolution and the formation of the different fracture sets (the order of formation could be determined) with hydrogeochemical indications (e.g. fracture minerals) of age. Although, such studies performed at Äspö HRL were rather inconclusive, they could nevertheless provide some insights into the validity of the conceptual model for groundwater flow and hydrogeochemical development.	There are no new data in Laxemar 1.2, which would necessitate an update of this evolutionary model.
Rock Mechanics	The stress model is consistent with the regional geological evolutionary model concerning the general stress direction in the latest period. But there has been no attempt to mechanically explain the creations of the deformation zones during previous periods.	No
During the Quaternary period		
Bedrock Geology	There is no information to support potential syn- or postglacial faulting. Near surface boulder “caves” and “assemblies” are an effect of glacial erosion and are not indications of post glacial seismic events /Lagerbäck et al. 2005/.	
Rock Mechanics	No reason to change current view of the conceptual model of stress. Implications from up-lift could possibly be assessed, but are not judged important in the Laxemar subarea.	No
Thermal model	Not assessed – there is also a lack of historical development data.	
Hydrogeology and Hydrogeochemistry	Groundwater flow and salinity transport simulations cover the period from the melting of the last glaciation, but not changes before that. Instead, the simulations have explored the impact of various assumptions made on initial conditions, properties, events and boundary conditions since the latest deglaciation (approximately 14,000 years ago). In general, analysing the impact of potential changes after the glaciation on the current day groundwater flow and distribution of groundwater composition will affect and support the conceptual groundwater flow model. The interaction between the evolution of the surface water composition and the evolution of the groundwater composition, is described concerning processes and origin of various water types (e.g. meteoric water, glacial melt water, Littorina water, brine).	There are large uncertainties in e.g. initial and boundary conditions: What is the time period for the existence of the Littorina sea, should the meteoric boundary conditions be divided into several time periods, what is the most appropriate origin of the water type “Marine sediments”, etc.
Surface System	We have a fairly good understanding of the last 14,000 years of development of the surface system, and the description of this historical development is consistent with the description of the present system.	No

Table A9-9. Changes since previous version.**List changes compared to previous model version (i.e. version Simpevarp 1.2)**

Geology	<ol style="list-style-type: none"> 1) Increased understanding and confidence of the 2D distribution of rock domains in the local scale model area – updating and refinement of 2D rock domain model due to new detailed bedrock map of the Laxemar subarea and surroundings. Apart from updating and refinement, the most conspicuous change compared to the Simpevarp 1.2 model is the definition of the two domains RSMP01 and RSMP02 (two branches of the Äspö shear zone). These are based on structural criteria (high frequency of ductile to brittle-ductile shear zones), and geographically, separate the Laxemar and Simpevarp subareas. 2) Increased understanding and confidence of the 3D geometry of rock domains in the local scale model volume – updating and refinement based on the new 2D rock domain model and new information from additional cored boreholes. 3) Increased understanding of rock domain properties in the local scale model area – new outcrop database for the Laxemar subarea and an increased number of modal, chemical and petrophysical analyses of rock types. 4) Deformation zones increased confidence in 2D zones along coastline, Ävrö and Simpevarp (bathymetric data). Alternative lineament interpretation increases confidence in previous lineaments identified on land. 5) Divided deformation zone confidence in existence into high, medium and low. 6) Subhorizontal zones assessed within the Laxemar subarea. 7) Evaluation modelling of the geological thickness of the high-confidence zones. 8) Updated -model of deformation zones. Increased number of high confidence zones in Laxemar subarea (but still many medium confidence zones). Some zones are now verified by targeted drillings. A new medium confidence zone is added. 9) Äspö shear zone is now modelled as two separate Rock Domains. 10) DFN model divided into rock domains and subareas – good agreement with fracture intensity to rock type.
Rock Mechanics	<ol style="list-style-type: none"> 1) Better data for rock mechanics properties increase confidence in intact Rock Mechanics properties description. Higher confidence in lab data for fracture tests. Better support for the empirical classification. 2) The theoretical approach is improved due to the rock domain specific DFN-model input. 3) Rock stress model is updated. The analysis considers additional zones- means that also Laxemar subarea is divided in to two stress domains. However, no new stress data. The stress model is updated based on evaluation of modelling results. 4) Quantified uncertainties for ALL aspects of the Rock Mechanics model. 5) Dilation angle include in the model.
Thermal	<ol style="list-style-type: none"> 1) Higher confidence in thermal conductivity rock type models. 2) Better understanding of spatial variability within domain RSMA. No significant change in mean thermal conductivity. 3) Mean thermal conductivity for domain RSMD is somewhat higher (2.70 W/m×K) in Laxemar 1.2 than in Simpevarp 1.2 (2.62 W/m×K) 4) Model results reported for domains RSMBA and RSMM, not modelled in Simpevarp 1.2. Potentially low thermal conductivity in domain M. 5) In Simpevarp 1.2 modelling results for domain RSMA were adjusted to take account of suspected bias (overestimation) in thermal conductivity values calculated from density. Results from Laxemar subarea require no such correction, even though contrary to what was found in Simpevarp 1.2, a slight underestimation of thermal conductivity is indicated by the density logging data. However, there are large uncertainties concerning calculated values for Ävrö granite with low thermal conductivity.
Hydrogeology	<ol style="list-style-type: none"> 1) A clearer picture of the definition of HRD and that they mainly coincide with the geological rock domains, even if there still are some data lacking to support this. 2) Assessed data from different scales and old data showing a tendency for depth dependence both in DZ and in the rock mass outside the DZ. This also concerns the spatial variability of properties with depth. 3) More data from Laxemar subarea, necessary for the hydraulic DFN model of Laxemar subarea.

- Hydro-geochemistry**
- 1) Only a few more water samples are available for the Laxemar subarea. The sharp depth trend suggested by KLX02 is not fully supported by the new data. There seems to be a more gradual increase in salinity.
 - 2) Improved understanding of the system from recharge of discharge, but still some key data on the recharge is missing.
 - 3) Improvement of the methodology and tools used in water/rock reaction modelling by conducting an analysis of sensitivity and uncertainty.
 - 4) ³H data evaluation has shown the limitations and possibilities in using such data for further modelling.
 - 5) Development of M3 modelling- reducing the uncertainties.
 - 6) Microbial evaluation assessing importance for redox conditions (but model still uncertain due to limited data).
 - 7) Re-assessing the data still suggests no evidence of Littorina water in Laxemar subarea (apart from some evidence in KLX01 which is located close to a Baltic Sea inlet).
 - 8) A few samples of matrix pore water.
- Transport**
- 1) Flow related transport parameters included in the analysis.
 - 2) Scale-up effects considered by flow path averaging over different rock types.
- Surface systems**
- 1) Soil model (GeoEditor)
 - 2) QD depth, stratigraphy and mapping
 - 3) Bathymetric model (part of DEM improved)
 - 4) Hydrology model over local model area (Larger model domains and use of more site data)
 - 5) Meteorological data from local stations
 - 6) Geometric data on watercourses
 - 7) Ecosystem models over local model area (enlarged area)
 - 8) Data on marine biota improved ecosystem description

Address whether there were any “surprises” connected to these changes

- Geology** No surprises in rock domain model. Mainly a combination of refinement and definition of new rock domains based on the available new detailed bedrock map of the Laxemar subarea and surroundings.
Increased uncertainty in coupling alteration to fracture intensity (affects the DFN model), but this is not a major surprise.
- Rock Mechanics** No real surprises.
- Thermal** No real surprises.
- Hydrogeology** Depth dependence not supported by Äspö data, but consistent with knowledge from most other sites.
- Hydro-geochemistry** No real surprises in overall chemistry
Generally no difference in salinity between matrix and flowing water down to about 500 m, (but below that the matrix is in cases more saline).
- Transport** Results broadly consistent with previous system knowledge.
- Surface system** No surprises in the surface system.

Address whether changes are significant or only concern details – is the model stabilising?

- Geology** Yes, the changes of the rock domains are significant in the local scale model volume, particularly in Laxemar subarea and in the area in between the latter and the Simpevarp subarea. The rock domain model is definitely stabilising but will certainly be refined by use of forthcoming data from cored boreholes.
The changes of the deformation zones in the Laxemar subarea mostly concern details, but there are still uncertainties (medium and low confidence zones).
The DFN model is judged better adapted to other user’s needs. There are still uncertainties and hypotheses left to explore.
- Rock Mechanics** The overall description is rather stable. However, the stress model is still uncertain, mainly due to lack of data.
- Thermal** Uncertainties remain, there is still potential for improving the model.
- Hydrogeology** Depth trends and the significant differences between the rock domains is a major change. Uncertainties remain, there is still potential for improving the model.

Hydro-geochemistry	Conceptual model appears stable (i.e. further evidence for non-marine waters in Laxemar subarea) – changes concern details. The updated information in ³ H could be significant.
Transport	For material property analysis it is a question of details. The inclusion of flow related parameters is significant from perspective of site knowledge and understanding. (Was previously only included in SA rather than in the SDM). Still significant uncertainties.
Surface system	Significant changes in all sub disciplines that constitutes the surface system. Model still under construction and areas not previously described have now been modelled. The description has by this version started to stabilise. Not all geographical areas covered.
